HYDRAULIC FLUID POWER

FUNDAMENTALS, APPLICATIONS, AND CIRCUIT DESIGN

ANDREA VACCA

GERMANO FRANZONI

WILEY

Hydraulic Fluid Power

Hydraulic Fluid Power

Fundamentals, Applications, and Circuit Design

Andrea Vacca
Maha Fluid Power Research Center
Purdue University
West Lafayette, Indiana, United States

Germano Franzoni
Global Mobile Systems, Parker Hannifin
Elk Grove Village, Illinois, United States

WILEY

Wiley also publishes its books in a variety of electronic formats and by print-on-demand. Some content that appears in standard print versions of this book may not be available in other formats.

Contents

Preface

The idea for this textbook came to the mind in the summer of 2003. At that time, as junior researchers at the University of Parma in Italy, the authors were tasked to learn more about hydraulic technology and gather material for a new course to be added to the mechanical engineering program.

Emilia Romagna in northern Italy, where Parma is located, is home to many proficient hydraulics manufacturers. To better connect with the surrounding industries, the Engineering Department of the University of Parma began teaching and doing research on hydraulics, a topic that was missing in the course offering.

The authors were challenged with preparing a material suitable for a college-level class and at the same time advertising the research capabilities of the university laboratory among the local fluid power companies.

After spending several hours online and in libraries searching for educational materials in fluid power, the authors immediately realized the absence of well-structured textbooks explaining the state-of-the-art of hydraulic technology. At the same time, by also interviewing hydraulic engineers in the workforce, they discovered how most knowledge on hydraulics seemed to belong to a restricted elite who learned through years of experience. This knowledge had been passed along within the same companies as a proprietary know-how, a kind of tribal knowledge.

Thanks to the "freedom of learning" allowed to young scholars in Italy, the authors started researching through existing literature and contacting Italian and international academic professors. Each book they had the chance to read and every class they could attend seemed to be focused only on certain aspects of hydraulics. Therefore, the authors started putting together different bits and pieces of a large collage, spending countless hours researching and animatedly debating on how to connect the dots.

The more their work was expanding, the more passionate they had become about hydraulics or better yet, "hydraulic fluid power." They quickly realized how this discipline has a huge technical implication and it often falls under the radar of many engineering departments. But it also is a very complex technology, which embraces bits and pieces of several other disciplines: structural mechanics, fluid mechanics, heat transfer, electrical engineering, control systems, product design, and others.

The authors also realized the difficulty to teach hydraulics, and the lack of structured teaching material was also probably the root cause for the decline in academic interest for fluid power. In fact, universities preferred to focus the attention on other technologies such as electronic controls and electric drives, which are more structured disciplines and benefit from the abundance of educational materials.

Also for this reason, the passion of the authors in their exciting hydraulics journey was fueled by a few individuals they had the good fortune to interact with. Prof. Nicola Nervegna, Prof. Gian Luca Zarotti, and Prof. Monika Ivantysynova are certainly among the pioneers of modern hydraulic education. Mr. Renato Casappa is an Italian entrepreneur who, like a modern-era Maecenas, promoted and financially supported several educational programs and symposiums. All of them felt that renewed interest on fluid power is needed to regain its lost inclusion in university curriculum. The authors feel lucky and privileged for having the chance to meet, interact, and in many cases closely work with these outstanding individuals. The level of the educational materials they produced or supported is among the best available today. Unfortunately, most of the materials created was not in English language, while some were not structured to reach the broader audience.

These are significant motivations for writing this book, aimed at filling the lack of educational materials suitable to train engineers in the field of hydraulic fluid power. However, all journeys come to an end, and both authors ended their shared research experience in Italy. While Dr. Vacca remained in the academia, Dr. Franzoni decided to pursue a career in the industry. However, as fate would have it, after several years, their paths crossed again in the American Midwest, a region that has a lot in common with the plains of Emilia Romagna in Italy where they originally met: hot, humid summers; modest, hardworking people; and a natural ingenuity born of necessity. Dr. Vacca joined one of the most important and advanced research labs in fluid power in the world, the Maha Fluid Power Research Center of Purdue University, while Dr. Franzoni joined Parker Hannifin, a global leader in hydraulics and motion control systems.

From here, the old idea of a textbook came back to life and both authors, during spring 2014, decided to seriously resume their old project. At this point, both authors could count on a much more solid base of experience. Dr. Vacca had become a well-respected faculty in the fluid power field, with numerous hours of teaching experience, organization of symposiums and conferences, as well as R&D collaborations with major fluid power companies and OEMs. He had the chance to work closely with and be mentored by Prof. Monika Ivantysynova until her tragic passing in 2018. On the other hand, Dr. Franzoni was fortunate to experience the current industrial environment and learn from customers' applications, as well as being mentored by two exceptional engineers: Jarmo Harsia and Leslie Claar. Both have contributed in building the solid application base which, according to the authors, is one of the essential features of the textbook.

The writing of this book was certainly "easier said than done." The authors spent more than 5 years of traveling between Lafayette, Indiana, and Chicago, to meet regularly, sacrificing family or leisure time and testing the patience of their significant others.

This book presents a new approach to the study of fluid power. Although there are parts inspired from material that can be found in other books, slides, classes or training manuals, the logic used to organize and present the design aspects of fluid power systems and the focus on real applications is completely original and unique. For these reasons, the authors are convinced that this manuscript is an excellent resource for both undergraduate and graduate level engineering classes. Furthermore, it is a reference guide that belongs on the desk of every hydraulic engineer in the industry.

Acknowledgments

The authors acknowledge many of the mentors that they had the privilege to work with: the already mentioned Prof. Nicola Nervegna, Prof. Gian Luca Zarotti, Jarmo Harsia, and Leslie Claar. More importantly, the authors firmly believe that this book would have never come to life if it had not been for Prof. Monika Ivantysynova. Both authors admired her passion and talent for fluid power research and credit her with many of the successes in their careers and personal lives. It is also thanks to her that both authors had the chance to reconnect in the USA.

The writing of the book involved also two co-authors who were very helpful in the development of some chapters. Gabriele Altare was part of the initial team and provided a tremendous support in the illustrations and writing of Chapters 4 and 5–9, while Lizhi Shang was instrumental in the chapter dedicated to hydrostatic pumps and motors (see chapter 6).

The authors' work was reviewed by several people: the graduate students of the Maha Fluid Power Research Center (class of 2019), Pradeep Gillella, Barun Acharya, and other members of Parker Hannifin, who all provided tremendous help with chapter reviews and suggestions for improvement.

Finally, both authors want to give a special thanks to their loving wives, Jing and Sarah, who supported us during this multiple years' journey and accepted us being away from home on numerous weekends.

Part I

Fundamental Principles

The first part of this book is dedicated to the description of the fundamental laws, concepts, and conventions that are necessary to comprehend the functioning of hydraulic circuits and hydraulic components.

Chapter 1 contains a brief introduction of the hydraulic control technology and an explanation of the symbology used to illustrate hydraulic circuits.

Chapter 2 gives an overview of the properties of hydraulic fluids and how their properties can affect the operation of a component or a circuit. It also illustrates the detrimental effects of fluid cavitation, aeration, and contamination.

Chapter 3 recalls fundamental concepts derived from fluid mechanics, which are useful to describe the operation of fluid power components.

Subsequently, Chapter 4 is dedicated to the orifice, which is one of the most important conceptual elements of hydraulic control circuits. Orifices can have multiple functions and variable orifices can be used to describe the operation of many hydraulic components. The orifice equation will be repeatedly used throughout the manuscript.

Although the focus of the book is on the steady-state operation of hydraulic machines and circuits, Chapter 5 introduces the reader to the basic analysis of transient operation of hydraulic circuits.

Objectives

Part I aims to familiarize the reader with the fundamental concepts and equations that will be used for the analysis of hydraulic circuits and hydraulic components. A reader already familiar with these concepts is still recommended to peruse the chapters of Part I, to be clear with the symbology and conventions used throughout the manuscript. After a thorough understanding of the contents presented in Part I, including the worked examples as well as the completion of the problems at the end of each chapter, the reader will be able to

1. Interpret circuits drawn with symbols of the ISO standard of representation.
2. Discuss the most common hydraulic fluids and describe the most important fluid properties affecting the operation of a hydraulic system.

3. Describe the concept of fluid cavitation or aeration and determine the effect on the fluid properties.
4. Describe the detrimental effects of solid contaminants in a hydraulic system.
5. Identify sources of energy loss, as turbulent or laminar hydraulic resistance.
6. Analyze flow forces in hydraulic components resulting from variation of fluid momentum.
7. Analyze the steady-state operation of a flow network, based on the pressure law and flow law.
8. Derive the orifice equation starting from the fundamental Bernoulli equation.
9. Recognize the function of a specific orifice in a hydraulic network.
10. Discuss the concept of hydraulic resistance, hydraulic capacitance, and hydraulic inductance and their effects on the transient response of basic hydraulic systems.
11. Apply the concept of hydraulic resistance, hydraulic capacitance, and hydraulic inductance for basic analyses of hydraulic transients.

Chapter 1

Introduction to Hydraulic Control Technology

Hydraulic control systems are used across many engineering applications to provide motion and force control of mechanical systems. With respect to competing technologies for transmitting mechanical power (i.e. mechanical drives or electrical drives), hydraulic drives offer favorable characteristics from both the power to weight ratio and control perspectives. State-of-art hydraulic systems can be up to 1 order of magnitude lighter than electric systems with the same power (or torque) level. Also, compared with mechanical drives, hydraulic systems offer a greater layout flexibility thanks to the versatile design of the piping or hose system that connects the hydraulic components. Hydraulic drive technology also easily offers solutions for advanced actuator control, in terms of output velocity and force, motion reversals, and safety functions. These mentioned features are particularly advantageous in applications involving the transmission of large amounts of power. For this reason, hydraulics is a consolidated technology in many heavy-duty applications, in manufacturing industry (hydraulic presses, molding machines, machining robots, etc.), and in mobile applications (construction, agriculture, aerospace, military, and marine). Recent progress in component miniaturization and interfacing with electronic controls have also brought hydraulic systems into emerging fields such as biomedical engineering (surgery robots, patient transfer and rehabilitation devices, etc.).

However, compared with other technologies for power transmission and motion control, hydraulics has some significant drawbacks, the most important one being the inevitable presence of energy losses. Depending on the application, other disadvantages might affect hydraulic systems, such as the high influence of temperature on the system behavior, the possible insurgence of leakages, and the limited duration of the working fluid, due to aging or contamination.

From the considerations made above, it appears clear how a "best technology" for transmitting mechanical power does not exist in absolute. The most suitable technology for a given application is usually the result of a compromise between initial and operating costs, functionality, durability, reliability, and safety. Consequently, it is very important for a designer to be fully aware of the possible technological alternatives that can be available for the system under evaluation from the early design stages. Too often a designer chooses the technology for which she/he has more experience, without considering alternatives. Due to the chronic lack in fluid power education in engineering schools, hydraulic control technology is seldom the preferred designer's choice. This book aims to fill this gap by educating current and future generations of designers on the potentials of hydraulic control technology.

1.1 Historical Perspective

The science of "hydraulic fluid power" (mostly known as "hydraulics") dates back from the ancient cultures. Earliest uses of hydraulic structures, such as dams, levees, and water distribution networks, were made by Egyptians, Romans, and Chinese populations even more than 2000 years ago. The term "hydraulics" originates from the Greek word hydraulikos compiled from hudôr (water) and autos (pipe).

> Fluid power is a discipline studying systems and machines that use fluids to perform mechanical actuations. Fluid power is subdivided into **hydraulics** and **pneumatics**. Hydraulic systems use liquids as fluid media. Instead, pneumatic systems use compressed air.

Basic principles for transferring fluids were already put in practice by Archimedes in the third century BCE. The first fundamental hydraulic laws were outlined in his work "Treatise on Floating Bodies." The principles discovered by Archimedes are the same that are governing the operation of modern-day hydrostatic units. However, his inventions did not reach the force multiplication potentials offered by fluid, as discovered by Blaise Pascal in the seventeenth century. In fact, it is the seventeenth century that marks the appearance of the first pumps or closed-circuit applications. The following discoveries have relevance in the history of fluid power:

- The first axial piston pump design was conceived by A. Ramelli (Figure 1.1) in the year 1588. The basic elements of a modern axial piston pump have not changed significantly from the first design idea by Ramelli.
- The first gear pump effectively used by Pappenheim in 1636.

The first machine that ushered in the modern era of hydraulics is the hydraulic press attributed to Joseph Bramah (1795). Many hydraulics machines assisted the industrial revolution in Europe, providing methods for power transmissions alternative to belts and mechanical drivetrains. Some European cities in the 1860s were equipped with central fluid power generating stations.

The major technological breakthrough in modern hydraulic technology was the introduction of oil as the working fluid in the early 1900s. The Waterbury Tool Company in 1905 introduced for the first time a variable flow rate pump operating with oil. The pump was capable of delivering about 120 l/min at 50 bar for a maximum shaft speed of 300 rpm, and it weighed about 300 kg. The use of oil in place of water, as in prior systems, permitted the hydrostatic units to operate reliably at higher pressure, thus reaching superior power to weight ratios. The first full hydraulic transmission system working with oil is considered to be the hydrostatic transmission system presented by Williams and Janney in 1905 to propel one of the first infantry tanks (Figure 1.2). Oil was also used for the first modern hydraulic system used in marine application in 1906. This was when a hydraulic system was developed to replace the electrical system that controlled the guns in the USS Virginia. This was the beginning of the modern era for fluid power.

After some decades of stagnation, during the great economic depression of the 1930s, renewed interest for fluid power technology emerged during the Second World War. This was driven by the need for high-power transmissions for ground and marine equipment, the requirement for precise and rapid aiming systems for heavy guns, and the need of precise control for aircraft fighters. It is during these years when fluid power technology moved from being a craft to becoming a serial
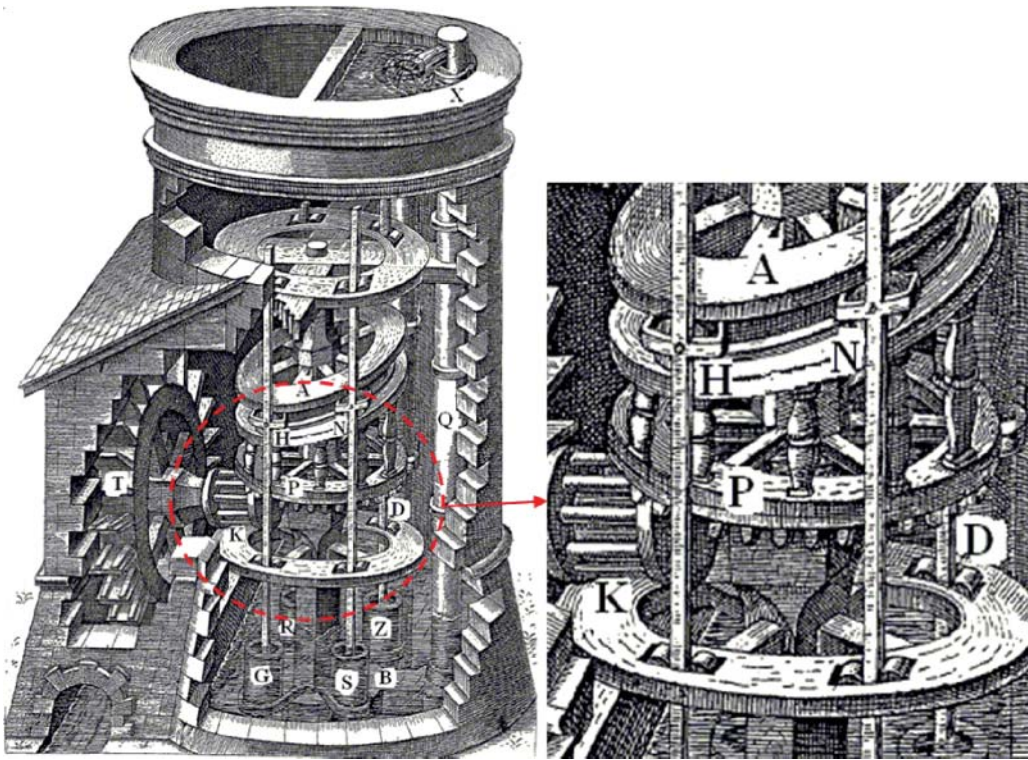
Figure 1.1 The axial piston pump sketched by A. Ramelli [1].

production industry. The decades following the Second World War are known as the *golden era* of fluid power; many entrepreneurs and inventors pioneered the creation of new components and technologies around the world. In this period before the advent of computers, control challenges were solved in many elegant ways, thanks to the creativity of some brilliant minds. For example, in the United States, Harry Vickers (1898–1977) is considered the greatest fluid power pioneer. He founded Vickers Corp. and performed many inventions such as the pressure balanced vane pump and the hydraulic power steering. Later in the years, Vickers Corp. acquired the electronic divisions of Sperry Corp. in 1978, which sparked several advancements made in the field of solenoid valves and proportional controls for industrial valves. Aeroquip-Vickers was acquired by Eaton Corp. in 1999.

In the United States, Arthur Parker (1885–1945) founded the Parker Appliance Company in 1918 (Figure 1.3). The firm started with producing pneumatic components for air compressors and moved into brake systems for vehicles. The success of the company strengthened in the 1930s shifting into the production of fittings for the aircraft industry. Today Parker Hannifin Corp. is a large group providing hydraulic, fluid connector, and motion control solutions for mobile, industrial, and aerospace businesses.

In the same century several individuals fueled the industrialization of hydraulics in Europe. For example, in Germany, Alfred Rexroth (1899–1978) led the company founded by his ancestor Georg Ludwig Rexroth in 1975 into the development of hydraulic components. Initially, in
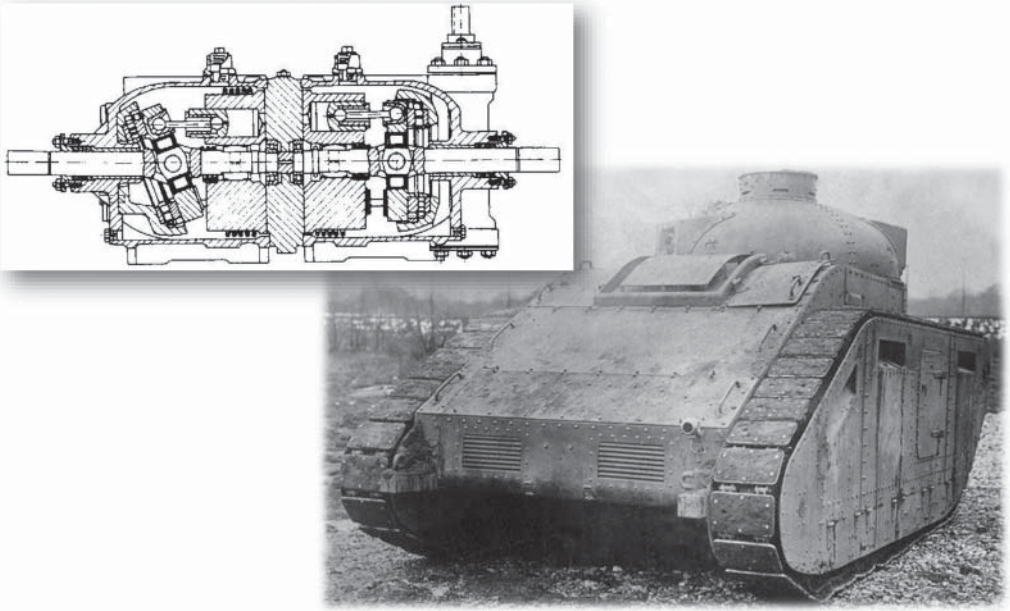
Figure 1.2 The Williams–Janney transmission was based on axial piston design units and used to propel one of the first infantry tanks (1905).

the 1950s, industrial production involved casted valves and gear pumps. In the first half of 1960s, industrial manifolds and mobile directional control spool valves were introduced. The second part of the decade instead saw the evolution of radial and axial piston pumps. In the 1970s hydraulics started merging with electronics; the first servo valves for industrial applications were introduced to the market. Also in Germany, Carl Von Linde founded with two other partners in 1904, the company known today as Linde Group. The company started specializing in refrigeration systems and introduced to the market hydrostatic-propelled vehicles in 1956. Linde Hydraulics launched the first load sensing (LS) valve in 1986. The industrialization of fluid power was not limited to Germany, but saw many historic contributions also in England, Italy, Sweden, and Eastern Europe.

Fluid power technology, including oil hydraulic and pneumatic systems, is recognized in academia as an independent discipline that has defined research and scholarly activities since the Second World War. In particular, the Massachusetts Institute of Technology (MIT) in the United States started working on the development of hydraulic control systems since 1939. An initially small team rapidly grew larger, making contributions in hydraulic components design and hydraulic control theories and calculation methods that are still considered fundament of fluid power discipline. Published in 1959, the work by MIT faculty Blackburn, Reethof, and Shearer [2] is perhaps the greatest technical manuscript ever written on fluid power technology, and it has influenced many following books, including this one.

Many other universities followed MIT and established research institutes expressly devoted to fluid power research. Many of these departments are still alive, shaping research on fluid power technology. A list of the most of these research centers can be found in [3].

The authors encourage the reader interested in learning more about the main historical passages of the hydraulic fluid power technology to consult Skinner's book [4].
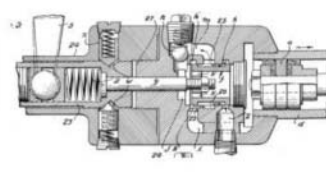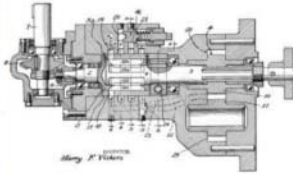
Harry Vickers and some of his patents (vane pump and power steering)

A view of the first "Parker appliance company" and their booth at the International Aircraft exposition in 1930
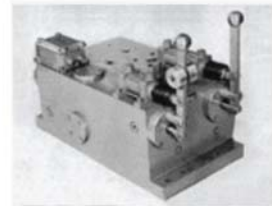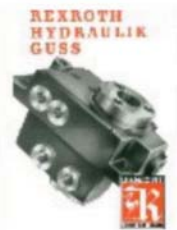
An old Rexroth catalog for cast iron valves, one of the first axial piston pumps, a three-piston radial piston pump and one of the first integrated manifolds (from left to right)

One of the first gear pumps and a mobile directional valve for a hydraulic excavator

Figure 1.3 A collage of pictures from historical moments of the fluid power industry. Sources: Various online sources.

1.2 Fluid Power Symbology and Its Evolution

One of the main barriers in the past for exchanging technical information related to hydraulics has been the lack of a common "language": a standard way to represent hydraulic circuits and systems. Figures 1.4 and 1.5 show two examples of hydraulic circuits represented in some "old fashion" styles. Even if the circuits are fairly simple, their representation is not of immediate understanding. They have different ways of indicating the components along with their functions in the circuit; one circuit shows component cutaways, while the other one describes the function of every part with
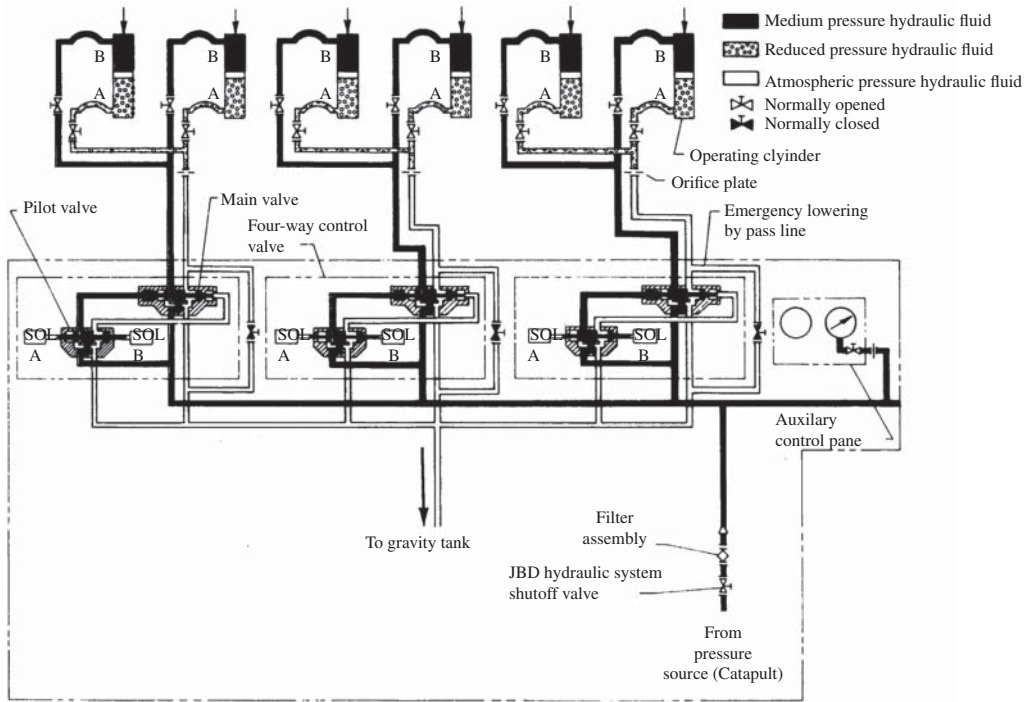
Figure 1.4 Hydraulic system of a jet blast deflector. Source: Beasley 1990.

arrowheads and text. Also, one circuit tries to give a detailed representation of the system layout and piping, while the other one uses straight lines between the ports.

A multitude of different approaches for representing hydraulic circuits were developed in the past by various companies and fluid power institutes. The aim was the same: representing on a single sheet of paper the system functions, the layout, and the design details of the components. However, the result was different. This lack of commonality represented an obstacle to the development of a common science.

The discussion on fluid power symbols and standards was initiated in the United States by the Joint Industry Conference (JIC) in 1944, and the first JIC-defined hydraulic symbols and standards were released in 1948. Soon after, the national standardization organizations took over: in 1958 the American Standards Association (ASA) released their revised version of the JIC standard. In Europe, the Comité Européen des Transmissions Oleohydrauliques et Pneumatiques (CETOP), founded in 1962, provided a series of recommendations on graphic symbols for fluid power that were received and approved by the International Organization for Standardization (ISO).

Finally, in 1976, the first version of ISO 1219 standard *Fluid Power Systems and Components: Graphic Symbols and Circuit Diagrams* was released. The ISO 1219 (parts 1 and 2) is frequently revised and updated. It is nowadays considered as the universal reference for representing hydraulic circuits.

ISO 1219 standard is the universal reference for representing hydraulic circuits. In engineering problems involving a hydraulic control system, it is always recommended to represent the system schematic using ISO symbols and following the criteria suggested by the standard.
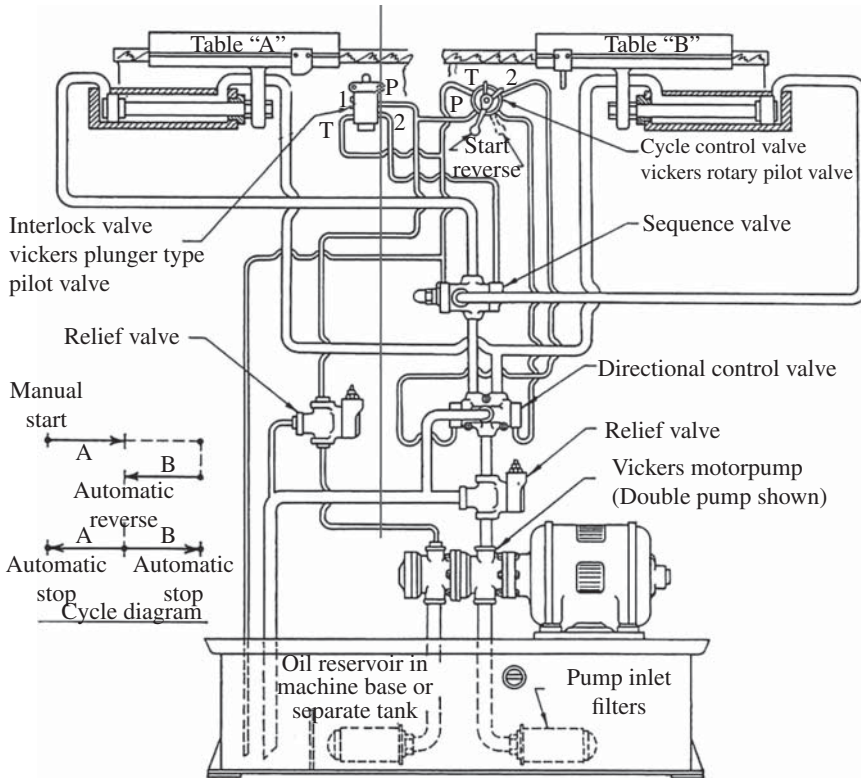
Figure 1.5 Hydraulic circuit with pilot-controlled sequence valve. Source: Harry Franklin Vickers, 1989.

The detailed description of the ISO 1219 standard is beyond the scope of this book; all rules and conventions can be found on these two ISO standards [5, 6]. However, it is still worthwhile to summarize the primary and most important aspects introduced by the standard:

- *Function representation.* The hydraulic circuit schematic should focus only on the functionality of both the components and system, whereas other information such as mechanical details of the parts or physical layout of the system should not be represented.
- *Symbols.* The standard includes precise recommendations about the symbol to be utilized to represent a specific component. The symbol itself contains relevant information necessary to understand the functionality of the component.
- *Additional information.* In the schematic of the system, each symbol needs to comprise information necessary to understand the operation. These include a label that uniquely identifies the component, particular function of the component, and sizing information.

All the systems presented in this book will adhere to the ISO standard of representation. The *additional information* will be often omitted for the sake of generality. However, it is important to point out how this information should never be neglected when the circuit is designed for an actual application.

These three aspects of the ISO standard can be described with the example of Figure 1.6, which represents a basic system to control a hydraulic cylinder. The components are laid out in a way that is very intuitive: the oil flows from tank to the actuator following a bottom-to-top path; vice versa, the return oil flows from top to bottom. This is the most popular way of representing circuits: all the actuators are clearly located at the top, the power source elements at the bottom, and the control

elements in the middle. An alternative layout can also follow a left-to-right path. Obviously, this is not related to the actual layout of the system.

The circuit comprises a hydraulic reservoir **1** that supplies flow to a fixed displacement pump **3** driven by an electric motor **2**. The pump outlet is connected to a four-way 3-position (4/3) solenoid-operated on/off directional control valve **5**, which in neutral position connects P to T, while the workports A and B are blocked. The pump outlet is also connected to an adjustable pressure relief valve **4**, which outlet is connected to the return line from **5** to tank. The workports A and B of valve **5** are supplying the linear actuator **6**: in particular A is connected to the bore and B to the rod side. When solenoid **Y1** is energized, the valve shifts in the "parallel arrows" position, and the pump outlet is connected to the cylinder bore, while the cylinder rod is connected to tank. In this situation, the cylinder extends. When solenoid **Y2** is energized, valve **5** shifts in the "crossed arrows" position, and the pump outlet flow is connected to the cylinder rod, while the bore discharges to tank; thus, the cylinder is retracted.

The circuit also provides the additional information needed to complete the understanding of the system operation. These include the size of the tank and the type of hydraulic fluid, the installed power of the electric motor, the shaft speed of the pump and the flow rate in the system, the maximum pressure in the system, the function of the valve solenoids, and reference to the electric connections. Even the size and length of the hydraulic lines are reported.

All essential features of the system operation should be derived from this information. For example, during cylinder extension, the velocity of the actuator is 0.24 m/s and the return flow 9.2 l/min, while during retraction these values are 0.47 m/s and 35.3 l/min. Similarly, the maximum power request can be estimated in 4 kW for the maximum allowed load at the cylinder.

The above description of the simple system of Figure 1.6 emphasizes the large amount of information provided by a schematic that complies with the ISO standard. Many designers often miss the advantages offered by a correct representation of a circuit, which is extremely helpful at various design and maintenance phases of a hydraulic-powered machine.
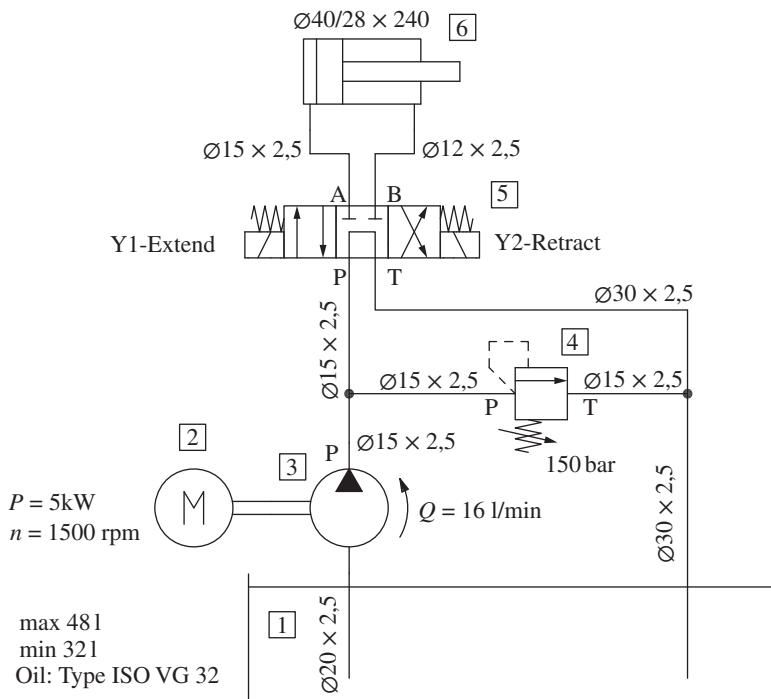
Figure 1.6 Hydraulic circuit for moving an actuator.
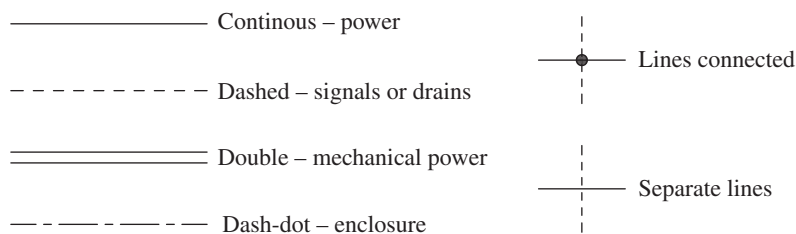
Figure 1.7   Meaning of different types of lines in hydraulic circuits.

1.3   Common ISO Symbols

The most common elements in hydraulic circuits are the hydraulic lines. As summarized in Figure 1.7, four line styles can be found in a schematic, and each one has a different meaning:

(1) *Continuous lines* represent working power lines; for example, these are the lines connected to the outlet and inlet of pumps and motors.
(2) *Dashed lines* represent pilot signals (for example, a load-sensing line between a LS pump and a valve) or drain lines (for example, the case drain of a variable displacement unit).
(3) *Double lines* represent mechanical power transmission, like in the case of a motor shaft.
(4) *Dash-dot lines* are instead used to indicate the physical layout of the system. When multiple components are enclosed in a dash-dot line, they are part of the same physical unit as, for example, a hydraulic manifold.

Another important rule is that the intersection of two or more lines needs to be represented by a dot. If two lines intersect on paper without a dot, it means that they remain physically separated.

Figure 1.8 represents the symbols for the most common prime movers (electric and motor and combustion engine) and for some elements that are often placed between the prime mover and the hydraulic energy conversion units. These can be gearboxes, clutches, or *power takeoffs* (PTOs) and can be equipped with different functionalities.

Figure 1.9 presents common symbols for energy conversion units. Rotary units are represented with circles, while linear actuators use rectangles. The reader can notice that each symbol emphasizes different characteristics. For example, the symbol of the fixed displacement pump is the only one highlighting the pump rotation. The first variable displacement pump does not mention anything about the type of control, while the second one emphasizes that the pump displacement is regulated based on the value of the outlet pressure. As it will be presented in Part 2, the representation
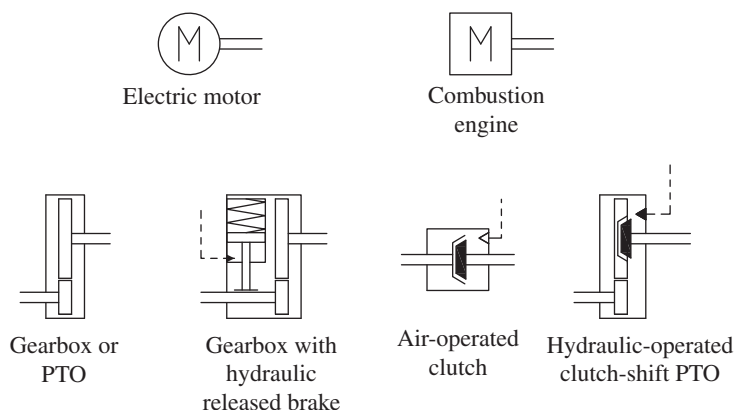
Figure 1.8   Common symbols for prime movers and mechanical rotary transmission elements.

CW fixed displ.
pump

Variable displ.
pump

Pressure compensated
variable displ. pump

Unidirectional fixed
displ. motor

Bidirectional
variable displ. motor

Bidirectional variable
displ. pump/motor

Double-acting
cylinder (single rod)

Double-acting
cylinder (dual rod)

Double-acting
telescopic cylinder
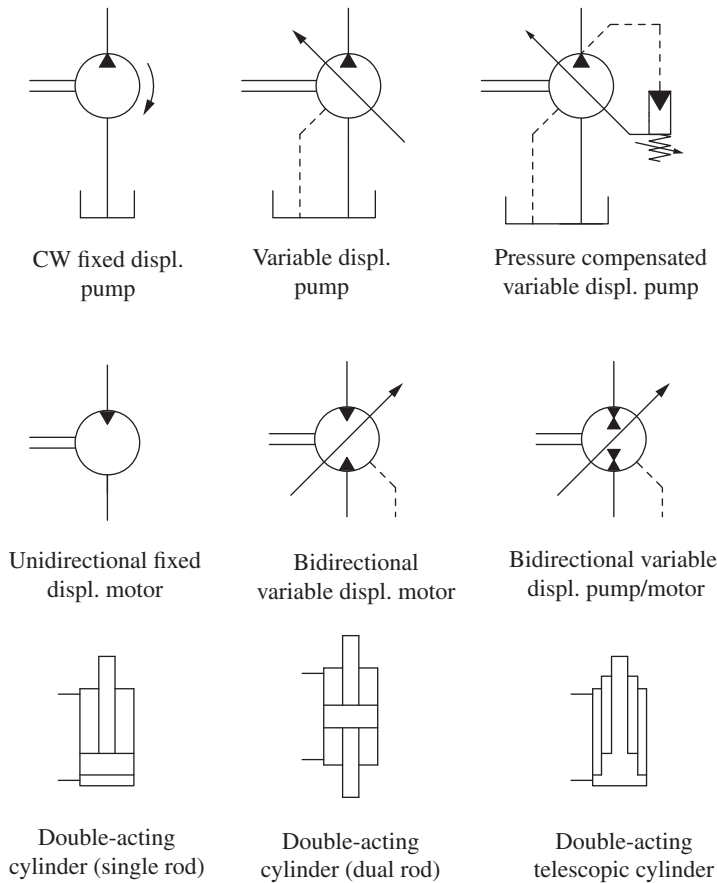
Figure 1.9 Common symbols utilized for prime movers and energy conversion units.

of the pump control can also be much more detailed. Depending on the case, the engineer can select the level of detail that needs to be presented in the hydraulic schematic.

Figure 1.10 reports some common symbols for pressure and directional control elements. These are always represented by squares that include arrows connecting the different ports. Each square represents the possible configurations of the valve. At the end of the squares, the actuation method is represented. This can be a solenoid, a spring, or an external or internal pilot pressure.

The elements on the first row of Figure 1.10 are three very common pressure control devices: relief, reducing, and counterbalance valves. Relief valves are used to protect circuits from over-pressurization and always discharge flow to tank. Reducing valves instead are used to reduce the supply pressure to a lower level. They are normally open valves where the spring is always drained to tank. Counterbalance valves are pressure control valves with two areas of influence that also include a check valve function. On the second row, three examples of two-way two-position valves are represented. Each valve has a different configuration and different control and implements a different application. The last row includes two examples of four-way three-position valves. The three squares indicate the neutral and the extreme positions. The first valve is a solenoid on/off valve, while the second one is a pilot-operated proportional valve. More details about the characteristic of these elements will be provided in the following chapters.

Finally, Figure 1.11 presents some symbols used for accessory elements and sensors. Accessories can be accumulators, coolers, filters, and breathers. These symbols can be simple or more articu-lated if it is necessary to identify additional features such as for the case of a filter with bypass valve

Pressure relief
valve

Pressure reducing
valve

Counterbalance
valve

2/2 manual
directional control
valve (N.O.)

2/2 ON/OFF solenoid
directional control
valve (N.C. with free
reverse flow)

2/2 poppet valve
(pilot to close)

4/3 ON/OFF solenoid-operated
directional control
valve (workports vented, P
blocked in neutral)

4/3 proportional hydraulic
pilot-operated directional
control valve (all ports
blocked in neutral)

Figure 1.10 Common symbols utilized for directional and pressure control elements.

Accumulator

Cooler

Filter

Breather

Filter with bypass and
differential pressure switch

Air-to-cooler with electric
fan and bypass valve

Pressure
gauge

Pressure
switch

Pressure
sensor

Temperature
sensor

Flow meter
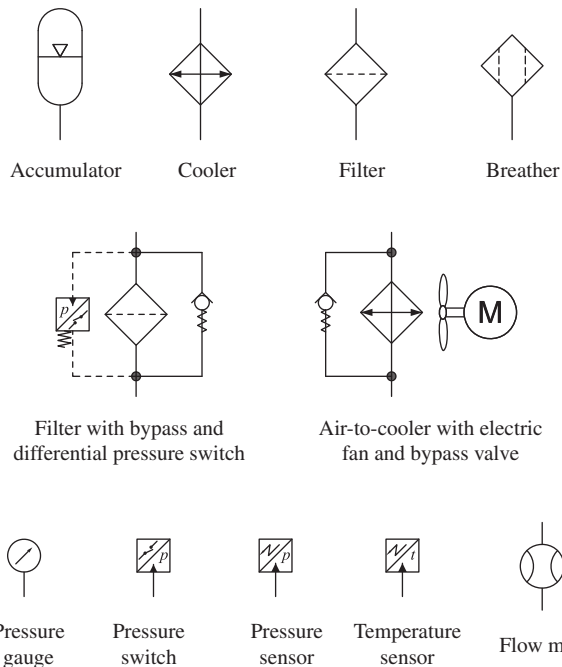
Figure 1.11 Symbols used for accessory elements and sensors.

and differential pressure switch. It is again a matter of the level of details that the designer wants to highlight in the circuit.

Example 1.1   Hydraulic schematic for a conveyor application

A hydraulic system is used to control a bidirectional conveyor. The system uses a 50 *kW* internal combustion engine (shaft speed of 1800 *rpm*) to drive a 35 cm^3/*rev* variable displacement axial piston pump. The conveyor is driven by a 20 cm^3/*rev* fixed displacement hydraulic motor (a bidirectional gear motor with a drain, rated speed of 1800 *rpm*). The control of the direction of rotation of the motor is achieved by means of 4/3 directional control valve, manually operated. The motor does not rotate in rest condition. The maximum system pressure has to be limited to 200 *bar*, and for this purpose one or more pressure relief valves can be used.

Draw the schematic of the circuit according to the basic rules of the ISO 1219 standard of representation, and comment on the operation of the system in standby conditions.

Given:
The generic description of a hydraulic system, which includes:

- a prime mover (internal combustion engine), with power $\dot{W} = 50$ *kW* and shaft speed of $n = 1800$ *rpm*;
- a variable displacement hydraulic pump (axial piston type) driven by the abovementioned engine, $V_p = 35$ cm^3/*rev*;
- a 4/3 directional control valve (details of the position not given), manually operated;
- a hydraulic bidirectional motor, $V_m = 20$ cm^3/*rev*, connected to the above valve; and
- one or more relief valves (pressure setting $p^* = 250$ *bar*), which accomplish the safety function (preventing excessive system pressurization).

Find:
The hydraulic schematic according to the ISO standard of representation.

Solution:
A possible representation of the hydraulic system is given by the figures below.
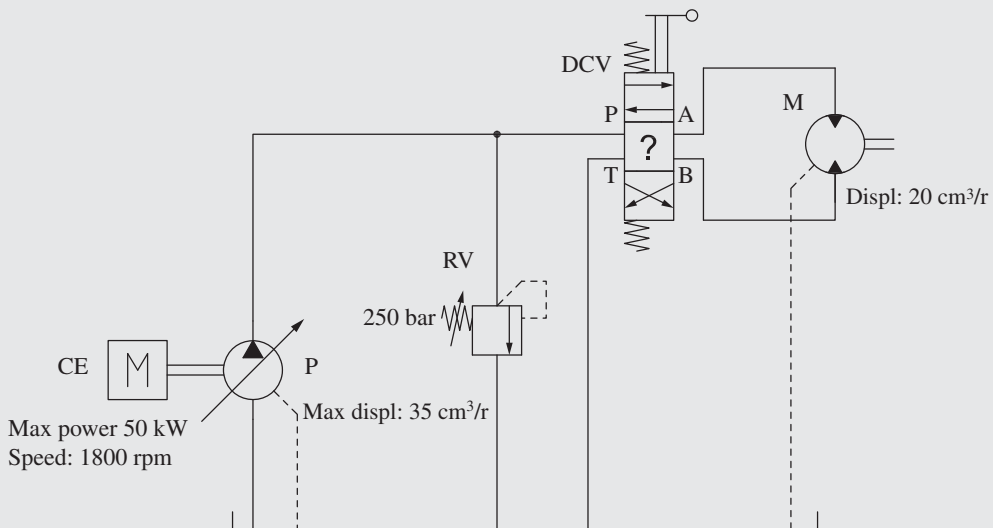
Alternative representation:
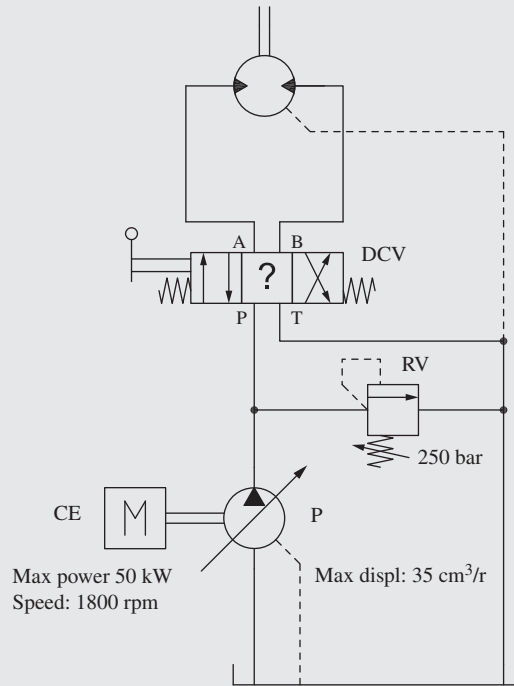
Remarks:

- The schematic in the top figure follows a left-to-right direction of representation. Starting from the prime mover positioned to the left, the schematic ends with the hydraulic function, or the actuator, at the right side of the schematic. As an alternative, the representation from bottom (prime mover) to top (actuator) is provided in the bottom figure.

  Either of these two options for representing a hydraulic system is acceptable, and it usually increases the readability and facilitates a quick understanding of the functioning of the system.

- The schematic must represent the operation of the system during rest condition. In other words, the connections of the supply pump and those of the actuator must be aligned to the central (or neutral position) of the directional control valve (DCV). These connections are indicated with the letters P (connection to the supply pump), T (connection to tank), A, and B (actuator workports). This central (or neutral position) corresponds to the configuration of the system when the DCV is not actuated. In position 1 (parallel arrow), the hydraulic motor rotates in one direction (i.e. clockwise). In position 2 (crossed arrows), the hydraulic motor rotates in the opposite direction (i.e. counterclockwise).
- Most of the component details defined in the problem statement are useful information for the analysis of the system, and therefore they are reported in the schematic as suggested by ISO 1219. The construction type of the pump (axial piston pump) and of the motor (gear motor) is not provided because it is not essential for a basic study of the system. This additional information, such as the component manufacturer and the component code, and other information, can be reported in a separated table.

Example 1.1 (Continued)

- The size of the component is not reflected in the size used for the corresponding symbol. For the case of this problem, the size of the circle used to represent the pump is the same of the one used to represent the hydraulic motor, even if the pump has a larger displacement.
- One pressure relief valve is used to protect the system against overpressurization. This relief valve is placed at the pump outlet, thus preventing the pump to supply fluid at a pressure higher than p^*. A sophisticated control of the pump displacement might integrate this feature (this will be seen in Part 3). However, since it is unknown if the pump has a pressure limiting device integrated into its design, a relief valve is included in the figure above.
- The problem statement does not specify the neutral position of the DCV, although it specifies that in neutral the fan speed should be null.

As it will be seen later (Chapter 8), DCV can easily implement different options for the rest position. For this problem, the designer could choose among the options below.
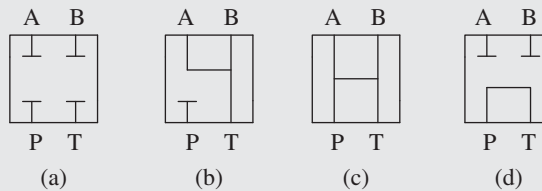
In the hydraulic schematic shown above, the selected neutral position is (c). In this position all ports P, T, A, B are connected to tank. This allows the pump to divert the flow to the tank (which is the path of minimum effort for the fluid), thus maintaining the outlet port P at a minimum pressure. The motor ports are also connected to tank; therefore the fan will not rotate since no flow energy is provided to the hydraulic motor. Position (b) would be another reasonable solution, although it would require a pump able to adjust its instantaneous displacement to zero in rest conditions. Otherwise, in rest conditions, the pump would supply flow to the relief valve RV, thus at the maximum allowable pressure, requesting high energy to the CE. Position (a) and (d) would block the motor ports; this would cause excessive pressure at the motor workports when the fan is brought to a sudden stop through the DCV. Such positions would require additional relief valves to handle these transients.

Problems

1.1 Using following symbols, represent a schematic of a hydraulic system that rotates the hydraulic motor in both directions. All the circuit branches need to be protected from overpressure using proper pressure relief valve(s). Symbols with (*) can have more instances. Use the minimum number of components.

Does the system have an "on/off" regulation nature, or does it implement a variable angular speed of the load?

Hydraulic pump
(with prime mover)

Pressure relief
valve* (discharges
to tank)

Hydraulic motor
(with load)

Directional valve
(manually operated)

Tank*
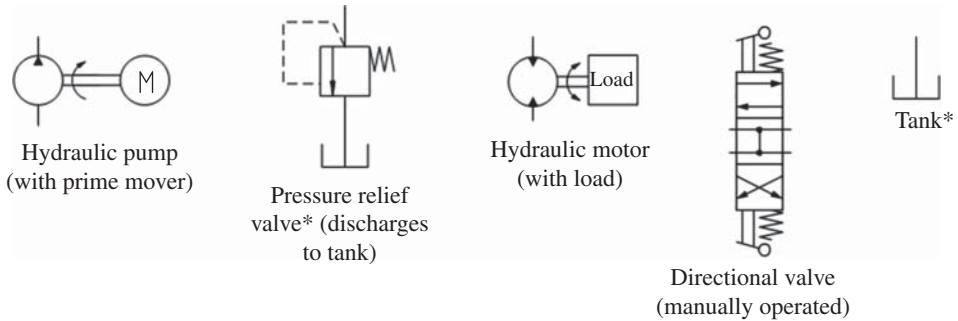
1.2 Solve again Problem 1.1. But instead of using the manually operated valve, use the electrically operated directional valve shown below.

Directional valve*
(electrically operated)
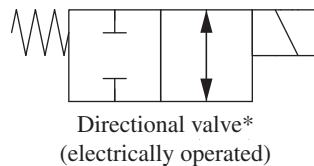
1.3 Consider the hydraulic system below. It includes two fluid sources (generically represented) that supply two circuits: one circuit is to pilot the actuation of valve 1, and one circuit supplies the main flow through the hydraulic actuator, cylinder 2. What happens to the cylinder 2 when the valve 1 is pushed and held?

   A It extends immediately and remains extended.
   B It extends after a certain time interval, necessary to fill the accumulator.
   C It remains in equilibrium, not moving at all.
   D It retracts immediately, and it remains retracted.
   E Retract immediately and extend after a certain time interval.
   Motivate your answer.

Accumulator,
initially discharged
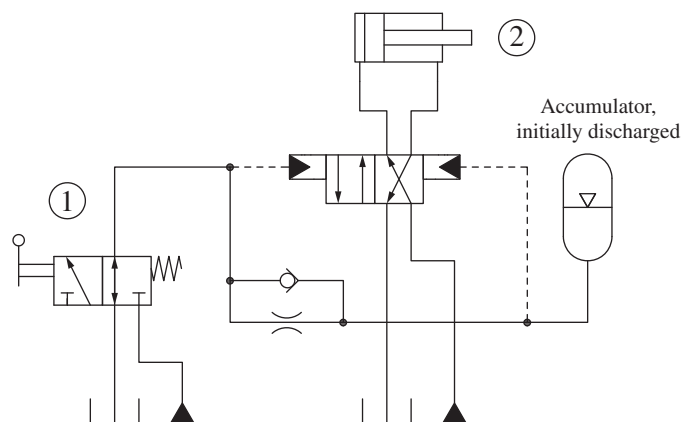
1.4 Consider again Problem 1.3, now with a modification of the hydraulic schematic as shown below. The pilot-operated valve includes now a spring. Does the behavior of the hydraulic cylinder 2 change? Motivate your answer.
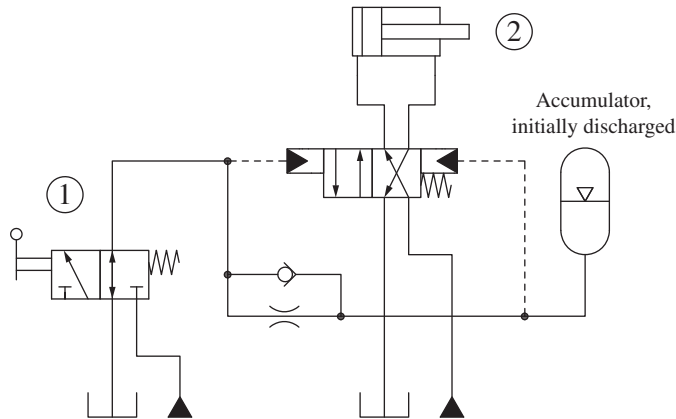
1.5 A hydraulic control system uses a 5 kW engine to drive a hydraulic motor ($10 \, \text{cm}^3$/rev, gear type with external drain) and a single-acting hydraulic cylinder (piston diameter: 80 mm, rod diameter: 40 mm). The single-acting cylinder is used to lift and lower a gravitational load. The two actuators are independently supplied by two fixed displacement gear pumps ($10 \, \text{cm}^3$/rev) both connected to the thermal engine. Both pumps are protected by system overpressurization through relief valves (pressure setting of 250 bar). Each pump is connected to the actuator through a directional valve that allows both directions of motion for the actuators. For controlling the hydraulic motor, a 4/3 valve is used. Instead, the single-acting cylinder is actuated through a 3/3 directional control valve. The retraction of the cylinder occurs through gravity. For this purpose, between the 3/3 valve and the cylinder, there is a check valve in parallel with a fixed orifice, calibrated for achieve a flow of 10 l/min during the lowering condition. Both directional control valves are solenoid operated. In rest conditions, no flow is supplied to both actuators, even if no load holding is achieved.

Represent the hydraulic schematic of the system, with particular attention to the positions of each directional control valve.

Chapter 2

Hydraulic Fluids

This chapter provides a brief description of the properties of hydraulic fluids. In general, the working fluid can be considered as the main component of the hydraulic system. The fluid is the media that transports the energy between different parts of the system; it can change its energy level as it flows through hydraulic components. Beyond this main function, the working fluid also lubricates the internal parts of the hydraulic components. Another important function of the hydraulic fluid is heat removal: the working fluid carries the heat that is generated within certain components of the hydraulic system and can be cooled using proper heat exchangers (HEs).

A deep analysis of the working fluid properties requires a solid base of chemistry, also because nowadays fluids are often a mix of several components and additives, in appropriate quantities to achieve the desired properties. For example, some fluids are fire resistant, while others are designed to work in some hazardous environments. However, the description of the fluid as energy transfer media requires only a limited number of fluid parameters. This chapter introduces these parameters, and it allows the reader to understand some considerations made throughout the next chapters of the textbook. Additional bibliographic references are provided for the reader that is interested in further studying the topic of hydraulic fluids.

2.1   Ideal vs. Actual Hydraulic Fluids

As mentioned before, the hydraulic fluid can be seen as a "distributed" component of the system. This concept can be described with the help of Figure 2.1, which shows a very simple hydraulic circuit that moves a linear actuator (CYL). The circuit is composed by a pump (P) driven by an electric motor (EM). The pump displaces fluid from the tank (T) to a directional control valve (DCV), which determines the direction of the flow from the pump to the actuator. Depending on the DCV configuration, the actuator rod (CYL) can move to the right, to the left, or remain at rest. A relief valve (RV) is used to limit the maximum pressure at the pump outlet, protecting it from overpressurization. The circuit also has a filter (F) that ensures the proper cleanness level of fluid, removing the solid contaminants coming from component wear or entering the circuit through the cylinder lip seals. Finally, an HE removes excess heat from the fluid. The hydraulic lines connecting all the components mentioned above represent pipes or hoses used to connect the different parts of the circuit.

A more detailed description of each component will be provided in the following chapters of the book; the reader at this point should not worry too much about having a full understanding of the operation of the above circuit. In general, each component has a certain function in the system operation, and its functionality can be studied by considering either its ideal behavior or its actual behavior. The ideal behavior represents the best possible scenario, i.e. it excludes the presence of
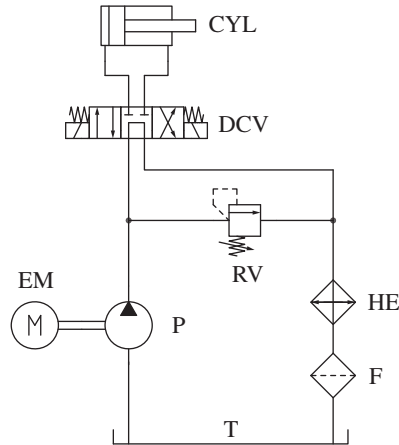
Figure 2.1 Example of simple hydraulic circuit. The hydraulic fluid can be imagined as an additional "distributed component" of the circuit.

undesirable – yet unavoidable – phenomena such as leakages, frictions, etc. Instead, the actual behavior is representative of the real-world operation, which accounts for the presence of these undesired effects. For example, the motion of the actuator (CYL) ideally occurs without frictional losses or leakages between the piston and the cylinder bore. In reality, these undesirable aspects are present during the operation of the system. Because of that, the energy required to generate the piston motion is higher than the energy that would be involved in the ideal case.

In the analysis of engineering problems, the use of ideal models greatly simplifies the circuit analysis. The ideal case is also useful to define a reference behavior that can be used to quantify the relative performance of an actual system or component. Important parameters such as energy efficiency will also be defined in this book by comparing the ideal use of energy of a system (or a component) with respect to the actual behavior.

Imagining the working fluid as a physical component of a hydraulic system might not be an obvious assumption. However, from a very high level, the hydraulic fluid can be seen as a physical element present everywhere in the circuit. Similar to other components of the entire system, the hydraulic fluid accomplishes specific functions, and its behavior can be described by either an ideal or a realistic model. In particular, the hydraulic fluid is a distributed "imaginary" component that accomplishes the following functions:

- *Energy transport*. With reference to Figure 2.1, the energy in the system flows from the prime mover (EM) through the pump (P) to the rest of the hydraulic system and finally to the end user (CYL). This transport occurs thanks to the fluid particles that travel and vary their energy level throughout the hydraulic system. This is the main function of the working fluid in a fluid power system. The lines dedicated to the transport of the energy are represented with continuous lines (see example in Figure 2.1).
- *Lubrication*. Many hydraulic components have internal parts in relative motion. The hydraulic fluid can lubricate these parts, avoiding solid-to-solid contacts that can lead to wear and energy dissipation. On the other hand, the fluid should be selected to avoid excessive leakages through the clearances between the solid part.
- *Heat removal*. The functioning of hydraulic systems often involves high levels of power. The energy dissipation present in the system, caused by mechanical friction, fluid shear, or throttling losses, often represents a significant portion of the overall power exchanged by the system. This energy dissipation is mainly converted into heat. Fortunately, the hydraulic fluid can carry

most of the generated heat. The ability of the fluid to carry heat permits the use of only one HE (in Figure 2.1), which can cool the working fluid to maintain its temperature within an acceptable range.

- *Signal transfer* (pilot lines). In addition to the working lines where the flow rate is significant, a hydraulic system often contains lines dedicated to the transmission of the pressure signals. Most of control strategies are implemented with components that sense the pressure at certain remote locations of the system. Dedicated lines are required to transmit this pressure information (pilot line). In these lines, the flow rate can usually be neglected, at least for a first understanding of the system operation. These pilot lines take advantage of the property of the fluid to transmit the pressure information rapidly and without significant energy consumption.

The **ideal fluid** accomplishes the above functions by:

- **avoiding irreversible interactions with the component materials**, such as oxidation or erosion;
- having an **infinite life**; and
- having **constant physical properties**, particularly as pertains to fluid compressibility and viscosity.

Instead, an **actual hydraulic fluid**:

- can be chemically reactive and interact with the material used to build the components;
- has physical properties that degrade with time; and
- has physical properties that strongly depend on the operating conditions, particularly on pressure and temperature.

Significant advancements in the formulation of hydraulic fluids have been made in recent years. This has led to the development of hydraulic fluids whose properties are very close to the ideal behavior. The features usually desired in a hydraulic fluid are:

- limited influence of pressure and temperature on fluid viscosity;
- high lubrication capacity;
- high bulk modulus (meaning low compressibility);
- long-life resistance and chemical stability;
- high flash point value (limiting risks of explosions and flammability);
- limited toxicity;
- high compatibility with the component material; and
- limited tendency to induce material corrosion.

2.2 Classification of Hydraulic Fluids

This section provides a high-level classification of the hydraulic fluids according to the current international standards. Details like formulation and chemical properties of each hydraulic fluid are out of the scope for this textbook. Nevertheless, it is important for the reader to understand that the panorama of the possible options for the working fluid is vast. Progress in various areas is constantly made by the industry to enhance the behavior of the commercially available hydraulic fluids. More details can be found in literature. Suggested readings are the book by Totten and De Negri [7] or by Zarotti [8].

Several standards have been formulated to classify the fluids currently available for hydraulic systems. The most important one is the ISO 6473 [9]. From this standard, a hydraulic fluid belongs to one of the following categories:

- mineral oil (the fluid identifier starts with H);
- fire-resistant fluid (the fluid identifier starts with HS);
- synthetic fluid.

2.2.1 Mineral Oils (H)

The most common hydraulic fluids in hydraulic systems for off-road (agricultural vehicles, construction, and mining machines) and industrial applications are mineral-based oils. These fluids have good operating features (according to the parameters described in the previous paragraphs) and are particularly economical in comparison with the other categories of hydraulic fluids. A good subclassification of the mineral oils can be represented by the schematic of Figure 2.2. From a base oil (HH), several other hydraulic fluids can be derived by using additives: HL implies an HH oil with anti-oxidation and anti-rust additives. From an HL oil, the use of additives that reduce the dependency of viscosity with temperature (VI improvers) leads to HR oils. If anti-wear additives are added to an HL oil, the fluid is then indicated with the letters HM (or HLP). HM oils are probably the most common fluids in today's hydraulic systems. More variants can be derived from the HM oils by adding VI improvers (HV oils) or with the use of additives that reduce the stick-slip effect that can occur inside hydraulic control valves.

The International Organization for Standardization (ISO) classification of Figure 2.2 is similar to the alternative DIN standard, which is still in use, especially in European countries. Table 2.1 shows the designations of the two standards for the most common oils.
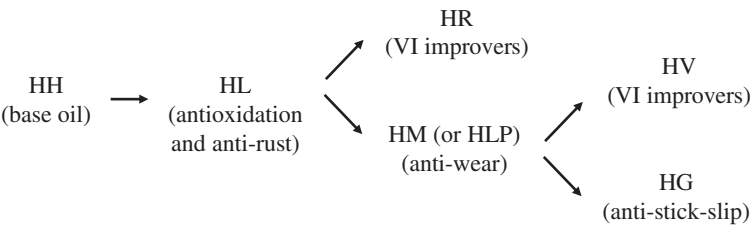
Figure 2.2 Classification of mineral oils according to ISO 6473-4. Source: Adapted from Zarotti [8].

Table 2.1 Correspondence between the DIN and the ISO standard for mineral oils.

DIN (code)	Additives	ISO
H	None	HH
HL	Anti-rust + antioxidant + antifoam	HL
HLP	Anti-rust + antioxidant + antifoam + anti-wear	HM
HLP-D	HLP + detergent + dispersant	Not envisaged
Not envisaged	HM + additives to improve viscosity index	HV

Source: Adapted from Assofluid [11].

2.2.2 Fire-Resistant Fluids (HF)

As the name of the category suggests, fire-resistant fluids are specifically used in applications where fire or explosion hazards must be limited. These fluids are in most cases water based. A basic classification of these fluids can be done according to ISO 7745 [10], summarized by the tree diagram of Figure 2.3.

HFA fluids contain at least 80% of water, and they can be further divided into HFAE, which are oil-in-water emulsions with anti-wear additives and HFAS, which contains other chemical solutions in water. HFB are emulsions of water in oil, with a minimum of 40% of water content. HFC are glycol-in-water solutions (from 35% to 60% of water content), and they also include additives to improve fluid viscosity. HFD fluids are synthetic products without water. In particular, the HFDR fluids are based on phosphate esters; the HFDS fluids are based on chlorinated hydrocarbons; the HFDT fluids are a base of a mixture of HFDR–HFDS fluids; finally, HFDU are fluids with other synthetic products (not further specified).

For HF fluids, especially those containing water, the maintenance or replacement of the working fluid is essential. It is also important to periodically monitor the composition of the fluid to ensure it has not been altered. Hydraulic fluids are often referred to with their commercial name rather than with the correct ISO denomination. A significant example in the fire-resistant fluid category is the Skydrol, which is a fire-resistant fluid used in aviation. This fluid belongs to the HFDR category.
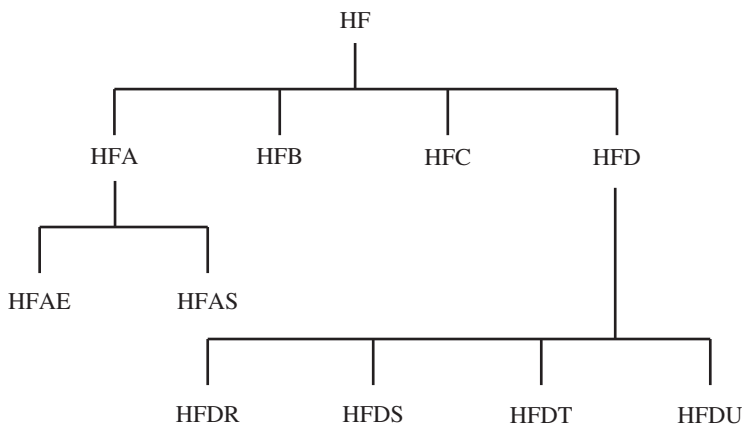
Figure 2.3 Classification of fire-resistant fluids according to ISO 7745. Source: Adapted from Zarotti [8].

2.2.3 Synthetic Fluids (HS)

ISO 6473 specifies the acronym for HS synthetics fluids, without further specifying their composition. Usually, these fluids are developed for specific applications. A typical example is the case of extreme temperature conditions. The technology for HS fluids is continuously evolving, and the number of options today available is too high to be summarized in a short list. Nevertheless, many current HS fluids are based on silicate esters and polyol esters.

2.2.4 Environmentally Friendly Fluids

In certain applications there is an increasing preference for using fluids that are environmentally friendly. In particular, a significant effort has been put in developing fluids that are highly biodegradable.

Synthetic fluids HPG (polyol esters) and HE (esters) and vegetable oils HTG (from sunflower and kale) belong to this category.

2.2.5 Water Hydraulics

Hydraulic control technology began and progressed with water as a working fluid until the beginning of the twentieth century, when mineral oil fluids became available. After that, the use of water for hydraulic control systems remained confined to very specific and limited applications, and basically all applications have been "oil hydraulics."

In the 1990s, the fluid power community renewed the interest for the use of water hydraulics for both mobile and industrial applications. This was mainly pushed by a couple of major players in the fluid power industry [12]. The main motivations for this renewed interest were driven by the following properties of water with respect to mineral oil:

– lower viscosity (about 30 times lower), which means less energy losses due to fluid shear;
– lower temperature dependency of viscosity;
– higher bulk modulus (about 50% higher);
– lower air release (up to 20 times); and
– higher specific heat (more than double) and higher thermal conductivity (about five times), which promote the cooling ability of the working fluid.

Additionally, one should not forget that water is inexpensive, and it does not pollute the environment. Despite these advantages, the following limitations have so far prevented the success of water hydraulics:

– *Lower viscosity*. Lower viscosity is a merit when it comes to frictions but is a limit for the lubrication ability of the fluid. Fluid lubricity is an essential property for guaranteeing the correct operation of fluid power components, particularly volumetric pumps and motors. These components present lubricating gaps in which the fluid has to generate a film able to avoid direct contact between the parts in relative motion.
– *Corrosion and oxidation*. While normal steel and iron can operate without durability problems with mineral oils, metals and other materials compatible with water tend to be more expensive in general.
– *Vapor pressure and freezing point*. The typical values of vapor pressure and freezing point limit the operating range of water hydraulic systems, particularly with respect to the fluid temperature. Normally, water hydraulic systems need to operate in the range of 4–50 °C.
– *Bacteria and fungi*. Water is the essence of life. This is not good news for a hydraulic machine. When the system is at rest, bacteria and fungi can grow in the different parts of the system, causing problems related to fluid contamination.

Because of these factors, components for water hydraulics applications need to have a special design, and they usually end up with high manufacturing costs. Consequently, water hydraulics is still considered to be a niche field, which is now almost limited to high-pressure washing systems, reverse osmosis water production systems, and some other marine applications.

2.2.6 Comparisons Between Hydraulic Fluids

A good summary of the main properties of different hydraulic fluids is provided in Table 2.2. This summarizes the data that can be found in literature [11], although one must consider that the use of additives can significantly alter the properties indicated in the table. Notwithstanding, the table

Table 2.2 Comparison between different hydraulic fluids.

Fluid	Density (kg/m³)	Viscosity Index (VI)	Lubricating power	Fire resistance	Antioxidizing power	Maximum temperature (°C)	Toxicity	Average cost
Mineral oil	870–900	70–100	Excellent	Poor	Excellent	−5 to 70	Low	100
Vegetable oil[a]	920	210	Excellent	Good	Fairly good	−10 to 70	No toxicity	250
Polyglycols[a]	1100	150–200	Excellent	Good	Good	−30 to 80	No toxicity	350
Synthetic esters[a]	920	200	Excellent	Good	Good	−30 to 100	No toxicity	700
Water-in-oil	915–940	High	Fairly good	Excellent	Good	0–50	Low	200
Water glycol	1060	High	Fairly good	Excellent	Good	0–50	Low	400
Chlorinated hydrocarbons	1430	Low	Good	Good	Fairly good	−5 to 70	High	700
Phosphoric esters	1270	Low	Excellent	Good	Fairly good	−5 to 70	High	500
Mixture of esters and chlorides	1150	Low	Excellent	Good	Fairly good	−5 to 70	High	600
Silicones	930–1030	High	Fairly good	Excellent	Fairly good	−5 to 90	Low	<700

a) Refers to biodegradable fluids.
Source: Adapted from Assofluid [11].

is particularly significant in its last column, which quantifies the relative costs of different fluids. Assuming the reference cost of a mineral oil being 100 (the actual value fluctuates depending on several economic factors), the cost of all other oils is at least double. This is the main reason for the popularity of mineral-based oils.

2.3 Physical Properties of Hydraulic Fluids

Properties of hydraulic fluids, such as density or viscosity, are usually tabulated (or expressed by analytical formulas) as functions of pressure and temperature. In order to justify the choice of pressure and temperature as independent variables, the Gibbs' phase law of thermodynamics should be considered:

$$f = n - \kappa + 2 \tag{2.1}$$

The Gibbs' rule defines the number of degrees of freedom, f, necessary to describe the state of a substance in thermodynamic equilibrium. The formula uses the number of components of the substance (n) and the number of phases in equilibrium (κ). The number of degrees of freedom is the number of independent intensive variables that can be varied simultaneously and arbitrarily without determining one another. An intensive variable does not depend on the size of the considered system. For the case of a hydraulic oil, specific volume, density, pressure, temperature, and viscosity are examples of intensive variables.

If we consider the hydraulic fluid as a single component matter (i.e. a pure chemical) even if it is usually a mixture of different components, then from Eq. (2.1), for a single-component system ($n = 1$) in the liquid phase ($\kappa = 1$), the number of degrees of freedom f is equal to two. This means that two intensive variables can be arbitrarily selected to completely determine the status of the fluid. Among all possible choices, choosing pressure and temperature is particularly convenient because:

- pressure and temperature are relatively easy to measure, with respect to other intensive properties of the fluid; and
- an engineer has a better ability or practical intuition to relate pressure and temperature to practical problems.

> Two intensive variables fully define the status of a liquid. In hydraulic, pressure and temperature are the typical choice for the independent variables used to express the functional between fluid properties.

2.4 Fluid Compressibility: Bulk Modulus

From the consideration made in the previous paragraphs, the functional dependence of the volume occupied by a certain amount of hydraulic fluid has the following form:

$$V = V(p, T) \tag{2.2}$$

The dependence of the volume on the variations of both pressure and temperature can be expressed made with a simple linear equation by considering the first-order Taylor series expansion:

$$V = V_0 + \left(\frac{\partial V}{\partial p}\right)\Big|_{T_0} (p - p_0) + \left(\frac{\partial V}{\partial T}\right)\Big|_{p_0} (T - T_0) \tag{2.3}$$

In other terms, the deviations from the initial volume V_0 (at the reference conditions p_0, T_0) can be expressed in a linear form by defining the coefficients:

$$B = -V_0 \left(\frac{\partial p}{\partial V} \right) \Big|_{T_0} \tag{2.4}$$

$$\gamma = -\frac{1}{V_0} \left(\frac{\partial V}{\partial T} \right) \Big|_{p_0} \tag{2.5}$$

So

$$V = V_0 \left[1 - \frac{(p - p_0)}{B} + \gamma \cdot \left(T - T_0 \right) \right] \tag{2.6}$$

> The parameter B is known as **isothermal bulk modulus** of the fluid, and it indicates the tendency of the fluid volume to vary under changes in pressure.

The negative sign in the definition of Eq. (2.4) implies an inverse type relationship, meaning that an increase of pressure causes a reduction in the fluid volume.

The reciprocal value $1/B$ is known as isothermal compressibility. In the fluid power field, however, the isothermal compressibility is not commonly used.

The parameter γ of Eq. (2.5) is known as **isobaric cubic expansion** coefficient (or simply volumetric expansion coefficient), and it expresses the tendency of the fluid volume to vary with temperature.

As it will be mentioned in the following chapter, pressure variations in the working fluid form the basis of the functioning of hydraulic systems. For this reason, the bulk modulus B is an important parameter that can be used to quantify the compressibility effects of the fluid. In the case of hydraulic systems, temperature effects on the fluid compressibility can be in most cases neglected. For this reason, the cubic expansion coefficient is a parameter rarely encountered when analyzing a fluid power system.

A practical definition for the bulk modulus is based on the finite form of Eq. (2.4), where finite differences are used instead of the differentials:

$$B = -V_0 \left(\frac{\Delta p}{\Delta V} \right) \tag{2.7}$$

The nature of the processes used to measure the pressure and volume variations (for example, isothermal or adiabatic), as well as the way of experimentally evaluating volume variations (secant or tangent methods), results in slightly different definitions for the bulk modulus. It is out of the scope for this book to discuss these details. However, the reader could refer to specific literature on fluid properties, such as [1].

Typical values for the bulk modulus of hydraulic fluids range between 15 000 bar and 20 000 bar. It can be interesting to note that typical hydraulic fluids are less stiff than water, which has a bulk modulus of about 22 000 bar.

Even if the concepts described in this book do not involve many considerations about fluid compressibility, it can be interesting to note how the bulk modulus of a fluid is in direct relation with the speed of sound within the fluid.

In fact, from the basic definitions of thermodynamics, the speed of sound c is defined as [13]

$$c = \sqrt{\frac{dp}{d\rho}} \tag{2.8}$$

Considering the definition of Eq. (2.4), after noticing that $\Delta V/V = \Delta\rho/\rho$ (the definition of fluid density, ρ, will be given in Section 2.5), the speed of sound results in

$$c = \sqrt{\frac{B}{\rho}} \tag{2.9}$$

2.5 Fluid Density

Density is an important intensive property of a fluid, and it can be defined as the ratio between the mass and the volume at a given state. Considering reference condition as (p_0, T_0), the density ρ_0 is given by

$$\rho_0 = \frac{m_0}{V_0} \tag{2.10}$$

Typical values of density of different fluids at room temperature and atmospheric conditions are given in Table 2.3.

Following the same line of reasoning presented in Section 2.4, density variations can also be related to pressure and temperature. The isothermal bulk modulus and the isobaric cubic expansion coefficient defined in Section 2.4 can be used to quantify the dependence of density on pressure and temperature.

The variation with respect to pressure (assuming constant temperature, T_0) is shown below:

$$\rho\,(p) = \frac{m_0}{V_0 + \Delta V|_{T_0}} = \frac{m_0/V_0}{1 + \frac{\Delta V}{V_0}|_{T_0}} = \frac{\rho_0}{1 - \frac{\Delta p}{B}} \tag{2.11}$$

However, the variation with respect to temperature (assuming constant pressure, p_0) is as follows:

$$\rho\,(T) = \frac{m_0}{V_0 + \Delta V|_{p_0}} = \frac{m_0/V_0}{1 + \frac{\Delta V}{V_0}|_{p_0}} = \frac{\rho_0}{1 + \gamma\Delta p} \tag{2.12}$$

The chart of Figure 2.4 shows the typical variation of fluid density for three different oils. The plot results from Eq. (2.11) using the following values for the parameters of Eq. (2.12) (values taken from [14]):

From Figure 2.4, one can notice that the change in density over a large pressure variation is not negligible. In particular, for a mineral oil, the same mass of fluid is exposed to a volume reduction (or a density increase) of about 0.7% every 100 bar of pressure variation. Using the same parameters from Table 2.4, the plot of Figure 2.5 can be derived from Eq. (2.12) to represent the variation of fluid density with temperature.

Table 2.3 Typical values for fluid density.

Fluid	Density [kg/m³]
Mineral oil	870–900
Water	1000
Water/glycol	1060
Water/oil emulsion	920–940
Vegetable oil	930
Chlorinated hydrocarbons	1400
Phosphoric esters	1150
Silicon-based fluid	930–1030
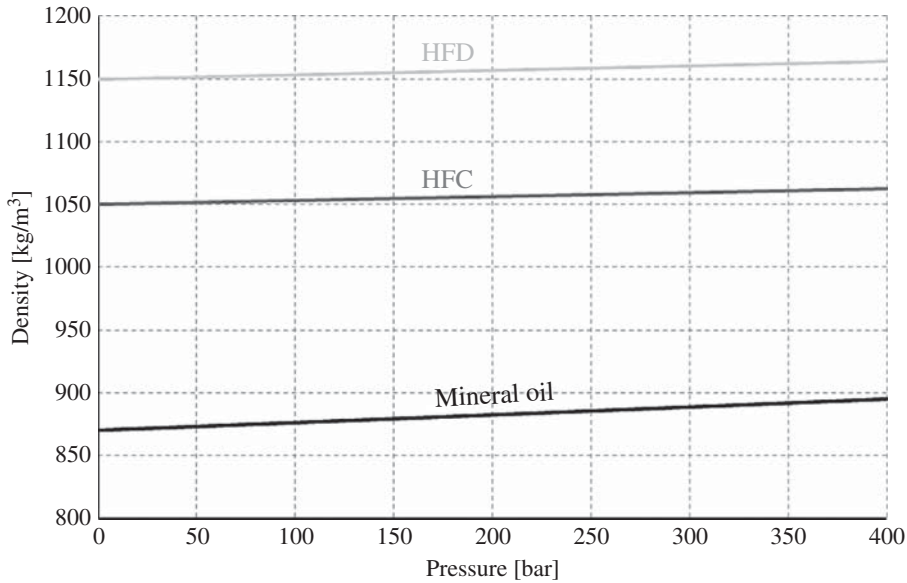
Figure 2.4 Density variation with pressure for three oils (parameters listed in Table 2.4).

Table 2.4 Fluid parameters used for the plot of Figure 2.4.

Fluid	ρ_0 [kg/m³]	$\frac{1}{B}$ [bar⁻¹]	γ [K⁻¹]
Mineral oil	870	$0.70 \cdot 10^{-4}$	$0.65 \cdot 10^{-3}$
HFC	1050	$0.30 \cdot 10^{-4}$	$0.70 \cdot 10^{-3}$
HFD	1150	$0.35 \cdot 10^{-4}$	$0.75 \cdot 10^{-3}$

Example 2.1 Liquid compressibility

A $10\,l$ rigid container is completely full of hydraulic fluid (density equal to $870\,kg/m^3$; bulk modulus equal to $1700\,MPa$). Calculate the volume of oil (in liters, l or cubic meters, m³) that must be introduced into the container to achieve a pressure increase from 0 to $200\,bar$.

Given:
The volume of a container $V = 10\,l$; the density of the fluid inside the container $\rho = 870\,kg/m^3$ and the bulk modulus $B = 1700\,MPa$; the pressure difference for the fluid inside the container $\Delta p = 200\,bar$.

Find:
The volume ΔV of fluid necessary to achieve the given Δp.

Solution:
The volume variation ΔV can be found straight from the definition of the bulk modulus:

$$B = -V\frac{\Delta p}{\Delta V}$$

(Continued)
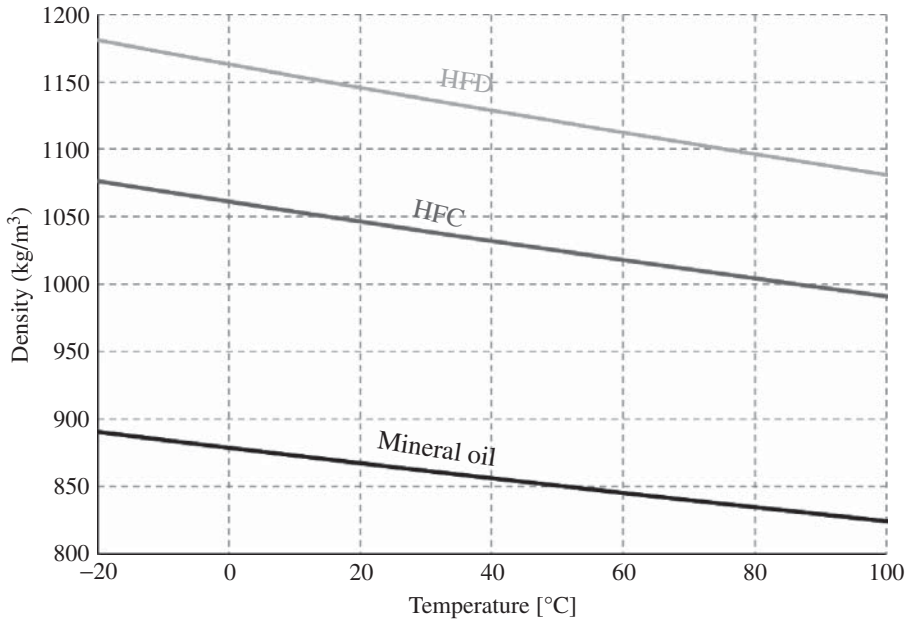
Figure 2.5 Density variation with temperature for three oils (parameters listed in Table 2.4).

Example 2.1 (Continued)

which gives

$$\Delta V = -V\frac{\Delta p}{B} = -0.010\,[m^3] \cdot \frac{2 \cdot 10^7\,[Pa]}{17 \cdot 10^8\,[Pa]}$$
$$= 0.117 \cdot 10^{-3}\,m^3 = 0.117\,l$$

2.6   Fluid Viscosity

Each fluid particle can experience surface forces, due to pressure or friction that are generated by contact with other particles or a solid surface. These surface forces lead to stresses. The concept of stress helps in describing how forces acting on the boundaries of a medium are transmitted throughout the medium itself. The concept of stress is very intuitive for a solid: stresses develop when the material is elastically deformed or strained. For example, when a force is applied to a solid part, such as a cantilever beam, stresses are generated within it. In contrast, if the medium is a fluid, stresses can be generated by motion rather than by deflection. In particular, shear stresses in fluids arise due to viscous flow. For this reason, while solids are *elastic*, fluids are *viscous*.

The shear effects can be visualized through the classic example of a flow between parallel plates (Figure 2.6). For a fluid at rest, there will be no shear stresses. This corresponds to the rest condition for a fluid element highlighted in Figure 2.6a. Now suppose that a rightward force dF is applied to the upper plate, dragging it across the fluid at a certain velocity. The relative shearing of the plates produces a shear stress τ, which acts on the fluid element:

$$\tau = \frac{dF}{dA} \tag{2.13}$$

where dA is the area of contact of the fluid element with the plate.
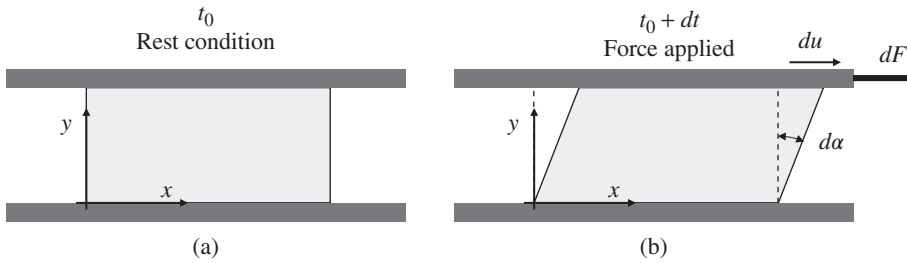
Figure 2.6 Shear stress in a fluid: initial rest condition (a) and (b) after a force is applied.

As one can guess from Figure 2.6, under the action of the force applied to the plate, the fluid element will continue deforming, with a rate that can be measured by the angle $d\alpha$. It is possible to demonstrate that deformation rate can be expressed in terms of the velocity of the upper plate du [15]:

$$\frac{d\alpha}{dt} = \frac{du}{dy} \tag{2.14}$$

Therefore, the fluid element subjected to a shear stress τ experiences a rate of deformation (or shear rate) given by du/dy. This fact is valid for any fluid. However, the relationship between τ and du/dy varies for different types of fluids. Fluids in which the shear stress is proportional to the shear rate are called **Newtonian fluids**. Common fluids, such as water and air, and hydraulic fluids behave as Newtonian fluids in most conditions.

The constant of proportionality between shear rate and shear stress is defined as absolute or **dynamic viscosity, τ**:

$$\tau = \mu \frac{du}{dy} \tag{2.15}$$

The value of dynamic viscosity can be reported with different units: the SI system uses kg/(m s) (or Pa · s), but it is also common to find the dynamic viscosity expressed in poise, where 1 P corresponds to 1 g/(cm s) [1]. One centipoise (cP) corresponds to 0.001 kg/(m s).

Sometimes, the viscosity can be expressed as ratio between absolute viscosity and density. This ratio is also referred to as **kinematic viscosity**:

$$\nu = \frac{\mu}{\rho} \tag{2.16}$$

The common unit for ν is the Stoke, where 1 Stoke corresponds to 1 cm^2/s. At room temperature (300 K), the dynamic viscosity of the water is 0.89 cP, while typically hydraulic fluids have much higher viscosity, typically higher than 30 cP.

Usually, viscosity cannot be estimated well from theoretical relations, and experimental devices (viscometers) are commonly used to determine the value of viscosity of a given fluid.

2.6.1 Viscosity as a Function of Temperature

For liquids, it is very important to consider that viscosity is strongly affected by temperature. For many fluids, an empirical correlation of the form of Eq. (2.17) can be used:

$$\mu = Ae^{B/(T-C)} \tag{2.17}$$

---

1 In the British units, the viscosity is expressed as (lbf · s)/ft.

where T is the absolute temperature (in K) and A, B, C are constants that can be determined once the value of viscosity at three different temperatures is known. For water, the values of these constants are [16]

$$A = 2.414 \cdot 10^{-5} \, \text{N} \cdot \text{s/m}^2$$
$$B = 247.8 \, \text{K} \tag{2.18}$$
$$C = 140 \, \text{K}$$

For mineral oils, it is very common to use Walter's relation:

$$\log_{10}\log_{10}(v + a) = k - m \cdot \log_{10} T \tag{2.19}$$

where v is the kinematic viscosity in mm^2/s, T is the temperature in K, and k, m, and a are constants dependent on the specific hydraulic fluid. For mineral oils

$$k \cong 0.97$$
$$m \cong 3.54 \tag{2.20}$$
$$a = 0.8$$

As reported in [17], some variants of Walter's relation have been developed to obtain a better match between numerical results and experimental data. Notwithstanding, the relation (2.20) is useful to understand the graphical dual-logarithm representation, typically used to describe the dependence of the viscosity on temperature (Figure 2.7). In this plot, the viscosity variation with
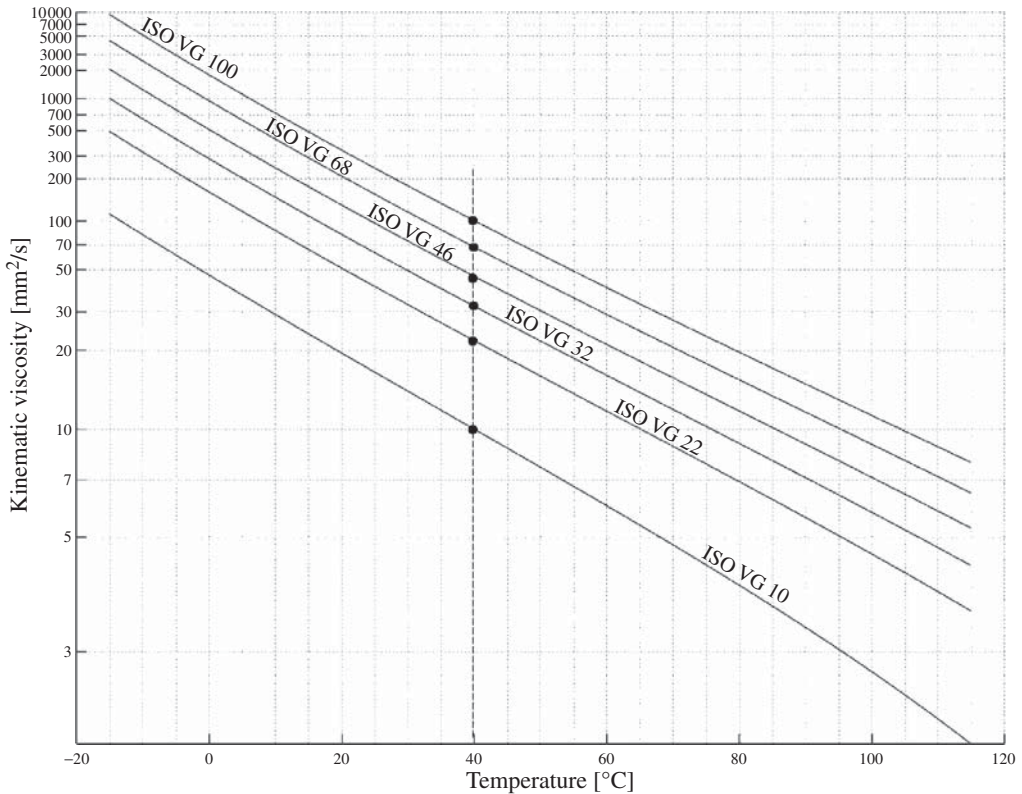
Figure 2.7 Viscosity of hydraulic fluids as a function of the temperature.

Table 2.5 ISO classes for hydraulic oils according to the viscosity grade.

ISO code	$v_{40°C}$ [mm^2/s]	v_{min} (−10%) [mm^2/s]	v_{max} (+10%) [mm^2/s]
VG10	10	9.0	11.0
VG22	22	19.8	24.2
VG32	32	28.8	35.2
VG46	46	41.4	50.6
VG68	68	61.2	74.8
VG100	100	90.0	110.0

temperature appears to be linear (because of the logarithmic scale), but in reality there is an exponential decay as expressed by Eq. (2.17).

The plot of Figure 2.7 reports curves for different fluids, identified by their viscosity grade (VG). This represents the ISO classification of hydraulic fluids based on the parameter VG. The VG of a hydraulic fluid is defined as the kinematic viscosity (in mm^2/s) at 40 °C. According to the ISO standard, there are six classes of oils, which are reported in Table 2.5.

As mentioned at the beginning of this chapter, an ideal hydraulic fluid maintains its properties constants, even under high temperature or pressure variations. However, as it is clearly visible from Figure 2.7, the large variations of fluid viscosity with temperature are far from the desirable ideal trend. This aspect has large implications in practical applications of hydraulic control technology. This is particularly true for machinery operating outdoor, which are affected by the seasonal or daily temperature changes. The viscosity of the working fluid in hot summer days can differ by orders of magnitude compared with the values reached in cold winter days. A designer needs to be mindful of this temperature dependence when selecting the proper fluid for the hydraulic system. Often the oil has to be changed with the season. For example, manufacturers can recommend a VG46 for summer use and a VG32 for the winter.

In many cases, it is possible to use oil additives that limit the viscosity variation with temperature. To compare the behavior of different oils in this regard, a parameter called **viscosity index** (VI) was introduced in 1929 [18], and it is nowadays defined by engineering standards [19, 20]. A high value for the VI indicates a limited dependence of viscosity with temperature. Vice versa, a low VI indicates a more pronounced variation of viscosity with temperature, as shown in Figure 2.8.
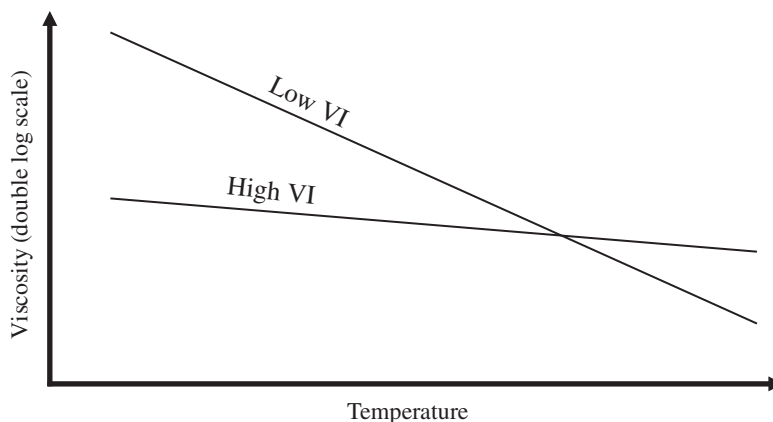
Figure 2.8 Qualitative representation of the viscosity index (VI).

Table 2.6 Typical values for the viscosity index.

Oil type	Viscosity index
Mineral oil	95–105
Multi-grade oil	140–200
Synthetic oils	200–400

Source: OelCheck [21].

The VI was originally defined as a dimensionless value on a 0–100 scale, being 100 the best VI. Nowadays, thanks to the progress in the formulation of VI improvers, much higher values can be achieved as shown in Table 2.6.

2.6.2 Viscosity as a Function of Pressure

For liquids, the viscosity increases with pressure. While this effect can be negligible for limited pressure variations (<200 bar), it might be relevant for hydraulic systems working at high pressure (>200 bar). A formula that can be used to approximate the variation of fluid viscosity with pressure is given by

$$\mu = \mu_0 \cdot e^{b \cdot p} \tag{2.21}$$

where μ_0 is the dynamic viscosity at atmospheric pressure (at a given temperature), p is the fluid pressure (in *bar*), and b is a coefficient that depends on the fluid. For mineral-based oils, $b = 1.7 \cdot 10^{-3}$ bar^{-1}; for HFC oils, $b = 3.5 \cdot 10^{-4}$ bar^{-1}; and for HFD oils $b = 2.2 \cdot 10^{-3}$ bar^{-1}. Relation (2.21) is plotted in Figure 2.9. As the reader can notice from the figure, for a mineral oil, there is an increase in viscosity of about 40% from atmospheric conditions to 200 bar.
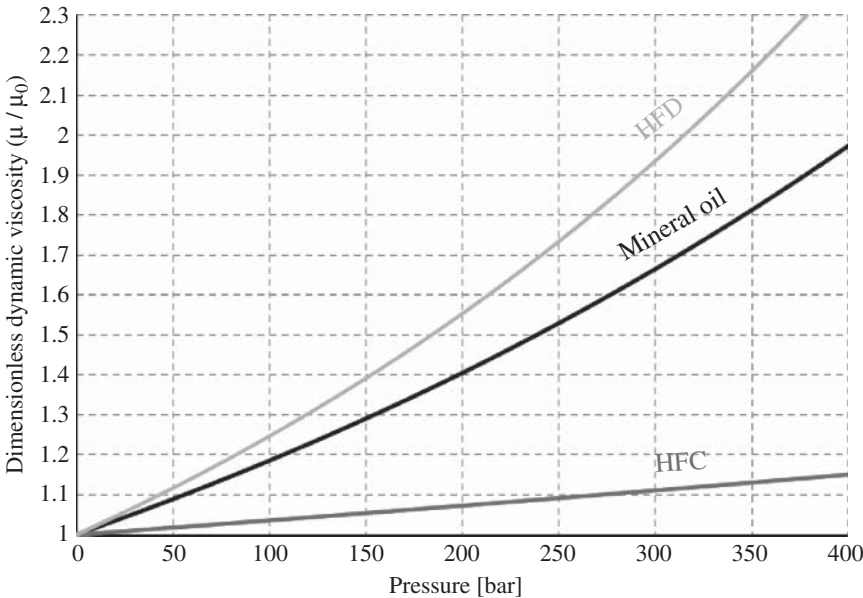
Figure 2.9 Viscosity as a function of pressure.

2.7 Entrained Air, Gas Solubility, and Cavitation

2.7.1 Entrained Air

> In some circumstances, the hydraulic fluid can entrain some air from the environment that can lead to suction condition issues for the pump(s). This is commonly referred as pseudo-cavitation.

This usually can occur in the reservoir (Figure 2.10a) or when gas leakages are present in low-pressure hydraulic lines, such as suction lines (Figure 2.10b). For example, the return line entering the reservoir might present a non-submerged pipe or a design creating a high amount of turbulence. In both cases the hydraulic fluid can entrap air that is then carried within the flow and can enter the hydraulic system. If the bubbles of air do not have enough time to settle within the reservoir, foam can accumulate on the surface.

The entrained air can lead to cavitation of the pump or to erratic phenomena such as a slow response of some functions. For this reason, it is always recommended to adopt all possible measures to avoid or limit the air entrainment.

2.7.2 Gas Solubility

> All liquids, including hydraulic fluids, normally contain dissolved incondensable gases (typically air taken from the environment).

The liquid absorbs the gas from the surroundings until the saturation state is reached. As long as the gas is dissolved, it does not influence the main properties of the fluid, particularly in terms of compressibility or viscosity.

The (maximum) volume of air dissolved in the liquid can be determined by the following equation, derived from the well-known Henry–Dalton law:

$$V_{\text{air},d} = V_0 \cdot \alpha_a \cdot \frac{p}{p_0} \tag{2.22}$$

It is important to remark that $V_{\text{air},d}$ represents the volume of air measured at the reference pressure p_0. This law states that the volume of air that the liquid can dissolve proportionally increases with pressure. For mineral oils, the coefficient α_a is also known as Bunsen coefficient and can vary
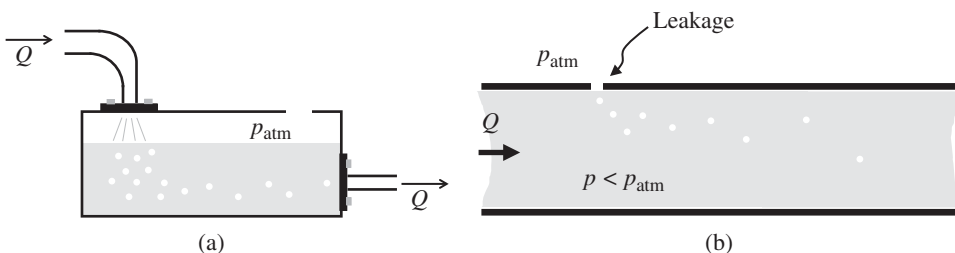
Figure 2.10 Typical causes of entrained air within the hydraulic fluid: (a) in a reservoir; (b) in a suction line.

from 0.06 to 0.09. This is not much affected by temperature or viscosity [22]. For water, the Bunsen coefficient is 0.04, which means that mineral-based oils tend to dissolve more air than water. To better understand the meaning of α_a and quantify the actual amount of incondensable gas that a hydraulic fluid can dissolve, one can consider the atmospheric pressure as the reference condition, p_0. This is the condition of most hydraulic fluids inside a reservoir open to atmosphere. In this situation, considering $p = p_0$ in Eq. (2.22), a volume of air corresponding to 6%, up to 9%, of the volume of the fluid V_0 could be held by the fluid. This amount of air is in equilibrium with the liquid, and it is not released unless the pressure of the fluid is reduced.

The air release phenomenon is similar to what anyone experiences when opening a bottle of carbonated drink. Before opening the bottle, the fluid in the bottle appears as uniform liquid; however, while opening the bottle, bubbles of gas can be observed while the internal pressure decreases. This means that before opening the bottle, the gas was in equilibrium with the liquid, entirely dissolved. As the pressure decreases, a certain amount of gas gets released, and bubbles start appearing within the liquid.

Considering the gas solubility of the fluid, three possible equilibrium states can be identified. These are graphically represented in Figure 2.11: Above the saturation pressure p_{SAT}, all the air is dissolved in the liquid without affecting the main properties of the fluid. However, below the saturation pressure, only a portion of the air remains dissolved as determined by the Henry–Dalton relation of Eq. (2.22). The rest of the air is released from the liquid and is in free state. In this condition, the fluid is a mixture of liquid and air, in the form of bubbles.
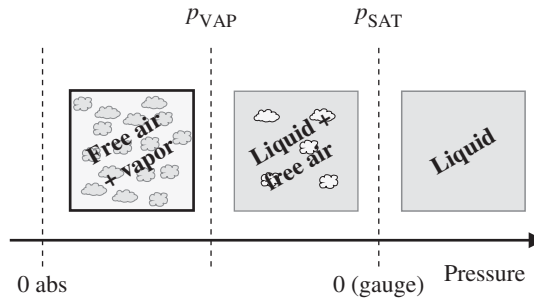
Figure 2.11 Equilibrium states for a liquid considering gas solubility.

> For hydraulic systems, the condition in which incondensable gases are released is generally referred to as *gaseous cavitation* or *aeration*.

The gaseous cavitation should be treated differently from the entrained air aspect described in Section 2.7.1, which is sometimes referred to as *pseudo-cavitation*.

Below the vapor pressure, p_{VAP}, the air is completely released, and the hydraulic fluid is in the vapor form. This condition for the hydraulic fluid is usually referred to as *vapor cavitation*.

Typical hydraulic oils are always a mixture of different components; therefore there is not a defined value of p_{VAP}, but rather an interval $[p_{VAP, L}, p_{VAP, H}]$ of pressure throughout which the vaporization of the fluid occurs. Typical values of $p_{VAP, L}$ and $p_{VAP, H}$ for mineral oils range between 15 000 and 30 000 Pa (absolute pressure) [23].

All the abovementioned cavitation phenomena can be detrimental to the operation of a hydraulic system. More than the formation of the vapor or of the gas bubbles, it is usually the opposite process

(that occurs in an abrupt manner), which causes erosion damages of the mechanical parts. For this reason, designers of hydraulic components normally put the highest attention in preventing cavitation phenomena. More specifically, the selection of hose diameters and length should avoid the fluid pressure to fall below vapor pressure and, if possible, below saturation pressure.

However, gaseous cavitation is often unavoidable, particularly in the lines connecting the reservoir (where the fluid is at saturation conditions) to the pump supply port. This is due to the frictional losses that cause the pressure to decrease as the fluid travels into the line. For this reason, the connection between the pump and the reservoir must be designed to limit these pressure losses as much as possible so that the pump can operate under a minimal (sometimes negligible) aeration condition.

Moreover, in certain parts of the hydraulic system, such as in hydraulic control valves or hydraulic pumps, there are sometimes violent flow restrictions where the fluid accelerates to high velocities, causing the static pressure to fall below the saturation pressure (see Bernoulli's equation, Chapter 3). All these reasons should give an idea why the cavitation is a very common issue in hydraulic control systems.

2.7.3 Equivalent Properties of Liquid–Air Mixtures

In presence of entrained air, or when vapor or air is released, the fluid becomes a mixture, and the equivalent density and bulk modulus significantly decrease with respect to the pure liquid condition.

Simple formulas can be derived based on the continuum fluid assumption. In this approach the different phases (gas and liquid) are considered to be the same media without a distinct separating interface [24]. Under this assumption, the fluid density can be calculated as a weighted average of the single densities:

$$\rho_{\text{tot}} = \alpha_g \rho_g + \alpha_v \rho_v + \left(1 - \alpha_g - \alpha_v\right) \rho_l \tag{2.23}$$

where α_g and α_v are, respectively, the volume fraction of the air and of the vapor:

$$\alpha_g = \frac{V_g}{V_{\text{tot}}}; \quad \alpha_v = \frac{V_v}{V_{\text{tot}}} \tag{2.24}$$

Similarly, for the viscosity,

$$\mu_{\text{tot}} = \alpha_g \mu_g + \alpha_v \mu_v + \left(1 - \alpha_g - \alpha_v\right) \mu_l \tag{2.25}$$

Also, for the bulk modulus, a similar expression can be found:

$$B_{\text{tot}} = \left[\frac{\alpha_g}{B_g} + \frac{\alpha_v}{B_v} + \frac{\left(1 - \alpha_g - \alpha_v\right)}{B_l}\right]^{-1} \tag{2.26}$$

An interpretation of the expression (2.26) is shown in Figure 2.12: according to the continuum assumption, all the undissolved gas particles can be treated as a single bubble with the overall volume V_g. With that in mind, it is possible to apply the definition of the bulk modulus (Eq. (2.4)) to the overall system of the two components, considering its total volume change under a certain pressure difference as the sum of the two contributions of the gas volume change and of the liquid volume change:

$$B_{\text{tot}} = -V_{\text{tot}} \left(\frac{dp}{dV_{\text{tot}}}\right) \tag{2.27}$$
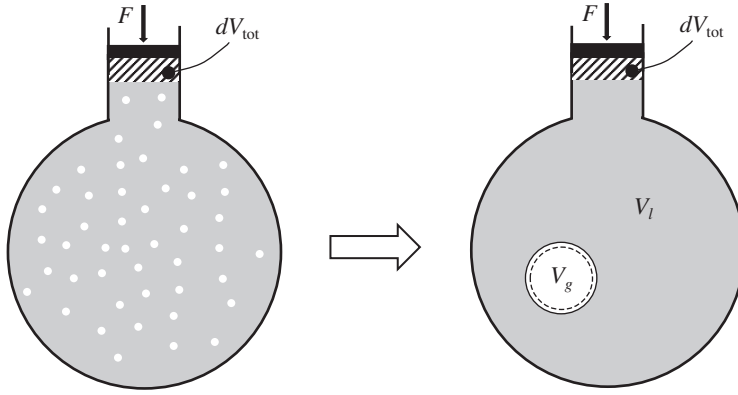
Figure 2.12 Compression of a mixture of liquid and undissolved gas.

With simple analytical passages, Eq. (2.26) can be derived from Eq. (2.27). The bulk modulus of the gas phases can be evaluated by considering an ideal gas behavior, according to which the pressure and volume variations follow the expression

$$p_g V_g{}^\gamma = \text{const} \tag{2.28}$$

where γ is the polytropic constant[2]. By differentiating the expression of Eq. (2.28),

$$dp_g V_g{}^\gamma + p_g \gamma V_g{}^{\gamma-1} dV_g = 0 \tag{2.29}$$

from which, by applying the general definition for the bulk modulus (Eq. (2.4)),

$$B_g = \gamma p_g \tag{2.30}$$

In order to evaluate the equivalent density, viscosity, and bulk modulus for the fluid mixture, by using the expressions presented in the previous paragraphs, it is necessary to first know the amount on undissolved gases. The simpler method for doing such estimation is based on the equilibrium assumption, according to which the gas and the vapor are released or dissolved instantaneously. In reality, these processes are not instantaneous, as they are characterized by time dynamics on the order of tens of milliseconds [25, 26]. It is documented that the air release or vaporization processes happen more rapidly than the opposite dissolving processes [23].

According to the equilibrium assumption, the amount of undissolved air or vapor can be evaluated according to the Henry–Dalton law (Eq. (2.22)), with the graphical representation of Figure 2.13. The saturation line represents the equilibrium states according to Eq. (2.22). For example, considering a hydraulic fluid with 9% of dissolved air at atmospheric pressure ($p_o \cong 1$ bar, state 0), if the pressure is brought to a lower pressure (state 1), the amount of air that can be dissolved is reduced ($V_{\text{air}, d, o} < V_{\text{air}, d, 1}$), meaning that a certain amount of air, $V_{\text{air}, r, 1}$, is released:

$$V_{\text{air},r,1} = V_{\text{air},d,0} - V_{\text{air},d,1} = V_{\text{sat}} - V_{\text{sat}} \left(\frac{p_1}{p_{\text{sat}}} \right) = V_{\text{sat}} \left(1 - \frac{p_1}{p_{\text{sat}}} \right) \tag{2.31}$$

In the process that brings the $V_{\text{air}, r, 1}$ from the saturation conditions ($p_{\text{sat}} = p_0$) to the actual pressure p_1, the calculated volume is subject to an expansion that can be approximated as polytropic;

---

2 The polytrophic constant can be assumed as a function of the dynamic of the process. For a fast compression or expansion process, $\gamma \cong 1.4$ (adiabatic); for a slow process, $\gamma \cong 1$ (isothermal). Intermediate choices, such as $\gamma = 1.2$, are often made to describe a more general situation.
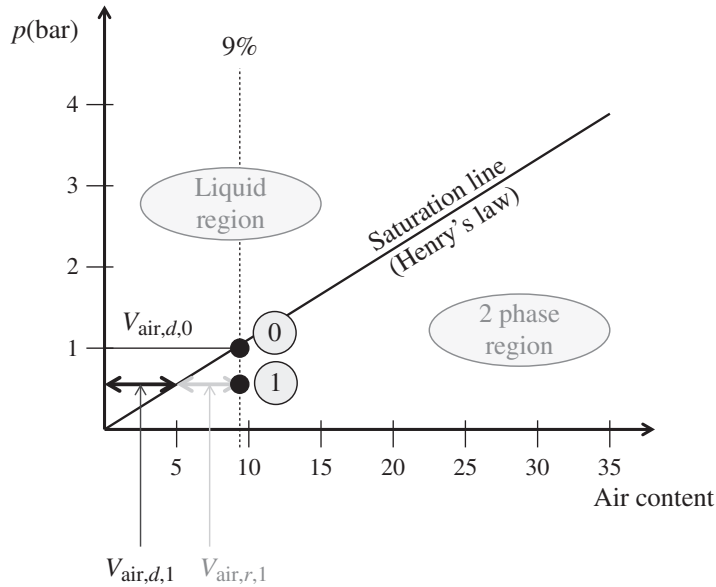
Figure 2.13 Graphical representation of the dissolved and undissolved air in a hydraulic oil. The volume in the x axis is referred to the reference pressure. Source: Adapted from Nervegna [14].

therefore the final expression that can be used to estimate the volume of undissolved air is

$$V_{air,r,1} = V_{sat} \left(1 - \frac{p_1}{p_{sat}} \right) \left(\frac{p_{sat}}{p_1} \right)^{\frac{1}{\gamma}} \tag{2.32}$$

This expression can then be used to evaluate the volume fraction α_g in the above expressions.

As previously discussed, in the majority of cases, hydraulic components do not see instances of vapor cavitation; therefore it can be usually assumed that $\alpha_v = 0$. However, in certain conditions, vapor cavitation can occur. If the reader has interest in these cases, for the evaluation of the parameter α_v, it is recommended to refer to more specialized literature, such as [25, 26].

Example 2.2 Volumetric flow rate of a hydraulic pump

In the field of hydraulics, it is very common to express flow rates as volumetric flow rates. As it will be discussed in the next chapter, there are two main reasons for that. First, it is straightforward to evaluate the motion velocity of a hydraulic actuator if the volumetric flow through it is known. Second, it is quite common to use volumetric flow meters for the measurement of the flow rate.

This example describes what is the effect of fluid compressibility on the volumetric flow rate.

A hydraulic pump supplies flow to a hydraulic cylinder that lifts a certain load. Due to this load, the pump outlet is pressurized at 100 *bar*. The inlet flow, from a tank open to atmosphere, is 100 *l/min*. Determine the volumetric flow exiting the pump. The density of the fluid is 870 *kg/m³*; bulk modulus of the fluid is 18 000 *bar*.

Consider the following cases:

a) The pump inlet pressure is the same as the tank pressure.
b) The pump inlet pressure is −0.3 *bar* gauge pressure.

(Continued)

Example 2.2 (Continued)
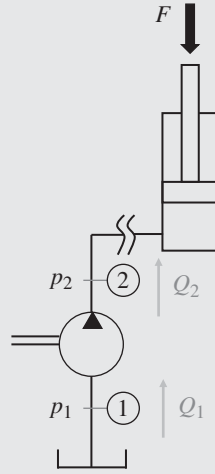
The Bunsen coefficient for the oil is 9%.

Given:
The pump inlet flow, $Q_1 = 100$ *l/min*; the pump outlet pressure $p_2 = 100$ *bar* (gauge pressure); the Bunsen coefficient of the oil, $\alpha_a = 9\,\%$; the density of the fluid, $\rho = 870$ [kg/m^3]; the bulk modulus of the fluid $B = 18\,000$ *bar*.

The inlet pump pressure in two cases: (a) $p_1 = p_T = 1$ *bar* (absolute pressure); (b) $p_1 = 0.7$ *bar* (absolute pressure).

Find:
The outlet pump flow rate, Q_2, for the two cases (a) and (b).

Solution
Case (a)
There is no pressure loss from the tank to the pump inlet. Therefore, assuming that the fluid is at saturation condition in the tank, there is no undissolved air at the pump inlet. This means that $\alpha_g = 0$ and the fluid is entirely liquid.

Assuming steady-state flow conditions, the same mass flows at the same rate at the inlet and outlet of the pump, so that

$$\rho_1 Q_1 = \rho_2 Q_2$$

Considering that

$$\rho_2 = \frac{\rho_1}{1 - \dfrac{\Delta p}{B_l}}$$

we have

$$Q_2 = Q_1 \left(1 - \frac{\Delta p}{B}\right) = 100\,[l/min] \cdot \left(1 - \frac{100\,[bar]}{18\,000\,[bar]}\right) = 99.44\,l/min$$

Due to the effect of the fluid compressibility, the volumetric flow rate at the pump outlet is lower than the volumetric flow rate at the inlet by 0.56%.

Case (b)

In this case, a certain amount of dissolved air is present at the pump inlet, being $p_1 < p_T = p_{SAT}$. The amount of air at the inlet port 1 can be evaluated as

$$V_{air,r,1} = V_{sat} \left(1 - \frac{p_1}{p_{sat}} \right) \left(\frac{p_{sat}}{p_1} \right)^{\frac{1}{\gamma}}$$

where $p_{sat} = p_T$, considering the process as isothermal ($\gamma = 1$):

$$V_{air,r,1} (\%) = 0.09 \left(1 - \frac{0.7}{1} \right) \left(\frac{1}{0.7} \right) = 0.09 \cdot 0.429 = 0.039$$

Therefore, the density of the fluid at the inlet section is

$$\rho_1 = \alpha_g \rho_g + \left(1 - \alpha_g \right) \rho_l = \frac{V_g}{(V_l + V_g)} \cdot \rho_g + \left(1 - \frac{V_g}{(V_l + V_g)} \right) \rho_l$$

$$= 0.0375 \cdot 1.225 \, [kg/m^3] + (1 - 0.0375) \cdot 870 \, [kg/m^3] = 837.4 \, kg/m^3$$

In the above expression, it is considered that the density of the air at standard conditions is $\rho_g = 1.225 \, kg/m^3$.

The density at the pump outlet can be calculated considering that at high pressure ($p_2 = 100 \, bar$) all the fluid is liquid:

$$\rho_2 = \frac{\rho_T}{1 - \frac{\Delta p}{B}} = \frac{870 \, [kg/m^3]}{1 - \frac{100 \, [bar]}{18\,000 \, [bar]}} = 874.9 \, kg/m^3$$

Therefore, from the expression

$$\rho_1 Q_1 = \rho_2 Q_2$$

we have

$$Q_2 = Q_1 \frac{\rho_1}{\rho_2} = 100 \, [l/min] \cdot \frac{837.4 \, [kg/m^3]}{874.9 \, [kg/m^3]} = 95.7 \, [l/min]$$

It is therefore possible to observe how, in this (gaseous) cavitation condition, the reduction in outlet flow is about 4.3%, much more pronounced with respect to the case (a), where there was no cavitation.

A final remark can be made on the evaluation of the equivalent (or effective) bulk modulus. For the typical operating pressure of hydraulic control systems, the elasticity of the material is also not negligible. Consider again the case of Figure 2.12 while also including the elasticity of the walls according to the bulk modulus of the material (similar to the Young modulus definition):

$$B_{mat} = -V_{tot} \left(\frac{\Delta p}{\Delta V_{mat}} \right) \tag{2.33}$$

The equivalent bulk modulus for the system becomes

$$B_{tot} = \left[\frac{\alpha_g}{B_g} + \frac{\alpha_v}{B_v} + \frac{(1 - \alpha_g - \alpha_v)}{B_l} + \frac{1}{B_{mat}} \right]^{-1} \tag{2.34}$$

2.8 Contamination in Hydraulic Fluids

A hydraulic oil is subject to various *forms of contamination*:

- *Solid contamination.* The solid contamination is the most common and intuitive form of contamination; it affects the operation and life of all hydraulic circuits. The solid contamination is due to the presence of undesired solid particles (metallic, plastic, fibers of different types, etc.) within the hydraulic fluid. These particles can accelerate the wear of the hydraulic components or produce the blockage of small flow connections (such as those of small hydraulic orifices). Solid contamination can cause malfunctioning of the hydraulic system and can also lead to the catastrophic failure of some components, like pumps and motors.
- *Liquid contamination.* In general terms, liquid contamination refers to the presence of other liquids in the working fluid that can either be chemically aggressive to the hydraulic components or can deteriorate the properties of the hydraulic fluid. In the majority of the cases, the liquid contaminant is water. For example, water causes rusting in hydraulic components (which can be visible, for example, in the reservoir of the system), reduces the lubrication characteristics of the oil, and can cause unwanted reactions leading to the formation of alcohols, acids, or sludges. In addition, water has a higher vapor pressure values when compared with typical oils. Therefore, the presence of water can lead to instances of vapor cavitation that can cause instabilities and damages of the mechanical parts.
- *Gas contamination.* Gas contamination usually refers the presence of undissolved or entrained air in the hydraulic oil. As mentioned before, this can lead to the premature wear of certain hydraulic components, caused by the implosion of the air bubbles, or can affect the controllability of parts of the hydraulic system. The physics behind the gas contamination phenomenon was described in detail in Section 2.7 of this chapter.

For every type of contaminant, three different sources can be distinguished:

1. *Native contamination.* Contaminant particles can be present in the system as residual from the manufacturing of the components or from the assembly or repair of the system. Residual from machining or welding processes, or excessive sealants, can also be present in a brand-new hydraulic system before the hydraulic fluid is introduced for the first time. Humidity from the environmental air can also cause undesired amount of water to condense in the components.
   It is also important to remark that a new hydraulic fluid may not be clean enough for a modern hydraulic system. Manufacturing, handling, and storage processes for the hydraulic fluids need to be strict enough to guarantee that the level of contaminants complies with the requirements of the hydraulic system.
2. *Ingressed contamination.* All the three types of contaminants (solid, liquid, gas) can enter the hydraulic system from the surrounding environment. The airflow into the reservoir, to compensate the changes in the fluid level during the operation of the system, might bring dirt particles and excessive humidity. The breather caps typically used in hydraulic reservoirs include filters to limit the amount of contaminants entering the system. Another typical source of ingressed contamination can be through hydraulic cylinders. Particularly when the cylinder is worn, the contaminants (dust and dirt particles) can enter from wiper seal during the retraction of the piston rod. This is a typical problem of many off-road hydraulic applications such as construction equipment.
3. *Internally generated contamination.* Many hydraulic components are subjected to wear. The most critical components subjected to wear are usually hydraulic pumps and motors. These

components have internal parts in relative motion, and consequently, particles can be removed from the interior parts. These particles can further promote wear or cause damage to other surfaces not subjected to wear.

Numerous studies have identified the fluid contamination as the most frequent cause of failure of a hydraulic system. Therefore, it is important to always take all possible precautions against possible cavitation damages when designing or maintaining a hydraulic system.

Necessary precautions against gas cavitation were already described in Section 2.7: the designer has to make every possible effort to eliminate or limit chances of entrained air or fluid pressure falling below the saturation conditions.

As pertains to liquid contamination, usually related to an undesired water content in the oil, it is important to maintain the water level below the saturation conditions. As a matter of fact, like air, water can also dissolve into the hydraulic fluid without interfering with the main fluid properties. For many hydraulic machines, the humidity of the surrounding air does not cause the water level within the working fluid to rise above saturation conditions. However, instances of water ingression from the reservoir or from worn cylinders can cause the water level to rise to levels that hamper the safe operation of the system.

Several techniques are nowadays available for removing water from hydraulic fluids using devices that are generally called "separators." Separating tanks are a common method based on the gravity and take advantage of the higher density of water with respect to most of the hydraulic fluids. If there is a sufficient resident time for the fluid in the hydraulic reservoir, water tends to settle at the bottom, which makes its removal possible. Other techniques include centrifugal separation, coalescing separation, and absorbent polymer separation [27]. These methods are sometimes used in special filters.

Solid contamination is always unavoidable in a typical hydraulic system due to all the three sources of contamination listed above. For this reason, one or more filter elements that ensure proper cleanliness level of the working fluid need to be present in a well-designed hydraulic system.

2.8.1 Considerations on Hydraulic Filters

The hydraulic components most affected by solid contaminants are those where mechanical parts are in relative motion with minimum clearances. This is the case of hydraulic pumps and motors, linear actuators, and hydraulic control valves. Ideally, a thin film of fluid is maintained in the gaps between the moving parts to avoid solid-to-solid contact. In presence of solid contaminant, the particles can cause erosion or abrasion or can even block the relative motion, as shown in Figure 2.14. The figure shows different particle sizes to make evident that the most dangerous particles are those of a size comparable with the gap height. Particles of the smallest size have high chances of passing through the gap without causing significant damages to the solid surfaces. Particles bigger than the gap height will not enter the gap, although they may cause erosion at the gap entrance regions. Finally, particles similar in size to the gap height will likely enter the gap and engage with frequent contacts with the surfaces. In the worst case they can get stuck between the mechanical parts and leave the gap region after causing severe abrasion damages.

When selecting the features of a hydraulic filter, it is important to keep in mind the geometrical clearances of the components used in each system. Table 2.7 gives a general reference on the typical clearances within hydraulic components. To provide the reader with a tangible reference for these values, it is worth mentioning that the diameter of a human hair ranges from 50 to 150 μm and the diameter of a grain of salt is from 80 to 200 μm. In inches, 10 μm corresponds to 0.000 39 in.
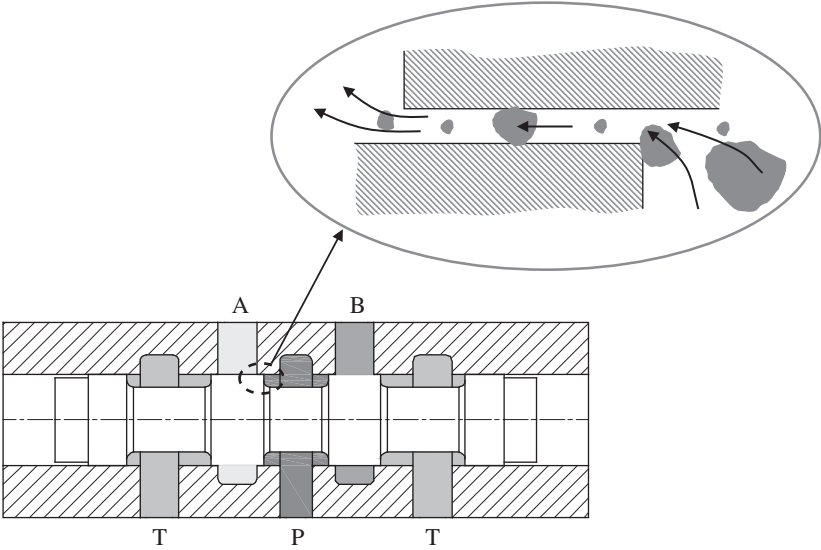
Figure 2.14 Solid particles entering the clearances of a hydraulic control valve.

Table 2.7 Typical clearances in hydraulic components.

Component	Clearance [μm]
Vane pumps (vane tip)	0.5–1
Gear pumps (side plates)	0.5–10
Piston pumps (piston to bore) (valve plate)	5–40 0.5–5
Servo valves (spool to sleeve)	1–4
Directional valves	2–20
Cylinders	50–250

Source: Assofluid [11] and Parker Hannifin [28].

Considering that a human cannot see objects smaller than 20–40 μm, the most dangerous particles cannot be seen by a naked eye!

ISO standard 4406 [29] defines a method for quantifying the solid contamination level of a hydraulic fluid. The standard is based on the counting, through proper experimental procedures, of the number of particles per milliliter of fluid. The contamination level is expressed by three numerical codes, which are determined according to the convention defined in Table 2.8.

Based on the number of particles counted in each size range, the corresponding codes are assigned according to Table 2.9.

Table 2.8 Codification of the fluid cleanliness according to ISO 4406, with the codes of Table 2.6.

First code	Second code	Third code
Number of particles per milliliter larger than 4 μm	Number of particles per milliliter larger than 6 μm	Number of particles per milliliter larger than 14 μm

Source: ISO 4406:2017 [29].

Table 2.9 Code for the cleanliness level of a hydraulic fluid according to ISO 4406.

Particles per milliliter		ISO code
More than	Up to	
80 000	1 600 000	24
40 000	80 000	23
20 000	40 000	22
10 000	20 000	21
5000	10 000	20
2500	5000	19
1300	2500	18
640	1300	17
320	640	16
160	320	15
80	160	14
40	80	13
20	40	12
10	20	11
5	10	10
2.5	5	9
1.3	2.5	8
0.64	1.3	7
0.32	0.64	6
0.16	0.32	5
0.08	0.16	4
0.04	0.08	3
0.02	0.04	2
0.01	0.02	1
0.005	0.01	0

Source: ISO 4406:2017 [29]

Example 2.3   Solid contamination of a hydraulic oil according to the ISO Standard

Determine the contamination level, in terms of particles per milliliter of fluid, of a hydraulic oil with a code 20/16/13 according to the ISO 4406.

(Continued)

Example 2.3 (Continued)

Given:
The ISO 4406 fluid specification, ISO 20/16/13.

Find:
The particle count, per milliliter of fluid.

Solution:
The answer is straightforward, after understanding Tables 2.7 and 2.8. In particular, per each ml the given fluid has:

- from 5000 to 10 000 particles larger than 4 μm;
- from 320 to 640 particles larger than 6 μm; and
- from 40 to 80 particles larger than 14 μm.

Hydraulic component manufacturers usually specify the maximum tolerable contamination level for the working fluid. An indicative list, adapted from [11, 28], is reported in Table 2.10. Obviously, the choice of the filter(s) to use in a hydraulic system should be based on the unit with the most stringent requirements. The units with stringent filtration requirements are typically the most expensive components of the system; therefore, preventing their failure is also justified from

Table 2.10 Suggested cleanliness code for typical hydraulic components according to ISO 4406 [11, 28].

	Low pressure (<70 bar)	Medium pressure (between 70 and 130 bar)	High pressure (>130 bar)
Pumps			
Gear pumps	21/18/16	20/17/15	20/17/14
Vane pumps fixed displacement	20/18/15	19/17/14	18/16/13
Vane pumps variable displacement	19/16/14	18/15/13	17/14/13
Piston pumps fixed displacement	19/17/15	18/16/14	17/15/13
Piston pumps variable displacement	18/16/14	17/15/13	17/14/12
Actuators			
Vane motors	20/18/15	19/17/14	18/16/13
Axial piston motors	19/17/15	18/16/14	17/15/13
Radial piston motors	20/18/16	19/17/14	18/16/14
Orbital motors	21/19/17	20/18/15	19/17/14
Cylinders	20/18/15	20/18/15	20/17/14
Valves			
Check valves	20/18/15	20/18/15	20/18/15
Pressure and flow control valves	19/17/14	19/17/14	19/17/14
Directional control valves – on/off	20/18/15	20/18/15	19/17/14
Directional control valve – proportional	18/15/13	17/15/12	17/14/11
Servo valves	17/14/12	16/13/11	16/12/10
Cartridge valves	20/17/15	19/17/14	19/16/13

Source: Assofluid [11] and Parker Hannifin [28].

an economical point of view. One should consider that the performance of the filter degrades with time, and it is based on the dirt holding capacity. It is common to require the replacement of the filter elements between 1000 and 10 000 hours, depending on the application and filter parameters.

The reader should know that there are different types of filter available on the market: each one can apply a different filtration technology, have a particular construction type, or integrate other accessories. Illustrating the details and the operating features of the different types of filters is beyond the scope of this chapter. A high-level description of the available options for filters is provided in [11, 28].

2.8.2 Filter Placement

It is important to comment on the application of filters in hydraulic circuits, since there are different alternative options. In general, filters can be classified based on their location in the circuit:

1. **Suction filters** (Figure 2.15) are placed between the reservoir and the pump inlet, which is usually the first component of the hydraulic system crossed by the hydraulic fluid after the tank.
2. **High-pressure filters** (Figure 2.16) are placed right after the pump outlet, before the working fluid can reach the control elements and the actuators of the hydraulic system.
3. **Return filters** (Figure 2.17) are placed on the return line, and they are the last component before the reservoir. These are often integrated in the reservoir.
4. **Offline filters** (Figure 2.18) are used within a separate circuit, created just for filtering the oil. In this case an auxiliary pump is used in a recirculation circuit including only the oil conditioning element(s). Often the filtration function is combined with thermal conditioning (oil cooling and or heating).

The reader could think that the best way to protect a system from external contamination is to put a filter right before the inlet of the pump (Figure 2.15). However, one should also consider that a real filter always induces a pressure drop, which, even if it is very small, can become very significant in suction lines. Here, the control of the pressure level is very important to avoid air release or vapor cavitation. Therefore, suction filters are rarely used, and most of the times they are
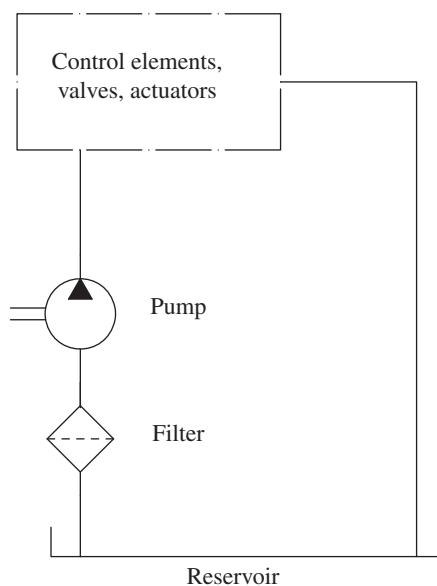
Figure 2.15 Suction filtration circuit.
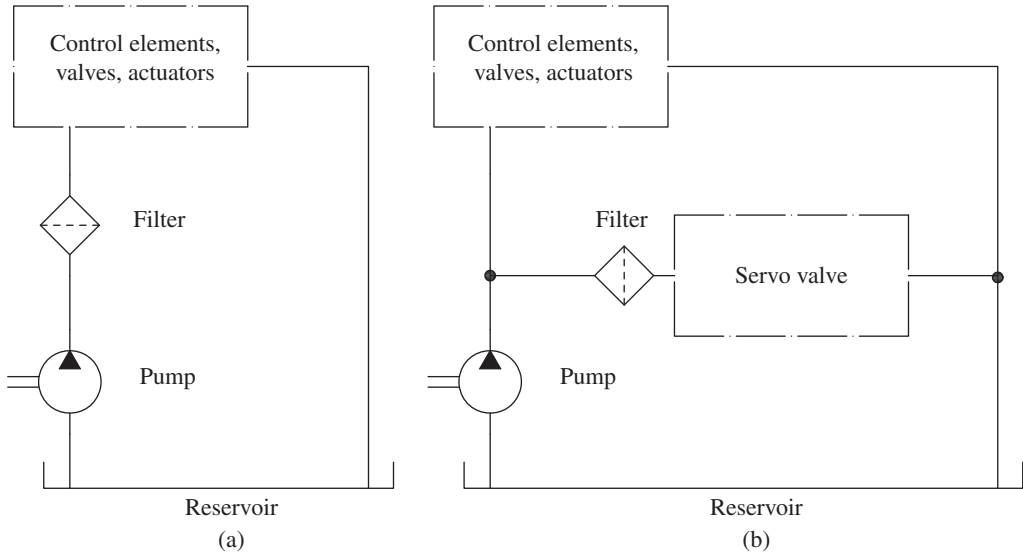
Figure 2.16 High pressure filtration circuit: (a) application to the whole circuit downstream the pump; (b) application to a specific branch of the circuit.

just strainers, designed to catch large particles, usually above 60–75 μm. Suction strainers always have to be combined with other types of filters in the system.

A high-pressure filter (Figure 2.16) can be used for two possible purposes: protecting some or all of the components located downstream of the pump or ensuring that a failure of the pump does not damage the rest of the system. The use of a high-pressure filter can be recommended when the hydraulic systems uses components with low internal clearances, such as servo valves. The drawback of high-pressure filters lies in their cost and weight. In fact, these filters need to be able to withstand high pressures and therefore need a properly sized cast iron housing.
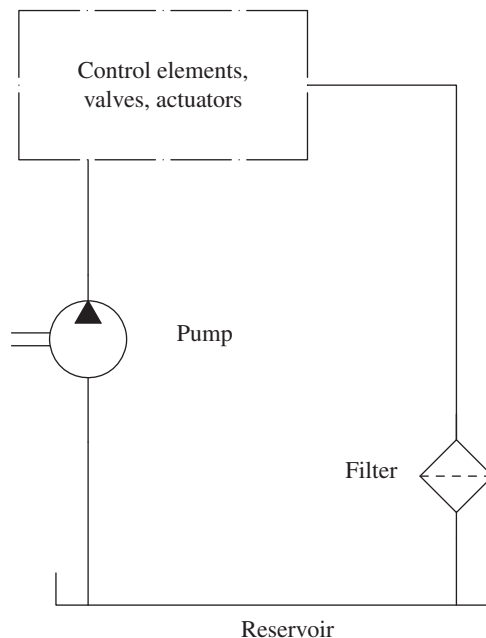
Figure 2.17 Return filtration circuit.
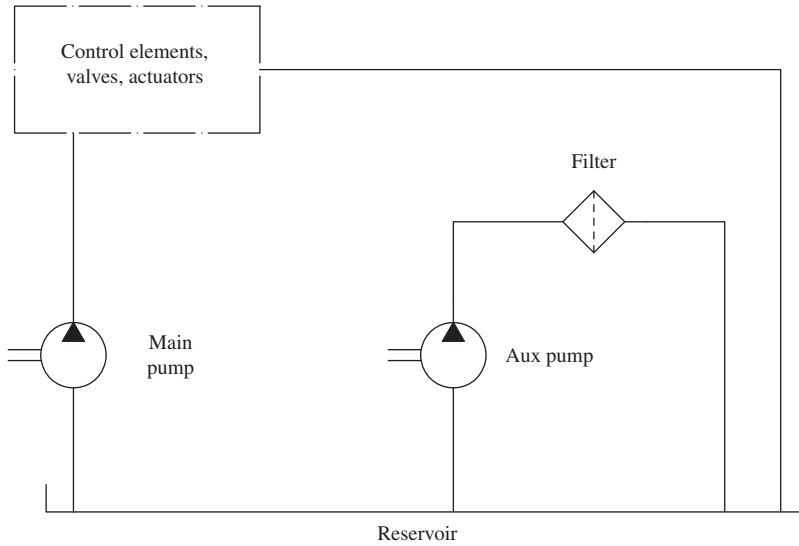
Figure 2.18   Offline filtration circuit.

Table 2.11   Typical pressure drops in filters depending on the filter installation choice.

Filter type	Typical pressure drop	
	Minimum [bar]	Maximum [bar]
Suction filters	0.02	0.1
Medium-/high-pressure filters	1	1.5
Return filters	0.3	0.5

Return filters (Figure 2.17) are often the preferred choice. This is because they are located in low-pressure lines (where the pressure is usually lower than 5 bar) and do not require a heavy housing. Furthermore, return filters can be easily integrated in the reservoir. The evident drawback of a return filter is that it cleans the working fluid after it has passed through the hydraulic system before returning to the tank. Therefore, this type of filtration is not effective against contamination introduced in the reservoir.

Table 2.11 summarizes the typical pressure drops of filters depending on their installation.

In the further chapters of this book, for sake of brevity and to better focus on the actual concepts, most of the hydraulic circuits will be illustrated often without hydraulic filters. However, the reader should always keep in mind that a real hydraulic system always requires proper filtration to guarantee the correct operation.

2.9   Considerations on Hydraulic Reservoirs

Tanks, also referred to as reservoirs, are a very important element of the hydraulic system, not only because they hold the hydraulic fluid but also because they affect the thermal properties of the system and they can be designed to separate solid, liquid, and gaseous contaminants from the oil.

2.9.1 Tank Volume

A high volume of the tank improves both the thermal and contaminant separation functions. However, it also increases the cost and the weight of the hydraulic system. Mobile applications usually require smaller tanks compared with industrial applications. As a general rule, the volume of the tank can be related to the flow rate that it exchanges with the system, i.e. the pump flow rate:

$$V_{\text{tank}} = \tau \cdot Q_p \tag{2.35}$$

Considering Q_p expressed in liter per minute and V_{tank} in liter, τ is the resident time in minute of hydraulic fluid in the tank. In other words, during the operation of the hydraulic system, each fluid particle spends an amount of time τ minute inside the reservoir before being reintroduced into the hydraulic circuit. This time interval should allow the working fluid to cool down, thanks to the heat exchange between the tank surfaces and the environment. For this reason, it is a good practice to locate the reservoir in a properly vented region of the hydraulic system.

During the time τ, the fluid should also be able to release both the entrained air and the undissolved air so that only liquid reenters the hydraulic system.

For industrial application with intermittent operation, the volume of the tank should ensure a value of τ between 2 and 3 minutes. In case of continuous operation, this value can be increased by two or three times. This means that for a system requiring 100 l/min of flow rate in continuous operation, the tank can be up to 900 l.

The size of the tank, and consequently its weight, is much more of an issue in mobile applications, which are sensitive to payloads and where often the available space is very limited. For this reason, proper design strategies have been developed to promote both the heat exchange and impurity separation functions within the reservoirs for mobile applications. These strategies include the use of external HEs and filters, as well as sophisticated internal air separators, and in some cases pressurized tanks. As a result, it is nowadays common to achieve time constants τ below 1 minute particularly for aerospace applications.

The reader shall understand that Eq. (2.35) represents only one of the design requirements that has to be satisfied for the tanks. In fact, during the operation of the system, the volume of hydraulic fluid in the tank can significantly vary due to the presence of accumulators or differential cylinders. These elements store variable amounts of fluid: for this reason, the reservoir has to accommodate for such variation while also allowing for a sufficient air cushion. Therefore, the designer needs to ensure that the value provided by Eq. (2.35) is well above the maximum volume variation ΔV that can be observed during the operation of the system. Otherwise, the volume of the tank has to be increased accordingly.

In case the tank is used as primary source of thermal conditioning of the fluid, to guarantee that the temperature of the working fluid remains stable during the operation of the hydraulic system, the volume of the tank needs also to allow a minimum heat exchange surface to the environment. An empirical formula, valid for parallelepiped-shaped tanks, is the following [11]:

$$V_{\text{tank}} = c \cdot \sqrt{\left(\frac{H/c_p}{T_f - T_{\text{amb}}} \right)^3} \tag{2.36}$$

where c_p [kJ/kgK] is specific heat capacity (can be assumed to be 4.187 kJ/kgK), T_f is the temperature of the working fluid, T_{amb} is the ambient temperature, H [kJ] is the heat to dissipate, and c is a constant that, with the above units, is equal to 1.25.

2.9.2 Basic Design of a Tank

The basic design of a hydraulic reservoir consists of a parallelepiped made of steel sheets. Small tanks (usually below 70 l) can be made of metal alloy or plastic. In a simplified cross-sectional view, the tank appears as shown in Figure 2.19. The suction duct and the discharge duct are usually placed at the opposite ends to increase the residence time of the working fluid inside the tank. Separator septs or baffles are used to prevent a straight flow path between the discharge and the suction pipe. In this way the fluid is forced to travel a longer path with reduced speed. In many cases, the septs force the fluid to flow vertically within the reservoir so that the release of the undissolved air is promoted by gravity. The discharge pipe is usually well below the free surface level of the fluid. This helps in preventing splashing of the fluid and whirls that would increase foam and entrained air. The pipes are often cut with angles greater than 45°. At the discharge pipe this further promotes a smooth entering of the fluid in the tank; but most importantly, at the suction pipe, it allows for a gradual acceleration of the fluid within the pipe, thus reducing the entrance losses.

The figure also shows an air breather element, which should always be present to allow the air to enter or leave the tank as the level of the fluid varies to accommodate volume variations driven by accumulators or differential cylinders.

Other accessories typically present in hydraulic reservoirs, not shown in Figure 2.19, include inspection ports, level indicators, filling inlet port and drainage or discharge caps, internal de-aeration separators (which are used to promote air separation and reduce foam), and magnets to capture contamination. The bottom of the tank is usually concave so that the solid impurities that remain at the bottom of the tank can be periodically drained through the discharge caps.
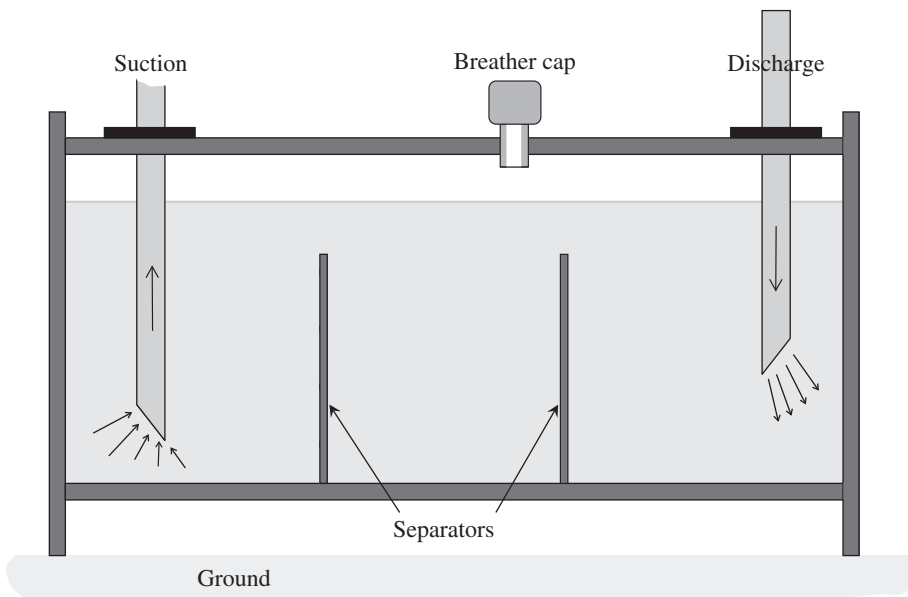
Figure 2.19 Typical design of a hydraulic reservoir.

Problems

2.1   A hydraulic cylinder is loaded such that the pressure in the piston chamber rises from 0 to 4000 psi (this chamber being blocked, for example, by a normally closed valve). Evaluate the motion Δx of the piston, in inches, as effect of oil compressibility. Assume no air entrapped in oil and $B_{liq} = 2.2 \cdot 10^5$ psi (bulk modulus). The rod chamber is connected to atmosphere at null pressure. Neglect compressibility of the material of the cylinder.
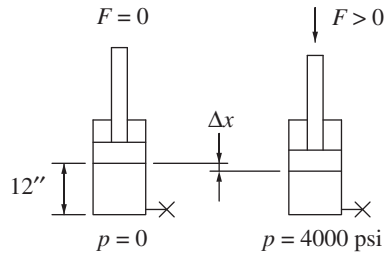
2.2   The cylinder in figure is loaded from 0 to 4000 psi keeping the bore port blocked. Evaluate the motion Δx of the piston from its initial position, in inches (in.), as effect of oil compressibility. Assume no air entrapped in oil and $B_{liq} = 2.2 \cdot 10^5$ psi (bulk modulus). The rod chamber is connected to atmosphere at null pressure. Neglect the compressibility of the material of the cylinder.
How much is the force F?
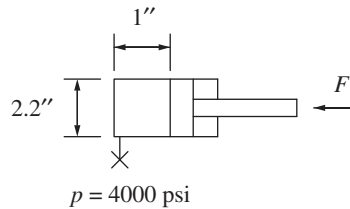
2.3   A cylinder with a 3 in bore and an extension of 1.42 in from the retracted position is loaded from 0 bar to 5000 psi while keeping the bore port blocked (as in the previous problem figure). Evaluate the motion Δx of the piston, as effect of oil compressibility. Assume 5% air entrained in oil and $K_{liq} = 2.2 \ 10^5$ psi. Neglect the compressibility of the material and of the cylinder walls. When evaluating the bulk modulus of the air, consider following two cases:
a) Gradual (slow) process (isothermal)
b) Fast process (adiabatic)

2.4   Measurements are taken on the piston chamber of a cylinder with a bore diameter of 250 mm. The bore port is blocked, and the rod chamber is connected to atmosphere (as in the previous problem figure). When the stroke (from retracted position) is 225 mm, the pressure is 70 bar. When the stroke is reduced to 222 mm, the pressure is 140 bar.
Determine the bulk modulus of the fluid.

Chapter 3

Fundamental Equations

The fundamental principles of fluid power are closely related to those of fluid mechanics: the basic relations used to analyze the operation of a fluid power system originate from the fundamental equations of fluid mechanics.

The basic concepts of hydraulic systems are usually presented with the simplified assumption of stationary conditions. This allows deriving very simple equations for the working fluid, which are particularly suitable to describe the functioning of even complex system layout architectures. This chapter describes how these simplified equations are derived from the classic equations of fluid mechanics of general validity. Readers with basic knowledge of fluid mechanics will appreciate and understand the derivation of these basic equations used throughout this book.

Knowledge of the tools used to perform a dynamic analysis is not necessary to understand the basic operation of a hydraulic circuit. This dynamic analysis becomes necessary when studying the system behavior during transients, for example, a sudden variation of the external load or the commutation of the system from one state to another (such as the sudden change in the commanded position of a hydraulic control valve). Some basic concepts pertaining to the dynamic behavior of hydraulic control systems during transients will be introduced in Chapter 5.

3.1 Pascal's Law

Pascal's law states that the pressure is transmitted undiminished in a confined body of fluid at rest.

> The Pascal's law of fluid statics is the foundation of what is considered by most engineers the modern era of fluid power technology.

The first hydraulic machines of the nineteenth century, such as the first hydraulic presses and hydraulic lifts, are based on this law.

The use of Pascal's law in an elementary hydraulic machine is shown in Figure 3.1. At level z^*, the fluid pressure must be equal in both the vertical branches of the apparatus. Therefore:

$$p_1 = \frac{F_1}{A_1} = \frac{F_2}{A_2} = p_2 \tag{3.1}$$

It is evident that the geometrical ratio of the areas of the two pistons is related to the ratio of the force applied:

$$\frac{F_2}{F_1} = \frac{A_2}{A_1} \tag{3.2}$$
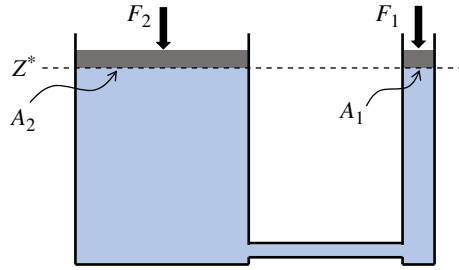
Figure 3.1 Basic hydraulic machine.

Equation (3.1) shows how it is possible to produce large loading forces using small geometrical areas and establishing high fluid pressures. This is based on power density, the main advantage of fluid power technology. Equation (3.2) is based on many hydraulic machines that require force multiplication, such as hydraulic brakes. For the practical applications of fluid power technology, the upper pressure limit (usually defined by the relief valve setting) is never given based on the fluid, but on the structural requirements of the components or of the machines. This also explains the current trend of increasing, where possible, the operating pressures of fluid power machines so that the power-to-weight ratio is reduced. A significant example for this is fluid power for aviation technology, where over the years the working pressure of the hydraulic actuation systems (flap and slat drives, landing gears, nose wheel steering, and many others) increased up to 210 bar, which is used in most commercial airliners. High performance military aircraft recently increased to 350 bar.

3.2 Basic Law of Fluid Statics

The Pascal's law presented in Section 3.1 is related to the basic equation of fluid statics:

$$\frac{dp}{dz} = -\rho \cdot g \tag{3.3}$$

Equation (3.3) implies that for a liquid at rest, the pressure linearly increases with depth, due to the effect of gravity. The integration of the differential Eq. (3.3) provides an expression for the pressure difference between two points at different elevation:

$$\Delta p = \rho \cdot g \cdot h \tag{3.4}$$

The concept expressed by the above Eq. (3.4) is illustrated in Figure 3.2.

Many hydraulic machines are often referred to as "hydrostatic machines" because their basic functioning can be evaluated using only static equations (not involving fluid velocity), as described in Section 3.1. Indeed, in almost all hydraulic components, the effect of fluid pressure is significantly higher than that of fluid velocity, thus making the latter negligible.
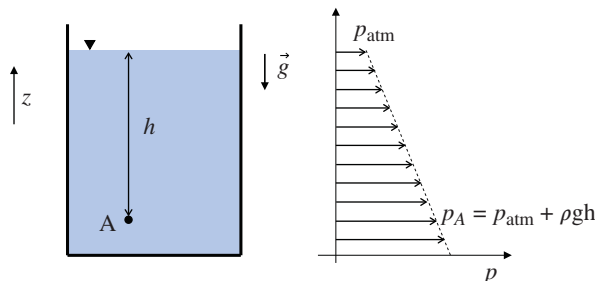
Figure 3.2 Fluid pressure increases with depth.
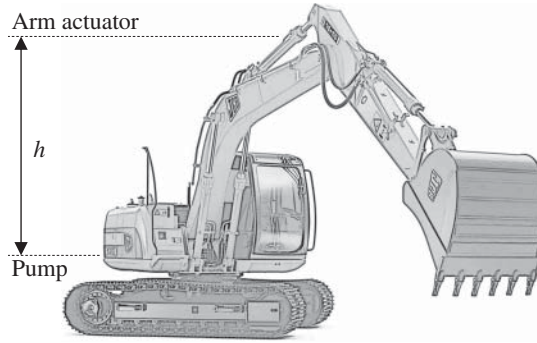
Figure 3.3 Elevation difference in the hydraulic circuit of a mobile application.

Despite this, the basic law of fluid statics is almost always omitted from the analysis of a fluid power system[1]. Neglecting elevation effects on fluid pressure is reasonable in all cases in which minimal variation of fluid pressure does not affect the operation of the systems. To better explain this concept, Figure 3.3 shows an example of a circuit of a mobile machine.

A reasonable value for h can be 3 m. Considering a fluid density of 870 kg/m³, which is typical for a hydraulic oil, the pressure difference between two points with the maximum elevation difference is

$$\Delta p = \rho \cdot g \cdot h = 870 \, [kg/m^3] \cdot 9.81 \, [m/s^2] \cdot 3 \, [m] = 25\,600 \, Pa = 0.256 \, bar \tag{3.5}$$

which is considerably lower than the typical operating pressure of the system, which is easily above 100 bar.

> The elevation difference in typical hydrostatic circuits can be neglected when calculating the system pressures. The effects of elevation become critical only when in parts of the system the pressure is close to the saturation conditions, such as at the suction of hydraulic pumps.

3.3 Volumetric Flow Rate

A hydraulic circuit comprises a network of components such as pumps, valves, cylinders, and filters, which are connected through fluid conveyance elements, such as hoses or pipes. The *flow rate* through the connecting hoses or pipes is a recurring parameter used in systems analysis. This section provides a high-level review of the concept of flow rate starting from the generic case of flow through a pipe, represented in Figure 3.4.

Before entering into more specific considerations for the hydraulic case, it is important to recall the definition of scalar product. Figure 3.4 shows the generic case of a pipe where a particle of fluid is traveling with a defined velocity along the direction of the pipe. The figure also represents a generic surface area defined by the section of the pipe with a generic plane. As shown in the figure, both are vector quantities: vector $\vec{v}$ denotes velocity, while vector $\vec{A}$ has the magnitude of the area A and it is perpendicular to the plane defining it. Their scalar product is

$$\vec{v} \cdot \vec{A} = v \cdot A \cdot cos \, \alpha \tag{3.6}$$

From the scalar product of Eq. (3.6), the convention for the flow crossing a surface can be defined: an in-flow is associated with a negative scalar product, while an out-flow has a positive scalar product.

---

1 A significant exception to this statement is the analysis of suction conditions at the inlet of hydraulic pumps. Considerations on the suction ability of pumps as well as the occurrence of gaseous or vapor cavitation should be taken into account when determining the elevation of the reservoir with respect to the inlet port.
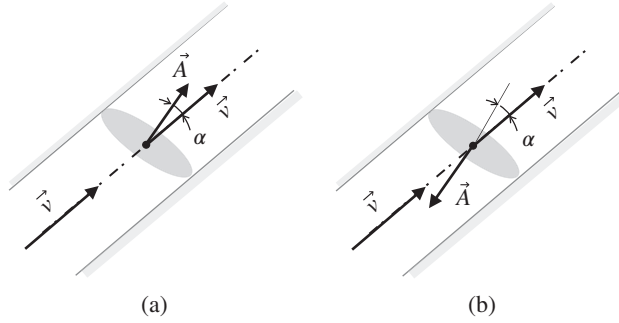
Figure 3.4 Flow through a pipe: velocity vector and surface area vector. (a) outflow; (b) inflow.

The scalar product in Eq. (3.6) is particularly important for the definition of volumetric flow rate across a section. In general:

$$Q = \int_A \vec{v} \cdot d\vec{A} \tag{3.7}$$

Figure 3.4 represents the case of a single fluid particle, Eq. (3.7) integrates this relationship to the whole section of the pipe. The velocity of each particle on the section is different and its profile depends on the flow regime. For laminar flow conditions, where viscous effects prevail over fluid inertia effect, the velocity profile resembles the parabolic distribution illustrated in Figure 3.5a.

For turbulent flow conditions (Figure 3.5b), the velocity profiles are fuller in the middle of the pipe while still satisfying the no-slip condition (zero velocity in proximity of the wall). The dimensionless Reynolds number is typically used to distinguish the flow regime conditions:

$$Re = \frac{\rho \cdot v_{avg} \cdot D_h}{\mu} \tag{3.8}$$

where, in Eq. (3.8), D_h represents the hydraulic diameter of the flow section:

$$D_h = \frac{4 \cdot A}{P_w} \tag{3.9}$$

A is the perpendicular cross-sectional area of the pipe, while P_w is the wetted perimeter. For circular pipes, the hydraulic diameter corresponds to the pipe's internal diameter.
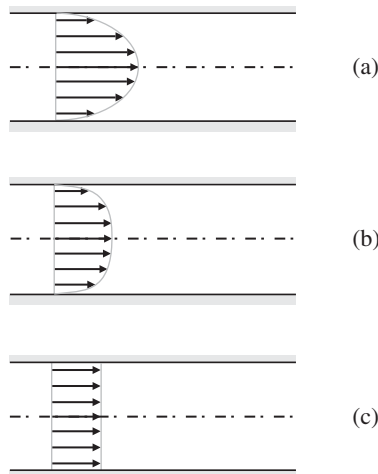
Figure 3.5 Actual velocity profile (laminar and turbulent flow) and uniform velocity profile. (a) Laminar regime. (b) Turbulent regime. (c) Uniform assumption approximation.

For circular pipes, $Re < 2300$ corresponds to laminar flow conditions, while $Re > 4000$ to turbulent flow conditions [15]. A transitional flow region is further defined between these flow regimes.

The average velocity value used for the calculation of the Reynolds number is defined as

$$v_{\text{avg}} = \frac{Q}{A} \tag{3.10}$$

The concept of average velocity can be illustrated with the *uniform flow distribution* in Figure 3.5b.

> The uniform flow distribution permits to describe the overall flow through a pipe section with a single value, which is also the representative fluid velocity, v_{avg}.

The v_{avg} will be used for deriving many features of pipe flows, particularly for describing phenomena with empirical correlations. A significant example, which will be further detailed in Section 3.5, is the case of the frictional losses in a pipe. These are calculated from the value of v_{avg}.

The average velocity v_{avg} is also often one of the main parameters to be considered when sizing certain hydraulic components. For example, when selecting the proper diameter of the pipes, or the diameter of the ports of pumps or motors, designers have to ensure that the maximum average velocity reached during the operation of the system is below certain values. Design guidelines usually recommend the following maximum values for average velocity [30]:

– Pressure lines – 25 ft/s or 7.62 m/s
– Return lines – 10 ft/s or 3.05 m/s
– Suction lines – 4 ft/s or 1.22 m/s

However, one must keep in mind that even when such requirement is met, the actual maximum fluid velocity at the centerline of the pipe is significantly higher.

3.4 Conservation of Mass

In fluid mechanics, the fundamental laws that describe flow can be expressed for a control volume (CV), which is a volume fixed in space or moving with a certain velocity through which the fluid flows.

The CV formulation of the mass conservation principle in fluid mechanics can be expressed by the following equation:

$$\frac{\partial}{\partial t} \int_{\text{CV}} \rho \, dV + \int_{\text{CS}} \rho \vec{v} \cdot d\vec{A} = 0 \tag{3.11}$$

The first term represents the rate of change of the mass in the CV, while the second term is the net rate of flux of mass across the bounding control surfaces (CS; Figure 3.6). Details on the derivation of Eq. (3.11) can be found in basic fluid mechanics textbooks [15].

In most hydraulics problems, it is convenient to assume incompressible flow, as well as uniform flow at each inflow or outflow section of the control surface, so that

$$\frac{\partial}{\partial t} \int_{\text{CV}} dV + \sum_{i=1}^{N} Q_i = 0 \tag{3.12}$$

Q_i represents all the flow rates exiting (positive) or entering (negative) the CV through the permeable surfaces. For stationary problems, the CV does not vary over time; therefore, the conservation of mass equation simply becomes

$$\sum_{i=1}^{N} Q_i = 0 \tag{3.13}$$
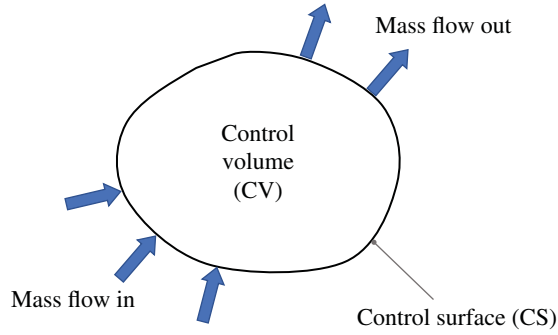
Figure 3.6   Control volume (CV) and bounding control surface (CS).

A direct application of the above equation is the case of a hydraulic junction (Figure 3.7) – the overall flow entering the junction equals the flow leaving the junction:

$$Q_3 = Q_1 + Q_2 \tag{3.14}$$

With this analogy, the law that applies in the flow in Eq. (3.14) is equivalent to Kirchhoff's current law applied to the nodes of electric circuits. Junctions in most of the hydraulic circuits are described in the following chapters, and the law that applies in Eq. (3.13) will be used frequently in describing the operation of the system.

3.4.1   Application to a Hydraulic Cylinder

Hydraulic cylinders are basic elements of a hydraulic system, and their function will be described in Chapter 7. This section is aimed to illustrate how the conservation of mass influences the derivation of the basic equation, which will be used throughout this book for describing the motion of the piston of a hydraulic cylinder.

In Figure 3.8, the cylinder is illustrated through its ISO symbol. Let us consider the case of cylinder extension, against a resistive force F. The fluid enters the piston chamber, causing the piston to move with a certain velocity $\dot{x}$. Because of the piston motion, the fluid exits the rod chamber. The piston area and the annular area at the rod chambers are also indicated in figure:

$$A = \pi \frac{D^2}{4} \tag{3.15}$$

$$a = \pi \frac{(D^2 - d^2)}{4} \tag{3.16}$$

where D and d are respectively the piston diameter and the rod diameter.
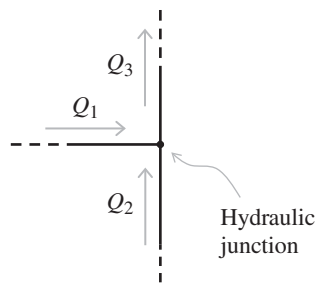
Figure 3.7   Conservation of mass in a hydraulic junction.
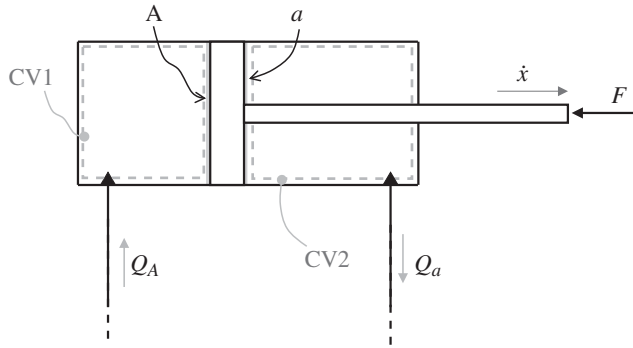
Figure 3.8 Representation of a hydraulic cylinder during the extension.

The conservation of mass (Eq. (3.11)) can be applied to CV1, which includes all the fluid at the piston chamber. The CV increases its size during the motion of the piston; therefore, the change in volume (first term of the conservation of mass) cannot be assumed to be zero. Considering the fluid density constant throughout CV1,

$$\frac{\partial}{\partial t}\int_{\text{CV1}} \rho dV = \rho A \dot{x} \tag{3.17}$$

The second term of Eq. (3.11) can be written with a simple expression considering that there is only one opening section in the CV1's control surface:

$$\int_{\text{CS1}} \rho \vec{v} \cdot d\vec{A} = -\rho Q_A \tag{3.18}$$

With these simplifications, and assuming constant fluid density, Eq. (3.11) applied to CV1 (bore side CV) becomes

$$\dot{x} = \frac{Q_A}{A} \tag{3.19}$$

A similar expression can be derived by applying the conservation of mass to the rod side CV, CV2:

$$\dot{x} = \frac{Q_a}{a} \tag{3.20}$$

From the results obtained for each CV, CV1 and CV2, a relation between the flow rates at the two cylinder ports can be derived:

$$\frac{Q_A}{Q_a} = \frac{A}{a} \tag{3.21}$$

Equation (3.21) is valid for both cases of extension and retraction of the linear actuator, and essentially it shows that the geometrical area ratio of the cylinder corresponds to the ratio of the flow rates at the two cylinder work ports.

It is important to notice that for a given flow rate entering the cylinder, the external load F applied to the piston does not have an impact on the cylinder motion. This is true when fluid compressibility effects can be ignored, as in most of the typical hydraulic control systems, the external load will instead have a direct impact on the fluid pressure inside the cylinder chambers.

3.5 Bernoulli's Equation

Bernoulli's equation is one of the most important equations in fluid mechanics.

Bernoulli's equation establishes the concept of energy conservation within a flow.

In textbooks on basic fluid mechanics, Bernoulli's equation is derived using two possible methods: one considers the conservation of mass and the momentum equation applied to a differential CV and another – perhaps more intuitively – starts from the principle of energy conservation. The reader can refer to [15] for more details. In this chapter, the classic form of the Bernoulli's equation is presented without discussing its derivation, in order to highlight its implications in hydraulic systems:

$$\frac{p}{\rho} + \frac{v^2}{2} + gz = const \tag{3.22}$$

This equation is valid under steady-state conditions, for incompressible and inviscid (frictionless) flows. Each term of the equation has units of energy per unit mass (J/kg) and summarizes three possible ways in which a fluid can store energy:

$$\frac{p}{\rho} \Rightarrow \text{flow (or pressure) energy}$$

$$\frac{v^2}{2} \Rightarrow \text{kinetic energy} \tag{3.23}$$

$$gz \Rightarrow \text{elevation (or potential) energy}$$

Equation (3.22) is used to describe the relation between pressure and fluid velocity in a flow stream:

$$\frac{p_1}{\rho} + \frac{v_1^2}{2} + gz_1 = \frac{p_2}{\rho} + \frac{v_2^2}{2} + gz_2 \tag{3.24}$$

As previously discussed, in hydraulic systems, the operating pressure is so high that even large differences in elevation are mostly negligible in fluid power machines. However, large variations in fluid velocities and in pressure can be found within hydraulic components. Neglecting the elevation contribution, Eq. (3.24) states that changes in fluid pressure in a fluid stream correspond to a quadratic change in fluid velocity.

In the presence of fluid contractions, where the fluid velocity increases, because of the conservation of mass, the pressure decreases. On the contrary, in case of expansions, the velocity decreases and the pressure rises. This is also illustrated in Figure 3.9.

Sharp contractions or expansions are often present within hydraulic components. It is therefore important to note the trend in the variation of fluid pressure and velocity as the flow crosses a certain geometric configuration. Equations (3.22) and (3.24) are valid for the ideal case of frictionless fluid (frictional effects due to viscosity negligible); and, strictly speaking, for flow particles along the same velocity streamline (an example of particle streamlines is represented in Figure 3.9). These ideal conditions are realistic for most contractions, where the frictional effects do not have
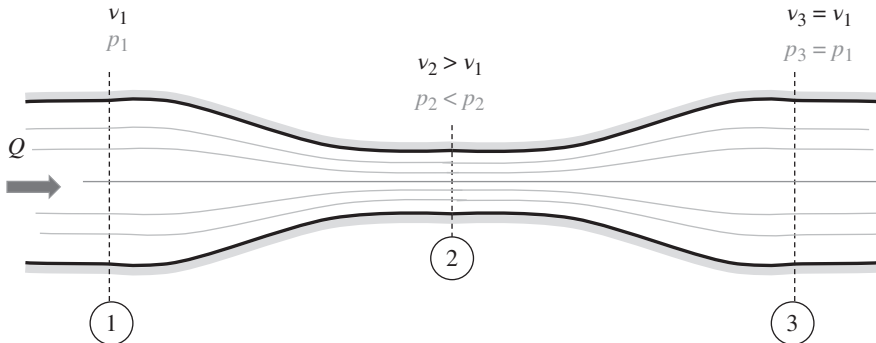
Figure 3.9 Venturi tube and representation of streamlines.

much influence on the velocity profile. However, at expansion, when the flow is on an adverse pressure gradient, frictional effects are more relevant, and conditions can be far from the ideal ones. If the geometrical area increases too rapidly, the boundary layer portion of the flow can grow in an unstable way and causes flow separation effects [15]. In simple terms, with reference again to Figure 3.9, the relations discussed above are valid for the convergent section up to section 2, while the actual pressure recovery at section 3 is much more limited ($p_3 < p_1$) and it depends on the how gradual is the area increase from section 2 to section 3.

3.5.1 Generalized Bernoulli's Equation

For the analysis of pipe flow problems, the basic Bernoulli's equation can be extended to its generalized form:

$$\left(\frac{p_1}{\rho} + \alpha_1 \frac{v_1^2}{2} + gz_1 \right) - \left(\frac{p_2}{\rho} + \alpha_2 \frac{v_2^2}{2} + gz_2 \right) = h_l - h_p \tag{3.25}$$

The generalized Bernoulli's equation (Eq. (3.25)) is written between two reference sections of a pipe flow stream: an upstream section (generally indicated with subscript 1), and a downstream section (subscript 2). At the second member, the equation includes terms denoting the presence of an energy loss, h_l, and of an energy generation, h_p. The term for energy loss represents the loss due to fluid shear between the control sections 1 and 2. The term for energy generation (h_p) includes the energy provided to the flow, for example, when pumps are present. This equation will also be used to introduce the hydraulic pumps in Chapter 6.

Here, the generalized Bernoulli's law is now applied to the whole pipe (delimited by the two control sections); the Bernoulli's equation discussed in the previous paragraph is valid only along a streamline. This implies a different evaluation for the kinetic energy. In Eq. (3.25), this kinetic energy contribution is calculated by considering the average velocity on the area, thus introducing a kinetic energy coefficient (α) to consider the actual velocity profile (Figure 3.10). Without going into the specifics of how α is calculated, which can be found, for example, in [15], one can just consider:

$$\begin{aligned} \alpha &= 2 \text{ for laminar flow} \\ \alpha &= 1 \text{ for turbulent flow} \end{aligned} \tag{3.26}$$

The energy loss per unit mass, h_l, is typically referred in fluid mechanics as head loss. It comprises two terms:

$$h_l = h_{\text{major}} + h_{\text{minor}} \tag{3.27}$$

The major loss, h_{major}, includes the friction effects generated in all the sections of the pipe (between the reference sections 1 and 2) with constant sectional areas and flow in fully developed

Laminar
(a)
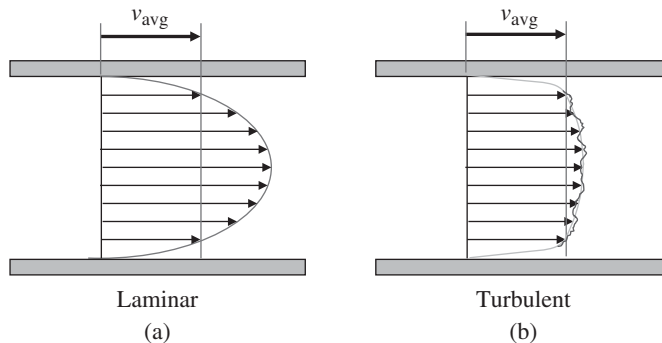
Turbulent
(b)

Figure 3.10 Laminar (a) and turbulent (b) velocity profiles in a pipe, with same average velocity.

conditions. On the other hand, the minor loss, h_{minor}, includes other frictional losses caused by singularities such as sectional discontinuities of fittings, bends, and entrances.

> The head loss h_l expresses the energy loss per unit mass in a defined flow section. It comprises two terms, the major loss (portions with constant sectional areas) and the minor loss (singularities).

Figure 3.11 clarifies how to identify the different loss terms in a pipe flow, between two reference sections 1 and 2. After every geometrical discontinuity in the piping system, such as at the entrance or after an elbow, or a fitting, the flow requires to travel a certain length before reaching fully developed conditions. Fully developed conditions are defined when the same velocity profile is held throughout the entire length of the constant area pipe. Figure 3.11 shows the entrance region of the flow getting into the first section of the pipe (length L_1) from the tank. After the entrance region, where the flow profile is still developing, the velocity profile is constant until the 180° bend is reached. The flow at the exit of the bend enters a second constant sectional portion (length L_2) and develops along a certain travel length before reaching fully developed conditions.

A detailed description of the entrance or the developing flow region is outside the scope of this chapter, but it has been a topic of interest in many fluid mechanics problems. Hence, it is important for the reader to understand the typical approach used in pipe flow problems to describe the energy loss associated with different portions of the pipe system.

3.5.2 Major Losses

For the regions of fully developed flow, it is possible to analytically demonstrate that for laminar flow conditions:

$$h_{\mathrm{major}} = \frac{64}{Re} \frac{L}{D_h} \frac{v^2}{2} \tag{3.28}$$
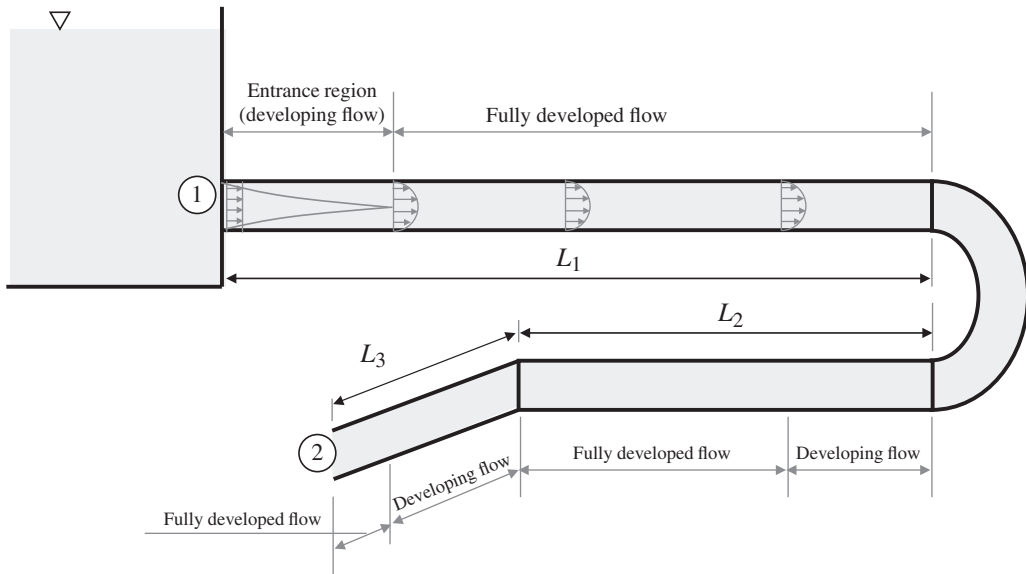
Figure 3.11 Example of analysis of major and minor losses in a pipe flow.

The velocity value v represents the average velocity over the section. From considerations based on dimensional analysis, it is possible to derive the Darcy-Weisbach equation, which has validity for both laminar and turbulent flow conditions:

$$h_{\mathrm{major}} = f \frac{L}{D_h} \frac{v^2}{2} \tag{3.29}$$

where the friction factor f is a function of the Reynolds number and the relative roughness of the pipe:

$$f = f\left(Re, \frac{e}{D_h}\right) \tag{3.30}$$

Figure 3.12 shows the results from the pioneering work performed by Moody [15] on the determination of the friction factor. The Moody's diagram is nowadays the most used chart for determining the major head losses in pipe flows. Analytical expressions for f can also be found in basic fluid mechanics textbooks. A widely adopted one is the Colebrook's formula:

$$\frac{1}{\sqrt{f}} = -2 \log\left(\frac{e/D}{3.7} + \frac{2.51}{Re\sqrt{f}}\right) \tag{3.31}$$

From Eq. (3.28), it is possible to conclude that the loss term h_{major} in laminar conditions is proportional to the average fluid velocity (v) because of the presence of the Reynolds number, Re, at the denominator of the expression. However, under conditions of complete turbulence, where the friction factor f is constant, the loss term follows a quadratic relation with v.

> The major loss term h_{major} is proportional to the average fluid velocity, v, in laminar conditions, and to v^2 in complete turbulent conditions.

3.5.3 Minor Losses

Minor losses are primarily caused by flow separation effects. Figure 3.13 illustrates the case of the flow separation in proximity of a pipe entrance from a reservoir: the streamlines qualitatively illustrated the mixing areas of the separated zones, where energy is dissipated.

Flow separation effects such as the case in Figure 3.13 occur at every geometrical discontinuity of the pipe flow system. The energy losses in these cases are described by two alternative formulas:

$$h_{\mathrm{minor}} = k\frac{v^2}{2} \tag{3.32}$$

or

$$h_{\mathrm{minor}} = f\frac{L_e}{D_h} \frac{v^2}{2} \tag{3.33}$$

As in the case of major losses, minor losses are quantified with respect to the kinetic term $v^2/2$, by means of empirical relations based on experimental data. For many cases, particularly for entrances, exits, or sudden contractions or expansions, it is common to find in the literature the k coefficients. In the case of an exit to a tank, it is intuitive to consider that all the kinetic energy of the fluid inside the pipe will be dissipated; therefore, $k_{\mathrm{exit}} = 1$. For other discontinuities, typically $k < 1$.

For other discontinuities, such as elbow or bends, it is more common to evaluate the friction coefficient f relative to the diameter representative of the discontinuity (i.e. the diameter of the curved pipe, for the case of an elbow) and use an empirical value of equivalent length L_e, which corresponds to the length of a straight pipe that would provide the same head loss.

The Moody diagram. Axes: Friction factor (vertical, left, 0.008 to 0.1), Reynolds number (horizontal, 10^3 to 10^8), Relative pipe roughness (vertical, right, 10^{-6} to 0.05).

Labels on the diagram: Transition region, Laminar Flow $\frac{64}{Re}$, Complete turbulence, Smooth Pipe, Friction factor $= \frac{2d}{\rho V^2 l}\Delta P$.

Material	ε [mm]
Concrete, coarse	0.25
Concrete, new smooth	0.025
Drawn tubing	0.0025
Glass, Plastic Perspex	0.0025
Iron, cast	0.15
Sewers, old	3.0
Steel, mortar lined	0.1
Steel, rusted	0.5
Steel, structural or forged	0.025
Water mains, old	1.0

Figure 3.12 Moody's diagram for the calculation of the friction factor. Source: Moody's diagram, Darcy–Weisbach friction factor, wikipedia. Licensed under CC BY-SA 4.0.
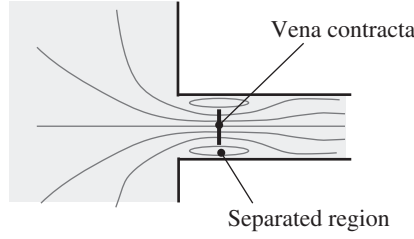
Figure 3.13 Example of separation region at a flow entrance.

A fluid power engineer must be ready to use both the formulas (3.32) and (3.33), depending on the data source that is available. For basic geometries, empirical data for minor losses can be found in the book of Idelchik [31].

It is important to point out that, in general, the minor losses include also the frictional effects of the developing flow region that follows the initial flow separation. This allows for a straightforward identification of the lengths to be used in the evaluation of the major loss terms. For example, with reference to the previous Figure 3.11, the entrance loss considers the additional losses associated to the entrance region in such a way that the evaluation of the major losses of the first straight section of the pipe is performed with the geometrical length L_1. Similarly, the lengths L_2 and L_3 will be used in Eq. (3.29) for the other major losses present between the reference sections.

> In most cases, the minor loss term h_{minor} is proportional to the term v^2.

3.6 Hydraulic Resistance

The generalized Bernoulli's law (Eq. (3.25)) can be written differently to break down the energy losses into three different contributions:

$$h_l = \frac{p_1 - p_2}{\rho} + \frac{\alpha_1 v_1^2 - \alpha_2 v_2^2}{2} + g(z_1 - z_1) \tag{3.34}$$

Equation (3.34) highlights the pressure, kinetics, and elevation terms contributing to h_{loss}. In hydraulic systems, it is very common to have the pressure differential term dominating the other two, which can easily be ignored. For this reason, it can often be assumed that

$$h_l \approx \frac{p_1 - p_2}{\rho} \tag{3.35}$$

> In hydraulic systems, the head loss term h_l ($= h_{major} + h_{minor}$) relates to a pressure loss.

Equations (3.25), (3.29) (major losses), and (3.32) (minor losses) highlight how the pressure drop due to frictional losses across a hydraulic element or a section of a pipe is proportional to v^2, for turbulent conditions:

$$\Delta p = p_1 - p_2 \propto v^2 \tag{3.36}$$

Common components of a hydraulic system such as valves and hydraulic fittings are mostly characterized by turbulent flow conditions. This is common for all sources of minor losses. Considering the relation between average velocity and volumetric flow rate (Eq. (3.10)), Eq. (3.36) can be written as follows:

$$\Delta p \propto Q^2 \tag{3.37}$$

The constant of proportionality in the quadratic equation between pressure can be referred to as **turbulent hydraulic resistance**, R_{turb}. The resistance term originates from the *electric analogy* approach. The value of the resistance sets the link between the generalized flow variable (electric current, in the electric domain, and volume flow rate, in the hydraulic domain) and the generalized effort variable (voltage, in the electric domain and pressure, in the hydraulic domain)[2]:

$$\Delta p = R_{turb} \cdot Q^2 \tag{3.38}$$

The hydraulic resistance R can be analytically derived from Eq. (3.29) (major losses) and Eq. (3.32) (minor losses), if the empirical friction factor or the loss coefficient is known. However, it is quite common for hydraulic components to find flow–pressure drop curves such as the one in Figure 3.14 (valid for a check valve), from which the resistance coefficient can be easily derived.

At this point, the reader should notice one major difference between the hydraulic and electrical resistances. In fact, in the hydraulic domain, the law is quadratic, while in the electrical one (Ohm's law), it is linear. This is because of the turbulent flow condition. The hydraulic–electrical analogy is completely accurate only for laminar flow conditions:

$$\Delta p = R_{lam} \cdot Q \tag{3.39}$$

where R_{lam} is the **laminar hydraulic resistance**. The subscript designation of the hydraulic resistance R is different between Eqs. (3.38) and (3.39) and refers to the type of flow inside the component. In hydraulic applications, laminar flow occurs only in particular cases, such as leakage flows inside the small gaps of pumps or spool valves.

The **hydraulic resistance** expresses the relation between flow rate Q and pressure drop Δp across a hydraulic element. For laminar flow conditions, the hydraulic resistance R_{lam} is a constant of proportionality between Q and Δp. In the more common case of turbulent conditions, the hydraulic resistance is a coefficient between Q^2 and Δp.

For simplified studies, or when linear relations are more convenient for applying control laws, it is possible to assume a linear relation between flow rate and pressure also for turbulent flow. This approximation is not recommended for general analysis, but it can be accurate enough to describe relative variations of pressure and flows in a small interval, as it is illustrated in Figure 3.15.
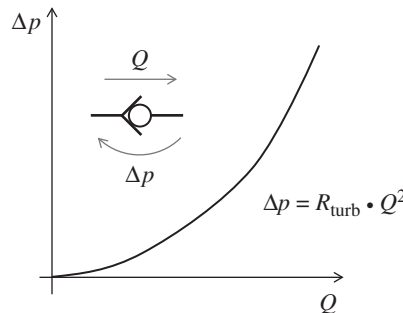
Figure 3.14 Resistance across a hydraulic check valve.

---

2 In the literature, it also common to find the hydraulic resistance generally defined as

$$R = \frac{\Delta p}{Q}$$
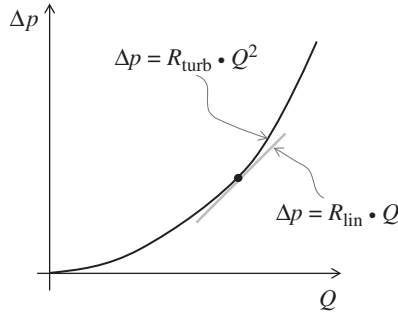
Figure 3.15 Linear approximation for the hydraulic resistance in turbulent flow conditions.

The linear hydraulic resistance (R_{lin}) can be calculated as

$$R_{lin} = \frac{d(\Delta p)}{dQ} = 2\sqrt{R_{turb} \cdot \Delta p} \tag{3.40}$$

3.7 Stationary Modeling of Flow Networks

The following chapters of the book focus on the analysis of hydraulic systems operating in steady-state conditions. Hence, after the presentation of the basic equations for hydraulic resistance and conservation of mass, it is now appropriate to provide the reader with the general approach that can be used to model a flow network.

A flow network can be defined as any collection of elements (valves, cylinders) and sources (pumps). The network interconnections are the fluid conveyance elements.

According to the approach also presented by Merritt [32], the flow and the pressure distribution within a network must satisfy three constraints:

1. Flow–pressure relationship
   Every element of the circuit is characterized by a flow–pressure relationship. The simplest example is the case of the hydraulic resistance that can be used to describe pipes, fittings, and certain hydraulic valves, previously shown in Eqs. (3.38) and (3.39). The next chapters will present also relations for other elements, such as pumps, motors, and linear actuators.
2. Flow law
   The flow law applies at any junction of pipes, and it was already presented as a direct consequence of the conservation of mass principle:

$$\sum Q_i = 0 \tag{3.41}$$

   Equation (3.41) can be seen as the equivalent of the Kirchhoff's current law in the electric domain. Essentially, this equation states that the sum of the flow rates entering a junction has to be equal to the sum of the flow rates exiting it (Figure 3.16a).
3. Pressure law
   The pressure law can be seen as the equivalent of the Kirchhoff's voltage law in the electric domain. It states that the overall pressure drop around any closed circuit has to be null:

$$\sum \Delta p_i = 0 \tag{3.42}$$

---

 which implies a linear relationship between flow rate and pressure drop. This will be the case of the laminar hydraulic resistance. In this book, the authors choose to distinguish the case of laminar hydraulic resistance from the case of turbulent hydraulic resistance.
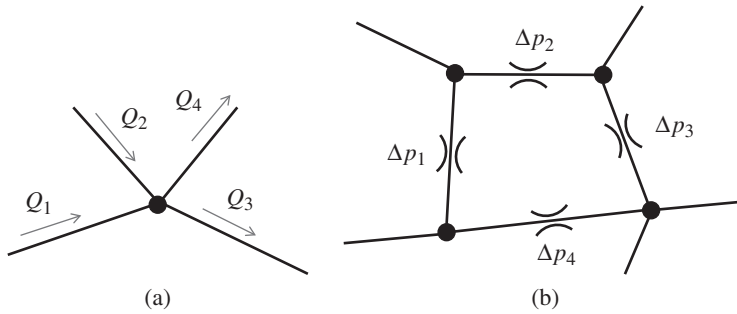
Figure 3.16 Graphical representation of flow law (a) and pressure law (b).

Example 3.1   Series and parallel hydraulic connections

The pressure drop–flow rate relation for three different pipes is known to be linear, as shown in the figure below. Find the pressure drop–flow rate relation for different configurations of the three pipes: (a) series; (b) parallel; and (c) series–parallel.

(a) Series   (b) Parallel   (c) Series–parallel
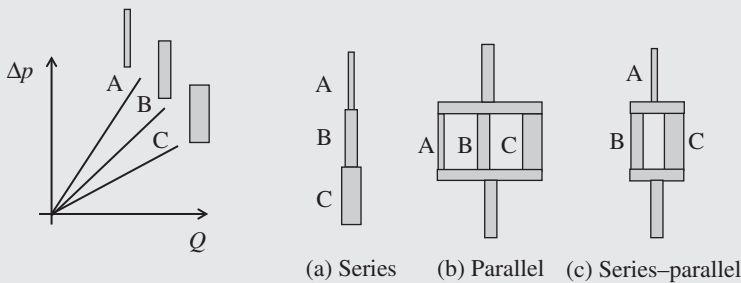
Given:
The linear characteristic of three pipe sections:
$\Delta p_A = R_A \cdot Q_A$; $\Delta p_B = R_B \cdot Q_B$; $\Delta p_C = R_C \cdot Q_C$

Find:
The equivalent hydraulic resistance for the three cases:
$\Delta p_{series} = R_{series} \cdot Q$; $\Delta p_{parallel} = R_{parallel} \cdot Q$; $\Delta p_{series/parallel} = R_C \cdot Q$

Solution:
Case (a) series
This case can be solved by considering the quantities shown in the figure below:
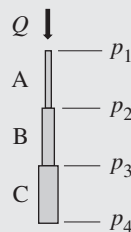
$$p_1 - p_2 = \Delta p_A = R_A \cdot Q_A; \quad p_2 - p_3 = \Delta p_B = R_B \cdot Q_B; \quad p_3 - p_4 = \Delta p_C = R_C \cdot Q_C$$

Therefore,

$$p_1 - p_4 = (R_A + R_B + R_C) \cdot Q$$

which means

$$R_{\text{series}} = R_A + R_B + R_C$$

Case (b) parallel

The approach is similar to case (a). With reference to the figure below,
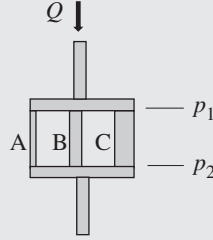
$$p_1 - p_2 = \Delta p_A = R_A \cdot Q_A = \Delta p_B = R_B \cdot Q_B = \Delta p_C = R_C \cdot Q_C$$

Considering the flow law,

$$Q = Q_A + Q_B + Q_C$$

which gives

$$Q = \frac{p_1 - p_2}{R_A} + \frac{p_1 - p_2}{R_B} + \frac{p_1 - p_2}{R_C}$$

or also

$$Q = (p_1 - p_2) \cdot \left(\frac{1}{R_A} + \frac{1}{R_B} + \frac{1}{R_C} \right)$$

which means

$$R_{\text{parallel}} = \left(\frac{1}{R_A} + \frac{1}{R_B} + \frac{1}{R_C} \right)^{-1}$$

Case (c) series–parallel

In this case, the reference schematic is shown below:
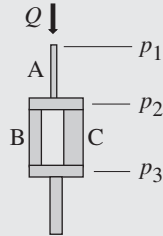
Pipe A is in series with B and C, which are in parallel. Using the relations derived above:

$$p_1 - p_3 = \left(R_A + \frac{1}{\frac{1}{R_B} + \frac{1}{R_C}} \right) \cdot Q$$

which means

$$R_{\text{series–parallel}} = R_A + \frac{1}{\frac{1}{R_B} + \frac{1}{R_C}}$$

3.8   Momentum Equation

The momentum equation is based on Newton's second law applied to a mechanical system, which states that the sum of all forces acting on the system is equal to the time rate of change of linear momentum of the system. In fluid mechanics problems, the same principle can be applied to a CV, having some bounding surfaces, CS, permeable to fluid:

$$\vec{F} = \vec{F}_S + \vec{F}_B = \frac{\partial}{\partial t} \int_{CV} \vec{v}\rho dV + \int_{CS} \vec{v}\rho\vec{v} \cdot d\vec{A} \tag{3.43}$$

The derivation of Eq. (3.43) can be found in basic fluid mechanics textbooks, such as [15]. The expression states that the sum of the forces acting on the CV is equal to the rate of change of momentum inside the CV (first term at the second member) added to the net rate at which momentum is leaving the CV through the CS (last term in the equation). The forces acting on CV can be of different nature: surface forces, $\vec{F}_S$, acting on the control surface, and body forces $\vec{F}_B$, acts throughout the volume. The surface forces are those related to fluid pressure and frictional effects, while the only body forces usually taken into consideration is gravity.

The above momentum equation is very useful to study the interaction between the fluid and the surrounding solid surfaces. In fluid power systems, the momentum equation is typically used to determine the force applied by the fluid in a piping system. The following problem provides a representative example.

Example 3.2   Force on an elbow

A 90° elbow is installed on a return line of a tank open to atmosphere. The areas at the elbow entrance and exit are respectively 5 and 3 cm^2. The return flow rate is 50 l/min. The pressure at the elbow entrance is 1 bar. Determine the overall force acting on the connecting bolts, assuming that no load is transmitted to piping upstream the elbow. Consider the frictional effects in the elbow negligible. The volume of the fluid contained in the elbow is 70 cm^3.
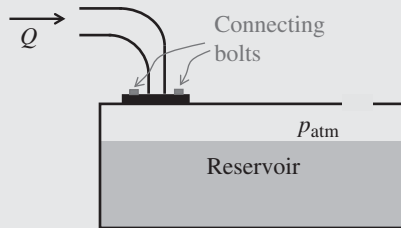
Given:
Flow rate $Q = 50$ l/min; elbow entrance cross-sectional area $A_1 = 5$ cm^2; elbow exit area $A_2 = 3$ cm^2; elbow turning angle $\alpha = 90°$; tank pressure $p_2 = p_{atm} = 1$ bar; pressure at elbow entrance $p_1 = 1$ bar; volume of the fluid in the elbow $V = 70$ cm^3; fluid density $\rho = 870$ kg/m^3

Find:
Forces acting on the elbow, F_x, F_y;

Solution:
The force components acting on the elbow can be found by applying the momentum Eq. (3.43) on the CV that includes the elbow. The CV is conveniently chosen to include control surfaces

(CS) where the fluid velocity is known. In particular, the CS includes the entrance and exit surfaces, A_1 and A_2, as well as surfaces where there is no flow (therefore with null fluid velocity).
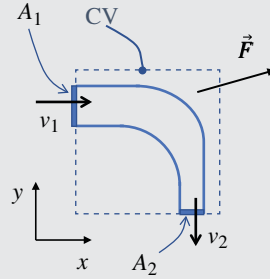
The velocities v_1 and v_2 can be calculated from the flow rates:

$$v_1 = \frac{Q}{A_1} = \frac{50 \, [l/min]}{5 \, [cm^2]} = 1.67 \, m/s$$

$$v_2 = \frac{Q}{A_2} = \frac{50 \, [l/min]}{3 \, [cm^2]} = 2.78 \, m/s$$

The momentum Eq. (3.43) can be solved separately in both the x and y components, considering the CV shown in the above figure.

x-component: For the calculation of the horizontal component of the total force, only the surface force term has to be considered. Neglecting frictional effects in the elbow, the only force component is given by the pressure force on the area A_1 and the force exerted by the elbow walls. Considering the elbow in atmosphere, it is convenient to use gage pressure instead of absolute pressure:

$$F_{S,x} = p_{1g}A_1 + R_x$$

where $R_x = -F_x$, meaning that the surface force seen by the fluid has equal but with opposite sign with respect to the force that the fluid exerts to the containing walls.

The x-component of the second member of Eq. (3.43) can be written by considering the assumption of stationary conditions, which implies that the momentum does not change over time. Therefore, the contribution from the control surfaces is the only one different from zero. Indicating the scalar horizontal velocity component with v_x, the terms at the second member of the momentum equation becomes

$$\int_{CS} v_x \rho \, \vec{v} \cdot d\vec{A}$$

There is only one section crossed by the flow where the u velocities are not null, namely, the entrance section A_1. Therefore, the CS term above reduces to the only section A_1. With the assumption of uniform flow,

$$\int_{CS} v_x \rho \, \vec{v} \cdot d\vec{A} = v_1(-\rho v_1 A_1)$$

Overall the x-component of the momentum equation becomes

$$p_{1g}A_1 + R_x = v_1(-\rho v_1 A_1)$$

Therefore,

$$R_x = -p_{1g}A_1 - \rho v_1{}^2 A_1 = -1 \, [bar] \cdot 5 \, [cm^2] - 870 \, [kg/m^3] \cdot 1.67^2 \, [m^2/s^2] \cdot 5 \, [cm^2]$$
$$= -51.21 \, N$$

Example 3.2 (Continued)

which means that the x-component of the force acting on the bolts is:

$$F_x = -R_x = 51.21 \, N$$

y-component: With the assumption of no frictional forces, and considering that the exit section A_1 is in atmosphere (gage pressure is null):

$$F_{S,y} = R_y$$

Due to gravity, the body force is given by the weight of the fluid inside the CV:

$$F_{B,y} = -\rho V_{\text{elbow}} g$$

The second term of the y-component of the momentum equation can be written under the same assumption of uniform flow, and considering that vertical components of the velocity at the control surface are present only at the section A_2 :

$$\int_{\text{CS}} v_y \rho \, \vec{v} \cdot d\vec{A} = -v_2(\rho v_2 A_2)$$

Overall,

$$R_y = -F_{B,y} - \rho v_2^2 A_2 = \rho V_{\text{elbow}} g - \rho v_2^2 A_2$$

$$R_y = 870 \, [kg/m^3] \cdot 70 \, [cm^3] \cdot 9.81 \, [m/s^2] + 870 \, [kg/m^3] \cdot 2.78^2 \, [m^2/s^2] \cdot 3 \, [cm^2] = -1.43 \, N$$

which means that the y-component of the force acting on the bolts is

$$F_y = -R_y = 1.43 \, N$$

The orientation of the force on the bolts is therefore similar to the one indicated in the image above, with a horizontal component more pronounced than the vertical one.

3.8.1 Flow Forces

Another important application of the momentum equation is for the determination of the so-called *flow forces* in hydraulic control valves.

The flow forces act on the moving element (generally a spool or a poppet) of the valve, and they are generated by the flow through the component. As it will be mentioned in Chapter 8, the presence of flow forces can significantly affect the operation of hydraulic control valves as well as the design of the valve actuation mechanism.

To understand the nature of flow forces and derive an analytical expression that can be useful to study most of the typical geometries of hydraulic control valves, the simplified case in Figure 3.17 is taken as reference. The figure represents a spool that varies the valve opening between the pump (1) supply and the work port (2). Specifically, the spool can move horizontally along the *x* axis, and in the position represented in the figure, it determines an effective opening area between the valve ports respectively at the sections indicated in figure with 1 (inflow) and 2 (outflow).

The figure considers the common situation of $A_1 \gg A_2$ so that, per the conservation of mass, higher exit velocities are obtained. This is a very typical working condition of many hydraulic control valves, when low flow areas are implemented to regulate the actuator speed. The figure clearly shows how the flow changes its velocity and direction (therefore, its momentum) as it crosses the
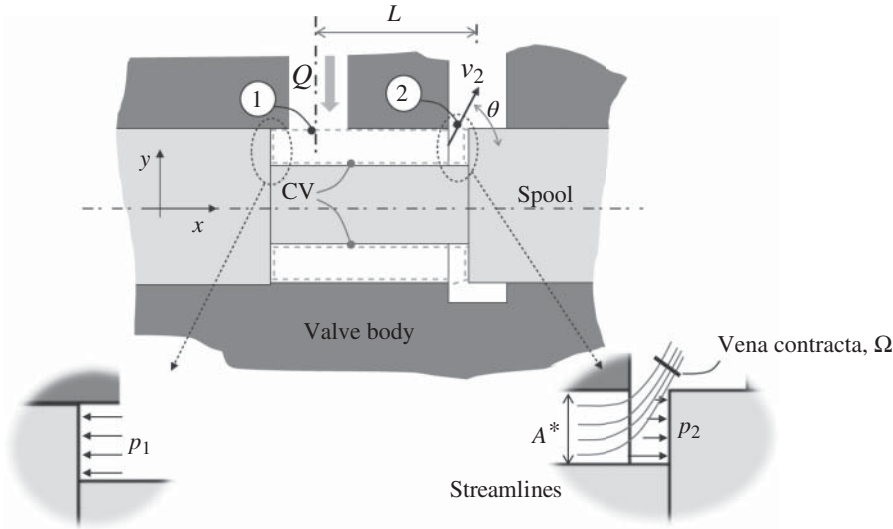
Figure 3.17 Reference geometry for the analysis of flow forces.

valve. Most of this momentum change is caused by the spool itself. The important question to be answered is: what is the force acting on the spool because of this momentum change? The answer is very important to understand how to size the valve actuation system, namely, the system that sets the position of the spool, which can be manually operated, electrically operated, or hydraulically operated. More details on the valve actuation systems will be provided in Chapter 8.

One possible way to answer this question consists in solving the pressure distribution at the spool walls, which is qualitatively shown in Figure 3.17. This approach requires a proper differential flow approach of analysis, where the governing equations are written for a differential fluid element and numerically integrated by mean of a computational fluid dynamics (CFD) tools. Numerical CFD techniques also allows studying more complex geometries that sometimes occurs in modern hydraulic control valves. However, the numerical CFD analysis can be time consuming, and it does not provide an analytical expression of the flow force. This analytical expression can be very useful to the valve designer to gain an intuitive understanding of the development of the flow forces, and more importantly it can be used if to formulate the proper controller parameters in case of hydraulic control valves using closed-loop controls.

An analytical expression can be easily calculated applying the momentum equation to a properly selected CV. By considering the annular shaped CV indicated in Figure 3.17, with constant fluid density, the equation becomes

$$\vec{F} = \rho \frac{\partial}{\partial t} \int_{CV} \vec{v} A^* dx + \int_{CS} \vec{v} \rho \vec{v} \cdot d\vec{A} \tag{3.44}$$

Assuming uniform flow at both inlet and outlet sections,

$$\iint_{CS} \vec{v} \rho \vec{v} \cdot d\vec{A} = \rho \left(\frac{Q}{\Omega} \right) \left(\frac{Q}{\Omega} \right) \Omega \, \cos \theta \hat{i} + \left[\rho \frac{Q^2}{A_1} + \rho \frac{Q^2}{\Omega} \sin \theta \right] \hat{j} \tag{3.45}$$

where $\hat{i}$ and $\hat{j}$ are the unit vectors, respectively, along the horizontal and vertical directions. For a rigorous application of the momentum Eq. (3.43), the CV extends outward from the spool exit section A_2, until the vena contraction, Ω. This section is defined when the flow is mono-dimensional (1D), which means parallel velocity streamlines. Only at Ω the uniform flow assumption is valid to describe the flow exiting the CV.

Therefore, from Eq. (3.44),

$$\vec{F} = \rho L \frac{\partial Q}{\partial t} \hat{i} + \rho \frac{Q^2}{\Omega} \, \cos \, \theta \, \hat{i} + \left[\rho \frac{Q^2}{A_1} + \rho \frac{Q^2}{\Omega} \sin \theta \right] \hat{j} \tag{3.46}$$

The objective of the flow force analysis usually corresponds to the force acting along the direction of motion of the moving element (in this case, the horizontal axis). This is the force that the actuation mechanism has to counter-react to balance the spool. The vertical force is usually compensated through symmetric design of the spool and housing. For example, in this case, a second exit area would be typically present in the lower end of the spool. Therefore, for the case in Figure 3.17, the attention is focused on the horizontal component of Eq. (3.46):

$$F_x = \rho L \frac{\partial Q}{\partial t} + \rho \frac{Q^2}{\Omega} \, \cos \, \theta \tag{3.47}$$

The term F_x corresponds to the forces acting on the CV through the CS. These include the pressure forces on the inlet and outlet sections, the pressure forces at the walls, and the frictional forces due to fluid shear. The pressure forces at both sections 1 and 2 can be considered as vertical[3], and typically the effects of the fluid shear inside the valve is negligible when compared to the flow forces. For this reason, the above expression (3.47) summarizes all the forces that the walls exert on the fluid inside the CV.

The flow force F_{fl} can be seen as the reaction force of the above F_x, which is the force that the fluid exerts to the bounding surfaces of the CV.

$$F_{fl} = -F_x = -\rho L \frac{\partial Q}{\partial t} - \rho \frac{Q^2}{\Omega} \, \cos \, \theta \tag{3.48}$$

The flow force presents both a stationary component and a transient component. The stationary component corresponds to a given position of the spool or the poppet of the valve and a constant flow rate. The transient component relates to variations of the spool (or poppet) position, as well as flow variations. In typical problems, the transient component is neglected.

The first term refers to transient conditions, and it can be neglected when studying a stationary condition. Therefore, when studying hydraulic control valves, the second term, is normally the most important one.

$$F_{fl,\text{steady}} = -\rho \frac{Q^2}{\Omega} \, \cos \, \theta \tag{3.49}$$

The negative sign in Eq. (3.48) implies that for the spool valve geometry of Figure 3.17, the flow force tends to reduce the opening area of the spool toward the outlet section 2. This is also qualitatively visualized in the details of Figure 3.17, which shows the two different pressure distributions at the two opposite spool lands: a uniform distribution at the left side, which comes from low fluid velocities, and a gradually decreasing pressure distribution at near the exit land, which results from an accelerating flow.

According to Eq. (3.48), the amount of the flow force is linked to the flow rate with a quadratic relation, meaning that flow forces can become severe at high flow rates. Additionally, the flow force depends on the exit angle θ of the flow, often referred as *flow jet angle*, which is usually a quantity difficult to estimate. Luckily, multiple studies on the flow jet angle for different valve geometries are available in the literature, with Merritt's textbook being a meaningful example [32]. According to this source, the angle to be used for geometries such as the one in Figure 3.17 is 69°. This value, however, can be slightly affected by the amount of opening and by the clearance between the spool and the valve body.

———
3 This is not exactly true for the exit section 2, as shown in the detail of the figure. However, it is usually a good approximation also because of the low velocity values that are typically present at the vena contraction.

The following example shows how the evaluation of the direction of the flow force might not be straightforward, even for very simple geometric cases.

Example 3.3   Flow force evaluation for two different valve designs

Two different poppet valve designs implement the same flow path. The two valve designs are shown in the figures below. The Case A uses a large diameter to guide the sliding element when compared to Case B.
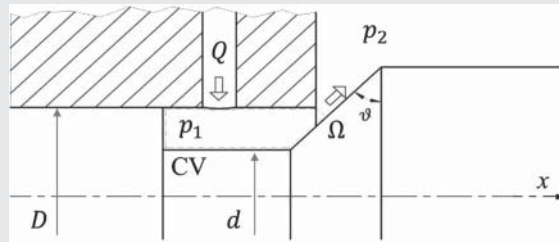
Case A
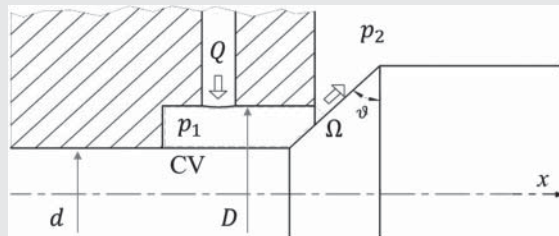
Case B

Determine an expression for the flow force acting on the valve poppet respectively for Case A and Case B. Assume that the valve poppet angle θ perfectly guides the flow at the valve exist section Ω.

Given:
Poppet valve geometry for two cases (figures above): flow rate Q; exit area Ω; jet force angle θ; and valve pressure drop $\Delta p = p_1 - p_2$

Find:
The expression and the direction of the flow force for Case A and Case B.

Solution:
This example shows two possible cases of poppet valve design. With poppet valves, the flow exit area can be almost perfectly sealed when the valve is closed (poppet against the seat). This feature is very difficult to achieve with the spool valve geometries in Figure 3.17, due to the necessary clearance between the spool and the valve body.

Flow force derivation – Case A
Equation (3.43) can be applied to the CV shown in the figure above, with the same assumptions illustrated in the previous paragraphs. This provides the expression of Eq. (3.48) for the flow

Example 3.3 (Continued)

force in steady state conditions:

$$F_{\text{fl,steady},A} = -\rho \frac{Q^2}{\Omega} \cos \theta$$

The flow force, in this case, tends to close the valve poppet.

Flow force derivation – Case B
Additionally, in this case, Eq. (3.43) can be applied to the CV shown in figure; however, it has to be noted that the Eq. (3.47) includes the overall contribution of the solid walls:

$$F_{x,\text{steady}} = \rho \frac{Q^2}{\Omega} \cos \theta$$

For this case, the pressure acting on CV at the left side (next to the entrance) is not acting on the sliding element, but on the valve body. It can be assumed that this pressure is equal to the entrance pressure p_1 and uniformly distributed at the surface (i.e. small opening area Ω). Next, assuming that with the whole poppet downstream, the flow area Ω is at the pressure p_2:

$$F_{\text{fl,steady},B} = \Delta p \frac{\pi(D^2 - d^2)}{4} - \rho \frac{Q^2}{\Omega} \cos \theta$$

For typical valve geometries, it is easy to show that the first term is generally higher than the second one so that in this case the flow force tends to open the poppet.

This can be proven by writing the orifice equation that relates Q and Δp:

$$Q = c_f \Omega \sqrt{\frac{2\Delta p}{\rho}}$$

and considering that generally

$$\frac{\pi(D^2 - d^2)}{4} \gg \Omega$$

Problems

3.1 The spool valve shown in the figure below has a maximum displacement of $x_v = 5$ mm. The area ratio for the valve, in terms of opening area per unit travel of the spool, is $w = 25$ mm. Determine the maximum steady state flow force, considering the max working pressure conditions of 200 bar. Assume the jet angle to be 69° and a valve orifice coefficient of 0.7.
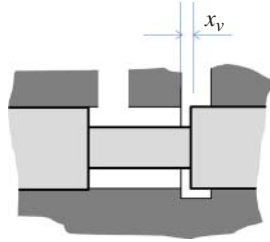
3.2 In an agricultural spraying system, the nozzles are supplied with water through 500 ft of aluminum (roughness, $e = 5 \ 10^{-6}$ ft) tubing from an engine driven pump. In its most efficient

operating range, the pump output is 1500 gpm at a discharge pressure not exceeding 65 psi. For satisfactory operation, the sprinklers must operate at 30 psi or higher pressure.

Minor losses and elevation changes may be neglected. Which is the smallest pipe size that can be used between: a 4-in., a 5-in., or a 6-in. internal diameter pipe?

3.3 Water is pumped from a reservoir on a construction job site using the pipe system of the figure below. The flow rate must be 600 gm and water must leave the spay nozzle at 120 ft/s. The tubing piping system consists of a re-entrant entrance, a regular 90°threaded elbow, two regular 45°threaded elbows, and a fully open gate valve (GV). The total length of the pipe is 700 ft, and the pipe has a diameter of 4 in.

1. Calculate the total head loss of the system, including major and minor losses.
2. Calculate the pump head required for the system.

The following data can be used:

Drawn tubing roughness: $5 \cdot 10^{-6}$ ft

Re-entrant entrance loss coefficient: 0.8

90° elbow loss coefficient: 1.5

45° elbow loss coefficient: 0.4

GV loss coefficient: 0.15
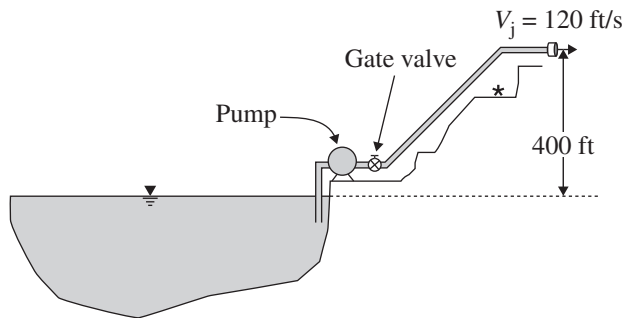
3.4 A pumping system is used to fill an elevated hydraulic tank as shown in the figure below. The hose used has a 1.91-cm (0.75 in.) diameter and 7.62-m (25 ft) length. The internal roughness is 0.5 mm ($1.97 \cdot 10^{-2}$ in) and the gage pressure of the oil at the pump outlet is 379 kPa (55 psi). The oil density is 900 kg/m^3 (62.4 lb$_m$/ft^3) and the viscosity of the oil is $4 \cdot 10^{-6}$ m^2/s ($1.20 \cdot 10^{-5}$ ft^2/s).
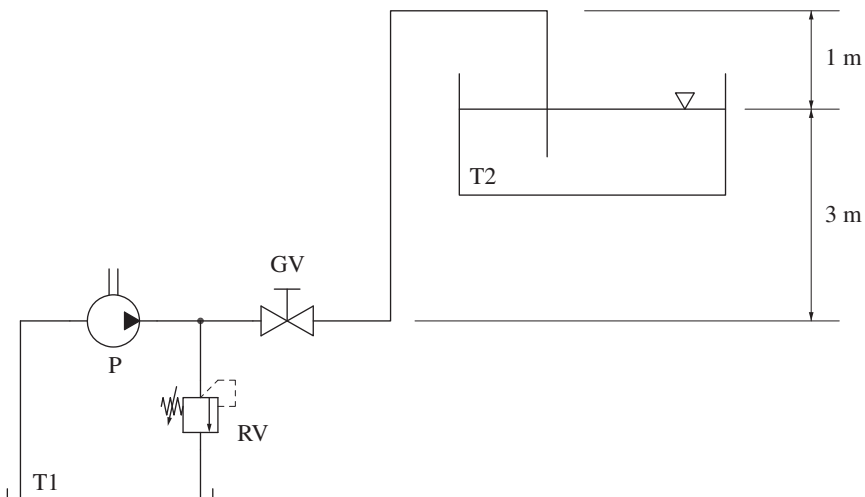
The minor loss coefficient due to the bends in the hose are much smaller than the minor loss coefficient due to the GV, positioned at the pump outlet. GV has a loss coefficient of 2. Determine the volumetric flow rate of the oil into the elevated tank.

3.5 Oil flows through two pipes with the same diameter, length, and friction factor. The flow rate through the second pipe is twice that through the first pipe. Both flows are turbulent and fully developed. Which statement is correct about the pressure drop over the pipe length, Δp, for the two pipes?
  a) $\Delta p_2 = 0.25 \Delta p_1$
  b) $\Delta p_2 = 0.5 \Delta p_1$
  c) $\Delta p_2 = \Delta p_1$
  d) $\Delta p_2 = 2 \Delta p_1$
  e) $\Delta p_2 = 4 \Delta p_1$

3.6 Oil of density 850 kg/m³ is flowing through the 180° elbow shown below. At the inlet of the elbow, the gage pressure is 1 bar. The oil discharges to the atmosphere. Assume properties are uniform over the inlet and outlet areas. Additionally, $A_1 = 25 \text{ cm}^2$ and $A_2 = 2.5 \text{ cm}^2$. The inlet velocity is 3.5 m/s. Find the horizontal component of the force to hold the elbow in place.
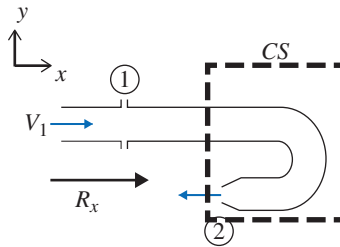
3.7 Water flows from a tank that sits on frictionless wheels. The pipe has a diameter of 0.5 m. The tank is open to atmospheric (location (1)) and it is connected with a 50-m-long pipe to a second pipe that is 75 m long, bolted at location (3). A filter with a loss coefficient $K = 8$ is placed along the second pipe and the flow exits to the atmosphere at location (2). All other minor losses are negligible.
  a) Use the generalized Bernoulli's equation to derive an expression for the velocity in the pipe as a function of the friction coefficient.
  b) Determine the pressure at the location (3), assuming a friction coefficient of 0.015.
  c) Use the CV approach and the momentum equation to determine the tension of the bolts of the flange at location (3).
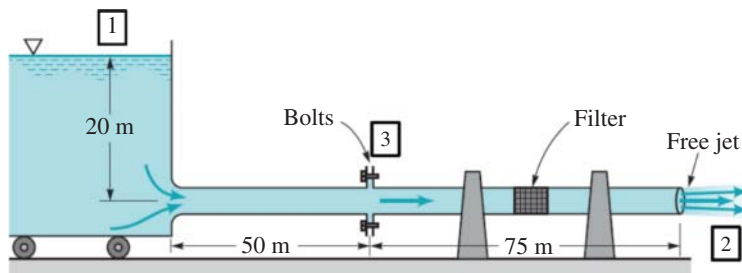
3.8 A pump is used for a fountain jet as in the schematic shown in the figure below. The pump is connected to an electric motor that rotates at 1000 rpm. Following data for the system are given: $D = 0.100$ m; $L = 1$ m (L is the length of each branch, as shown in the figure); and relative roughness, $\varepsilon/D = 0.02$, for all pipe sections. The inlet of the pump is at the same elevation as the free surface of reservoir, as shown in the figure.

Factors for minor losses are $K_{in} = 0.5$; $K_{bend} = 1$, $K_{conv} =$ negligible

For the water, assume $\rho = 1000$ kg/m^3; $\mu = 1 \times 10^{-3}$ N s/m^2
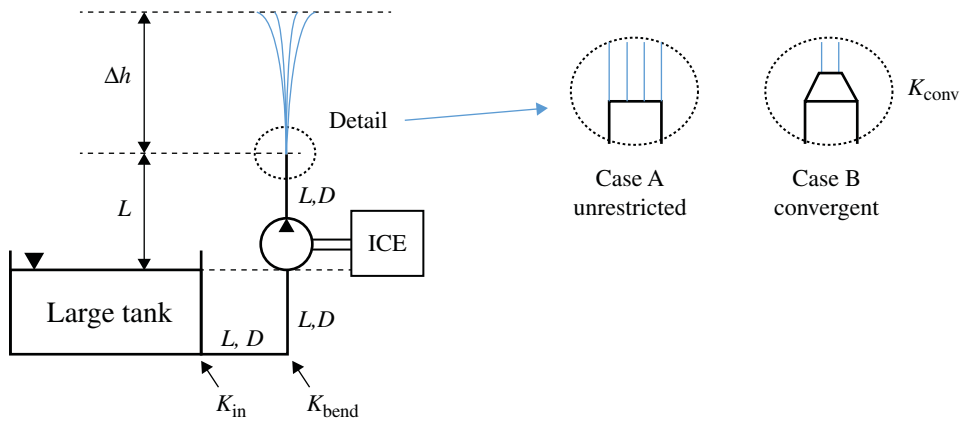
Knowing that the pump characteristic curve is given by following equation:

$$h_p = 10 - 625 \cdot Q^2$$

$[H_p] = m$, $[Q] = $ m^3/s, the units of the coefficients 10 and 625 are not written for convenience.

a) Find the flow rate through the pump, in m^3/s for Case A.

b) Indicate the operating point of the system, in a (Q, H) plot (qualitative representation), for Case A.

c) Find the elevation of the jet, Δh, in m, for Case A.

d) Does the value of Δh increase/decrease, for the Case B? Calculate the Δh you get for Case B.

e) Calculate the power requested by the electric motor.

Assume the total efficiency of the pump $\eta = 0.8$.

Chapter 4

Orifice Basics

Flow restrictions such as orifices, flow nozzles, and venturis are known for introducing pressure losses associated with flow rate. In hydraulic control systems, the relationship between pressure drop and flow rate established by these restrictions (generally referred to as **orifices**) is the basis of the operating principle accomplished by most of the control elements in hydraulic systems, such as hydraulic control valves. Therefore, an entire chapter is dedicated to the orifice equation and its uses in hydraulic systems.

4.1 Orifice Equation

> The orifice equation provides the relationship between the flow rate through a generic restriction and the pressure drop across it.

In this section, the orifice equation is derived for the particular case of a sharp orifice (Figure 4.1). As shown in the figure, the internal flow is characterized by different phases. At first, the fluid stream accelerates approaching the restriction. Afterward, the flow separates from the sharp edge of the orifice, which causes recirculation zones downstream of the restriction. In this phase, the mainstream flow still continues to accelerate from the nozzle throat to form a *vena contracta* at section 2, where the flow area is minimum. The flow then decelerates to fill the duct section. At vena contracta, the flow streamlines are essentially straight, and the pressure is uniform across the section.

This flow condition can be well studied using the continuity and Bernoulli's equations. Then, empirical correction factors may be applied to estimate the correct flow rate, or to consider different geometrical conditions.

Under the assumption of incompressible flow, the mass conservation written between sections 1 and 2 of Figure 4.1 gives

$$\overline{v_1}\Omega_1 = \overline{v_2}\Omega_2 \tag{4.1}$$

Bernoulli's equation applies to both sections 1 and 2 under the additional assumptions of stationary conditions, frictionless flow, and uniform velocities at each section[1]. Moreover, these sections are properly considered where no streamline curvature is present so that the pressure is uniform across the sections:

$$\frac{p_1}{\rho} + \frac{\overline{v_1}^2}{2} + gz_1 = \frac{p_2}{\rho} + \frac{\overline{v_2}^2}{2} + gz_2 \tag{4.2}$$

---

1 It should be noticed that the velocity profile approaches uniform flow only at high Reynolds numbers (turbulent conditions).
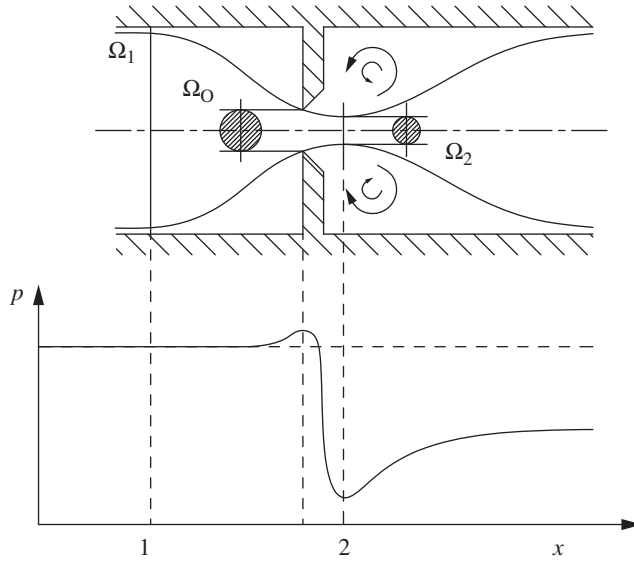
Figure 4.1 Flow through a sharp orifice.

The elevation term in Eq. (4.2) can be simplified by assuming $z_1 = z_2$.

From Eqs. (4.1) and (4.2), it is possible to obtain the following expression for the volume flow rate $Q = Q_1 = Q_2$:

$$Q = \frac{\Omega_2}{\sqrt{1 - (\Omega_2/\Omega_1)^2}} \sqrt{\frac{2(p_1 - p_2)}{\rho}} \tag{4.3}$$

The actual flow area Ω_2 in the vena contracta is unknown. Therefore, an empirical coefficient called the coefficient of discharge C_d is introduced in order to write the equation referring to the known value Ω_O:

$$Q = \frac{C_d \Omega_O}{\sqrt{1 - \left(\Omega_O/\Omega_1\right)^2}} \sqrt{\frac{2\Delta p}{\rho}} \tag{4.4}$$

The coefficient of discharge not only is a pure geometrical ratio but also accounts for other secondary but non-negligible aspects that affect the actual flow conditions through the orifice. These are the frictional effects due to fluid viscosity and the approximated flow uniformity. For these reasons, the empirical formulas available for C_d show a primary dependency of the coefficient of discharge with the Reynolds number. Empirical formulas for C_d are available in the literature, such as in the Miller handbook [38] or the ASME standards [39].

The term $1/\sqrt{1 - (\Omega_O/\Omega_1)^2}$ is also referred to as the *velocity of approach factor*. Usually, the velocity of approach factor and the coefficient of discharge are combined in a single coefficient, often indicated as the *flow coefficient* or the *orifice coefficient*. Equation (4.4) then becomes[2]

$$Q = C_f \Omega_O \sqrt{\frac{2\Delta p}{\rho}} \tag{4.5}$$

---

2 With commonly used metric or standard units:

$$Q\,[l/min] = 18.97 \cdot C_f \cdot \Omega_O\,[mm^2] \sqrt{\frac{2\Delta p\,[bar]}{\rho\,[kg/m^3]}}$$

$$Q\,[gpm] = 211.9 \cdot C_f \cdot \Omega_O\,[in^2] \sqrt{\frac{2\Delta p\,[psi]}{\rho\,[lb/ft^3]}}$$
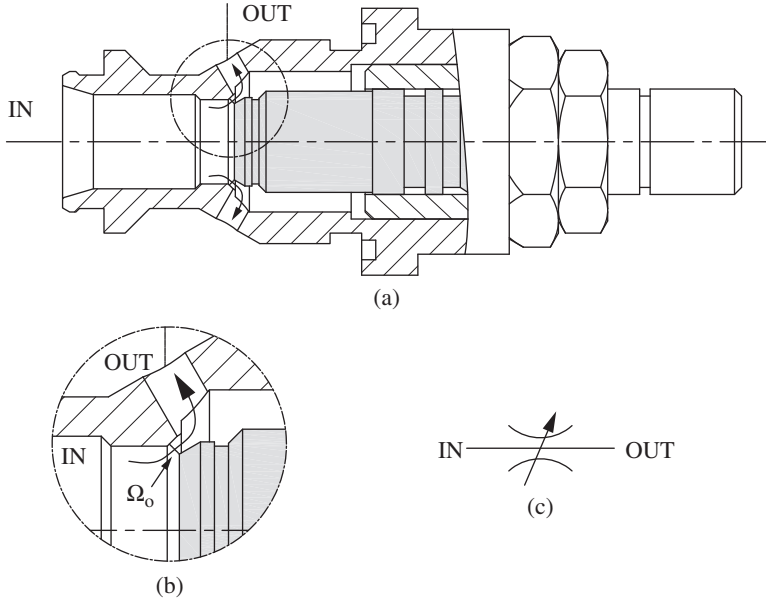
Figure 4.2 Orifice area for a poppet needle valve. (a) Entire popper valve. (b) Eetail on the throat flow area. (c) ISO symbol.

The same abovementioned references collected empirical formulas for the orifice coefficient for various geometries and sizes. In many cases, it can be simply assumed that $\Omega_1 \gg \Omega_O$: hence, the effects of velocity of approach are negligible and the value of C_f can be approximated with the coefficient of discharge C_d.

The orifice equation has a very broad application in hydraulics because it can be used to describe the flow through any element of the system introducing one or more flow restrictions. Figure 4.2 shows the example of a needle valve based on a poppet design. The orifice area Ω_O is represented by the minimum flow area and, in this case, it has an annular shape.

For any specific geometric case, the orifice coefficient should be determined experimentally. Several authors report the theoretical evaluation of such a coefficient for different geometries, under the assumptions of frictionless, incompressible and irrotational flow. For example, Von Mises [40] provided the analytical results for the flow coefficient for several different orifice geometries. A comparison between Von Mises' results and experimental data is also extensively discussed in [36].

As shown in [2, 32, 36], typical values for C_f are in the range of 0.6–0.8. In particular, 0.611 is the von Mises' theoretical value for a circular sharp edge orifice (Figure 4.1).

The value of the C_f coefficient can be considered constant only for high Reynolds numbers (turbulent flow conditions). In case of laminar flow, the flow through an orifice can be solved analytically from Navier-Stokes equations. In the case of a circular sharp edge orifice, the relationship becomes [41]

$$Q = \frac{\pi d^3}{50.4\mu} \Delta p \tag{4.6}$$

Figure 4.3 shows the trend for the C_f coefficient as a function of the Reynolds number, *Re*. In the figure, both theoretical solutions (Von Mises and Eq. (4.6)) are reported along with experimental results, as described in [36]. The measured trend for C_f shows a smooth transition from the laminar behavior, typical of low fluid velocities, and the turbulent conditions. Qualitatively, the same trend represented in Figure 4.3 applies to the orifice geometries and shape characteristics of common hydraulic control elements.
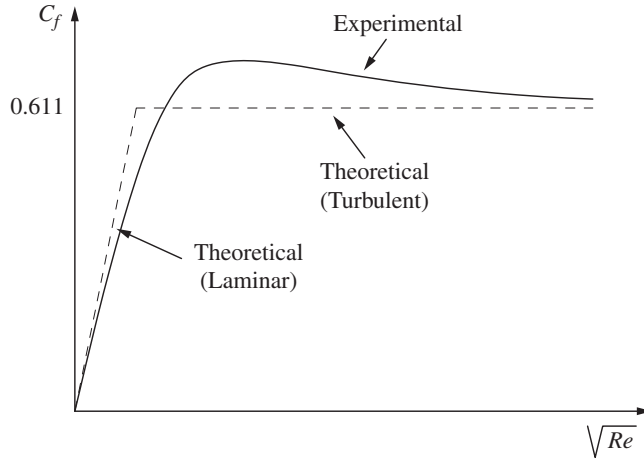
Figure 4.3 Theoretical and experimental trends of the flow coefficient vs. the Reynolds number.

The general orifice equation (Eq. 4.5) shows how an orifice can be seen as a hydraulic resistance, according to the definition provided in Chapter 3 (Eq. (3.38)):

$$\Delta p = R_{turb} \cdot Q^2$$

Therefore,

$$R_{\text{turb}} = \frac{\rho}{2C_f{}^2\Omega_O{}^2} \tag{4.7}$$

4.2   Fixed and Variable Orifices

> A *fixed orifice* is a hydraulic element characterized by a specific throat area Ω_O; in a *variable orifice*, the area Ω_O can vary according to the instantaneous geometric configuration.

Figure 4.2 gives an example of a needle valve, which is an adjustable orifice. The characteristics of both fixed and variable orifices are represented in Figure 4.4. The relationship between pressure drop and flow rate for turbulent flow conditions is parabolic, and the curves show the trend for different orifice areas. The component working conditions pertain only to the first (positive flow) and the third quadrant (negative flow). The figure also highlights the symbols used to indicate both the fixed and the variable orifice cases.

It is important to remark the square root dependence between Δp and Q highlighted in Figure 4.4. Because of this dependence, in order to double the flow across the orifice, it is necessary to increase the pressure by four times.

In hydraulic control valves, variable orifices are often used to represent the positions and the connections implemented by the valve. Figure 4.5 shows the example of two proportional valves, one is a two-position two-way (a) and the other one is a three-position four-way (a). In both cases, each square represents the possible configurations of the port connections obtained by the valve, and the continuous lines above and below the symbols indicate that the orifice area of every connection can be continuously varied.

The valve symbol includes different details when compared to the representation with basic orifices. For instance, in Figure 4.5, the information about the closed configuration (all ports completely closed $\Omega_O = 0$) is not provided by the basic orifice symbols.
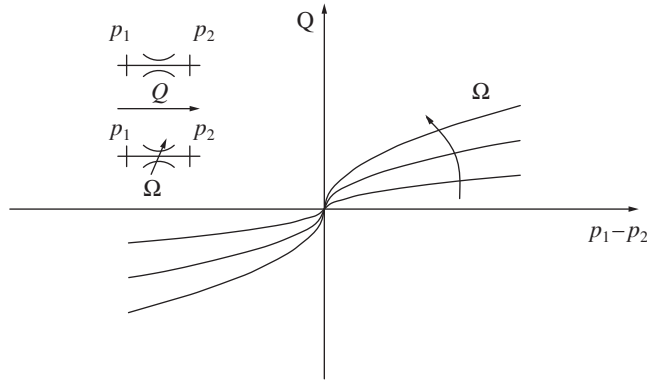
Figure 4.4 Orifice equation plotted in a (p, Q) layer for different area openings.

4.3 Power Loss in Orifices

As explained in Chapter 3, the product $Q \cdot \Delta p$ represents hydraulic power. For the case of an orifice, this product represents the power dissipation introduced by the orifice itself:

$$P_{OR} = Q_{OR} \cdot \Delta p_{OR} \tag{4.8}$$

This power dissipation mostly goes into heat generation within the fluid. In most cases, the portion of heat exchange with the external environment (through the solid walls of the components in the system, including the orifice) is minimal and negligible. The temperature increase of the fluid can be calculated from the energy balance:

$$Q_{OR} \cdot \Delta p_{OR} = \rho \, Q_{OR} \, c_p \Delta T + \frac{1 - \alpha T}{\rho} \Delta p_{OR}$$

$$\Delta T = \frac{(1 - \alpha T) \, \Delta p_{OR}}{\rho \, c_p} \approx \frac{\Delta p_{OR}}{\rho \, c_p} \tag{4.9}$$
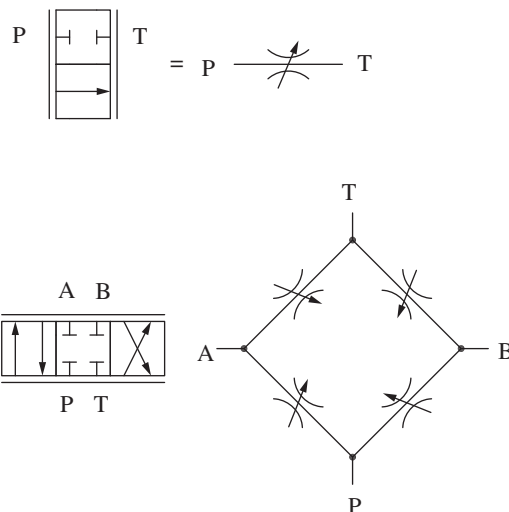
Figure 4.5 Hydraulic symbol of two valves and equivalent orifice networks.

The Eq. (4.9) points out how the effects due to the thermal expansion of the fluid can be neglected. This is a reasonable assumption for oils, which have a thermal expansion coefficient, α, typicall of $7 \cdot 10^{-4}$ [1/K].

Assuming common properties for mineral based oil, the value of ΔT is approximately 5 to 6 degrees Celsius per 100 bar of pressure drop.

Example 4.1   Orifice Flow, Power Dissipation and Temperature Rise

An orifice is used in a pilot line of a system, connected to tank. The pressure in the line, upstream the orifice, is 190 *bar*, while the tank pressure is atmospheric. If the diameter of the orifice is $D = 0.5$ *mm*, evaluate the flow rate lost through it at maximum pressure and the power dissipated through it. Assume oil density $\rho = 850$ *kg/m³* and $C_f = 0.62$. If the constant specific heat of the oil is 1.8 *kJ/kg K*, estimate the temperature rise for the fluid across the orifice.

Given:
The pressure drop across the orifice $\Delta p_{OR} = 190$ *bar*; the orifice diameter $D = 0.5$ *mm*; the orifice coefficient $C_f = 0.62$; the fluid density $\rho = 850$ *kg/m³* and the specific heat coefficient $c_p = 1.8$ *kJ/kg K*

Find:

a) the flow rate through the orifice Q_{OR}
b) the power dissipated by the orifice P_{OR}
c) temperature rise of the fluid through the orifice

Solution:
The ISO schematic of the system can be represented by the figure below. Note that the pilot line is represented as dashed line, according to the standard of representation.
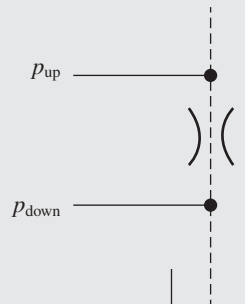
a) Q_{OR} can be simply calculated by using the orifice equation (4.5), being the Δp across the orifice given by the problem data

$$Q_{OR} = C_f \cdot \frac{\pi \cdot D^2}{4} \cdot \sqrt{\frac{2 \cdot \Delta p_{OR}}{\rho}} = 0.62 \cdot \frac{\pi \cdot (0.5 \, [mm])^2}{4} \sqrt{\frac{2 \cdot 190 \, bar}{850 \left[\frac{kg}{m^3}\right]}} = 2.5 \, 10^{-5} \left[\frac{m^3}{s}\right]$$

$$= 1.5 \, l/min$$

b) The power dissipated is calculated from Eq. (4.8):

$$P_{OR} = Q_{OR} \cdot \Delta p_{OR} = 1.5 \left[\frac{L}{min}\right] \cdot 190 \ [bar] = 489 \ W$$

c) The temperature rise experienced by the fluid through the orifice can be estimated from Eq. (4.9), under the assumption that the entire heat dissipation increases the internal energy of the fluid

$$\Delta T = \frac{\Delta p_{OR}}{\rho \, c_p} = \frac{190 \ [bar]}{850 \left[\frac{kg}{m^3}\right] 1.8 \left[\frac{kJ}{kg \ K}\right]} = 12.4°C$$

4.4 Parallel and Series Connections of Orifices

In some hydraulic circuits, orifices appear in series or in parallel configuration (Figure 4.6). In these cases, it can be useful to evaluate the overall behavior of the system of orifices.

One way to address this problem is to consider the definition of hydraulic resistance for an orifice. Then, consider that

$$R_{\text{parallel}} = \sum_i \left(\frac{1}{R_i}\right)^{-1} \tag{4.10}$$

and

$$R_{\text{series}} = \sum_i R_i \tag{4.11}$$

where the hydraulic resistance of the orifice has the expression of Eq. (4.7).

From Eqs. (4.10) and (4.11), the area of the equivalent orifice can be calculated. Another way for determining the area of the equivalent orifice is to directly derive the relationship between Q and Δp of the set of orifices, as shown in the figure.
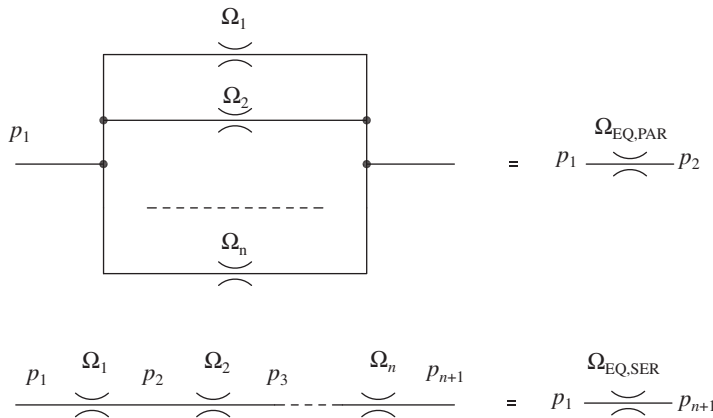
Figure 4.6   Orifice in parallel and in series.

For orifices connected in parallel, the overall flow is the sum of the individual flows, while the upstream and downstream pressures are equal for all:

$$Q = \sum_i \Omega_i \, C_{f,i} \sqrt{\frac{2\,(p_1 - p_2)}{\rho}} \tag{4.12}$$

Therefore, if the same flow coefficient is assumed for all orifices, the area of the equivalent orifice is represented by the sum of the individual areas, and the equivalent diameter is square root of the sum of the square of the individual diameters:

$$\Omega_{\text{eq,par}} = \sum_i \Omega_i \;;\;\; d_{\text{eq,par}} = \sqrt{\sum_i d_i^2} \tag{4.13}$$

For orifices in series, the flow across the orifices is constant, while the Δp at each orifice is different:

$$Q = \Omega_i \, c_f \sqrt{\frac{2\,(p_i - p_{i+1})}{\rho}}; \quad i = 1, 2, \dots n \tag{4.14}$$

By definition, the equivalent orifice satisfies the equation:

$$Q = \Omega_{\text{eq,ser}} \, c_f \sqrt{\frac{2\,(p_1 - p_{n+1})}{\rho}} \tag{4.15}$$

By equating the last two equations, it is possible to provide the expression for $\Omega_{\text{eq, ser}}$. This can be shown for the case of two orifices below, assuming again the same flow coefficient for all orifices:

$$\frac{\rho}{2}\left(\frac{Q}{\Omega_{\text{eq,ser}}\, C_f}\right)^2 = (p_1 - p_3) = (p_1 - p_2) + (p_2 - p_3) = \frac{\rho}{2}\left(\frac{Q}{C_f}\right)^2 \cdot \left(\frac{1}{\Omega_1^2} + \frac{1}{\Omega_2^2}\right) \tag{4.16}$$

Therefore, the equivalent orifice area is

$$\Omega_{\text{eq,ser}} = \sqrt{\frac{1}{\left(\dfrac{1}{\Omega_1^2} + \dfrac{1}{\Omega_2^2}\right)}} \tag{4.17}$$

This equation can easily be generalized for more orifices:

$$\Omega_{\text{eq,ser}} = \sqrt{\frac{1}{\sum_i \dfrac{1}{\Omega_i^2}}}; \quad d_{\text{eq,ser}} = \left(\frac{1}{\sum_i \dfrac{1}{d_i^4}}\right)^{1/4} \tag{4.18}$$

Example 4.2   Orifice Sizing

An emergency supply system uses an accumulator pressurized at 100 *bar* to extend a cylinder. This has a piston diameter $D = 15$ *cm* and sees a force of 50 *kN*. The connection between the cylinder and the accumulator is managed through a normally closed solenoid valve. The valve, when energized, implements a restriction equivalent to an orifice (this feature is represented in the valve symbol) with diameter of 4.4 *mm* and flow coefficient of 0.7. Assuming the accumulator is large enough to maintain a constant supply pressure, calculate the cylinder extension speed. Elaborate a simple system modification (without changing any of the existing components) for reducing the extension velocity to 60% of the previous value. Assume the pressure of the accumulator constant during the cylinder extension.
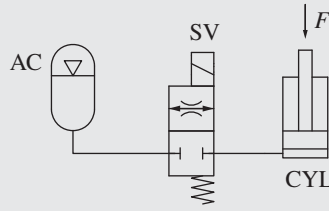
Given:

The ISO schematic of the hydraulic emergency system, which includes an accumulator as energy source, an on/off valve, and a linear actuator. The upstream pressure of the accumulator, constant, $p_{acc} = 100\ bar$; the orifice diameter $d_0 = 4.4\ mm$ and the flow coefficient $C_f = 0.7$. The load on the actuator is $F = 50\ kN$ and the piston diameter, $D = 15\ cm$.

Find:

The extension velocity of the piston, $\dot{x}$

Solution:

The system contains a solenoid valve (SV; which will be further described in Chapter 8), which when energized opens an accumulator to the piston chamber of a linear accumulator. For simplicity, the accumulator can be seen as a constant pressure source. In reality, the pressure inside the accumulator will decrease as the accumulator releases flow, as it will be better described in Chapter 9.

When the valve is energized, the flow rate across it is defined by the orifice equation:

$$Q = \frac{\pi \cdot d_O^2}{4} \cdot C_f \cdot \sqrt{\frac{2(p_{acc} - p_{cyl})}{\rho}}$$

The pressure inside the cylinder is given by the external force:

$$p_{cyl} = \frac{F}{A_{cyl}} = \frac{F}{\pi \dfrac{D^2}{4}} = \frac{50\,000\ [N]}{\pi \dfrac{(0.15\ [m])^2}{4}} = 28.3\ bar$$

Therefore, the actuator speed is

$$\dot{x} = \frac{Q}{A} = \frac{\dfrac{\pi \cdot d_O^2}{4} \cdot C_f \cdot \sqrt{\dfrac{2(p_{acc} - p_{cyl})}{\rho}}}{\pi \dfrac{D^2}{4}} = \left(\frac{4.4\ [mm]}{150\ [mm]}\right)^2 \cdot 0.7 \sqrt{\frac{(100 - 28.3) \cdot 10^5\ [N/m^2]}{850\ [kg/m^3]}}$$

$$= 0.08\ m/s = 8\ cm/s$$

In order to reduce the actuator's speed, there are possible alternatives:

1. Increase the piston diameter.
2. Decrease the valve size, thus reducing the valve coefficient k.
3. Reduce the accumulator pressure.
4. Add an orifice in series with the valve (see figure below).

All mentioned solutions are reasonable; however, solutions 1, 2, and 3 require modifications to the existing components. Solution 4 can be a simple way to modify an existing system.

Example 4.2 (Continued)
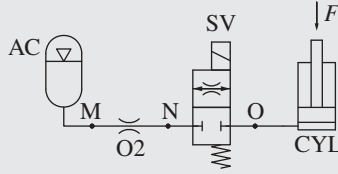
The flow rate through the orifice and the valve can be written as

$$Q = \frac{\pi \cdot d_{\text{eq}}^2}{4} \cdot C_f \cdot \sqrt{\frac{2(p_{\text{acc}} - p_{\text{cyl}})}{\rho}}$$

d_{eq} is the diameter of the equivalent orifice given by the series connection of SV and O2. The desired speed of the actuator corresponds to the following flow:

$$Q_2 = \dot{x}_2 \cdot \frac{\pi \cdot D^2}{4} = 0.6 \cdot 0.08 \,[m/s] \cdot \frac{\pi \cdot (0.15)^2 \,[m^2]}{4} \cdot 60\,000 = 50.9 \,l/min$$

The equivalent series orifice diameter results:

$$d_{\text{eq}} = \sqrt{\frac{4 \cdot Q_2}{\pi \cdot C_f \cdot \sqrt{\frac{2(p_{\text{acc}} - p_{\text{cyl}})}{\rho}}}} = \sqrt{\frac{4 \cdot 50.9/60\,000 \,[m^3/s]}{\pi \cdot 0.7 \cdot \sqrt{\frac{2 \cdot (100 - 28.7) \cdot 10^5 \,[N/m^2]}{850 \,[kg/m^3]}}}} = 3.44 \,mm$$

Assuming that both orifices have the same flow coefficient ($C_f = 0.7$), the diameter of orifice O2 results:

$$d_{O2} = \left(\frac{1}{\dfrac{1}{d_{\text{eq}}^4} - \dfrac{1}{d_O^4}} \right)^{1/4} = \left(\frac{1}{\dfrac{1}{(3.4\,[mm])^4} - \dfrac{1}{(4.4\,[mm])^4}} \right)^{1/4} = 3.86 \,mm$$

4.5 Functions of Orifices in Hydraulic Systems

Even though the orifice element is described by a single equation (Eq. (4.5)), an orifice can assume different roles in a hydraulic circuit. A first way to classify an orifice function is based on its location in the system: in fact, orifices can be present either in the *working and return lines* or on the *pilot lines* of the systems. The working and return lines are represented by the connections to/from the actuators of the system; the power transfer functions achieved by the system occur in these lines. Thus, these lines are usually characterized by significant values of flow rate and pressure. Pilot lines are instead used to transmit pressure information to different locations of the system. These latter lines usually have negligible flow rates and are used for control purposes. According to ISO1219-1 [1], pilot lines are always indicated with dashed lines, while working and return lines with a solid line.

4.5.1 Orifices in Pressure and Return Lines

When an orifice is used in the working or the return line of a system, it can operate as *metering* or *compensating* element.

In principle, if an orifice establishes the flow rate, for a given pressure drop, it functions as a metering element; however, if the orifice defines a certain pressure drop for a given flow rate, it

functions as a compensator. In both cases, the relation between pressure drop and flow rate across the orifice is given by Eq. (4.5).

This classification is important to understand several control strategies used in hydraulic systems, as it will be shown in Part II and Part III of the book. A significant example is now provided to clarify the distinction between these different behaviors of an orifice.

Example 4.3   Orifice as a Metering Element or a Compensator

The system in figure consists of a fixed displacement pump and a variable orifice in parallel with a pressure relief valve. The pressure relief valve limits the maximum pressure at the pump outlet to p^*. The pump delivers a fixed flow rate Q_P independently of the pump outlet pressure. Find the flow rate through the orifice, Q_O, as well as the pump outlet pressure p_P, as a function of the orifice area opening, Ω. Describe also the function of the orifice, which can either be metering or compensator.
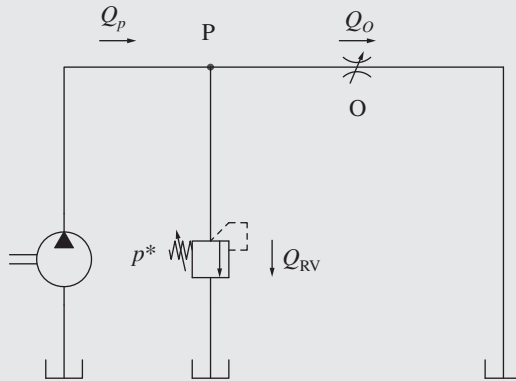
Given:
The pump flow rate, Q_P; the setting of the relief valve p^*.

Find:

a) The flow rate through the orifice, Q_O
b) The pressure at pump outlet, p_P
c) The orifice function (metering/compensator)

Solution:
Point P is located at the junction of the three main elements of the system (the pump, the relief valve, the variable orifice). Therefore, the operating pressure at point P can be found by intersecting the characteristics curves of these components, while also satisfying the constraints of maximum allowed pressure and available flow.

To clarify this statement, the characteristic curves of the three components in the $(\Delta p, Q)$ chart are shown in the figure below. In particular,

- the orifice characteristic curves are plotted according to the orifice equation 4.5 for decreasing values of the area Ω ($\Omega_1 > \Omega_2 > \Omega_3 \ldots$). This trend is as also shown in the plot of Figure 4.4. It is important to observe that, in this case, the pressure drop across the orifice equals p_P, since the pressure downstream the orifice is $p_T = 0$ bar.
- the pump curve represented by a horizontal line (constant flow rate). In fact, for this problem the pump provides a constant flow independent on the system pressure.

(Continued)

Example 4.3 (Continued)

- the relief valve curve, represented by a vertical line. The relief valve, which will be explained more in detail in Chapter 8, limits the maximum pressure at the junction point P to p^*.
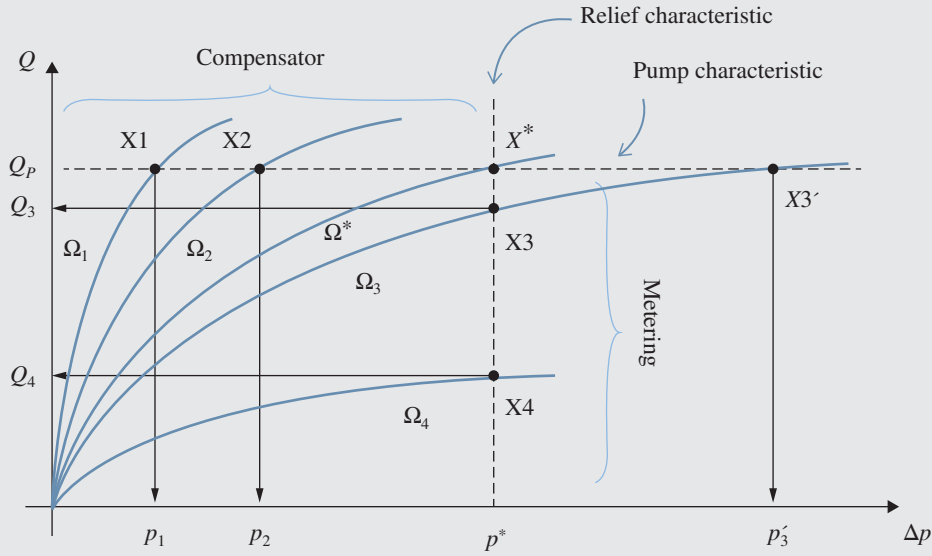
The behavior of the system can be analyzed for different openings of the variable orifice O.

In case of a large orifice area ($\Omega = \Omega_1$), the intersection between the pump characteristic and the orifice curve is at X1. This point is located at a pressure lower than p^*: the entire pump flow rates Q_P goes to the orifice ($Q_P = Q_O$); and the relief valve is closed ($Q_{RV} = 0$). In this case, the orifice Eq. (4.5) can be used to find the pressure at the point P:

$$p_P = p_1 = \frac{\rho}{2} \cdot \left(\frac{Q_P}{C_f \Omega_1} \right)^2$$

In this condition, the orifice O behaves as a *compensator*, since it establishes a pressure drop for a given flow rate.

The situation is similar for the smaller opening area $\Omega_2 < \Omega_1$: the operating point shifts from X1 to X2 at a higher pressure. The relief valve remains closed and the orifice equation can be used again to find p_2.

The orifice maintains the compensator function until it reaches the opening area Ω^*. This area value is critical, as it corresponds to a pressure at point P equal to p^*. When the opening area is Ω^*, the full pump flow is still passing through the orifice.

For area values smaller than Ω^*, as in the case of Ω_3, the intersection between the orifice curve and the pump curve would result in the operating point X3′, which corresponds to a system pressure p_3', greater than p^*. As a consequence, when $\Omega = \Omega_3$ the operating point is defined by the intersection of the orifice curve with the relief characteristic (point X3). In other words, the relief valve opens, relieving a portion of the pump flow to tank, so that the pressure is limited to $p_P = p^*$. The flow passing through the orifice is Q_3, while the relief valve discharges the flow $Q_{RV,3} = Q_P - Q_3$.

The orifice equation in this case can be used to find the flow rate Q_3, knowing that the pressure drop across the orifice is defined as $\Delta p_3 = p^* - p_T = p^*$

$$Q_3 = C_f \cdot \Omega_3 \sqrt{\frac{2\,p^*}{\rho}}$$

A further reduction of the opening area of the orifice ($\Omega_4 < \Omega_3$) results in a reduction of the orifice flow, as visible by the location of the intersection point X4 in the figure.

In these conditions, the orifice behaves as *metering*, since it establishes a flow rate as a consequence of a given pressure drop.

This example shows how a metering element can be used to regulate flow in a hydraulic system. In this simple case, the orifice flow is directed to tank at null pressure. In general, an actuator can be located downstream of the metering element, which is ultimately used to adjust its speed.

4.5.2 Orifices in Pilot Lines

Pilot lines are used to transmit the value of pressure to different locations of a circuit. In such lines, it is very rare to find orifices working as metering or compensator devices. Instead,

Orifices are used in pilot lines to manipulate the pressure signal, according to two possible function purposes: *pressure separators* or *dynamic orifices*.

A *pressure separator* is an orifice used to decouple the pressure in the working line – where the pilot line is connected – and the pressure transmitted by the pilot line itself, downstream the orifice.

A *dynamic orifice* is utilized with to modify the rate at which the pressure information is transmitted through the pilot line. Dynamic orifices dampen the pilot pressure information, acting as hydraulic low pass filters. Typically, dynamic orifices are accomplished with two different layout configurations. In the first layout, they are located next to closed-end connections of the pilot line. Therefore, they do not affect the operation of the system in steady-state operation, being crossed by zero flow rate in this condition. This kind of dynamic orifice can be neglected while studying the main steady-state system operation. In the second layout, the dynamic orifice is used in an additional pilot line connection to the reservoir (bleed orifice). Also, a bleed orifice does not affect the steady-state operation of the system, but it introduces a constant dissipation by bleeding fluid to tank.

Understanding the function of orifices in working lines and pilot lines is not always simple, particularly for the cases of pressure separators and dynamic orifices. For this reason, this book will often point out the function accomplished by the various orifices present in a certain component or system. In this way, the reader will progressively become more familiar with recognizing the different roles of orifices in hydraulic systems.

Example 4.4   Leakage in a Cylinder

Consider the hydraulic system in the figure below. The system is used to lift and lower a vertical load. The system requirement is that no leakage should occur while the system is in rest

Example 4.4 (Continued)

or standby (directional control valve (DCV) in neutral position). However, the cylinder seal is damaged so that leakages can occur between its piston chamber and its rod chamber. Assuming that the DCV can perfectly block the cylinder work ports, what happens to the piston when the valve is in rest position? Does it fall? Or it remains stand still? Also, provide the value of the reading of the two pressure gages A and B in such condition.

The following data are given: equivalent orifice resistance of the internal cylinder leakage = 50 $(bar \cdot min)/l$; mass = 1000 kg; piston diameter 100 mm; rod diameter 40 mm.
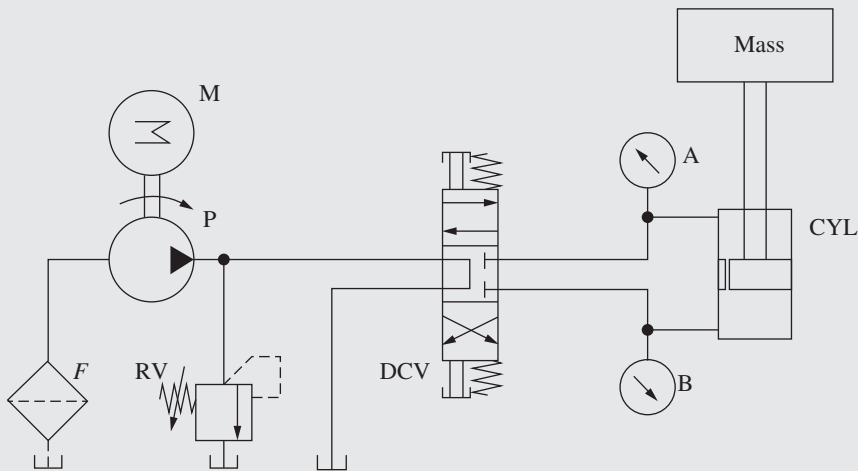
Given:
The hydraulic schematic of a hydraulic lifting system, the piston diameter of the cylinder $D = 100$ mm and the rod diameter $d = 40$ mm. The gravitational load is known $M = 10\,000$ kg. The internal leakage of the cylinder expressed as equivalent orifice resistance $(\Delta p_{O, LAM} = R_{LAM}Q_{LEAK})$ $R_{LAM} = 50$ $[(bar \cdot min)/l]$.

Find:

a) The motion of the cylinder in rest condition (vertical velocity)
b) The reading of the pressure gages A and B

Solution:
The hydraulic schematic of the lifting system considered in this problem introduces the symbolic representation of components that will be described in more detail in the next chapter of this book. However, for the reader, the functioning of the system should be quite intuitive: a hydraulic pump P is driven by a prime mover (an electric motor) M to supply flow to a hydraulic control valve, DCV. The hydraulic control valve is manually activated, and it determines the direction of the supply flow: in one position, it implements the cylinder extension, and in the other, the retraction. Centering springs ensure the valve blocks the cylinder work ports in case of no valve actuation.

A pressure relief valve is installed at the pump outlet, to protect the pump from overpressurization.

Considering the rest position, the supply part of the hydraulic system is isolated through the DCV, so that the problem can be simplified by considering the following schematic:
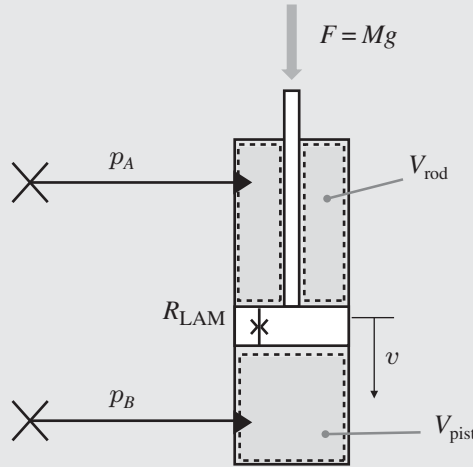
a) If a motion of the piston would occur in rest conditions the steady-state form of the conservation of mass at both V_{pist} and V_{rod} would apply:

$$\dot{x} \cdot A_{pist} = Q_{LEAK} \tag{E4.4.1}$$

$$\dot{x} \cdot A_{rod} = Q_{LEAK} \tag{E4.4.2}$$

The above equations were derived in Chapter 3, when analyzing the basic functioning of a linear actuator. The flow Q_{LEAK} is the flow rate through the laminar orifice that represents the internal leakages inside the cylinder.

$$Q_{LEAK} = \frac{(p_{pist} - p_{rod})}{R_{LAM}} \tag{E4.4.3}$$

From the above (E4.4.1) and (E4.4.2), being $A_{pist} \neq A_{rod}$, it is clear that the only possible solution for the leakage flow is $Q_{LEAK} = 0$ *l/min*. This means that even if there is an opening between the two chambers of a differential cylinder actuator, there are no internal leakage inside the actuator. This means that $v = 0$ *m/s*, meaning that the piston will remain in standstill.

b) The above equation (E4.4.3) implies that

$$p_{pist} = p_{rod}$$

Recognizing that $p_{rod} = p_A$ and $p_{pist} = p_B$, we have

$$p_A = p_B = p$$

The two pressure gages will give the same reading, which can be determined by the force balance of the piston (assuming no friction):

$$p = \frac{F}{(A_{pist} - A_{rod})} = \frac{M \cdot g}{\frac{\pi}{4}D^2 - \frac{\pi}{4}(D^2 - d^2)} = \frac{10\,000 \, \text{kg} \cdot 9.81 \, [m/s^2]}{\frac{\pi}{4}(0.04^2) \, [m^2]} = \frac{98\,100 \, [m/s^2]}{0.001\,257 \, [m^2]}$$

$$= 7.804 \, MPa = 78.04 \, bar$$

(Continued)

Example 4.4 (Continued)

Further considerations:

- This example shows how the presence of internal leakages paths inside a differential cylinder do not prevent realizing a perfect load holding, as long as the hydraulic circuit properly blocks the cylinder work ports. This is why load handling hydraulic machines can safely use even worn cylinders, as long as the connecting hydraulic valves can achieve a perfect sealing.
- The answer $\dot{x} = 0\,m/s$ is true only after the system reaches a stationary condition. A very fast transient will actually happen when the valve is brought to rest, or in case of a variation of the load. During this transient, the pressure inside the piston and rod chamber will equalize. This process involves a small mass exchange between V_{pist} and V_{rod} (therefore a $Q_{\text{LEAK}} \neq 0$ for a short interval) related to the compressibility of the fluid.

Problems

4.1   An orifice is used in a system to discharge pressure to the tank from a hydraulic line. The pressure in the line (upstream the orifice) can reach 190 bar (gage pressure) during the operation of the system, while the tank pressure can be considered constant at 0 bar (gage pressure). If the diameter of the orifice is $D = 0.5$ mm, evaluate the flow rate through the orifice at the maximum pressure condition, as well as the energy dissipated through it. Assume the oil viscosity $\rho = 850$ kg/m³ and the orifice coefficient $C_f = 0.62$.

4.2   An orifice in parallel with a check valve is used to control the velocity of an actuator during its lowering, as shown in the figure below. Determine the diameter of the orifice to accomplish the complete lowering in 10 seconds starting from actuator fully extended. During lowering, the external load is such that the piston chamber is pressurized at constant pressure of 80 bar. The cylinder parameters are piston diameter = 63.5 mm, rod diameter 44.5 mm, and stroke 965 mm. The oil has a density of 880 kg/m³. The orifice coefficient is 0.65.
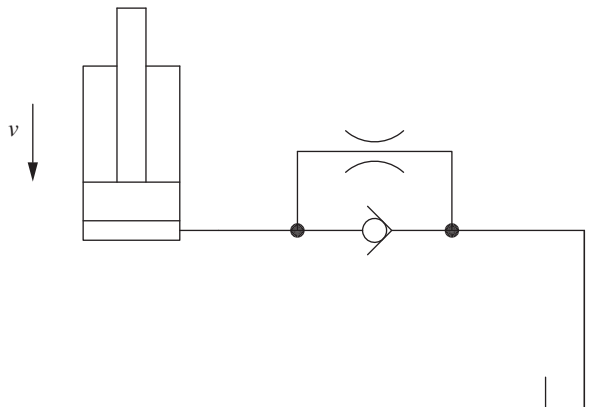
4.3   Consider again the system of the previous problem, but this time the orifice diameter is given $d_{\text{orif}} = 2$ mm. What is the lowering time in this case?

Introduce an additional orifice in series or in parallel to the given orifice to achieve a lowering time of 10 seconds. What is the diameter of this additional orifice?

4.4 Consider the system described in Example 4.4. With the same system data, consider now the case of a double rod cylinder instead of a single rod one. Will the system behave in the same way? What would be the pressure reading of the pressure gages in this case?

4.5 Consider again the problem described in Example 4.4. The system is brought to rest immediately after the raising of the 10 000 kg load by switching the position of the valve DCV. The piston will interrupt abruptly its upward motion and stop. Will the piston remain in standstill exactly at the position it reached when the DCV was switched? Or it will end up remaining stand still at a different position? Motivate your answer. If oil properties are needed, refer to the data below:

Density	850 kg/m^3
Bulk modulus	15 000 bar
Kinematic viscosity	40 cSt

4.6 A valve experiences a pressure drop of 100 psi (687 kPa) for a flow rate of 25 gpm (98.4 l/min). The fluid is hydraulic oil with a specific gravity (sg) of 0.90 ($r_{oil} = sg\ r_{water}$). Determine the capacity coefficient k ($Q = k\sqrt{\Delta_p}$). Determine also the area of the equivalent orifice, assuming $C_d = 0.65$.

4.7 For the six cases (a) to (f) shown below, indicate if the orifice behaves as a metering orifice or a compensator. *Hint*: Always consider the pump as a flow generator. For this problem, the accumulator can be considered as a constant pressure source.
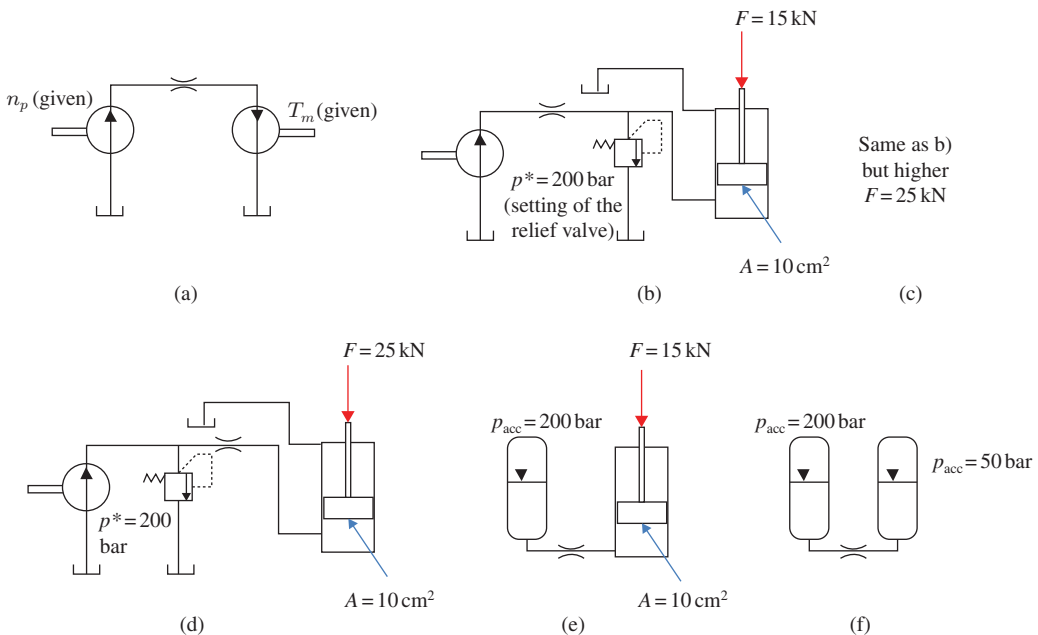
4.8 For the two systems in figure below:
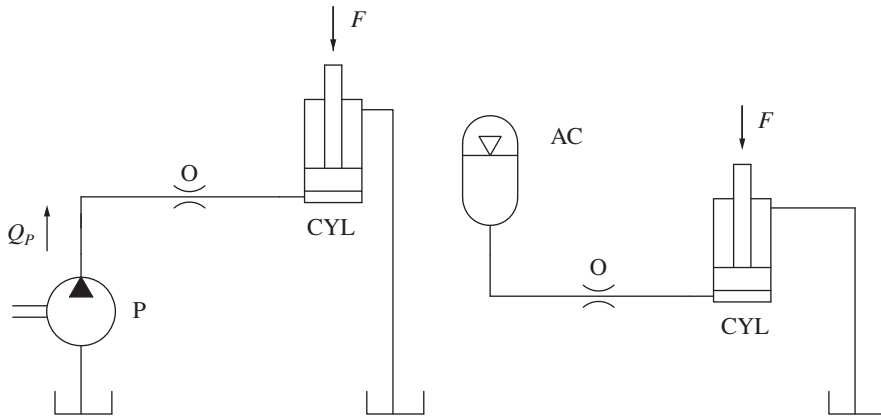
Determine if the orifice O operates as a metering or as a compensator (give separate answers for the two systems).

Considering $F = 1$ kN, $d_{\text{piston}} = 10$ mm; $d_{\text{orifice}} = 1$ mm for both systems; $p_{\text{acc}} = 200$ bar for the accumulator circuit; $n = 500$ rpm and $V_{D\text{pump}} = 5$ cm^3/rev for the pump circuit, determine the extension speed of the cylinder for the two cases. You can assume $C_f = 0.7$, $\rho = 800$ kg/m^3. If an additional 3 mm orifice is put in series to the orifice O, does the cylinder velocity will change for the two cases?

Chapter 5

Dynamic Analysis of Hydraulic Systems

Complementing Chapter 3, which was discussed the concepts of fluid mechanics necessary to understand the operation of hydraulic circuits in stationary conditions, this chapter starts from the same fundamental equations. The authors would derive here the equations and parameters that can be used for simple analyses of the transient operation of hydraulic systems. The technique used for the analyses is called **lumped parameter** modeling approach.

The equations that will be presented are the *pressure build-up equation*, which comes from the conservation of mass, and the *fluid inertia equation*, which is derived from the momentum equation. The pressure build-up equation is useful to describe the changes in pressure inside a specific volume of the system, based on flow rates and fluid compressibility. The fluid inertia equation instead relates the momentum changes of the fluid with pressure variations. From these equations, it will be possible to define the *hydraulic capacitance* and the *hydraulic inductance*, which, along with the hydraulic resistance introduced in Chapter 3, are the basis of the set of equations that can be used to describe the transient behavior of a generic flow network. This chapter will also show how these equations are analogous to the equations used to describe electric network formed by resistor, capacitors, and inductors.

5.1 Pressure Build-up Equation: Hydraulic Capacitance

This equation addresses the characterization of a transient pressure inside a control volume (CV, Figure 5.1). The derivation starts from the basic conservation of mass (Eq. (2.11)):

$$\frac{\partial}{\partial t}\int_{CV}\rho dV + \int_{CS}\rho\vec{v}\cdot d\vec{A} = 0 \tag{5.1}$$

The first term in the conservation of mass equation can be further simplified by assuming uniform fluid density throughout the CV:

$$\frac{\partial}{\partial t}\int_{CV}\rho dV = \frac{\partial}{\partial t}(\rho\cdot V) = \rho\frac{\partial V}{\partial t} + V\frac{\partial\rho}{\partial t} \tag{5.2}$$

The second term of Eq. (5.1) can be simplified assuming uniform flow at the permeable surfaces:

$$\int_{CS}\rho\vec{v}\cdot d\vec{A} = \sum\rho Q_{OUT} - \sum\rho Q_{IN} \tag{5.3}$$

By combining the two equations above,

$$\frac{V}{\rho}\frac{\partial\rho}{\partial t} = \sum Q_{IN} - \sum Q_{OUT} - \frac{\partial V}{\partial t} \tag{5.4}$$
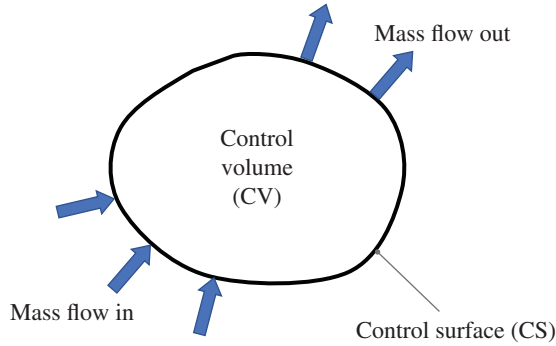
Figure 5.1 Control volume (CV) and bounding control surface (CS).

The change in density can be expressed by considering the generic function $\rho = \rho(p, T)$:

$$\frac{\partial \rho}{\partial t} = \frac{\partial \rho}{\partial p}\bigg|_T \frac{\partial p}{\partial t} + \frac{\partial \rho}{\partial T}\bigg|_p \frac{\partial T}{\partial t} \tag{5.5}$$

Considering the definition of the bulk modulus,

$$B = -V\frac{dp}{dV} \tag{5.6}$$

The (5.5) becomes

$$\frac{\partial \rho}{\partial t} = \frac{\rho}{B_T} \frac{\partial p}{\partial t} + \frac{\partial \rho}{\partial T}\bigg|_p \frac{\partial T}{\partial t} \tag{5.7}$$

where B_T implies using the bulk modulus definition of Eq. (5.6) assuming an isothermal process (isothermal bulk modulus).

By substituting Eq. (5.7) in Eq. (5.4), it is possible to get

$$\frac{\partial p}{\partial t} = \frac{B_T}{V}\left(\sum Q_{\text{IN}} - \sum Q_{\text{OUT}} - \frac{\partial V}{\partial t}\right) - \frac{B_T}{\rho} \frac{\partial \rho}{\partial T}\bigg|_p \frac{\partial T}{\partial t} \tag{5.8}$$

The above expression (*thermal pressure build up equation*) can be further simplified by neglecting the last term at the second member, which relates to the temperature variation within the CV. In fact, the isothermal assumption is applicable to most hydraulic control systems problems, where the effects of fluid temperature variations are negligible with respect to those due to temperature variations.

Therefore, the isothermal assumption yields to

$$\frac{\partial p}{\partial t} = \frac{B_T}{V}\left(\sum Q_{\text{IN}} - \sum Q_{\text{OUT}} - \frac{\partial V}{\partial t}\right) \tag{5.9}$$

Equation (5.9) is often referred to as the *pressure build-up equation*, and it is suitable to describe the pressure evolution inside a CV where it is reasonable to assume uniform fluid density. If the volume of CV is not changing, as it happens to a rigid pipe, the term $\partial V/\partial t$ is null. When the volume varies with time (e.g. a CV used to describe the chambers inside a hydraulic cylinder during its stroke motion), the term $\partial V/\partial t$ cannot be neglected. The pressure build-up equation can be used in various instances to describe the pressure transients in a circuit.

> The pressure build-up equation describes the pressure variations inside a CV resulting from flow rates entering or leaving the volume, as well as due to volume variations.

The bulk modulus to be used in the pressure build-up equation is the isothermal bulk modulus, B_T. In fact, the bulk modulus value depends on the process at which the term dp/dV is measured

in Eq. (5.9). In other words, in the pressure build-up equation used in the following chapters, the bulk modulus will be simply denoted by *B*.

Example 5.1   Simple dynamic model of a cylinder

The analysis of the dynamic behavior of a hydraulic actuator needs to consider the transient equations for both the fluid and the actuator. In this example, the capacitance effect of the fluid of the linear actuator are coupled with the basic law of motion of the piston (Newton's second law).

In particular, this example illustrates the equations necessary to solve the dynamic behavior of the system shown in the figure below:
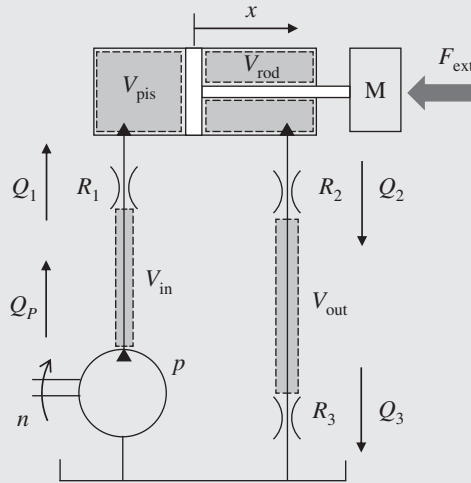
The system has known hydraulic resistances R_1, R_2, and R_3 between the pump P and the cylinder bore port and the cylinder rod port and tank. These hydraulic resistances can represent, for example, the restrictions given by a directional control valve in a certain restrictive position. The connecting lines have known volumes. The pump displacement is also known. The shaft speed of the pump varies with a known relationship $n = n(t)$, so that the piston extends against a fixed load with a variable velocity $\dot{x}$.

Given:

- The cylinder fluid areas A (piston side) and a (rod side), and the initial volumes of the piston chamber ($V_{pis,\,0}$) and rod chamber ($V_{rod,\,0}$).
- The pump displacement $V_{D,\,pump}$.
- The hydraulic resistances R_i, where $\Delta p_i = R_i \cdot Q_i^2$
- The volumes of the connecting lines V_{in} and V_{out}
- The external force F_{ext} and the mass connected to the piston
- The friction coefficient opposing the motion of the piston, c
- The fluid bulk modulus B
- The pump shaft speed as a function of time $n = n(t)$

Find:

The system of equations describing the piston motion, $x = x(t)$, as well as the flow rates and the pressures within the system.

Example 5.1 (Continued)

Solution:

The piston motion can be described with the Newton's second law:

$$-M\ddot{x} = F_{\text{ext}} - p_{\text{pis}}A + p_{\text{rod}}a + c\dot{x}$$

The differential equation can be solved to find $x = x(t)$ as long as proper expressions for the pressures in the piston and rod chamber can be found.

These expressions are given by the pressure build up equations written for the whole system:

Piston chamber

$$\frac{\partial p_{\text{pis}}}{\partial t} = \frac{B}{V_{\text{pis}}}\left(Q_1 - \frac{\partial V_{\text{pis}}}{\partial t}\right)$$

where

$$\frac{\partial V_{\text{pis}}}{\partial t} = A\dot{x}$$

$$V_{\text{pis}} = V_{\text{pis,0}} + A\dot{x}$$

Similarly, for the rod chamber,

$$\frac{\partial p_{\text{rod}}}{\partial t} = \frac{B}{V_{\text{rod,0}} - ax}(-Q_2 + a\dot{x})$$

The two chambers V_{in} and V_{out} are rigid pipes; therefore,

$$\frac{\partial p_{\text{in}}}{\partial t} = \frac{B}{V_{\text{in}}}(Q_P - Q_1)$$
$$\frac{\partial p_{\text{out}}}{\partial t} = \frac{B}{V_{\text{in}}}(Q_2 - Q_3)$$

The system of differential equations can be solved with the knowledge of the flow rates:

Pump. The pump flow rate can be expressed as a function of time:

$$Q_P = V_{D,\text{pump}} \cdot n(t)$$

Hydraulic resistances

$$p_{\text{in}} - p_{\text{pis}} = R_1 \cdot Q_1{}^2$$
$$p_{\text{rod}} - p_{\text{out}} = R_2 \cdot Q_2{}^2$$
$$p_{\text{out}} - p_{\text{tank}} = R_3 \cdot Q_3{}^2$$

The system of equations to solve therefore becomes

$$- M\ddot{x} = F_{\text{ext}} - p_{\text{pis}}A + p_{\text{rod}}a + c\dot{x}$$

$$\frac{\partial p_{\text{pis}}}{\partial t} = \frac{B}{V_{\text{pis,0}} + A\dot{x}}(Q_1 - A\dot{x})$$

$$\frac{\partial p_{\text{rod}}}{\partial t} = \frac{B}{V_{\text{rod,0}} - a\dot{x}}(-Q_2 + a\dot{x})$$

$$\frac{\partial p_{\text{in}}}{\partial t} = \frac{B}{V_{\text{in}}}(Q_P - Q_1)$$

$$\frac{\partial p_{\text{in}}}{\partial t} = \frac{B}{V_{\text{in}}}(Q_P - Q_1)$$

$$\frac{\partial p_{\text{out}}}{\partial t} = \frac{K}{V_{\text{in}}}(Q_2 - Q_3)$$

$$Q_P = V_{D,\text{pump}} \cdot n(t)$$

$$Q_1 = \sqrt{\frac{p_{in} - p_{pis}}{R_1}}$$

$$Q_2 = \sqrt{\frac{p_{rod} - p_{out}}{R_2}}$$

$$Q_3 = \sqrt{\frac{p_{out} - p_{tank}}{R_3}}$$

The systems of equations cannot be solved in an explicit form, and computational tools are necessary to model the dynamic behavior.

The isothermal pressure build-up equation describing the variation of the pressure inside a CV is similar to an equation describing the charge of an electric capacitor. Hence, the **hydraulic capacitance**, C_H, is defined as

$$C_H = \frac{V}{B} \tag{5.10}$$

For a CV that is not changing over time,

$$\frac{\partial p}{\partial t} = \frac{1}{C_H}\left(\sum Q\right) \tag{5.11}$$

This hydraulic equation is very similar to the electric equation for a capacitor:

$$\text{Hydraulic equation} \rightarrow p(t) = \frac{1}{C_H}\int \sum Q(t)$$

$$\text{Electric equation} \rightarrow V(t) = \frac{1}{C}\int i(t) \tag{5.12}$$

Equation (5.12) underlines the analogy of fluid pressure with electric voltage (effort variables) and flow rate with electric current (flow variables).

One can also say that the fluid capacitance is a measure of potential energy stored in a fluid, such as the electrical potential energy stored in an electric capacitor. The capacitance is quantified by the Δp associated with a certain amount of fluid introduced into the system. This Δp is related to the energy given by the compression of the fluid, but it can also include the elasticity effects of the walls. These latter effects can be significant if, for example, flexible hoses are used in the circuit. Instead of accounting for the CV variations due to the hose elasticity, a simpler approach utilizes a properly modified expression for the bulk modulus, B_{eq}. Therefore, the equivalent bulk modulus includes in a single parameter the compressibility of the fluid (in certain conditions also the additional compressibility effect of the undissolved gases) as well as of the containing walls. Expressions for the equivalent bulk modulus were described in Chapter 2.

The hydraulic capacitance is the hydraulic analog of the electric capacitance. It expresses the relationship between pressure changes and net flow rate entering a fluid volume.

5.2 Fluid Inertia Equation: Hydraulic Inductance

The momentum equation introduced in Part I describes the relationship between pressure and momentum changes in the fluid. In this section, the equation is applied to the particular case of a constant diameter section of a pipe, represented in Figure 5.2. The resulting expression is suitable to quantify the fluid inertia effects, and the following considerations can be applicable to other cases.
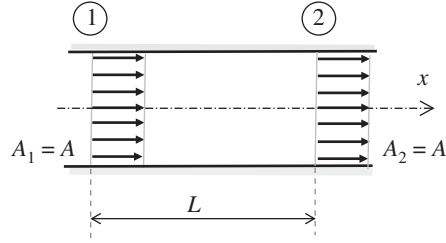
Figure 5.2 Constant section pipe with uniform velocity profile.

Equation (5.13) below is the expression for the momentum equation already presented in Part I:

$$\vec{F} = \overrightarrow{F_S} + \overrightarrow{F_B} = \frac{\partial}{\partial t}\int_{CV}\vec{v}\rho dV + \iint_{CS}\vec{v}\rho\vec{v}\cdot d\vec{A} \tag{5.13}$$

Equation (5.13) is a vector equation; when applied to the CV shown in Figure 5.2, its most significant term is represented by the horizontal component (x axis). In particular, the following assumptions can be made.

- Gravity effects and frictional effects can be neglected. These latter, if significant, can be evaluated through the hydraulic resistance. The component of the external forces F_x on the CV becomes

$$F_x = (p_1 - p_2)A \tag{5.14}$$

- The rate of change of momentum inside the CV can be written as follows:

$$\frac{\partial}{\partial t}\int_{CV}\vec{v}\rho dV = m\frac{\partial v_x}{\partial t} \tag{5.15}$$

where $m = \rho LA$ is the mass of the fluid inside the CV.

- Under the assumption of uniform flow at the permeable surfaces of the CS, the net rate at which the momentum is leaving the CV across its control surface (CS) is

$$\iint_{CS}\vec{v}\rho\vec{v}\cdot \overrightarrow{dA} = \rho\cdot v_2\cdot Q_2 - \rho\cdot v_1\cdot Q_1 \tag{5.16}$$

This last term can be considered null, under the further assumption that spatial variation of the fluid velocity has a faster dynamic than the time variation of the velocity.

Given these assumptions, the momentum equation then becomes

$$(p_1 - p_2) = \frac{\rho L}{A}\cdot\frac{\partial Q}{\partial t} \tag{5.17}$$

The term $\rho L/A$ is usually referred to as **hydraulic inductance**, L_H:

$$L_H = \frac{\rho L}{A} \tag{5.18}$$

The hydraulic inductance is a measure of the fluid inertia effect: it quantifies the pressure forces developed when a fluid accelerates in a pipe or a flow passage. As shown in Eq. (5.17), the inertia effect corresponds to the Δp across the considered section, which cannot be ignored if the changes in flow rates are very rapid.

This term "inductance" originates from the analogy with the electrical equation describing the relationship between electric voltage and current for an inductor:

$$\text{Hydraulic equation} \rightarrow p(t) = L_H\frac{\partial Q(t)}{\partial t}$$
$$\text{Electric equation} \rightarrow V(t) = L\frac{\partial i(t)}{\partial t} \tag{5.19}$$

The hydraulic inductance is the hydraulic analog of the electric inductance and it measures the fluid inertia effects. It expresses the relationship between pressure changes resulting from flow transient variations.

Example 5.2   Pressure spike occurring at a cylinder end-stop

The system in the figure below actuates a hydraulic cylinder in extension and retraction. Considering the extension (directional valve (DV) in position 1), describe the equations characterizing the pressure spike that occurs during the transient conditions corresponding to the piston reaching the full extension end-stop. Given data are the pump flow rate, the volume of the hydraulic lines, the oil properties, the cylinder size, the cylinder loading, the setting, and the design features of the pressure relief valve (direct acting type). Neglect frictional effects in the DV and within the connecting lines.
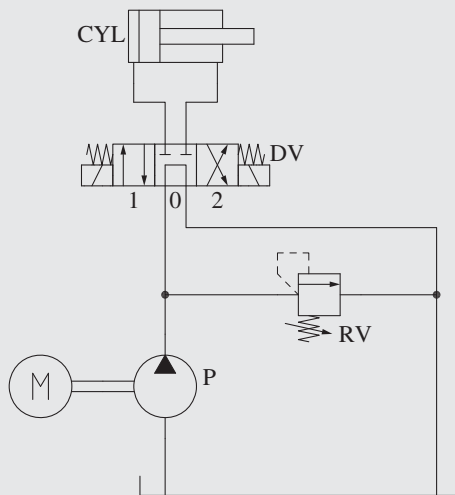
Given:
Following parameters are given: the pump flow rate, Q_p; the cylinder loading, F; the cylinder dimensions (piston area A, annular rod area a, piston stroke s); oil density, ρ, and bulk modulus, B; overall line volume between the pump and the cylinder V_{line}; and pressure relief valve setting, p^*.

The following detains for the pressure relief valve are also known: the poppet mass, m; spring stiffness, k; poppet friction, c; and the opening area function of the poppet, $\Omega = \Omega(x)$.

Find:
The pressure function $p = p(t)$ corresponding to extension end-stop event

Solution:
The equations governing the system dynamics can be easily found by considering the following figure, which simplifies the layout configuration corresponding to the cylinder extension. The

(Continued)

Example 5.2 (Continued)

main assumption made here is that the valve does not introduce any pressure drop for the flow reaching the cylinder.
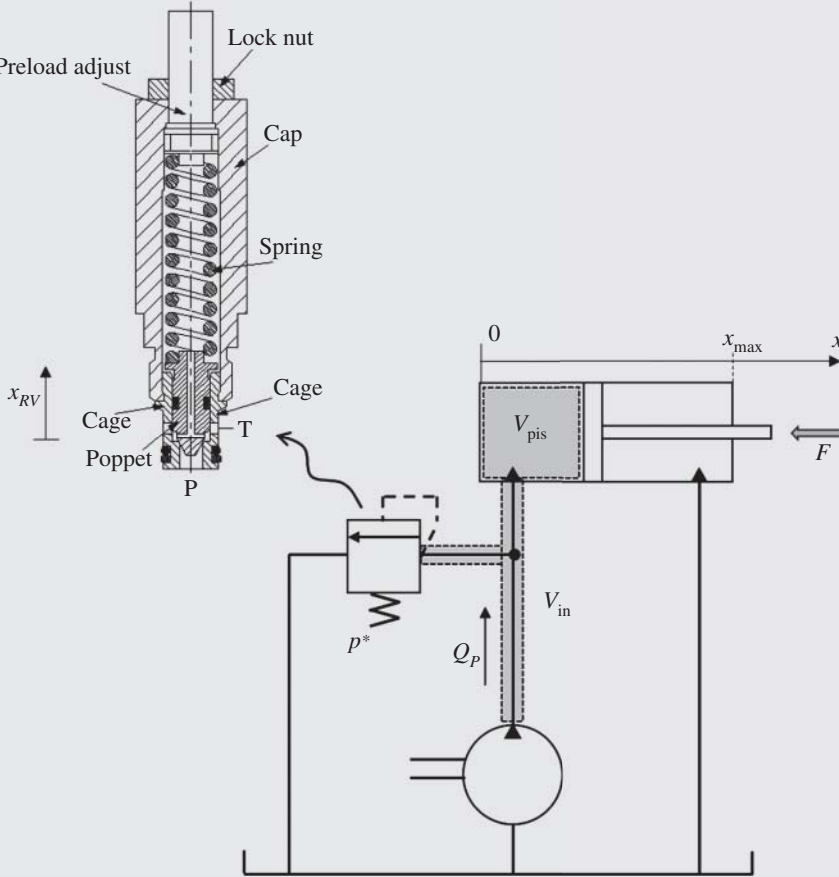
First, it can be useful to describe the operation of the system according to steady-state equations.

During the extension, the pressure at the supply and inside the cylinder is simply given by (assuming a null return pressure):

$$p_{P,0} = \frac{F}{A}$$

while the extension velocity of the piston is

$$\dot{x} = \frac{Q_p}{A}$$

After the piston reaches the end-stop, the whole pump flow is diverted to the pressure relief valve, and consequently the system pressure ideally goes to p^*.

In reality, as observed in Chapter 3, the actual steady-state behavior of the valve implies a higher system pressure due to the effect of the spring compression and of flow forces. By ignoring flow forces, and assuming that the opening area of the relief valve is a linear function of the poppet position,

$$\Omega_{RV}(x_{RV}) = w_g \cdot x_{RV}$$

where w_g is the area gradient (constant), with units [mm^2/mm].

The flow diverted to the relief valve $Q_{RV} = Q_p$ forces the opening of the valve to a position x_{RV} determined by the orifice equation:

$$Q_{RV} = c_f w_g x_{RV} \sqrt{\frac{2 p_{p,1}}{\rho}}$$

where $p_{p,1}$ is the system pressure after reaching the end-stop. Another equation is necessary to find both $p_{p,1}$ and x_{RV}. This comes from the RV poppet balance (in this case, flow forces are neglected).

$$p_{p,1} = \frac{F_0 + k x_{RV}}{A_{RV}}$$

where A_{RV} is the area of influence of the pressure inside the RV and $F_0 = p^* \cdot A_{RV}$

The system of equation has the graphical solution represented in the plot below.
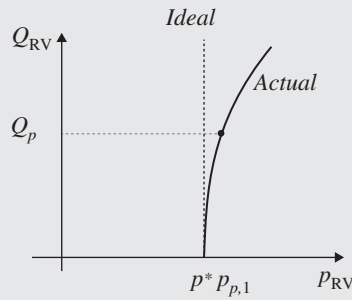
From the stationary analysis, at the instant t^* when the piston hits the end-stop, the system pressure jumps from $p_p = F/A$ to $p_p = p_{p,1}$. This transition happens as a step due to the stationary assumptions. In reality, the pressure transient develops continuously, as qualitatively shown in the figure below.
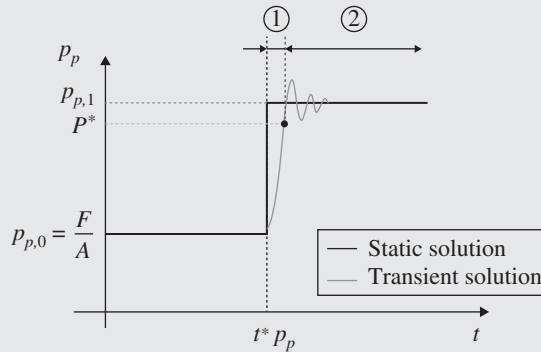
To find the transient solution after the piston reaches the end-stop, it should be considered that in the first part of the transient, the system pressure rises while the RV remains closed (part indicated with "1" in figure). In this time interval, the RV does not have any effect on the pressure transient of the system. However, after reaching cracking pressure, p^* the spool of RV opens, and its dynamic affects the system.

Example 5.2 (Continued)

Therefore, the transient can be fully described by considering the governing equations for these two regions.

Region 1 (RV closed)
If momentum effects and pressure losses are neglected, the system pressure can be described by the pressure build-up equation of the overall volume formed by the connecting lines and the piston chamber at full stroke:

$$\frac{dp_p}{dt} = \frac{K}{(V_{in} + V_{pist})} Q_p$$

The pressure rise is therefore linear, and its gradient is determined by the overall volume, the pump flow rate, and the bulk modulus of the fluid.

Region 2 (RV open)
After the opening of the RV, the system pressure is instead described by

$$\frac{dp_p}{dt} = \frac{K}{(V_{in} + V_{pist})} (Q_p - Q_{RV})$$

where Q_{RV} is again given by the orifice equation:

$$Q_{RV} = c_f w_g x_{RV} \sqrt{\frac{2p_p}{\rho}}$$

To find x_{RV}, the poppet balance needs to be written considering all the terms of the Newton's second law:

$$m_{RV} \ddot{x}_{RV} = p_p A_{RV} - (F_0 + k x_{RV}) - c \dot{x}_{RV}$$

where c is the viscous friction coefficient opposing the poppet motion. For simplicity, static friction terms and flow forces are neglected.

The system contains nonlinear differential equations. Describing the methods for solving these equations falls of the scope of this book. In fact, several authors, including [14, 33], present the analytical analysis of the system linearized about one operating point (usually at the RV cracking), showing that the transfer function of the system, in terms of spool motion versus system pressure, is of the second order. This means that the design parameters of the valve, such as mass of the poppet, spring stiffness, and the area of influence, are responsible for the type of transient behavior in region 2. The resulting response can be underdamped, thus with a pressure overshoot as shown in the figure above, or overdamped, as shown in the figure below.
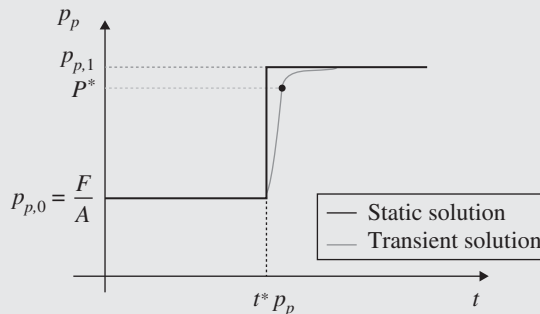
5.3   Modeling Flow Network: Dynamic Considerations

Chapter 3 illustrated the basic laws for modeling flow networks under stationary conditions. As already mentioned, most of the considerations made in the rest of the book are based on the stationary assumption, thus neglecting transient effects. In other words, only the pressure and the flow equations presented in Chapter 3 will be considered, along with the hydraulic resistance effects. However, once the hydraulic system layout is defined, a design engineer may need to study the transient behavior of the system, thus considering both compressibility and momentum effects. Several approaches of analysis are available in fluid mechanics. Pure numerical approaches are usually based on solving the differential form of the momentum equation and continuity equations. These formulations constitute the basis of computational fluid dynamics (CFD), which nowadays has become a standard tool for studying the dynamic behavior of components. However, CFD approaches are computationally expensive, and they are often unsuited for a comprehensive analysis of the entire hydraulic circuit. When analyzing a complete system, a simpler analytical formulation, based on ordinary differential equations, is convenient and, most of the times, accurate enough.

For this purpose, researchers have developed *lumped parameter* modeling approaches, based on the CV method. The system is divided in different CVs and inside each one of them, properties are uniform, and vary only with time. In hydraulics, lumped parameter approaches are mostly based on the concepts of hydraulic resistance, capacitance, and inductance, ruled by the Eqs. (5.11) and (5.17). Table 5.1 summarizes the lumped parameter elements and their governing equations; these can be used to describe the effect of friction (hydraulic resistance), fluid compliance and inertia in a hydraulic line (or in a hydraulic volume inside a certain component). This original approach was well described by Merritt [32]. The table also highlights hydraulic-electric analogy for each element.

The electric analogy can be very useful especially to professionals with electric engineering (EE) background. In fact, thanks to this analogy, the tools available for the analysis of electric circuits can be used for the study of hydraulic systems. However, it is important to note that turbulent conditions, which usually occur in most parts of a hydraulic system, imply a quadratic relation between the flow and effort variables. This is also clarified in Table 5.1, which highlights the cases of laminar and turbulent flow. For this reason, the turbulent flow hydraulic systems are nonlinear, and the approaches valid for linear systems can be used only as an approximation. This was also mentioned in Chapter 3, where the process for linearizing a turbulent resistance was shown in Figure 3.15.

The electric analogy also yields the definition of **hydraulic impedance**, Z_H. The introduction of this parameter elevates the concept of flow resistance to the dynamic domain, considering the behavior of the hydraulic element in terms of frequency response.

The impedance Z_H can be considered as a complex number $Z_H = Z_H(s)$, representative of the transfer function between the pressure and the flow rate across the considered element.

$$p = Z_H \cdot Q \tag{5.20}$$

The hydraulic impedance is the analog of the electric impedance. It is a complex number that can be used to relate the pressure variations with the flow variations in the frequency domain.

As shown in Table 5.2, a pure hydraulic resistance does not imply any dynamic effect between the flow rate crossing the element and the pressure drop. This is reflected by the constant magnitude

Table 5.1 Lumped parameter elements for a hydraulic line and electric equivalent.
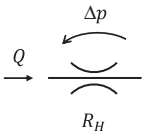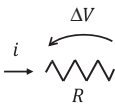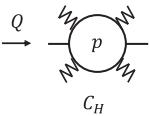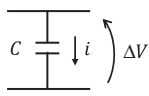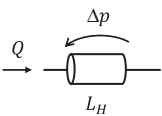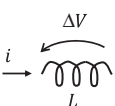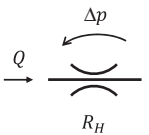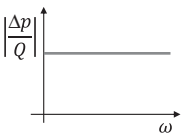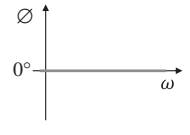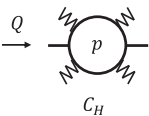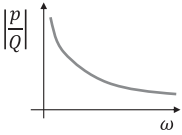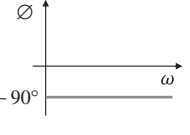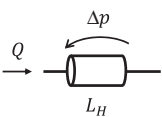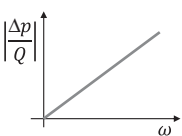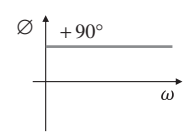
Element	Symbolic representation	Formula	Electric analog	Symbolic representation	Formula
Hydraulic resistance		$\Delta p_{\mathrm{LAM}} = R_{\mathrm{LAM}} Q$ $\Delta p_{\mathrm{TUR}} = R_{\mathrm{TUR}} Q^2$	Electric resistance		$\Delta V = Ri$
Hydraulic capacitance		$\dfrac{dp}{dt} = \dfrac{1}{C_H} Q$	Electric capacitance		$\Delta V = \dfrac{1}{C} \int i\, dt$
Hydraulic inductance		$\Delta p = L_H \dfrac{dQ}{dt}$	Electric inductance		$\Delta V = L \dfrac{di}{dt}$

Table 5.2 Hydraulic impedance and transfer function representation of a hydraulic resistance, capacitance and inductance.

Element	Symbolic representation	Impedance	Magnitude	Phase
Hydraulic resistance		$\dfrac{\Delta p}{Q}(s) = R$		
Hydraulic capacitance		$\dfrac{p}{Q}(s) = \dfrac{1}{sC_H}$		
Hydraulic inductance		$\dfrac{\Delta p}{Q}(s) = L_H s$		

plot and the zero-phase lag used to provide a full representation of Z_H in the frequency domain. A transfer function is usually represented through the Bode diagrams: these represent magnitude and phase with respect to frequency. Those not familiar with these concepts could refer to any basic textbook on dynamics and control systems, particularly Lumkes [34] with its large number of examples applied to hydraulic systems.

The frequency diagrams of the hydraulic resistance indicate that for any possible input flow rate function, the pressure drop across it follows the same shape of the input function, and it differs only by a constant factor.

In contrast, the hydraulic capacitance presents a decreasing amplitude with frequency. Qualitatively, this means that the instantaneous pressure in the fluid element responds well to low-frequency flow variations. However, pressure variations resulting from high-frequency flow variations are attenuated. Moreover, these pressure variations occur with a delay (90° phase delay) with respect to the flow variation.

The hydraulic inductance has qualitatively the opposite trend of the capacitance. A flow variation in a hydraulic inductor occurs as a result of a pressure variation (Eq. (5.17)), and this can explain while the flow variation is now delayed with respect to the pressure variation. The increasing amplitude trend shown in Table 5.2 also reflects the physical nature of the inductor: the faster the flow variation, the higher is the pressure drop according to the momentum equation (5.17).

The dynamic behavior for the flow through a hydraulic element can be described with the impedance approach. In general, all the three effects in Table 5.2 – resistive, capacitive, and inductive – can be present, which should be considered while evaluating the overall impedance. Following approximations are normally accepted while modeling a system with the impedance approach:

Flow restrictions. When modeling the restriction of an orifice, the sole orifice equation can be used neglecting other dynamic effects (fluid capacitance and inductance). In other words, the impedance of a flow restriction is only given by its hydraulic resistance. This assumption can be justified by considering that the volume of fluid between the control sections used to write the orifice equation is very small. These small volumes (CV1 and CV2 in Figure 5.3) have negligible hydraulic capacitance. Eventually their capacitive effect can be integrated within the upstream and downstream lines shown in the same figure. The length of CV1 and CV2 is also very small, so that fluid inductance can be also neglected.

Hydraulic lines. In a hydraulic line, the resistive, capacitive, and inductive effects can be significant. Figure 5.4 illustrates how the impedance is divided into the three contributions; this model is suitable to study a generic hydraulic line.

The resistance[1], R_H, is associated with the frictional losses within the line, introduced in Chapter 3. The hydraulic capacitance of the line, C_H, considers all the compressibility effects of the line. For an infinitely rigid line, the capacitance is given by Eq. (5.10). Actual lines also show compliance effects, meaning that the containing walls also deform under the fluid pressure, altering the fluid volume. Moreover, the presence of undissolved air within the fluid can also affect the overall
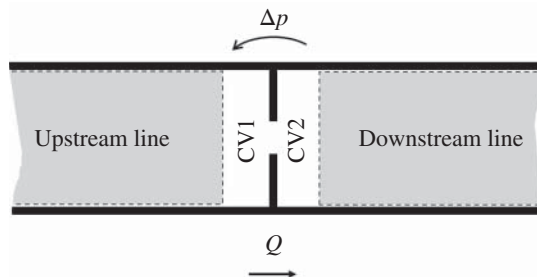
Figure 5.3 An orifice connected to upstream and downstream lines is a pure resistive element.

---

1 For the frictional effects in hydraulic lines, several studies have demonstrated frequency dependent friction phenomena. This causes the hydraulic resistance not to be constant with the frequency. However, these effects are usually negligible in the majority of the cases; they can become relevant in short lines and for high viscosity conditions. Some expressions that can be used in these cases are available in [29].
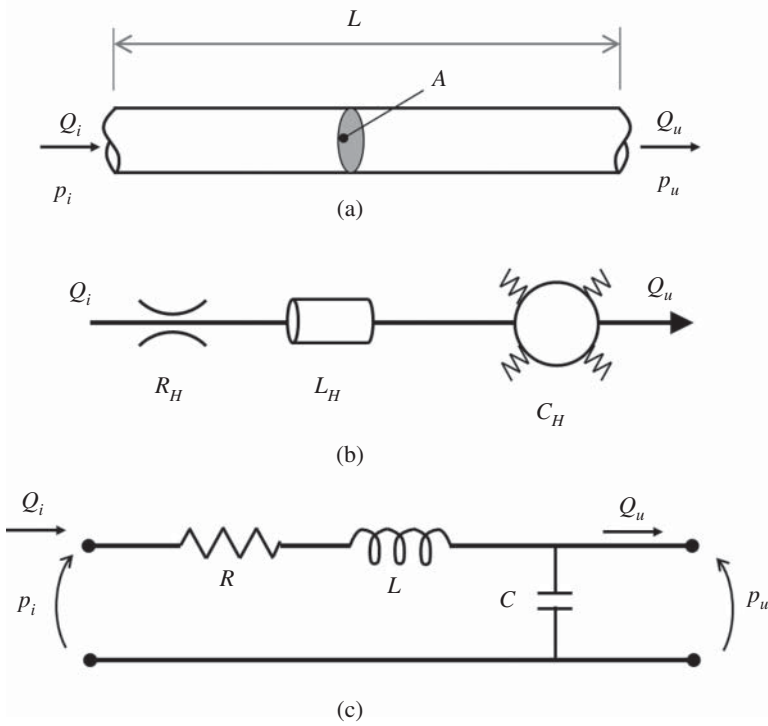
Figure 5.4 Impedance model for a hydraulic line. (a) Real system, (b) Lumped parameter form, (c) electric analog.

hydraulic capacitance. When these effects are important, the overall hydraulic capacitance is calculated through the equivalent bulk modulus (the bulk modulus that includes wall deformation and presence of undissolved air) in the expression of Eq. (5.10). More details can be found in [14]. The hydraulic inductance becomes important for long lines, and its expression is given by Eq. (5.18).

The overall dynamic model of the line results as the hydraulic equivalent of the electric RLC circuit of Figure 5.4. A RLC circuit is an electrical circuit consisting of a resistor (R), an inductor (L), and a capacitor (C). In contrast to the steady-state modeling assumption in Chapter 3, where only the hydraulic resistance was considered along with the flow and pressure laws, for the dynamic case, the effects of inductance and capacitance should also be considered.

The impedance approach is a simple lumped parameter modeling method for estimating the dynamics of flow and pressure in hydraulic systems. The approach "consolidates" the main flow parameters (i.e. pressure, flow rate) as lumped parameters. This approach loses the actual "distributed" nature of the system; however, it represents a relatively simple and convenient method. The lumped parameter approach uses few ordinary and differential equations (summarized Table 5.2) to describe complex systems.

Distributed approaches for analyzing hydraulic lines can also be found in literature [15, 35]. Most of these are based on the CFD solution of the 1D Navier-Stokes equation:

$$\frac{\partial \rho}{\partial t} + \frac{\partial(\rho V_x)}{\partial x} = 0$$
$$\frac{\partial(\rho V_x)}{\partial t} + \frac{\partial(\rho V_x^2 + p)}{\partial x} + f_{fr} = 0$$

(5.21)

The term f_{fr} is representative of the frictional forces due to shear.

It is not within the scope of this chapter to further explore these CFD 1D methods, which are often necessary to obtain accurate solutions for fast dynamic processes, such as the response to a flow or pressure impulse. In fact, the lumped parameter approach is easier to implement, much faster and in most cases accurate enough to study the main dynamic aspects occurring in a hydraulic system.

5.3.1 Validity of the Lumped Parameter Approach

The hydraulic impedance lumped parameter approach is considered to be valid when the time required for a pressure wave to travel the length of the line is short with respect to the period of the highest frequency wave that is to be transmitted [36].

In other words, basic lumped parameter models are useful to study frequency response characteristics of the flow over frequency ranges considerably below the natural frequency of the line. An expression for the natural frequency of a line will be shown in Section 5.3.2.

Some commercial software, such as Siemens Amesim [37], suggests using simple lumped parameter models only when

$$L/D < 6 \tag{5.22}$$

More accurate considerations are based on the time required for a pressure wave to travel along a pipe. Considering the definition of the speed of sound for a liquid,

$$c = \sqrt{\frac{K}{\rho}} \tag{5.23}$$

A dimensionless parameter often referred as Damping number can be defined:

$$D_n = \frac{\mu L}{c\left(D/2\right)^2} \tag{5.24}$$

The Damping number results from a non-dimensional expression of the Eq. (5.21), and it quantifies the viscous friction effects. Low values for D_n means that there is no significant effect of friction in the line, but wave propagation effects can be important. Instead, $D_n > 1$ means that wave effects are not important, and friction and compressibility dominate the flow solution. This is the region where the lumped parameter model provides an accurate solution.

Some software packages, such as Siemens Amesim [37], also propose the so called "lumped distributive" models, which consist multiple lumped parameter elements to represent a single hydraulic line. The basic idea is represented in Figure 5.5. This approach has to be used with particular care, because it can misrepresent the highest frequencies components of the flow.

5.3.2 Further Considerations on the Line Impedance Model

The schematic of Figure 5.4 shows how two impedances can be defined for one hydraulic line (or more in general a hydraulic connection). These two impedances can be obtained by looking at the input terminals or the output terminals.

For the *input impedance*,

$$Z_i = \frac{p_i}{Q_i} = \left(R_H + L_H s + \frac{1}{C_H s} \right) \tag{5.25}$$

while, for the *output impedance,*

$$Z_u = \frac{p_u}{Q_u} = \frac{1}{C_H s} \tag{5.26}$$
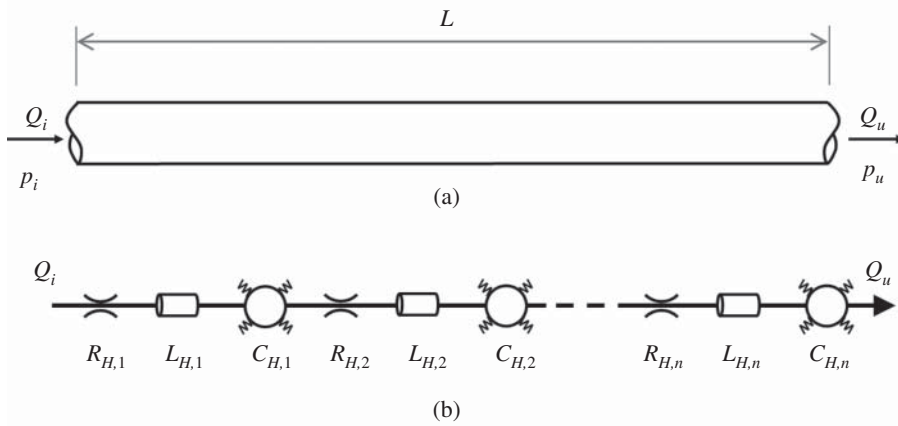
Figure 5.5 Lumped distributive model for a hydraulic line. (a) Real system, (b) Distributed line model.

Now, considering that for the pipe section, we have $Q_i = Q_u$, it is possible to define a transfer function for the pressure in the pipe:

$$\frac{Z_u}{Z_i} = \frac{p_u}{p_i} = \frac{1}{L_H C_H s^2 + R_H C_H s + 1} \tag{5.27}$$

which can also be written in the form of a classic second-order transfer function:

$$\frac{p_u}{p_i} = \frac{1}{\dfrac{1}{\omega_n} s^2 + \dfrac{2\xi}{\omega_n} s + 1} \tag{5.28}$$

where the natural frequency ω_n and the damping of the line are given by

$$\omega_n = \frac{1}{\sqrt{L_H C_H}}; \quad \xi = \frac{R_H}{2} \sqrt{\frac{C_H}{L_H}} \tag{5.29}$$

The equations above indicate that the line, with respect to the relation between the output pressure and the inlet pressure, behaves as a second-order vibrating system, and the natural frequency and the damping ration of the line are expressed in Eq. (5.29).

The impedance approach is useful for frequency analyses of hydraulic components. For a hydraulic connection, the ratio between the input impedance and the output impedance provides the transfer function between the input and output pressures, as a second-order transfer function.

5.4 Damping Effect of Hydraulic Accumulators

The dynamic equations and the related parameter definitions given in this chapter can also be useful to describe one of the typical uses of hydraulic accumulators: the pressure dampening function.
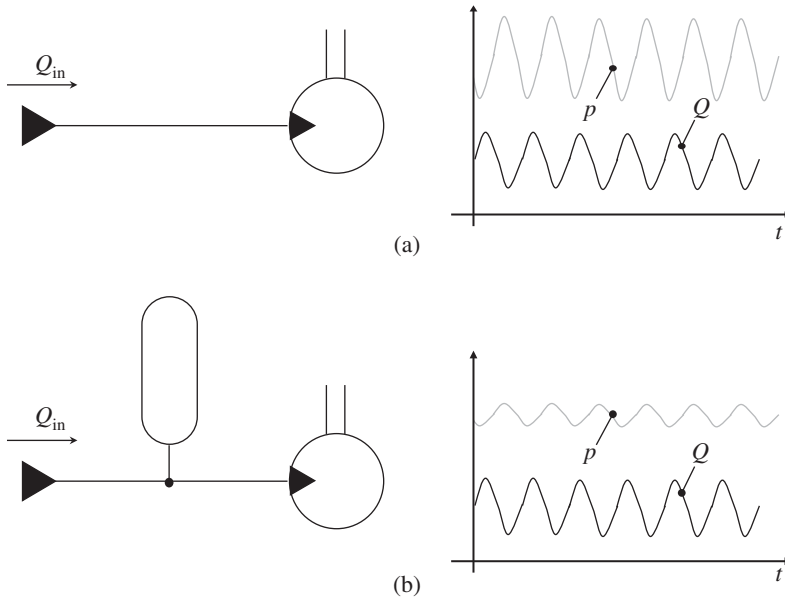
Figure 5.6 Conceptual representation of using of a hydraulic accumulator for pressure dampening. Qualitative pressure ripples without accumulator (a) and with accumulator (b).

As it will be discussed in Part II (Chapter 9), an accumulator can operate in a system that can attenuate the pressure and flow fluctuations in a certain hydraulic line.

As in a hydraulic motor, Figure 5.6 shows the use of an accumulator for reducing the pressure oscillations at the inlet of a certain component. However, in practice, this reduction applies to other components such as control valves. In the figure, excessive inlet pressure oscillations can cause undesired output shaft torque oscillations. The inlet flow ripple is typically generated by the flow supply, which consist of a positive displacement machine.

If the flow function $\sum Q(t) = Q_n - Q_{out}$ is known, the pressure in the line, neglecting frictional and inertial effects is, from Eq. (5.9):

$$\frac{dp}{dt} = \frac{1}{C_H}\left(\sum Q\right) \tag{5.30}$$

where $C_H = V/K$ is the hydraulic capacitance. If an accumulator is added to the pressure line, the overall capacitance becomes

$$C_H = C_{H,\text{line}} + C_{H,\text{acc}} \tag{5.31}$$

It is therefore obvious that the increased capacitance due to the presence of the accumulator is beneficial to reduce the pressure variations within the system.

To find an expression of the capacitance of the accumulator, we can consider the definition of the bulk modulus:

$$K = -\frac{dp}{dV/V} \tag{5.32}$$

It can be inferred that

$$dV = -\frac{V}{K}dp \tag{5.33}$$

Therefore,

$$C_H = -\frac{dV}{dp} \tag{5.34}$$

This last expression is useful to find $C_{H,\,acc}$, from the evaluation of the internal volume changes within it. Considering a typical gas charged accumulator, the polytropic relation applies to the gas volume. The process from the precharge condition to a generic pressure p is

$$pV^\gamma = p_0 V_0^{\,\gamma} \tag{5.35}$$

from which

$$V = \left(\frac{p_0}{p}\right)^{\frac{1}{\gamma}} V_0 \tag{5.36}$$

Therefore, the capacitance of the accumulator can be derived as

$$C_{H,acc} = -\frac{\partial}{\partial p}\left(p_0^{\frac{1}{\gamma}} \cdot p^{-\frac{1}{\gamma}} \cdot V_0\right) \tag{5.37}$$

which, after proper simplifications, becomes

$$C_{H,acc} = \frac{V_0}{\gamma} \cdot \sqrt[\gamma]{\frac{p_0}{p^{1+\gamma}}} \tag{5.38}$$

Given the average working pressure of the system at which the oscillations are occurring, p, the volume of the accumulator that can reduce the pressure oscillation at an acceptable level can be determined by using this last formula.

Further considerations on the use of the accumulator for pulsation dampening will be made in Chapter 9.

Problems

5.1 For the pressure receiver tank shown below, the following values are known: the flow rate entering the inlet port, the flow velocity at the outlet port, and the inner diameter of the outlet pipe. Determine the rate at which the recipient gains or loses fluid. Assume: $Q_{in} = 22\,\text{l/min}$, $v_{out} = 1.4\,\text{m/s}$, $d_{out} = 32\,\text{mm}$, fluid density to be $900\,\text{kg/m}^3$.
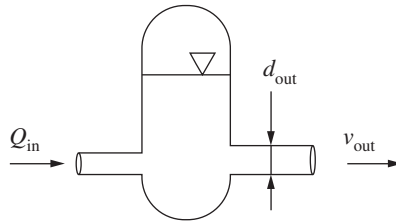
5.2 A cylindrical tank of 15-cm-diameter drains through an opening with a diameter of 0.6 mm located at the bottom of the tank. The speed of the liquid leaving the tank is $v = \sqrt{2gy}$ where y is the height from the tank bottom to the free surface. If the tank is initially filled with oil to 1 m, determine the oil depth after one minute. Plot the function of the depth versus time.

5.3 Use the approach presented in Example 5.1 to study the response of the actuation system in the figure below. The system has a pump and a relief valve set at p^*. The pump provides flow to a dual rod actuator, via a directional control valve. Although these two elements will be further discussed in Part II, for the sake of this problem, the reader can assume that the valve opens the connections as shown in figure. In particular, the valve lifts the load in position (1) and lowers the load in position (2). All the area openings of the valve are proportional to the valve travel, x_v. The constant of proportionality is indicated as valve area gradient. The orifice equation can be used to express the flow across the valve ports.

Using the data reported in the table, and the valve opening shown in the plot, derive the expression for the pressure in the piston chambers, $p_1 = p_1(t)$ and $p_2 = (t)$, and for the for the cylinder motion, $\dot{x}_{cyl} = \dot{x}_{cyl}(t)$. These expressions will have the form of differential equations, as in Example 5.1.

Using a numerical solver, plot the time course for p_1, p_2, and $\dot{x}_{cyl}$.

Note that the valve shifts from one position to another with linear ramps, not instantaneously. In solving the problem, assume that

– the pump flow is always larger than the flow requested by the valve so that the relief valve is always open, and the pump delivery is always at a constant pressure p^*.
– the volumes of the supply (upstream the valve) and the return (downstream the valve) very large so that a constant pressure can be assumed at the valve supply and return ports.
– the mass of the piston is negligible compared to the mass attached to it (load).
– there are no frictional effects in the lines.

Neglect frictional effects in lines and in the piston motion.
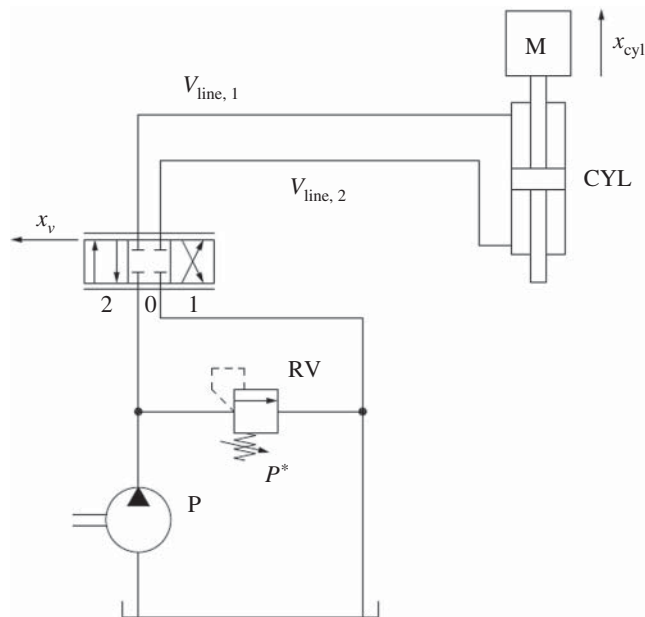
Parameter	Symbol	Value	Unit
Mass	m	1000	kg
Volume of the line connecting to valve, upper port	$V_{\text{line, 1}}$	20 10^{-5}	m^3
Volume of the connection cylinder to valve, lower port	$V_{\text{line, 2}}$	20 10^{-5}	m^3
Piston diameter	D	0.05	m
Rod diameter	d	0.028	m
Stroke	l	0.8	m
Piston thickness	s	0.02	m
Dynamic friction opposing the piston motion	s	1	Ns/m
Maximum valve travel (both directions)	$x_{v,\text{ max}}$	0.008	m
Neutral position (all connections closed)	$x_{v,\text{ neutral}}$	0	m
Valve area gradient (both directions)	w	0.01	m
Orifice coefficient	C_F	0.65	—
Relief valve setting	p^*	250	bar (gage)
Tank pressure	p_T	0	bar (gage)
Valve ramp time	t_{ramp}	50	ms
Lift time	t_{lift}	1	s
Lower time	t_{lower}	1	s
Rest time	t_{rest}	1	s
Fluid density	ρ	870	kg/m^3
Bulk modulus	B	1500	bar

5.4 From Problem 5.3, consider working a fixed amount of undissolved air, which is equal to 0.1% at atmospheric (tank) conditions. Use the formulas in Chapter 2 to derive the fluid properties to use in the dynamic equations.
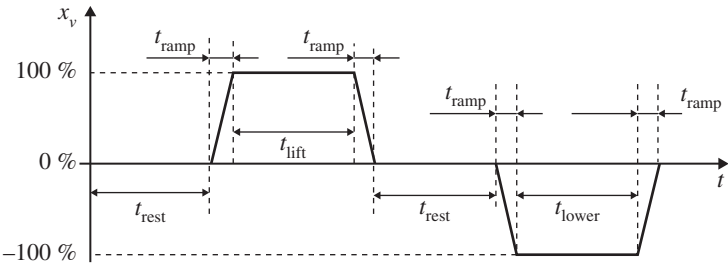
References

1 Ramelli, A. and Gniudi, M.T. (1994). *The Various and Ingenious Machines of Agostino Ramelli: A Classic Sixteenth-Century Illustrated Treatise on Technology*. Dover Publications.

2 Blackburn, J.F., Reethof, G., and Shearer, J.L. (1959). *Fluid Power Control*. The M.I.T. Press.

3 Global Fluid Power Society. *Homepage*. www.gfpsweb.org

4 Skinner, S. (2014). Hydraulic Fluid Power – A Historical Timeline. http://lulu.com

5 ISO 1219-1 (2012). *Fluid power systems and components—Graphical symbols and circuit diagrams—Part 1: Graphical symbols for conventional use and data-processing applications*.

6 ISO 1219-2 (2012). *Fluid power systems and components—Graphical symbols and circuit diagrams—Part 2: Circuit diagrams*.

7 Totten, G.E. and De Negri, V.J. (2011). *Handbook of Hydraulic Fluid Technology*, 2e. CRC Press.

8 Zarotti, G.L. (1998). *Fluidi Oleodinamici, Quaderni Tematici*. IMAMOTER CNR.

9 ISO 6473 (2007). *Lubricants, industrial oils and related products*.

10 ISO 7745:2010 (2010). *Hydraulic fluid power – Fire-resistant (FR) fluids*. Switzerland.

11 Assofluid (2007). Hydraulics in Industrial and Mobile Applications. Milan, Italy: Assofluid.

12 Trostmann, E. (1995). *Water Hydraulics Control Technology*. CRC Press.

13 Cengel, Y. and Boles, M. (2014). *Thermodynamics: An Engineering Approach*, 8e. McGraw-Hill.

14 Nervegna, N. and Rundo, M. (2020). *Passi nell'oleodinamica* vol. 1–2, Epics.

15 Pritchard, P.J. (2016). *Fox and McDonald's Introduction to Fluid Mechanics*, 8e. Wiley.

16 Touloukian, Y.S., Saxena, S.C., and Hestermans, P. (1975). *Thermophysical Properties of Matter, the TPRC Data Series, Vol. 11–Viscosity*. New York Plenum Publishing Corp.

17 Seeton, C.J. (2006). Viscosity-temperature correlation for liquids. *Tribology Letters* 22: 67–78.

18 Cragg, J.C. and Evans, E.A. (1943). Viscosity measurement and viscosity index. *Journal of the Institute of Petroleum* 29 (232): 99–123.

19 ISO—International Organization for Standardization (2002). *ISO 2909:2002 Petroleum products – Calculation of viscosity index from kinematic viscosity*.

20 ASTM D7042-20 (2020). *Standard test method for dynamic viscosity and density of liquids by Stabinger viscometer (and the calculation of kinematic viscosity)*. West Conshohocken, PA: ASTM International.

21 OelCheck (2012). *Viscosity – the single most important physical characteristic of any oil*, pp. 5–8. Brannenburg, Germany. https://en.oelcheck.com/fileadmin/user_upload/pdf/oelchecker/en/2012/oelchecker_summer_2012_EN.pdf.

22 Backe, W. (1988). *Grundlagen der Olhydraulik, Umdruck zur Vorlesung, 7 Auflage*. RWTH Aachen.

23 Tillner, W., Fritsch, H., Kruft, R. et al. (1993). *The Avoidance of Cavitation Damage*. London: MEP.

24 Vacca, A., Klop, R., and Ivantysynova, M. (2010). A numerical approach for the evaluation of the effects of air release and vapour cavitation on effective flow rate of axial piston machines. *International Journal of Fluid Power* 11 (1): 33–45.

25 Shah, Y.G., Vacca, A., and Dabiri, S. (2018). Air release and cavitation modeling with a lumped parameter approach based on the Rayleigh–Plesset equation: the case of an external gear pump. *Energies* 11 (12): 3472.

26 Zhou, J., Vacca, A., and Manhartsgruber, B. (2013). A novel approach for the prediction of dynamic features of air release and absorption in hydraulic oils. *ASME Journal of Fluid Engineering* 135 (9): 091305. https://doi.org/10.1115/1.4024864.

27 Fitch, J. (2001). Vacuum distillation for the removal of water and other volatile contaminants. *Practicing Oil Analysis magazine* (March–April).

28 The Handbook of Hydraulic Filtration. Parker Hannifin. Available online https://www.parker.com/literature/Hydraulic%20Filter%20Division%20Europe/fdhb289uk.pdf.

29 ISO 4406:2017 (2017). *Hydraulic fluid power – Fluids – Method for coding the level of contamination by solid particles*. Switzerland: ISO.

30 Parker Hannifin Technical Catalog 4400 US. Available online https://www.parker.com/literature/Hose%20Products%20Division/Catalog%204400%20PDF%20Files/Section_E_Technical.pdf.

31 Idelchik, I.E. (2008). *Handbook of Hydraulic Resistance*, 4e. BHB. ISBN: ISBN-13: 978-1567002515.

32 Merrit, H.E. (1967). *Hydraulic Control System*. Wiley.

33 Manring, N.D. (2013). *Fluid Power Pumps and Motors: Analysis, Design, and Control*. Mcgraw Hill.

34 Lumkes, J.H. *Control Strategies for Dynamic Systems: Design and Implementation*. Dekker Mechanical Engineering.

35 Streeter, E.B. and Wylie, V.L. (1967). *Hydraulic Transients*. McGraw-Hill.

36 McCloy, D. and Martin, H.R. (1980). *Control of Fluid Power*. Ellis Horwood Limited.

37 Simcenter Amesim (2017). Hydraulic Library 16 User's guide, Siemens Industry Software NV.

38 Miller R. W., 1996. *Flow Measurement Engineering Handbook*, 3 McGraw-Hill Companies, Inc., Boston, MA.

39 Bean, H.S. (1971). Formulation of equations for orifice coefficients. *Journal of Basic Engineering* 93 (2): 97–98.

40 Mises, R.V. (1917). Berechnung von Ausflum- und Uberfallzahlen. Zeit. des Vereines deutscher Ingenieure 61. Reprinted in (1963). *Selected Papers of Richard von Mises* (eds. P. Frank et al.). American Mathematical Society.

41 Wuest V.W. (1954). Ingenieur Arch.22, 357.

Part II

Hydraulic Components

Part II of the book presents the basics of the operation of the main components used in hydraulic circuits. These are generally classified in three categories: energy conversion units (hydraulic pumps and actuators), control valves, and hydraulic accessories.

Energy conversion units include all the elements that convert energy between the mechanical and the hydraulic domains. Hydraulic pumps convert mechanical into hydraulic energy. Hydraulic motors and linear actuators follow the opposite path, transforming hydraulic into mechanical energy. The first chapter of this part focuses on pumps and motors, establishing discussion from the general principles in Part I and also emphasizes on the differences between the real and the ideal components, which therefore defines energy efficiency parameters. The main architectures of pumps and motors are then presented and briefly analyzed. Chapter 7 concentrates on linear actuators, presenting the different available types and their operating principles. The ideal case is compared to the real one, which considers the influence of frictions and leakages.

Chapter 8 presents the basics of hydraulic control valves. Initially, some basic components are analyzed: check and shuttle valves are mostly used as logic elements of a circuit. Relief and reducing valves are used to limit or control the pressure of a part of a circuit. Flow control valves regulate the flow rate inside some branches of a hydraulic system. Finally, some generic principles of directional control valves are presented. Directional valves will be further discussed also in the next parts of the book, when the different metering control concepts will be analyzed for single and multiple actuators.

The last chapter of this part (Chapter 9) covers hydraulic accumulators, presenting the different architectures and their applications, the generic operating principles, and the selection and sizing methods. Accumulators are often considered as part of the hydraulics accessories group, together with filters, coolers, and reservoirs. The fundamentals of these latter accessories have been briefly covered in Part I.

Objectives

After an in-depth reading of Part II, including the worked examples and the proposed end of chapter problems, the reader will be able to

1. Define the concept of hydraulic power and power conversion in a hydraulic system.
2. Describe the equations governing the steady-state operation of pumps and motors in the ideal case.

3. Define the concepts of volumetric and hydromechanical (or torque) efficiency for a hydraulic pump and for a hydraulic motor.
4. Recognize and describe the phenomena leading to losses in hydraulic pumps, motors, and linear actuators.
5. Describe the main design architectures for pumps and motors, as well as the different features of each one of them.
6. Size and select the right pump or actuator (cylinder or motor) for a given applications.
7. Illustrate the functions and the operation of springs in hydraulic valves.
8. Describe the function of check and shuttle valves in a hydraulic circuit.
9. Explain the purpose of relief valves and the difference between real and ideal valves.
10. Describe the difference between direct acting and pilot operated valves.
11. Select the correct valve for the application.
12. Illustrate the features of pressure reducing valves and flow control valves.
13. Build the circuit equivalent to a directional control valve using variable orifices.
14. Explain the different actuation methods for directional control valves.
15. Recognize the equivalent schematic or symbol from the cross-sectional view of a hydraulic valve.
16. Recognize the different architectures of hydraulic accumulators.
17. Size and select an accumulator for a specific application.

Chapter 6

Hydrostatic Pumps and Motors

This chapter describes the theory and design of the main types of pumps and motors used in hydraulic control systems. Hydraulic pumps and motors are energy conversion elements and play a fundamental role in a fluid power transmission system. A hydraulic system is always supplied by a hydraulic pump connected to an internal combustion engine or an electric motor (prime mover). Hydraulic systems always control actuators, either linear (cylinder) or rotary (hydraulic motor). This chapter will present hydraulic motors together with hydraulic pumps due to their design similarities. Linear actuators will be described in Chapter 7.

The ideal functioning – assuming no losses – of pumps and motors will be illustrated here as well as their actual operation. Actual components are characterized by defining energy efficiency parameters, such as the volumetric and the hydromechanical (or torque) efficiency. These are useful to quantify the performance of an actual unit with respect to the desirable ideal case. Next, the main source of power loss occurring in the positive displacement machines used to implement hydraulic pumps and motors will be described with illustrations of the most successful construction types of units. The chapter does not dive into many design details and the design procedures for these units. Proper references will be provided to the reader interested in further learning design methods for modern positive displacement machines for fluid power applications.

6.1 Introduction

The general operation of a hydraulic system is represented in Figure 6.1. The input is provided in the form of mechanical energy by the "prime mover," usually an electric motor, an internal combustion engine, or a turbine engine. This is converted within the hydraulic circuit in the form of hydraulic energy, which can be defined as "moving pressurized fluid.". Hydraulic energy is then properly transmitted throughout the circuit and converted again into mechanical energy to be provided to the actuators of the system.

> The mechanical-to-hydraulic conversion element is indicated as **pump**, while the opposite hydraulic-to-mechanical conversion unit is indicated as **actuator**.

Actuators can be further subdivided according to the nature of their motion as rotary actuators (motors) or linear actuators (cylinders).

Figure 6.1 also points out the physical quantities used to express the power in both the mechanical and hydraulic domains. In particular, for a rotating shaft, the power is given by the product of the torque and the angular velocity; for a linear actuator, it is given by the force and the linear
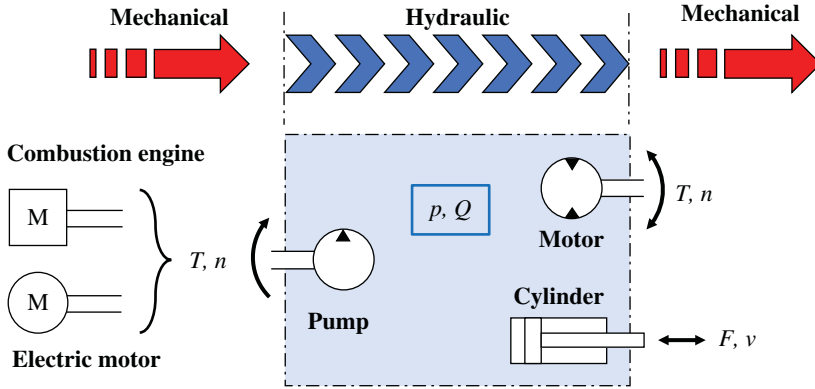
Figure 6.1 Power flow in a hydraulic system.

velocity. In the hydraulic domain, within the common operating pressure ranges, the power can be approximated as the product of the pressure and the volumetric flow rate and it will be discussed in the next section.

6.2 The Ideal Case

Hydraulic pumps and motors are units that enable the energy conversion from/to the mechanical domain to/from the hydraulic domain.

The generic ISO symbols for a pump and a motor are shown in Figure 6.2. The figure also gives an idea of the energy conversion occurring in these units. The shaft mechanical power is defined as the product of the shaft speed and torque[1]:

$$P_{\text{mech}} = T \cdot \omega = T \cdot n \, \frac{2\pi}{60} \tag{6.1}$$

(a)   (b)
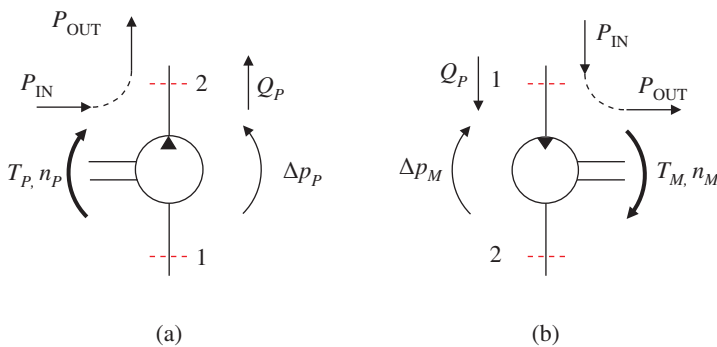
Figure 6.2 Representation of power flow and input-output energy parameters in hydraulic pumps (a) and motors (b).

---

1 with the common units used in hydraulics:

$$P_{\text{mech}}(\text{kW}) \cong T \, [Nm] \cdot n \, [rpm] \cdot \left(\frac{\pi}{30\,000} \right) \left[\frac{kW}{rpm \cdot Nm} \right]$$

$$P_{\text{mech}}(\text{hp}) \cong T \, [ft\,lbs] \cdot n \, [rpm] \cdot \left(\frac{\pi}{16\,494} \right) \left[\frac{hp}{rpm \cdot ft\,lbs} \right]$$

The hydraulic power is defined considering the difference of the energy level at the inlet and outlet ports of the unit. This energy equation can be written as follows for pumps (Figure 6.2a) and motors (Figure 6.2b):

$$h_p = \left(\frac{p_2}{\rho} + \frac{v_2^2}{2} + gz_2 \right) - \left(\frac{p_1}{\rho} + \frac{v_1^2}{2} + gz_1 \right) \tag{6.2a}$$

$$h_m = \left(\frac{p_1}{\rho} + \frac{v_1^2}{2} + gz_1 \right) - \left(\frac{p_2}{\rho} + \frac{v_2^2}{2} + gz_2 \right) \tag{6.2b}$$

The equations above correspond to the generalized Bernoulli's equation presented in Chapter 3, with the exception that h_p and h_m are no longer head loss terms. Here they represent the energy contribution of the pump (h_p), or of the motor (h_m); the net change of the energy of the fluid at the unit ports is the difference between the two terms in parentheses.

Each term is calculated as the sum of flow energy, kinetic energy, and potential energy (expressed as energy per unit mass). In particular, the energy contribution of the pump is calculated as the difference between fluid energy at the outlet and inlet. For the motor, the energy contribution has the opposite sign. Note that for the ideal case, the fluid is considered to be as ideal, incompressible.

Equations (6.2a) and (6.2b) can be significantly simplified after a few considerations (according also to ISO 4391 [1]). In fact, in all hydraulic systems, the predominant characteristic is a high working pressure, with relatively low fluid speeds. In other words, the pressure difference across the ports of the units in Figure 6.2 is significantly higher than both the elevation and kinetic energy differences. These can be ignored in the energy balance. In the ideal case, there are no energy losses between sections 1 and 2, and the expression of the hydraulic power simply becomes[2]:

$$P_{\text{hyd},p} = \dot{m}_p \cdot h_p \cong Q_p \cdot (p_2 - p_1) \tag{6.3a}$$

$$P_{\text{hyd},m} = \dot{m}_m \cdot h_m \cong Q_m \cdot (p_1 - p_2) \tag{6.3b}$$

Two important remarks follow Eq. (6.3):

- The equations governing the operation of a pump and a motor are generic and not specific to the unit architecture.
- The equations justify why hydraulic pumps and motors are often referred to as **hydrostatic units**: the work associated with their operation is solely related to fluid pressure change.
- $Q \cdot \Delta p$ is used to identify forms of power in all hydraulic components: it is also used to estimate the power loss across a valve as well as the power loss associated with internal leakage.

6.3 General Operating Principle

The units applied in hydraulic circuits are always positive displacement machines. This technology is best suited to operate at the common levels of pressure and flows encountered in hydraulic systems. On the other hand, dynamic machines (e.g. impeller pumps) are instead suitable for operations with high flows and lower pressures, such as in hydrogeological applications.

------

2 With the common units used in hydraulics:

$$P_{\text{hyd}}(\text{kW}) \cong Q_p(\text{l/min}) \cdot (p_2 - p_1)[bar] \cdot \left(\frac{1}{600} \right) \left[\frac{kW}{l/min \cdot bar} \right]$$

$$P_{\text{hyd}}(\text{hp}) \cong Q_p(\text{gpm}) \cdot (p_2 - p_1)[psi] \cdot \left(\frac{1}{1714} \right) \left[\frac{hp}{gpm \cdot psi} \right]$$

Positive displacement pumps and motors work according to a reciprocating cycle in which variable volumes (displacement chambers) are properly set into communication with the inlet or the outlet port in such a way that the fluid is moved from inlet to outlet.

> The volume of fluid displaced per revolution is called **displacement** of the hydraulic pump or motor and it is indicated as V_D.[3]

This concept can be understood referring to the simple example shown in Figure 6.3. This represents a positive displacement pump comprising a plunger moving along the cylinder bore and a spool controlling the flow connection between the chamber and the A and B ports.

The spool shown in Figure 6.3 is at the neutral position, which completely isolates the chamber from both ports. When the spool is at the upper position, the chamber connects to port A, and when it is at the lower position, the chamber connects to port B.

Figure 6.4 demonstrates four significant states of the plunger pump. One displacing cycle is completed when the pump transitions through states (a), (b), (c), and (d). From (a) to (b), the plunger moves outward and pulls fluid from port B to the chamber. The fluid pressure in the chamber is equalized to the port B pressure, p_B. From (b) to (c), the spool moves from the lower position to the upper position and connects the chamber to the port A. The pressure in the chamber then becomes the port A pressure, p_A. The plunger moves inward from (c) to (d) and pushes the fluid from the chamber into the port A. During this cycle, a finite amount of fluid is *displaced* from one port to the other.

In case that p_A is greater than p_B, the transition from (a) through (b) and (c) to (d) can be illustrated with the rectangular path of Figure 6.5. The plunger pulls fluid from low pressure (p_B) and displaces it into higher pressure (p_A). The energy is transferred from the mechanical domain to the hydraulic domain and the unit works as a pump. The amount of energy transferred at every cycle
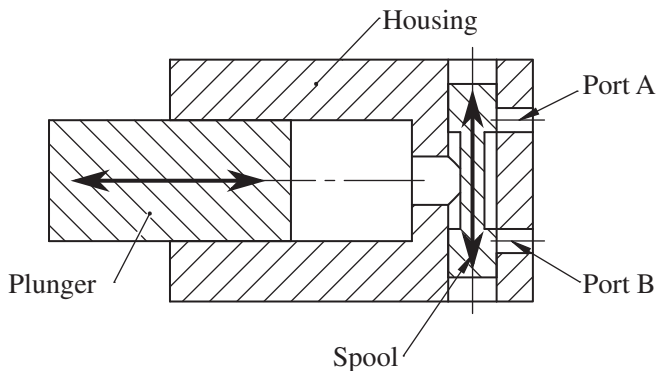
Figure 6.3 Plunger pump with port selection spool.

---

3 The definition of the displacement of a pump or a motor is not always straightforward. In fact, in most cases V_D is assumed equal to the *geometric displacement*, this being defined as "the calculated total of all changes in volume of pressure chambers originating from the movement of displacement elements during one revolution of the input (pumps) or output (motors) shaft, or one double stroke of an oscillating drive. Tolerances, clearances, distortions or deformations are not considered" (ISO 3662 [2]). In reality, the displacement of a unit is affected by other factors such as the manufacturing tolerances and the timing of the internal connections (for example, the valve plate of an axial piston unit); therefore, the correct value for the displacement of a single unit is the so-called *derived displacement,* which can be evaluated experimentally as described in standard ISO 8426 [3].
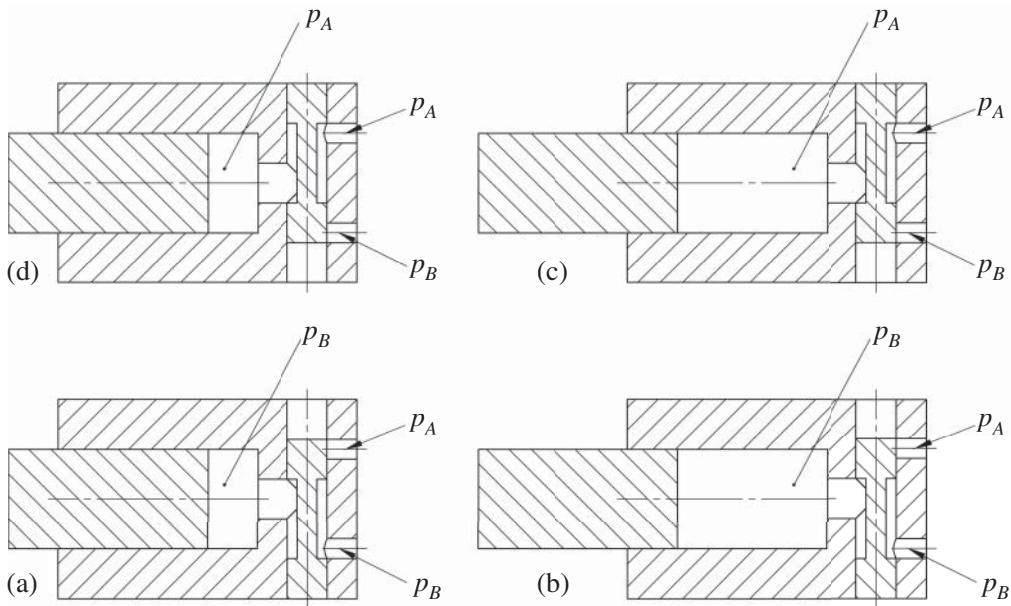
Figure 6.4 Commutation points for a plunger pump, starting from the bottom left figure, following counterclockwise order: (a) minimum volume– port B open; (b) maximum volume – port B open; (c) maximum volume – port A open; (d) minimum volume – port A open.

equals the work done by the plunger:

$$E = p_A \cdot (V_{\max} - V_{\min}) + p_B \cdot (V_{\min} - V_{\max}) = (p_A - p_B) \cdot (V_{\max} - V_{\min}) \tag{6.4}$$

Equation (6.4) is also the formula of the area of the rectangle used to illustrate the plunger cycle.

When the plunger operates in the opposite order, from (d), through (c), (b), and (a), in a clockwise direction (Figure 6.5), the plunger becomes a motor. In fact, the fluid is taken from high pressure and displaced to low pressure. In other words, hydraulic energy is converted into mechanical energy. The energy transferred by the motor at every cycle also follows Eq. (6.1), except that the work is done by the fluid instead of the plunger.
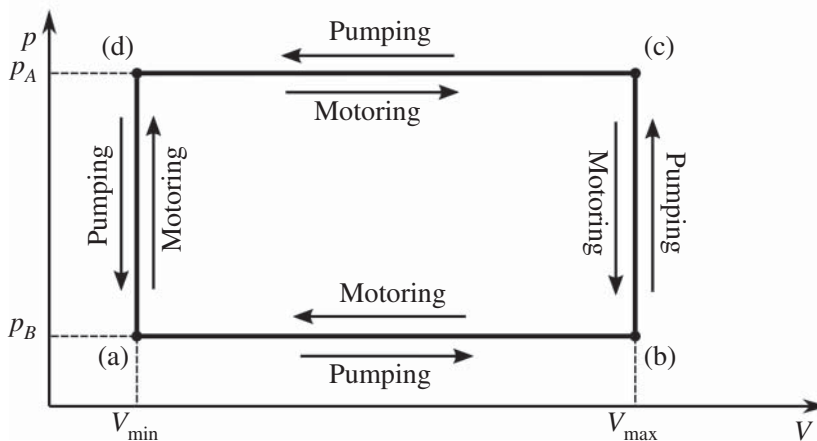
Figure 6.5 Ideal working cycle of the plunger pump.
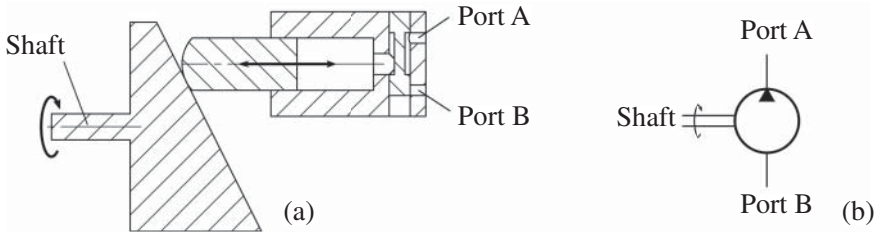
Figure 6.6 Wobble plate pump (a) and ISO pump symbol (b).

Even though the general definition of hydrostatic pumps and motors does not specify the form of mechanical drive, the terms *pump* and *motor* are commonly referring to devices using a driveshaft to take/deliver mechanical power. As shown in Figure 6.6a, a plunger pump can be driven by a shaft with a wobble plate modification. As the plate rotates around the shaft axis, the plunger remains in contact with the plate creating a reciprocating motion.

For every rotation of the shaft, the plunger completes one full cycle. Therefore, if n is the shaft rotational speed, the flow rate associated with the pump or motor unit is:

$$Q_p = n \cdot (V_{\max} - V_{\min}) \tag{6.5}$$

Figure 6.7 shows the trend of the plunger volume during a rotation, which usually can be approximated with a sinusoidal curve. For a pump, the flow rate generated by the unit also follows a sinusoidal trend over time, similar to the volume trend. The value expressed by Eq. (6.5) represents the average flow value over a cycle. In contrast, for a motor that is supplied with a constant flow, the shaft speed oscillates around an average value following the same sinusoidal trend.

According to the Eq. (6.5) and to the definition introduced at the beginning of this section, the displacement of the wobble plate pump equals:

$$V_D = V_{\max} - V_{\min} \tag{6.6}$$

Equation (6.6) refers to the case of a single plunger pump. In general, hydraulic pumps or motors contain multiple displacement chambers. The displacement of the unit then becomes

$$V_D = z \cdot (V_{\max} - V_{\min}) \tag{6.7}$$
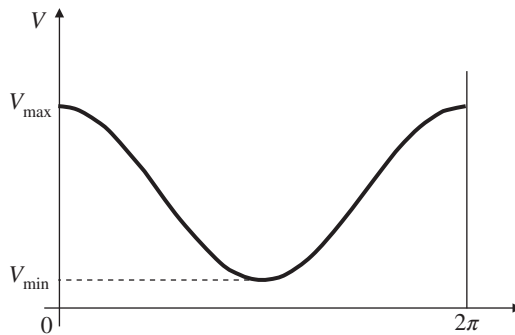
Figure 6.7 Displacement chamber volume as a function of the shaft angular position.

The use of multiple displacement chambers with proper phase lag increases the unit displacement. The multiple chamber arrangement design based on the inclined surface such as the wobble plate of Figure 6.6 is the basis of the axial piston pump design that will be further detailed later in this chapter. It is possible to demonstrate that having multiple chambers reduces the amplitude of the oscillation of the flow rate (as well as the shaft torque) around the average value. The demonstration can be found on the Ivantysyn and Ivantysynova's book [4], where it is also shown the convenience of using an odd number of pistons rather than an even number to further reduce the flow rate oscillations.

In the case of multiple stroke architectures, which are common in internal support radial piston machines and vane type machines, the displacement chamber volumes cycle between the maximum and the minimum volume multiple times in a single shaft revolution. The displacement of multiple stroke unit then becomes

$$V_D = z \cdot N_{\text{cycle}} \cdot (V_{\max} - V_{\min}) \tag{6.8}$$

Certain unit designs allow for variation of the displacement. For the simplistic design in Figure 6.6, this would mean varying the inclination angle of the wobble plate. These designs are called **variable displacement units**. For these, the *instantaneous displacement* can be defined as follows:

$$V_D(\varepsilon) = \varepsilon \cdot V_{D,\max} \tag{6.9}$$

ε is the *fractional displacement* parameter and ranges within the interval (0, 1). It can be also be expressed as percentage.

6.4 ISO Symbols

The ISO symbol summarizes all main functionalities of a pump, or a motor, in the system. The only aspect not described by the symbol is the type of architecture. Figure 6.8 shows the features that should be included as a symbol for a pump. Examples of the most common pump symbols are represented in Figure 6.9. Similarly, Figure 6.10 displays the symbolic representation of a hydraulic motor.
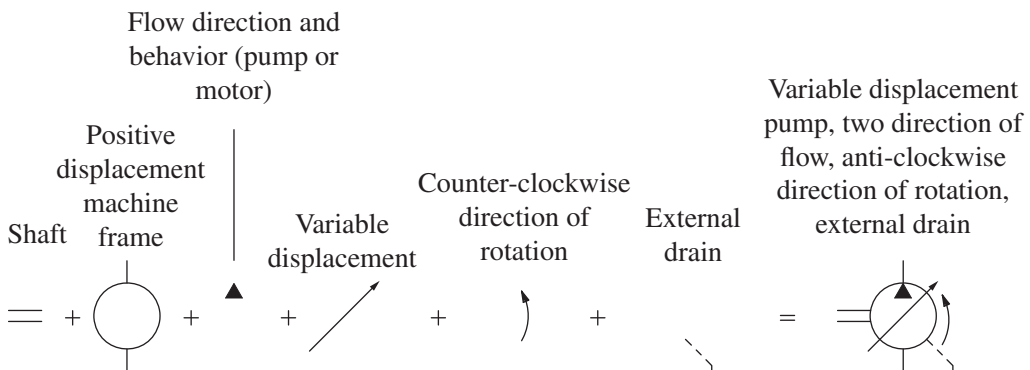
Figure 6.8 Procedure for assembling a pump symbol. The factors to be considered are the direction of the flow, the fixed or variable displacement nature of the unit, the direction of rotation, and the presence of an external drain.

	Fixed Displacement		Variable Displacement	
	One direction of flow	Two direction of flow	One direction of flow	Two direction of flow
Pump				

Figure 6.9   ISO symbols of the most common pumps.

6.5 Ideal Equations

As clearly shown by the wobble plate pump example, the ideal – or theoretical – flow rate of pumps and motors is proportional to the shaft speed and the unit displacement. Considering that the primary function of a pump (P) is to generate flow, while for a motor (M) is to produce shaft

	Fixed Displacement		Variable Displacement	
	One direction of flow	Two direction of flow	One direction of flow	Two direction of flow
MOTOR				
	One direction of flow	Two direction of flow	One direction of flow	Two direction of flow
PUMP/MOTOR				

Figure 6.10   Symbol breakdown for a hydraulic motor (top) and ISO symbols of the most common motors in hydraulic applications (bottom table).

speed, relations (6.10a) and (6.10b) are used respectively for describing the operation of pumps and motors[4]:

$$Q_{P,i} = V_{D,P} \cdot n_P \tag{6.10a}$$

$$n_{M,i} = \frac{Q_M}{V_{D,M}} \tag{6.10b}$$

The subscript i stands for *ideal*.

The value of V_D is the actual displacement. In case of a variable displacement unit this is determined with Eq. (6.9). With reference to Figure 6.2, by equating the input and output power terms of Eq. (6.3a), it is possible to derive the following ideal relationships between the shaft torque and the port pressure difference[5]:

$$T_{p,i} = V_{D,p} \cdot (p_2 - p_1)_p \tag{6.11a}$$

$$(p_1 - p_2)_{m,i} = \frac{T_m}{V_{D,m}} \tag{6.11b}$$

Equations (6.11a) and (6.11b) reflect the different nature of pumps and motor and also show their different logic of operation: a pump requires input torque to generate flow against the load (which sets the pressure). A motor needs a high enough supply pressure in order to rotate the shaft against a resistive torque.

6.6 The Real Case

The cases analyzed so far assumed that the energy conversion happens without losses. In other words, all the mechanical power is transferred to useful hydraulic power (or vice versa). In the real case, energy losses are present in the operation of pumps and motors. These phenomena negatively affect the energy conversion ability of the unit, causing a lower power output respect to the ideal

---

4 with the units commonly used in hydraulics:

$$Q_{P,i}(l/\min) = V_{D,P}[cm^3/rev] \cdot n_P[rpm] \cdot \left(\frac{1}{1000}\right) \left[\frac{l/min}{cm^3/rev \cdot rpm}\right]$$

$$n_{M,i}(rpm) = \frac{Q_M[l/min]}{V_{D,M}[cm^3/rev]} \cdot (1000) \left[\frac{cm^3/rev \cdot rpm}{l/min}\right]$$

$$Q_{P,i}(gpm) = V_{D,P}[cm^3/rev] \cdot n_P[rpm] \cdot \left(\frac{1}{3785}\right) \left[\frac{gpm}{cm^3/rev \cdot rpm}\right]$$

$$n_{M,i}(rpm) = \frac{Q_M[gpm]}{V_{D,M}cm^3/rev} \cdot (3785) \left[\frac{cm^3/rev \cdot rpm}{gpm}\right]$$

5 with the units commonly used in hydraulics

$$T_{P,i}(Nm) = V_{D,P}[cm^3/rev] \cdot (p_1 - p_2)_p[bar] \left(\frac{1}{20 \cdot \pi}\right) \left[\frac{Nm}{cm^3/rev \cdot bar}\right]$$

$$(p_1 - p_2)_{M,i}(bar) = \frac{T_M(N \cdot m)}{V_{D,M}[cm^3/rev]} (20 \cdot \pi) \left(\frac{bar \cdot cm^3/rev}{Nm}\right)$$

$$T_{P,i}(ft \cdot lbf) = V_{D,P}[cm^3/rev] \cdot (p_1 - p_2)_p[psi] \left(\frac{1}{1235}\right) \left[\frac{ft \cdot lbf}{cm^3/rev \cdot psi}\right]$$

$$(p_1 - p_2)_{M,i}(psi) = \frac{T_M[ft \cdot lbf]}{V_{D,M}[cm^3/rev]} (1235) \left[\frac{psi \cdot cm^3/rev}{ft \cdot lbf}\right]$$

case (Figure 6.2). The energy conversion performance of a hydrostatic unit is quantified by the overall efficiency:

$$\eta_t = \frac{P_{out}}{P_{in}} \tag{6.12}$$

By expressing the mechanical and hydraulic power, the formulas for the overall efficiencies of real pumps and motors can be calculated as follows[6]:

$$\eta_{t,P} = \frac{(p_2 - p_1) \cdot Q_{P,e}}{T_{P,e} \cdot n_P} \tag{6.13a}$$

$$\eta_{t,M} = \frac{T_M \cdot n_{M,e}}{(p_1 - p_2)_e \cdot Q_M} \tag{6.13b}$$

The notation used in Eqs. (6.13a) and (6.13b) highlights with the subscript "*e*" the actual values, which differ from the ideal one. In particular, an actual pump working at a given pressure $(p_2 - p_1)$ and shaft speed n_p delivers a lower flow $Q_{P,e}$ and requires more shaft torque $T_{P,e}$ with respect to the ideal case. For an actual motor working with a given resistant torque T_M that receives an input flow rate Q_M, the pressure level $(p_1 - p_2)_e$ is higher than the ideal case, while the actual rotation speed $n_{M,e}$ is lower.

6.7 Losses in Pumps and Motors

The case of the plunger pump previously presented can be useful to describe the different sources of energy loss in energy conversion units. These losses can be generically associated with three possible sources:

- Fluid compressibility
- Internal and external leakage
- Viscous and turbulence resistance

The detailed analysis of the losses occurring in a hydrostatic pump or motor is a topic deeply studied by several researchers. A detailed description of these losses, along with extensive numerical approaches for their evaluation, is reported in specialized books such as references [4–6] and numerous research papers. Among others, important authors in this field are Ivantysynova, Manring, Bergada, Yamaguchi, Hooke for the case of axial piston machines, and Vacca, Mucchi, Borghi for the case of gear machines. As concerns experimental methods for measuring efficiencies of hydrostatic units, the reader is encouraged to refer to the standard ISO 4409 [7].

The following sections only provide the essential aspects of the losses occurring in hydrostatic units so that the reader can gather a general understanding of the factors affecting the actual performance of a hydrostatic pump or motor. For more details, the reader is encouraged to refer to the abovementioned references.

---

6 With the units commonly used in hydraulics

$$\eta_{t,P} = \frac{(p_2 - p_1)\,[bar] \cdot Q_{P,e}\,[l/min]}{T_{P,e}\,[Nm] \cdot n_P\,[rpm]} \cdot \frac{50}{\pi} \left[\frac{Nm \cdot rpm}{bar \cdot l/min} \right]$$

$$\eta_{t,M} = \frac{T_M\,[Nm] \cdot n_{M,e}\,[rpm]}{(p_2 - p_1)_e\,[bar] \cdot Q_M\,[l/min]} \cdot \frac{\pi}{50} \left[\frac{bar \cdot l/min}{Nm \cdot rpm} \right]$$

$$\eta_{t,P} = \frac{(p_2 - p_1)[psi] \cdot Q_{P,e}\,[gpm]}{T_{p,e}\,[ft\,lbf] \cdot n_P\,[rpm]} \cdot 8.4 \left[\frac{ft\,lbf \cdot rpm}{psi \cdot gpm} \right]$$

$$\eta_{t,M} = \frac{T_M\,[ft\,lbf] \cdot n_{M,e}\,[rpm]}{(p_2 - p_1)_e\,[psi] \cdot Q_M\,[gpm]} \cdot \frac{1}{8.4} \left[\frac{psi \cdot gpm}{ft\,lbf \cdot rpm} \right]$$

6.7.1 Fluid Compressibility

As explained in Chapter 2, the relationship between the pressure and the volume of a fluid is expressed by the bulk modulus:

$$B = -V_0 \left(\frac{\Delta p}{\Delta V} \right) \tag{6.14}$$

The rectangular shape of the pressure/volume relationship for an ideal pump was shown in Figure 6.5. In the real case, this chart becomes the one shown in Figure 6.11 because of the volume changes of the fluid during the compression and expansion phases. The displacement chamber is closed to both inlet and outlet ports during the compression and expansion process[7].
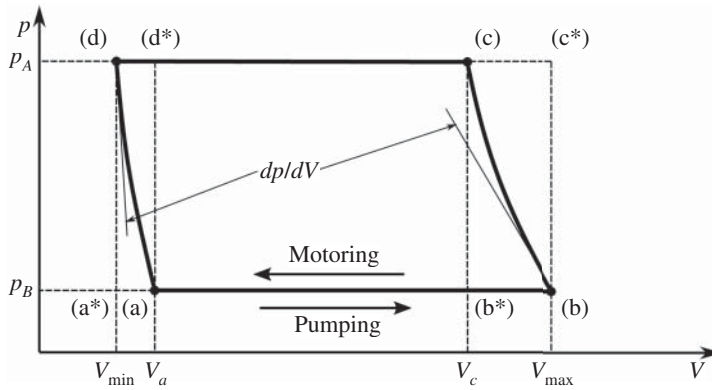
Figure 6.11 Displacing cycle of an ideal hydrostatic machine with compressible fluid.

The inclination on the (b) to (c) side is always greater than that on the (d) to (a) side because the fluid volume is greater on the (b) to (c) side.

In the case of the pump, the displacement chamber only opens to the outlet port from (c) to (d). Therefore, the output energy, E_{out}, can be represented by the rectangular *area* (a*) to (b*) to (c) to (d):

$$E_{\text{out}} = (p_A - p_B) \cdot (V_c - V_d) \tag{6.15}$$

The input energy E_{in} is instead represented by the area enclosed by the trapezoidal path (a) to (b) to (c) to (d). Comparing to the area that illustrates the output energy, the triangular area on the right side (b*) to (b) to (c) is the energy used to compress the fluid and it is equal to

$$E_{\text{cp}} = \int_{V_b}^{V_c} p dV \tag{6.16}$$

The triangular area on the left side (a*) to (a) to (d) is instead an energy that is recovered, due to the fluid expansion:

$$E_{\text{ep}} = \int_{V_d}^{V_a} p dV \tag{6.17}$$

Therefore, the input energy of the pump using compressible fluid is

$$E_{\text{in}} = E_{\text{out}} + E_{\text{cp}} - E_{\text{ep}} \tag{6.18}$$

———

7 In the ideal case (incompressible fluid), as shown in Figure 6.4, the commutation of the spool corresponds to the plunger dead end positions. In the real case (compressible fluid), however, the commutation happens only when the piston chamber has equalized the port pressure. Therefore, at the dead ends, there are instances where the cylinder chamber remains isolated from A and B.

According to the definition of the ISO standard, the power loss due to the compression effect is

$$P_{L,\text{compr},P} = \dot{E}_{\text{cp}} - \dot{E}_{\text{ep}} \tag{6.19}$$

where $\dot{E}_{\text{cp}}$ and $\dot{E}_{\text{ep}}$ are the time derivatives of the terms E_{cp} and E_{ep}.

The power loss expressed by Eq. (6.19) can be further divided into a volumetric and a mechanical contribution. The volumetric one represents the flow rate loss due to the fluid compressibility and it is equal to

$$\Delta V_{\text{compr},P} = V_{\text{max}} \cdot \frac{p_A - p_B}{B} \tag{6.20}$$

This expression can be derived from the bulk modulus definition of Eq. (6.14).

In terms of flow rate, the volumetric loss becomes

$$Q_{\text{compr},P} = n \cdot V_{\text{max}} \cdot \frac{p_A - p_B}{B} \tag{6.21}$$

Therefore,

> For a hydrostatic pump, the volumetric loss due to the compression effect is proportional to the pressure difference as well as the shaft speed.

Considering the usual symbol to indicate proportionality,

$$\begin{aligned} Q_{\text{compr},P} &\propto \Delta p \\ Q_{\text{compr},P} &\propto n \end{aligned} \tag{6.22}$$

The torque loss due to the compression effect can be calculated from the power loss in Eq. (6.19) and the volumetric loss in Eq. (6.21):

$$T_{\text{compr},P} = \frac{P_{L,\text{compr},P} - \Delta p \cdot Q_{\text{compr},P}}{n} \tag{6.23}$$

With reference to Figure 6.11, the power loss due to the compression effect $P_{L,\,\text{compr}}$ can be defined from the areas $A_{\text{bcb}*}$, $A_{\text{ada}*}$:

$$Pl_{\text{compr},P} = A_{\text{bcb}*} - A_{\text{ada}*} \tag{6.24}$$

The power loss associated with the compressive volumetric loss is also

$$Pl_{\text{compr,vol},P} = \Delta p \cdot Q_{\text{compr},P} = A_{\text{bc}*\text{cb}*} \tag{6.25}$$

By comparing the areas in Eq. (6.24) and Eq. (6.25), the torque loss due to the compression effect T_{compr} can be found negative, which, due to compressibility, the torque required for an ideal pump operating with a compressible fluid is less than the value obtained with an incompressible fluid.

The above analysis was for the case of a pump. In case of a motor, the direction of the power flow is opposite to the pump case. Therefore, the previous equations change as follows:

$$\begin{aligned} E_{\text{in}} &= (p_A - p_B) \cdot (V_c - V_d) \\[4pt] E_{\text{ep}} &= \int_{V_b}^{V_c} p\,dV \\[4pt] E_{\text{cp}} &= \int_{V_b}^{V_c} p\,dV \\[4pt] E_{\text{out}} &= E_{\text{in}} + E_{\text{ep}} - E_{\text{cp}} \\[4pt] P_{L,\text{compr},M} &= \dot{E}_{\text{cp}} - \dot{E}_{\text{ep}} \end{aligned} \tag{6.26}$$

Note that for an ideal motor, the energy required to compress the fluid is less than the energy that is recovered during the expansion. Therefore, the power loss due to the compression effect in an ideal motor is negative.

In other words,

> The hydrostatic motor benefits from the effects of fluid compressibility. This is one of the reasons motors usually have better efficiencies than pumps.

Furthermore, for a motor the volumetric loss due to the compression effect is

$$Q_{\text{compr},M} = n \cdot (V_c - V_{c*}) \tag{6.27}$$

The volumetric loss due to the compression effect for a motor can be found negative. Like the power gain, this volumetric gain is due to the expansion of the fluid in the displacement chamber.

The torque loss due to the compression effect for a motor also follows an equation similar to Eq. (6.23):

$$T_{\text{compr},M} = \frac{P_{L,\text{compr},M} - \Delta p \cdot Q_{\text{compr},M}}{n} \tag{6.28}$$

6.7.2 Internal and External Leakage

Any positive displacement pump is formed by elements in relative motion. For example, in the case of the plunger pump, both the plunger and the spool move into the bores. The relative motion between the elements is made possible because of the gaps between the mechanical parts. These gaps also represent tiny restrictions, separating chambers at different pressure levels. This fact inevitably causes leakages. In general, leakages can be classified into two categories: external and internal.

Internal leakages occur between displacement chambers or between the inlet and outlet ports of the unit, for example, leakages across the spool of Figure 6.12 recirculating oil from port A to port B. **External leakages** occur toward a separate volume, which is usually the pump case, which is separately drained to the tank. For example, the leakages escaping between the plunger and its bore are collected in the pump case. Not all pump architectures (e.g. gear or vane) present external leakages.

> Internal leakages occur between displacement chambers or between the inlet and the outlet port. Instead, external leakages are collected to a separated volume and drained to tank.
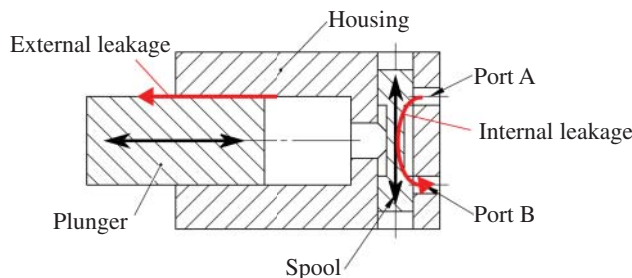
Figure 6.12 Examples of external leakage and internal leakage.

Leakages are undesirable because they decrease the volumetric performance of the machine. However, they also provide some benefits, and for most pumps and motors, they have a functional behavior. In fact, with the reference to the case of Figure 6.12, the oil lost between the plunger and its bore lubricates and cools the elements in relative motion. Furthermore, the internal leakage between high- and low-pressure ports can smoothen pressure spikes occurring inside the displacement chambers, during the commutations between the inlet and outlet ports. These details apply, for example, to the case of axial piston pumps and will be explained later in this Chapter. In general, the power loss due to leakages is given in Eq. (6.29):

$$P_{L,\text{leak}} = Q_{\text{leak}} \cdot \Delta p \tag{6.29}$$

The leakage flow is in most cases laminar, therefore Q_{leak} is linearly proportional to the pressure difference Δp according to Eq. (3.39). In a typical situation, the leakage flow Q_{leak} develops through a rectangular flow passage. This is usually a good assumption since the gap height, h, is very small (in order of few microns). Therefore:

$$Q_{\text{leak}} = \frac{b \cdot h^3 \cdot \Delta p}{12 \cdot \mu \cdot L} \tag{6.30}$$

In Eq. (6.29), b represents the width of the gap, while L the length of the gap. Therefore, the hydraulic resistance representing the leakage is:

$$R_{\text{lam}} = \frac{b \cdot h^3}{12 \cdot \mu \cdot L} \tag{6.31}$$

For gap geometries significantly different than a rectangular shape, other expressions for R_{lam} can be found. A good set of examples can be found in [8].

> Internal and external leakages are proportional to the gap height and to the pressure difference at the unit ports. They are inversely proportional to fluid viscosity.

6.7.3 Friction

As mentioned before, pumps and motors are based on elements in relative motion. The gap between the parts in relative motion is very tight, normally in the order of magnitude of few microns. The fluid in the gap together with the two solid boundaries forms a lubricating interface. The viscous friction in the lubricating interface is responsible for most of the friction losses in hydrostatic pumps or motors.

By setting the coordinate system on one of the solid boundaries, the other boundary moves at the relative velocity v_r. As explained in Chapter 2, the fluid velocity in the gap (which height is h) follows a linear relationship with the vertical position z:

$$v = v_r \cdot \frac{z}{h} \tag{6.32}$$

A typical hydraulic oil follows the Newtonian behavior; therefore, the shear stress on the moving boundary is a function of the fluid viscosity μ:

$$\tau = \mu \cdot \frac{dv}{dz} = \mu \cdot \frac{v_r}{h} \tag{6.33}$$

The shear stress is proportional to the relative velocity and the reciprocal of the gap height. The friction force on the moving boundary is then

$$F_T = \int_A \tau \cdot dA \tag{6.34}$$

The power loss due to this friction force is then

$$P_{L,\text{friction}} = F_T \cdot v_r \tag{6.35}$$

The torque loss at the shaft, due to the friction force is instead

$$T_\mu = C_{T\mu} \cdot \frac{\mu}{h} \cdot n \tag{6.36}$$

where $C_{T\mu}$ is a constant. For a pump, the term T_μ is an additional torque requested at the shaft. For a motor, it represents a value that needs to be subtracted at the output shaft.

> Frictional losses in a hydrostatic unit occur between the parts in relative motion. They affect the actual shaft torque and are proportional to the shaft speed and to the fluid viscosity. The frictional losses depend on the geometric clearance, and they reduce with an increasing gap height.

It can be interesting to note the opposing effects that geometrical clearance have on the power loss of hydrostatic units. From the volumetric standpoint, the clearances defining the gaps between moving parts needs to be small, to limit the volumetric losses Q_{leak}. Instead, from the mechanical point of view, it is convenient to operate with large gaps to reduce frictions. As one can observe from Eq. (6.31), the term R_{lam} has cubic dependence to the gap height, which dominates over the linear trend of Eq. (6.32). Therefore, it is more important to implement units with minimum gap heights (in order of microns).

Fluid viscosity is also present with opposite effects in both loss terms, due to leakage and friction. The opposite tendency is linear in both cases, as it can be observed from Eqs. (6.31) to (6.32). Therefore, for this case, the optimal fluid viscosity for a hydrostatic unit results from a trade-off between these two loss terms. Since viscosity is highly dependent on temperature (see Chapter 2), it is important to operate a hydraulic unit within the optimal range of temperature. The energy efficiency of a hydrostatic pump or motor highly depends on fluid viscosity and therefore fluid temperature. The operation of the hydraulic system at a controlled temperature (possibly near the optimal energy efficiency point) is often a requirement for many hydraulic machines. Heater and coolers can be used to serve this purpose.

6.7.4 Other Types of Losses

Turbulent Losses
The flow through positive displacement machines is subjected to losses due to the connections between the displacement chambers and the inlet and outlet ports. These connections can be viewed as orifices, whose area depends on the machine design. For the wobble pump used as reference example, the area opening of the spool valve determines the orifice area.

The presence of these orifices results in a pressure differential between the pressure value at the port and the pressure inside the displacement chamber, as shown in Figure 6.13. This pressure differential is regulated by the orifice equation presented in Chapter 4, and it has a quadratic dependence with the pump flow. According to Eq. (6.10a), the flow is proportional to the pump speed. Therefore, the above pressure differential is proportional to the unit shaft speed.

The pressure differential translates into a torque loss. In fact, a pump must pressurize the displacement chambers to a higher level than the outlet. For a motor, the actual pressure differential available to produce torque is lower than the value that can be calculated from the port pressures.
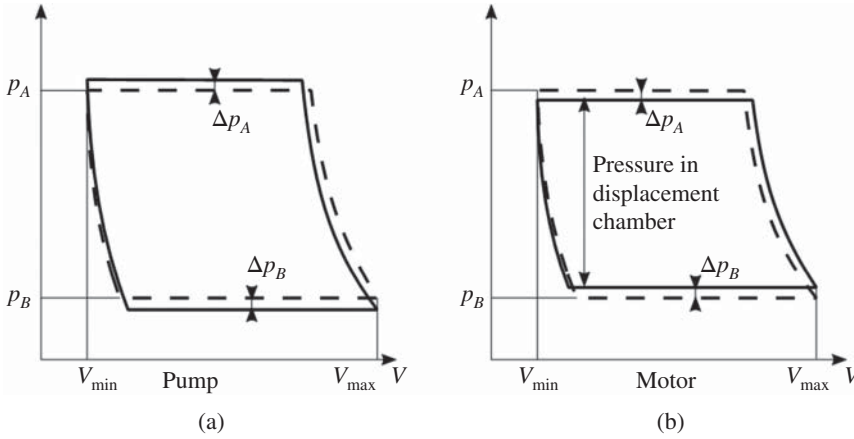
Figure 6.13 Effect of turbulent losses: (a) pump; (b) motor.

Following the relationship in Eq. (6.32), the torque loss due to turbulent resistance can be generally expressed as

$$T_\rho = C_{T\rho} \cdot \rho \cdot n^2 \tag{6.37}$$

where $C_{T\rho}$ is also a constant factor.

Churning Losses

Churning loss is another type of torque loss. These losses are caused by the motion of all the rotating parts in the machine housing filled with fluid [4]. This term is proportional to the square of the relative velocity:

$$F_\rho = \int_A \rho \cdot v_r^2 \cdot c_d \cdot dA \tag{6.38}$$

It is clear that the churning losses have the same relation of the turbulent losses. Therefore, Eq. (6.37) can be used to include also churning losses.

Pressure-Dependent Torque Loss

A torque loss univocally dependent on the operating pressure is also very common in hydrostatic pumps and motors. Even though the torque loss has no direct relationship with the operating pressure of the machine, higher pressure normally cause higher load on the lubricating interfaces. This results in lower gap height h and consequently higher shear stresses (Eq. (6.33)). This torque loss linearly dependent on pressure can be expressed as

$$T_p = C_{Tp} \cdot \Delta p \tag{6.39}$$

where $C_{T\rho}$ is another constant factor.

Incomplete Filling

A volumetric loss due to *incomplete filling* occurs when a hydrostatic unit (either pump or motor) operates at a very high speed and the fluid entering the inlet port cannot completely fill the displacement chamber.

The relationship between the volumetric loss due to incomplete filling and the pump speed is qualitatively shown in Figure 6.14 where the incomplete filling effects only occurs in the high shaft speed regions.
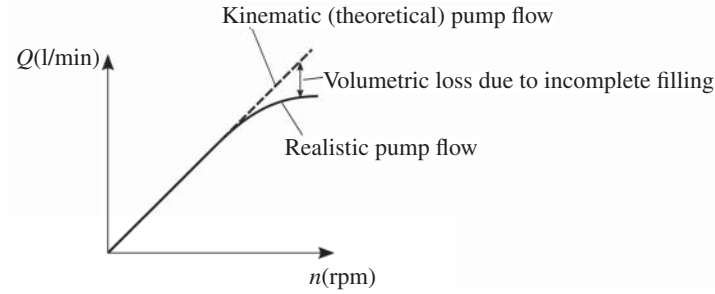
Figure 6.14 Incomplete filling.

6.8 Volumetric and Hydromechanical Efficiency

The previous section highlighted how losses occurring in hydrostatic units can impact the flow rate across the unit (volumetric losses) or the torque at the unit's shaft (mechanical losses). The contribution of these losses on the unit's efficiency can be separately analyzed by considering the volumetric and hydromechanical efficiency. Also, in this case, these definitions follow standard ISO 4391 [1].

The leakages and the compressibility losses affect the so-called volumetric performance of the machine, which can be quantified by the parameter *volumetric efficiency*. For a pump, this equates[8]:

$$\eta_{v,P} = \frac{Q_{P,e}}{n_P \cdot V_{D,P}} \tag{6.40}$$

Since for an actual motor the leakages cause a lower rotational shaft speed, with respect to the ideal case, the volumetric efficiency is defined as

$$\eta_{v,M} = \frac{n_{M,e}}{n_{M,i}} = \frac{n_{M,e} \cdot V_{D,M}}{Q_{M,e}} \tag{6.41}$$

The last equation implies that the actual input flow rate to a motor to achieve a target shaft speed is higher than the ideal flow rate.

For a pump, the **volumetric efficiency** is the ratio between the actual output flow and the ideal one. For a motor, the volumetric efficiency is the ratio between the actual shaft speed and the ideal one. In both cases the volumetric efficiency is a measure of the leakage loss occurring in the machine.

Frictional losses due to the presence of parts in relative motion and due to fluid shear cause a higher torque necessary to drive a pump working at a given pressure, with respect to the ideal

---

8 With the units commonly used in hydraulics

$$\eta_{v,P} = \frac{Q_{P,e}[l/min]}{n_P[rpm] \cdot V_{D,P}[cm^3/rev]} \cdot 1000 \left[\frac{cm^3/rev \cdot rpm}{l/min} \right]$$

$$\eta_{v,M} = \frac{n_{M,e}[rpm] \cdot V_{D,M}[cm^3/rev]}{Q_{M,e}[l/min]} \cdot \frac{1}{1000} \left[\frac{l/min}{cm^3/rev \cdot rpm} \right]$$

$$\eta_{v,P} = \frac{Q_{P,e}[gpm]}{n_P[rpm] \cdot V_{D,P}[cm^3/rev]} \cdot 3785 \left[\frac{cm^3/rev \cdot rpm}{gpm} \right]$$

$$\eta_{v,m} = \frac{n_{m,e}[rpm] \cdot V_{D,m}[cm^3/rev]}{Q_{m,e}[gpm]} \cdot \frac{1}{3785} \left[\frac{gpm}{cm^3/rev \cdot rpm} \right]$$

case. This aspect is measured by the so-called *torque efficiency* (also often referred as *hydraulic mechanical efficiency*, or *hydromechanical efficiency*). For a pump, this is[9]

$$\eta_{hm,P} = \frac{T_{P,i}}{T_{P,e}} = \frac{V_{D,P} \cdot (p_2 - p_1)}{T_{P,e}} \tag{6.42}$$

For a motor working with a given torque load, the presence of frictional losses implies a higher supply pressure; therefore, the torque efficiency can be expressed as

$$\eta_{hm,M} = \frac{(p_1 - p_2)_i}{(p_1 - p_2)_e} = \frac{T_{M,e}}{V_{D,M} \cdot (p_1 - p_2)_e} \tag{6.43}$$

> For a pump, the **torque efficiency** is the ratio between the ideal shaft torque and the actual one. For a motor, it represents the ratio between the actual shaft torque and the ideal one. In both cases the torque efficiency is a measure of the torque loss occurring in the machine.

The reader can easily verify the relationship between the three efficiencies (overall, volumetric, and hydraulic mechanical), for both the cases of pump and motor:

$$\eta_t = \eta_v \cdot \eta_{hm} \tag{6.44}$$

> The overall energy efficiency of a hydrostatic unit is the product between the volumetric efficiency and the torque efficiency.

Example 6.1   Flow, torque and power consumption of an hydraulic pump

A 75 cm^3/rev fixed displacement pump rotates at 1800 rpm and supplies a hydraulic actuator with flow. The load on the actuator pressurizes the pump outlet at 180 bar (gage pressure). The pump inlet port is connected to a reservoir at atmospheric pressure. Draw an ISO schematic of the system and calculate

a) The flow rate delivered by the pump in the ideal case
b) The torque at the pump shaft in the ideal case
c) The power consumption in the ideal case
   A flow meter and a torque meter are used to measure the actual values of flow rates and shaft torque. The sensor readings are 127 l/min and 234 Nm. Determine
d) The volumetric efficiency of the pump
e) The hydromechanical efficiency of the pump

---

9 With the units commonly used in hydraulics

$$\eta_{hm,P} = \frac{V_{D,P}[cm^3/rev] \cdot (p_2 - p_1)[bar]}{T_{P,e}[Nm]} \cdot \frac{1}{20 \cdot \pi} \left[\frac{Nm}{cm^3/rev \cdot bar} \right]$$

$$\eta_{hm,M} = \frac{T_{M,e}[Nm]}{V_{D,M}[cm^3/rev] \cdot (p_1 - p_2)_e[bar]} \cdot 20 \cdot \pi \left[\frac{cm^3/rev \cdot bar}{Nm} \right]$$

$$\eta_{hm,P} = \frac{V_{D,P}[cm^3/rev] \cdot (p_2 - p_1)[psi]}{T_{P,e}[ft \cdot lbf]} \cdot \frac{1}{1235} \left[\frac{ft \cdot lbf}{cm^3/rev \cdot psi} \right]$$

$$\eta_{hm,M} = \frac{T_{M,e}[ft \cdot lbf]}{V_{D,M}[cm^3/rev] \cdot (p_1 - p_2)_e[psi]} \cdot 1235 \left[\frac{cm^3/rev \cdot psi}{ft \cdot lbf} \right]$$

f) The overall efficiency of the pump
g) The actual power consumption of the pump

Given:

Pump displacement $V_D = 75\ cm^3/rev$; pump differential pressure $(p_2 - p_1)_P = 180\ bar$; measured torque $T_{P,e}$; and measured flow rate $Q_{P,e}$

Find:

a) Ideal pump flow rate, $Q_{P,i}$
b) Ideal pump torque, $T_{P,i}$
c) The volumetric efficiency of the pump, $\eta_{v,P}$
d) The hydromechanical efficiency of the pump, $\eta_{hm,P}$
e) The overall efficiency of the pump, $\eta_{tot,P}$
f) The actual power consumption of the pump, $P_{in,e}$

Solution:

The system can be represented by the following ISO schematic:
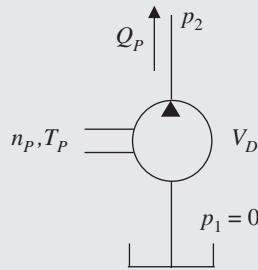
a) The ideal pump flow rate can be determined from Eq. (6.10a):

$$Q_{P,i} = V_{D,P} \cdot n_P = 75\ [cm^3/rev] \cdot 1800\ [rpm] \left(\frac{1}{1000}\right) = 135\ l/min$$

b) The ideal torque can be determined from Eq. (6.11a):

$$T_{P,i} = V_{D,P} \cdot (p_2 - p_1)_P = 75\ [cm^3/rev] \cdot 180\ [bar] \left(\frac{1}{20\cdot\pi}\right) = 214.9\ Nm$$

c) In the ideal case, the pump converts the whole mechanical power at the shaft into hydraulic power. Therefore, the power consumption can be determined by evaluating both terms:

$$P_{in} = T_{P,i} \cdot n_P = 214.9\ [Nm] \cdot 1800\ [rpm] \cdot \left(\frac{\pi}{30\,000}\right) = 40.5\ kW$$

$$P_{out} = Q_{P,i} \cdot (p_2 - p_1)_P = 135\ [l/min] \cdot 180\ [bar] \cdot \left(\frac{1.66}{1000}\right) = 40.5\ kW$$

d) The sensors measure the actual pump flow rate and shaft torque; therefore, according to Eq. (6.40):

$$\eta_{v,P} = \frac{Q_{P,e}}{n_P \cdot V_{D,P}} = \frac{Q_{P,e}}{Q_{P,i}} = \frac{127\ [l/min]}{135\ [l/min]} = 0.941\ (or\ 94.1\%)$$

e) The hydro-mechanical efficiency can be calculated with Eq. (6.42):

$$\eta_{hm,P} = \frac{T_{P,i}}{T_{P,e}} = \frac{214.9\ [Nm]}{234\ [Nm]} = 0.918\ (or\ 91.8\%)$$

Example 6.1 (Continued)

f) In this problem, the total efficiency can be calculated in two ways: the easiest one is through formula (6.44), using the values of the efficiencies above calculated:

$\eta_t = \eta_v \cdot \eta_{hm} = 0.941 \cdot 0.918 = 0.864$ (*or* 86.4%)

Alternatively, formula 6.13a can be used

$$\eta_{t,P} = \frac{(p_2 - p_1) \cdot Q_{P,e}}{T_{P,e} \cdot n_P} = \frac{180\,[bar] \cdot 127\,[l/min]}{234\,[Nm] \cdot 1800\,[rpm]} \cdot \frac{50}{\pi} = 0.864\,(or\,86.4\%)$$

g) The actual power consumption can be calculated with Eq. (6.13a) or simply by using the ideal power (c) and the total efficiency:

$$P_{in,e} = \frac{P_{in,i}}{\eta_{t,P}} = \frac{40.5\,[kW]}{0.864} = 46.9\,kW$$

In many fluid power problems, as in Example 6.1, the efficiency of actual units can be approximated using a constant value, as will be often assumed in the next chapters. However, the efficiency of an actual unit depends on several operating parameters, such as pressure, speed, position of the setting, temperature, and fluid type.

6.8.1 Trends for Volumetric and Hydromechanical Efficiencies

The typical graphical trends for the volumetric and the torque efficiencies can be found by considering the loss terms previously discussed.

The volumetric loss includes the loss due to compressibility, to the leakages in laminar and turbulent flow, and to the loss due to incomplete filling. Figure 6.15 shows the relationships between the different types of volumetric losses and the operating pressure and speed. These trends can be derived from Eqs. (6.21), (6.27), and (6.29).

The hydraulic-mechanical (or torque) loss in a positive displacement machine includes the loss due to compressibility, the viscous friction, the churning motion, and the pressure dependent loss. Figure 6.16 shows the trends of these losses with the operating pressure and speed. These relationships can be derived from Eqs. (6.23), (6.28), (6.36), (6.37), and (6.39).
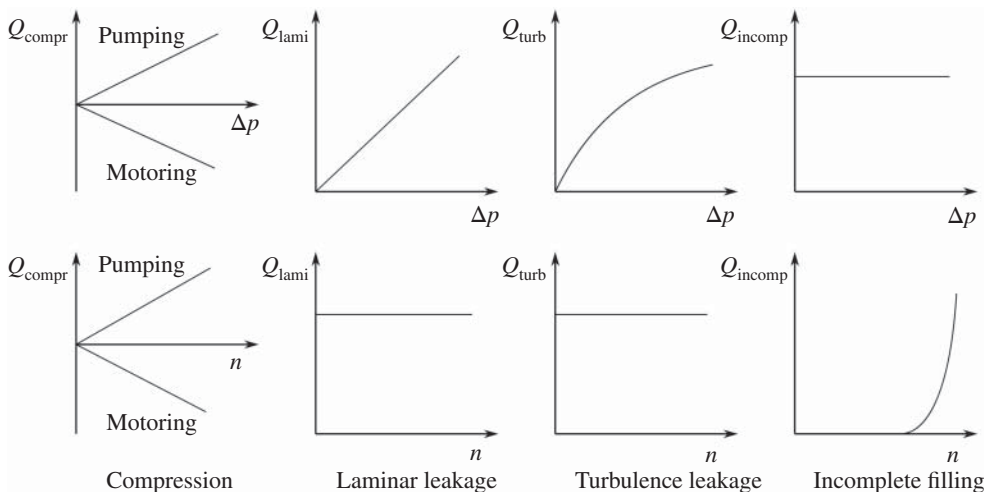
Figure 6.15 Trends for the volumetric losses.
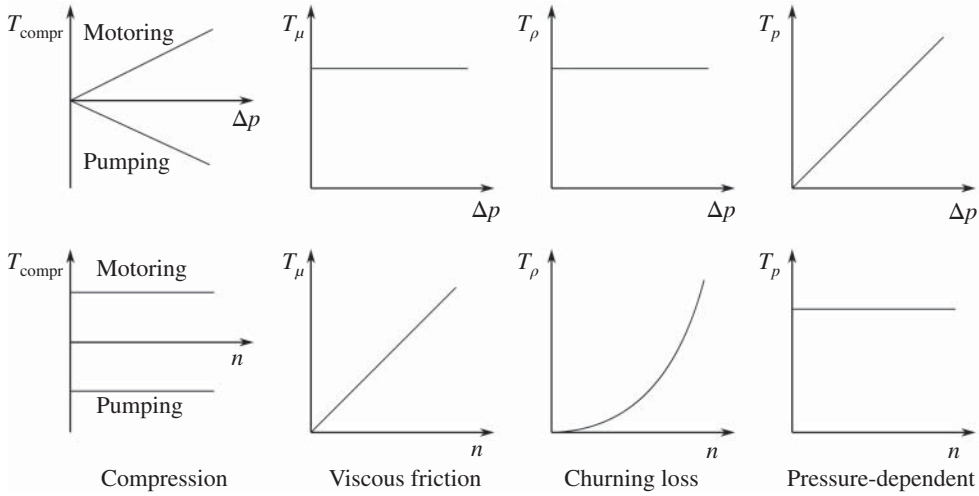
Figure 6.16 Trends for the hydraulic-mechanical losses.

The total volumetric loss of a hydrostatic pump or motor is the sum of the previously mentioned four types of volumetric losses:

$$Q_{\text{loss}} = Q_{\text{compr}} + Q_{\text{lami}} + Q_{\text{turb}} + Q_{\text{incomp}} \tag{6.45}$$

The total hydraulic-mechanical loss of a hydrostatic pump or motor is the sum of the previously mentioned four types of hydraulic-mechanical losses:

$$T_{\text{loss}} = T_{\text{compr}} + T_{\mu} + T_{\rho} + T_{p} \tag{6.46}$$

Combining Figures 6.15 and 6.16, the qualitative trends for volumetric efficiency, torque efficiency, and the total efficiency with respect to the operating pressure and speed for a hydrostatic pump can be shown in Figure 6.17. The volumetric efficiency decreases with the pressure and
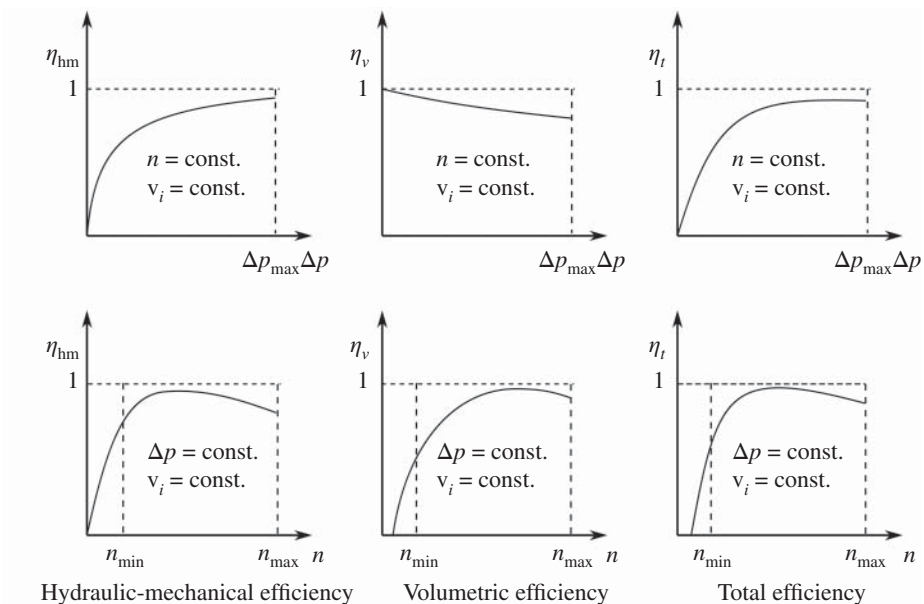
Figure 6.17 Qualitative representation of volumetric, hydraulic-mechanical, and overall efficiency of a pump as a function of operating pressure and operating speed.
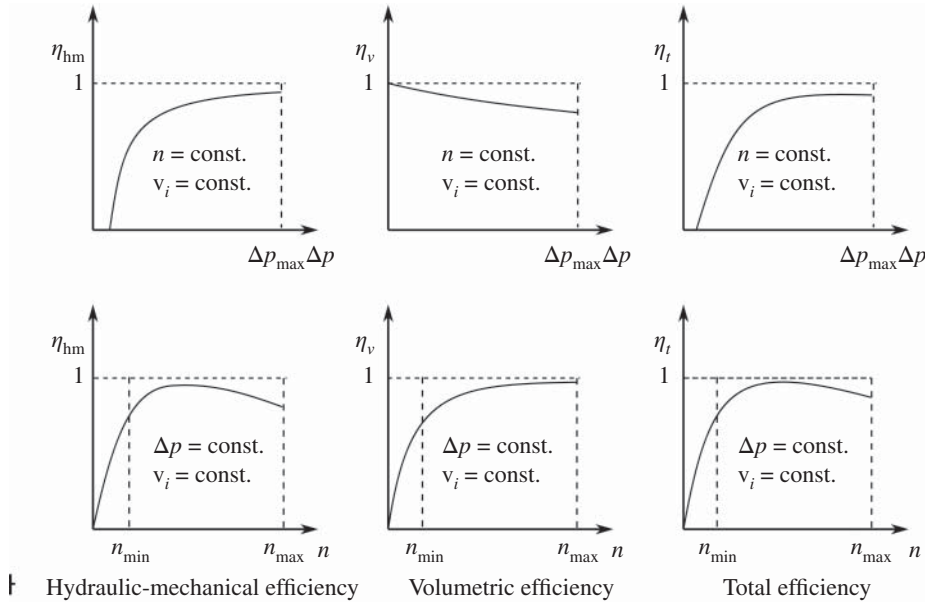
Figure 6.18 Qualitative representation of volumetric, hydraulic-mechanical, and overall efficiency of a motor as a function of supply pressure and operating speed.

increases with the speed considering that a higher pressure implies more leakage losses. However, a higher working speeds decreases the weight of the leakage losses with respect to the outlet flow.

The value of the hydraulic-mechanical efficiency is null at zero pressure and increases as the outlet pressure increases: this is because the internal frictions of the pump are only slightly affected by pressure and become less important as the working pressure rises. On the other hand, the same efficiency has a different trend with respect to the pump speed: when this is below the value of the minimum operating speed (dotted line), the hydraulic mechanical efficiency is very low. As the speed increases, the efficiency rapidly increases to its peak and then slowly decays. This trend can be explained as an effect of the fluid shear or churning losses.

The overall efficiency is the product of the two: its trend is shaped as a convex curve reaching a peak at approximately 75% of the rated pressure and 50% of the rated speed.

Figure 6.18 shows the same efficiency trends for the case of a hydraulic motor. The behavior is very similar to the case of a pump, with some minor differences.

First of all, the volumetric efficiency of the motor is null at very low speeds and starts increasing only when the supply flow is enough to overcome the internal leakages.

Second, the hydraulic-mechanical efficiency of the motor is null at very low pressure and starts increasing after a minimum pressure level, which illustrates an effect of the internal frictions that needs to be overcome by the pressure before the unit starts turning (startup torque). In addition, in the case of motors, it is important to consider the minimum operating speed, which can vary depending on the motor architecture (e.g. axial piston vs. radial piston motor).

Finally, it is useful to remark that motors usually have slightly higher volumetric efficiencies than pumps because the compressibility effect of the fluid acts against the pump efficiency and in favor of motor efficiency.

Example 6.2 Hydraulic winch system

A 20 cm^3/rev hydraulic motor drives a winch through a gearbox with ratio $i = n_{in}/n_{out} = 10$. The winch drum has a diameter $D = 200$ mm. The return line pressure $p_{out} = 10$ bar. Operating condition: The winch is lifting a load of 8000 N at 2.5 m/s.
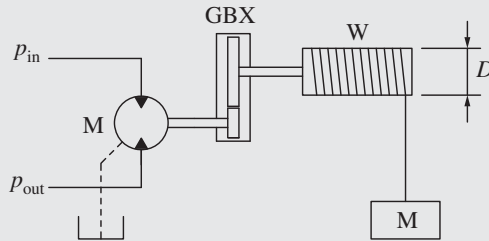
Calculate:

a) The flow rate required by the motor in the ideal case
b) The inlet pressure p_{in} required by the motor in the ideal case
c) The hydraulic power required by the motor in the ideal case

In the real case, the gearbox efficiency is 0.97. The hydraulic motor hydraulic-mechanical efficiency and volumetric efficiency can be found with the following efficiency maps:

Example 6.2 (Continued)
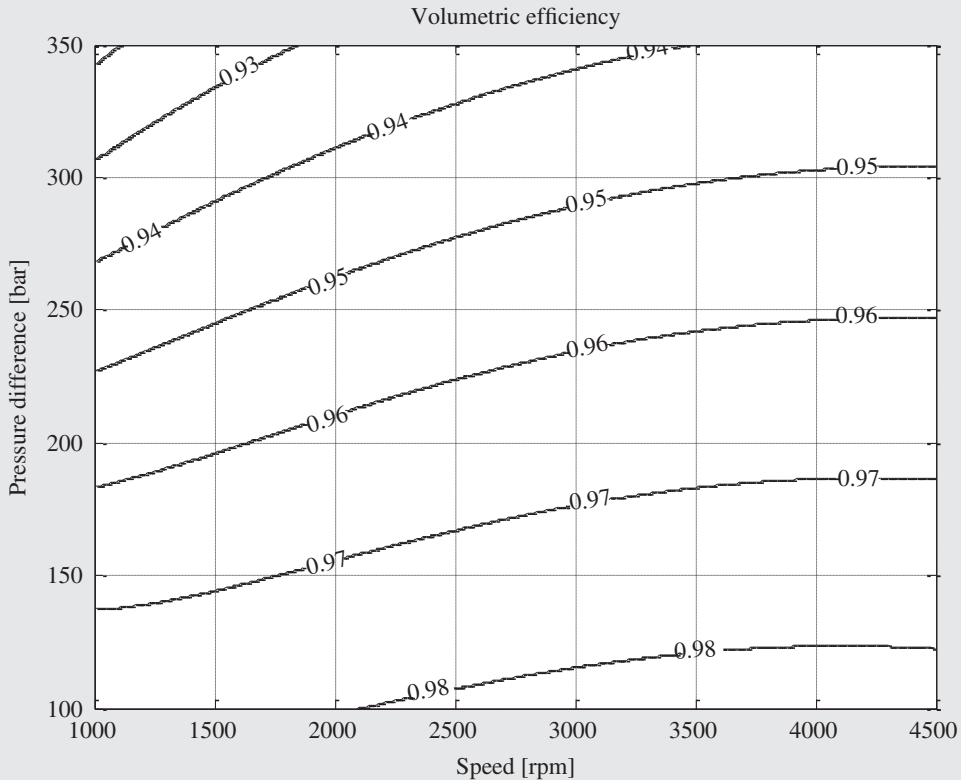
Hydraulic mechanical efficiency
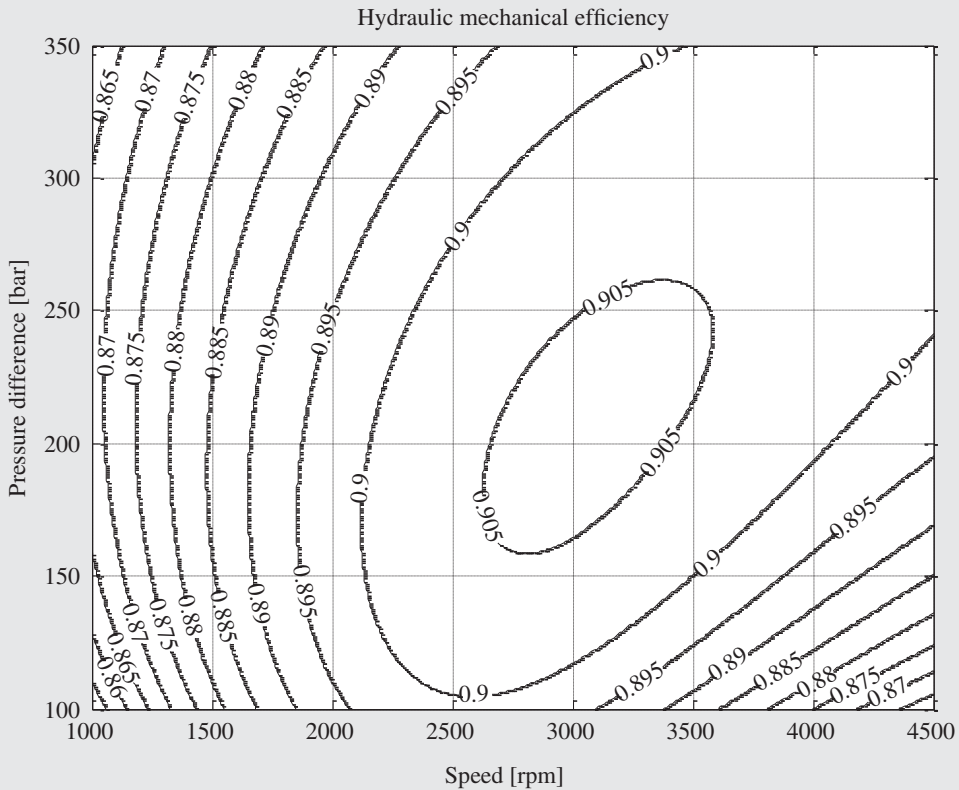
Find the volumetric efficiency and hydraulic-mechanical efficiency from the maps for the given operating condition and calculate

d. The flow rate required by the motor in the real case
e. The inlet pressure p_{in} required by the motor in the real case
f. The hydraulic power required by the motor in the real case
g. The total efficiency of the hydraulic motor

Given:
Motor displacement, $V_D = 20\ cm^3/r$; gearbox with ratio, $i = 10$; Diameter of the winch drum, $D = 200\ mm$; the return line pressure, $p_{out} = 10\ bar$; load, $F = 8000\ N$; load speed, $v = 2.5\ m/s$; gearbox efficiency, 0.97; motor efficiency plots.

Find:

a) Ideal motor flow rate, $Q_{M, i}$
b) Ideal motor inlet pressure, p_{in_i}
c) Ideal hydraulic power, P_i
d) Effective motor flow rate, $Q_{m, e}$
e) Effective motor inlet pressure, p_{in_e}
f) Effective hydraulic power, P_e
g) Total motor efficiency η_{tot}

Solution:

a) The winch drum rotational speed is

$$n_D = \frac{v}{\pi \cdot D} = 2.5 \,[m/s] \cdot \frac{60\,000}{\pi \cdot 200 \,[mm]} = 239 \, rpm$$

The motor speed is

$$n_M = n_D \cdot i = 239 \,[rpm] \cdot 10 = 2390 \, rpm$$

The ideal motor flow rate follows Eq. (6.10a):

$$Q_{M,i} = V_{D,M} \cdot n_M = 20 \,[cm^3/rev] \cdot 2390 \,[rpm] \left(\frac{1}{1000}\right) = 47.8 \, l/min$$

b) The torque on the winch drum is

$$T_D = \frac{F \cdot D}{2} = \frac{8000 \,[N] \cdot 200 \,[mm]}{2000} = 800 \, Nm$$

The ideal motor torque, neglecting the losses at the gearbox, is

$$T_{M,i} = \frac{T_D}{i} = \frac{800 \,[Nm]}{10} = 80 \, Nm$$

The ideal motor inlet pressure can be determined from Eq. (6.11b):

$$(p_{in} - p_{out})_{M,i} = \frac{T_{M,i}}{V_D} = \frac{80 \,[Nm] \cdot 20 \cdot \pi}{20 \,[cm^3/rev]} = 251 \, bar$$

$$p_{in,i} = (p_{in} - p_{out})_{M,i} + p_{out} = 251 + 10 = 261 \, bar$$

c) The hydraulic power for the motor follows Eq. (6.3a):

$$P_{hyd,i} = Q_{M,i} \cdot (p_{in} - p_{out})_i = 47.8 \,[l/min] \cdot 251 \,[bar] \cdot \left(\frac{1.66}{1000}\right) = 19.92 \, kW$$

d) With the motor operating condition of 2390 *rpm* and 261 *bar*, the motor volumetric efficiency η_v can be found around 0.95 in the volumetric efficiency map. The effective motor flow rate $Q_{M,e}$ follows Eq. (6.41):

$$Q_{M,e} = \frac{n_M \cdot V_{D,M}}{\eta_{v,M}} = \frac{47.8}{0.95} = 50.3 \, l/min$$

e) The effective motor torque is calculated considering the gearbox efficiency:

$$T_{M,e} = \frac{T_D}{i \cdot \eta_{GB}} = \frac{800 \,[Nm]}{10 \cdot 9.7} = 82.5 \, Nm$$

f) With the motor operating condition of 2390 *rpm* and 261 *bar*, the motor hydraulic-mechanical efficiency η_{hm} can be found around 0.9 in the hydraulic-mechanical efficiency map. The effective motor inlet pressure $p_{in,e}$ follows Eq. (6.43):

$$(p_{in} - p_{out})_e = \frac{T_{M,e}}{V_{D,M} \cdot \eta_{hm,M}} \frac{82.5 \,[Nm] \cdot 20 \cdot \pi}{20 \,[cm^3/rev] \cdot 0.9} = 288 \, bar$$

$$p_{in,e} = (p_{in} - p_{out})_e + p_{out} = 288 + 10 = 298 \, bar$$

(Continued)

Example 6.2 (Continued)

g) The effective hydraulic power for the motor follows Eq. (6.3a):

$$P_{\text{hyd},e} = Q_{M,e} \cdot (p_{\text{in}} - p_{\text{out}})_e = 50.3 \, [l/min] \cdot 288 \, [bar] \cdot \left(\frac{1.66}{1000} \right) = 24.05 \, kW$$

h) The total motor efficiency η_t follows Eq. (6.44):

$$\eta_t = \eta_{\text{hm}} \cdot \eta_v = 0.9 \cdot 0.95 = 0.855 \; or \; 85\%$$

6.9 Design Types

The principle of operation of a positive displacement machine was previously introduced for the case of a wobble pump. This example, because of its straightforward geometry, is particularly suitable to familiarize the reader with the general concept of displacing fluid between two different pressure levels. In real life, the same principle can be implemented with many different pump or motor architectures. Nowadays, the most successful design types are as follows:

- Axial piston machines
  - o Swashplate type axial piston machines[10]
  - o Bent axis type axial piston machines
- Radial piston machines
- Gear machines
  - o External gear machines
  - o Internal gear machines
  - o Gerotors
- Vane-type machines

Each design type presents unique features that will be briefly summarized in the following paragraphs. The reader is encouraged to consult more specific technical literature for more details for each one of these designs. Great sources are the books by Ivantysyn and Ivantysynova [4] and Manring [5]. However, many peculiar features of modern designs can be found only in technical papers or manufacturer catalogs.

6.9.1 Swashplate-type Axial Piston Machines

Figures 6.19 and 6.20 show the structure of a swashplate-type axial piston machine. The first cross-section is perpendicular to the rotation axis of the swashplate, showing the fluid displacement principle. To rotate around the main axis, the shaft drives the cylinder block, which houses several pistons that at one end, are coupled with slippers through a ball-type joint. The slippers are held against the swashplate by the pressure in each displacement chamber. When the swashplate is at an inclined position, as shown in Figure 6.19, the rotational motion of the cylinder block causes a reciprocating motion of the pistons relative to the cylinder bore. This concept is very similar to the wobble pump example, except that now the pistons are rotating and the swashplate is still. The pump shown in Figure 6.19 has a variable displacement. The instantaneous pump displacement is adjusted by changing the inclination of the swashplate using two control pistons. Different types of swashplate adjustment systems are available. Some of the most common examples will be presented throughout Parts IV and VI.

---

10 Also often referred to as "in-line" piston machine.
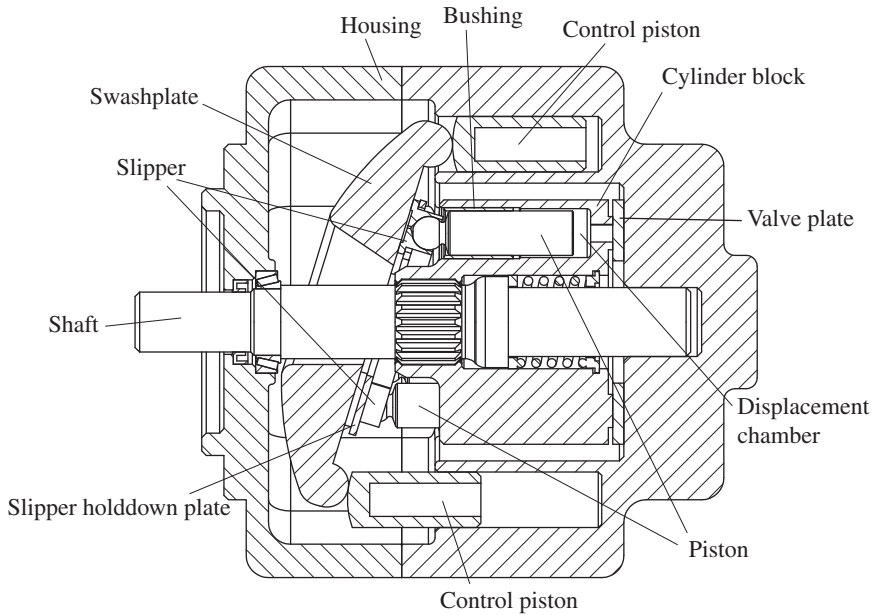
Figure 6.19 Swashplate-type axial piston machine vertical cross-section.

In an axial piston machine, the displacement chambers are connected to the suction and delivery ports through the valve plate; this is clearly visible from the cross section in Figure 6.20, where the section plane is parallel to the swashplate rotation axis. In particular, Figure 6.21 illustrates the geometry of the valve plate and the displacement chamber opening. The displacement chamber connects to port A in the first half turn and to port B in the second half turn within each shaft revolution.

In Figure 6.21, each displacement chamber, when transitioning around the 12 and 6 o'clock positions, is instantaneously connected to both ports. This effect is achieved through four port timing grooves. This is common in valve plate designs and serve the purpose to smooth out the transition when the chamber switches between different pressure levels.
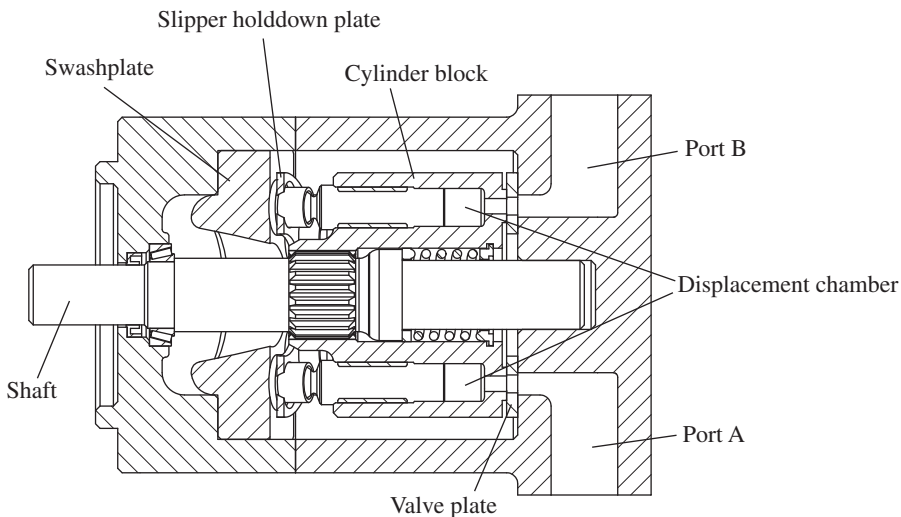
Figure 6.20 Swashplate-type axial piston machine horizontal cross-section.
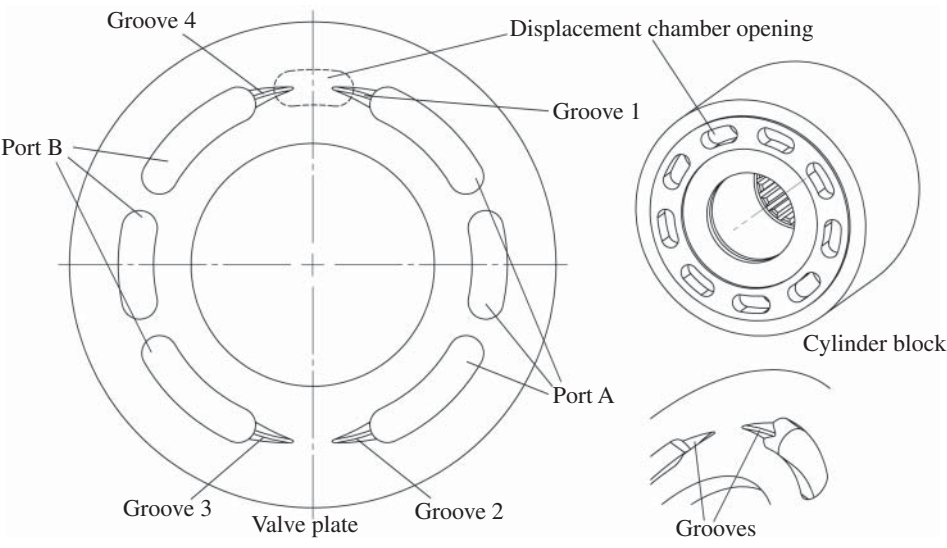
Figure 6.21 Valve plate geometry example for a bidirectional motor.

Figure 6.21 shows a symmetric valve plate, typical of a bidirectional motor. This is not necessarily the case for all piston units: in fact, one can design the kidney slots of the valve plate differently for the suction and delivery phases, or the timing grooves can also be different for the two transitions between high and low pressures. The valve plate is usually nonsymmetrical when the unit is unidirectional. In this case, only two grooves can be implemented instead of four.

The pressure in the displacement chamber pushes the piston against the swashplate. Slippers are located between the piston and the swashplate. Common designs present a slipper pocket that connects the displacement chamber through a series of channels and orifices, as represented in Figure 6.22. The orifice in the slipper works as a pressure separator and controls the height of the slipper sealing gap. When the height of the gap between the slipper and the swash plate is very short, the flow through the slipper orifice is low due to the low leakage. This situation almost corresponds to a static scenario in which the pocket pressure is almost equal to the displacement chamber pressure. The increased pocket pressure then pushes the slipper away from the swashplate, thus
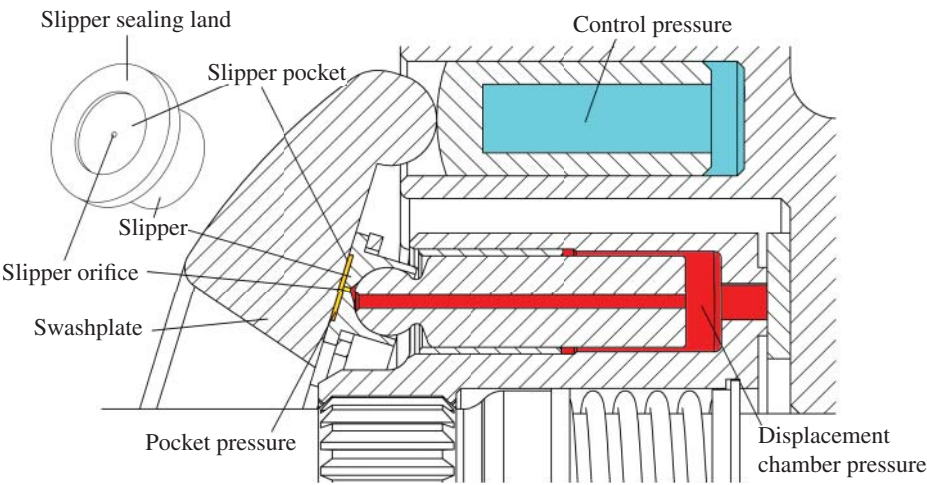
Figure 6.22 Pressures in a swashplate axial piston machine.
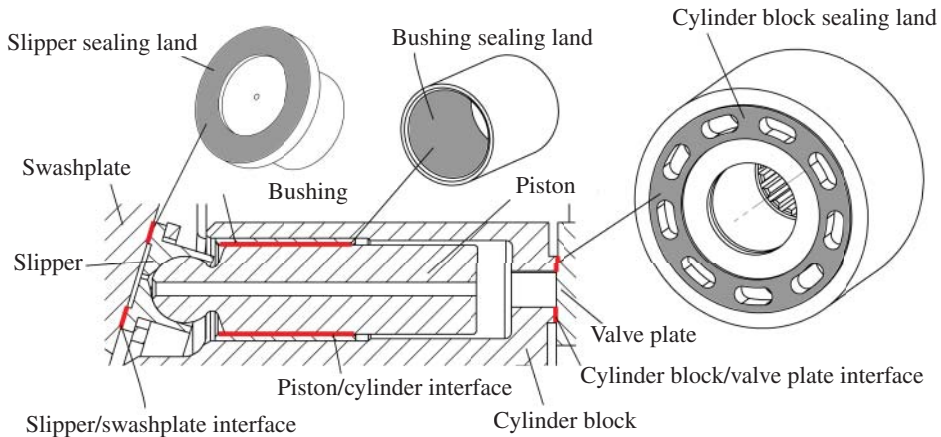
Figure 6.23 Three lubricating interfaces in swashplate-type axial piston machines.

increasing the gap. On the other hand, when the slipper is too far from the swashplate, the leakage flow causes a pressure drop through the slipper orifice (which works as a pressure separator). The pocket pressure decreases, which then brings the slipper closer to the swashplate. In this way, the slipper/swashplate gap is self-regulated depending on the operating conditions. Furthermore, there is a slipper hold down plate that prevents the slipper from lifting away from the swashplate in some specific transitory conditions, for example, when the case pressure exceeds the suction pressure.

There are three main lubricating interfaces in swashplate-type axial piston machines: between the piston and cylinder, the slipper and swashplate, and the valve plate and cylinder block (Figure 6.23). The piston/cylinder interface separates the piston and cylinder bore. The inclined swashplate causes a side force applied through the center of the piston ball joint. This side force and other inertia forces are balanced by the pressure distribution in the piston/cylinder interface. This force-carrying capability requirement for the piston/cylinder interface is the key of the pump or motor design. The slipper/swashplate interface and the cylinder block/valve plate interface follow the hydrostatic bearing principle. When designing such interfaces, a hydrostatic balancing factor is commonly used to predefine the load-carrying capability solely from hydrostatic effects in the percentage of the total external load. A balancing factor from 80% to 90% is commonly used in both interfaces. The remaining 10–20% external load is balanced by the hydrodynamic effect.

6.9.2 Bent Axis-type Axial Piston Machines

Figure 6.24 shows a cross-section of a bent axis-type axial piston machine. Similar in the swashplate-type axial piston machine, the reciprocating motion of the pistons leads to the change of the displacement volumes. With the rotation of the cylinder block, each displacement chamber opens to the inlet or the outlet port through the valve plate, similar to Figure 6.21.

The reciprocal motion of the bent axis machine pistons is created by the rotation of the driving flange. Unlike the swashplate-type machine, the pistons in a bent axis machine must be able to tilt from the bore axis.

Since the pistons are free to tilt in the cylinder bore, the displacement chamber pressure forces transfer through the pistons and the driving flange to the machine shaft as side loads. These side loads are supported by the bearings which, in bent axis machines, are visibly larger than other pump types. Comparing to the swashplate-type machines, the piston/cylinder interface in bent axis machines presents less challenges for the load-bearing function, thanks to the relatively small cylinder block torque and the tilting freedom (unlike the swashplate type, which uses the block to drive the pistons, the driving flange drives the pistons in the bent axis type). This allows the
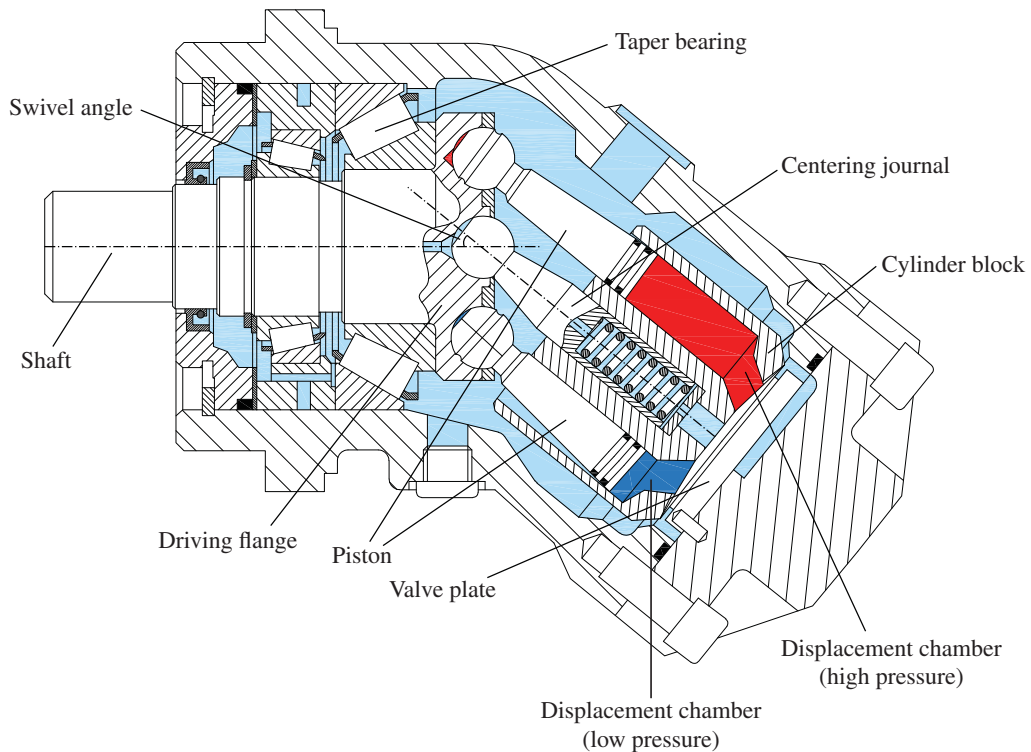
Figure 6.24 Bent axis-type axial piston machine.

piston/cylinder interface design to have tighter clearance or piston rings to reduce the leakage from this interface. Thus, the overall efficiency of a bent axis machine is normally better than that of a swashplate-type machine. Finally, the slipper/swashplate interface is also eliminated from the bent axis design and it is replaced by a ball/socket joint that also needs lubrication (often achieved with a small axial hole in each piston.

There are two ways to synchronize the cylinder block. Connections such as universal joint, bevel gear, or double joint are often used in many bent axis machines to transmit the torque. In other designs, such as the one shown in Figure 6.24, the torque is directly transmitted using the pistons.

Varying the displacement for bent axis-type axial piston machine is possible. The most common way is to change the swivel angle by moving the cylinder block and the valve plate. Comparing to the swashplate-type axial piston machine, the displacement adjustment systems in the bent axis type are more complicated and less responsive and take more space.

In usual applications, it is very common to encounter swashplate axial piston units as pumps, due to the flexibility of the controls and the possibility of implementing a drive-through layout for mounting multiple units on a single shaft. Bent axis units are also available as pumps but they are mostly applied as motors, thanks to the high-speed capabilities (some small motors can reach up to 14 000 rpm) and to the high-power density.

6.9.3 Radial Piston Machines

In radial piston machines, as shown in Figure 6.25, the cylinders are radially arranged with respect to the main rotating shaft. Following the piston support, radial piston machines can be divided into two groups: external support and internal support radial piston machines. Figure 6.25 is an
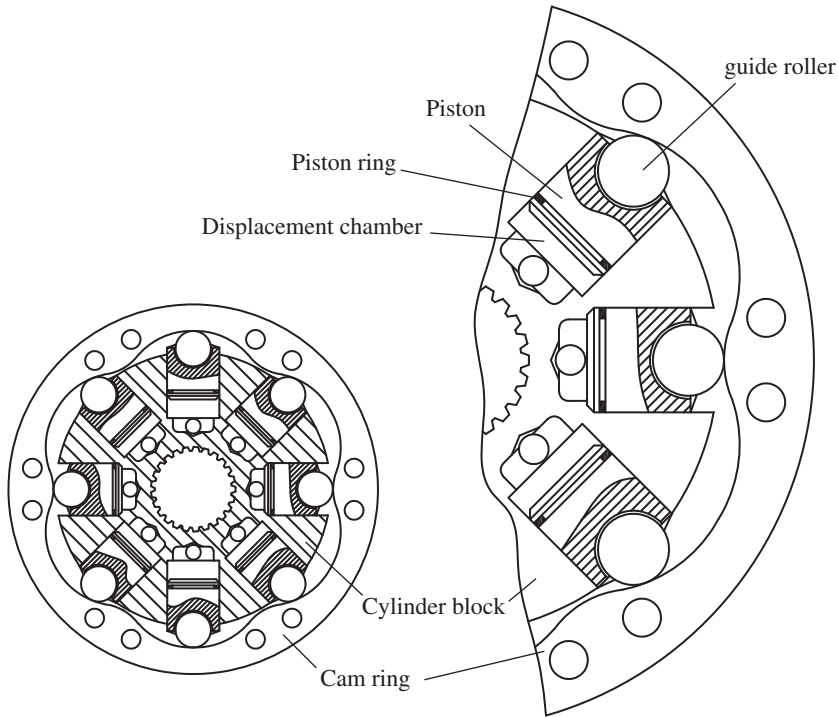
Figure 6.25 Radial piston machine.

example of an external support radial piston machines. With the rotation of the cylinder block, the roller follows the cam ring, which drives the piston in a reciprocal motion within the cylinder bore. Like the axial piston machines, the reciprocal motion creates the change of the displacement chamber volume. The distribution function is performed mostly by a control journal, not represented in the figure. The fluid is supplied from the pump connections to the distribution through axial bores in the control journal. The external support radial piston machine shown in Figure 6.25 is a multistroke machine; in fact, following the external cam ring, the piston completes 6 cycles per revolution.

Referring to Eq. (6.8), the multistroke design increases the displacement volume of the machine. In addition, radial piston machines can be designed for very high pressure (over 700 bar) and are available as pumps or motors. While the pumps are used in special very high-pressure applications, the motors are more useful due to their advantage: radial piston motors can generate very high torques (high displacements are achievable in a very compact design) with low pulsations at speeds below 1 rpm.

Internal support radial piston machines share the same principle as the external support radial piston machines. The fluid distribution to the cylinder chamber is provided from the outer circumference of the cylinder block. The piston motion is created from the internal camshaft.

6.9.4 Gear Machines

Gear machines can be classified as

- External gear machines
- Internal gear machines
- Gerotor and Orbit machines

Gear machines are perhaps the most common fixed displacement hydrostatic machines, thanks to their manufacturing simplicity and low cost. This is particularly true for external gear pumps and motors, as well as for Gerotors. In fact, only few parts are necessary to build a pump (the two rotors and the unit case). An external gear pump can be made of less than 15 individual components (including nuts and bolts).

External Gear Machines

Figure 6.26 shows an example of an **external gear machine**. The drive and the driven gear rotate in opposite directions. The unit moves fluid from the low-pressure port (left side) to the high-pressure port (right side): the drive gear rotates clockwise, and the driven gear counterclockwise. The driven gear is often referred as pinion. The meshing between the two gears and the tight radial gap between the gear tip and the housing separate the high- and low-pressure regions.

Each displacement chamber is defined by the tooth space volume between two neighboring teeth. The process of displacing the fluid follows two separate stages: the transfer of the fluid from the inlet to the outlet, followed by the actual displacement occurring in the meshing region. For a pump (as the one represented in Figure 6.26), during the transfer stage, the tooth space volume is completely filled by fluid and moves from the low- to high-pressure port along the outer profile of the gear housing. In this phase, the displacement chamber (tooth space volume) is sealed, thanks to the small clearances between the housing, the lateral bushings (if present), and the gears.

Subsequently, the displacement chamber enters the meshing zone. During meshing, a tooth from the opposite gear enters into the tooth space volume, forcing the fluid to escape toward the outlet.
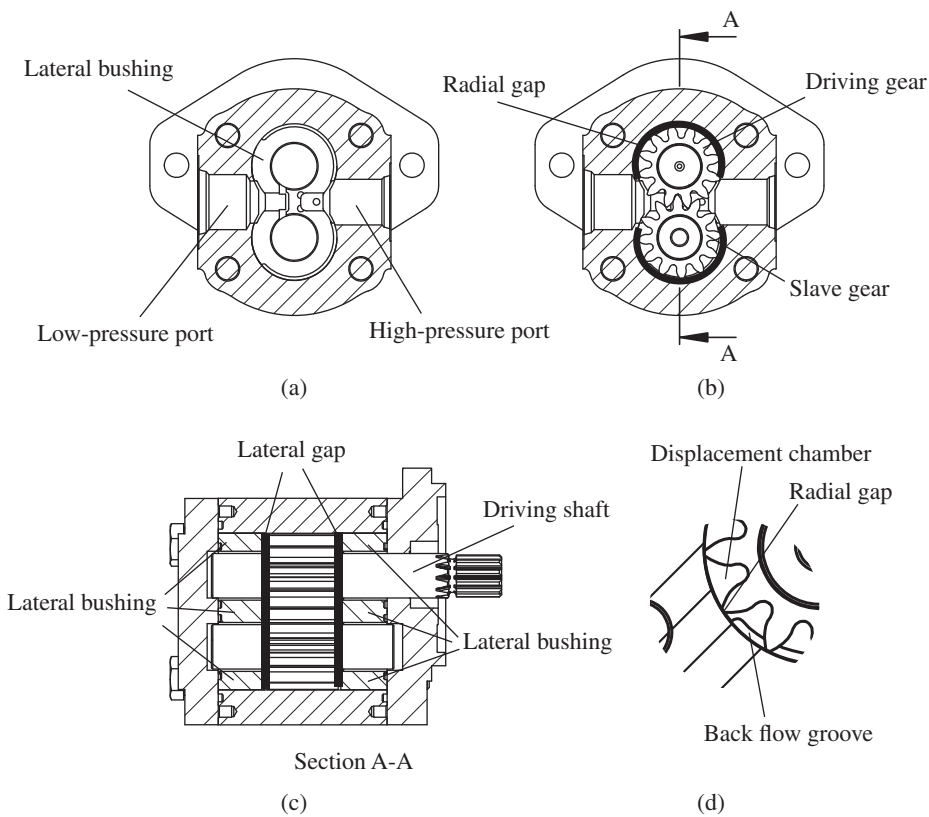
Figure 6.26 External gear machine: (a) view of the lateral bushing surface facing the gears; (b) gears and tooth tip circumferential gap; (c) section A-A of figure (b) detail on the lateral gap; (d) detail on the backflow groove used to influence the tooth space volume pressure.

When contact between the teeth occurs, the displacement chamber is not isolated because a lateral connection is always implemented (in the machine housing or in the lateral bushings) so that the fluid can still communicate to either the inlet or the outlet port, until the minimum volume value is reached. These lateral connections are shown in Figure 6.27 as relief grooves.

After the chamber has reached the minimum volume, there is a commutation of the port connection (from outlet to the inlet port), as the tooth space volume starts increasing. Therefore, as the tooth leaves the meshing region, its volume is again filled with fluid.

The behavior of a motor is intuitive and very similar, with the difference that the power flow is opposite (from the fluid to the gears).

As shown in Figure 6.26, the two gears present a circumferential gap, between housing and gear tips, and a lateral gap, between the lateral face of the gears and the sidewall.

In low-pressure external gear machines (usually below 150 bar), the side walls are typically integrated into the machine housing to reduce the cost. For high-pressure applications (up to 350 bar), pressure compensation design for the lateral gap is normally required to reduce the leakage through the gap.

The pressure compensation for the lateral gap is achieved with floating elements: lateral bushings, if they also include the bearings that support the gear shaft, or pressure plates, if otherwise. These change the height of the lateral gap according to the operating pressure.

Figure 6.27 shows the detail of the lateral bushings present in the unit in Figure 6.26. The bushing position is determined by the forces acting on the two opposite sides. At the balance side, a low-pressure area and a high-pressure balance area are established through proper connections with the inlet and outlet ports. These two areas are separated by a seal, which is shaped like a pair of glasses. At the opposite side of the bushing, a pressure field develops from the tooth space volumes. The forces and moments at the balance side counteract those from the opposite gap side. A proper sizing of the balance areas on the lateral bushings guarantees minimum gap heights, thus reducing leakages. At the same time, contacts between the gears and the lateral bushing can be avoided. More details on the lateral balancing features of pressure compensated gear pumps can be found in [9].

Figure 6.27 details also the relief grooves mentioned earlier. These grooves are responsible for the timing of the connection of the tooth space volumes with either the inlet port or the outlet port during the meshing process. In gear machines, circumferential grooves, indicated as back flow grooves in the figure, can be present. These grooves regulate the pressurization of the tooth space volumes during the transfer phase. This method is generally used to control the radial forces acting on each gear, in both amount and direction [10].
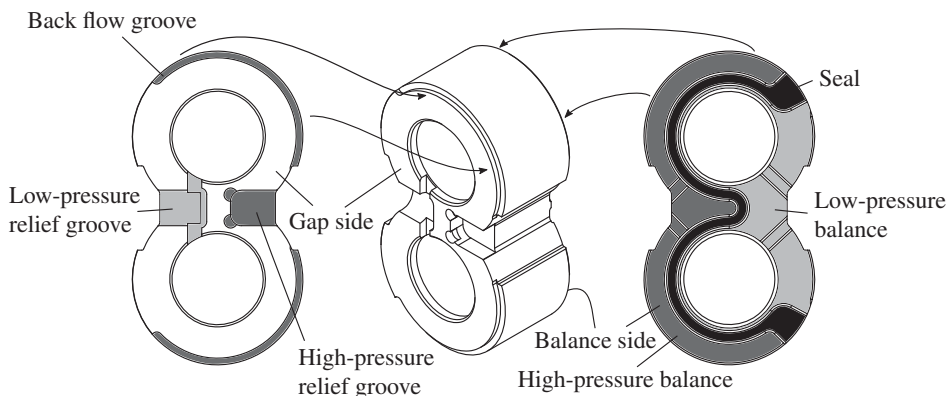
Figure 6.27 External gear machine lateral bushing.

Internal Gear Machines

Similar to the external gear machines, **internal gear units** also have two gears: the inner external gear (connected to the shaft) meshes with an outer internal gear. The two gears are eccentric, and a crescent is interposed between the two elements, as shown in Figure 6.28. The crescent can float subject to the different pressure forces, achieving a tight sealing effect. The process for displacing fluid is very similar to the previous case, presenting a transfer phase followed by a meshing phase. The connection between the displacement chambers (tooth space volumes) and the inlet and outlet ports can occur through axial connections or radial connections. The drawings in Figure 6.28 shows the case of radial connections. The radial openings allow the displacement chambers to connect to the high-pressure and low-pressure ports, through proper channels implemented in the housing.

Lateral gap compensation through floating elements, similar to that of external gear machines, can also be used in internal gear machines to limit the lateral gap leakage.

Internal gear machines are more difficult to manufacture than external gear units, thereby making them significantly more expensive. However, they are more compact, less noisy and can reach higher operating pressures.
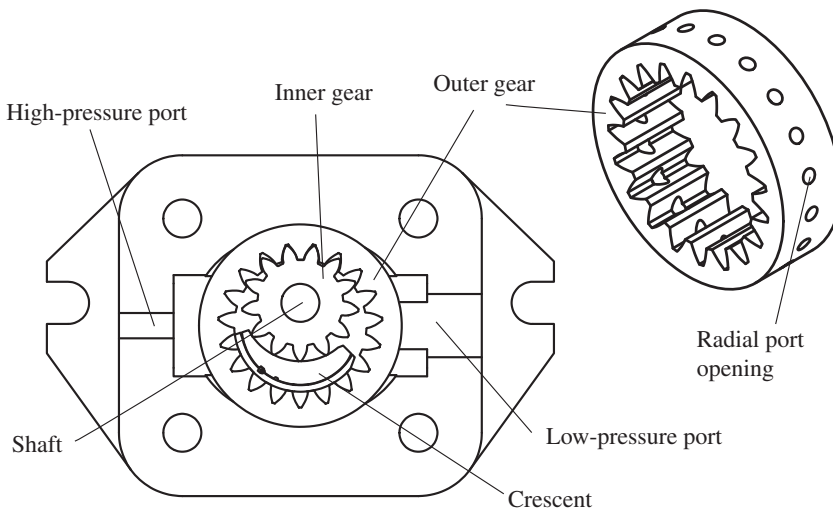
Figure 6.28 Internal gear machine.

Gerotors and Orbit type machines

Different from internal gear units, which use a crescent and involute teeth, **gerotor machines** use two conjugated profiles for both the inner rotor and the outer ring gears. Infinite profile morphologies can be utilized to design the gears. However, most of the commercially available units utilize circular, cycloidal, or hypotrochoidal profiles [11].

Figure 6.29 shows the cross-section of a gerotor design. Both inner gear and outer gear rotate in the same direction to displace fluid from the lower port to the upper port. The ports are connected to the displacement chambers by two slots in the end cover of the unit. This port configuration implements an axial opening, as opposed to the radial opening of the unit shown in Figure 6.28.

The outer gears in internal gear machines or gerotor machines are commonly supported by journal bearing. The inner gear is connected to the shaft, which is supported by either journal bearing or roller element bearing.
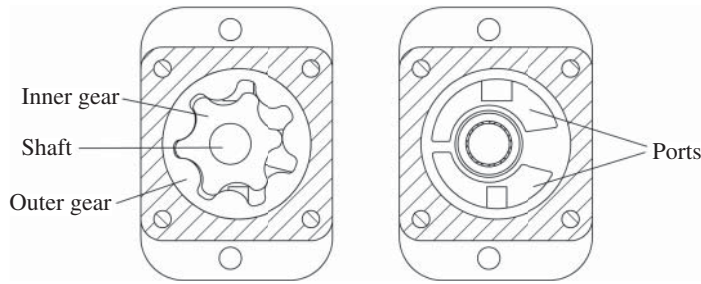
Figure 6.29 Gerotor cross-section.

One of the features of gerotor pumps is their capability of achieving very high speeds. They are often used as steering pumps in car engines, which can range from 300–500 to 6000 rpm. A variation of the gerotor concept can be used to design orbit motors and power steering units, where the inner gear is connected to the shaft and a special valve plate distribution pressurizes alternately the inner chambers. In this design, the outer profile is fixed, and the inner gear follows a trajectory similar to an orbit. More details on the features of orbit motors can be found in [12] and an example further described in Chapter 22, which discusses the steering units. The design of the orbit motors is also more efficient due to high torques and low speeds. Though its efficiency and pressure level are not at par with those of a radial piston unit, but an orbit motor is economical and very simple to manufacture.

6.9.5 Vane-type Machines

Vane-type machines are compact units that are characterized by low flow pulsations (therefore low noise) and high mechanical efficiencies. On the other hand, they cannot reach very high operating pressures (maximum of 280 bar) and are very sensitive to cavitation or quick pressure gradients. As shown in Figure 6.30, the vanes are housed in the rotor and can move radially. They
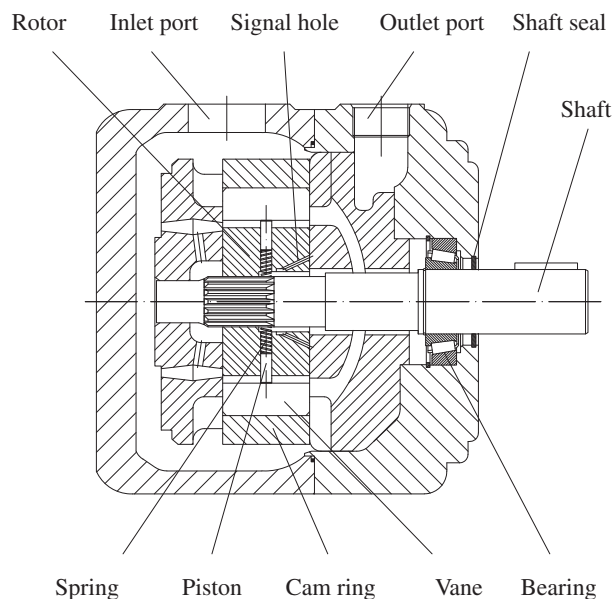
Figure 6.30 Vane pump cross-section.
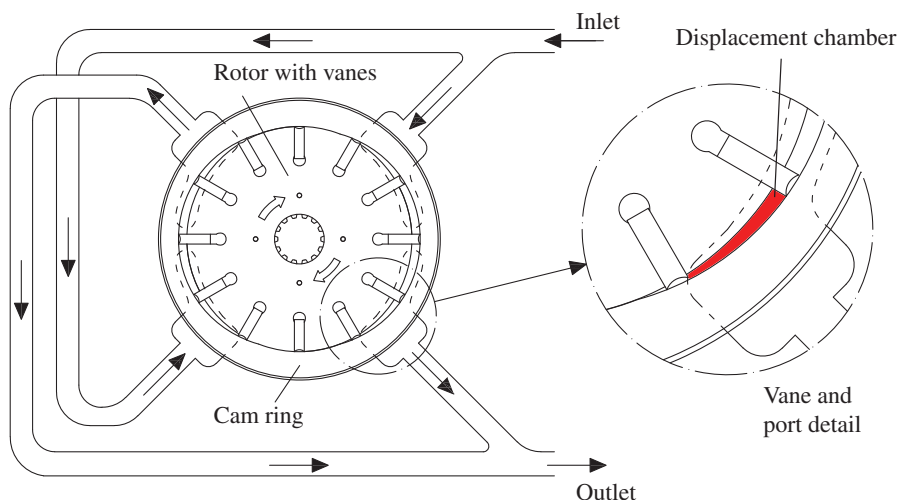
Figure 6.31 Vane pump port flow.

are pressed against the cam ring by springs and pistons. Each piston is exposed to the operating pressure. Each displacement chamber is enclosed by two neighboring vanes, the cam ring and the rotor, as shown in Figure 6.31. The geometry of the cam ring controls the variation of the displacement chamber volume.

Most of the vane machines present a design similar to Figure 6.31: each displacement chamber displaces oil from suction to delivery twice in each shaft revolution. Thanks to the symmetric pressure loading on the shaft, the pump is perfectly balanced, and no side load is transmitted to the shaft, thus resulting in very high mechanical efficiency. Another advantage of this type of vane units is that the displacement is univocally determined by the cam ring shape. Therefore, the same pump housing can carry multiple displacement cam ring, which can be easily interchanged.

The double stroke architecture in Figure 6.31 is very common for high-pressure applications (up to 280 bar). Figure 6.32 shows the design principle of a single stator vane machine. In single stator vane machines, the displacement chamber completes one cycle in each shaft revolution. The advantage of the single stator vane machine is that the displacement can be varied by adjusting the eccentricity of the rotor relative to the stator. This type of machine is often used as boost pump to improve the suction capability of the main circuit pump.
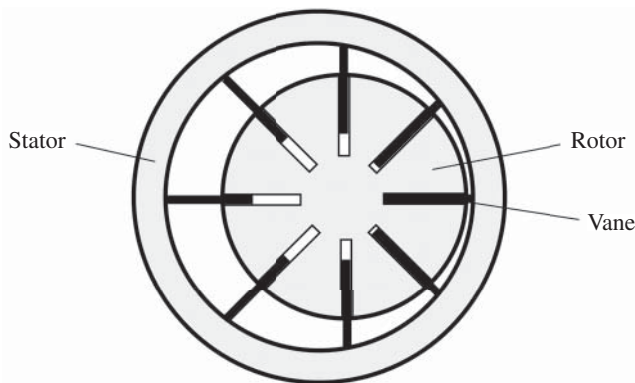
Figure 6.32 Single stator vane machine.

Table 6.1 Features and main operating parameters of the most common positive displacement machines.

Type of machine	Merits	Demerits	Speed (rpm)		Max pressure [bar]
			Minimum	Maximum	
Swashplate-type axial piston machine	• High pressure level • Variable displacement • Good efficiency • Through-shaft possible	• High production cost • High shear forces and side loads on piston	5–20	300–18 000	420
Bent axis-type axial piston machine	• High pressure level • Variable displacement • Best efficiency • Low shear forces and loads on piston	• High production cost • High control force in case of variable machines	5–20	500–8000	420
Radial piston machine	• Very high pressure level, high power density • Good efficiency • High torque at lowest speeds	• High production cost • Not as compact as axial piston machine • Low speed	1–10	120–400	700
External gear machine	• Very simple design, economical • Robust, suited for hard application • High power density	• Fixed displacement • High efficiency only with complexity • High noise	300–700	2000–8000	300
Internal gear machine	• Compact design, high power density • Low flow pulsations, very low noise emission, long life • Robust	• Fixed displacement • More expensive than external gear machine	300–1500	2000–5000	320
Gerotor	• Small size, high power density • Simple design • Robust • Relatively large displacement volume	• Fixed displacement • Unfavorable efficiency	10–50	200–2000	200
Vane machine	• Compact • Low flow pulsation, low noise level • Variable displacement	• Sensitive against pressure peaks • Unfavorable efficiencies • Relatively low pressure level	10–400	1000–4000	50–250

The following table gives a brief summary of the features and characteristics of the most common positive displacement machines, classified by design type (Table 6.1).

Problems

6.1 A pump has a displacement of 75 cm^3/rev. It delivers 70 l/min at 1000 rpm and 210 bar. Evaluate the volumetric efficiency of the pump. Additionally, calculate the torque Nm required

to operate the pump for the ideal case (100% efficiency). If the torque actually measured at the pump shaft is 270 Nm, what is the overall efficiency of the pump?

6.2 A 75 cm^3/rev fixed displacement pump rotates at 1800 rpm and supplies a hydraulic actuator. The load on the actuator pressurizes the pump outlet at 180 bar (gage pressure). The pump suction is connected to a reservoir at atmospheric pressure. Draw the ISO schematic of the system and calculate
a) The flow rate delivered by the pump in the ideal case
b) The torque at the pump shaft in the ideal case
c) The power consumption in the ideal case
  A flow meter and a torque meter are used to measure the actual values of the port flow rates and the shaft torque. The sensor readings are 127 l/min and 234 Nm. Determine
d) The volumetric efficiency of the pump
e) The hydromechanical efficiency of the pump
f) The overall efficiency of the pump
g) The actual power consumption of the pump

6.3 A 63 cm^3/rev hydraulic motor works under a differential pressure between the inlet port and the outlet port of 180 bar, and it receives 60 l/min flow from a pump. Calculate the shaft speed [rpm], the torque [Nm], and power [kW]. Consider the motor as ideal (unitary volumetric and hydromechanical efficiencies).

6.4 A hydraulic motor has a displacement of 90 cm^3/rev and delivers 280 Nm at the shaft. The shaft speed is 2000 rpm, the supply pressure 210 bar and the outlet is connected to a tank at atmospheric pressure. If the flow rate through the motor is 200 l/min, find
1. The volumetric efficiency of the motor
2. The hydromechanical efficiency of the motor
3. The overall efficiency of the motor
4. The actual power delivered by the motor

6.5 A hydraulic motor drives a winch through a gearbox with ratio $i = \frac{n_{in}}{n_{out}} = 20$. The maximum pressure at the inlet is $p_{in} = 210$ bar.
Determine the minimum motor displacement to lift a load of $F = 50\,000$ N. The winch drum has a diameter $D = 260$ mm, and the pressure in the return side of the motor is $p_{out} = 10$ bar. The gearbox has mechanical efficiency of 0.97.
- *Case* 1. Assume an ideal hydromechanical efficiency of the motor, $\eta_{hm} = 1$.
- *Case* 2. Assume a hydromechanical efficiency of the motor, $\eta_{hm} = 0.9$.
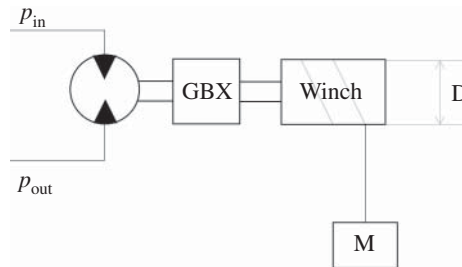
6.6 An open circuit pump is driven by a power take off (PTO) connected to a truck transmission. The truck idles at 800 rpm and the maximum engine speed is 2000 rpm. The pump has to

provide 35 gpm at idle. The PTO can be selected with the following available ratios (pump vs engine speed): 87%, 99%, 115%, 132%, and 161%. From the catalogs of commercially available pumps, select the most compact pump displacement to provide the required flow without exceeding the maximum pump speed.

6.7 A feller-buncher uses a circular saw to cut trees. The saw is powered by a hydraulic motor and it rotates at a very high speed, together with a large flywheel. The tree-cutting action is provided by the flywheel inertia. Assume that the motor has a 6 cm³/rev displacement, while the flywheel has a rotary inertia of 1.2 kg·m². The motor is supplied with a fixed flow of 54 l/min and the pressure is limited to 180 bar by a relief valve. Calculate the time required for the motor to reach steady-state speed once it is activated.

6.8 Looking at the figure below, answer the following questions: What type of displacement machine is represented? Is it a fixed or variable displacement unit? Name the components numbered from 1 to 10.
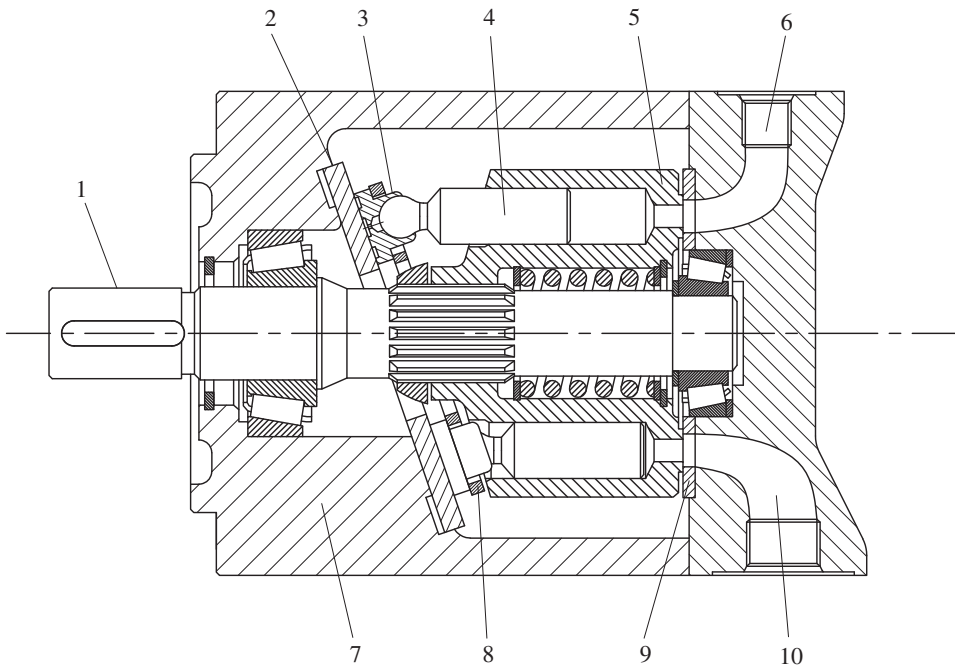
Chapter 7

Hydraulic Cylinders

Hydraulic linear actuators, or hydraulic cylinders, are used to achieve linear motion using hydraulic control systems. They convert hydraulic energy into translational kinetic energy. Therefore, they are energy conversion elements, such as hydrostatic pumps and motors. This chapter presents an analysis of hydraulic cylinders and describes both the ideal behavior and the actual features of operation.

7.1 Classification

The high-power density and the simplicity and robustness of the design of a hydraulic cylinder are some factors behind the success of hydraulic technology in general. In fact, other technologies (e.g. electromechanical or purely mechanical) have not yet produced competitive solutions for linear motion capable to compete with hydraulics in terms of complexity, cost, and packaging. An example of hydraulic cylinder architecture, along with the ISO symbol, is represented in Figure 7.1.

Fundamentally, a hydraulic cylinder consists of a cylinder body (or barrel), a moveable piston, and a piston rod attached to the piston. End caps are attached to the cylinder body barrel by threads, tie rods, or weldments. Dynamic seals on the piston prevent fluid from leaking from one chamber into the other, while static seals are used to prevent leakages between the rod and the rod-side end cap.

Figure 7.2 summarizes the most common linear actuator architectures, represented with their ISO symbols. One of the most important classification criteria divides cylinders in double acting and single acting. In a double acting cylinder, the sliding piston divides the barrel into two volumes, each one connected to a different hydraulic port. Each port is used to perform one of the two possible motions (extension or retraction).

In a single acting cylinder, the piston motion is controlled by using only one hydraulic port. The opposite chamber is usually vented to the reservoir.

Double acting cylinders are used in applications where the force acting on the cylinder can change direction during the operation. Typical examples are cylinders used to control the motion of the arms in cranes or excavators. Single acting cylinders are utilized in cases where the load always acts in one direction, as in dump trucks.

Hydraulic cylinders can also be of single rod or double rod type. Single rod cylinders are the most common, while double rod cylinders (often referred as differential cylinders) are used in applications where a symmetry operation is required for each direction of motion, such as in most hydraulic power steering systems.

Another important category of linear actuators is represented by telescopic actuators, which consist of multiple stages combined in a single architecture.

Base cap   Extended port   Piston   Barrel   Rod   Retract port   Box gland

Cylinder stroke

Piston bearing   Piston seal   Gland bearing   Gland seal   Rod wiper

Bore chamber   Rod chamber

Rod

Bore port   Piston   Rod port
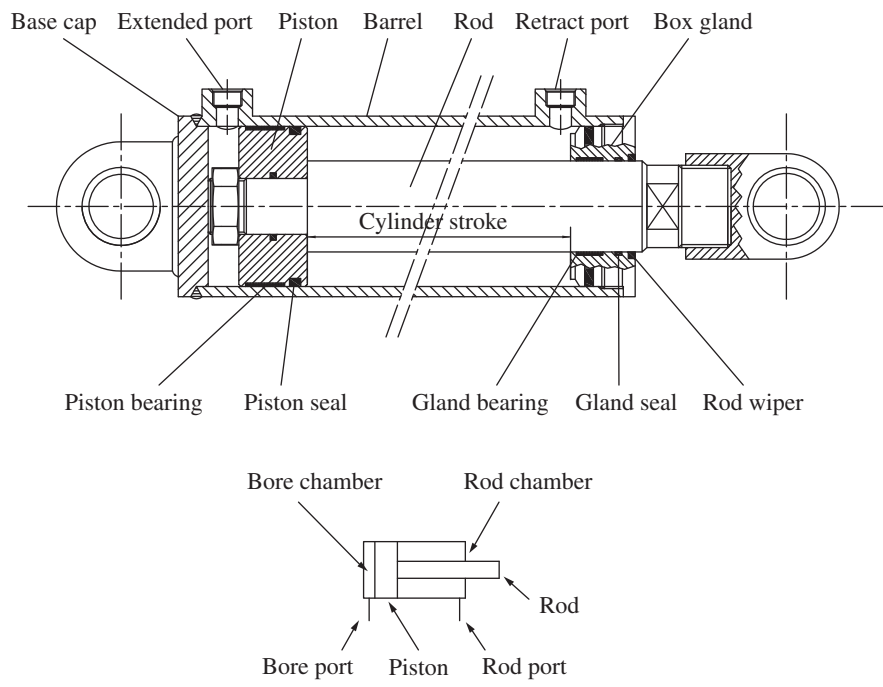
Figure 7.1   Linear actuator architecture and ISO symbol.

More exhaustive information about cylinder types and constructions can be found in references [13, 14].

7.2   Cylinder Analysis

The following pages will take as reference a single stage, single rod, double acting cylinder, which represents the most frequent case in hydraulic machines. However, all the considerations made

Double-acting, single rod
cylinder

Telescopic cylinder,
single-acting

Telescopic cylinder,
double-acting

Double-acting, single rod
cylinder with cushioning

Double-acting, double rod
cylinder

Single-acting, single rod
cylinder, return stroke by spring force,
spring chamber with connection
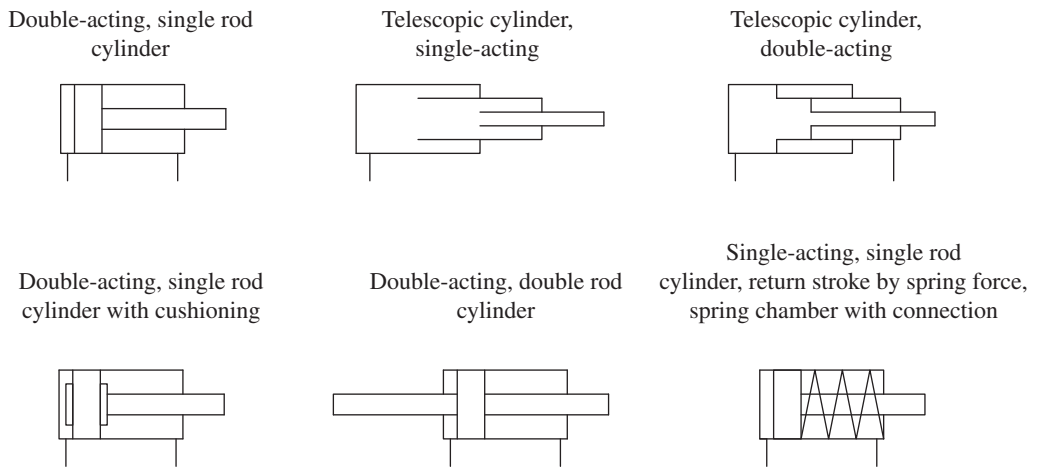
Figure 7.2   ISO symbols of various linear actuators.

Significant dimensions
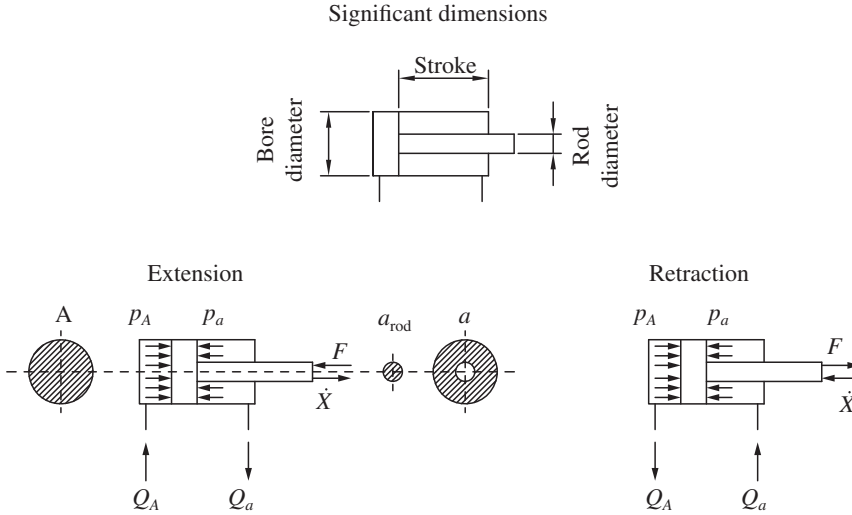
Figure 7.3 Cylinder areas, forces, and pressure. The sign convention for the piston velocity (positive for extension) and for the external force (positive when toward the bore) is also shown.

can be easily extended to other cylinder architectures. The typical parameters characterizing this cylinder, as shown in Figure 7.3, are

- the piston stroke, which represents the maximum linear travel of the piston;
- the bore inner diameter, which defines the bore influence area, A;
- the rod diameter, which defines the rod side influence area, a, given by the difference between the bore area and the rod area (this area has an annular shape);
- the parameter φ, defined as the ratio between A and a (its value is greater than 1). Given D the bore diameter and d the piston diameter, φ can be defined as

$$\varphi = \frac{A}{a} = \frac{\frac{\pi}{4}D^2}{\frac{\pi}{4}(D^2 - d^2)} = \frac{D^2}{(D^2 - d^2)} \tag{7.1}$$

The standard ISO 3320 [15] reports the common values for φ to be found in commercial units.

The velocity of the piston can be determined from the continuity equation applied at both piston and rod chambers, as it was described in depth in Chapter 3:

$$\dot{x}_i = \frac{|Q_A|}{A} = \frac{|Q_a|}{a} \tag{7.2}$$

where Q_A and Q_a are the flow rates respectively at the piston side and at the rod side ports. The subscript i specifies that the expression of Eq. (7.2) is valid for the ideal case. Additionally, in Eq. (7.2), the absolute value of the flow is used in order to generalize the expression for both retraction and extension cases. However, both situations could be differentiated by using a conventional direction for the velocity (for example in Figure 7.3, a positive velocity is used for extension).

Depending on the direction of the external force acting on the piston, F in Figure 7.3, the linear actuator can operate as a motor or as a pump. In more detail, if the force opposes the piston motion (**resistive** force) *the cylinder behaves as a motor*: the hydraulic power P_f is converted in mechanical power P_m:

$$P_f = Q_{in} \cdot p_{in} - Q_{out} \cdot p_{out} \tag{7.3}$$

$$P_m = |F \cdot \dot{x}| \tag{7.4}$$

where, for the case of Figure 7.3, $Q_{in} = Q_A$ and $Q_{out} = Q_a$.
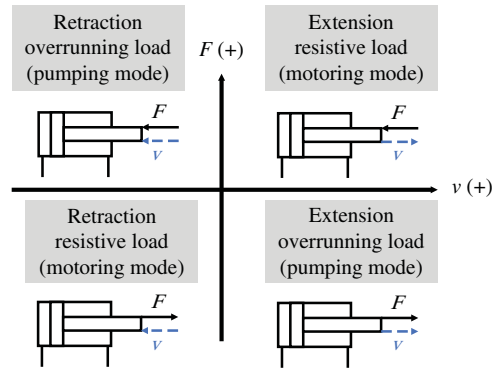
Figure 7.4 Definition of resistive and overrunning loads for a hydraulic cylinder. When the load is resistive, the cylinder is in motoring mode. When the load is assistive, the cylinder operates in pumping mode.

A typical example of a resistive load case is the lifting a gravitational load connected to the hydraulic cylinder.

If the external load F has the same direction of the piston velocity (opposite direction for the force F in Figure 7.3), the load is **overrunning** (or assistive). In this case, the energy conversion is opposite: the energy of the external load is converted into fluid energy. *The linear actuator then behaves as a pump*. The different operating modes of the linear actuator can be summarized with the four-quadrant representation of Figure 7.4.

The lowering of a hydraulic actuator under a gravitational load is a typical case of an overrunning load. In this case, the energy of the load "enters" the hydraulic system, providing energy to the hydraulic fluid in terms of pressure as can be inferred from Eqs. (7.3) and (7.4).

Example 7.1   Supply pressure of a differential cylinder

Calculate the extension velocity and the supply pressure for a differential cylinder in two different configurations, as shown in the figure below. The load is 20 *kN*, always opposing the piston motion. The supply flow rate is 20 *l/min* and return pressure is 5 *bar*. The piston diameter is 10 *cm*, and the rod diameter is 5 *cm*. Neglect frictional effects associated with the piston motion.
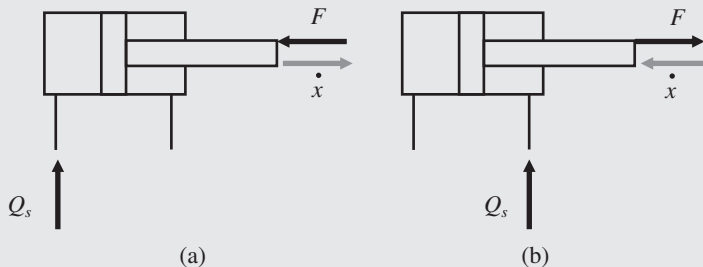
Given:
A differential cylinder, supplied in two different configurations: (a) extension and (b) retraction. The following data are given:

Force (resistive), $F = 20$ *kN*; piston diameter, $D = 10$ *cm*; rod diameter, $d = 5$ *cm*; supply flow rate, $Q_S = 20$ *l/min*; and return pressure, $p_R = 5$ *bar*.

Find:
The cylinder velocity $\dot{x}$ and the supply pressure, p_S for the cases (a) and (b).

Solution:

The problem requires the evaluation of the piston area A and the annular area a:

$$A = \frac{\pi}{4}D^2 = \frac{\pi}{4}(0.1\,[m])^2 = 0.00785\,m^2$$

$$a = \frac{\pi}{4}(D^2 - d^2) = \frac{\pi}{4}(0.1^2 - 0.05^2)\,[m^2] = 0.00589\,m^2$$

a) Extension

For this case, the extension velocity is given by

$$\dot{x} = \frac{Q_s}{A} = \frac{20\,[l/min]}{0.007\,85\,[m^2]}\frac{1}{60\,000} = 0.042\,m/s = 4.2\,cm/s$$

From the force balance of the piston $F = p_A A - p_a a$, considering that $p_a = p_R$ and $p_A = p_S$:

$$p_S = \frac{F + p_R a}{A} = \frac{20\,000\,[N] + 500\,000\,[Pa] \cdot 0.005\,89\,[m^2]}{0.00785\,[m^2]} = 2.697\,MPa = 26.7\,bar$$

b) Retraction

For the retraction case, the velocity is

$$\dot{x} = \frac{Q_s}{a} = \frac{20\,[l/min]}{0.005\,89\,[m^2]}\frac{1}{60\,000} = 0.0566\,m/s = 5.66\,cm/s$$

From the force balance of the piston $F = p_a a - p_A A$, where now that $p_A = p_R$ and $p_a = p_S$,

$$p_S = \frac{F + p_A A}{a} = \frac{20\,000\,[N] + 500\,000\,[Pa] \cdot 0.007\,85\,[m^2]}{0.00589\,[m^2]} = 3.662\,MPa = 36.6\,bar$$

It can be noticed how the area ratio of the cylinder, $\varphi = A/a = 1.33$ determines the difference between extension and retraction velocities, as well as supply pressure.

7.3 Ideal vs. Real Cylinder

In the ideal case, there are no leakages between the two piston chambers, and the velocity of the piston is given by Eq. (7.2). For most commercial cylinders, the no-leakage assumption is a good approximation, since the internal seals usually guarantee a very low level of bypass flow between the piston and the rod chamber.

However, an internal leakage connecting the piston and the cylinder chamber affects the piston velocity. Figure 7.5 illustrates this, with the leakage indicated as Q_{leak}. This leakage can be approximated as the flow across an orifice, where direction is driven by the pressure difference between the piston chamber p_A and the rod chamber p_a. Therefore, the direction of Q_{leak} depends on the direction of the external load. This situation is summarized in Figure 7.5. In case of a resistive load (or light overrunning loads, for a differential cylinder), $p_A > p_a$, the internal leakage has a detrimental effect on the effective piston velocity $\dot{x}_e$:

$$\dot{x}_e = \frac{Q_A - Q_{\text{leak}}}{A} \tag{7.5}$$

Therefore, $\dot{x}_e < \dot{x}_i$. The ratio between the actual velocity and the ideal velocity is sometimes referred as volumetric efficiency for the linear actuator. For the case of resistive load, this becomes

$$\eta_{v,\text{cyl,res}} = \frac{\dot{x}_e}{\dot{x}_i} \tag{7.6}$$
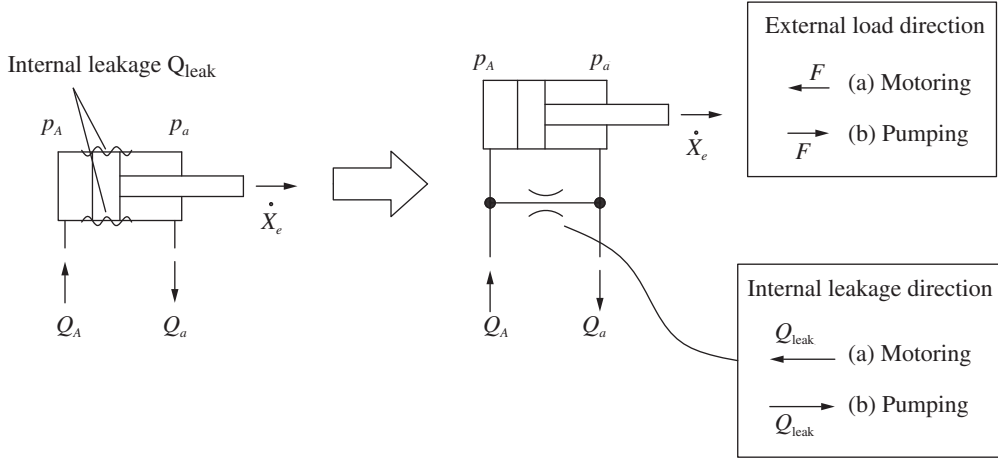
Figure 7.5 Schematic for the definition of volumetric efficiency for a hydraulic cylinder.

The above definition of volumetric efficiency (Eq. (7.6)) is valid only when $p_A > p_a$, which is typical for the motoring mode.

In case of $p_a > p_A$, as it occurs in typical overrunning conditions, the leakage has opposite sign, and it contributes in establishing an effective piston velocity higher than the actual velocity:

$$\dot{x}_e = \frac{Q_A + Q_{\text{leak}}}{A} \tag{7.7}$$

In this case, the actuator behaves as a pump, and its volumetric efficiency is defined in terms of expected outlet flow:

$$\eta_{v,\text{cyl,ovr}} = \frac{Q_a}{\dot{x}_e \cdot a} = \frac{\dot{x}_i}{\dot{x}_e} \tag{7.8}$$

The determination of the pressure in the cylinder chambers is based on the force balance of the piston considering the external force F as well as the pressure forces and the friction at the sealing elements:

$$F + F_{\text{fr}} \frac{\dot{x}}{|\dot{x}|} + p_a \cdot a - p_A \cdot A = M \cdot \ddot{x} \tag{7.9}$$

Equation (7.9) represents a generic case of an accelerating piston, as shown by the second member of the equation, according to the sign convention in Figure 7.3. However, in this analysis, the steady-state condition is considered[1]. Eq. (7.9) can then simplified as follows:

$$F + F_{\text{fr}} \frac{\dot{x}}{|\dot{x}|} + p_a \cdot a - p_A \cdot A = 0 \tag{7.10}$$

The term F_{fr} is present only when the actuator is moving, and its direction is always opposite to the piston velocity. The frictional force implies an increase in the chambers pressure, with respect to the ideal situation.

The mechanical efficiency of the cylinder, for the case of a resistive load, can then be expressed as follows:

$$\eta_{\text{hm,cyl,res}} = \frac{(p_A \cdot A - p_a \cdot a)_i}{(p_A \cdot A - p_a \cdot a)_e} = \frac{F}{F + F_{\text{fr}} \dfrac{\dot{x}}{|\dot{x}|}} \tag{7.11}$$

The evaluation of F_{fr} is a complicated tribology problem. In many cases, as in many examples provided in this book, F_{fr} can be simply neglected. In reality, the internal seals used in commercial

---

1 Alternatively, one can say that if the inertia of the load is considerable, the inertial force can be included as part of the external load F.

cylinders guarantee high volumetric efficiency at expenses of frictional losses. Therefore, the frictional term F_{fr} might not be negligible. A very common, yet effective method for modeling F_{fr} consists in considering it proportional to the piston velocity. This is a good approximation for many problems, particularly when it is not important to study the initial transient of piston accelerating from rest.

A more complex approach is based on a combined evaluation of both the static and the dynamic contributions of F_{fr} according to the Stribeck method. In this method, F_{fr} is a function of the piston velocity $\dot{x}$, which is expressed in terms of empirical coefficients that can be found in the specialized literature [16, 17]. However, for single stage commercial cylinders, it is possible to simply assume $\eta_{hm, c}$ constant, within the range of 0.94–0.98. For telescopic cylinders, this value should be lowered to 0.80–0.88 [18].

At this point, it is appropriate to expand the application of the efficiency equations for the analysis of cylinders. One important aspect is given by the differential flow rate at the cylinder ports. From Eq. (7.12), for a given cylinder velocity, there is an imbalance of the supply and return flow rates caused by the area ratio φ:

$$\left| \frac{Q_A}{Q_a} \right| = \frac{A}{a} = \varphi \tag{7.12}$$

Equation (7.12) highlights that when the cylinder is retracting the return flow from the bore can be significantly higher than the supply flow. This phenomenon is critical in the case of telescopic cylinders, where the value of φ can be very high for the first stages.

Another important consideration involves the use of Eq. (7.11) for the determination of the pressure at the cylinder ports or for selecting the cylinder areas. Usually, one of the two port pressures is known from the layout of the hydraulic circuits (e.g. the return port is often connected to tank[2]). In these cases, the pressure at the opposite port is

$$p_A = \frac{1}{A} \cdot \left(\frac{F}{\eta_{mh,c}} + p_a \cdot a \right) \tag{7.13}$$

$$p_a = \frac{1}{a} \cdot \left(p_A \cdot A - \frac{F}{\eta_{mh,c}} \right) \tag{7.14}$$

Also in this case, the differential area has to be carefully accounted for. The rod and bore pressures are always different, due to the area ratio φ:

$$\frac{p_A}{p_a} = \frac{a}{A} = \frac{1}{\varphi} \tag{7.15}$$

For example, a null external force on the actuator does not imply null pressures. In such a situation, there can be a pressure imbalance between p_A and p_a because of the back pressure created by the circuit[3].

The overall efficiency of a linear actuator is given by the ratio between the useful power output and the net hydraulic power input:

$$\eta_{t,c} = \frac{F \cdot v_e}{Q_A \cdot p_{A,e} - Q_a \cdot p_{a,e}} \tag{7.16}$$

By using the above definitions for $\eta_{v, c}$ and $\eta_{hm, c}$, it is easy to verify that

$$\eta_{t,c} = \eta_{v,c} \cdot \eta_{hm,c} \tag{7.17}$$

---

2 This is not a valid assumption for those systems in which the return line has a pressure controlled by metering or compensator elements.
3 This term could represent a substantial contribution to the force balance and neglecting it would lead to a wrong evaluation of the pressure p in the circuit.

Example 7.2   Supply pressure of two cylinders in series

For the system in the figure below, determine the pressure at the supply of the two cylinders and the piston velocity of each cylinder. The two cylinders have same piston diameter and rod diameter (120 and 80 *mm*, respectively). An external load of 4000 *N* is acting on the second cylinder, while the first cylinder moves without any load. The supply flow is known (50 *l/min*). Which one of the two configurations requires the lowest low pump pressure? Which one of the two solution provides a higher speed for the second actuator?

(a)   (b)
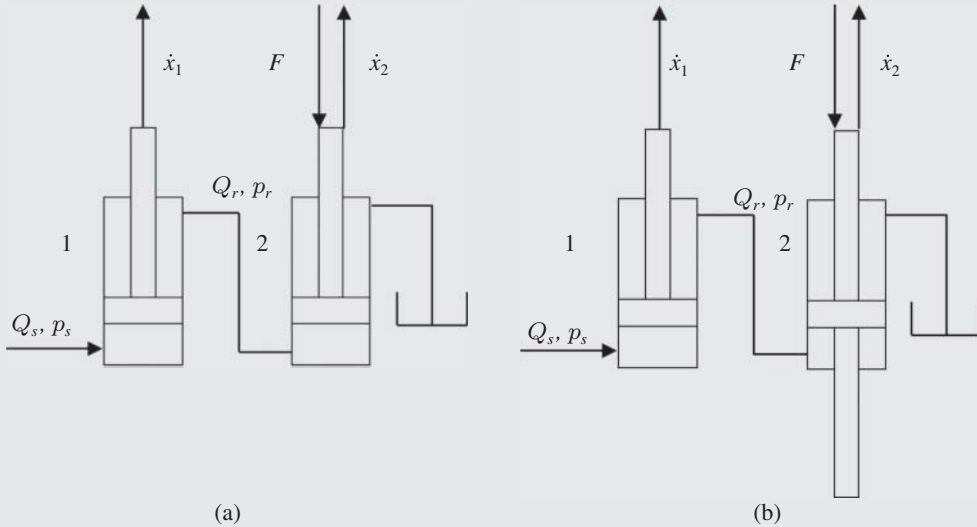
Given:
Two cylinders in series, in case (a) both cylinders are single rod, while in case (b) one cylinder is double rod. Inlet supply flow $Q = 50$ *l/min*; force acting on the second cylinder $F = 4000$ *N*; piston diameter $D = 120$ *mm*; and rod diameter $d = 80$ *mm*.

Find:
The supply pressure p_S and the extension velocity of the second actuator $\dot{x}_2$ for both cases (a) and (b). Both cylinders are single rod in case (a), while in case (b) the second cylinder is a double rod.

Solution:
To solve this problem, it is useful to first calculate the bore area and the annular rod area:

$$A = \frac{\pi}{4}D^2 = 113\,09.73 \; mm^2$$

$$a = \frac{\pi}{4}(D^2 - d^2) = 6283.19 \; mm^2$$

from which the area ratio φ can be calculated

$$\varphi = \frac{A}{a} = 1.80$$

Case (a)

The piston velocity of the first actuator is

$$\dot{x}_1 = \frac{Q_S}{A} = 0.074 \, m/s$$

The flow rate discharged by the rod side of the first actuator is equal to the flow entering the bore side of the second actuator. Therefore, the speed of the second actuator is

$$\dot{x}_2 = \frac{Q_S}{\varphi \cdot A} = 0.041 \, m/s$$

The pressure on the bore side of the second actuator is equal to the pressure on the rod side of the first actuator:

$$p_{\text{rod},1} = p_{\text{bore},2} = \frac{F}{A} = 35.37 \, bar$$

Therefore, the pressure at the supply delivery is

$$p_S = p_{\text{bore},1} = \frac{p_{\text{rod},1}}{\varphi} = 19.65 \, bar$$

Case (b)

The piston velocity of the first actuator is the same as in the case (a). Since the annulus area of the second actuator is the same of the annulus area of the first actuator, we have

$$\dot{x}_1 = \dot{x}_2 = 0.074 \, m/s$$

The pressure on the rod side of the second actuator is equal to the pressure on the rod side of the first actuator:

$$p_{\text{rod},1} = p_{\text{rod},2} = \frac{F}{a} = 63.66 \, bar$$

while the pressure at the pump delivery is

$$p_S = \frac{p_{\text{rod},1}}{\varphi} = 35.37 \, bar$$

Therefore, Case (a) allows a lower supply pressure, but case (b) gives a faster speed for the second actuator.

7.4 Telescopic Cylinders

Telescopic cylinders are used in applications where a long stroke is required while the space available for the installation is small. In fact, telescopic cylinders are extremely compact reaching a collapsed length up to 20% of the extended dimension. On the other hand, these components present a complex design and have some technical limitations due to the structural characteristics. Nevertheless, the application of telescopic cylinders is often more complex than traditional cylinders and the designer should carefully consider factors as buckling and return flow amplification, not covered in the present book.

A telescopic cylinder is built with several coaxial sections of steel tubing of different diameters. Each section defines a different stage of the cylinder. The stages are numbered from the largest to the smallest. Usually telescopic cylinders exist up to six stages. As a traditional cylinder, every stage

can be individually studied and characterized by a bore and a rod side area of influence. The bore area is circular, while the rod area is annular.

The first stages are characterized by larger areas of influence. Therefore, for a given value of the external load, they are associated to lower operating pressures. On the other hand, for a given supply flow rate, they correspond to lower actuator velocities. For this reason, it can be intuitive to observe that while extending a telescopic cylinder the first stage is also the first one to move. This because it is associated to the easiest path for the incoming flow. After one stage completes its stroke, the following stage extends. Every stage is associated with a higher extension velocity. The case of cylinder retraction is more complex and needs to be distinguished between single and double acting type.

7.4.1 Single Acting Telescopic Cylinder

A cross section of a single acting telescopic cylinder is represented in Figure 7.6 The reader should notice how the different steel tubes are internally connected. The two parameters d_1 and d_2 are enough to define the circular area of influence of each stage.

This type of components is very popular in truck applications where they are used to lift and lower the dump body. Here, the load generated by the truck body weight is unidirectional, and the lowering is controlled by gravity, as it will be explained in Chapter 13.

7.4.2 Double Acting Telescopic Cylinder

A cross section of a double acting telescopic cylinder is represented in Figure 7.7. Here, the reader can observe how the location of the hydraulic port is different from the previous case. A separate tube welded inside the second stage allows to keep the chambers separate. When the cylinder extends, the mechanism is similar to the case of the single rod, even if the location of the port is different. Also in this case, the larger stage extend first. Instead, for the retraction, the location of the side holes in the tubes causes the opposite sequence, where the last stage extends first and the other follow in sequential order.

The figure also highlights the areas of influence for extension and retraction. In the figure, d_1 and d_2 represent the diameters of the two stage rods, while d_B and d_{B1} are the diameters of the barrels.
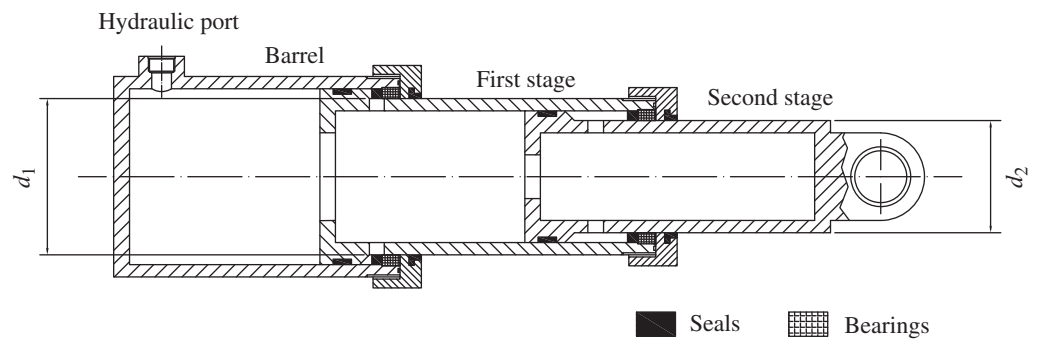
Figure 7.6 Conceptual cross-section of a two-stage single acting telescopic cylinder
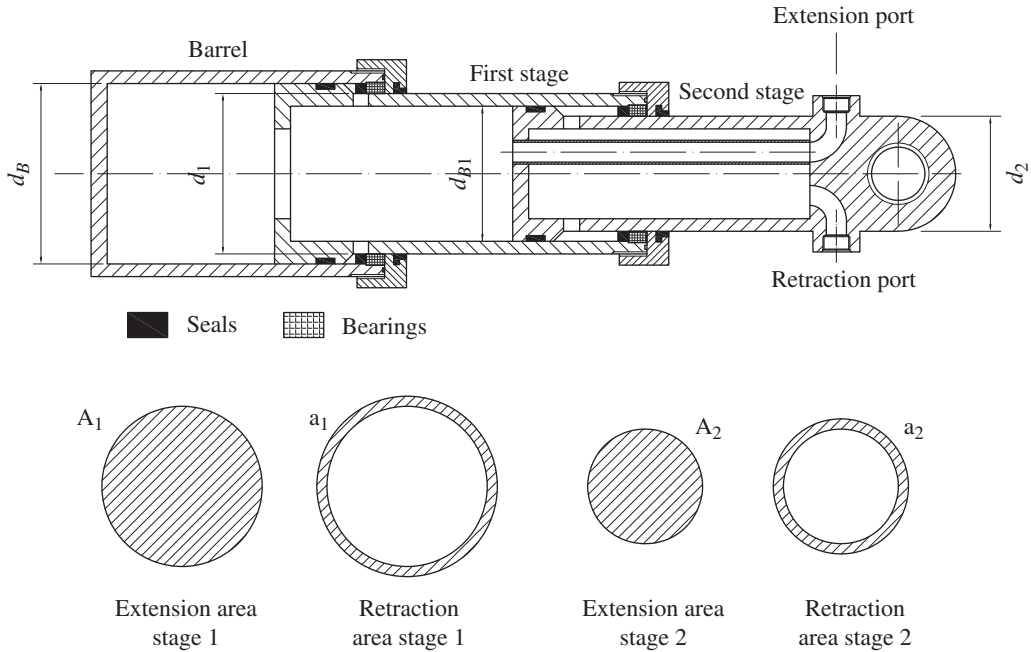
Figure 7.7 Conceptual cross-section of a two-stage double acting telescopic cylinder

The areas result to be:

$$A_1 = \frac{\pi \cdot d_1^2}{4} \quad \text{and} \quad a_1 = \frac{\pi \cdot \left(d_B^2 - d_1^2\right)}{4}$$

$$A_2 = \frac{\pi \cdot d_2^2}{4} \quad \text{and} \quad a_2 = \frac{\pi \cdot \left(d_{B1}^2 - d_2^2\right)}{4}$$

The reader can immediately observe how the value of the two area ratios (φ_1 and φ_2) can be significantly high. In particular, the design of the inner tube connected to the extension port can create a restriction and cause significant return pressures when the cylinder is retracted because of flow amplification phenomena. This situation is analyzed in the following example.

Example 7.3   Double acting telescopic cylinder

A three-stage double acting telescopic cylinder is controlled with the circuit represented below. The supply pump has a displacement of 9 *cm³/rev* and it rotates at a speed of 2000 *rpm*. The cylinder rods have diameters of 100 *mm*, 80 *mm* and 60 *mm*. The barrel diameters are instead 110 *mm*, 90 *mm* and 70 *mm*. When extending, the cylinder sees a resistive force of 28 *kN*, while when retracting the external load is null. Calculate the extension and retraction velocities and the pressures in two separate cases:

a) No restrictions present in the lines
b) The tube connected to the supply port (as shown in Figure 7.2) is equivalent to a 5 *mm* orifice

Assume an oil density equal to 850 *kg/m³* and the orifice coefficient 0.7. The relief valve is set to 150 *bar*.

Example 7.3 (Continued)
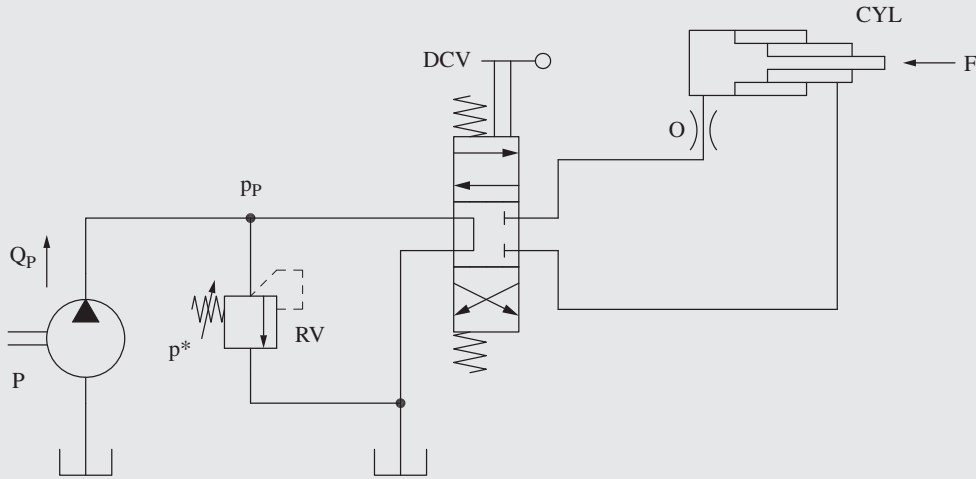
Given:

pump displacement $V_D = 8\ cm^3/rev$; pump speed $n_P = 2000\ rpm$; first stage rod $d_1 = 100\ mm$, second stage rod $d_2 = 80\ mm$, third stage rod $d_3 = 60\ mm$, first stage barrel $d_B = 110$ mm, second stage barrel $d_{B1} = 90\ mm$, third stage barrel $d_{B2} = 70\ mm$; external load during extension $F = 28000\ N$. Oil density: $\rho = 850\ kg/m^3$, flow coefficient $C_f = 0.7$. Relief valve setting $p^* = 150\ bar$.

Find:

a) Extension speeds $\dot{x}_{E1}, \dot{x}_{E2}, \dot{x}_{E3}$
b) Retraction speeds $\dot{x}_{R1}, \dot{x}_{R2}, \dot{x}_{R3}$
c) Pump pressure during extension and retraction ($p_{P,E}, p_{P,R}$)
d) Repeat calculations in case the inner tube presents a resistance equivalent to $d_O = 5\ mm$. Calculate the cylinder pressure $p_{C,R}$ and the pump pressure $p_{P,R}$ during retraction.

Solution:

a) The pump flow can be easily calculated as follows:

$$Q_P = V_D \cdot n_P = 9\ \left[cm^3/rev\right] \cdot 2000\ [rpm]\left(\frac{1}{1000}\right) = 18\ l/min$$

The bore areas of the three stages of the cylinder are:

$$A_i = \frac{\pi}{4}d_i^{\,2}\ ,\quad i = 1, 2, 3$$

These leads to the three values: $A_1 = 7854\ mm^2, A_2 = 5027\ mm^2, A_3 = 2827\ mm^2$. The three speeds are therefore:

$$\dot{x}_{Ei}\ [m/s] = \frac{Q_P}{A_i} = \frac{18\ \left[l/min\right]}{A_i\ \left[mm^2\right]}\frac{1}{0.06}$$

The three speeds result: $\dot{x}_{E1} = 0.04\ m/s, \dot{x}_{E2} = 0.06\ m/s, \dot{x}_{E3} = 0.11\ m/s$. For example, the cylinder speed in the last stage is almost three times the one in the first stage.

b) The rod areas of the three stages of the cylinder are:

$$a_i \left[mm^2\right] = \frac{\pi}{4} \left(d_{B(i-1)}^2 - d_i^2\right)$$

These leads to the three values: $A_1 = 1649\ mm^2$, $A_2 = 1335\ mm^2$, $A_3 = 1021\ mm^2$. The three speeds are therefore:

$$\dot{x}_{Ri} \left[m/s\right] = \frac{Q_P}{a_i} = \frac{18\ \left[l/min\right]}{a_i\ \left[mm^2\right]}\frac{1}{0.06}$$

The three speeds result: $\dot{x}_{R1} = 0.18\ m/s$, $\dot{x}_{R2} = 0.22\ m/s$, $\dot{x}_{R3} = 0.29\ m/s$. The values of the retract speeds are much higher than the extension. The three cylinder ratios equal:

$$\varphi_i = \frac{A_i}{a_i}$$

Where: $\varphi_1 = 4.76$, $\varphi_2 = 3.76$, $\varphi_1 = 2.77$.

c) The pump pressures during extension are the following:

$$p_{P,Ei}\ [\text{bar}] = \frac{F}{A_i} = \frac{28000\ \left[N\right]}{A_i\ \left[mm^2\right]} \cdot 10$$

The three values are $p_{P,E1} = 35.7\ bar$, $p_{P,E2} = 55.7\ bar$, $p_{P,E3} = 99.0\ bar$. Since the load during extension is null and the inlet restriction is neglected, the ideal pump pressure during retraction is also null.

d) In reality, the inlet tube creates a restriction that affects the cylinder operation both in extension and in retraction. The pressure drop across the inlet orifice is calculated from the orifice equation:

$$\Delta p\ [\text{bar}] = \frac{\rho\ \left[kg/m^3\right]}{2} \cdot \left(\frac{Q\ \left[l/min\right]}{18.97 \cdot C_f \cdot \Omega_O\ \left[mm^2\right]}\right)^2$$

During the extension, the flow across the orifice is equal to $Q_P = 18\ l/min$, therefore the corresponding pressure drop is:

$$\Delta p_E\ [\text{bar}] = \frac{850\ \left[kg/m^3\right]}{2} \cdot \left(\frac{18\ \left[l/min\right]}{18.97 \cdot 0.7 \cdot 19.6\ \left[mm^2\right]}\right)^2 = 2.0\ bar$$

For each stage of the extension, the pump pressure is increased by 2.0 bar, which seems a pretty negligible value. However, the interesting phenomena happens during the cylinder retraction. The pressure inside the cylinder chamber is in fact affected by the high area ratios. The pressure drop across the orifice is a function of the stage:

$$\Delta p_{R,i}\ [\text{bar}] = \frac{850\ \left[kg/m^3\right]}{2} \cdot \left(\frac{18\ \left[l/min\right]}{18.97 \cdot 0.7 \cdot 19.6\ \left[mm^2\right]}\right)^2 \cdot \varphi_i^2$$

The pressure drop is a function of the square value of the cylinder area ratio, therefore the retraction pressures inside the cylinder become: $p_{C\,R1} = 46.0\ bar$, $p_{C\,R2} = 28.2\ bar$, $p_{C\,R3} = 15.3\ bar$. The pump pressure is even higher. In fact, according to the cylinder force balance equation:

$$p_{P\,Ri} = p_{C\,Ri} \cdot \varphi_i$$

> **Example 7.3 (Continued)**
>
> The three pump pressures become: $p_{P\,R1} = 219\ bar$, $p_{P\,R2} = 106.0\ bar$, $p_{P\,R3} = 42.4\ bar$. The reader can notice that the pump pressure during the first stage is higher than the relief setting, even if the load on the cylinder is null. During this phase the relief valve will be open, and the cylinder will retract at a lower speed than the theoretical value previously calculated. This simple example shows how restrictions in the return line, which can be in the cylinder, in the directional control valve or in the fluid conveyance, can cause significant issues when telescoping cylinders are used.

Problems

7.1 A single acting cylinder (50-mm internal diameter) is used to lift a 500-kg gravitational load for 500 mm of stroke. The lifting phase is performed in 20 seconds. Estimate the following:
  a) the flow rate of the pump connected to the cylinder, in liter per minute
  b) the displacement of the pump, if the shaft rotates at 1000 rpm, for the ideal pump (unit efficiency)
  c) the displacement of the pump if its volumetric efficiency is 0.95
  d) hydraulic power requested by the pump, in kilowatt, for the ideal pump (unit efficiency)
  e) the mechanical power (in kilowatt) requested by the engine, for the pump with a volumetric efficiency of 0.95 and a torque (hydromechanical) efficiency of 0.92
  f) set pressure of the relief valve (considering a value 25% higher than the operating pressure) used to protect the pump, in bar.

7.2 A double acting single rod cylinder extends with a speed of 0.3 m/s. Calculate the required flow Q_B l/min at the bore chamber to reach the desired speed. Determine the return flow rate from the rod side. The piston diameter is $D = 75$ mm and the rod diameter is $d = 48$ mm. Assume no internal leakage inside the cylinder.

7.3 A double acting single rod cylinder moves with speed of 5 cm/s. Calculate required flow deliveries Q_1 and Q_2 at the cylinder ports if the piston area is $A1 = 20\ cm^2$ and the area of the annulus is $A2 = 10\ cm^2$. Assume no internal leakage inside the cylinder.

7.4 The dump body of a truck is lifted with a three-stage telescopic plunger cylinder and it is controlled with the circuit represented below. The cylinder bore is 5 in., the rod of the first stage is 4 in., the second is 3 in., and the third is 2 in. Each stage has a stroke of 2 ft. The body is lifted by shifting the directional control valve (DCV) to the right position (P-A). The body creates a load of 20 000 lbf and it is supposed constant during the lift. Calculate the pressure at the pump outlet at each stage (neglect the pressure drop caused by the DCV). Calculate the pump flow in order to execute the full lift in 35 seconds. After the body is lifted, the load is released, and the new weight of the empty body is 5000 lbf. At this point the body is lowered by shifting the DCV in the left position (A-T). In this position, the valve creates a restriction equivalent to a 4-mm orifice. Calculate the amount of time necessary for lowering the dump body.
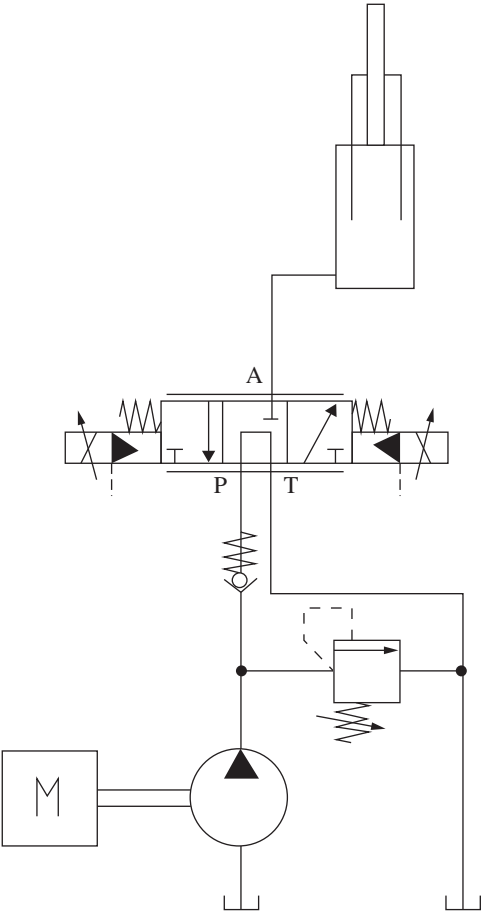
Chapter 8

Hydraulic Control Valves

The motion control of a hydraulic actuator can be achieved in many different ways; this will be further discussed in the later chapters. Some solutions heavily rely on metering elements, such as directional valves, while others on other control principles. Nevertheless, despite the control principle implemented, every hydraulic circuit uses some hydraulic control valves. For this reason, before stepping into a deeper analysis of each control concept, it is important to introduce the basic operating features of the most common *hydraulic control valves*. Hydraulic valves embrace a large number of components with various different features. A possible classification of hydraulic control valves can be based on different criteria:

- Type of control (directional, pressure control, flow control valves)
- Internal construction (spool, poppet-seat, ball, rotary type)
- Actuation method (manual, mechanical, pneumatic, hydraulic, electric actuated)
- Number of ports (two-way, three-way, etc.)
- Number of positions (two-position, three-position, etc.)
- Discrete or proportional position control
- Mounting (cartridge type, sub-plate mount, inline, etc.)

The number of options for the control valves is extremely wide, and providing a complete analysis is beyond the scope of this book. However, the operation of most hydraulic control elements can be condensed into few basic principles. This chapter illustrates these principles through examples using the most common architectures.

8.1 Spring Basics

Before analyzing the functioning of hydraulic valves, it is useful to recall some concepts about mechanical springs. The spring is very often an element playing a crucial role in a valve. The spring generates the mechanical force that is usually opposed to the control force generated either by the fluid pressure or the actuation mechanism on the sliding element (spool or poppet) inside the valve.

The force generated by a spring can be determined with Hooke's law. Figure 8.1 illustrates the force associated with the compression of a spring from its free length status:

$$F = k \cdot (L_f - L) \tag{8.1}$$

where L is the final spring length, L_f is the spring free length, and k is the spring stiffness defined as

$$k = \frac{G \cdot d_W^4}{8 \cdot D_S^3 \cdot i} \tag{8.2}$$
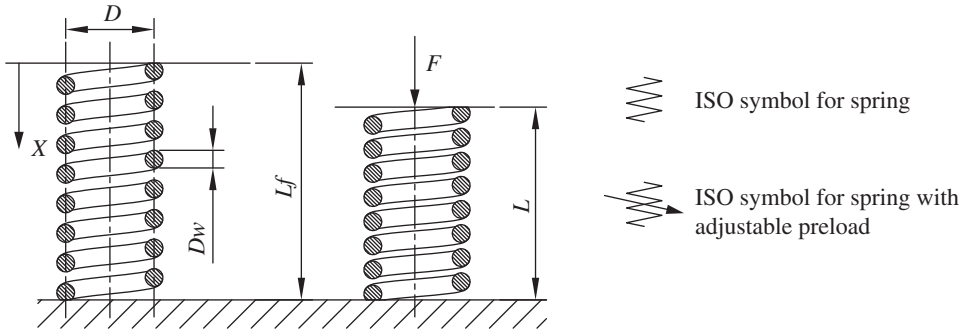
Figure 8.1 Generic parameters of springs used in hydraulic components and, in particular, in valves.

G is the material shear modulus, i the number of active coils, D_S the spring mean diameter, and d_W the wire diameter.

Equation (8.1) is always used to determine the spring force in a valve element. In most hydraulic component, the spring is not found at its free length since it is geometrically constrained between two elements capable of relative motion. With L_0 as the spring length in the neutral configuration, the spring generates a preload F_0 defined as:

$$F_0 = k \cdot (L_f - L_0) \tag{8.3}$$

During the component operation, an additional force can be then generated by a further motion of the two constraining elements, measured by the travel x:

$$F = F_0 + kx \tag{8.4}$$

In many cases, such as for pilot operated pressure control valves, the travel of the sliding element is negligible with respect to the change in force of the spring. Therefore, the spring force can be assumed constant and equal to the preload F_0. In some cases, such as for the piloting of proportional spool valves, this variation is a preferred feature of the component.

8.2 Check and Shuttle Valves

8.2.1 Check Valve

A check valve is a two-port element that allows flow only in one direction.

The symbols used to indicate check valves are shown in Figure 8.2: the expanded symbol (on the right) is often replaced by the two simplified symbols (on the left).

Common design architectures for check valves are represented in the cross-sectional views in Figure 8.3: one uses a poppet and the other a ball element. In both cases, free flow occurs from port A to port B. However, the valve does not allow flow from port B to port A. This functionality is achieved by having the sliding element (poppet or sphere) held by a spring against a seat in the valve body. The pressure at port A can easily overcome the spring, thus opening the valve and allowing the flow to port B. Vice versa, higher pressure at port B forces the sliding element against the seat.

Typically, check valves have a "soft" spring, meaning a spring with low stiffness, lightly preloaded, and not adjustable. Therefore, a minimum pressure difference between A and B (usually ranging from 0.1 up to 20 bar, depending on the design selection) is enough to overcome
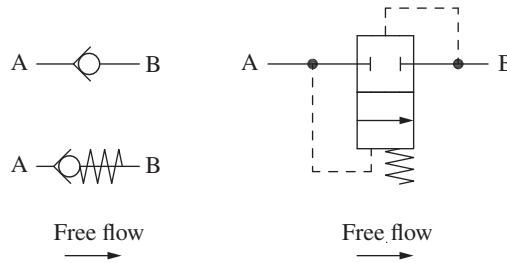
Figure 8.2 Possible symbols for a check valve.

the spring force and therefore open the valve. In most cases, check valves are applied with the weakest spring (0.1–0.2 bar), which exerts a negligible force. They work as a pure unidirectional element. In these cases, the spring can be omitted from the symbolic representation as in the top left symbol of Figure 8.2. Even if the symbol does not show any spring element, a spring is always necessary for the correct functioning of the valve. For example, it guarantees that the valve returns to the normally closed position when the system is turned off.

In some other cases, the check valve utilizes a spring with a significant preload so that the flow can cross the valve only when a certain pressure difference is reached. In this case, it is recommended to use the symbolic representation that includes the spring.

Figure 8.4 represents a typical flow–pressure characteristic of a check valve: the *x-axis* depicts the flow through the valve, while the *y-axis* the pressure drop across the element. The valve presents a cracking pressure p^* (visible from the detail view): below this value, the flow is null because the valve is closed. As soon as the pressure increases above cracking, the check valve behaves like a fixed orifice in the free flow direction. This under the assumption that the spring has a very low stiffness (as previously mentioned), so for pressures above p^*, the sliding element (ball or poppet) immediately reaches the mechanical end-stop, which limits its travel. On the other hand, in a relief valve, as shown in the next paragraphs, the spring stiffness cannot be ignored while determining the characteristic curve. The steepness of the parabola in Figure 8.4 depends on the size of the valve in consideration, which drives the equivalent orifice diameter.

8.2.2 Pilot Operated Check Valve

A pilot operated check valve (PO check) includes a third port (pilot port), which is capable to act on the sliding element in conjunction with the pressure differential previously described. In particular, two types of PO checks can be encountered in hydraulic systems (as shown in Figure 8.5): pilot-to-open and pilot-to-close check valves.
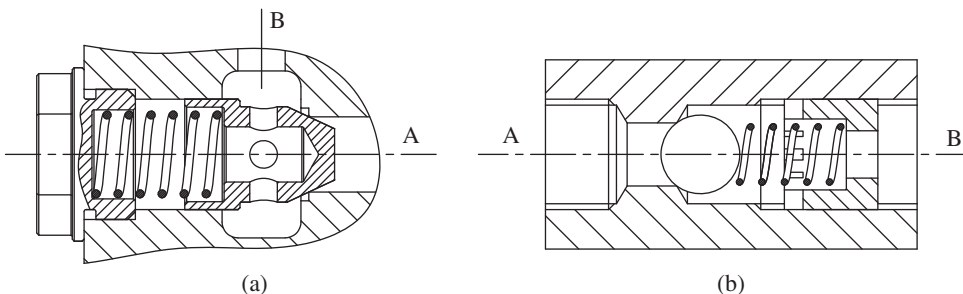
Figure 8.3 Architectures for a check valve. (a) Poppet-seat type. (b) Ball-seat type.
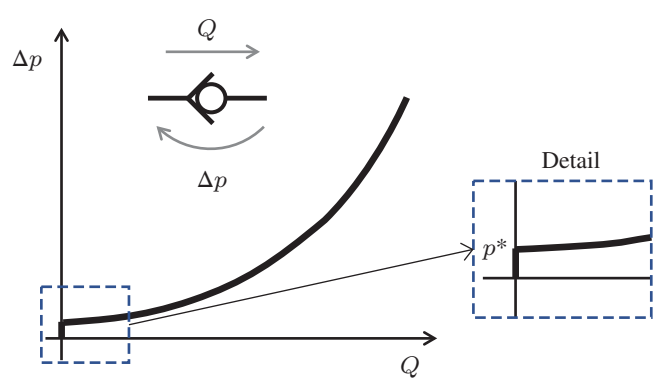
Figure 8.4 Flow–pressure characteristic of a check valve.
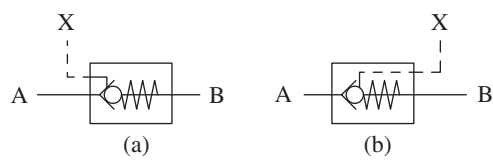
Figure 8.5 Pilot-to-open (a) and pilot-to-close (b) check valves.

A pilot-to-open check works as a regular check valve when no pressure is applied to the pilot port. However, when this is sufficiently pressurized, the sliding element is forced to open the passage between A and B, thus allowing free flow in both directions. The pilot-to-close valve instead presents the opposite behavior: pilot pressure causes the element to stay closed, blocking flow in both ways.

The pilot operated check valves will be further discussed, in more detail in Chapter 14, with examples of their application on hydraulic circuits.

8.2.3 Shuttle Valve

A shuttle valve is a three-port element that connects one port (port 2, in Figure 8.6) with either port 1 or port 3. The selection is based on the pressure present at ports 1 and 3:

- 2 is connected to 1 if $p_1 > p_3$
- 2 is connected to 3 if $p_3 > p_1$
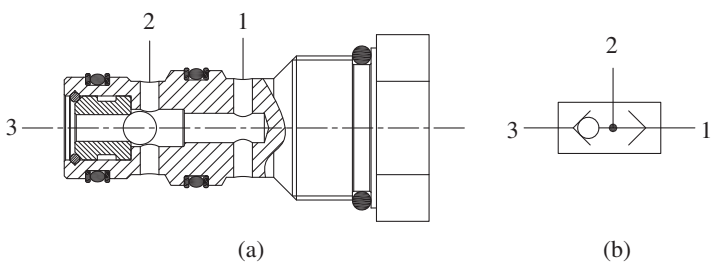
Figure 8.6 Symbol and cross-section of a shuttle valve. Cross section (a) and symbolic representation (b) of a shuttle valve.

Therefore, the shuttle valve operates as a logic element, and it is often used to select the highest pressure between two different signals.

The typical architecture of a shuttle valve is shown in Figure 8.6: a spherical element is pushed by the highest of the pressures between port 1 and port 3 blocking the port with the lower pressure. The ISO symbol is quite intuitive and reflects the typical valve architecture.

8.3 Pressure Control Valves

Although the system pressure is usually established by the loads at the actuators, hydraulic pressure control valves can be used to set or limit the pressure in a specific part of the circuit. There are several types of pressure control valves that can be found in modern hydraulic systems. This section covers the two most basic kinds of pressure control valves: pressure relief valves and pressure-reducing valves. The detailed description provided for these components will provide the key operating principles that can easily be expanded to other types of pressure control valves.

8.3.1 Pressure Relief Valve

Pressure relief valves are very common elements in hydraulic systems and are used to limit the maximum pressure in a hydraulic circuit or in a limited section of it.

> A pressure relief valve limits the maximum pressure in a hydraulic circuit or in a limited section of it.

The relief valve is normally closed, and it opens a connection to the reservoir when the pressure reaches the valve set pressure, p^*. Pressure relief valves can be direct acting or pilot operated.

Direct Acting Pressure Relief Valve
A direct acting relief valve consists of a sliding element (poppet, ball, or spool) held against a seat by spring compressed with a certain preload. Figure 8.7 shows the ISO symbol and the building blocks for a direct acting relief valve. One can notice that the relief valve is always discharging flow to tank. The functioning of a poppet type relief valve is depicted in Figure 8.8.

Architecture. The valve represented in Figure 8.8 is a cartridge-type direct acting pressure relief valve. Port P is at the bottom of the valve and connected to the high-pressure line, while port T is directly connected to the tank. This type of design is commonly defined as "nose to side" flow path. The sliding element of the valve is a poppet, which has a cylindrical top portion and a conical bottom portion. The poppet seats into the valve cage, whose upper part is also cylindrical, therefore serving as a guide for the poppet. The manufacturing accuracy of the guide is very important in
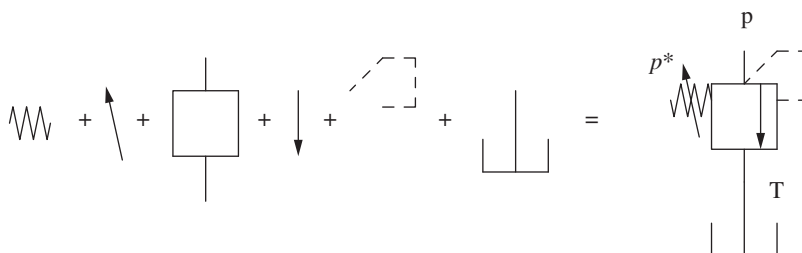
Figure 8.7 ISO symbol and its breakdown for a direct acting pressure relief valve.
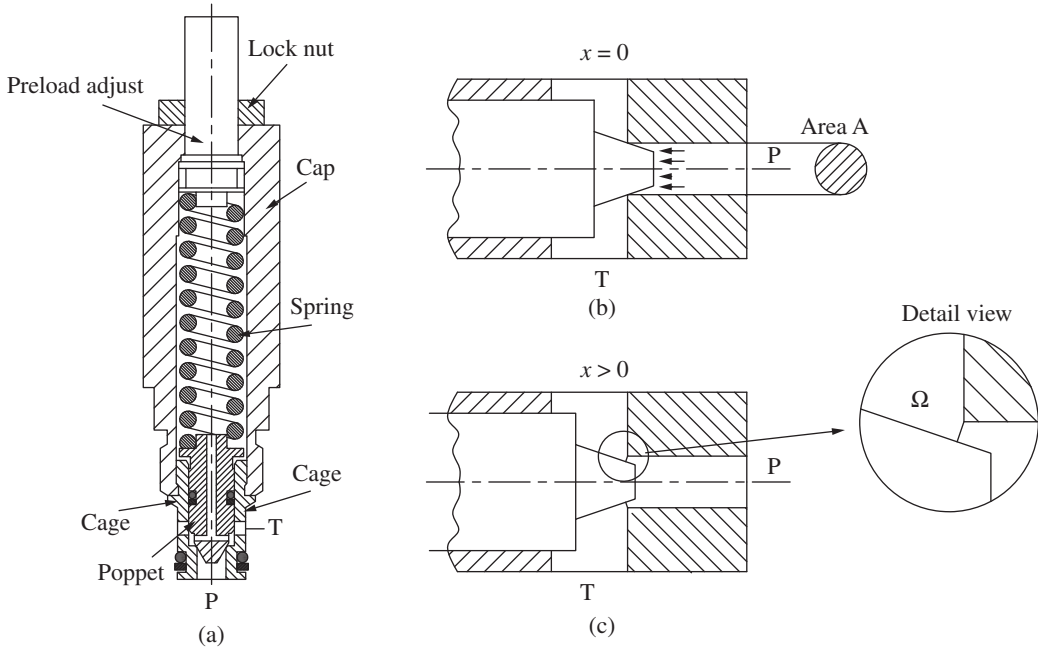
Figure 8.8 Direct acting pressure relief valve, poppet type. (a) Cross sectional view; (b) Closed position and area of influence for the opening pressure; (c) Open position, with detail on the fluid passage area.

order to allow the valve to reseat in the same configuration. The valve cage presents a seat with a reduced diameter, which is normally held in contact with the conical portion of the poppet by the spring. The upper face of the poppet is shaped in order to function as a guide for the valve spring, which is contained in a hollow cap. The upper face of the cap is threaded in order to house the manual spring adjustment mechanism, allowing the user to adjust the spring preload by changing the spring length. The adjustment screw is held in place by a lock-nut, which prevents the undesired effect of vibrations that can cause retention problems. In pressure relief valves, the spring chamber is always connected to the tank. In Figure 8.8, this is done through the axial and radial holes machined in the poppet.

This type of valve is normally used in manifolds, where the valve is threaded into a cavity machined in the block. The cage presents also a seal on the outer diameter, which acts between the cartridge and the cavity and prevents oil leakage from P to T.

The pressure at port P acts on the influence area A of the poppet, generating a force opposite to the spring force. When this force exceeds the spring preload, the poppet opens the connection P-T. Thus, the functioning of a pressure relief valve is described by two states:

- valve closed, when $p < p^*$
- valve regulating, when $p \geq p^*$

where:

$$p^* = \frac{F_0}{A} \tag{8.5}$$

The pressure p^* is referred as *cracking pressure,* or *set pressure* of the relief valve.

Equation (8.5) shows that the set pressure is directly related to the spring preload and the valve design parameter A. For this reason, in hydraulics, it is very common practice to refer to the spring preload (or force) by using a pressure value, without specifying F_0 and A.
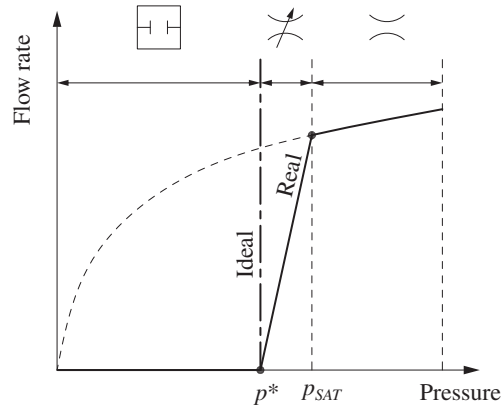
Figure 8.9 Steady-state characteristic of a direct acting pressure relief valve.

Operation. The steady-state operation of a pressure relief valve can be represented in the (p, Q) plane of Figure 8.9, where p is the pressure at port P, considered independent variable, and Q is the flow rate resulting by the control action of the valve[1]. Several aspects of valve operation are highlighted in Figure 8.9. First, when the pressure is below p^*, the valve is equivalent to a closed connection, so the discharged flow is null. For $p \geq p^*$, the valve behaves as a variable orifice, with features that are described below. The figure points out the ideal characteristic of the relief valve (vertical dash-dot line): ideally the valve can discharge any amount of flow Q while keeping the cracking pressure at port P. In this case, the equivalent variable orifice becomes infinitely open.

However, in reality, the flow discharged by the valve increases with the pressure at port P. This trend is practically linear and can be explained by the orifice equation in Eq. (4.5), applied to the valve flow area Ω, and the spring force in Eq. (8.4). As the valve opens (acting like a variable orifice), the poppet moves against the spring to establish a larger flow area; consequently both p and Q increase, with a slope related to the spring stiffness[2]. The lower the spring stiffness value, the more the valve approximates, the ideal the valve characteristic. This condition is in general difficult to achieve from a design standpoint, especially if high forces are required (Eq. (8.3)). In fact, the spring stiffness can be reduced by using springs with a high number of coils (Eq. (8.2)), as in Figure 8.8, which can become excessively long. In this area, a significant role is also played by the flow forces, which can modify the slope of the line, depending on the geometrical design of the valve.

As the pressure increases further, the valve reaches its *saturation* condition: this is because the valve cannot further increase the flow area Ω when the pressure at port P increases. Here the valve starts behaving as a fixed orifice and the characteristic follows the typical orifice parabolic curve. Reaching saturation can be due to various reasons, such as the sliding element hitting a mechanical end-stop, or also an insufficient area for the valve ports. Saturation of a pressure relief valve is detrimental for the hydraulic circuit: in these conditions, the valve can discharge an additional flow only if the pressure at port P increases drastically. Thus, it is always important to carefully select the maximum rated flow, to guarantee that saturation conditions are never reached during the operation of the system.

---

1 Although the (p, Q) representation for a relief valve is formally more correct than the equivalent (Q, p) representation, on product data sheets, the (Q, p) is the preferred one.
2 In reality, the slope of the (p, Q) valve characteristic does not depend only by the linear $F(x)$ function of the spring. Depending on the valve design, other forces need to be considered in the force balance of the sliding element. These include fluid momentum (flow forces, described in Chapter 3), and frictional forces.

An interesting remark pertains to the definition of the valve-cracking pressure p^*. Although this value theoretically divides the two states of the valve (open or closed), the practical difficulties associated with measuring tiny flow rates are usually solved by providing a set pressure value that corresponds to a pre-determined Q through the valve (in the order of few liters per minute).

Despite the advantages of a very simple and reliable design and a fast dynamic response, direct acting relief valves encounter the limits to their application when the valve needs to discharge high flows at high pressures. In these cases, in order to work below the saturation condition, the valve has to be capable of high flow areas Ω. This can be obtained by increasing the sliding element size, thus increasing the influence area A. Therefore, the forces involved in the spring setting can easily grow. This leads to assembly and adjustment issues, besides the increase in size of the overall valve. This problem is overcome by using pilot operated relief valves.

Pilot Operated Pressure Relief Valve

Architecture. Figure 8.10 depicts an example of pilot operated pressure relief valve: port P is at the bottom of the valve and it is connected to the pressure line, while ports T and Y are on the side of the valve. In this particular design, ports T and Y are both connected to the tank externally, since there is no sealing element between the two, while there is a seal between P and T. This valve design presents two springs and two sliding elements: a poppet V1 and a spool V2. The flow discharged from P to T is controlled by V2, where four radial holes can open a connection with respect to a port machined in the cage.

The pressure at P is acting on the right end of V2. This spool presents a small axial drilling (equivalent to an orifice marked as O) connecting P to the chamber X. This latter is sealed from T, due to the tight tolerances between V2 and the valve cage. In the neutral condition, the pressure at P is pushing both ends of V1 (with an equal area of influence A_{V1}). Chamber X contains a spring, which keeps V2 against the retaining ring and ensures that the connection between P and T is closed.

The left side of chamber X serves also a seat to the second sliding element, V1. The sliding element is held against the seat by the force of a second spring, which can be adjusted by a screw. This design is very similar to the direct acting relief valve of Figure 8.9: V1 opens the connection between X and Y when the pressure in X overcomes the spring force.

V2 is usually defined as the main stage of the valve, while V1 is the valve pilot stage. It is immediately noticeable how the pilot stage spring has a much thicker wire than the main stage. This is general guideline useful to distinguish pilot from the main stage.

Operation. Figure 8.11 represents the generic ISO symbol for a pilot operated relief valve. The labeling in Figure 8.11 is consistent with that in Figure 8.10, to facilitate the understanding of the link
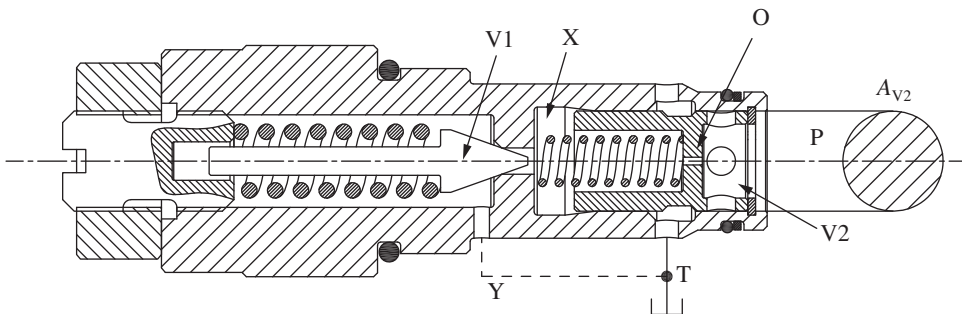
Figure 8.10 Pilot operated pressure relief valve.
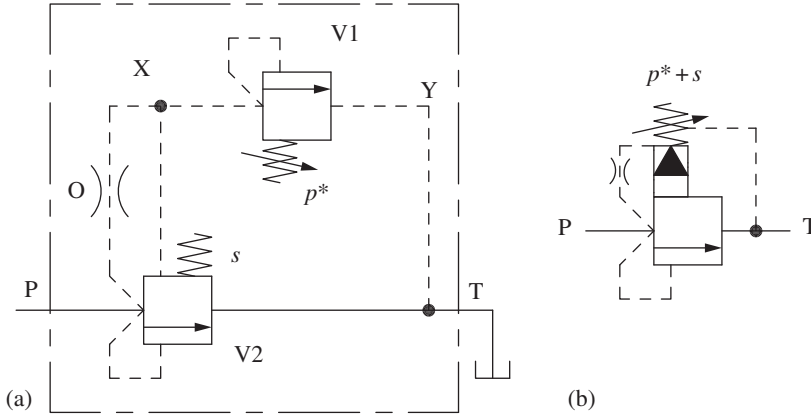
Figure 8.11 Detailed ISO representation of a pilot operated relief valve (a) and a simplified ISO symbol (b).

between the symbolic representation and the physical design. The pilot stage (V1) creates a connection to the reservoir (port Y) through the pilot (dotted) line. In this pilot line, a fixed orifice (O) is installed with the function of a *pressure separator*. A pressure drop between port P and point X is created in case the pilot stage (V1) opens establishing a flow through it. The main stage (V2) is similar to a direct operating relief valve, but it uses an additional pilot connection from point X to pressurize the spring chamber.

The functioning of the pilot operated pressure relief valve can be shown in the (p, Q) plane of Figure 8.12, and it can be described by analyzing its states corresponding to different levels of the pressure at port P:

– $p_P < p^*$ (valve closed). In this condition, the pilot stage is closed, and there is no flow through the orifice O. Due to the spring s, the sliding element of the main stage remains at its neutral position (closed), since the pressures at its opposite sides, p_X, p_p are equal.

– $p^* \leq p_P < p^* + s$. In this condition, the pilot stage opens discharging flow to tank through port Y. The pressure at point X is limited by the pilot stage setting ($p_X = p^*$). The main stage is still closed because the closing force is still greater than the opening force:

$$p_P \cdot A_{V1} < p^* \cdot A_{V1} + F_s \tag{8.6}$$
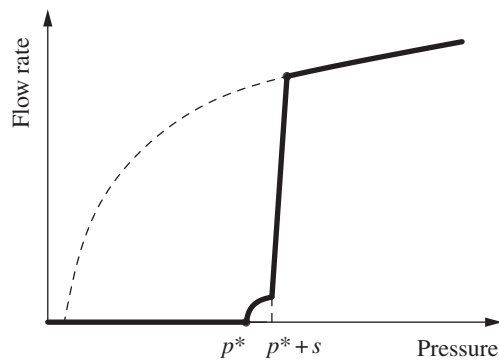
Figure 8.12 Steady-state characteristic of pressure relief valves: qualitative comparisons between pilot operated and direct acting valves.

where $F_s = s\,A_{V1}$. The flow is discharged by the valve only through the pilot line, and it is given by the pressure drop $p_P - p^*$ across the orifice O. Therefore, the valve characteristic in this region resembles the parabolic trend of an orifice with a small flow area[3]. The curve starts at p^*, the minimum pressure at which V1 opens.

– $p_P \geq p^* + s$ (valve open). In this case, both stages are open. The opening and closing forces acting on the sliding element of the main stage are now in equilibrium:

$$p_P \cdot A_{V1} = p^* \cdot A_{V1} + F_s \tag{8.7}$$

This is because the pilot stage still limits the pressure at X ($p_X = p^*$). Therefore, the main stage adjusts its opening to maintain a specific set pressure at port P:

$$p_P = p^* + s \tag{8.8}$$

Typically, when the valve enters into this state, the contribution of the pilot stage on the overall discharged flow is negligible because the main stage offers a larger P-to-T connection area.

The valve operation provided above highlights the convenience of utilizing small spring preloads for the main stage, s. In fact, a small value of s implies:

– a negligible influence of the transition region between the opening and closing of the valve ($p^* \leq p_P < p^* + s$), in which only the pilot stage is open and the valve characteristic is far from the ideal one (vertical line, in Figure 8.12)
– an almost ideal (vertical) characteristic of the valve when its main stage is open. This is possible because the small preload s can be achieved with a soft spring (low k), according to Eq. (8.2).

In this way, the pilot operated design offers an elegant solution to the conflicting requirements for the spring stiffness k, pointed out when describing the characteristic of the direct acting relief valve (Figure 8.9). In fact, in the pilot operate valve, the high valve settings p^* is achieved with a stiff pilot spring. The pilot poppet allows very short travels, usually negligible, when the valve opens. On the other hand, a very soft (low k) spring is used at the main stage, whereas the sliding element is need for high travels in order to discharge high flow rates.

For the reasons explained above, pilot operated pressure relief valves are commonly used for high flow ($Q \gg 40\,\mathrm{l/min}$) and high pressure ($p^* > 100\,\mathrm{bar}$) settings. Valve saturation can still occur when the main stage reaches its maximum travel (Figure 8.12).

With respect to the direct acting design, a possible disadvantage of pilot operated pressure relief valves is the higher leakage rate, due to the presence of multiple sealing regions, as pointed out when describing the architecture in Figure 8.10.

8.3.2 Pressure-reducing Valve

> A pressure-reducing valve sets the pressure of a portion of the hydraulic circuit located downstream the valve itself.

A pressure relief valve is normally closed and controls the pressure upstream, whereas the pressure-reducing valve is normally open and controls the downstream pressure. Brake circuits and pilot supply lines for directional control valves (DCVs) are typical applications of these components. Similarly to the case of pressure relief valves, pressure reducing valves can also be implemented with a direct acting or pilot operated design.

---

3 Pilot lines are used to transfer pressure information at low flow rates, so that their power level as well as the physical size of the pilot stages are minimized. Consequently, small orifices (diameter lower than 1 mm) are used in these lines.
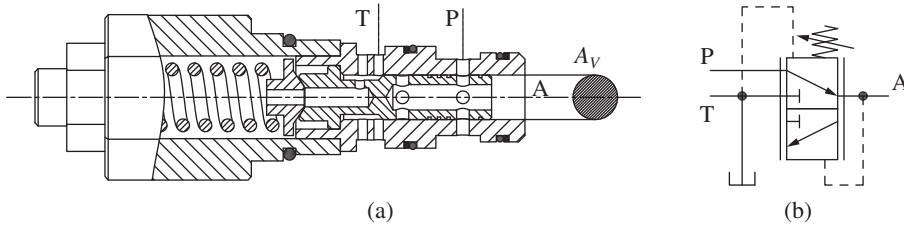
Figure 8.13 Direct acting pressure reducing and relieving valve: cross sectional view (a) and equivalent ISO symbol (b).

Direct Acting Pressure-reducing Relieving Valve

Architecture. Figure 8.13 shows a cross-section of a typical direct acting pressure-reducing valve and its equivalent ISO schematic. The valve has three ports: P is the supply line, A is the controlled pressure line, and T is connected to the tank. The sliding element is a spool, which is held against a mechanical stop by the force generated by an adjustable spring. The spring chamber is always connected to the tank, through the axial and radial drillings in the spool and spring guide. In the neutral position, as displayed in the figure, port A is connected to port P through the radial holes in the spool. With further travel of the spool against the spring, the connection $P \rightarrow A$ gradually closes as the spool land covers the radial holes of port P in the cage. After the complete closure of $P \rightarrow A$, a second spool land opens a connection $A \rightarrow T$ through a second set of radial holes in the cage.

Operation. Figure 8.14 represents the ideal operating characteristic of the valve in a (p_A, Q_A) plane, which can be described by three different states according to the pressure at the valve outlet:

– $p_A < p^*$ (valve open). This situation occurs in two possible cases: when the supply pressure at P is lower than p^* or when pressure cannot build at the port A. In both cases, the pressure at port A, acting on the area of influence A_V, generates a force lower than the spring force $F = p^* \cdot A_V$. Thus, the spring prevails and the flow area of the connection $P \rightarrow A$ is completely open. The valve behaves as a fixed orifice between P and A.

– $p_A = p^*$ (valve regulating – reducing). In this condition the ports involved in the valve operation are P (inlet) and A (outlet): the valve maintains p_A at the set value p^* by throttling flow from port P. The spool travels establishing a proper restriction for the connection $P \rightarrow A$, so that the forces acting on the spool are balanced:

$$p_A \cdot A_V = F \tag{8.9}$$

– $p_A \geq p^*$ (valve regulating – relieving). In this state, the valve limits the pressure at port A to the set value p^* by relieving flow to port T, connected to the tank. In this case, the valve behaves similarly to a pressure relief valve and prevents over-pressurization of the downstream circuit caused by external events.

To implement this functionality, the valve spool can further travel and completely close the connection $P \rightarrow A$. Simultaneously, a variable connection $A \rightarrow T$ is created to drain flow from A to T. In this state, flow Q_A is considered with a negative sign since it is in the opposite direction with respect to the previous state. The presence of this state is the reason this type of valve is commonly designated as *pressure-reducing and -relieving valve*.

Pressure relief valves (Figure 8.8) are two-way valves (P, T) because the downstream port is always connected to the tank. However, pressure-reducing valves, beside ports P and A, need an additional third port T in order to refer the spring chamber to a known pressure value. This available connection can be used to implement the additional relief functionality of the device.
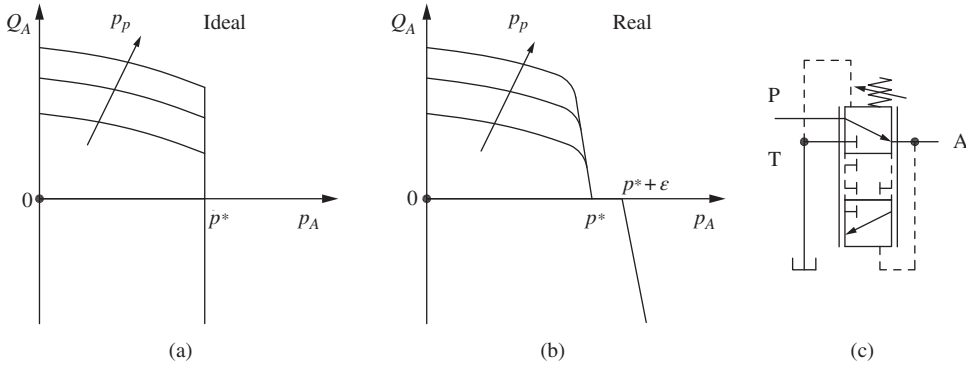
Figure 8.14 Ideal (a) and real operating characteristics (b) of a pressure reducing and relieving valve. The ISO symbol (c) indicates the transition position.

Figure 8.14 shows the real characteristic of the reducing relieving valve. To describe the real trend, two factors have to be considered. The first is the stiffness of the spring, which determines an inclination of the characteristic when the valve is regulating. The second one is the overlapping of the spool lands and the port in the valve body, which implements the $P \rightarrow A$ and $A \rightarrow T$ openings. In this case, after the $P \rightarrow A$ connection is fully closed, the spool has to further travel before the $A \rightarrow T$ connection opens. The length of this travel is normally indicated as *positive overlap*, which, in this case, is a desired feature because it avoids a direct connection between P and T that would waste flow during regulation. When this feature is relevant for the circuit operation, the transition between two valve positions can be indicated in the symbol using dotted lines, as represented in Figure 8.14. The positive overlap of the valve is the reason for which the relieving characteristic starts at $p^* + \varepsilon$.

Pilot Operated Pressure Reducing Valve

Architecture. Figure 8.15 shows the cross-section of a cartridge-type pilot operated pressure-reducing valve and its equivalent ISO schematic. In Figure 8.10, the valve presents two stages, each one with a sliding element and springs. The main stage V2 is a three-way spool valve connecting P, A, and T and realizing the same configuration of the direct acting case. This spool presents a small drilling, which represents the orifice O between port A and chamber X. Chamber X, delimited by the spool and a fixed disc rigidly connected to the valve body, contains a soft spring, which holds the main spool against a mechanical stop. The fixed disc also serves as seat for the valve pilot stage V1, which in this case is a ball-type relief valve set at p^*. The spring chamber of the pilot stage is drained to T through the clearances between the valve elements, as shown in the figure.

Operation. With reference to the ISO schematic of Figure 8.15, the valve operation in the ideal case can be defined by the following states:

- $p_A < p^*$ (valve open). The pressure at port A is equal to the pressure at chamber X because the pilot relief is closed and there is no flow across the orifice O. The connection $P \rightarrow A$ is fully open. $p^* < p_A < (p^* + s)$ (valve open). The pilot relief is now open and the pressure at port X is limited to p^*. The flow discharged from A-T is given by the pressure drop $(p_A - p^*)$ across the orifice O. However, the flow discharged by the pilot element does not affect the valve operation, which stays open.
- $p_A = (p^* + s)$ (valve regulating). The pilot stage is still limiting the pressure $p_X = p^*$ but now the main spool is regulating and reduces the P→A area. The pilot stage is consuming oil Q_Y,
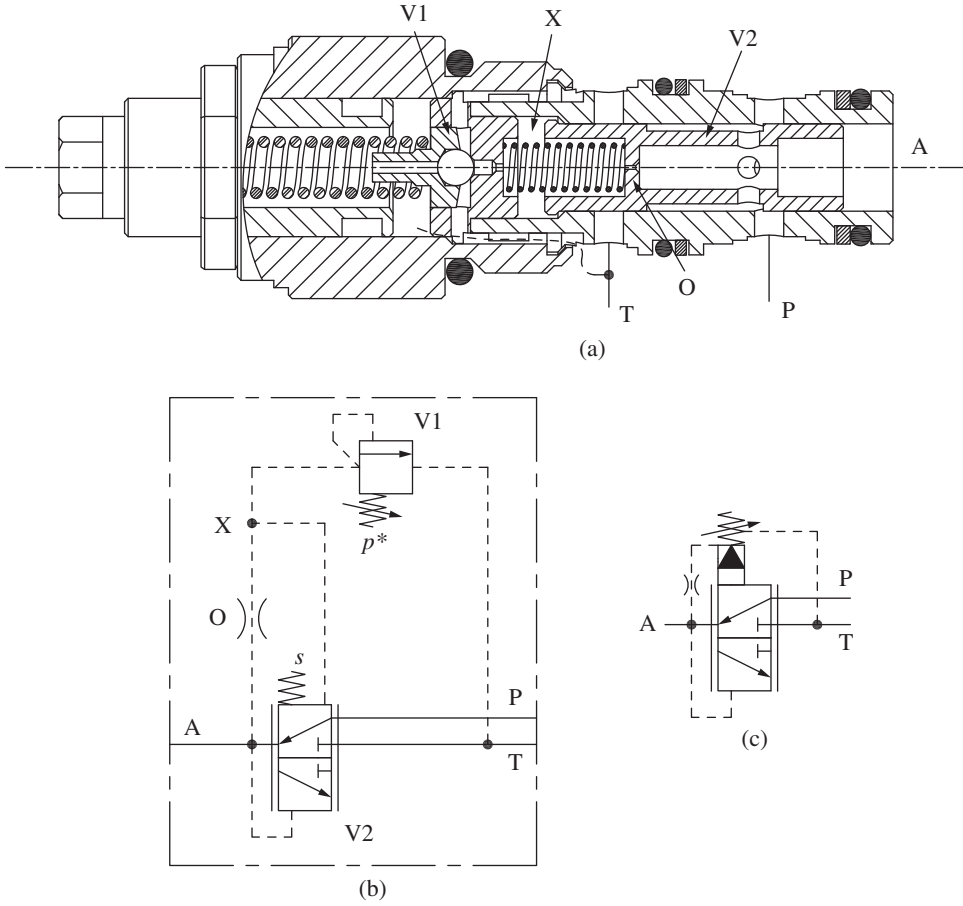
Figure 8.15 Pilot operated pressure reducing valve: cross sectional view (a), detailed ISO representation (b), simplified ISO symbol (c).

according to the following:

$$Q_Y = C_f \Omega_O \sqrt{\frac{2(p_A - p_X)}{\rho}} = C_f \Omega_O \sqrt{\frac{2s}{\rho}} \tag{8.10}$$

– $p_A \geq (p^* + s)$ (valve relieving). As in the case of the direct acting pressure-reducing relieving valve, the main stage three-way spool can prevent over-pressurization of port A by connecting it to the tank.

The same considerations done for the real vs. ideal characteristic of the direct acting valve can be done for the pilot operated reducing valve, considering the spring effect and the positive overlap.

As for the case of the relief valve, the pilot operated pressure-reducing valve can operate discharging higher flows, since the main spool is acting only on the soft spring. The pilot operated reducing valve, as highlighted in Eq. (8.10), always consumes a pilot flow when it is regulating. As this flow taken from port P, therefore, the power loss associated with this flow is equal to:

$$P_{L,Y} = Q_Y \cdot p_P \tag{8.11}$$

This value can be significant, affecting the efficiency of the system. Therefore, when it is an option, the use of direct acting pressure-reducing valves is often preferable.

8.4 Flow Control Valves

> Flow control valves (FCVs) are used to control the amount or the direction of flow at the down-stream section of the hydraulic circuit.

A common way to classify these valves is based on their ability to perform their function independently of the downstream pressure, which is normally created by external loads. *Pressure-compensated FCVs* control the flow independently of the downstream pressure.

Fixed or variable orifices, such the needle valve shown in Chapter 4, are typical *non-compensated* elements. In this case, the flow rate through the valve depends not only on the area setting but also on the upstream and downstream pressures, according to the orifice equation.

This section illustrates two basic methods to control flow independently of pressure. As it will be described in following chapters, these principles of flow regulation often occur also in more complex valve architectures.

8.4.1 Two-way Flow Control Valve

> A two-way FCV, from a conceptual standpoint, is achieved with two orifices in series: one working as metering and the other as compensator.

According to their relative position, the valve can be *pre-compensated* or *post-compensated* (Figure 8.16).

Architecture. An example of post-compensated valve is shown in Figure 8.17. The flow enters axially through the inlet port A and exits the valve through port B, via axis-symmetric radial holes machined into the valve body. The inlet flow passes through a calibrated orifice O1 entering an intermediate chamber X. O1 is the metering orifice of the valve. The spool position determines the area for the connection $X \rightarrow B$: this restriction becomes the compensator orifice of the FCV. The pressure in X is transmitted through a dynamic orifice O2 to the spring chamber, at the side of the spool opposite to the inlet port A. The spool equilibrium depends on the pressure at its opposing end surfaces p_A, p_X and the spring force.

Operation. The functional principle of the two-way FCV is given by the force balance of the sliding element of the compensator and the orifice equation applied to the metering element. Figure 8.18 provides also a detailed ISO schematic representative of the component, alternative to the one of Figure 8.16c. The balance of the sliding element when the valve is regulating is given by:

$$p_A \cdot A_O = p_X \cdot A_C + F \tag{8.12}$$

(a)	(b)	(c)
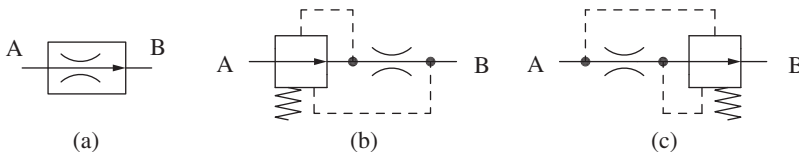
Figure 8.16 ISO representation of a two-way flow control valve: simplified symbol (a), a detailed representation for a pre-compensated (b), and a post-compensated valve (c).
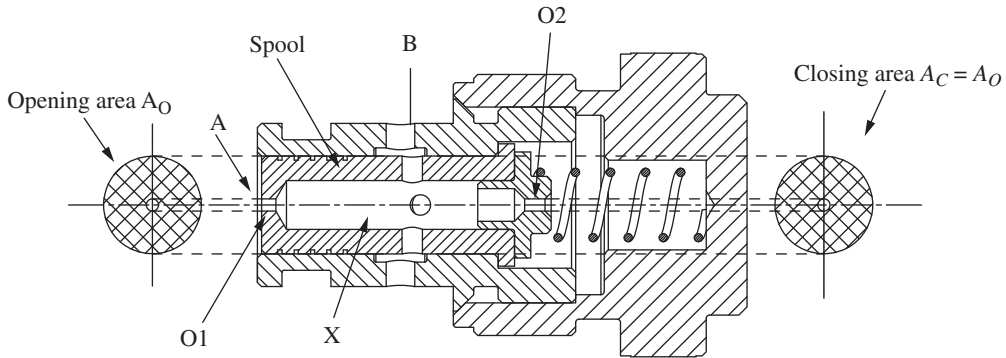
Figure 8.17 Cross-section of a post-compensated two-way flow control.

By indicating the spring force in terms of pressure,

$$s = \frac{F}{A_C} \tag{8.13}$$

In the majority of the cases, the two areas of influence are equal ($A_O = A_C$), therefore:

$$p_A - p_X = s \tag{8.14}$$

This permits to simplify the equation for the metering orifice O1 as follows:

$$Q = C_f \cdot \Omega_{O1} \cdot \sqrt{\frac{2(p_A - p_X)}{\rho}} = C_f \cdot \Omega_{O1} \sqrt{\frac{2s}{\rho}} \quad (= Q^*) \tag{8.15}$$

Equation (8.15) summarizes the basic functionality of the two-way FCV and highlights the independence of the regulated flow from the system pressure. Equation (8.14) summarizes the *pressure compensation* principle demonstrated by the valve: the compensator orifice establishes a defined Δp (equal to the spring force s) across the metering orifice. In this way, the flow rate through the valve is only function of design parameter (being Ω_O the most important one).

The characteristic of the two-way FCV is represented in the Q vs. $(p_A - p_B)$ plane, in the plot of Figure 8.19.

For $(p_A - p_B) < s$, the valve is not regulating because the sliding element is held at its neutral position against the end-stop. In this condition, the valve flow rate is lower than the rated flow Q^*. For $(p_A - p_B) \geq s$, the ideal characteristic is a horizontal line, although the real trend can differ from the ideal one due to the effects of spring compression or flow forces. In case the compensator
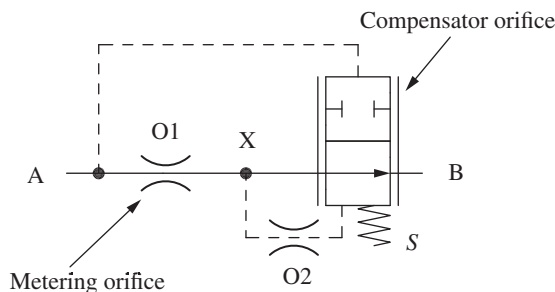
Figure 8.18 Detailed ISO symbol for the valve of Figure 8.17.
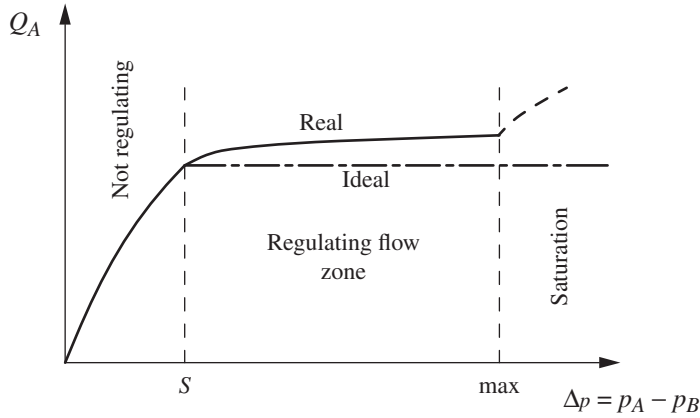
Figure 8.19 Characteristic of a two-way pressure compensated valve.

cannot completely close because of mechanical end-stops, the valve saturation can be reached for high values of $(p_A - p_B)$. This is not the case of the example shown in Figure 8.17.

Two-way FCVs can also be found with adjustable flow setting; Figure 8.20 shows two different architectures where the setting Q^* can either be varied by adjusting the area of the orifice or by varying the spring setting *s*.

One important aspect of FCVs is the analysis of the power consumption of the valve, as both the compensator and metering elements introduce a pressure drop between inlet and outlet:

$$P_{L,V} = Q_A s + Q_A(p_A - p_B - s) = Q_A(p_A - p_B) \tag{8.16}$$

Equation (8.16) shows the expression of the power loss highlighting the contribution of the metering element $Q_A s$ and of the compensator $Q_A(p_A - p_B - s)$.

An important remark concerning two-way FCVs is that they should not be used in cases in which the flow rate is already determined by another element upstream the valve.

8.4.2 Fixed Displacement Pump Circuit with a Two-way Flow Control Valve

This example illustrates how the two-way FCV operates to regulate the flow provided to a generic consumer (e.g. a motor, a cylinder, or a leg of hydraulic circuit).

The circuit in Figure 8.21 includes a fixed displacement pump (P1) supplying flow to an adjustable two-way FCV (V1). Downstream V1, a generic consumer U is located, which imposes a load pressure p_U. Between the outlet of P1 and the inlet of V1, a pressure relief valve, set at p^*, is located. The outlet flow generated by the pump is indicated as Q_P, while the setting of the valve V1 is Q^*. The operating condition of the circuit depends on the setting Q^* of the FCV:
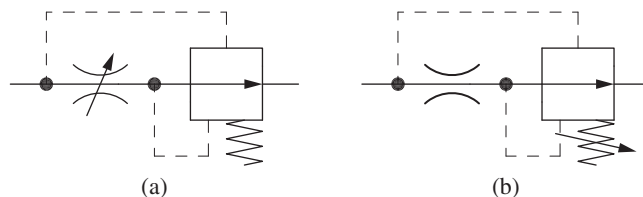
Figure 8.20 Examples of variable setting two-way flow control valves.
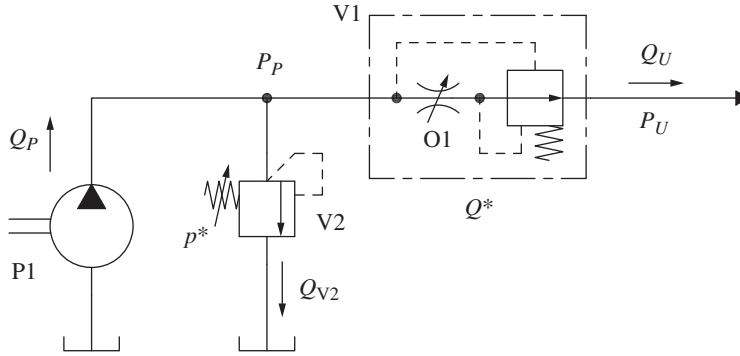
Figure 8.21 Circuit with a two-way flow control supplied by a fixed displacement pump.

a) $Q^* \geq Q_P$. In this case, the valve V1 is not regulating, and the compensator is wide open. All the flow is going to the consumer $Q_U = Q_P$. The pressure at the pump outlet is the sum of p_U and the pressure drop across the orifice O1:

$$p_P = p_U + \frac{Q_P{}^2}{C_f{}^2 \cdot \Omega_{O1}{}^2} \frac{\rho}{2} \tag{8.17}$$

This latter equation is valid under the assumption that the pump pressure remains lower than the maximum pressure p^* allowed by the relief valve V2, so that $Q_{V2} = 0$.

b) $Q^* < Q_P$. In this case, the valve V1 is regulating, and the compensator restricts the flow area in order to maintain the desired pressure drop across the metering orifice O1. The excess flow $(Q_P - Q^*)$ generated by the pump can only be discharged through the relief V2. This condition can only be achieved if the outlet pressure of the pump reaches p^*.

When the valve is regulating, the power consumed by the system is given by the sum of the useful power P_U and the power loss P_L:

$$P = P_U + P_L = Q_U \cdot p_U + \{Q_U \cdot (p^* - p_U) + (Q_P - Q_U) \cdot p^*\} \tag{8.18}$$

Equation (8.18) highlights the power dissipation introduced by circuit, where the term $Q_U \cdot (p^* - p_U)$ represents the contribution of the two-way flow control, while the term $(Q_P - Q_U) \cdot p^*$ is the loss on the relief valve. It is important to note that in case 1), the valve V2 does not perform its flow regulation function and represents only a power dissipation element.

Due to these losses, the circuit in Figure 8.21 does not represent an energy efficient application of the two-way FCV since the valve conflicts with the pump operation as they both function as flow-regulating elements in series. The circuit efficiency can be improved by using a three-way FCV, as explained in the following section.

Example 8.1   Velocity control of a hydraulic motor

Consider the hydraulic circuit of the figure below. The system is supplied by a 50 cm^3/r pressure-compensated variable pump (P) rotating at 1800 *rpm*. The pressure setting of the pump is 150 *bar*. The pump supplies a 50 cm^3/r motor (M), which has a resistive torque of 50 *Nm*. A two-way FCV is located between the pump and the motor and it is set to 40 *l/min*. The spring setting of FCV is 5 *bar*. A manual valve (MV) is used to bypass the motor and divert the flow directly to the tank.

Example 8.1 (Continued)
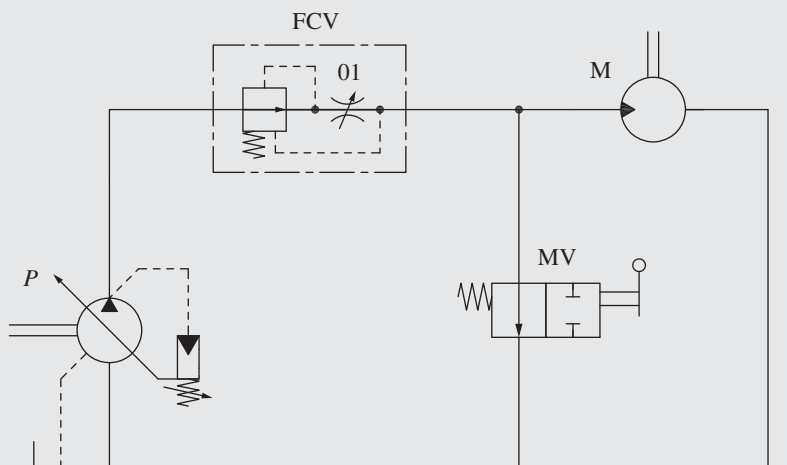
Assume the ideal operation of the system (no pressure losses in the lines, ideal pump, and motor efficiencies).

Calculate:

a. The pump flow rate and pump pressure when MV is in neutral and shifted position
b. The displacement setting of the pump and the shaft speed and supply pressure of the motor when MV is actuated
c. The useful power (power consumption of the motors) and the input power (power consumption of the pump), in kilowatt. Calculate the system efficiency, as a ratio of the two calculated powers, in percentage.

Given:

The hydraulic schematic of a hydraulic system supplying flow to one motor. The displacement of the hydraulic motor, $V_m = 50 \ cm^3/r$; the torque at the motor (resistive), $T_m = 50 \ Nm$. The setting of a two-way FCV $Q^* = 40 \ l/min$, with spring setting $s = 5 \ bar$. The displacement of the supply pump, $V_p = 50 \ cm^3/r$ the pump shaft speed $n_p = 1800 \ rpm$, the setting of the pressure compensator at $p^* = 150 \ bar$. Assume an ideal behavior for the components (no energy loss at the pumps, motors, and lines).

Find:

a) The flow rate of the pump, Q_p when MV is in neutral or shifted position
b) The displacement setting of the pump, ε, the shaft speed n_m and supply pressure p_m of the moor
c) The output power P_{out}, the input power, P_{in} and the system efficiency η_{SYS}

Solution:

The motor has a flow supply based on a variable displacement pump and a two-way FCV. A 2/2 manual operated valve can enable the motor when actuated. In normal position, it diverts the flow to the tank.

a) Under the assumption that the pressure at the motor is lower than $p^* - s = 145 \ bar$, when MV is shifted (which will be later verified), the pump output flow always matches the setting of the FCV. Therefore,

$$Q_p = Q^* = 40 \ l/min$$

b) The pressure at the motor inlet can be calculated from the given torque and displacement:

$$p_m = \frac{T_m}{V_m} = \frac{50\,[Nm]}{50\,[cm^3/r]} \cdot 20\pi = 68.2\,bar$$

The value of p_m is lower than $p^* - s$. This confirms answer (a) is correct. The motor rotates at the following speed:

$$n_m = \frac{Q^*}{V_m} = \frac{40\,[l/min]}{50\,[cm^3/r]} \cdot 1000 = 800\,rpm$$

The pump operates at a displacement setting equal to

$$\varepsilon = \frac{Q^*}{n_p \cdot V_p} \cdot 100 = \frac{40\,[l/min]}{1800\,[rpm] \cdot 50\,[cm^3/r]} \cdot 10^5 = 44.4\%$$

c) The useful power of the system is the motor output power:

$$P_m = Q_m \cdot \Delta p_m = 40\,[l/min] \cdot 68.2\,[bar] \cdot \frac{1}{600} = 4.19\,kW$$

The pump sits at the compensated pressure, equal to 150 *bar*. The power input to the system is

$$P_p = Q_p \cdot p^* = 40\,[l/min] \cdot 150\,[bar] \cdot \frac{1}{600} = 10.0\,kW$$

Therefore, the system efficiency is

$$\eta_{SYS} = \frac{P_m}{P_p} = \frac{4.19\,[kW]}{10.0\,[kW]} = 41.9\%$$

As a further consideration, since all components are assumed to have an ideal behavior, the power loss in the system is all concentrated to the two-way FCV. In fact, although the load at M requires 68.1 bar, the pump is required to work at the maximum pressure ($p^* = 150\,bar$). Therefore, it is important to remark that this low energy efficiency is not due to a poor performance of the components, but to the functional operation of the system.

8.4.3 Three-way Flow Control Valve

A three-way FCV is also composed of a metering orifice, O1, and a compensator (or *unloader*). With respect to the two-way FCV, in this configuration the elements are connected in parallel, forming a three-port layout.

The metering orifice connects the valve inlet P to the controlled flow port A, while the compensator connects the port P to an additional outlet port T, usually connected to tank, as shown in Figure 8.22. The different design of this compensator (normally closed) can be observed with respect to the previous one (normally open, shown in Figure 8.16). The compensating element can control the flow across the metering element by discharging the exceeding portion of the flow entering from P to the tank. When used in this configuration, the compensator is also referred as *unloader*.

Architecture. An example of three-way FCV architecture is shown in the cross-sectional view in Figure 8.23. The image reports also its equivalent ISO symbol. The inlet flow enters axially through port P, while the two outlet ports A and T are accessible by radial holes machined in
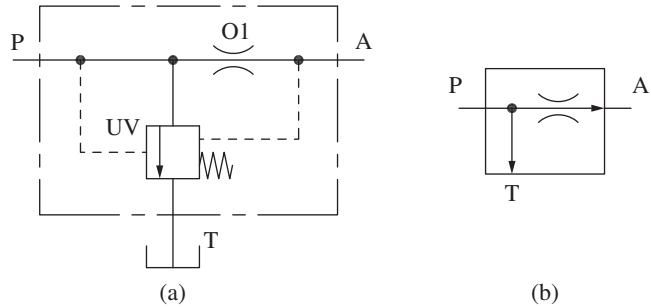
Figure 8.22 Detailed (a) and simplified (b) ISO representations of a three-way flow control valve.

an axis-symmetric configuration in the valve body. The valve spool is hollow, and it houses two calibrated orifices: O1 (metering), which connects the inlet port P with the internal chamber X, and O2 (dynamic orifice), which connects X with the spring chamber. In the neutral configuration, the valve spool closes the connection to port T. The force resulting from the different pressures at the spool ends (p_P, p_X) can make it travel against the spring, opening of the connection $P \rightarrow T$. The spool motion, however, does not affect the connection between the internal chamber X and the port A.

Operation. The principle of operation of the valve is based on the force balance of the spool, which determines the flow area of the compensator orifice between port P and port T. This balance reads as:

$$p_P \cdot A = p_B \cdot A + F \tag{8.19}$$

where A represents the areas of influence of the pressure at the compensator. Also in this case, the spring force F can be expressed as a pressure value:

$$s = \frac{F}{A} \tag{8.20}$$

so that the balance implemented by the compensator becomes:

$$p_P - p_A = s \tag{8.21}$$
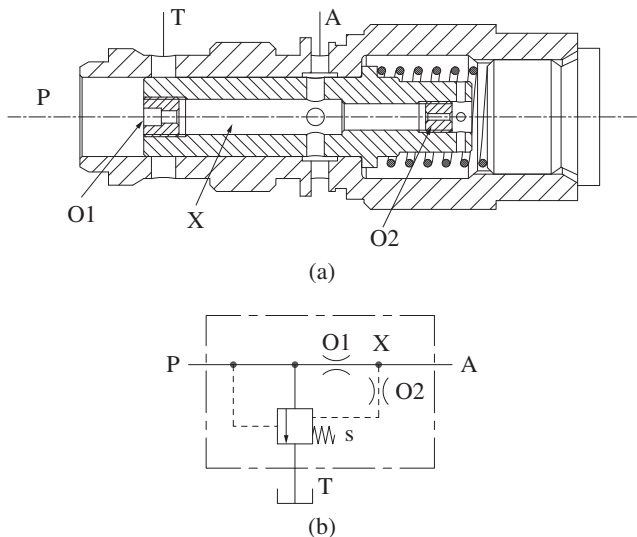
Figure 8.23 Three-way flow control valve: cross-section and equivalent symbol.
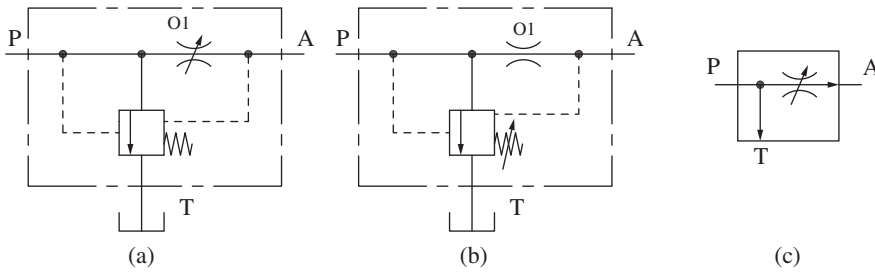
Figure 8.24 Different solutions for adjustable three-way flow control valves (a, b) and simplified ISO symbol (c).

The equation for the metering orifice O1 can be expressed as follows:

$$Q = C_f \cdot \Omega_{O1} \cdot \sqrt{\frac{2(p_P - p_A)}{\rho}} = C_f \cdot \Omega_{O1} \sqrt{\frac{2 \cdot s}{\rho}} \, (= Q^*) \tag{8.22}$$

Equation (8.22) summarizes the function of the three-way control valve, which can establish the flow rate at the port A to a set value Q^* by maintaining a constant pressure drop across the metering orifice O1. Three-way FCVs are usually adjustable, and their setting Q^* can be varied by changing either the value of the spring force or the metering orifice area, as shown in Figure 8.24.

The principle of operation of the three-way FCV appears to be equal to one of the two-way FCV, as evident by comparing Eqs. (8.15) and (8.22). However, the additional T connection of the three-way FCV permits to discharge the excess flow without overpressurizing the port P. In general, this permits a more energy efficient way to control the flow rate, as it will be described in the following example.

8.4.4 Fixed Displacement Pump Circuit with a Three-way Flow Control Valve

The control of the flow rate to a generic consumer by using a three-way FCV is illustrated in Figure 8.25, with a reference circuit: a fixed displacement pump P1 generates the flow rate Q_P, while the three-way FCV V1 is used to set the desired value of flow rate Q^* to the actuator. A pressure relief valve (V2) is used as a safety element, to limit the maximum pressure in the circuit to p^*.
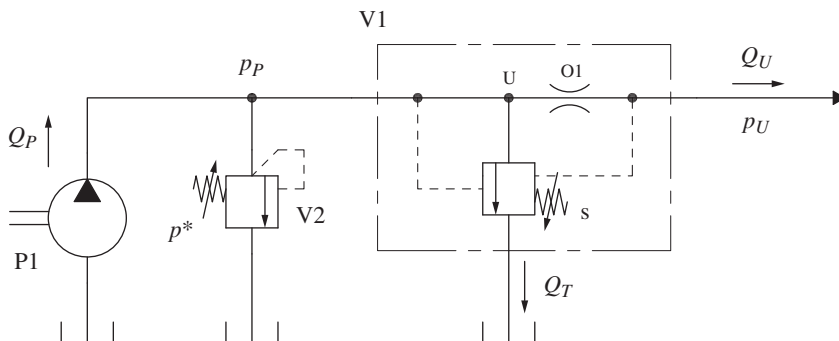
Figure 8.25 Circuit with a two-way flow control supplied by a fixed displacement pump.

The circuit operation can be described as a function of the setting of the three-way FCV:

a) $Q_P < Q^*$. In this case, the compensator is not regulating, and the connection to tank is closed ($Q_T = 0$) because:

$$p_P - p_U = \frac{Q_P{}^2}{C_f{}^2 \cdot \Omega_{O1}{}^2} \frac{\rho}{2} < \frac{Q^{*2}}{C_f{}^2 \cdot \Omega_{O1}{}^2} \frac{\rho}{2} = s \tag{8.23}$$

This means that the pressure difference $p_P - p_A$ is not sufficient to move the spool against the spring. The entire flow generated by the pump goes to the actuator ($Q_P = Q_U$) and the pump pressure is:

$$p_P = p_U + \frac{Q_P{}^2}{C_f{}^2 \cdot \Omega_{O1}{}^2} \frac{\rho}{2} \tag{8.24}$$

b) $Q_P \geq Q^*$. The excess flow generated by the pump is discharged to the tank through the compensator:

$$Q_T = Q_P - Q^* \tag{8.25}$$

The compensator sets a constant pressure drop across the metering orifice O1, according to Eq. (8.14). Therefore, the pump pressure is:

$$p_P = p_U + s \tag{8.26}$$

The power consumed by the system when the valve is regulating the flow is given by the useful power term, P_U, and the power loss term, P_L:

$$P = P_U + P_L = Q_U \cdot p_U + \{Q_U \cdot s + (Q_P - Q^*) \cdot (p_U + s)\} \tag{8.27}$$

By comparing the power losses associated with the circuits of Figure 8.21 (two-way) and Figure 8.25 (three-way), it is evident the advantage of the three-way flow control concept:

$$P_{L,\text{two-way}} = Q_U \cdot (p^* - p_U) + (Q_P - Q^*) \cdot p^* \tag{8.28}$$

$$P_{L,\text{three-way}} = Q_U \cdot s + (Q_P - Q^*) \cdot (p_U + s) \tag{8.29}$$

In the three-way flow control circuit in Figure 8.25, the relief valve V2 is not involved in the normal circuit operation, unlike the two-way circuit in Figure 8.21. This is why Eq. (8.29) does not involve the setting of the relief valve p^*, which can easily be much higher than the value of $(p_U + s)$.

Furthermore, the compensator of a three-way flow control can be also used as part of the relief functionality: Figure 8.26 shows how the valve compensator in combination with the pilot stage V2 also fulfills the function of a pilot operated relief valve. In this case, the orifice O2 works as *pressure separator* (similarly to what was described in the pilot operated pressure relief valve) in case V2 enters in regulation.
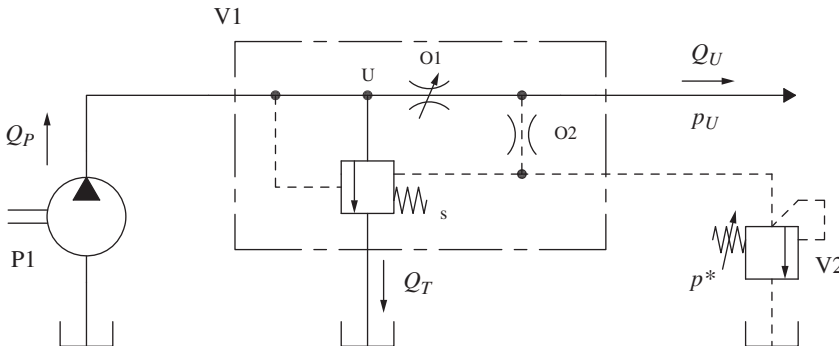
Figure 8.26 Circuit where the three-way flow control is also used for accomplishing the relief functionality.
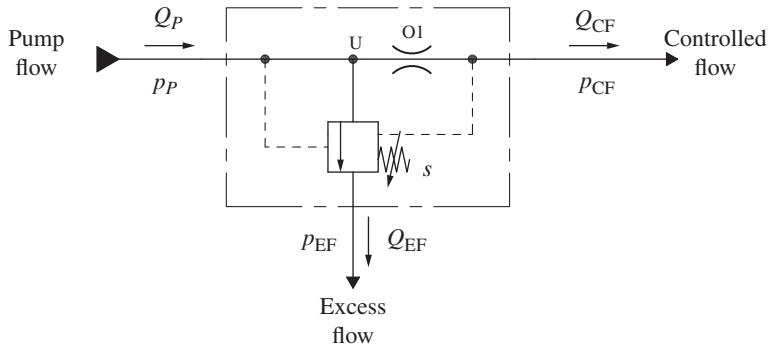
Figure 8.27 Three-way priority flow control valve.

In some applications, the same layout of a three-way FCV is used to implement a priority flow control logic (Figure 8.27). The flow at the port CF (*controlled flow*) is defined by the valve setting Q^*, while the excess flow is provided to the port EF (*excess flow*), which can be connected to a second actuator. This type of functionality will be better discussed in Chapter 22.

Example 8.2   – Flow rate of a three-way flow control valve

For the system represented in the figure below, assuming $C_f = 0.65$ (orifice coefficient) and an oil density of $\rho = 870\,kg/m^3$, determine the flow rate to the cylinder as well as the inlet pressure for following cases:

1. $Q_{in} = 60\,l/min$ and $F_{load} = 5000\,N$
2. $Q_{in} = 60\,l/min$ and $F_{load} = 25\,000\,N$
3. $Q_{in} = 20\,l/min$ and $F_{load} = 5000\,N$
4. $Q_{in} = 10\,l/min$ and $F_{load} = 5000\,N$
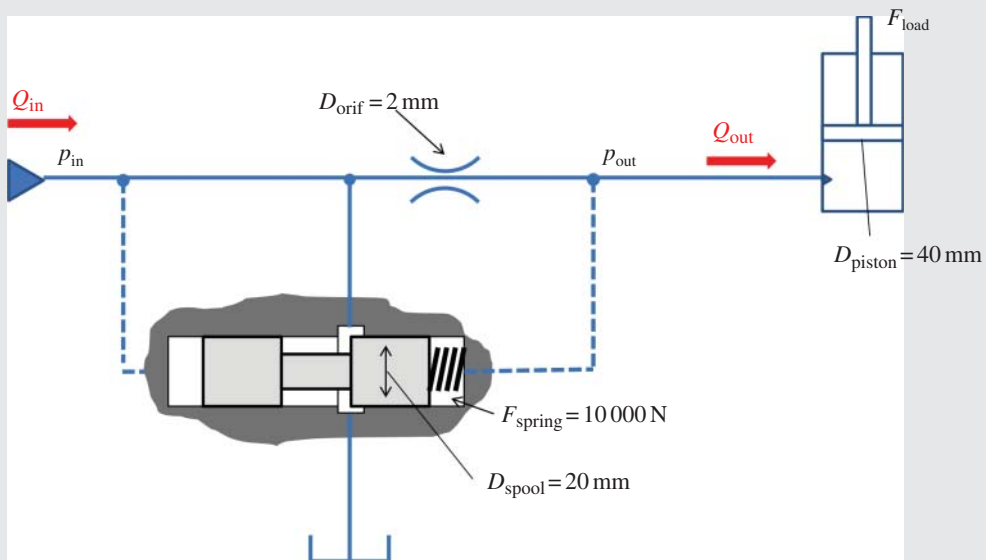
(Continued)

Example 8.2 (Continued)

For each case, determine the useful power to the load as well as the power dissipated in the hydraulic components shown in the figure.

Given:

A three-way FCV, with a metering orifice of diameter, $D_{orif} = 2\ mm$; a spool compensator of diameter, $D_{spool} = 20\ mm$; and a spring, $F_{spring} = 1000\ N$ (the spring force can be assumed constant). The outlet port of the three-way valve is connected to a single acting cylinder with piston diameter $D_{piston} = 40\ mm$. Four different scenarios are given for the inlet flow and the load acting on the cylinder:

1. $Q_{in} = 60\ l/min$ and $F_{load} = 5000\ N$
2. $Q_{in} = 60\ l/min$ and $F_{load} = 25\,000\ N$
3. $Q_{in} = 20\ l/min$ and $F_{load} = 5000\ N$
4. $Q_{in} = 10\ l/min$ and $F_{load} = 5000\ N$

Find:

For all the given conditions, determine the flow rate to the cylinder, Q_{out}; the pressure at the inlet of the three-way FCV, p_{in}; and the useful power P_u and the power dissipated in the three-way FCV, P_{loss}.

Solution:

Case 1 ($Q_{in} = 60\ l/min$ and $F_{load} = 5000\ N$)

The inlet pressure can be found by considering the spool balance of the compensator of the three-way FCV:

$$p_{in}A_{spool} = F_{spring} + p_{out}A_{spool}$$

so that

$$p_{in} = \frac{F_{spring}}{A_{spool}} + p_{out} = \frac{F_{spring}}{\frac{\pi}{4}D_{spool}^2} + p_{out}$$

p_{out} can be found from the given load:

$$p_{out,1} = \frac{F_{load,1}}{A_{piston}} = \frac{F_{load,1}}{\frac{\pi}{4}D_{piston}^2} = \frac{5000\ [N]}{\frac{\pi}{4}(40\ [mm])^2} = \frac{5000\ [N]}{12.56 \cdot 10^{-4}\ [m^2]} = 39.8\ bar$$

The inlet pressure is therefore

$$p_{in,1} = \Delta p_{orif} + p_{out,1} = \frac{F_{spring}}{\frac{\pi}{4}D_{spool}^2} + p_{out,1} = \frac{1000\ [N]}{\frac{\pi}{4}(20\ [mm])^2} + 39.8\ bar$$

$$= \frac{400\ [N]}{3.14 \cdot 10^{-4}\ [m^2]} + 39.8\ [bar] = 12.7\ [bar] + 39.8\ [bar] = 52.5\ bar$$

The flow to the cylinder can be calculated by applying the orifice equation at the metering orifice:

$$Q_{out,1} = C_f\Omega_{orif}\sqrt{\frac{2(p_{in,1} - p_{out,1})}{\rho}} = C_f\left(\frac{\pi}{4}D_{orif}^2\right)\sqrt{\frac{2\Delta p_{orif}}{\rho}}$$

$$= 0.65\left[\frac{\pi}{4}(3\ [mm])^2\right]\sqrt{\frac{2 \cdot 12.7\ [bar]}{870\ [kg/m^3]}}$$

$$= 0.65 \cdot 7.06 \cdot 10^{-6}\ [m^2] \cdot 54.03\ [m/s] = 2.48 \cdot 10^{-4}\ [m^3/s] = 14.9\ l/min$$

The piston extension velocity can be calculated as

$$\dot{x}_{\text{piston},1} = \frac{Q_{\text{out},1}}{A_{\text{piston}}} = \frac{14.9\,[l/min]}{12.56 \cdot 10^{-4}\,[m^2]} = 0.20\,m/s$$

This value is useful to calculate the useful power:

$$P_{u,1} = F_{\text{load},1} \cdot \dot{x}_{\text{piston},1} = 5000\,[N] \cdot 0.20\,[m/s] = 0.99\,kW$$

The power loss is given by the product between flow and pressure across the metering orifice and the compensator of the three-way FCV:

$$P_{\text{loss},1} = Q_{\text{out},1}(p_{\text{in},1} - p_{\text{out},1}) + (Q_{\text{in},1} - Q_{\text{out},1})(p_{\text{in},1} - p_T)$$
$$= 14.9\,[l/min](52.5\,[bar] - 39.8\,[bar]) + (60\,[l/min] - 14.9\,[l/min])\,(52.5\,[bar] - 0\,[bar])$$
$$= 0.315\,[kW] + 3.946\,[kW] = 4.26\,[kW]$$

Case 2 ($Q_{\text{in}} = 60\,l/min$ and $F_{\text{load}} = 25\,000\,N$)
For this case

$$p_{\text{out},2} = \frac{F_{\text{load},2}}{A_{\text{piston}}} = \frac{25\,000\,[N]}{12.56 \cdot 10^{-4}\,[m^2]} = 199.0\,bar$$

and, similarly to the previous case,

$$p_{\text{in},2} = \Delta p_{\text{orif},2} + p_{\text{out},2} = 12.7\,[bar] + 199.0\,[bar] = 211.7\,bar$$

The flow rate has the same value of the previous case 1:

$$Q_{\text{out},2} = C_f \Omega_{\text{orif}} \sqrt{\frac{2(p_{\text{in},2} - p_{\text{out},2})}{\rho}} = C_f \Omega_{\text{orif}} \sqrt{\frac{2\Delta p_{\text{orif},2}}{\rho}} = 14.9\,l/min$$

The useful power is

$$P_{u,2} = F_{\text{load},2} \cdot \dot{x}_{\text{piston},2} = 25\,000\,[N] \cdot 0.20\,[m/s] = 5.00\,kW$$

The power loss has the same expression as for the case 1:

$$P_{\text{loss},2} = Q_{\text{out},2}(\Delta p_{\text{orif},2}) + (Q_{\text{in},2} - Q_{\text{out},2})(p_{\text{in},2} - p_T) = 14.9\,[l/min] \cdots 12.7\,[bar]$$
$$+ (60\,[l/min] - 14.9\,[l/min])\,(199.0\,[bar] - 0\,[bar]) = 0.315\,[kW] + 14.958\,[kW]$$
$$= 15.27\,kW$$

Although the flow sent to the consumer is the same as in case 1, the power dissipated in case 2 is much higher due to the high pressure of the flow that is diverted to tank by the compensator of the three-way FCV.

Case 3 ($Q_{\text{in}} = 20\,l/min$ and $F_{\text{load}} = 5000\,N$)
The formulas here are the same as those in cases 1 and 2:

$$p_{\text{out},3} = \frac{F_{\text{load},3}}{A_{\text{piston}}} = \frac{25\,000\,[N]}{12.56 \cdot 10^{-4}\,[m^2]} = 39.8\,[bar]$$

$$p_{\text{in},3} = \Delta p_{\text{orif},3} + p_{\text{out},3} = 12.7\,[bar] + 39.8\,[bar] = 52.5\,bar$$

$$Q_{\text{out},3} = C_f \Omega_{\text{orif}} \sqrt{\frac{2\Delta p_{\text{orif},3}}{\rho}} = 14.9\,l/min$$

$$P_{u,3} = F_{\text{load},3} \cdot \dot{x}_{\text{piston},3} = 5000\,[N] \cdot 0.20\,[m/s] = 0.99\,kW$$

Example 8.2 (Continued)

$$P_{\text{loss},3} = Q_{\text{out},3}(\Delta p_{\text{orif},3}) + (Q_{\text{in},3} - Q_{\text{out},3})(p_{\text{in},3} - p_T)$$
$$= 14.9\,[l/min]\,12.7\,[bar] + (20\,[l/min] - 14.9\,[l/min])\,(52.5\,[bar] - 0\,[bar])$$
$$= 0.315\,[kW] + 0.446\,[kW] = 0.761\,kW$$

For case 3, the power lost at the FCV is much less compared to the previous case due to the lower flow that the compensator needs to divert to the tank.

Case 4 ($Q_{\text{in}} = 10\,l/min$ and $F_{\text{load}} = 5000\,N$)
This case is of particular interest because the inlet flow is not enough to open the compensator stage of the valve, which is normally closed.

In fact, the whole flow goes through the orifice, causing a pressure drop of

$$\Delta p_{\text{orif},4} = (p_{\text{in},4} - p_{\text{out},4}) = \left(\frac{Q_{\text{orif}}}{C_f \Omega_{\text{orif}}}\right)^2 \frac{\rho}{2} = \left(\frac{10\,[l/min]}{0.65 \cdot 7.06 \cdot 10^{-6}\,[m^2]}\right)^2 \frac{870\,[kg/m^3]}{2}$$
$$= 5.74\,bar$$

This $\Delta p_{\text{orif},4}$ represents the pressure acting at the two spool sides of the compensator stage, and being

$$(p_{\text{in},4} - p_{\text{out},4})A_{\text{spool}} < F_{\text{spring}}$$

the compensator will not open. In fact, to open, there must be enough inlet flow to establish a Δp_{orif} equal to $12.7\,bar$ as in the previous cases. In this case, the whole flow rate entering the valve goes through the actuator:

$$Q_{\text{in},4} = Q_{\text{out},4} = 10\,[l/min]$$

The functional behavior of the fixed orifice of the three-way FCV is now as compensator. The actuator velocity is now

$$\dot{x}_{\text{piston},4} = \frac{Q_{\text{out},4}}{A_{\text{piston}}} = \frac{10.0\,[l/min]}{12.56 \cdot 10^{-4}\,[m^2]} = 0.13\,m/s$$

Therefore, the useful power is

$$P_{u,4} = F_{\text{load},4} \cdot \dot{x}_{\text{piston},4} = 5000\,[N] \cdot 0.13\,[m/s] = 0.65\,kW$$

while the power dissipated at the three-way FCV is represented only by the loss at the fixed orifice, $P_{\text{loss},4} = Q_{\text{out},4}(\Delta p_{\text{orif},4}) = 10\,[l/min] \cdot 5.74\,bar = 0.096\,kW$

8.5 Directional Control Valves

A DCV is an element used to control the direction and the amount or simply the direction of the flow to one or more hydraulic actuators.

The family of the DCVs consist of many valve types, each with something different from the others. DCVs can be classified or grouped according to many criteria, which includes their functionality.

> DCVs can be separated in *on/off* valves and *infinite positioning* valves, commonly known as *proportional* DCVs. On/off valves control only the direction of the flow and, ideally, they create flow paths with either a null (when closed) or infinitely large flow area (when open) between the ports.

On/off valves are used in circuits where the amount of flow is controlled by other elements, such as a pump or a FCV.

> Proportional directional valves control both the direction and the amount of flow.

Proportional directional valves accomplish this functionality by generating restrictions to the flow path. A particular case of infinite positioning valves is represented by *discrete positioning valves*. These work within a discrete number of positions as on/off valves. However, when actuated, they create restrictions designated to control the flow to the functions. Figure 8.28 shows the different symbols adopted for on/off, discrete, and proportional DCVs. In particular, orifices are represented within the arrows of discrete position valves. Infinite positioning valves, but are represented with two additional lines above and below the symbol and the work-ports.

A particular case of infinite positioning valves is represented by *servovalves*, which differ from proportional DCVs because they implement an internal closed-loop architecture to accurately control of the spool position. Servovalves will be further discussed in a separated section of this chapter.

Other criteria for classifying the different types of DCVs consider the number of ports of the valve, the layout of the connections enabled by the working positions, and the type of actuation. In the current common mobile and industrial applications, the vast majority of DCVs are spool-type proportional valves. They are usually identified by the following features: a supply port P (usually connected to the pump outlet), a return port T (usually connected to tank), and two work-ports A and B, connected to the actuator ports. Such component is usually referred as a four-way three-position (4/3) proportional DCV. The general considerations in the following are illustrated by simple examples. However, they are also valid for other more complex types of valves, which will be covered in the chapters focused on metering controls.

Figure 8.29 shows a basic schematic and a cross-section of a 4/3 DCV. As mentioned, 4/3 indicates the number of ports and the number of possible positions implemented by the valve. In this case, in neutral (or central) position, the valve blocks all the ports, and no internal connection is made. When actuated in position 1, the valve establishes a connection between the inlet P and the work-port A and between the work-port B and the return port T. In position 2 (crossed arrows), the DCV connects P to the work-port B and the work-port A to T.

The design architecture in Figure 8.29 is suitable for on/off, discrete, and infinite position configurations. In the infinite position case, the valve and the spool are meant to operate in any relative position between spool and body. On the other hand, in the on/off case, the DCV is designed to operate only at three given positions: the center and the two extreme shifting positions (where the flow areas are maximized). In the discrete positioning configuration, the valve still works at three given positions of the spool but realizing some controlled restriction of the ports, as indicated in Figure 8.28.
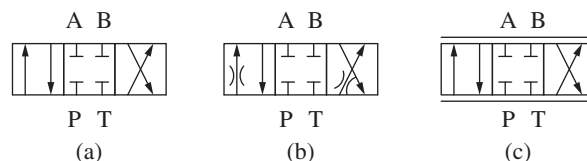
Figure 8.28 ISO symbols used for (a) on/off, (b) discrete position, and (c) infinite position DCVs.
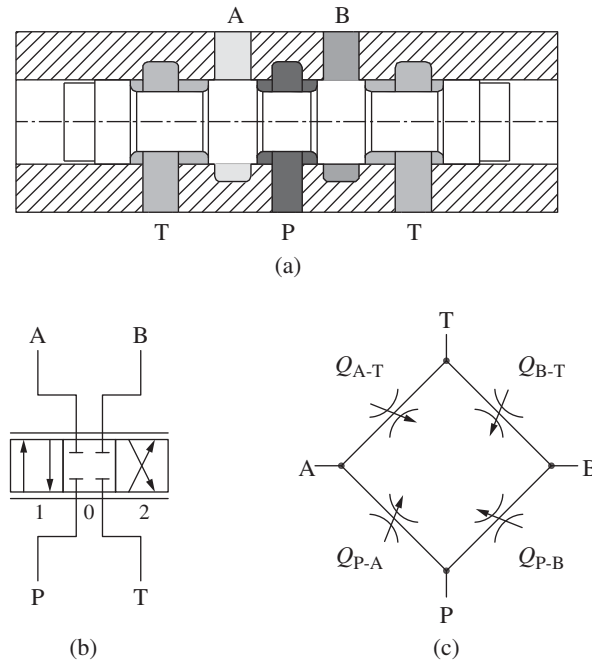
Figure 8.29 Example of a 4/3 spool directional control valve (a): simplified cross-sectional view (b); ISO symbol; equivalent representation with variable orifices (c).

8.5.1 Meter-in and Meter-out Configurations

Figure 8.29 also shows how the represented 4/3 DCV is equivalent to a combination of four variable orifices in a bridge configuration. They are gradually opened or closed as the spool travels toward each position. The area of these orifices is determined, as shown in Figure 8.30, by the relative position of metering lands on the spool with respect to the lands in the spool bore, machined in the body. In particular, two of the orifices O_{P-A} and O_{P-B} are located between the inlet port P and the work-ports A and B, while orifices O_{A-T} and O_{B-T} are located between the work-ports and the return line T. The first orifices determine the *meter-in* characteristic of the DCV, while the second ones the *meter-out* characteristic[4]. While this paragraph focuses on the DCV architecture, Chapter 12 will provide a detailed analysis of metering control aspects.

Figure 8.31 represents an example of the four orifice areas trends, as a function of the spool travel, for a specific spool design. For achieving a good control of the actuator, particularly important are the fine metering area regions of the valve. These are the small area regions in Figure 8.31, which correspond to the initial openings around the neutral position. For this purpose, *metering notches* are often present in the spool lands, as in Figure 8.32. The use of notches allows a very precise and repeatable control of the initial area openings of the spool equivalent orifices.

In any DCV, the spool design parameters allow limitless combinations of possible area functions. The design and selection of the correct area functions for each application is not an exact science, and it is one of the most difficult aspects in the design of hydraulic systems. These are affected

---

4 It is important to highlight that the terms "meter-in" and "meter-out" refer to the location of the variable orifice of the valve with respect to the actuator, and they do not correspond to the function of the orifice (metering or compensator, as defined in Chapter 4). The function of the meter-in and meter-out orifice will be discussed extensively in Part IV.
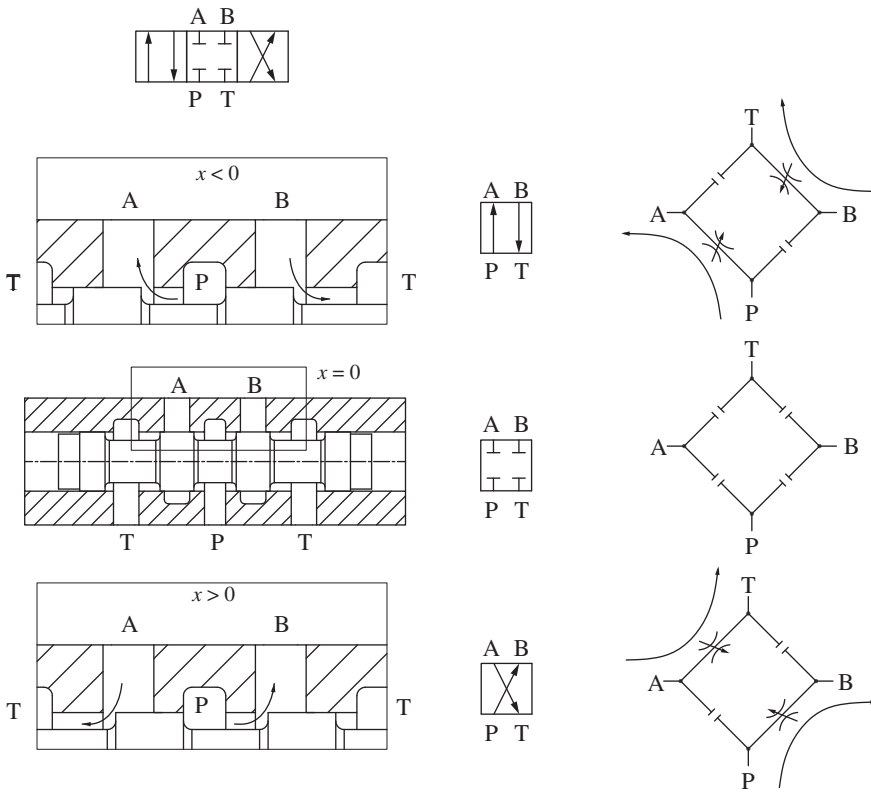
Figure 8.30 Orifice connections implemented through spool and bore lands.
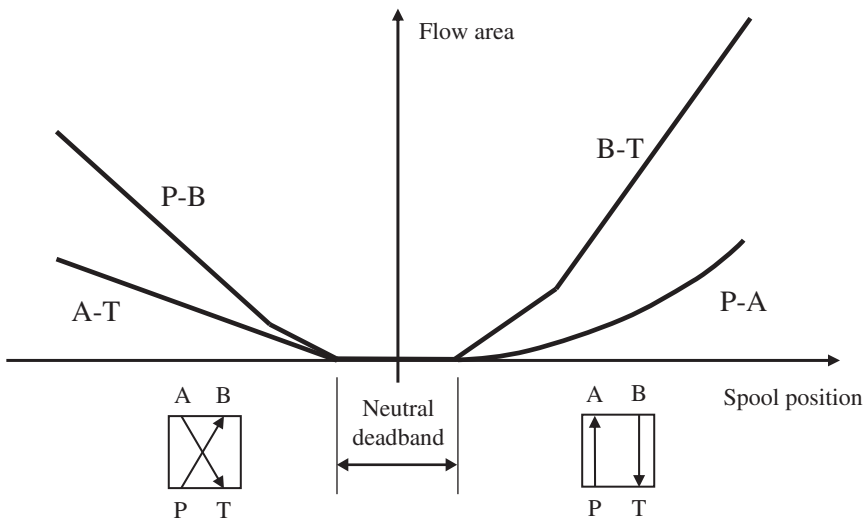
Figure 8.31 Example of opening area vs. spool position for the meter-in and meter-out orifices of a 4/3 infinite position DCV.

(a)

(b)
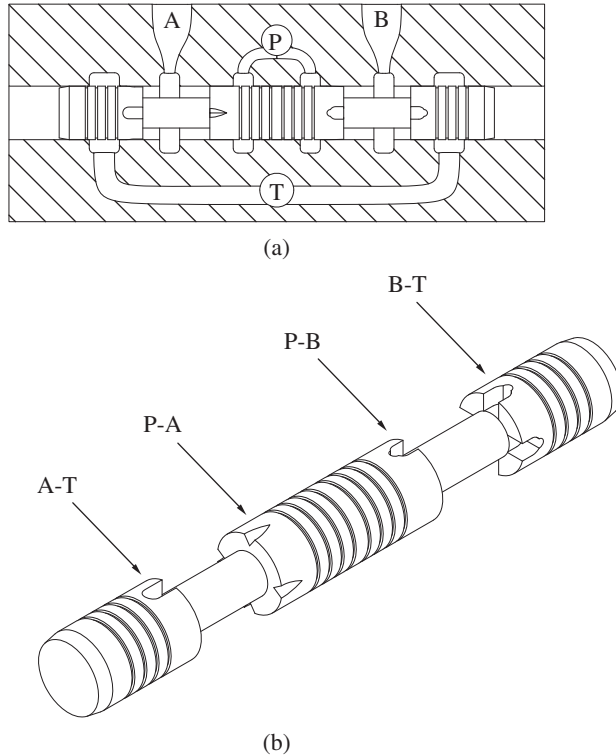
Figure 8.32 Spool with metering notches to obtain fine regulations: cross sectional view (a) and 3D image of the spool (b). The balancing grooves are used to facilitate an axis-symmetric distribution of the pressure around the spool and help reducing frictional and hysteresis effects.

by the type of actuator, by the type and magnitude of the external loads and by the presence of other control elements between the work-ports and the actuator. In this section, only few basic concepts of the spool metering are presented, a deeper application-based analysis will be pursued the following chapters.

8.5.2 Neutral Position

An important parameter for all DCV types is the configuration achieved in the neutral position. Typically, multiple designs for the spool are available within the same valve body, offering different options for the neutral position, as shown in Figure 8.33. This figure presents some of the most common cases for proportional DCVs:

a) The work-ports A and B are normally connected to the tank, while the P port is blocked. This configuration is often referred to as floating or free flow center and spools with such feature are usually known as *motor spools*. This configuration is often used in combination with rotary actuators where the spool is not designed for holding the load in neutral. Furthermore, as visible in the cross-section, the meter-out orifices O_{A-T} and O_{B-T} are already open in neutral with a relatively large area, their area increases even further when the spool is shifted. Motor spools can only provide a control on the meter-in side, restriction on the meter-out side has to be provided, if needed, by external elements, such as counterbalance valves (as explained in Chapter 13).

(a)

(b)

(c)

(d)
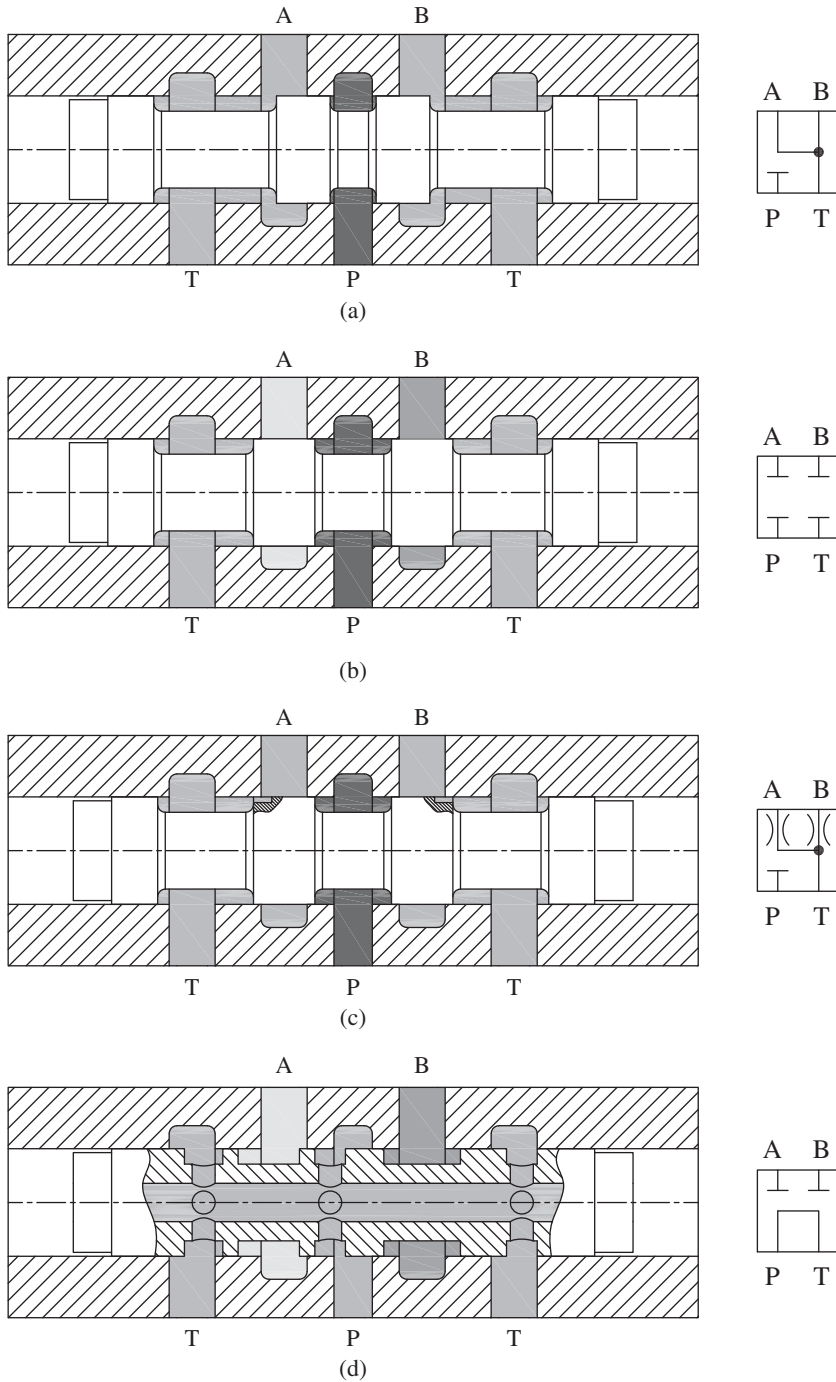
Figure 8.33 Example of possible neutral configurations of a 3/4 DCV: (a) motor spool; (b) cylinder spool; (c) bleeder spool; (d) series spool.

b) All ports are blocked in neutral position, this configuration is normally referred as closed center design. This configuration is referred to as *cylinder spool,* as it is often used in combination with linear actuators where the spool is capable of holding a load in neutral. Furthermore, this design allows to control both meter-in and meter-out equivalent orifices during the spool stroke.

c) In this neutral configuration, P is blocked while A and B ports are connected to the tank through two small orifices, made with two notches in the spool. This configuration is usually identified as *bleeder spool* and it is different from a motor spool because it vents A and B to the tank while keeping the possibility of implementing meter-out restrictions during the spool travel.

d) Work-ports A and B are blocked, and port P is connected to T. This configuration is achieved through a hollow spool and is often identified as *series spool*. This is often used when multiple DCVs are connected in series, where the T port of one valve supplies the P port of the following one. More on series connection is available at Chapter 18.

The valve of Figure 8.31 presents a closed center spool with a neutral deadband, sometimes also referred to as positive overlap. In other words, the spool must accomplish a certain travel before areas start opening. The presence and amplitude of this deadband varies from case to case. For example, servovalves are designed to have no transition deadband between the working positions (zero overlap). On the other hand, many mobile control valves purposely have a relatively wide transition deadband.Actuation Methods

> The actuation method for a DCV refers to the technique used to control the spool travel *x*, which defines the flow area of the different port connections. Typically, the actuation method can be either mechanical, hydraulic, or electric.

The actuation is usually achieved through an external axial force applied to the spool, which acts against one or more centering springs. In DCVs, these springs keep the valve in the neutral position when the force applied is null. When a force is applied, they establish a relationship between the actuation force and the spool position.

Figure 8.34 represents a cross-section of a 4/3 DCV, where the spool is centered by two springs and it is moved by the two possible actuation forces: F_{a1} moves the spool to the right and F_{a2} to the left. Normally, there is no interaction between the two actuation forces, as when one force is applied, the other one is null.

Equation (8.30) gives the ideal relationship between the applied actuation force and the corresponding spool travel in either direction:

$$x = \begin{cases} 0; F_a \leq F_0 \\ \dfrac{F_a - F_0}{k}; \ \ F_a > F_0 \end{cases} \tag{8.30}$$
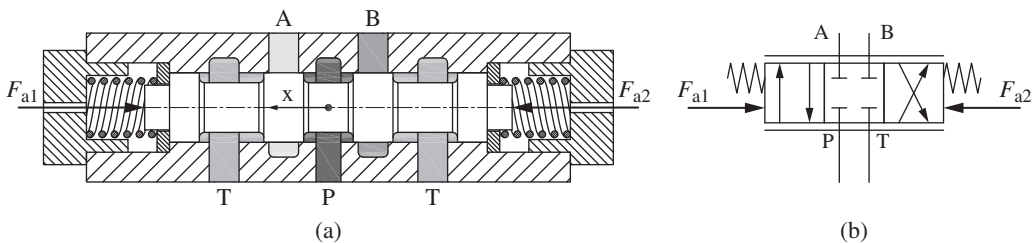
Figure 8.34 Spool actuation principle for a hydraulic pilot operated 4/3 DCV: cross sectional view (a) and ISO symbolic representation (b). It is noticeable how the washers maintain each spring at a preload. The actuating force works only against one spring, depending on the direction of travel.

As described in the previous section on spring basics, F_0 is the spring preload and k is the spring constant. Two important considerations can be made from Eq. (8.30). First, the equation is a good approximation of the spool positioning even if it does not consider other external forces that can be applied on the spool (such as the *flow forces*, which can be particularly relevant at high flow rates as described in Chapter 3). Second, in the case of spool actuation, the spring constant cannot be neglected even in the ideal case. This is different from the case, for example, of the ideal pressure relief valve, where the term *kx* was neglected and the spring force was considered constant.

In most cases, the actuating force can have two different sources: mechanical or hydraulic[5].

> When the mechanical force has human origin, it is transmitted to the spool through a linkage and a lever, which is pushed or pulled by the operator. This type of actuation is often defined as *manual actuation*.

Alternatively[6], the actuating mechanical force can also be generated by a solenoid, which is controlled by an electric signal.

> Direct *electric actuation* is normally implemented by a solenoid connected to the valve spool.

The solenoid (represented in Figure 8.35) is made of an *electromagnetic coil* wound around a cylindrical element, referred to as a *tube,* and contained in a high permeability *core*. Inside the tube, an armature (or plunger) can axially slide. When current is sent through the coil, a magnetic field is generated and directed by the core, causing an axial force on the armature. The armature is in contact with one of the spool ends and transmits the force to the spool causing its travel. Extensive details on the architecture and operation of solenoids can be found in [19]. For the sake of simplicity, in this book, solenoids will be considered elements generating a force proportional to the current sent through the coil. The spool actuation controlled by solenoid force is often referred to as *direct solenoid actuation*. Figure 8.36 shows two examples of ISO symbols for mechanically actuated DCVs.
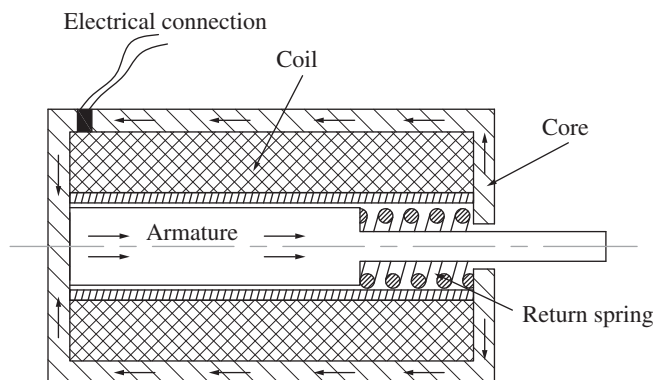
Figure 8.35   Solenoid basic architecture and operating principle and ISO symbol.

---

5 Pneumatic actuation can also be encountered; however, this has been omitted from the chapter because of its decreasing popularity.

6 The mechanical force can also be generated through a cam actuator, however this type of actuation is becoming less and less popular displaced by electro-hydraulic controls driven by sensor inputs.
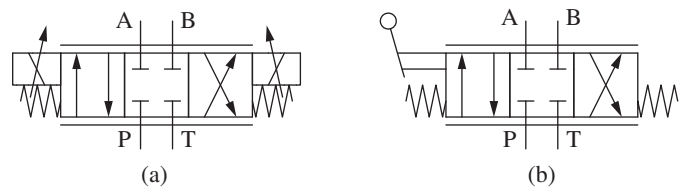
Figure 8.36 ISO symbols of a DCV with (a) manual and (b) direct solenoid actuation.

Ideally, the preload and stiffness of the centering springs of DCVs should be minimal, in order to also minimize the actuation force needed by levers or solenoids. However, as mentioned before, during valve operation, the fluid flow controlled by the spool also generates flow forces, which have an axial component transmitted to the spool, as described in Chapter 3. This force component should also be part of the spool force balance equation (Eq. (8.30)) with the result of affecting the spool travel. In order to minimize the effect of flow forces, the preload and stiffness of the centering springs need to be properly selected. In general, the higher the flow controlled by the DCV, the stiffer and larger the springs.

In the case of the direct solenoid actuation, the force generated by the solenoid is proportional to the coil size. Therefore, larger flows require large coils, which penalizes the space claim and the cost of the DCV. In general, direct electric actuation is suitable for DCVs rated for low flows, in the order of magnitude of 50 l/min or less. DCVs rated for higher flows require a more power dense source of actuation, based on hydraulic pressure. Hydraulic actuation is instead achieved by controlling pressure acting on one of the spool ends and generating a force opposed to the centering spring(s). This pressure is often referred to as *pilot pressure*. Hydraulic actuation can be further classified into two types (hydraulic pilot actuation and electro-hydraulic actuation), depending on how the pilot pressure is controlled.

When the pilot pressure is controlled by a manually adjustable external pressure reducing valve, this is called *hydraulic remote pilot actuation*, or simply *hydraulic pilot actuation*. In this case, the pressure reducing valve is usually part of a hydraulic joystick, and its setting is changed by moving the joystick handle. A longer travel of the handle causes a higher pilot pressure, which in turn increases the DCV spool travel. Figure 8.37 shows the schematic of a hydraulic pilot actuated DCV
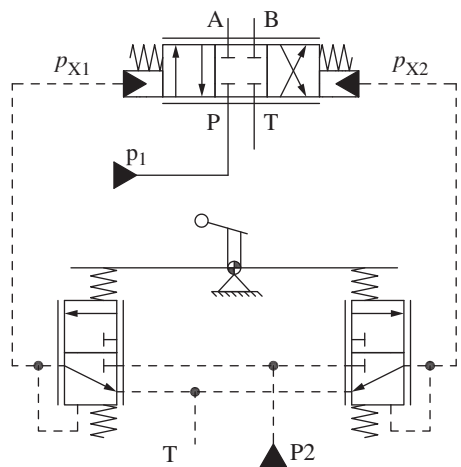
Figure 8.37 ISO schematic of a DCV with hydraulic remote pilot actuation controlled with a hydraulic joystick.
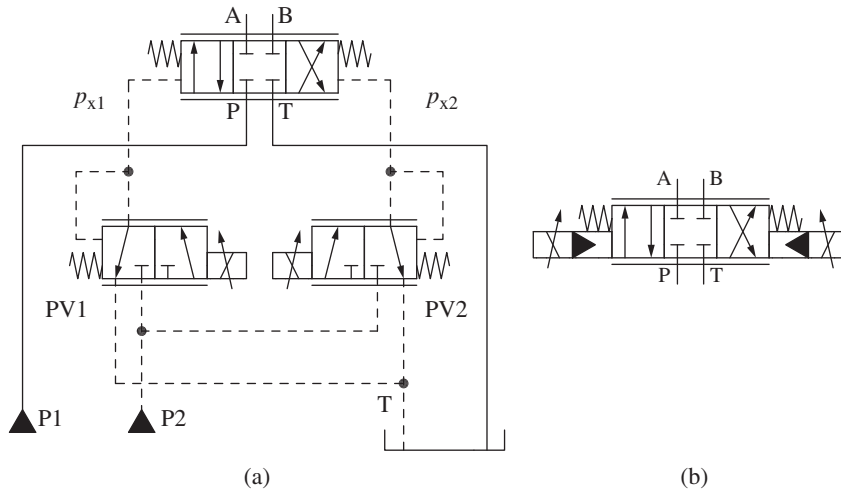
Figure 8.38 (a) ISO expanded circuit representing an electro-hydraulic actuated DCV and (b) simplified symbol.

with a single-axis hydraulic joystick, consisting of two pilot reducing valves. DCVs are usually designed so that the pilot pressure necessary for a complete spool travel is approximately between 15 and 30 bar. The hydraulic joystick is supplied by the line P2, which is normally limited to 35–50 bar; P2 is part of the pilot supply circuit.

Alternatively, the pilot pressure can be controlled by an electrically adjusted pressure-reducing valve. In this case, the pilot pressure is varied by changing the current sent to a proportional solenoid, which controls the setting of this reducing valve. This is called *electro-hydraulic actuation,* or simply *EH actuation*. Figure 8.38 shows the expanded schematic and the simplified symbol of a
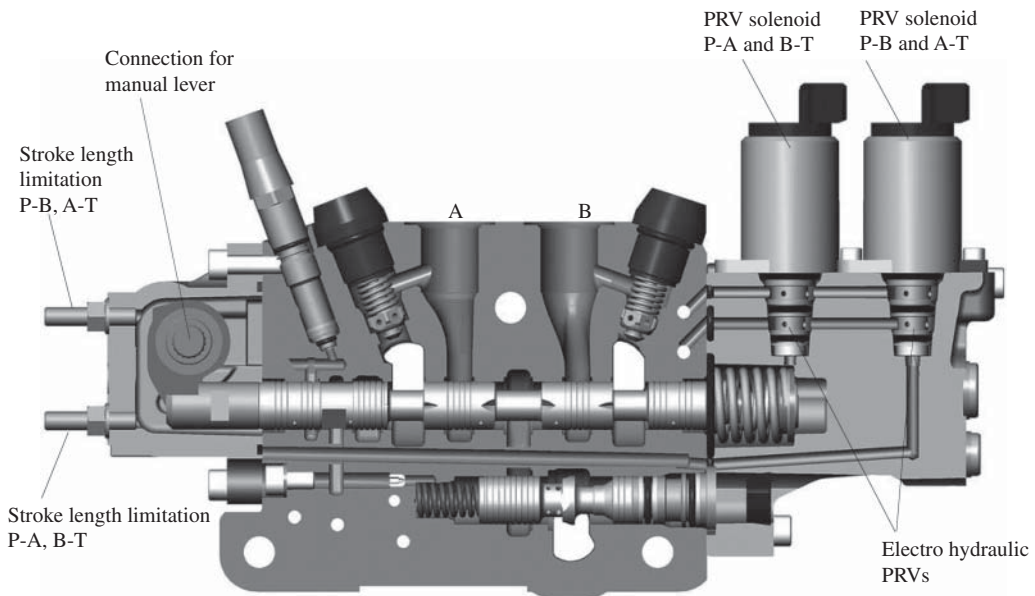
Figure 8.39 Cross-section and equivalent schematic of a DCV with manual and EH actuation. Courtesy of Parker Hannifin Corp.

proportional DCV with electrohydraulic actuation. The two proportional pilot valves PV1 and PV2 are pressure-reducing valves in which the downstream pressure p_X acts against the solenoid force. The spring force, in this case, is acting concordant to p_X and its value is tiny as it is used to restore a zero values for the valve pilot pressure when the solenoid current is null. In the same figure, the pilot supply line P2 supplies PV1 and PV2, while the DCV is connected to the pump line P1.

> Hydraulic actuation is achieved through a pilot pressure signal acting on the spool. There are two types of hydraulic actuation: hydraulic pilot actuation and electrohydraulic actuation.

The solenoid valves used in EH actuation are usually very compact and integrated in the DCV architecture. Many DCVs are designed in a way that more than one actuation system can be simultaneously implemented. For example, Figure 8.39 shows a proportional DCV where the spool has electrohydraulic and manual actuation.

8.6 Servovalves

Servovalves are a particular type of "high performing" infinite positioning DCVs. They allow very precise accuracy and repeatability of the controlled flow, with a very fast response time coupled with minimal hysteresis. They are widely used in aerospace and industrial applications, but they are rarely adopted in mobile machinery.

Servovalves have a unique yet very distinct architecture based on a pilot and a main stage, which are coupled through a mechanical-hydraulic feedback. These features allow high control accuracy and response. A typical design of a nozzle flapper servovalve is shown in Figure 8.40.

> A servovalve is an infinite positioning DCVs with high control bandwidth and accuracy. It formed by a pilot stage (torque motor) and a main stage (spool valve).

The pilot stage is normally referred to as **torque motor**: this is an electromagnetic device that is located on top of the valve. When energized, the torque motor determines the rotation of a mechanical element called push rod. The push rod controls the opening of the main stage of the servovalve, through a mechanism that will be described in the following. The actuation of the push rod is achieved by two permanent magnets that compose the frame of the torque motor, a central mobile core rigidly connected to the push rod, and two coils with opposite polarization between the core and the frame. The mobile core can pivot, realizing the rotation of the push rod. By energizing the coils, a magnetic field is established at the core so that the push rod is tilted in one direction or the opposite according to the polarization of the current. The intensity of the current determines the inclination of the push rod.

Thus, the torque motor can be seen as an element similar to the solenoid of a conventional proportional valve, although it implements a rotation of the control element instead of a linear motion. The torque motor of a servovalve usually requires a lower current (thus a lower electric power) with respect to a proportional DCV. Both electromagnetic devices (the torque motor and the proportional solenoid) can have a similar electronic control, which can include electric ramps, dithering, etc. For more details on these features of the electric control system, the reader is advised to consult specific literature, such as [20–25].

The main stage of the servovalve is typically a 4/3 spool, such as in Figure 8.30, but with critical (or close to critical) lapping. This means that the connections implemented by the equivalent
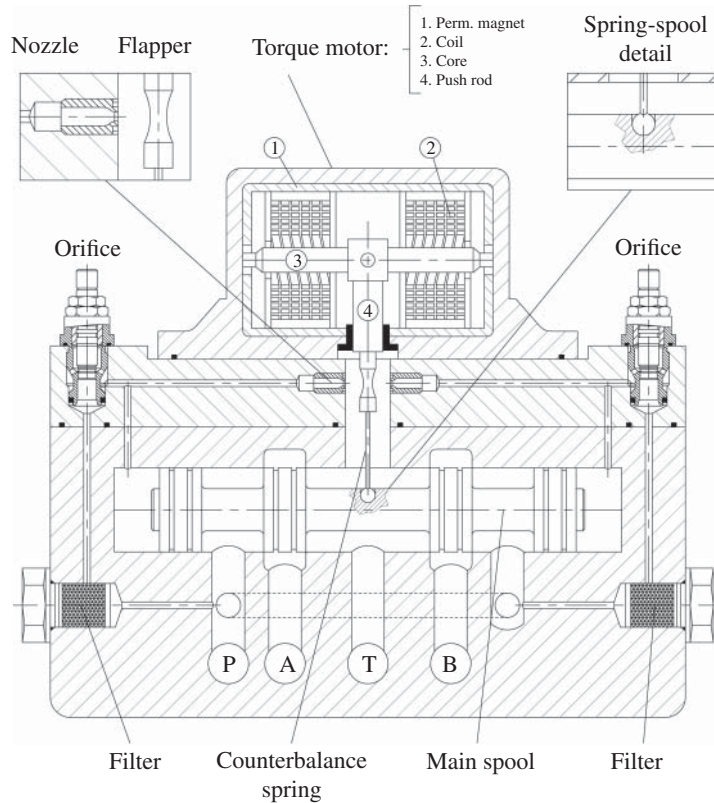
Figure 8.40   Architecture of a servovalve (flapper/nozzle type).

orifices O_{P-A}, O_{P-B}, O_{A-T}, and O_{B-T} are null in neutral position, but they become nonzero as soon as the spool travels. In fact, servovalves are designed to often operate near the center position of the main spool, to guarantee a continuous position control of the controlled hydraulic function. In reality, the main stage of commercial servovalves is often implemented with a small overlap or underlap. The definition of these lapping conditions between the spool land and the bore edges is clearly represented in Figure 8.41. In the literature related to servovalves, the positive lap condition is sometimes referred as "closed-center," while the negative lap condition as "open-center." However, this book will not use these denominations, since "open-center" is also commonly used for a particular type of conventional DCVs.

The effect of different lapping on the valve porting areas and the related flow characteristic of the servovalve is shown in Figure 8.42: positive lapping leads to a control deadband, while negative lapping leads to leakage flow in neutral position. Both situations introduce nonlinearities in the flow control curve. This explains why the critical lapping is the desired condition for precise servovalves, often affecting the high manufacturing cost.

The control mechanism for positioning the main spool includes the flapper and the counterbalance spring connected to the push rod of the torque motor. The flapper has normally a cylindrical shape and it is located next to two nozzles. The counterbalance spring is connected to the flapper and to the main spool, so that when the spool travel, it creates an opposing force to the flapper and the push rod.

The spool can travel when the two pilot pressures on its extreme sides are different. For this purpose, as it is visible from the simplified cross-sectional view in Figure 8.40, two small channels
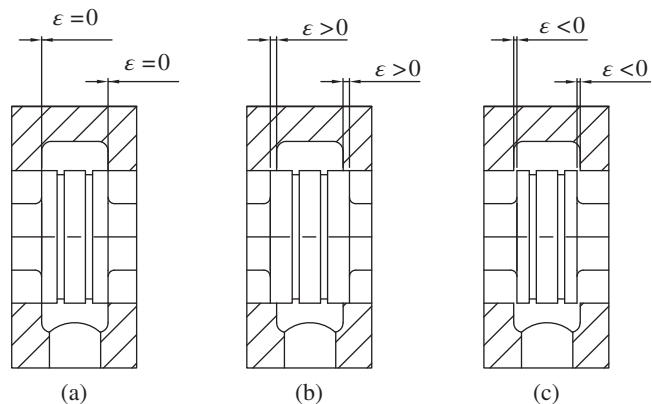
Figure 8.41 Spool lapping around the center positions for servovalves. (a) Critical lap (zero lap). (b) Positive lap (overlap). (c) Negative lap (underlap).

are derived from port P to pilot the motion of the main spool. These two channels connect P to T, through two orifices in series: the first one is an adjustable orifice (set during valve initial tuning) and the second is the nozzle orifice. Therefore, the pilot pressures acting on the left and right chambers of the main spool depend on the opening of the nozzle orifices. In neutral condition, the two nozzle orifices have the same opening area because the flapper is in the center position, symmetric to the two nozzles. Therefore, the two pilot pressures are equal, and the spool is centered.

When the torque motor is energized, the push rod rotates toward one side, causing the flapper to vary the opening areas of the two nozzles. As a consequence, the two pressures at the pilot chambers of the main spool become different, causing the spool to travel (Figure 8.43, top). As the spool travels the counterbalance spring moves the flapper back to the symmetric position between the nozzles, causing a new hydraulic balance of the main spool at a position different that the neutral one (Figure 8.43, bottom). In this new equilibrium position, the counterbalance spring force equals the force of the torque motor on the push rod. Therefore, there is a unique (linear) relation between the spool position and the command given to the torque motor.
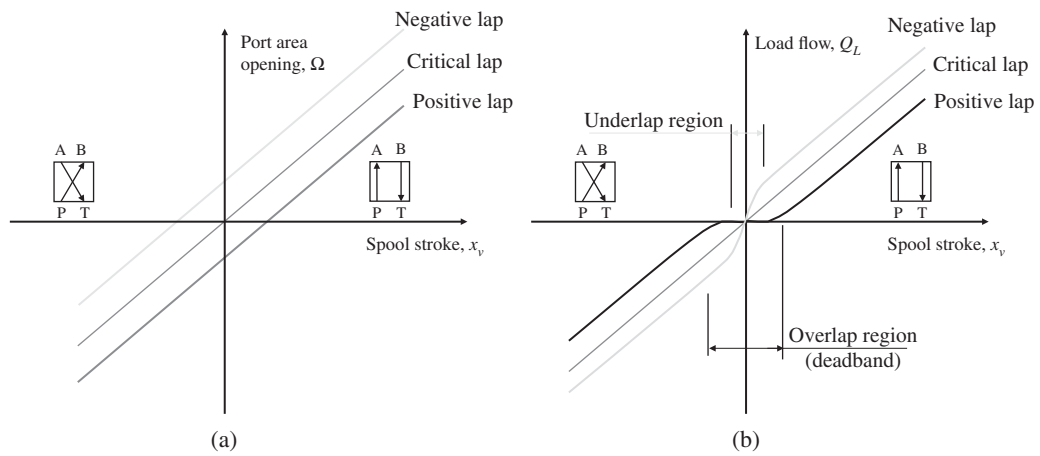
Figure 8.42 Opening area (a) and Flow characteristic (b) of a servovalve as a function of the center position of the main spool. Source: Derived from Merritt 1966 [24]. Copyright 1966, John Wiley & Sons.
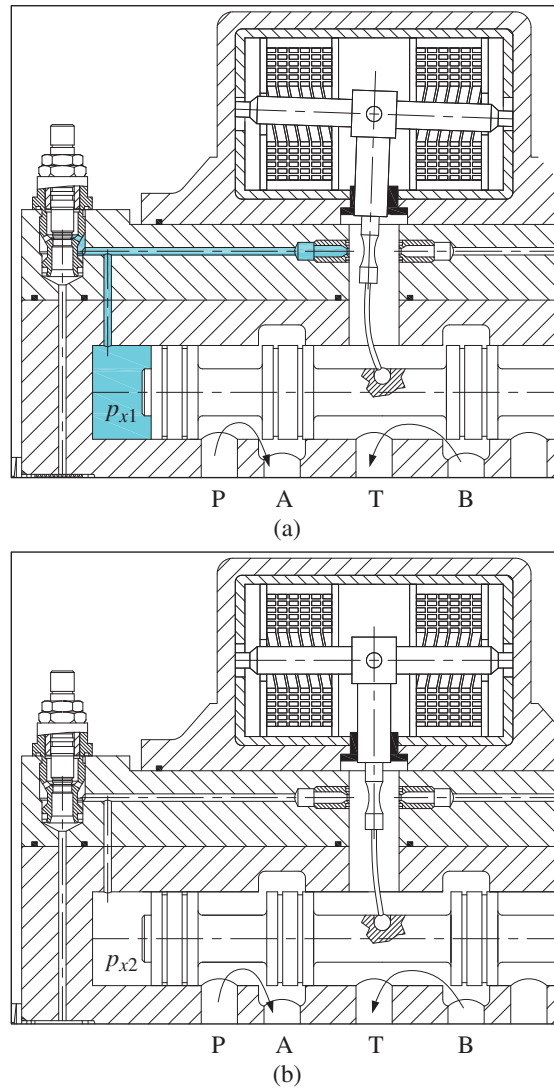
Figure 8.43 Control mechanism of the servovalve (flapper-nozzle type): (a) initial configuration after the electric command; (b) equilibrium configuration.

The flapper-nozzle design of Figure 8.40 represents one of the most popular architectures of servovalves. However, there are other servovalve designs that implement a similar feedback mechanism to accurately control the main spool. Among these designs, particularly successful is the jet-pipe one. The reader can refer to specialized literature for understanding the details of these different servovalve designs [20, 25].

8.6.1 Characteristic of Servovalves

As described in the previous section, the control of the position of the main spool of a servovalve is achieved through a hydromechanical closed loop control, implemented by the counterbalance spring and the flapper. A servovalve, and sometimes also a conventional proportional valve, is further controlled using a close loop electronic control system. This electronic control system targets at controlling the actuator in either position, velocity, or force. For a servovalve, these different
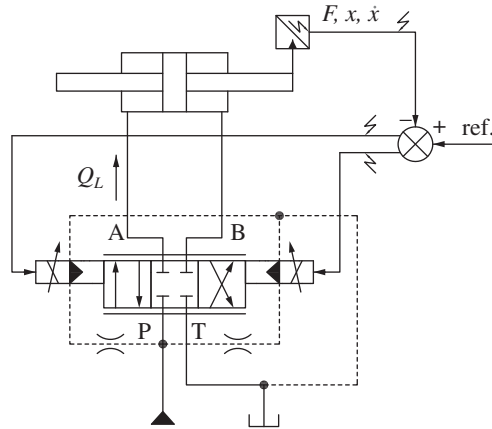
Figure 8.44 Use of a servovalve for controlling and actuator. Depending on the feedback, the system can be a "position servo" system, a "velocity servo" system, or a "force servo" system.

strategies are summarized in Figure 8.44, which also shows a common ISO symbolic representation for servovalves, highlighting the two orifices that represent the internal mechanical-hydraulic feedback that controls the main spool.

In the figure, the system requires a feedback sensor depending on the controlled variable, a position sensor for the position servo system, a force sensor for a force servo system, or a velocity sensor for a velocity servo system[7].

It is important to remark that, as shown in Figure 8.44, servo-controlled systems using servovalves typically use a constant pressure supply system. A typical supply pressure level for most industrial and aerospace applications is 210 bar (or 3000 psi). Constant pressure systems will be also further described in Parts III and IV.

In designing the controller of one of the servo systems represented in Figure 8.44, it is useful to know the "plant" characteristic, which includes the behavior of the servovalve. With reference to Figure 8.45, such characteristic corresponds to the relation between flow and command, for a given load condition of the actuator. Considering the relationship between input command to the valve and spool position, this relation can be expressed in general as:

$$Q_L = Q_L(x_v, p_L) \tag{8.31}$$

For control purposes, most of the time it is enough to approximate th e expression of Eq. (8.31) with the Taylor series expansion, limited to the first-order terms:

$$Q_L = Q_{L,0} + \frac{\partial Q_L}{\partial x_v}\bigg]_0 \Delta x_v + \frac{\partial Q_L}{\partial p_L}\bigg]_0 \Delta p_L \tag{8.32}$$

This last relation is useful to define the valve chara cteristic parameters, also known as valve flow gain and valve flow–pressure coefficient:

$$\Delta Q_L = Q_L - Q_{L,0} = K_Q \Delta x_v - K_c \Delta p_L \tag{8.33}$$

where:

$$K_Q = \frac{\partial Q_L}{\partial x_v} \text{ valve flow again}$$
$$K_c = \frac{\partial Q_L}{\partial p_L} \text{ valve flow – pressure coefficient} \tag{8.34}$$

---

7 In the case of a rotary actuator, the sensors to be used to implement the different servo systems would be respectively an angular sensor (position servo), a torque sensor (torque servo), and an angular speed sensor (shaft speed servo).
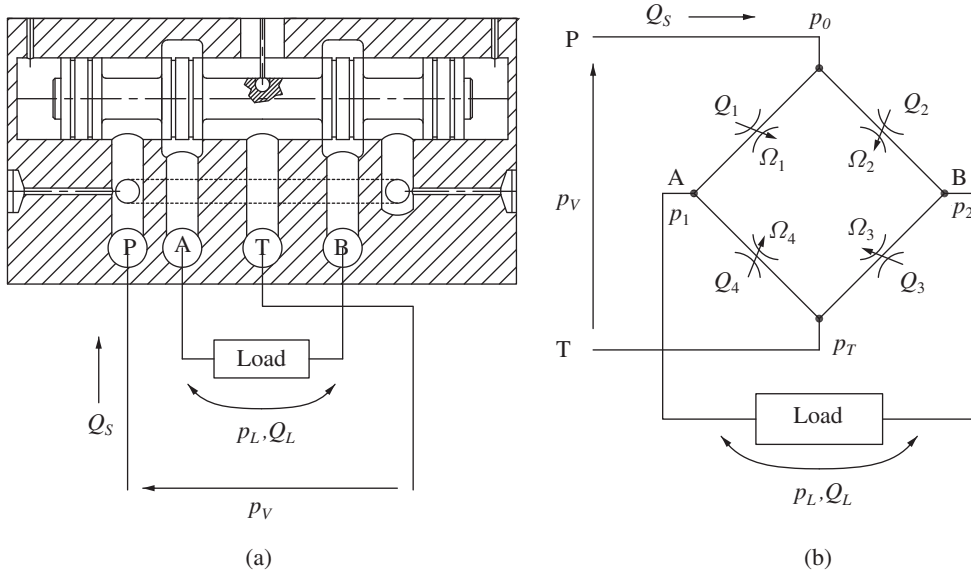
Figure 8.45 Parametrization of the servovalve: (a) cross sectional view; (b) equivalent orifice representation.

The negative sign in the coefficient K_c is due to the negative relation between actuator flow and actuator pressure: the higher the load, the lesser the flow that the valve, for a given supply pressure, will be able to provide to the actuator. The literature often defines a third parameter for a FCV:

$$K_p = \frac{\partial p_L}{\partial x_v} = \frac{K_Q}{K_c} \text{ valve pressure sensitivity} \tag{8.35}$$

Depending on the architecture of the controller used to implement the servo-system in Figure 8.44, the above coefficients play a relevant role in the system dynamic response, affecting also the system stability. Without discussing the basic control theories, which are beyond the scope of this book, in general the valve flow gain K_Q affects not only the system stability but also its promptness. The valve flow–pressure coefficient K_c relates to the damping of the system response. More details on these dynamic aspects can be found in [24, 25]. It can be interesting to observe that these coefficients are not constant for a valve, but they depend on the operating points. This is due to the nonlinear analytical relationship between pressure, flow, and spool position. However, often the control designer can obtain good controllers by approximating these coefficients as constant, choosing a particular operating condition as linearization point. The most common condition for determining K_Q, K_c, and K_p is the null condition, where $x_v = 0$, $p_L = 0$, $Q_L = 0$. If the valve geometry is known, namely, the valve opening areas Ω_1, Ω_2, Ω_3, and Ω_4, it is possible to analytically derive an expression for the valve flow characteristics Eq. (8.31), with respect to the valve opening and the actuator load. This can be done by considering the orifice equations for the meter-in and meter-out orifices as well as the basic pressure–flow relations that can be derived from Figure 8.45. The system of equations that can be derived is as follows:

$$Q_1 = C_f \Omega_1 \sqrt{\frac{2(p_0 - p_1)}{\rho}}$$

$$Q_2 = C_f \Omega_2 \sqrt{\frac{2(p_0 - p_2)}{\rho}}$$

$$Q_3 = C_f \Omega_3 \sqrt{\frac{2(p_2 - p_T)}{\rho}}$$

$$Q_4 = C_f \Omega_4 \sqrt{\frac{2(p_1 - p_T)}{\rho}}$$

$$Q_L = Q_1 - Q_4$$

$$Q_L = Q_3 - Q_2$$

$$p_L = p_1 - p_2$$

(8.36)

A simple solution is presented here under three assumptions:

1) Symmetrical areas: the spool opens the same port areas independently on the travel direction, $\Omega_1(x_v) = \Omega_2(-x_v)$ and $\Omega_3(x_v) = \Omega_4(-x_v)$;
2) Matching orifices: for every spool opening, $\Omega_1 = \Omega_3$ and $\Omega_2 = \Omega_4$
3) Linear area trends:

$$|\Omega_i| = \pi D(x_v - \epsilon) \qquad for \ i = 1, 2, 3, 4$$

(8.37)

The parameter ϵ refers to the spool lapping according to the definition in Figure 8.41 (all the spool lands have the equal lapping).

These simplifications allow finding a first representation of the valve characteristic. The system of Eq. (8.36) leads to the following:

$$Q_L = Q_1 - Q_4 = C_f \Omega_1 \sqrt{\frac{2(p_0 - p_1)}{\rho}} - C_f \Omega_4 \sqrt{\frac{2(p_1 - p_T)}{\rho}}$$

$$Q_L = Q_3 - Q_2 = C_f \Omega_3 \sqrt{\frac{2(p_2 - p_T)}{\rho}} - C_f \Omega_2 \sqrt{\frac{2(p_0 - p_2)}{\rho}}$$

(8.38)

This clearly implies that a relation between the system pressure needs to be satisfied:

$$p_0 - p_1 = p_2 - p_T$$

(8.39)

which, considering that $p_L = p_1 - p_2$, means that:

$$p_1 = \frac{1}{2}(p_0 + p_T + p_L)$$

$$p_2 = \frac{1}{2}(p_0 + p_T + p_L)$$

(8.40)

so that:

$$Q_L = C_f \Omega_1 \sqrt{\frac{(p_0 - p_T - p_L)}{\rho}} - C_f \Omega_4 \sqrt{\frac{2(p_0 - p_T + p_L)}{\rho}}$$

(8.41)

By defining the pressure drop across the valve as $p_V = (p_0 - p_T)$,

$$Q_L = C_f \Omega_1 \sqrt{\frac{(p_V - p_L)}{\rho}} - C_f \Omega_4 \sqrt{\frac{2(p_V + p_L)}{\rho}}$$

(8.42)

The last relationship depends on valve size and operating pressures, but it can be written in a more generic form. This can be done by normalizing the operating features according to the dimensionless parameters first introduced by Blackburn et al. [8]:

$$v = \frac{Q_L}{Q_{max}} \quad normalized \ valve \ flow$$

$$\pi = \frac{p_L}{p_V} \ \ \text{normalized load}$$

$$\lambda = \frac{x_v}{x_{v,\max}} \ \ \text{normalized travel} \tag{8.43}$$

$$\lambda_0 = \frac{\varepsilon}{x_{v,\max}} \ \ \text{normalized valve lapping}$$

where:

$$Q_{\max} = C_f \Omega_{\max} \sqrt{\frac{p_V}{\rho}} \tag{8.44}$$

Now, if we first consider the case of a critical center valve ($\varepsilon = 0$), considering Eq. (8.37), it is possible to write, for Ω_1:

$$\begin{cases} \dfrac{\Omega_1}{\Omega_{\max}} = \lambda \ \text{for} \ \lambda > 0 \\[3mm] \dfrac{\Omega_1}{\Omega_{\max}} = 0 \ \text{for} \ \lambda \leq 0 \end{cases} \tag{8.45}$$

and, for Ω_4,

$$\begin{cases} \dfrac{\Omega_4}{\Omega_{\max}} = 0 \ \text{for} \ \lambda > 0 \\[3mm] \dfrac{\Omega_4}{\Omega_{\max}} = -\lambda \ \text{for} \ \lambda \leq 0 \end{cases} \tag{8.46}$$

The two equations above imply null leakages inside the servovalve. In this way, the flow characteristic of the critical center valve can be expressed in a simple form as:

$$\begin{cases} \nu = \lambda \sqrt{1-\pi} \ \ \text{for} \ \lambda > 0 \\ \nu = \lambda \sqrt{1+\pi} \ \ \text{for} \ \lambda \leq 0 \end{cases} \tag{8.47}$$

The graphical representation of the valve characteristic of Eq. (8.47) is shown with the four-quadrant representation in Figure 8.46. The x-axis reports the dimensionless load at which the valve is subjected (π), while the y-axis refers to the dimensionless flow to the load, ν. Positive and negative flows refer to opposite commanded flow directions, as shown in the simplified schematic in Figure 8.47. Positive and negative loads refer to the load direction in terms of pressurization at the valve port. In this way, the 1st and 3rd quadrants refer to load conditions opposing the flow direction (resistive loads); while the 2nd and the 4th quadrants refer to conditions of assistive (or overrunning) loads. More considerations on resistive and assistive loads will be made in Part III. The plot in Figure 8.46 reports also the characteristic lines corresponding to a certain commanded position λ. Therefore, the 1st and 2nd quadrant correspond to a positive spool travel (servovalve commanded in position 1, in Figure 8.47), while the 3rd and 4th quadrants pertain to the commanded position 2.

When the valve is commanded in position 1, the flow sent to the hydraulic function connected to the servovalve depends on the load pressure. From the values corresponding to null loads (the y-axis region delimiting the 1st and 2nd quadrants), the flow reduces as the load increases, up to a null flow condition when the load pressure reaches the limit pressure of the valve supply. Overrunning load conditions promote greater flows, as it appears from the curves in the 2nd quadrant.

The 3rd and 4th quadrant of the characteristic of Figure 8.46 can be interpreted in a similar fashion, considering that the servovalve is now actuated in the opposite position.
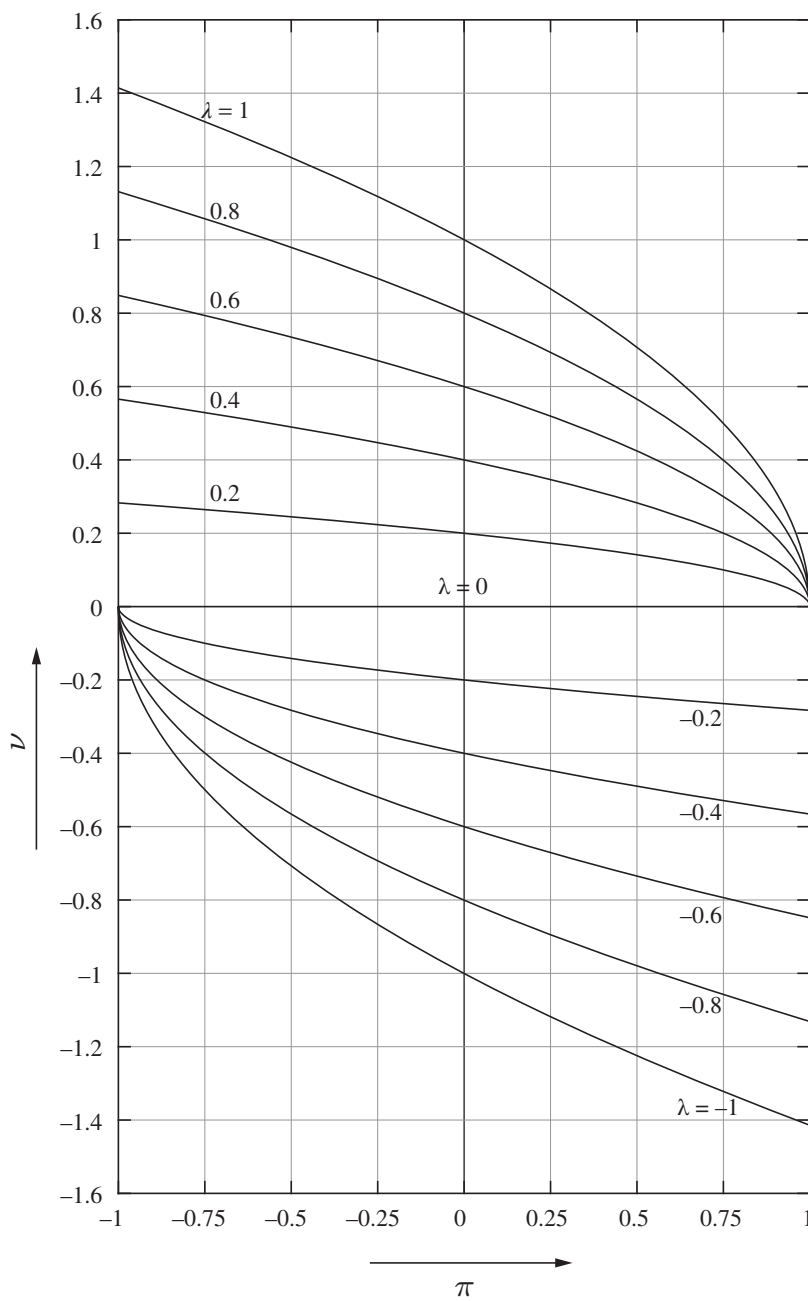
Figure 8.46 Characteristic curve of a servovalve.

Another typical representation of the characteristic of servovalves, and sometimes even of proportional valves, is the alternative to that in Figure 8.48. In this case, the dimensionless flow is plotted against the dimensionless spool travel, and the curves represent the effect of different loading conditions. With the linear area functions assumed in Eq. (8.37), all curves appear to be linear, and each slope depends on the load value.
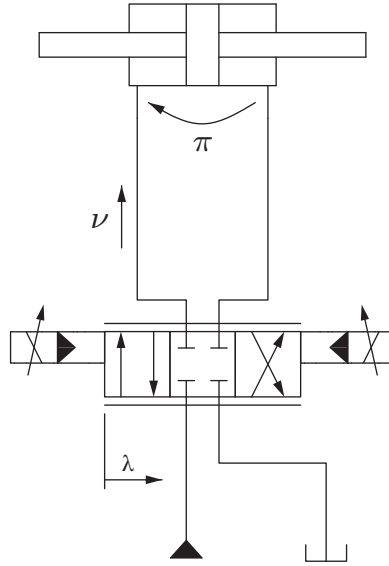
Figure 8.47 Simplified schematic for understanding the servovalve characteristic.

The cases of spool design with overlap ($\varepsilon > 0$) or underlap ($\varepsilon < 0$) are represented respectively in Figure 8.49 and Figure 8.50.

For the case of positive lapping, $\lambda_0 > 0$, according to Eq. (8.43). This means that instead of Eqs. (8.45) and (8.46), the area functions are given by:

$$\begin{cases} \dfrac{\Omega_1}{\Omega_{\max}} = \lambda - \lambda_0 \text{ for } \lambda > \lambda_0 \\[4mm] \dfrac{\Omega_1}{\Omega_{\max}} = 0 \text{ for } \lambda \leq \lambda_0 \end{cases} \tag{8.48}$$

For Ω_1 and for Ω_4,

$$\begin{cases} \dfrac{\Omega_4}{\Omega_{\max}} = 0 \text{ for } \lambda > -\lambda_0 \\[4mm] \dfrac{\Omega_4}{\Omega_{\max}} = -\lambda - \lambda_0 \text{ for } \lambda \leq -\lambda_0 \end{cases} \tag{8.49}$$

This brings to the following expression for the valve characteristic (positive lapping):

$$\begin{cases} v = (\lambda - \lambda_0)\sqrt{1 - \pi} \text{ for } \lambda > \lambda_0 \\ v = 0 \text{ for } -\lambda_0 \leq \lambda \leq \lambda_0 \\ v = (\lambda + \lambda_0)\sqrt{1 + \pi} \text{ for } \lambda \leq -\lambda_0 \end{cases} \tag{8.50}$$

The expression of Eq. (8.50) is used in the representation in Figure 8.49.
For the case of negative lapping ($\lambda_0 < 0$), the area functions become:

$$\begin{cases} \dfrac{\Omega_1}{\Omega_{\max}} = \lambda - \lambda_0 \text{ for } \lambda > -\lambda_0 \\[4mm] \dfrac{\Omega_1}{\Omega_{\max}} = 0 \text{ for } \lambda \leq -\lambda_0 \end{cases} \tag{8.51}$$
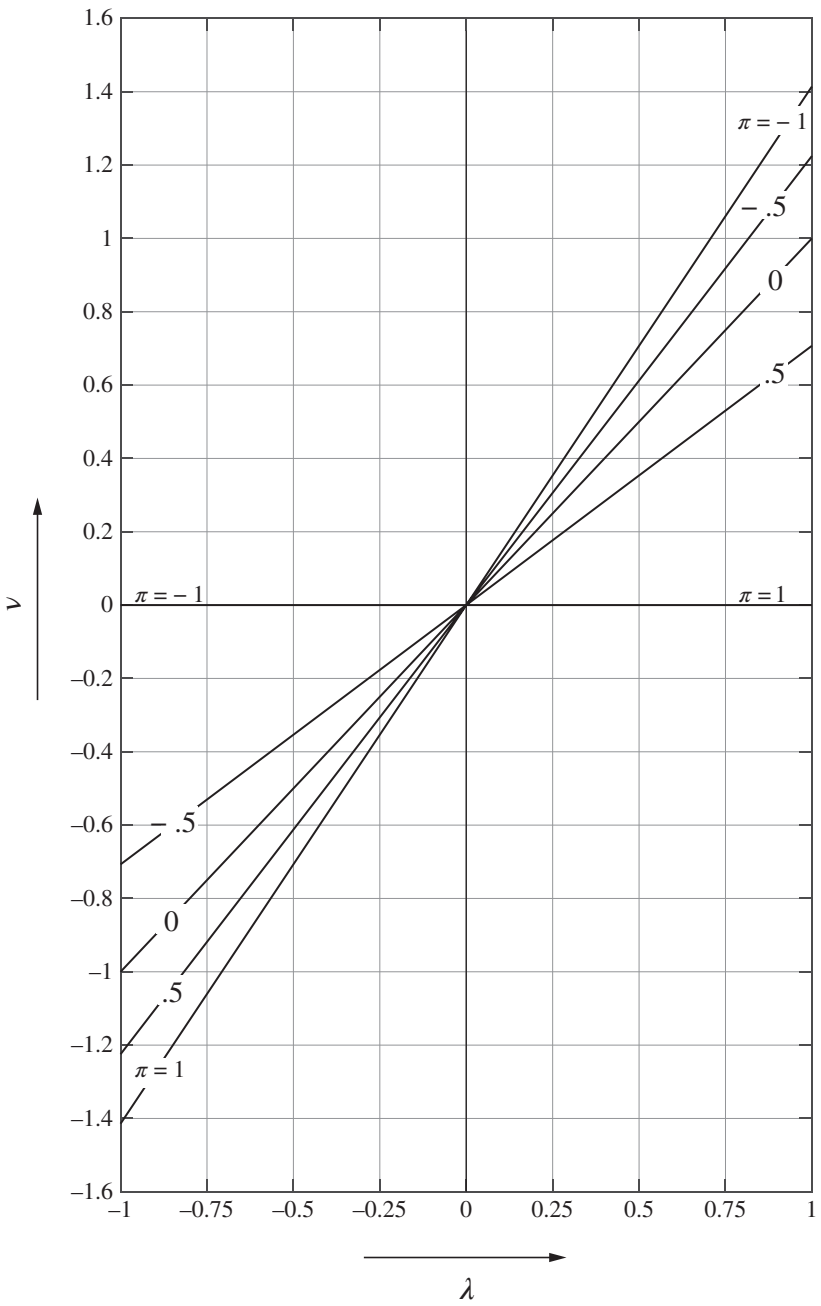
Figure 8.48 Characteristic curve of a servovalve (alternative).
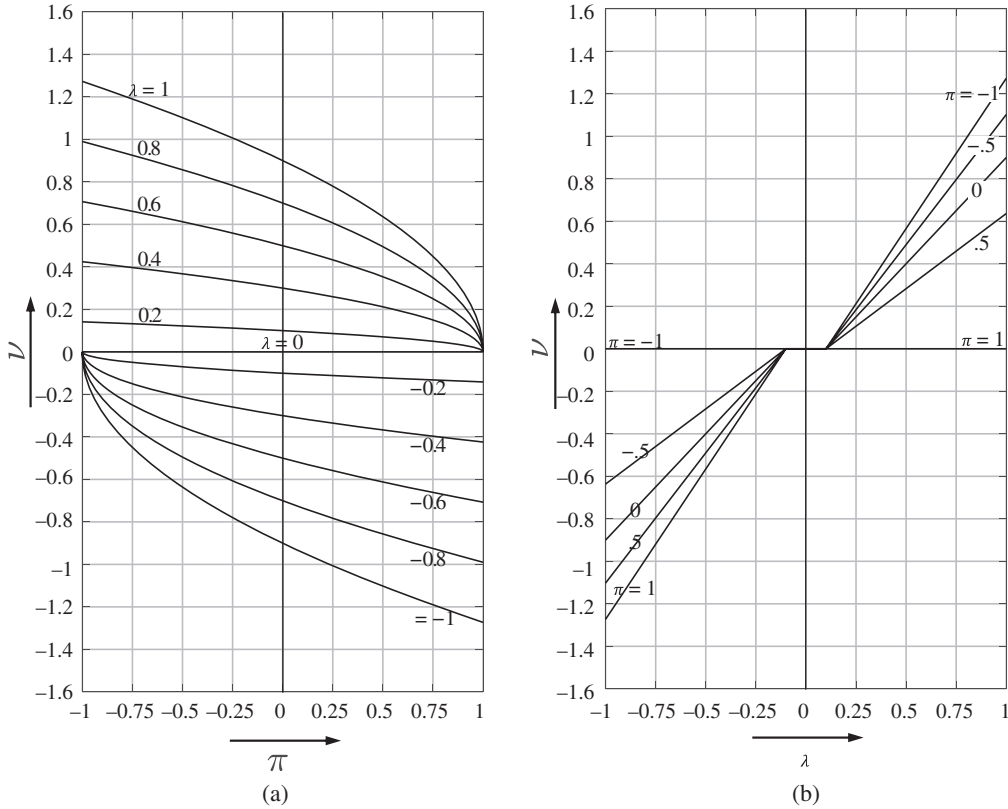
Figure 8.49 Characteristic curve of a servovalve with positive lapping (closed center) ($\lambda_0 = 0.1$): (a) as a function of the load; (b) as a function of the valve opening).

For Ω_1 and for Ω_4,

$$\begin{cases} \dfrac{\Omega_4}{\Omega_{max}} = 0 \text{ for } \lambda > \lambda_0 \\[2mm] \dfrac{\Omega_4}{\Omega_{max}} = \lambda + \lambda_0 \text{ for } \lambda \leq \lambda_0 \end{cases} \tag{8.52}$$

This brings to the following expression for the valve characteristic (positive lapping):

$$\begin{cases} \nu = (\lambda - \lambda_0)\sqrt{1 - \pi} \text{ for } \lambda > -\lambda_0 \\ \nu = (\lambda - \lambda_0)\sqrt{1 - \pi} + (\lambda + \lambda_0)\sqrt{1 + \pi} \text{ for } \lambda_0 \leq \lambda \leq -\lambda_0 \\ \nu = (\lambda + \lambda_0)\sqrt{1 + \pi} \text{ for } \lambda \leq -\lambda_0 \end{cases} \tag{8.53}$$

It is important to point out that the analysis made above was based on several assumptions, including the valve spool parameters (symmetric spool with matched orifices) and the actuator type (symmetric, with return flow equal to the supply flow). However, following a similar procedure as described above, it is possible to derive the characteristic also for different servo-system configurations.
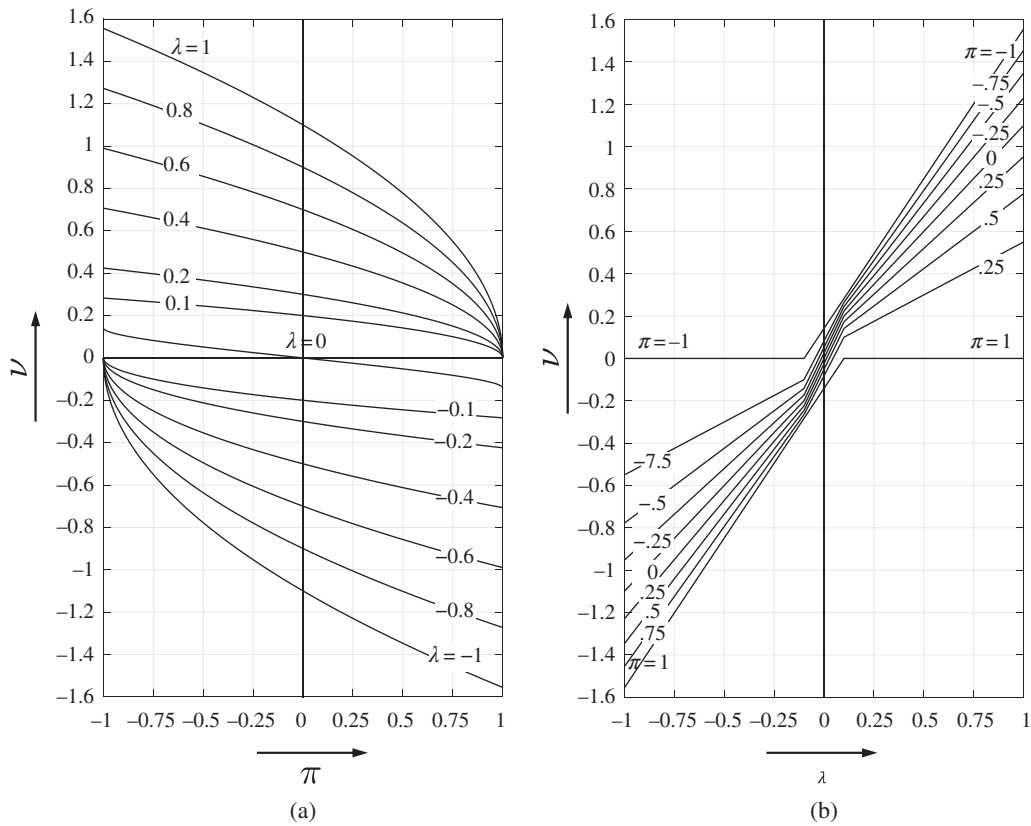
Figure 8.50 Characteristic curve of a servovalve with negative lapping (open center) ($\lambda_0 = -0.1$): (a) as a function of the load; (b) as a function of the valve opening).

Table 8.1 Main differences between conventional proportional DCV and servovalves.

	Conventional proportional DCV	**Servovalves**
Type of control	Open loop	Closed loop (feedback sensor required)
Control accuracy	Moderate (error $\geq 3\%$)	Very high (error $<1\%$)
Frequency response	Low ($<10\,\text{Hz}$)	High (60-400 Hz)
Cost	Moderate	High
Tolerance to contamination	Moderate	Low

8.6.2   Servovalves vs. Proportional Valves

Despite the architecture of the valve actuation described earlier in this chapter, there are several differences between conventional solenoid actuated DCVs and servovalves. The main differences between the two valve technologies can be summarized in Table 8.1.

First, conventional DCV are usually utilized for open loop regulations, where the input command to the valve is determined by the human operator rather than processing a feedback sensor

that monitors the actuator. Moreover, conventional DCVs are in most cases used for velocity control of the actuator, while servovalves are more frequently used for position servo-systems or force servo-systems. This implies different designs for the center position of the spools. In fact, for position servo or force servo, the valve often operates in regions near null flow Q_L, therefore near the center position. While for a velocity control system, the valve operates around higher values for Q_L, therefore at larger port opening. Therefore, while the critical center position is a preferred requirement for a servovalve, it is actually not required for a conventional DCV. Consequently, conventional DCV can correctly function with significant control deadbands.

The internal hydraulic-mechanic control loop that control the spool of the main stage in a servovalve (which is absent in a proportional DCV) is very fast. It is also very accurate because it creates a unique relationship between torque motor excitation and spool position. Certain proportional DVC achieve a similar control strategy electronically, by using a sensor that measures the spool position as a feedback. However, this electric control is typically much slower that the mechanical-hydraulic one present in a servovalve. The dynamic response of a servovalve is much faster than the response of a conventional proportional DCVs rated for the same flow rate.

Proportional DCV normally do not attempt realizing the same control accuracy in the outlet flow rate as servovalves. For this reason, larger clearances are used in the manufacturing of the spool and the bore. The pilot control system of the spool of the main stage of a servovalve works with small nozzle diameters and nozzle-flapper clearances, requiring a stricter filtration than conventional DCVs. Obviously, the overall cost of a servovalve is much higher than the cost of a conventional DCV (often about 10 times higher).

As shown in the valve characteristics presented earlier, servovalves follow a very linear characteristic, with respect to traditional proportional DCVs. This linearity is the main driver for their success in precision applications. However, this feature is achieved at the expense of a usually large valve size. In other words, in order to preserve a linear behavior, the servovalve needs to maintain a certain size with respect to the application in which it is utilized. This can be better understood by referring to Figure 8.51, which represents the valve operation for a given opening of the main spool.

Considering one of the work-port connections, for example, the supply $P \rightarrow A$, the equivalent circuit can be represented with the schematic also reported in Figure 8.51, showing the additional fixed orifice between the load and the spool areas. This orifice is enabled by the inner restrictions of the valve housing. These are in series with the variable orifice determined by the spool and bore lands. This fixed orifice depends on the valve size: the bigger the valve, the larger the orifice.

The presence of the orifice Ω_0 affects the expected behavior of the valve. In fact, the variable orifice created by the spool lands does not see the supply pressure (indicated as p, in Figure 8.51), but rather a smaller pressure value. The deviation caused by this undesired pressure drop is described equating the flow–pressure equations for both orifices:

$$Q = c_f \Omega_0 \sqrt{\frac{(p - p_{\text{int}})}{\rho}} = c_f \Omega(i) \sqrt{\frac{2p_{\text{int}}}{\rho}} \tag{8.54}$$

This flow rate apparently differs from the expected one, which would be:

$$Q_{\text{exp}} = c_f \Omega(i) \sqrt{\frac{2p}{\rho}} \tag{8.55}$$
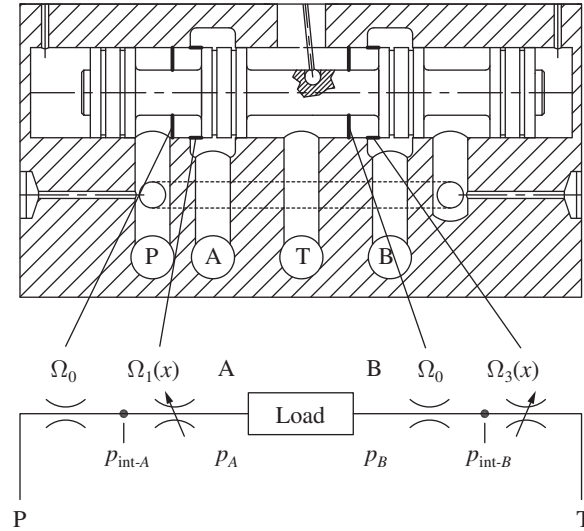
Figure 8.51 Valve open at an intermediate position.

The nonlinearity deviation caused by internal restrictions of the valve is graphically represented in Figure 8.52. In order to keep the linearity error below 1%, the variable orifice areas created by the spool need to be below 25% of value Ω_0, representative of the valve internal restrictions.

For this reason, to achieve a strict linearity in servovalves, it is necessary to use large spool diameters to achieve high values for Ω_0, and at the same time the maximum spool travel needs to be limited. Spools of servovalves are normally between 6 and 50 mm of diameter. This corresponds to maximum spool travels respectively of 0.3 and 2.26 mm, which is a very limited spool travel compared with the typical values for proportional valves, where the spool can travel easily above 8 mm.

To avoid designing very large servovalves, an alternative way to keep low the linearity error consists on working with large pressure drops, p_V, across the valve. On the other hand, for standard
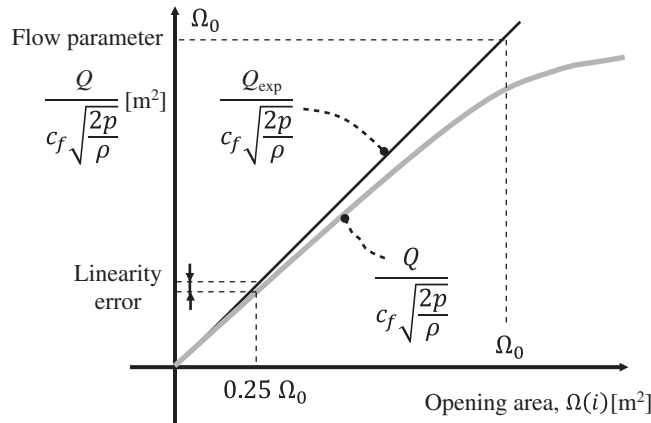
Figure 8.52 Linearity error in a spool valve.

proportional DCVs, the linearity is not so important, and therefore overall valve size can be more compact.

Example 8.3   Maximum power delivered by a servovalve.
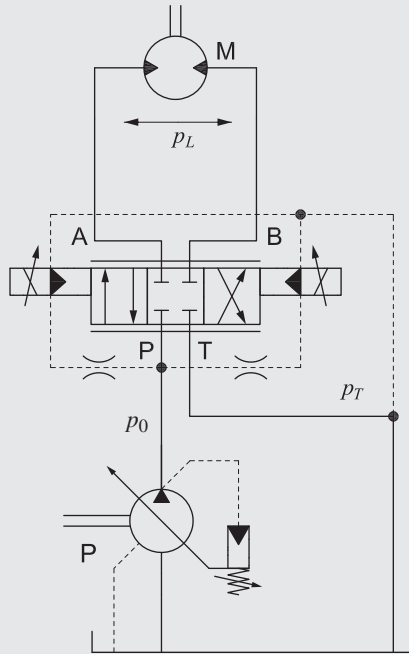
Determine the relation between the supply pressure and the load pressure that maximizes the hydraulic power at the load for a symmetric servovalve open at a given position.

Given:

A symmetric servovalve at a given position, $\Omega_{PA}(x) = \Omega_{BT}(x) = \Omega(x)$

The load at the actuator $p_L = p_A - p_B$
The supply pressure p_0
The return pressure $p_T = 0$

Find:

the ratio between the p_0 and p_L for which the power at the load ($P_L = Q_L \cdot p_L$) is maximum

Solution:

The servovalve circuit can be represented with the simplified schematic in the figure below.

(Continued)

Example 8.3 (Continued)
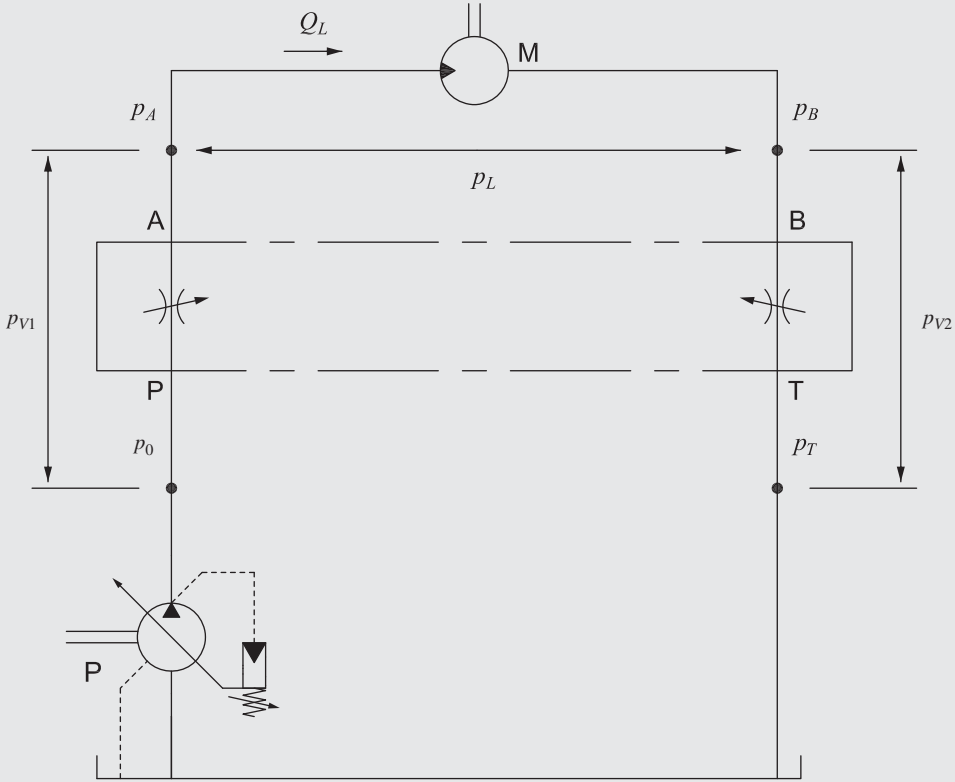
The following considerations can be made to find a suitable expression for both the hydraulic power at both the supply and at the load.

First, the pressure drop at the valve p_V can be expressed as:

$$p_V = p_{V1} + p_{V2} = (p_0 - p_T) - p_L$$

The flow rate is given by

$$Q_L = C_f\, \Omega\,(x) \sqrt{\frac{2p_{V1}}{\rho}} = C_f\, \Omega\,(x) \sqrt{\frac{2p_{V2}}{\rho}}$$

From the expression above, it can be observed that: $p_{V1} = p_{V2} = p_V/2$

Therefore

$$Q_L = C_f\, \Omega\,(x) \sqrt{\frac{p_V}{\rho}} \qquad\qquad (*)$$

The hydraulic power at the load is given by

$$P_L = p_L \cdot Q_L = p_L C_f\, \Omega\,(x) \sqrt{\frac{p_V}{\rho}} = C_f\, \Omega\,(x)\, p_L \sqrt{\frac{p_0 - p_T - p_L}{\rho}}$$

The hydraulic power dissipated by the servovalve (i.e. by the two orifices in the figure) is equal to the power at the supply (when $p_T = 0$ and $p_L = 0$) is instead given by

$$P_0 = (p_0 - p_T) \cdot C_f \, \Omega(x) \sqrt{\frac{p_0 - p_T}{\rho}}$$

The latest expression can be found by assuming a zero load ($p_L = 0$) and considering that the two orifices of the servovalve $\Omega_{PA}(x), \Omega_{BT}(x)$ have the same area, as in the given problem.

From the two expressions above, it can be demonstrated that the ratio of the two hydraulic powers, which can be represented by the dimensionless parameter Π, is given by:

$$\Pi = \frac{P_L}{P_0} = \pi \sqrt{1 - \pi}$$

Where

$$\pi = \frac{p_L}{p_0 - p_T}$$

To find the maximum value for Π, the first derivative of its expression can be set equal to zero:

$$\frac{d\Pi}{d\pi} = 0 \qquad ==> \qquad \frac{2 - 3\pi}{2\sqrt{1 - \pi}} = 0 \qquad ==> \qquad \pi = \frac{2}{3}$$

To verify that this value for π corresponds to a maximum, the second derivative value calculated for $\pi = \frac{2}{3}$ must be negative.

$$\left.\frac{d^2\Pi}{d\pi^2}\right|_{\pi=\frac{2}{3}} = \left.\left(\frac{9\pi - 8}{4(1 - \pi)\sqrt{1 - \pi}}\right)\right|_{\pi=\frac{2}{3}} = \frac{-3\sqrt{3}}{2}$$

This means that the maximum power transmitted to the load by the servovalve is maximum when the ratio between the load pressure p_L and the supply pressure (considered as $p_0 - p_T$) is 2/3. In other words,

$$\left. p_L \right|_{P_{L,max}} = \frac{2}{3}(p_0 - p_T)$$

This explains why for the typical systems using servovalves that operate at 3000 psi (210 bar), the ISO 10770 suggests using a value of 70 bar as reference value for p_V to provide the steady state valve characteristics.

Problems

8.1 Create the equivalent ISO schematic of the following valves and explain the operation. What is the feature that all these valves have in common? (Drawings courtesy of Parker Hannifin).
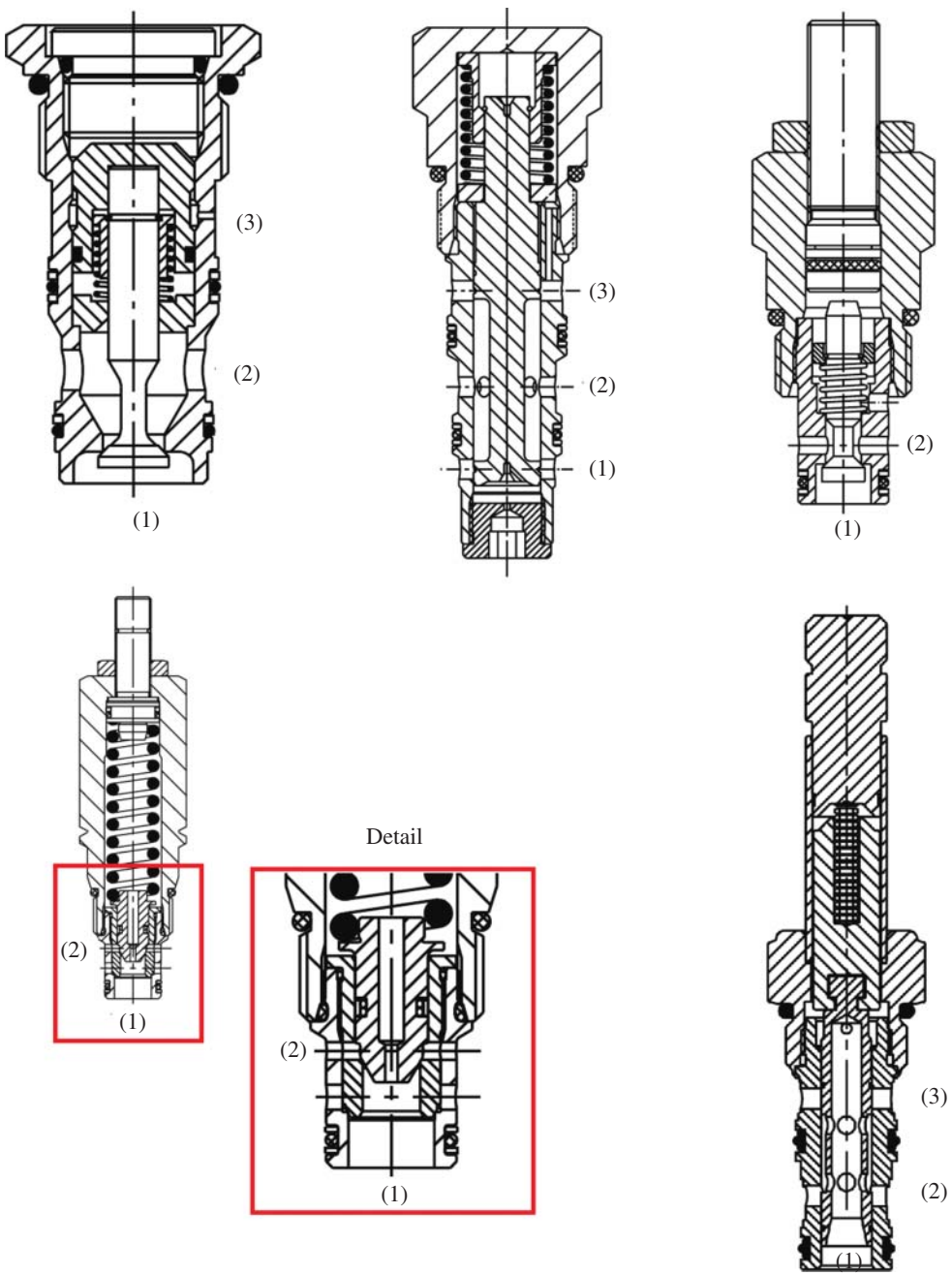
8.2 Create the equivalent ISO schematic of the following valves and explain the operation. What all these valves have in common? (Drawings courtesy of Parker Hannifin).
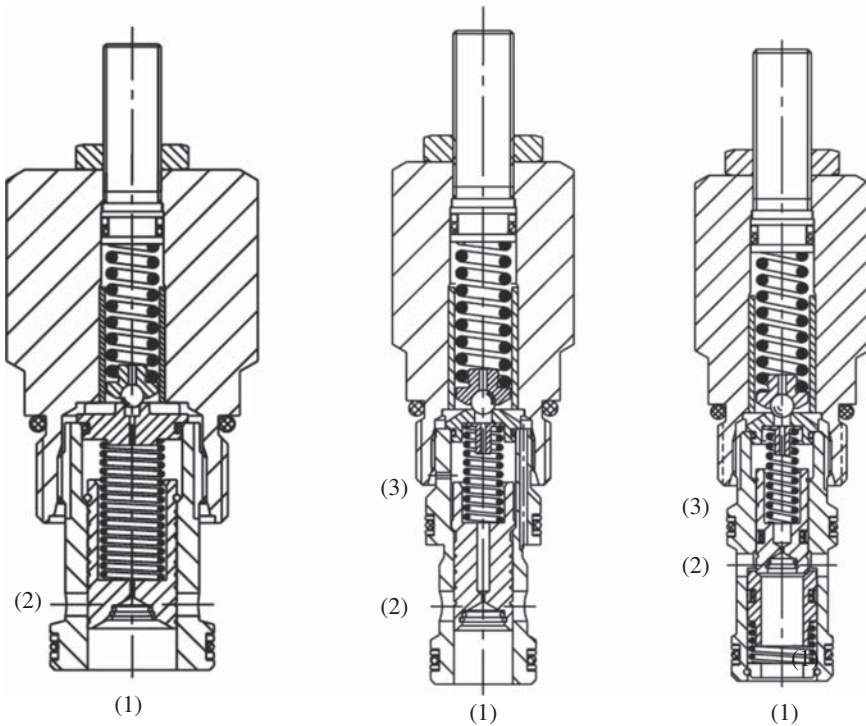
8.3 Consider the system in the figure, at rest conditions (no current provided to the valve solenoids).

Does the load move down because of gravity in the ideal case of no internal leakages in the cylinder? What is the pressure at pressure at the cap side of the cylinder (p_H) in this ideal case? (Show both formula and result.)

Does the load move down because of gravity in the real case of internal leakages in the cylinder? pressure at the cap side of the cylinder (p_H) in this real case? (Show both formula and result.)

If needed, you can assume realistic values for the parameters not expressly indicated in the figure.

Mass: 52 000 Ib

Bore: 6″
Rod: 3″
Stroke: 55″
Initial pos: 50%
Stroke

P   T
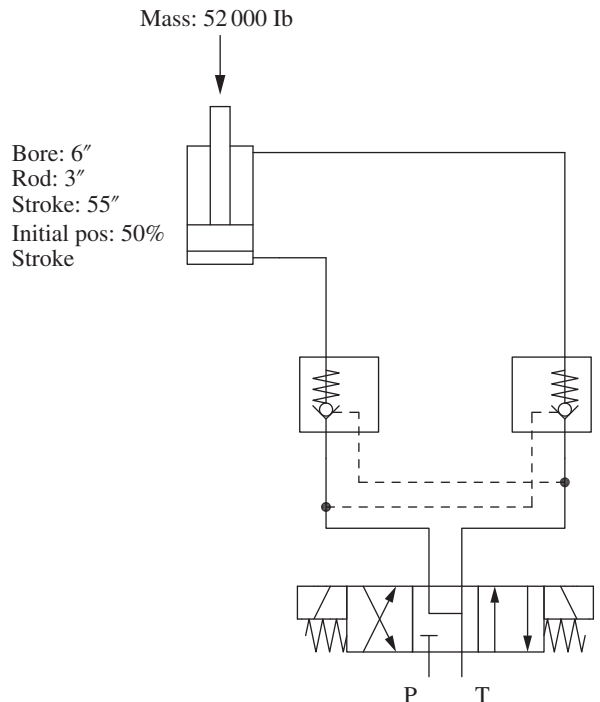
8.4 A direct operated pressure relief valve is used to limit the pressure in a circuit where the flow rate generated by the pump is 100 l/min. The influence area A on which the pressure acts is 78.54 mm^2, the spring preload gives a cracking pressure of 180 bar. The spring stiffness is 20 N/mm, the tank pressure is at 0 bar, the fluid density is 850 kg/m^3, and the flow coefficient is 0.62. Determine the travel of the poppet when the valve is discharging half of pump flow and the full pump flow. The maximum flow area corresponding to the maximum poppet travel of 10 mm is 28.27 mm^2. Assume a linear relationship between flow area and poppet travel. Neglect the effect of flow forces.

8.5 The figure below shows a two-way FCV. The value of the diameter is $d = 1$ mm of the orifice downstream the compensator. The flow rate established by the valve is $Q = 40$ l/min. The force of the compensator spring is $F_s = 100$ N.
Assuming the coefficient of discharge for the orifice, $C_d = 0.65$, and the density of the fluid, $\rho = 850$ kg/m^3, calculate the area of influence A of the pressure compensator. This area is equal on both sides.

A

Q

F_S

A

8.6 The figure below shows a three-way FCV. The diameter is $d = 1$ mm of the orifice after pressure compensated stage. The flow rate established by the valve is $Q = 40$ l/min. The force of the spring in the pressure compensated stage is $F_s = 10\,000$ N.

Assuming the coefficient of discharge for the orifice, $C_d = 0.65$, and the density of the fluid, $\rho = 850$ kg/m³, calculate the area of influence A for the pressure, in the pressure compensated stage, in mm².

Neglect pressure losses in the connecting lines. Any value of pressure pout can be assumed.

8.7 The following ISO schematic is used in a system for feeding two consumers: U1 and U2. The port P is connected at the pump delivery while the port T at the reservoir (tank pressure 0 bar). The pump delivers a fixed amount of fluid equal to 80 l/min. By reading the ISO schematic and considering ideal springs, determine the flow rate going to the consumer U2 and the flow rate discharged by the relief valve, knowing that U1 is taking 30 l/min.

8.8 For the system represented in the figure, determine the spring force necessary to get $Q = 40$ l/min. The fluid density is $\rho = 870$ kg/m³ (mineral oil). Assume the orifice coefficient to be 0.65. Is the flow rate Q function of the inlet pressure p_{in}?

8.9 In the figure below, the mass is lifted to the position shown and then the valve is switched to neutral position. Now the mass is suddenly dropped (say, the rope by which the mass is hanging is cut off). What happens to the piston position in the hydraulic cylinder? Does it retract, extend, or stay the same? If your answer is retraction, or extension, what is the magnitude of that? Also determine the pressure in bore and rod side chamber.
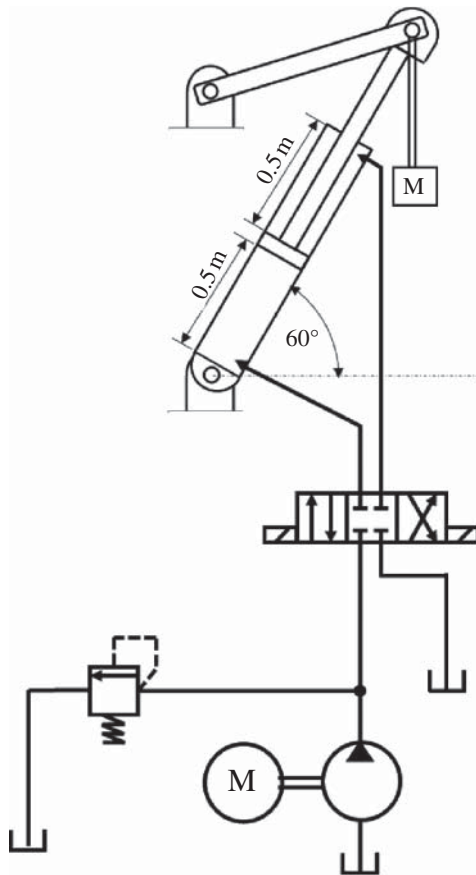
Use the following data:

$M = 8000$ kg
Acceleration due to gravity $= 9.81$ m/s^2
Hydraulic cylinder:
$\qquad D_{bore} = 60$ mm
$\qquad D_{rod} = 30$ mm
Stroke $= 1$ m

Assume zero leakage through the directional control valve.

Chapter 9

Hydraulic Accumulators

An accumulator is a device that can store and release energy in the form of a pressurized fluid. Thus, an accumulator is the hydraulic equivalent of an electric capacitor, involving fluid energy instead of electric energy. It is used in hydraulic systems not only as energy storage elements but also for pulsation dampening, suspension, and emergency supply.

   This chapter provides a brief classification of the existing architectures for hydraulic accumulator and describes their main use in hydraulic systems.

9.1 Accumulator Types

> Hydraulic accumulators store energy in the form of a pressurized fluid.

There are three main architectures available: *gravity* or *weight-loaded* accumulators, *spring-loaded* accumulators, and *gas-loaded* accumulators. Modern hydraulic circuits mostly use the last type.

9.1.1 Weight-loaded Accumulators

Weight-loaded accumulators represent an ancient hydraulic technology. Their design consists of a vertical cylinder, where the piston is loaded with a series of weights. The weights produce a constant pressure independent of the volume of fluid inside the cylinder. A famous example of a weighted-loaded accumulator is in the original hydraulic system for raising or lowering the Tower Bridge in London [21]. Weight-loaded accumulators have very limited energy storage, so they are not used in common hydraulic systems.

9.1.2 Spring-loaded Accumulators

While weight-loaded accumulators use the gravitational energy of a mass, spring-loaded accumulators store energy by compressing a mechanical spring. Their architecture resembles a single acting cylinder without a rod, using a spring-returned piston (Figure 9.1).

   The pressure of the fluid inside a spring-loaded accumulator depends on the compression of the spring. Therefore, there is a relationship between the energy E of the fluid stored inside the accumulator and its volume:

$$E = p \cdot V = \left(\frac{F_s}{A}\right) \cdot (A \cdot x) = \left(F_0 + kx\right) \cdot x \qquad (9.1)$$

Equation 9.1 uses Hooke's law to calculate the spring force, where k is the spring stiffness and x is the travel of the piston from the fully extended position, represented in Figure 9.1. The pressure of
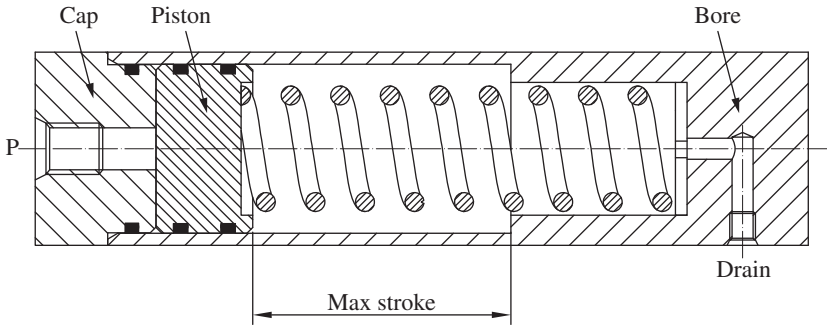
Figure 9.1 Cross-section of a spring-loaded accumulator. The supply port P is connected to the hydraulic circuit, while the drain is connected to a tank or vented to the atmosphere.

the fluid varies linearly with the position of the piston, and the energy stored inside the accumulator increases with the volume following a quadratic relation, as shown by Eq. (9.1).

The use of spring-loaded accumulators (sometimes also referred as *spring charged* accumulators) is limited to specific applications where small amounts of energy need to be stored. For example, they are used in some anti-lock braking system (ABS) system for cars and sport utility vehicle (SUVs).

9.1.3   Gas-charged Accumulators

Gas-loaded (or *gas-charged*) accumulators are by far the most common type of accumulators used in modern hydraulic systems. In such components, the compressive energy is provided by a gas, typically nitrogen, or in some cases argon, since they are inert gases. Gas-loaded accumulators are classified in three common architectures depending on the method used to separate the hydraulic fluid from the gas: *piston*, *bladder*, and *diaphragm* accumulators.

9.1.4   Piston-type Accumulators

The design of a piston-type accumulator is similar to the spring-loaded one, and it is represented in the cross section of Figure 9.2. The accumulator has one port for the hydraulic fluid (at the bottom) and one port at the top for "charging" the gas (i.e. setting the initial pressure). The moving piston has proper seals to separate the fluid from the gas. To guarantee effective sealing and durability, the internal surface of the barrel requires smooth surface finishing. In any gas charged accumulator, the precharge value is defined as the pressure in the gas chamber when the piston is at rest in the bottom position. The precharge can be adjusted by introducing or relieving gas from the top valve.

9.1.5   Diaphragm-type Accumulators

Diaphragm accumulators use a diaphragm (usually made of rubber or neoprene) to separate the fluid from the compressed gas. The structure of a diaphragm accumulator is shown in Figure 9.3. The body (usually carbon steel, but lightweight fiber accumulators are also available) is separated into two parts that are welded or bolted together to allow the assembly or replacement of the diaphragm. Diaphragm accumulators have a simple and more economical design compared with
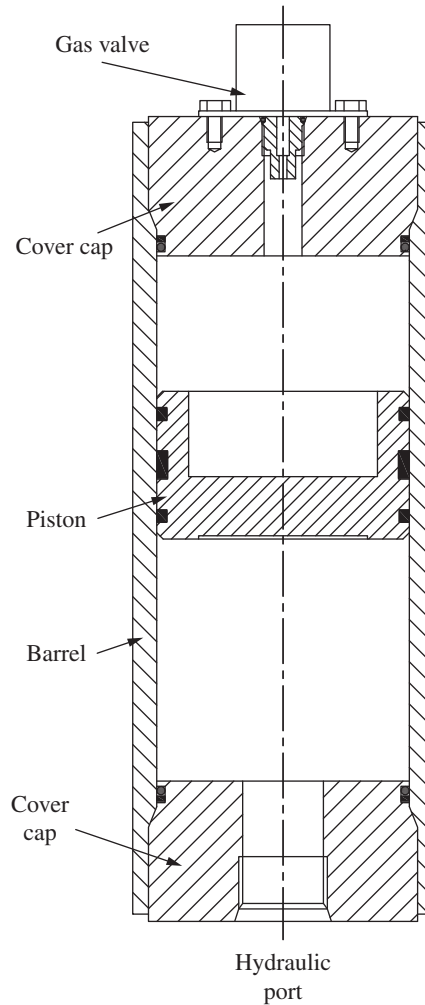
Figure 9.2 Piston-type gas-loaded accumulator.

piston accumulators. However, due to its elastomeric material, these accumulators have a limited life span, thus making them less suitable for heavy-duty applications.

Diaphragm accumulators allows very high ratios between the maximum operating pressure and the initial precharge. As it will be discussed at the next section, this establishes an advantage from the energy density standpoint. However, they are only commercially available in small sizes (up to 5 l).

9.1.6 Bladder-type Accumulators

Bladder accumulators are similar to diaphragm accumulators. They are made of a shell in which an elastomeric bladder is located (Figure 9.4). The bladder is filled with gas from the gas valve located at the top of the accumulator. At the bottom, a properly designed valve allows the connection with
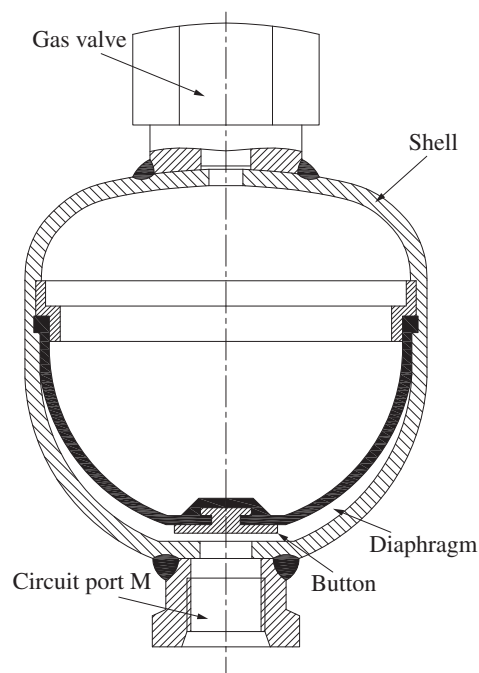
Figure 9.3 Diaphragm-type gas-loaded accumulator.
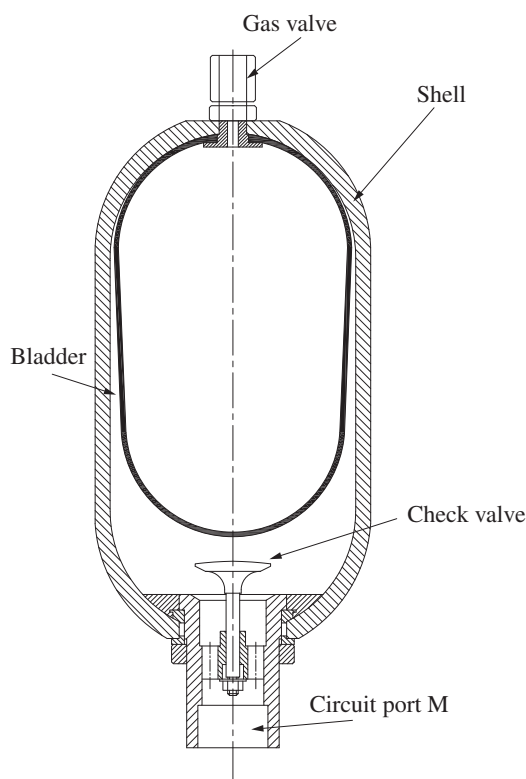
Figure 9.4 Bladder-type gas-loaded accumulator.

the fluid side and prevents the extrusion of the bladder into the hydraulic lines. The bladder can be replaced when it reaches the end of its life span.

Bladder accumulators is available to all possible sizes, from typical minimum size of 1–2 l up to 500 l as in special cases. The shell material is normally steel, but lightweight carbon fiber accumulators are also available for weight-sensitive applications.

9.2 Operation of Gas-charged Accumulators

> Gas-charged accumulators store fluid energy by compressing gas.

The gas used in hydraulic accumulators is an inert gas, usually nitrogen. Air cannot be used because it would introduce corrosion problems and risk of explosions due to spontaneous combustion if the oil enters in contact with the air at high pressure.

The gas inside the accumulator is initially pressurized at a level called *precharge pressure, p_0*. The precharge is set while the system is at rest. The accumulator is selected to work in a pressure range where p_2 is the maximum and p_1 is the minimum value. The three most significant operating states, for the case of a bladder accumulator, are shown in Figure 9.5.

Different architectures allow to achieve different operating ranges, usually defined by the compression ratio p_2/p_0. In particular,

i)   Bladder accumulators allow $p_2/p_0 < 4$.
ii) Diaphragm accumulators allow $p_2/p_0 < 8$.
iii) Piston accumulators does not have p_2/p_0 limitations.

For the optimal energy utilization of the accumulator, the value for the precharge pressure p_0 should theoretically be equal to the minimum operating pressure p_1. This is possible with piston accumulators, but it should be avoided in diaphragm and bladder accumulators because the elastomer separating element could be damaged as a result of a frequent contact with the anti-extrusion valve present at the fluid port of the accumulator. Typically, the precharge is selected as follows:

– Bladder and diaphragm accumulators, $p_0 \cong 0.9\, p_1$
– Piston accumulators, $p_0 \cong p_1$

The considerations above are typical for the applications of accumulators as energy storage devices, working between two known pressure levels. Accumulators can also be used as elements that stabilize the pressure within the system. For these pseudo-constant pressure applications (at a value p_{sys}), it is instead typical to have:

$$p_0 \approx 0.7\, p_{sys} \tag{9.2}$$

9.3 Typical Applications

Hydraulic accumulators can be encountered in hydraulic systems for accomplishing different functionalities. While energy accumulation is, at this point, the most intuitive one, other common functionalities are mentioned in the next paragraphs and throughout the rest of the book.
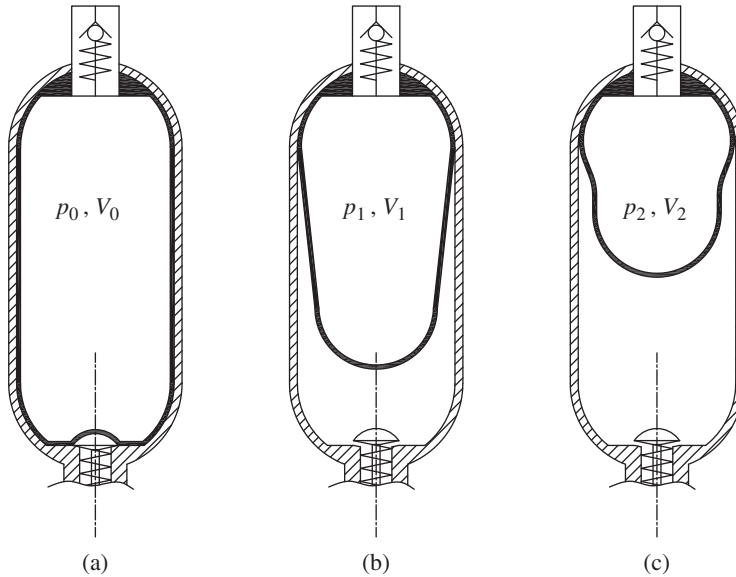
Figure 9.5 Operating conditions for a bladder accumulator: precharge condition (a), minimum operating pressure condition (b), *and* maximum operating pressure condition (c).

9.3.1 Energy Accumulation

In most applications, accumulators are used as energy storage devices that can supply additional flow to the primary pump. This is very useful in applications undergoing working cycles characterized by a short period of high flow demand alternating with longer periods of rest. In fact, in such applications, the use of accumulators reduces the size of the primary flow supply, i.e. the pump and, eventually, the prime mover. Common examples are circuits to supply hydraulic brakes (Figure 9.6).

The pump, P, is supplying the accumulator (AC) through a check valve (CV), and a 3/2 directional control valve (DCV). The pump flow is also supplying other secondary hydraulic functions not represented in the circuit. The position of the DCV influences the flow to the accumulator and the other functions: In neutral position, the DCV supplies both lines but restricts flow toward the secondary circuit, but when the DCV is shifted, the pump flow is free to reach the secondary circuit. The accumulator supplies a brake-modulating valve (BV), which is the equivalent of a pressure-reducing valve with a setting that is proportional to the position of the foot pedal. The valve BV finally supplies the brake cylinder (BC). This is a single rod actuator, which contains a spring returning it to the neutral position. The valve DCV is monitored by a pressure sensor, which measures the state of the charge of the accumulator. If the accumulator pressure is below the minimum value, p_1, the DCV stays in neutral and part of the pump flow is diverted to the accumulator, because of the valve restriction. The valve is maintained in such position until the maximum pressure value p_2 is reached in the break circuit. At this point, the valve can shift and the pump flow is free to reach the secondary circuit. The CV prevents leakages of the oil trapped in the accumulator through the spool element of DCV. Each time the brakes are pushed, a portion of oil is lost, thereby reducing accumulator pressure. When the pressure is below the minimum value p_1, the DCV returns to neutral and the accumulator is charged.

The brake circuit presented in Figure 9.6 is simplified and based on an electric control of the charge valve. In reality, brake circuits can become much more complex due to safety requirements.
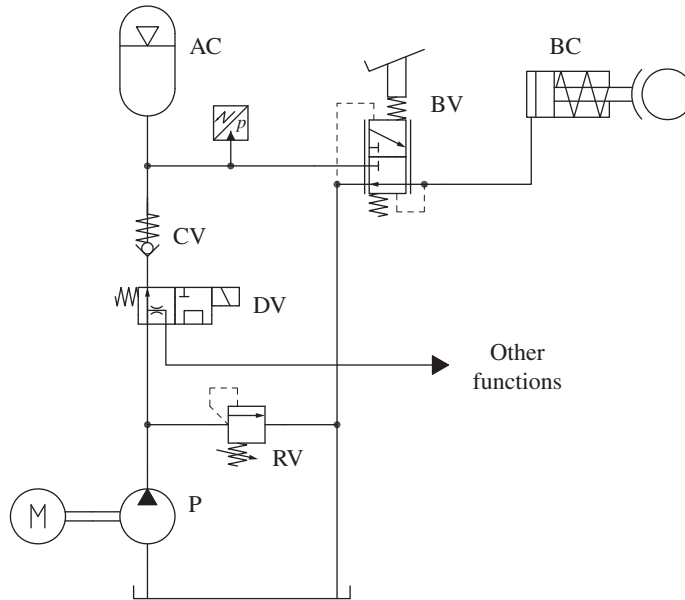
Figure 9.6 Simplified circuit for hydraulic brakes.

More on this topic can be found in [14]. A more detailed example of brake supply circuit is also reported in Chapter 17, where constant pressure systems are presented.

9.3.2 Emergency Supply

The accumulator presented in the circuit in Figure 9.6 also has an emergency functionality: in case of failure of the pump or the prime mover, the vehicle can still perform a number of braking maneuvers.

Other instances of emergency functionality are encountered in circuits using piloted directional control valves, such as in Figure 8.37 and Figure 8.38. In such components, the main spool can be operated only if the machine is running and pilot pressure is present. However, sometimes, the machine is required to perform some emergency maneuvers (e.g. lowering the boom or the hoist) after the engine is turned off. This is accomplished with a small accumulator connected to the pilot supply circuit, capable of maintaining pilot pressure for some time after the vehicle is turned off.

9.3.3 Energy Recuperation

Accumulators can be used as energy storage element in circuits with *energy regeneration* function. In these circuits, the accumulator has the function to recover energy from overrunning load conditions (this topic will be extensively covered in Part III). Examples of overrunning load conditions include the lowering of a boom arm under gravity, the lowering of load through a hydraulic winch, or the braking of a vehicle wheel connected to a hydraulic motor.

In most actuation systems (not only hydraulic systems), the energy associated with overrunning load conditions is dissipated within the actuation system. However, energy recuperation derived from overrunning conditions through accumulators is often allowed. A clear example is presented by the secondary controlled hydrostatic transmissions, which are presented in Chapter 27.

9.3.4 Hydraulic Suspensions

In many off-road vehicles, such as agricultural tractors, accumulators are used as a suspension element. The basic idea is represented in Figure 9.7: a hydraulic cylinder mechanically connects the vehicle chassis with the wheel axle. The shocks caused by uneven ground conditions are damped in a circuit including an accumulator (hydraulic capacitance), a CV, and an orifice (hydraulic resistance). When the vehicle runs into a bump, the energy of the shock is captured in the accumulator (the flow moves freely through the CV). Subsequently, when the vehicle overcomes the obstacle, the accumulator returns the flow to the cylinder through the orifice and uses the stored energy. Without the orifice, the accumulator would return the stored energy to the cylinder, which would cause a continued oscillation of the vehicle.

The performance of the suspension has to match the mass of the vehicle, the traveling speed, and the ground conditions. This can be achieved by properly sizing the accumulator and the orifice.

Hydraulic suspensions are not only used in axles but also to other parts of the machine. For example, wheel loaders present a boom suspension system often referred to as *ride control* [26].
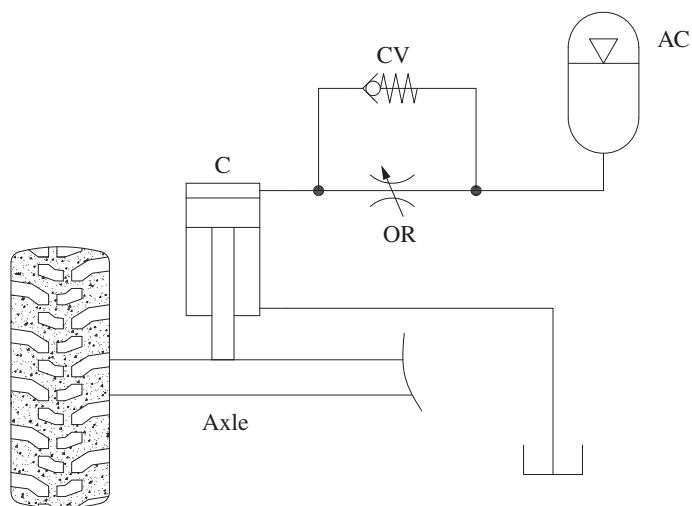
Figure 9.7   Accumulator in a vehicle suspension circuit.

9.3.5 Pulsation Dampening: Shock Attenuation

The flow within the lines of a hydraulic system is not continuous but presents ripples that can interact with the machine structure and create an audible noise. The first and most common source of irregularity is the flow supply. As described in Chapter 6, hydraulic pumps are positive displacement machines, so their design intrinsically provides an irregular outlet flow. Hydraulic lines also have their own frequency responses; the pressure waves traveling inside the lines can amplify certain frequencies in an undesired manner. Other hydraulic components, such as hydraulic control valves, are also subjected to resonances that normally need to be avoided. Hydraulic accumulators can be used to attenuate these irregularities with a basic concept illustrated in Figure 9.8.

In this kind of application, the accumulator serves as an element that produces a large increase of the capacitance: the system at the outlet of the pump becomes less stiff and it responds to flow variations gently. Small size accumulators (typically of the diaphragm type) are used to implement the pressure dampening function because, at a very small volume, the gas can be sufficient to
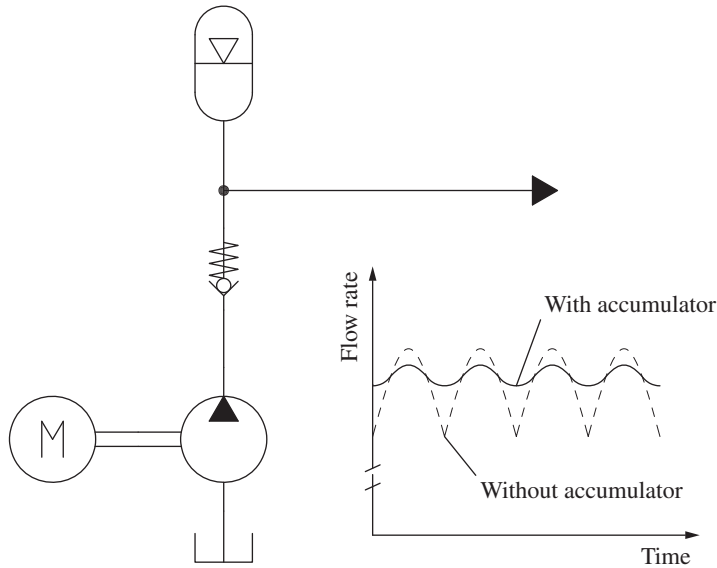
Figure 9.8 Use of an accumulator for pulsation dampening.

increase the overall compressibility of the hydraulic lines connected to the accumulator. Hydraulic systems very sensitive to flow irregularities, such as systems requiring operation at high frequencies using servovalves, typically require small accumulators with the pulsation dampening function.

As previously stated, the main focus of this book is on the stationary operation of hydraulic control systems, and therefore dynamic conditions typical of transients are considered out of the scope of this book. Nevertheless, Chapter 5 covers the main elements for performing a dynamic analysis of a generic hydraulic system, including an example of the pulsation dampening achieved with an accumulator.

9.4 Equation and Sizing

9.4.1 Accumulator as Energy Storage Device

In general, sizing an accumulator means finding its optimal volume and precharge pressure, for a given set of operating conditions. In Figure 9.5, the three main states of a gas-charged accumulator are characterized by the following parameters:

i) At rest condition, the gas pressure equals the precharge p_0, while the gas volume V_0, is equal to the full accumulator volume.
ii) At the minimum working pressure, p_1, the volume of the gas is V_1.
iii) At the maximum working pressure, p_2, the volume of the gas is V_2.

As stated earlier, $V_0 \cong V_1$ only for piston accumulators, while for bladder or diaphragm accumulators V_1 can be significantly smaller than V_0. The ratio between the two volumes is determined according to the pressure guidelines for p_0 and p_1 provided earlier, according to equations that will be further discussed.

During its regular operation, ΔV is the volume of fluid that the accumulator is expected to exchange with the hydraulic system:

$$\Delta V = V_2 - V_1 \tag{9.3}$$
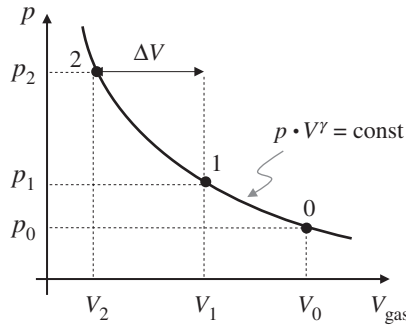
Figure 9.9 Polytropic behavior of the gas inside the accumulator.

Usually, the design engineer can evaluate the quantity ΔV by analyzing the hydraulic system and its working cycle. For example, in sizing a brake circuit, the engineer is given the number of brake applications that need to be performed using oil in the accumulator. The designer can also establish the pressure levels at which the system operates to use the actuator loads. These data can be used along with pressure and volume to determine the optimal accumulator volume V_0.

In the sizing calculations, the assumption of ideal gas following polytropic processes is usually considered a good approximation of the actual behavior of the gas[1]. According to this hypothesis,

$$p_0 \cdot V_0^\gamma = p_1 \cdot V_1^\gamma = p_2 \cdot V_2^\gamma = \text{constant} \tag{9.4}$$

The constant γ is the polytropic index for the gas. Equation 9.4 can be represented graphically in Figure 9.9. The polytropic coefficient depends on the nature of the compression and expansion processes inside the accumulator, and it is sometimes difficult to estimate. A slow charging and discharging process (in the order of minutes) can be approximated by an isothermal process ($\gamma = 1$). This assumption considers that the gas inside the accumulator has enough time during the process to dissipate the generated heat to the surroundings without varying its temperature. In contrast, a fast process (in the order of seconds) can be considered adiabatic. Typical values of γ are the following:

$$
\begin{aligned}
\gamma &= 1 && \text{(isothermal)} \\
\gamma &= 1.4 && \left(\text{adiabatic} - \text{nitrogen}\right) \\
\gamma &= 1.67 && \left(\text{adiabatic} - \text{argon}\right)
\end{aligned}
\tag{9.5}
$$

Many actual processes happen under intermediate conditions between the isothermal and adiabatic conditions. For this it is often reasonable to assume intermediate values of $\gamma \cong 1.2$.

From Eq. 9.5, it is possible to derive expressions relating the volumes V_1 and V_2 to V_0:

$$
\begin{aligned}
V_2 &= V_0 \cdot \left(\frac{p_0}{p_2}\right)^{\frac{1}{\gamma}} \\
V_1 &= V_0 \cdot \left(\frac{p_0}{p_1}\right)^{\frac{1}{\gamma}}
\end{aligned}
\tag{9.6}
$$

Working on the two expressions in Eq. 9.6, it is possible to derive ΔV as

$$\Delta V = V_0 \cdot p_0^{\frac{1}{\gamma}} \cdot \left(\frac{p_2^{\frac{1}{\gamma}} - p_1^{\frac{1}{\gamma}}}{p_2^{\frac{1}{\gamma}} \cdot p_1^{\frac{1}{\gamma}}}\right) \tag{9.7}$$

---

1 The results found with the polytropic relation for ideal gas are usually considered accurate for nitrogen. However, particularly for applications above 200 bar, a better accuracy can be achieved by applying proper correction coefficients that consider the real gas behavior. Such correction coefficients can be found by applying the known real gas relations, but they are sometimes provided by the accumulator manufacturers. Examples of such coefficients are in [8, 9].

which, in terms of the accumulator volume V_0, becomes:

$$V_0 = \frac{\left(\dfrac{p_2}{p_1}\right)^{\frac{1}{\gamma}} \cdot \Delta V}{\left(\dfrac{p_o}{p_1}\right)^{\frac{1}{\gamma}} \cdot \left[\left(\dfrac{p_2}{p_1}\right)^{\frac{1}{\gamma}} - 1\right]} \tag{9.8}$$

Equation 9.8 can be used to calculate the ideal accumulator volume as a function of known parameters. In fact, the precharge p_o can be selected according to the pressure ranges previously indicated for p_o, p_1, and p_2.

9.4.2 Accumulator as a Dampening Device

The sizing of a gas-charged accumulator for pulsation dampening is a typical dynamic problem, which can be addressed with a lumped parameter approach. Chapter 5 has been fully dedicated to the dynamic equations suitable to describe the transient within a hydraulic system. This includes the analysis of the dampening effect of an accumulator within the hydraulic system. Simply, for the system in Figure 9.10, the pressure derivatives in the line can be reduced by acting on the system capacitance:

$$\frac{dp}{dt} = \frac{1}{C_H}\left(\sum Q\right) \tag{9.9}$$

where:

$$C_H = C_{H,\text{line}} + C_{H,\text{acc}} \tag{9.10}$$

If an accumulator is used, the line capacitance can easily prevail. The formula derived for the accumulator capacitance is

$$C_{H,acc} = -\frac{V_0}{\gamma} \cdot \sqrt[\gamma]{\frac{p_0}{p^{1+\gamma}}} \tag{9.11}$$

(a)

(b)
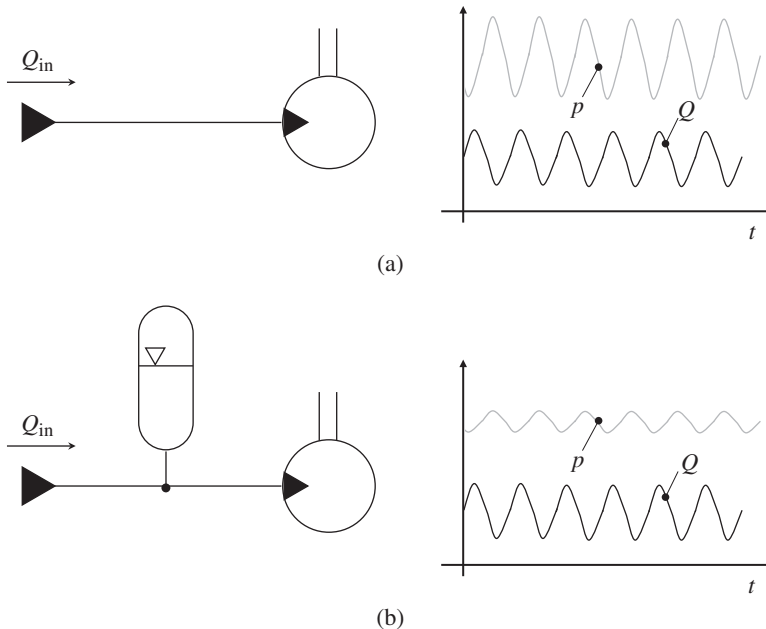
Figure 9.10 Accumulator for pressure dampening.

where p represents the level of the pulsating pressure within the system. Typically, for pressure damping application, the precharge pressure is set between 60% and 75% of the average system pressure. Therefore, the volume of the accumulator can be found depending on the severity required by the application. Since the pressure pulsations normally occur with a fast dynamic, it is typical to adopt high values for the polytropic coefficient γ (close to 1.4).

Example 9.1   Using an accumulator to reduce the input power of a cyclic operation

A hydraulic system is used to control the motion of a double rod actuator according to a repetitive cycle of 60 seconds duration. Within each cycle, the actuator completes first a left stroke in three seconds, then pauses for 27 seconds, then a right stroke of three seconds, and another pause for 27 s. Each stroke is 250 *mm*, and the force acting on the rod is 300 *kN*, always resistive (opposing the motion of the rod). The cylinder annular area is 200 *cm²*. The hydraulic schematic of the system is shown in the figure below. The system uses a fixed displacement pump providing 18 *l/min* of flow and uses a sequence valve (SV) with external pilot set at 200 *bar*. Calculate the volume of the accumulator necessary to perform the cycle above described. Plot the qualitative trend for the system pressure and flow rates during the cyclic operation of the system (problem derived from [27]).
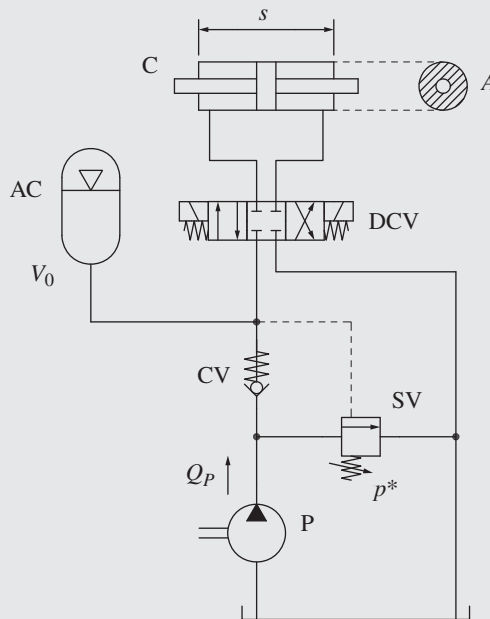
Given:
A schematic of a hydraulic system performing a cyclic operation of a double rod actuator. The actuator annular area, $A = 200$ *cm²*; the actuator stroke, $s = 250$ *mm*; the actuator load, $F = 200$ *N* (resistive); the pump flow rate, $Q_p = 18$ *l/min*; and the setting of the externally piloted pressure SV, $p^* = 200$ *bar*. The cycle time, $t_{cycle} = 60$ s, which includes two full strokes completed in $t_{stroke} = 3$ s each; each stroke is followed by a rest time of $t_{rest} = 27$ s.

Find:

a) The size of the accumulator necessary to complete the cycle, V_0
b) Graphically represent the trend of the system pressure (p_p, p_{acc}) as well as the flow rates (Q_{cyl}, Q_{acc})

Solution:

To solve this problem, it is useful to visualize the duty cycle of the system in the figure below. The figure also shows the position of the directional control valve that is used to achieve the stroking motion of the linear actuator.
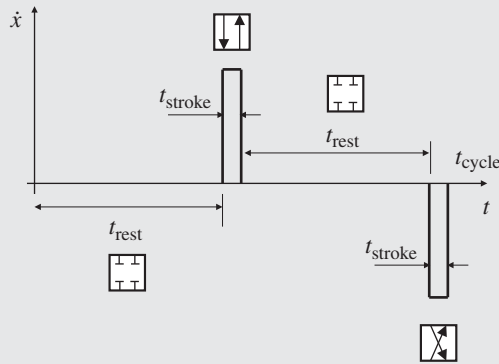
When DCV is at rest (neutral position), the pump supplies flow to the accumulator until its pressure reaches the setting of the sequence valve, set at p^*. At this point, the sequence valve opens and diverts the pump flow to the tank when the accumulator pressure reaches p^*. The reader should notice that the SV is different from a traditional relief valve (where the pilot pressure is picked up internally). In fact, the pressure at the accumulator, isolated by the CV, allows to fully unload the pump at ideally zero pressure. Mode details on accumulator unloading valves are presented in Chapter 17.

a) To find the accumulator volume, it is important to first find the volume of fluid required by a single stroke of the actuator.

$$V_{stroke} = A \cdot s = 200\,[cm^2] \cdot 250\,[mm] = 5\,l$$

The average flow reaching the actuator during a single stroke is therefore

$$Q_{stroke} = \frac{V_{stroke}}{t_{stroke}} = \frac{5\,[l]}{3\,[s]} = 100\,l/min$$

It is clear how the pump, which provides $Q_p = 18\,l/min$, would not be able to move the cylinder in $t_{stroke} = 3\,s$. The volume contribution of the pump during the stroke is

$$V_p = Q_p \cdot t_{stroke} = 18\,[l/min] \cdot 3\,[s] = 0.9\,l$$

Therefore, the accumulator needs to provide the remaining volume:

$$\Delta V_{acc} = V_{stroke} - V_p = 5\,[l] - 0.9\,[l] = 4.1\,l$$

This accumulator volume is provided while the pressure decreases from the maximum working pressure p_2 to the minimum working pressure, p_1, as represented in the figure below that shows the locus of the pressure levels inside the accumulator.

Example 9.1 (Continued)
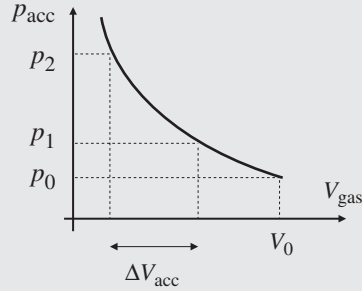
In this problem, the maximum pressure reached in the accumulator is given by the setting of the pressure SV: $p_2 = p^*$. The minimum pressure inside the accumulator during the working cycle, p_1, is the minimum value of pressure that still allows winning the resistance force on the actuator:

$$p_1 = p_{cyl} = \frac{F}{A} = \frac{300\,[kN]}{200\,[cm^2]} = 150\ bar$$

As mentioned previously, a common value for the precharge of a bladder accumulator is 90% the minimum working pressure:

$$p_0 = 0.9 \cdot p_1 = 0.9 \cdot 150\,[bar] = 135\ bar$$

From these values, it is possible to find the volume of the accumulator, which corresponds to the volume of the gas inside it at precharge conditions:

$$V_0 = \frac{\left(\dfrac{p_2}{p_1}\right)^{1/\gamma} \cdot \Delta V_{acc}}{\left(\dfrac{p_0}{p_1}\right)^{1/\gamma}\left[\left(\dfrac{p_2}{p_1}\right)^{1/\gamma} - 1\right]} = \frac{\left(\dfrac{200\,[bar]}{150\,[bar]}\right)^{1/1.4} \cdot 4.1\,[l]}{\left(\dfrac{135\,[bar]}{150\,[bar]}\right)^{1/1.4}\left[\left(\dfrac{200\,[bar]}{150\,[bar]}\right)^{1/1.4} - 1\right]} = 23.8\ l$$

In the above expression, it is assumed a polytropic coefficient or the gas processes are equal to $\gamma = 1.4$. This means assuming adiabatic conditions, which might be reasonable for a fast process ($t_{stroke} = 3\ s$).

It should be observed that the accumulator has a large volume, $V_0 = 23.8\ l$, even if the volume flowing in and out the accumulator during the cycle is only $\Delta V_{acc} = 4.1\ l$.

The accumulator has permitted a considerable reduction of the system installed power. The power needed for a system with a similar circuit but without accumulator would be

$$\dot{W}_{w/o\ acc} = Q_{stroke} \cdot p_{cyl} = 100\,[l/min] \cdot 150\,[bar] = 25\ kW$$

Instead, thanks to the use of the accumulator,

$$\dot{W}_{w\ acc} = Q_p \cdot p_2 = 18\,[l/min] \cdot 200\,[bar] = 6\ kW$$

The installed power is reduced by 76%. However, this advantage comes at the price of a significant increase in size and weight.

b) The qualitative trend for both the pressures and the flow rates within the system during one cycle are represented in the figure below.
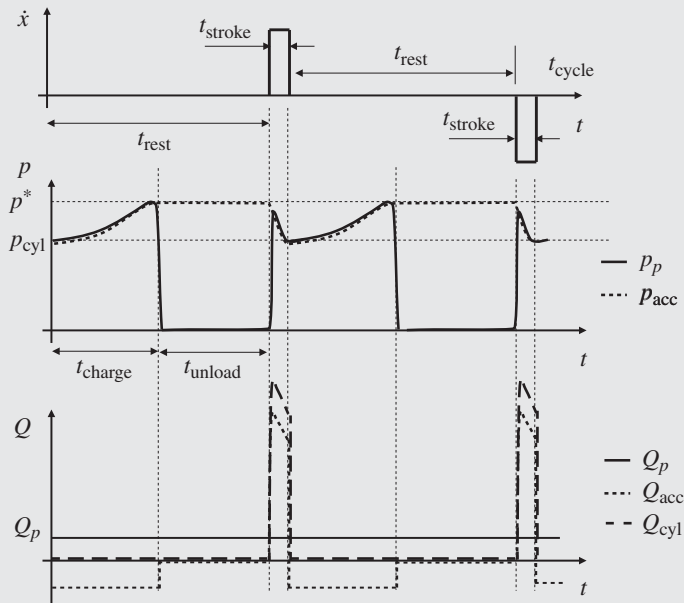
During each rest time phase, the accumulator first increases its pressure tanks to the pump flow. This period is indicated with t_{charge}. During the charge, both the accumulator and the pump delivery have the same pressure. As soon as the accumulator reaches the setting of the sequence valve, p^*, the pump pressure decreases to tank pressure thanks to the sequence valve externally piloted. The sequence valve in this case behaves as an unloader. The charge time can be calculated as:

$$t_{charge} = \frac{\Delta V_{acc}}{Q_p} = \frac{4.1 \ [l]}{18 \ [l/min]} = 13.7 \ s$$

The remaining period of the resting time occurs with the pump unloaded:

$$t_{unload} = t_{rest} - t_{charge} = 27 \ [s] - 13.7 \ [s] = 13.3 \ s$$

When the directional control valve is activated to perform each of the two strokes, the accumulator discharges the volume ΔV_{acc}, reaching its minimum pressure $p_1 = p_{cyl}$. The cycle then restarts, following the same trend described before.

The bottom plot shows the flow rates. While the pump flow rate is constant, the accumulator flow rate is negative (flow rate entering the accumulator) during the charge time interval, null during the t_{unload}, and then positive when the cylinder is actuated.

The system presented in this example has some very specific features that fit the use of an accumulator: the operation of the cylinder is repetitive and alternates long pauses between each movement. Furthermore, the loads on the cylinder are predictable and they are the same in both directions. If, for example, the load in one direction would have been much smaller than the one in the other direction, the system would have required more power to charge the accumulator and then completed a movement with much smaller power demand.

Problems

9.1 The system in the figure below uses a fixed displacement pump connected to an accumulator to drive a fixed displacement hydraulic motor. By using a 4/3 directional control valve (DCV) in series with a two-way flow control valve, a cyclic operation of the motor is performed as shown in the plot below.

In the drive cycle, the motor spins clockwise for 10 seconds (t_{cw}), rests for t_{rest} seconds, spins counterclockwise for other 10 seconds (t_{ccw}), and rests again for t_{rest} seconds. The torque acting on the motor is 200 Nm and is always resistive. The motor displacement is 100 cm³/rev. The pump flow is 10 l/min.

The two-way flow control valve upstream the directional control valve is set to provide 40 l/min.
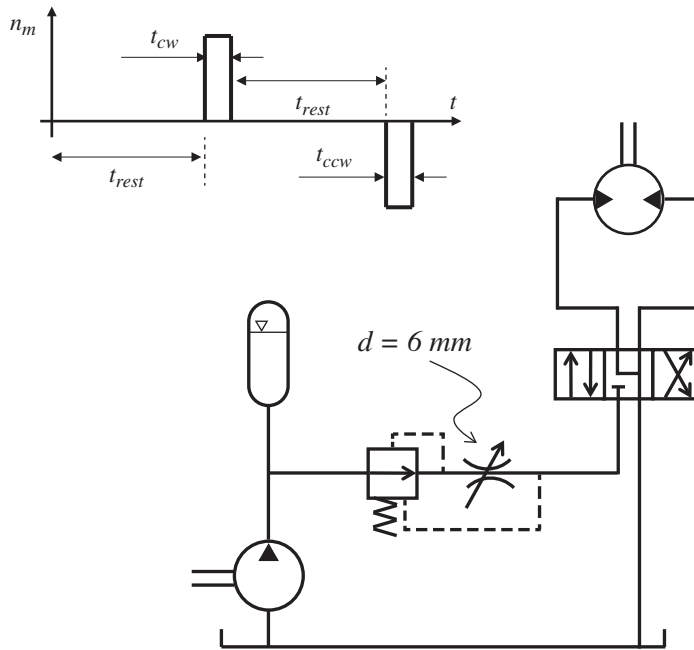
Perform the following tasks:

a) In the ISO schematic of the system, place the minimum number of relief valve(s), set at $p^* = 250$ bar to limit the maximum pressure of the system.

b) Calculate the pressure level of the hydraulic motor when it is operated by the DCV.

c) Calculate the shaft speed of the motor when it is operated by the DCV.

d) Find the volume of the accumulator necessary to guarantee the five seconds duration of each cycle. The formula you can use is

$$V_0 = \frac{\left(\dfrac{p_2}{p_1}\right)^{1/\gamma} \cdot \Delta V_{acc}}{\left(\dfrac{p_0}{p_1}\right)^{1/\gamma} \left[\left(\dfrac{p_2}{p_1}\right)^{1/\gamma} - 1\right]}$$

where p_1 and p_2 are the minimum and the maximum pressures, respectively, during the working cycle in the accumulator. p_0 is the precharge pressure (you can assume 90% of

the minimum pressure p_1), and γ is the polytropic coefficient (assume 1.4). ΔV_{acc} is the volume change inside the accumulator between the two pressure levels p_1 and p_2.

e) The minimum value achievable by the system for t_{rest} for the two rest intervals of the duty cycle.

f) Represent the qualitative trends for the pump pressure, accumulator pressure, and accumulator flow (in/out) in a time plot.

9.2 The system shown in the figure is used for car metal sheet press. In order to keep the pump size at a minimum value, an accumulator is used.

Determine

1. The pump displacement [cc/rev] necessary to fulfill the cycle requirement if the accumulator is not present in the circuit and if the electric motor is rotating at 1500 rpm.

2. The power absorbed by the electric motor for the configuration of part 1, assuming the relief valve is working [kW].

3. If $V_p = 15$ cc/rev and the electric motor rotates at 1500 rpm, evaluate the accumulator volume V_0 [l] to fulfill the cycle requirement.

Assume that the pump volumetric and hydromechanical efficiency as in the table below.
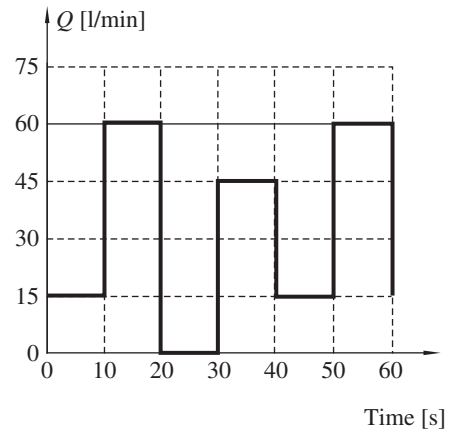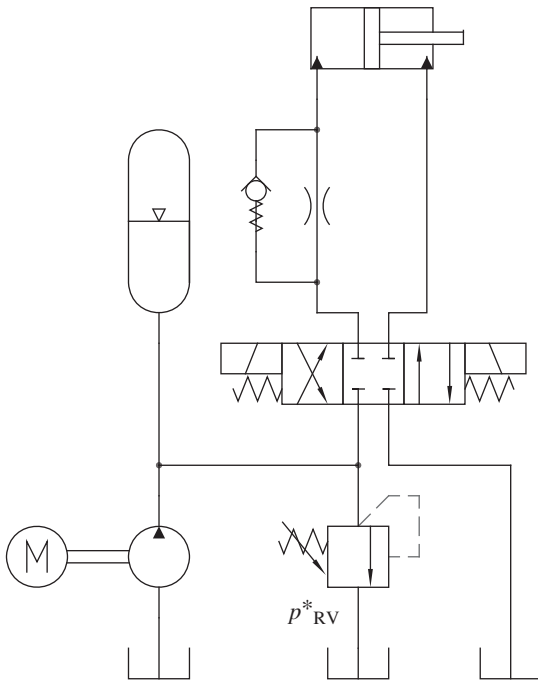
$\eta_{v, pump}$	0.93	
$\eta_{hm, pump}$	0.91	
$n_{polytrophic}$	1.3	
p^*_{RV}	210	*bar*
p_{tank}	0	*bar*
p_{min}	80	*bar*
$P_{recharge\ pressure} = 0.9 \cdot p_{min}$		

References

1 ISO 4391:1983 (1983). *Hydraulic Fluid Power—Pumps, Motors and Integral Transmissions—Parameter Definitions and Letter Symbols*. Switzerland: ISO.

2 ISO 3662:1976 (1976). *Hydraulic Fluid Power—Pumps and Motors—Geometric Displacements*. Switzerland: ISO.

3 ISO 8426:2008 (2008). *Hydraulic Fluid Power—Positive Displacement Pumps and Motors—Determination of Derived Capacity*. Switzerland: ISO.

4 Ivantysyn, J. and Ivantysynova, M. (2003). *Hydrostatic Pumps and Motors: Principles, Design, Performance, Modelling, Analysis, Control and Testing*. Tech Books International.

5 Manring, N. (2003). *Fluid Power Pumps and Motors: Analysis, Design and Control*. McGraw Hill Professional.

6 Merritt, H.E. (1991). *Hydraulic Control Systems*. Wiley.

7 ISO 4409:2019 (2019). *Hydraulic Fluid Power—Positive-Displacement Pumps, Motors and Integral Transmissions—Methods of Testing and Presenting Basic Steady State Performance*. Switzerland: ISO.

8 Blackburn, J.F., Reethof, G., and Shearer, J.L. (1959). *Fluid Power Control*. The M.I.T. Press.

9 Dhar, S. and Vacca, A. (2013). A fluid structure interaction-EHD model of the lubricating gaps in external gear machines: formulation and validation. *Tribology International* 62: 78–90.

10 Vacca, A. and Guidetti, M. (2011). Modelling and experimental validation of external spur gear machines for fluid power applications. *Simulation Modelling Practice and Theory* 19: 2007–2031.

11 Robison, A. and Vacca, A. (2018). Multi-objective optimization of circular-toothed gerotors for kinematics and wear by genetic algorithm. *Mechanism and Machine Theory* 128: 150–168.

12 Manne, V., Pellegri, M., and Vacca, A. et al. (2019). Fluid dynamic simulation of hydraulic orbital motors. *The Sixteenth Scandinavian International Conference on Fluid Power*, Tampere, Finland (May 22–24, 2019).

13 Parker Hannifin Corp (2002). *Design Engineers Handbook Volume 1 – Hydraulics*. Parker Hannifin Corp.

14 Assofluid (2007). *Hydraulics in Industrial and Mobile Applications*. Milan, Italy: Assofluid.

15 ISO 3320:2013 (2013). *Fluid Power Systems and Components—Cylinder Bores and Piston Rod Diameters and Area Ratios—Metric Series*. Switzerland: ISO.

16 Stribeck, R. (1902). The key qualities of sliding and roller bearings. *Zeitschrift des Vereines Seutscher Ingenieure* 46 (38, 39): 1342–1348, 1432–1437.

17 Armstrong-Helouvry, B. (1991). *Control of Machines with Friction*. Norwell, MA: Kluwer Academic Publishers.

18 Nervegna, N. and Rundo, M. (2020). *Passi nell'oleodinamica* vol. 1–2, Epics.

19 Gomis-Bellmunt, O. and Campanile, L.F. (2010). *Design Rules for Actuators in Active Mechanical Systems*. London: Springer-Verlag.

20 Plummer, A. (2016). Electrohydraulic servovalves – past, present, and future. *Proceedings of 10th International Fluid Power Conference IFK2016*, Dresden, Germany (March 8, 2016).

21 Clack, D. C. (1969). Selection and performance criteria for electrohydraulic servodrives. *25th National Conference on Fluid Power* (October 15–16, 1969). Chicago, IL.

22 Neal, T. P. (1974). Performance estimation for electrohydraulic control systems. *National Conference on Fluid Power* (November 1974). Chicago, IL.

23 Moog (2018). Moog 72 Series Flow Control Servo Valves, Rev V (June 2018). https://www.moog.com/literature/ICD/Moog_ServoValves_72Series_Catalog_en.pdf.

24 Merritt, H.E. (1966). *Hydraulic Control Systems*. Wiley.

25 Watton, J. (2009). *Fundamentals of Fluid Power Control*. Cambridge Press.

26 Rahmfeld, R. and Ivantysynova, M. (2004). An overview about active oscillation damping of mobile machine structure. *International Journal of Fluid Power* 5 (2): 5–24.

27 Stecki, J.S. and Garbacik, A. (2002). *Design and Steady-State Analysis of Hydraulic Control Systems*. Cracow: Fluid Power Net Publications.

28 BS ISO 10770-1:2009 *Hydraulic Fluid Power. Electrically Modulated Hydraulic Control Valves*. Test Methods For Four-Port Directional Flow-Control Valves (British Standard)

Part III

Actuator Control Concepts

Every hydraulic control system transfers the power generated from a primary source (an internal combustion engine or an electric machine) to one or more actuators. The accurate control and distribution of this power is generally the most important and challenging design feature of the system. In fact, hydraulic technology offers multiple solutions to control the power transfer to the actuators; each solution presents some strengths and some drawbacks. Often, the designer, before selecting and sizing each component, is challenged in choosing the most suitable layout for the hydraulic circuit. This choice on the circuit architecture is not unique. Almost always, alternative concepts can be utilized to accomplish the same operational features. Part III introduces the general control concepts available to control a hydraulic actuator. In particular, Chapter 10 introduces the basic control concepts for an actuator depending on its loading conditions: speed vs. force control, resistive and overrunning loads, and steady state vs. dynamics. Chapter 11 provides an overview of the most important and common hydraulic system architectures. These are presented with simplified hydraulic schematics, for the case of single actuator. The actual schematics used in real applications are then explored in the following parts of this book. Chapter 12 is dedicated to regeneration, an actuator control concept specific to differential cylinders. Regeneration allows increasing the extension velocity of linear actuators without increasing the supply flow demand.

Objectives

The goal of Part III is to familiarize the reader with the basic concepts of controlling a hydraulic actuator, as well as the main layout architectures that can be utilized to implement a certain control strategy. With a careful reading of the chapters of this part, and by practicing with the presented concept through both the worked examples as well as the completion of the proposed end of chapter problems, the reader will be able to:

1. Define the concept of velocity, pressure, and position control for a hydraulic actuator.
2. Recognize the occurrence of resistive or overrunning loads.

3. Formalize the case of actuator dynamics.
4. Recognize the difference between a flow and a pressure type supply.
5. Define the different features of primary, metering, and secondary control as alternative methods for controlling hydraulic actuators.
6. Recognize the use of regeneration in hydraulic circuits.
7. Determine the required flow and the transmissible force limits of regenerative circuits.

Chapter 10

Basics of Actuator Control

This chapter defines the concept of "controlling an actuator." The term "control" can appear – at first – vague. Therefore, it is necessary to first provide a specific meaning for it, for the case of a hydraulic function. In addition, for a hydraulic system, it is important to distinguish the case of resistive loads from that of overrunning (or assistive) loads. The load condition usually affects the behavior of the hydraulic system, as well as the energy flow within it.

10.1 Control Methods: Speed, Force, and Position Control

As mentioned so far, a hydraulic system transfers power from a prime mover to one or more actuators. Therefore, controlling an actuator implies controlling the power delivered to it, according to a certain command. As the actuator power is a result of its speed and force (or torque, in case of rotary actuators), the control of the power is usually achieved by controlling either one of them. Hence, *speed* or *force* (torque) are the typical outputs of the control system. The type of control can be different depending on the application.

> Input signals to the hydraulic control system are usually generated by the operator (by means of a lever, a joystick, a potentiometer) or via an electronic control unit. These input signals are used to vary the configuration of the hydraulic system by adjusting the setting of the main *control element*.

This control element, for example, can be a hydraulic control valve, the setting mechanism of a variable displacement unit, or the speed of the prime mover.

Figure 10.1 summarizes the common variables involved in the motion of linear and rotary actuators.

> The actuator is *velocity controlled* when the hydraulic system sets the flow rate supplied to it.

The common steady-state relationships between the actuator (linear or rotary) velocity and the input flow Q are

$$\dot{x} = \frac{Q}{A}; \quad n = \frac{Q}{V_D} \tag{10.1}$$
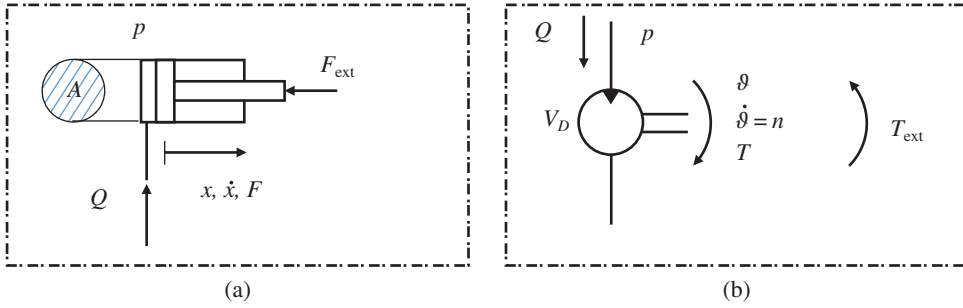
Figure 10.1 Control variables for a linear (a) and rotary (b) actuators.

In *force (or torque) controlled* actuators, the force (on a cylinder) or the torque (on a motor shaft) are controlled by modulating the supply pressure.

This is possible according to the basic equation:

$$F = pA; \qquad T = pV_D \tag{10.2}$$

It is important to remark that in most fluid power machines, the hydraulic system does not govern the value of the force or torque on the actuator, which is determined by external conditions. This concept is very intuitive in the case of an excavator: the load at the boom cylinders depends on the mass of dirt in the bucket, on the configuration of the arm, and on the direction of motion. Thus, actuators of this type of machines are usually speed controlled, and the force on the actuator, from a control standpoint, is a variable external to the hydraulic system.

However, there are certain applications where the load is predictable, and it is strictly correlated to one or more actuator variables (position or velocity) with a monotonic relation. Figure 10.2 shows two examples: a hydraulic press or a hydraulic fan drive. In the case of the press, the compressed material generates the load on the linear actuator. The load can be represented as a spring[1]: the more it is compressed, the higher the external force generated. In this case, the external force of the load can be a function of the actuator position. Figure 10.2 shows also the case of a hydraulic fan drive: here, the properties of the fan blades define a relationship (predominantly quadratic) between the torque demanded and the rotational speed. Therefore, applying the torque equation of the motor, the fan speed is uniquely dependent on the pressure supplied at the motor inlet. In the
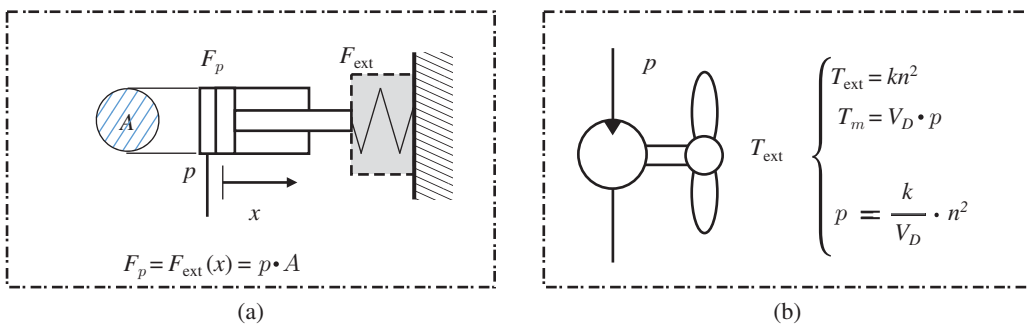
Figure 10.2 A cylinder compressing material (a), or a rotary actuator driving a fan (b) are examples of possible force and torque control.

---

1 Depending on the material being pressed, the spring law can also be nonlinear.

case of fans, once the speed–torque law is known, the control of the speed of the actuator can be achieved through the control of the torque, based on adjusting the supply pressure. More on this topic will be covered in Chapter 24.

> A hydraulic system achieving either velocity or pressure control can generally be used also to implement *position control*.

Usually, this is only possible through closed loop architecture, feeding back the actuator position to the controller. In this case, the control input signal, which determines the actuator velocity or force, is properly manipulated to obtain a desired actuator position.

10.2 Resistive and Overrunning Loads

Figure 10.3 shows a very simple example of a hydraulic system for controlling a single actuator. P is a fixed displacement pump driven by an electric motor running at constant speed. The directional control valve (DCV) is a 4/3 on/off solenoid actuated valve. The load is pushing on the bore side with a force F, generated, for example, by a mass lifted in the air.

In neutral position (0), DV diverts the pump flow Q_P back to tank, while ports A and B are blocked so the load and the actuator is locked in its position. If solenoid Y1 is energized, the valve shifts to position (1) (parallel arrows) and the pump flow is now diverted to port A, i.e. to the bore of C. The pump flow is in control of the actuator speed, equal to $\dot{x} = Q_P/A$, while the pressure at the pump outlet is $p = F/A$. In this condition, the actuator is extending against the load F; in other words, the vector representing the actuator velocity has the opposite direction with respect to the vector of the load. In this case the force F behaves as a *resistive load*.
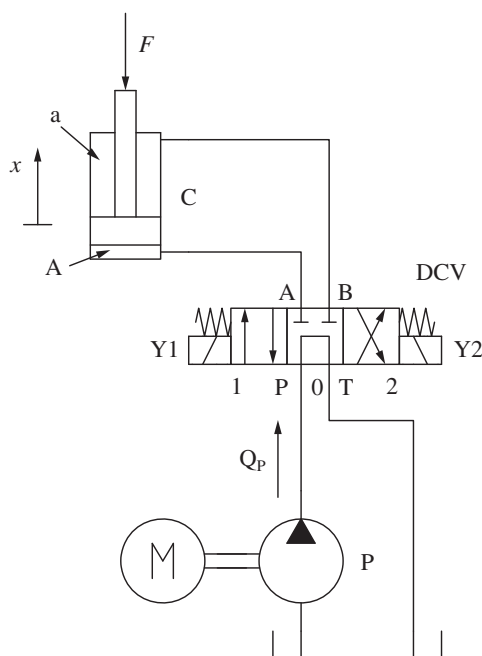
Figure 10.3 Simple example for understanding resistive and overrunning loads.

On the contrary, when the solenoid Y2 is energized, the valve DV shifts to position (2) (crossed arrows) and the pump flow is now diverted toward port B, connected to the rod chamber. At the same time, port A, i.e. the actuator bore chamber, is connected to tank. The actuator is retracting, and the load and speed vectors are concurrent: in this case F behaves as an *overrunning* (or *assistive*) *load*. Assuming the on/off valve DV does not present any significant restriction between B and T, the load is free to fall, driven by gravity. In other words, the system of Figure 10.3 does not provide any control of the actuator speed when it is retracting. Subsequent paragraphs of this chapter will cover extensively the problem of controlling overrunning loads.

> A load (force for cylinders, torque for motors) is *resistive* when it opposes the motion of the actuator. Instead, the load is *overrunning* when it aids the motion of the actuator.

Figure 10.4 summarizes all the four possible load configurations for a linear actuator, depending on the load direction and the actuator motion (extension or retraction).
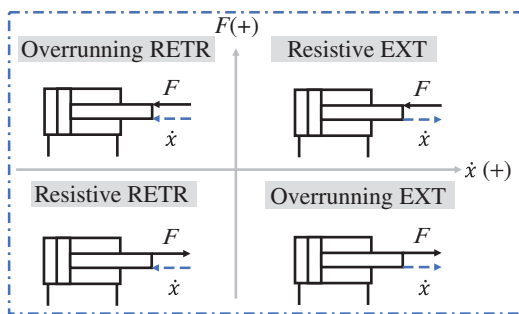
Figure 10.4 Resistive and assistive loads for linear actuators.

Similarly, rotary actuators can see four different configurations (summarized in Figure 10.5), depending on the direction of the torque and the actuator shaft rotation clockwise or counterclockwise (CW or CCW). Examples of overrunning loads for rotary actuators can be a winch lowering a load or the wheel motor of a vehicle traveling downhill.
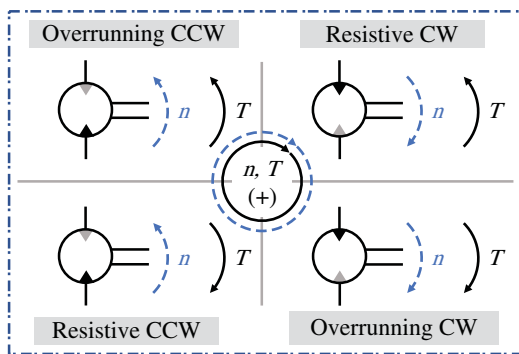
Figure 10.5 Resistive and assistive loads for motors.

10.2.1 Power Flow Depending on the Load Conditions

A very important feature differentiating the cases of resistive and overrunning loads is the opposite direction of the power flow. In fact, the mechanical power of the load (P_{load}) is expressed with the

scalar product of the actuator force (or torque) and its linear (or angular) velocity.

$$P_{\text{cyl}} = \vec{F} \cdot \dot{\vec{x}}; \qquad P_{\text{motor}} = \vec{T} \cdot \vec{\omega} \tag{10.3}$$

Therefore, the sign of P_{load} is opposite in the case of resistive or overrunning load. This mathematical difference has a very important physical meaning: in the case of resistive load, P_{load} is the power the hydraulic circuit transfers to the mechanical actuator.

> The power transferred by the hydraulic system to the load in case of resistive load conditions is the *useful power* as it represents the actual work of the machine or system.

On the contrary, in the case of an overrunning load, P_{load} represents the mechanical power transferred by the actuator into the hydraulic circuit. Therefore, in the overrunning load case, the hydraulic system must achieve the control of the function by consuming the overrunning load power. In principle, the hydraulic system can consume the overrunning power in two ways: either by dissipating it, as in most of today's circuits, or by recovering it. Energy dissipation occurs through fluid throttling, thus generating heat transfer to the fluid or the surrounding environment. Energy recovery is possible when the hydraulic system can store the energy within hydraulic accumulators or directly utilize such energy in other hydraulic actuators.

> The power transferred by the actuator to the hydraulic system in case of overrunning load conditions must either dissipated, reused, or stored to maintain control of the actuator.

Problems

10.1 Hydraulic cylinders are commonly used to control the flaps present in aircraft wings. These are highlighted in the picture. What kind of control is used for these actuators? With reference to the figure, determine the type of load (resistive or overrunning) during the extension and the retraction.

10.2 The figure below represents the three linear actuators of an excavator: boom, arm, and bucket. Each actuator can extend or retract. Analyze each actuator individually and identify which one can see resistive and overrunning loads depending on the direction of motion or on the configuration of the machine. *Hint*: First, assume the situation where the excavator arm is lifted in the air. Second, assume the case when it is in the ground digging a trench.
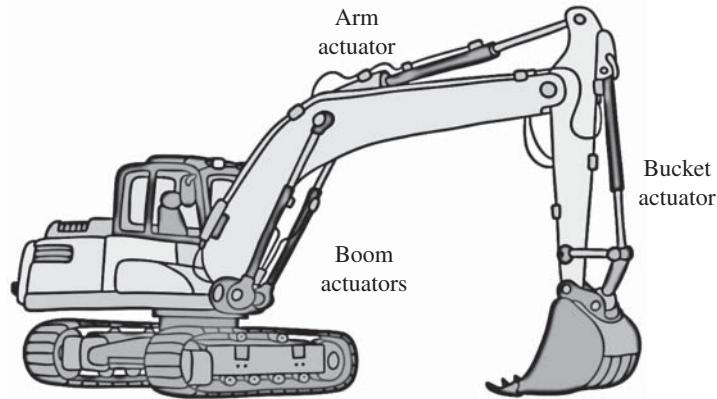
10.3 Determine the type of load for the boom actuator and the fork actuator in a telehandler (see figure). In normal operation, is the load resistive or overrunning during the extension and the retraction of these actuators?

Chapter 11

General Concepts for Controlling a Single Actuator

Hydraulic control systems offer multiple possible layouts and architectures to control hydraulic functions. Very often, these present substantial differences regarding the control features as well as hydraulic components utilized in the system. In the literature, it is possible to find different sources that report detailed descriptions for each one of these architectures. However, it is very difficult to find an organic classification of the options that can be available to the designer to implement a hydraulic control system. In this chapter, the authors made the effort of classifying the available architectures, according to well-defined criteria such as the type of hydraulic supply and the hydraulic control element used to accomplish the control function. With this classification, the available concepts are here presented using simplified schematics, which are very easy to understand, although they neglect many elements necessary for an actual implementation.

The purpose of the simple classification provided in this chapter is to make the reader aware of the possible options that hydraulic control technology offers for controlling actuators and understand the basic functional differences among them. After Part III, the chapters of the book are then dedicated to the actual implementation of the architectures more commonly used in the modern machines.

11.1 Supply and Control Concepts

After introducing the basic concepts of speed, position, and force control of an actuator, the focus of this and the next chapters shifts to the rest of the hydraulic system. There are, in fact, several different ways to implement the hydraulic control of an actuator. Even if the outcome looks the same, every architecture has some unique features and drawbacks that will be analyzed from here until the end of the book.

Hydraulic systems used to control a single actuator can be classified according to two criteria, as also outlined by Murrenhoff [1]. The first criterion is the *supply concept*, which pertains to the way the mechanical energy is converted to fluid energy by the supply system. The fundamental element of a supply system is always a pump. As mentioned in Chapter 2, a pump always generates flow; however, different layouts can be used to implement:

– a **flow supply**, a supply system imposing a defined flow rate
– a **pressure supply**, a supply system setting a defined pressure value

The second criterion is the ***control concept***. According to the location of the control element, the system architecture can implement

- a **primary control**, when the control element directly affects the output (pressure or flow) of the supply. For example, a primary control on a flow supply varies the output flow rate depending on the input command. Similarly, a primary control on a pressure supply varies the output pressure value.
- a **metering control**, when the control element is interposed between the supply system and the actuator. The control element is usually a hydraulic control valve that can adjust the metering area as a function of the input control signal (operator command). The architecture of this control valve varies depending on the application; in general terms, this valve can be represented as one or more variable orifices.
- a **secondary control**, when the control element directly affects the configuration of the actuator. The secondary control applies only to rotary actuators and it is usually achieved by varying the motor displacement.[1]

Figure 11.1 groups in a single figure all the abovementioned concepts. The same figure also visualizes the power flow within the system, from the prime mover to the actuator. It is important to remark how the primary or secondary control concepts are inherently more efficient as they do not involve throttling or flow losses through metering elements. In the case of ideal components without mechanical and volumetric losses, the mechanical input power $P_{mech, in}$ equals $P_{hyd, supply}$ in the case of regulation with primary control. Similarly, in the case of secondary control, the hydraulic power to the actuator, $P_{hyd, act}$, equals $P_{mech, out}$, the mechanical output power. However, for the case of metering control, the hydraulic power to the actuators, $P_{hyd, act}$, is generally lower than $P_{hyd, supply}$, the hydraulic power supplied to the system.

Each type of supply type (pressure or flow) can be matched to all control concept options (primary, secondary, or metering). All possible combinations are summarized in Figures 11.2 and 11.3. Figure 11.2 represents the different architectures based on flow supply and Figure 11.3 shows the options with a pressure supply. Both figures also display the enabling architectures for the supply
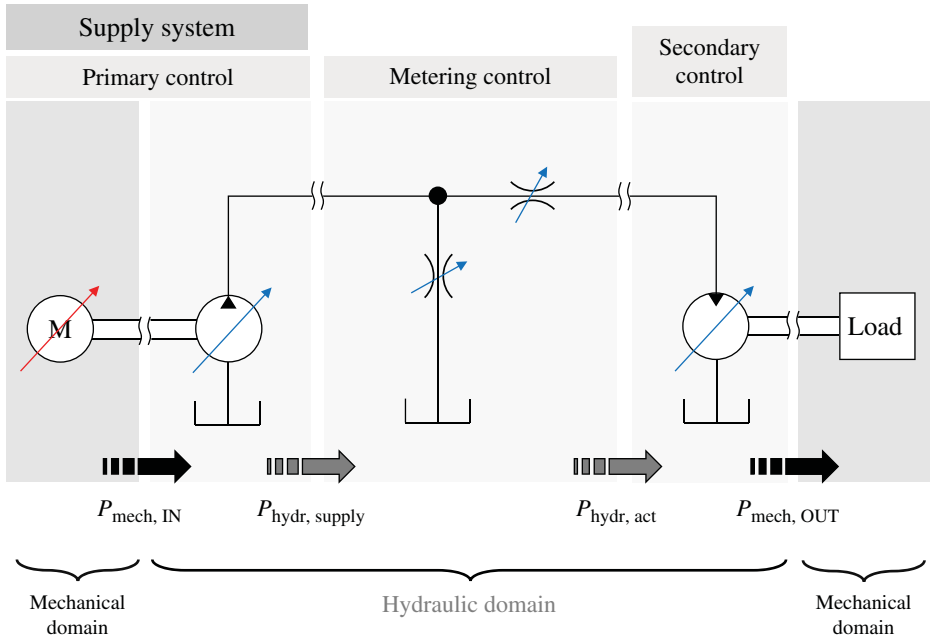
Figure 11.1 The basic control concepts involved in the control of a single actuator.

---

1 Common linear actuators do not allow a variation of the rod or bore areas.
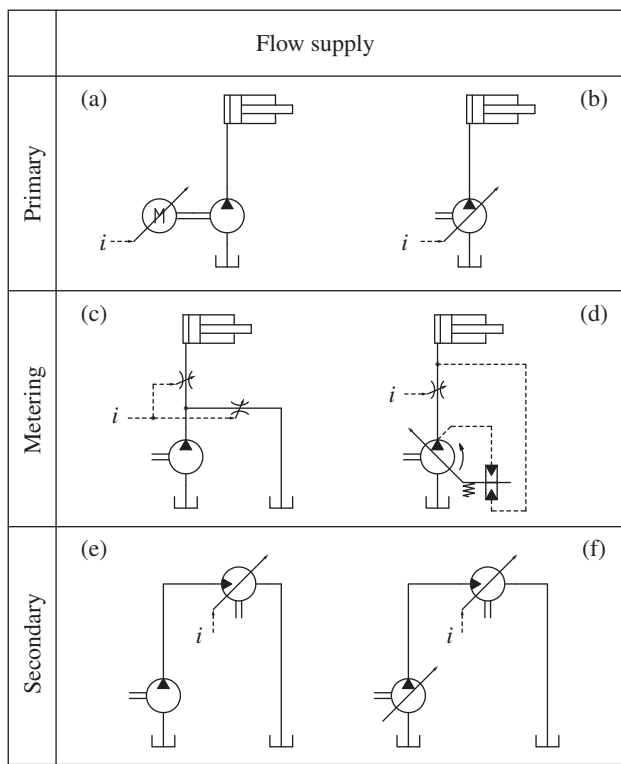
Figure 11.2 Control concepts in case of flow supply. Each architecture is represented for the cases of fixed (a, c, e) or variable (b, d, f) pumps.

system, which can use a fixed or a variable displacement pump. The two figures highlight the control element that receives the input signal *i* to accomplish the control action. The figure represents only one type of actuator for each illustration; however, rotary actuators could be used instead of linear actuators.

The next paragraphs give deeper insights on every possible configuration of the hydraulic control systems summarized in Figures 11.2 and 11.3. The hydraulic circuits shown in the next paragraphs are simplified schematics used to describe the basic principle behind every individual concept. In reality, sometimes hydraulic circuits can potentially implement more than one type of control concept, depending on the configuration of their elements and the operating conditions. This concept will be further clarified in later chapters.

11.2 Flow Supply – Primary Control

Figure 11.4 shows this architecture for the case of fixed and variable displacement pump. Both solutions are suitable for speed control of the actuator. The figure highlights the nature of the control command generated by the operator. In the case of a fixed displacement pump, the operator command adjusts the speed of the prime mover, thus regulating the flow to the actuator. The prime mover needs to be a variable speed electric motor. An internal combustion engine is not suitable for this control concept because of the limitations on its operating range (i.e. idle speed). Many applications, such as industrial injection molding machines or compact electrohydraulic actuators, utilize this solution.
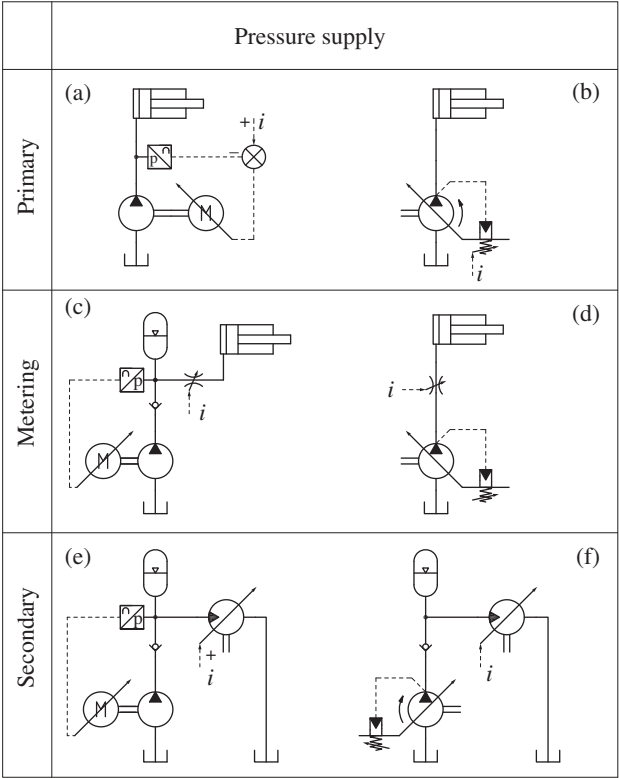
Figure 11.3 Control concepts in case of pressure supply. Each architecture is represented for the cases of fixed (a, c, e) or variable (b, d, f) pumps.

In the case of a variable displacement pump (also shown in Figure 11.4), a constant speed prime mover drives the unit and the operator command adjusts the pump displacement. This determines the amount of flow delivered to the actuator.

In the ideal case, both solutions of Figure 11.4 do not introduce power losses associated with the regulation.

> **Primary controls** do not have power losses associated with regulation. For this reason, they are considered among the most efficient control alternatives for controlling a single actuator.
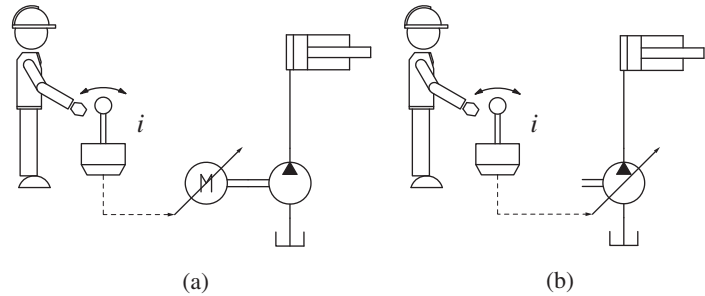
Figure 11.4 Primary control with fixed (a) or variable displacement flow (b) supply.

However, in the real case, the pump efficiency might cause significant power losses in primary controlled systems. As described in Chapter 6, variable displacement units typically suffer from low energy efficiencies at low instantaneous displacement; therefore, the primary control will have low energy efficiency when the flow demand is low. The situation is not much better when fixed displacement pumps are used in primary controlled systems. In fact, their limited range of the operating speeds (i.e. the minimum and maximum allowed speed) is often an issue because the system cannot provide flow below a defined minimum value and the pump efficiency at low shaft speeds is usually particularly low.

Primary controlled circuits are analyzed in detail in Part VI, where they are further divided in flow supply primary controlled systems and pressure supply primary controlled systems. In particular, primary controlled circuit with flow supply will be classified in hydrostatic transmissions (rotary actuators) and hydrostatic actuators (linear). Primary controlled circuits with pressure supply will be presented as secondary controlled hydrostatic transmissions.

11.3 Flow Supply – Metering Control

Figure 11.5 highlights two possible solutions for this architecture based on fixed displacement pumps. In both cases, the supply unit is rotating at constant speed and delivering a constant flow. Connected to the supply, the hydraulic circuit presents two parallel flow paths, one to the actuator and one to the tank. The control signal to the valve determines the portion of the inlet flow sent to the consumer and the portion discharged to the tank. In the first case, the control signal acts only on the restriction located in the path toward the tank, while the other is open to the actuator. This type of circuit is commonly referred as **bleed off**. In the second circuit instead, both paths present variable restrictions that are commanded by the operator. This type of circuit is commonly referred as **open center**. Both layouts are suitable for velocity or force controls, depending on the nature of the metering elements.

Figure 11.6 highlights two possible strategies for a flow supply-metering control solution using variable displacement pumps. In this case, the control signal from the operator acts on one or two variable orifices located between the pump and the actuator, to achieve a flow or a pressure control. In both cases, the pump displacement varies based on internal signals, which are mostly pressure information. In the schematic on the left, the two metering orifices have the same open-center layout as before. The pump setting is controlled by the pressure in the return side, generated by an
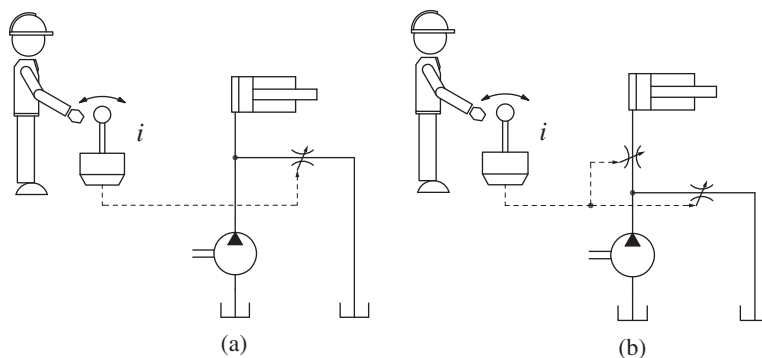
Figure 11.5 Metering controls with fixed displacement flow supply: the concept of bleed off system (a) and of open center system (b).
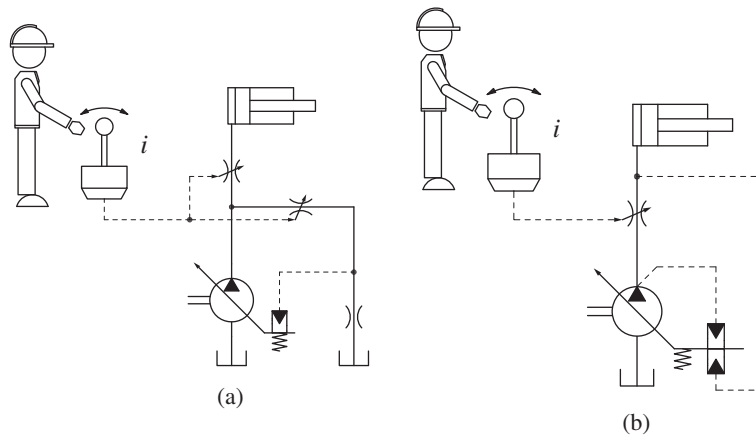
Figure 11.6 Metering controls with variable displacement flow supply. Advanced open center (a) and load sensing (b).

additional fixed orifice. This type of architecture is known as *negative flow control* and belongs to the category of **advanced open center** systems.

In the second architecture in Figure 11.6, there is only one metering element, which is controlled by the operator. The pump receives the pressure information downstream of the metering element and adjusts its displacement by comparing the load pressure with its own outlet pressure. This type of architecture is known as **load sensing** system.

Open center, **bleed off**, or **load sensing** are among the most common types of systems and will be thoroughly analyzed in Parts IV and V for the case of single and multiple actuators, respectively. They are easy to implement and tune and very favorable when multiple actuators need to be controlled from a single source. However, in terms of energy, the metering control always introduces throttling losses, which are usually more significant than the inefficiencies of pumps and actuators.

> **Open center**, **bleed off**, and **load sensing** systems are very common solutions to control hydraulic actuators based on the metering principle. To achieve the regulation, the circuit introduces power losses due to fluid throttling across the metering orifice.

One final remark needs to be addressed about the variable displacement solutions presented in Figure 11.6. In both cases, the pump adapts its displacement to match the flow requested by the operator through the metering control. However, the pump itself adjusts its displacement based on internal pressure signals. Therefore, this layout could also be interpreted as a "pressure supply" type. There is therefore a fine line between the two interpretations. The authors have preferred to classify these concepts as "flow supply" type, because the overall result of the pump displacement regulation is the matching of the flow commanded by the metering control element. The pump supplies flow "on-demand."

11.4 Flow Supply – Secondary Control

This architecture is suitable for speed control of rotary actuators, and it is also used in hydrostatic transmissions, as it will be seen in Part VI. As shown in Figure 11.7, in the case of fixed or variable pump, the speed of the actuator is controlled to adjust the motor displacement. If the flow supply is
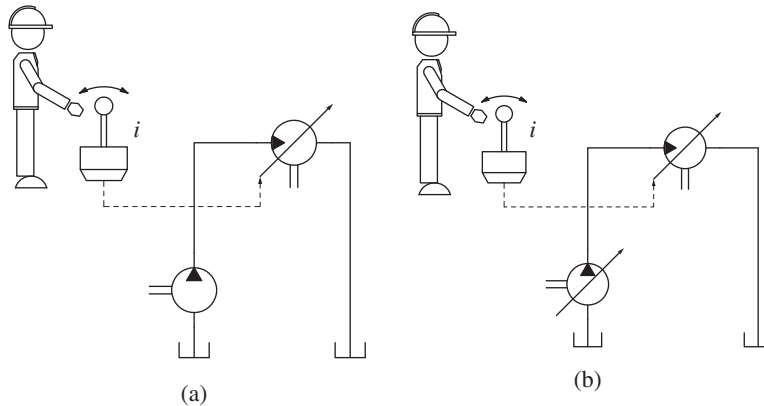
Figure 11.7 Secondary control with flow supply with fixed displacement pump (a) and variable displacement pump (b). This concept is applicable only to rotary actuators.

based on a fixed displacement pump, the velocity control range is limited by the allowable range of variation of the actuator displacement (usually the ratio of maximum and minimum displacement is 5 : 1 or lower). In the case of a variable displacement pump, the flow supply is actually adjusted by a primary control, in addition to the actuator secondary control regulation. In this case, the system can achieve a wider control range for the motor velocity, acting on both the pump and motor displacements.

Similarly, to the case of primary control, secondary control does not involve throttling losses and the only losses are caused by the inefficiencies of the components in the system.

11.5 Pressure Supply – Primary Control

This type of solution is suitable for force or torque control of the actuator. Figure 11.8a, shows a pressure supply with primary control, using a fixed displacement pump driven by a variable speed
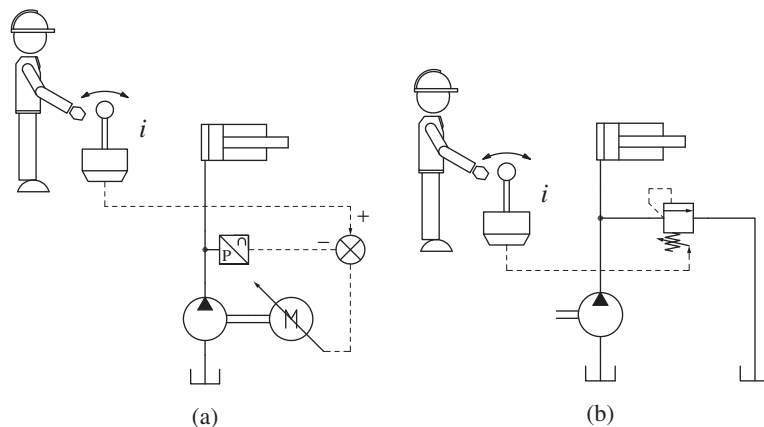
Figure 11.8 Primary control with pressure supply circuits using fixed displacement pumps. Solution based on shaft speed regulation (a) and with variable setting relief valve (b).

motor. A closed loop control external to the hydraulic system (simplified in the representation used in the figure) is necessary to implement this solution. The input signal is a pressure value (controller set point) requested by the operator. The feedback information comes from a pressure sensor located at the actuator inlet (i.e. pump delivery). The automatic controller adjusts the speed of the electric motor, which regulates the instantaneous pump output flow in order to match the pressure set point. This fixed pump-variable speed motor layout is theoretically possible; however, from a practical standpoint, it is not the most suitable solution to achieve force control of an actuator. In fact, the design of the controller presents significant challenges and the solution does not offer significant advantages with respect to simpler solutions (e.g. using variable pumps), in terms of cost or dynamic performance.

An alternative and more practical solution for implementing this control logic with a fixed displacement pump is shown in Figure 11.8b. The fixed displacement pump is combined with a relief valve, in this case. The relief valve can be considered as a part of the supply system, to implement the pressure supply concept. The supply pressure is adjusted by setting of the relief valve. This system is extremely simple, but when the flow consumption of the actuator is low and the pressure is high, the system efficiency is very poor because a large portion of the pump flow is diverted to the tank through the pressure relief valve, not contributing to useful work.

In the case of a variable pump (Figure 11.9), the unit rotates at constant speed and is equipped with a hydromechanical pressure limiter. This type of internal control adjusts the pump displacement to maintain a constant outlet pressure. The input signal coming from the operator acts on the setting of the pressure limiter. In many cases, the adjustment of the pump pressure limiter can be varied electronically, and it is referred as electrohydraulic pressure limiter. More details on this type of pump control will be given in Chapters 17 and 24.

In terms of energy consumption, the considerations made for the flow supply of primary control circuits also apply for the circuit in Figures 11.8 and 11.9.

> Primary controlled circuits based on pressure supply do not have power losses associated with the regulation. This is not valid if the circuit uses external elements (relief valves) to control the supply pressure.

This type of architectures will be further analyzed in Part VI, dedicated to hydrostatic transmissions. An example will be given on the case of fan drives using open circuit hydrostatic transmissions.
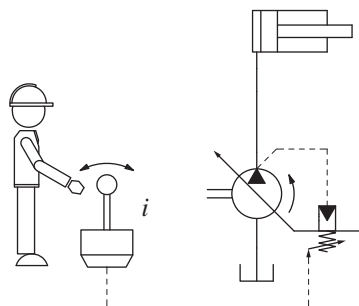
Figure 11.9 Pressure supply of primary control with a variable displacement pump.

11.6   Pressure Supply – Metering Control

This concept is suitable for both velocity and force control. The input signal acts on a metering element. In the case of force control, the metering element reduces the supply pressure to the pressure set point at the actuator. However, in the case of velocity control, the metering element is used to control the flow to the actuator.

The circuits for implementing this layout using fixed displacement pumps are represented in Figure 11.10: both circuits present an accumulator, which is common for this kind of applications. The left circuit utilizes a variable speed prime mover to control the pump outlet flow. The speed of this element is controlled based on the feedback of a pressure sensor located at the accumulator. A check valve is used to isolate the accumulator from the pump. The circuit in Figure 11.10b shows a more common application of this control strategy. The pump rotates at constant speed and an on/off valve is used to maintain the accumulator pressure within a certain range. When the accumulator pressure drops below a minimum threshold, the on/off valve is energized to provide flow to the accumulator. Consequently, the accumulator charges until it reaches the desired pressure. The pump, the on/off valve, and the accumulator are part of the supply system, which approximates the constant pressure operation.

The circuit using a variable displacement pump is represented in Figure 11.11. In this case, the circuit uses, as in Figure 11.9, a pump with a pressure limiter to maintain a constant pressure supply.

The circuits in Figure 11.10 and Figure 11.11 are often referred as ***constant pressure systems***. They are found in many marine and industrial systems and also used in many mobile applications. In terms of energy consumption, this architecture has the same features of the flow supply of a metering control: the presence of the metering element introduces inevitable energy losses.

Pressure supply of metering control circuits are commonly referred as **constant pressure systems**. Their control strategy inevitably introduces power losses due to the regulation concept based on metering orifices.

Constant pressure systems will be covered in chapters 17 and 19, for the case of single and multiple actuators, respectively.
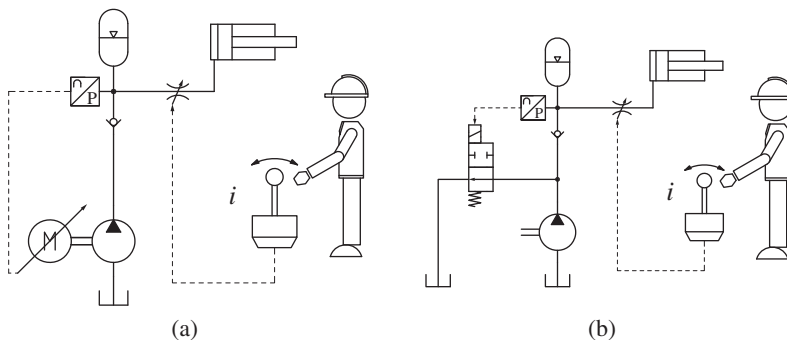
Figure 11.10   Pressure supply, metering controls using fixed displacement pump. (a) solution with variable speed prime mover. (b) solution with constant shaft speed.
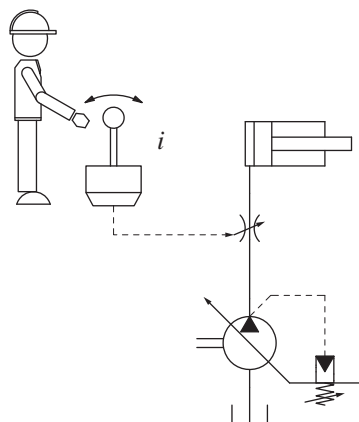
Figure 11.11 Pressure supply of metering control with a variable displacement pump.

11.7 Pressure Supply – Secondary Control

This architecture implements a significantly different control strategy of the actuator, with respect to the previous concepts. In fact, in primary and metering controls, as well as in secondary controls based on flow supply, the system imposes the flow to the actuator, while the load determines the actuator operating pressure. Vice versa, in secondary controls with pressure supply, the actuator supply pressure is constant, and its speed is adjusted by controlling the torque on the secondary element. The actuator speed is then a result of the balance between the torque generated by the load and the toque generated by the secondary hydraulic unit. This latter consists of a variable displacement unit with over-center capability, allowing the unit to reverse the direction of rotation by reversing the displacement and the handling of overrunning loads by reversing the unit's operation (motoring vs. pumping mode). The energy generated by the overrunning load is captured by the accumulators present in the system. The circuits respectively for the cases of fixed (a) and variable displacement (b) pumps are represented in Figure 11.12.

Pressure supply – secondary controlled circuits can be implemented only with variable displacement hydraulic motors, and they represent a very easy solution to perform energy recovery during overrunning load instances.
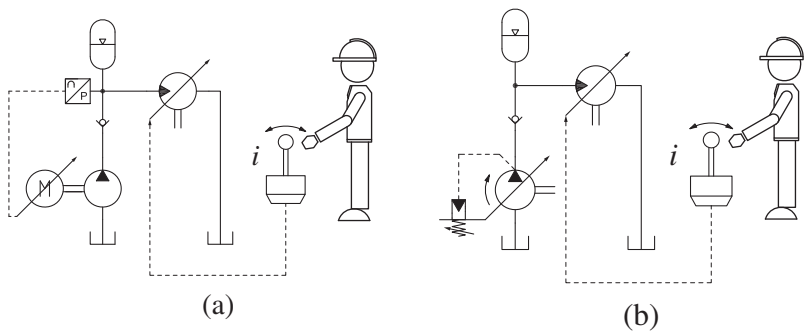
Figure 11.12 Pressure supply of secondary controlled circuits. The circuits represent the solutions using fixed (a) or variable (b) displacement pumps.

Secondary control systems can alternatively be classified as a particular case of hydrostatic transmission in open circuit configuration. Therefore, they are treated in Chapter 27, which is fully dedicated to the hydrostatic transmissions.

11.8   Additional Remarks

The conceptual circuits presented here highlight that power losses associated with the actuator control are present only in the systems based on metering controls. In principle, both primary and secondary controls do not introduce regulation losses. This consideration is true at least for ideal components, when the unit efficiencies (i.e. volumetric and hydromechanical efficiency) are not considered as part of the equations.

This important observation influences the analysis of the actual circuits that implement these control concepts. For metering circuits, it will be important to discuss the losses associated with the control regulation, with respect to the useful power at the actuator. The chapters in Parts IV and V, which are dedicated to metering control systems, will put emphasis on the analysis of this regulation losses.

On the other hand, when analyzing primary and secondary controlled systems, these regulation losses will not be present, but the effect of the actual component efficiency on the overall power transmission efficiency may become important. This will be highlighted in Part VI, dedicated to these systems.

In favor of the hydraulic control circuits based on metering control, it is important to remark that

Metering control systems are in general more economical than primary and secondary controlled systems. They also allow to easily control multiple actuators with a single supply.

Chapter 12

Regeneration with Single Rod Actuators

All the control concepts illustrated in the previous Chapter 11 implicitly assume that the velocity of the actuator controlled by the system is univocally defined by the flow supplied to the bore or rod chamber, e.g. by the primary or metering elements. This assumption is generally valid, but there is an exception that applies to differential cylinders, for which the *regenerative* control is a possibility. The regeneration is possible only during the piston extension, and it allows reaching higher velocities with respect to the normal control configuration. This chapter illustrates the main features of regenerative circuits.

12.1 Basic Concept of Regeneration

The concept of regeneration in the control of a linear actuator can be illustrated with the general schematic of Figure 12.1. Both schematics of the figure refer to the case of the extension of a differential cylinder, with area ratio $\varphi = A/a$. For the standard case (a), as already discussed in Chapter 3:

$$\dot{x}_{\text{std}} = \frac{Q_P}{A} \left(= \frac{Q_A}{A} = \frac{Q_a}{a} \right) \tag{12.1}$$

For the right schematic, which is representative of the regenerative configurations, the extension velocity can be found by first showing flow law at the junction node:

$$Q_A = Q_P + Q_a = Q_P + \frac{Q_A}{\varphi} \tag{12.2}$$

This last equation results from the fact that in regeneration, the flow exiting the rod chamber of the actuator merges with the supply flow entering the piston chamber. In other words, the return flow from the rod is re-used (from here the term regeneration) for the control function. The expression of the flow entering the cylinder bore is:

$$Q_A = \frac{\varphi}{\varphi - 1} \cdot Q_P \tag{12.3}$$

By dividing the last expression by the piston area A:

$$\dot{x}_{\text{reg}} = \frac{Q_A}{A} = \frac{\varphi}{\varphi - 1} \cdot \frac{Q_P}{A} \tag{12.4}$$
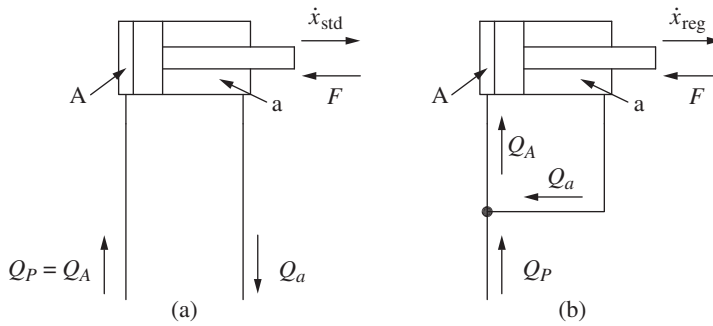
Figure 12.1 Basic illustration of the regeneration concept: (a) standard extension (no regeneration); (b) regenerative extension.

By comparing the last Eq. (12.4) with Eq. (12.1), it is possible to obtain a relation between the velocity in the two extension cases:

$$\frac{\dot{x}_{\text{reg}}}{\dot{x}_{\text{std}}} = \frac{\varphi}{\varphi - 1} \tag{12.5}$$

Being $(\varphi/(\varphi - 1)) > 1$ it is clear how the extension velocity is greater in the regeneration case, although for both cases there is the same supply flow. The amount of extension velocity increase depends on the area ratio φ. The higher is the ratio (large bore and small rod), the more is the velocity increment with respect to the standard actuation. Obviously, for a linear actuator the value of φ is limited by structural reasons (e.g. buckling).

By expressing the value of $(\varphi/\varphi - 1)$ as a function of the cylinder areas $((\varphi = A/a)$, Eq. (12.3) can also be written as follows:

$$\dot{x}_{\text{reg}} = \frac{\varphi}{\varphi - 1} \cdot \frac{Q_P}{A} = \frac{Q_P}{A - a} = \frac{4 \, Q_P}{\pi \cdot d_{\text{rod}}^2} \tag{12.6}$$

Equation (12.6) shows the physical meaning of regeneration: the extension speed of the cylinder is inversely proportional to the difference between the bore and rod effective area. This difference is equal to the rod cross sectional area (which is different than a, representing the annular area). In other words, it is like the pump flow is pushing only on the rod diameter area. For this reason, the incremented extension velocity comes at the cost of a reduced force capability of the actuator. In fact, for the standard actuation, the external load is related to the actuator pressures according to the following relation:

$$F_{\text{std}} = p_A A - p_a a = p_P A \tag{12.7}$$

Note that, for simplicity, frictional effects are neglected in the force balance of Equation (12.7). Also, it is assumed that the return pressure is null ($p_a = 0$), as in a "return to tank" condition.

For the case of regeneration, Figure 12.1b:

$$F_{\text{reg}} = p_A A - p_a a = p_P \cdot (A - a) = p_P \cdot \frac{\pi \cdot d_{\text{rod}}^2}{4} \tag{12.8}$$

Again, Eq. (12.8) shows how the area of influence of the pressure is also equal to the cylinder rod sectional area. The two above equations imply that, for the same supply pressure, the force exerted by the actuator is lower for the regenerative configuration. In particular:

$$\frac{F_{\text{reg}}}{F_{\text{std}}} = \frac{\varphi - 1}{\varphi} = \frac{A - a}{A} \tag{12.9}$$

Regeneration occurs only with resistive load conditions. As a matter of fact, from the above Eq. (12.8) it is clear that overrunning load conditions cannot be handled in a condition where both pressures at the piston and at the rod chamber of the actuator are equalized.

Summarizing,

Regeneration is a control concept that allows primary or metering controlled circuits to increase the extension velocity under resistive load conditions. In regenerative mode, the hydraulic control system can overcome lower resistive loads than in non-regenerative mode. This because during regeneration, the area of influence of the pressure in the cylinder is reduced.

Example 12.1 Supply pressure of a differential cylinder

Calculate the extension velocity and the supply pressure for a differential cylinder in two different configurations for the extension, as shown in figure below. The load is 20 *kN* (resistive). The supply flow rate is 20 *l/min* and return pressure is 5 *bar*. The piston diameter is 10 *cm*, and the rod diameter is 5 *cm*. Determine the maximum resistive force that the system can overcome, if the maximum supply pressure is 210 *bar*.

(a)

(b)
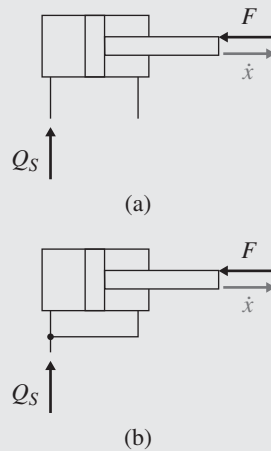
Given:
A differential cylinder, controlled in extension in two alternative configurations: (a) standard extension; (c) regenerative extension. Following data are given:

Force (resistive), $F = 20$ *kN*
Piston diameter, $D = 10$ *cm*
Rod diameter, $d = 5$ *cm*
Supply flow rate, $Q_S = 20$ *l/min*
Return pressure, $p_R = 5$ *bar*
Maximum supply pressure, $p^* = 210$ *bar*.

Find:
The extension velocity $\dot{x}$ and the supply pressure, p_S for the cases (a) and (b). Determine the maximum cylinder force, F_{max} for the two cases.

(Continued)

Example 12.1 (Continued)

Solution:

This problem is similar to the Example 7.1, but now the focus is in the additional regenerative control position. The problem requires the evaluation of both the piston area A and the annular area a:

$$A = \frac{\pi}{4}D^2 = \frac{\pi}{4}(0.1\ [m])^2 = 0.00785\ m^2$$

$$a = \frac{\pi}{4}(D^2 - d^2) = \frac{\pi}{4}(0.1^2 - 0.05^2)\ [m^2] = 0.00589\ m^2$$

a) Extension

For this case, the extension velocity is given by:

$$\dot{x} = \frac{Q_s}{A} = \frac{20\ [l/min]}{0.00785\ [m^2]}\frac{1}{60\,000} = 0.042\ m/s = 4.2\ cm/s$$

From the force balance of the piston $F = p_A A - p_a a$, considering that $p_a = p_R$ and $p_A = p_S$:

$$p_S = \frac{F + p_R a}{A} = \frac{20\,000\ [N] + 500\,000\ [Pa] \cdot 0.00589\ [m^2]}{0.00785\ [m^2]} = 2.697\ MPa = 26.7\ bar$$

The maximum load is given by the force balance, assuming $p_S = p^*$:

$$F_{\max} = p^* A - p_R a = 21\,000\,000\ [Pa] \cdot 0.007\,85\ [m^2] - 500\,000\ [Pa] \cdot 0.00589\ [m^2]$$
$$= 161\,905\ N = 161.9\ kN$$

b) Regenerative extension

The situation for the configuration (c) can be summarized by the figure below:
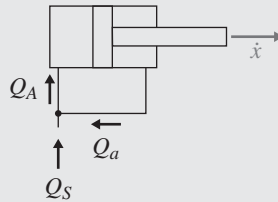
The extension velocity can be determined by solving the system of equations below:

$$\begin{cases} Q_A = Q_S + Q_a \\ Q_A = \dot{x}A \\ Q_A = \dot{x}a \end{cases}$$

which has three unknowns: $\dot{x}, Q_A, Q_a$.

The solution for the extension velocity is:

$$\dot{x} = \frac{Q_s}{A - a} = \frac{20\ [l/min]}{(0.00785 - 0.00589)\ [m^2]}\frac{1}{60\,000} = 0.17\ m/s = 17\ cm/s$$

The extension velocity is therefore higher than the basic extension of case (a).

The extension velocity gain, with respect to the basic extension case, goes with the price of a higher pressurization of the supply. In fact, now we have $p_A = p_a = p_S$. Therefore:

$$p_S = \frac{F}{A - a} = \frac{20\,000\ [N]}{(0.00785 - 0.00589)\ [m^2]} = 10.24\ MPa = 102.4\ bar$$

The maximum load in the regenerative configuration is given by:

$$F_{\max} = p^*(A - a) = 21\,000\,000\,[Pa] \cdot (0.007\,85 - 0.00589)\,[m^2] = 411\,160\,N = 41.2\,kN$$

which shows how the regenerative system has much lower load capability with respect to the standard actuation of case (a).

12.2 Actual Implementation

Regenerative circuits can be implemented in several variants. This section discusses some of the most popular implementations, as presented in [2–4].

12.2.1 Directional Control Valve with External Regeneration Valves

In this case the cylinder is controlled with a traditional 4/3 directional control valve (DCV) and two external valves are used to implement the regenerative extension (Figure 12.2). The first valve is a check valve (CV) and the second is a pilot-to-close check valve (PCV). When extension is commanded, CV prevents the flow exiting the rod from returning to the DCV. The flow is then forced to pass through PCV to the bore side, realizing the regenerative configuration. PCV is open because the pilot signal is vented to tank through DCV. Instead, in retraction mode, the flow from the pump crosses CV and enters the rod chamber without crossing through PCV. This latter is closed because the pilot signal is equal to the pump pressure.
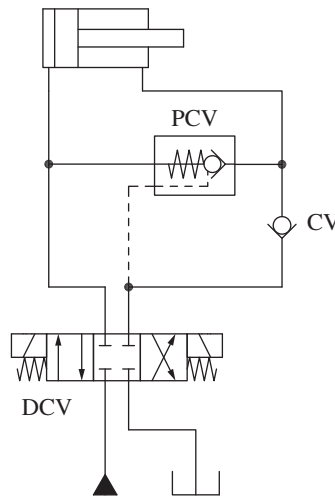
Figure 12.2 Regeneration achieved using a standard DCV and two external valves.

12.2.2 Directional Control Valve with Regenerative Extension Position

In this case, the connection between rod and bore chamber is implemented internally in the valve spool, through a proper regenerative position. Figure 12.3 shows two possible implementations. In Figure 12.3a, the 4/3 DCV implements the regenerative position every time the extension stroke is commanded. In the circuit of Figure 12.3a the valve DCV is represented as on/off but it could also
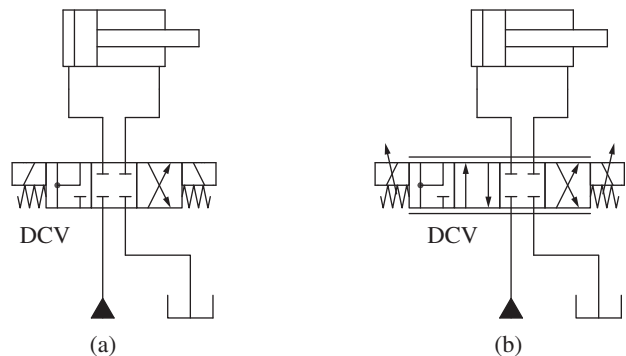
Figure 12.3 Example of spools with regenerative extension. Standard 4/3 DCV (a) or and 4/4 DCV with dual extend position (b).

be proportional. Figure 12.3b shows another the DCV is proportional. As the spool shifts towards the right, the extension is initially achieved in a traditional manner (parallel arrows). After a certain spool travel the configuration shifts and the extension is now achieved in regenerative mode. This layout is often referred to as directional valve with "regenerative fourth position".

The concept of regeneration can be implemented also in more complex architectures for the DCV. The next Part IV will discuss control metering architectures, such as Load Sensing systems and Open Center Systems. Both architectures allow implementing regenerative extensions. The Figure 12.4 shows an example of a 6/3 DCV used in Open Center Systems. More details on this control architectures will be provided in Chapter 15.
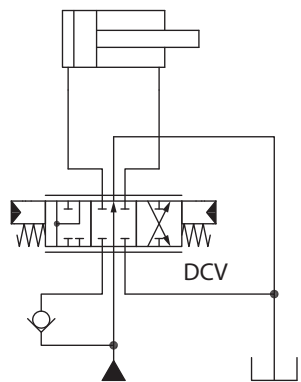
Figure 12.4 Example of open-center type spool with regenerative extension position.

12.2.3 Solution with Automated Selection of the Regeneration Mode

As discussed in the Section 12.1, the regenerative extension is characterized by a higher extension velocity and a lower force potential than the standard extension position. In certain cases, it can be convenient to implement circuits where the actuator has a fast motion under no load, and a slower motion under load. This could be for example the case of certain industrial machines which have work cycles made of a fast positioning and slow work phase. In these cases, it is convenient to implement a circuit able to automatically switch between regenerative extension and standard extension. An example of such circuit is given in Figure 12.5.

The circuit of Figure 12.5 has two check valves (CV1 and CV2) and a remote pressure control valve SQ: this work as a piloted sequence valve and it is represented in the schematic as a 2/2
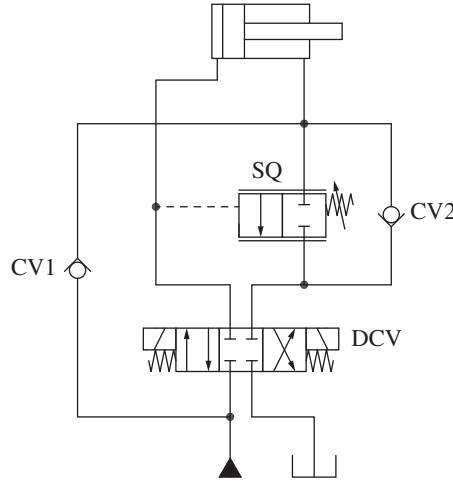
Figure 12.5 Circuit with automatic selection of the regenerative extension depending on the load.

infinite position spool. This valve has a pressure setting of p_{SQ}^* and the pilot signal is connected to the cylinder bore side. The regenerative extension is activated based on the external force level. In particular:

- *Fast extension (low loads).* In this condition, the pump pressure is lower than the setting of the sequence valve, $p_P < p_{SQ}^*$. Therefore, the sequence valve SQ is closed. The fluid returning from the rod chamber cannot return to the DCV and it is forced back to the piston chamber of the actuator, through the CV1. In this case, the circuit allows regeneration. The system operates in this configuration for forces such that:

$$F < F^* = p_{SQ}^* \cdot (A - a) \tag{12.10}$$

In this region, the pressures inside the cylinder are equal ($p_A = p_a$) as shown in the plots of Figure 12.6a.

- *Slow extension (intermediate loads).* If the load is higher than F^*, the valve SQ is regulating, implementing a variable orifice between the rod chamber and the return of the DCV. The value of the pressure at the piston chamber p_A remains at p_{SQ}^*, to keep the valve SQ open, while the value of p_a is lower than p_{SQ}^*, to balance a force higher than F^*. Therefore, the CV valve is closed and the
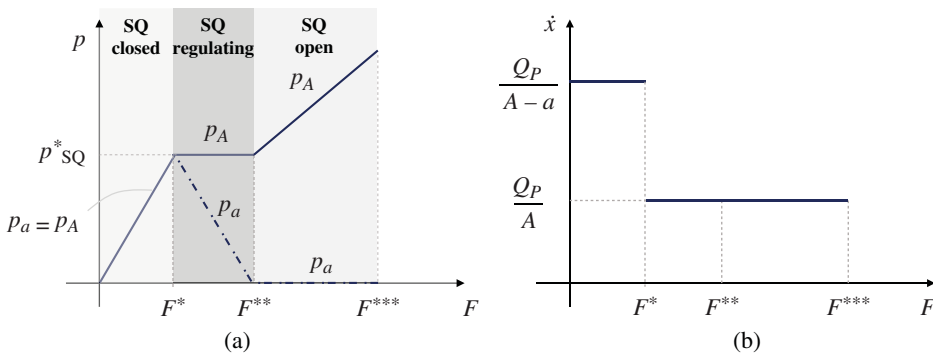
Figure 12.6 Characteristics of the automated regenerative circuit of Figure 12.5: (a) pressure vs external load; (b) extension velocity vs external load.
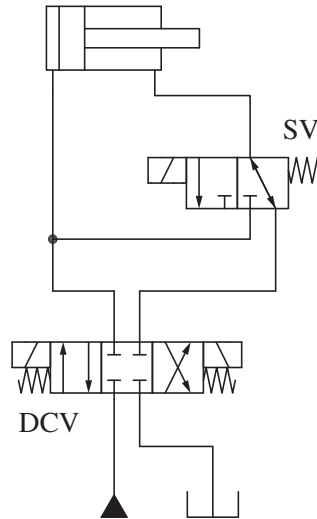
Figure 12.7 "On demand" regeneration circuits solenoid actuated.

actuator velocity is determined by the standard configuration. This behavior is represented by the central region of the characteristics of Figure 12.6a.

The SQ is regulating until the rod pressure reaches the null value ($p_a = 0$). This means a value of force in the interval:

$$p_{SQ}^* \cdot (A - a) = F^* < F < F^{**} = p_{SQ}^* \cdot A \qquad (12.11)$$

- *Slow extension (high loads).* If the load exceeds F^{**}, it means that SQ is fully open and p_a is ideally equal to tank pressure. The increasing force on the cylinder is counteracted by the pressure p_A ($=p_P$) acting on the full bore area. This behavior is represented with the right region of the plots of Figure 12.6b. Figure 12.6b provides a summary of the actual cylinder extension speed for the different values of external force: the regenerative speed is attained only for values of $F < F^*$.

The circuit described in the previous paragraphs is sometimes referred as *low-pressure regeneration*. Sometimes, the valve SQ can be replaced with an orifice; this layout is often referred as *semi-regenerative circuit* and can be found in some machine functions such as the dipper arm of excavators.

In other instances, the regenerative configuration can be an option activated by an external command. An example of a possible configuration implementing such functionality is shown in the Figure 12.7. In this circuit, the 2/3 solenoid valve (SV) can select the path of the return flow from the rod, thus realizing regeneration.

Problems

12.1 For the system in figure, determine the pressure in psi at the pump outlet for the position 1, 2, 3 of the directional control valve. Assume:

$D = 4$ in. (piston diameter)

$d = 2$ in. (rod diameter);

$F = 5000$ lbf. (load, assume always resistant, opposite to piston velocity)

$Q = 10$ gal/min

Set pressure of the relief valve = 500 psi
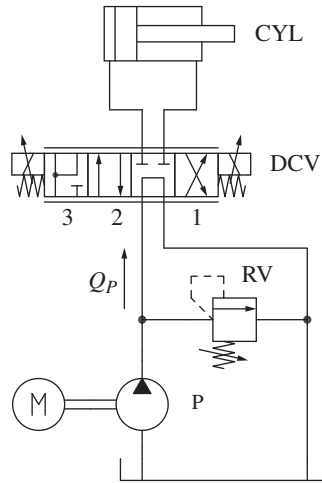
12.2 Consider the circuit of Figure 12.5, with a vertical cylinder lifting or lowering a vertical load. With the following data:

Parameter	Symbol	Value	Unit
Piston diameter	D	0.05	m
Rod diameter	d	0.028	m
Sequence valve setting pressure	p_{SQ}^*	200	bar

Plot the trends for the cylinder pressures and of the piston extension velocity with respect to the external load, F.

If the mass is equal to 1000 kg, does the extension occur in regenerative condition?

References

1 Murrenhoff, H., Sgro, S., and Vukovic, M. (2014). An overview of energy saving architectures for mobile applications. *9th International Fluid Power Conference (IFK)*, Aachen, Germany (March 24–26).

2 Nervegna, N. and Rundo, M. (2020). *Passi nell'oleodinamica* vol. 1–2, Epics.

3 Assofluid (2007). Hydraulics in Industrial and Mobile Applications.

4 Zarotti, G.L. (1997). *Circuiti Oleodinamici, Nozioni e Lineamenti Introduttivi*. Italy: Quaderni Tematici, Cemoter.

Part IV

Metering Controls for a Single Actuator

Part III introduced the different hydraulic system concepts that can be implemented for controlling an actuator. Among these, the metering control is one of the most common concepts adopted in modern hydraulic machines, and thus deserves a particular attention. Starting from the basic idea of using orifices to achieve regulation, many different metering control architectures can be derived. Part IV thus focuses on the most popular metering control methods, applied for the case of a single actuator. The extension to the case of multiple actuators will be done in Part V.

The first chapter of this part (Chapter 13) presents the fundamental concepts of metering control, an covers the differences between meter-in and meter-out architectures. Followed by that, the control of overrunning loads is further explored in Chapter 14, which covers the topic of counterbalance valves. Chapter 15 goes over the first two important metering control concepts: Bleed-Off and Open Center circuits. Subsequently, in Chapter 16 the load sensing (LS) systems are introduced, again for the case of a single actuator. This Chapter 15 also illustrates the implementations with both fixed displacement pumps and variable displacement pumps. The following Chapter 17 covers the so-called constant pressure circuits, which can again be implemented with both variable pump or fixed displacement pumps, using accumulators.

Objectives

This part builds the fundamentals for metering control systems. With focus to a single actuator (the extension to multiple actuators will be done in the next part), the chapters of this part will make the reader familiar with the basics metering concept as well as the more advanced metering concept used in today's hydraulic control systems. The reader, after carefully reading the chapters of the Part IV, and by practicing with the proposed worked examples and the end of chapter problems, will be able to:

1) Analyze and design basic metering control configurations, which include elementary meter-in, meter-out and mixed metering control strategies.
2) Describe the function of anti-cavitation valves in hydraulic control circuits based on metering concepts.
3) Design basic metering control circuits, determining the main control valve features.
4) Identify the need of using methods for controlling overrunning loads, such as counterbalance valves.
5) Describe the operation of counterbalance valves.

6) Analyze and design basic open-center and bleed-off systems.
7) Describe the architecture of an open center spool valve.
8) Describe the operation of advanced open-center architectures: positive and negative flow control.
9) Analyze and design basic LS systems based on either fixed or variable displacement pumps.
10) Describe the operation of a LS pump controller.
11) Recognize the architecture of a basic LS spool valve.
12) Analyze and design constant pressure systems.
13) Identify the theoretical energy efficiency and the source of energy loss for the different metering circuits: open center systems, LS systems, constant pressure systems.

Chapter 13

Fundamentals of Metering Control

Architectures based on metering control represent the most common solutions utilized in hydraulic machines, particularly in mobile applications. Metering control implies using a hydraulic control valve between the supply system and the actuator. This valve is implemented in such a way that its command affects the opening of a metering orifice, thus regulating the actuator flow. This chapter introduces some general concepts on metering control and describes the features of the system as a function of the location of the metering element with respect to the actuator. Emphasis is given to the cases of resistive and overrunning loads, which can be handled with different types of metering solutions. The chapter also discusses the energy consumption of each basic metering control concept presented.

13.1 Basic Meter-in and Meter-out Control Principles

Metering controls can be attained by implementing either *meter-in* or *meter-out* strategies, depending on the location of the control element with respect to the actuator (Figure 13.1).

> In the case of **meter-in** control, the hydraulic control element is located at the inlet of the actuator with respect to the direction of the flow. **Meter-out** control is achieved when the orifice is located at the outlet port of the actuator.

Meter-in and the meter-out strategies have different capabilities of controlling resistive or overrunning loads. This section describes the principles of the meter-in and meter-out concepts by considering basic circuits used to control the velocity of an actuator. In these examples, the meter-in and the meter-out elements are simply represented by variable orifices. In real applications, metering elements are usually implemented with more complex valve architectures, the details of which will be described in the later chapters of Part IV.

In order to show the differences from the energy consumption standpoint, two types of supply circuits are referenced, i.e. with a fixed displacement pump and with a variable displacement pump. The actuator type chosen to present the basic meter-in and meter-out concepts is a linear actuator with a single rod. This has an area ratio, $\varphi = A/a$, between bore and rod side which is greater than 1. The concepts that are presented can easily be extended to the case of rotary actuators or linear actuators with double rod. In these cases, where present in the formulas, the coefficient φ should be unitary.
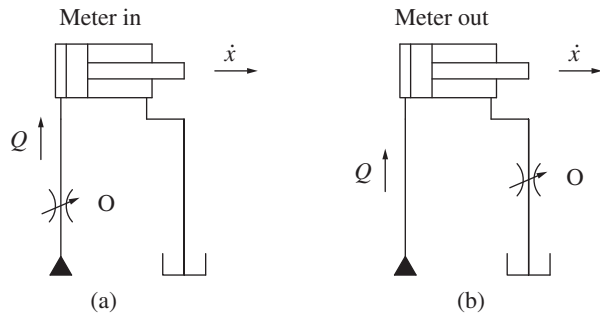
Figure 13.1 General layout for the meter-in (a) and the meter-out (b) control circuits.

13.1.1 Meter-in Control

Figure 13.2 shows two simple circuits for explaining the meter-in control concept. Figure 13.2a represents a layout based on a fixed displacement pump and a relief valve, while Figure 13.2b shows the case of a variable displacement pump with constant pressure regulator. In both cases, the pressure setting of the system is indicated as p^*. The meter-in element is the variable orifice O, while the directional valve (DV) is an on/off valve that determines the extension or retraction of the actuator. The load F, as represented in Figure 13.2, acts against the bore side of the actuator; therefore, it is resistive when the actuator extends and overrunning when it retracts. The pump flow is fixed, $Q_P = Q_{P,\max}$ for the case of Figure 13.2a (fixed displacement pump), while it varies between 0 and $Q_{P,\max}$ for the case of Figure 13.2b (variable displacement pump).
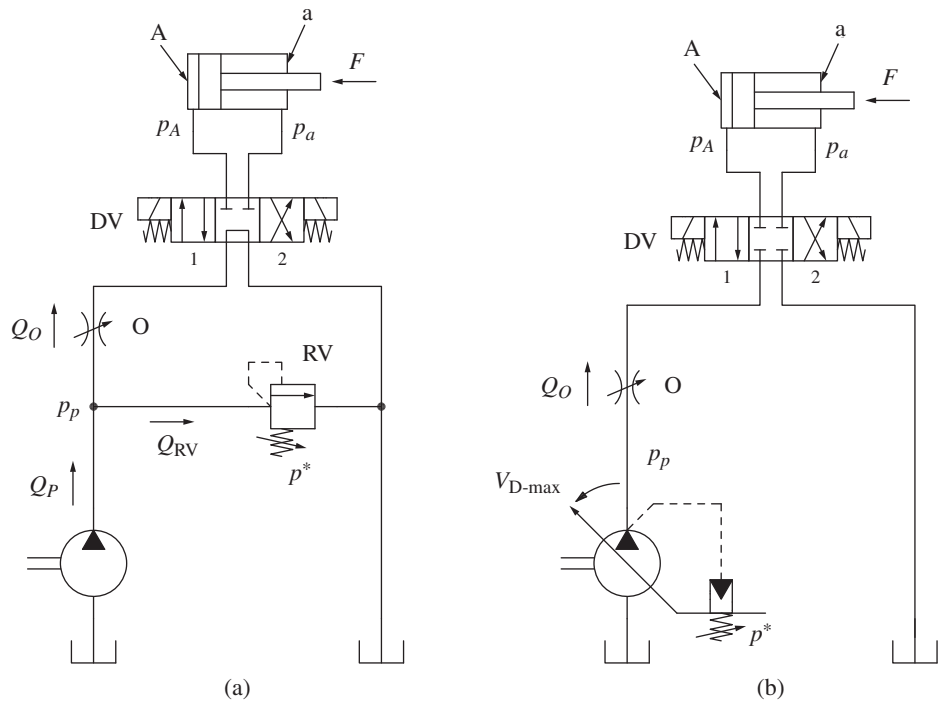
Figure 13.2 Meter-in control concept using a fixed (a) and a variable (b) displacement pump.

Extension with Resistive Loads (DV in Position 1)

When the valve DV shifts to position 1, the cylinder extends, and the load is resistive. Assuming a motion of the piston with constant velocity and no frictional losses in the cylinder and in the hydraulic components, the pressures at the cylinder chambers are:

$$p_a = 0 \,\text{bar} \;\; ; \;\; p_A = \frac{F}{A} \tag{13.1}$$

All pressures are considered as gage pressure (the tank pressure, p_T is 0 bar).

If Δp_O indicates the pressure drop across the orifice, the pressure at pump outlet is

$$p_p = p_A + \Delta p_O \tag{13.2}$$

The orifice equation correlates the pressure drop across the control orifice with the flow rate through it (the orifice area is indicated as usual with Ω):

$$\Delta p_O = \frac{\rho Q_O{}^2}{2C_f{}^2 \Omega^2} \tag{13.3}$$

Therefore, combining Eqs. (13.3 and 13.4) the pump pressure becomes:

$$p_p = \frac{F}{A} + \frac{\rho Q_O{}^2}{2C_f{}^2 \Omega^2} \tag{13.4}$$

For a given load condition, pump speed and displacement, the orifice area Ω becomes the only independent variable describing the system state. Therefore, the operation of the system in Figure 13.2 with DV in position 1 can be covered by analyzing all possible values for the orifice area Ω. The analysis can be made first considering the orifice fully open ($\Omega = \Omega_{max}$) and then gradually closing it, up to the minimum value ($\Omega = 0$). Intuitively, when the orifice is fully open all the pump flow goes to the actuator. As the orifice area decreases, the pressure at the pump increases until the relief valve starts opening, for the fixed pump case (or the pressure limiter starts reducing the pump flow, for the variable case).

Naturally, the reader can understand that a critical situation in Eq. (13.4) is reached when, simultaneously, $p_p = p^*$ and $Q_O = Q_{P,\max}$. In this condition the pump reaches the max pressure, but full flow is still going to the actuator. This condition is identified by a specific orifice area Ω^*_{IN}, calculated considering

$$p^* = \frac{F}{A} + \frac{\rho Q_{P,\max}{}^2}{2C_f{}^2 \Omega^*_{\mathrm{IN}}} \tag{13.5}$$

so that:

$$\Omega^*_{\mathrm{IN}} = \frac{Q_{P,\max}}{C_f} \frac{1}{\sqrt{\dfrac{2}{\rho}\left(p^* - \dfrac{F}{A}\right)}} \tag{13.6}$$

according to the value of Ω with respect to Ω^*_{IN}, two different behaviors can be defined for both systems in Figure 13.2:

- *No regulation ($\Omega^*_{IN} < \Omega < \Omega_{max}$).* For large openings of the orifice, the pump outlet pressure p_P does not reach the pressure setting p^*. This is because the pressure drop across the orifice, Δp_O, is lower than ($p^* - F/A$). Therefore, all pump flow is diverted to the actuator. In the case of the system with fixed displacement pump (Figure 13.2a), this happens because the relief valve is closed. For the case of variable displacement pump (Figure 13.2b), the pump regulator keeps it at full displacement, since the pressure signal sent to the regulator is below its setting. For both

cases in Figure 13.2, $Q_O = Q_{P,\text{max}}$. Therefore, the actuator velocity is simply determined by the pump flow, and not by the variable orifice. The actuator velocity is at its maximum value:

$$\dot{x}_{\text{max}} = Q_{P,\text{max}}/A \qquad (13.7)$$

The orifice O works as a compensator: it creates a pressure drop, Δp_O, without affecting the actuator speed. This is why this condition is identified as "no regulation." The value of Δp_O changes with the flow area Ω according to Eq. (13.3).

> In the basic meter-in architecture, for large orifice openings ($\Omega > \Omega_{\text{IN}}^*$), the meter-in orifice does not affect the actuator velocity, which is just a function of the pump flow. In such case, the meter-in orifice behaves as a compensator.

- *Meter-in regulation ($\Omega \leq \Omega_{IN}^*$).* As the orifice area is restricted below Ω_{IN}^*, the relief valve opens and diverts some flow to the tank ($Q_{\text{RV}} > 0$), for the system in Figure 13.2a. Instead, for the system in Figure 13.2b, the pump reduces its displacement since the regulator acts to maintain the setting p^* at the pump outlet.

  In both cases, the pump pressure p_P is kept at the setting p^* and the flow through the orifice Q_O is lower than $Q_{P,\text{max}}$. As a consequence, the actuator velocity is lower than $\dot{x}_{\text{max}}$ of Eq. (13.6). The orifice O accomplishes the regulation based on its opening area, and it works as a metering element. In fact, the value of Δp_O is constant:

$$\Delta p_O = p^* - \frac{F}{A} \qquad (13.8)$$

In this second situation, the system changes configuration of the supply and control type. In fact, here the supply becomes a constant pressure type with metering control achieved on the meter-in side.

> In the basic meter-in architecture, regulation is achieved for orifice openings smaller than the critical value ($\Omega < \Omega_{\text{IN}}^*$). In this condition, the meter-in orifice behaves as metering element and it is controlling the actuator speed.

Figure 13.3 shows the actuator speed and pump pressure as a function of the orifice area Ω. This plot summarizes the considerations on the meter-in control of resistive loads: if the orifice area is smaller than Ω_{IN}^*, the actuator speed increases linearly with Ω while the pump pressure stays constantly at p^*. If the area is larger than Ω_{IN}^*, the velocity stays constant and the pressure drop decreases with a quadratic relationship to the area. Figure 13.3 shows how, with this solution, it is possible to achieve a full range of velocities from 0 to $\dot{x}_{\text{max}} = Q_{P,\text{max}}/A$. The reader should notice that the value of Ω_{IN}^* depends on the load F and the actuator size (i.e. area A).

Figure 13.4 shows the power consumed by the meter-in circuits in Figure 13.2 as a function of the orifice area. In the case of the fixed displacement pump (Figure 13.2a), when the orifice is in regulation, the pump pressure equals p^*, and the power contributions are:

$$
\begin{aligned}
P_{\text{load}} &= F \cdot \dot{x} = F \cdot \frac{Q_o}{A} \ \ \text{mechanical power at load} \\
P_o &= \left(p^* - \frac{F}{A}\right) \cdot Q_o \ \ \text{power loss at the orifice} \\
P_{\text{RV}} &= p^* \cdot (Q_{p,\text{max}} - Q_o) \ \ \text{power loss at the relief valve} \\
P_p &= p^* \cdot Q_{p,\text{max}} = P_{\text{load}} + P_o + P_{\text{RV}} \ \ \text{overall power consumed}
\end{aligned}
\qquad (13.9)
$$
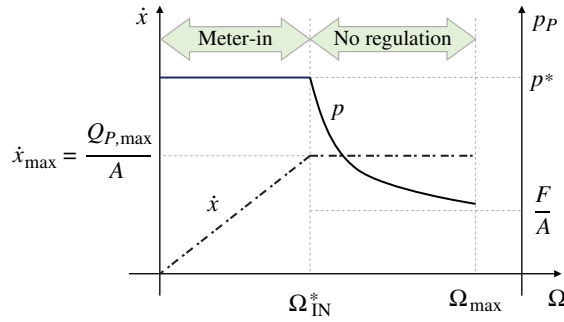
Figure 13.3 Control modes for the actuator in the circuits shown in Figure 13.2 (resistive load).

On the other hand, for the variable displacement pump circuit in Figure 13.2b, the power contributions during regulation are:

$$P_{\text{load}} = F \cdot \dot{x} = F \cdot \frac{Q_o}{A} \text{ mechanical power at load}$$

$$P_o = \left(p^* - \frac{F}{A} \right) \cdot Q_o \text{ power loss at the orifice}$$

$$P_p = p^* \cdot Q_o = P_{\text{load}} + P_o \text{ overall power consumed}$$

(13.10)

(a)

(b)
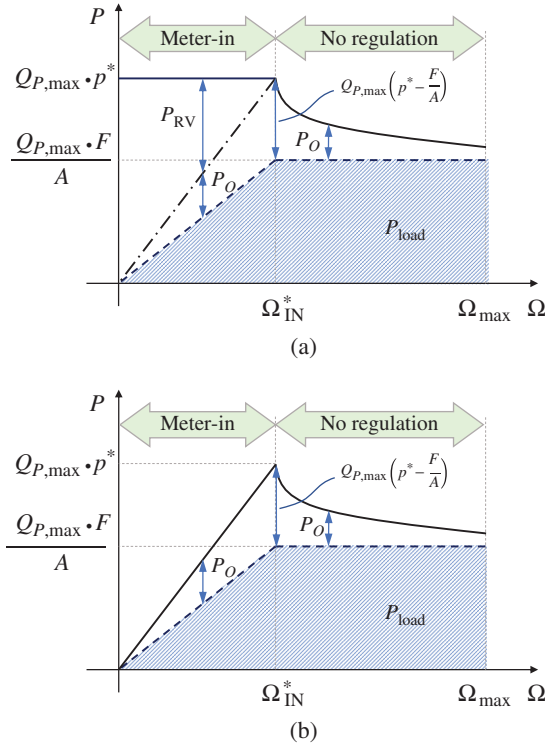
Figure 13.4 Power consumption analysis for the circuits of Figure 13.2 : (a) with a fixed displacement pump, (b) with a variable displacement pump.

When both systems are in no regulation, the situation is the same for types of power supplies:

$$P_{\text{load}} = F \cdot \dot{x} = F \cdot \frac{Q_{P,\max}}{A} \text{ mechanical power at load}$$

$$P_o = \Delta p_o \cdot Q_{P,\max} \frac{\rho Q_{P,\max}{}^3}{2C_f{}^2\Omega^2} \quad \text{power loss at the orifice} \tag{13.11}$$

$$P_p = \left(\frac{F}{A} + \Delta p_o\right) \cdot Q_{p,\max} = P_{\text{load}} + P_o \quad \text{overall power consumed}$$

Retraction with Overrunning Loads (DV in Position 2)

In the circuits in Figure 13.2, when the DV shifts to position 2 (crossed arrows), the cylinder retracts and the load becomes overrunning. The external force and the actuator velocity both have the same direction. In this case, the simplified force balance at the cylinder becomes:

$$p_A A - p_a a - F = 0 \tag{13.12}$$

Considering that the piston chamber is connected to the tank, the solution would be:

$$p_a = -\frac{F}{a}; \quad p_A = 0 \, \text{bar} \tag{13.13}$$

This solution is impracticable since it implies a negative value of the pressure p_a.[1] Therefore, one can briefly conclude that meter-in technique does not permit the control of the actuator when the load is overrunning. This situation is equivalent to the case in Figure 10.3 when the valve DV shifts to position 2 and the actuator retracts. The absence of restrictions on the return side of the circuit causes the load to free fall without control of its speed.

> The basic **meter-in** control architecture does not allow controlling overrunning loads. To control overrunning loads using a meter-in layout, additional elements must be introduced in the system.

13.1.2 Meter-out Control

Figure 13.5 illustrates two basic circuits implementing a meter-out control, again for the two cases, i.e. using a fixed displacement pump and a variable displacement pump. The hydraulic circuits are similar to the meter-in case with the difference that the orifice O is placed after the return port of the valve DV. In addition, a check valve (CV) prevents the pump outlet pressure to fall below the tank pressure. The functionality of CV is explained further as this section develops. Like in the pure meter-in case, the operation of the system can be described by separating the cases of resistive and overrunning load.

Extension with Resistive Loads (DV in Position 1)

When DV is actuated to position 1, corresponding to the cylinder extension, the pressure at both cylinder chambers can be calculated by applying the orifice equation to O and the force balance equation to the actuator:

$$\begin{aligned} p_a &= \Delta p_o = \frac{\rho Q_o{}^2}{2C_f{}^2\Omega^2} \\ p_A &= \frac{\rho Q_o{}^2}{2C_f{}^2\Omega^2}\frac{1}{\varphi} + \frac{F}{A} \end{aligned} \tag{13.14}$$

where, in Eq. (13.14), φ is the area ratio of the cylinder $\varphi = A/a$, as defined in Chapter 7.

---

1 In reality, small overrunning loads could be balanced by the pressure in the rod chamber because the pressure in Eq. (13.10) is expressed as gage pressure; therefore, negative pressures up to –1 atm (≈ -1 bar) are physical. However, as explained in Chapter 2, it is recommended to not operate below atmospheric pressure to avoid cavitation issues.
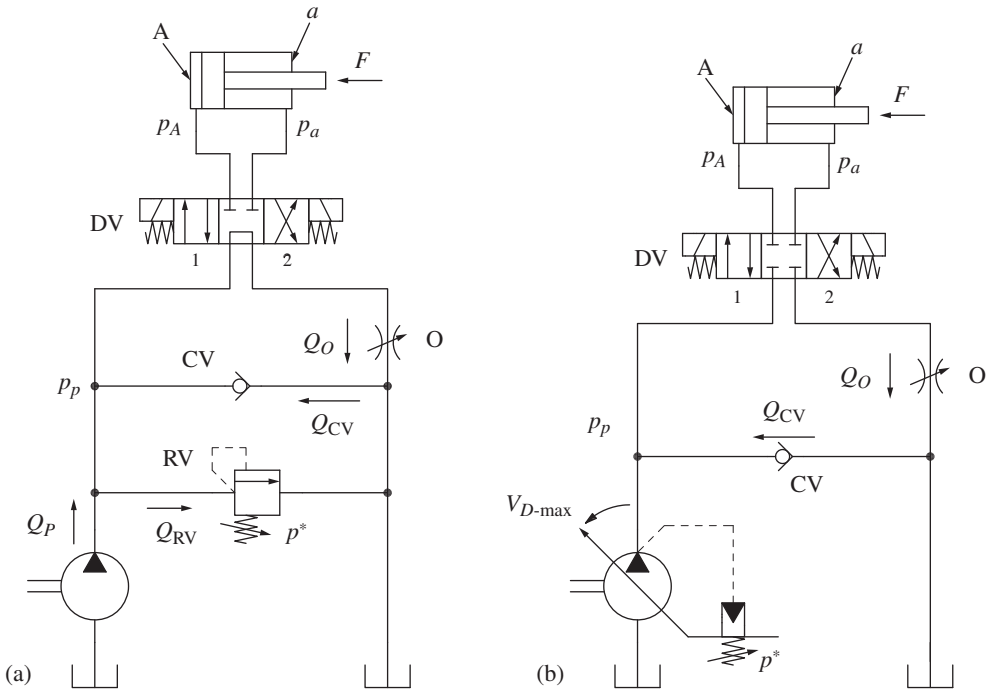
Figure 13.5 Meter-out control concept using a fixed (a) and a variable (b) displacement pump. It is assumed that the DV can handle a pressurized return port.

In Figure 13.5, it is evident that the pump pressure, p_P is equal to the pressure at the piston chamber, p_A.

In this condition, the operation of the system is once again determined by the opening area, Ω, of the control orifice. Starting from the largest value of Ω and gradually decreasing it, two different behaviors are encountered:

- *No regulation ($\Omega_{OUT}^* < \Omega < \Omega_{max}$).* For high Ω values, the pressure drop across the orifice, Δp_O, is not high enough to cause the pump outlet pressure to be larger than the pressure setting of the system, p^*. In this case, $Q_O = Q_{P,max}$, and the actuator velocity is at its maximum value, $\dot{x}_{max} = Q_{P,max}/A$. In this condition, the pump flow controls the actuator velocity (as in the case of primary regulation), while the orifice O behaves as compensator just creating a pressure drop: Δp_O varies according to the area Ω as shown in Eq. (13.14).
- *Meter-out regulation ($\Omega \leq \Omega_{OUT}^*$).* For small opening areas of the orifice O, the pressure at the pump outlet reaches its critical value p^*. The relief valve in Figure 13.5a opens and diverts some flow to the tank ($Q_{RV} > 0$), or the pump regulator in Figure 13.5b decreases the pump displacement. This causes a reduction of the flow through the orifice Q_O, thus reducing the actuator velocity, with respect to $\dot{x}_{max}$. The orifice O behaves as metering, being Δp_O constant:

$$\Delta p_O = p_a = p^* \varphi - \frac{F}{a} \tag{13.15}$$

Therefore, the orifice area Ω determines the flow to the actuator, Q_O. The pump outlet pressure is constant and equal to p^*, the circuit behaves as a pressure supply metering control where the metering element is on the meter-out side.

The flow area Ω_{OUT}^* at which the transition between the two operating modes (meter-out regulation, no regulation) occurs, corresponds again to the simultaneous conditions $p_p = p^*$ and
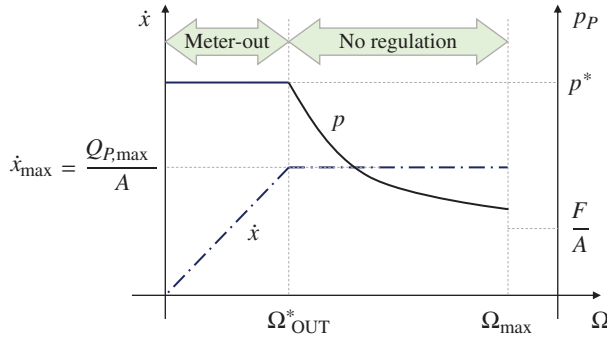
Figure 13.6 Control of the actuator velocity with the circuits in Figure 13.5 (resistive load).

$Q_O = Q_{P,\max}$ applied to Eq. (13.14):

$$\Omega_{\mathrm{OUT}}^* = \frac{Q_{P,\max}}{\varphi C_f} \frac{1}{\sqrt{\frac{2}{\rho}\varphi\left(p^* - \frac{F}{A}\right)}} \tag{13.16}$$

Figure 13.6 summarizes the considerations on the meter-out control of resistive loads. The shape of the curves is very similar to that in Figure 13.3, with a key difference: i.e. for a given actuator, the transition value Ω_{OUT}^* is smaller than the equivalent for the meter-in case Ω_{IN}^* because of the actuator geometry. Using the approach described earlier, the power analysis for the meter-out case is summarized in Figure 13.7.

Equation (13.15) highlights a very important aspect of the meter-out control: in regulation, the value of the pressure at the cylinder rod chamber p_a is generally different than p^*. This is due to two effects: first, the load term F, which is always present and, second, the cylinder area ratio φ (which is greater than 1), which causes a *pressure amplification* effect. The relief valve (for the fixed pump circuit) or the pressure regulator (for the variable pump case) is limiting the pressure only at the outlet of the pump, while the highest pressure in the system might be located elsewhere[2].

> The basic **meter-out** control architecture behaves similarly to the meter-in for resistive load conditions. Regulation occurs only for small opening of the meter-out orifice, when the orifice becomes a metering device. Differently from the meter-in architecture, the meter-out architecture can induce pressure amplification, which needs to be carefully considered when analyzing the maximum system pressure.

Figure 13.7 shows the power consumption of the circuits of Figure 13.5, in resistive load conditions. In case of regulation with fixed displacement pump, the power consumption is summarized by following terms:

$$
\begin{aligned}
P_{\text{load}} &= F \cdot \dot{x} = F \cdot \frac{Q_o}{a} \quad \text{mechanical power at load} \\
P_o &= \left(p^*\varphi - \frac{F}{a}\right) \cdot Q_o \quad \text{power loss at the orifice} \\
P_{\text{RV}} &= p^*(Q_{P,\max} - Q_o\varphi) \quad \text{power loss at the relief valve} \\
P_p &= p^* \cdot Q_{P,\max} = P_{\text{load}} + P_o + P_{\text{RV}} \quad \text{overall power consumed}
\end{aligned}
\tag{13.17}
$$

---

2 In the case of opposite connection of the cylinder (resistive load at the rod side), the cylinder geometry causes a pressure mitigation effect. Therefore, the maximum pressure is located at the pump outlet.

(a)

(b)
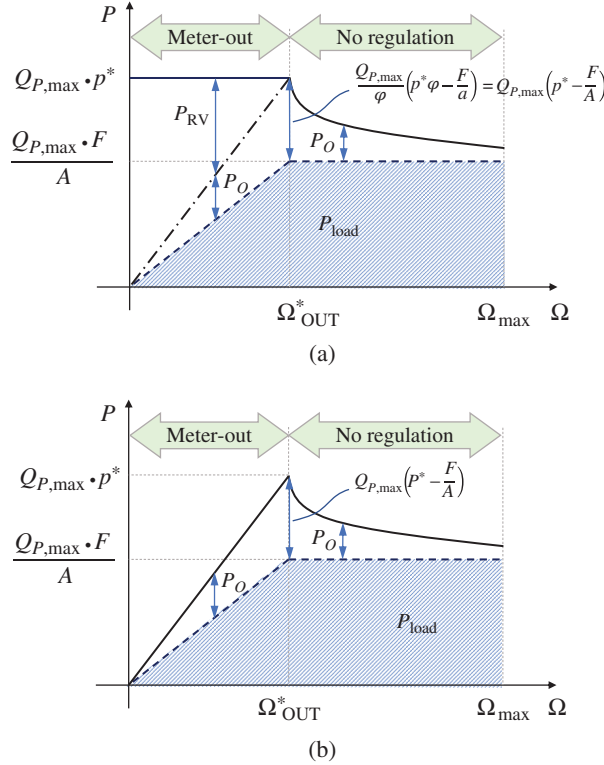
Figure 13.7 Power consumption analysis for the circuits in Figure 13.5 for resistive loads: (a) fixed displacement pump, Figure 13.5a; (b) variable displacement pump, Figure 13.5b.

On the other hand, for the variable displacement pump circuit, the power contributions during regulation are:

$$P_{\text{load}} = F \cdot \dot{x} = F \cdot \frac{Q_o}{a} \quad \text{mechanical power at load}$$

$$P_o = \left(p^*\varphi - \frac{F}{a}\right) \cdot Q_o \quad \text{power loss at the orifice} \tag{13.18}$$

$$P_p = p^* \cdot Q_{P,\text{max}} = P_{\text{load}} + P_o \quad \text{overall power consumed}$$

When both systems are in primary regulation, the situation is the same in both cases:

$$P_{\text{load}} = F \cdot \dot{x} = F \cdot \frac{Q_{P,\text{max}}}{A} \quad \text{mechanical power at load}$$

$$P_o = \Delta p_o \cdot Q_o \quad \text{power loss at the orifice} \tag{13.19}$$

$$P_p = \left(\frac{F}{A} + \frac{\Delta p_o}{\varphi}\right) \cdot Q_{P,\text{max}} = P_{\text{load}} + P_o + P_{\text{RV}} \quad \text{overall power consumed}$$

Retraction with Overrunning Loads (DV in Position 2)

In the circuits in Figure 13.5, when the DV shifts in position 2 the cylinder retracts and, as before, the load becomes assistive. The external force and the actuator velocity have same direction. Differently from the meter-in case, the meter-out architecture always allows for controlling overrunning loads. This can be shown with the force balance at the actuator:

$$p_A A - p_a a - F = 0 \tag{13.20}$$

The pressure at the piston chamber is determined by the orifice equation applied at the orifice O:

$$p_A = \frac{\rho Q_O{}^2}{2C_f{}^2\Omega^2} \tag{13.21}$$

By combining Eqs. (13.20) and (13.21), the pressure at the pump outlet becomes:

$$p_P = p_a = \frac{\rho Q_O{}^2}{2C_f{}^2\Omega^2}\varphi - \frac{F}{a} \tag{13.22}$$

The expression for p_a ($=p_P$) in Eq. (13.22) is useful to summarize the operating cases for the system. As before, the analysis of the system behavior can be done starting from the case of orifice fully open and then gradually close it:

- *Pump unloaded meter-out regulation* ($\Omega_U < \Omega < \Omega_{max}$). For large openings of the orifice area, Eq. (13.22) could be satisfied only if p_P were null or negative. This occurs when the area Ω is larger than Ω_U, where:

$$\Omega_U = \frac{\varphi Q_{P,\max}}{C_f}\sqrt{\frac{\rho A}{2F}} \tag{13.23}$$

Ω_U is calculated imposing the condition $p_a = 0$ and $Q_O = \varphi Q_{P,\max}$ to Eq. (13.22). In particular, when $\Omega > \Omega_U$ the actuator moves at a speed $\dot{x}$, where $\dot{x} \cdot a > Q_{P,\max}$. If the circuits in Figure 13.5 were not equipped with the CV, the actuator rod chamber (i.e. the pump outlet) would fall below atmospheric pressure. However, the CV makes up for the flow difference (Q_{CV}), so that the rod chamber stays at the tank pressure. For this reason, CV is usually referred to as *anticavitation valve*. With $p_a = 0$, in this condition, $p_A = F/A$ and consequently:

$$Q_O = c_f\Omega\sqrt{\frac{2F}{\rho A}} \tag{13.24}$$

When $\Omega > \Omega_U$, the make-up flow passing through the CV is:

$$Q_{CV} = \frac{Q_O}{\varphi} - Q_{P,\max} \tag{13.25}$$

For $\Omega = \Omega_U$ the orifice flow given by Eq. (13.24) is $Q_O = \varphi Q_{P,\max}$. This means that the flow Q_O exiting from the actuator balances the flow entering to it, Q_P, with $Q_{CV} = 0$. During the pump unloaded metering control, the orifice O behaves as a metering element controlling the actuator velocity $\dot{x} = Q_O/A$, while the pump is not consuming any power, i.e. its outlet pressure equal to tank pressure. Sections 13.1.3 and 13.3 will provide more details about the use of anticavitation valves and their operation.

> The meter-out architecture combined with the use of an anticavitation check valve allows controlling overrunning loads without pressurizing the flow supply. This case is referred to as **unloaded meter-out regulation**. The meter-out orifice is a metering orifice that allows reaching actuator velocities higher than the value corresponding to the maximum pump flow.

- *No regulation* ($\Omega^*_{OUT} < \Omega < \Omega_U$). If the orifice area is smaller than Ω_U and the pump pressure (Eq. (13.22)) is positive, but lower than p^*, there is no regulation achieved by the meter-out orifice. This is a consequence of the value of the pressure drop, Δp_O, produced by the orifice. The full pump flow enters the actuator rod chamber and $Q_O = Q_{P,\max} \cdot \varphi$. Therefore, the actuator velocity is given by the pump flow rate $\dot{x} = Q_{P,\max}/a$. In this condition, the orifice O works as compensator. Differently from the previous cases where no regulation is seen for the meter-in and meter-out architectures in resistive load conditions, in this case the pressure drop Δp_O has a necessary function. It is not just a power loss, but it is a pressure drop that allows balancing

the actuator under overrunning load conditions. This behavior is similar to the operation of counterbalance valves, which will be presented in Chapter 14.

The "no regulation" region occurs until the meter-out orifice closes reaching a value Ω^*_{OUT}. The expression for Ω^*_{OUT} is slightly different than the resistive load case (Eq. (13.16)) because the cylinder is retracting:

$$\Omega^*_{OUT} = \frac{\varphi \, Q_{P,\max}}{C_f} \frac{1}{\sqrt{\frac{2}{\rho}\left(\frac{p^*}{\varphi} + \frac{F}{A}\right)}} \tag{13.26}$$

Equation (13.26) calculates the value of Ω^*_{OUT} by imposing the condition $p_P = p_a = p^*$ to Eq. (13.22). Being the pump pressure lower than p^*, there is no flow discharged to the tank through the relief valve.

- *Pump-loaded meter-out regulation ($\Omega \leq \Omega^*_{OUT}$).* For orifice areas lower than Ω^*_{OUT}, the pump pressure in the systems in Figure 13.5 remains at p^*. This means that either the relief valve opens, for the fixed displacement pump circuit in Figure 13.5a, or the pump regulator reduces the pump displacement, as in Figure 13.5b. The supply operates at a constant pressure, and the orifice O works as a metering element, with a Δp_O equal to:

$$\Delta p_O = p_A = \frac{p^*}{\varphi} + \frac{F}{A} \tag{13.27}$$

The flow across the orifice O (which in turn gives the actuator speed) is reduced with respect to the previous condition, and it becomes a function of the area Ω:

$$Q_O = C_f \Omega \sqrt{\frac{2}{\rho}\left(\frac{p^*}{\varphi} + \frac{F}{A}\right)} \tag{13.28}$$

By observing carefully Eq. (13.27), the reader can realize that, in the case of meter-out control of overrunning loads, the maximum pressure in the cylinder rod side can exceed the pump set pressure p^*.

The basic meter-out architecture allows controlling overrunning loads. The actuator velocity is regulated for small areas of the meter-out orifice, which behaves as metering. For larger openings, there is no regulation but still the meter-out orifice has the important function of balancing the actuator, acting as a compensator. If an anticavitation valve is used, the meter-out orifice allows implementing regulation without pressurizing the pump.

Figure 13.8 provides a summary of the three scenarios described: during the two meter-out regulation intervals, the actuator speed increases linearly with the value of Ω. The slope of these straight lines is higher for the case of the pump-loaded meter-out, as is evident by comparing Eq. (13.24) with Eq. (13.28). In the no regulation region, the actuator speed is a constant value defined by the pump flow. During pump-loaded meter-out, the pump pressure is constant, equal to p^*. In the no regulation region, the pump pressure decreases with a quadratic relationship until it reaches a null value, at $\Omega = \Omega_U$. Finally, in the pump-unloaded meter-out zone, the pump pressure remains constant at the value of the tank (zero-gage pressure), making this region very interesting from an energy consumption standpoint. In fact, under this condition, the pump requires (ideally) no power to the prime mover. However, the careful reader should notice that in this area the actuator velocity can reach very high values.

Figure 13.9 summarizes the power analysis for the circuits in Figure 13.5, in overrunning load conditions. As mentioned in Chapter 5, in this situation the hydraulic system should be able to consume the mechanical power at the actuator to be able to maintain its control. In the case of the
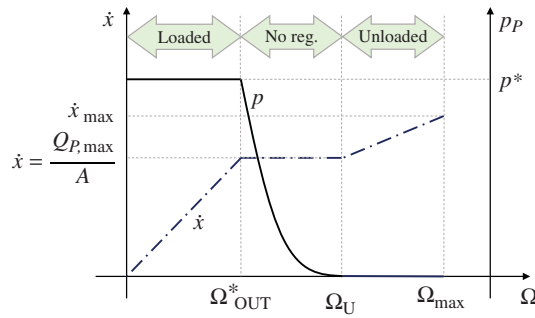
Figure 13.8 Control of the actuator velocity with the circuits in Figure 13.5 (assistive load).

simple circuits in Figure 13.5, the actuator power (represented in Figure 13.9 with a dash-dot line) is entirely dissipated within the hydraulic system. On top of this, in certain conditions, the pump requires additional input power to the prime mover to guarantee a proper control of the actuator velocity (represented in Figure 13.9 by a continuous line). The control orifice serves as a dissipation element: it consumes the mechanical overrunning power P_{load} and a portion or all the pump power, as it will be detailed by the following equations. Thus, in terms of energy consumption, one can think the meter-out solution is not a good strategy for controlling hydraulic actuators. However, because of its simplicity, accuracy of control, and ease of implementation, the meter-out control is

(a)

(b)
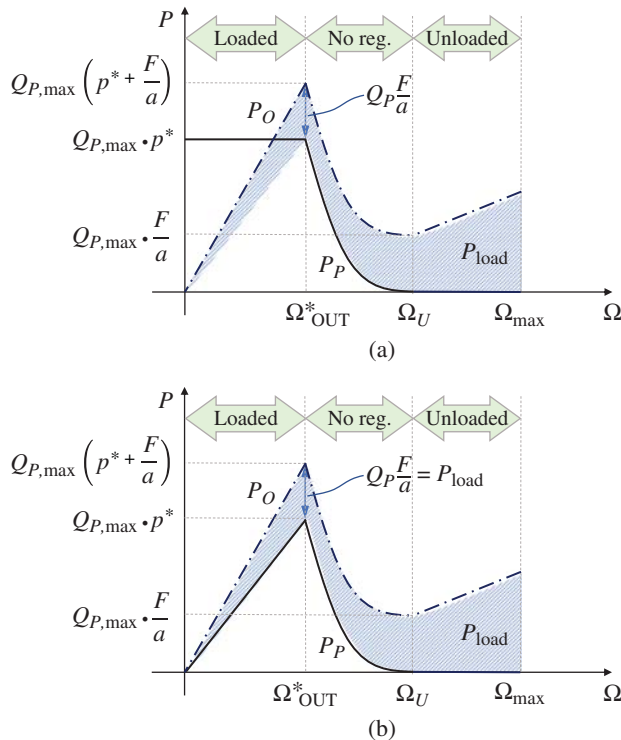
Figure 13.9 Power consumption analysis of the basic meter-out control circuits in Figure 13.5 for overrunning loads: (a) fixed pump, Figure 13.5a; (b) variable displacement pump, Figure 13.5b. The dash-dot line represents the power dissipated at the orifice, while the continuous line represents the power consumed by the pump.

widely used in many applications. Figure 13.9 details the abovementioned aspects, by showing the different power terms in pump-loaded regulating conditions ($\Omega < \Omega_{\text{OUT}}^*$):

$$P_{\text{load}} = F \cdot \dot{x} = F \cdot \frac{Q_{P,\text{max}}}{a} \quad \text{mechanical power at load}$$

$$P_o = Q_o \cdot \left(\frac{p^*}{\varphi} + \frac{F}{A} \right) \quad \text{power loss at the orifice}$$

$$P_{\text{RV}} = p^* \left(Q_{P,\text{max}} - \frac{Q_o}{\varphi} \right) \quad \text{power loss at the relief valve}$$ \hfill (13.29)

$$P_p = p^* \cdot Q_{P,\text{max}} \quad \text{power consumed by the pump}$$

where, in the above Eq. (13.29), the term P_{RV} is present only for the case of fixed displacement pump (Figure 13.5a).

In the primary regulating conditions ($\Omega_{\text{OUT}}^* < \Omega < \Omega_U$),

$$P_{\text{load}} = F \cdot \dot{x} = F \cdot \frac{Q_{P,\text{max}}}{a} \quad \text{mechanical power at load}$$

$$P_o = \frac{\rho Q_{P,\text{max}}{}^3 \varphi^3}{2C_f{}^2 \Omega^2} \quad \text{power loss at the orifice}$$ \hfill (13.30)

$$P_p = p_P \cdot Q_{P,\text{max}} = \left(\frac{\rho Q_{P,\text{max}}{}^2}{2C_f{}^2 \Omega^2} \varphi^3 - Q_{P,\text{max}} \frac{F}{a} \right) \quad \text{pump power}$$

Finally, for the pump unloaded regulation ($\Omega > \Omega_U$):

$$P_{\text{load}} = F \cdot \dot{x} = F \cdot \frac{Q_o}{a} \quad \text{mechanical power at load}$$

$$P_o = Q_o \cdot \frac{F}{A} \quad \text{power loss at the orifice}$$ \hfill (13.31)

$$P_p = p_P \cdot Q_{P,\text{max}} = 0 \quad \text{power consumed by the pump}$$

13.1.3 Remarks on the Meter-in and the Meter-out Controls

Section 13.1 introduced the elementary concepts of metering control by using the simple circuits in Figure 13.2 (meter-in) and Figure 13.5 (meter-out). These circuits are based on the simplest configurations of pressure supply and primary flow supply. However, the concepts highlighted in the previous pages can be further generalized to other circuit layouts. To begin, Section 13.1 discussed the case of resistive loads for the cylinder extension and the case of overrunning loads for the retraction. The table in Figure 13.10 summarizes the mathematical formulas reporting also the opposite case.

To conclude, for all the meter-in and meter-out control situations discussed so far, the following remarks can be made:

- When metering elements are used to control an actuator, these elements achieve control of the actuator velocity only in specific ranges for the metering area. Outside these ranges, other elements in the system are in control of the actuator velocity.
- The implementation of the metering controls for the circuits in Figure 13.2 (meter-in) or Figure 13.5 (meter-out) generally involves an additional power consumption because the regulation happens most of the time when the pump is at the maximum pressure. These dissipations are not related to component inefficiencies (losses in the pump, valves, or connecting lines), but they are inherent to the control concept.
- The pure meter-in control solution does not allow to handle overrunning loads.

- The meter-out control permits the control of both resistive and assistive load conditions. However, meter-out control can create pressure amplification at the cylinder ports, when the area ratio φ is greater than 1.
- Meter-out control of overrunning loads can take place in two alternative ways: loaded meter-out control and unloaded meter-out control. The second case usually requires the use of additional anticavitation valves, but it is more convenient because of two reasons: the maximum controlled velocity is not limited by the maximum pump flow rate and the power dissipation in the hydraulic system is reduced to the minimum.
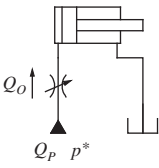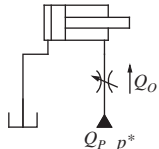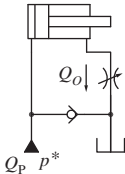
	Load direction (F) ⟵	Load direction (F) ⟶
Meter-in extend	<u>Resistive load</u> $\Omega \in [0, \Omega^*_{IN}]$ meter-in reg. $\Omega > \Omega^*_{IN}$ no regulation $\Omega^*_{IN} = \dfrac{Q_{P,max}}{C_f} \dfrac{1}{\sqrt{\frac{2}{\rho}\left(p^* - \frac{F}{A}\right)}}$	<u>Overrunning load</u> Not allowed
Meter-in retract	<u>Overrunning load</u> Not allowed	<u>Resistive load</u> $\Omega \in [0, \Omega^*_{IN}]$ meter-in reg. $\Omega > \Omega^*_{IN}$ no regulation $\Omega^*_{IN} = \dfrac{Q_{P,max}}{C_f} \dfrac{1}{\sqrt{\frac{2}{\rho}\left(p^* - \frac{F}{a}\right)}}$
Meter-out Extend	<u>Resistive load</u> $\Omega \in [0, \Omega^*_{OUT}]$ meter-out reg. $\Omega > \Omega^*_{OUT}$ no regulation $\Omega^*_{OUT} = \dfrac{Q_{P,max}}{\varphi C_f} \dfrac{1}{\sqrt{\frac{2}{\rho}\varphi\left(p^* - \frac{F}{A}\right)}}$	<u>Overrunning load</u> $\Omega \in [0, \Omega^*_{OUT}]$ loaded meter-out $\Omega \in [\Omega^*_{OUT}, \Omega_U]$ no regulation $\Omega > \Omega_U$ unloaded meter-out $\Omega^*_{OUT} = \dfrac{Q_{P,max}}{\varphi C_f} \dfrac{1}{\sqrt{\frac{2}{\rho}\varphi\left(p^* + \frac{F}{A}\right)}}$ $\Omega_U = \dfrac{Q_{P,max}}{\varphi C_f} \sqrt{\dfrac{\rho a}{2F}}$

Figure 13.10 Summary of the possible meter-in and meter-out control situations. The load direction is shown in the first row of the table.
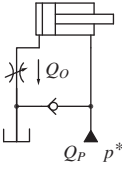
Meter-out retract	Overrunning load	Resistive load
	$\Omega \in [0, \Omega^*_{OUT}]$ loaded meter-out	$\Omega \in [0, \Omega^*_{OUT}]$ meter-out reg.
	$\Omega \in [\Omega^*_{OUT}, \Omega_U]$ no regulation	$\Omega > \Omega^*_{OUT}$ no regulation
	$\Omega > \Omega_U$ unloaded meter-out	
	$\Omega^*_{OUT} = \dfrac{\varphi Q_{P,\max}}{C_f} \dfrac{1}{\sqrt{\dfrac{2}{\rho}\left(\dfrac{p^*}{\varphi} + \dfrac{F}{A}\right)}}$	$\Omega^*_{OUT} = \dfrac{\varphi Q_{P,\max}}{C_f} \dfrac{1}{\sqrt{\dfrac{2}{\rho}\left(p^* - \dfrac{F}{a}\right)}}$
	$\Omega_U = \dfrac{\varphi Q_{P,\max}}{C_f} \sqrt{\dfrac{\rho A}{2F}}$	

Figure 13.10   (*Continued*)

Some of the abovementioned drawbacks of the basic meter-in and meter-out circuits can be addressed by using more complex system architectures to implement metering control. These are, for example, represented by the open center architecture (Chapter 15) and the load sensing systems (Chapter 16). Nevertheless, the basic principles described in the previous paragraph still apply – with proper variants – to all possible ways of implementing meter-in or meter-out controls.

Example 13.1   Loaded meter-out control

From the previous considerations, loaded meter-out control appears to be a poor design choice. However, in several applications, it represents the only viable metering solution. The following problem represents a very common scenario in systems design.

Problem: Design a hydraulic circuit for controlling the extension of a telescopic arm. Choose a basic meter-in or meter-out architecture as described in Section 13.1. The arm can be tilted by another actuator (not represented in the figure) from the horizontal. The two extreme inclinations α for the arm are +45° and −45°. Assume the maximum pump pressure p^* is equal to 120 *bar*. Other known data are the following: the mass M is 900 *kg*, the cylinder bore diameter is 40 *mm*, and the rod diameter is 25 *mm*. Assume an orifice flow coefficient equal to 0.65.
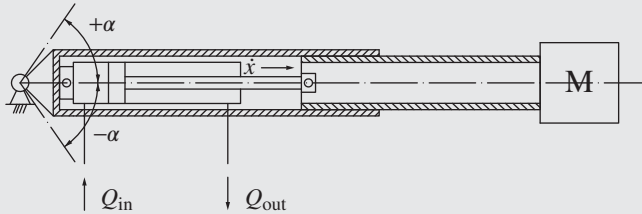
Answer the following questions:

1) Determine the pump flow necessary to reach the extension speed $\dot{x}_{\max} = 0.5$ *m/s* and select the proper basic metering architecture from Figures 13.2 and 13.5.
2) Determine the maximum pressure in the system.

(Continued)

Example 13.1 (Continued)

Given:

Inclination of the arm: α varies between $+45°$ and $-45°$.
Maximum pump pressure, $p^* = 120\ bar$
Mass acting on the actuator, $M = 900\ kg$
Cylinder bore diameter, $d_B = 40\ mm$
Cylinder rod diameter, $d_R = 25\ mm$
Maximum extension speed, $\dot{x}_{max} = 0.5\ m/s$
Orifice flow coefficient, $C_f = 0.65$

Find:

1) The required pump flow Q_P
2) The suitable control architecture between the basic meter-in and meter-out circuits described in Section 13.1. Define the orifice area openings.
3) The maximum pressure in the system.

Solution:

First, the extension speed requirement determines the maximum pump flow:

$$Q_P = \dot{x}_{max} \cdot A = \dot{x}_{max} \cdot \frac{\pi\ d_B^2}{4} = 0.5\ [m/s] \cdot \frac{\pi \cdot 1600\ [mm^2]}{4} \cdot 0.06 = 37.7\ l/min$$

As noticeable from the figure, when the arm is tilted upward ($\alpha > 0$), the extension load is resistive, while when the arm is tilted downward ($\alpha < 0$), the load is overrunning. Therefore, the meter-in control layouts in Figure 13.2 cannot be chosen, because it would not handle the negative tilts of the telescopic arm. Therefore, the arm control needs a meter-out arrangement, such as in Figure 13.5.

For the $\alpha = +45°$ case (resistive load), the actuator velocity is controlled when the meter-out orifice area varies between 0 and $\Omega^*_{OUT,+45}$, where $\Omega^*_{OUT,+45}$ is given by Eq. (13.16):

$$\Omega^*_{OUT,+45} = \frac{Q_P}{\varphi C_f} \frac{1}{\sqrt{\frac{2}{\rho}\varphi\left(p^* - \frac{Mg \cdot \cos(\alpha)}{A}\right)}} = \frac{37.7\ [l/min]}{1.64 \cdot 0.65 \cdot 60\,000} \cdot$$

$$\frac{1}{\sqrt{\frac{2 \cdot 1.64}{850\ [kg/m^3]}\left(120\ [bar] \cdot 10^5 - \frac{8829\ [N] \cdot 0.7}{1256\ [mm^2] \cdot 10^{-6}}\right)}} = 3.6\ mm^2$$

The coefficient φ is calculated as follows:

$$\varphi = \frac{d_B^2}{d_B^2 - d_R^2} = \frac{40^2\ [mm^2]}{40^2 - 25^2\ [mm^2]} = 1.64$$

In regulation, the pressure at the piston chamber is equal to $p^* = 120\ bar$, while the pressure at the rod chamber is

$$p_a = \left(p^* - \frac{Mg \cdot \cos(\alpha)}{A}\right)\varphi = \left(120\ [bar] - \frac{8829\ [N] \cdot 0.7}{1256\ [mm^2]} \cdot 10\right) \cdot 1.64 = 116.1\ bar$$

For the $\alpha = -45°$ case (overrunning load), the pump loaded meter-out control occurs when the orifice area varies between 0 and $\Omega^*_{OUT,-45}$. The expression for $\Omega^*_{OUT,-45}$ pertains to the case

of overrunning load during cylinder extension, and with the help of Figure 13.10:

$$\Omega^*_{OUT,-45} = \frac{Q_P}{\varphi c_f} \frac{1}{\sqrt{\frac{2}{\rho}\varphi\left(p^* + \frac{F}{A}\right)}} = 2.3 \ mm^2$$

In regulation, the pressure at the piston chamber is equal to $p^* = 120 \ bar$, while the pressure at the rod chamber is

$$p_a = \left(p^* + \frac{F}{A}\right)\varphi = 169 \ bar$$

Therefore, p_a is the maximum pressure in system, and its value is higher than p^*. During the $\alpha = -45°$ case, the area $\Omega_{U,-45}$ that would give pump-unloaded control is equal to

$$\Omega_{U,-45} = \frac{Q_P}{\varphi c_f}\sqrt{\frac{\rho a}{2F}} = \frac{37.7 \ [l/min]}{1.64 \cdot 0.65 \cdot 60\,000} \cdot \sqrt{\frac{850 \ [kg/m^3] \cdot 766 \ [mm^2] \cdot 10^{-6}}{2 \cdot 8829 \ [N] \cdot 0.7}} = 4.3 \ mm^2$$

In summary, the maximum metering area for controlling the arm extension has to be equal to the highest between $\Omega^*_{OUT,+45}$ and $\Omega^*_{OUT,-45}$, which is $\Omega_{max} = \Omega^*_{OUT,+45} = 3.6 \ mm^2$. When the arm is in the upper position, the operator adjusting the metering area will have full control range from zero up to Ω_{max}. As the arm lowers from its highest position, the control range reduces, and the operator will feel a deadband as the system switches from meter-out regulation to primary regulation (as represented in the figure below). During primary regulation, the actuator speed does not change and stays equal to $\dot{x}_{max}$. Pump unloaded meter-out cannot be implemented with the selected areas.
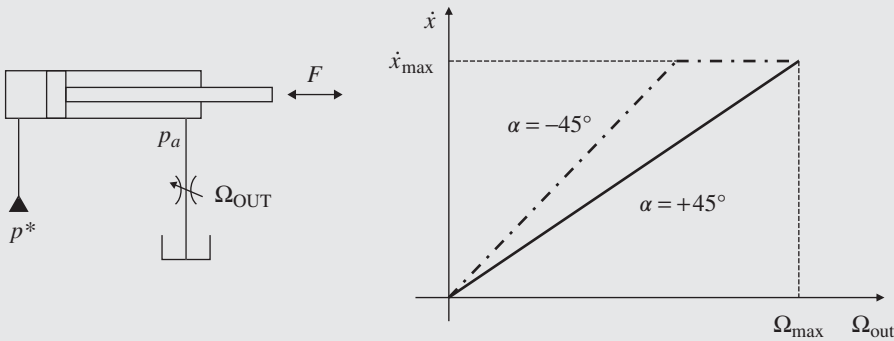
In general, meter-in control is the preferred strategy for controlling the velocity of a hydraulic actuator because it allows an easier implementation for multi-actuator systems (this will be addressed in Part V). Furthermore, the meter-in control does not present the risks of pressure amplification, which is a limiting factor for the use of meter-out, especially in the case of resistive loads.

Many hydraulic circuits (such as in Example 13.1) use a combination of meter-in and meter-out control elements, to achieve a force (or torque) balance at the controlled actuator in case of overrunning loads. In these cases, the meter-in element still determines the flow rate to the actuator, and thus the actuator velocity, while the meter-out element adjusts the pressure at the actuator ports to guarantee force balance.

Example 13.2   Analysis of meter-in and meter-out orifice

Consider a simple hydraulic mass lifting system as shown in the figure below. The arm motion is obtained through a hydraulic motor and a mechanical gearbox that reduces the motor shaft speed.
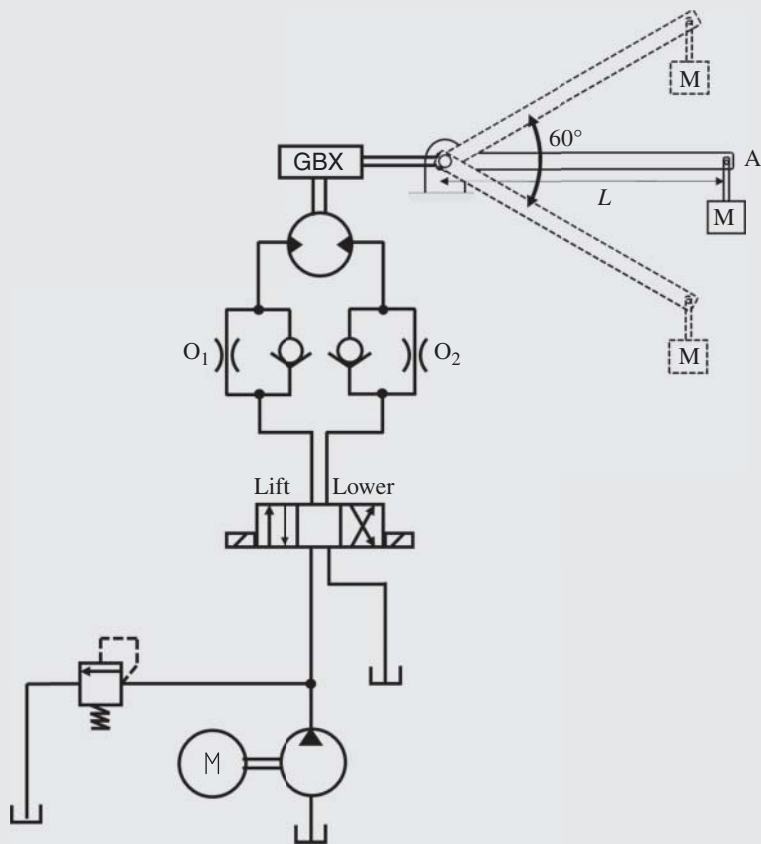
A summary of the known data for the system is given in the table below.

Arm length $= 2\ m$	Payload $= 1000\ kg$
Motor displacement $= 50\ cc/rev$	Gear box ratio $= 250$
Electric motor speed $= 1000\ rpm$	Relief valve setting $= 140\ bar$
Orifice coefficient, $C_f = 0.65$	Area of orifice O2, $\Omega_{O2} = 10\ mm^2$
Area of orifice O1, $\Omega_{O1} = 4\ mm^2$	Acceleration of gravity $= 9.81\ m/s^2$

The arm is required to lift the payload in five seconds.
Answer to the following questions:

a) From the options provided below, choose the neutral position of the directional control valve that can hold the mass in position while dissipating the minimum amount of energy at the pump.

b) Calculate the torque exerted by the mass when the mass is at position A.

For all the questions below, assume the load torque to be constant and same as the value calculated in part (b).

c) Size the pump assuming ideal behavior of the components
d) Size the pump if the volumetric efficiencies of pump and motor are 95% and 90%, respectively.

For all the questions below, use the volumetric efficiencies mentioned above in your calculations.

e) Determine the power delivered by the electric motor to the pump if the hydromechanical efficiency for both pump and motor is 90%.
f) Is O1 really needed in the circuit? Why?
g) Is O2 really needed in the circuit? Why?
h) Is O1 metering or compensator? And O2?
i) Determine the size of O1 to have pressure at the pump outlet to be 0 bar.
j) Determine the size of O2 to have the lowering time equal to 10 s.

The main oil properties are given in the table below:

Density	$850\ kg/m^3$
Bulk modulus	$15\,000\ bar$
Kinematic viscosity	$40\ cSt$

Given:
A crane lifting system using a proper configuration of meter – in and meter – out orifices. The given data, with the proper symbolic representation are given in the list below:

Feature	Symbol	Value
Crane angular span	α	60°
Crane arm length	L	$2\ m$
Crane max payload	M	$1000\ kg$
Gearbox ratio	i_{GBX}	250
Crane required lift time	t_{lift}	$5\ s$
Acceleration of gravity	g	$9.81\ m/s^2$
Displacement of the hydraulic motor	V_m	$50\ cm^3/rev$
Relief valve setting	p^*	$140\ bar$
Electric motor speed	n_p	$1000\ rpm$
Area of orifice 1 (O1)	Ω_{O1}	$4\ mm^2$
Area of orifice 2 (O2)	Ω_{O2}	$10\ mm^2$
Orifice coefficient	c_f	0.65
Oil bulk modulus	K	$15\,000\ bar$
Oil kinematic viscosity	ν	$40\ cSt$
Oil density	ρ	$850\ kg/m^3$

(Continued)

Example 13.2 (Continued)

Find:

a) The neutral position of the directional control valve to allow load holding with minimum energy dissipation, among three possible choices: N1, N2, and N3.

b) The torque at the gearbox exerted by the payload, T_{arm}.

c) Pump displacement, V_p, assuming ideal efficiencies for both the pump and the hydraulic motor.

d) Pump displacement, V_p, considering a volumetric efficiency of the pump $\eta_{v,p} = 0.95$ and a volumetric efficiency of the motor $\eta_{v,m} = 0.90$.

e) The power delivered by the prime mover $\dot{W}_{em}$, considering a torque efficiency $\eta_{hm} = 0.90$ for both the hydraulic pump and the hydraulic motor.

f) An assessment on the need of the orifice O1 for the operation of the crane.

g) An assessment on the need of the orifice O2 for the operation of the crane.

h) The functional behavior of orifice O1 and O2 (metering or compensator).

i) The orifice area Ω_{O1} to achieve a null pump outlet, $p_p = 0\ bar$.

j) The orifice area Ω_{O2} to attain a lowering time of $t_{lower} = 10\ s$.

Solution:

First, it is useful to summarize the operation of the system with the two figures below, which visualize the direction of the flow in the lift and the lower operation of the crane.
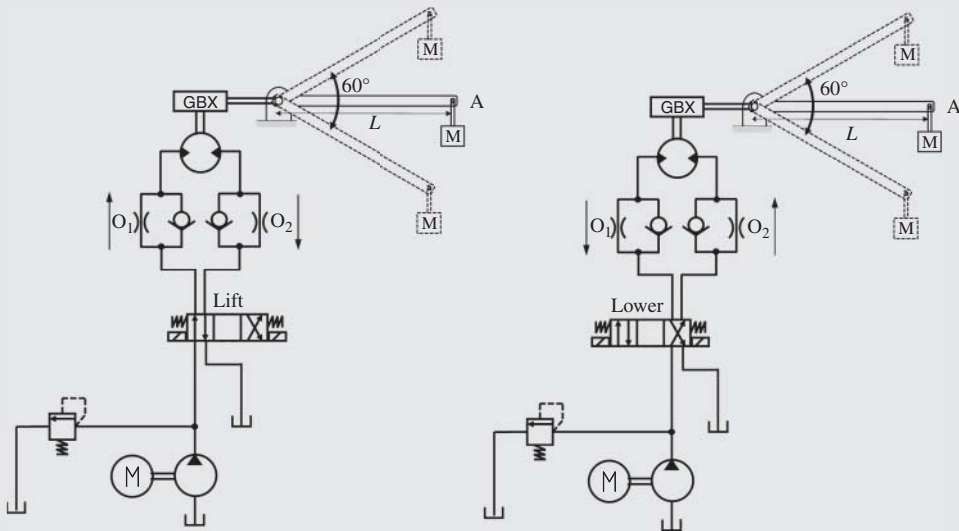
Due to the presence of CVs in parallel with the orifices O1 and O2, the orifice O1 is crossed by flow only during the lowering operation, while the orifice O2 is active only during the lifting phase. This consideration will be very important to answer the questions of the problem.

a) Among the three options for the neutral position of the directional control valve, only N1 and N2 have closed work-ports to the hydraulic motor, which hold the load in position. With positions N1 and N3 the pump port is blocked in neutral. This means that the pump flow is forced to go through the relief valve, demanding maximum electric power. The position N2 allows the pump to discharge the flow to tank in neutral position, while both motor

work-ports are blocked. Therefore, this position allows holding the load, while maintaining a minimum value for the pump outlet pressure (ideally zero). The answer to question a) is therefore N2.

As a complement to this question, it should be observed that a DV, which is normally a spool valve, usually does not guarantee a perfect holding of the load, and small leakages through the spool valve will result in a slow lowering of the load. In case there is a strict requirement for holding the load, additional poppet type components should be used such as pilot operated CVs or counterbalance valves (which will be described in Chapter 14).

b) The torque at the gearbox shaft can be calculated as

$$T_{\mathrm{arm}} = M \cdot g \cdot L = 1000\,[kg] \cdot 9.81\,[m/s^2] \cdot 2\,[m] = 19\,620\,Nm$$

c) The size of the pump, assuming ideal behavior of both the pump and the hydraulic motor, can be determined by first estimating the flow demand of the motor. For this purpose, we need to first calculate the motor speed at the most stringent lift requirements. The angular speed of the arm, in rpm, can be calculated from the t_{lift} requirement:

$$n_{\mathrm{arm}} = \frac{\alpha}{t_{\mathrm{lift}}} = \frac{60\,[deg]}{5\,[s]} \cdot \frac{1\,[rev]}{360\,[deg]} \cdot \frac{60\,[s]}{1\,[min]} = 2\,rpm$$

$$n_m = n_{\mathrm{arm}} \cdot i_{\mathrm{GBX}} = 2\,[rpm] \cdot 250 = 500\,rpm$$

Once the speed of the motor is determined, the flow rate of the motor can be calculated from the motor displacement:

$$Q_{m,i} = n_m \cdot V_m = 500\,[rpm] \cdot 50\,[cm^3/rev] \cdot \frac{1}{1000} = 25\,l/min$$

As $Q_{p,i} = Q_{m,i}$ (this assumes that the whole pump flow is used to satisfy the maximum lifting velocity condition, this assumption will be further discussed in points *e* and *g*), the pump displacement is given by

$$V_{p,i} = \frac{Q_{p,i}}{n_p} = \frac{25\,[l/min]}{1000\,[rpm]} \cdot 1000 = 25\,cm^3/rev$$

d) Considering the given values for the volumetric efficiencies, the number above need to be revised:

$$Q_{m,e} = \frac{Q_{m,i}}{\eta_{v,m}} = \frac{25\,[l/min]}{0.9} = 27.78\,l/min$$

Again $Q_{p,e} = Q_{m,e}$, therefore,

$$V_{p,e} = \frac{Q_{p,e}}{n_p \cdot \eta_{v,p}} = \frac{27.78\,[l/min]}{1000\,[rpm] \cdot 0.9} \cdot 1000 = 29.24\,cm^3/rev$$

e) The power required at the electric motor to drive the pump can be found after evaluating the torque at the pump shaft. In order to do so, the pressure loading at the pump has to be found. The pressure loading at the pump results from the sum pressure drop across the hydraulic motor and the pressure drop across the orifice O2. Therefore,

$$T_{m,e} = \frac{T_{m,i}}{\eta_{\mathrm{hm},m}} = \frac{T_{\mathrm{arm}}/i_{\mathrm{GBX}}}{\eta_{\mathrm{hm},m}} = \frac{19\,620\,[Nm]}{250 \cdot 0.9} = 87.2\,Nm$$

Example 13.2 (Continued)

$$\Delta p_{m,e} = \frac{T_{m,e}}{V_m} = \frac{87.2 \, [Nm]}{50 \, [cm^3/rev]} \cdot 20\pi = 109.6 \, bar$$

In the lift position of the directional flow control valve, the flow crosses orifice O2 after the motor. Therefore, Δp_{O2} has to be considered as well:

$$\Delta p_{O2} = \frac{\rho}{2} \cdot \left(\frac{Q_{m,e}}{c_f \cdot \Omega_{O2}} \right)^2 = \frac{850 \, [kg/m^3]}{2} \cdot \left(\frac{27.78 \cdot 1/60\,000 \, [m^3/s]}{0.65 \cdot 10 \cdot 10^{-6} \, [m^2]} \right)^2 \cdot \frac{1 \, [bar]}{10^5 \, [Pa]}$$

$$= 21.6 \, bar$$

Consequently,

$$\Delta p_{p,e} = \Delta p_{O2} + \Delta p_{m,e} = 109.6 \, [bar] + 21.6 \, [bar] = 131.2 \, bar$$

For a better understanding, these results are also visualized in the schematic of the system in the figure below.
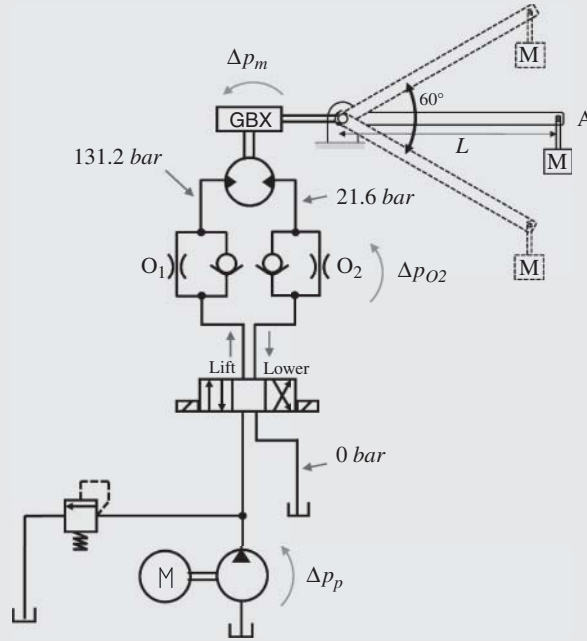
Assuming the tank pressure equal to zero (gauge pressure), the pump pressure is

$$p_p = \Delta p_{p,e} = 131.2 \, bar < p^* = 140 \, bar$$

This means that the relief valve is not open. If this condition was not verified, the assumption made in (c) and (d) $Q_p = Q_m$ would not be valid. A case where the relief valve is open will be analyzed later in this problem.

After the pump delivery pressure is known, the shaft torque can be calculated as

$$T_{p,e} = \frac{V_{p,e} \cdot \Delta p_{p,e}}{\eta_{hm,p}} = \frac{29.24 \, [cm^3/rev] \cdot 131.2 \, [bar]}{0.9} \cdot 20\pi = 67.8 \, Nm$$

Therefore,

$$\dot{W}_{em} = T_{p,e} \cdot n_p = 67.8 \, [Nm] \cdot 1000 \, [rpm] \frac{\pi}{30\,000} = 7.1 \, kW$$

f) O1 is crossed during the lowering operation of the crane, which correspond to an over-running load condition. The orifice O1 is therefore necessary to build the necessary pressure downstream the hydraulic motor, to counter-reach the load. To better explain the operation of the system in both the lifting and lowering cases, the following figure shows the pressure level (high, H and low, L) at the ports of the hydraulic motor. For the lifting case previously analyzed, the hydraulic motor pressurizes its inlet port, to exert a shaft torque $T_{m,e}$ that raises the arm. Since the load is gravitational (it keeps the same vertical direction), during the lowering, the shaft torque maintains the same sign. Therefore, the pressure drop at the motor ($\Delta p_{m,e}$) is still the same, and the pressure is still high (p_H) at the left port, and low (p_L) at the right port. Since the flow through the hydraulic motor is opposite with respect to lift phase, the motor now behaves as a pump: it pressurizes the fluid using the gravitational energy of the load.

Since the return of the motor during lowering is connected to the tank, at zero gage pressure, an element is needed to dissipate the flow energy produced by the hydraulic motor working in pumping mode.

For this reason, the orifice O1 is necessary to guarantee a torque equilibrium at the hydraulic motor. Without O1, the shaft torque would not be balanced by the pressure at the motor work-ports; as result, the arm would have a downward acceleration (payload fall), and not a lowering with constant velocity.

g) As shown at the beginning of the solution, O2 is crossed by the flow during the lift phase, which is a resistive load condition. The calculation explained in (e) shows that the setting of the orifice is such that the whole pump flow goes to the hydraulic motor. Therefore, O2 does not have a regulation function. With these considerations, the presence of O2 seems to be inappropriate. Without O2, the same lifting velocity would be achieved, at less expense of power at the prime mover.

Therefore, O2 appears to be not necessary.
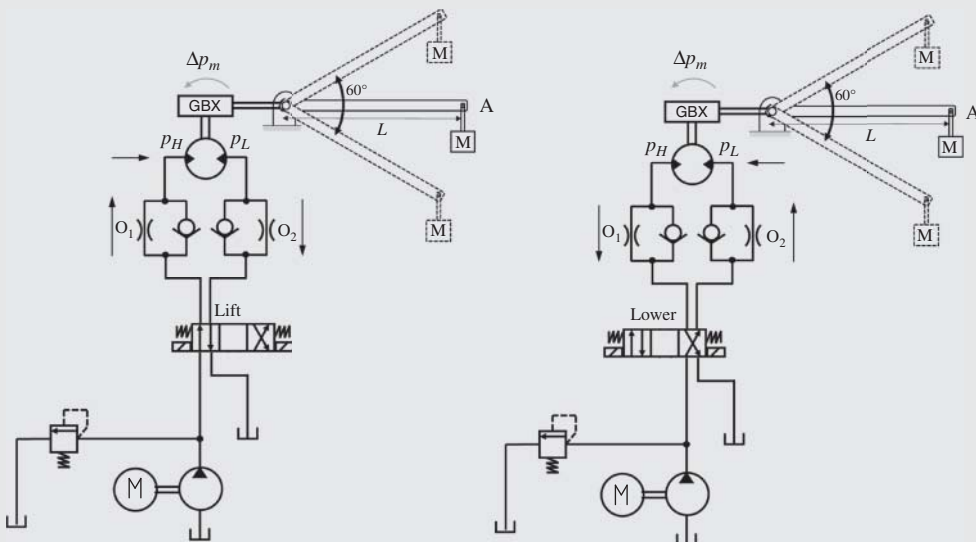
h) First, let us discuss the function of O2, which is active during the lifting.

O2 behaves as compensator. In fact, as shown in (e), it is crossed by a given flow (the flow Q_m) and as a result it establishes a certain Δp_{O2}.

Example 13.2 (Continued)

This behavior is at least true for the given orifice size: $\Omega_{O2} = 10\ [mm^2]$. A more restricted area of this orifice might cause the pump pressure p_p to reach the relief valve pressure p^*. In such chase, a portion of the pump flow would be diverted to tank though the relief valve, and O2 would behave as a metering orifice.

Pertaining to O1, which is active during lowering, we need to understand if its restriction is such to engage the relief valve during the lowering phase. In other terms, if $\Delta p_{O1} < p^*$, then the whole pump flow is received by the hydraulic motor, and the orifice O1 behaves as a compensator. However, if $\Delta p_{O1} = p^*$, then O1 will behave as metering orifice. Therefore, to determine in which case the orifice O1 operates, we evaluate the pressure drop considering the whole pump flow:

$$\Delta p_{O1} = \frac{\rho}{2} \cdot \left(\frac{Q_{p,e}}{c_f \cdot \Omega_{O1}} \right)^2 == \frac{850\ [kg/m^3]}{2} \cdot \left(\frac{27.78 \cdot 1/60\,000\ [m^3/s]}{0.65 \cdot 4 \cdot 10^{-6}\ [m^2]} \right)^2 \cdot \frac{1\ [bar]}{10^5\ [Pa]}$$

$$= 134.8\ bar$$

Given the value of the pressure drop across the motor found in (e), $\Delta p_{m,e} = 109.6\ bar$, the pump pressure is

$$p_p = \Delta p_{O1} - \Delta p_{m,e} = 134.8\ [bar] - 109.6\ [bar] = 25.2\ bar$$

Therefore, $p_p < p^*$: the relief valve is closed and the whole pump flow is used for the lowering. The lowering time will equal the lifting time (5 s) and the orifice O1 behaves as a compensator.

The pressure values are also represented in the figure below:
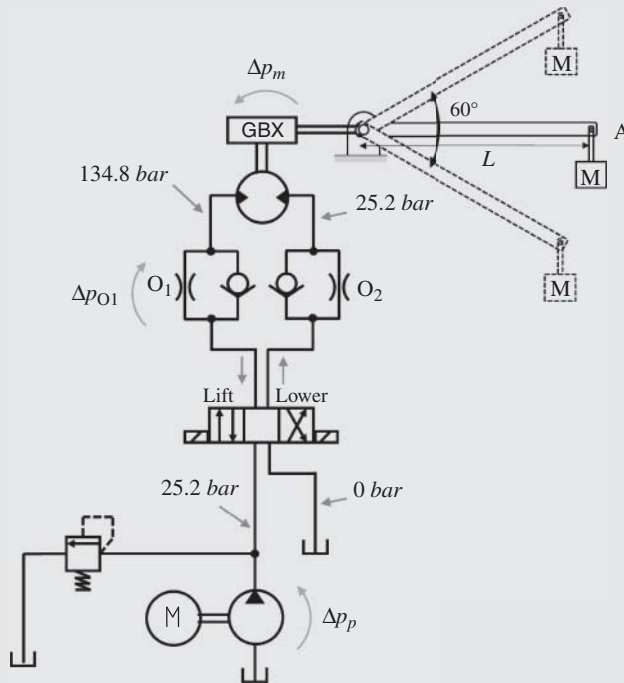
i) With the given size of the orifice O1, the lowering phase occurs with a pump pressure $p_p = 25.2\ bar$, which means that the pump still requires energy from the prime move to perform the lowering of a gravitational load.

The orifice size O1 could be further increased to lower this pressure, ideally to the limit $p_p = 0\ bar$. In practice, it is safer to ensure few bar of pressure above the zero gage pressure to avoid possible cavitation during the operation of the circuit.

To find the orifice area that would bring to a zero pressure level at the pump, the pressure drop across the orifice should equal the pressurization of the motor:

$$\Delta p_{O1} = \Delta p_{m.e}$$

Therefore,

$$\Omega_{O1} = \frac{Q_{m,e}}{c_f \sqrt{\frac{2 \cdot \Delta p_{m.e}}{\rho}}} = \frac{27.78 \cdot 1/60\,000\ [m^3/s]}{0.65 \sqrt{\frac{2 \cdot 109.6 \cdot 10^5\ [Pa]}{850\ kg/m^3}}} \cdot 10^{-6} = 4.436\ mm^2$$

i) The size of O1 can be restricted to achieve a shorter lowering time. As explained above, in this case O1 works as a metering orifice.

To achieve half lowering time (10 s instead of 5 s), the flow rate through both the motor and the orifice is

$$Q_{m,e,10s} = \frac{Q_{m,e,5s}}{2} = \frac{27.78\ [l/min]}{2} = 13.89\ l/min$$

The relief valve has to divert to tank the flow:

$$Q_{RV,10s} = Q_{p,e} - Q_{m,e,10s} = 27.78\ [l/min] - 13.89\ [l/min] = 13.89\ l/min$$

Since the relief valve is open, $p_p = p^*$, the pressure drop at O1 is

$$\Delta p_{O1} = p_p + \Delta p_{m.e} = 140\ [bar] + 109.6\ [bar] = 249.6\ bar$$

The orifice area is

$$\Omega_{O2} = \frac{Q_{m,e,10s}}{c_f \sqrt{\frac{2 \cdot \Delta p_{O1}}{\rho}}} = \frac{13.89 \cdot 1/60\,000\ [m^3/s]}{0.65 \sqrt{\frac{2 \cdot 249.6 \cdot 10^5\ [Pa]}{850\ [kg/m^3]}}} \cdot 10^{-6} = 1.47\ mm^2$$

Example 13.2 (Continued)

The pressure in the system in this operating condition are shown in the figure below:
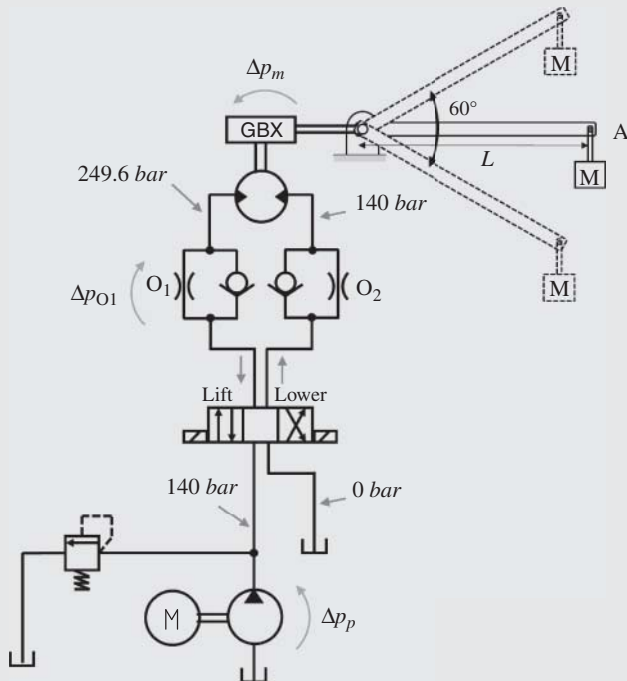
It is important to remark that the maximum pressure of the system in this condition is higher than the pressure set by the relief valve. This pressure amplification aspect was introduced earlier, when presenting the meter-out control architecture. When using a meter-out control architecture, it is always important to verify that the pressure at the return port of the actuator is lower a maximum limit, since the relief valve at the supply side does not limit this pressure value.

Further considerations

The three meter-out conditions examined in the problem, with $\Omega_{O1} = 4$ mm^2; $\Omega_{O1} = 4.436$ mm^2 (*i*); $\Omega_{O1} = 1.47$ mm^2 (*j*) can be represented in a plot that shows the crane arm lowering time as well as the pump pressure:
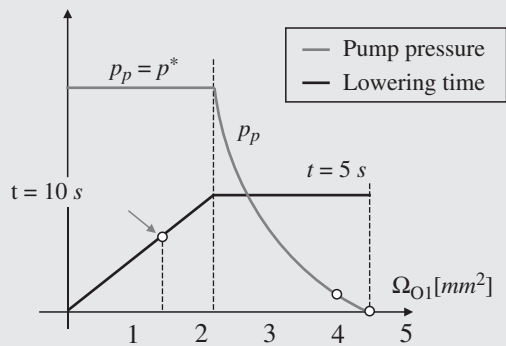
A continuous regulation system could be achieved by using an infinite position directional control valve (DCV), which integrates the orifice O1. Below is a schematic of the system that would allow for such regulation, which could be applied also to the lift and permits a similar reduction of the lift velocity.
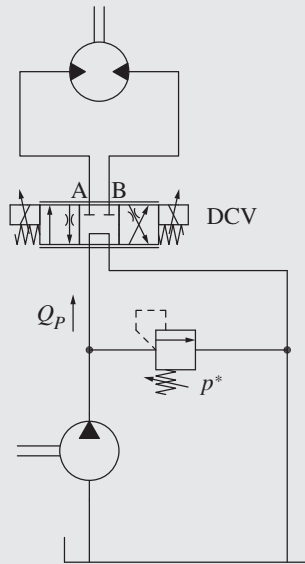
13.2 Actual Metering Control Components

In the basic architectures taken as reference in Figure 13.2 (meter-in) and Figure 13.5 (meter-out), the metering control elements are represented by variable orifices as separated components, while the direction of the actuators flow is determined with simple on/off DCVs. In reality, these two functionalities are usually integrated within the component that controls both the metering and the flow direction. Such components are referred as *proportional directional control valves*. A further distinction can be made between the more common proportional DCVs based on a single spool, which handles both the inflow and the return from the actuator, and *independent metering elements*, which control the meter-in and the meter-out area by means of separate elements.

13.2.1 Single Spool Proportional DCVs

Chapter 8 has given a high-level overview of proportional DCVs. Each valve is presented as a combination of orifices equivalent to the shifted positions of the valve. The valve control signal (such as a current, a pilot pressure, or a force on a handle) defines the relative position of the spool with respect to the lands in the bore, defining equivalent orifices on the supply and return side. The design of the spool of a metering DCV can achieve pure meter-in control, pure meter-out control, or a combination of both. Figure 13.11 shows a simple schematic highlighting the orifice areas.

Figure 13.11 also shows the simplified schematic representative of the cylinder extension, which happens when the solenoid Y1 is energized. Ω_{PA} represents the area on the supply side, while Ω_{BT} the one on the return side. The case of constant pressure supply, p_P, is considered. Applying the
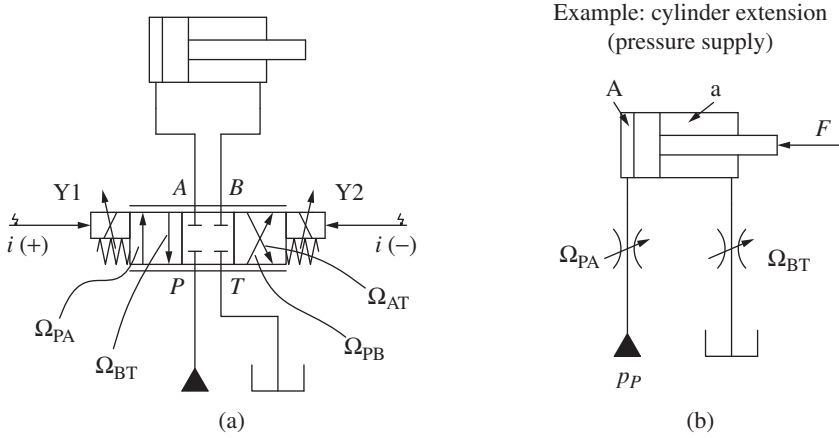
Figure 13.11 Proportional DCV with meter-in and meter-out areas and simplified schematic for the extension. (a) Proportional DCV with meter-in and meter-out areas and (b) Simplified schematic for the extension.

cylinder force balance and the two orifice equations, the expression of the cylinder speed $\dot{x}$ is

$$\dot{x}(i) = \frac{C_f}{A} \sqrt{\frac{2(A \cdot p_P - F)}{\rho \left(\dfrac{A}{\Omega_{PA}^2} + \dfrac{a}{\varphi \cdot \Omega_{BT}^2} \right)}} \tag{13.32}$$

Equation (13.32) shows how $\dot{x}$ is affected by both supply and return orifices (Ω_{PA} and Ω_{BT}) implemented by the valve; in other words, it is a combination of meter-in and meter-out controls. Furthermore, the value of $\dot{x}$ is a function of the input signal i (the solenoid current, in this case), as also Ω_{PA} and Ω_{BT} vary with i. In general, for a proportional DCV, the parameter ξ defines the *metering area ratio*:

$$\xi_A(i) = \frac{\Omega_{PA}}{\Omega_{BT}} \tag{13.33}$$

ξ_A refers to the situation where port A is connected to the supply and port B to the return. Vice versa, when the spool is shifted in the opposite direction, Ω_{PB} is the orifice area on the supply side, while Ω_{AT} on the return side. Here, ξ_B is defined as

$$\xi_B(i) = \frac{\Omega_{PB}}{\Omega_{AT}} \tag{13.34}$$

Equation (13.32) shows that, theoretically, the same value of $\dot{x}$ corresponds to an infinite combination of Ω_{PA} and Ω_{BT}; the spool designer can select the metering notches in order to obtain the most appropriate laws, depending on speeds, type of actuator, and type of loads.

If the load is known to be always resistive, the value of Ω_{BT} should be as large as possible so that the value $1/\Omega_{BT}^2$ tends to zero. If this happens, Eq. (13.32) can be simplified such that it is equivalent to Eq. (13.4), valid for the pure meter-in regulation. Meter-in is always preferred for the control of resistive loads because it does not result in pressure amplification. In fact, the pressure at the rod chamber follows Eq. (13.35):

$$p_a = \frac{1}{\varphi^2 \cdot \dfrac{\Omega_{PA}^2}{\Omega_{BT}^2} + \dfrac{1}{\varphi}} \cdot \left(p_p - \frac{F}{A} \right) \tag{13.35}$$

Equation (13.35) shows how the pressure at the rod chamber increases with the meter-out portion of the control, according to the pressure amplification principle typical of the meter-out control.

If the load can be overrunning, the value of Ω_{BT} should be lower, such that it enables the use of meter-out regulation or unloaded lowering strategies. The design of the metering areas of a proportional DCV is a very delicate topics of hydraulics. Example 13.3 will give an idea concerning a possible strategy to use for designing the valve areas. The actual strategy for designing the metering area of a valve often varies from engineer to engineer, and in many cases the approach is largely driven by experience and empirical knowledge.

> Proportional DCVs can implement meter-in, meter-out, or a combination of both with a high degree of freedom. The meter-in regulation is often the preferred choice since it does not introduce pressure amplification effects, making the solution easier to design and control.

13.2.2 Independent Metering Control Elements

A 4/3 DCV spool controls the flow direction to an actuator, establishing well-defined area laws based on its geometry. Alternatively, simpler valve elements (e.g. proportional 2/2 valves) can be used with multiple instances to achieve the same functionality. This solution adds circuit complexity, but it allows implementing flexible metering laws. Therefore, architectures that implement meter-in and meter-out with separate components are usually referred as *independent metering* systems. Figure 13.12 shows typical design solutions for this type of systems. An advantage of certain independent metering systems, such as in Figure 13.12a, is the use of metering poppets, which can also accomplish a tight seal and thus results in a low leakage when in neutral position. Although poppets have the zero-leak advantage, they present challenges in terms of control of the flow area gain with respect to spools. This aspect contributed to the limited commercial success of the solution in Figure 13.12a. However, some valve manufacturers recently introduced to the market solutions such as in Figure 13.12b.

Independent metering systems usually offer the advantage of a flexible circuit layout. For example, on the basis of measurements of the work-port pressure, the control unit can determine the load condition at the actuator (resistive or overrunning). Therefore, the control unit can implement the most suitable and efficient control strategy among meter-in and meter-out, according to the summary table in Figure 13.10, or a combination of the two.

Although the first independent metering concepts were proposed in the late 1970s, until now the use of independent metering has not encountered a significant commercial success equipment due to the following reasons:

- Independent metering requires solenoid actuation, and the solenoids are usually controlled with closed loop architectures, based on the feedback given by sensors (usually pressure sensors to measure the instantaneous pressure drop across the valve, or position sensors of the valve poppet/spool). This limits the use of independent metering system only to electrohydraulic (EH) systems. However, many hydraulic machines still utilize traditional pilot operated actuation of the hydraulic control valves (see Chapter 8) and avoid the use of EH technology.
- Advanced EH components, such as independent metering valves that integrate additional sensors, usually increase the overall cost of the machine and also decrease the system reliability. However, the latest tendency toward automation and remote operation of hydraulic machines demands for the more advanced EH systems. For this reason, several commercial solutions are currently available for valves (similar to those shown in Figure 13.12).
- For an EH machine, the use of independent metering valves requires more solenoids than a comparable solution based on traditional EH DCVs. Therefore, the independent metering technology is considered to be among the most expensive of the available EH technologies.
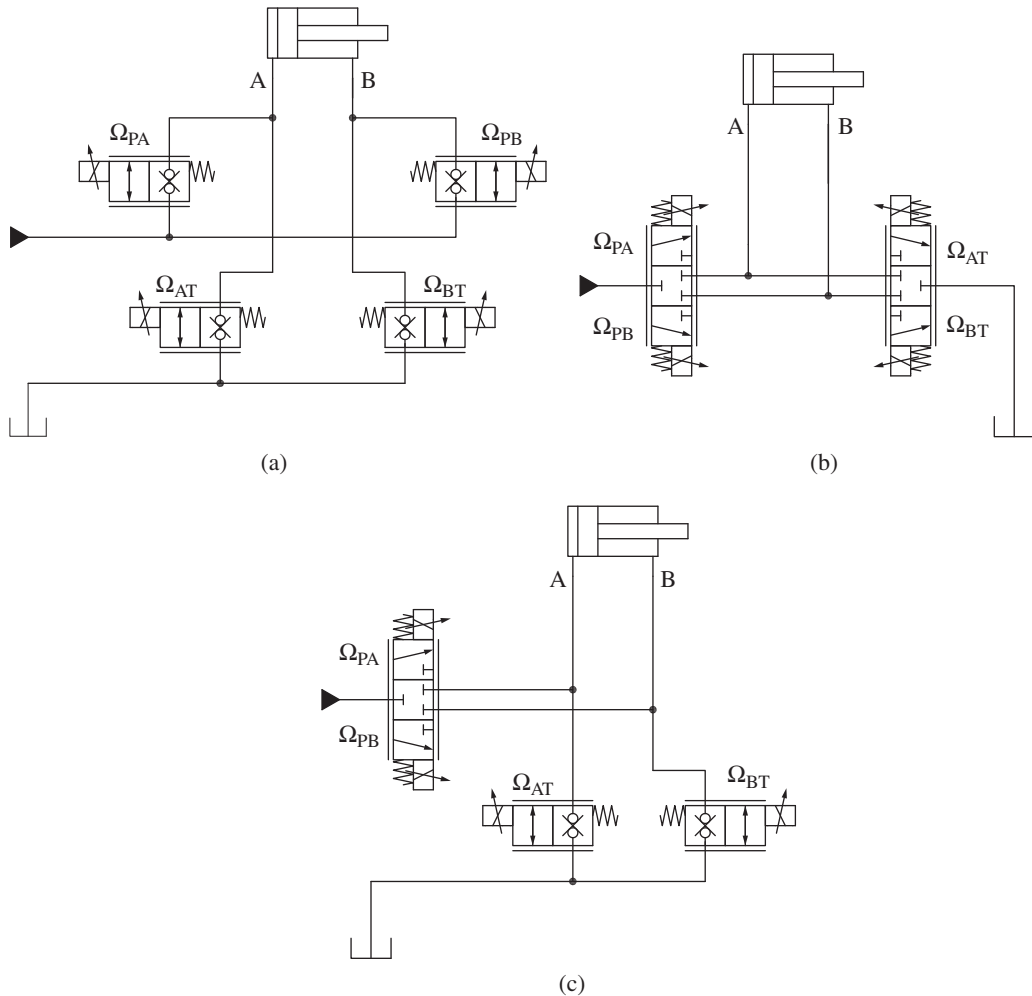
Figure 13.12 Different designs of independent metering elements: (a) metering poppets, (b) split spools concept, (c) hybrid solution.

- In traditional spool valves, the allowable machining tolerances on the spool/sleeve permits to implement accurate ratios between the different valve porting areas, thus permitting fine regulation of the actuator velocities. In the case of independent metering valves, realizing area ratios with similar accuracy requires a proper coordination between the commands given to the two separate spools/poppets, which is difficult to consistently repeat among several specimens.

Example 13.3   Metering control of a forklift mast

Problem: A forklift mast is operated in lifting and lowering with two single-acting cylinders with bore diameter of 80 *mm*. The hydraulic system uses a 3/3 directional proportional control valve, solenoid operated. To accomplish the lift, a constant pressure supply of 140 *bar* is used. The lowering is achieved through gravity. Calculate the metering areas of the valve spool to control the mast of a forklift truck, knowing that the overall load lifted by the mast is 2000 *kg*. The maximum lifting speed requirement is 0.5 *m/s*, while the requirement for the maximum lowering speed is 0.65 *m/s*.

For the calculations, assume an orifice flow coefficient equal to 0.65 and an oil density of 850 *kg/m³*.

Considering the case of empty forks, when the pressure at the cylinder bore is only 30 *bar*, what is the performance of the hydraulic system in terms of lifting and lowering speed?

Represent the hydraulic schematic of the system. Furthermore, consider how to modify it in case there is a zero-leakage requirement for the cylinder (which is not possible to satisfy by using a spool valve).

Given:

A hydraulic system for lifting and lowering a forklift mast based on a 3/3 directional control valve. Following parameters are known:

Bore diameter of the single acting cylinder, $d_B = 35$ *mm*
Mass lifted by the cylinders, $M = 2000$ *kg*
Supply pressure, $p^* = 140$ *bar*
Maximum lifting speed, $\dot{x}_{up} = 0.5$ *m/s*
Maximum lowering speed, $\dot{x}_{dn} = 0.65$ *m/s*
Orifice coefficient, $C_f = 0.65$
Oil density, $\rho = 850$ *kg/m³*
Acceleration of gravity, $g = 9.81$ *m/s²*
Cylinder pressure without load, $p_{A, light} = 30$ *bar*

Find:

a) The hydraulic schematic of the system.
b) The DCV port areas for both lifting and the lowering functions, Ω_{P-A} and Ω_{A-T} at the maximum velocity requirements.
c) Describe a possible solution for the spool area timing function, $\Omega_{P-A} = \Omega_{P-A}(x)$ and $\Omega_{P-T} = \Omega_{A-T}(x)$ for a continuous regulation.
d) Evaluate the system performance at empty load: $\dot{x}_{up,light}$, $\dot{x}_{down,light}$.
e) Discuss possible solutions for a leakage-free case (using additional poppet valves).

Solution:

(Continued)

Example 13.3 (Continued)

a) The figure above shows the ISO schematic for controlling the forklift: the mast is controlled using a three-position three-way proportional spool DCV with electric control. Although the supply is limited at p^*, a relief valve is used to protect the actuators against overloads when the DCV is in neutral position.

P indicates the pressure supply port of the DCV, while T the return port. The only work-port to the single acting cylinder is A.

b) The area Ω_{P-A} controls the lifting through a meter-in control, while the lowering occurs by gravity through the area Ω_{A-T} (meter-out control). To calculate these areas, it is first necessary to evaluate the flow rates in lift and lower operation. The required cylinder bore flow rates in lifting and lowering conditions are

$$Q_{up} = 2 \cdot \dot{x}_{up} \cdot A = 2 \cdot 0.5 \, [m/s] \cdot \frac{\pi \cdot 1225 \, [mm^2]}{4} \cdot 0.06 = 57.7 \ l/min$$

$$Q_{dn} = 2 \cdot \dot{x}_{dn} \cdot A = 2 \cdot 0.65 \, [m/s] \cdot \frac{\pi \cdot 1225 \, [mm^2]}{4} \cdot 0.06 = 75.0 \, l/min$$

The pressure at the cylinder bore generated by the load is

$$p_A = \frac{Mg}{2A} = \frac{2000 \, [kg] \cdot 9.81 \, [m/s^2]}{2 \cdot \frac{\pi \cdot 35^2}{4} \, [mm^2]} \cdot 10 = 102 \ bar$$

To meet the lifting speed requirement, the meter-in area Ω_{P-A} needs to be equal to

$$\Omega_{P-A} = \frac{Q_{up}}{C_f} \sqrt{\frac{\rho}{2(p^* - p_A)}} = \frac{57.7 \, [l/min]}{0.65 \cdot 60\,000} \sqrt{\frac{850 \, [kg/m^3]}{2 \cdot (140 - 102) \, [bar] \cdot 10^5}} \cdot 10^6 = 15.6 \ mm^2$$

Similarly, the meter-out area to achieve the desired lowering speed is

$$\Omega_{A-T} = \frac{Q_{dn}}{C_f} \sqrt{\frac{\rho}{2p_A}} = \frac{75.0 \, [l/min]}{0.65 \cdot 60\,000} \sqrt{\frac{850 \, [kg/m^3]}{2 \cdot 102 \, [bar] \cdot 10^5}} \cdot 10^6 = 12.4 \ mm^2$$

In these conditions, both orifices Ω_{P-A} and Ω_{A-T} are metering orifices.

c) The spool design should achieve the metering areas for lifting and lowering found in (b) at maximum stroke. The simplest design of the spool would implement linear area trends. However, in forklifts, it is critical for the operator to have the ability to achieve fine adjustments of the forklift mast position. For this purpose, the spool design can be optimized by implementing a nonlinear curve where the area increase is small in the first part of the stroke, and it becomes steeper in the second part of the stroke. In this way, the control resolution can be improved for fine movements. As shown in the figure below, the spool notches can be easily shaped to achieve such characteristic.
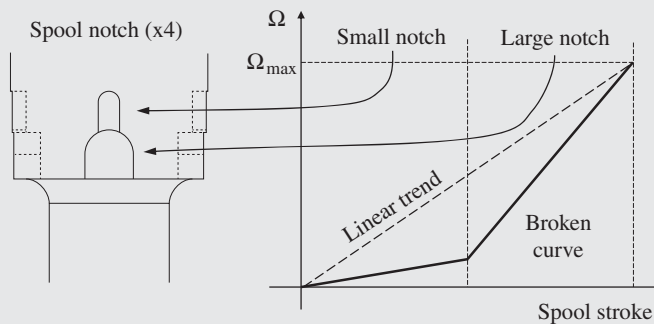
d) When the forks are unloaded, with the DCV valve described above the machine operates differently. In fact, the maximum lifting and lowering speed become

$$\dot{x}_{\text{up,light}} = \frac{C_f \Omega_{P-A}}{2A}\sqrt{\frac{2(p^* - p_{A,\text{light}})}{\rho}} = \frac{0.65 \cdot 15.6\,[mm^2]}{2 \cdot \dfrac{\pi \cdot 35^2}{4}\,[mm^2]}\sqrt{\frac{2 \cdot (140 - 30)\,[bar] \cdot 10^5}{850\,[kg/m^3]}}$$

$$= 0.84\,\text{m/s}$$

$$\dot{x}_{\text{dn,light}} = \frac{C_f \Omega_{A-T}}{2A}\sqrt{\frac{2 p_{A,\text{light}}}{\rho}} = \frac{0.65 \cdot 12.4\,[mm^2]}{2 \cdot \dfrac{\pi \cdot 35^2}{4}\,[mm^2]}\sqrt{\frac{2 \cdot 30\,[bar] \cdot 10^5}{850\,[kg/m^3]}} = 0.35\,m/s$$

As one can immediately notice, the lifting speed is higher than that in the previous case of full load, while the lowering is slower. The lowering speed is almost reduced to half of the previous value. This finding reflects the load dependency effects also highlighted by all formulas involving the actuator velocity in the basic meter-in and meter-out control architectures described in Section 13.1.

This feature makes designing a spool for this application sometimes challenging: if the fully loaded case is taken as reference, the empty forks performance might not be acceptable. Vice versa, if the empty case is taken as the design reference, the loaded lowering speeds could present a dangerous situation. This issue can be addressed in several ways, the easiest one can be to size the spool for an intermediate load value and eventually prevent excessive lowering speeds by using a two-way flow control valve (FV) or a pressure control valve (PV) as shown in the two schematics below.
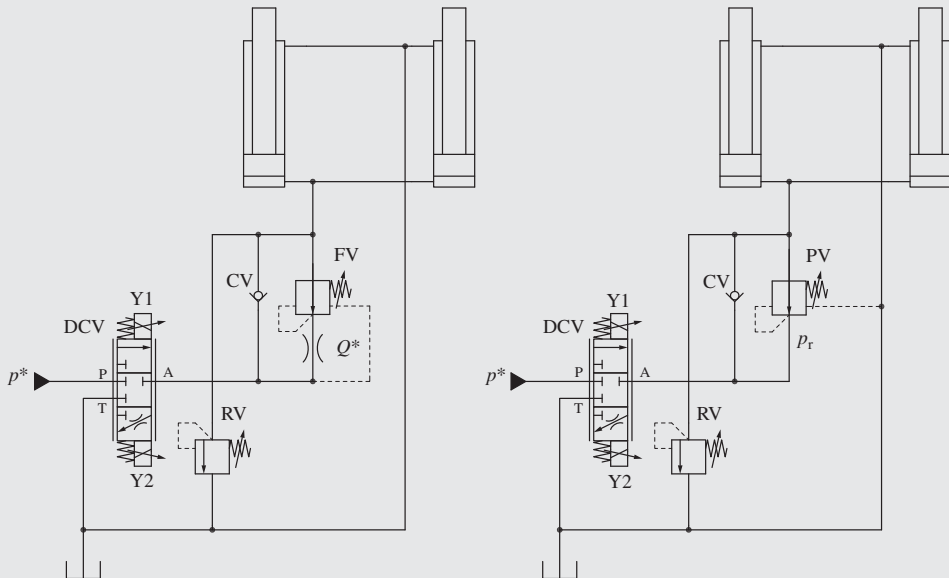
In both cases, these additional valves are active only during lowering, thanks to the CV. In the case of the left figure (valve FV), the valve limits the lowering flow to Q^* and it is fully open if the flow is below its setting. This is consistent with the behavior of two-way flow control valves as presented in Chapter 8.

(Continued)

Example 13.3 (Continued)

In a similar way, the reducing valve PV of the schematic at the right side of the figure limits the pressure at port A of the main spool during the lowering phase to the setting value p_r, therefore preventing excessive lowering speeds.

e) In case the machine had a zero-leakage requirement, a poppet valve needs to be used to prevent drifting of the mast. The simplest way to achieve this feature is to include an additional solenoid valve (SV), as shown in the figure below (left circuit). However, many times, adding a solenoid is not an option (for example when the main spool has manual control). In this case, the main spool design needs to change. A possible solution is shown in the figure below (right-side circuit): the main DCV becomes a four-way valve, where port B is used to open a pilot operated CV, whenever lowering is commanded. Load holding valves will be described in more details in the next chapter.
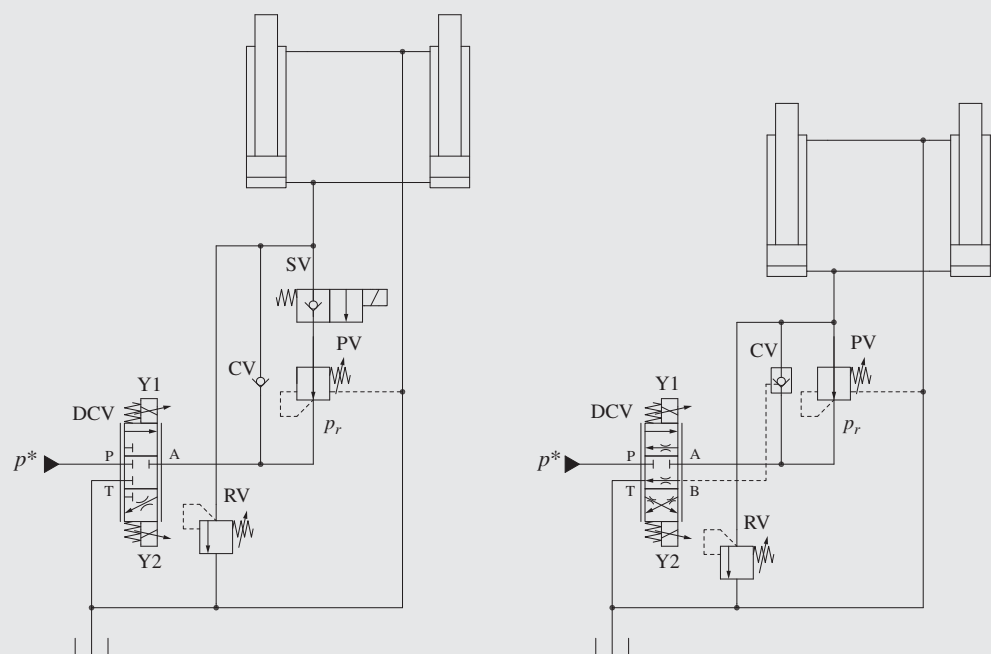
The chart below summarizes the functionality of the main DCV spool for the four-way operation. The connection B-T is open in neutral and when lifting is commanded. When the operator commands the lowering of the forks, initially B-T transitions to the close position, and then it is connected to P through a small notch, since it is just a signal line. Only after this connection is generated, the main notch A-T starts opening.
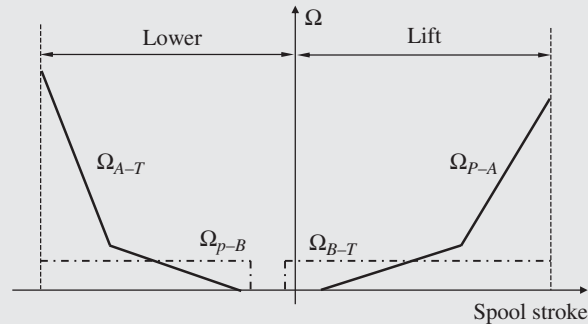
13.3 Use of Anticavitation Valves for Unloaded Meter-out

The circuit in Figure 13.5 used to illustrate the main features of the meter-out control highlighted the particular role that the anticavitation valve plays during overrunning loads. By connecting the return of the system to the supply, the anticavitation valve avoids cavitation at the actuator, but it also allows controlling the actuator velocity without pressurizing the supply. This is a very attractive feature for a designer, because

- Anti-cavitation valves used for unloaded meter-out allows reaching high actuator velocity independent on the available pump flow
- There is (ideally) no energy request at the supply

The basic architecture in Figure 13.5 establishes the unloaded lowering condition only for a large opening of the meter-out orifice ($\Omega > \Omega_U$). However, different meter-out architectures can be used to achieve unloaded lowering for a wider range.

A realistic example is the boom of a tractor loader attachment (Figure 13.13). At first, one could think that cavitation during the lowering phase of the implement (solenoid Y1 energized) would not cause significant harm. In fact, during the lowering of the boom, without CV, the cavitation that would occur in the cylinder rod chamber would not prevent the boom from lowering. Additionally, cylinders may be quite resistant to the structural damages due to the air and vapor bubbles collapse that occur during cavitation. If so, why is the anticavitation valve needed?
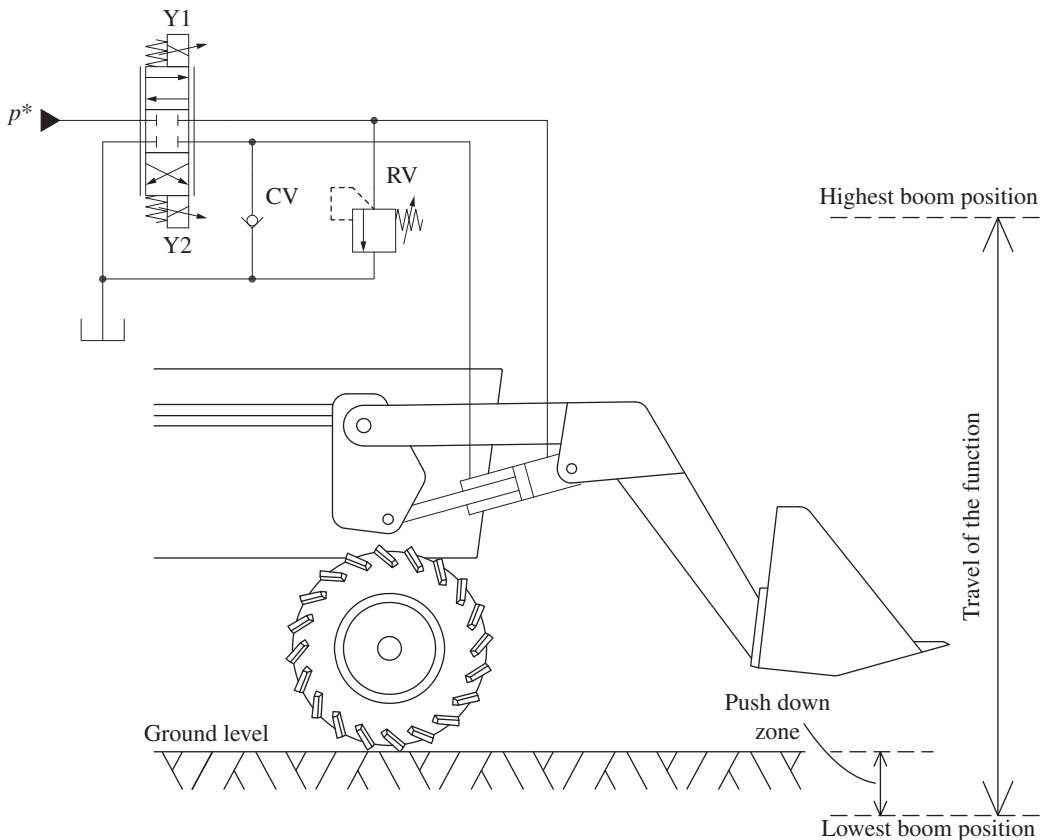
Figure 13.13 The loader attachment for a tractor is a typical example of use of anticavitation valves to achieve unloaded lowering.

When the operator commands a fast lowering of the boom, perhaps with the engine at low idle (thus with the supply pump spinning at low engine rpm), the boom cylinder retracts at a high speed causing an unloaded meter-out situation. This is because the pump supply is not capable of providing the necessary make up flow on the rod side, implying that the pressure in the rod chamber falls below the atmospheric value, resulting with the oil releasing air and eventually vaporize, as described in Chapter 2. When the boom touches the ground, the load turns from overrunning to resistive. At this point, the loader would not be able to push down on the soil until the supply provided the fluid necessary for filling the voids. It is only when the fluid completely returns to the liquid phase, the system can build enough pressure to generate a downward force. This would cause a significant time delay in the boom motion, negatively perceived by the operator. The anti-cavitation valve, if used, maintains the fluid in the rod chamber near the tank pressure so that when the load changes direction, the system can immediately build pressure to oppose the resistive force.

So far, the anticavitation CV has been considered as an ideal component, assuming a null pressure drop for the flow crossing it. Figure 13.14 shows a realistic characteristic of a check valve (CV1) used as anticavitation: the pressure drop raises as the flow increases. If Q_M is the make-up flow across the valve, the corresponding pressure drop is p_M. In other words, the tank pressure p_0 has to be greater than p_M in order for the system to be able to provide the necessary make-up flow Q_M to the cylinder bore side.

Hydraulic circuits are often equipped with solutions for increasing the return or tank pressure in order to ensure the necessary make-up flow through the anticavitation valves. The first solution consists of pressurizing the reservoir, for example, by means of a source of pressurized air, when already available on the application (pressurized air can be available in several off-road vehicles). This solution is relatively simple, although it might require reinforcements to the oil tank structure.

Alternative solutions are represented in Figure 13.15a,b. Here, a counterpressure valve is placed between the anticavitation CV and the reservoir. The purpose of such element is to increase the return line pressure so that the anticavitation CV uses a higher pressure downstream it. In this way, a higher pressure drop can be established at the anticavitation valve. In the first case (a), the counterpressure valve CV2 has a fixed setting p_R. This solution is very simple, but it introduces a constant pressure drop in the tank line, which causes a power loss, since the return pressure p_R is always present (in the case of the loader, for example, also during load lifting). This is why, sometimes, it can be convenient to have a counterpressure valve with a variable setting, as in case (b). In this case, the valve V2 is controlled with an external signal p_X. The return pressure maintained by this valve is $p_X + s$. The signal p_X can be electrically controlled (e.g. applied on demand)

(a) (b)
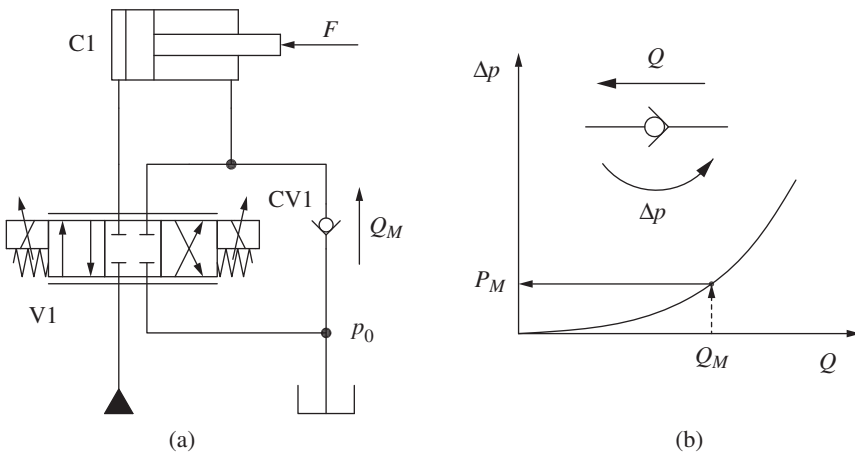
Figure 13.14 Anticavitation valve: schematic (a) and real valve characteristic (b).
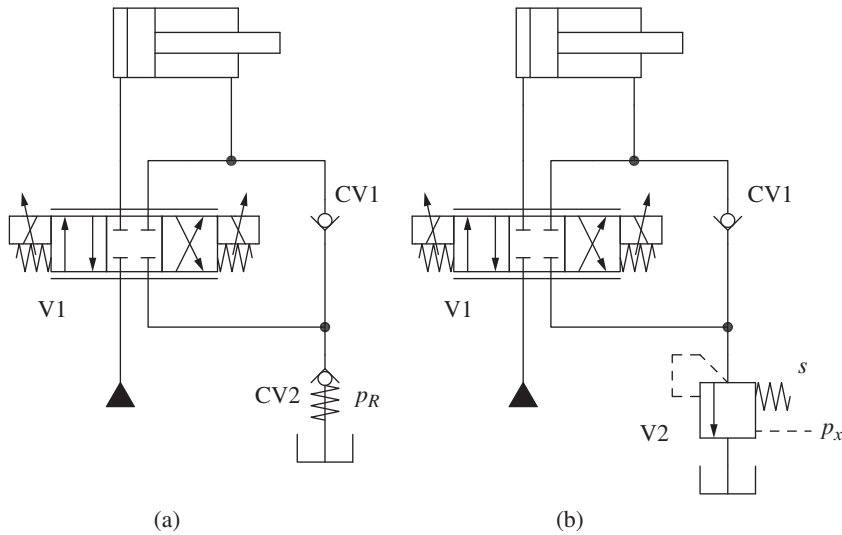
Figure 13.15 Pressurization of return lines for anti-cavitation function using a fixed (a) or a variable (b) setting pressure control valve.

or can also be connected to one of the pilot pressures of the main DCV spool (the one connected to the lowering configuration).

Problems

13.1 The system in the figure below is designed to control the velocity of a cylinder loaded with 50 kN. Consider only position 1 of the directional control valve (extension), in overrunning load conditions. Determine the area range for the meter-out orifice necessary to obtain a regulation from zero to the maximum speed allowed by the 100 cm³/rev variable displacement pump. Determine also the maximum area of the meter-out orifice, which permits to extend the overrunning load at the maximum speed with minimum pump pressure. Assume the orifice coefficient to be 0.7 and the fluid density as 850 kg/m³.
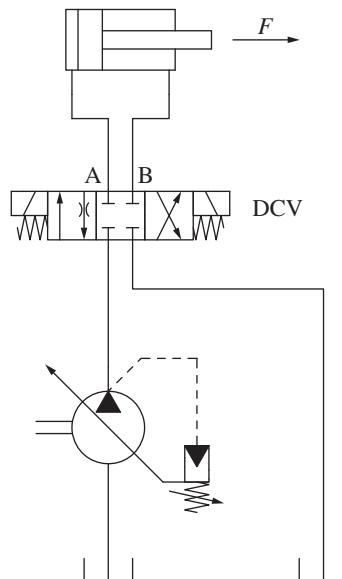
13.2 For the system in figure, consider
- Load, F of 9.1 kN
- Piston diameter, $d_{BORE} = 40/\sqrt{\pi}$ mm
- Rod diameter, $d_{ROD} = 20/\sqrt{\pi}$ mm
- Pressure setting of relief valve, $p^* = 300$ bar
- Inlet flow rate (rod side), $Q_{ROD} = 30\,l/min$
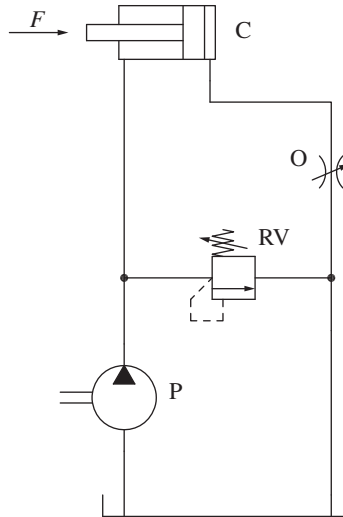
Determine
a) The cylinder pressure (piston side, p_A) in bar, if the inlet pressure (rod side, p_a) is 30 bar
b) The piston velocity, v, in m/s, for condition (a)
c) The cylinder pressure (piston side, p_A) if the inlet pressure (rod side, p_a) is 300 bar (relief valve open)
d) Determine the area Ω in mm^2 of the orifice if the piston velocity, v, has the value of 1.5 m/s. Assume the fluid density, ρ, equal to 900 kg/m^3, and the orifice coefficient, C_f, equal to 0.7.
e) How is the area reduction/increase of the variable orifice W if we want to reduce the piston velocity by 50%? (1) Same area; (2) Half area; (3) 1/4 of the area; (3) Square of the area; (4) Square root of the area. Justify the answer.
f) What is the function of the orifice in the system above (metering, compensator, dynamic orifice)? Does the answer depend on the orifice opening area? *Assume that if the behavior of the orifice changes for small opening areas/large opening areas.*

13.3 Consider the hydraulic system in the figure below.
a) Fill the boxes associated with all the system sensors with the proper number.
b) Find the diameter of the orifice ($D_{orifice}$) that can allow to move the cylinder at 0.45 m/s.
c) Calculate the system efficiency (ratio between power output and power input) in the two values of $D_{orifice}$, assuming ideal components.
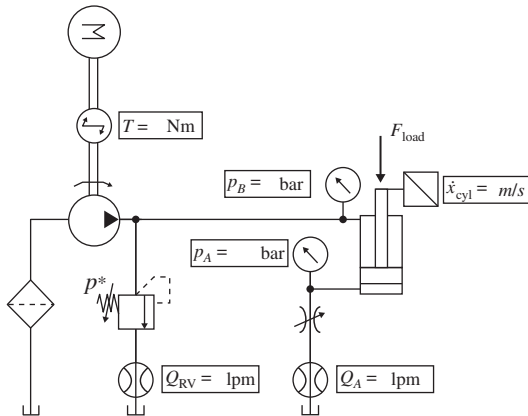
Cylinder parameters:
D = 90 mm (piston diameter)
d = 65 mm (rod diameter)

V_{pump} = 200 cc
pump speed = 1000 rpm

$\eta_{v\,pump} = \eta_{hm\,pump} = 1$
F_{load} = 15 kN
$D_{orifice}$ = 3 mm; $C_{d\,orifice}$ = 0.65
p^* = 150 bar
ρ_{oil} = 850 kg/m^3

13.4 A needle valve is used to control the extending speed of a hydraulic cylinder. It is placed in the outlet line of the hydraulic cylinder as shown in the figure. The following data are given:

1. Desired cylinder speed = 10 in/s
2. Cylinder piston diameter = 2 in
3. Cylinder rod diameter = 1 in
4. Cylinder load = 1000 lb
5. Density of oil = 56 lb/ft^3
6. Pressure relief valve (PRV) setting = 500 psi

Determine the required capacity coefficient of the needle valve, and the flow area of the valve, Assuming C_d = 0.62,
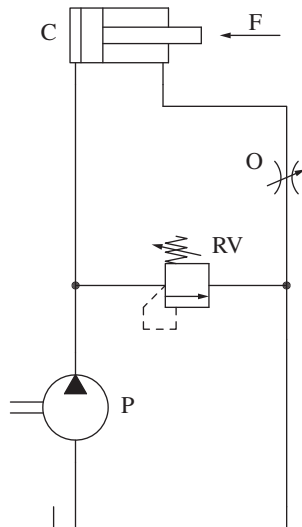
13.5 The hydraulic system shown in the figure is used to operate a winch that pulls logs up to hills. During the lifting, the load is always resistant.
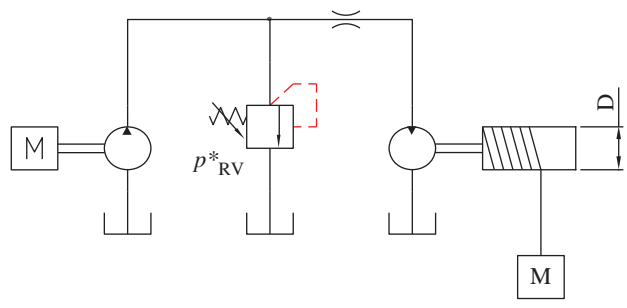
Determine
1. The pressure at the inlet of the motor $p_{\text{motor,IN}}$ $[bar]$
2. The pressure at the pump delivery p_{delivery} $[bar]$
3. The flow rate passing through the orifice Q_{orif} $[l/min]$
4. The flow rate discharged by the relief valve Q_{RV} $[l/min]$
5. The power requested to the engine W_{request} $[kW]$
6. For the condition at point 2, the speed of the motor $[rpm]$
7. For the conditions at the point 2, the overall efficiency (η_{overall}) of the system (power$_{\text{out}}$/power$_{\text{in}}$)
8. For the conditions at the point 2, the linear speed of the log (v_{log}) $[m/s]$

The following data are given for the transmission:

$\eta_{v,\text{pump}}$	0.93		Winch diameter, D	50	mm
$\eta_{\text{hm,pump}}$	0.91		Mass, m	600	kg
$\eta_{v,\text{motor}}$	0.95		A_{orifice}	6	mm^2
$\eta_{\text{hm,motor}}$	0.94		g	9.81	m/s^2
p^*_{RV}	210	bar	p_{tank}	0	bar
V_p	20	cc/rev	n_{engine}	2000	rpm
V_m	60	cc/rev	C_d	0.62	
ρ	850	kg/m^3			

Chapter 14

Load Holding and Counterbalance Valves

This chapter focuses on two common elements often present in hydraulic systems designed to control actuators that handle gravitational loads: load-holding valves and counterbalance valves (CBVs). Both valves are used to maintain a certain pressure level within the actuator such that the hydraulic control system (either a meter-in control or a primary control) can function properly even for overrunning loads.

Load-holding valves are used to maintain the position of an actuator under an external load by ensuring that there is no flow through the valve. Essentially, these valves achieve zero leakage, but they cannot be used as metering or compensator elements. On the other hand, CBVs can implement multiple functionalities, including load holding, zero leak, and pressure relief. Additionally, CBVs provide a robust solution to achieve the control of overrunning loads with primary or meter-in control.

14.1   Load-holding Valves

A very common requirement of certain hydraulic machines is the holding of suspended loads, especially when the equipment is off or in standby mode. This can be seen as a special case of actuator control with zero commanded velocity but requiring no power consumption.[1] Load holding is often a functional requirement. However, in some applications such as hydraulic cranes, it can be mandated by safety standards. In many of these cases, load holding must be guaranteed not only during normal operation of the equipment but also in case of hose failure. In the circuits in Figures 13.11 and 13.13 of the previous chapter, when no movement is commanded, the spool valve in neutral configuration holds the cylinder at zero speed. However, if by accident, the hose or pipe connecting the valve to the pressurized side of the actuator was damaged, the load would be free to fall due to gravity. This represents a very dangerous situation in applications where people or other objects could be present near the suspended load, for example, in the case of material handling cranes.

In general, hydraulic control valves are always characterized by sliding elements, which move inside a sleeve or a bore. The relative motion of these sliding elements requires clearances, which in turb leads to a certain amount of leakage. Therefore, ideal load holding (i.e. exact zero leakage) is not achievable but can only be approximated. The amount of leakage allowed by hydraulic valves

---

1 This case is different from the position servo system explained in Chapter 8. In fact, for the servovalve to maintain a position control with varying loads, the spool continuously meters the flow to the actuator work-ports, thus leading to a nonzero power consumption at the supply system.
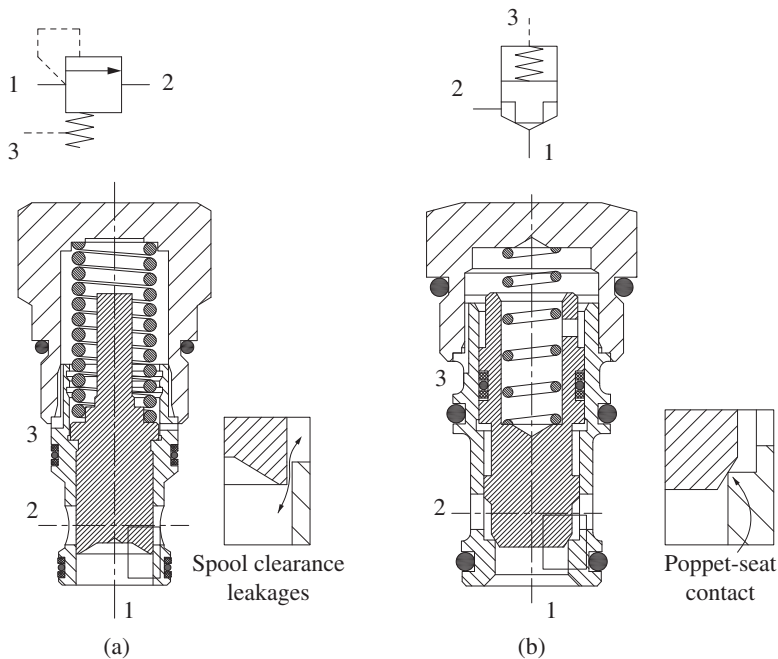
Figure 14.1 Spool (a) and poppet (b) elements achieving a similar functionality.

varies with the type of sliding element. The most common ones are the spool type and the poppet type, which, in terms of holding, have significant differences. The two valves represented in Figure 14.1 achieve very similar functionality, in terms of circuits. They are both two-way valves, normally closed with a spring chamber supplied by an external pilot pressure. The spring force and the pilot pressure keep the valve in neutral position, blocking the passage from port 1 to port 2. The pressure on the nose side (1) has the effect of opening the valve. The two sliding elements have a different design: the left valve is spool type, while the right valve is poppet type. From the magnified view, it is possible to see the two leakage paths for the oil (port 1 is supposed at higher pressure than 2), which are quite different from each other. The spool has a circumferential clearance with the bore, which creates a leak path between the pressurized cylinder port and the tank port. Usually, the value of the clearance in mobile spool valves is between 2 and 20 μm with respect to the diameter. On the other hand, the poppet is held on the seat by the fluid pressure and the spring thereby realizing metal-to-metal contact between the two parts. The leakage in this case is caused only by the imperfections in the manufacturing of the parts, and it is at least one order of magnitude smaller than the spool valve.

In the case of spool valves, the leakage rate is usually provided in cubic centimeter per minute, while in the case of poppet valves, it is measured in drops per minute where one cubic centimeter is equivalent to approximately 20 drops. When a valve limits leakage rates in the order of drops per minute, it is commonly referred as a *zero-leakage valve*, and it is suitable for load holding functionality.

Poppet-type valves typically allow much lesser leakages than spool valve. **Zero-leakage valves** (with actual leakages in the order of few *drops/min*) can be used for load holding.

14.1.1 Pilot Operated Check Valve

The simplest hydraulic components used for load holding is the pilot operated (PO) check valve (Figure 14.2). The valve presents two sliding elements: a poppet, which separates ports A (usually connected to the valve) and B (usually connected to the cylinder), and a piston, connected to an external pilot pressure through port X. If the pressure at p_X is null, the valve operates as a simple check valve, allowing free flow from A to B and blocking flow in the opposite direction. The piston, in this case, does not have any effect on the valve operation.

When pressure is applied at port X and it is greater than p_A, the piston moves in contact with the poppet and they can be treated as a single body. The closing force, F_c, and the opening force, F_o, on the poppet can be calculated as follows:

$$F_c = p_B \cdot A_2 + F_{\text{spring}}$$
$$F_o = p_X \cdot A_1 - p_A \cdot (A_1 - A_2) \tag{14.1}$$

In this simplified analysis, the effect of friction forces on the poppet or of flow forces is neglected. The two forces in Eq. (14.1) equalize when the pilot pressure is equal to p_X^*:

$$p_X^* = \frac{1}{A_1} \left(p_B \cdot A_2 + F_{\text{spring}} + p_A \cdot (A_1 - A_2) \right) \tag{14.2}$$

Introducing the parameter $\alpha = A_1/A_2$ (known as *pilot ratio*[2]) and assuming $F_{\text{spring}}/A_1 \cong 0$ (the springs used in check valves usually establish relatively low force), p_X^* becomes

$$p_X^* = p_A + \frac{p_B - p_A}{\alpha} \tag{14.3}$$

If $p_X < p_X^*$, the component still behaves as a check valve blocking the flow from B to A. However, if $p_X > p_X^*$, the piston pushes the poppet to a completely open position allowing free flow from B to A.

It is very important to remark that PO check valves are designed with low spring forces and therefore work practically as on/off devices. In other words, these valves are not suitable to operate as either metering or compensator element in the circuit.

Figure 14.3 represents a typical application of a PO check valve for holding a differential cylinder. During cylinder lowering, the orifice O needs to implement a pump-loaded lowering condition, working either as metering or compensator. As described in Chapter 13, for low areas, the orifice O will work as a metering orifice, affecting the actuator velocities. For larger areas, the orifice will work as a compensator, creating enough pressure to balance the actuator. Since anti-cavitation valves are not used, too large an area will lead to a non-controlled lowering condition.
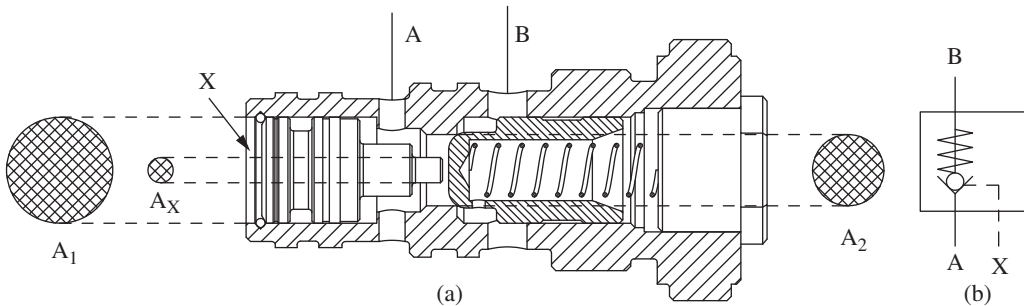
Figure 14.2 Pilot operated check valve (a) and equivalent symbol (b).

---

2 The pilot ratio is greater than 1 and typical values for pilot operated check valves are in the range of 3–10.
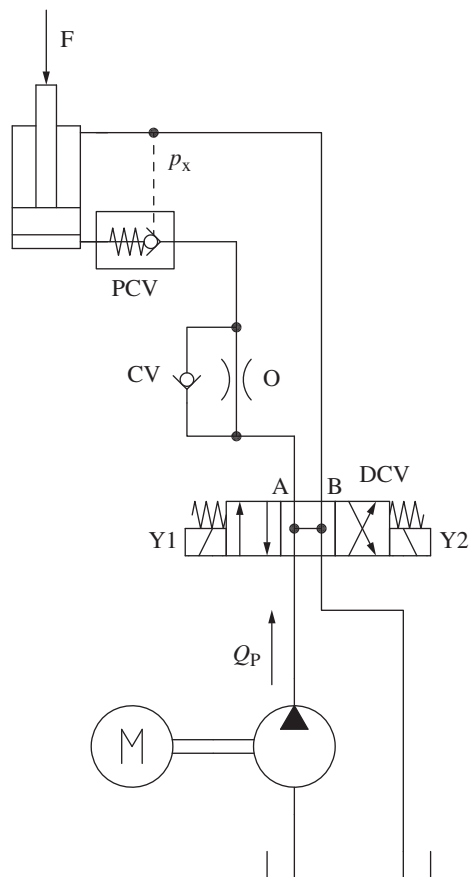
Figure 14.3 Typical circuit utilizing a pilot operated check valve for load holding. The orifice O deserves special attention as it is a necessary element to avoid chattering during lowering.

The orifice O will establish a pressure p_X high enough to keep the piloted check valve (PCV) open. If the orifice O was either absent or too large, the lowering of the cylinder would be characterized by instability and chattering as the valve HV would repetitively open and close. In particular, when HV is closed, the system would build up pressure until it opens. Then, when HV is opened, the load would free fall, which causes the pilot pressure to decrease and the HV to close suddenly. In order to avoid this undesirable situation, PO check valves are used in combination with flow restrictions in the return line (for example, with unidirectional orifices or with proper directional control valve with proper DCV spools). Alternatively, the PO check valves can be replaced by load-holding valves with compensator characteristics, such as CBVs.

Similar to other load holding devices, PO check valves are also usually mounted directly on the actuator. This enables the system to comply with safety requirements that demand the load-holding condition to be maintained regardless of hose failures.

Example 14.1   Application of a PO check valve

With reference to the circuit below, a cylinder with a 40 *mm* bore and a 25 *mm* rod is used to control a 2000 *kg* load. A PO check with a 4:1 pilot ratio is used as load-holding device mounted on the cylinder bore port. The pump maximum flow is 50 *l/min*, while its pressure compensator

is set to 180 bar. Find the maximum diameter for the orifice O that allows a stable lowering of the load.
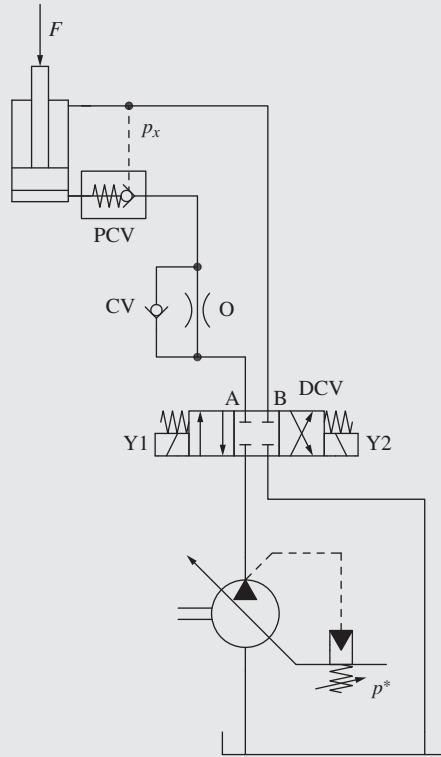
Given:

Cylinder bore diameter, $d_B = 40\,mm$
Cylinder rod diameter is, $d_R = 25\,mm$
Pump compensator pressure, $p^* = 180\,bar$
Mass on the actuator, $M = 2000\,kg$
Maximum pump flow, $Q = 50\,l/min$
PO check pilot ratio, $\alpha = 4$

Find:
Orifice diameter d_O that allows stable lowering of the load

Solution:
As a PO check is not a metering device, to achieve a stable lowering, the orifice should be sized to maintain a positive pump pressure when the lowering solenoid Y2 is activated. In particular, the following equation needs to be satisfied during lowering:

$$p_x \geq \frac{1}{\alpha} \cdot p_B$$

p_B represents the pressure at the cylinder bore. The balance of the forces on the cylinder during lowering is the following:

$$p_B = \frac{F}{A} + \frac{1}{\varphi} \cdot p_x$$

Example 14.1 (Continued)

Combining the two equations, the following condition needs to be satisfied:

$$p_B \left(\varphi - \frac{1}{\alpha} \right) \geq \frac{F}{A}$$

In the limit case where the full pump flow is diverted to the rod side during lowering, the bore pressure is established by the pressure drop across the orifice O caused by the return flow from the bore to the tank:

$$p_B = \left(\frac{\varphi \cdot Q_p}{C_f \cdot \Omega_O} \right)^2 \cdot \frac{\rho}{2}$$

Substituting this equation into the previous, one can find the sizing condition for the orifice O:

$$\frac{1}{\Omega_O} \geq \frac{C_f}{Q_p} \cdot \sqrt{\frac{2F}{A \cdot \varphi \cdot \left(\varphi - \frac{1}{\alpha} \right) \cdot \rho}}$$

The value of the cylinder ratio φ becomes

$$\varphi = \frac{d_B^2}{d_B^2 - d_B^2} = \frac{40^2 \, [mm^2]}{40^2 - 25^2 \, [mm^2]} = 1.64$$

Therefore, the solution becomes

$$\frac{1}{\Omega_O} \geq \frac{0.65 \cdot 60\,000}{50 \, [l/min]} \cdot \sqrt{\frac{2 \cdot 196\,20 \, [N] \cdot 10^6}{\frac{\pi \cdot 40^2}{4} [mm^2] \cdot 1.64 \cdot (1.64 - 0.25) \cdot 850 \, [kg/m^3]}}$$

The result is

$$\Omega_O \leq 10.1 \, mm^2$$

This area corresponds to an orifice diameter $d_O = 3.6 \, mm$. In this condition, the pressure at the cylinder bore during lowering is approximately 183 *bar*, while the pressure p_x is 45 *bar*.

14.2 Counterbalance Valves

CBVs are elements usually placed in proximity of actuators. They can implement three important functions:

1) hold the load with zero-leakage
2) protect the actuator from over-pressurization
3) guarantee the actuator force equilibrium under overrunning load conditions

For this last feature (3), a CBV functions as a compensator orifice. A CBV establishes a counter-pressure at the outlet port of the actuator, allowing the hydraulic control system (based on either a primary control or a metering control) to govern the actuator speed, independent of the load magnitude.

Figure 14.4 shows the typical hydraulic symbol used for a CBV: port C connects to one of the actuator ports, port V to a DCV or flow supply and X is a pilot signal usually connected to the opposite actuator port. The valve is normally closed, as a result of a spring, F_{CBV}. The CBV can
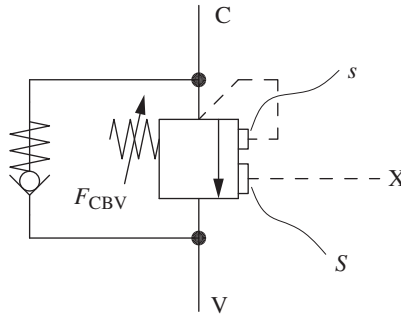
Figure 14.4 ISO symbol for a counterbalance valve.

be forced to open either by the pressure at port C, which acts on an area of influence s, or by the pressure at port X, acting on the area S, or a combination of the two pressures. The ratio of the two areas of influence is a characteristic parameter of each CBV and it is usually referred to as **pilot ratio**:

$$\alpha = S/s \tag{14.4}$$

The CBV accomplishes also the check valve functionality, allowing free flow from V to C.

14.2.1 Basic Operating Principle

The concept of overrunning loads was introduced in Chapter 10 (Part III), where the simple example of a free-falling cylinder was presented. The same circuit is presented again here, in Figure 14.5 (left). When the solenoid Y2 is actuated, the system loses control of the motion. As mentioned in Chapter 13, the circuit can be corrected by introducing a meter-out control element. So far, meter-out elements have been presented as either a fixed or a variable flow restriction, set by an external command.

CBVs achieve the same concept of a variable restriction (compensator) with an opening that is automatically set hydraulically, by a combination of pressure signals. In this sense, a CBV can be viewed as somewhat equivalent to a pressure relief valve, located on the overrunning side of a load. As shown in Figure 14.5 (right), the relief valve creates a restriction on the lowering side, which allows the pump to always see a positive pressure. In this way, a stable lowering piston velocity is always guaranteed. However, this functionality can be achieved by a pressure relief valve with has a fixed setting, determined for the worst-case scenario:

$$p^*_{\text{relief}} \geq \frac{F_{\max}}{A} \tag{14.5}$$

so that if the load corresponds to the maximum value $F_{\max}$, the minimum pressure required at the actuator supply side is minimum (ideally null).

Therefore, the system using a relief valve to balance the load in overrunning conditions becomes very inefficient, particularly when the external load is not at the maximum value. In fact, the lower the F, the higher the pressure at the supply. This implies a substantial energy request at the pump shaft also when lowering a load.

The CBV acts similarly to a relief valve whose setting is not fixed, but it rather "adapts" to the current load situation. In particular, the increased pressure at the supply side in the case of partial loads is used as a signal to further open the valve. This helps to minimize the pump pressure and thus the energy required at the supply pump. Therefore, this "adaptable setting" feature is achieved by a pilot line, which senses the pressure on the opposite side of the cylinder.
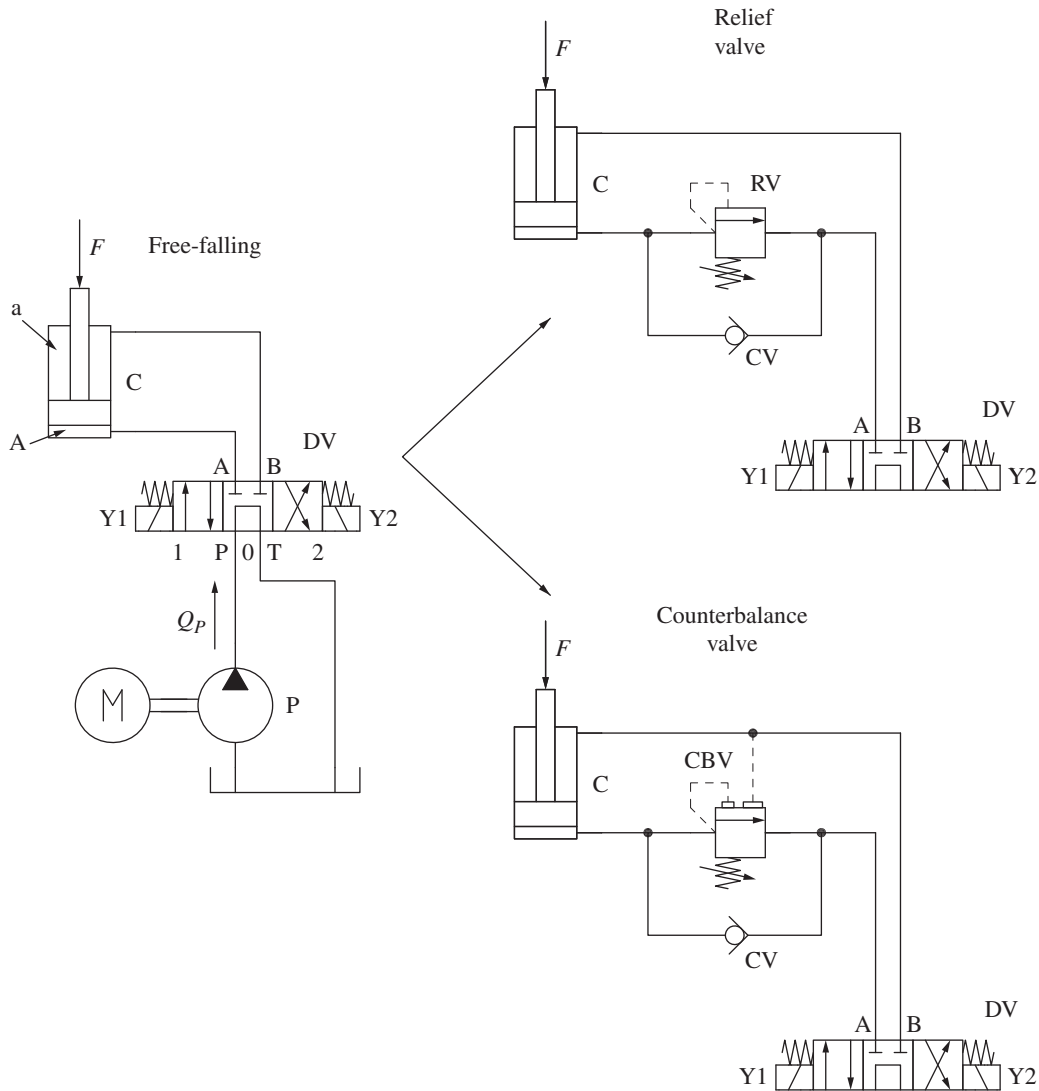
Figure 14.5 Working principle of a counterbalance valve.

With reference to the circuit in Figure 14.5, during cylinder lowering, the return flow always needs to cross the CBV. Therefore, the CBV always needs a positive pump pressure value to remain open. This pump pressure is dictated by the load, in the case of resistive load conditions. For overrunning loads, when the pump pressure decays, the CBV tends to close and thus helps to maintain a positive pressure at the supply side.

The ideal pump pressure during lowering is identified by the spring setting of the CBV, divided by its pilot ratio. This operation will be better analyzed in the following sections.

14.2.2 CBV Architecture

Figure 14.6 shows one of the common architectures used to implement a CBV. The three ports C, V, and X are connected to internal volumes separated by seals. The valve presents two sliding elements: a movable sleeve and a poppet. In addition, two springs are present: a strong spring
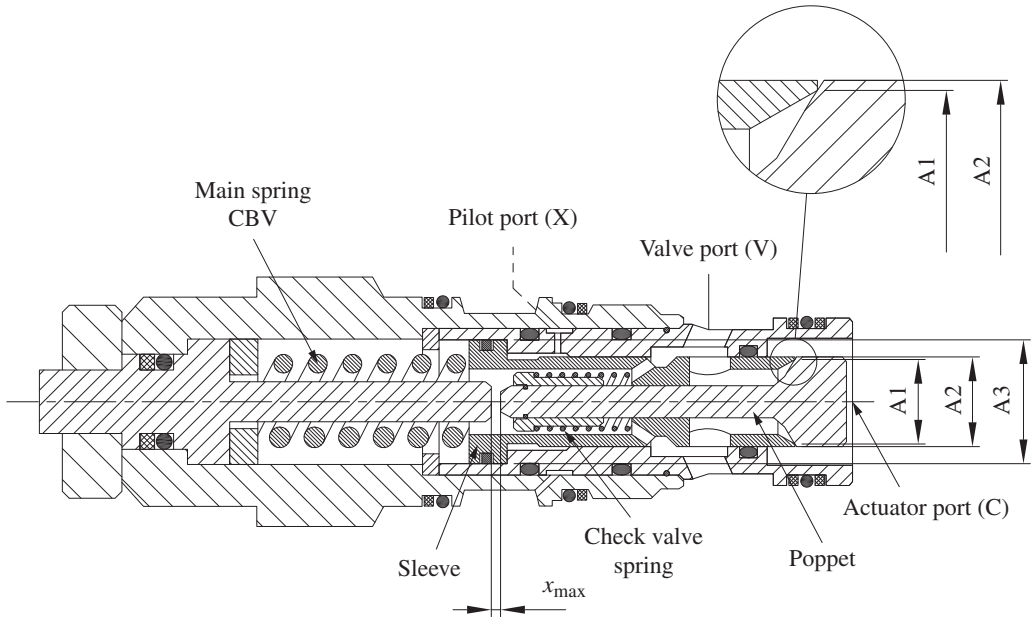
Figure 14.6 Typical architecture of a CBV.

F_{CBV} acts against the movable sleeve, while a tiny spring acts against the check valve poppet. One important detail resides in the spring guide and the adjustment mechanism, which also provides a stroke limitation to the poppet element. In this CBV design, both spring chambers are connected to V.

Check Valve Operation

If the pressure at port V is higher than the pressure at port C (the preload of the soft spring is generally negligible), the poppet slides to the right and it opens a connection from V to C (Figure 14.7). This is how the component implements the check valve functionality. The figure highlights how the CBV normally opens a large flow area so that the pressure drop across the valve is kept minimum.

Pressure Relief Operation

If both the pressures at X and V are null, the pressure at port C (p_C) acts against the poppet, on the area of influence A_2. When $p_C \geq F_{\text{CBV}}/A_2$, both poppet and sleeve move toward the left, but no flow passage opens as they jointly shift. After a certain travel x_{max}, the poppet hits the mechanical stop created by the spring guide. At this point, only the sleeve can travel further. The situation is
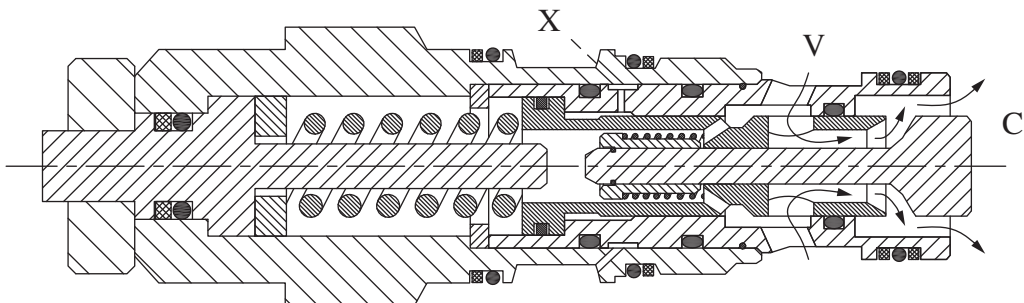
Figure 14.7 CBV during the check valve operation.
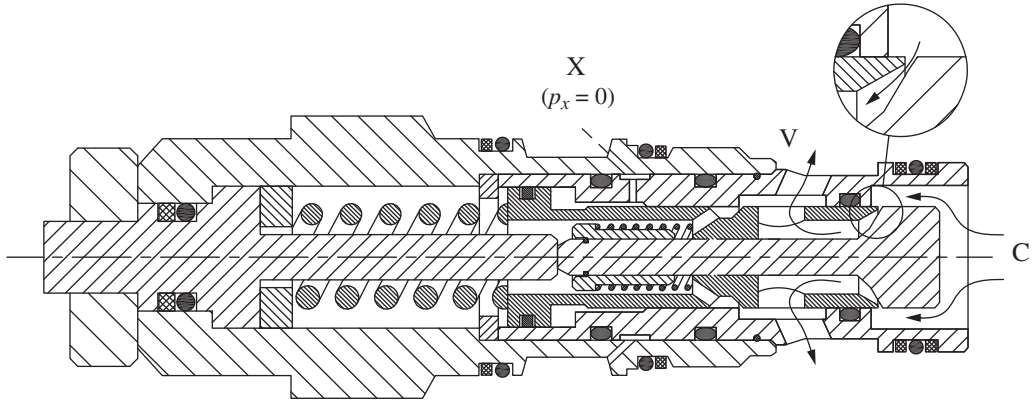
Figure 14.8 CBV during the pressure relief operation.

represented in Figure 14.8. It is very important to understand that, once this condition is reached, the area of influence of the pressure p_c on the sleeve changes and it becomes equal to the annular area $s = A_2 - A_1$. This is due to the geometry of the sleeve, with respect to the poppet in the zone of the contact, as shown by the magnified view in Figure 14.6. In this situation, the CBV operates as a pressure relief valve, with setting given by:

$$p_{CBV}^* = \frac{F_{CBV}}{s} = \frac{F_{CBV}}{A_2 - A_1} \tag{14.6}$$

As qualitatively shown in Figure 14.8, the flow area in this operating mode are usually small so that a high pressure drop is established by the valve.

Once p_{CBV}^* is reached, the valve discharges flow from C to V because the sleeve can further shift to the left while the poppet is blocked. The function of relief valve ($p_C = p_X = 0$) typically occurs when the hydraulic system is at rest or in idle. The value p_{CBV}^* is commonly referred as the *setting* (or *cracking pressure*) of the CBV, and it determines the maximum load that the hydraulic system can hold, using the CBV. In most typical applications, the CBV setting is usually adjusted to be slightly above (20–30%) the maximum pressure, which can be expected in the actuator under normal operating conditions. In other words, the load itself can never open the valve, unless severe overload conditions occur. Finally, yet importantly, when the relief valve is closed, the poppet element allows zero-leakage from C to V, thus acting as load-holding device.

Pilot Pressure Operation

When the pressure at port X (p_X) is greater than zero (a condition typically associated with the actuator movement), there is an additional opening force on the movable sleeve. The area of influence of the pilot pressure p_X is given by $S = A_3 - A_2$, visible in Figure 14.6.

The configuration for the internal elements of the CBV in this operating mode is shown in Figure 14.9, which points out the region of the valve pressurized by the pilot pressure p_X. The geometrical parameter α is indicated as *pilot ratio* of the CBV:

$$\alpha = \frac{S}{s} = \frac{A_3 - A_2}{A_2 - A_1} \tag{14.7}$$

Usually the pilot ratio of a CBV is greater than 1 and can reach values up to 20 or higher.

The pilot ratio α, as well as the setting p_{CBV}^*, is the main design parameters for the CBV. Their values determine both the range of possible operation and the behavior of the CBV in the system.
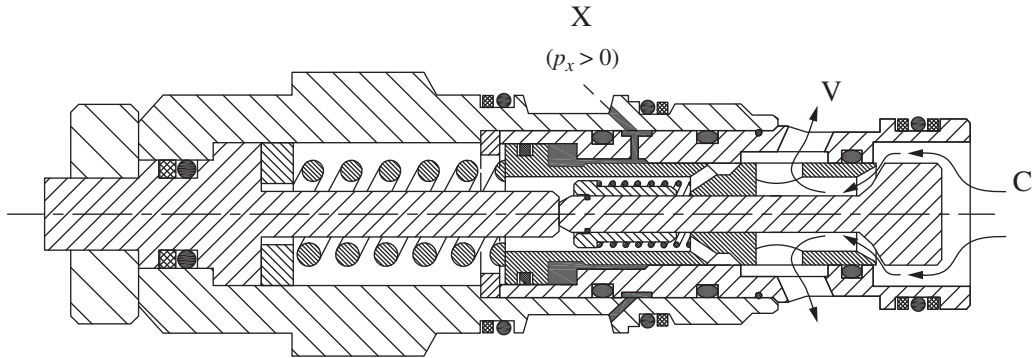
Figure 14.9 CBV during the pilot pressure operation.

> The two main design parameters of the CBV are the **cracking pressure** and the **pilot ratio**. The cracking pressure corresponds to the setting of the CBV when functioning as pressure relief valve. Both cracking pressure and pilot ratio affect the operation of the CBV when controlling overrunning loads.

14.2.3 Detailed Operation of CBV

The simple schematic in Figure 14.10 depicts a very common application, which is useful to understand the steady-state operation of CBVs. Here, CBV1 and CBV2 are installed at each port of a linear actuator.[3] This is subject to a load F, whose direction can vary. Therefore, depending on the orientation of F and on the cylinder motion, the load can be resistive or overrunning. As visible in the figure, the pilot port of each CBV (the one indicated in Figure 14.10 with X) senses the pressure from the supply port of the opposite counterbalance (indicated in Figure 14.10 as port V). Here, an on/off DCV controls the direction of motion of the actuator, while a primary flow control determines the supply flow Q_P. As an alternative, one could also select a meter-in control architecture for handling the flow supply. A pressure relief valve is present at the pump outlet, limiting the supply pressure to p^*.

Before analyzing the operation of the CBVs in Figure 14.10, some assumptions and conventions should be clarified. First, the following analysis will refer to the case of cylinder extension (solenoid Y1 energized). The load, F, is considered positive when pushing against the bore and negative in the opposite direction. The analysis will cover both sign directions for the load, during the extension of the actuator. The conclusions that will be drawn are general enough to cover all the operating modes of the CBV. Similar considerations (with proper adjustments for the areas of the cylinder) are valid for the cylinder retraction.

When Y1 is energized, the cylinder velocity $\dot{x}$ is given by $\dot{x} = Q_P/A$. The check valve integrated in CBV1 allows free flow to the cylinder, while the check valve of CBV2 is closed. Therefore, the fluid exiting the rod side of the cylinder has to be throttled through CBV2. As mentioned before, CBV2 opens a flow passage only if the combined force generated by the bore chamber pressure p_A,

---

3 To describe the operation of CBVs, a rotary actuator, or a double rod cylinder, could also have been used in Figure 14.5. The resulting considerations would be very similar; however, the case of a single rod cylinder is more generic because it highlights the additional effects due to the differential areas of the cylinder on the CBV operation.
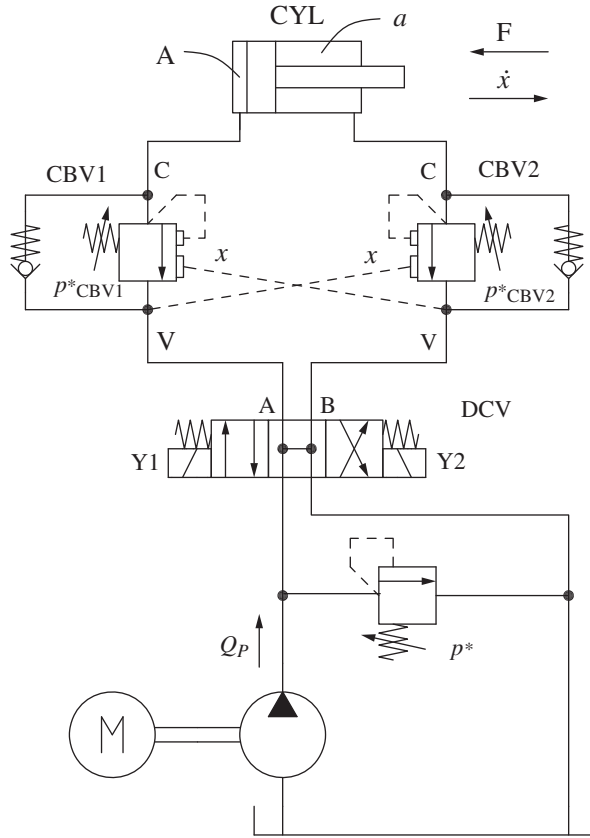
Figure 14.10 Application of CBVs for controlling the motion of a linear actuator subject to a generic load.

acting on the area of influence S, and the rod chamber pressure p_a, acting on s, is greater than or equal to the spring force F_{CBV}.[4]

The system is analytically described by the force balance at the actuator, as well as the force balance at CBV2, both under stationary flow conditions, i.e. constant external load, F and constant extension velocity, $\dot{x}$:

$$\begin{cases} A \cdot p_A - a \cdot p_a = F \\ S \cdot p_A + s \cdot p_a = s \cdot p_{CBV2}^* \end{cases} \tag{14.8}$$

The value of the load F is positive for the resistive case and negative for the overrunning one. Solving for the pressure at the cylinder chambers, p_A and p_a, and considering that the pressure at the cylinder chambers cannot fall below the tank pressure:

$$\begin{cases} p_A = \dfrac{a \cdot p_{CBV2}^* + F}{A + a \cdot \alpha} \\ p_a = \max \left(\dfrac{A \cdot p_{CBV2}^* - \alpha \cdot F}{A + a \cdot \alpha}, 0 \right) \end{cases} \tag{14.9}$$

---

4 Additional forces, such as friction and flow forces can affect the CBV balance. In this simplified analysis, these additional terms are neglected. It is also assumed that F_{CBV} is constant, while in reality this value varies with the position of the valve sleeve.
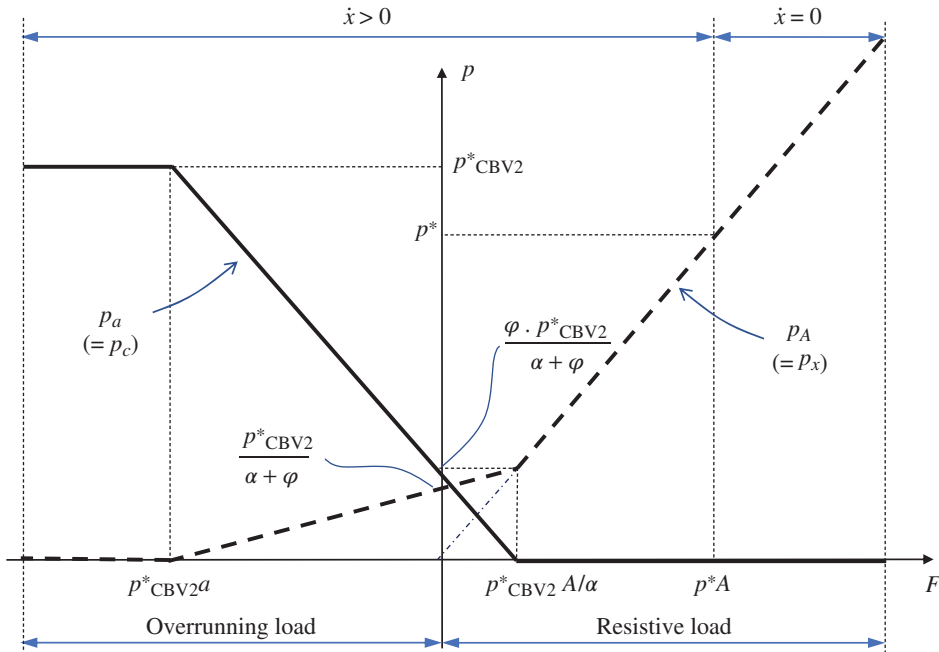
Figure 14.11 Steady-state operation of a counterbalance valve for different loads. The curves refer to CBV2 of Figure 14.10, for the case of cylinder extension with constant velocity $\dot{x}$.

The system of Eq. (14.9) is useful to describe the operation of CBVs. Figure 14.11 provides the graphical representation of the actuator work-port pressures p_A and p_a as a function of direction and magnitude of the load F.

The chart in Figure 14.11 can be broken down into three different areas, depending on the load value (F):

Null load ($F = 0$). Although there is no external force on the actuator, the pump outlet is pressurized because of the restriction created by the valve CBV2. The two actuator pressures are:

$$
\begin{cases}
p_A = \dfrac{a \cdot p^*_{\text{CBV2}}}{A + a \cdot \alpha} = \dfrac{p^*_{\text{CBV2}}}{\varphi + \alpha} \\[4mm]
p_a = \dfrac{A \cdot p^*_{\text{CBV2}}}{A + a \cdot \alpha} = \dfrac{\varphi \cdot p^*_{\text{CBV2}}}{\varphi + \alpha}
\end{cases}
\tag{14.10}
$$

Here, all the power consumed by the pump is considered a loss, since the actuator is moving under no external load. This is a direct result of the action of the CBV:

$$
P_P = P_{L,\text{CBV2}} = Q_P \cdot p_A = \frac{Q_P \cdot p^*_{\text{CBV2}}}{\varphi + \alpha}
\tag{14.11}
$$

Resistive loads ($F > 0$). in this case, two different operating modes can be distinguished, depending on the load value:

Low resistive loads. For low external loads F, CBV2 is not fully open, and it is throttling the flow returning to tank from the rod chamber. The pressure at the cylinder rod side p_a (port C of the valve) is not null, ($p_a > 0$), and consequently $p_A > F/A$. In this case, the hydraulic power at the pump is equal to $P_P = Q_P \cdot p_A$ and the power loss introduced by CBV2 is given by the

difference between P_P and the useful power to move the load, P_U:

$$P_{L,\text{CBV2}} = P_P - P_U = Q_P \left(p_A - \frac{F}{A} \right) = Q_P \left(\frac{A \cdot p^*_{\text{CBV2}} - \alpha \cdot F}{\varphi \left(A + a \cdot \alpha \right)} \right) \tag{14.12}$$

For higher resistive load, pressure p_A increases and, in turn, the value of p_a decreases (Eq. (14.8)). This happens until the value of p_A alone is high enough to overcome the spring force of CBV2. In this situation,

$$F = \frac{A \cdot p^*_{\text{CBV2}}}{\alpha} \quad \rightarrow \quad \begin{cases} p_A = \dfrac{F}{A} \\ p_a = 0 \\ \alpha > 1 \end{cases} \tag{14.13}$$

High resistive loads. If the load is greater than the value given by Eq. (14.13), the counterbalance valve (CBV2) fully opens and hence does not introduce any pressure drop for the flow crossing it. Therefore, the system is governed by the following equations:

$$\begin{cases} p_A = \dfrac{F}{A} \\ p_a = 0 \end{cases} \tag{14.14}$$

If the load increases further, the actuator extends in the same conditions of constant velocity until the pump pressure reaches the setting of the relief valve p^*. In the system of Figure 14.10, the pressure at the actuator p_A during the extension can theoretically increase above p^*. This is because the spring chamber of CBV1 (the other CBV in the circuit) has the same pressure at the pump through port V, as shown in Figure 14.6. In this case, the valve CBV1 remains closed preventing the oil from relieving through the main circuit relief valve. As it will be described in Section 14.2.5, this potential issue can be avoided with a different design for the CBV.

Overrunning loads ($F < 0$). In overrunning load conditions, the system of Eq. (14.9) again describes the system behavior (considering that now the value of F has a negative sign). As shown in Figure 14.11, the value of p_a is directly proportional to the magnitude of the assistive load. On the other hand, p_A decreases with the load magnitude but maintains a positive value. In this situation, CBV2 operates as a compensator on the return side, introducing a proper counter-pressure that allows the flow supply (primary, in this case) to remain in control of the actuator speed. The counterbalance valve (CBV2) causes the pump to consume power, being $p_A > 0$:

$$P_P = P_{L,\text{CBV2}} = Q_P \cdot p_A = Q_P \cdot \frac{a \cdot p^*_{\text{CBV2}} - |F|}{A + a \cdot \alpha} \tag{14.15}$$

Equation (14.15) gives an expression for the power consumed by the pump but does not include the throttling loss due to CBV2. If these are included, the overall power loss of the system (which turns into heat) becomes:

$$P_L = Q_P \left(p_A + \frac{p_a}{\varphi} \right) \tag{14.16}$$

If the load magnitude increases above the valve setting ($|F| \geq a \cdot p^*_{\text{CBV2}}$), the valve CBV2 starts relieving as it will limit the value of the cylinder rod pressure $p_a = p^*_{\text{CBV2}}$. In this case, the control of the actuator is lost, and the actuator starts accelerating.

In summary, CBVs enable the adjustment of the system pressures in order to satisfy the steady-state balance of the actuator, for different conditions of external load (resisting or overrunning) and input flow.

Therefore, CBVs can be used along with meter-in or primary supply concepts, which by themselves cannot handle overrunning loads. In comparison with the use of alternative elements downstream the actuator (such as the orifice in Figure 13.5, the spool in Figure 13.11, or the independent metering scheme in Figure 13.12), the CBVs have the inherent feature of self-adapting to the load condition. On the other hand, these alternative systems need to be designed or controlled based on the specific operating conditions (load, flow, area ratio).

Example 14.2   Counterbalance valve application vs. fixed orifice in the return line

A 50 *cm³/r* pump is driven by an electric motor rotating at 1000 *rpm*. The same pump is used in two different circuits to supply a cylinder with a bore diameter of 50 *mm* and a rod diameter of 25 *mm*. In both cases, the cylinder is subjected to an external load equal to 15 000 *N*, pulling from the bore toward the rod side. The first circuit uses a DCV with a restriction (orifice O) between ports B and T during extension. This restriction is equivalent to a 2.5 *mm* diameter orifice. In the second circuit, however, the DCV presents no work-port restrictions along with a CBV on the rod side. The CBV has a pilot ratio of 5 : 1, and it is set to 200 *bar*.
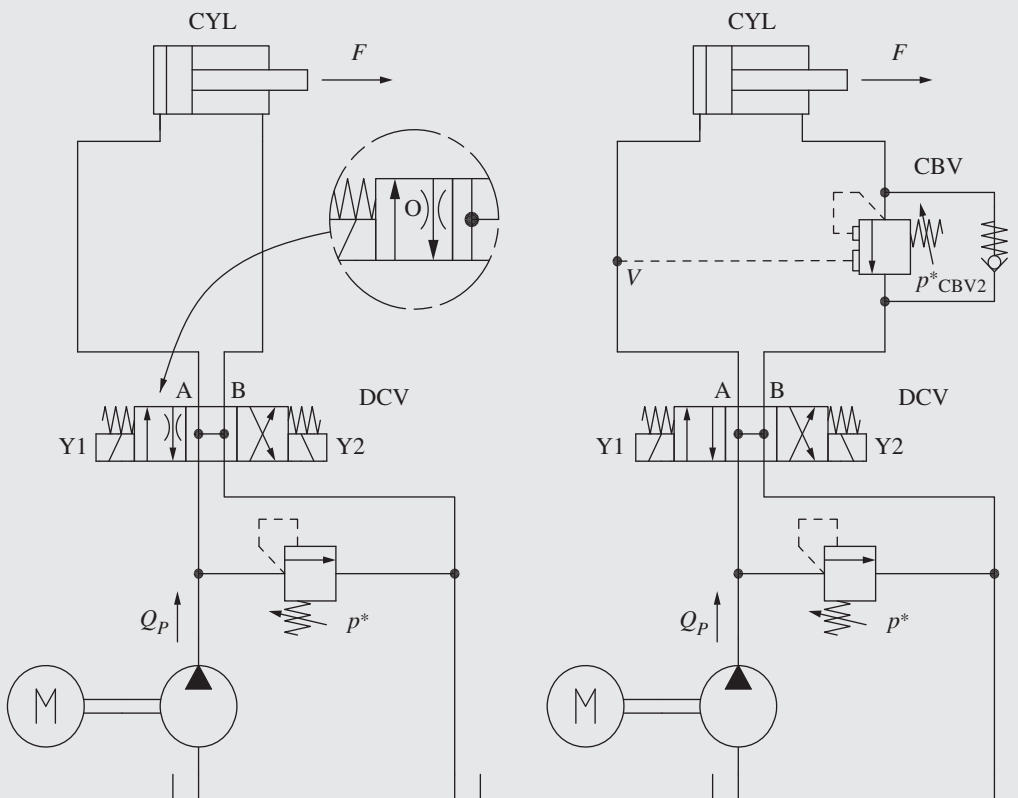
Calculate the pump pressure, the rod-side pressure, and the cylinder velocity for both circuits when the cylinder is extending (Y1 energized). Repeat the calculations in case the pump speed increases by 30%.

Example 14.2 (Continued)

Given:

Cylinder bore diameter, $d_B = 50\,mm$
Cylinder rod diameter, $d_R = 25\,mm$
Force on the actuator, $F = 15\,000\,N$
Pump speed, $n_p = 1000\,rpm$
Pump displacement, $V_p = 50\,cm^3/r$
Orifice diameter, $d_O = 2.5\,mm$
Counterbalance pilot ratio, $\alpha = 5$
Counterbalance setting, $p_{CBV}^* = 200\,bar$
Oil density, $\rho = 850\,kg/m^3$
Orifice coefficient, $C_f = 0.65$

Find:

1) Pump pressure p_P, rod-side pressure p_R, and cylinder velocity $\dot{x}$ for the initial case during cylinder extension
2) Pump pressure p_P', rod-side pressure p_R', and cylinder velocity $\dot{x}'$ for the case where the pump flow is increased by 30%

Solution:
The bore and rod-side areas of the cylinder are

$$A = \frac{\pi \cdot d_B^2}{4} = \frac{\pi \cdot 50\,[mm^2]}{4} = 1963\,mm^2$$

$$a = \frac{\pi\,(d_B^2 - d_R^2)}{4} = \frac{\pi\left((50\,[mm])^2 - (25\,[mm])^2\right)}{4} = 1471\,mm^2$$

The value of the cylinder ratio φ is

$$\varphi = \frac{A}{a} = \frac{1963\,[mm^2]}{1471\,[mm^2]} = 1.33$$

In the first case, the system needs to be analyzed considering the force balance at the actuator together with the orifice equation at its the return side:

$$\begin{cases} p_P \cdot A + F = p_R \cdot a \\[2mm] \dfrac{Q_P}{\varphi} = C_f \cdot \Omega_O \cdot \sqrt{\dfrac{2\,p_R}{\rho}} \end{cases}$$

The pressure at the rod side is calculated from the second equation:

$$p_P = \frac{\rho}{2} \cdot \left(\frac{Q_P}{\varphi \cdot C_f \cdot \Omega_O}\right)^2 = \frac{850\,[kg/m^3]}{2} \cdot \left(\frac{50\,[l/min]/60\,000}{1.33 \cdot 0.65 \cdot \dfrac{\pi(2.5)^2}{4} \cdot 10^{-6}}\right)^2 \cdot 10^{-5} = 158\,bar$$

The pressure at the pump outlet, i.e. at the bore side, instead is

$$p_P = \frac{p_R}{\varphi} - \frac{F}{A} = \frac{158\,[bar]}{1.33} - \frac{15\,000\,[N]}{1963\,[mm^2]} \cdot 10 = 42.3\,bar$$

In the case of the second system (using a CBV), the system can be analyzed using Eq. (14.8):

$$\begin{cases} p_P \cdot A + F = p_R \cdot a \\ \alpha \cdot p_P + p_R = p_{\text{CBV}}^* \end{cases}$$

Substituting the second equation into the first one,

$$p_P = \frac{a \cdot p_{\text{CBV}}^* - F}{A + \alpha \cdot a} = \frac{1471\,[mm^2] \cdot 200\,[bar] \cdot 0.1 - 15\,000\,[N]}{1963\,[mm^2] + 5 \cdot 1471\,[mm^2]} \cdot 10 = 24\,bar$$

The rod-side pressure is obtained as

$$p_R = p_{\text{CBV}}^* - \alpha \cdot p_P = 200\,[bar] - 5 \cdot 24\,[bar] = 80\,bar$$

In both cases the resulting cylinder speed is

$$\dot{x} = \frac{Q_P}{A} = \frac{50\,[l/min]/60\,000}{1963\,[mm^2] \cdot 10^{-6}} = 0.42\,m/s$$

In case the pump speed increases by 30%, the new pump flow becomes $Q'_P = 65\,l/min$. For the first circuit (orifice), the new rod-side pressure becomes

$$p'_R = \frac{\rho}{2} \cdot \left(\frac{Q'_P}{\varphi \cdot C_f \cdot \Omega_O} \right)^2 = \frac{850\,[kg/m^3]}{2} \cdot \left(\frac{65\,[l/min]/60\,000}{1.33 \cdot 0.65 \cdot \frac{\pi(2.5)^2}{4} \cdot 10^{-6}} \right)^2 \cdot 10^{-5} = 277\,bar$$

The new pump pressure is

$$p'_P = \frac{p'_R}{\varphi} - \frac{F}{A} = \frac{277\,[bar]}{1.33} - \frac{15\,000\,[N]}{1963\,[mm^2]} \cdot 10 = 131.8\,bar$$

In the circuit using the CBV, however, the system maintains the same pressure levels, since the pump flow is not part of the equilibrium equations. The new cylinder speed becomes

$$\dot{x}' = \frac{Q'_P}{A} = \frac{65\,[l/min]/60\,000}{1963\,[mm^2] \cdot 10^{-6}} = 0.55\,m/s$$

In conclusion, this example highlights how the control of the overrunning load with a CBV operates consistently and independently of the actuator velocity. Contrary to this, the use of a fixed restriction on the return side operates properly only for a narrow range of speeds.

Example 14.3   Counterbalance valve application vs. relief valve in the return line

A pump delivering 50 *l/min* is used in two different circuits to supply a cylinder with a bore diameter of 50 *mm* and a rod diameter of 25 *mm*. In both cases, the cylinder is subject to an external load equal to 15 000 *N*, pulling from the bore toward the rod side. The first circuit uses a relief valve located between the cylinder rod port and the valve B port (per figure below, left circuit). This relief valve is set to 200 *bar*. In the second circuit (same figure on the right side), a CBV with 8 : 1 pilot ratio and same pressure setting is used, instead of the pressure relief valve.

Example 14.3 (Continued)
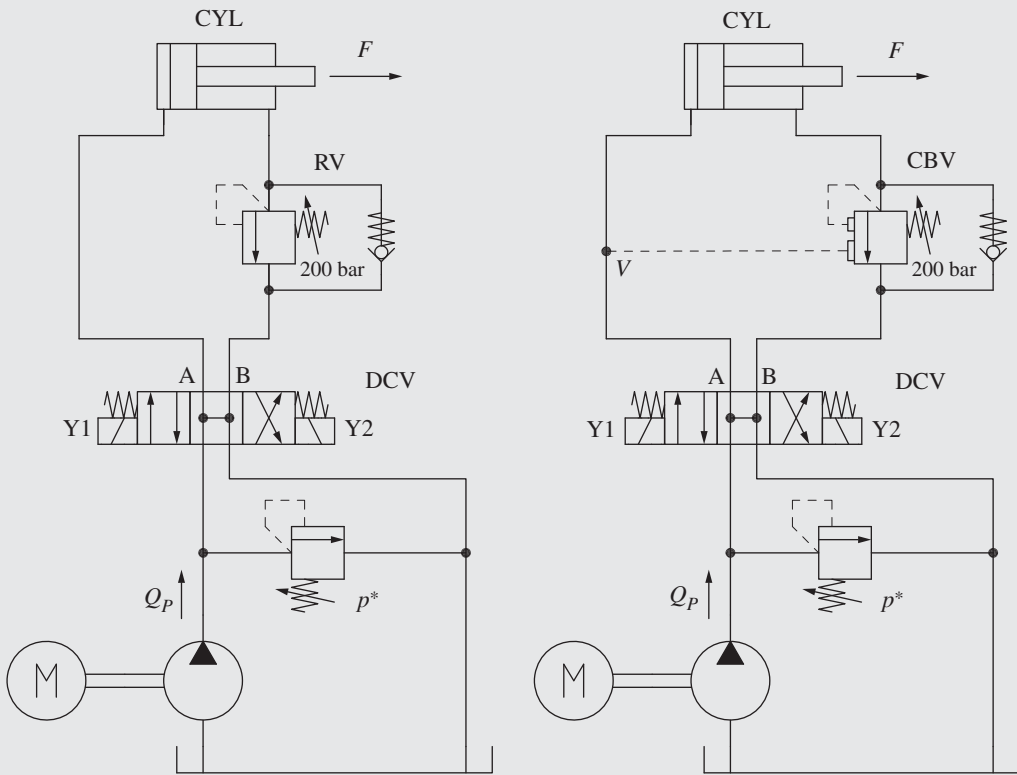
Calculate the pump pressure and rod-side pressure for both circuits when the cylinder extends (Y1 energized). Repeat the calculations in case the external force increases by 40%.

Given:

Cylinder bore diameter, $d_B = 50\,mm$
Cylinder rod diameter, $d_R = 25\,mm$
Force on the actuator, $F = 15\,000\,N$
Pump flow, $Q_p = 50\,l/min$
Relief valve setting, $p_R^* = 200\,bar$
Counterbalance pilot ratio, $\alpha = 8$
Counterbalance setting, $p_{CBV}^* = 200\,bar$
Oil density, $\rho = 850\,kg/m^3$

Find:

1) Pump pressure p_P and rod-side pressure p_R for both circuits during cylinder extension.
2) Pump pressure p'_P and rod-side pressure p'_R for the case where the load is increased by 40%

Solution:

As in the previous case, the bore and rod-side areas of the cylinder are

$$A = \frac{\pi \cdot d_B^2}{4} = (\frac{\pi \cdot (50\,[mm])^2}{4} = 1963\,mm^2$$

$$a = \frac{\pi \left(d_B^2 - d_R^2\right)}{4} = \frac{\pi \left((50\,[mm])^2 - (25\,[mm])^2\right)}{4} = 1471\,mm^2$$

The value of the cylinder ratio φ becomes

$$\varphi = \frac{A}{a} = \frac{1963\,[mm^2]}{1471\,[mm^2]} = 1.33$$

The theoretical pressure caused by the force at the rod side would be

$$p_{load-rod} = \frac{F}{a} = \frac{15\,000\,N}{1471\,[mm^2]} \cdot 10 = 102\,bar$$

This is below the pressure setting of 200 *bar* of the relief and CBVs. This ensures that both the systems are capable of controlling the overrunning load.

In the circuit using the relief valve, when extension is commanded, the pressure in the cylinder rod chamber is controlled by the relief. Therefore, $p_R = p_R^* = 200\,bar$. The pump pressure can be easily calculated from the cylinder force balance:

$$p_P = \frac{p_R \cdot a - F}{A} = \frac{p_R}{\varphi} - \frac{F}{A} = \frac{200\,[bar]}{1.33} - \frac{15\,000\,[N]}{1963\,[mm^2]} \cdot 10 = 74\,bar$$

In the case of the second system (using a CBV), the system can be analyzed using Eq. (14.8):

$$\begin{cases} p_P \cdot A + F = p_R \cdot a \\ \alpha \cdot p_P + p_R = p_{CBV}^* \end{cases}$$

Substituting the second equation into the first one,

$$p_P = \frac{a \cdot p_{CBV}^* - F}{A + \alpha \cdot a} = \frac{1471\,[mm^2] \cdot 200\,[bar] \cdot 0.1 - 15\,000\,[N]}{1963\,[mm^2] + 8 \cdot 1471\,[mm^2]} \cdot 10 = 10.5\,bar$$

The rod-side pressure is

$$p_R = p_{CBV}^* - \alpha \cdot p_P = 200\,[bar] - 8 \cdot 10.5\,[bar] = 116\,bar$$

In case the external force increases by 40%, the new value becomes $F = 21\,000\,N$. The systems can be studied with the same equations.

For the circuit using a relief valve,

$$p_R' = p_R^* = 200\,bar \text{ and } p_P' = 43.4\,bar$$

In the second circuit (CBV), the pressures change slightly to the following values:

$$p_R' = 151\,bar \text{ and } p_P' = 6.1\,bar$$

Both circuits can control the overrunning load under all the desired speed conditions. However, the circuit using a relief valve is very inefficient, because the control of the actuator is achieved with high pump pressures. The lower the force, the higher the pump pressure. Contrary to this, the CBV can "adapt" to the load conditions and maintain a rod pressure slightly higher than the theoretical rod pressure (indicated with $p_{load-rod}$). The resulting pump pressure is fairly low. A part of this can be attributed to the high pilot ratio selected.
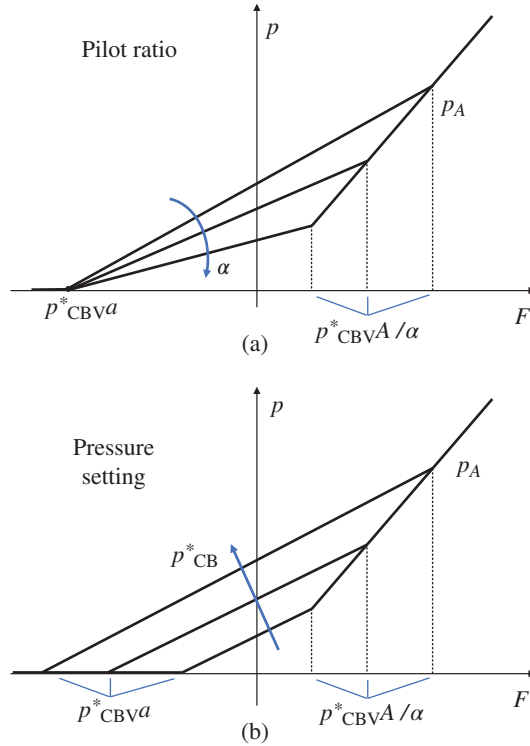
Figure 14.12 CBV steady state characteristic for different valve settings: (a) pilot ratio, (b) pressure setting.

14.2.4 Effect of the Pilot Ratio and of the Pressure Setting

Equations (14.8) and (14.9) highlight the two parameters that characterize a CBV: the pilot ratio α and the pressure setting p_{CBV}^*. These two parameters affect the slope and the intercept of the straight lines describing the CBV behavior in its operating range in Figure 14.11. Equation (14.9) can be also written as follows, to highlight the straight-line trend:

$$\begin{cases} p_A = \dfrac{1}{\beta} \cdot F + \dfrac{a}{\beta} \cdot p_{CBV}^* \\ p_a = -\dfrac{\alpha}{\beta} \cdot F + \dfrac{A}{\beta} \cdot p_{CBV}^* \end{cases} \quad ; \quad \beta = (A + a \cdot \alpha) \tag{14.17}$$

Figure 14.12 shows how the parameters α and p_{CBV}^* affect the value of p_A, which is usually indicative of the power loss introduced by the CBV in the system, according to Eqs. (14.12) and (14.15). By changing the value of α, p_A describes a family of straight lines centered in the point $\left(-a \cdot p_{CBV}^*; 0\right)$[5]. In particular, higher values of α result in lower values of p_A. Similarly, by changing the pressure setting p_{CBV}^*, the resulting p_A can be represented as a family of parallel straight lines.

Selection of CBV Parameters

As mentioned earlier, the CBV setting (p_{CBV}^*) is usually chosen considering the maximum load the actuator must hold and multiplying it by a safety coefficient (usually +30%). On the other hand, the value of α is a design parameter that can be selected. Theoretically, in order to minimize the energy consumption during overrunning load situations, α should be selected as high as possible. However, one more factor should be considered: Figure 14.13 shows how a CBV can be approximated as

---

5 It is assumed here that α is varied, while p_{CBV}^* remains constant.
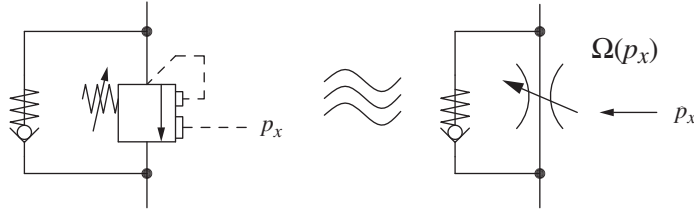
Figure 14.13 A counterbalance valve can be approximated as a variable orifice where the opening area is function of the pilot pressure p_X.

a variable orifice where the opening area Ω is a monotonically increasing function of the pilot pressure p_X. Under this assumption, the area gain of the valve is directly proportional to the pilot ratio:

$$G_{CBV} = \frac{\partial \Omega}{\partial p_X} \propto \alpha \tag{14.18}$$

Contrary to a spool valve (see Chapter 8, DCV actuation methods), where the pilot pressure is generated by an external steady source, for CBVs p_X is the pressure in the line supplying the other actuator port. Therefore, the value of p_X is part of the actuator dynamic, as defined in Chapter 8. In other words, the value of G_{CBV} affects the actuator dynamic behavior: the higher the value of G_{CBV} (i.e. the pilot ratio), the easier the occurrence of oscillation when overrunning loads are handled. In other words, the stability of the system is a requirement that usually detracts from the energy efficiency.

14.2.5 Counterbalance Valve with Vented Spring Chambers

All the CBVs analyzed in the Section 14.2 are assumed to be constructed as in Figure 14.6. In that case, the spring chamber internally connects to the V port of the valve. This is the most common and economical design for CBVs. However, other types of CBVs are built with the spring chamber vented to the atmosphere or to the tank (via a separate drain line). The hydraulic symbols used for possible CBV architectures are represented in Figure 14.14.

The use of a separate drain for the spring chamber allows the valve to be independent from possible backpressures. This can have some functional advantages. In the diagram shown in Figure 14.11, which describes the behavior of the circuit in Figure 14.10, it was highlighted how the circuit could lose the protection from overloading during the cylinder extension because CBV1 loses its relief functionality during the cylinder extension. In fact, for the CBVs used in Figure 14.10, the spring chamber is drained internally (Figure 14.6). In other words, the pressure at port V adds to the spring force. The CBV force balance equation during regulation for the valve in Figure 14.6 should be described as follows:

$$p_x \cdot (A_3 - A_2) + p_C \cdot (A_2 - A_1) = F_{CBV} + p_V \cdot A_3 \tag{14.19}$$
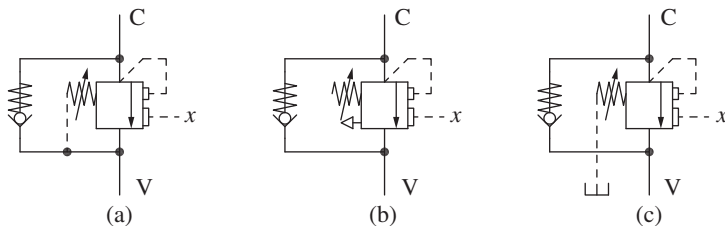
Figure 14.14 Different solutions for CBV spring chamber drain: internal drain (a), atmospheric vent (b), and external drain (c). Usually if the drain is omitted from the symbol, the CBV is internally drained.
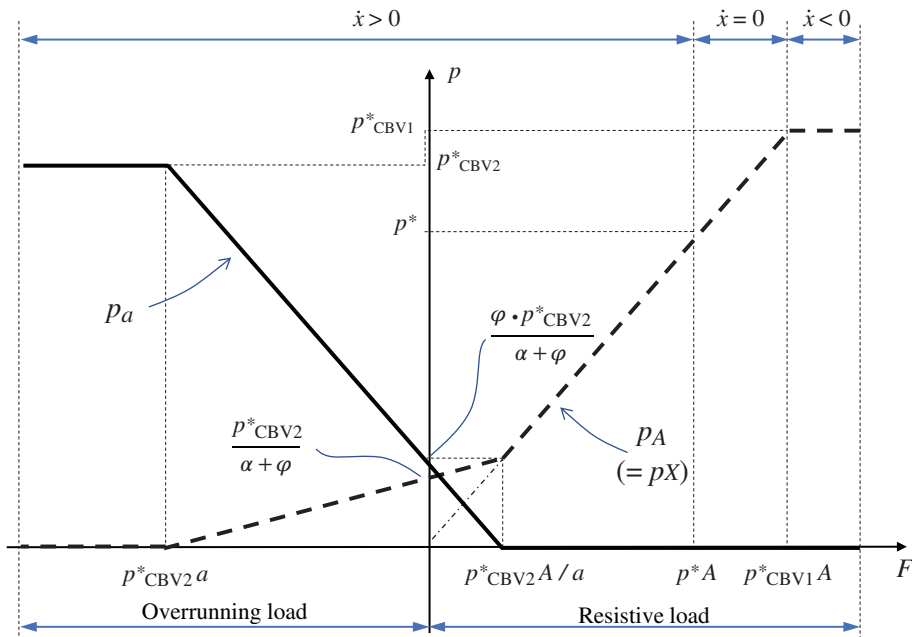
Figure 14.15 Operating characteristic of the circuit in Figure 14.10 with vented counterbalances.

While in overrunning load conditions the value of p_V can be assumed null, in resistive load conditions this is not true. Especially during extension, the setting of valve CBV1 is affected by p_V. In other words, if the load increases above the safety limit, $p_V = p^*$, the valve CBV1 would stay closed even if the load increased to value much higher than p^*_{CBV1}. This risk can be avoided by using a CBV with vented spring chamber. In this case, the setting of the relief function is p^*_{CBV1} and is independent from the value of p_V. Figure 14.15 shows how the operating characteristic of the same circuit would change by using vented CBVs. When the resistive load overcomes the value $p^*_{CBV1} \cdot A$, CBV1 relieves limiting the value of $p_A = p^*_{CBV1}$. The flow relieved by CBV1 discharges to the tank through the main relief.

In addition to the abovementioned advantages, vented CBVs are also interesting for two other aspects: first, they are not affected by pressure perturbations in the return line that can be generated by other parts of the hydraulic circuit. Second, they can be used in combination with other restrictions in the return line, such as meter-out orifices or spools. Therefore, the CBV can then be combined with other strategies for controlling overrunning loads.

Problems

14.1 In the circuit shown below, a cylinder with a bore of 35 mm and a rod of 20 mm is subject to a pulling load of 36 kN. The CBV has a spring setting of 4000 psi and a pilot ratio of 3.5. The pressure compensated pump is large enough to satisfy the required supply flow and maintains a constant supply pressure of 185 bar. Calculate the cylinder extension speed if the needle valve is set to an area of 5 mm². How does the answer change if the CBV pilot ratio is increased to 10?

14.2 For the system shown in the figure, in which a double acting single rod cylinder is subjected to gravity force, calculate the pilot pressure p_s of the PO check valve controlling the lowering operation when the external force is known (provide the analytical expression).
Ignore the friction and flow forces in each component, and assume the flow control valve working with a given $\Delta p = p_2 - p_2'$.

14.3 A hydraulic winch is used to lift or lower a payload of 100 kN. The winch has a drum diameter of 0.5 m and it is connected to a fixed displacement hydraulic motor through a gearbox that reduces the angular speed of the motor by 30 times. In both raising and lowering, the velocity of the payload is 0.3 m/s. A fixed displacement pump rotating at 2000 rpm is used in combination with a 4/3 DCV to accomplish the lift, lower, and rest functions. The maximum pressure at which the pump can operate is 200 bar. A CBV with a pressure setting of 250 bar and a pilot ratio of 4 : 1 is used to control the motion of the winch. Determine

a) The system schematic

b) The displacement of the pump and the motor

c) The pressures at the motor port during lifting and the lowering

Assume ideal unit efficiency, and neglect pressure losses at the DCV and the connecting lines.

Chapter 15

Bleed-off and Open Center Systems

Bleed-off and open center circuits represent popular hydraulic control strategies that implement meter-in velocity control of actuators in combination with a flow supply. This chapter introduces both circuit layouts and then presents various characteristics of each approach such as the energy consumption and the controllability of the system. The chapter begins with a discussion on the basic system architectures and later proceeds to introduce more advanced systems that are commonly found in today's state-of-the-art machines.

Resistive loads are always taken as a reference for the sake of simplicity. For overrunning loads, the resulting systems tend to be more complicated, due to the integration of the meter-out solutions similar to those presented in Chapters 13 and 14.

15.1   Basic Bleed-off and Open Center Circuits

The basic operating principle (shown in Figure 15.1) of *bleed-off* and *open center* systems consists of providing two possible paths for the pump flow, which are characterized by different throttling areas. The first path connects to the actuator, while the second one connects to the return to tank. The actuator speed is determined by how the pump outlet flow is split between the two paths. This split is governed by the throttling areas and the load pressure. While a majority of these systems are used in combination with a fixed displacement pump, in some cases (which will be presented at the end of this chapter) variable displacement pumps can also be utilized to improve the energy efficiency.

Although they are implemented by different architectures, from a conceptual point of view, the two control concepts are very similar. The bleed-off circuit can be classified as a special case of an open center circuit. In particular, bleed-off circuits utilize a variable restriction only at the line connecting the pump outlet to tank (orifice O_T in Figure 15.1a), while the flow path to the actuator is always open. On the other hand, open center circuits present flow restrictions on both paths (orifices O_U and O_T in Figure 15.1b). The command signal determined by the operator controls the opening area of the different restrictions. Hence, the actuator speed is a result of the pump flow, the area openings, and the actuator load.

> Bleed-off and open center system have a similar principle of operation. The pump outlet flow is split into two possible paths, one connected to the actuator and the other one to the tank. The **bleed-off** solution utilizes only one regulating orifice placed at the line returning to tank. The **open center** solution uses two variable orifices, one on the line to the actuator, and another on the return line to the tank.
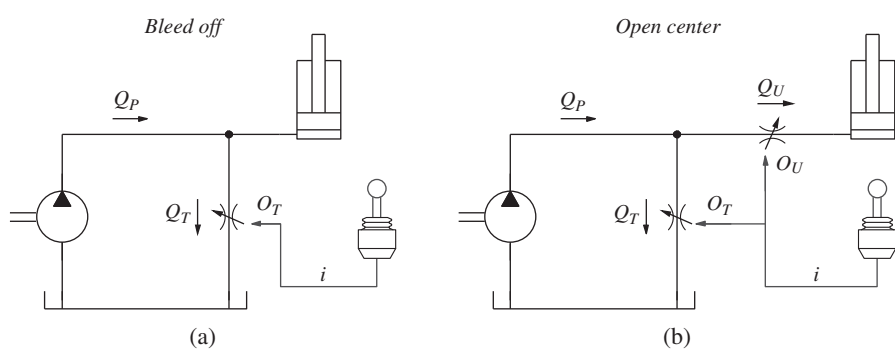
Figure 15.1 Principle of operation of bleed-off (a) and open center (b).

15.2 Bleed-off Circuit Operation

Figure 15.2 represents a typical bleed-off circuit application: the speed of the motor, M, is controlled by the proportional throttling valve labeled in the circuit as PV. This valve "bleeds off" part of the flow supplied by the pump. The DCV is an on/off valve and it is used to control the flow direction to the actuator. For simplicity, this example assumes that the torque at the motor shaft is always resistive and remains constant over the whole speed range, so that $p_U = T/V_D$.

Figure 15.3 shows the pump pressure p_P and the actuator flow Q_U for different values of the input signal i in the system shown in Figure 15.2. The value of i is the current sent to the proportional solenoid of PV, which determines the throttling area of the valve. The valve PV, which is normally open, closes as the current i increases.

Neutral position. When $i = 0$, PV is fully open ($\Omega_T = \Omega_{max}$) and the DCV is in neutral position: all the pump flow Q_P returns to the tank through PV. Ideally this happens at zero pressure (tank pressure). In reality, the standby pressure p_0 is greater than zero because of the pressure drop
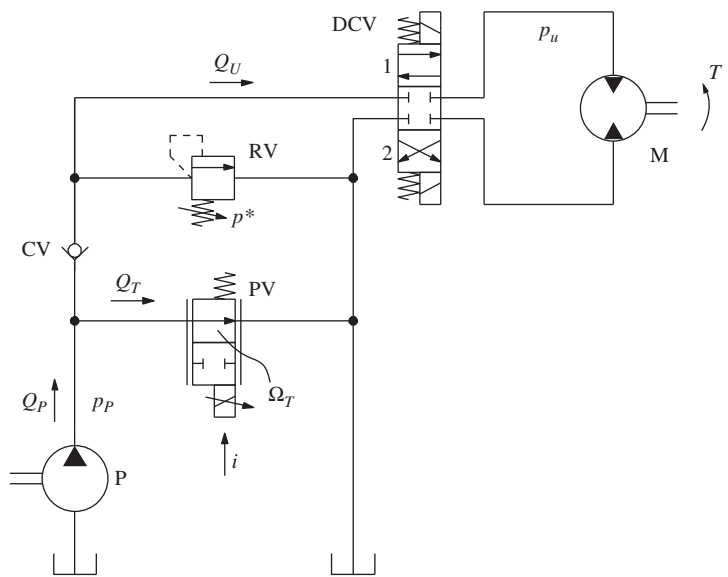
Figure 15.2 Typical circuit applying a bleed-off strategy to control the speed of a hydraulic motor.
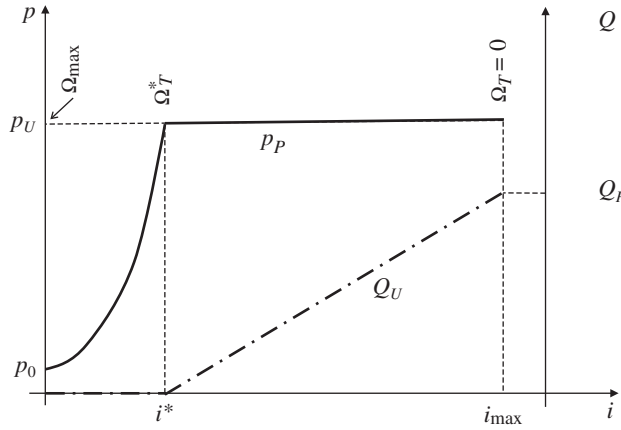
Figure 15.3 Pressure and flows in the bleed-off system, for different input signals.

across PV, which has a maximum opening area Ω_{max}:

$$p_0 = \frac{\rho Q_P{}^2}{2C_f{}^2\Omega_{max}^2} \tag{15.1}$$

Non-regulating region ($0 \leq i < i^*$). If the directional control valve (DCV) is shifted to position 1, while PV is not energized, the pump flow continues returning to the tank through PV, while the outlet pressure of the pump stays at p_0. This is because the check valve labeled in the circuit as CV separates the load pressure, p_U, from the pump pressure, p_P, and thus prevents the motor from rotating backward and feeding the pump line. This CV is commonly referred to as a *load drop check valve* and it is present as an internal element in a majority of DCVs.

When $0 \leq i < i^*$, the bleed-off area $\Omega_T(i)$ decreases from its initial value and the pump pressure p_P increases. Initially, all the pump flow still returns to the tank (i.e. $Q_U = 0$), because the pump pressure p_P is lower than p_U. This situation persists until the input signal reaches the value i^*, at which point the pump pressure becomes equal to the load pressure. The input i^* corresponds to the bleed-off area Ω_T^*, defined as follows:

$$\Omega_T^* = \frac{Q_P}{C_f}\sqrt{\frac{\rho}{2p_U}} \tag{15.2}$$

In the basic bleed-off circuit, the region of "no regulation" corresponds to large openings of the bleed-off element (PV). In this situation no flow is sent to the actuator. In this case, the variable orifice PV works as a compensator.

Regulating region ($i > i^*$). When $i > i^*$, the area Ω_T further decreases, and part of the pump flow is directed to the actuator. In this situation, PV acts as a metering element working between p_U and tank pressure. In this control interval, the relations between the metering area Ω_T and the values of Q_U and Q_T are given by

$$\begin{cases} Q_T = C_f\Omega_T(i)\sqrt{\dfrac{2p_u}{\rho}} & \text{for } \Omega_T(i) \leq \Omega_T^* \\ Q_U = Q_P - Q_T \end{cases} \tag{15.3}$$

The formulas of Eq. (15.3) are valid under for the cases where $p_U < p^*$, where p^* is the maximum pressure allowed by the relief valve (RV).

> In the case studied, the basic bleed-off circuit controls the flow to the actuator only when the bleed-off element (PV) reaches area openings small enough to overcome the load pressure. In this case the variable orifice PV is a metering orifice.

15.2.1 Energy Analysis

Figure 15.4 shows the energy plot of the bleed-off system: P is the operating point of the pump, while U correspond to the actuator. The different power contributions are as follows:

$$P_P = Q_P \cdot p_U \quad \text{pump power}$$

$$P_U = Q_U \cdot p_U \quad \text{useful power} \tag{15.4}$$

$$P_L = (Q_P - Q_U) \cdot p_U \quad \text{power loss}$$

The efficiency of the system is defined as follows:

$$\eta_S = \frac{P_U}{P_P} = \frac{Q_U}{Q_P} \tag{15.5}$$

It is important to note that, even under the assumption of ideal components, the system efficiency can be far from the ideal case of 100%. Furthermore, another drawback for this type of system is the power consumed during standby conditions. In this case, the pump power is $P_P = Q_P \cdot p_0$ where p_0 is the one calculated in Eq. (15.1). This power consumption can be significant, especially in applications where the pump speed, and consequently Q_P, can reach high values.

Other important observations about this control technique can be made by looking at Figure 15.3. The control of the actuator speed happens only between i^* and i_{max}. When the command signal ranges below i^*, the actuator does not move ($Q_U = 0$) and thus results in a control *deadband zone*. The difference $i_{max} - i^*$ defines the range in which the command effectively modulates the actuator speed. It is usually desirable to have a wide control range to improve the sensitivity of the input command, which in turn means having a reduced deadband zone. Besides this, the value of i^* is load dependent (Eq. (15.2) gives the relationship between Ω_T^* and p_U). Therefore, the deadband zone and the control range change with the load.
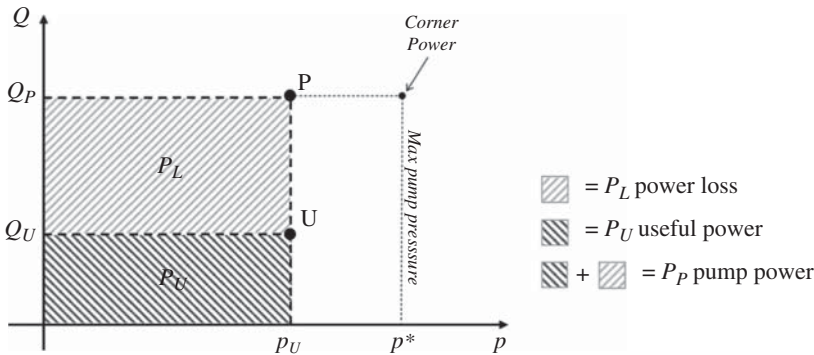
Figure 15.4 Energy plot for the bleed-off circuit in Figure 15.2.

Example 15.1   Bleed-off circuit to extend an actuator

The following circuit is used to extend a cylinder where the external load generates a bore pressure of 150 *bar*. The pump flow is 60 *l/min*, the cylinder bore diameter is 50 *mm*, and the setting of the pressure relief valve is 250 *bar*. Answer to the following questions:

a) At what bleed-off area will the cylinder start moving?
b) What value of the bleed-off area does ensure a standby pump pressure of 10 *bar*?
c) What is the bleed-off area that corresponds to half of the maximum achievable speed? What is the system efficiency under this condition?
d) What would be the system pressure if the cylinder reaches full extension under this condition?
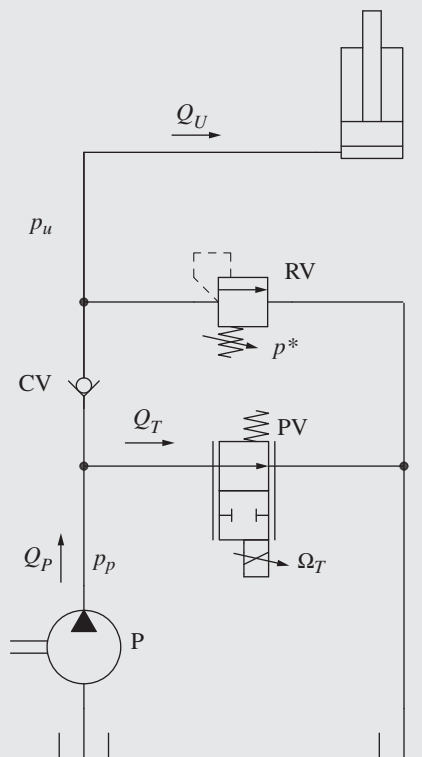
Assume no losses in the connecting lines, and consider an oil density of 850 *kg/m³*. The orifice coefficient of the PV is 0.65.

Given:

Cylinder bore diameter, $d_B = 50$ *mm*
Load pressure, $p_U = 150$ *bar*
Pump flow, $Q_P = 60$ *l/min*
Pressure relief valve setting, $p^* = 250$ *bar*
Orifice coefficient, $C_f = 0.65$
Oil density, $\rho = 850$ *kg/m³*

Example 15.1 (Continued)

Find:

a) The area Ω_T^* (start metering).
b) The area Ω_0 that corresponds to a standby pressure $p_0 = 10\ bar$.
c) The area $\Omega_{1/2}$ corresponding to half of the maximum cylinder speed.
d) The system efficiency η_S.
e) The pump pressure p_P, when the cylinder reaches the end of stroke and $\Omega_T = \Omega_{1/2}$.

Solution:

a) The value of Ω_T^* can be calculated using Eq. (15.2):

$$\Omega_T^* = \frac{Q_P}{C_f}\sqrt{\frac{\rho}{2p_U}} = \frac{60\ [l/min]}{60\,000 \cdot 0.65} \cdot \sqrt{\frac{850\ [kg/m^3]}{2 \cdot 150\ [bar] \cdot 10^5}} \cdot 10^6 = 8.2\ mm^2$$

b) The value of Ω_0 is obtained from Eq. (15.1):

$$\Omega_0 = \frac{Q_P}{C_f}\sqrt{\frac{\rho}{2p_0}} = \frac{60\ [l/min]}{60\,000 \cdot 0.65} \cdot \sqrt{\frac{850\ [kg/m^3]}{2 \cdot 10\ [bar] \cdot 10^5}} \cdot 10^6 = 31.7\ mm^2$$

A careful reader can immediately notice the significant difference between the standby and the start of the regulation.

a) The actuator runs at 50% of the maximum speed when $Q_U = Q_T = 0.5 \cdot Q_P = 30\ l/min$. This corresponds to an opening area of

$$\Omega_{1/2} = 0.5 \cdot \Omega_T^* = 0.5 \cdot 8.2\ [mm^2] = 4.1\ mm^2$$

b) Under this condition the system efficiency is

$$\eta_S = \frac{P_U}{P_P} = \frac{Q_U}{Q_P} = 50\%$$

c) If the actuator reaches maximum extension while $\Omega_T = \Omega_{1/2}$, the pressure at the pump is equal to the minimum value between p^* and p_{max} where p_{max} equals to

$$p_{max} = \frac{\rho}{2} \cdot \left(\frac{Q_P}{C_f \cdot \Omega_{1/2}}\right)^2 = \frac{850\ [kg/m^3]}{2} \cdot \left(\frac{60\ [l/min]/60\,000}{0.65 \cdot 4.1\ [mm^2]/1000^2}\right)^2 \cdot 10^{-5} = 598\ bar$$

The value of p^* is significantly lower; therefore, the resulting pump pressure is equal to $p^* = 250\ bar$.

15.3 Basic Open Center System

Figure 15.5 shows a typical circuit layout for an open center system: the most important element is represented by the DCV, which has a 6/3 proportional spool. In fact, besides the typical P, T, A, and B ports, the spool includes an additional connection to tank through the so-called open center gallery. The open center gallery and port P are both connected to the pump outlet and represent the two possible paths for the pump flow. In addition, a load drop check valve CV is placed between the pump and port P in a very similar fashion to the bleed-off circuit.

Open center systems are very common in hydraulic applications mainly for two reasons. First, the valve layout is very simple as the metering functions can be achieved with a single spool, contrarily
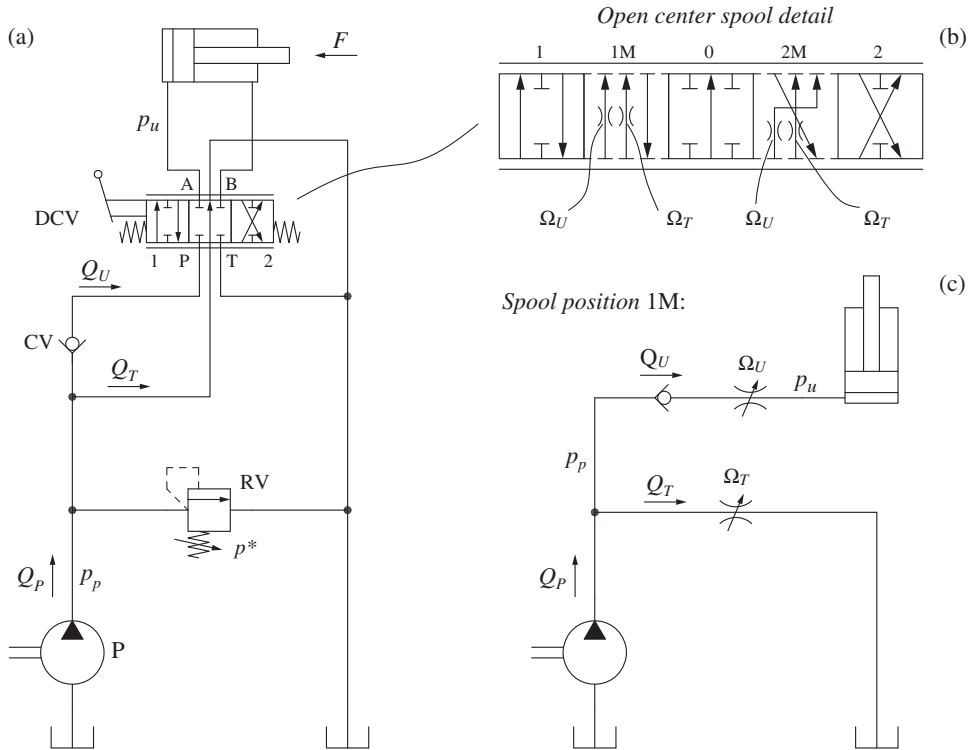
Figure 15.5 Typical layout of an open center system (a) with detailed view of the DCV spool (b) and equivalent configuration for the position 1 M (c).

to the bleed-off circuit where two valves are needed (PV and DCV in Fig1ure 15.2). Second, the operation based on the combination of two metering orifices determining the flow split between open center gallery and actuator provides a dynamic control of the actuator which is favored by many operators. However, the selection of the spool throttling areas is critical in order to optimize the control resolution and the system efficiency.

15.3.1   Operation

Neutral position. In neutral configuration (spool in position 0), ports P, T, A, and B are blocked; therefore, all the pump flow passes through the open center gallery of the open center valve, and it returns to the tank. The standby pressure of the valve is determined by $\Omega_{T-\max}$, and it has the same expression of Eq. (15.1) found for the bleed-off circuit. Therefore, this area should be large to minimize the pump standby pressure.

Non-regulating region ($0 \leq i < i^*$). When the valve is commanded toward position 1, the spool moves to the intermediate configuration 1 M (represented in the detailed view in Figure 15.5). As the command signal increases, the area Ω_T rapidly decreases, while the connection to the work-port Ω_U remains closed. This causes a rapid increase of the pump pressure p_P, until the condition at which both areas are finely determined by the spool notches (the actual valve section will be presented later). At this point, the open center flow area restricts (Ω_T decreases), while the connection P → A opens (Ω_U increases). It is assumed here that the decrease of $\Omega_T(i)$ and the increase of $\Omega_U(i)$ are characterized by linear functions. In reality, the trends of the areas $\Omega_T(i)$ and $\Omega_U(i)$ and their relative timing is an important design aspect of open center valves, which has a significant impact on the control characteristics.

For low command values, $\Omega_T(i)$ is large and consequently $p_P < p_U$. Similarly to the case of the bleed-off circuit, all the pump flow returns to tank through the open center gallery, and the load drop check valve prevents the actuator from retracting. This situation occurs until the input command reaches i^*, where $\Omega_T(i) = \Omega_T^*$ (whose value has the same expression of Eq. (15.2)), and consequently $p_P = p_U$.

Regulating region ($i > i^*$). For input commands higher than i^*, $\Omega_T(i) < \Omega_T^*$. The pump pressure exceeds the load pressure ($p_P > p_U$) and the actuator starts moving. Different from the bleed-off concept, here the flow to the actuator results from a combination of flow throttling through the areas Ω_U and Ω_T. With reference to the simplified circuit depicting the configuration implemented by the spool in position 1 M in Figure 15.5, the status of the system is governed by the following equations:

$$\begin{cases} Q_T = C_f \Omega_T(i) \sqrt{\dfrac{2p_P}{\rho}} \\[2mm] Q_U = C_f \Omega_U(i) \sqrt{\dfrac{2\left(p_P - p_U\right)}{\rho}} \\[2mm] Q_U = Q_P - Q_T \end{cases} \tag{15.6}$$

The unknowns of this system of equations are Q_T, Q_U, and p_P and a mathematical solution can be found for any spool configuration. A qualitative trend for the three variables as a function of the spool stroke i (i.e. input command) is represented in Figure 15.6.
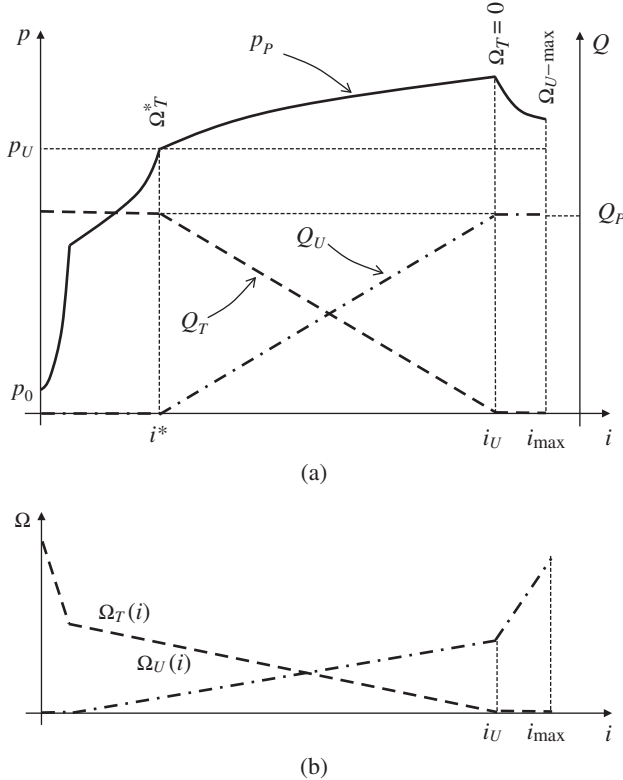
Figure 15.6 Pump pressure and flow (a), and area (b) trends for an open center system at different spool strokes.
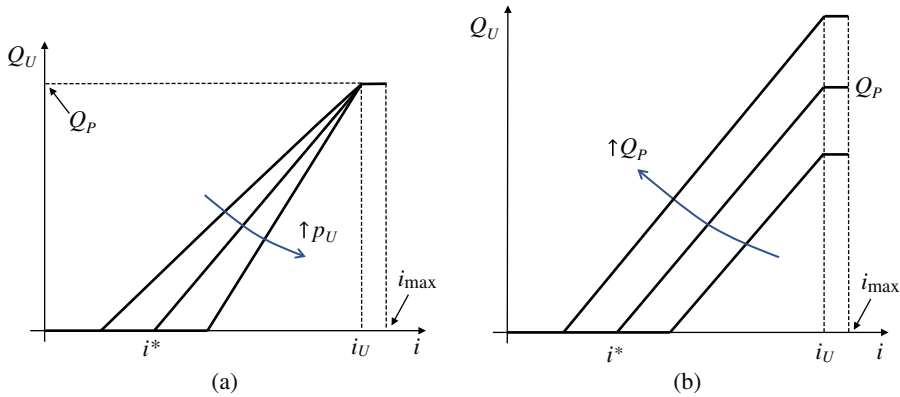
Figure 15.7 Influence of load pressure (a) and pump flow (b) on the control characteristic of an open center valve.

To summarize the operation of the system in Figure 15.5, when $i = 0$, the pump pressure is equal to the standby value p_0. If $0 < i < i^*$, the pump pressure increases, while no flow goes to the actuator. If $i^* < i < i_U$, the pump flow splits between the open center gallery and the actuator. During this regulation range, the pump pressure p_P slightly increases as the spool shifts and remains relatively close to the load value.

Figure 15.6 shows how the valve spool can be designed in such a way that the control range is limited between i^* and i_U, so that an additional control interval ($i_U < i < i_{max}$) is available for reducing the power losses when the entire pump flow is sent to the actuator. To obtain this feature, the valve flow area is designed with the trend represented in Figure 15.6: for $i \geq i_U$, the open center gallery completely closes ($\Omega_T = 0$), while the value of Ω_U rapidly increases (this can be achieved by opening the spool annular area), with the effect of significantly reducing the value of p_P.

Figure 15.6 shows the flow and pressure characteristic for a generic open center spool. As in the case of bleed-off circuits, the control range is a function of the values of Q_P and p_U. These trends are represented in Figure 15.7. In order to optimize the control of the actuator, the design of an
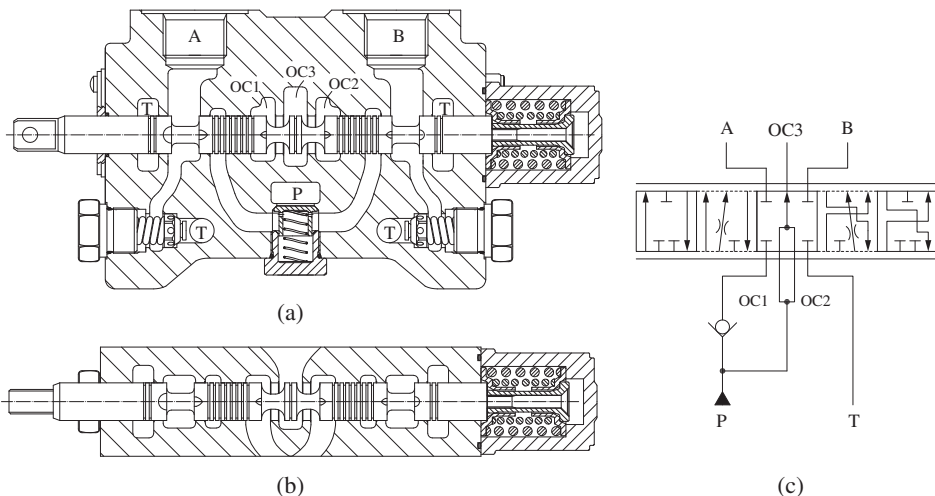
Figure 15.8 Cross sections (a, b) of an open center valve and equivalent spool symbol (c). The equivalent symbol does not show the port relief valves at both work-ports visible in the cross-sectional view.

open center spool (namely, the values of areas Ω_U and Ω_T) needs to be tailored to the operating conditions at which the actuator runs.

15.3.2 Open Center Valve Design

Figure 15.8 shows a cross section of a typical open center valve, where it is possible to notice the architecture of the open center gallery. As shown in the more detailed equivalent spool ISO schematic (symbol at the right of the figure), the open center gallery consists of three ports realizing a "Y" connection. This is also visible at the lower cross section (Figure 15.8b). In particular, the supply to the open gallery splits between ports OC1 and OC2. When the spool shifts in either direction, the area Ω_T is given by a combination of the flow areas between ports OC1-OC3 and OC2-OC3.

15.3.3 Energy Analysis

Figure 15.9 shows the energy plot for the circuit of Figure 15.5. The losses of the system are due to the flow loss through the open center gallery and to the metering loss across the area Ω_U. In fact, the energy performance of the open center system is affected mainly by two parameters: Q_P and p_U. The value of the flow areas can be selected around specific values of pump flow and load pressure in order to minimize the difference $p_P - p_U$, thus maximizing the energy efficiency. However, a change in load or a change in pump flow (i.e. engine speed increase) can significantly deteriorate the performance of the system as $p_P - p_U$ can easily increase.
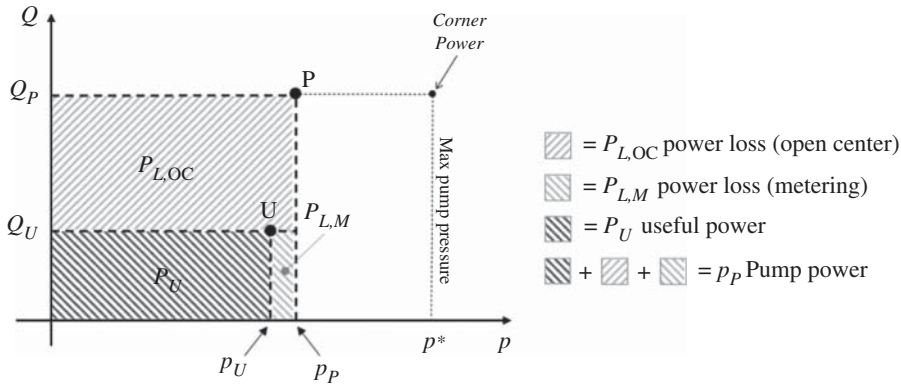
Figure 15.9 Energy plot for the open center circuit in Figure 15.5.

Similar with that of the bleed-off circuit, the energy efficiency of a basic open-center circuit tends to be low when the actuator is requiring only a part of the available flow. The energy efficiency is high when the commanded flow is close to the flow rate provided by the supply pump.

Example 15.2   Open center system to control an actuator

An open center valve is used to control the lifting of a cylinder. The pump flow is 35 *l/min*, and the cylinder pressure is 150 *bar*. The spool is moved to an intermediate position where the area to the cylinder is $\Omega_U = 10\,mm^2$ and the area to tank is $\Omega_T = 2.5\,mm^2$. Determine

a) The flow to the actuator, the flow back to tank and the pump pressure
b) The system efficiency
c) Repeat the calculations in case the pump flow rate doubles and also in the case that the load increases by 50% (keeping the same initial flow value)
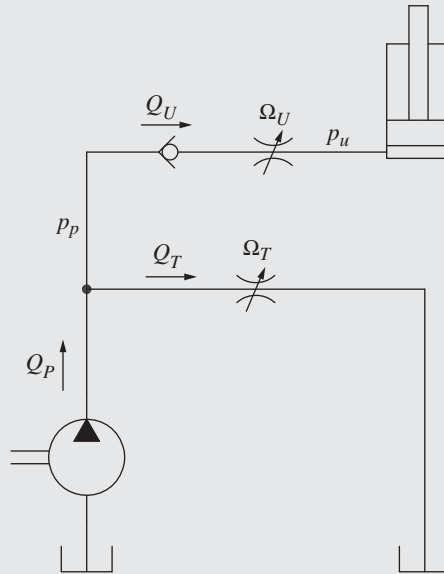
Consider no energy losses outside the orifices, and assume an orifice coefficient of 0.65 and oil with a density of 850 kg/m^3.

Given:
Load pressure, $p_U = 150\ bar$
Pump flow, $Q_P = 35\ l/min$
Area, $\Omega_T = 2.5\ mm^2$
Area, $\Omega_U = 10\ mm^2$
Orifice coefficient, $c_f = 0.65$
Oil density, $\rho = 850\ kg/m^3$

Find:
a) Flow to the actuator Q_U, flow back to tank Q_T, and pump pressure p_P
b) Repeat calculation for increased pump flow
c) Repeat calculations for increased load

Solution:

a) The circuit can be solved using the system of equations for an open center circuit (Eq. (15.6)):

$$
\begin{cases}
Q_T = C_f \Omega_T \sqrt{\dfrac{2p_P}{\rho}} \\[3mm]
Q_U = C_f \Omega_U \sqrt{\dfrac{2\left(p_P - p_U\right)}{\rho}} \\[3mm]
Q_U = Q_P - Q_T
\end{cases}
$$

Example 15.2 (Continued)

Substituting the values, the results are obtained as

$$
\begin{cases}
Q_T = 0.65 \cdot \dfrac{2.5\,[mm^2]}{10^6} \cdot \sqrt{\dfrac{2 \cdot 10^5 \cdot p_P\,[bar]}{850\,[kg/m^3]}} = 2.5 \cdot 10^{-5} \sqrt{p_P} \\[4mm]
Q_U = 0.65 \cdot \dfrac{10\,[mm^2]}{10^6} \cdot \sqrt{\dfrac{2 \cdot 10^5 \cdot (p_P - 150\,[bar])}{850\,[kg/m^3]}} = 10^{-4} \sqrt{p_P - 150} \\[4mm]
Q_U = 35\,l/min - Q_T = 35 - Q_T
\end{cases}
$$

The solution of this system can be found analytically through some mathematical manipulations and by solving the resulting second-order equations. However, considering the tools available currently, the numerical solution using a simulation model is recommended. Running the numbers on a numerical model, the results are obtained as

$$
\begin{cases}
Q_T = 18.7\,l/min \\
Q_U = 16.3\,l/min \\
p_P = 157.3\,bar
\end{cases}
$$

The reader can notice that the system pressure is just slightly above the load pressure.

b) The efficiency of the system is

$$
\eta_S = \frac{P_U}{P_P} = \frac{Q_U \cdot p_U}{Q_P \cdot p_P} = \frac{16.3\,[l/min] \cdot 150\,[bar]}{35\,[l/min] \cdot 157.3\,[bar]} = 44.4\%
$$

c) Using the same simulation model of (a), if the pump flow doubles to 70 *l/min*, the results are the following:

$$
\begin{cases}
Q_T = 21.8\,l/min \\
Q_U = 48.2\,l/min \\
p_P = 213.9\,bar
\end{cases}
$$

In the same way, if the cylinder pressure increases to 225 *bar* (while the pump flow is 35 *l/min*):

$$
\begin{cases}
Q_T = 22.6\,l/min \\
Q_U = 12.4\,l/min \\
p_P = 229.2\,bar
\end{cases}
$$

15.4 Advanced Open Center Control Architectures

The biggest limitation of a traditional open center system (based on the architecture in Figure 15.5) is the poor efficiency achieved during partial metering situations because the portion of the flow that was not used by the actuators is diverted back to tank through the open center gallery. This flow constitutes a power loss, and it can become quite significant. With reference to the chart of Figure 15.9, this loss equals:

$$
P_{L,OC} = (Q_P - Q_U) \cdot p_P \tag{15.7}
$$

The higher the value of $Q_P - Q_U$[1], the worse is the system efficiency. This can also create significant overheating issues, especially in systems where large amounts of flow is moved and not always used. This issue can be overcome by coupling an open center valve with a variable displacement pump. It is then possible to minimize the difference between the flow delivered with the flow requested by the actuator $Q_P - Q_U$, which in turns leads to minimizing the value of $P_{L,\,\text{OC}}$. Many designs have been developed throughout the years for achieving this feature and they are usually referred as *advanced open center systems*. Among these, the most common and most significant are the *negative flow control* and *positive flow control* systems.

> Standard open center systems have poor energy efficiency at partial flow commands due to the large amount of supply flow returned through the open center gallery. Advanced open center systems use variable displacement pumps to address this issue and achieve higher energy efficiency.

15.4.1 Negative Flow Control

Basic Schematic
The basic schematic of a negative flow control circuit is represented in Figure 15.10: the unique elements of this circuit are the variable displacement pump P and the orifice O placed on the open center gallery downstream of the DCV spool, before merging with the tank gallery.

The pump P contains a displacement control mechanism where the pilot pressure p_s acts against the spring ε. The spring force pushes the pump on-stroke, and the pilot pressure acts in the opposite way, decreasing the pump displacement.

Operation
The relationship between the pump displacement and pilot pressure can be simplified by the following equations:

$$\begin{cases} p_s \cdot A = F_\varepsilon + k_\varepsilon \cdot x \\ V_P = V_{P,\text{max}} - \lambda \cdot x \end{cases} \tag{15.8}$$

where A is the area of influence of the pressure p_s, F_ε, and k_ε are the preload and coefficient of the spring ε, and λ is a geometrical constant defining the relationship between x and V_P. Solving the system of Eq. (15.8), the pump displacement can be expressed as:

$$V_P\left(p_s\right) = V_{P,\text{max}} - \lambda \cdot \left(\frac{p_s \cdot A - F_\varepsilon}{k_\varepsilon} \right) \tag{15.9}$$

The chart in Figure 15.11 represents the trend described by Eq. (15.9): the pump displacement starts decreasing linearly when the pilot pressure overcomes the spring preload. Therefore, the minimum pressure at which the regulation starts is $p_{s,\,\text{min}} = F_\varepsilon / A$. However, the pump displacement never reaches the null value. In fact, the pump typically contains a minimum displacement mechanical stop, set at $V_{P,\,\text{min}}$.

Figure 15.10 also shows how the pilot pressure p_s is generated. The open center gallery flow Q_T is directed through the fixed orifice O, which has a cross-section Ω. The pressure p_s is taken from

---

1 The value of $Q_P - Q_U$ is critical not only in situations where the flow commanded is small (i.e. partial metering situations) but also when the amount of flow produced by the pump becomes high. This should be considered for the cases where the open center system is sized for a specific engine speed (e.g. engine idle), but the supply pump encounters also instances at which it spins at a much higher speed.

Figure 15.10 Basic architecture of a negative flow control system. The pump displacement control mechanism is represented with a simplified symbol.

the open center gallery, between the valve DCV and the orifice O. The value of the pilot pressure p_s sent to the pump is a function of the area Ω and the flow rate Q_T:

$$p_s = \frac{\rho}{2} \left(\frac{Q_T}{C_f \cdot \Omega} \right)^2 \tag{15.10}$$

Neutral position (i = 0). In standby conditions, the DCV is in its neutral position and the pump outlet is connected to the tank through the open center gallery and the orifice O. In this condition, the pump sets its displacement at $V_{P,0}$, in order to provide the flow $Q_{P,0} = Q_{T,0}$. The value $V_{P,0}$ corresponds to the standby value of the pilot pressure $p_{s,0}$, as it is represented in the chart in Figure 15.11. The exact values of standby flow and pressure can be found by combining Eqs. (15.9) and (15.10) and considering that $Q_{T,0} = n \cdot V_{P,0}$. It can be seen that $V_{P,0}$ is directly related the orifice area Ω. Hence the size of this orifice can be selected based on the desired amount of standby flow.

Obviously, in standby condition, it is desirable to have $\Omega_T \gg \Omega_O$, so that the standby pressure at idling conditions $p_{s,0}$ is at minimum.

Regulation. When the spool is moved from its neutral position by a command $i > 0$, part of the flow is instantaneously subtracted from the open center gallery and diverted to the actuator. This situation is similar to what happens in the standard open center system (Figure 15.6). As the flow to the actuator increases, the value of Q_T decreases. In turn, the value of p_s also decreases
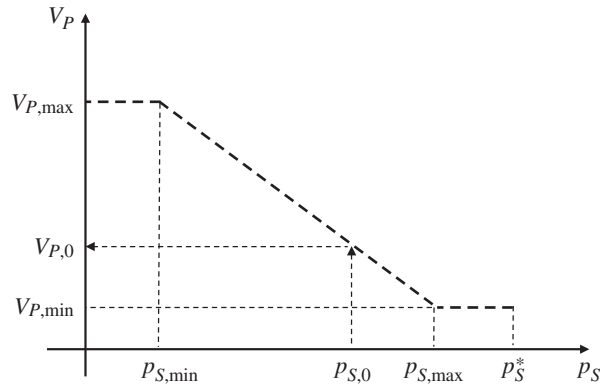
Figure 15.11 Relationship between displacement V_p and pilot pressure p_s in a negative flow control pump.

(according to the above Eq. (15.10)), and the pump control reacts increasing the displacement of the unit, until a new equilibrium condition is reached.

The overall behavior of the system is represented in Figure 15.12, which correlates the value of the input command i – i.e. the spool position – to the different steady-state flows and pressures. The representation is similar to Figure 15.6, given that for the open center system, a fixed displacement pump is used. In the negative flow control circuit, as i increases, more flow is provided to the consumer Q_U, while the flow through the open center gallery Q_T gradually reduces
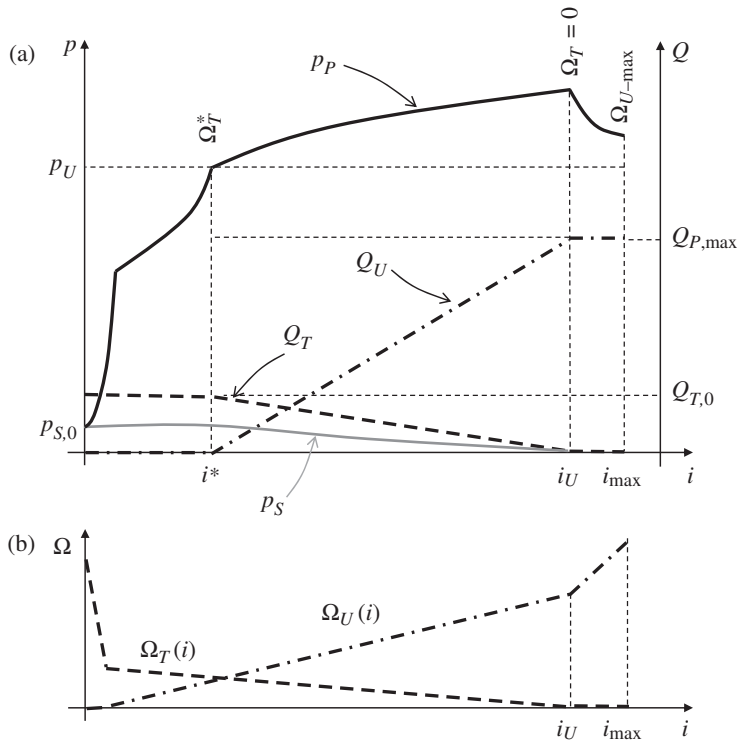
Figure 15.12 Pump pressure and flow (a) and area (b) trends for an open center system with negative flow control.

from the standby condition $Q_{T,0}$. In other words, the standby condition has the highest flow through the open center gallery. The trend of Q_T leads to a decreasing control pressure p_s, which means increasing the pump displacement. A proper timing of the areas Ω_T and Ω_U can help to accomplish a gradual (almost linear) relation between the input command, i, and the output flow Q_U.

As i increases, the open center valve will rapidly decrease the open center gallery area Ω_T, entering into the metering notches configuration. This significantly increases the pump pressure, while the flow through the orifice O remains constant (Q_T). At this point, the valve also gradually opens a connection area to the actuator Ω_U. As soon as the pump pressure equals the load pressure p_u, the check valve CV will allow a portion of the pump flow to be sent to the function. As before, the condition $Q_U > 0$ occurs at a certain command i^*, which depends on the load pressure.

A particular situation is reached when the valve DCV is fully shifted and the open center gallery is closed. In this case, $Q_T = 0$ and the pump is driven at its maximum displacement.

The relief valve RV2 indicated in Figure 15.10 is present only to limit the maximum value of p_s and protecting the displacement adjustment mechanism of the pump, especially during transients, like a sudden closure of the DCV spool.

Pump Displacement Setting Mechanism

The circuit in Figure 15.10 gives an intuitive representation of the pump control. In reality, the displacement setting mechanism used in negative flow control pumps is quite complex because the pilot pressure p_s alone, whose maximum values are in the range of 20–30 bar, is not capable of adjusting the pump displacement quickly enough to follow the spool command. Second, the negative flow control concept requires a properly damped control mechanism in order to avoid instability issues. These two problems can be overcome by a control mechanism equipped with an internal feedback, as represented in Figure 15.13.

The pump displacement is controlled with the differential area control piston, labeled as CD. The rod side is connected to the pump outlet pressure and also includes a spring, which is used to bias
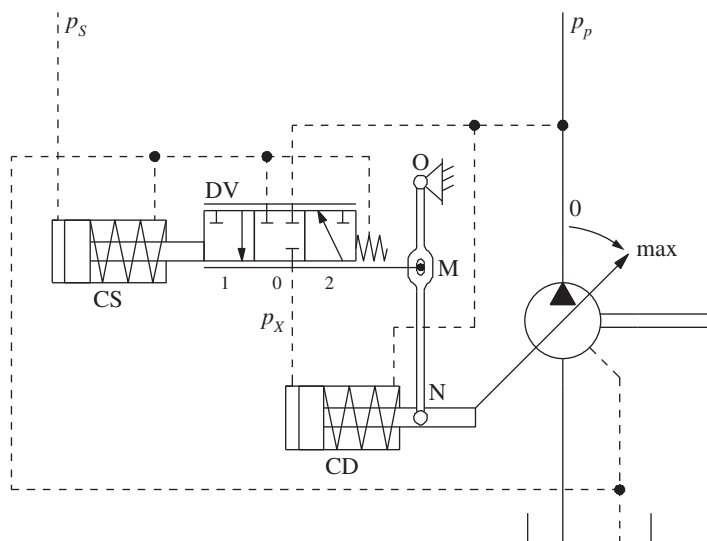
Figure 15.13 Detailed view of a possible control concept for negative flow control pumps.

the displacement to its maximum value in neutral configuration. The bore side of CD is supplied with the pressure p_x, which is controlled by the 3/3 proportional valve, labeled as DV. The spool of DV is actuated by the plunger, labeled as CS, which is supplied by the pilot pressure p_s. The plunger is used to amplify the force generated by p_s with respect to the small diameter of the spool DV. When the spool DV is in neutral position (0), all ports are blocked and the pump is held at constant displacement. When DV is in position 1, pump pressure is sent to the CD and the pump reduces its displacement. Vice versa, in position 2, p_x is relieved and the displacement is increased by the pump pressure acting on the rod side of CD.

The control schematic in Figure 15.13 also presents a mechanical feedback between the displacement of the pump and the sliding sleeve of the valve DV. This is represented by the linkage $\overline{ON}$: the point O is fixed, while N is connected to the stroking piston CD. The sleeve of DV follows the linkage in its intermediate point M. When the spool DV shifts toward the right, DV is moved into configuration 1, the path from P to X is open and the pump decreases its displacement. Consequently, the linkage in M pulls the sleeve also toward the right (following the movement of the spool) until the neutral configuration is restored. The travel of the spool is proportional to the value of p_s, which is acting against the spring contained in CS. Therefore, displacement setting is also proportional to the value of p_s.

Figure 15.14 presents the actual implementation of the control described in Figure 15.13. The structure of the control is rather complex and includes additional elements with respect to the simplified schematic. However, it achieves the same functionality. The spool DV, represented in position (1), slides into a sleeve (2). A spring pushes the spool toward the left side by acting on the sleeve and on a washer locked on the spool left end. A second outer spring (coaxial to the previous
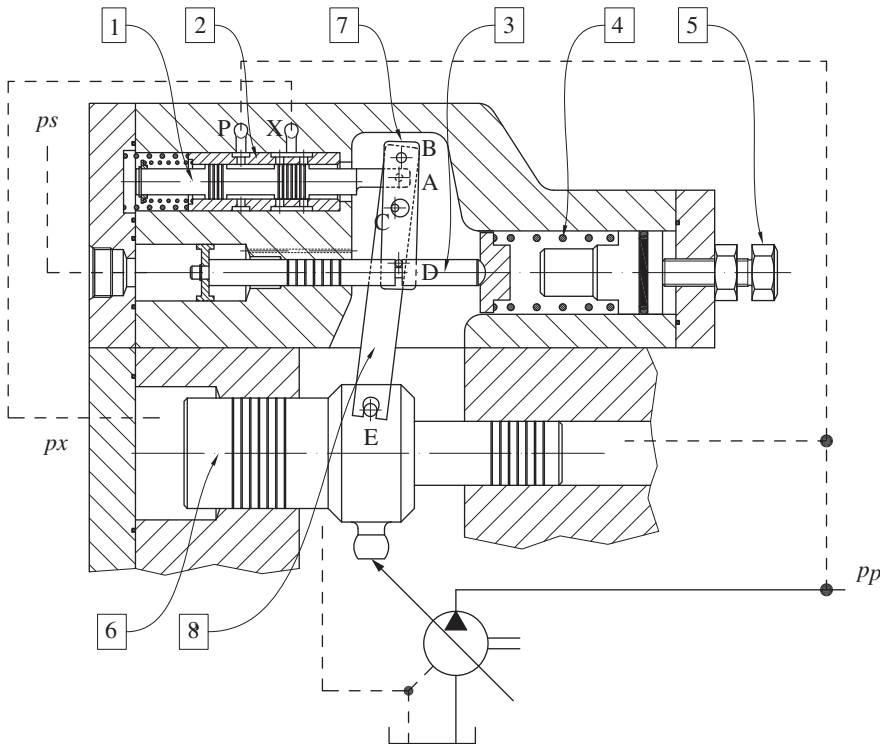
Figure 15.14 Actual implementation of the negative flow control for an axial piston pump.

one) is used to lock the sleeve in place[2]. The sleeve connects ports P and X from the control housing to the spool bore through three calibrated radial holes and two circular slots on the outer diameter. The spool metering lands (represented in neutral position) block both holes connected to the X port (positive overlap). If the spool travels to the right, P is connected to X; vice versa, when the spool shifts left, X is vented to the case of the pump (T port), through the sleeve bore clearance. Below the spool and the sleeve, the plunger CS (3) slides on a parallel axis. The pressure p_s acts on the large area of the plunger pushing against the spring (4), which has an adjustable preload, by acting on the cap screw (5). Below the plunger, the swash plate control piston CD (6) is subject to the pressure p_X on the large area of the left chamber, and to the pressure p_P in the right chamber, with smaller area. The control piston is connected via a spherical joint to the pump swash plate, on which inclination determines the fractional displacement ε of the pump. The three main elements (1, 3, and 6) are linked together by two lever arms (7 and 8). These present five significant pivot points with an equal number of pins. The long lever arm (8), which, as in Figure 15.14, is located behind the lever (7) and the plunger (3). It connects with the spool at point A, with the short lever (7) at points B and C and with the stroking piston (6) at point E. The short lever arm (7) connects with the long lever (8) at points B and C and with the plunger 3 at point D (this pin seats into a slot machined in the plunger). In particular, the connection at point C is rigid only in one direction, since the slot in (7) is larger than the pin in (8).

In the initial configuration, port X is closed and the control piston is locked in position. If the pressure p_s increases, the plunger (3) shifts to the right, until the pressure force is balanced by the action of the spring (4). As a consequence, the short lever (7) translates to the right, held in position by the pins B and C. In turn, the long lever (8) slightly rotates clockwise around the fixed point E. In this situation, point A shifts slightly to the right which causes spool (1) to also move right, thus opening an area between P and X. The left chamber of piston (6) is pressurized, causing it to move right, thus reducing the pump displacement. As (6) moves, the pin E also moves and the lever (8) rotates counterclockwise pivoting around B. In this motion, pin C detaches from the contact point with lever (7): the spool, pulled by its spring, shifts to the left, until the connection P-X is closed and the spool returns in the neutral position. With this motion, (7) and (8) also rotate slightly around A returning to the initial relative configuration.

If pressure p_s decreases, the plunger (3) shifts to the left, because of the action of spring (4). Lever (7) initially rotates clockwise around point B, while pin C detaches from the seat. The spool moves left pulled by its spring and the long lever (8) slightly rotates counterclockwise until pin C regains contact with the larger seat. In this position, the spool vents port X to tank T and the piston (6) is free to shift to the left, thereby increasing the pump displacement. While doing so, the spool is also shifted in the opposite direction as the long lever (8) rotates around points A and E, until the neutral configuration is established at an increased pump displacement.

15.4.2 Positive Flow Control

Basic Schematic

Figure 15.15 represents the basic positive flow control circuit: the DCV is an open center type and the spool control is hydraulic pilot. The pilot pressures p_{XA} and p_{XB} comes from a remote pilot actuation of the function, as described in Figure 8.37. The source of the pilot pressure (not shown in

---

2 Contrary to what Figure 15.10 depicts, the sleeve is actually not moving. The position feedback is achieved with a series of levers which are ultimately acting on the spool.
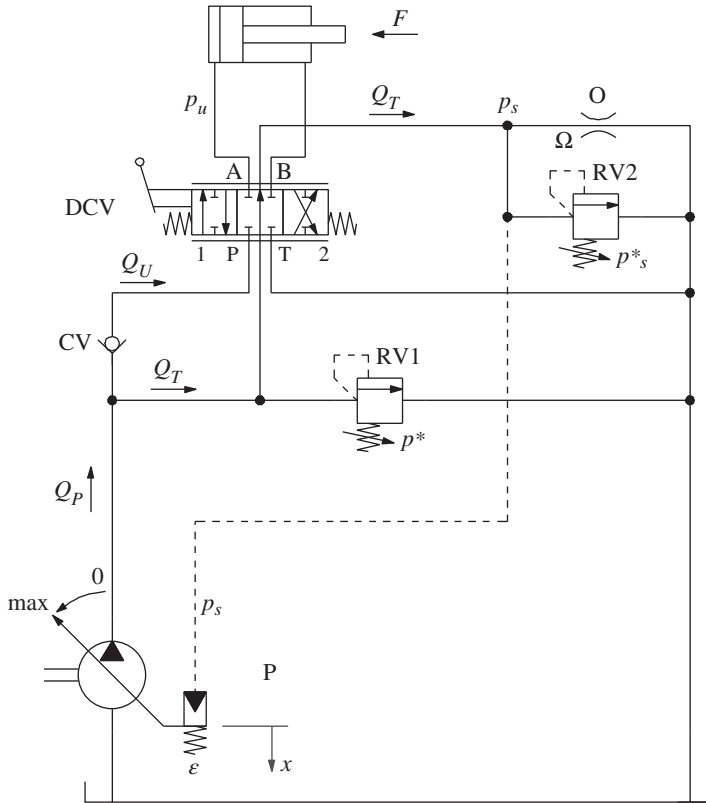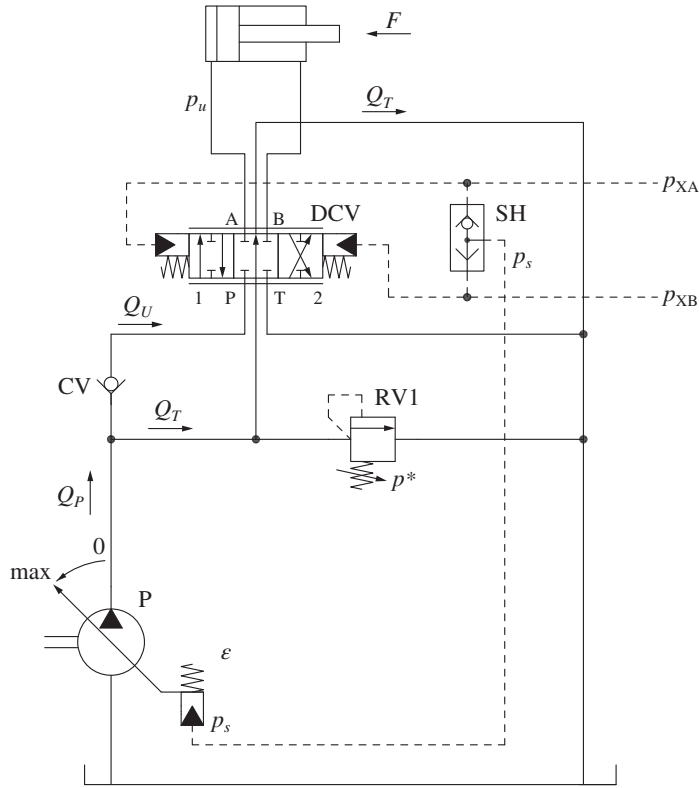
Figure 15.15 Basic architecture of a positive flow control system. The pump displacement control mechanism is represented with a simplified symbol.

figure) is usually implemented by a dedicated circuit. The pilot pressures p_{XA} and p_{XB} are compared through the shuttle, labeled as SH and the highest of the two p_s is sent to the pump control mechanism. In this way, the pump displacement increases along with the pilot pressure commands, as more flow is commanded to the function.

Operation

The pump control mechanism is similar to the one described in Figure 15.10 (negative flow control), but it operates with the opposite operating principle with respect to the pilot pressure. In particular, the spring ε biases the pump to its minimum displacement, while the force generated by the pressure p_s increases the displacement setting:

$$\begin{cases} p_s \cdot A = F_\varepsilon + k_\varepsilon \cdot x \\ V_P = V_{P,\min} + \lambda \cdot x \end{cases} \tag{15.11}$$

which gives:

$$V_P\left(p_s\right) = V_{P,\min} + \lambda \cdot \left(\frac{p_s \cdot A - F_\varepsilon}{k_\varepsilon}\right) \tag{15.12}$$

The relationship between p_s and pump displacement V_P is represented in Figure 15.16. The relationship is linear with direct proportionality for pilot pressures between $p_{s,0}$ and $p_{s,\max}$. A minimum displacement value $V_{P,\min}$ is typically kept to achieve a better system performance, in terms of control accuracy and dynamic response.
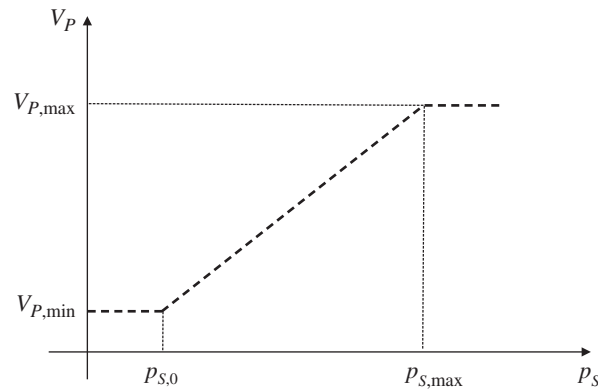
Figure 15.16 Relationship between displacement V_p and pilot pressure p_s in a positive flow control pump.

Pump Displacement Setting Mechanism

The detailed schematic of the pump control mechanism is depicted in Figure 15.17: the schematic is very similar to Figure 15.13, except here the plunger CS is not acting directly on the spool but, by means of the linkage with pivot point U, its action has the opposite effect with respect to the previous case. In other words, increasing the value of p_s causes the pressure p_X to be relieved, therefore causing the pump displacement to increase. In the layout of Figure 15.14, this change can be implemented by changing the location of pin B, positioning it between C and D.

15.4.3 Energy Analysis for Advanced Open Center Architectures

Figure 15.18 shows the energy plot for the two concepts. When compared to the open center case of Figure 15.9, the area indicative of power loss in the open center gallery $P_{L,OC}$ is significantly smaller. This because the value of Q_P is lower than $Q_{P,\max}$. In the negative flow control circuit, the pump control mechanism automatically sets the displacement in order to have a residual flow $(Q_P - Q_U)$ through the open center gallery, unless it is closed (i.e. in the case of full flow condition). For the positive flow control case, the situation is more complex. In fact, the valve spool and its control need to be designed in order to match the pump displacement command range, in both directions of movement. The energy plot Figure 15.18 assumes that the system is designed with the pump
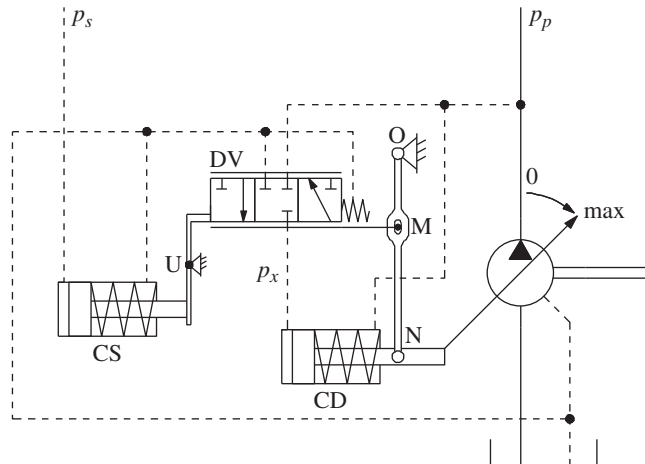
Figure 15.17 Detailed view of a possible control concept for positive flow control pumps.
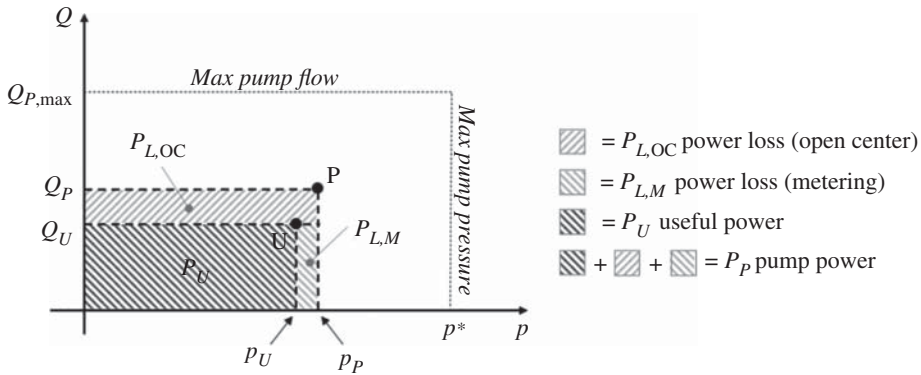
Figure 15.18 Energy plot for the advanced open center systems.

being always "ahead" of the demand from the consumer (i.e. $Q_P > Q_U$), which is the common case for these types of systems.

Problems

15.1 Consider a circuit such as in Figure 15.2. The pump has a displacement of $75\,\text{cm}^3/\text{r}$ rotating at 1000 rpm. The motor has a displacement of $300\,\text{cm}^3/\text{r}$ and drives a broom, which requires an external torque of 550 Nm. The torque is resistive in both directions of rotation. Calculate
   1) The flow area Ω_0 corresponding to a standby pressure of 12 bar
   2) The flow area Ω^* at which the motor starts rotating (when DCV is actuated)
   3) The useful and wasted energy when the area Ω is equivalent to a 2.8-mm orifice diameter (flow coefficient 0.67)
   4) Repeat the same calculations for the case where the pump speed is increased to 1750 rpm.

15.2 Consider the bleed-off circuit below. The torque at the hydraulic motor (size: 10 cc/rev) is 15.9 Nm. The pump flow is $Q_p = 20\,\text{l/min}$.
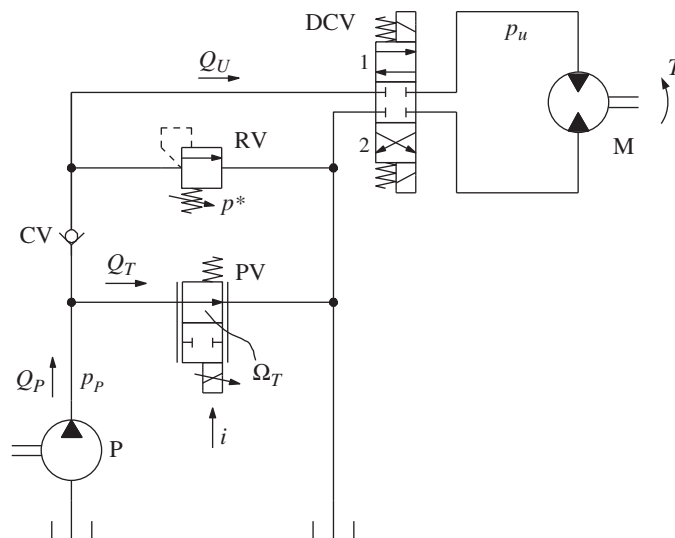
    a) Find the range of equivalent orifice area of the bleed off valve that allows controllability of the motor.

       Consider a case where the equivalent orifice area of the bleed-off valve is 1 mm².

    b) Draw the energy plot with proper labels and numbers.

    c) Determine the system efficiency.

    Assume that the motor is 100% efficient, as well as following values: $C_f = 0.7$, $\rho = 850 \text{ kg/m}^3$, $p^* = 150$ bar

15.3 In the simplified basic open center circuit represented below, the pump provides 70 l/min to the two areas Ω_T and Ω_U. The cylinder has a bore diameter of 45 mm and works against a load of 5670 lbf. Calculate the two combinations of areas Ω_T and Ω_U, which would lead to a cylinder extending speed of 0.45 m/s for the following cases. The first combination of values should have a pressure drop of 5 bar across Ω_U, and the second one, a pressure drop of 20 bar across Ω_U. Calculate useful power and power loss of the system for both cases.
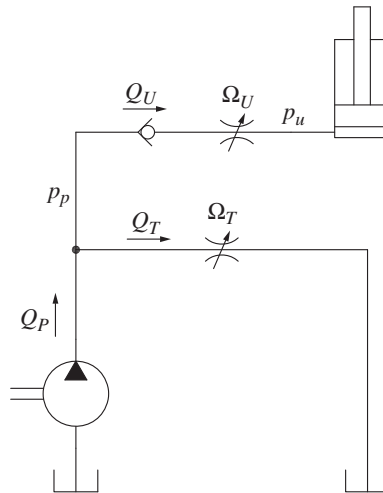
Chapter 16

Load Sensing Systems

Load sensing (LS) control is a very energy-efficient method for metering control of hydraulic actuators and relatively simple for single and multiple actuators. Thus, the popularity and success of LS systems have been rapidly increasing across multiple applications, especially on mobile equipment, in the past 30 years.

This chapter illustrates the basic concepts of LS systems and then presents its application with both fixed and variable displacement pumps. The chapter also provides insights on the architectures of the main components that operates in an LS system: the LS valve and the LS pump.

16.1   Basic Load Sensing Control Concept

The term "load sensing" (LS) refers to a metering control concept in which the load pressure information is continuously used by a hydraulic control system to regulate the velocity of an actuator. This type of feedback within the metering control enables two important and desirable features. First, the actuator velocity is not influenced by the pressure induced by the load and is only a function of the operator command. Second, the supply pressure always follows the load pressure, which minimizes the power loss associated with the metering control. Therefore, an LS system is the most energy-efficient implementation of metering control.

LS controls are used in combination with a particular type of flow supply (as defined in Chapter 11), which can be implemented either with a fixed or with a variable displacement pump.

In metering control, from the basic metering schemes of Chapter 13 to the open center systems of Chapter 15, the actuator velocity is not uniquely determined by the operator command. In fact, in all these metering concepts, the actuator velocity is a result of both the control command, i, and the actuator load, p_U:

$$Q_U = Q_U\left(i, p_U\right) \tag{16.1}$$

However, in an LS system, the flow rate sent to the actuator (thus its velocity) is a unique function of the control signal and is independent of the load:

$$Q_U = Q_U\left(i\right) \tag{16.2}$$

Therefore, LS systems permit a straightforward control of the actuators, without requiring specific customization of the control elements based on the application. This aspect, along with the abovementioned energy efficiency advantage, have contributed to the commercial success of LS systems.

> **Load sensing systems** are an energy-efficient method for implementing metering control. They achieve flow regulation independent of the actuator load.

In many applications characterized by highly variable loads and requiring accurate velocity control of the actuator, the dual dependence of Q_U with i and p_U (summarized by Eq. (16.1)) is undesirable. Consider, for example, the case of a hydraulically driven conveyor, which needs to maintain a constant speed independent of the amount of material on the conveyor belt. For such application, the LS circuit is a perfect fit because, with an open center system, the operator (or the electronic controller) would have to continuously adjust the command in order to maintain a constant actuator velocity. However, it is also important to understand that, for some applications, such as hydraulic backhoes or excavators, the influence of the load on the controlled actuator velocity can actually be a desirable feature for an expert operator. This is because it provides the operator with a feeling of the load encountered by the actuator, and it can help to promptly perceive any sudden changes in operating conditions (such as encountering a metal pipe while digging).

16.2 Load Sensing System with Fixed Displacement Pump

16.2.1 Basic Schematic

The operating concept of an LS system with a fixed displacement pump is represented in Figure 16.1. The flow provided to a generic actuator (or consumer, U) is controlled with an adjustable orifice O. The orifice throttling area is proportional to the command i and a compensator C (commonly referred to as an *unloader*) that senses the load pressure p_U.

16.2.2 Operation

The unloader C compares the pump pressure p_P with the load pressure p_U, biased by the equivalent pressure of the spring, s, and controls the flow rate Q_T that is discharging to the tank, such that
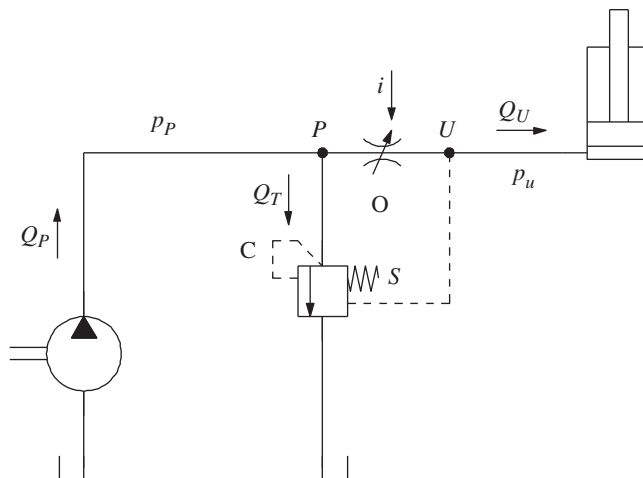
Figure 16.1 Load sensing principle (flow supply, fixed displacement pump) for a single actuator.

following condition is satisfied:

$$p_P = p_U + s \tag{16.3}$$

The orifice O is the metering control element. In fact, according to the definition given in Chapter 4, the pressure drop across the orifice $(p_P - p_U)$ is regulated by the compensator. Consequently, the flow rate through the orifice (whose opening area is Ω_U) to the actuator becomes

$$Q_U = C_f \cdot \Omega_U(i) \cdot \sqrt{\frac{2\left(p_P - p_U\right)}{\rho}} = C_f \cdot \Omega_U(i) \sqrt{\frac{2 \cdot s}{\rho}} \tag{16.4}$$

Equations (16.3) and (16.4) together show how the supply pressure follows the load, and also the actuator flow is only a function of the orifice area, which is directly related to the input command, *i*. As mentioned in the introduction, these are the main features of a LS system.

One can observe that the LS principle shown in Figure 16.1 accomplishes the equivalent function of a three-way flow control valve with the adjustable setting placed between the pump and the hydraulic consumer. This can be observed by comparing Figure 8.25 with Figure 16.1. Furthermore, Eq. (16.4) coincides with the expression of Eq. (8.22), which was provided for a three-way flow control valve.

Figure 16.2 shows two alternative solutions for limiting the pressure in an LS system. These are equivalent to the solutions described in Chapter 8 (Figures 8.25 and 8.26) for the case of three-way

(a)

(b)

Figure 16.2 Limiting the maximum pressure in the LS system of Figure 16.1: with a pressure relief valve on the main flow line (a); with a pressure relief valve in the pilot line (b).

flow control valves. It is important to describe the function of the orifice O_S in Figure 16.2b. This orifice works as a *pressure separator* when the relief valve (RV) enters into regulation. The use of pressure separators is necessary when a pressure control valve, in this case a pressure relief valve, is used to limit the pressure in a pilot line. This was also discussed in Chapter 8, for the case of pilot operated relief valves. Obviously, with respect to the solution of Figure 16.2a, the system of Figure 16.2b permits to use a smaller pressure relief valve, since the valve has to handle tiny flow rates in the pilot line.

16.2.3 Energy Analysis

The energy analysis of the system can be performed by expressing the power consumed by the pump:

$$P_P = Q_P \cdot (p_U + s) \tag{16.5}$$

and the power utilized by the actuator:

$$P_U = Q_U \cdot p_U \tag{16.6}$$

These terms are represented by rectangular areas in the energy plot in Figure 16.3. As shown in the figure, the power dissipated by the LS metering system, P_L, is given by two terms. The first one is the unloader dissipation, $P_{L,C}$ (due to the unloader throttling the excess flow generated by the pump to tank). The second one is the throttling loss of the metering orifice, $P_{L,M}$:

$$P_L = P_{L,C} + P_{L,M} = (Q_P - Q_U) \cdot (p_U + s) + Q_U \cdot s \tag{16.7}$$

The system efficiency becomes

$$\eta_S = \frac{P_U}{P_P} = \frac{Q_U \cdot p_U}{Q_P \cdot (p_U + s)} \tag{16.8}$$

From Eqs. (16.7) and (16.8), it appears convenient, in terms of energy, to reduce the unloader settings (also referred as *load sensing margin*) to a low value. Typical values for the spring setting of a compensator range between 5 and 20 bar.[1] Also, the lower the difference between the pump flow Q_P, and the flow request, Q_U, the higher the system efficiency.

Figure 16.3 Energy plot of the LS system in Figure 16.1.

---

1 As it will be explained in the following paragraphs, a low value of the LS margin improves the system efficiency but has also some disadvantages. Therefore, the value of the LS margin is rarely lower than 10 bar, even with fixed displacement pumps.

Figure 16.4 Flow rate provided to the actuator by the LS system in Figure 16.2.

16.2.4 Saturation Conditions

The flow vs. pressure chart of Figure 16.3 (energy plot) outlines the upper bounds for the operating points U and P of the system. The *pressure saturation* condition starts when the load pressure p_U reaches the maximum pressure allowed by the relief valve, p^*. In this case, the pump is limited to its maximum pressure $(p^* + s)$, due to the action of the unloader and the relief valve in the pilot line. For a further increase of the load, the flow Q_U progressively decreases until becoming null, when $p_U = p^* + s$. For higher load pressure, the control action of the system is lost $(Q_U < 0)$ and the actuator velocity becomes opposite to the command. This condition can be avoided by using a load drop check, as it was shown for the open center circuits. The load drop check valve (CV) will be shown specifically for the LS system later in this chapter.

As it pertains to the maximum flow rate, it is clear that $Q_{U, \max} = Q_P$. This condition will be reached for the maximum opening of the metering orifice O:

$$\Omega_{\max} = \frac{Q_P}{C_f} \sqrt{\frac{\rho}{2s}} \tag{16.9}$$

For $0 < \Omega \le \Omega_{\max}$, the flow rate to the function increases linearly, as shown in Figure 16.4. If the relation $\Omega = \Omega(i)$ is also linear, Q_U, and therefore the actuator velocity, will result in a linear function of the command i, independent on the load pressure. For this reason, the performance of a LS valve can ideally be considered independent from the external forces on the actuators. This is different from other metering concepts, such as open center systems, where the load affects the control characteristics of the valve.

In case the orifice O allows for openings $\Omega > \Omega_{\max}$, the condition of *flow saturation* is reached: Q_U remains at its maximum value $(Q_U = Q_P)$, and the point P in the energy plot of Figure 16.3 tends to overlap the point U. In other words, $p_P < p_U + s$ and the condition of Eq. (16.3) is no longer satisfied. In flow saturation, the unloader is closed $(Q_T = 0)$ and the orifice O behaves as a compensator. Flow saturation is likely to happen in systems where the pump speed is variable, when the pump rotates at a speed lower than the design point (e.g. vehicle idle conditions).

16.3 Load Sensing Valve

A practical implementation of the LS principle from Figures 16.1 and 16.2 is shown in the schematic of Figure 16.5, which allows for the bidirectional control of the actuator velocity using a 5/3 spool
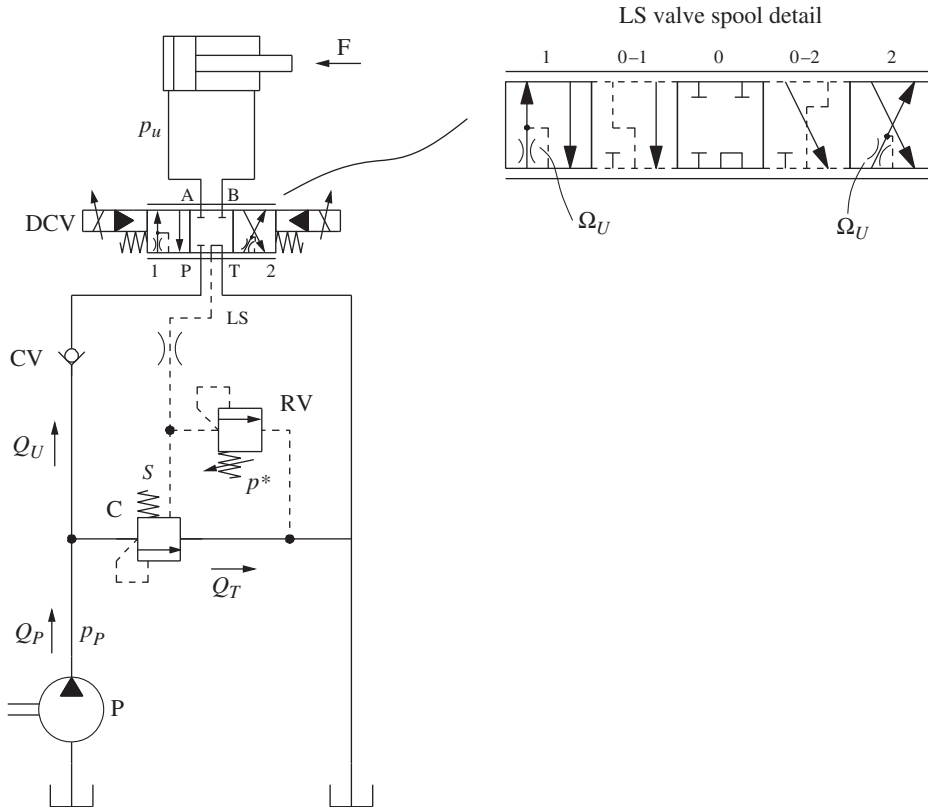
Figure 16.5 LS system with fixed displacement pump using a 5/3 proportional LS valve.

valve (DCV, commonly indicated as *LS valve*). This spool valve has four power ports: the supply connection to the pump (P) and the return to the tank (T) and the two actuator connections A and B. The additional port is the LS signal (LS port), which is connected to the external unloader C to replicate the principle of Figure 16.2. In neutral position, the LS valve ports P, A, and B are closed, while the LS port is connected to T. In this situation, all the pump flow is diverted to the tank through the unloader and the pump pressure equals the LS margin *s*. This minimizes the energy dissipation when the actuator is not operated.

When the LS valve operates at one of the two working positions, the connection P opens to one of the actuator work-ports ($P \rightarrow A$ for the extension; position 1; $P \rightarrow B$ for the retraction; position 2), with an opening area Ω_U proportional to the command *i*. The opposite work-port is connected to the tank port T, with a large area. The variable flow areas to the work-ports implement the metering orifice of the LS concept: $\Omega_U = \Omega_{PA}(i)$ when the LS valve in position 1, $\Omega_U = \Omega_{PB}(i)$ in position 2. As indicated in the spool symbol, while opening the metering orifice, the spool also connects the LS signal port to the work-port being supplied, downstream of the metering orifice. This enables the valve to "read" the load pressure and send this information to the compensator. A load drop check valve (CV) is also present next to the inlet port P to prevent the load from moving in the opposite direction in case of overload conditions (as described in Section 16.2.4 for the case of pressure saturation conditions).

The detail of the LS valve shown at the right of Figure 16.5 also highlights a peculiar feature of the spool design, in the intermediate positions (indicated as positions 0-1 and 0-2). These are interposed between the neutral position and the working positions. These intermediate configurations are indicated using dotted lines and represent the connections implemented by the valve, right after the spool is moved from the neutral position. In particular, before the port P is connected to either one of

the two work-ports, A or B, the LS valve first connects the LS port to the actuator work-port. This permits the unloader to establish the pressure $(p_U + s)$ at the pump outlet before the connecting the port P to the load. If this condition were not implemented, the pump would be connected to the actuator when its delivery line is still at the low pressure (corresponding only to s). This could cause a transient in the actuator motion, which is undesirable to the operator.

An example of typical LS valve architecture is represented in the cross-section of Figure 16.6. The LS valve spool is maintained in the neutral position by two centering springs located in the pilot chamber X. The springs are coupled to the spool with two washers and a cap screw so that the same springs are compressed when the spool travels in either direction. When the spool shifts to the right the outer washer is held in position against the cap. Similarly, in the opposite direction, the inner washer is held against the valve housing. When the pilot pressure at X or Y exceeds the centering

Figure 16.6 5/3 Proportional LS valve architecture, with integrated work-port relief valves and with LS pressure limitation at port A: (a) cross section, (b) detailed schematic.

spring preload, the spool starts to move opening the connections $P \to A$ and $B \to T$ (when p_X is increased) or $P \to B$ and $A \to T$ (when p_Y is increased). The springs force increases with the travel, so that the spool position is proportional to the pilot pressure. Typically, the pilot pressure range is between 5 bar (minimum pilot pressure) and 20 bar (maximum pilot pressure). The minimum pilot pressure is mainly related to the preload of the centering springs in neutral and the spool underlap. It corresponds to the pressure at which the valve starts to open and deliver flow to one of the two work-ports. The maximum pilot pressure corresponds to the full travel of the spool, in either direction, where maximum opening area of the valve is reached. As shown in the figure, it is typical to have multiple nested centering springs to meet the requirements in terms of spool travel, pilot pressure range, and available space.

The spool of the LS valve shown in Figure 16.6 also presents metering notches that allow a controlled opening of the metering areas of the valve, for the connections $P \to A$ and $P \to B$.

An interesting feature of the valve is the solution used for handling the LS signal, which follows a complex path. The main spool is hollow, and the internal axial channel is used for carrying the load signal to the LS channel located in the valve housing. The load pressure is picked by two small radial holes in the spool (*LS pickup holes*), located close to the A and B ports. A third radial hole (located close to the Y end-cap on the left side) carries the pressure signal to the LS port. In addition, there are three additional spool lands (*LS selecting lands*) which can connect the LS signal to the tank or to one of the two volumes, LS-A or LS-B.

In the neutral position, the two LS pickup holes are blocked, and the spool internal channel is connected to the return (port T), using the LS selecting lands. After a small travel of the spool in either direction, the LS selecting lands close the passage to the tank. At the same time, the LS pickup holes are connected to either the A or B work-port while the LS path is connected to LS-A or LS-B where signal relief valves can be located. In the valve of Figure 16.6, the valve RV_{LS} is limiting the signal on the A side, while no relief valve is located on the B side. The configuration just mentioned corresponds to the spool intermediate positions represented with dotted lines, i.e. where the work-ports are still closed, and no flow is being directed to the actuator.

If the spool travel increases, the spool opens the metering area $\Omega_{P \to A}$ (when p_X is piloted) or $\Omega_{P \to B}$ (when p_Y is piloted) proportional to the pilot pressure. The absence of metering notches at the spool lands realizing the return connections $\Omega_{A \to T}$ and $\Omega_{B \to T}$ permit to achieve large openings at the return port, thus reducing throttling losses on the return side.[2]

The embodiment of the LS valve typically includes additional features, which can vary according to the configuration selected for the application. In Figure 16.6, a load drop CV is present between port P of the valve and the inlet chamber of the main spool. Two pressure relief valves RV_A, RV_B (work-port reliefs) are used to prevent overpressurization at the two work-port lines.[3] Furthermore, as mentioned before, a signal pressure relief valve (RV_{LS}) is used to limit the signal pressure in the LS line, similar to the concept in Figure 16.2b.

In a nutshell, LS valves offer different options for limiting the maximum pressure in the system:

- RV_{LS} signal relief connected to the LS signal line. In this case, the LS signal pressure cannot be greater than the set pressure of RV_{LS}, thus limiting the pressure supplied to the actuator. The valve RV_{LS} can be connected to the common LS port (thus realizing the configuration of

2 The configuration of the LS valve in Figure 16.3 is suitable for a meter-in control, in which counterpressure at the return port is not necessary (only resistive loads) or is achieved with external components such as counterbalance valves. In some cases, it is possible to obtain a counterpressure within the LS valve by restring the return connection $\Omega_{A \to T}$ or $\Omega_{B \to T}$ by means of metering notches in the spool lands.
3 Since the valve represented blocks all ports A, B, and P is in neutral and is equipped by load drop check valve CV, overpressurization of the actuator caused by external conditions cannot be avoided just by limiting the supply pressure.

Figure 16.2b) or it can be connected to the individual chambers LS-A (as in Figure 16.6) and LS-B, allowing separate supply pressure limits for each direction of operation. Two signal pressure limiters RV_{LS-A} and RV_{LS-B} can also be installed simultaneously.

- $RV_{A,B}$ work-port reliefs. These valves act on the main flow to the actuator. They are commonly used to avoid overpressurization in neutral configuration or to prevent the effect of external loads.

Certain applications might require the use of both types of pressure limitation, presenting up to four relief elements in a single valve section. In case a signal relief and a work-port relief are both used, the setting of the work-port relief needs to be higher than the other one.

Example 16.1   Hydraulic winch – LS system with fixed displacement pump

A hydraulic winch is installed in a mobile crane and it is used to lift or lower payloads up to 100 kN. The winch can be represented as in the figure below: it has a drum diameter of 0.5 m and it is connected to a fixed displacement hydraulic motor through a gearbox that divides the angular speed of the motor by a ratio of 30. The maximum velocity of the payload is 0.3 m/s.

A load sensing system with a fixed displacement pump and a LS valve is used to control the hydraulic motor of the winch. The pump is driven by a combustion engine rotating at 2000 rpm, and its maximum pressure is limited to 200 bar. The LS margin of the system is 20 bar.
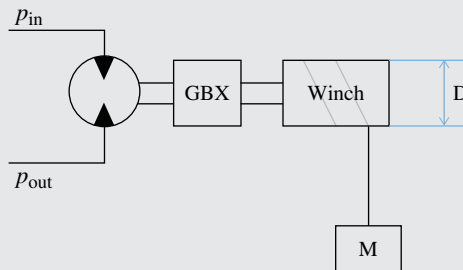
a. Represent the schematic of the complete hydraulic system, including a proper solution for controlling the overrunning load condition (lowering).

Additionally, determine

b. The displacement of the hydraulic units (motor and pump)
c. The power demand at the engine and the hydraulic system efficiency, in two lifting conditions: co*ndition* 1 payload of 50 000 N at 0.15 m/s and *condition* 2 payload 80 000 N at 0.15 m/s
d. The energy plot for the two conditions 1 and 2
e. The opening area of the LS valve for the conditions 1 and 2

Assume ideal hydraulic components and pressure drops only across the hydraulic units and functional orifices. The hydraulic fluid has a density of 850 kg/m^3. All orifice coefficients equal 0.62.

Given:
Drum diameter, $D = 0.5\,m$; maximum payload, $F_{max} = 100\,000\,N$; maximum lifting velocity, $v_{max} = 0.3\,m/s$; gearbox ratio, $i = \dfrac{n_{in}}{n_{out}} = 30$; ideal hydraulic components, $\eta = 1$ for the pump

---

(Continued)

Example 16.1 (Continued)

and the motor; maximum pump pressure, $p_{max} = 200\,bar$; pressure margin of the LS system, $s = 20\,bar$; pump shaft speed, $n_p = 2000\,rpm$; orifice coefficient, $C_f = 0.62$; fluid density, $\rho = 850\,kg/m^3$.

Operating conditions, c1: $F_{c1} = 50\,000\,N$; $v_{c1} = 0.15\,m/s$; c2: $F_{c2} = 80\,000\,N$; $v_{c2} = 0.15\,m/s$

Find:

a. The schematic of the hydraulic LS system with a fixed displacement pump
b. The pump displacement $V_{D,p}$ and the motor displacement $V_{D,m}$
c. The power at the combustion engine, P_{Eng}, and the system efficiency η_S for the conditions c1 and c2
d. Energy plot (p, Q), representing the operating points for the pump and the motor for the conditions c1 and c2
e. Opening area of the metering orifice of the LS valve for c1 (Ω_{c1}) and c2 (Ω_{c2})

Solution:

a) Schematic

The ISO schematic of the system can be derived from Figure 16.5, substituting the linear actuator with the hydraulic winch given in the example:
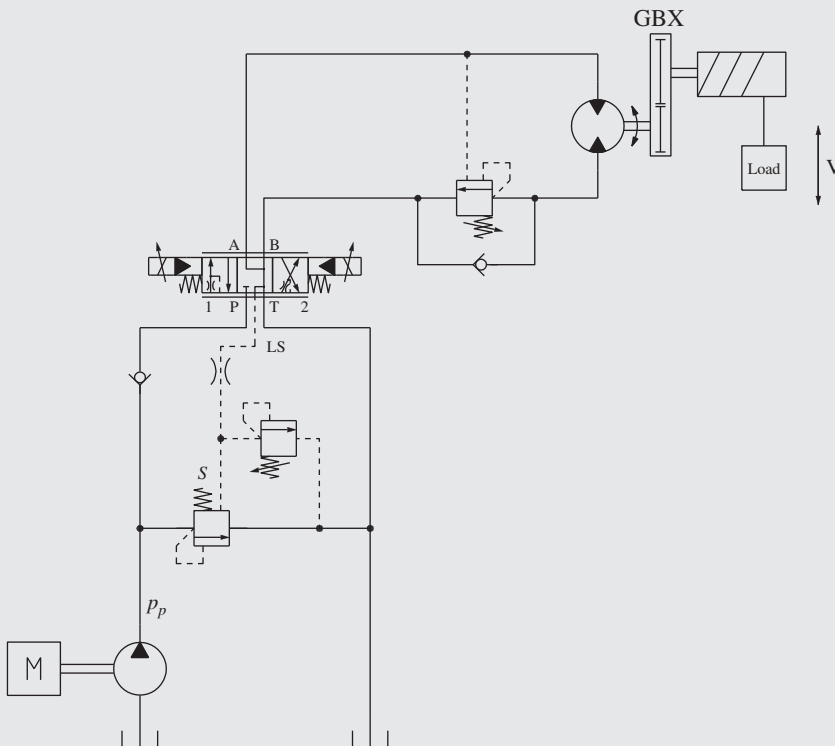
The figure shows the use of a counterbalance valve, CBV, at the work-port B. This is a typical solution to handle overrunning load in hydraulic winches, as it was presented in Chapter 14. The check valve of the CBV permits to have ideally no pressure drop through the CBV during lifting (resistive load), when the LS valve is commanded to position 2. During lowering (overrunning load), when the LS valve is in position 1, the CBV controls the counterpressure at

the motor outlet to a value suitable to balance the external load. More details on the operation and sizing of counterbalance valves have been given in Chapter 14. This example involves only resistive loads (lifting phases); therefore, there will be no further considerations involving the CBV.

To handle overrunning load conditions, a designer could also choose to have a meter-out orifice with a fixed area instead of a CBV. This solution might not be optimal from the energy point of view, since the orifice area must be sized for the highest overrunning load conditions. However, a fixed orifice could be a more economical solution, which also allows a better dynamic behavior of the system.

b) Pump and motor sizing

The size of the hydraulic motor, or the motor displacement, can be found by first evaluating the torque at the motor shaft:

$$T_{m,\max} = F_{\max} \cdot \frac{D}{2 \cdot i} = 100\,000\,[N] \cdot \frac{0.5\,[m]}{2 \cdot 30} = 833\,Nm$$

Considering the maximum pressure at which the supply pump can operate, and the given LS margin, the maximum pressure drop[4] across the hydraulic motor is

$$\Delta p_{m,\max} = p_{in} - p_{out} = p_{\max} - s = 200\,[bar] - 20\,[bar] = 180\,bar$$

The motor displacement is therefore

$$V_{D,m} = \frac{T_{m,\max}}{\Delta p_{m,\max}} = \frac{833\,[Nm]}{180\,[bar]} \cdot 20\pi = 290.8\,cm^3/r$$

The rotation speed of the motor to lift the load at maximum speed is

$$n_{m,\max} = \frac{2 \cdot v_{\max} \cdot i}{D} = \frac{2 \cdot 0.3\,[m/s] \cdot 30}{0.5\,[m]} \cdot \frac{60}{2\pi} = 343.8\,rpm$$

The flow rate required by the motor to rotate at $n_{m,\,max}$ is

$$Q_{m,\max} = V_{D,m} \cdot n_{\max} = 290.8\,[cm^3/s] \cdot 343.8\,[rpm] \cdot \frac{1}{1000} = 100.0\,l/min$$

Under the assumption of ideal components, the flow $Q_{m,\,max}$ corresponds exactly to the flow that supply pump needs to deliver, $Q_p = Q_{m,\,max}$. Therefore, the displacement of the hydraulic pump is

$$V_{D,p} = \frac{Q_p}{n_p} = \frac{100\,[l/min]}{2000\,[rpm]} 1000 = 50\,cm^3/r$$

c) Power demand and system efficiency

The power demand at the engine can be evaluated after calculating the loading pressure for the two given operating conditions c1 and c2:

$$\Delta p_{m,c1} = \frac{T_{m,c1}}{V_{D,m}} = \frac{F_{c1} \cdot \frac{D}{2 \cdot i}}{V_{D,m}} = \frac{50\,000\,[N] \cdot \frac{0.5\,[m]}{2 \cdot 30}}{290.8\,[cm^3/rev]} 20\pi = 90\,bar$$

$$\Delta p_{m,c2} = \frac{T_{m,c2}}{V_{D,m}} = \frac{F_{c2} \cdot \frac{D}{2 \cdot i}}{V_{D,m}} = \frac{80\,000\,[N] \cdot \frac{0.5\,[m]}{2 \cdot 30}}{290.8\,[cm^3/rev]} 20\pi = 144\,bar$$

(Continued)

---

4 This is the maximum pressure drop that still guarantees maximum load speed of 0.3 m/s.

Example 16.1 (Continued)

Considering that there are no pressure losses within the circuit (ideal components), $\Delta p_p = \Delta p_m + s$. The pump always provides a fixed flow $Q_p = 100$ *l/min*, so that the power at the engine shaft becomes, under the assumption of ideal pump efficiency:

$$P_{\text{Eng,c1}} = Q_p \cdot \Delta p_{p,c1} = Q_p \cdot \left(\Delta p_{m,c1} + s\right) = 100 \, [l/min] \cdot 110 \, [bar] \cdot \frac{1}{600} = 18.3 \, kW$$

$$P_{\text{Eng,c2}} = Q_p \cdot \Delta p_{p,c1} = Q_p \cdot \left(\Delta p_{m,c2} + s\right) = 100 \, [l/min] \cdot 164 \, [bar] \cdot \frac{1}{600} = 27.3 \, kW$$

The useful power can be calculated directly considering the motion of the payload:

$$P_{U,c1} = F_{c1} \cdot v_{c1} = 50\,000 \, [N] \cdot 0.15 \, [m/s] \cdot \frac{1}{1000} = 7.5 \, kW$$

$$P_{U,c2} = F_{c2} \cdot v_{c2} = 80\,000 \, [N] \cdot 0.15 \, [m/s] \cdot \frac{1}{1000} = 12.0 \, kW$$

Therefore, the system efficiency for the system for the two considered conditions is

$$\eta_{S,c1} = \frac{P_{U,c1}}{P_{\text{Eng,c1}}} = \frac{7.5 \, [kW]}{18.3 \, [kW]} = 0.41$$

$$\eta_{S,c2} = \frac{P_{U,c2}}{P_{\text{Eng,c2}}} = \frac{12.0 \, [kW]}{27.3 \, [kW]} = 0.44$$

The efficiency tends to increase with the useful power. However, even assuming ideal components, the efficiency calculated for this example is relatively low (little higher than 40%).

d) Energy plot for the c1 and c2 operating conditions
The operating points for the two conditions can be represented in the energy plot as shown below:

Energy Plot – Fixed Displacement Pump
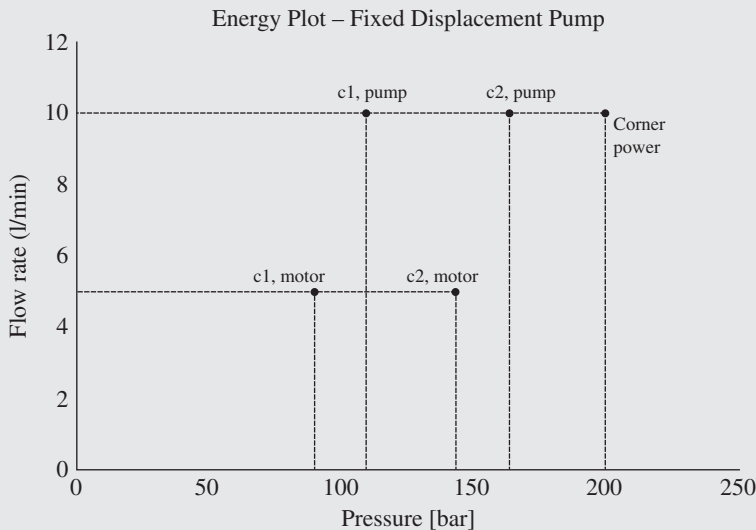
e) Opening areas of the LS valve for c1 and c2
The opening area of the metering orifice of the LS valve, when commanded to position 2 to perform the lifting at conditions c1 and c2, can be calculated with the orifice equation.

First, the flow rate can be determined from the motor request:

$$Q_{m,c1} = V_{D,m} \cdot n_{m,c1} = V_{D,m} \cdot \frac{2 \cdot v_{c1} \cdot i}{D}$$

$$= 290.8 \; [cm^3/r] \cdot \left[\frac{2 \cdot 0.15 \; [m/s] \cdot 30}{0.5 \; [m]} \cdot \frac{60}{2\pi} \right] [r/min] \cdot \frac{1}{1000} = 50 \; l/min$$

$Q_{m,c2} = Q_{m,c1}$, because $v_{c2} = v_{c1}$. The pressure drop across the metering orifice is equal to the LS margin. Therefore, the opening area is

$$\Omega_{c1} = \Omega_{c2} = \frac{Q_{m,c1}}{C_f \cdot \sqrt{\frac{2 \cdot s}{\rho}}} = \frac{50 \; [l/min] \; \frac{1}{60\,000}}{0.62 \cdot \sqrt{\frac{2 \cdot 20 \; [bar] \cdot 10^5}{850 \; [kg/[m^3]]}}} \cdot 10^6 = 19.6 \; mm^2$$

16.4 Load Sensing System with Variable Displacement Pump

16.4.1 Basic Schematic

The LS principle becomes even more effective when implemented in combination with a flow supply based on a variable displacement pump. The conceptual schematic for this principle is shown in Figure 16.7a, while a more realistic implementation based on the use of a LS valve (the same valve of Figure 16.5), which permits the bidirectional control of the actuator, is shown in Figure 16.7b.

When a variable displacement pump is used, the circuit does not need an unloader to maintain the constant pressure drop across the metering orifice, O. The condition $p_P - p_U = s$ is now achieved

Figure 16.7 LS system with a variable displacement pump: (a) conceptual schematic; (b) implementation with a 5/3 proportional LS valve and maximum pressure limitation.

through a proper displacement control system equipped on the pump, commonly indicated to as a *LS regulator* or *differential pressure limiter*.

A pump with such a displacement adjustment system is typically referred as *load-sense controlled pump* or simply *LS pump*. The simplified representation of this regulator is shown next to the pump symbol in both Figure 16.7a,b. The arrow indicating the variability of the pump displacement is connected to a mechanism including two hydraulically piloted actuators and a spring with an equivalent pressure setting *s*. An internal pilot line connects the actuator located on the top side to the pump outlet. With this setup, the pump outlet pressure p_P acts to reduce the pump displacement. A second pilot line links the actuator located at the opposite side of the mechanism to the load pressure, p_U. This is often referred to as the *LS line* and it appears as an external connection to the pump. The bottom actuator acts together with the spring *s* to increase the pump displacement. The pump regulator finds an equilibrium position when the following condition is satisfied:

$$p_P = p_U + s \tag{16.10}$$

Figure 16.7b shows a more realistic implementation of the LS principle where a LS pump is combined with a LS valve. In this case, the LS port of the valve is connected to the LS line going to the pump control mechanism. The LS line is a signal type connection, meaning that it is used only to transmit the load pressure information.

16.4.2 Operation

In the hydraulic circuit in Figure 16.7a, the variable orifice O is located between the pump and the actuator. Therefore, thanks to the differential pressure limiter explained above, the pump adjusts its displacement to establish a proper flow through the orifice O, so that

$$\Delta p_O = p_P - p_U = s \tag{16.11}$$

Consequently, the flow to the actuator (which equals the pump flow), again obeys the relation of Eq. (16.4):

$$Q_U = C_f \cdot \Omega_O(i) \sqrt{\frac{2 \cdot s}{\rho}} \tag{16.12}$$

Equation (16.12) has the same expression calculated for the fixed displacement pump circuit. However, here the LS margin, *s*, is set by the pump LS regulator, and the pump flow Q_P is equal to the flow supplied to the actuator Q_U, without the need of an unloader. In other words, the displacement adjusting system of the pump varies its instantaneous displacement, V_D, to satisfy Eq. (16.10). Therefore, the fractional displacement of the LS pump, ε, is directly related to the command *i*:

$$V_D(i) = \varepsilon(i) \cdot V_{D,\max} \tag{16.13}$$

Figure 16.7b also shows how the use of a pressure relief valve in the LS pilot line can be an effective solution to limit the maximum pressure at the pump outlet, for the variable displacement pump case. Specifically, when the load reaches or overcomes the relief valve setting p^*, the LS signal seen by the pump regulator remains p^* and the pump outlet pressure becomes

$$p_{P,\max} = p^* + s \tag{16.14}$$

Similar to the example of Figure 16.2b, where a relief valve was used in the pilot line, an orifice is also necessary in Figure 16.7b. This is located upstream the relief valve and functions as pressure separator in case the relief valve becomes active.

16.4.3 Energy Analysis

The energy consumption of the LS system that uses a variable displacement pump can be significantly smaller than the LS solution based on a fixed displacement unit. This is shown in the energy

plot of Figure 16.8, which represents the power consumed by the pump:

$$P_P = Q_U \cdot (p_U + s) \tag{16.15}$$

as well as the power utilized by the actuator:

$$P_U = Q_U \cdot p_U \tag{16.16}$$

Since there is no flow generated by the pump in addition to the request, the power loss is determined only by the LS margin:

$$P_L = Q_U \cdot s \tag{16.17}$$

The system efficiency becomes

$$\eta_S = \frac{P_U}{P_P} = \frac{p_U}{p_U + s} \tag{16.18}$$

Therefore, in the case of ideal components, the energy efficiency of a LS system based on a variable displacement pump depends only on the load pressure and the LS margin. In Eq. (16.18), one could assume that the margin should be kept as low as possible to maximize the system efficiency and minimize the throttling losses across the metering orifice. However, two factors must be taken into account when selecting the LS margin. First, a tiny LS margin would require very large spool valves, in order to achieve the metering areas necessary to generate the desired flow (as can be seen from Eq. (16.12)). Second, the effective pressure drop across the metering orifice is always lower than the pump margin because of the losses that the pump flow encounters between the pump and the valve. The lower the LS margin, the higher the influence of this pressure loss on the controlled flow. Therefore, normal applications use LS margin values between 10 and 25 bar.
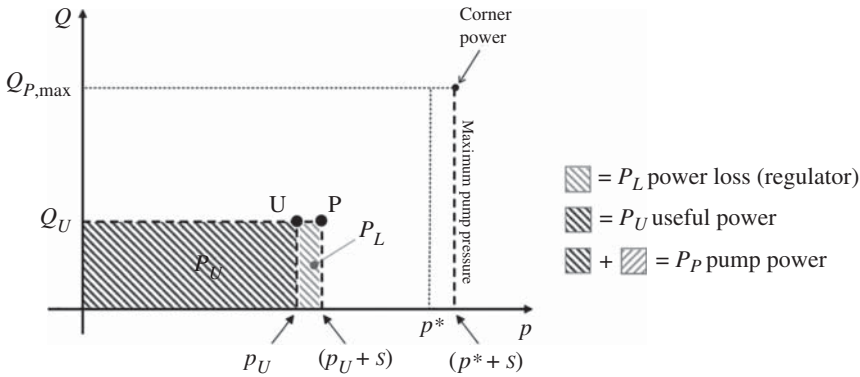
Figure 16.8 Energy plot of the LS system in Figure 16.7

16.4.4 Saturation Conditions

The conditions of pressure or flow saturations described in Section 16.2.4 for the case of an LS system based on a fixed displacement pump also apply to the system based on a variable displacement LS pump. *Pressure saturation* occurs when the load pressure, p_U, hits the maximum pressure allowed by the relief valve of Figure 16.7b, p^*. In this case the pump maintains the pressure $(p^* + s)$ at its outlet, and consequently $\Delta p_O < s$. This causes a reduction of the pump flow rate and thus decreases the actuator velocity.

Flow saturation can be reached with a LS pump if the LS valve opening area exceeds the value $\Omega_{\max}$, defined as

$$\Omega_{\max} = \frac{Q_{p,\max}}{C_f} \sqrt{\frac{\rho}{2s}} \tag{16.19}$$

where $Q_{p,\,\mathrm{max}} = n_p \cdot V_{D,\,\mathrm{max}}$. In case of flow saturation, Q_U remains at its maximum value $(Q_U = Q_{P,\,\mathrm{max}})$, as in Figure 16.4.

Example 16.2   Hydraulic winch: LS system with variable displacement pump

Consider the same system of Example 15.1 (hydraulic winch), but assume now to have a LS system based on a variable displacement pump. Using the same given data,

a. Draw the new schematic of the hydraulic circuit.
b. Find the power demand at the engine, the overall hydraulic system efficiency, in the following lifting situations: c1, 50 000 N at 0.15 m/s and c2, 80 000 N at 0.15 m/s.
c. Represent the energy plot for two conditions c1 and c2.
d. Compare the system efficiency with respect to the solution of the Example 16.1 for the following conditions: c3, 50 000 N at 0.05 m/s and c4, and 80 000 N at 0.21 m/s.
e. Consider the case in which the hydraulic pump and the motor are not ideal, with efficiencies given by the plots below. Calculate the overall system efficiency for c3 and c4.

(a)

(b)

Pump, full displacement ε = 100%

(c)

Pump, reduced displacement ε = 20%

(d)

Motor

(e)

Example 16.2 (Continued)

Motor

(f)
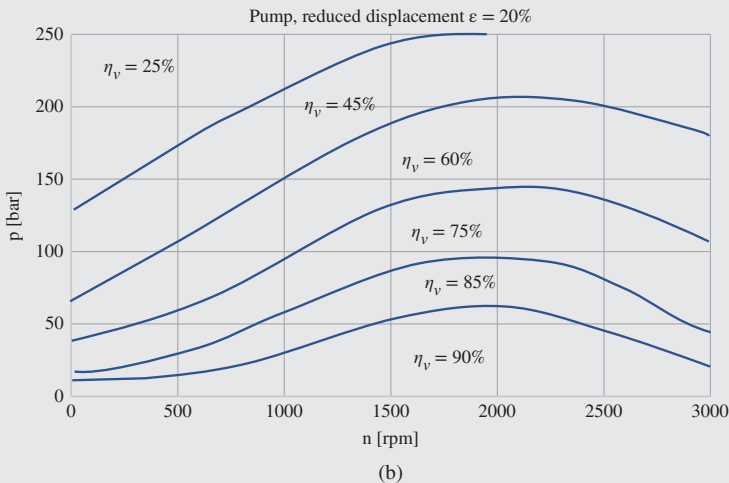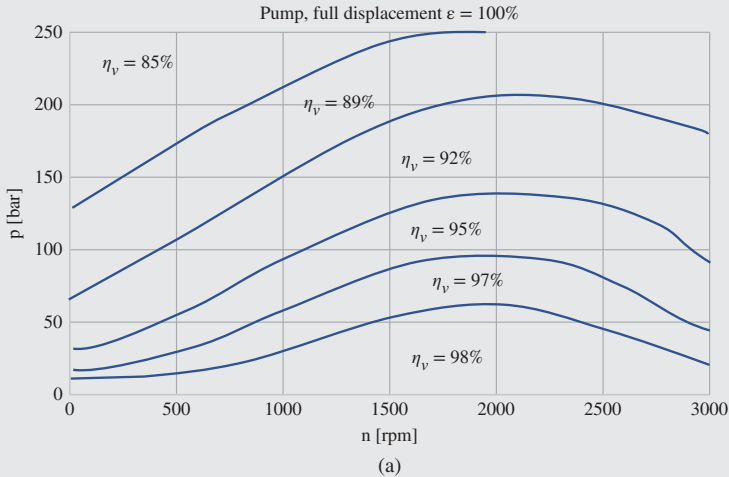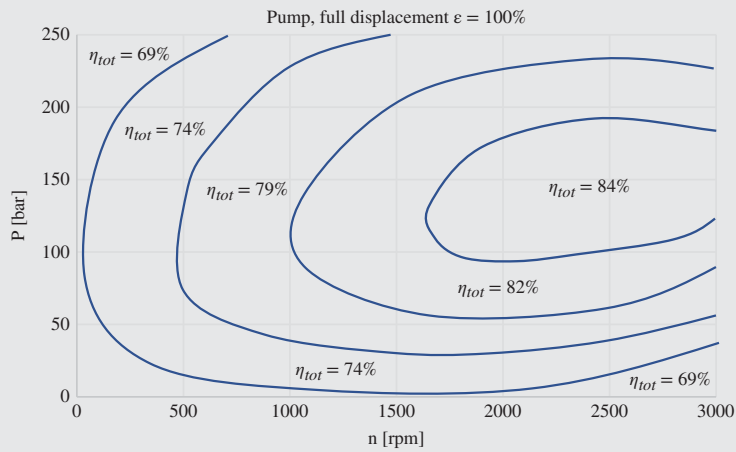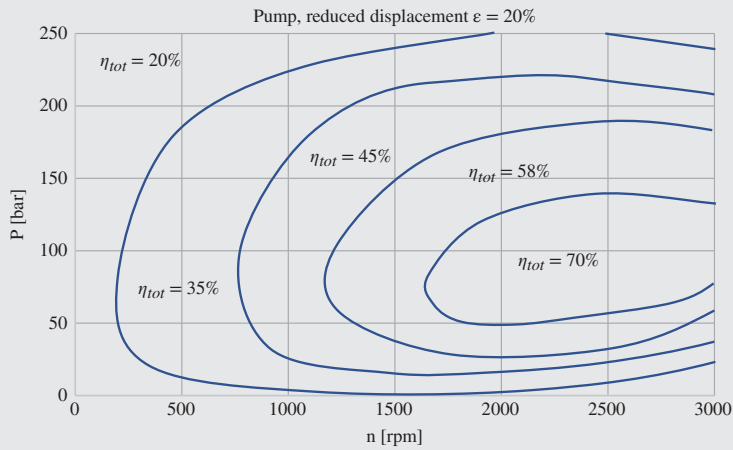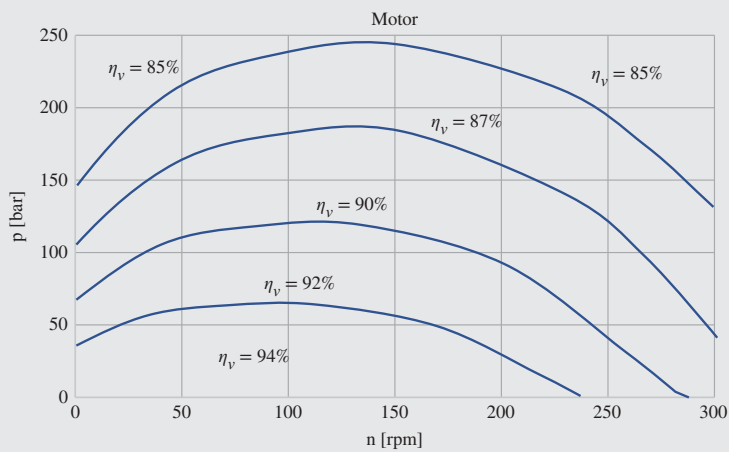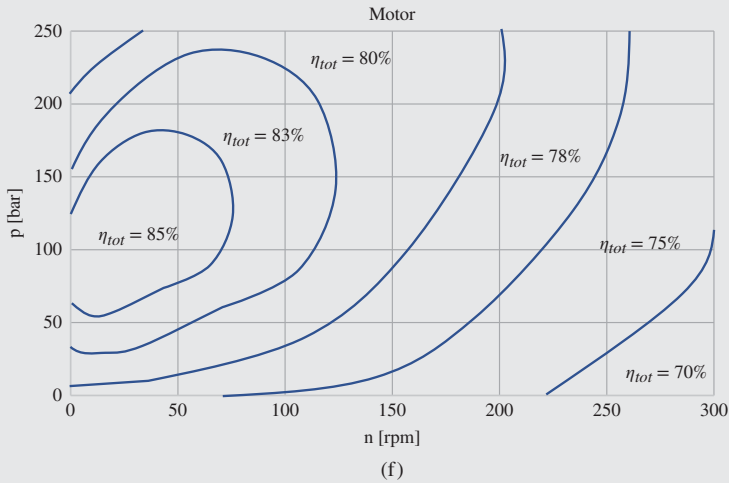
Pump energy efficiency plots at 100% displacement (left) and 20% displacement (right). The first row shows the volumetric efficiency, the second row the torque efficiency, and the third row the overall efficiency.

Given:

Drum diameter, $D = 0.5\,m$; maximum payload, $F_{max} = 100\,000\,N$; maximum lifting velocity, $v_{max} = 0.3\,m/s$; gearbox ratio, $i = \frac{n_{in}}{n_{out}} = 30$; ideal hydraulic components, $\eta = 1$ for the pump and the motor; maximum pump pressure, $p_{max} = 200\,bar$; pressure margin of the LS system, $s = 20\,bar$; pump shaft speed, $n_p = 2000\,rpm$; orifice coefficient, $C_f = 0.62$; fluid density, $\rho = 850\,kg/m^3$.

Operating conditions: c1, $F_{c1} = 50\,000\,N$; $v_{c1} = 0.15\,m/s$; c2, $F_{c2} = 80\,000\,N$; $v_{c2} = 0.15\,m/s$; c3, $F_{c3} = 50\,000\,N$; $v_{c3} = 0.05\,m/s$; c4, $F_{c4} = 80\,000\,N$; $v_{c4} = 0.21\,m/s$.

Efficiency plots for the pump (for $\varepsilon = 100\%$ and $\varepsilon = 20\%$) and for the fixed displacement motor.

Find:

a. The schematic of the hydraulic LS system with a variable displacement pump
b. The power at the combustion engine, P_{Eng}, and the system efficiency η_S for the conditions c1 and c2
c. Energy plot (p, Q), representing the operating points for the pump and the motor for the conditions c1 and c2
d. The overall system efficiency for the conditions c3 and c4. Compare the values with respect to the case of fixed displacement pump (Example 16.1)
e. The overall system efficiency for c3 and c4, when considering actual efficiency plots for the pump and the motor

Solution:

a) Schematic

The ISO schematic of the system resembles the one of Example 16.1, but it has the variable displacement LS pump as in Figure 16.7b:
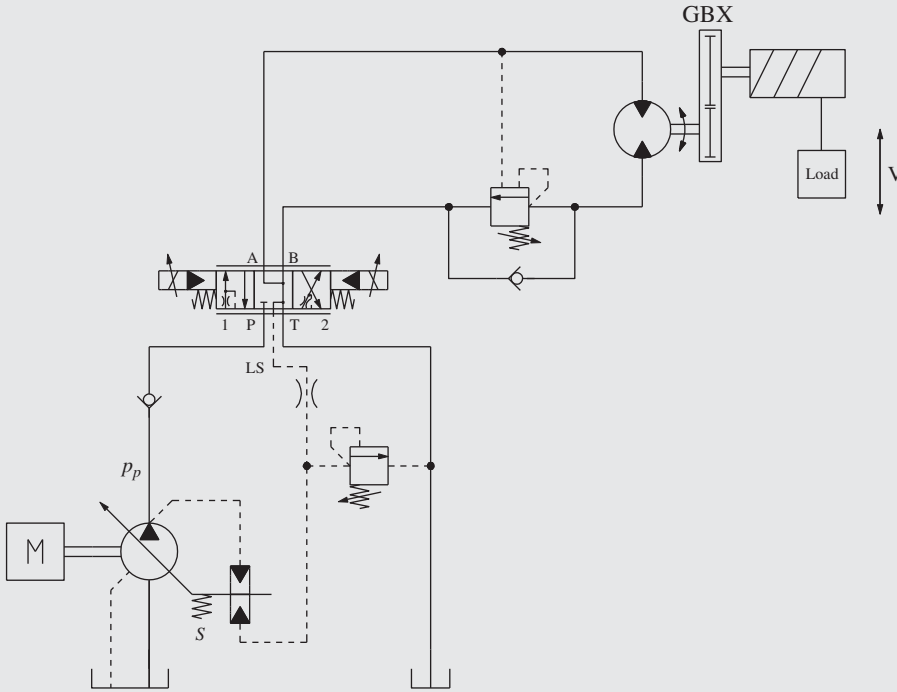
b) Power calculations (c1 and c2)

The sizing of the variable displacement pump and of the hydraulic motor follows the same calculations of Example 10.1: $V_{D,m} = 290.8\ cm^3/r$; $V_{D,p} = 50\ cm^3/r$;

The load pressures for conditions c1 and c2 were already calculated in Example 16.1:

$$\Delta p_{m,c1} = 90\ bar; \Delta p_{m,c2} = 144\ bar$$

Also for the case of LS system with the variable displacement pump, $p_p = \Delta p_m + s$, as in the case of the previous Example 16.1. However, the variable displacement pump adjusts its displacement to provide exactly (for the ideal case) the flow rate requested by the hydraulic motor that drives the winch. To quantify this flow rate request for each condition, it is necessary to first calculate the speed of the hydraulic motor at each operating condition:

$$n_{m,c1} = n_{m,c2} = \frac{2 \cdot v_{c1} \cdot i}{D} = \frac{2 \cdot 0.15\ [m/s] \cdot 30}{0.5\ [m]} \cdot \frac{60}{2\pi} = 171.9\ rpm$$

Then, the flow rate at the motor for the conditions c1 and c2 becomes

$$Q_{m,c1} = Q_{m,c2} = V_{D,m} \cdot n_{m,c1} = 290.8\ [cm^3/r] \cdot 172.0\ [rpm] \cdot \frac{1}{1000} = 50.0\ l/min$$

Therefore, for both conditions c1 and c2: $Q_{p,c1} = Q_{p,c2} = 50.0\ l/min$

The power request at the engine shaft for the two conditions under consideration is

$$P_{Eng,c1} = Q_{p,c1} \cdot p_{p,c1} = Q_{p,c1} \cdot \left(\Delta p_{m,c1} + s\right) = 50\ [l/min] \cdot 110\ [bar] \cdot \frac{1}{600} = 9.2\ kW$$

$$P_{Eng,c2} = Q_{p,c2} \cdot p_{p,c1} = Q_{p,c2} \cdot \left(\Delta p_{m,c2} + s\right) = 50\ [l/min] \cdot 164\ [bar] \cdot \frac{1}{600} = 13.7\ kW$$

(Continued)

Example 16.2 (Continued)

Considering the values for the useful power already calculated in Example 16.1:

$$\eta_{S,c1} = \frac{P_{U,c1}}{P_{Eng,c1}} = \frac{7.5 \, [kW]}{9.2 \, [kW]} = 0.81$$

$$\eta_{S,c2} = \frac{P_{U,c2}}{P_{Eng,c2}} = \frac{12.0 \, [kW]}{13.7 \, [kW]} = 0.87$$

It is important to notice how, for the two considered conditions, the efficiency of the system has doubled with respect to the case of fixed displacement pump of Example 16.1!

c) Energy plots (c1 and c2)
The energy plots for the configurations c1 and c2 is visible in the figure below:

Energy Plot – Fixed Displacement Pump
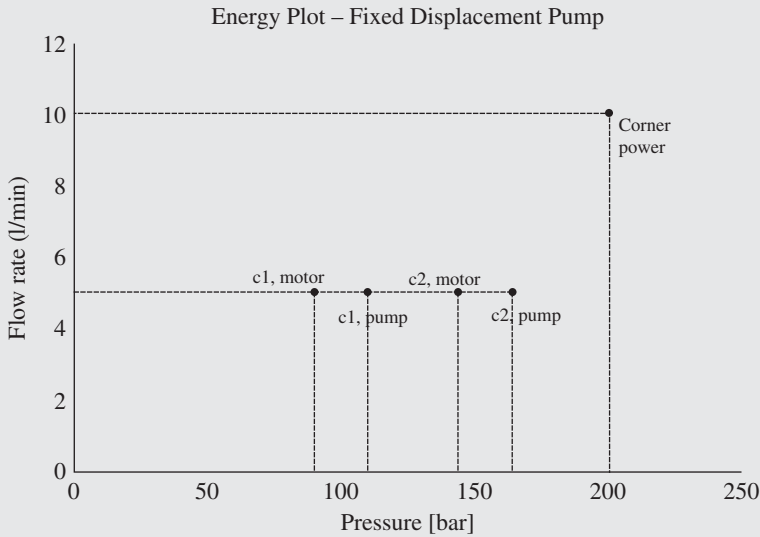
d) System efficiency (c3 and c4, ideal units)
The operating conditions c3 and c4 differ significantly from c1 and c2 especially as it pertains the payload lifting velocity. Following the same procedure used above to estimate the system efficiency,

$$n_{m,c3} = \frac{2 \cdot v_{c3} \cdot i}{D} = \frac{2 \cdot 0.05 \, [m/s] \cdot 30}{0.5 \, [m]} \cdot \frac{60}{2\pi} = 57.3 \, rpm$$

$$n_{m,c4} = \frac{2 \cdot v_{c4} \cdot i}{D} = \frac{2 \cdot 0.21 \, [m/s] \cdot 30}{0.5 \, [m]} \cdot \frac{60}{2\pi} = 240.6 \, rpm$$

$$Q_{m,c3} = V_{D,m} \cdot n_{m,c3} = 290.8 \, [cm^3/r] \cdot 57.3 \, [rpm] \cdot \frac{1}{1000} = 16.7 \, l/min$$

$$Q_{m,c4} = V_{D,m} \cdot n_{m,c4} = 290.8 \, [cm^3/r] \cdot 240.6 \, [rpm] \cdot \frac{1}{1000} = 70.0 \, l/min$$

Consequently, $Q_{p,c3} = Q_{m,c3}$; $Q_{p,c4} = Q_{m,c4}$. The pump fractional displacement is $\varepsilon_{c3} = 16.7\%$ for c3, and $\varepsilon_{c4} = 83.3\%$ for c4.

$$\Delta p_{m,c3} = \frac{T_{m,c3}}{V_{D,m}} = \frac{F_{c3} \cdot \dfrac{D}{2 \cdot i}}{V_{D,m}} = \frac{50\,000 \, N \cdot \dfrac{0.5 \, [m]}{2 \cdot 30}}{290.8 \, [cm^3/rev]} 20\pi = 90 \, bar$$

$$\Delta p_{m,c4} = \frac{T_{m,c4}}{V_{D,m}} = \frac{F_{c4} \cdot \dfrac{D}{2 \cdot i}}{V_{D,m}} = \frac{80\,000\,\text{N} \cdot \dfrac{0.5\,[m]}{2 \cdot 30}}{290.8\,[cm^3/rev]} 20\pi = 144\,bar$$

$$P_{\text{Eng,c3}} = Q_{p,c3} \cdot \Delta p_{p,c3} = Q_{p,c3} \cdot \left(\Delta p_{m,c3} + s\right) = 16.7\,[l/min] \cdot 110\,[bar] \cdot \frac{1}{600} = 3.1\,kW$$

$$P_{\text{Eng,c4}} = Q_{p,c4} \cdot \Delta p_{p,c4} = Q_{p,c4} \cdot \left(\Delta p_{m,c4} + s\right) = 70.0\,[l/min] \cdot 164\,[bar] \cdot \frac{1}{600} = 19.1\,kW$$

While the useful power is

$$P_{U,c3} = F_{c3} \cdot v_{c3} = 50\,000\,[N] \cdot 0.05\,[m/s] \cdot \frac{1}{1000} = 2.5\,kW$$

$$P_{U,c4} = F_{c4} \cdot v_{c4} = 80\,000\,[N] \cdot 0.21\,[m/s] \cdot \frac{1}{1000} = 16.8\,kW$$

the overall system efficiency, considering a variable displacement LS pump (subscript vp) becomes

$$\eta_{S,c3,\text{vp}} = \frac{P_{U,c3}}{P_{\text{Eng,c3}}} = \frac{2.5\,[kW]}{3.1\,[kW]} = 0.80$$

$$\eta_{S,c4,\text{vp}} = \frac{P_{U,c4}}{P_{\text{Eng,c4}}} = \frac{16.8\,[kW]}{19.1\,[kW]} = 0.88$$

Results above and from (b) show that as the useful power decreases, the overall energy efficiency of the LS system also decreases. However, using a variable displacement pump the ideal efficiency value is always relatively high (higher than 80%, for the data given in this example).

Using the system of Example 10.1, with the fixed displacement pump (subscript fp):

$$P_{\text{Eng,c3,fp}} = Q_p \cdot p_{p,c3} = Q_p \cdot \left(\Delta p_{m,c3} + s\right) = 100\,[l/min] \cdot 110\,[bar] \cdot \frac{1}{600} = 18.3\,kW$$

$$P_{\text{Eng,c4,fp}} = Q_p \cdot p_{p,c4} = Q_p \cdot \left(\Delta p_{m,c4} + s\right) = 100\,[l/min] \cdot 164\,[bar] \cdot \frac{1}{600} = 27.3\,kW$$

Finally, the overall system efficiency is

$$\eta_{S,c3,\text{fp}} = \frac{P_{U,c3}}{P_{\text{Eng,c3,fp}}} = \frac{2.5\,[kW]}{18.3\,\text{kW}} = 0.14$$

$$\eta_{S,c4,\text{fp}} = \frac{P_{U,c4}}{P_{\text{Eng,c4,fp}}} = \frac{16.8\,[kW]}{27.3\,[kW]} = 0.62$$

It can be noted that $\eta_{S,c4,\text{fp}}$ is close to $\eta_{S,c4,\text{vp}}$, meaning that for high motor flow rates, the two systems of Examples 16.1 and 16.2 operate at a similar efficiency. $\eta_{S,\text{fp}} = \eta_{S,\text{vp}}$ for the case of maximum lifting velocity ($Q_p = Q_{m,\text{max}}$). However, $\eta_{S,c3,\text{fp}}$ is significantly lower than $\eta_{S,c3,\text{vp}}$. Therefore, while the system with variable displacement pump maintains the overall system efficiency at levels always higher than 80% for all considered lifting conditions, the system with fixed displacement pump can operate in a wide range of energy efficiency, from 14% to 62%! In general, systems with variable displacement pump are more energy efficient that system with fixed displacement pumps. However, in the case where a system operates mostly with actuator flow rates near the maximum, a solution based on fixed displacement pump can be a better compromise between cost of the components and energy efficiency.

e) System efficiency (c3 and c4, real units)
   In this case, the comparison between the system of Example 16.1 and the one with variable displacement pump is performed considering realistic efficiency plots.

(Continued)

Example 16.2 (Continued)

Condition c3

The motor, at 90 *bar* and 57.3 *rpm* has following efficiencies: $\eta_{v,m,c3} = 0.92$; $\eta_{t,m,c3} = 0.85$. There-fore, $\eta_{hm,m,c3} = \eta_{t,m,c3}/\eta_{v,m,c3} = 0.92$.

The effective motor Δp and flow rate are obtained as

$$\Delta p_{m,c3,e} = \frac{\Delta p_{m,c3,i}}{\eta_{hm,m,c3}} = \frac{90\,[bar]}{0.92} = 97.8\,bar$$

$$Q_{m,c3,e} = \frac{Q_{m,c3,i}}{\eta_{v,m,c3}} = \frac{16.7\,[l/min]}{0.92} = 18.5\,l/min$$

Even if the effective pressure is different from the ideal pressure of the motor, iterations for recalculating the values of the motor efficiencies at c3 are not needed. In fact, the efficiency maps at the re-calculated effective conditions would provide approximately the same values for the component efficiency.

The pump now operates at $p_{p,c3,e} = (105.6 + 20)\,[bar] = 125.6\,bar$.

Since the pump must provide only 18.5 *l/min*, it operates at a fractional displacement of $\varepsilon_{c3,e} = 24.7\%$ (for the ideal case, it was $\varepsilon_{c3,i} = 16.7\%$). In this case, the volumetric efficiency plot given for $\varepsilon = 20\%$ can be used with good approximation. The pump volumetric efficiency is $\eta_{v,p,c3} = 0.75$. The overall efficiency is $\eta_{t,p,c3} = 0.70$. Therefore, the mechanical efficiency is $\eta_{hm,p,c3} = \eta_{t,p,c3}/\eta_{v,p,c3} = 0.93$.

Note that $\varepsilon_{c3,e} = (Q_{p,c3,e}/V_{D,p} \cdot n_p \cdot \eta_{v,p,c3})$.

In this case, the effective power demand at the engine is

$$P_{Eng,c3,vp,e} = \frac{Q_{p,c3} \cdot P_{p,c3}}{\eta_{t,p,c3}} = \frac{18.5\,[l/min] \cdot 125.6\,[bar]}{0.70}\frac{1}{600} = 5.5\,kW$$

The overall system efficiency becomes

$$\eta_{S,c3,vp} = \frac{P_{U,c3}}{P_{Eng,c3,vp,e}} = \frac{2.5\,[kW]}{5.5\,[kW]} = 0.45$$

It is important to point out how, introducing the pump and motor efficiency, the system efficiency for the case c3 has reduced from 80% to 45%.

Condition c4

The motor, at 144 *bar* and 240.6 *rpm* has following efficiencies: $\eta_{v,m,c4} = 0.87\,\%$; $\eta_{t,m,c4} = 0.78\%$. Therefore, $\eta_{hm,m,c4} = \eta_{t,m,c4}/\eta_{v,m,c4} = 0.90$.

$$\Delta p_{m,c4,e} = \frac{\Delta p_{m,c4,i}}{\eta_{hm,m,c4}} = \frac{144\,[bar]}{0.90} = 160.0\,bar$$

$$Q_{m,c4,e} = \frac{Q_{m,c4,i}}{\eta_{v,m,c4}} = \frac{70.0\,[l/min]}{0.87} = 80.5\,l/min$$

Iterations for recalculating the values of the motor efficiencies at c4 are not needed.

The pump now operates at $p_{p,c4,e} = (160 + 20)\,[bar] = 180\,bar$.

To satisfy the speed requirement of the load in condition c4, the pump fractional displacement increases to $\varepsilon_{c4,e} = 87.5\%$ from the value $\varepsilon_{c4,i} = 83.3\%$ of the ideal case. It is clear that to meet the maximum requirement of $v_{max} = 0.3$ *m/s* with $F_{max} = 100$ *kN* with real components, a resizing of the pump and of the motor would be required. The pump maximum displacement would need to be higher than 100 cm^3/r! In condition c4, the pump

efficiencies can be calculated from the full displacement plots. The volumetric efficiency is $\eta_{v,p,c4} = 0.92$. The overall efficiency is $\eta_{t,p,c4} = 0.82$. Therefore, the mechanical efficiency is $\eta_{hm,p,c3} = \eta_{t,p,c3}/\eta_{v,p,c3} = 0.89$. Note that $\varepsilon_{c4,e} = (Q_{p,c4,e}/V_{D,p} \cdot n_p \cdot \eta_{v,p,c4})$.

In this case, the power request at the engine is

$$P_{\mathrm{Eng},c4,vp,e} = \frac{Q_{p,c3} \cdot p_{p,c3}}{\eta_{t,p,c3}} = \frac{80.5 \,[l/min] \cdot 180.0 \,[bar]}{0.89} \frac{1}{600} = 27.1 \,kW$$

The overall system efficiency becomes

$$\eta_{S,c4,vp} = \frac{P_{U,c4}}{P_{\mathrm{Eng},c4,vp,e}} = \frac{16.8 \,[kW]}{27.1 \,[kW]} = 0.62$$

For condition c4, introducing the pump and motor efficiency, the overall system efficiency has reduced from 88% to 62%!

For the sake of clarity, this textbook illustrates all the basic concepts of each hydraulic control solution assuming ideal hydraulic components. However, as clearly illustrated with this example, the actual sizing of a hydraulic system, cannot neglect using realistic values for the component efficiencies.

16.5 Load Sensing Pump

At this point, it is interesting to understand how the actual displacement regulating mechanism of an LS pump is implemented and operated. In fact, Figure 16.7 provided a simplified and intuitive representation of the displacement adjustment system, which focused on the operating principle rather than the real architecture. Figure 16.9 shows a detailed schematic of the most common method for implementing an LS control of a variable pump. Typically, LS pumps are swash plate type axial piston units, as shown in the cross-section of Figure 16.10.[5] With this architecture, the instantaneous pump displacement is determined by the swash plate angle β, which is set by the combined action of two single acting hydraulic linear actuators: the control cylinder (CC) and the bias cylinder (BC). The bias cylinder, connected to the pump delivery and aided by an integrated spring, increases the pump displacement, by increasing the swash plate angle β. The control cylinder acts against the bias cylinder and thus reduces the swash plate angle. The pilot pressure supplying the control cylinder (also indicated as *control pressure*, p_C) is determined by the action of two spool valves V1 and V2, which are hydraulically connected in series and manipulate the pump delivery pressure, p_P. In general, $p_C < p_P$, since the control cylinder can overcome the force of the bias cylinder, thanks to the higher influence area, as in Figure 16.10.[6]

The key elements in the control operation are the two spool valves, commonly referred as *differential pressure limiter* (or LS regulator, V1) and *absolute pressure limiter* (V2). These two valves are shown in both Figure 16.9 (schematic) and Figure 16.10 (cross-section). Both figures are inspired from the description of LS systems provided by Nervegna [2] and Zarotti [3].

---

5 Other pump architectures, such as bent axis axial piston pumps, are also available in the market as LS pump. In this case, the ISO schematic of Figure 16.4 might no longer be suitable for representing the displacement adjusting system.

6 The equilibrium of the swash plate is given by the action of the control and bias cylinders and the forces generated by the piston chambers transmitted to the swash plate through the slippers. More details can be found in [1].

Figure 16.9 Detailed ISO schematic of a variable displacement pump with pressure limiter and differential pressure limiter (LS pump).

LS regulator V1. This valve implements the LS principle, according to Eq. (16.10). The functioning of this regulator is based on the equilibrium of the spool, which is subjected to the action of the pressure in the LS input port (p_{LS}) and of the spring (with an equivalent pressure setting s) pushing the spool toward the neutral position (A connected to D and P blocked). On the other end, the pump delivery pressure (p_P) pushes the spool toward the opposite configuration (A connected to P and D blocked). In steady-state regulation, the swash plate angle is held constant and the spool holds the intermediate position represented in detail in Figure 16.11. Here, the spool lands achieve a simultaneous restricted connection of the port A between the inlet port P and the outlet port D. In other words, in this configuration the spool works in the pressure gain region due to an underlapped configuration. This results in a value of $p_C = p_A$ smaller than p_P, which is transmitted downstream to the pump CC, through the pressure limiter V2. As long as the outlet pressure is $p_P < p^*$, the spool V2 stays in neutral configuration, causing the value of p_C to be the same as p_A that is established by V1.

If p_{LS} increases, the LS pressure and the spring force prevail. Therefore, the spool moves and restricts the connection A → D, and thus reduces p_A. This results in a decrease in the force of the CC, which in turn increases the swash angle β, and consequently the pump displacement. With an augmented flow delivered by the pump, p_P tends to increase: i.e. it tends to follow the increment of p_{LS} according to the LS principle. This continues until a new equilibrium is found and the spool returns to the intermediate holding position.

Pressure limiter. The pressure limiter is used to modify the swash plate angle in order to prevent over pressurization of the pump outlet. The layout presented here (Figures 16.9 and 16.10) has a different operating principle with respect to the pilot relief valve in Figure 16.7b.

Figure 16.10 Variable displacement pump with pressure limiter and differential pressure limiter (LS pump).

The pressure limiter is accomplished through valve V2, whose spool has two input signal ports (A, from the upstream LS regulator, and P, from the pump outlet) and one output signal port (C, to the control cylinder). As mentioned above, during the normal operation of the LS pump ($p_P < p^*$), the spring with equivalent setting p^* keeps the spool of V2 in its neutral configuration, realizing an open connection between the inlet port A and the outlet to the control cylinder. In this condition, $p_C = p_A$.

When the pump outlet pressure, which acts on the right side of the spool against the spring, reaches p^*, the spool opens the connection $P \to C$, increasing the value of p_C with respect to p_A. In this way the pump reduces its displacement. It is therefore clear that the pressure limiter can "override" the LS regulator, in case the output p_A would produce a pump delivery pressure greater than p^*.

The operation of the pressure limiter is controlled by spool V2; when this is in regulation, it controls the value of p_C in a similar fashion to the operation of V1 represented in Figure 16.11.
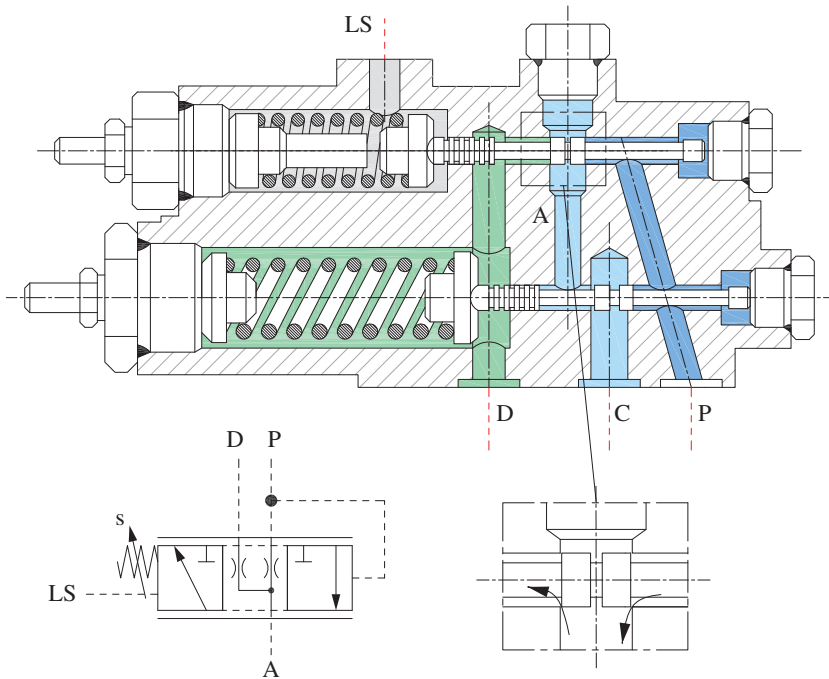
Figure 16.11 Detail of the differential pressure limiter during regulation.

On the other hand, since the pump displacement is reduced, the LS condition of Eq. (16.10) is not valid anymore. In other words, $p_P < p_{LS} + s$; therefore, the spool of V1 returns to the neutral configuration, thereby opening the connection between A and D.

The LS regulator presented in this section (the schematic is shown in Figure 16.9) also includes two orifices O1 and O2, located between the points A and C and the drain line D. From a theoretical standpoint, these elements are not necessary for the operation of the pump displacement adjustment system. However, they are frequently seen as they play a very important role for the dynamic stability of the LS pump. The drawback is given by the fact that these orifices create a leakage path to the tank, subtracting oil flow from the pump outlet. The leakage flow rate through O1 and O2 along with the leakage caused by the spool V1 in regulation, and the flow lost in the spool-bore clearances of V1 and V2, all add up to the overall volumetric loss. In today's state of the art LS pumps, the value of the flow lost in the pump displacement adjustment system (commonly referred as *control leakage*) is in the order of 1.0–1.25 l/min for every 100 bar of outlet pressure. This control leakage can have a significant impact on the pump volumetric efficiency, especially when the pump works at high pressure and low displacements.

Example 16.3   Operation of a differential pressure regulator

Consider the differential pressure regulator of the variable displacement axial piston pump represented below.
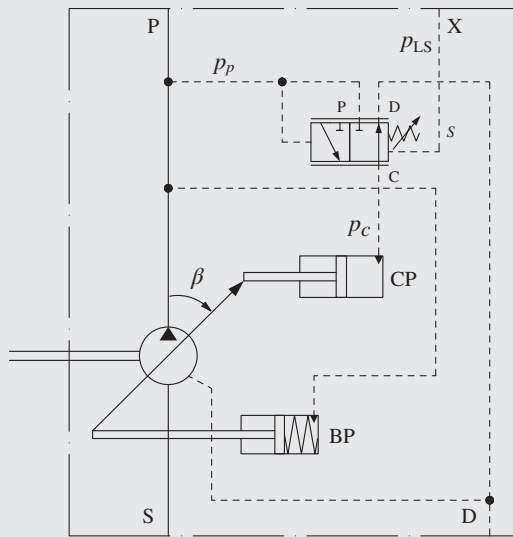
Calculate:

a) The pressure in the control piston to hold the displacement at a constant value, if the outlet pressure of the pump is 180 *bar* and the internal swash plate moment, resulting from the pressure forces acting on the pistons of the pump is 10 *Nm*, acting in the same direction of the moment generated by the force on the control piston.
b) The angular velocity of the swash plate if the control spool defines a connection with the pump outlet equivalent to 0.8 *mm²*. Assume that the control piston pressure is the same as in the previous point a. Is the pump increasing or decreasing displacement?
c) The angular velocity of the swash plate if the control spool implements an area opening equivalent to 2.5 *mm²* to the case drain. Assume that the control piston pressure is the same as in the previous points a. and b. Is the pump increasing or decreasing displacement?

Assume:

Control piston diameter: 25 *mm*, bias piston diameter: 12 *mm*, control and bias piston arm: 110 *mm*, bias spring force: 140 *N* (constant), Orifice flow coefficient 0.7. The forces generated by the pistons and spring are parallel to their axes and act on the swashplate at an angle. For simplicity, assume these forces to be perpendicular to the swash plate.[7]

Given:

A variable displacement pump with a differential pressure limiter, pump pressure, $p_P = 180$ *bar*. Swash plate moment, $\mathcal{M} = 10$ *Nm*, control piston diameter, $d_{cp} = 25$ *mm*, bias piston diameter, $d_{bp} = 12$ *mm*, control and bias piston arm, $l = 110$ *mm*, bias spring force, $F_{bs} = 140$ *N* (constant), Orifice flow coefficient, $C_f = 0.7$, oil density, $\rho = 850$ *kg/m³*.

Operating modes:

Case 1 – pump holding a constant displacement
Case 2 – pump changing displacement with a control spool; equivalent area $\Omega_{cs} = 0.8$ *mm²*. Assume the same control piston pressure as in Case 1.

Example 16.3 (Continued)

Case 3 – pump changing displacement with a control spool equivalent area $\Omega_{cs}= 2.5 \, mm^2$. Assume the same control piston pressure as Case 1.

Find:

Case 1 – Control piston pressure p_x

Case 2 – Swash plate angular velocity and displacement direction

Case 3 – Swash plate angular velocity and displacement direction

Solution:

Case 1 – The pump is holding a constant displacement. The forces acting on the swash plate are the control piston force F_{cp}, the bias piston force F_{bp}, and the bias spring force F_{bs}. All these forces create a moment through the arm $l = 110 \, mm$. The other force acting on the swash plate are the pistons internal forces that create a moment $\mathcal{M} = 10 \, Nm$. The situation is summarized in the figure below:
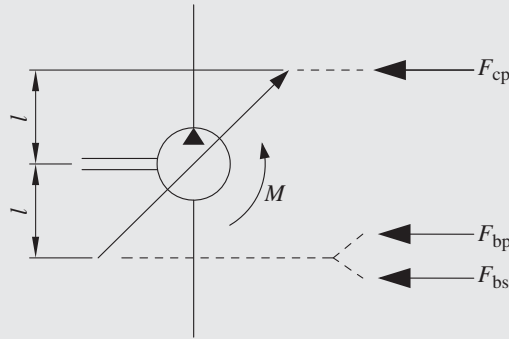
The swash plate balancing equation is

$$\left(F_{cp} - F_{bp} - F_{bs}\right) \cdot l + \mathcal{M} = 0$$

In particular, the two piston forces are equal to $F_{cp} = \Omega_{cp} \cdot p_x$ and $F_{bp} = \Omega_{bp} \cdot p_P$. Therefore, the control piston pressure is

$$p_x = \frac{\left(\Omega_{bp} \cdot p_P + F_{bs}\right) - (\mathcal{M}/l)}{\Omega_{cp}}$$

Substituting the values into the formula,

$$p_x = \frac{\left(\frac{\pi \cdot 12^2}{4}[mm^2] \cdot \frac{180}{10} \, [N/mm^2] + 140 \, [N]\right) - \left(\frac{10 \cdot 1000 \, [N \cdot mm]}{110 \, [mm]}\right)}{\frac{\pi \cdot 25^2}{4} \, [mm^2]} \cdot 10 = 42 \, bar$$

The pressure in the control piston is approximately 23% of the outlet pressure.

Case 2 – In this case, the pump is reducing its displacement, which moves toward the min position (as per the represented schematic). The control spool defines a metering area of $0.8 \, mm^2$

between the outlet and control piston. The flow going through the control spool is

$$Q_{cp} = C_f \cdot \Omega_{cs} \sqrt{\frac{2\,(p_P - p_x)}{\rho}} = 0.7 \cdot \frac{0.8}{10^6}\,[m^2] \sqrt{\frac{2 \cdot (180 - 42) \cdot 10^5\,[Pa]}{850\,[kg/m^3]}} \cdot 60\,000 = 6\ l/min$$

The linear speed of the control piston is

$$\dot{x}_{bp} = \frac{Q_{bp}}{\Omega_{bp}} = \frac{\dfrac{6}{60\,000}\,[m^3/s]}{\dfrac{\pi \cdot 25^2}{4} \cdot \dfrac{1}{10^6}\,[m^2]} = 0.2\ m$$

The angular velocity of the swashplate (in degrees per second) is then equal to

$$\omega_{sw} = \frac{\dot{x}_{bp}}{l} = \frac{0.2\,[m/s]}{\dfrac{110}{1000}\,[m]} \cdot \frac{180}{\pi} = 104\ deg/s$$

Assuming, for example, that the maximum displacement of the pump corresponds to a swash plate inclination of 24°, in this condition, the pump requires approximately 230 *ms* to completely de-stroke. Another important consideration is that during this transient, the control piston is subtracting Q_{bp} from the pump outlet flow. This amount is only partially compensated by the additional flow pushed to the outlet by the bias piston:

$$Q_{bp} = Q_{cp} \cdot \frac{\Omega_{bp}}{\Omega_{cp}} = Q_{cp} \cdot \left(\frac{d_{bp}}{d_{cp}}\right)^2 = 6\,[l/min] \cdot \left(\frac{12}{25}\right)^2 = 1.4\ l/min$$

A pump with the given geometrical parameters should not exceed 30 cm^3/r displacement. Therefore, the flow "robbed" by the control mechanism during this transition (approximately 4.6 l/min) represents a significant portion of the outlet flow.

Case 3 – In this case the pump is increasing its displacement, which moves toward the max position (as per the represented schematic). The control spool defines a metering area of 2.5 mm^2 between the outlet and the case drain. The flow going through the control spool is

$$Q_{cp} = C_f \cdot \Omega_{cs} \sqrt{\frac{2p_x}{\rho}} = 0.7 \cdot \frac{2.5}{10^6}\,[m^2] \sqrt{\frac{2 \cdot 42 \cdot 10^5\,[Pa]}{850\,[kg/m^3]}} \cdot 60\,000 = 10.5\ l/min$$

The linear speed of the control piston becomes

$$\dot{x}_{bp} = \frac{Q_{bp}}{\Omega_{bp}} = \frac{\dfrac{10.5}{60\,000}\,[m^3/s]}{\dfrac{\pi \cdot 25^2}{4} \cdot \dfrac{1}{10^6}\,[m^2]} = 0.35\ m/s$$

The angular velocity of the swashplate (in degrees per second) is then equal to

$$\omega_{sw} = \frac{\dot{x}_{bp}}{l} = \frac{0.35\,[m/s]}{\dfrac{110}{1000}\,[m]} \cdot \frac{180}{\pi} = 182\ deg/s$$

Under the same assumption that the maximum displacement of the pump corresponds to a swash plate inclination of 24°, in this condition, the pump requires approximately 132 *ms*

Example 16.3 (Continued)

to completely stroke-up. During this transient, the control piston is releasing Q_{cp} through the pump case drain. The case drain ports in axial piston pumps are usually sized for the transient flows caused by the control mechanism, and not for the leakage flow that is usually much smaller.

16.6 Load Sensing Solution with Independent Metering Valves

Independent metering valves have been introduced in Chapter 13, as a method to accomplish a flexible combination of throttling areas using valves controlled by separated solenoids. An independent metering system can be used to directly implement the basic LS principles in Figure 16.1 (fixed displacement pump) or Figure 16.7 (variable displacement pump), using an architecture that is different when compared to the traditional LS valve. There are multiple variants of independent metering solutions for LS systems, and a possible example of implementation is given in Figure 16.12, for the case of fixed displacement pump. In this system, four solenoid actuated 2/2 proportional valves are used to control the actuator velocity. VPA and VPB connect the supply to the actuator work-port and are energized to control the cylinder extension and the retraction, respectively, as meter-in orifices according to the LS principle. Therefore, the operator command is sent either to VPA (extension) or VPB (retraction). The load pressure is sent to the unloader C (or to the differential pressure regulator, in case of a variable displacement pump), so that the pump outlet pressure becomes $p_P = p_U + s$, as in Eq. (16.10). CVA and CVB, in series with VPA and VPB, respectively, ensure that the value of p_U used to determine the pump pressure is always the pressure
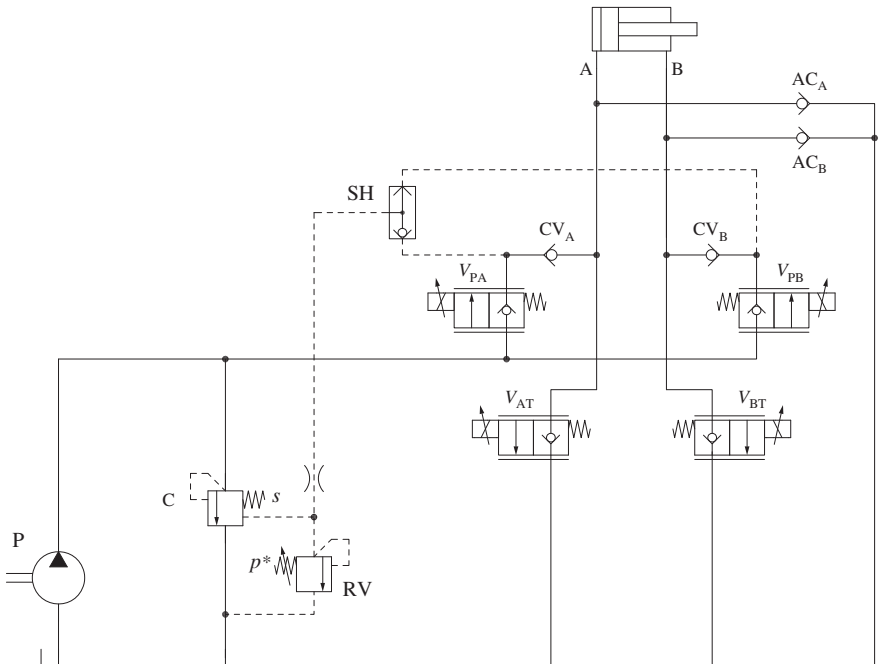
Figure 16.12 Load sensing system using independent metering elements.

at the actuator supply port. In fact, for certain external load conditions (such as resistive loads), the pressure at the return port could be higher than the pressure at the supply port. The bleed orifice O permits to not have residual pressures trapped in the pilot lines that carry the load signal. The pressure drop across the commanded VP valve is maintained at s, so that the flow sent to the actuator is a function only of the valve opening (Ω_{PA} or Ω_{PA}), as expressed in Eq. (16.12).

The flow returning from the actuator goes to VTA for the case of retraction and VTB for the case of extension. Both VTA and VTB are proportional valves, and their opening (Ω_{TA} or Ω_{TB}) affects the pressure at the return work-port. While the supply valves VP are directly controlled by the operator (command i), the opening of the return valves VT is performed separately, usually independent of the operator command. In the case of resistive loads, it is convenient to fully open the return valve VT, so that the supply pressure is minimized to operate the system with minimum energy consumption. However, in the case of overrunning loads, a proper opening of VT creates a counterpressure that balances the load and avoids losing control of the actuator, as described in Chapter 13. In these conditions, the optimal opening of the return orifice corresponds to the minimum positive pressure at the supply work-port. If the return orifice area is lower than the optimal value, the actuator velocity is controlled at a cost of a higher energy consumption due to an unnecessary pump overpressurization. To achieve this functionality, independent metering systems such as in Figure 16.12 requires pressure sensors at the actuator work-ports, as feedback signal to the controller that handles the return valves VT. For simplicity, these pressure sensors are not shown in Figure 16.12. A simpler alternative for controlling the system under overrunning load conditions would consist in using two counterbalance valves to replace VTA and VTB.

The independent metering system in Figure 16.12 also allows controlling the actuator in meter-out mode, in cases of assistive loads. To enable this mode, anticavitation check valves AC are present to allow the supply flow from the tank, bypassing the VP valve. The flow regulation is performed using the return valve as meter-out. In this case, the system works as pure meter-out (as described in Chapter 13), and not as an LS system.

An alternative LS independent metering architecture, which uses a variable displacement pump, will be illustrated in Chapter 19, for the case of multiple actuators.

16.7 Electronic Load Sensing (E-LS)

In all LS circuits presented so far in this chapter, the load pressure information is always transmitted from the actuator to the pump regulator, or unloader, through a hydraulic signal line i.e. the hydraulic LS connection. In the concept of electronic LS (E-LS), the hydraulic pressure signal is replaced by an electric signal and thus eliminates the hydraulic LS connection. A typical implementation circuit of E-LS is represented in Figure 16.13. Here the actuator is controlled with an LS valve, similar to Figure 16.5. The LS port of the valve is connected to a pressure transducer, which reads the load pressure p_U.

The pump is a variable displacement unit equipped with a differential pressure limiter (as the one presented in Figure 16.7). Here, the LS pressure signal is "artificially" generated through a proportional pressure relief valve (PRV), whose setting p^* is a function of the input signal i_R. This valve is supplied from the pump delivery through a pressure separator O_S. With such a layout, the pump always "chases" the PRV pressure, therefore implementing the condition:

$$p_P = p^* + s = f\left(i_R\right) + s \qquad (16.20)$$

Usually the proportional relief valve PRV allows to continuously change the pressure setting between zero and a maximum value, p_{max}. In most of the cases, the relationship between the command i_R and the set pressure p^* is linear. Some PRVs have a directly increasing relationship between
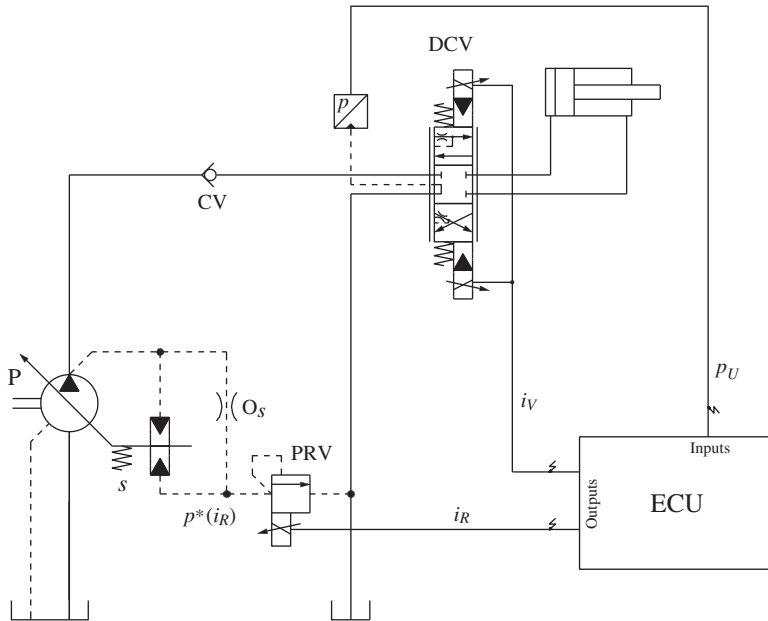
Figure 16.13 Circuit implementing the electronic LS principle.

current and pressure; others have an inverse relationship between the two. For the first type of PRVs, the relationship between the set pressure and current i_R is

$$p^* = f\left(i_R\right) = \min\left(p_{\max}, k \cdot \left(i_R - i_0\right)\right) \tag{16.21}$$

For the second type of PRVs (inverse relationship between current and pressure), this is

$$p^* = f\left(i_R\right) = \max\left(0, p_{\max} - k \cdot \left(i_R - i_0\right)\right) \tag{16.22}$$

In Eq. (16.21), if $i_R = 0$, then $p^* = 0$; in Eq. (16.22) if $i_R = 0$, then $p^* = p_{\max}$.

The logic of operation of the E-LS circuit is implemented by an electronic control unit (ECU), which receives two inputs (the operator command and the reading of the pressure transducer) and commands two outputs (the command signal to the LS DCV and the signal i_R to the PRV). To implement the LS principle, the ECU sends a signal to the PRV that is equal to

$$i_R = f^{-1}\left(p_U + \varepsilon\right) \tag{16.23}$$

f^{-1} is the inverse function of the characteristic of PRV (described by Eq. (16.21)); ε is a value that can be added (or subtracted, if negative) to the measured load pressure, p_U. Substituting Eq. (16.23) into Eq. (16.20), the pump outlet pressure becomes

$$p_P = p_U + (s + \varepsilon) \tag{16.24}$$

The value of ε is a parameter that can be changed by the controller to modulate the effective margin pressure at the LS valve. For example, if the value of ε is null, the system implements the typical LS condition $p_P = p_U + s$, as in Eq. (16.10). If the value of ε is greater than zero, the margin pressure is increased. Therefore, more flow is commanded to the actuator, for a given opening area of the LS valve. Vice versa, if ε is negative, the margin pressure can be reduced, to obtain a more efficient control because of the reduced pressure drop across the metering element.

In general, the E-LS has the advantage of allowing an additional degree of flexibility in the control architecture. The commands in this case are i, the LS valve opening, and i_R to influence the

pressure margin across the LS valve. This enables additional control strategies when compared to a traditional LS system. Possible examples are as follows:

- *Variable maximum flow*. The value of ϵ determined by i_R allows varying the maximum flow capability of the LS valve. The maximum flow that the LS valve can send to the actuator is given by

$$Q_{\max} = C_f \Omega_{\max} \sqrt{\frac{2(s + \epsilon)}{\rho}} \qquad (16.25)$$

where $\Omega_{\max}$ corresponds to the maximum opening of the LS valve, and it is directly related to the maximum command $i_{\max}$. For a traditional LS system, the value of $Q_{\max}$ corresponds to the maximum flow rate of the supply pump, to avoid flow saturation (Eq. (16.9)). However, for an E-LS, the above relation can be used to conveniently scale the maximum flow rate of the LS valve. This can be convenient for using small LS valves in applications only occasionally require high flow rates. For low flow demand conditions, the LS margin $(s + \epsilon)$ is set to a small value to reduce the energy loss across the metering orifice in the LS valve. For high flow demand conditions, the LS margin is increased to allow for higher flor rates at expenses of higher throttling losses.
- *Variable standby pressure*. In terms of energy consumption, when a function is not activated, it is convenient to minimize the energy consumption of the pump by reducing its outlet pressure. E-LS permits to further reduce the setting of the differential flow limiter s, so that the standby pressure can be raised only when needed.

On the other hand, E-LS have some drawbacks and challenges. First, in the circuit of Figure 16.13, a constant flow rate is continuously lost through the pressure separator orifice O_S (which is always exposed to the differential pressure s). This reduces the system efficiency with respect to a traditional LS circuit. Second, the key element of the system is the proportional PRV, which must closely follow the load pressure with a good degree of accuracy. Especially when the system is working at low margin pressures, the nonideal characteristic of the PRV (valve hysteresis, nonlinearities, sample to sample variations, etc.) can significantly affect the system performance and pose challenges for a robust implementation of this concept.

Problems

16.1 An engine powered scissor lift uses an LS system supplied with a gear pump to control the hydraulic functions. In particular, the lift function uses a cylinder with a 50 *mm* bore and a 30 *mm* rod. The stroke of the cylinder is 700 *mm*. The force necessary to lift the platform is 160 *kN* and can be considered constant during the operation. The pump has a displacement of 21 *cm³/r* and rotates at 1500 *rpm*. The LS valve uses an unloader with a 7 *bar* spring. The platform needs to be lifted in eight seconds and lowered in 12 *s*.
   1) Represent the hydraulic circuit.
   2) Determine the meter-in area of the spool to achieve the desired lifting speed.
   3) Determine the energy utilized and dissipated during the lifting operation.
   4) Calculate the system efficiency during lifting.
   5) Calculate the optimal design of the LS valve (meter-in and meter-out) in order to optimize the system efficiency during the lowering phase.

16.2 A hydraulic cylinder is controlled with a LS valve and a variable displacement pump. This has a displacement of 45 *cm³/r*, rotates at 2000 *rpm*, and has a margin setting of 18 *bar*. The

cylinder force generates a load pressure of 120 *bar*. When actuated, the LS valve opens a metering area of 25 mm^2. Calculate

1) The fractional displacement ε at which the pump operates in normal conditions
2) The pump fractional displacement and outlet pressure if the pump speed is reduced to 1200 *rpm*

Assume an orifice flow coefficient equal to 0.7 and fluid density of 850 kg/m^3.

16.3 A hydraulic motor is controlled using an LS system based on a variable displacement pump. This has a displacement of 75 cm^3/r, rotates at 2000 *rpm*, and has a margin setting of 15 *bar*. The pump and the valve are located at the opposite ends of the vehicle and, therefore, the pressure losses in the lines and connectors between the two are not negligible. The hydraulic turbulent resistance of the lines between the pump and the valve is 0.001 $bar/(l/min)^2$. What is the maximum flow that can be achieved at the hydraulic consumer? Assume an orifice flow coefficient equal to 0.7 and fluid density of 850 kg/m^3.

Chapter 17

Constant Pressure Systems

Constant pressure systems usually indicate metering control concepts based on a constant pressure supply. In general, two types of constant pressure systems are encountered, depending on the supply type, which can be implemented by a variable displacement pump or by a fixed displacement pump with one or more accumulators. The simplified circuits of such systems were already introduced in Chapter 11. This chapter presents additional details about the actual implementation of this hydraulic control strategy, for both types of flow supply, i.e. fixed displacement pump and variable displacement pump. As it will be described in Part V, constant pressure systems are particularly suitable for applications with multiple actuators. In fact, with this simple architecture, there is no interference between controlled actuators with different loads.

17.1 Constant Pressure System with Variable Displacement Pump

17.1.1 Basic Schematic and Operation

Figure 17.1 shows both the simplified schematic and the detailed circuit for the case of a constant pressure system that uses a variable displacement pump. These circuits show the displacement adjusting mechanism usually common for a swash plate-type axial piston pump.[1] This adjustment mechanism regulates the pump displacement in order to keep its outlet pressure p_P at the setting p^*. This is achieved by the use of an absolute pressure limiter, the operation of which was introduced during in Chapter 16 (valve V2 of Figure 16.9). The system operates with a constant pump outlet pressure, and the flow to the actuator is set by a proportional DCV that functions as a metering element. Therefore, the flow to the actuator is given by the orifice equation applied to the metering element:

$$Q_U = C_f \Omega_U (i) \sqrt{\frac{2 \left(p^* - p_U \right)}{\rho}} \tag{17.1}$$

The metering area Ω_U is a function of the input command i. Therefore, if $\Omega_U(i)$ is linear, the controlled actuator velocity also varies linearly with the input command. Consequently, the actuator starts moving as soon as the area Ω_U opens. Contrarily to the cases of open center and bleed-off systems (Chapter 14), the constant pressure system architecture does not present a load dependent regulation deadband. However, the flow sent to the actuator, Q_U, and thus the actuator velocity, depends on the load p_U. In addition to this, the control range is also affected by the load. In fact,

---
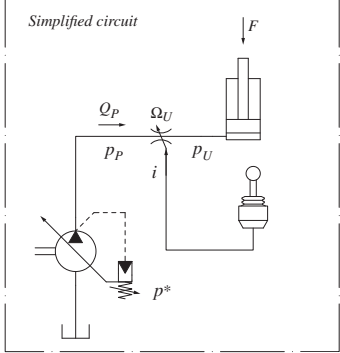
Figure 17.1 Constant pressure system using a variable displacement pump.

the actuator speed is input-dependent until *flow saturation* is reached. This happens when $\Omega_U \geq \Omega^*$ where Ω^* is a function of p_U:

$$\Omega^* = \frac{Q_{P,\max}}{C_f} \sqrt{\frac{\rho}{2\left(p^* - p_U\right)}} \tag{17.2}$$

Constant pressure systems allow precise control of the actuator speed without any deadband in the command. However, the flow rate to the actuator is influenced by the value of the actuator load.

Figure 17.2 shows the pressure, flow, and area trends typical of a constant pressure system. The pump flow (equal to the actuator flow) increases linearly from $i = 0$ until $i = i^*$ (which corresponds to Ω^*), under the assumption that $\Omega_U(i)$ also follows a linear trend. For values $\Omega_U(i) > \Omega^*$ the *flow saturation* condition is reached where the pressure drop across the control orifice is not high enough to keep the pump pressure at p^*. In this condition, the displacement adjustment system leaves the pump at its maximum displacement $V_{D,\max}$. As a result, for $i > i^*$, the flow to the actuator remains constant and the pump pressure decreases for increasing values of i. In this range, the control element transitions from being a metering element to a compensator, since $Q_U = Q_{P,\max} = \text{const}$).

For some constant pressure applications, the saturation condition can be part of the duty cycle. This happens when the duty cycle requires phases of maximum velocity. In these cases, it can be convenient to use a control orifice that has an area trend where the slope drastically changes for $i > i^*$. Physically, this can be achieved by a spool design where the opening is through metering notches, for $i \leq i^*$, while the opening is through the annular area when $i > i^*$. This feature leads to a significant decrease of the pump pressure during saturation conditions and thus reduces power losses due to throttling. Since the value of i^* depends on p_U, the actual command at which the area trend changes should be evaluated considering the maximum load conditions, $p_{U,\max}$:

$$i_1 = i^*|_{p_{U,\max}} \tag{17.3}$$

Figure 17.2 Pump pressure (a), flow, and area trends (b) for a constant pressure system for different input commands (p_U = const).

Therefore, when $p_U < p_{U,\max}$, then $i^* < i_1$. This means that in general, in the interval $i^* < i < i_1$ of flow saturation, the pressure drop across the control orifice only decreases slightly, as shown in Figure 17.2.

The above described effect of the load on the flow controlled by the system is shown in the plot of Figure 17.3. The figure shows the outlet flow curves for different levels of the input command i, including the case of flow saturation $i > i^*$.

Figure 17.3 Influence of the load on the actuator flow in a constant pressure system.

Figure 17.4 Energy plot for the constant pressure circuit of Figure 17.1.

17.1.2 Energy Analysis

The energy plot for the constant pressure circuit during normal operation (not in saturation conditions), is shown in Figure 17.4. The energy efficiency of the system is obtained as:

$$\eta_S = \frac{P_U}{P_P} = \frac{p_U}{p^*} \tag{17.4}$$

> The energy efficiency of a constant pressure system is poor when the pressure at the actuator is low. However, the efficiency of the system improves for high actuator loads.

17.2 Constant Pressure System with Unloader (CPU)

An important consideration about the constant pressure system in Figure 17.1 pertains to the standby condition (directional control valve, DCV, in neutral position). When the DCV is not commanded, ideally the pump should require a null power, because it delivers zero flow at the set pressure p^*. In reality, two important aspects should be considered:

- An actual pump needs to make up for the leakage flow, necessary for a proper lubrication of the internal parts, and for the flow consumed by the absolute pressure regulator. Therefore, the displacement is always maintained at a nonzero value, and thus the actual power consumption of the system in standby conditions can be significant. For example, a commercially available 75 cm³/rev piston pump equipped with such regulator running at 1800 rpm with blocked delivery port (i.e. zero outlet flow) requires about 4 kW at 200 bar and 1.5 kW at 25 bar.
- During each start-up event, the pump rapidly reaches its pressure setting. This can be undesirable for both the prime mover (due to the high torque request at start-up), as well as for the pump (due to insufficient lubrication of the internal sliding elements). Therefore, it is desirable to achieve start-up conditions with low pressure at pump outlet.

Thus, constant pressure systems with the layout shown in Figure 17.5 are often preferred.

In this case, the pump displacement adjustment mechanism consists of a differential pressure limiter (V1), which maintains the following condition:

$$p_P = p_X + s \tag{17.5}$$
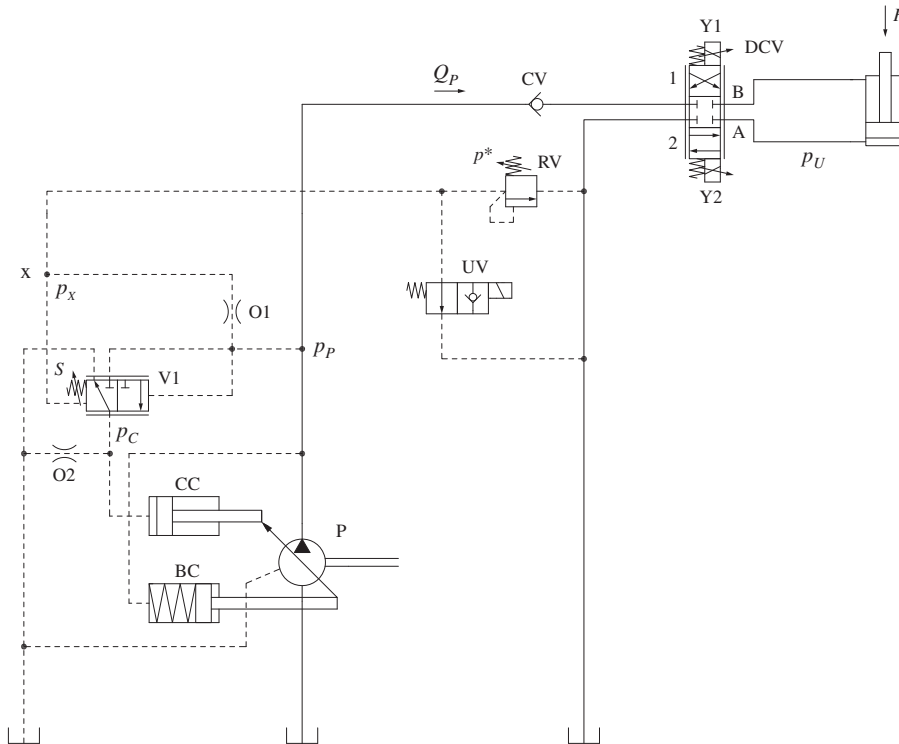
Figure 17.5 Constant pressure system with unloader and variable setting pressure.

This pressure limiter is similar to the one present in load sensing (LS) pumps, as described in Chapter 16. The pilot pressure p_X is taken from the pump outlet, through a pressure separator, O1. Furthermore, the point X is connected to a relief valve RV set to p^* and to a 2/2 on/off valve known as unloading valve (UV). When the UV is in its neutral configuration, the pressure at point X is null because the pilot line is connected to the tank. Therefore, the pump outlet pressure is $p_P = s$. This condition, along with the DCV being in neutral, permits to have a low standby power consumption since typical values of s are 10–15 bar.

If UV is energized, the relief valve RV takes control of the pressure p_X. Thus, the pump pressure is $p_P = p^* + s$. In this situation, the valve DCV can be energized to control the actuator velocity. All the considerations made above for the system in Figure 17.1 also apply to this case. The correct pump outlet pressure value here is equal to $p^* + s$.

The transition between the two states happens when the valve UV is energized, the pilot line X is closed, and its pressure starts increasing. This happens because the pump outlet pressure is statically transmitted, through the orifice O1, to the valve V1. The valve V1 is therefore in neutral position,[2] with the effect of increasing the pump displacement. This dynamic situation, which lasts only a few milliseconds, returns to the steady-state condition when the pressure at point X reaches the setting of the relief valve (RV). At this point, the RV opens and the pressure p_X remains steadily at p^*, thanks to the pressure separator orifice O1. The differential pressure limiter V1 then

---

2 In this situation, V1 ensures the pump pressure and the spring force are applied on the left side, and the pump pressure on the right side. In other words, the two pressures balance out and the spring force determines the position of the spool.

maintains the pump displacement, in order to satisfy the condition $p_P = p^* + s$. This condition is also known as the *constant pressure condition*.

The pilot flow consumed by the displacement adjustment system includes the flow rate across the orifice O1, which always sees a constant pressure difference equal to the spring rate *s*. Typical values for the diameter of O1 are within 0.7–1.0 mm, and for *s* are 10–15 bar, thus leading to a pilot flow consumption between 0.8 and 2.0 l/min. This value needs to be added to the flow loss through the orifice O2 (present for dynamic stability, as bleed orifice), and to the leakage across spool V1 when in regulation. The overall pilot flow consumption of this type of regulator can be significant, i.e. up to 2–4 l/min.

Once the system is in constant pressure condition, the flow to the actuator can be adjusted by proportionally shifting the DCV.

One important observation is that during flow saturation the pump pressure is lower than $p^* + s$. Thus, the variable displacement pump remains at maximum displacement, behaving as a fixed displacement unit. The orifice Ω_u then behaves as a compensator. Under this condition, the pump regulator (Figure 17.5) stays in neutral position (control cylinder [CC] connected to the tank) and, since $p_P < p^* + s$, the flow across the orifice O1 is null as well as the cross-port leakage of V1. In other words, the pilot flow consumption of the regulator is minimal and limited only to the clearance leakage of the spool V1.

17.3 Constant Pressure System with Fixed Displacement Pump

17.3.1 Basic Schematic and Operation

A constant pressure system can also be achieved with a fixed pump architecture. In this case, the system comprises at least one accumulator. The accumulator functions as an energy storage device. Different from the case of a flow variable displacement pump, this circuit does not maintain an exact constant pressure. Rather, it approximates the ideal case by maintaining a pressure between two reference values.

Figure 17.6 shows a typical hydraulic circuit used for implementing a constant pressure system with a fixed displacement pump. Besides the pump P, the system also includes an accumulator (ACC) and a check valve (CV) located to allow free flow from the pump to the accumulator. The
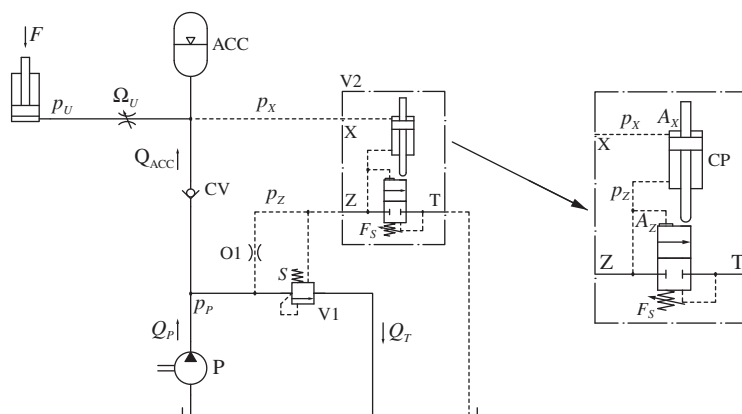

Figure 17.6 Typical layout of a constant pressure system supplied by a fixed displacement pump. A detailed view of the charging control valve schematic is included.

charging of the accumulator is controlled with two valves, V1 and V2. V1 is a 2/2 pilot operated valve. This is equivalent to the unloader described in Chapter 16, for the case of LS system with fixed displacement pump.

The key element of the circuit is the *accumulator charging control valve*, V2, which, in one possible architecture, is formed by two elements: a 2/2 normally closed spool (or poppet) and a plunger. The peculiar architecture of V2 is represented in detail in Figure 17.6. O1 is a pressure separator orifice, located between the pump outlet and the port Z of V2. The function speed is controlled with a generic valve (in the schematic shown as a variable orifice Ω_U), which is placed between the accumulator and the actuator.

Accumulator Charging Control Valve

The spool of V2 opens or blocks the connection between port Z and port T (connected to tank at null pressure). This connection is normally closed due to the effect of the spring force F_s. The plunger CP is represented as a double rod cylinder, where the lower chamber is supplied by the pressure at port Z (p_Z), and the top chamber by the pressure at port X (p_X). The plunger is normally free, but if $p_X > p_Z$, it mechanically engages with one side of the spool. Therefore, the spool of V2 can open the flow passage in two ways:

1) $p_X \leq p_Z$, and $p_Z < p_1^*$. In this case, the plunger is disengaged and the pressure at port Z generates a force able to overcome the spring. Using A_Z to denote the area of influence of the pressure p_Z, the maximum value for the pressure p_Z to maintain this condition is

$$p_1^* = \frac{F_s}{A_Z} \tag{17.6}$$

2) $p_X > p_Z$ and $p_X > p_2^*$. If the combined force of the plunger and of the pressure p_Z overcome the force of the spring. As mentioned before, this condition can happen only if $p_X > p_Z$. Indicating with A_X the area of the cylinder PC, this opening condition is reached if

$$(p_X - p_Z) \cdot A_X + p_Z A_Z \geq F_s \tag{17.7}$$

A particular case of Eq. (17.7) can be derived for the condition $p_Z = 0$. In this case, the spool is shifted only under the action of the plunger. This condition is reached if $p_X > p_2^*$, where

$$p_2^* = \frac{F_s}{A_X} \tag{17.8}$$

One important note is that usually $A_X > A_Z$. The parameter $\tau = A_Z/A_X$ represents the ratio between the two areas and the ratio of the two charging pressures. Usual values of τ are $0.75 \div 0.9$.

Once the operation of the accumulator-charging control valve V2 is clear, it can be easy to understand the operation of the whole constant pressure system in Figure 17.6. Figure 17.7 summarizes the trends of both the pump and the accumulator pressures in the system, starting from a condition of empty accumulator.

Figure 17.7 can be divided into different time intervals:

- $0 \leq t < t_1$ *Charging phase*. At $t = 0$, the accumulator pressure is null ($p_X = 0$). Also, the metering valve to the actuator is closed ($\Omega_U = 0$). The pump flow Q_P is then diverted to the accumulator. In fact, in this situation, $p_X = p_Z$ (so the plunger has no effect on the spool of V2) and $p_Z < p_1^*$. The valve V2 is closed, and the pressure is statically transmitted across O1 and therefore V1 is also closed. In this interval, the pump pressure p_P follows the increasing accumulator pressure p_X.
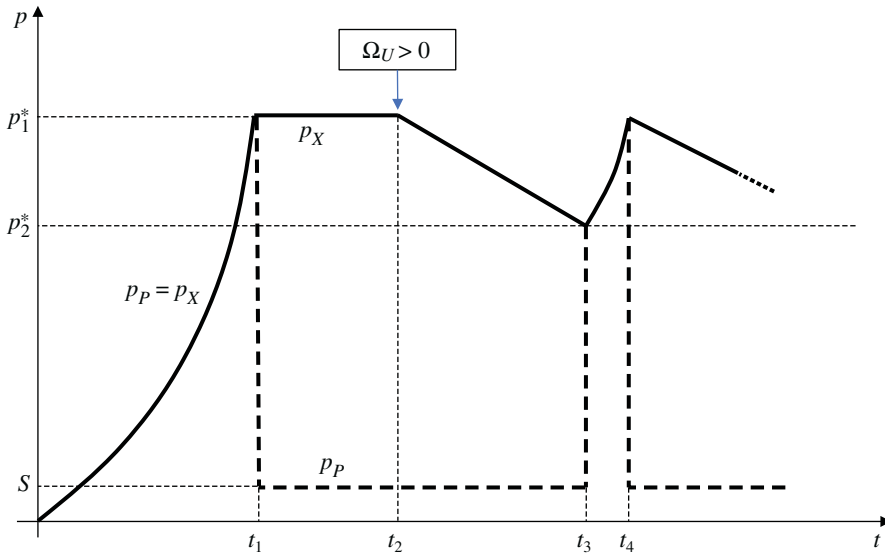
Figure 17.7 Pressure trends in the circuit, starting from an empty accumulator condition.

- $t_1 \leq t < t_3$ *Pump unloaded*. At $t = t_1$ the accumulator pressure reaches p_1^*. At this point, valve V2 starts acting as a pressure relief valve, opening an area in order to maintain the condition $p_Z = p_1^*$. However, the unloader V1 is still closed due to the effect of the spring *s*. Therefore, the accumulator pressure keeps increasing, and $p_X > p_Z$. At this point, the plunger starts pushing on the spool of V2; when $p_X = p_1^* + \varepsilon$ (where ε is a small value depending on the compressibility of the spring of V2), then Eq. (17.7) is satisfied and the spool of V2 is completely open. Consequently, $p_Z = 0$, and the valve V1 unloads the pump to the tank, at a small pressure level, $p_P = s$. However, per effect of the check valve, CV, the accumulator maintains its pressure equal to p_1^*. p_1^* also acts on the area A_X of the plunger of V2. Since $A_X > A_Z$, the pressure $p_X = p_1^*$ is high enough to keep the valve V2 open (even if $p_Z = 0$).
  From t_1 onward, the situation is steady until $t = t_2$, when the input command opens the metering valve ($\Omega_U > 0$) and the pressure in the accumulator starts decreasing. During $t_2 \leq t < t_3$, both valves V2 and V1 are open because $p_X > p_2^*$ and the force of the plunger is still greater than F_s.

- $t_3 \leq t < t_4$ *Recharging phase*. When $t = t_3$, the pressure in the accumulator reaches the second critical value p_2^*. As soon as $p_X = p_2^* - \varepsilon$, the force of the spring overcomes the force of the plunger and the valve V2 closes. Consequently, V1 also closes and the pump flow is sent back to the accumulator. At $t = t_4$, the upper charging pressure is reached again and the cycle repeats.
  In case the actuator control valve (Ω_U) is still open, the recharging phase can happen as represented in Figure 17.7 only under the assumption that the flow request $Q_U < Q_P$. Otherwise, the flow saturation condition is reached, and the pump would not be able to charge the accumulator.

17.4 Application to Hydraulic Braking Circuits

Constant pressure systems using accumulators are commonly encountered in hydraulic brake circuits. Here, the accumulator serves both as an energy storage and an emergency device that guarantees a safe and consistent supply that is independent of the planned or unplanned operating conditions of the machine. Braking, together with steering (an entire chapter will be dedicated to
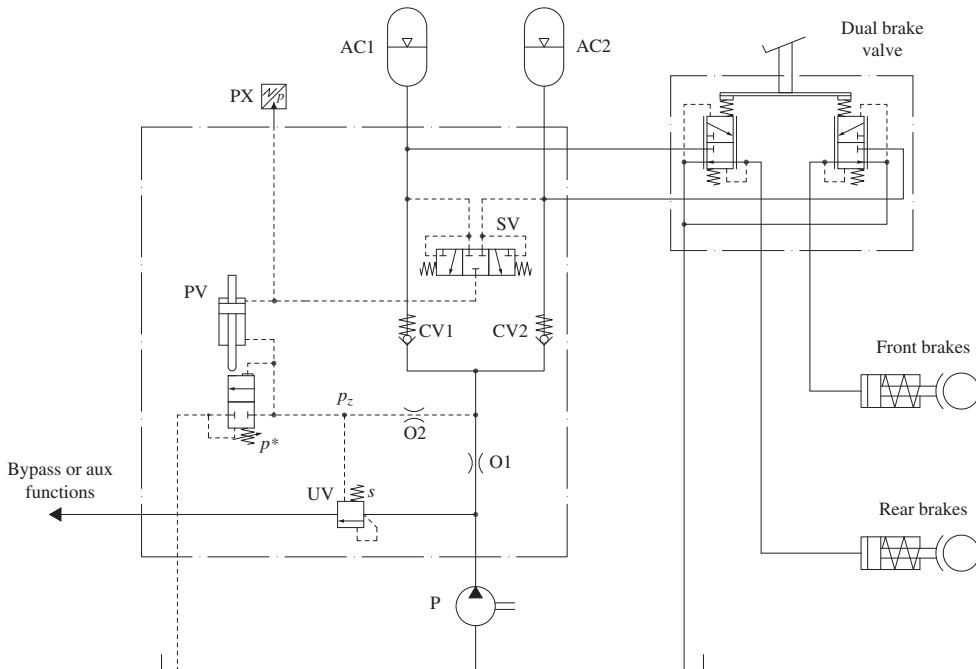
Figure 17.8 Constant pressure circuit for braking applications.

steering systems in Part V), is a critical function of a vehicle. The design of the circuit is strongly driven by safety and emergency operation. More information on the requirements for braking circuits can be found in the ISO standard 3450 [4] or in the references [5, 6].

An example of a hydraulic brake circuit is presented in Figure 17.8: the layout is very similar to the circuit of Figure 17.6, where the valves PV and UV controls the charge of the accumulators.

The system in Figure 17.8 presents a dual accumulator layout. The two accumulators, AC1 and AC2, belong to two independent circuits, which are separated by the check valves, CV1 and CV2. The brake valve includes two spools, each one for different axels: AC1 supplies the rear brakes, while AC2 supplies the front brakes. The accumulator charge circuit is controlled by the lowest of the two accumulator pressures, which is selected by the inverse shuttle valve (SV). When the accumulators are charged, PV is open and the signal pressure p_z is null. The orifice O2 works as a pressure separator and small amount of flow is lost through the pilot circuit. When the accumulators need charge, PV closes and the orifice O1 is in control of the amount of flow going to the accumulators: the pressure drop across O1 equals the spring s of the unloader valve, UV.

In this circuit, the failure of one accumulator or valve can be detected by the pressure sensor PX, but the vehicle will still partially maintain the functionality of the brake system.

Problems

17.1 A constant pressure circuit uses a 45 cm^3/r variable displacement pump with a pressure setting of 150 bar rotating at 1800 rpm. The system supplies a 200 cm^3/r hydraulic motor moving a load generating a torque, which varies with the motor speed according to the following: $T_M = T_0 + k \cdot n_M$. The value of T_0 is 264 Nm, while k is 0.3 Nm/rpm. Calculate the

metering area that corresponds to a motor speed of 200 rpm. Calculate the pump fractional displacement and the system efficiency.

17.2 A hydraulic cylinder operates following a repetitive duty cycle. The extension phase requires 30 l/min and 120 bar for 15 seconds. This is followed by a retraction phase of 9 seconds, requiring 22 l/min and 75 bar. The system rests for 45 seconds before restarting the same cycle. The system is supplied by a constant pressure circuit using a 60 cm^3/r variable displacement pump with a pressure setting of 180 bar rotating at 1800 rpm. The pump has a volumetric efficiency of 93% and a hydromechanical efficiency of 88%. Furthermore, the real pump requires torque even when it stays at standby condition (zero outlet flow). The requested torque varies with the outlet pressure and is represented in the chart below.

Shaft torque for a 60 cm^3/r pump at 1800 rpm and zero outlet flow
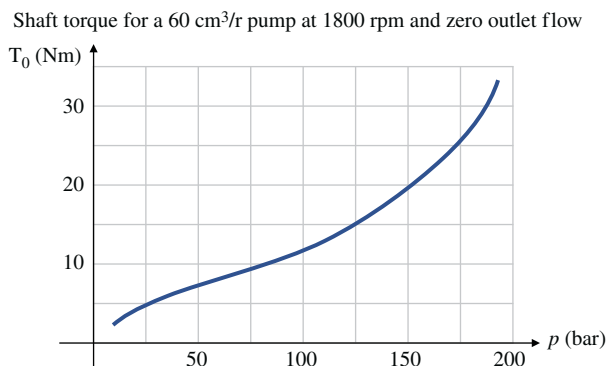
For the described duty cycle, compare the performance of a standard 180 bar constant pressure system (Figure 17.1) and a constant pressure system with unloader (CPU) system (Figure 17.5) that unloads the pressure to 15 bar and has a bleed orifice of 0.6 mm.
Calculate the flow areas to achieve the desired cycle and the energy used by the two systems for a single cycle. Which of the two is the more efficient circuit?

References

1 Ivantysyn, J. and Ivantysynova, M. (2003). *Hydrostatic Pumps and Motors: Principles, Design, Performance, Modelling, Analysis, Control and Testing*. Tech Books International.

2 Nervegna, N. and Rundo, M. (2020). *Passi nell'oleodinamica* vol. 1–2, Epics.

3 Zarotti, G.L. (1997). *Circuiti Oleodinamici—Nozioni e lineamenti introduttivi*. Cemoter.

4 ISO 3450:2011 (2011). *Earth-Moving Machinery—Wheled or High-Speed Rubber-Tracked Machines—Performance Requirements and Test Procedures for Brake Systems*.

5 Keyser, D.E. and Hogan, K. (1992). *Full Power Hydraulic Brake Actuation, Circuit Design Considerations for Off-Highway Vehicles and Equipment*. Mico Inc.

6 Middendorf, R. and Keyser, D. E. (1992). Reverse modulating brake valves, circuit design considerations and applications. SAE Technical Paper 920908.

Part V

Metering Controls for Multiple Actuators

The chapters of Part IV has presented different types of metering control concepts available for hydraulic systems, applied to circuits with a single actuator. The single actuator case is very seldom encountered in real applications. However, as mentioned before, presenting the control concepts on a single actuator was a very useful way to discuss the operating principles and the pros and cons of each concept. In most hydraulic applications, a single supply is used to drive multiple actuators. This allows reducing the cost, the space claim, and the weight of the system. In some cases, the capability of easily controlling multiple actuators with a single power supply is one of the advantages of hydraulic systems over other technologies.

In the scenario of multiple actuator systems, the metering control concepts represents the easiest and most common way to control the actuators from a single supply. Open center, constant pressure, and load sensing (LS) systems can all be extended to multiple actuators, each one of them presenting some unique advantages and challenges. For example, most excavating machines use open center circuits, while hydraulic cranes or forklifts are mostly based on LS systems. On the other hand, industrial or naval applications prefer constant pressure circuits.

Part V presents an analysis of each different technology, from the efficiency and controllability points of view. Chapter 18 introduces the basic concept of connecting multiple actuators, in either series or parallel configuration. Chapter 19 extends the case of constant pressure systems to multiple actuators. Chapter 20 focuses on open center systems. Chapter 21 covers the load sensing systems for multiple actuators, detailing the features of the pre-compensated and the post-compensated solution. The final Chapter 21 is dedicated to power steering and hydraulic systems with priority functions, which is a special case of multi-actuator system.

Many of the concepts presented in the chapters in Part V are inspired by the work of Nervegna [1] and Zarotti [2].

Objectives

Part V focuses on the features of circuits that use a single hydraulic supply to control multiple actuators. This kind of arrangement is typical of metering control systems. The reader, after a

careful understanding of the chapters here, and after working on the proposed examples and the end-of-chapter problems for practice, will be able to

1) Identify the generic layout architecture in multiple actuator circuits.
2) Recognize the phenomenon of load interference and, where this is an issue, implement the preferred method to address it.
3) Illustrate the different operation of metering and volumetric flow dividers.
4) Describe the operating features of constant pressure circuits for multiple actuators.
5) Describe the features of operation of open center circuit, including tandem, series, and parallel configuration.
6) Design a basic open center circuit for multiple actuators.
7) Identify the spool design characteristics that can improve the controllability of an open center circuit.
8) Recognize the different types of LS architecture for multiple actuators.
9) Define the features of LS compensators in load sensing pressure compensated (LSPC) circuits.
10) Describe how different LSPC circuits address the flow saturation issue. Define the flow sharing feature and the different ways to accomplish it.
11) Design the main components of LS circuits.
12) Describe the operation of power steering circuits.
13) Recognize the features of hydraulic power steering. Size a power steering unit for a given application.
14) Define the concept of priority in hydraulic systems and the different ways this can be achieved.
15) Design a priority circuit for a power steering application.

Chapter 18

Basics of Multiple Actuator Systems

Before presenting the different design architectures available to control multiple actuators with a single supply, it is important to first provide some considerations about the possible methods that can be used to connect actuators to the supply. This chapter first presents the series and parallel configurations, highlighting the main advantages and disadvantages of each basic layout. The concept of load interference is also illustrated for parallel actuators, thus introducing the methods for achieving a synchronism between multiple actuators. Different types of flow dividers are presented as a mean to realize synchronous motion. Finally, flow saturation is analyzed for the generic case of multiple actuators.

18.1   Actuators in Series and in Parallel

When connecting two (or more) actuators to a single supply, a *series* or *parallel* connection is be an option. The basic concept of series or parallel architectures is illustrated in Figure 18.1. Depending on the control concept selected for the actuators (e.g. metering or primary), series and parallel connections can be implemented in slightly different ways, some of which will be illustrated in the next chapters.

> In general, in the **series** configuration (cases a and c in Figure 18.1), the flow returning from the first actuator is connected to the supply port of the following one, located downstream in the hydraulic circuit. In the **parallel** configuration (cases b and d in Figure 18.1), all the actuator supply ports are connected to a common line, and similarly the return ports are merged in a single return line.

Figure 18.1 presents the case of two actuators; however, these concepts can be easily extended to a higher number of elements.

Figure 18.1 represents the flow supply connected the left side of each schematic, realizing only one direction of motion (i.e. extension, for the linear actuators). However, all the schematics represented can realize a bidirectional motion of the actuators, for example, by connecting supply and return ports to the work-ports of a directional control valve (DCV).

18.1.1   Series Configuration

The main feature of the series configuration can be easily understood by looking at Figure 18.1a (series connection of motors): the same flow Q_P is supplied to all actuators; therefore, each
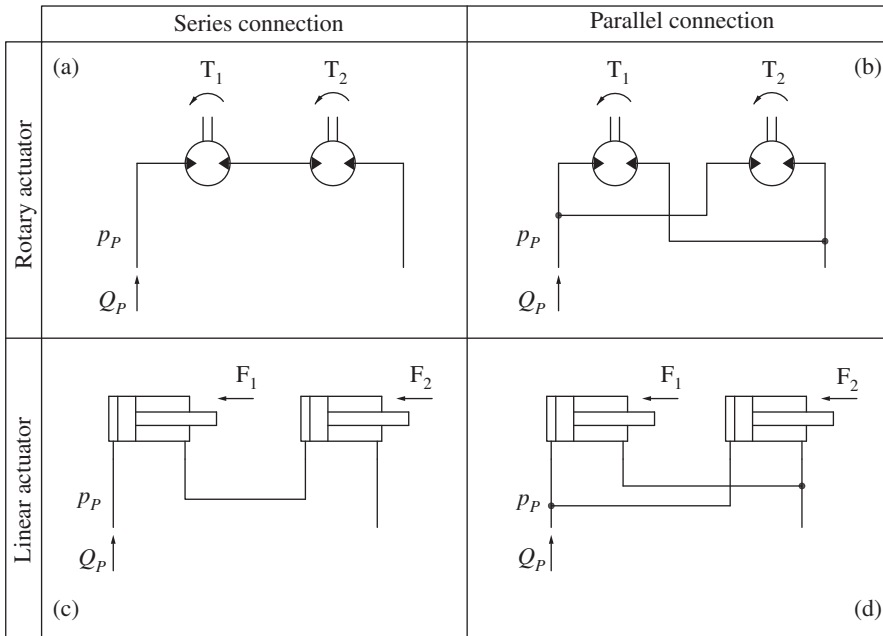
Figure 18.1 Basic concepts for series (a, c) and for parallel (b, d) connections. The top figures (a, b) are rotary actuators, and the bottom figures (c, d) are linear actuators.

individual motor speed is

$$n_i = \frac{Q_P}{V_{\text{Di}}} \tag{18.1}$$

The supply pressure p_P is defined by the *summation* of all the individual pressure drops at each actuator. Under the assumption that the return of U2 is connected to tank, the supply pressure is

$$p_P = \sum_i \frac{T_i}{V_{\text{Di}}} = \frac{T_2}{V_{\text{D2}}} + \frac{T_1}{V_{\text{D1}}} \tag{18.2}$$

The reader can notice how U2 is discharging flow to tank, while actuator U1 is working between the pump pressure and the supply pressure of U2. In other words, the return of U1 is connected to a positive pressure. This can sometimes be a limiting factor for certain actuator types, which are not suited for this type of circuit because of the limited return pressure capability.

The same concepts shown for rotary actuators also apply for linear actuators (Figure 18.1b). Here, the considerations regarding the flow rate must account for the effect of the differential areas of the cylinders. In Figure 18.1b, the two actuator speeds and the supply pressure are

$$\dot{x}_1 = \frac{Q_P}{A_1}; \quad \dot{x}_2 = \frac{Q_P}{\varphi_1 \cdot A_2}$$
$$p_P = \frac{F_2}{\varphi_1 \cdot A_2} + \frac{F_1}{A_1} \tag{18.3}$$

An important advantage of the series configuration is the **absence of pressure interference**. Pressure (or load) interference occurs when a load change on one actuator alters the controlled velocity of the other ones.
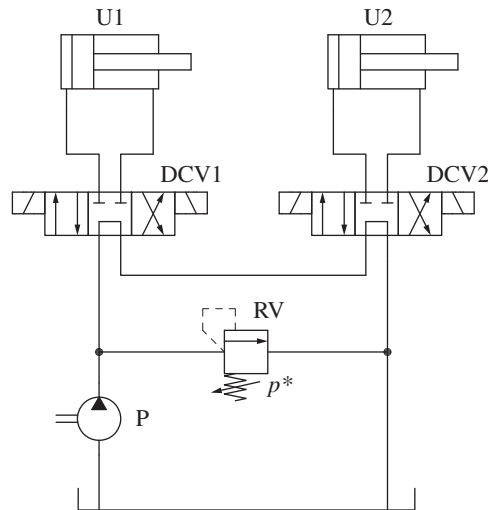
Figure 18.2 Circuit with two actuators in series.

For the series configuration, the hydraulic connections ensure a direct flow coupling between the actuators. The flow returning from one actuator goes to the supply of the downstream actuator. Consequently, a change in load on one actuator affects the system supply pressure but not the flow rate to each actuator. Therefore, the series configuration is the preferred layout to realize *synchronous motion* of actuators. The actuator velocity is not affected by the loads, under the assumption that the system pressure remains below the relief settings.

> The **pressure summation** of a system with multiple actuators in series is usually its limiting factor. It implies that the available working pressure needs to be split among multiple actuators, therefore penalizing the power density of the system.

The series connection can be also problematic for the first actuators because they have to work with high supply and high return pressures. This can limit the life and the performance of the units, especially the rotary ones. It can also lead to pressure amplification issues when linear actuators are used. Finally, the series connection is not suitable for actuators where the velocity needs to be independently modulated.

Figure 18.2 represents a more complete schematic of a circuit with multiple actuators in series, inclusive of the directional control elements. In this circuit, U2 is downstream of U1, realizing a series connection. The two actuators can be controlled simultaneously or independently, in both extension and retraction modes with the two DCV (devices for controlling overrunning load conditions are not shown for simplicity). In simultaneous actuation, synchronism between the motions of both actuators is guaranteed independently on the load.

Example 18.1 – Agricultural machine with three augers

An agricultural machine uses three augers driven by hydraulic motors to transfer corn seeds. The first auger moves the seeds along the bottom of a trailer, while the second and third augers move the seeds inside a chute. In order to operate correctly and avoid clogging, the three augers need to rotate at the same speed. Select the correct architecture for controlling them.

With heavy loading, the torque is 150 *Nm* on the first auger, 400 *Nm* on the second auger, and 280 *Nm* on the third auger. Size the three motors in order to not exceed the supply pressure of 280 *bar*. Which is the preferred layout of the three motors in the hydraulic circuit?

Given:

– The description of a hydraulic system, including three hydraulic motors
– Loading condition of $T_1 = 150$ *Nm*, $T_2 = 400$ *Nm*, $T_3 = 280$ *Nm*.
– Maximum supply pressure of $p^* = 280$ *bar*

Find:

– The hydraulic layout satisfying the simultaneous operation requirements
– The displacement of the three hydraulic motors V_{M1}, V_{M2}, and V_{M3}.

Solution:

In order to operate properly, the machine requires synchronous control of three actuators under different loads. The series connection is the preferred layout.
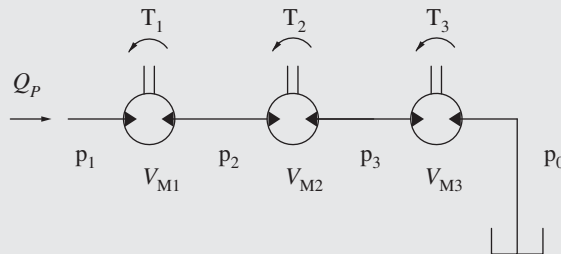
In particular, the three augers need to rotate at the same speed for a given supply flow rate. This implies the three hydraulic motors need to have the same displacement.

The torque equation can be written for this specific circuit in order to find the desired motor displacement V_M:

$$p^* = p_1 - p_0 = (p_1 - p_2) + (p_2 - p_3) + (p_3 - p_0) = \frac{T_1 \cdot 2\pi}{V_{M1}} + \frac{T_2 \cdot 2\pi}{V_{M2}} + \frac{T_3 \cdot 2\pi}{V_{M3}}$$

$$= \frac{(T_1 + T_2 + T_3) \cdot 2\pi}{V_M}$$

Therefore,

$$V_M = \frac{(150 + 400 + 280) \, [Nm] \cdot 20\pi}{280 \, [bar]} = 186.3 \; cm^3/r$$

Assuming the initial layout, the intermediate pressures are $p_2 = 229.4$ *bar* and $p_3 = 94.5$ *bar*. In other words, the first motor is working between 280 and 229.4 *bar*. This condition can limit the motor life because of the excessive return pressure. A better layout should have the load motor with the highest pressure first, followed by the other load motors in descending order. Therefore, the preferred order becomes M2, M3, and M1. Under this layout, the intermediate pressures become 145 and 50.6 *bar*.

18.1.2 Parallel Configuration

In the parallel configuration, actuators share a common inlet as well as a common return port (Figure 18.1b,d). In this layout, all actuators are subject to the same supply pressure p_P and the pump supply flow Q_P is the sum of all the actuators individual flows.

The parallel configuration takes better advantage of the power density; in fact, actuators can be sized for the full pump pressure, with smaller space claim. Furthermore, if not all actuators are always required to run at full speed at the same time, the pump size can be lower than the maximum theoretical value[1].

> Actuators in parallel configuration are subject to the effect of **load interference**. In other terms, in a parallel circuit the velocity of each actuator is a function of the load distribution among all consumers. Additional elements need to be added in the circuit to improve the controllability of each actuator and limit the load interference effects.

It is important to point out that the effects of load interference are not always undesired. In other words, in some applications, it is acceptable or even preferred to see functions slowing down or speeding up depending on the loads. In other cases, these need to be minimized and ideally a pressure-independent actuator speed is required.

The load interference within the basic parallel circuit configuration can be explained by analyzing the circuit in Figure 18.3, which reproduces the equivalent situation in Figure 18.1d. Ideally, the inlet flow Q_P should split between the two actuators U1 and U2. However, this condition cannot be achieved with the simple circuit in Figure 18.3.
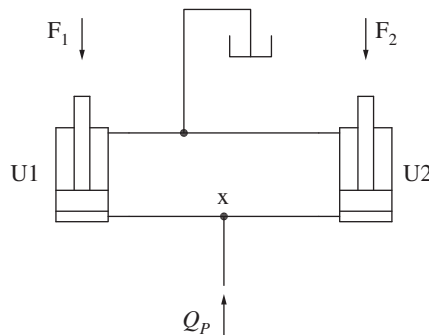
Figure 18.3　Analysis of the motion of two actuators in parallel.

Both Actuators Moving
This condition is achieved only if $F_1/A_1 = F_2/A_2$; the two cylinders generate the same pressure. In this case, the pressure at the junction X is well defined:

$$p_X = p_{U1} = \frac{F_{U1}}{A_1} = p_{U2} = \frac{F_{U2}}{A_2} \tag{18.4}$$

---

1 In hydraulic applications it is very common to encounter parallel multi-actuator systems where the pump is not sized for the worst-case scenario. In these cases, the phenomenon of flow saturation can occur when the actuator individual speeds cannot reach the desired values because the pump is over-demanded. This concept will be further discussed in the next chapters.
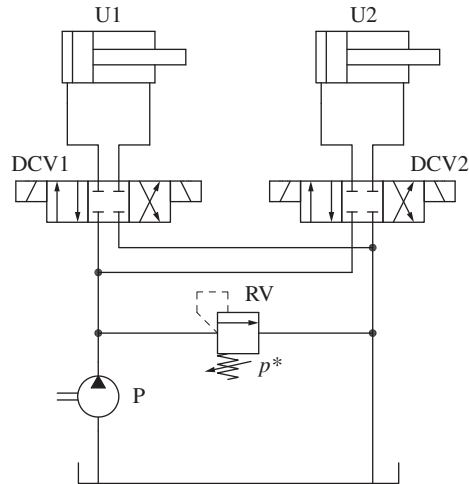
Figure 18.4 Circuit with two actuators in parallel and directional control valves.

The inlet flow can equally split between the two actuators U1 and U2, thus realizing a coordinated control of the two actuators. This situation, however, pertains to a very specific condition, which is very rarely met.

Only One Actuator Moves

In most of the cases $F_1/A_1 \neq F_2/A_2$ and Eq. (18.4) is no longer valid. This means that the pressure at the supply (node X of Figure 18.3) is now defined only by one load. The flow from the supply follows the most favorable path, toward the least loaded actuator. The pressure at node X is

$$p_X = \min\left(\frac{F_1}{A_1}, \frac{F_2}{A_2}\right) \tag{18.5}$$

Under the assumption that $F_1/A_1 > F_2/A_2$, the pressure at node X propagates to the most loaded actuator U1, without balancing the external load F_1. Since a load drop check valve is not used in the circuit, the actuator U1 retracts under the external force F_1. The returning flow from U1 merges with the supply flow and goes to U2. Therefore, although an extension of both actuators is desired, the circuit of Figure 18.3 realizes only the extension of one actuator, while the most loaded actuator retracts uncontrolled.

Once the extending actuator U2 reaches the end of stroke, it stops. The value of p_X increases until the value F_1/A_1 is reached. At this point, the actuator U1 finally starts extending supplied by the flow Q_P.

A more realistic schematic for a system with two actuators in parallel is given in Figure 18.4. Directional control valves are used to permit control of the actuators in both directions.

Example 18.2 – Fan motor in parallel with actuator

A hydraulic pump supplies a flow rate of 60 *l/min* to two actuators in parallel. The first is a motor driving a blower fan, while the second is a cylinder lifting a load. The blower fan induces a torque on the motor that is proportional to the square value of the rotational speed according to the following law: $T = n_M^2 \cdot 3.5 \cdot 10^{-5}$ *Nm*. The blower motor has a displacement of 25 *cm³/r*.

The cylinder has a bore diameter of 50 *mm* and its load is 4000 *kg*. Calculate the pump outlet pressure, the speed of the motor and the speed of the cylinder. How would the system work if the pump flow is decreased to 30 *l/min*?

Given:

- Pump flow, $Q_P = 60$ *l/min*
- Blower torque law, $T_1 = n_{M1}^2 \cdot 3.5 \cdot 10^{-5}$ *Nm*
- Blower motor displacement, $V_{M1} = 25$ *cm³/r*
- Cylinder bore, $d_B = 50$ *mm*
- Weight on cylinder, $M = 4000$ *kg*
- Reduced pump flow, $Q_P' = 30$ *l/min*

Find:

- Pump outlet pressure, p_P
- Blower speed, n_{M1}
- Cylinder extension speed, $\dot{x}_2$
- System operation under reduced pump flow

Solution:

With respect to the previous cases of actuators in parallel, here the load on the first actuator is not fixed but a function of the speed. In other words, the pressure in the system is set by the linear actuator and the flow to the rotary actuator is a consequence of this value. In other words, the pump pressure becomes

$$p_P = \frac{Mg}{A_2} = \frac{4000 \cdot 9.81 \, [N]}{\pi \cdot 50^2/4 \, [mm^2]} \cdot 10 = 200 \, bar$$

At this point, the speed of the blower fan can be easily calculated:

$$n_{M1} = \sqrt{\frac{V_{M1} \cdot p_P}{2\pi} \cdot \frac{1}{3.5 \cdot 10^{-5}}} = \sqrt{\frac{25 \, cm^3/r \cdot 200 \, [bar]}{20 \cdot \pi} \cdot \frac{1}{3.5 \cdot 10^{-5}}} = 1508 \, rpm$$

The corresponding flow to the motor is equal to

$$Q_{M1} = V_{M1} \cdot n_{M1} = \frac{25 \, [cm^3/r] \cdot 1508 \, [rpm]}{1000} = 37.7 \, l/min$$

The cylinder extension speed is

$$\dot{x}_2 = \frac{Q_P - Q_{M1}}{A_2} = \frac{60 - 37.7 \, [l/min]}{\pi \cdot 50^2/4 \, [mm^2]} \cdot \frac{10^6}{60} = 189 \, mm/s$$

If the flow of the pump is reduced to 30 *l/min*, one can immediately see that the pump flow is not enough to move both actuators at the same time because even if the full pump flow is going through the blower motor, the system pressure is not enough to overcome the weight on the cylinder. In fact, with a 30 *l/min* flow, the resulting blower speed is

$$n_{M1}' = \frac{30 \, [l/min]}{25 \, [cm^3/r]} \cdot 1000 = 1200 \, rpm$$

The torque generated by the blower on the hydraulic motor is

$$T_1' = n_{M1}'^2 \cdot 3.5 \cdot 10^{-5} = 50.4 \, Nm$$

> **Example 18.2 (Continued)**
>
> This corresponds to a system pressure of
>
> $$p_P' = \frac{2\pi \cdot T_1'}{V_{M1}} = \frac{20\pi \cdot 50.4\,[Nm]}{25\,[cm^3/r]} = 126.7\,bar$$
>
> In conclusion, if the pump flow is reduced to 30 *l/min*, the outlet pressure is 126.7 *bar*. This is not enough to move the cylinder; therefore, all the flow goes to the motor. When the pump flow is reduced, flow saturation occurs in the system. In this specific case, the flow saturation causes the actuator with the highest load to stop.

18.2 Elimination of Load Interference in Parallel Actuators

Section 18.1.2 discussed how the two circuits for actuators in parallel (Figures 18.3 and 18.4) cannot be controlled simultaneously if they are carrying different loads. The load distribution at the actuators is responsible for their velocity, depending on the type of loads. This phenomenon is generally referred to as **load interference**. Sometimes load interference is desired in the machine operation, while in other times it needs to be reduced or eliminated. In this section, the two main high-level concepts that can be used to achieve simultaneous control of actuators connected in parallel are presented: the use of compensators and the implementation of a volumetric coupling.

18.2.1 Solving Load Interference Using Compensators

The function of a compensator used to synchronize the speed of two actuators with different loads is shown in Figure 18.5.

> In parallel configurations, a restriction can be placed in the line supplying the actuator with the lower load to achieve synchronization. This restrictor behaves as a compensator.

Under the condition $F_1/A_1 > F_2/A_2$, as in Figure 18.3, the orifice O is placed at the side of the actuator with lighter load, to create an additional resistance for the flow directed toward U2 so the flow equally splits between U1 and U2. In other words, the orifice O compensates for the load imbalance between U1 and U2, so that the system establishes an equal split of the supply. Since the desired flow through the orifice O is known ($Q_p/2$), O behaves as a compensator. The area of the
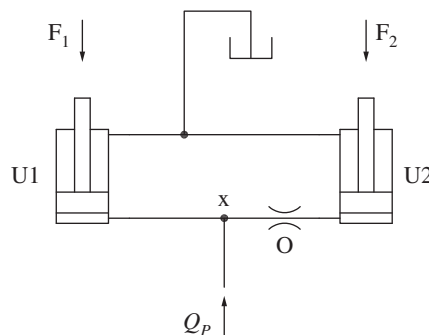

Figure 18.5 Use of a compensator for synchronizing the motion of two actuators in parallel.

orifice O can be derived from the orifice equation:

$$\frac{Q_p}{2} = 2 \cdot C_f \cdot \Omega_O \sqrt{\frac{2 \cdot \left(\frac{F_1}{A_1} - \frac{F_2}{A_2}\right)}{\rho}}$$

$$\xrightarrow{\text{yields}} \Omega_O = \frac{Q_p}{4 \cdot C_f} \sqrt{\frac{\rho}{2 \cdot \left(\frac{F_1}{A_1} - \frac{F_2}{A_2}\right)}} \tag{18.6}$$

The solution of Eq. (18.6) contains the values of the two loads F_1 and F_2; therefore, the orifice area is valid only for one load condition. In general, to achieve a continuous synchronization of the two actuators, the area Ω_O of orifice O should adapt to the changing load conditions and to the inlet flow rate.

In hydraulic systems based on metering control, compensation is achieved with the same principle described in Figure 18.5. However, the implementation of the compensator is specific to the system architecture. For example, in open center valves, the compensation is achieved by the design of the spool areas; however, in load sensing systems, pressure compensators automatically adjust the compensating orifice size depending on the loads.

Sometimes, the supply flow needs to be divided among two actuators with a predefined and constant ratio. This is the case for two wheels that need to be turning at the same speed even if on different grounds. In this case, the function of compensators can be realized through a *resistive flow divider*, which will be described later in this chapter.

18.2.2 Solving Load Interference with a Volumetric Coupling

The load interference between multiple actuators can be overcome also by utilizing a volumetric device, located between the pump and the actuators, which imposes a pre-determined flow split, regardless of the pressure imbalance.

The most intuitive schematic describing this solution is represented in Figure 18.6. In this schematic, the two actuators (U1 and U2) are connected to two double rod actuators (A1 and A2), which rigidly constrain the rods. For each double-rod actuator (A1 and A2), one chamber is connected to the flow supply, and the opposite chamber is connected to the actuator (bore chambers of U1 and U2). Therefore, A1 and A2 are supplied in parallel from the same supply, but the rods move together at the same velocity $\dot{x}_A$. Accordingly, the following equations can be written for the system in Figure 18.6:

$$\begin{cases} Q_{A1} = \dot{x}_A \cdot A_1 \\ Q_{A2} = \dot{x}_A \cdot A_2 \\ Q_{A1} + Q_{A2} = Q_p \end{cases} \tag{18.7}$$

Solving the previous system of equations, the flow delivered to each actuator becomes

$$\begin{cases} Q_{U1} = Q_{A1} = Q_p \cdot \dfrac{A_1}{A_1 + A_2} \\[2mm] Q_{U2} = Q_{A2} = Q_p \cdot \dfrac{A_2}{A_1 + A_2} \end{cases} \tag{18.8}$$

Equation (18.8) shows that the inlet flow rate split depends only on the geometric areas of the double rod actuators. The values of the loads, p_{U1} and p_{U2} do not influence the actual flow sent to the actuators.
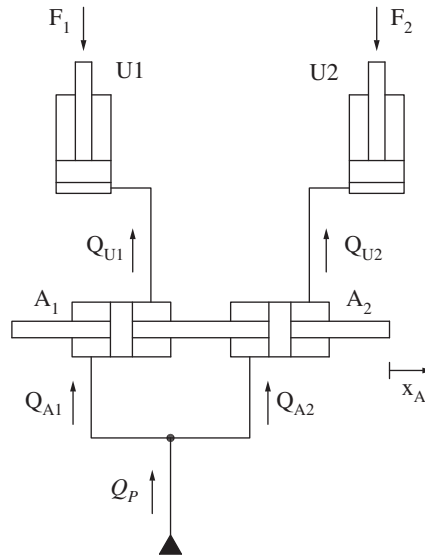
Figure 18.6 Volumetric coupling to achieve synchronism between actuators in parallel.

It is interesting to discuss on the value of the pressures at the different points of the system, particularly at the actuators and at the flow supply. The equilibrium of the double rod actuators leads to the following equations:

$$\begin{cases} p_p \cdot A_1 - p_{U1} \cdot A_1 & = F \\ p_p \cdot A_2 - p_{U2} \cdot A_2 & = -F \end{cases} \tag{18.9}$$

so that

$$p_p = \frac{p_{U1} \cdot A_1 + p_{U2} \cdot A_2}{A_1 + A_2} \tag{18.10}$$

Equation (18.10) shows how the supply pressure is the weighted average of the load pressures, with weights given by the areas of the double rod cylinders utilized for realizing the volumetric flow split. In other words, the supply pressure is lower than the highest actuator pressure. The pressure equilibrium of Eq. (18.9) also demonstrates that one double rod actuator (A_1, in case $p_{U1} > p_{U2}$) is "helped" by the other one (A_2), thus realizing a mechanical power exchange within the double rod actuators. This power exchange is internal to the system and transfers the excess of power at the U2 side $Q_{U2} \cdot (p_p - p_{U2})$ to the higher load side, compensating its power deficit $Q_{U1} \cdot (p_{U1} - p_p)$.

The above described solution represents one of the possible manners for achieving *volumetric coupling*. In general, the devices accomplishing this functionality are referred to as *volumetric flow dividers*. Flow dividers are encountered in different architectures, which are described in Section 18.3.

> Flow dividers achieve synchronization of actuators in parallel through the principle of volumetric coupling. The incoming flow is split into two paths according to the ratio of the volume of the internal chambers of the flow divider.

18.3 Synchronization of Parallel Actuators Through Flow Dividers

Flow dividers are simple hydraulic components that allow synchronization of parallel actuators by implementing the concepts illustrated in Sections 18.2.1 and 18.2.2. Their function can be realized through compensators or volumetric coupling.

18.3.1 Spool-type Flow Divider

> A spool type flow divider achieves synchronism between two actuators independent of the loads, using the basic concept of the pressure compensation.

Pressure compensation to achieve synchronism has been introduced with the conceptual schematic of Figure 18.5. The basic schematic of the spool-type flow divider can be represented in Figure 18.7a. which shows the simplified ISO schematic of the component (referred in the figure as FD) and the detailed representation. From the detail view, one can notice how the flow divider consists of two fixed orifices O1 and O2, and an infinite position 4/3 spool valve. The spool position is determined by the two pressures downstream of the two orifices. If the two loads are equal, $p_{U1} = p_{U2}$ and the spool stays in the neutral position allowing free flow through both paths. In cases where $p_{U1} > p_{U2}$, the spool shifts to the right, restricting the more favorable path to U2. The operation of the component in this case is explained by Figure 18.7b: the spool creates an additional restriction C2 to the paths toward U2, in series with O2. The additional orifice C2 achieves the condition of $p_{X2} = p_{U1} = p_{X1}$. In this situation, orifices O1 and O2 operate as metering devices under the same pressure drop $p_p - p_{U1}$. The orifice C2 behaves instead as a compensator.

The flow rate at the two actuators U1 and U2 is determined by the ratio between the two orifice areas Ω_1 and Ω_2:

$$\begin{cases} Q_{U1} = C_f \cdot \Omega_1 \sqrt{\dfrac{2 \cdot (p_p - p_{U1})}{\rho}} \\[4mm] Q_{U2} = C_f \cdot \Omega_2 \sqrt{\dfrac{2 \cdot (p_p - p_{U1})}{\rho}} \\[4mm] Q_{U1} + Q_{U2} = Q_p \end{cases} \qquad (18.11)$$
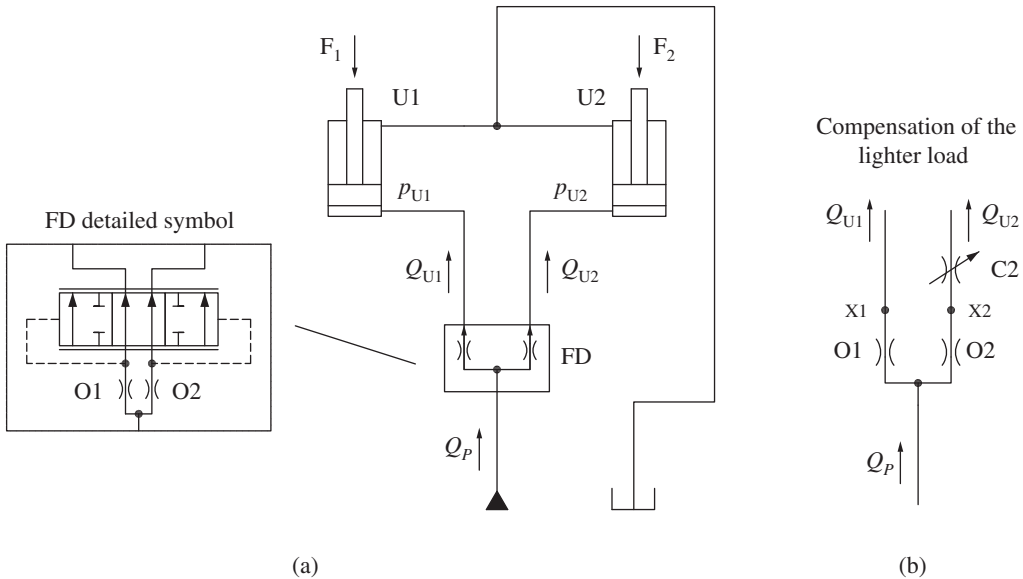

(a) (b)

Figure 18.7 Spool type flow divider: (a) simplified ISO symbol, detailed schematic, and operation in a simple circuit; (b) equivalent orifice representation when compensating the line of U2.
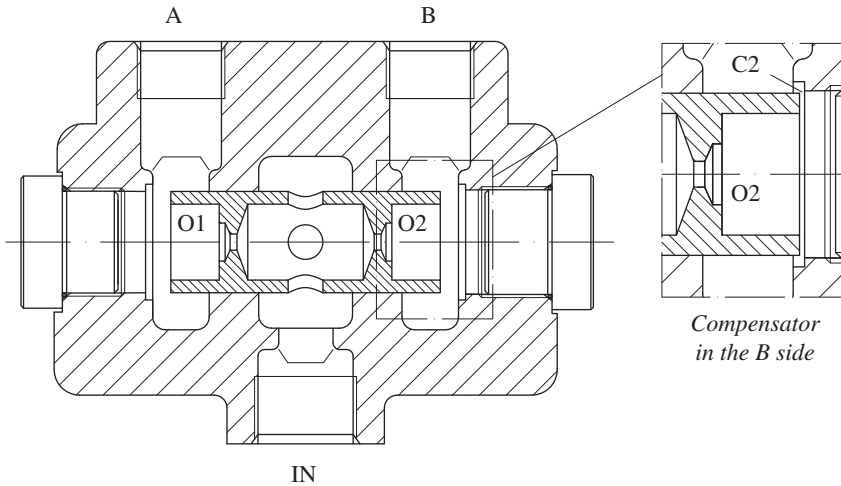
Figure 18.8 Cross-sectional view of a spool-type flow divider.

which yields to

$$
\begin{cases}
Q_{U1} = Q_p \cdot \dfrac{\Omega_1}{\Omega_1 + \Omega_2} \\[2mm]
Q_{U2} = Q_p \cdot \dfrac{\Omega_2}{\Omega_1 + \Omega_2}
\end{cases}
\tag{18.12}
$$

The last Eq. (18.12) shows how the split of the entering flow depends on the metering areas of the two fixed orifices, and it is not affected by the different loads on the actuator. Intuitively, equal orifice areas lead to a 50–50 flow split between the actuators.

Figure 18.8 shows a cross-sectional view of a spool type flow divider: the flow enters the inner cavity of the spool and splits between two fixed orifices: O1 at the left side and O2 at the right side. These two orifices are located between the inlet IN port and two chambers at each side of the spool. When the pressures at the spool ends are different, the spool moves and creates additional restrictions between the lateral chambers and the A and B ports. Figure 18.8 represents how the spool flow divider realizes the restriction C2, when the spool shifts in the right direction.

18.3.2 Spool-type Flow Divider/Combiner

The spool-type flow divider works only when the flow supply is connected to IN. The component does not have the ability of maintaining the actuator synchronization when the cylinders are retracting, and the direction of the flow is reversed. Many applications require synchronization between two actuators in both directions of motion.

In Figure 18.7, if the flow direction were reversed, the spool would keep restricting (variable orifice C2) until closing the side connected to the actuator with the lower load (U2). As a result, the actuator with the higher load would move freely, since its returning flow is not restricted by a variable orifice. The actuator with lower load would stay blocked until the other reaches the end of stroke.

Thus, the flow dividers in Figure 18.8 are rarely used in fluid power systems. However, the flow dividers that can operate in both directions are more common. Such elements are usually referred as *flow dividers/combiner*s. Figure 18.9 represents a typical circuit application.

Figure 18.10 shows the simplified ISO symbol of the components together with a detailed schematic, useful to understand its operating principle.
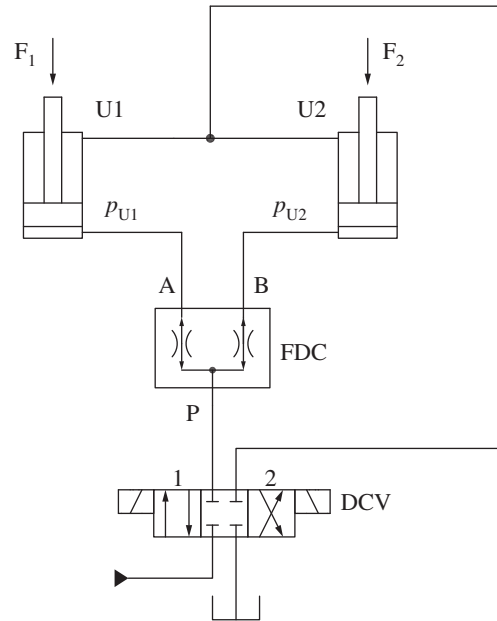
Figure 18.9 Application of a flow divider combiner (FDC) to control the extension and retraction of two cylinders.

The flow divider/combiner has two separate modes of operations, depending on the direction of the flow. The component uses two spools (V1 and V2): one operating between ports P and the port A and the other between P and B. The two spools mechanically interact with each other using three springs and two "L-shaped" connecting rods.

When the flow is supplied to port P (cylinder extension, in Figure 18.9), the valve operates in the flow divider mode, as shown in Figure 18.11. The pressure p_P at the inlet port P is higher than both p_{X1} and p_{X2}; therefore, the spools V1 and V2 are rigidly maintained at the maximum distance allowed by the mechanical link. V1 and V2 operate as a single spool, whose configuration is the same as the one described for the simple flow divider (Figure 18.7).

On the contrary, when the DCV in Figure 18.9 is shifted in position 2 (retraction), the flow returns from the actuators, entering the valve at the work-ports A and B and exiting at P. The valve works as a flow combiner, as shown in Figure 18.12. In this case, the pressures p_{X1} and p_{X2} are higher than p_P. Spools V1 and V2 are locked at their minimum relative distance allowed. The two spools V1 and

Figure 18.10 Spool type flow divider/combiner: detailed and simplified ISO schematic.
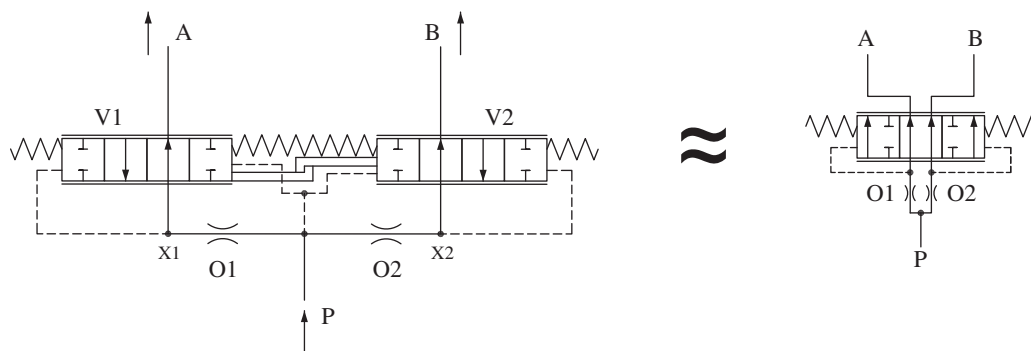
Figure 18.11 Flow divider/combiner: operation as a flow divider.

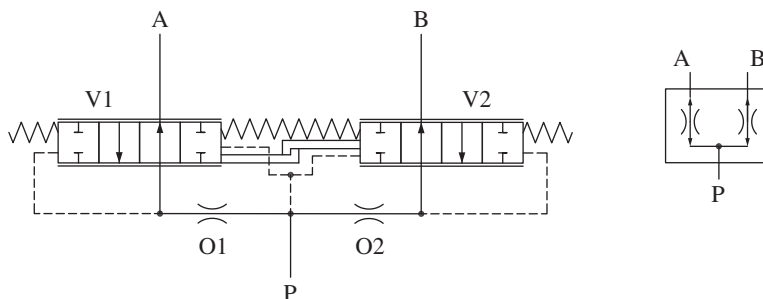V2 also in this condition are rigidly connected and work as a single spool, whose configuration is represented in Figure 18.12.

The cross-sectional view of a cartridge style flow divider/combiner is represented in Figure 18.13. The fixed orifices O1 and O2 are obtained by two pairs of small holes machined in each spool. The chambers X1 and X2 inside the spools are connected to the work-ports A and B through variable orifices whose areas are defined by the relative position of the lands machined in each spool and by radial holes machines in the valve sleeve. Depending on the operating mode, these compensator areas behave differently with respect to pressure changes. In the flow divider mode, a reduction of the pressure p_{X1} (or p_{X2}) tends to reduce the variable orifice area to the work-port A (or B); vice versa, in flow combiner mode, the same reduction of the variable orifice area is caused by an increase of the pressure p_{X1} (or p_{X2}).
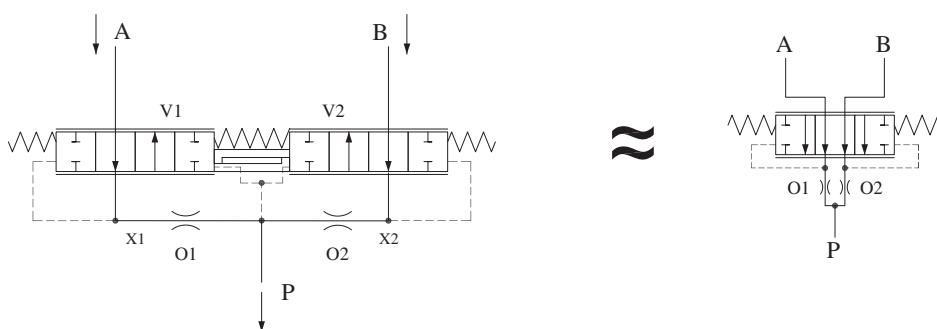
Figure 18.12 Flow divider/combiner: operation as a flow combiner.

18.3.3 Volumetric Flow Divider/Combiner

A volumetric flow divider/combiner implements the same *flow coupling* principle on the double rod cylinders. This architecture also maintains a precise flow split between different actuators, independently of the individual loads.

A volumetric flow divider/combiner achieves the synchronism by means of a flow coupling principle. Volumetric flow dividers usually achieve a more accurate split with respect to spool type flow dividers/combiners.
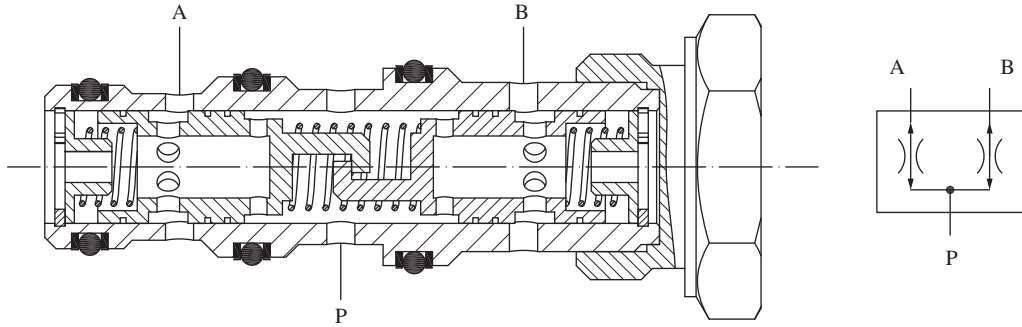
Figure 18.13 Cross-sectional view of a spool type flow divider-combiner

The use of **linear flow dividers/combiners** (dual road actuators), as in Figure 18.6, is limited to very few industrial applications, where high accuracy in the flow division is required. In fact, the tight manufacturing tolerance achievable in hydraulic cylinders allow very low leakages between chambers. Linear flow dividers achieve a level of precision much higher than spool or rotary designs. However, the limitation of these component is that the flow division is not continuous but is limited by the displaced volume of the linear actuator.

Figure 18.14 shows a linear flow divider architecture, similar to the conceptual schematic of the previous Figure 18.6. An important remark about the volumetric flow divider in Figure 18.6, or Figure 18.14, is that they work equally for both cases of flow split, and flow merge. This can be seen from Eq. (18.8), which describes the operation of the device: no assumption was made on the flow direction through the element. Therefore, volumetric flow dividers can also operate as flow combiners.
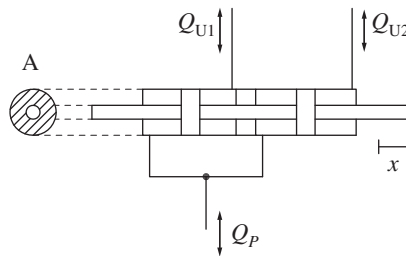
Figure 18.14 Volumetric flow divider/combiner using intermediate dual rod cylinders.

**Rotary flow dividers/combiners** represent the most common type of volumetric flow dividers. These units implement the same basic principle of the unit in Figure 18.6, but using rotary actuators to displace fluid, instead of double rod linear actuators. The ISO schematic of a two-way flow divider/combiner with rotary actuators is shown in Figure 18.15. Since the shafts of the pump/motor units are rigidly connected, they both rotate at the same speed n. Therefore, the flow at each port are

$$\begin{cases} Q_{U1} = Q_P \cdot \dfrac{V_{D1}}{V_{D1} + V_{D2}} \\ Q_{U2} = Q_P \cdot \dfrac{V_{D2}}{V_{D1} + V_{D2}} \end{cases} \tag{18.13}$$

Equation (18.13) is very similar to Eq. (18.8): the geometric displacement of the rotary actuators is used instead of the cylinder areas. The energy flow between the two rotary actuators is the same
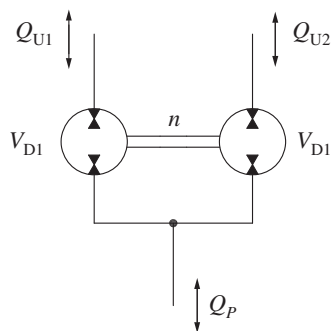
Figure 18.15 Two-way rotary flow divider/combiner.

as was previously described for the case of the dual-rod actuators: one unit works as hydraulic motor (connected to lower load) and provide power to the other unit working as pump (higher load). Thus, when the flow enters from P, the pressure at the inlet port reaches an intermediate value between the two ports U1 and U2, following a relation similar to Eq. (18.10):

$$p_P = \frac{p_{U1} \cdot V_{D1} + p_{U2} \cdot V_{D2}}{V_{D1} + V_{D2}} \tag{18.14}$$

Ideally, any positive displacement machine design could be used to realize rotary flow dividers/combiners. However, the most successful design architecture is based on external gear units. This design allows compact packaging where multiple ratios of flow split can be easily combined. In fact, different displacements can be realized by just changing the gear width, without changing the radial dimensions of the unit. For example, it is easy to stack multiple sections, realizing compact solutions for splitting/merging flow rates to/from a high number of actuators. Figure 18.16 represents an example of four-way rotary flow divider.
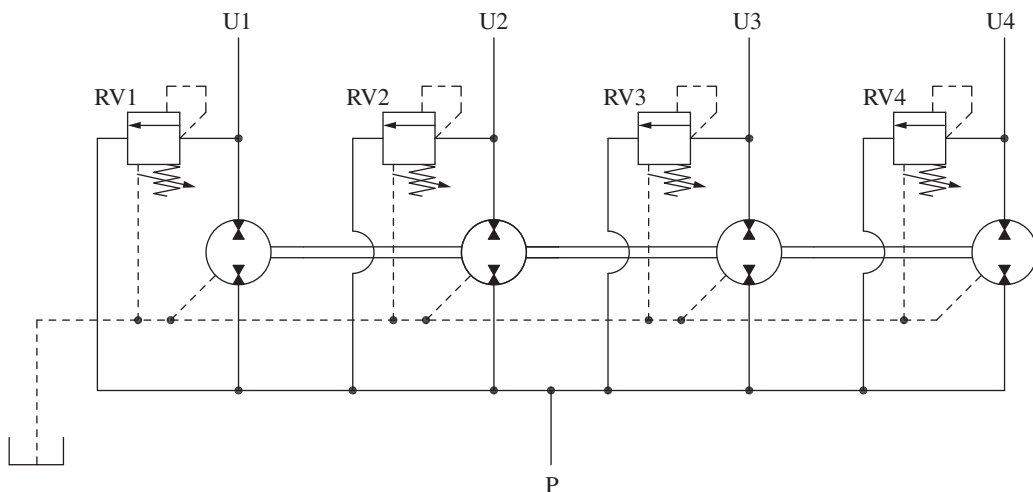
Figure 18.16 Example of four-way rotary flow divider/combiner. Each line is also equipped with relief valves. Note that the spring chamber of each relief is vented to the case drain of the unit.

Example 18.3 – Flow dividers

Two equal actuators (U1 and U2) are supplied in parallel from a single flow supply ranging from 0 to 40 *l/min*. The actuators should move with a 70–30 speed ratio, where 70% of the flow should go to U1 and 30% to U2.

In the first case, a spool type flow divider is used, like the one in Figure 18.8. Calculate the size of the two orifices, assuming a maximum pressure drop of 20 *bar*.

In the second case, a gear type flow divider is used, and it is sized to work at a maximum speed of 2800 *rpm*. Calculate the displacements of the gear units.

In the assumption that the load on U1 generates a pressure of 85 *bar*, while U2 requires 135 *bar*, calculate the operating conditions of the two flow dividers when the actuator moves at maximum speed. Considering all units as ideal, what is the useful power versus the input power in the two cases? Assume orifice coefficients equal to 0.7 and oil density of 850 *kg/m³*

Given:

- Max pump flow, $Q_{P,\,max} = 40$ *l/min*
- Flow split, 70–30
- Spool flow divider max pressure drop, $\Delta p_{max} = 20$ *bar*
- Gear flow divider max speed, $n_{max} = 2800$ *rpm*
- U1 pressure, $p_{U1} = 85$ *bar*
- U2 pressure, $p_{U2} = 135$ *bar*
- Orifice coefficient, $C_f = 0.7$
- Oil density, $\rho = 850$ *kg/m³*

Find:

- Diameters of O1 and O2 in spool flow divider (d_{O1}, d_{O2})
- Displacements of gear flow divider (V_{D1}, V_{D2})
- Pump pressure for the working condition
- Useful vs. input power for the working condition

Solution:
The orifice diameters of the spool flow divider can be calculated using Eqs. (18.11) and (18.12):

$$
\begin{cases}
Q_{U1} = Q_p \cdot \dfrac{\Omega_1}{\Omega_1 + \Omega_2} \\[2mm]
Q_{U1} = C_f \cdot \Omega_1 \sqrt{\dfrac{2 \cdot (p_p - p_{U1})}{\rho}}
\end{cases}
$$

In the given case, $Q_{P,\,max} = 40$ *l/min* and $Q_{U1,\,max} = 28$ *l/min* (70%). Under this condition, $p_p - p_{U1} = \Delta p_{max} = 20$ bar. Therefore,

$$
\Omega_1 = \frac{Q_{U1}}{2 \cdot C_f \sqrt{\dfrac{2 \cdot \Delta p_{max}}{\rho}}} = \frac{28\,[l/min]/60\,000}{0.7 \cdot \sqrt{\dfrac{40\,[bar] * 100\,000}{850\,\,[kg/m]}}} \cdot 10^6 = 9.7\ mm^2
$$

(Continued)

Example 18.3 (Continued)

This corresponds to a $d_{O1} = 3.5\ mm$ orifice. The second orifice area results equal to

$$\Omega_2 = \frac{(Q_p - Q_{U1})}{Q_{U1}} \cdot \Omega_1 = \frac{Q_{U2}}{Q_{U1}} \cdot \Omega_1 = \frac{12\ [l/min]}{28\ [l/min]} \cdot 9.7\ [mm^2] = 4.15\ mm^2$$

This corresponds to a $d_{O2} = 2.3\ mm$ orifice.

In the case of rotary flow dividers, the maximum operating speed of the unit is known. Therefore, the displacement of the first gear unit is

$$V_{D1} = \frac{Q_{U1}}{n_{max}} = \frac{28\ [l/min]}{2800\ [rpm]} \cdot 1000 = 10\ cm^3/r$$

The displacement of the second unit results:

$$V_{D2} = \frac{Q_{U2}}{Q_{U1}} \cdot V_{D1} = \frac{12\ [l/min]}{28\ [l/min]} \cdot 10\ [cm^3/r] = 4.3\ cm^3/r$$

When the flow dividers are operating under the given conditions, this results in the following.

Spool flow divider

The spool of the divider is open toward U2 and restricts the flow going to U1, which is the lowest load. Under the assumption of $\Delta p_{max} = 20$ bar the pump pressure results equal to 155 *bar*. The useful and input power are

$$\begin{cases} P_U = 28\ [l/min] \cdot 85\ [bar] + 12\ [l/min] \cdot 135\ [bar]) \cdot (1/600) = 6.6\ kW \\ P_{IN} = 40\ [l/min] \cdot 155\ [bar]) \cdot (1/600) = 10.3\ kW \end{cases}$$

One can notice that the efficiency of this simple circuit is already 64% because of the orifice pressure drop and the compensating losses introduced by the flow divider.

Rotary flow divider

In this case, the supply pressure can be calculated using Eq. (18.14):

$$p_P = \frac{p_{U1} \cdot V_{D1} + p_{U2} \cdot V_{D2}}{V_{D1} + V_{D2}} = \frac{85\ [bar] \cdot 10\ [cm^3/r] + 135\ [bar] \cdot 4.3\ [cm^3/r]}{10\ [cm^3/r] + 4.3\ [cm^3/r]} = 100\ bar$$

The useful power is the same as in the previous case P_U= 6.6 kW, while the input power is

$$P_{IN} = 40\ [l/min] \cdot 100\ [bar] \frac{1}{600} = 6.6\ kW$$

The reader can immediately observe that the system using a rotary flow divider has a 100% efficiency, much higher than the previous case.

Problems

18.1   A hydraulic system with two cylinders connected in a series is shown in figure. Following data are available:

Piston areas for the cylinder 1 (left) $A_{11} = 20\,cm^2$, $A_{12} = 15\,cm^2$

Piston areas for the cylinder 2 (right) $A_{21} = 14\,cm^2$, $A_{22} = 10\,cm^2$

Length of stroke is $s = 50\,cm$ for both cylinders

Forces acting on cylinders: $F_1 = F_2 = 15\,kN$

Pump displacement $= 15\,cm^3/rev$

Pump rotation speed $n = 2800\,rpm$

Pump volumetric efficiency 0.85

Assume both pistons at the bottom end position. Assume no volumetric losses except for the volumetric pump losses. Ignore pressure losses in the DCV.

Calculate the difference between the pistons position when one of the pistons reaches its end position. Assume a lifting condition for both cylinders (valve in parallel arrows position), when they start from the bottom end stop position.
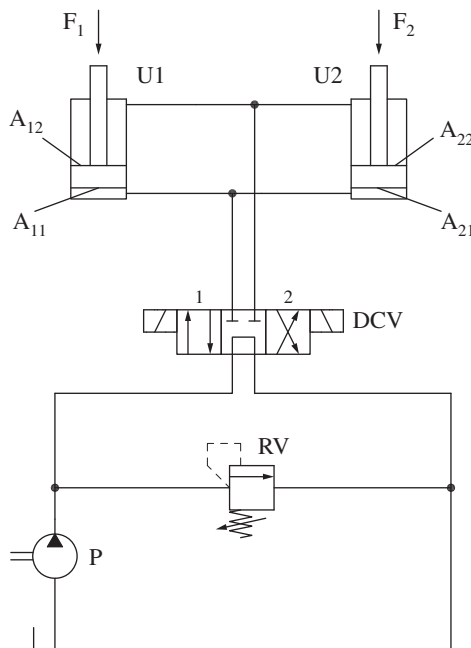
18.2   Two hydraulic motors are used to run two different conveyor belts to extract rocks from a rock crusher. The first conveyor motor (M1) rotates at 1500 rpm, while the second (M2) at 1800 rpm. The torque is 170 ft lbs on the first conveyor, while 80 ft lbs on the second. The supply pump is capable of 3500 psi continuous pressure, with a relief valve set at 3800 psi. Select what type of layout is suitable for this type of system and size the pumps and motors. When defining the layout, it is critical that, in case of overloading, the M1 maintained its speed (at the expense of M1) in order to avoid jamming of the material between the conveyors. Assume ideal units.

18.3 The circuit represented below presents two motors, M1 and M2, connected through a 3/2 solenoid valve (SV). Describe the functionality of SV. Each motor has a displacement of 150 cm^3/r, the torque on each motor is 200 Nm and the pump supply flow is 200 l/min. Determine the speed of each motor and the pump pressure in two cases: SV in neutral, SV energized.
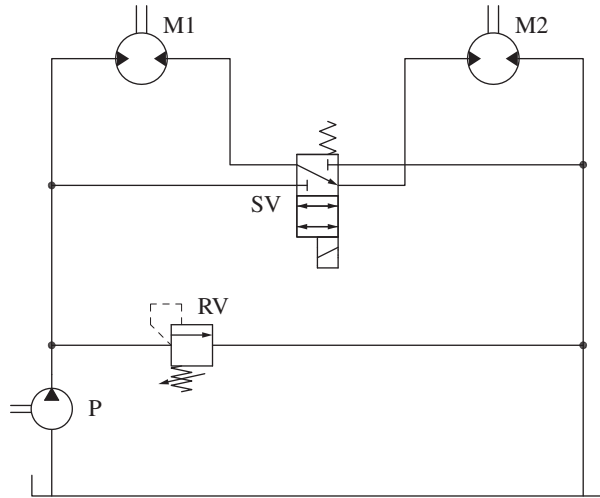
18.4 Two motors, M1 and M2, are supplied in parallel by a common pump, P. The shafts of M1 and M2 are driving a winch from each end, as if they are rigidly connected. The torque generated by the winch is 800 Nm. M1 and M2 have the same displacement of 100 cm^3/r but they have different efficiencies. In particular, $\eta_{v1} = 0.92$ and $\eta_{T1} = 0.85$ while $\eta_{v2} = 0.89$ and $\eta_{T2} = 0.83$. The pump is supplying 20 l/min. Calculate the speed and torque generated by each motor.
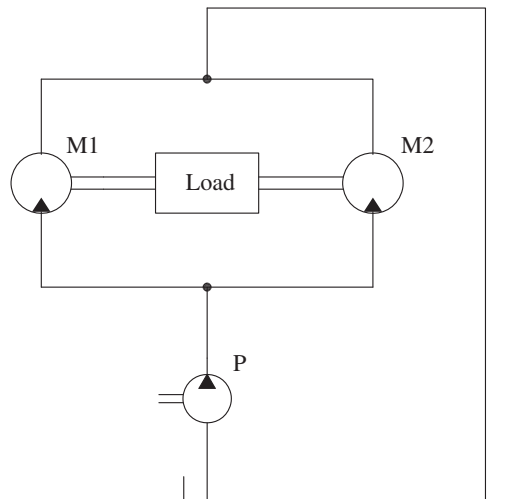
18.5 Repeat the previous problem under the assumption that now the two motors M1 and M2 are supplied through a flow divider, which allows the motors to rotate at the same speed and introduces a pressure drop of 5 bar. Which one of the two solution is the best one? Why?
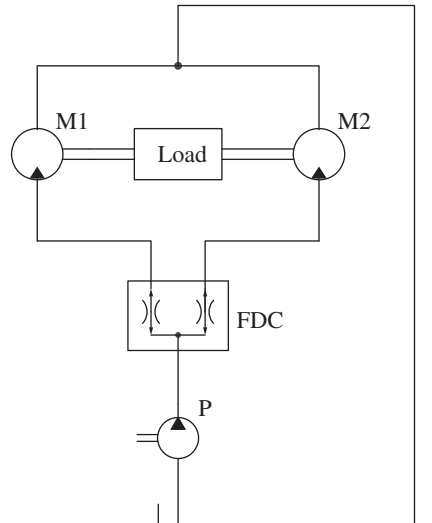
18.6 The hydraulic circuit represented below uses a rotary flow divider to synchronize the motion of two linear actuators. Each cylinder has a bore diameter of 50 mm, but the two loads are different: $F_1 = 17\,000$ lbs and $F_2 = 4000$ lbs. The pump provides 30 gpm, the relief valve RV is set 3500 psi and the two gear units of the flow divider have a displacement of 45 cm^3/r. Calculate the operating condition of the system: pressures and flows at the three ports of the flow divider, and speed of actuators and flow divider. What comments can be made regarding the system operation? How can the issues be improved?
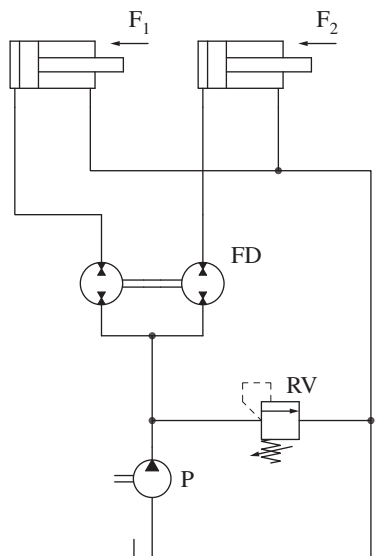
18.7 For the system represented below, which controls the speed of the two single acting cylinders connected in parallel,
  (a) indicate the missing element (necessary to regulate the flow when the cylinders extend)
  (b) determine the diameter of the orifice necessary to obtain a flow equal to 5 gpm through the flow regulating valve. (Assume a oil density of 53 lb/ft³, mineral oil)
  (c) if a relief valve with a pressure of 3500 psi is used to limit the maximum pressure at pump outlet, which is the pressure at pump outlet during the lifting phase?
  (d) Are the two cylinders lifting together? If not, which one moves first?
  (e) What is the pressure at point G during the lifting of the two cylinders?
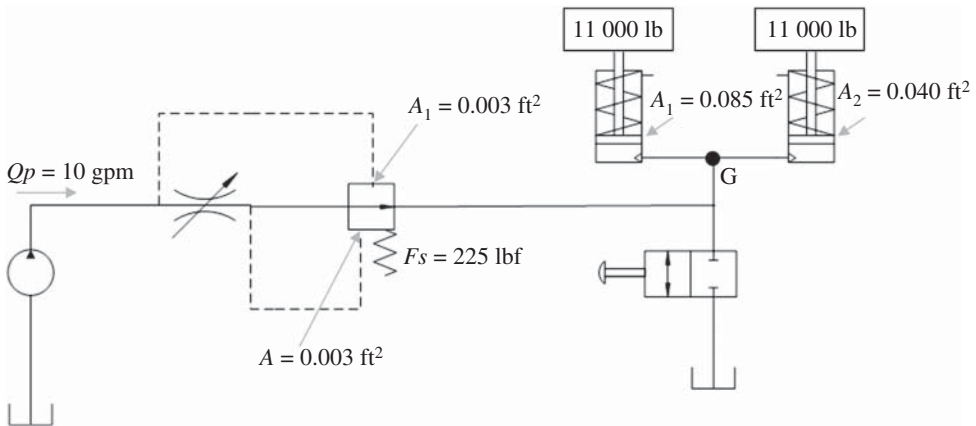
Chapter 19

Constant Pressure Systems for Multiple Actuators

Constant pressure systems represent the simplest metering concept for controlling multiple actuators. A single constant pressure supply provides flow to several actuators in parallel. The flow to each actuator is controlled simply using a proportional throttling device, such as a spool valve. Compensators are not necessary to address the load interference. In fact, the flow to each actuator depends only on its load and the opening of the metering device. This flow is not affected by the configuration of the other actuators. The system layout is very straightforward; however, the system efficiency is not always high because of the high pressure drops that can be established at the metering elements. After showing how the basic control concept of a constant pressure system can be extended to multiple actuators, this chapter illustrates the advantages and functional limitations of this control solution.

19.1 Basic Concepts for a Multi-Actuator Constant Pressure System

19.1.1 Basic Schematic

Figure 19.1 illustrates the simplified schematic of a constant pressure circuit serving two actuators, U1 and U2. In this case, the system is supplied with a variable displacement pump, equipped with an absolute pressure limiter set to p^*. The two cylinders are supplied by two generic metering elements. The orifice equation applied to each metering element gives the flow to each actuator:

$$Q_{U1} = C_f \Omega_{U1} \left(i_1 \right) \sqrt{\frac{2 \left(p^* - p_{U1} \right)}{\rho}}$$

$$Q_{U2} = C_f \Omega_{U2} \left(i_2 \right) \sqrt{\frac{2 \left(p^* - p_{U2} \right)}{\rho}}$$

(19.1)

Equation (19.1) shows that the flow to each actuator is a function of the throttle area Ω_U and the actuator pressure p_U, as it was demonstrated in Chapter 17 for the case of a single actuator.

> In the basic constant pressure system, the flow to each actuator is a function of the area of the corresponding control orifice. This flow is also affected by the actuator pressure. For a multi-actuator system, the governing equation for the flow to each actuator is the same as for the case of a constant pressure system with a single user, as long as flow saturation does not occur.
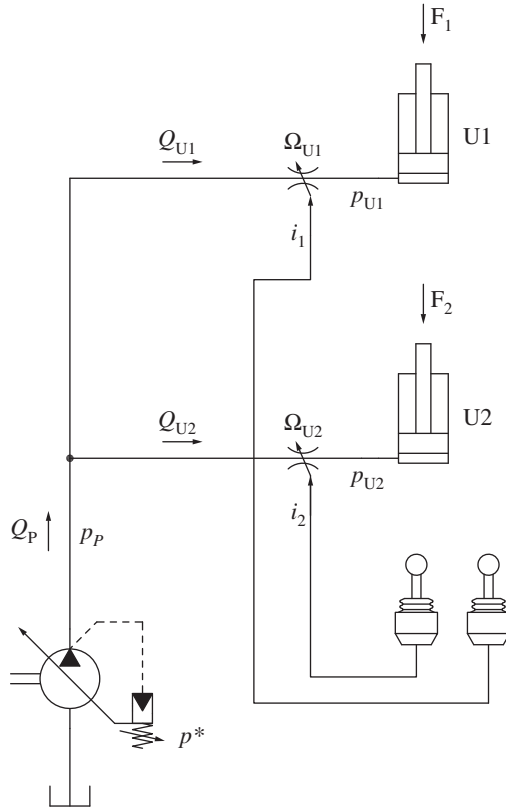
Figure 19.1 Simplified circuit of a constant pressure system with multiple actuators.

This is valid until flow saturation occurs. Flow saturation occurs when the overall flow requested by the actuators exceed the pump flow. When saturation occurs, the pump is no longer able to maintain an outlet pressure equal to p^*, as will be discussed below. Eq. (19.1) is written for two actuators but it can be extended to a larger number.

When the system is running, the flow instantaneously provided by the pump equals the sum of the two actuators flow:

$$Q_P = Q_{U1} + Q_{U2} = C_f \left(\Omega_{U1} \sqrt{(p^* - p_{U1})} + \Omega_{U2} \sqrt{(p^* - p_{U2})} \right) \sqrt{\frac{2}{\rho}} \qquad (19.2)$$

19.1.2 Flow Saturation

The system is free from load interference until flow saturation occurs. In this situation, the sum of the actuator theoretical flows (Eq. (19.1)) becomes higher than the pump maximum flow. This situation occurs if

$$\Omega_{U1} \sqrt{(p^* - p_{U1})} + \Omega_{U2} \sqrt{(p^* - p_{U2})} \geq \frac{Q_{P,\max}}{C_f} \sqrt{\frac{\rho}{2}} \qquad (19.3)$$

Equation (19.3) shows that saturation can be caused either by excessive opening of the throttling areas, Ω_U, by a decay of the load pressures, p_U, by a reduction of the available flow, $Q_{P,\max}$, or by a combination of all these factors. In the case of flow saturation conditions, the pump operates at its maximum displacement, while its outlet pressure p_p is lower than p^*. The value of the pump

pressure p_p can be calculated solving the following implicit equation:

$$\Omega_{U1}\sqrt{(p_p - p_{U1})} + \Omega_{U2}\sqrt{(p_p - p_{U2})} = \frac{Q_{P,\max}}{C_f}\sqrt{\frac{\rho}{2}} \tag{19.4}$$

> During flow saturation, the constant pressure system cannot keep anymore a constant pressure supply, therefore enabling load interference.

All functions slow down with respect to the theoretical flow value, the actuator with the highest load being the most penalized. This concept is also illustrated in Figure 19.2, which highlights the flow reductions for two actuators U1 and U2 at a known pressure ($p_{U1} > p_{U2}$), undergoing a reduction of the supply pressure from p^* to p_{sat}. Simply, the plot in Figure 19.2 assumes constant values for Ω_{U1} and Ω_{U2}. Therefore, in this case, the flow saturation can be caused by a reduction of the pump shaft speed and not by an increased request at U1 or U2.
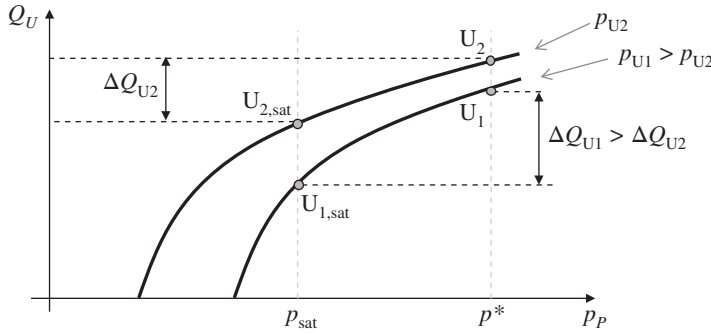
Figure 19.2 Flow rate reduction of a multi-actuator constant pressure system under flow saturation.

19.1.3 Energy Analysis

The energy plot reported in Figure 19.3 analyzes the constant pressure system during regular operation (no flow saturation). It is possible to observe how the power loss at the metering orifices can become significant, especially if the functions demand high flow and work at low pressure. In Figure 19.3, the power loss can easily be higher than the useful power.
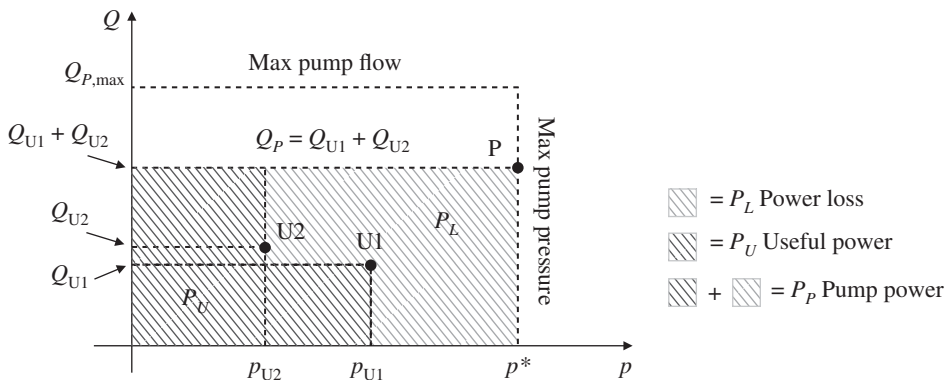
Figure 19.3 Energy plot for a constant pressure system with two actuators.

19.2 Complete Schematic for a Multi-Actuator Constant Pressure System

Figure 19.4 shows a detailed schematic of a constant pressure system for multiple actuators. To simplify, the figure includes only two actuators, which are controlled by two 4/3 proportional directional control valves (DCVs). The check valves prevent the loads from dropping, in case the actuator pressure exceeds the value provided by the supply. In the schematic, the maximum pressure at both work-ports A and B of the actuator U2 is limited by two relief valves.

Constant pressure systems have a very simple layout and provide a very accurate control of the actuator because the load interference does not affect the regulation, at least during regular operation, when no flow saturation occurs. Additionally, constant pressure systems provide a very quick response, as each valve is always supplied at the maximum system pressure. In other words, the pump does not have to raise its pressure level, as in load sensing systems, once the DCV is actuated. This feature is very useful for distributed systems where the valves and the control elements can be very far from the supply pump. This is, for example, the case of a ship or a large industrial plant where many functions in very large applications are usually served from a single constant pressure source.
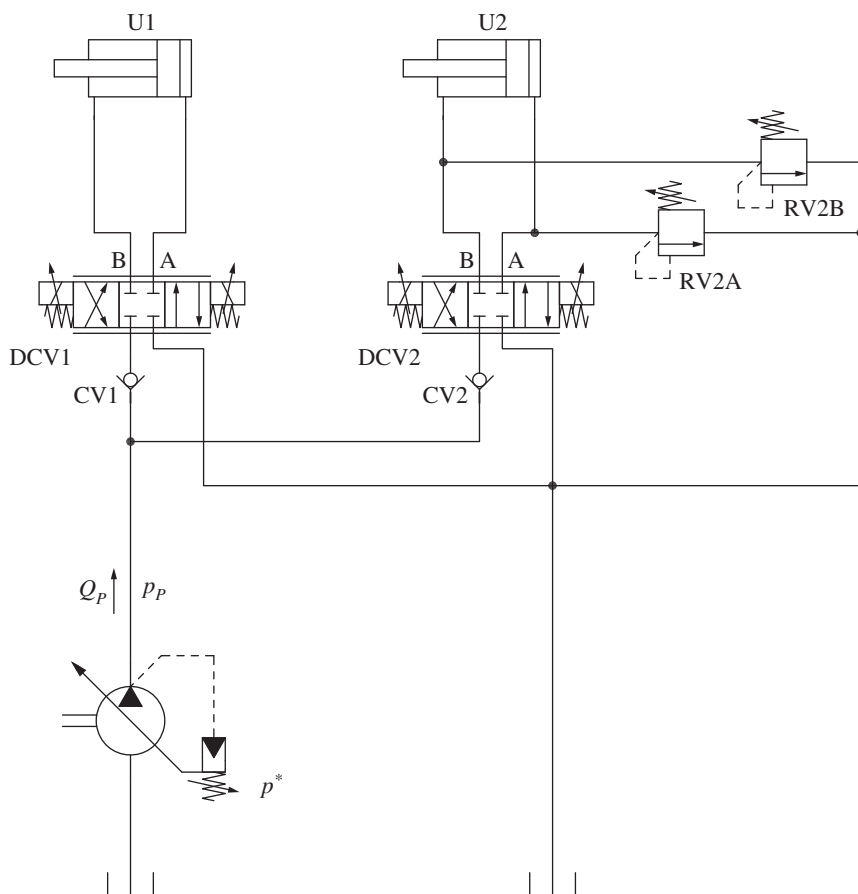
Figure 19.4 Complete schematic of a constant pressure system.

On the other hand, this type of layout can be characterized by poor efficiency, especially if the actuators are used in conditions of high flow demands under low loads. This can be a concern for high productivity mobile equipment, such as wheel loaders or forestry cranes. Therefore, constant pressure systems are seldom used in equipment with intensive duty cycles. However, constant pressure systems, in their constant pressure unloaded (CPU) variant, as described in Chapter 17, is a valid option for mobile equipment that have seldom operation, such as aerial lifts or material handling cranes.

Example 19.1   Constant pressure system

A constant pressure circuit as in Figure 19.4 is used to control a cylinder lift function and a rotary conveyor. The pump has a flow capacity of 35 *gpm* and its pressure compensator setting is 3000 *psi*. The load on the lift cylinder generates a pressure equal to 2600 *psi*, while to conveyor needs 1200 *psi* to rotate. Calculate the opening area of the two spools to provide 15 *gpm* to the conveyor and 8 *gpm* to the lift. Calculate the system efficiency in this case. What happens to the system if the flow area to the conveyor doubles its value? What happens to the system if then the lift cylinder reaches end of stroke? Assume an oil density of 53 *lb/ft*^{3} and orifice flow coefficients of 0.65.

Given:

- Max pump flow, $Q_{P,\max} = 35 \, gpm$
- Pump compensator pressure, $p^* = 3000 \, psi$
- Lift actuator pressure, $p_{U1} = 2600 \, psi$
- Lift actuator flow, $Q_{U1} = 8 \, gpm$
- Conveyor motor pressure, $p_{U2} = 1200 \, psi$
- Conveyor motor flow, $Q_{U2} = 15 \, gpm$
- Orifice coefficient, $C_f = 0.65$
- Oil density, $\rho = 53 \, lb/ft^3$

Find:

- Valve areas Ω_{U1} and Ω_{U2}
- System efficiency
- System behavior if $\Omega'_{U2} = 2 \cdot \Omega_{U2}$
- System behavior if lift reaches the end of stroke

Solution:
The orifice diameters of the spools can be calculated using Eq. (19.1) with the proper unit conversion factor (as indicated in Chapter 4):

$$\Omega_{U1} = \frac{Q_{U1}}{C_f\sqrt{\frac{2(p^*-p_{U1})}{\rho}}} = \frac{8 \, [gpm]}{0.65 \cdot \sqrt{\frac{2 \cdot (3000 - 2600) \, [psi]}{53 \, [lb/ft^3]}}} \cdot \frac{1}{211.9} = 0.015 \, in^2$$

In the same way, one can calculate that $\Omega_{U2} = 0.013 \, in^2$. Even if the conveyor requires more flow, the area Ω_{U2} is smaller than Ω_{U1} because of the high pressure drop at which the conveyor spool is working.

(Continued)

Example 19.1 (Continued)

The system efficiency is calculated as follows:

$$\eta_S = \frac{Q_{U1} \cdot p_{U1} + Q_{U2} \cdot p_{U2}}{(Q_{U1} + Q_{U2}) \cdot p^*} = 56\%$$

As mentioned before, the efficiency of the constant pressure systems is generally not very high due to the high pressure drops that can be involved in the metering. The value of 56% is based on ideal units and, in reality, it is even lower.

If the conveyor spool doubles its metering area to $\Omega'_{U2} = 2 \cdot \Omega_{U2}$, the theoretical flow required by the actuator becomes

$$Q'_{U2,th} = C_f \Omega'_{U2} \sqrt{\frac{2\left(p^* - p_{U2}\right)}{\rho}} = 0.65 \cdot 0.026 \,[in^2] \sqrt{\frac{2 \cdot (3000 - 1200) \,\left[psi\right]}{53 \,\left[lb/ft^3\right]}} \cdot 211.9$$

$$= 29.5 \, gpm$$

Under this condition, the theoretical demanded flow becomes $Q'_{U2,th} + Q_{U1} = 37.5 \, gpm$, greater than the available pump flow, $Q_{P,max}$. The system reaches flow saturation and it can be described by Eq. (19.4). Using a numerical solver, one can easily find that the pump pressure lowers to $p'_P = 2869 \, psi$. Applying the orifice equation, the two actuator flows become $Q'_{U1} = 6.6 \, gpm$ and $Q'_{U1} = 28.4 \, gpm$. Their sum equals the total pump flow.

When the lift actuator reaches the end of stroke, the system returns to working in the constant pressure mode with a flow demand of 29.5 gpm from the conveyor motor.

Problems

19.1 A constant pressure circuit as in Figure 19.4 is used to control two motors. The first motor has a displacement of 60 cm³/r and runs an underwater propeller. The torque at the propeller shaft varies linearly with the speed and equals 150 Nm when the motor runs at 1800 rpm. The second motor instead runs a winch and requires 50 l/min at 45 bar. The pump has a capacity of 150 l/min and its pressure compensator setting is 180 bar. Calculate the maximum metering area of the winch spool that allows the propeller to run at full power. Calculate the system efficiency in such condition. If both spools are fully open with a maximum area of 20 mm², what is the operating condition of the circuit (pump flow and pressure, function flows)? Assume an oil density of 850 kg/m³ and orifice flow coefficients of 0.65.

19.2 In the circuit represented below, the pump P (100 cm³/r, rotating at 1800 rpm) maintains a maximum pressure of 3000 psi. The two orifices O1 and O2 are used to control the flow to M1 and M2. In particular, M1 has a load of 900 psi, while M2 of 1800 psi. O2 has a diameter d_2 of 2.5 mm. Calculate:
- The value d_1^*, diameter of O1, which allows the maximum speed of M1 while maintaining 3000 psi at the pump outlet.
- How the value d_1^* changes as a function of p_2, i.e. the inlet pressure of motor M2. Represent the qualitative trend of $d_1^*\left(p_2\right)$ in a chart.
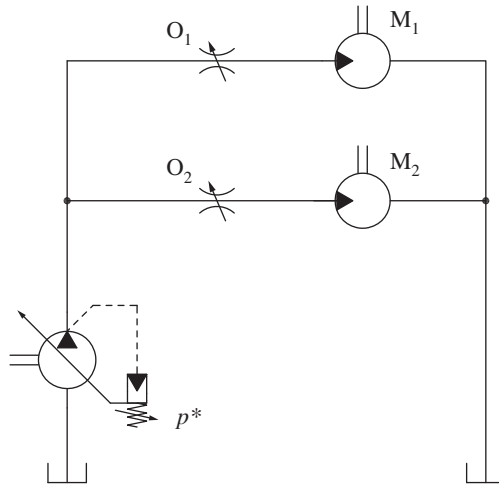
19.3 In the circuit represented below, the pump P (50 cm^3/r, rotating at 2000 rpm) maintains a maximum pressure of 4000 psi. At the outlet of the pump, an accumulator (volume 3.78 l and precharge of 1300 psi) is located. Orifice O1 ($d_1 = 1.8$ mm) controls the flow to motor M1 (10 cm^3/r), which is subject to a pressure of 1600 psi. Orifice O2 ($d_2 = 0.13''$) +is instead connected to the tank through the solenoid valve (SV). Calculate

- The speed of M1 when SV is closed.
- If SV is actuated, for how long can M1 maintain its previous speed?
- Steady-state operation of M1 after SV is actuated.
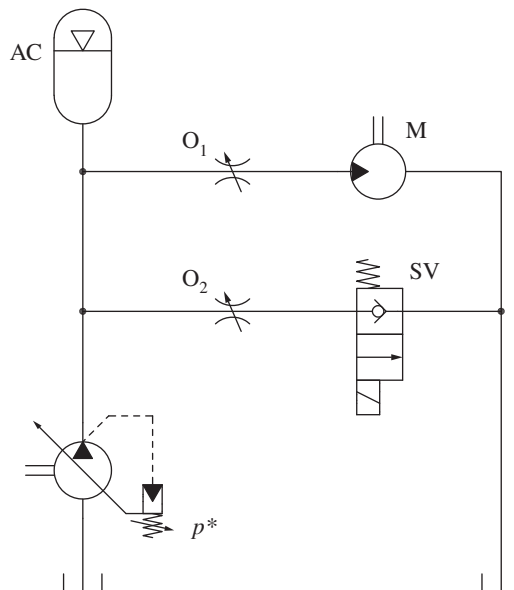
Chapter 20

Open Center Systems for Multiple Actuators

The open center concept presented in Chapter 15 for a single actuator can be easily extended to multiple actuators in parallel. Like the constant pressure system of Chapter 19, an open center circuit supplying multiple actuators consists of several proportional spool valves laid out sequentially and supplied by a single pump, working as a flow supply. However, an open center circuit for multiple actuators becomes more complex to analyze than a constant pressure system. In fact, while for the constant pressure system the operation of one or more actuators does not affect the status of the pressure supply (assuming no flow saturation), in an open center system the value of the supply pressure changes depending on how many and which actuators are being moved. This causes the system to be more efficient, because the supply tends to match the highest load of the circuit. However, it creates several control challenges because the phenomenon of the load interference can become significant.

20.1 Parallel Open Center Systems

20.1.1 Operation

In open center systems serving multiple actuators, the DCVs can be configured in different ways. The most common and simple layout is the parallel configuration, which is represented in Figure 20.1. In this configuration, the pump outlet supplies in parallel the power lines the two spools DCV1 and DCV2 through the check valves CV1 and CV2. However, the open center path realizes a series connection of the two spools: the OC outlet of the first spool feeds the inlet of the other one. This mix of parallel and series connections influences the unique features of open center circuits. Figure 20.1 represents the layout for a circuit based on a fixed displacement pump; a similar circuit could be arranged in an "advanced open center" architecture using a variable displacement pump.

The circuit in Figure 20.1 can be studied through the simplified schematic in Figure 20.2. Two variable orifices (Ω_{U1} and Ω_{U2}) are connected in parallel between the pump line and the actuators, while other two orifices in series (Ω_{T1} and Ω_{T2}) connect the pump to the tank.

In the circuit in Figure 20.2, each of the input commands (i_1 and i_2) controls two variable orifices: one orifice connects the pump to the work-port (*power line*), while the other one connects the pump
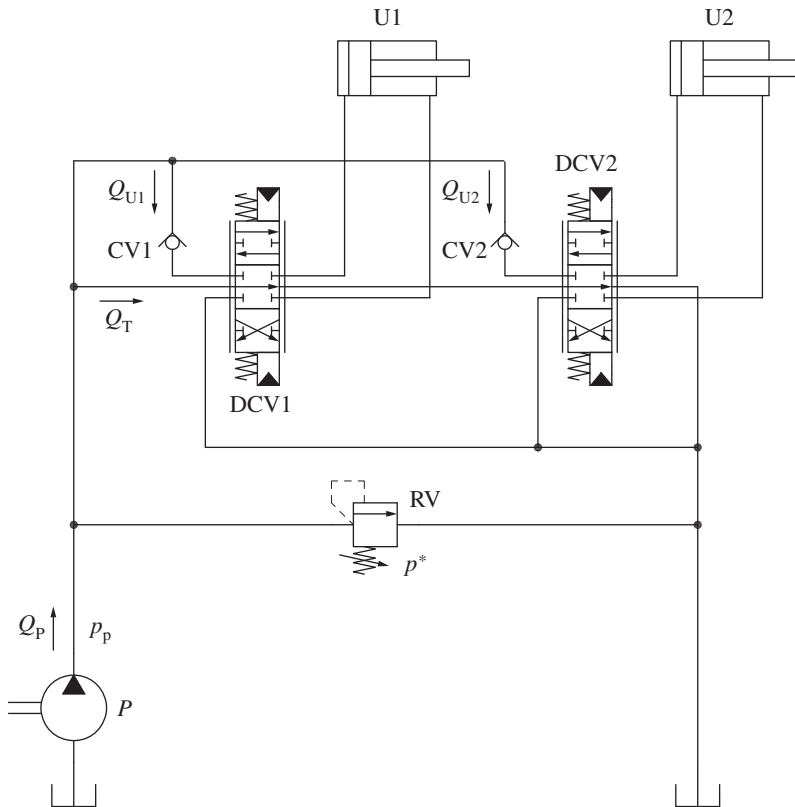
Figure 20.1 Open center circuit with two actuators connected in parallel.
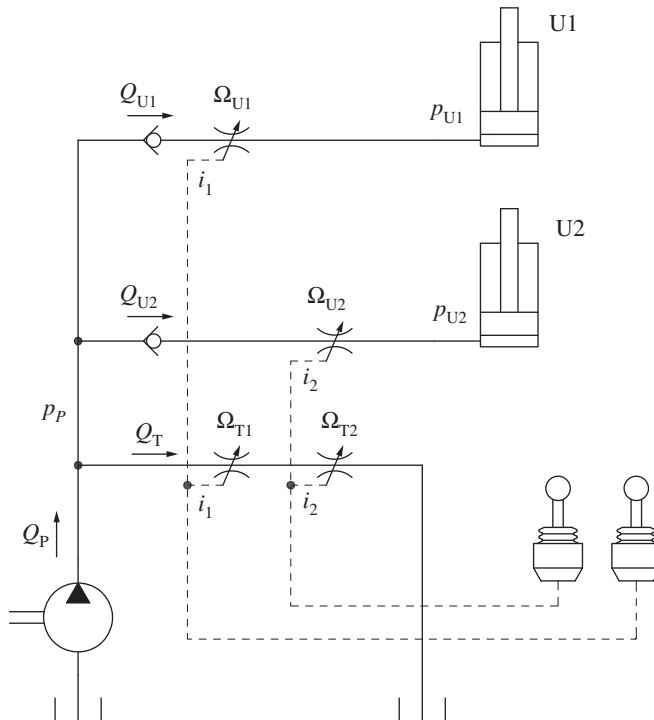
Figure 20.2 Simplified schematic of the open center parallel connection.

to tank (*open center line*). The system operation can be described by the following set of equations:

$$\begin{cases} Q_{U1} = C_f \Omega_{U1} \sqrt{\dfrac{2\left(p_P - p_{U1}\right)}{\rho}} \\[2ex] Q_{U2} = C_f \Omega_{U2} \sqrt{\dfrac{2\left(p_P - p_{U2}\right)}{\rho}} \\[2ex] Q_T = C_f \Omega_{eq,T} \sqrt{\dfrac{2 p_P}{\rho}} \\[2ex] Q_P = Q_{U1} + Q_{U2} + Q_T \end{cases} \tag{20.1}$$

The unknowns of the system of Eq. (20.1) are Q_{U1}, Q_{U2}, Q_T, and p_P As the system is analyzed under given loads and operator commands. The commands i_1 and i_2 define the valve opening areas. The area $\Omega_{eq,\,T}$ represents the equivalent orifice to Ω_{T1} and Ω_{T2}, which are in series. $\Omega_{eq,\,T}$ can be calculated by applying the formula derived for orifices in series in Chapter 5.

The solution of the system of Eq. (20.1) could be written in an explicit form using a computational solver. However, the explicit solution is long and complex, thus not reported here. The set of Eq. (20.1) is useful to understand qualitatively the system behavior.

20.1.2 Energy Analysis

The energy plot in Figure 20.3 represents the steady-state operation of the system under the assumptions that both actuators are moving under different resistive loads, with $p_{U1} > p_{U2}$. It is also assumed that the two spools supplying U1 and U2 are identical (same flow areas), with linear area functions similar to those in Chapter 15.

In Figure 20.3, a significant amount of power, indicated as P_L, is lost. The value of P_L is given by three contributions: the throttling losses on the two spools (with the one on DCV2 being higher the one on DCV1) and the power loss caused by the excess flow to tank Q_T through the open center. The value of this last contribution can be reduced with an "advanced open center" architecture, as shown in Figure 20.4. This architecture is implemented with a variable displacement pump, realizing a negative flow control.
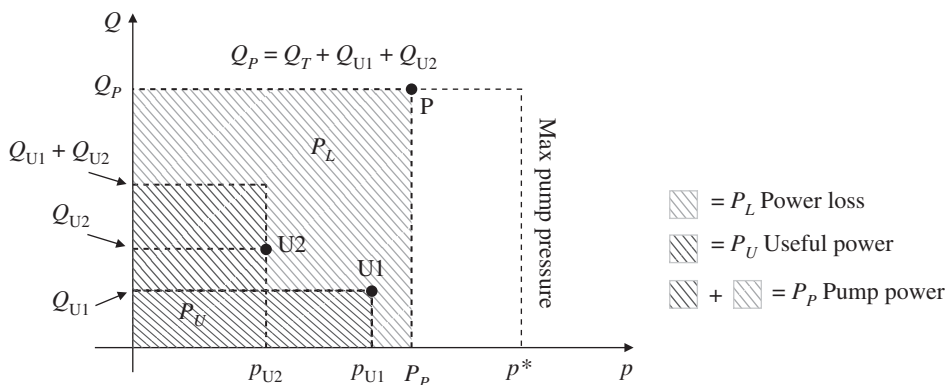
Figure 20.3 Energy plot representing a parallel open center system supplying simultaneously two actuators at different pressures.
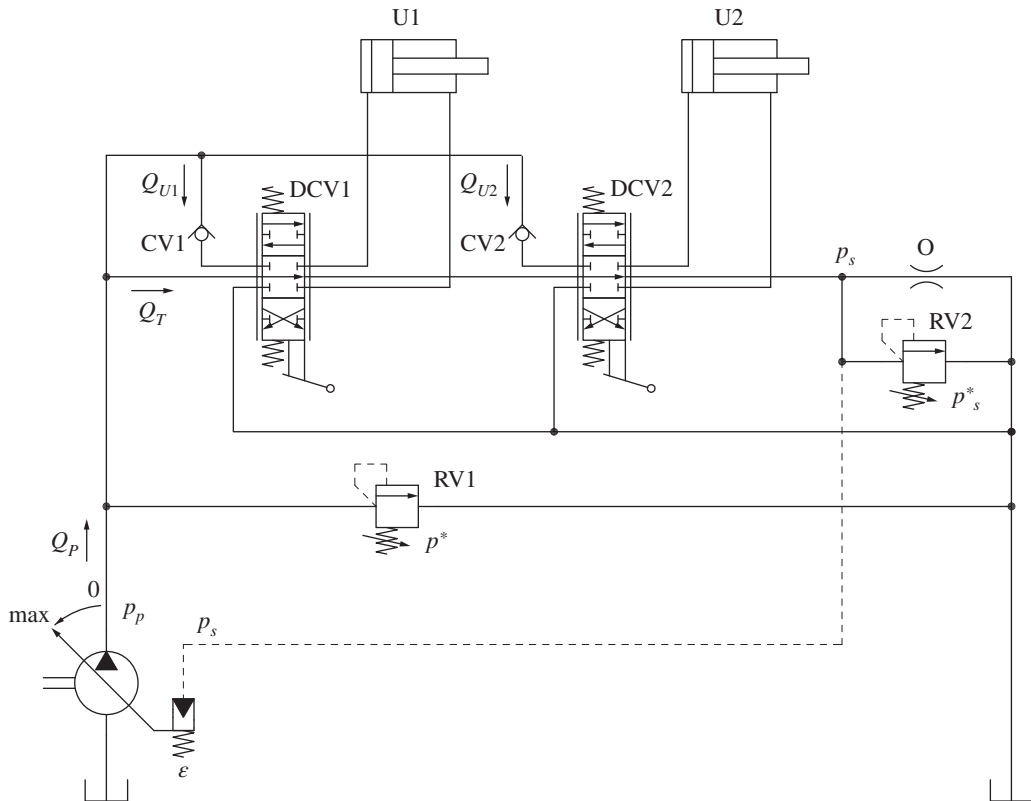
Figure 20.4 Advanced open center system with a variable displacement pump.

20.1.3 Flow Saturation

In this layout, when the throttle areas open above the flow saturation limit, the distribution of the loads determines which actuators are penalized from flow saturation. As in the constant pressure case, the actuator with the highest load is the one slowing down the most.

20.1.4 Considerations On the Open Center Spool Design

The system of Eq. (20.1) is useful to qualitatively analyze the behavior of the system with respect to the load interference. A change in any load, or in any throttling area, affects all the other variables of the hydraulic circuit. For example, a variation in p_{U1} affects Q_{U2}. However, the open center circuit can limit the load interference problem by a proper design of the metering elements. In order to understand how this can be implemented, it is necessary to recall the case of a single actuator controlled with an open center system (as studied in Chapter 15) and make additional considerations about the design of the spool defining the metering areas. The case of the open center system with a single actuator as studied in Chapter 15 is depicted in Figure 20.5.

The flow supplied to the actuator was previously analyzed as a function of the opening areas $\Omega_U(i)$ and $\Omega_T(i)$, which depend on the command i provided to the open center valve. The system of Eq. (20.2) was then written to derive the plots of Figure 20.5b, which describes how the pump flow splits between the actuator U and the tanks T as a function of the actuator pressure to satisfy the
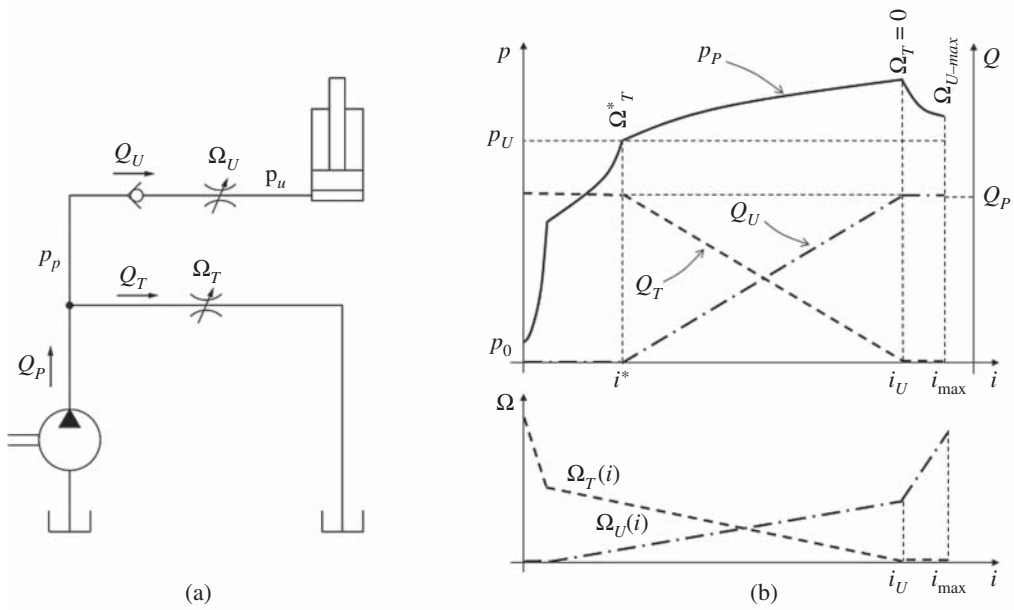
Figure 20.5 Simplified schematic of a single actuator open center system (a) and its operating features (b). See also Chapter 15.

operator command.

$$
\begin{cases}
Q_T = C_f \Omega_T\,(i)\,\sqrt{\dfrac{2p_P}{\rho}} \\[2mm]
Q_U = C_f \Omega_U\,(i)\,\sqrt{\dfrac{2\,(p_P - p_U)}{\rho}} \\[2mm]
Q_U = Q_P - Q_T
\end{cases}
\tag{20.2}
$$

In more detail, the unknowns of the system of Eq. (20.2) are Q_U, Q_T, and p_p, while the independent variables are Ω_U, Ω_T, and Q_P. The system of Eq. (20.2) is useful for making further qualitative considerations on the effects of the main design parameters of the spool, which will help understanding the behavior of the open center system with multiple actuators.

Opening Areas

The split of the pump flow Q_P between the actuator line, Q_U, and the tank line Q_T, is realized by the areas Ω_U and Ω_T, which have opposite trends with respect to the valve command i, as shown in Figure 20.5b. As the spool moves, one area (Ω_U) increases while the other (Ω_T) decreases.

The expression for the flow to the actuator[1], Q_U is:

$$
\frac{Q_U^2}{C_f^2\Omega_U^2} - \frac{\left(Q_P - Q_U\right)^2}{C_f^2\Omega_T^2} + \frac{2p_U}{\rho} = 0
\tag{20.3}
$$

──────────

1 To obtain this expression, the last equation of the system should be substituted into the first one. The resulting equation is then resolved to calculate p_p. This expression of p_p is then substituted into the second equation of the system.

Equation (20.3) is a second-order equation, which can be solved to find Q_U:

$$Q_U = \frac{\Omega_U}{\Omega_U^2 - \Omega_T^2} \left(\Omega_U Q_P - \Omega_T \sqrt{\frac{2 C_f^2 p_U}{\rho} \left(\Omega_U^2 - \Omega_T^2 \right) + Q_P^2} \right) \tag{20.4}$$

Equation (20.4) shows that, for a given operating condition (specified by Q_P, p_U), the same value of Q_U can be obtained by an infinite combination of flow areas (Ω_U, Ω_T), defined by the spool geometry. Different pairs of values (Ω_U, Ω_T) realizing the same Q_U are characterized by a different pump pressure p_P.[2] The same consideration is valid also for Q_T, which equals $Q_P - Q_U$.

In general, one can observe that the same flow characteristic $Q_U(i)$ and $Q_T(i)$ can be obtained by different combinations of Ω_U and Ω_T and therefore by different spool geometries. For example, Figure 20.7 compares the flow and pressure characteristics (lower charts) of two spools with different flow areas (top charts). The two considered spools have the same trend for the area functions (linear, in the case of the figure, although other trends are possible), but the spool at the left side of the figure implements larger areas than the spool at the right side.

The spool with larger flow areas presents a lower pump pressure within the operating range. For a single actuator circuit, it is obviously convenient to select a spool which gives the minimum pressure drop across the area Ω_U in order to reduce the throttling losses and maximize the system efficiency.

Besides the different area values, which imply different operating pressures, there is another important difference between the two charts in Figure 20.6: the value of the input command at which the actuator starts seeing flow, indicated as i^*. The spool with smaller throttle areas
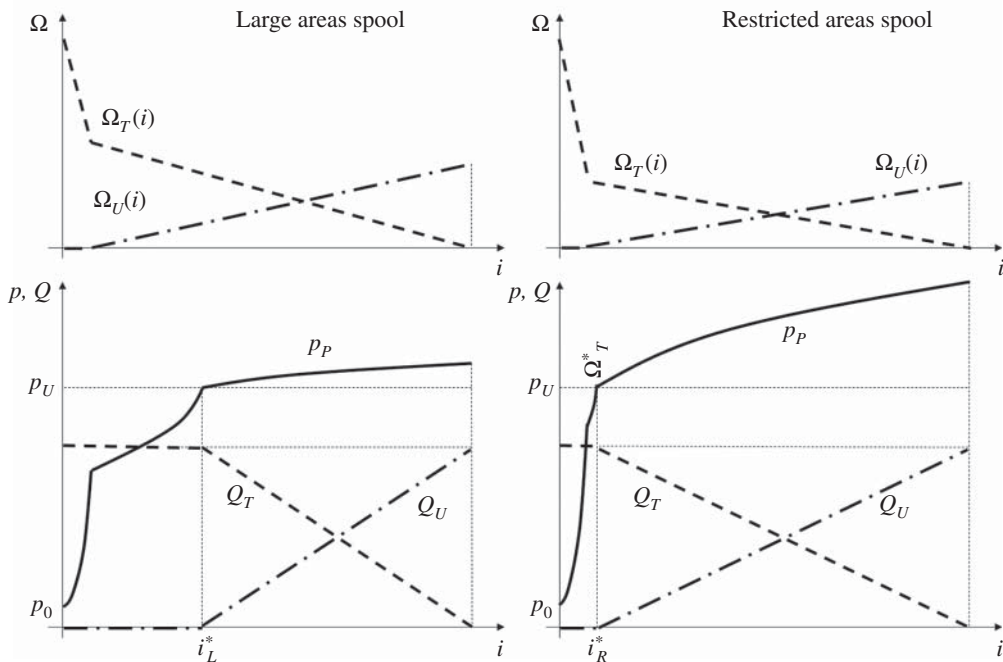

Figure 20.6 Flow rates and pressure trends for two open center spools (large opening areas at the left, small opening areas at the right).

---

2 The relation between p_p and the two areas Ω_U, Ω_T is given by the first two equations of the system of Eq. (20.2).
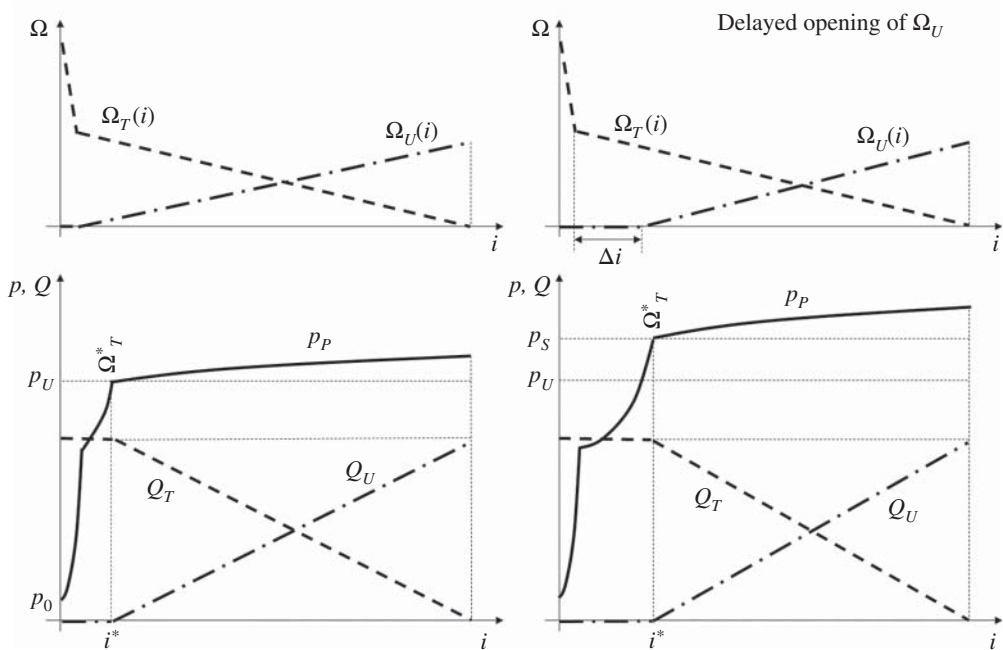
Figure 20.7 Comparison of flow and pressure curves for two spools with similar area curves but with different timing in the opening of Ω_U: simultaneous port opening at the left, delayed opening of Ω_U at the right.

(right-side charts) starts moving the actuator for $i = i_R^*$, which is significantly lower then i_L^*, the equivalent point for the larger area spool (left side).

Opening Delay (Valve Timing)

In the open center characteristic plots shown so far, the values of Ω_U and Ω_T start varying simultaneously. In other words, when Ω_T starts decreasing, the value of Ω_U starts increasing. In reality, open center spools can be designed with a delay in the opening of Ω_U, with respect to the closing of Ω_T (Figure 20.7). The right chart refers to a spool design that presents a delay Δi in the opening of Ω_U. This delay in the opening affects the value of the dead-band, i.e. the value of i^*, as well as the trend of p_P. In the spool with simultaneous area trends, the actuator starts seeing flow when the value of p_P equals p_U. However, with a spool with delayed opening, it is possible to have the pump pressure to raise to a value $p_S > p_U$ before the actuator moves. As the spool further opens Ω_U, the pump pressure p_P remains above the level of p_S.[3]

20.1.5 Load Interference in Open Center Systems

The valve geometry parameters discussed in the previous sections, such as opening areas, timing, and delayed opening, have important implications on the behavior of open center systems for multiple actuators, during the simultaneous actuation of multiple functions, which can be described by considering a case of simultaneous actuation of two functions, U1 and U2, with Figure 20.8. For the case of the figure, it can be assumed that the load in U1 is higher than the one in U2 ($p_{U1} > p_{U2}$).

---

3 While the previous note provides a condition for Ω_T, the desirable condition of $p_P > p_S$, for any value of i, gives a requirement for $\Omega_U(i)$, which cannot increase too rapidly. A sudden opening of Ω_U after the delay would cause p_P to drop.

Figure 20.8 Open center circuit for the analysis of the simultaneous actuation of two functions: identical spools (a); different spools (b).

The operator initially commands DCV2 and controls Q_{U2} to a steady-state condition. At a given instant t^*, the spool DCV1 is also shifted, so that U1 starts moving. What happens to U2?

The dynamic behavior of the system is summarized in Figure 20.9, for two different cases.
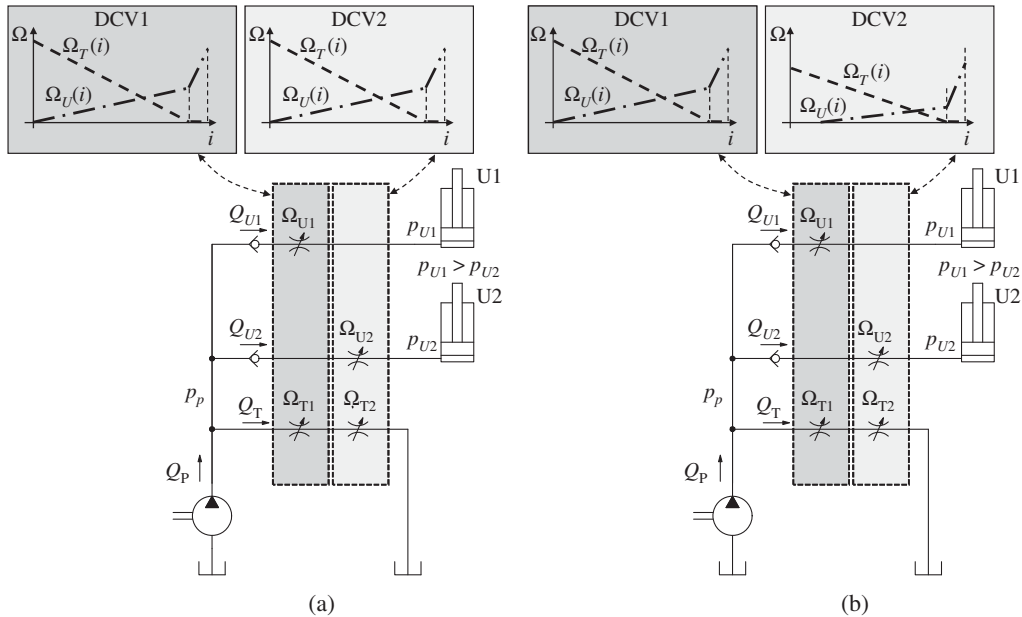
Identical Spools

In the first case, Figure 20.9a, the two spools DCV1 and DCV2 are identical, with the opening areas shown in Figure 20.8a. When only DCV2 is shifted, the pump pressure is slightly above p_{U2}, giving a flow rate to U2 equal to Q'_{U2}. At t^*, when DCV1 is also actuated, the additional restriction introduced by Ω_{T1} causes the pump pressure to increase to a value higher than p_{U1}, so that a flow to Q_{U1} is established. Consequently, since the throttle area to U2 remains unchanged, the value of the flow rate to U2 jumps to Q''_{U2}, which is higher than the previous value Q'_{U2}. In other words, when U1 is actuated, the operator perceives an unexpected acceleration of U2. The operator can counter act to this behavior by modulating the position of DCV2 to reduce the throttling area Ω_{U2} to return U2 to the desired speed, although this may further affect the actual value of Q_{U1}.

Different Spools

In the second case, Figure 20.9b, the control valves have two different spools. DCV1 is identical to the previous case, while DCV2, which supplies the lower load, has a more restricted area and a delayed opening of Ω_U. In the initial stage ($t < t^*$), only U2 is moving with a supply flow equal to Q'_{U2}. In this condition, the design of the DCV2 spool is such that the pump pressure, p_P is significantly higher than p_{U2}. At t^*, DCV1 is shifted, and the actuator U1 starts moving. In this case, the pump pressure has only a slight change in value, because DCV1 has larger areas ($\Omega_{T2} \ll \Omega_{T1}$). Consequently, Q''_{U2} is only slightly affected by this change and the load interference effect is significantly reduced with respect to the initial case. In this case the machine operator does not require significant corrections of the DCV2 command to correct the U2 velocity to the desired speed.

The situation just described is summarized in Figure 20.9. The solution using different spool shows a very small change in Q_{U2} when DCV1 is actuated. This system achieves improvements on the controllability side at the expense of the system efficiency. In fact, DCV2 is more restrictive,
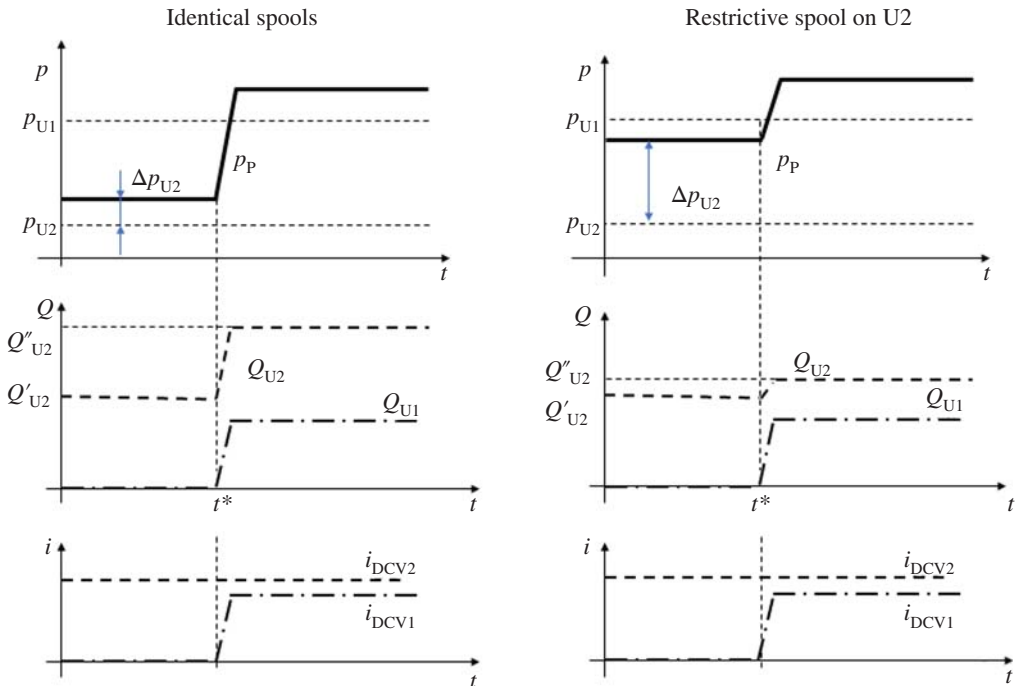
Figure 20.9 Load interference example with two different spool combinations.

causing higher throttling losses when controlling U2. This is clearly visible in the first part of Figure 20.9 ($t < t^*$): the same value of Q'_{U2} is achieved at higher pump pressure because of the restrictive spool design.

The careful reader should notice that the behavior of the system described in Figure 20.9 is also a result of the actuation sequence (U1 is activated while U2 is running). If the opposite situation happened, the system would behave differently. Usually these different behaviors are compensated by the operator, which is the element closing the loop in the actuation process.

In conclusion, open center parallel circuits are a simple architecture that can successfully be used to control multiple actuators. Compared to more complex architectures using dedicated components to manage the effects of load interference (load sensing compensators, as explained in Chapter 21), the open center circuit is almost always the most economical solution. Furthermore, the metering characteristic of open center valves is often appreciated by many machine operators. A customized design for the DCVs metering areas can significantly limit the interference between the controlled flow rates during the simultaneous actuation of the machine functions.

When attempting to reduce the load interference, the following important factors need to be accounted for:

- *Increased energy consumption*. From one side, the use of restrictive spools at each function with low load functions limits the load interference. However, this is achieved at the expense of a higher pump pressures, reducing the overall efficiency of the open center system.
- *Predictable loads*. The method outlined is effective only when the load conditions at each actuator can be somehow predicted. Many machines, such as backhoes or wheel loaders, operate with repetitive duty cycles with predictable loads. In such cases, strategies on the spool design can be very effective in limiting the load interference. However, this is not the case for all applications and the spool design cannot be an effective method. To understand this last consideration, one can think about the system in Figure 20.8b, undergoing the cycle in Figure 20.9b, under

a condition where $p_{U2} > p_{U1}$. In this case, the load interference effect would be amplified with respect to that in the case of equal valves (Figure 20.9a).

Open center parallel system is a quite mature technology, but it is still successfully applied on many pieces of equipment, especially on excavating machines. All crawler excavators are controlled with advanced open center architectures. In addition, this technology has been applied in backhoes and wheel loaders for decades.

Example 20.1 Open center parallel system for multi-actuator

A conveyor is controlled with an open center system comprising a 50 cm^3/r gear pump rotating at 1500 rpm, and a two-section open center valve with parallel layout. The system schematic is shown below. The first valve section controls the motor rotation, while the second section controls the cylinder used to raise or lower the conveyor. The conveyor motor is 300 cc/r and works under a resistive torque of 860 Nm. The lifting cylinder has a bore diameter of 50 mm and is subject to a force of 25.8 kN caused by the conveyor weight.
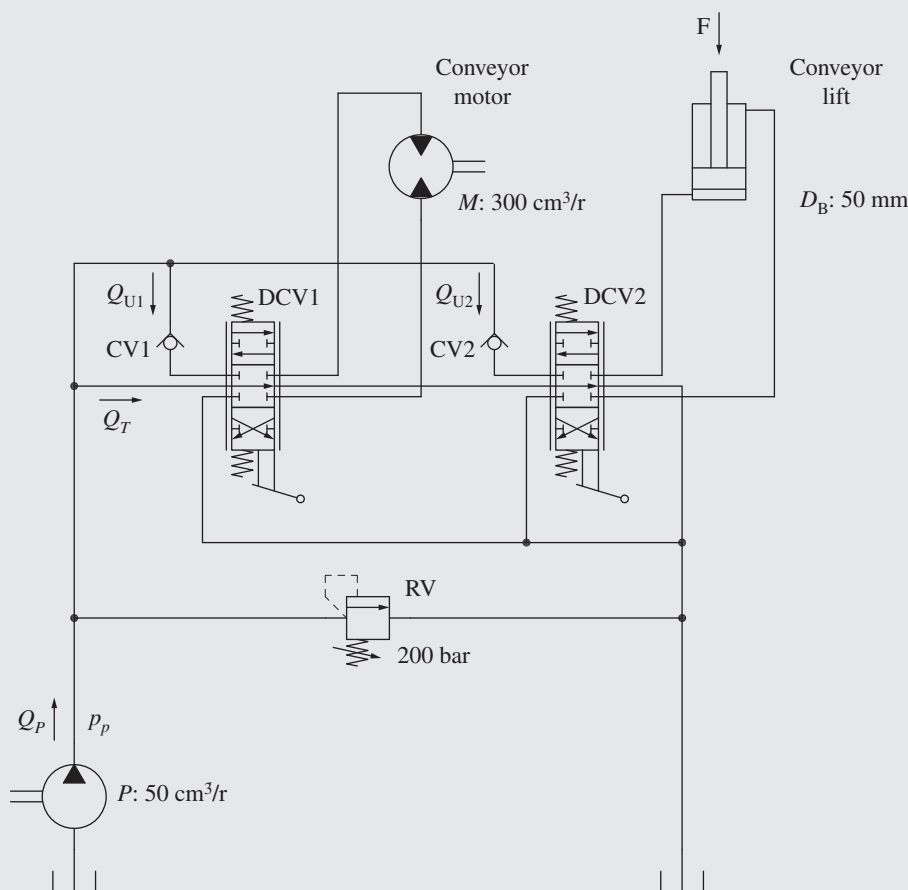
Answer the following questions:

(1) Calculate the standby power consumption of the system considering that both spools have a maximum throttle area $\Omega_T = 40$ mm^2.

(2) If the operator activates the conveyor motor opening the following areas $\Omega_{U1} = 26\ mm^2$ and $\Omega_{T1} = 2.8\ mm^2$, what is the resulting conveyor speed?

(3) If the operator keeps the conveyor spool at the previous position and moves also the conveyor lift sections realizing $\Omega_{U2} = 2.0\ mm^2$ and $\Omega_{T1} = 35\ mm^2$, what will be the lifting speed? Will the conveyor speed be affected?

(4) The operator shifts only the conveyor spool to full stroke, realizing $\Omega_{U1} = 35\ mm^2$ and $\Omega_{T1} = 0\ mm^2$. The conveyor starts loading heavier material and increases its weight by 40% (assume the motor torque constant). If the operator moves the conveyor lift spool to the same position of the previous point, will the cylinder move?

(5) What changes can be done in the system to allow the operator to lift the conveyor under the previous conditions?

(6) Consider a situation where the valve has six sections, instead of the two sections shown in the figure. Such valve would control four additional actuators (not shown in the figure). Consider all the valve sections identical. What would be the stand-by power consumption in this case?

Consider the pump and motor as ideal units, and neglect pressure losses in the pipes. Assume a flow coefficient $C_f = 0.7$ though the flow passage areas in the hydraulic control valves.

Given:

Pump $V_d = 50\ cm^3/r$; $n_P = 1500\ rpm$.
Motor $V_M = 300\ cm^3/r$; $T_M = 860\ Nm$
Cylinder $d_B = 50\ mm$; $F = 25800\ N$

(1) Spools in neutral, flow area $\Omega_{T1} = \Omega_{T2} = 40\ mm^2$
(2) Additional four spool section case
(3) Only spool 1 shifted, $\Omega_{U1} = 26\ mm^2$; $\Omega_{T1} = 2.8\ mm^2$
(4) Both spools shifted: $\Omega_{U1} = 26\ mm^2$; $\Omega_{T1} = 2.8\ mm^2$; $\Omega_{U2} = 2.0\ mm^2$; $\Omega_{T1} = 35\ mm^2$
(5) Spool 1 fully shifted: $\Omega_{U1} = 35\ mm^2$; $\Omega_{T1} = 0$. Load on the cylinder increases to $F = 36\,120\ N$

Find:

(1) Pump power consumption, $P_{sb,2}$
(2) Motor speed, n_M
(3) Cylinder lifting speed, v, and conveyor speed, n_M
(4) Cylinder lifting speed, v
(5) Solutions for improving the simultaneous controllability
(6) Pump power consumption, for the case of six sections $P_{sb,6}$

Solution:

(1) The two spools realize a series connection for the orifices $\Omega_{T1} = \Omega_{T2}$. The equivalent area of two orifices in series (see Chapter 5) is

$$\Omega_{T,eq} = \sqrt{\frac{1}{\left(\dfrac{1}{\Omega_{T1}^2} + \dfrac{1}{\Omega_{T2}^2}\right)}} = \sqrt{\frac{1}{\left(\dfrac{1}{40^2} + \dfrac{1}{40^2}\right)}}[mm^2] = \frac{40}{\sqrt{2}}[mm^2] = 28.2\ mm^2$$

Example 20.1 (Continued)

The pump flow rate is

$$Q_P = V_d \cdot n_P = 50 \left[cm^3/r\right] \cdot 1500 \, [rpm] \frac{1}{1000} = 75 \, l/min$$

The pump standby pressure is

$$p_{sb} = \left(\frac{Q_P}{C_f \cdot \Omega_{T,eq}}\right)^2 = \left(\frac{75 \, [l/min]}{0.7 \cdot 28.2 \, [mm^2]}\right)^2 \cdot 1.19 = 17.3 \, bar$$

The pump standby power is

$$P_{sb} = Q_P \cdot p_{sb} = 75 \, [l/min] \cdot 17.3 \, [bar] \cdot \frac{1}{600} = 2.2 \, kW$$

(2) The pressure required by the conveyor motor is

$$p_{U1} = 2\pi \frac{T_M}{V_M} = \frac{860 \, [Nm]}{300 \, [cm^3/r]} \cdot 20\pi = 180 \, bar$$

When only one spool is shifted, the flow rate to the conveyor motor can be calculated applying Eq. (20.4):

$$Q_U = \frac{\Omega_U}{\Omega_U^2 - \Omega_T^2} \left(\Omega_U Q_P - \Omega_T \sqrt{\frac{2 \cdot c_f^2 p_U}{\rho} \left(\Omega_U^2 - \Omega_T^2 \right) + Q_P^2} \right)$$

$$= \frac{26}{26^2 - 2.8^2} \left[\frac{1}{[mm^2]}\right] \left(26 \cdot 75 \, [l/min \cdot mm^2] \right.$$

$$\left. - 2.8 \, [mm^2] \sqrt{\frac{2 \cdot 0.49 \cdot 180 \, [bar]}{850 \, [kg/m^3]} (26^2 - 2.8^2)[mm^4] \cdot 360 + 75^2 [l^2/min^2]} \right)$$

$$= 50 \, l/min$$

The number 360 in the formula is a conversion factor and has the dimension of $[(l/min)^2 \cdot kg/m^3 \cdot mm^4/bar]$. Furthermore, the area Ω_{T2} is still equal to 40 mm^2 but it can be ignored in the calculation because Ω_{T1} dominates the restriction to the tank. With this flow rate the conveyor operates at

$$n_M = \frac{Q_M}{V_M} = \frac{50 \, [l/min]}{300 \, [cm^3/r]} \cdot 1000 = 166.7 \, rpm$$

(3) When the cylinder is lifted, the pressure demanded by the function is

$$p_{U1} = \frac{4 \cdot F}{\pi \cdot d_B^2} = \frac{4 \cdot 28\,500 \, [N]}{\pi \cdot 2500 \, [mm^2]} \cdot 10 = 145 \, bar$$

The operation of the system can be now defined using Eq. (20.1). As mentioned, the explicit solution of system becomes rather complex to write and it is easier to utilize a numerical solver or a simulation model. This leads to the following values:

$$\begin{cases} Q_{U1} = 42.0 \, l/min \\ Q_{U2} = 8.3 \, l/min \\ p_P = 186.4 \, bar \end{cases}$$

Under these conditions, the cylinder lifts with a speed of 70 *mm/s* and the motor rotates at 140 *rpm*. Therefore, by actuating the lift cylinder, the conveyor speed reduces by 16%.

(4) If the conveyor spool alone is shifted to its full stroke position, all the pump flow goes to the conveyor motor since $\Omega_{T1} = 0$. The restriction Ω_{U1} acts as a compensator and the pump pressure becomes

$$p_P = p_{U1} + \frac{\rho}{2} \cdot \left(\frac{Q_P}{C_f \cdot \Omega_{U1}} \right)^2 = 180 \,[bar] + \frac{850 \,[kg/m^3]}{2} \left(\frac{75 \,[l/min]}{0.7 \cdot 35 \,[mm^2] \cdot 18.97} \right)^2$$

$$= 191 \, bar$$

If the cylinder load increases to 36 120 *N*, the pressure required by the cylinder increases to 203 *bar*. Then, if the cylinder spool is shifted, the load pressure becomes higher than the pump pressure. In other words, the cylinder will not move.

(5) In order to satisfy the previous load condition, the spool of DCV1 can be selected with a more restrictive area toward the actuator. In other words, Ω_{U1} could be smaller for the fully shifted position. This would allow control of the two functions under heavy load, but it will also reduce the efficiency of the system, increasing the pressure drop across the metering orifice. Another potential solution is represented by a different layout of the valve, selecting a tandem connection between the two spools. This topic will be explained in Section 20.2.

(6) If the number of spool sections in the valve increases to a total of 6 with identical spools, then

$$\Omega_{T,\text{eq}} = \frac{40}{\sqrt{6}}[mm^2] = 16.3 \, mm^2$$

$$p_{\text{sb}} = \left(\frac{75 \,[l/min]}{0.7 \cdot 16.3 \,[mm^2]} \right)^2 \cdot 1.19 = 51.4 \, bar$$

$$P_{\text{sb}} = 75 \,[l/min] \cdot 51.4 \,[bar] \cdot \frac{1}{600} = 6.3 \, kW$$

The pressure drop across the valve in standby increases linearly with the number of sections.

20.2 Tandem and Series Open Center Systems

In the open center systems described so far, all actuators were connected in parallel to the pump outlet through the throttle areas Ω_U. In this layout, all actuators appear "equal" with respect to the flow supply, and no one has priority over the others. When flow saturation occurs, the actuator with the highest load is penalized and will receive a flow rate lower than the commanded value.

20.2.1 Tandem Configuration

One of the advantages of open center circuits is the possibility to easily realize priority among functions by implementing a tandem layout. The tandem layout is represented in the circuit in Figure 20.10: the spool DCV2 is not supplied directly by the pump outlet (as in Figure 20.1) but by the open center gallery of DCV1. It is intuitive to see that the spool DCV1 has priority over DCV2, as DCV2 is supplied with the flow Q_{T1} which is not used by DCV1.

The **tandem** layout for open center systems with multiple actuators permits to achieve priority among different functions.
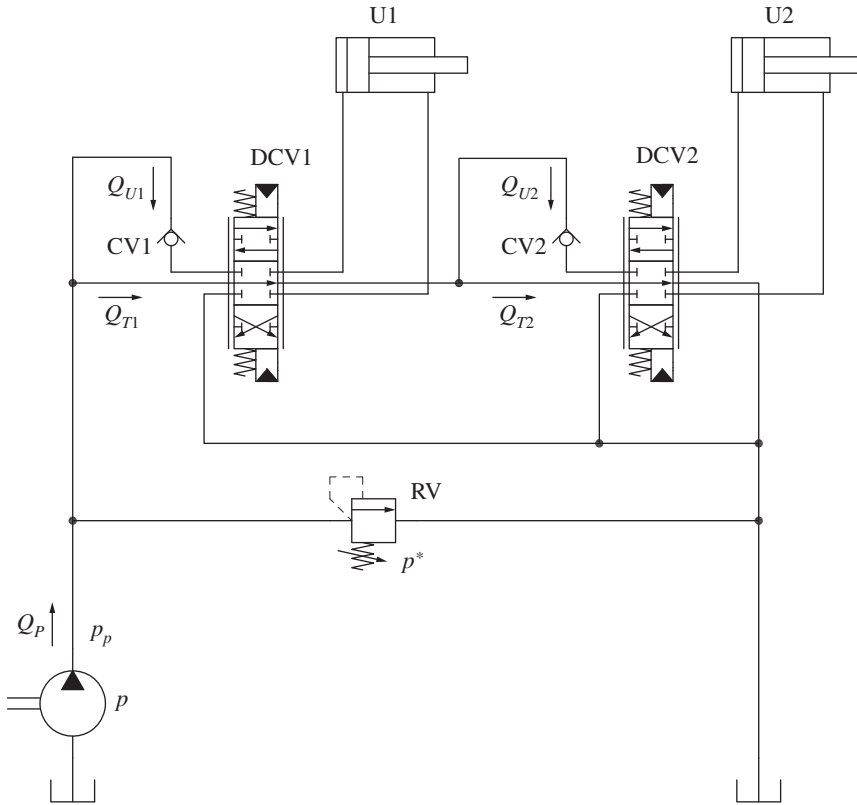
Figure 20.10 Tandem open center circuit. U1 has the priority over U2.

The tandem circuit can be studied with the simplified schematic in Figure 20.11. The system can be characterized solving the six equations grouped in Eq. (20.5). The unknowns are Q_{U1}, Q_{T1}, Q_{U2}, Q_{T2}, p_P, p_X.

With reference to the circuit of Figure 20.11, the equations describing the system are

$$
\begin{cases}
Q_{U1} = c_f \Omega_{U1} \sqrt{\dfrac{2\left(p_P - p_{U1}\right)}{\rho}} & ; & Q_{U2} = c_f \Omega_{U2} \sqrt{\dfrac{2\left(p_X - p_{U2}\right)}{\rho}} \\[3mm]
Q_{T1} = c_f \Omega_{T1} \sqrt{\dfrac{2\left(p_P - p_X\right)}{\rho}} & ; & Q_{T2} = c_f \Omega_{T2} \sqrt{\dfrac{2p_X}{\rho}} \\[3mm]
Q_P = Q_{U1} + Q_{T1} & ; & Q_{T1} = Q_{U2} + Q_{T2}
\end{cases}
\tag{20.5}
$$

From Eq. (20.5) it is intuitive to see how U1 is governed by the same equations as the open center system with a single actuator, with the only difference in the term p_X used in the expression of Q_{T1}. Also, U2 is governed by similar equations, using Q_{T1} instead of Q_P and p_X instead of p_P. A particular situation occurs when DCV1 is fully shifted: here $\Omega_{T1} = 0$, therefore $Q_{U2} = Q_{T2} = 0$, independently on the position of the DCV2.

20.2.2 Series Configuration

Open center valves also allow to easily implement series connections. In this type of circuit, as represented in Figure 20.12, the spool DCV2 is supplied by the return port and by the open center gallery of DCV1.
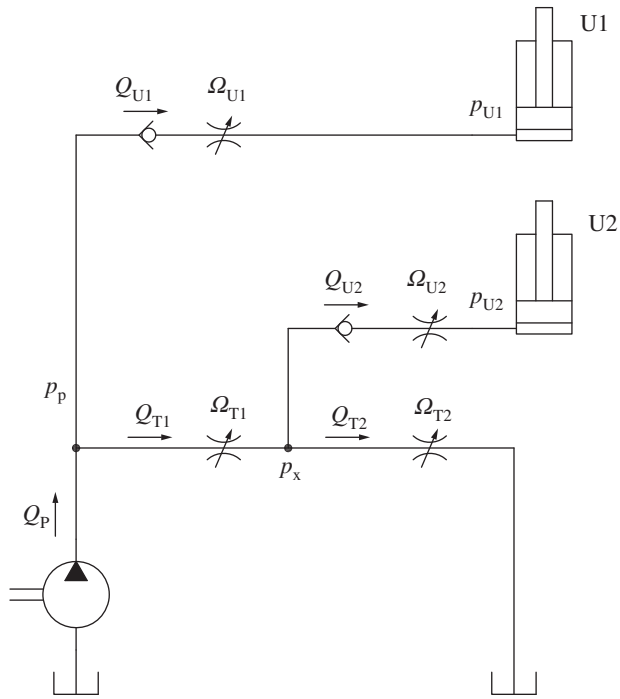
Figure 20.11 Simplified circuit of an open center system with tandem connection.
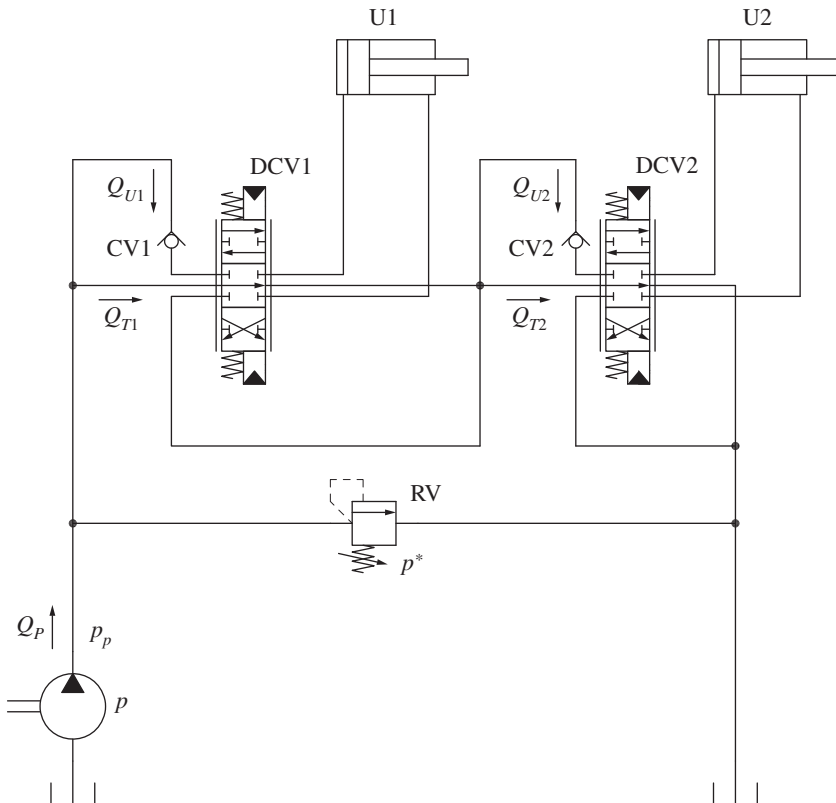
Figure 20.12 Open center circuit with series spool connection.

In other words, DCV1 operates as a standard single actuator open center system. If DCV2 is actuated, this spool also works as an independent open center circuit, being supplied with the residual open center flow of DCV1 (if DCV1 is partially stroked) added to the return flow from the actuator U1. When both actuators are run, the pump pressure is additive as described in Chapter 18.

Besides the effect of the differential area and eventually of the relief valve (RV) (which can open if the pressure raises to p^*), the series configuration is not subject to load interference. This type of circuit is often used on compact construction equipment, where the loads are relatively small with respect to the size of the cylinders and therefore the pressure summation is not limiting the machine performance.

20.3 Advanced Open Center Circuit for Multiple Actuators: The Case of Excavators

As previously discussed, despite being considered an old technology, open center valves are still very popular among many applications. A significant example is the case of excavators, where throughout the years manufacturers developed and perfected a purpose-designed system based on advanced open center architecture with tandem piston pumps. Actual systems are usually relatively complex and every machine has its own custom features. However, the basic layout – shown in Figure 20.13 – is relatively simple and, due to its good performance and operator friendliness, has become a standard for most of these machines.

The system represented in Figure 20.13 is based a negative flow control architecture with two piston pumps and two open center valve banks combined within a single body.

In each valve, the first sections (DCV1a and DCV1b) are dedicated to the travel functions. The travel functions have priority because of the tandem connection implemented with respect to the downstream sections. This means that when the machine is traveling, P1 is dedicated to the left track and P2 to the right track. This allows for a precise control of the drive and straight tracking at full speed. The excess flow from each travel section reaches the spools downstream, which control the excavator functions. Each valve bank presents spools with different properties: DCV2a, DCV4a, DCV2b, DCV3b, and DCV5b are primary spools dedicated to swing, arm, aux, boom, and bucket, respectively. However, DCV3a and DCV4b are secondary spools dedicated to boom and arm, which are the functions with higher flow demand. The timing and pilot thresholds of the secondary spools are designed so that, when the excavator is multifunctioning, the left valve bank (supplied by P1) is dedicated to the swing and arm, while the right valve bank (supplied by P2) is dedicated to boom and bucket[4]. The two circuits work independently, thus reducing the effects of the load interference and of flow saturation. The two independent circuits also allow achieving a good level of energy efficiency. However, when the two high flow functions (boom and arm) are demanding maximum speed, the secondary spools can participate in supplying additional flow to the functions, if available, thus increasing the actuators speed.

The reader can observe other details in the open center valve. For example, the secondary boom spool, DCV3a, participates only in the boom lifting phase, while the lowering occurs only through DCV3b. However, regarding the arm, DCV4a realizes the cylinder extension through a semi-regenerative spool (the concept of regeneration explained in Chapter 12).

As stated, actual excavator valves are more complex than those in Figure 20.13, but their basic layout follows the one shown in the circuit. Furthermore, the same layout can also be applied to a positive flow control architecture, where the pumps are now piloted from the joystick signals.

---

4 This functionality is usually achieved with additional elements (not represented in the simplified circuit) that disable the secondary spools during multifunctioning.
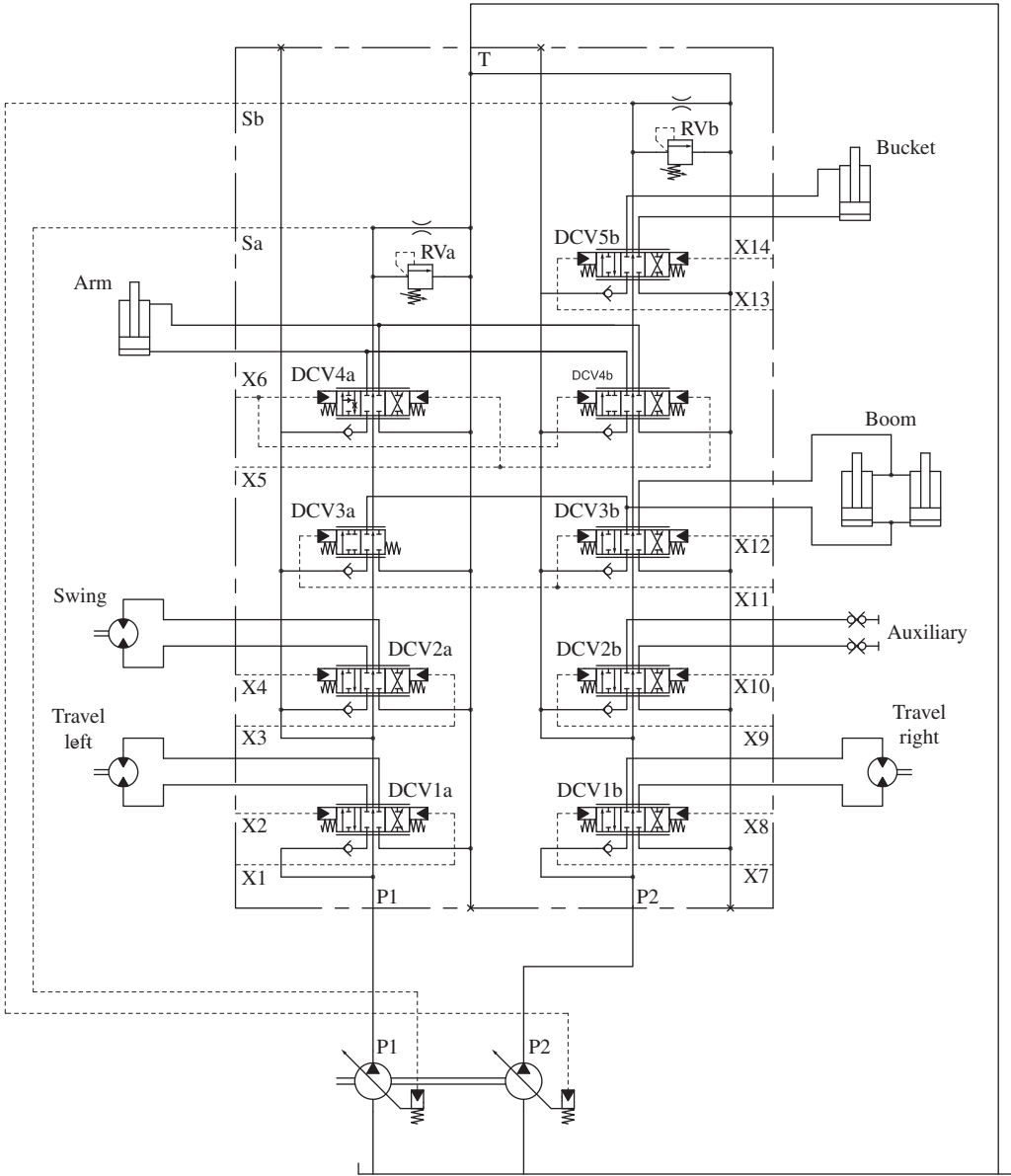
Figure 20.13 Simplified open center architecture for excavators.

Problems

20.1 A small crane is controlled with an open center system comprising a $45\,\text{cm}^3/\text{r}$ gear pump rotating at 2100 rpm, and a three-section open center valve with parallel layout. The first valve section controls the swing, the second one the hoist, and the third one the winch. In the current load configuration, the swing motor is $180\,\text{cm}^3/\text{r}$ and works under a resistive torque of 470 Nm. The lifting cylinder has a bore diameter of $50\,\text{mm}^2$ and is subject to a force of 20 600 N, while the winch sees a pressure of 45 bar. The three valve spools are shifted realizing the following work-port throttling areas: swing area, $3.5\,\text{mm}^2$; hoist area, $4.2\,\text{mm}^2$; and winch area, $2.45\,\text{mm}^2$. The equivalent throttling area of the open center gallery is $2.9\,\text{mm}^2$. Calculate the flow reaching each function, the pump pressure and the flow lost through the open center. How do the function flows change if the load to the winch increased by 50%? What if now the load to the swing is reduced by 30%? Finally, what happens if the pump speed decreases by 20%?

20.2 A two-section open center valve is supplied with $100\,\text{l/min}$. The first section has a work-port throttling area of $12.5\,\text{mm}^2$ and has a resistive load of 2000 psi. The second section is $2.4\,\text{mm}^2$ and has a resistive load of 1000 psi. The open center gallery area is $9.6\,\text{mm}^2$. Calculate the flow reaching each of the functions, the flow returning to the tank, and the pump pressure. At this point, calculate an alternative configuration of the areas, in which the flow split is approximately the same ($\pm5\%$ vs. the previous case), but where the pump supply pressure is 2800 psi.

20.3 Consider the circuit of the previous problem, system A corresponds to the initial throttling areas, and system B corresponds to the calculated areas to obtain a pump pressure of 2800 psi. Compare the behavior of the two systems in the following cases:
   i) Pressure on first function: 2300 psi; pressure on second function: 1000 psi
  ii) $p_1 = 1700\,\text{psi}$, $p_2 = 1000\,\text{psi}$
 iii) $p_1 = 2000\,\text{psi}$, $p_2 = 250\,\text{psi}$
  iv) $p_1 = 2000\,\text{psi}$, $p_2 = 1600\,\text{psi}$
Which of the two systems behaves better in terms of % of flow variation with respect to the baseline? What about the system efficiencies in the two cases?

Chapter 21

Load Sensing Systems for Multiple Actuators

The load sensing (LS) control concept, which has been introduced in Chapter 16 in relation to a single actuator, finds its most suitable application with multiple actuators. In systems with multiple actuators, the LS concept provides the advantages of low energy consumption and load-independent function control, almost with a plug-and-play architecture. This feature is behind the success of LS systems in many hydraulic applications, especially in the field of mobile equipment. For example, LS systems are used to control the implements of construction and agricultural machines, the booms of hydraulic cranes or aerial platforms, or the functions of truck mounted equipment.

Usually, the *LS principle*, applied to multiple actuators, refers to a family of solutions, each a different variant of the same concept and features different design details and functional enhancements. This chapter illustrates the basic principles of the most common LS architectures.

As in Part V, each design variant is presented as a basic concept and subsequently applied to a system including two single rod cylinders connected to a single hydraulic supply. This simple case can easily be generalized to more complex architectures, some of which are presented in the examples or in the end-of-chapter problems. The two main variants for the flow supply of an LS system are "with fixed displacement pump" or "with variable displacement pump," which have been illustrated in detail in Chapter 16. In this chapter, most hydraulic circuits will use either a variable or a fixed displacement pump.

21.1 Load Sensing Systems Without Pressure Compensation (LS)

21.1.1 Basic Circuit

The principle of a multi-actuator LS system is described with the schematic in Figure 21.1. Figure 21.1 is an extension of the single actuator circuit presented in Chapter 16. This was used to illustrate the LS regulation method with a variable displacement pump.

In Figure 21.1, the variable orifices O1 and O2 meter the flow to the two actuators U1 and U2. The shuttle valve SH selects p_{LS}, equal to the highest of the two load pressures:

$$p_{LS} = \max(p_{U1}, p_{U2}) \tag{21.1}$$

The p_{LS} signal is conveyed to the pump supply, i.e. to the differential pressure limiter of the variable displacement pump (as in Figure 21.1) or to the unloader valve, in the case of fixed displacement pump. The regulator sets the pump displacement to achieve the outlet pressure p_P, which is greater than the maximum load, by the value of the spring s:

$$p_P = p_{LS} + s \tag{21.2}$$
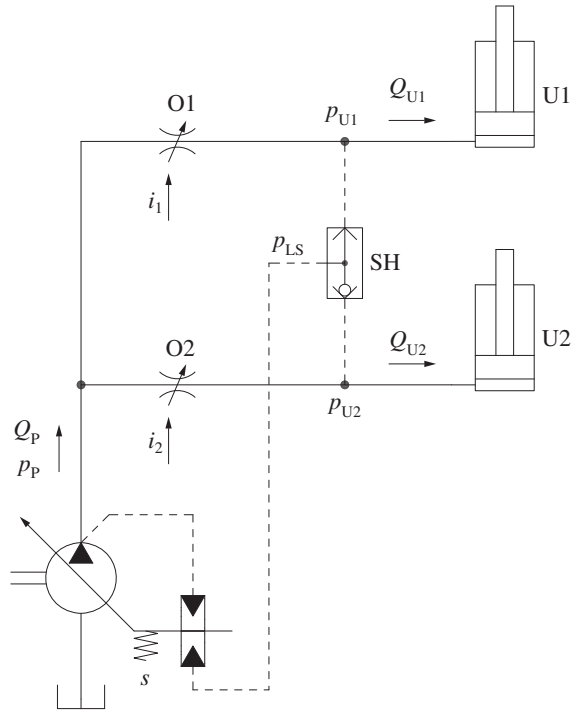
Figure 21.1 Principle of load sensing control of multiple actuator.

As defined in Chapter 16, *s* is the *LS margin pressure* setting of the variable displacement pump.

The speed of each actuator is proportional to the flow rate in the corresponding leg of the circuit, to Q_{U1} and Q_{U2}. The values of Q_{U1} and Q_{U2} can be calculated through the orifice equation applied to the metering orifices O1, O2:

$$Q_{U1} = C_f \cdot \Omega_{O1}(i_1) \cdot \sqrt{\frac{2(p_P - p_{U1})}{\rho}}$$
$$Q_{U2} = C_f \cdot \Omega_{O2}(i_2) \cdot \sqrt{\frac{2(p_P - p_{U2})}{\rho}}$$

(21.3)

As presented again in Chapter 16, the LS principle applied to the case of a single actuator ensures the flow rate sent to the actuator is a function only of the metering orifice area, which, in turn, is proportional to the operator command. In other words, the magnitude of the load does not affect the actuator speed[1]. In the case of multiple actuators, as in the system in Figure 21.1, the condition of load-independent flow is valid only for the actuator with the highest load. For example, assuming a load at U1 higher than the load at U2 ($p_{U1} > p_{U2}$), from Eq. (21.3):

$$Q_{U1} = C_f \cdot \Omega_{O1}(i_1) \cdot \sqrt{\frac{2s}{\rho}}$$

(21.4)

Therefore, the flow rate to U1 is univocally determined by the opening area of O1 and, of course, by the value of the margin pressure *s*. However, the actuator U2 with lower load is supplied with a flow rate equal to

$$Q_{U2} = C_f \cdot \Omega_{O2}(i_2) \cdot \sqrt{\frac{2[s + (p_{U1} - p_{U2})]}{\rho}}$$

(21.5)

---

1 As long as pressure or flow saturation conditions are not reached.

Equation (21.5) shows how the flow rate to U2 is a function of two variables: the opening area of O2, Ω_{O2}, and the difference between the two load pressures, $(p_{U1} - p_{U2})$. This latter represents the *load imbalance* between the two actuators, which leads to interference. In fact, the flow rate to the actuator U2 is higher than the theoretical value Q_{U2t}, which corresponds to the value calculated for the case of single actuator:

$$Q_{U2t} = C_f \cdot \Omega_{O2}(i_2) \cdot \sqrt{\frac{2s}{\rho}} \tag{21.6}$$

In the LS circuit as in Figure 21.1, U2 would receive the flow rate Q_{U2t} in case U2 had a load higher than U1 $(p_{U1} \geq p_{U2})$ or in case no flow was commanded to U1 $(i_1 = 0)$.

Load interference can be very significant with LS valves: the metering elements are usually designed to work over relatively low-pressure drops (i.e. the margin *s*). The value of the load imbalance $(p_{U1} - p_{U2})$ can assume values much higher than the margin *s* andthus can cause undesired accelerations of the functions (Example 21.1).

> In summary, for the basic LS circuit without pressure compensators, only the actuator with the highest load is always controlled at the theoretical flow value (determined by the area of the metering element). This load is also the one driving the pump pressure. All remaining actuators with lower loads will receive a flow rate higher than the theoretical values.

21.1.2 Energy Analysis

Figure 21.2 shows the operating points of the described system in the (p, Q) plane. The conditions assumed in the figure are that $p_{U1} > p_{U2}$ and also that $Q_{U1t} < Q_{U2t}$. The plot shows how the actuator with the lower load operates with a higher flow rate with respect to the theoretical case of single actuator, under the effect of the load imbalance. In Figure 21.2, the power transmitted by the system, the power request at the supply, and the power loss can be easily observed. In particular, the mechanical power transferred to the actuator (useful power) is given by

$$P_U = P_{U1} + P_{U2} = Q_{U1} \cdot p_{U1} + Q_{U2} \cdot p_{U2} \tag{21.7}$$

The losses in the metering elements of the systems are

$$P_L = Q_{U1} \cdot s + Q_{U2} \cdot (s + p_{U1} - p_{U2}) \tag{21.8}$$

The overall power consumed by the system equals the pump power:

$$P_P = P_U + P_L = (Q_{U1} + Q_{U2}) \cdot (p_{U1} + s) \tag{21.9}$$

Figure 21.2 Energy plot for the LS system of Figure 21.1 assuming $p_{U1} > p_{U2}$ and $Q_{U1} < Q_{U2t}$.

The energy efficiency of the system is given by the ratio between the useful and consumed power:

$$\eta_S = \frac{P_U}{P_P} = \frac{Q_{U1} \cdot p_{U1} + Q_{U2} \cdot p_{U2}}{(Q_{U1} + Q_{U2}) \cdot (p_{U1} + s)} \tag{21.10}$$

> The energy efficiency of the LS system depends on two important factors. First is the value of the LS margin: a higher LS margin reduces the system efficiency. The second factor affecting η_S is the load imbalance: for a given value of Q_{U2}, the greater the difference between the actuator pressures, the lower the system efficiency.

21.1.3 Valve Implementation and Extension to More Actuators

The conceptual schematic in Figure 21.1 is very useful to explain the basic principle of the LS regulation for the case of multiple actuators, because it highlights the metering orifices as separated elements. However, as it was already described in Chapter 16 for a single actuator, the function of each metering orifice is accomplished by a directional control valve, which also controls the direction of movement of the actuator (extension/retraction, in case of a cylinder). This element is usually referred as an LS valve. Figure 21.3 shows the detailed LS circuit for controlling two actuators.
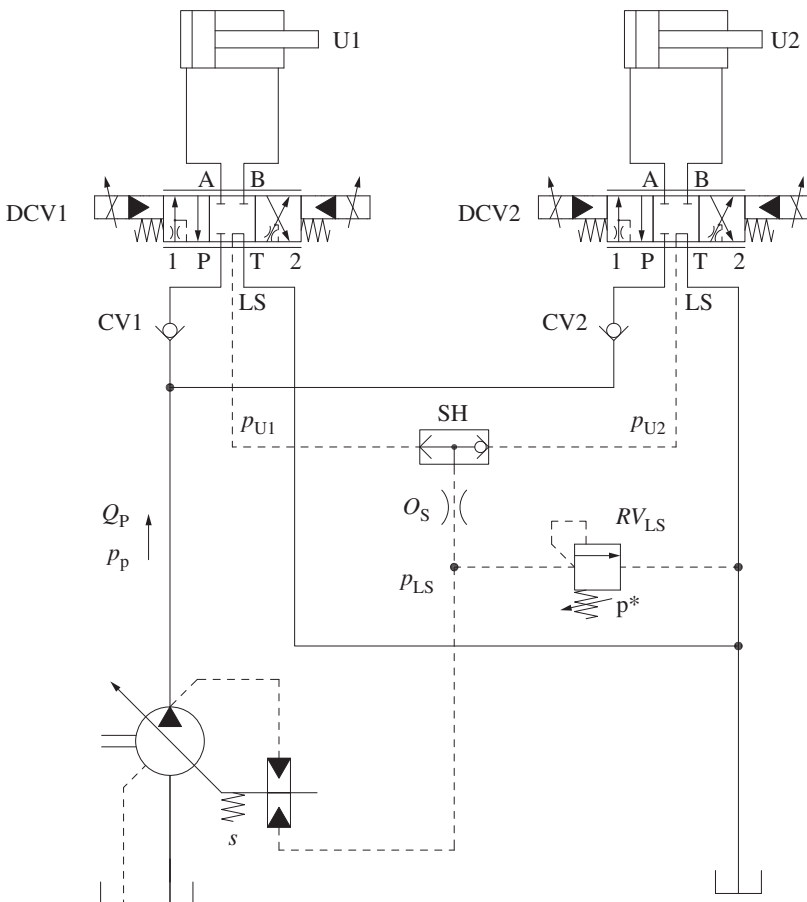

Figure 21.3 Multi-actuator LS system with LS pump and LS valve.
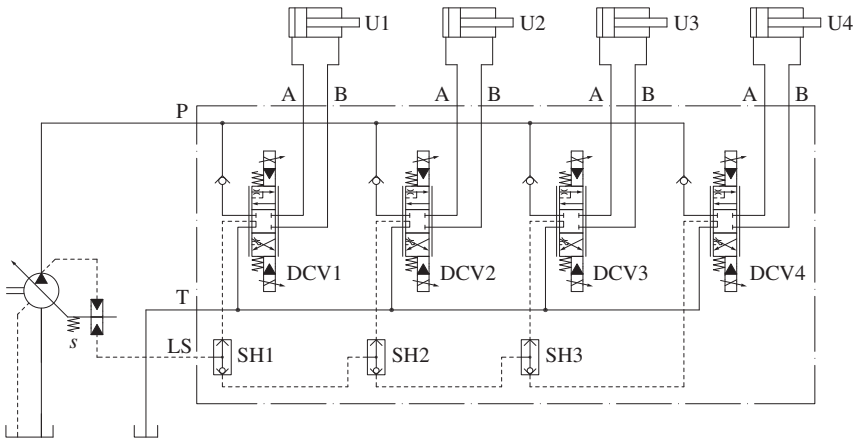
Figure 21.4 LS system with four actuators: the shuttle network comprises three elements used to select the highest load as signal to the LS pump.

In general, for N actuators, $N-1$, shuttle valves are required to select the highest actuator pressure to be sent to the pump as an LS signal. This can be realized with the cascade configuration shown in Figure 21.4. The shuttle valve at each valve section compares the pressure at the section with the resolved value of the previous ones.

Example 21.1   Load sensing system without pressure compensators

A mobile crane is used to move and position various loads. The three main functions of the crane are the boom, actuated by a hydraulic cylinder, and the swing and the winch, actuated by hydraulic motors. In this example, the operation of the winch is not considered for sake of simplicity.
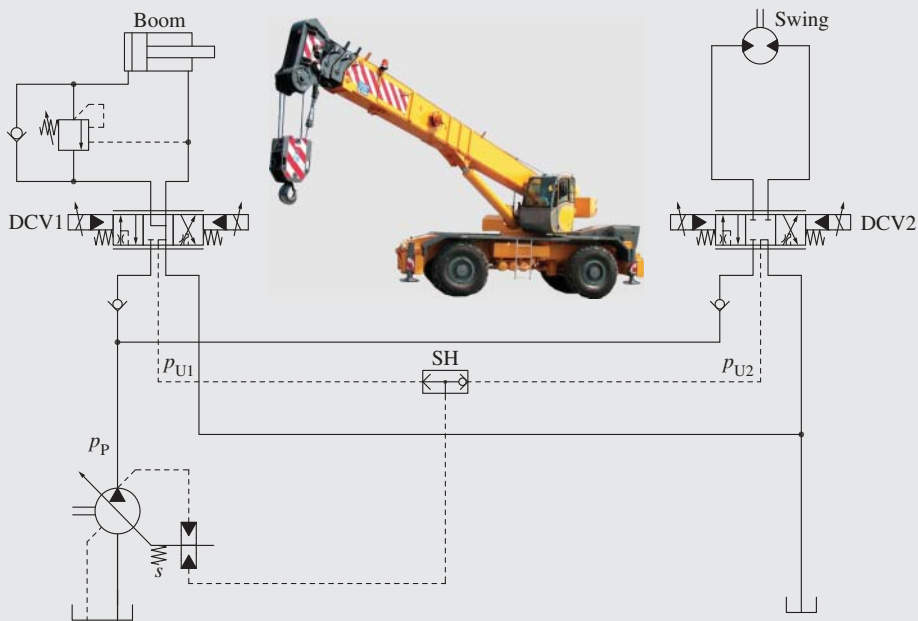
(Continued)

Example 21.1 (Continued)

A 75 cm^3/r load sensing variable displacement pump – limited to 300 *bar* – rotates at 1500 *rpm* and supplies the hydraulic system. The boom and swing functions are controlled with two load sensing proportional DCVs (DCV1 for boom, DCV2 for swing). The highest actuator load is selected with a shuttle valve (SH) and sent to the pump regulator through the LS line. The pump LS margin is 20 *bar*. The schematic of the system is given above.

In the first operating mode, the operator is positioning a load and moving the swing. In this situation the swing pressure at 75 *bar* and the spool of DCV2 open a metering area of 7 mm^2. Calculate the swing motor speed, given the motor displacement is 150 cm^3/r.

In the second mode, the operator, while keeping the swing joystick in the same position (i.e. DCV2), lifts the load to avoid an obstacle. The operator commands the boom extension by opening the spool of DCV1 with a metering area of 15.5 mm^2. The load imposes a lifting pressure equal to 225 *bar*. Calculate the swing speed under this operating condition.

To what value should the opening area of DCV2 be changed to maintain the same swing speed while lifting the boom?

Assume the oil density equal to 850 kg/m^3 and the orifice coefficient equal to 0.64.

Both the pump and the hydraulic actuators can be assumed as ideal units.

Given:
A LS system without pressure compensators supplied by a variable displacement pump, controlling two actuators: a differential cylinder (U1) and a hydraulic motor (U2).

System data: Pump maximum displacement, $V_p = 75$ cm^3/r; pump operating speed, $n_p = 1500$ *rpm*; swing motor displacement, $V_m = 150$ cm^3/r; pump LS margin, $s = 20$ *bar*; pump max pressure, p_{max} 300 *bar*; oil density, $\rho = 850$ kg/m^3; orifice coefficient, $C_f = 0.64$.

Operating modes:

Case 1: DCV1 in neutral position; DCV2 open with $\Omega_2 = 7$ mm^2; $p_{U2} = 75$ *bar*
Case 2: DCV1 open with $\Omega_1 = 15.5$ mm^2; DCV2 open with $\Omega_2 = 7$ mm^2; $p_{U1} = 225$ *bar*; $p_{U2} = 75$ *bar*
Case 3: DCV1 open; DCV2 open with $\Omega_2 = 7$ mm^2; $p_{U1} = 225$ *bar*; $p_{U2} = 75$ *bar*; swing speed $n_{m, case1} = n_{m, case3}$

Find:

Case 1: swing speed, $n_{m, case1}$
Case 2: swing speed, $n_{m, case1}$
Case 3: metering area Ω_1

Solution:
Case 1
According to Eqs. (21.1) and (21.14), the pump pressure equals: $p_p = p_{U2} + s = 75$ *bar* + 20 *bar* = 95 *bar*. The pressure drop across the metering area Ω_2 is 20 *bar*, so the flow to the swing actuator is (Eq. (21.3))

$$Q_{U2} = C_f \cdot \Omega_2 \cdot \sqrt{\frac{2(p_P - p_{U2})}{\rho}} = 0.64 \cdot 7 \cdot 10^{-6} \, [m^2] \cdot \sqrt{\frac{40 \cdot 10^5 \, [Pa]}{850 \left[\frac{kg}{m^3}\right]}} = 307 \cdot 10^{-6} \frac{m^3}{s}$$

$$= 18.4 \, l/min$$

The speed of the hydraulic motor becomes

$$n_{m,\text{case1}} = \frac{Q_m}{V_{D,m}} = \frac{18.4 \ [l/min]}{150 \ [cm^3/rev]} \cdot (1000) = 122 \ rpm$$

Case 2

According to Eqs. (21.1) and (21.14), the pump pressure equals: $p_p = \max(p_{U1}, p_{U2}) + s = 225 \ bar + 20 \ bar = 245 \ bar$. The pressure drop across the metering area Ω_1 is $20 \ bar$, so the flow to the boom actuator is (Eq. (21.3))

$$Q_{U1} = C_f \cdot \Omega_1 \cdot \sqrt{\frac{2(p_P - p_{U1})}{\rho}} = 0.64 \cdot 15.5 \cdot 10^{-6} \ [m^2] \cdot \sqrt{\frac{40 \cdot 10^5 \ [Pa]}{850 \left[\frac{kg}{m^3}\right]}}$$

$$= 680 \cdot 10^{-6} \frac{m^3}{s} = 40.8 \frac{l}{min}$$

Since the LS valve does not have compensators, $p_P - p_{U2} = 170 \ bar$ and the flow across Ω_2 equals

$$Q_{U2} = C_f \cdot \Omega_2 \cdot \sqrt{\frac{2(p_P - p_{U2})}{\rho}} = 0.64 \cdot 7 \cdot 10^{-6} \ [m^2] \cdot \sqrt{\frac{340 \cdot 10^5 \ [Pa]}{850 \left[\frac{kg}{m^3}\right]}} = 896 \cdot 10^{-6} \frac{m^3}{s} = 53.8 \frac{l}{min}$$

The swing motor speed becomes

$$n_{m,\text{case2}} = \frac{Q_m}{V_{D,m}} = \frac{53.8 \ [l/min]}{150 \ [cm^3/rev]} \cdot (1000) = 358 \ rpm$$

It is important to notice that the swing speed tripled with respect to the case 1!

Case 3

In order to maintain the same swing speed, the value of Ω_2 needs to be reduced to satisfy the following equation:

$$\Omega_2 = \frac{Q_{U2}}{C_f} \cdot \sqrt{\frac{\rho}{2(p_P - p_{U2})}} = \frac{307 \cdot 10^{-6} \left[\frac{m^3}{s}\right]}{0.64} \cdot \sqrt{\frac{850 \left[\frac{kg}{m^3}\right]}{340 \cdot 10^5 \ [Pa]}} = 2.4 \cdot 10^{-6} \ m^2 = 2.4 \ mm^2$$

This problem highlights that the load interference effect can cause unwanted and dangerous situations, particularly for load handling machines such as cranes, which operates heavy loads in proximity of obstacles or people. The system proposed in the example is not an acceptable design for such application! In other cases, such as tractor loader attachments, or compact earthmoving equipment the load interference phenomenon might not represent a relevant issue for the operators. In these cases, the LS system without compensators still represents an energy efficient and, at the same time, cost-effective solution.

21.2 Load Sensing Pressure Compensated Systems (LSPC)

Almost all hydraulic powered machines operate more than one actuator at the same time. Many applications also require an accurate and repeatable control of the simultaneous movements. For

systems that are affected by load interference, the operator can compensate for flow variation to a certain actuator by changing the input command. However, for some applications, this operator correction might not be sufficient, as in the case of the crane presented in Example 18.1. The LS concept explained in the previous section is not suited for these cases, because of the load interference effect that can lead to non-commanded speed changes of the load.

> When accurate control is required in a multi-actuator LS system, the load interference issue can be overcome using the pressure compensated load sensing pressure compensated (LSPC) system architecture. With this concept, the LS valve integrates the use of *compensators*.

In general, the compensator is a variable orifice positioned in series with the metering element of a LS valve. Compensators, during the simultaneous operation of multiple actuators, generate an additional restriction in the lines supplying the lower loads. They offset the pressure differences between the loads, eliminating the interference effect on the metering element.

LSPC metering valves are classified in two families, depending on the position of the compensator with respect to the metering element. In ***post compensated*** LS systems, the compensator is located downstream the metering element, while in ***pre compensated*** LS systems, the layout is opposite.

21.2.1 LSPC with Pre-compensated Valve Technology

Basic Circuit

Figure 21.5 shows the conceptual schematic of a pre-compensated LS system controlling two actuators (U1 and U2), with a variable displacement pump used as a flow supply. The figure uses the same notation used before in this chapter (Figure 21.1): O1 and O2 are the two metering elements and the shuttle valve SH selects the highest pressure between the two actuators.

Compensators C1 and C2 are represented as normally open 2/2 infinite positioning valves. They are located between the flow supply and the metering orifices. Each compensator spool is piloted by two pressures: the actuator pressure, p_U (p_{U1} or p_{U2}) acts on the opening side together with the spring s_C. The pressure upstream the metering orifice (and just downstream the compensator), p_X (p_{X1} or p_{X2}), acts on the closing side.

Therefore, the equation realized by each compensator is

$$p_X = p_U + s_C \tag{21.11}$$

Under this condition, the flow to each actuator can easily be calculated applying the orifice equation to O1 and O2:

$$
\begin{aligned}
Q_{U1} &= C_f \cdot \Omega_{O1}(i_1) \cdot \sqrt{\frac{2(p_{X1} - p_{U1})}{\rho}} = C_f \cdot \Omega_{O1}(i_1) \cdot \sqrt{\frac{2s_c}{\rho}} \\
Q_{U2} &= C_f \cdot \Omega_{O2}(i_2) \cdot \sqrt{\frac{2(p_{X2} - p_{U2})}{\rho}} = C_f \cdot \Omega_{O2}(i_2) \cdot \sqrt{\frac{2s_c}{\rho}}
\end{aligned}
\tag{21.12}
$$

Equation (21.12) clearly shows how the flow to both the actuators are independent of the load pressure, being a function of the orifice area commanded by the operator and the compensator spring s_c (which is constant). The load interference effect, which is present in the LS system without compensator, is now eliminated, and the flow rate to each actuator is well defined:

$$Q_U = Q_{Ut,pre} = C_f \cdot \Omega_O(i) \cdot \sqrt{\frac{2s_c}{\rho}} \tag{21.13}$$

This equation corresponds to the theoretical flow defined early in Eq. (21.6), with the only difference on the term under the square root (s_c instead of s).

It is interesting to observe how the compensator and the related variable orifice on each actuator line functions exactly as a pressure compensated two-way flow control valve, which was described in Chapter 8. This is also highlighted in Figure 21.5, with the "alternative" symbol indicated on the top part.

The operating condition described by Eqs. (21.11) and (21.12) is met because the LS pump ensures that:

$$p_P = p_{LS} + s \tag{21.14}$$

where s is greater than s_c so that p_P is greater than both p_{X1} and p_{X2}. In general, the pressure drop across each compensator is:

$$\Delta p_C = p_P - p_X = (p_P - p_U) - s_C = (p_{LS} - p_U) + (s - s_C) \tag{21.15}$$

In particular, under the assumption that the loads are such that $p_{U1} > p_{U2}$, and $p_{LS} = p_{U1}$, the pressure drop across the two compensators is:

$$\begin{aligned} \Delta p_{C1} &= s - s_C \\ \Delta p_{C2} &= (p_{U1} - p_{U2}) + (s - s_C) \end{aligned} \tag{21.16}$$
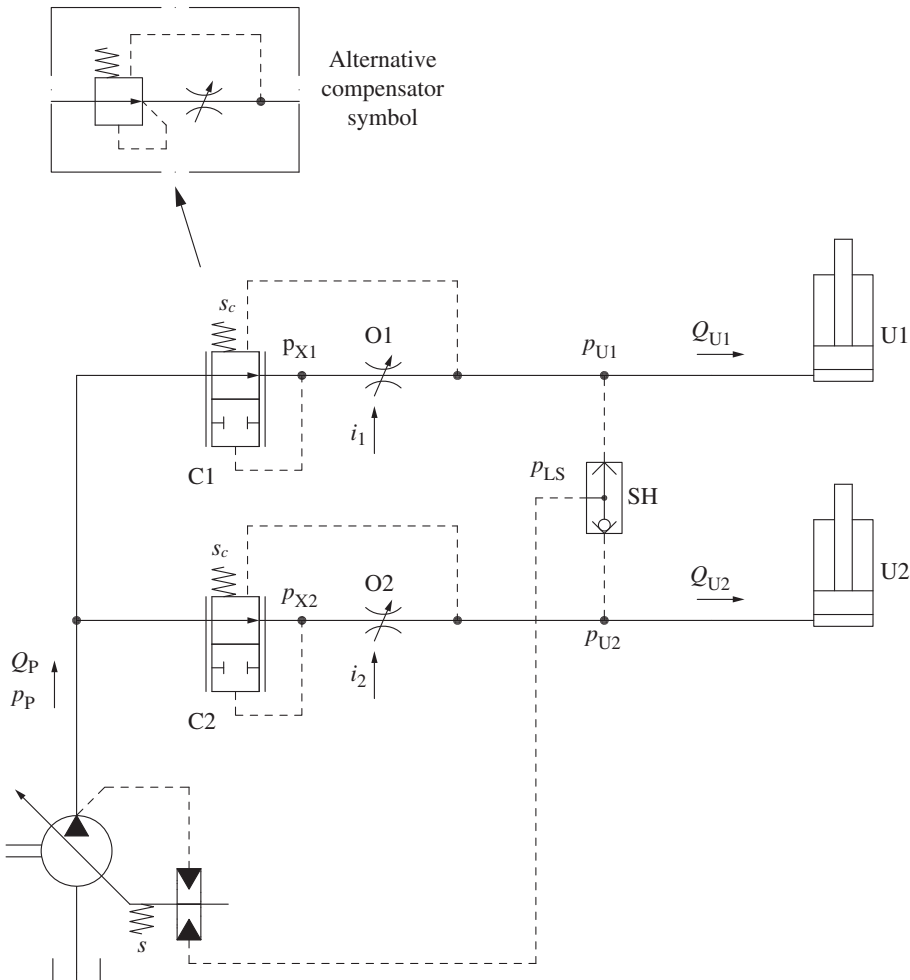

Figure 21.5 Simplified representation of the LSPC pre-compensated concept.
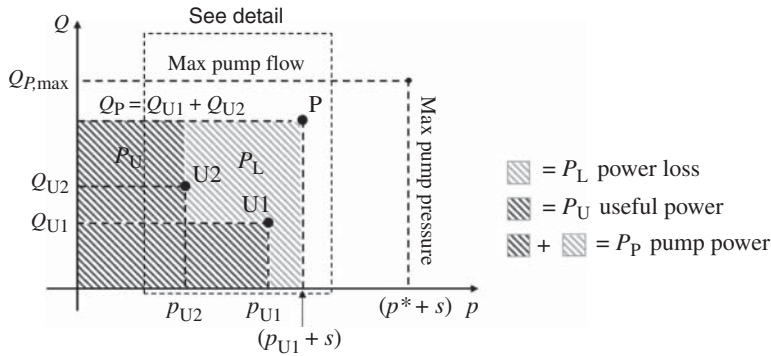
Figure 21.6 Energy plot for the pre-compensated LS system of Figure 21.5, assuming $p_{U1} > p_{U2}$ and $Q_{U1} < Q_{U2}$.
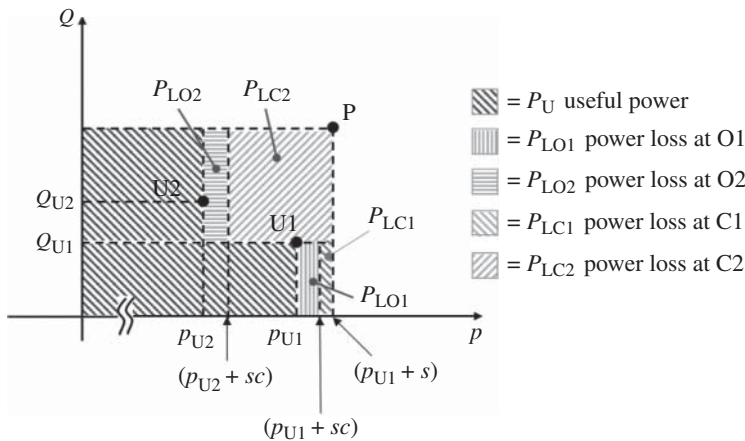

Figure 21.7 Detailed representation of the Power loss term for the pre-compensated LS system of Figure 38 (detail of Figure 21.6).

Energy Analysis

By knowing the pressure drops across the compensators (Eq. (21.16)), and considering that the pressure drop across the two metering orifices is $\Delta p_O = s_c$ (Eq. (21.12)), it is easy to describe the power consumption of the system. This can be shown graphically in Figure 21.6, which highlights the useful power, the power loss, and the power request at the flow supply and by Figure 21.7, which shows the detail of the various contributions to the total power loss.

The useful power is given by the same expression of Eq. (21.7) of the non-compensated LS system:

$$P_U = P_{U1} + P_{U2} = Q_{U1} \cdot p_{U1} + Q_{U2} \cdot p_{U2} \tag{21.17}$$

The losses now include the power consumed at the metering elements as well as those in the compensators:

$$P_L = P_{LO1} + P_{LO2} + P_{LC1} + P_{LC2} = Q_{U1} \cdot s_c + Q_{U2} \cdot s_c + Q_{U1} \cdot (s - s_c) + Q_{U2} \cdot$$
$$[(p_{U1} - p_{U2}) + (s - s_C)] = Q_{U1} \cdot s + Q_{U2} \cdot [(p_{U1} - p_{U2}) + s] \tag{21.18}$$

The overall power consumed by the system equals the pump power:

$$P_P = P_U + P_L = (Q_{U1} + Q_{U2}) \cdot (p_{U1} + s) \tag{21.19}$$

Finally, the energy efficiency of the system is given by the ratio between the useful and consumed power:

$$\eta_S = \frac{P_U}{P_P} = \frac{Q_{U1} \cdot p_{U1} + Q_{U2} \cdot p_{U2}}{(Q_{U1} + Q_{U2}) \cdot (p_{U1} + s)} \tag{21.20}$$

It can be noted that all power terms P_U, P_L, P_P, and consequently η_S for the pre-compensated LS system have the same expressions of the non-compensated LS system. However, while the pre-compensated solution ensures $Q_{U2} = Q_{U2t}$, for the non-compensated solution $Q_{U2} > Q_{U2t}$. This makes the result of Eq. (21.20) different from the results of Eq. (21.10) valid for the non-compensated solution.

Ideally, the value of s_c should be equal to the pump margin pressure s, to reduce the power loss in the system. However, it is always recommended to select s greater than s_c to ensure that the pressure upstream each compensator is equal or greater than $p_{LS} + s_C$. In fact, the losses occurring between the pump and the compensators in the real operation (losses in lines, fittings, internal passages in the valve housing, etc.) reduce the actual pressure at each compensator inlet. This can affect the correct operation of the system. Typical values for s_C range from 3 to 15 bar.

Valve Implementation and Architecture

Figure 21.8 shows the schematic of an actual LSPC system with pre-compensated valves. The symbols of the spools are the same as the ones shown for the non-compensated case (Figure 21.3). The only difference is given by the compensators C1 and C2 located before each DCV. The load-drop check valve functionality is usually accomplished by the compensator, which prevents the reverse flow in case the load pressure exceeded the pump pressure.

The same figure shows an extra feature of the pre-compensated LS valves: individual LS pressure relief valves can be added in the pilot line of each section, and they can be set to different pressure levels. In the case of Figure 21.8, RV_{LS} limits the maximum value of p_{LS} to p^*; instead RV_{LS2} is set to p_2^*, which is lower than p^*. This can be a convenient way of limiting the maximum supply pressure at each actuator to different values, without using in-line pressure relief valves. It is possible to observe that C2 acts in conjunction with RV_{LS2} similar to the example of the pilot operated pressure reducing valve presented in Figure 8.15. If the load pressure of the second actuator p_{U2} rises to the setting of the limiter p_2^*, the compensator C2 closes, reducing or, eventually blocking, the flow supply to U2. In the meanwhile, U1 continues its motion undisturbed.

Figure 21.9 shows an example of the architecture of a pre-compensated LS directional control spool valve and its equivalent schematic. In Figure 21.9, the spool, the load sense galleries, and reliefs (LS and work-port) are the same as in Figure 16.6, which referred to the case of a non-compensated LS valve. The design and operation of these elements follow the same description provided in the same chapter.

In Figure 21.9, the element that is different from the same valve presented in Chapter 16 is the compensator[2], with a detailed illustration in Figure 21.10. The compensator is a spool that operates over two metering edges: one implements the load drop check functionality and the other the compensator function. The spool position is determined by the action of the spring s_c aided by the LS pressure p_{LS} (acting on the left side) and by the pressure measured after the compensator notches p_Z, which is reported to the right side of the spool via a cross drilling.

In neutral position, for example, when the system is turned off, the compensator spool seats toward the right so that the load drop edge is closed and the edge that determines the compensator area is widely open. If the system is turned on, but the function is not energized (standby

---

2 The cross-section in Chapter 16 had simply a load drop check in the same cavity where here the compensator is housed. SImilar valve sections can be specified with or without compensator and assembled in a single valve unit.
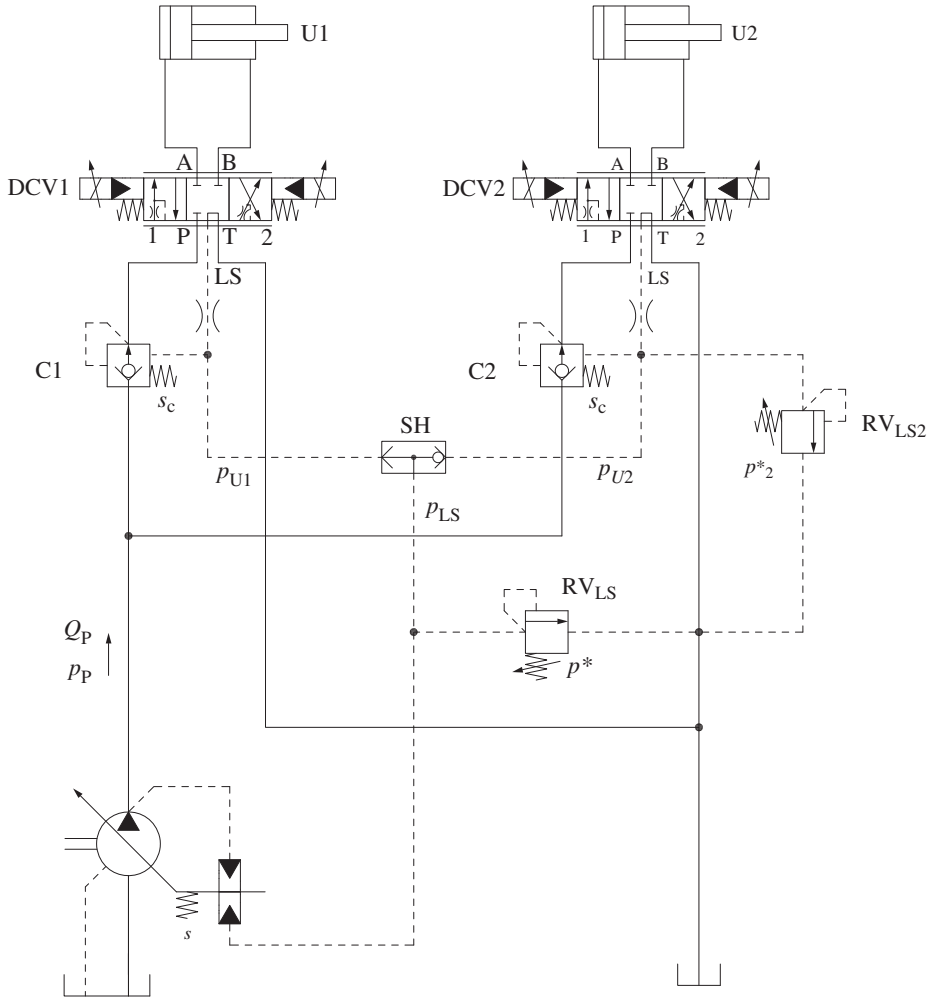
Figure 21.8 Multi-actuator pre-compensated PCLS system.

condition), p_Z equals the pump pressure, and p_{LS} is null. The load drop check area opens, while the compensator edge area reduces, to satisfy the relationship:

$$p_Z = s_c \tag{21.21}$$

When the function is energized, i.e. the main valve spool is shifted, p_{LS} equals the load pressure (denoted by p_U in Figures 21.5 and 21.8) and the compensator spool ensures the condition:

$$p_Z = p_{LS} + s_c \tag{21.22}$$

The compensator edge area is therefore an orifice operating as compensator (from here the general name of compensator for this valve). During its operation, the spool reduces the supply pressure p_P to the value p_Z, thanks to the action of the compensator metering edge and the compensator notches.

If the LS pressure increases above the value of p_Z, the compensator spool is shifted back to the neutral position preventing flow to go from the load into the P gallery of the valve. This situation can occur, for example, during flow saturation and it will be described later in this chapter.
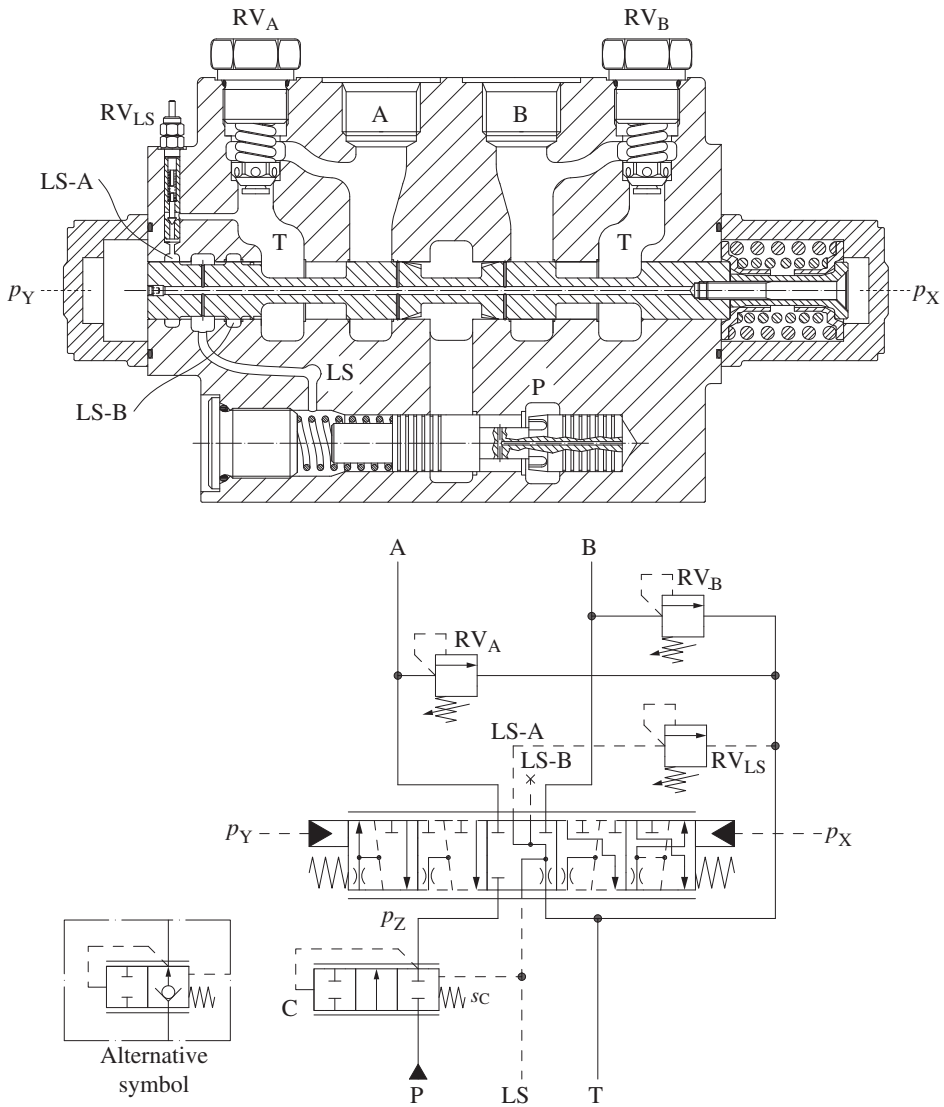
Figure 21.9 Cross-section and equivalent schematic of a pre-compensated directional control valve.
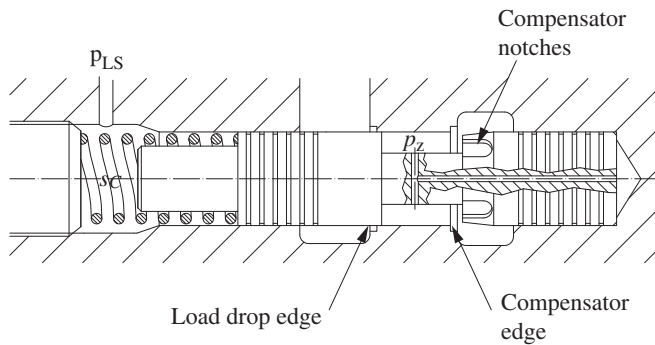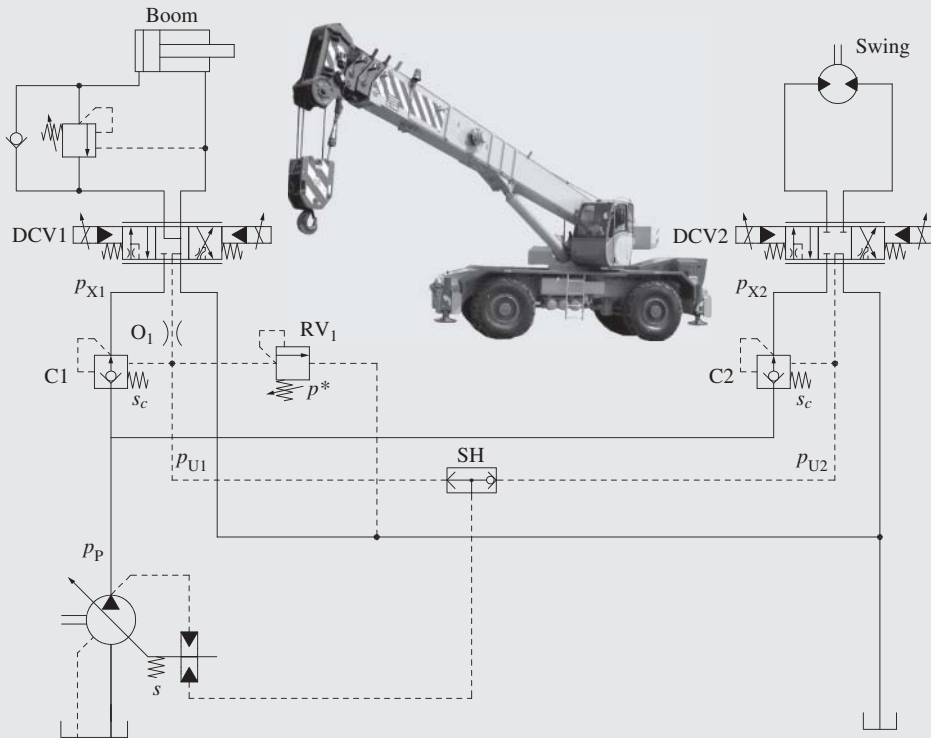

Figure 21.10 Detailed view of the compensator.

Example 21.2   Pre-compensated load sensing system

The same crane application presented in Example 21.1 is now controlled with an LSPC system utilizing a pre-compensated valve technology. The system schematic is represented below.

Also in this case, the system is supplied with a 75 cm^3/r load sensing variable displacement pump – pressure limited to 300 *bar* – rotating at 1500 *rpm*. The pump LS margin is 20 *bar*. The boom and swing functions are controlled with two load sensing proportional DCVs (DCV1 for boom, DCV2 for swing) equipped with pre-compensators.

In the valve, the setting of each compensator spring is 8 *bar*. The boom section is also equipped with an individual pressure limiter set to 260 *bar*.

In the first operating mode, the operator runs the 150 cm^3/r swing motor at 122 *rpm* at an operating pressure of 75 *bar*. Calculate the opening area of DCV2 to obtain such condition.

In the second operating mode, while the swing is running in the same condition as before, the operator runs the boom extension by opening the spool of DCV1 of a metering area of 15.5 mm^2. Knowing that the boom pressure is equal to 225 *bar*, calculate the flow to the boom cylinder and the swing flow in this new condition. How much is the pump power versus the useful power transmitted to the actuators in this condition? What is the system efficiency in this case?

Subsequently, in a different operation of the crane, the operator attempts to lift (swing is not moving) a heavy load, which would require 280 *bar* lifting pressure. Also in this case, the DCV1 is open with a metering area of 15.5 mm^2. What is the power consumption of the system during this operation?

Assume the oil density equal to 850 kg/m^3 and the orifice coefficient equal to 0.64. Pumps and motor are ideal units. The boom counterbalance valve has a cracking pressure setting of 350 *bar*. The diameter of the orifice O_1 is 0.8 *mm*.

Given:

An LSPC system with pre-compensated valves supplied by a variable displacement pump, controlling two actuators: a differential cylinder (U1) and a hydraulic motor (U2).

System data: Pump maximum displacement, $V_p = 75$ cm^3/r; pump operating speed, $n_p = 1500$ *rpm*; swing motor displacement, $V_m = 150$ cm^3/r; pump LS margin, $s = 20$ *bar*; compensator spring, $s_c = 8$ *bar*; pump max pressure, p_{max} 300 *bar*; oil density, $\rho = 850$ kg/m^3; orifice coefficient, $C_f = 0.64$.

Operating modes:

Case 1: DCV1 in neutral position; $p_{U2} = 75$ *bar*; $n_m = 122$ *rpm*
Case 2: DCV1 open with $\Omega_1 = 15.5$ mm^2; DCV2 open with $\Omega_2 = \Omega_{2, case1}$; $p_{U1} = 225$ *bar*; $p_{U2} = 75$ *bar*; $n_m = 122$ *rpm*
Case 3: DCV1 open with $\Omega_1 = 15.5$ mm^2

Find:

Case 1: DCV2 opening area Ω_2
Case 2: boom flow Q_{U1}; swing speed, $n_{m, case2}$; pump power P_P; useful power P_U; system efficiency η_S
Case 3: pump power P_P

Solution:
Case 1
The swing motor is running at 122 *rpm*, so the flow supplied to the motor is

$$Q_{U2} = n_m \cdot V_{D,m} = 122 \, rpm \cdot 150 \, [cm^3/rev] \cdot \left(\frac{1}{1000} \right) = 18.3 \, l/min$$

In the case of the pre-compensated valve, the flow across the spool is defined by compensator spring s_c. In other words, the pump sees an outlet pressure of $p_p = p_{U2} + s = 75$ *bar* + 20 *bar* = 95 *bar*; however, the compensator reduces the supply pressure to the spool of DCV2 to $p_{x2} = p_{U2} + s_c = 83$ *bar*. The opening area of Ω_2 becomes

$$\Omega_2 = \frac{Q_{U2}}{C_f} \cdot \sqrt{\frac{\rho}{2s_c}} = \frac{305 \cdot 10^{-6} \left[\frac{m^3}{s} \right]}{0.64} \cdot \sqrt{\frac{850 \left[\frac{kg}{m^3} \right]}{16 \cdot 10^5 \, [Pa]}} = 11 \cdot 10^{-6} \, m^2 = 11 \, mm^2$$

Case 2
When the boom is actuated with a pressure $p_{U1} = 225$ *bar*, the pump sees an outlet pressure equal to $p_p = \max(p_{U1}, p_{U2}) + s = 225$ *bar* + 25 *bar* = 245 *bar*. The compensator C1 reduces the supply pressure of DCV1 to the value $p_{x2} = p_{U1} + s_c$; therefore, the flow to the boom actuator becomes

$$Q_{U1} = C_f \cdot \Omega_1 \cdot \sqrt{\frac{2s_c}{\rho}} = 0.64 \cdot 15.5 \cdot 10^{-6} \, [m^2] \cdot \sqrt{\frac{16 \cdot 10^5 \, [Pa]}{850 \left[\frac{kg}{m^3} \right]}} = 430 \cdot 10^{-6} \frac{m^3}{s} = 25.8 \frac{l}{min}$$

(Continued)

Example 21.2 (Continued)

The compensator C2 still reduces the supply pressure of DCV2 to $p_{x2} = p_{U2} + s_c = 83$ *bar*, as in the previous condition. Therefore, the flow to the swing function remains equal to $Q_{U2,\,case1} = 18.3$ *l/min*, as the pressure drop across DCV2 remains $s_c = 8$ *bar*.

The total pump outlet flow equals the sum of the two actuator flows:

$$Q_P = Q_{U1} + Q_{U2} = 44.1 \; l/min$$

The pump power is

$$P_P = Q_P \cdot p_P = 44.1 \, [l/min] \cdot 245 \, [bar] \cdot \frac{1}{600} = 18.0 \; kW$$

The useful power becomes

$$P_U = Q_{U1} \cdot p_{U1} + Q_{U2} \cdot p_{U2} = \left(18.3 \left[\frac{l}{min} \right] \cdot 75 \, [bar] + 25.8 \left[\frac{l}{min} \right] \cdot 225 \, [bar] \right) \frac{1}{600}$$

$$= 12.0 \; kW$$

The system efficiency becomes

$$\eta_S = \frac{P_U}{P_P} = \frac{12 \, [kW]}{18 \, kW} = 66\%$$

Case 3

In this case, the operator shifts the spool of DCV1 and the system can produce a maximum lifting pressure limited to the setting of the individual pressure limiter RV_1. In other words, the LS pressure to the pump goes up to $p_{U1} = p^* = 260$ *bar*. Therefore, the outlet pump pressure is $p_p = 260 \; bar + 20 \; bar = 280 \; bar$. The pressure downstream the compensator C1 becomes $p_{x1} = p^* + s_c = 260 \; bar + 8 \; bar = 268 \; bar$. This is the pressure also seen in the lifting cylinder, which will not move because the supply pressure is not enough to lift the load. The pump will not deliver any flow to the function, except for the small flow discharged through the pressure separator orifice O1, which diameter is 0.8 *mm* (area $\Omega_O = 0.50 \; mm^2$):

$$Q_{U1} = C_f \cdot \Omega_O \cdot \sqrt{\frac{2s_c}{\rho}} = 0.64 \cdot 0.5 \cdot 10^{-6} \, [m^2] \cdot \sqrt{\frac{16 \cdot 10^5 \, [Pa]}{850 \left[\frac{kg}{m^3} \right]}} = 13.9 \cdot 10^{-6} \frac{m^3}{s} = 0.8 \frac{l}{min}$$

The power consumption of the pump in this case is

$$P_P = Q_P \cdot p_P = 0.8 \, [l/min] \cdot 280 \, [bar] \cdot \frac{1}{600} = 0.4 \; kW$$

21.2.2 LSPC with Post-Compensated Valve Technology

LSPC with post-compensated technology represents an alternative architecture to overcome the load interference issue. Post-compensated valves can sometimes be an alternative to pre-compensated ones. However, they present some different characteristics, which will be analyzed in the following sections.
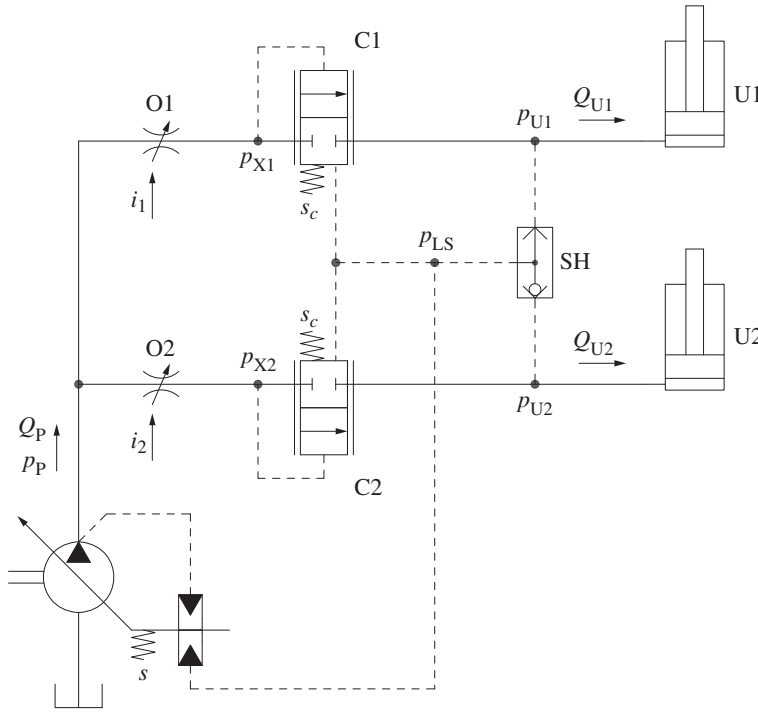
Figure 21.11 Simplified representation of the LSPC post compensated concept.

Basic Circuit

The basic concept of LSPC system with post-compensators is represented in Figure 21.11. As in Figure 21.1 (basic LS system) and Figure 21.5 (basic LS system with pre-compensators), O1 and O2 indicate the metering elements, and the shuttle valve SH is used to select the highest load pressure to use as LS signal for the flow supply.

The two compensators C1 and C2 are now located between the actuators and the metering orifices. In the post-compensated architecture, the compensators are normally closed 2/2 infinite positioning valves. The upstream pressure p_X (p_{X1} or p_{X2}) is used to pilot the opening of the compensator, while and the highest load pressure p_{LS} pilots the closing, together with the spring s_C.

The equation realized by each compensator is

$$p_X = p_{LS} + s_C \tag{21.23}$$

When both actuators are moving at the same time, under the assumption that U1 is the highest of the two loads, the LS resolved pressure is $p_{LS} = p_{U1}$ and, therefore, the pump outlet pressure is $p_P = p_{U1} + s$.

Both C1 and C2 compensators impose the condition of Eq. (21.23) in their lines; therefore, the pressures at the two points X1 and X2 equally become

$$p_{X1} = p_{X2} = p_{U1} + s_C \tag{21.24}$$

In turn, the flow rates Q_{U1} and Q_{U2} become

$$Q_{U1} = C_f \cdot \Omega_{O1}(i_1) \cdot \sqrt{\frac{2(s - s_C)}{\rho}}$$

$$Q_{U2} = C_f \cdot \Omega_{O2}(i_2) \cdot \sqrt{\frac{2(s - s_C)}{\rho}}$$

$$(21.25)$$

Equation (21.25) demonstrates how this type of LSPC system eliminates the load interference effect between multiple actuators working at different pressures. In fact, both flow rates are independent of the pressure values being only function of the area opening of the metering orifices, i.e. of the operator command:

$$Q_U = Q_{Ut,\text{post}} = C_f \cdot \Omega_O(i) \cdot \sqrt{\frac{2(s - s_C)}{\rho}} \tag{21.26}$$

As shown in Eq. (21.26), the relation for the actuator flow in the post-compensated LSPC differs from the case of the basic, non-compensated LS system (Eq. (21.27)), where s is the pressure differential term inside the square root function. It differs also from the case of the pre-compensated solution (Eq. (21.13)), where s_c is the pressure differential term.

In the line supplying U2, the lowest of the two loads, the compensator C2 throttles the flow and then realizes a pressure drop Δp_{C2} that compensates the load imbalance between the two actuators:

$$\Delta p_{C2} = p_{X2} - p_{U2} = p_{U1} - p_{U2} + s_C \tag{21.27}$$

In the other line supplying U1, the compensator C1 instead realizes a pressure drop Δp_{C1} equal to the spring setting:

$$\Delta p_{C1} = p_{X1} - p_{U1} = s_C \tag{21.28}$$

Energy Analysis
The energy plot of the post-compensated LS system of Figure 21.11 is shown in Figure 21.12. If the same conditions are assumed for the pre-compensated solution of Figure 21.5, the two plots look identical. However, as highlighted by the detail of Figure 21.13, the breakdown of the power losses through the metering orifices and the compensator is different for the post-compensated solution, with respect to the pre-compensated arrangement (Figure 21.7).

The useful power, the power loss, and the pump power terms have the same expressions presented before for both the non-compensated LS system and for the pre-compensated solution:

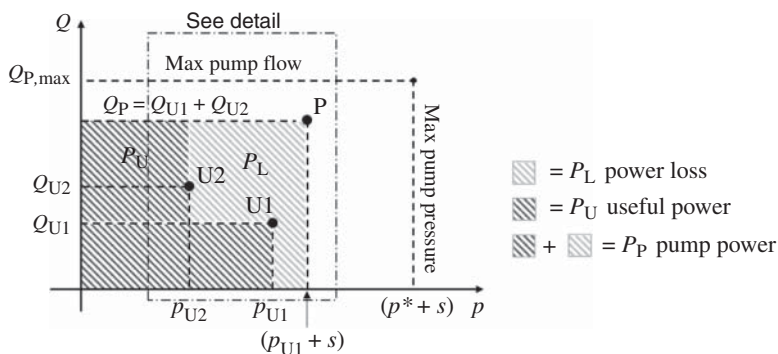$$P_U = P_{U1} + P_{U2} = Q_{U1} \cdot p_{U1} + Q_{U2} \cdot p_{U2} \tag{21.29}$$

Figure 21.12 Energy plot for the post compensated LS system of Figure 21.11, assuming $p_{U1} > p_{U2}$ and $Q_{U1} < Q_{U2}$.
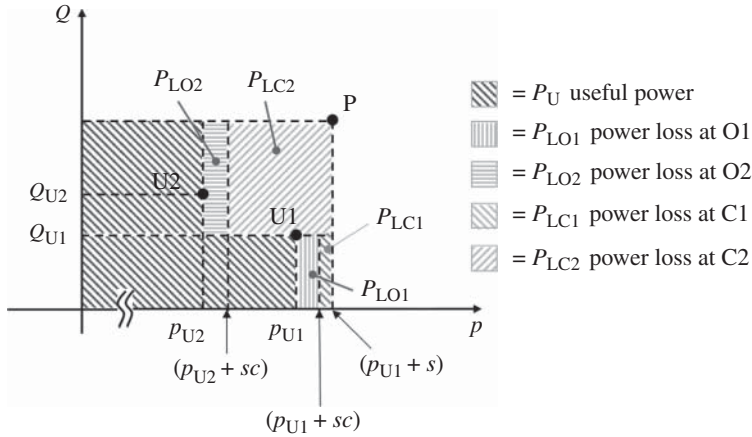
Figure 21.13 Detailed representation of the Power loss term for the post-compensated LS system in Figure 21.11, detail of Figure 21.12.

The losses now include the power consumed in the metering elements as well as those in the compensators:

$$P_L = Q_{U1} \cdot s + Q_{U2} \cdot [(p_{U1} - p_{U2}) + s] \tag{21.30}$$

The overall power consumed by the system equals the pump power:

$$P_P = P_U + P_L = (Q_{U1} + Q_{U2}) \cdot (p_{U1} + s) \tag{21.31}$$

Consequently, the energy efficiency of the system is given again by

$$\eta_S = \frac{P_U}{P_P} = \frac{Q_{U1} \cdot p_{U1} + Q_{U2} \cdot p_{U2}}{(Q_{U1} + Q_{U2}) \cdot (p_{U1} + s)} \tag{21.32}$$

> In terms of system efficiency, there is no difference between the different LS system solutions presented so far, which used different compensator architectures (pre or post).

From a theoretical point of view, the value of s_C could be null: the compensator could implement this function even without this spring element. In reality, a very soft spring is used to ensure the return in neutral (closed) position once the function is turned off. Usually the value of s_C is in the neighborhood of 0.5–3 bar, and it is often neglected in the flow calculations (Eq. (21.26)). Under this assumption, the pressure drop impressed by C1 is negligible; in other words, the compensator associated with the highest load stays in the fully open position.

Valve Implementation and Architecture

Figure 21.14 shows the typical schematic of an LSPC post compensated valve and highlights its enabling architecture. The metering control element are two directional control valves, DCV1 and DCV2. These are 6/3 infinite positioning spool valves with, in this case, electrohydraulic proportional actuation. The detailed view in the same figure depicts the six ports: P is the supply, T is the tank, A and B are the work-ports, and X and U are internal flow passages. From the schematic one can immediately notice how, when the spool is energized, the flow from the pump to the actuator crosses the spool twice: initially from P to X and then from U to the selected work-port. In the first passage (P → X) the spool realizes the metering area that controls the flow to the function (equivalent to orifices O1 and O2 of Figure 21.11). This area is proportional to the spool stroke.
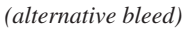
Figure 21.14 Schematic of a two section post compensated valve.

After exiting port X, the flow goes through the compensator (C1 or C2). Downstream the compensator, the load pressure is connected to the shuttle valve SH, which selects the highest load. After this point, the flow passes through the load drop check valve (CV1 or CV2) and returns to the spool port U. Finally, depending on the direction the spool is shifted, the flow is diverted to the work-port A or B. An aspect to notice is that this second passage U → A or U → B shall not create any restriction to the flow. It is a design feature to simply achieve both the metering and the directional control in a single spool.

In Figure 21.14 there are three relief valves. RV_{LS} is the signal relief in the LS line and limits the max system pressure to $p_{max} = p^* + s$. This works in conjunction with the pressure separator orifice O_S. The maximum pressure supplied to the actuator U1 then becomes $(p^* - s_C)$. Vice versa, actuator U2 is equipped with port reliefs RV_A and RV_B, which are used to limit the actuator pressure to a different value. The necessity of using port relief valves, instead of relief valves in pilot lines (as it was seen in the case of the pre-compensated LS solution, Figure 21.8) is one of the significant differences between pre-compensated and post-compensated LS architectures. In fact, in the post-compensated solution each compensator uses the highest load pressure (i.e. the selected LS pressure signal) – instead of the actuator pressure – to control its opening area. Therefore, it is not possible to limit the actuator pressure by limiting the pressure the pilot signal controlling the compensation closure.

Another important feature of the post compensated LSPC is represented by the orifice O_B. This is a bleed orifice located between the LS line and the tank. The function of this orifice is to relieve

the LS pressure when the DCVs return to a neutral position. In fact, the spool port U is closed in such position and the load pressure p_U can remain trapped in the line from U to the pump LS port. Unfortunately, the orifice O_B also bleeds oil during regular operation and the flow loss across it can be significant when the operating pressure gets high. In many cases, O_B is replaced with a pressure compensated flow control valve discharging a small flow rate to tank. This is represented in Figure 21.14 and labeled as FCV (alternative bleed). The flow discharged to tank by FCV becomes independent on the LS pressure value.

Figure 21.15 represents an example of post compensated valve architecture. The spool can connect or block a number of different galleries in the valve housing. As usual, P is connected to the
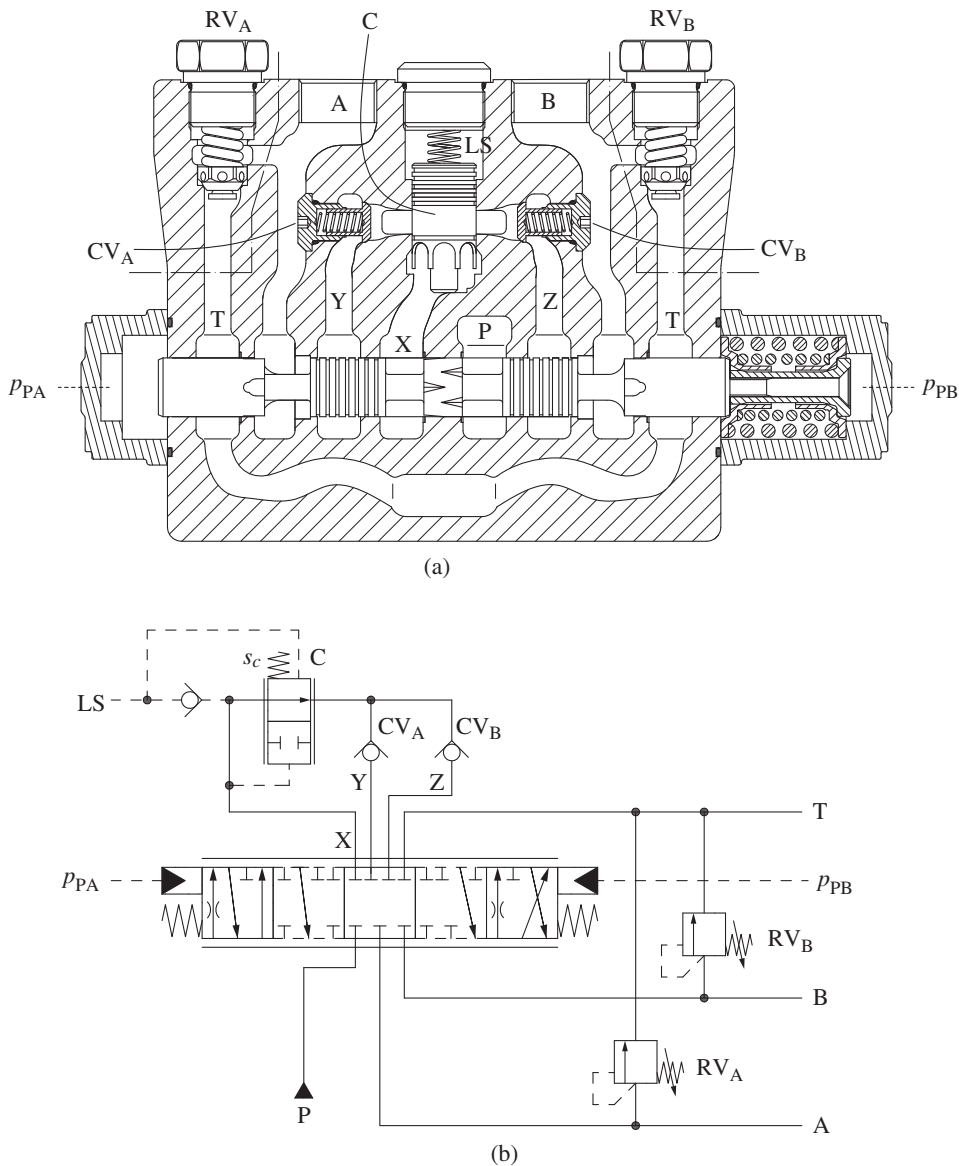

(a)

(b)

Figure 21.15 Section view of a post-compensated proportional directional control valve (a), ISO schematic (b).

pump outlet, T to the tank and A and B to the two work-ports. When the pilot pressure p_{PA} is applied, the spool shifts toward the right. The triangular notches located on the X side open a connection between chamber P and X. The flow passing through X encounters the compensator C, which is housed in a bore perpendicular to the spool. The compensator is a normally closed element, where the LS pressure p_{LS} acts on the top, together with a soft spring (with equivalent pressure setting s_C). The pressure in the chamber X (p_x) pushes the compensator upward, until the semicircular notches open a flow path in the perpendicular direction, toward the two check valves CV_A and CV_B. The compensator equilibrium realizes the pressure balance of Eq. (21.23) ($p_x = p_{LS} + s_C$).

After passing the compensator, the flow goes to the chambers Y and Z, through the check valves CV_A and CV_B, which implement the load drop check functionality. However, since the spool is shifted to the right, the spool still blocks the chamber Z, while chamber Y is connected to work-port A. On the opposite side, work-port B is connected to the tank through the spool circular notches.

It is important to remark how the supply flow goes through the spool twice, before reaching the work-port. The first passage is from P to X, which realizes the metering function, where the metering area is defined by the triangular notches. The second passage (Y to A) defines the direction of the flow to the actuator work-port, and it occurs at a much larger annular flow area, defined by the spool travel. The pressure drop across this area represents a loss, usually negligible.

When the opposite pilot pressure is generated (p_{PB}), the spool moves to the left. The flow goes from P to Z through the triangular notches located on the P side. After that, it passes through CV_B and Z before reaching the work-port B.

Example 21.3   Post-compensated load sensing system

The same crane application presented in the previous Examples 21.1 and 21.2 is now controlled with a LSPC system utilizing a post-compensated valve technology. The system schematic is represented below.

Also in this case, the system is supplied with a 60 cm^3/r load sensing variable displacement pump – pressure limited to 300 bar – rotating at 1500 rpm. The pump LS margin is 20 bar. The boom and swing functions are controlled with two load sensing proportional DCVs (DCV1 for boom, DCV2 for swing) equipped with post-compensators equipped with a 2 bar spring.

In the valve, the boom section is also equipped with a relief valve limiting the maximum lifting pressure limiter to 260 bar.

In the first operating mode, the operator runs the 150 cm^3/r swing motor at 250 rpm at an operating pressure of 75 bar. At the same time, the boom extension is run by opening the spool of DCV1 of a metering area of 15.5 mm^2. The boom lifting pressure is equal to 225 bar. Calculate the opening area of DCV2 and the flow resulting to the boom actuator. How much is the pump power vs. the useful power transmitted to the actuators in this condition? What is the system efficiency in this case?

Subsequently, the operator attempts to lift (swing is not moving) a different load, which would require 280 bar lifting pressure. Also in this case DCV1 is open with a metering area of 15.5 mm^2. What is the power consumption of the system during this operation?

Assume the oil density equal to 850 kg/m^3 and the flow coefficients across the spool area equal to 0.64. All hydraulic components can be assumed as ideal. The counterbalance valve installed at the boom has a cracking pressure setting of 350 bar. The diameter of orifice O_B is 0.6 mm, for which the flow coefficient is 0.7.
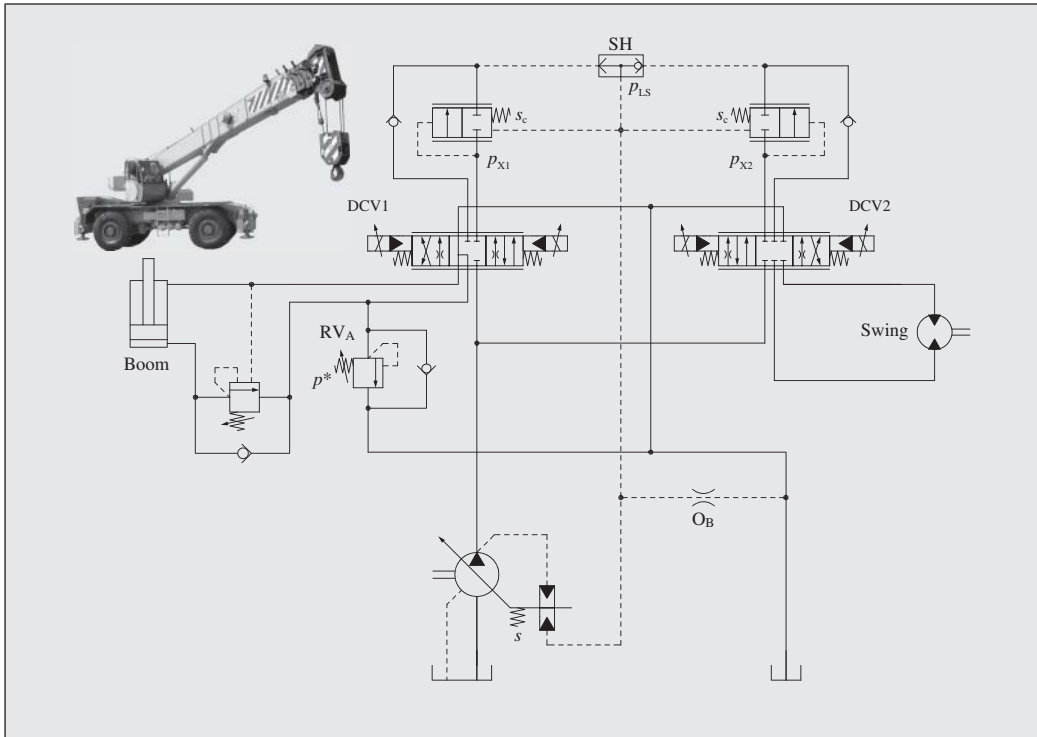
Given:

An LSPC system with post-compensated valves supplied by a variable displacement pump, controlling two actuators: a differential cylinder (U1) and a hydraulic motor (U2).

System data: pump maximum displacement, $V_p = 60 \ cm^3/r$; pump operating speed, $n_p = 1500 \ rpm$; swing motor displacement, $V_m = 150 \ cm^3/r$; pump LS margin, $s = 20 \ bar$; compensator spring, $s_c = 2 \ bar$; pump max pressure, p_{max} 300 bar; oil density, $\rho = 850 \ kg/m^3$; orifice coefficient, $C_f = 0.64$; bleed orifice diameter, $d_B = 0.6 \ mm$; orifice coefficient for OB, $C_f = 0.7$.

Operating modes:

Case 1: DCV1 opens with $\Omega_1 = 15.5 \ mm^2$; DCV2 open; $p_{U1} = 225 \ bar$; $p_{U2} = 75 \ bar$; $n_m = 250 \ rpm$; $n_P = 1500 \ rpm$

Case 2: DCV1 opens with $\Omega_1 = 15.5 \ mm^2$; maximum boom pressure $p^* = 260 \ bar$.

  Find:

Case 1: DCV2 opening area Ω_2, boom flow Q_{U1}; pump power P_P; useful power P_U; system efficiency η_S

Case 2: pump power P_P

Solution:

Case 1

The swing motor is running at 250 rpm, therefore the flow supplied to the motor is

$$Q_{U2} = n_m \cdot V_{D,m} = 250 \ [rpm] \cdot 150 \left[\frac{cm^3}{rev} \right] \cdot \left(\frac{1}{1000} \right) = 37.5 \ l/min$$

Example 21.3 (Continued)

In the case of the post-compensated valve, the flow across the swing spool DCV2 is defined by the difference between the pump pressure and pressure p_{x2}. The value of p_{x2} is imposed by the compensator that implements the equation: $p_{x2} = p_{LS} + s_c$. The value of $p_{LS} = \max(p_{U1}, p_{U2})$. In this case, $p_{LS} = 225\ bar$, $p_P = 245\ bar$, and $p_{x2} = 227\ bar$. The area opening Ω_2 becomes

$$\Omega_2 = \frac{Q_{U2}}{C_f} \cdot \sqrt{\frac{\rho}{2(s - s_c)}} = \frac{625 \cdot 10^{-6}\ \left[\frac{m^3}{s}\right]}{0.64} \cdot \sqrt{\frac{850\ \left[\frac{kg}{m^3}\right]}{36 \cdot 10^5\ [Pa]}} = 15 \cdot 10^{-6}\ m^2 = 15\ mm^2$$

For the same reason, the flow to the boom extension is

$$Q_{U1} = C_f \cdot \Omega_1 \cdot \sqrt{\frac{2(s - s_c)}{\rho}} = 0.64 \cdot 15.5 \cdot 10^{-6}\ [m^2] \cdot \sqrt{\frac{36 \cdot 10^5\ [Pa]}{850\ \left[\frac{kg}{m^3}\right]}} = 645 \cdot 10^{-6}\frac{m^3}{s}$$

$$= 38.7\frac{l}{min}$$

One important thing to notice is that Q_{U1} is the flow going through the spool of DCV1. However, not all this flow reaches the actuator. In fact, a portion of this flow is lost through the bleed orifice O_B on the LS line. This orifice has a diameter of 0.6 *mm*, corresponding to an area $\Omega_O = 0.28\ mm^2$. The flow lost through the bleed is equal to

$$Q_O = C_f \cdot \Omega_O \cdot \sqrt{\frac{2 \cdot p_{U1}}{\rho}} = 0.7 \cdot 0.28 \cdot 10^{-6}\ [m^2] \cdot \sqrt{\frac{225 \cdot 10^5\ [Pa]}{850\ \left[\frac{kg}{m^3}\right]}}$$

$$= 31.9 \cdot 10^{-6}\frac{m^3}{s} = 1.9\frac{l}{min}$$

Therefore, the flow that reaches the boom actuator is

$$Q_{boom} = Q_{U1} - Q_O = 36.8\ l/min$$

The pump outlet flow equals the sum of the Q_{U1} and Q_{U2}:

$$Q_P = Q_{U1} + Q_{U2} = 76.2\ l/min$$

In this condition, the power requested by the pump is

$$P_P = Q_P \cdot p_P = 76.2\ [l/min] \cdot 245\ [bar] \cdot \frac{1}{600} = 31.1\ kW$$

Instead, the useful power provided to the actuators is

$$P_U = Q_{boom} \cdot p_{U1} + Q_{U2} \cdot p_{U2} = \left(37.5\ \left[\frac{l}{min}\right] \cdot 75\ [bar] + 36.8\ \left[\frac{l}{min}\right] \cdot 225\ [bar]\right)\frac{1}{600}$$

$$= 18.5\ kW$$

The system efficiency becomes

$$\eta_S = \frac{P_U}{P_P} = \frac{18.5\ [kW]}{31.1\ [kW]} = 59.5\%$$

Case 2

In this case, the swing is not running and the operator attempts to lift a load that requires a system pressure above the maximum limit imposed by RV_A. In this case, DCV2 produces the

same flow calculated for case 1 and the boom lift cylinder pressure is limited to the value of $p^* = 260$ *bar* by the port relief. In other words, the pump flow is

$$Q_P = Q_{U1} = 38.7 \ l/min$$

The pump pressure is $p_P = p_{U1} + s = 260 \ bar + 20 \ bar = 280 \ bar$. The pump power is

$$P_P = Q_P \cdot p_P = 38.7 \ [l/min] \cdot 280 \ [bar] \cdot \frac{1}{600} = 18.1 \ kW$$

As one can easily observe, this value is much higher than the power required to the pump in the case of a pre-compensated solution (Example 21.2), where the pump outlet flow is negligible.

21.3 Flow Saturation and Flow Sharing in LS Systems

As also previously mentioned, flow saturation is a condition that occurs when the theoretical combined flow demand of the actuators is higher than the maximum flow the supply can provide. Although one can think that flow saturation is an undesired condition that should be avoided when designing a hydraulic system, many hydraulic circuits are designed to properly handle flow saturation. For example, in an excavator, several hydraulic functions (e.g. boom, bucket, and dipper) can individually demand all the pump flow. Therefore, when they run simultaneously, flow saturation is very easily reached. Sometimes the loss of control of some functions during saturation is acceptable (or can be corrected by the operator) or undesired. In this latter case, a helpful feature for the hydraulic system is the so-called *flow sharing*.

Flow sharing implies that, during flow saturation events, the operation of all commanded functions is maintained at a lower speed. The pump flow is divided between the actuators proportionally to the operator commands.

In some sizing problems, flow sharing can permit to maintain the full functionality of the machine, limiting the pump size and consequently the power request at the prime mover.

The LS circuits previously introduced in this chapter have different behaviors under flow saturation conditions, and different ways of implementing flow sharing. For the sake of clarity, all considerations will be made with reference to the simplified schematics using orifices instead of spools. However, these considerations apply also to more complex schematics.

21.3.1 Flow Saturation with Pre-Compensated LSPC

With reference to Figure 21.16, the saturation condition is reached when

$$Q_{U1t,pre} + Q_{U2t,pre} > Q_{P,\max} \tag{21.33}$$

The system is described by calculating how the pump flow splits between the two actuators. Among the multiple possible combinations of flow demands and loads, the system is first described under the following assumptions:

$$Q_{U1t,pre} < Q_{P,\max}$$
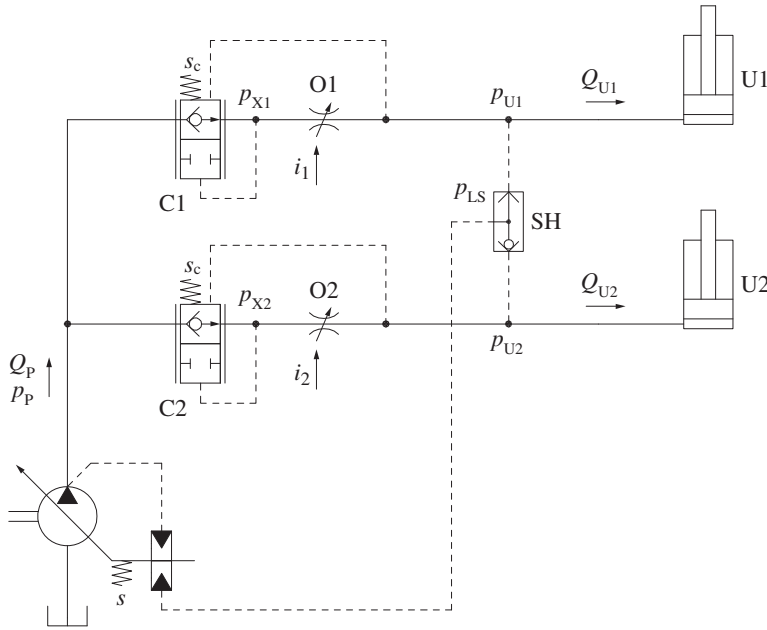$$Q_{U2t,pre} < Q_{P,\max} \tag{21.34}$$
$$p_{U1} > p_{U2}$$

Figure 21.16 Basic circuit for the pre-compensated LSPC.

It is important to remark that Eq. (21.34) states that each theoretical flow demand cannot individually exceed the available pump flow. In this case, the LS signal sent to the pump equals the highest load, $p_{LS} = p_{U1}$. The differential pressure limiter of the pump sets the displacement to the maximum. However, the condition $p_P = p_{LS} + s$ cannot be met because the flow demand is higher than $Q_{P,max}$. This was also observed in Chapter 16, when the flow saturation was analyzed for the case of a LS system with a single actuator.

The pump pressure is

$$p_P = p_{LS} + \Delta p_x \tag{21.35}$$

where $\Delta p_x < s$. This value of p_P allows meeting the theoretical LS flow demand at actuator U2, at the lower pressure. In fact, the compensator C2 operates under the pressure drop:

$$\Delta p_{C2} = p_P - (p_{U2} - s_c) \tag{21.36}$$

while the metering orifice O2 operates under the theoretical pressure drop s_c, which satisfies the equation for $Q_{U2t, pre}$, Eq. (21.13).

Consequently, the flow to U1 is lower than the theoretical value $Q_{U1t, pre}$, and equals

$$Q_{U1} = Q_{P,max} - Q_{U2t,pre} \tag{21.37}$$

The compensator C1 is fully open, resulting in the pressure drop across the control orifice O1 being lower than s_c.

The pressure drop across O1 becomes

$$\Delta p_{O1} = p_P - p_{U1} = \Delta p_x \tag{21.38}$$

By combining the last two equations, considering also the orifice equation, the expression of the pressure drop across the control orifice O1, $\Delta p_{O1} < s_c$, can be found as

$$\Delta p_{O1} = \Delta p_x = \frac{\rho}{2}\left(\frac{Q_{P,max} - Q_{U2t,pre}}{c_f \Omega_{O1}}\right)^2 \tag{21.39}$$

The orifice O1, in such conditions, works as a compensator.

In case of saturation conditions with a pre-compensated LSPC, the actuator with the highest load is penalized: its flow is lower than the commanded value. The flow demand to the other actuators is met, as long as the pump provides enough flow to satisfy them.

Another interesting case is when the flow demand on the second actuator alone is higher than the pump flow:

$$Q_{U2t,pre} > Q_{P,\max}$$
$$p_{U1} > p_{U2}$$

(21.40)

Equation (21.39) can be applied here showing how the pressure drop across O1 becomes null: no flow is sent to U1. The load drop check valve prevents the actuator U1 to backflow into the circuit. All the pump flow is sent to U2, the compensator C2 is fully open, while O2 operates as a compensator, under the pressure drop:

$$\Delta p_{O2} = \frac{\rho}{2} \left(\frac{Q_{P,\max}}{c_f \Omega_{O2}} \right)^2$$

(21.41)

The pump pressure becomes

$$p_p = p_{U2} + \Delta p_{O2}$$

(21.42)

It is interesting to note that in this condition, the LS signal sent to the pump is still equal to p_{U1}. Therefore, the pump pressure p_p given by Eq. (21.42) is lower than the LS pressure. The pump displacement is at maximum and the differential pressure limiter cannot satisfy its normal operating condition.

This analysis can be extended for systems with more than two actuators. The pump flow meets the demand of the actuator with the lowest load. The remaining flow (if any), goes to the actuator with the second lowest load, and so on.

The LSPC pre-compensated solution is not capable of implementing flow sharing in case of over demand.

Some valve designs address this issue equipping the compensators with a plunger that acts on the spring load. This element reduces the value of s_c to all compensators if the over demand condition is realized. Consequently, the flow sharing condition is met.

A simpler method can be applied to electrically controlled LS valves. In fact, the control unit, knowing the pump available flow and the actuator commands, can modify the signals to the individual metering orifices according to the following formula[3]:

$$Q_{Uim} = Q_{Uit} \cdot \frac{Q_{P,\max}}{\sum_n Q_{Uit}}$$

(21.43)

Q_{Uim} is the modified signal, which is equal to the theoretical flow value multiplied by a coefficient smaller than one and represents the "amount of overdemand." This method is also known as ***electronic flow sharing***.

---

3 Calculated under the assumption of linear relationship between flow and input command.

21.3.2 Flow Saturation with Post-Compensated LSPC

In the generic LSPC post-compensated circuit in Figure 21.17, the saturation condition is reached when

$$Q_{U1t,post} + Q_{U2t,post} > Q_{P,max} \tag{21.44}$$

Under the assumption that $p_{U1} > p_{U2}$, the LS signal sent to the pump is $p_{LS} = p_{U1}$. Also in the post-compensated case, the pump, when over-demanded, sets the displacement to the maximum value. Under this condition it cannot satisfy the condition $p_P = p_{LS} + s$ because the flow demand is higher than $Q_{P,max}$. The pump pressure is

$$p_P = p_{LS} + \Delta p_x \tag{21.45}$$

where $\Delta p_x < s$. Differently from the pre-compensated case, the reduction in margin pressure affects equally both functions, independently of the load pressure. In fact, both metering orifices O1 and O2 are exposed to the pump pressure p_P, and to p_{X1} and p_{X2}, respectively. Equation (21.24) previously calculated the value of these two pressures. This equation does not change for the case of flow saturation:

$$p_{X1} = p_{X2} = p_{U1} + s_C \tag{21.46}$$

Therefore, it is easy to calculate the value of Q_{U1} and Q_{U2}:

$$Q_{U1} = C_f \cdot \Omega_{O1}(i_1) \cdot \sqrt{\frac{2(\Delta p_x - s_C)}{\rho}}$$
$$Q_{U2} = C_f \cdot \Omega_{O2}(i_2) \cdot \sqrt{\frac{2(\Delta p_x - s_C)}{\rho}} \tag{21.47}$$
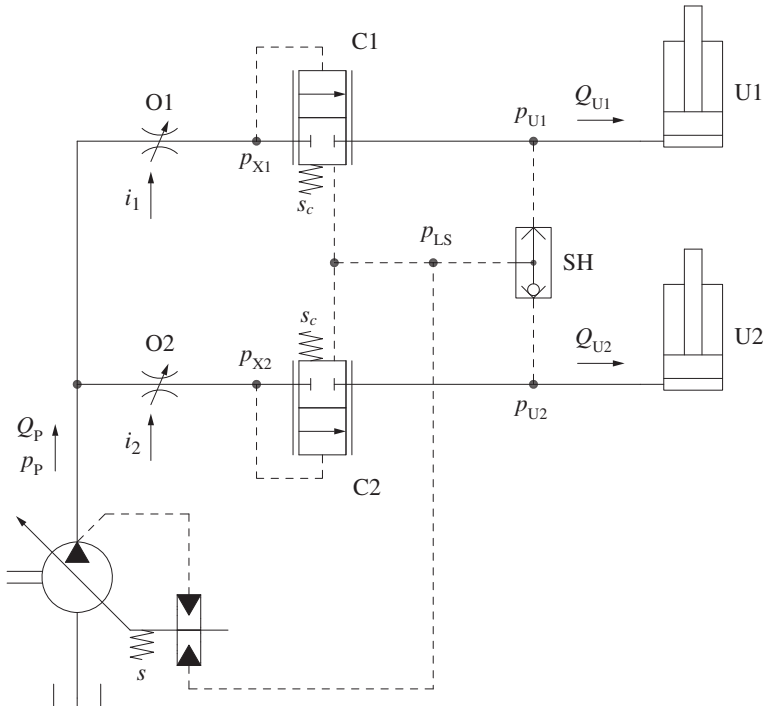

Figure 21.17 Simplified representation of the LSPC post compensated concept.

Equation (21.47) is very similar to Eq. (21.25), calculated for the non-saturated case. The only difference is that Eq. (21.47) uses Δp_x in lieu of s. The value of Δp_x can be calculated imposing the condition that $Q_{U1} + Q_{U2} = Q_{P,\,max}$ and becomes

$$\Delta p_x = s_C + \frac{\rho}{2} \left(\frac{Q_{P,max}}{C_f \cdot (\Omega_{O1} + \Omega_{O2})} \right)^2 \tag{21.48}$$

The value of Δp_x is lower than the pump margin pressure s, and the ratio between the theoretical flow and the real flow during saturation is the same for all functions:

$$\frac{Q_{U1}}{Q_{U1t,post}} = \frac{Q_{U2}}{Q_{U2t,post}} = \sqrt{\frac{\Delta p_x - s_C}{s - s_C}} \tag{21.49}$$

> In conclusion, the post-compensated LS technology addresses the flow saturation by proportionally reducing the flow delivered to all functions by the same coefficient. This feature is known as flow sharing and it is achieved independently of the number of actuators or individual flow demands.

21.4 Pre- vs. Post-compensated Comparison

This section will attempt to address one of the largest debates among hydraulic engineers: which valve architecture is better? The authors believe there is no unique answer, and most of the time the right choice is related to the application and to other "environmental" factors related to the application field. However, the two different technologies can be compared and ranked according to three different criteria:

(1) Pressure saturation
(2) Flow saturation
(3) Control accuracy

21.4.1 Pressure Saturation

The condition of pressure saturation occurs when one – or more – actuators reaches the maximum allowable pressure. As shown in the circuits in Figures 21.8 and 21.14, in both the pre-compensated and post-compensated LSPC system, the valve LS pressure can be limited using a relief valve RV_{LS} in the signal line. If the pressure of a load reaches that value, the pump outlet pressure is limited to $p^* + s$ and the system interrupts the flow supply to such load. However, the difference between the two technologies is evident when the pressure to a single function needs limited to a value lower than p^*. This situation is very common in systems with a single valve bank serving multiple actuators.

The pre-compensated valve can use individual pressure limiters (e.g. the valve RV_{LS2} in Figure 21.8) that shut off the compensators if the pressure reached the maximum permitted value. This is a very efficient way for limiting the individual pressure, since no oil is wasted over work-port relief valves (except for the loss through the small signal relief) and more flow is available for the other functions.

On the other hand, the post-compensated valve does not allow using individual pressure limiters on the functions, because the compensator is controlled by the upstream pressure p_X and by the LS

pressure p_{LS}. In other words, the compensator does not have any information of the downstream pressure (the load) and cannot be used for pressure limiting. Therefore, the individual pressure of each function can only be limited by full flow relief valves located at the work-ports (valves RV_A and RV_B in the schematic of Figure 21.14).

21.4.2 Flow Saturation

The previous section deeply analyzed the behavior of pre- and post-compensated valves when flow saturation occurs. Post-compensated technology easily realizes flow sharing. On the contrary, pre-compensated valves can achieve it if the spool control is electrohydraulic by changing the control logic to implement electronic flow sharing. Some more complex pre-compensated LS valves can implement flow sharing similarly to a post-compensated valve, but these solutions usually imply a higher complexity.

21.4.3 Control Accuracy

Accurate delivery of flow to the functions independently of their load is one of the main features of LSPC valves. This feature is a key the success of LS systems in many applications.

In pre-compensated valves, the setting of the compensator spring s_c defines the flow to the actuator in conjunction with the metering orifice, as shown in Eqs. (21.12) and (21.13). This concept makes the valve extremely accurate independent from external conditions (i.e. oil temperature).

However, in post compensated valves, both the settings of the pump margin pressure s and of the compensator spring s_c define the flow to the function, in conjunction with the metering orifice. First, the value of $(s - s_c)$ across the metering orifice can be affected by environmental conditions. In fact, the pump is usually located at a certain distance from the valve, connected by hoses or pipes and fittings. These elements cause major and minor pressure losses that follows well know relations of pipe flows. Therefore, the actual pressure differential at the metering orifice is always lower than the ideal: $(s - s_c - \varepsilon)$. The value of ε is representative of these losses, and it varies with the flow rate as well as the temperature, which affects the fluid viscosity. In other words, the accuracy of a post-compensated valve section is affected by the oil temperature and by the amount of flow demanded by other functions.

Second, in a post-compensated system the setting of the pump margin contributes to the pressure drop across the metering orifice. This makes the system highly sensitive to maintenance or to the replacement of the main pump, while this is not the case for the pre-compensated LS solution.

Example 21.4   Flow saturation with LS systems

The same crane application presented in Example 21.3, which system schematic is represented also below, is studied in case of flow saturation.

The system is supplied with a 60 cm^3/r load sensing variable displacement pump – pressure limited to 300 bar. The pump LS margin is 20 bar. The boom and swing functions are controlled with two load sensing proportional DCVs (DCV1 for boom, DCV2 for swing) equipped with post-compensators equipped with a 2 bar spring. In the valve, the boom section is also equipped with a relief valve limiting the maximum lifting pressure limiter to 260 bar.
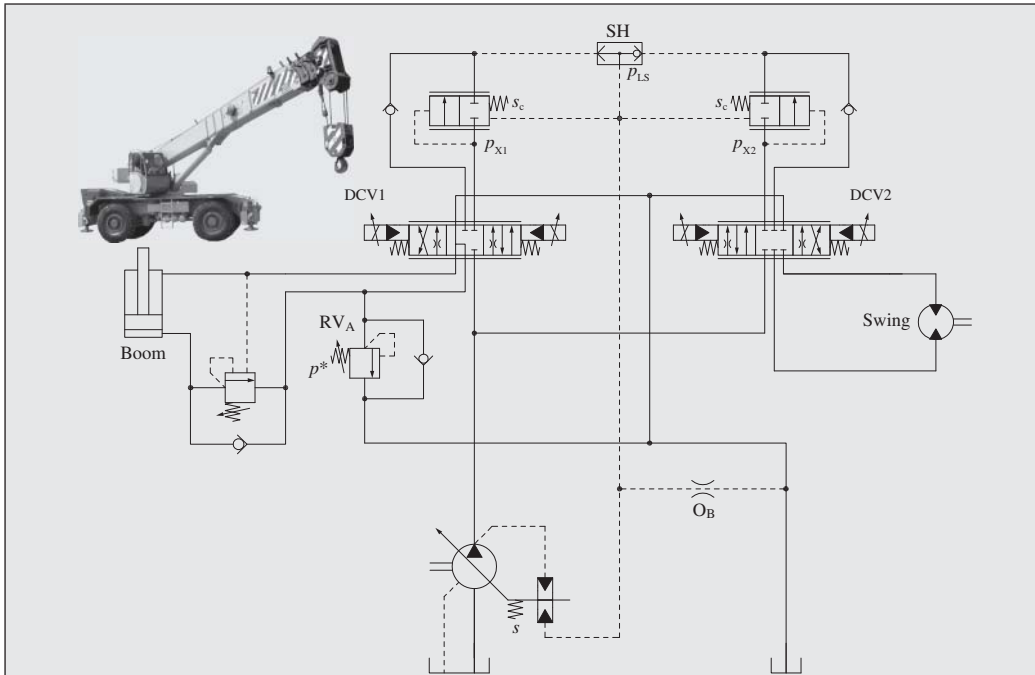
Initially, as in the previous Example 21.3, the operator runs the 150 cm^3/r swing motor at 250 rpm at an operating pressure of 75 bar, with the − rotating at 1500 rpm. At the same time, the boom extension is activated by opening the spool of DCV1 of a metering area of 15.5 mm^2. The boom lifting pressure is equal to 225 bar. During this latter operation, the engine speed drops to 1000 rpm. Calculate the flow delivered to each section and the value of the pressure drops across each metering spool.

Assume the oil density equal to 850 kg/m^3 and the flow coefficients across the spool areas equal to 0.64. All the hydraulic components can be assumed as ideal. The counterbalance valve at the boom actuator has a cracking pressure setting of 350 bar. The diameter of the bleed orifice O_B is 0.6 mm, and its flow coefficient is 0.7.

Given:

An LSPC system with post compensated valves supplied by a variable displacement pump, controlling two actuators: a differential cylinder (U1) and a hydraulic motor (U2).

System data: pump maximum displacement, $V_p = 60$ cm^3/r; pump operating speed, $n_p = 1500$ rpm dropping to 1000 rpm; swing motor displacement, $V_m = 150$ cm^3/r; pump LS margin, $s = 20$ bar; compensator spring, $s_c = 2$ bar; pump max pressure, $p_{max} = 300$ bar; oil density, $\rho = 850$ kg/m^3; orifice coefficient for the metering valve, $C_f = 0.64$; bleed orifice OB diameter, $d_B = 0.6$ mm; orifice coefficient for OB, $C_f = 0.7$.

Operating modes: DCV1 opens with $\Omega_1 = 15.5$ mm^2; DCV2 open; $p_{U1} = 225$ bar; $p_{U2} = 75$ bar; $n_m = 250$ rpm; pump speed n_P drops from to 1500 to 1000 rpm

Find:
Boom flow Q_{U1}; swing flow Q_{U2}

Example 21.4 (Continued)

Solution:

When the pump (engine) is still running at 1500 *rpm*, the flow to each function is the same as calculated in Example 21.3:

$$Q_{U2} = n_m \cdot V_{D,m} = 250 \, [rpm] \cdot 150 \left[\frac{cm^3}{rev} \right] \cdot \left(\frac{1}{1000} \right) = 37.5 \, l/min$$

$$Q_{U1} = C_f \cdot \Omega_1 \cdot \sqrt{\frac{2(s - s_c)}{\rho}} = 0.64 \cdot 15.5 \cdot 10^{-6} \, [m^2] \cdot \sqrt{\frac{36 \cdot 10^5 \, [Pa]}{850 \left[\frac{kg}{m^3} \right]}} = 645 \cdot 10^{-6} \frac{m^3}{s}$$

$$= 38.7 \frac{l}{min}$$

The pump flow is $Q_P = Q_{U1} + Q_{U2} = 76.2 \, l/min$. The pump has a maximum displacement of 60 cm^3/r rotating at 1500 *rpm* and therefore has a flow capacity of $Q_{P,max} = 90 \, l/min$. Since the flow demand is less than the maximum flow capacity, the pump instantaneous displacement can be calculated as 84.6% (i.e. 50.8 cm^3/r).

When the pump speed drops to 1000 *rpm*, the maximum pump flow becomes $Q_{P,max} = 60 \, l/min$. The system enters in flow saturation as the flow demanded by the two DCVs exceeds the pump capacity. Under this condition, the flow split between the two functions can be calculated through Eq. (21.25), which determines the reduced pump margin Δp_x during saturation:

$$\Delta p_x = s_C + \frac{\rho}{2} \left(\frac{Q_{P,max}}{C_f \cdot (\Omega_1 + \Omega_2)} \right)^2 = 2 \cdot 10^5 \, [Pa] + \frac{850}{2} \left[\frac{kg}{m^3} \right]$$

$$\cdot \left(\frac{1 \cdot 10^{-3} \left[\frac{m^3}{s} \right]}{0.64 \cdot (15 + 15.5) \cdot 10^{-6} \, [m^2]} \right)^2$$

$$= 13.1 \cdot 10^5 \, Pa = 13.1 \, bar$$

In other words, the pump pressure during saturation is $p_P = \max(p_{U1}, p_{U2}) + \Delta p_x = 225 \, bar + 13.1 \, bar = 238.1 \, bar$. The pressure drop across each spool is equal to $\Delta p_x - s_c = 11.1 \, bar$.

Knowing the value of Ω_1 and Ω_2, the flow through each valve spool section is

$$Q_{U1} = C_f \cdot \Omega_1 \cdot \sqrt{\frac{2(\Delta p_x - s_c)}{\rho}} = 0.64 \cdot 15.5 \cdot 10^{-6} \, [m^2] \cdot \sqrt{\frac{22.2 \cdot 10^5 \, [Pa]}{850 \left[\frac{kg}{m^3} \right]}}$$

$$= 506 \cdot 10^{-6} \frac{m^3}{s} = 30.5 \frac{l}{min}$$

$$Q_{U2} = C_f \cdot \Omega_1 \cdot \sqrt{\frac{2(\Delta p_x - s_c)}{\rho}} = 0.64 \cdot 15 \cdot 10^{-6} \, [m^2] \cdot \sqrt{\frac{22.2 \cdot 10^5 \, [Pa]}{850 \left[\frac{kg}{m^3} \right]}}$$

$$= 490 \cdot 10^{-6} \frac{m^3}{s} = 29.5 \frac{l}{min}$$

> The sum of the two flows matches the pump output. Both functions are affected by the engine speed reduction, but the ratio between the two flows remains the same.
>
> It is important to remark that if the same problem of flow saturation was given using the schematic in Example 21.2 (pre-compensated LSPC), the flow rate split between the two functions would significantly differ: the actuator U1 will have the commanded flow up to $Q_{P, \max}$, while U2 only the remaining flow.

21.5 Independent Metering Systems with Load Sensing

The concept of independent metering control illustrated for the case of a single actuator in Chapter 8, can be extended to multiple actuators. The main idea of an independent metering system is to control the hydraulic actuators through multiple proportional valves installed at each actuator work-ports. These valves permit to realize variable flow areas at the both the actuator supply and return lines with a high degree of freedom, usually through external electric control signals. In this way, the control unit can select the best metering control (meter-in or meter-out) according to the instantaneous load conditions on the actuator.

Several concepts for implementing independent metering systems have been proposed over the last years, and the main concepts have been schematically illustrated in Chapter 13, for the case of single actuator. These circuits require control architectures based on feedback sensors (usually pressure sensors) to determine the opening area according to the type of load. The same circuits could be extended to the case of multiple actuators. However, in this case the level of complexity of the controller further increase due to the effects of load interference between functions. A simplification of the controller can be achieved by implementing the concept of independent metering with an LSPC layout, using compensators to eliminate the problem of the load interference. Multiple implementation variants are possible, depending on the technology used for the control valves (spool or popper type), and the location of the compensators.

Figure 21.18 illustrates a significant example of a post-compensated LS independent metering system with 2/2 poppet valves. The figure shows the case of two actuators, a differential cylinder and a hydraulic motor. In the valve assembly within the dash-dotted line, each actuator work-port (A, B) has two separate flow paths: one connecting the work-port to the pump P and another to the tank (T).

The first flow path to the actuator work-port connects the supply line P to a proportional 2/2 valve, VP, followed by a compensator, C, and a check valve (CV). The post-compensator C ensures that the pressure drop across every valve VP commanded by the operator is constant, equal to $(s - s_C)$. In accordance to Eq. (21.25), valid for a generic post-compensated LS system, this establishes a flow rate to the actuator dependent only on the opening area of the valve VP and independent on the load pressure. Thanks to the check valve (CV), the line connecting VP, C, and CV can only establish a flow to the actuator work-port, and it cannot be crossed by a flow returning from the actuator. A network of pilot lines with check valves, CV_{LS}, selects the highest work-port pressure to the supply pump LS line. The LS line is also drained (bleed orifice O_B) to avoid residual pressure being trapped on the pilot lines when no function is activated.

The second flow path is for the flow returning from the actuator. Each work-port (A, B) is connected to the tank, T, through another 2/2 proportional valve, VT.

In the case of resistive loads, the velocity at each actuator is determined by the opening of the meter-in orifice VP. In this condition, it is convenient to set the corresponding VT valve to its
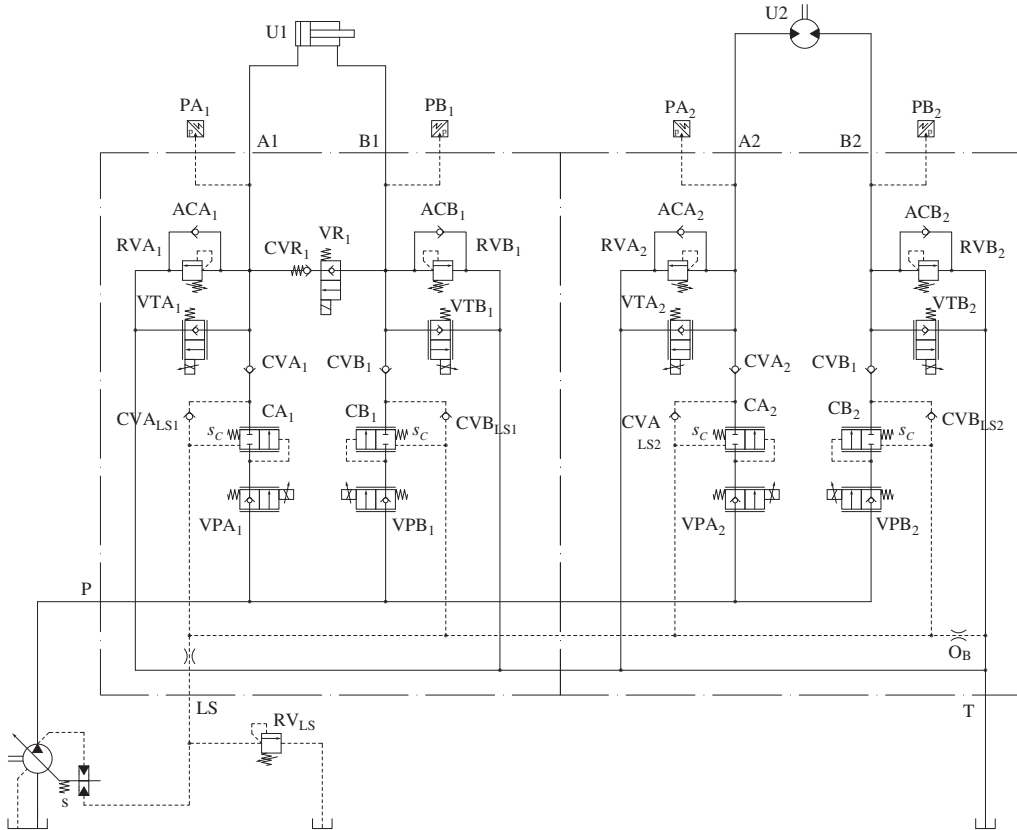
Figure 21.18 Post-compensated LS independent metering system.

maximum opening, so that the pressure at the supply port is minimum as well as the energy consumption.

In the case of overrunning loads, the opening area of VT is selected in order to guarantee the control of the actuator velocity. The determination of the opening area of VT can be discussed with considerations in line with the basic concepts of meter-out control done in Chapter 6. A first mode of controlling the system under overrunning load conditions uses VT as a compensator. In this mode, VP still determines the actuator velocity, as in the case of resistive loads, while the valve VT controls the pressure at the actuator work-ports. In particular, considering the extension for the differential cylinder in Figure 21.18 (valve VPA_1 energized) under overrunning load conditions, the pressure at the piston chamber is[4]

$$p_A = -\frac{F}{A} + \frac{a}{A}\frac{\rho \cdot Q_{VP}^2}{2c_f \Omega_{VT}^2} \tag{21.50}$$

Equation (21.50) follows the nomenclature of Figure 21.19 and shows the relation between the opening area Ω_{VT} and the pressure at the supply actuator work-port. The minimum energy consumption is achieved for the minimum positive pressure at the supply work-port, which depends on the load and the flow established by VP. A pressure sensor at the supply work-port can be used

---

4 Equation (21.50) results from the static equilibrium of the linear actuator, assuming a frictionless motion of the piston and no losses on the connecting lines. Unphysical negative absolute pressures for p_A correspond to an uncontrolled motion of the actuator.
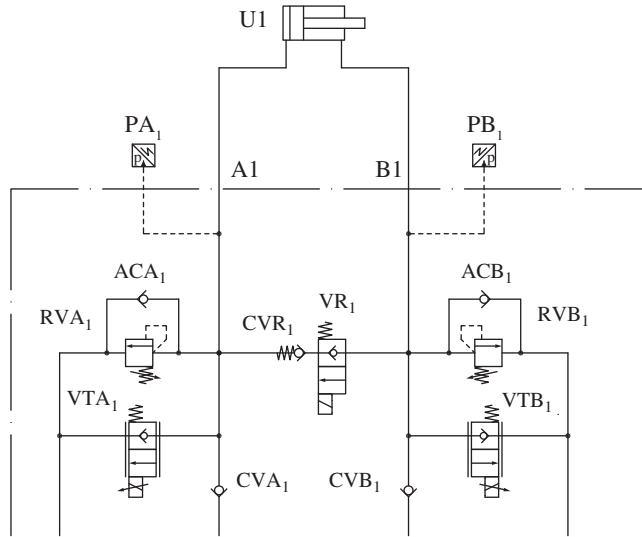
Figure 21.19 Regenerative feature with independent metering circuit.

as feedback signal to determine the maximum Ω_{VT} that still ensures a meter-in control. Hence, independent metering LS systems usually require the pressure sensors at the actuator work-ports, as also shown in Figure 21.18.

The second operating mode for controlling the actuator during an overrunning load condition is the "pump unloaded meter-out," already presented in Chapter 6. Here, the VT valve behaves as a meter-out element: the flow rate through the valve (and thus the actuator velocity) is determined by the opening area Ω_{VT} and p_a. At the same time, VP is completely closed, so that there is no pump flow consumption, and the supply workport is connected to T through the anticavitation valve AC[5]. This operating mode can be particularly convenient for two reasons: first, it allows for actuator velocities higher than those corresponding to the maximum pump flow. Second, it makes more pump flow available to the remaining functions, leading to a better machine productivity.
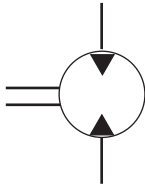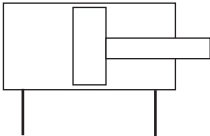
Figure 21.18 also includes anti-shock valves, RV, to protect the hydraulic circuit from instantaneous overpressurizations.

An additional feature of the independent metering system in Figure 21.18 is given by a supplementary regeneration line at the differential actuator. This line includes a check valve CVR and an on/off valve VR. The valve VR can be energized to activate a regenerative extension mode. This mode can increase the extension velocity of the actuator though recirculation of the return flow, which merges the inlet flow provided by the opening of VPA. In this case, both VTB and VPB are closed. The flow regeneration concept have been discussed in detail in Chapter 12.

Problems

21.1 An LS system with a variable displacement pump needs to be designed to control the following two actuators.

---

5 In certain cases, it can be convenient to supply a certain portion of the actuator flow through the VP valve also during the "pump unloaded meter-out operation." This permits to avoid a complete stop of the actuator, in case the load suddenly switches from overrunning to resistive.

$T_{m,max}$ = 200 Nm (motor torque) V_m = 100 cm³/r (motor displacement) n_m = 1000 rpm (shaft speed of the motor)	$F = k\,Tm$ N (cylinder load) k = 250 1/m (load factor) v = 0.3 m/s (piston velocity)

For both actuator, the load is always resistive.

Draw the ISO schematic of the system that permits the control in both directions of each actuator, limiting the number of hydraulic components as much as possible.

Assuming ideal component, and the maximum pressure of the system equal to 225 bar. Determine

1. The proper size of the cylinder with three available options:

| Cylinder A	Cylinder B	Cylinder C
D_a = 40 mm (bore diameter)	D_b = 50 mm (bore diameter)	D_c = 60 mm (bore diameter)
d_a = 18 mm (rod diameter)	d_b = 22 mm (rod diameter)	d_c = 26 mm (rod diameter)

2. The minimum size (displacement) of the pump, knowing that the pump is connected to an engine that rotates at n_p = 2000 rpm.
3. At the maximum load condition for both actuators, indicate the pressure at the main locations of the system: at pump outlet, upstream/downstream the directional control valves. Assume an LS margin of 7 bar.
   Are pre-compensators (or post-compensator) necessary? If yes, at which actuator?
4. Represent in the energy plot (p,Q) the operating points of the pump (P), the motor (M) and the cylinder-extension (C), at maximum load conditions. Represent and calculate the power loss in kW.
5. Calculate the input power a torque at the pump.
6. Is an additional orifice in the main line necessary in case the load at the cylinder C is resistive? If yes, what is the size of the orifice necessary to balance the maximum overrunning load condition?

21.2 The system in the figure below has four actuators (M1, C1, C2, C3), controlled by LS proportional valves. Considering following data:

Torque on motor M1, resistive	T_1	250 Nm
Load on C1	F_1	20 kN
Load on C2	F_2	15 kN
Load on C3	F_3	10 kN
Bore diameter cylinder a	D_a	40 mm
Rod diameter cylinder a	D_a	18 mm
Bore diameter cylinder b	D_b	50 mm
Rod diameter cylinder b	D_b	22 mm
Bore diameter cylinder c	D_c	63 mm
Rod diameter cylinder c	D_c	36 mm
Speed of pump	N	2000 rpm
Max pressure of pump	p_{max}	120 bar
LS pressure margin,	S	8 bar
Compensators pressure setting	s_c	8 bar
Flow rate of all LS valves PVBs	Q_{PVB}	30 l/min
Displacement of motor GU1	V_m	160 cc/rev

Assume all components as ideal.

All cylinders a, b, and c are present in the system, but the location of each one has to be determined according to the data provided in the problem.
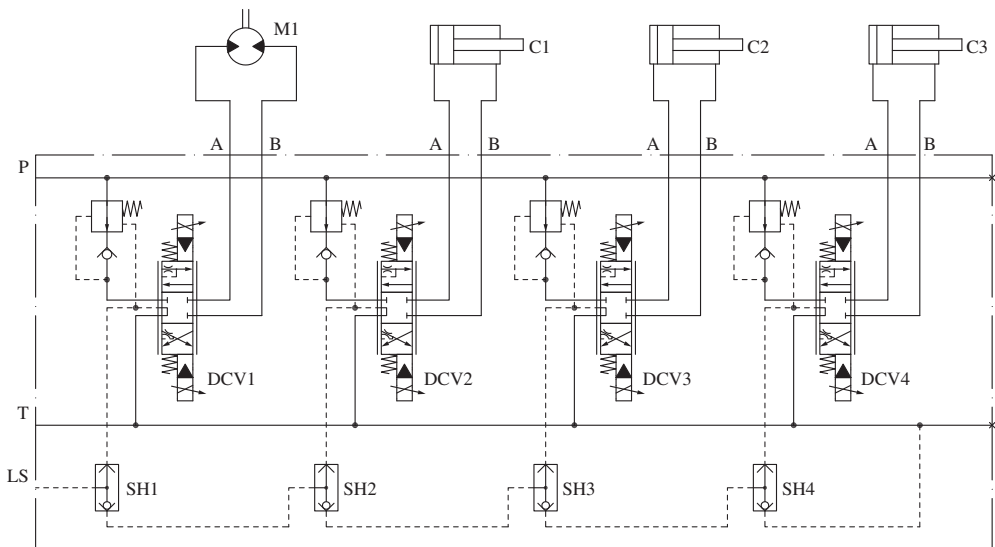
Reference system

1. Represent the ISO schematic of the supply system, considering a variable displacement pump with LS flow regulator.
2. Evaluate the maximum pressure at which each load can operate.
3. Evaluate which one of the three available cylinder (a,b,c) is suitable for C1.
4. Evaluate the speed of extension of C1, in m/s.
5. Identify the cylinders (among a, b, c) to use for C2 and C3 considering that all cylinders C1, C2, and C3 are actuated in retraction and M1 (motor) is at rest. The choice should optimize energy consumption.
6. Calculate the minimum pump displacement, considering that the simultaneous extension of C1, C2, C3 is requested.
7. Calculate the pressure in bar at each cylinder during the extension phase of the three cylinders (in simultaneous actuation). For this condition, evaluate also the pressure in bar at pump delivery and the power requested by the pump in kW.
8. In the energy plane (Q-p), show the point of operation of each cylinder for the previous point 6. Indicate useful power and power dissipated in kW.
9. Evaluate the speed of the motor (M1) in rpm and the pressure in bar at the inlet of the motor.

21.3 A load sensing (LS) system without pressure compensators is used to control two identical cylinders ($A = 500\,\text{mm}^2$, $a = 250\,\text{mm}^2$). The cylinders are arranged vertically, and the downward load on them is $F_1 = 5000\,\text{N}$ and $F_2 = 8000\,\text{N}$, respectively. The maximum pump flow rate is $Q_P = 10\,\text{l/min}$. The LS directional control valve, at maximum opening, is rated for providing $10\,\text{l/min}$ when the differential pressure across the valve equals the pump LS margin of $s = 20\,\text{bar}$. Determine

  (a) The maximum extension velocity for each cylinder, when the directional control valve is fully open (assume the other one closed)
  (b) The pressure at the piston side of each cylinder, in the LS pilot line, and at the pump delivery when both LS valves are commanded in extension with 30% opening
  (c) If the two cylinders move at the same extension velocity, cylinder 1 moves faster than cylinder 2, and cylinder 1 moves slower than cylinder 2, when both LS valves are commanded in extension with 30% opening
  (d) The area Ω_O of the return orifice that permits to have a pump supply pressure of 0 bar (absolute pressure), considering cylinder 1 in lowering conditions (and DCV2 not actuated), $\rho = 900\,\text{kg/m}^3$, and $c_f = 0.65$.
  (e) The retraction (lowering) velocity for cylinder 1 (DCV2 not actuated)
  (f) Another possible solution for doubling the lowering velocity for cylinder 1 besides increasing the pump displacement

For all the points of the problem, consider ideal components (no undesired pressure or torque losses).
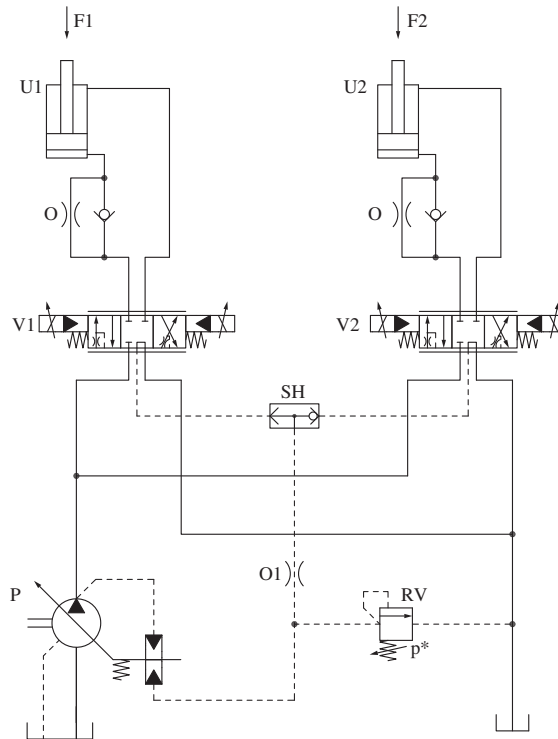

21.4 Considering the system below (load sensing, pre-compensated), operating under the conditions specified in the table, answer the following questions:

1. What is the maximum pressure the pump can reach (*independently from the specific p_{CYL} values reported in the table*)?
2. What is the maximum load pressure at which the loads can operate steadily *independently from the specific p_{CYL} values reported in the table)*?

Assuming that all cylinders are actuated through V1, V2, V3, with the PCYL values reported in the table below:

3. What is the Δp across V3?
4. What are the Δp's across the pressure compensators 1, 2, and 3?
5. What is the pump delivery pressure?
6. What is the function of CV1.6 and RV1.6?

What is the function of O1?
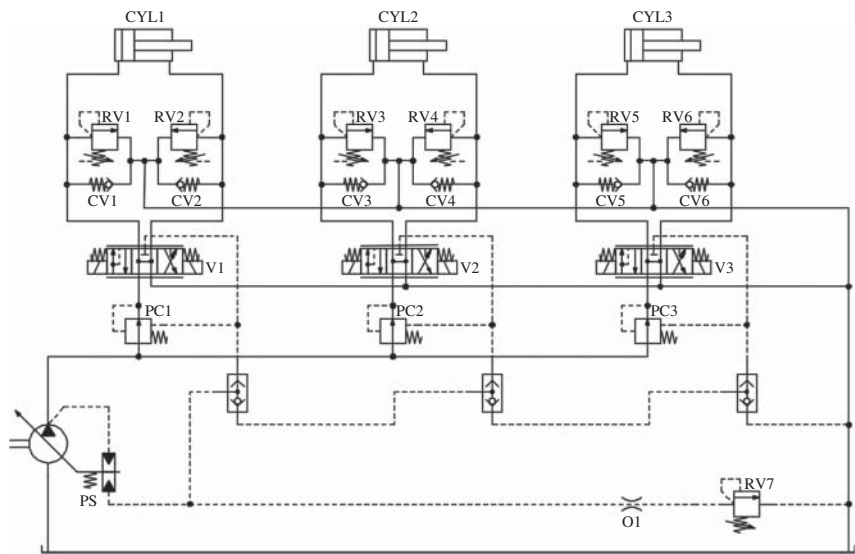
O1 (Orifice)		
PC1, PC2, PC3 (pressure compensator setting)	p_c^*	20 bar
PS (pump margin)	p_{LS}^*	20 bar
RV1… RV6 (pressure relief valve)	$p_{RV1}, p_{RV2}, p_{RV3}, p_{RV4}, p_{RV5}, p_{RV6}$	300 bar
RV3 (pressure relief valve)	p_{RV7}	270 bar
CV1…CV6 (Check valves)		
CYL1 (load pressure for cylinder 1)	p_{CYL1}	150 bar
CYL2 (load pressure for cylinder 2)	p_{CYL2}	95 bar
CYL3 (load pressure for cylinder 3)	p_{CYL3}	200 bar

21.5   The hydraulic system in Figure 1 is used to perform the simultaneous actuation of two cylinders, according to a 15 s cycle as shown in Figure 2.

The load on the cylinder is given, and it is always resistive, for both extension and retraction strokes.

A fixed displacement pump along with an accumulator is used to supply flow to the two cylinders. An unloading valve UV is used to lower the pump pressure in case the accumulator is full.

The accumulator size is given. The accumulator is used to lower the pump displacement, so that the pump flow can fill the accumulator (up to the maximum pressure p_2) during the phase of the cycle where no flow is sent to the actuators. The cycle repeats over time, so that the state of charge of the accumulator at the end of the cycle has to be the same as the initial condition.

Two pre-compensated load sensing valves are used to overcome load imbalance.

Following data are given for the system below.

Compensator C1 and C2 setting	s	15 bar
CYL1 and CYL2 stroke	L	1 m
CYL1 and CYL2 rod diameter	d	50 mm
CYL1 and CYL2 diameter	D	100 mm
Load CYL1	F1	50 000 N
Load CYL2	F2	30 000 N
CYL1 and CYL2 velocity at 100% command	v	0.2 m/s
Cycle time	Δt	60 s
Accumulator volume	V_0	10 l
Polytrophic coefficient	n	1.25
Accumulator precharge pressure	p_0	90 bar
Accumulator maximum pressure	p_2	350 bar
Pump shaft speed	n_p	1000 rpm

Find:
1. The pressure at CYL1 and CLY2, during the actuation phases.
2. The flow rate to each cylinder Q_{CYL1}, Q_{CYL2}, during the actuation phases.
3. In a (Q,p) plot, the operating points of the accumulator, CYL1 and CYL2, when the pressure in the accumulator is $p_2 = 350$ bar. Clearly indicate in the plot the useful power, and the power losses at LSV1, LSV2, C1, and C2.
4. The minimum pressure at the accumulator, p_1, necessary to guarantee the supply to both actuators CYL1 and CYL2. *Consider that the accumulator works between p_1 and p_2.*
5. The nitrogen volume inside the accumulator, at p_1 (assume $p_1 = 100$ bar).
6. The volume of oil released by the accumulator, $\Delta V = V_1 - V_2$ (assume $p_1 = 100$ bar).
7. The minimum size of the pump (V_p, in cm^3/rev) to guarantee the system functionality over the 15 s cycle. *Consider that the accumulator discharges flow during the actuation phases.*
8. The pressure setting p^* of the unloading valve.
9. Represent in a time diagram the qualitative trend of the pressures at the accumulator and, at the pump outlet, for the 15 s cycle. Highlight the effect of the unloading valve.
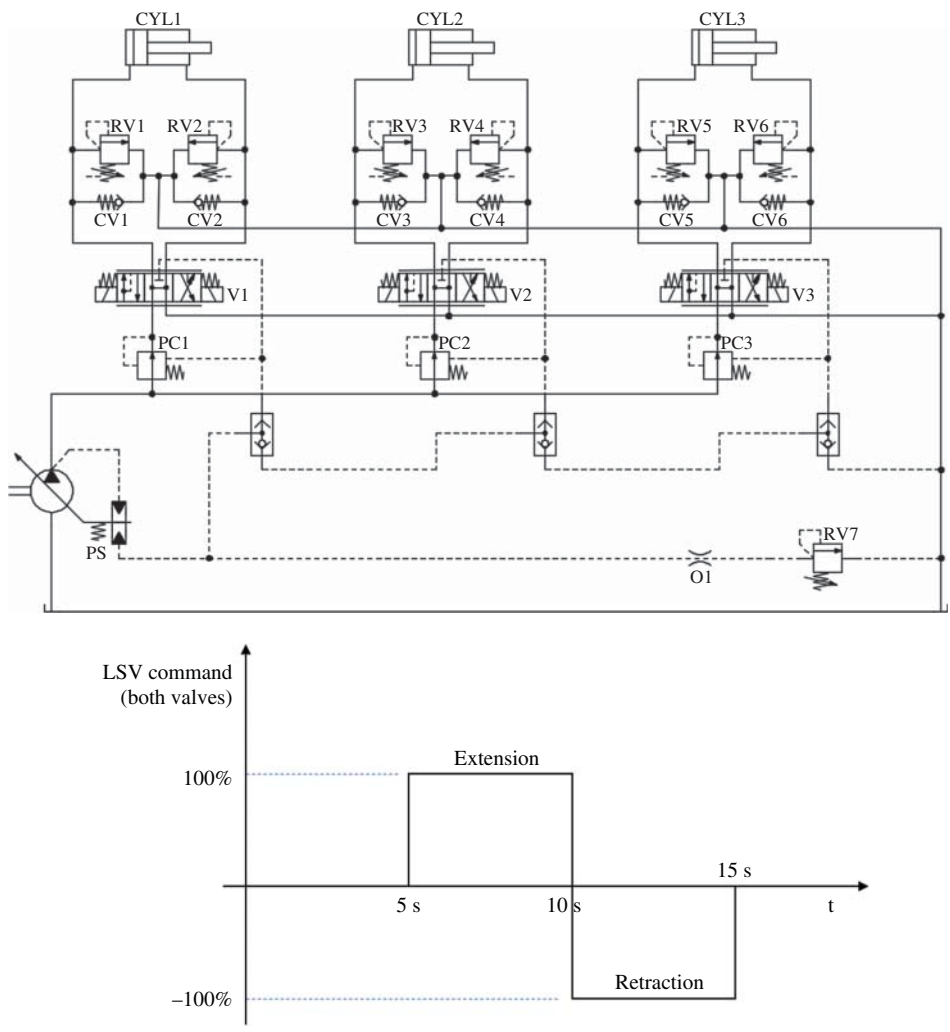
Drive cycle (perpetual cycle).

21.6 A load sensing system includes two actuators: one bidirectional motor and one through a rod cylinder. They are controlled by two LS proportional pre-compensated valves.

1. Represent a working ISO schematic of the system considering a variable displacement pump supply.
2. Determine the pressure of the two actuators in bar.
3. Determine the flow rate at each actuator, in l/min.
4. Determine the shaft speed of the hydraulic motor, in rpm.
5. Calculate the flow rate delivered by the pump, in l/min.
6. Calculate the instantaneous displacement of the pump ($V_{p,\mathrm{ist}}$), cm^3/rev, and the value of α $\alpha = V_{p,\mathrm{ist}}/V_{p,\mathrm{max}}$.
7. Determine the pressure at pump delivery, in bar.
8. Determine the torque at the pump shaft in Nm.
9. Determine the useful power, and the dissipated power in kW. Represent these quantities in a flow – pressure diagram ($Q – p$).

10. Determine which hydraulic components introduce power loss during the operation of the system. Quantify the power loss, in kW.

Data to be used:

Torque at hydraulic motor (T_m)	140	Nm
Diameter piston/rod (D_p/D_r)	63/45	mm
Force applied to cylinder (F)	25	kN
Pump shaft speed (n_p)	1100	rpm
Flow Rate hydraulic motor (Q_m)	15	l/min
Pump load sensing margin p^*_{LS}	12	bar
Piston velocity (v_p)	0.2	m/s
Displacement of the hydraulic Motor (V_m)	180	cm³/rev
Maximum pump displacement ($V_{p,max}$)	50	cm³/rev

- Assume all components with ideal behavior (es: $\eta_v = \eta_{hm} = 1$).
- Assume also resistive load conditions at both actuators.
- Assume backpressure of the LS proportional valves and tank pressure equal to 0 bar.
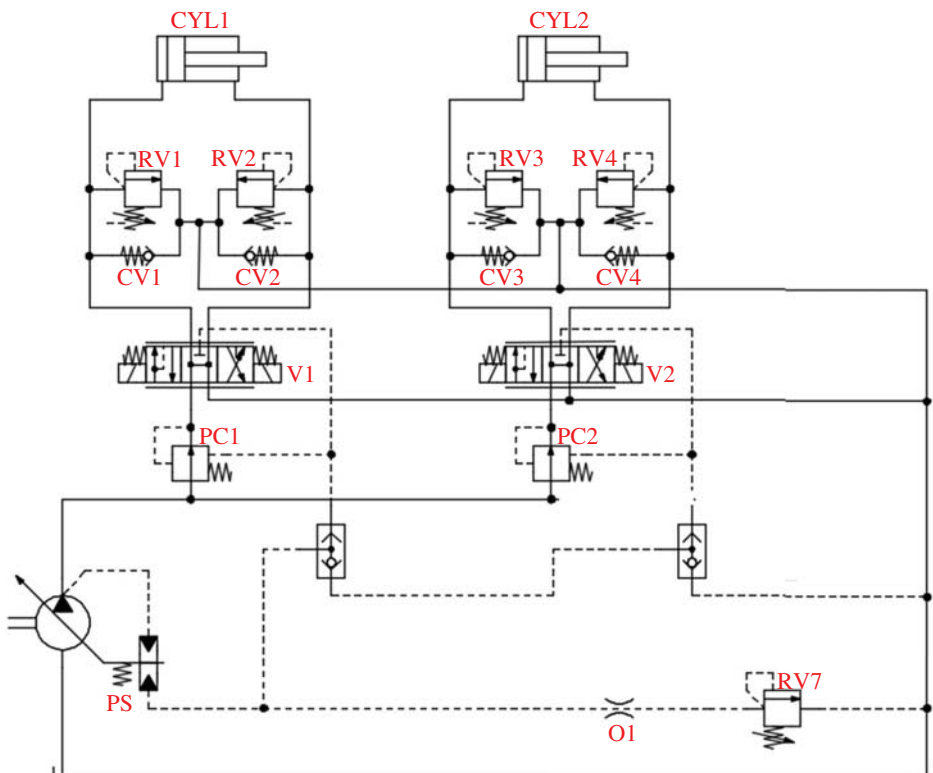
21.7 Consider the above system (load sensing, pre-compensated), with two actuators. The following data are provided.

Abbreviation (Description)	Symbol	Value
PC1, PC2 (pressure compensator setting)	p_c^*	12 bar
PS (pump margin)	p_{LS}^*	20 bar
RV1, RV2, RV3, RV4 (pressure relief valve)	$p_{RV1}, p_{RV2}, p_{RV3}, p_{RV4}$	290 bar
RV7 (pressure relief valve)	p_{RV7}	270 bar
Rod diameter (both CYL1 and CYL2)	D	20 mm
Piston diameter (both CYL1 and CYL2)	D	40 mm
Max velocity for extension and retraction (both CYL1 and CYL2)	v	0.1 m/s
CYL1 load (resistive in both extension and retraction)	p_{CYL1}	95 bar
CYL2 load (resistive in both extension and retraction)	p_{CYL2}	200 bar
Pump shaft speed	N	1000 rpm

Assuming ideal energy efficiencies for each component,

(a) Determine the minimum pump size (displacement) that allows for simultaneous operation of both cylinder (either extension or retraction).

(b) For the case of retraction of both cylinders, indicate the pressure at each piston chamber, at the pump outlet and between each compensators (PC) and the directional valve (V).

(c) Assuming that each directional valve (V) is sized reaching 0.1 m/s with the compensator setting of $p_c^* = 12$ bar (as indicated in the table), describe what happens if the compensator setting is reduced to $p_c^* = 6$ bar:

c1. Does the system still operate as a LS system? If not, why?

c2. What is the maximum extension/retraction velocity for both the cylinders?

21.8 Sketch the complete ISO schematic of a load sensing system that needs to control following actuators

(a)	(b)	(c)
maximum load = 100 bar	maximum load = 100 bar	maximum load = 150 bar
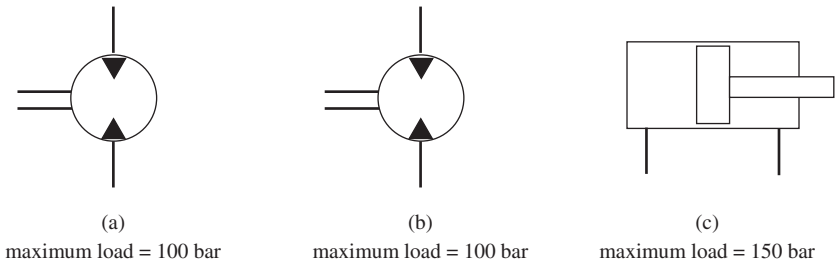
The two hydraulic motors are identical, and they need to rotate always in a synchronized way.

The two motors (a and b) use a series connection, while the hydraulic cylinder (c) is in parallel with respect to the two motors.

The system uses a variable displacement pump, which has a load sensing margin of 20 bar, and pressure compensated (pre-compensated) valves, with a setting of 10 bar. The system also includes a pressure limitation to 300 bar.

a) Draw the complete hydraulic schematic

b) For the maximum load condition and the simultaneous actuation of all a, b, c, indicates:
1. The pressure at the inlet port of each actuator
2. The pressure at the inlet and outlet port of each LS valve
3. The pressure at the pump delivery
4. The pressure at the pump LS line

c) Determine the setting of the pressure relief valve you indicated in the schematic

Chapter 22

Power Steering and Hydraulic Systems with Priority Function

In all systems analyzed so far, actuators are subject to the same set of rules in the event of flow saturation. In other words, in a circuit using non-flow-sharing valves, the load on each actuator determines which one loses speed during over-demand. However, in flow-sharing circuits, all functions slow down proportionally, independent of the load distribution.

In some cases, it is instead desired to create a hierarchy among the actuators so that one (or sometimes more than one) function has priority over the remaining ones. In case of flow saturation, the priority function shall maintain the desired amount of flow, while the remaining available flow is shared among the other functions.

The most common example of such a priority function is vehicle steering. While some circuits use a separate steering pump, it is very common to encounter circuits where steering shares the same flow supply with other hydraulic functions. In these cases, it is important to ensure that the steering function is always supplied with the correct amount of flow, independent of machine condition (i.e. engine speed).

This chapter illustrates the main solutions utilized to achieve priority between functions, focusing on the steering application. The first part of the chapter describes different types of steering solutions, covering various architectures and functionalities. The second part focuses on priority circuits for steering applications. Since priority is usually achieved through an element referred as priority valve, different types of priority valves will be analyzed. However, it should be noted that priority valves are not the only elements capable of creating priority into a circuit. In fact, there are other solutions that can achieve similar results, such as the tandem circuits for open center systems that have been presented in Chapter 20.

22.1 Hydraulic Power Steering

Steering is one of the most common applications for hydraulics. The need for hydraulic power assisted steering is justified by the fact that human effort alone is not enough to steer the tires of large vehicles, like off-road equipment. In general, the effort to steer a vehicle increases with the vehicle mass. It also depends on various factors, such as the geometry of the suspension system, the placement of the steering linkages, and the tire size. Manual steering systems were adequate in the early industrial development stages of the last centuries, when vehicles were still relatively small. The industrial trend to make vehicles larger, faster, and safer, however, required an additional power source to assist the driver in the steering effort.

Initially, hydraulic power steering technology conquered most on-road and off-road vehicle applications. However, in the last decade, pure electric power steering technology has become increasingly popular in the light-duty automotive industry, replacing hydraulic power steering. This new technology allows the parasitic losses associated with the hydraulic power steering pump to be eliminated and the fuel consumption to be decreased (gains can be up to 1 mpg). However, electric power steering systems have not been successfully applied to larger vehicles, where the power requirement for steering is higher and where the steering linkages are different than a car (e.g. articulated steering). Thus, hydraulic power steering is and will remain the dominant technology for off-road vehicle and the trucking industry.

The purpose of this section is to provide the reader with an overview of the main hydraulic concepts used to supply and power the steering function, covering the case of on- and off-highway applications. This section focuses only on the steering function as a single actuator system.

22.2 Classification of Hydraulic Power Steering Systems

The design of a hydraulic power steering system includes two unique challenges: maintaining the same level of safety of a mechanical steering system and providing the operator with the same feeling. A failure in the hydraulic system should still allow the operator to maintain a certain level of control of the vehicle, avoiding dangerous accidents. However, the operator feel is also very important, because the driver controlling the steering needs to feel the vehicle, and the control he/she exerts over it, without delay. Three main concepts of hydraulic power steering can be implemented to satisfy these challenges.

Hydromechanical Power Steering
This category is often referred to as *on-highway* power steering. In hydromechanical power steering systems, the motion is transmitted from the prime mover (steering wheel) to the wheels using hydraulic power. However, this layout also includes a mechanical connection between the steering wheel and the steered components. The manual effort of the operator and the hydraulic power are managed through the steering unit, often referred as steering gear. Steering gears are often based on a rack and pinion feedback device. These are used on cars or trucks and usually require relatively low flows and pressures.

Hydrostatic Power Steering
This category is often referred to as *off-highway* power steering. In a hydrostatic power steering system, instead of a mechanical link, a hydraulic connection is used between the steering wheel and the vehicle. In case of loss of power from the steering pump, the hydrostatic steering unit acts as a manually operated pump, allowing a reduced performance of the steering system. Off-highway units are encountered in vehicles of any size, from a small forklift to a large mining truck.

Electrohydraulic Power Steering
This category includes two families: traditional steering systems supplied through an electro hydraulic power supply, and *steer-by-wire* systems. In the first case, the power supply is decoupled from the main engine and the flow supply can be varied with the steering demand. This leads to significant savings in term of energy consumption and to some additional safety features. Steer-by-wire instead heavily relies on electronics (sensors, actuators, electronic control units) and

control algorithms to perform the power steering function. This allows for a very high degree of flexibility and for automation (autonomous driving).

Besides this first, general classification, there are other criteria that can be used to classify different types of hydraulic power steering. For example, a second possible classification of hydraulic steering systems can be made according to how the function is supplied within the vehicle system. In some cases, the steering system has a dedicated flow supply, separate from the rest of the hydraulic circuit (if present). In these cases, steering can be considered a single actuator system. In other cases, steering is not the only hydraulic function on the machine, and the hydraulic supply is shared with the rest of the actuators. Here, in order to meet the safety requirements, steering needs to have priority over the remaining functions.

A third classification of hydraulic power steering systems pertains to the design of the steering unit, dividing them into open center and closed center steering units. The first one requires a constant flow supply, while the second one requires flow "on demand" only when the steering is actuated.

Finally, a fourth way to classify hydraulic power steering units is based on the action of the forces on the steered wheels and thus on the steering actuator. A nonreactive steering unit blocks the steering ports in neutral, holding the wheel position when the operator releases the steering wheel. In a reactive steering unit, the ground forces are allowed to return the steering wheel to its approximate straight position when the steering wheel is released. This behavior is comparable to automobile steering.

22.3 Hydromechanical Power Steering

Hydromechanical power steering systems are used in vehicles designed to travel mostly on the road and capable of achieving relatively high speeds (greater than 50 km/h). This type of solution always maintains a mechanical connection between the actuators and the steering wheel to ensure the safety of operation. On-highway steering systems are open center units with a dedicated flow supply. It is important that the flow supplied to an open center power steering system is constant, in order for the operation of the steering function to be consistent and repeatable at various conditions. Figure 22.1 shows the schematic of a typical power steering system used in on-highway applications. The first element of the circuit is the pump: this is a fixed displacement unit (in most cases vane type) and includes some valve elements for controlling the outlet flow while limiting the maximum pressure.

The pump in Figure 22.1 is driven by a variable speed engine, and two facts should be noted:

(1) The pump displacement must be sized for engine idle speed: it is in this condition that full steering flow is required. This can be understood by thinking about a car: the parking maneuvers require high steering flows with low engine speeds.
(2) In vehicles such as a car or an on-highway truck, the speed variations of the engine are very relevant. Especially for gasoline engines, the speed can range from 800 up to 5000 rpm. Therefore, at high engine speeds, the fixed pump will circulate a large amount of flow.

These two facts are the reasons the steering pump should be equipped with valves capable of providing the steering unit with the correct flow at all speeds. The elements V1, V2, O1, and O2 in Figure 22.1 realize a three-way flow control with pressure limitation, as described in Chapter 8. Here, the bypass flow is recirculated to the pump inlet. This solution allows the size of the pump inlet connections to be reduced, since this is sized only for the steering flow.
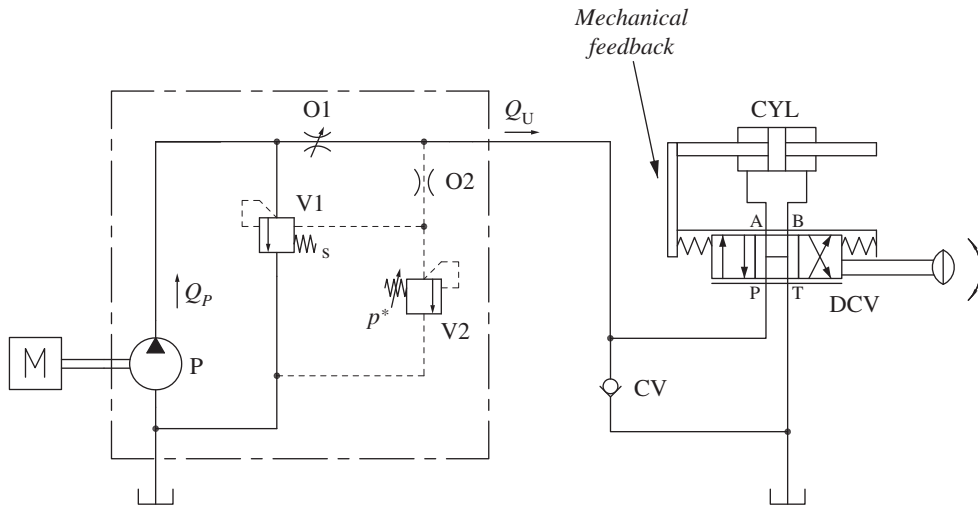
Figure 22.1 Example of typical open center steering system for on-highway applications. Source: Nervegna [1].

The second element of the circuit in Figure 22.1 is the power steering device, which consists of the steering cylinder, CYL, and an infinite position directional control valve (DCV). The DCV is manually actuated by turning the steering wheel. This valve is equipped with a movable sleeve, which is mechanically linked to the steering cylinder CYL. When the operator turns the steering wheel, the spool is shifted to a power position and supplies flow to CYL. As the cylinder moves, the vehicle steers, and the sleeve moves accordingly, returning the valve into the neutral position. In this way, for a given turning angle of the steering wheel, the cylinder CYL moves a corresponding travel. This type of device is a typical example of a servo-mechanism; other examples include the servovalve and the negative flow controlled pump that have already been presented.

Figure 22.2 gives insight into the architecture of the steering actuator: it is a double rod cylinder, whose chambers L and R are supplied by the work-ports of the hydraulic control valve. The actuator, in particular, represents a "rack and pinion" type connection between the steering rod and the control valve element: a linear movement of the actuator corresponds also to an angular rotation of the pinion. In Figure 22.2, the dash-dot line X-X indicates the cross-sectional planes of the steering control valve represented in Figure 22.3.
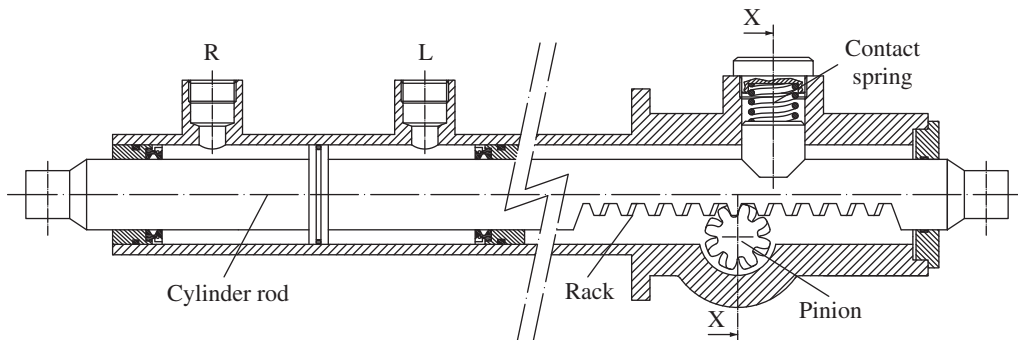
Figure 22.2 Detailed view of the power steering actuator.
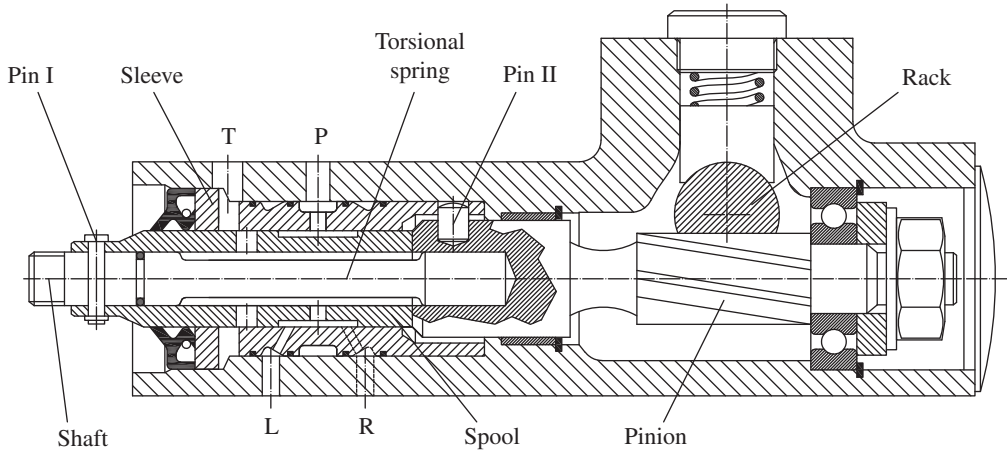
Figure 22.3 Cross-section (X-X) of the hydraulic servo system controlling the power steering.

Figure 22.3 shows a sectional view of the power steering valve. The housing holds four ports: supply, P, return, T, and the actuators, L and R. The valve body houses two main elements:

(1) The **sleeve**: on its outer diameter, there are four seals separating the four chambers connected to the work-ports. A series of radial holes connects the chambers on the outer diameter to axial slots on the inner diameter, where the spool sits.

(2) The **spool**: the edges of the axial slots machined into this component, depending on the relative angular position with respect to the edges of the slots in the sleeve, can connect the P and T ports to L or R, respectively.

The second important aspect of the control element is the actuation with feedback:

- The rotary spool is actuated by the steering shaft on the left side: this is rigidly connected to the valve spool with a radial pin (Pin I). Therefore, the spool turns with the steering wheel.
- The feedback elements are located at the opposite end: a pinion shaft with helical gears is supported by a ball bearing and a bushing. This element is rigidly coupled to the valve sleeve, also by a radial pin (Pin II).
- The pinion shaft and the steering rod are also connected by an inner elastic element, which works as a torsional spring. The spring is pressed into the pinion element, with which it creates a rigid connection. This spring gives the force feedback on the steering wheel when the operator turns the vehicle and provides the resistance to the operator action.
- The cylindrical rod and the spool each feature two flat surfaces (not represented in Figure 22.3). When the relative angular position of these two elements reaches a set angle ($\pm 7°$ in this case), the flats become in contact, and the steering shaft rigidly connects to the pinion. This allows the steering system to be operable also in case of a loss of pump pressure.
- The figure shows also a contact spring which pushes on a small piston and ensures the rack is always engaged with the pinion.

The general operation of the unit is intuitive: a rotation of the spool commanded by the driver causes a motion of the actuator, which in turn, moves the sleeve until the system returns to its neutral position; however, a complete analysis of the steering operation is quite complex.

Figure 22.4 shows a cross-section of the spool–sleeve combination: from this diagram, it can be understood how the edges of the axial slots in the spool determine the opening area of the valve between the work-ports, pressure, and tank. In particular, Figure 22.4 shows how the timing of
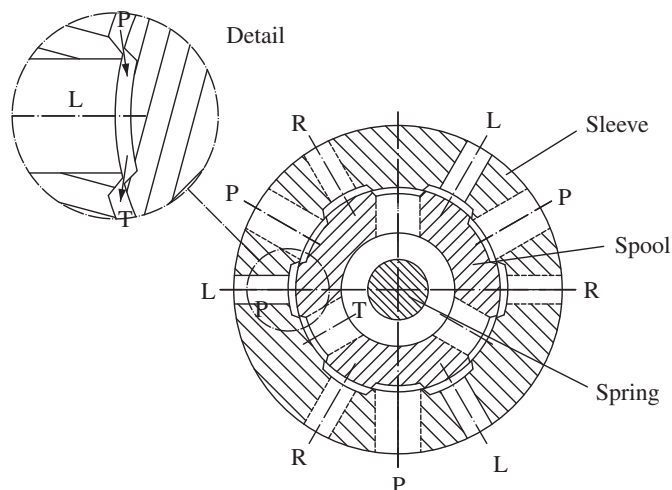
Figure 22.4 Cross-section of the spool and sleeve in neutral position.

these edges realize a negative lapping (visible in the detailed view). That is, the distance between the edges on the sleeve is smaller than the width of the slots in the spool. This leaves an open passage for the oil in neutral position, as represented in Figure 22.1. In neutral, all ports P, T, A, and B are connected.

When the wheels are centered, the valve is in neutral position: the supply flow enters from port P, as shown in detail in Figure 22.4, crosses the area between the P-R and R-T slot edges and returns to the tank through the T connection. The same path is also followed on the other side of the slots, between P-L and L-T. These areas work as a combination of orifices in series (P-R and R-T) and in parallel (R and L paths), creating a pressure drop in the system, between P and T.

If the operator starts turning the wheel to the left, the spool rotates counter-clock wise (CCW), reducing the area of the P-R and L-T connections (turning clockwise [CW] would open them more). As a result of this, the restriction to the flow at the P-R and L-T connections causes the pump pressure to rise. This pressure is also seen at the L work-port, while the R port opens toward T. When the pressure difference between L and R is enough to win the resistance of the tires on the ground, the vehicle starts turning to the left. In this situation, the steering is being operated slowly, and all the connections between the ports are still open. In other words, the valve is operating in the pressure control zone by modulating the various restrictions (which, again, are all still open). If the driver's effort is limited to the small spool rotation just described (which can be the case for a small steering correction), the sleeve follows the wheels and rotates CCW until the effect of the increase of pressure is neutralized by the re-balancing of the flow areas toward the neutral condition.

Vice versa, if the steering effort is more important, for example, a parking maneuver, the spool keeps rotating CCW until the P-R and L-T lands close completely. Thus, the P-L and R-T connections are fully open prior to steering, and the supply flow is completely diverted toward the left chamber of the steering actuator. Also, in this case, the motion of the steering actuator moves the sleeve CCW, until the valve returns to neutral position. If the driver keeps turning the wheel, the steering linkage ultimately reaches its end of stroke. In this case, the connection between the flat surfaces of the rod and sleeve causes the steering wheel also to stop. However, in this case, the valve is kept open toward L, because the sleeve cannot travel anymore. The system then needs to discharge the pump flow over a relief valve.

One last observation about this steering system should be made, with regard to the neutral position configuration of the valve-sleeve combination: when the vehicle is traveling, and the steering is kept at an angle (for example, while traveling along a left curve), the vehicle dynamics causes

a reaction force on the steering actuator pointing toward the right. Therefore, in order to hold the steering position, the valve does not set in a perfectly centered condition. Rather, as described above, the spool is slightly rotated toward the left, in order to restrict the flow path such as to increase the pressure on the L port and balance the dynamic force on the steering linkage. The relative rotation between spool and sleeve causes the torsional spring to generate a torque, which will need to be counteracted by the driver. This torque is also known as the *steering effort*.

If the driver leaves the steering wheel, the spring tends to re-center the spool, opening the L-T connection. At this point, the force on the steering actuator causes the oil to move from L to T and, at the same time, the sleeve rotates CW, and the spool follows its movement. This continues, until the dynamic reaction on the steering linkage is null, which corresponds to a parallel straight position of the wheels. In other words, if the driver does not hold the steering wheel, the vehicle attempts to return to being straight: this type of system is known as *reactive style* steering system.

22.4 Hydrostatic Power Steering

As mentioned before, off-highway vehicles, because of their size, weight, and ground conditions, require a large force to turn the steering wheels. Furthermore, the layout of the vehicle often makes it very difficult, sometimes impossible, to create a mechanical connection between the steering actuator and the operator cabin. A typical example is a wheeled excavator, where the cab is located on a turret that can swing 360°. In such cases, a hydrostatic power steering system is normally used to control the vehicle direction.

Hydrostatic steering units are also referred as orbital steering units and are characterized by a hydraulic feedback device between the wheels and the operator. These steering units can be used in open center or closed center configurations; the supply can be provided by a dedicated steering pump or by a pump shared with other functions. In the latter case, a priority valve is often used to ensure the correct operation of the steering in all conditions. More details on priority circuits are provided in Section 22.5.

Figure 22.5 represents a conceptual schematic of a hydrostatic open center steering mechanism. The system consists of three main elements: a manually actuated spool, i.e. DCV, sliding into a moving sleeve; a "measuring" actuator, denoted MA, rigidly connected to the sleeve, and a steering cylinder, CYL.

The spool of the DCV has a six-way configuration: the bottom ports are P (pump supply) and T (tank), while the top ports are A, X, Y, and B. A and B are connected to the chambers of the
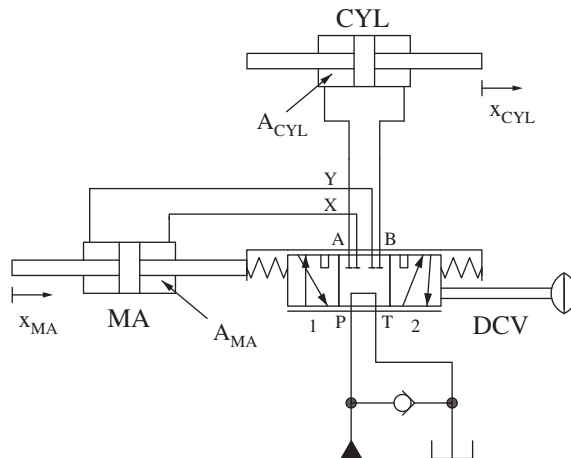

Figure 22.5 Operational diagram of a hydrostatic linear steering unit.

steering actuator, while X and Y are connected to the chambers of the measuring actuator. As for the on-highway devices, the operation of the unit is intuitive: when the operator shifts the spool by a certain travel, the pump flow is diverted to one chamber of the measuring actuator; the return oil from the measuring device is then diverted to steering cylinder. The oil returning from the opposite chamber of the steering cylinder goes back to tank. While the oil flows and the steering moves, the measuring actuators moves together with the sleeve, bringing it back to the neutral position. As in the previous case, for a given travel of the spool, a given volume of oil is transferred to the steering cylinder. The feedback between steering cylinder and actuator is purely hydraulic, realized by the fluid exchanged between the supply and the measuring actuator.

With reference to Figure 22.5, the area of the measuring actuator is A_{MA}, and its position is x_{MA}; the area of the steering cylinder is A_{CYL} and its position is x_{CYL}. If the spool of DCV is shifted by a stroke equal to ε, a portion of the inlet flow is diverted toward the actuator:

$$Q = f(\varepsilon) = A_{MA} \cdot \dot{x}_{MA} = A_{CYL} \cdot \dot{x}_{CYL} \tag{22.1}$$

As the actuators move, the sleeve follows until DCV returns to the neutral position. At this point, the measuring actuator will have traveled for an amount equal to ε. Integrating Eq. (22.1) over this operation, one obtains the volume of oil displaced during the steering operation:

$$V = A_{MA} \cdot \varepsilon = A_{CYL} \cdot x_{CYL} \tag{22.2}$$

Equation (22.2) highlights the linear relationship between the input command and steering travel, where the gain of the system is the ratio between the areas of the two cylinders:

$$x_{CYL} = \frac{A_{MA}}{A_{CYL}} \cdot \varepsilon \tag{22.3}$$

Figure 22.5 is based on linear actuators and provides a clear view of the device's operation. However, this schematic does not give a complete view of the architecture that constitutes a hydrostatic steering unit. This is better represented in Figure 22.6: here, the measuring device is not a linear actuator, but a bidirectional pump/motor unit. The spool and sleeve are again actuated by rotating about their axis, just as in the case of the on-highway steering gear. This type of device is often referred as a rotary (or orbital) steering unit.

The operation of the rotary steering unit is similar to the linear steering unit previously explained. In this case, however, the relationship between the measuring actuator and the steering cylinder is different:

$$V_{MA} \cdot \vartheta_{MA} = A_{CYL} \cdot x_{CYL} \tag{22.4}$$
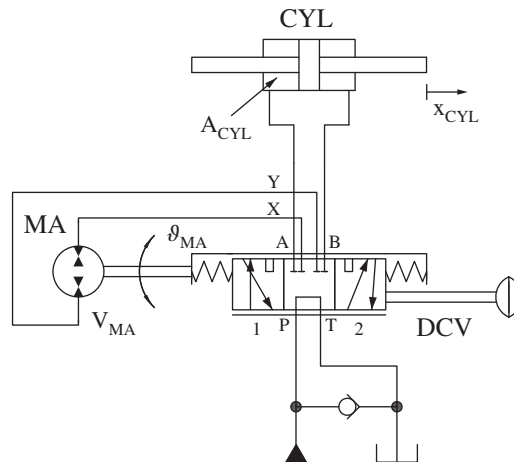

Figure 22.6 Equivalent schematic of an open center rotary steering unit. Source: Nervegna [1].

V_{MA} is the displacement of the rotary actuator, while ϑ_{MA} is its angular position. Equation (22.4) is used to size the steering unit's displacement (usually, the designer knows the number of turns of the steering wheel from lock to lock and the overall steering cylinder stroke). How exactly this is done will be clearer after the next numerical example.

22.4.1 Hydrostatic Steering Unit Description

Figure 22.7 shows a simplified cross section of an open center hydrostatic steering unit. Its main elements can be divided in two functional groups: directional and feedback. Among the directional elements, the main rotary spool is coupled to the steering wheel through a female spline. A rotary sleeve is located between the spool and the housing and is rigidly connected to the internal cardan shaft through a radial pin. The pin passes through some slots in the spool, whose width defines the maximum angular lag between the spool and the sleeve. The cardan shaft links the sleeve to the orbit pump-motor, which functions as feedback device. The orbit unit is built by a rotor and a stator. The different chambers of this motor are connected to the ports of the sleeve by several drillings in the unit housing.

Figure 22.7 represents the steering unit in its rest position: the spool is centered with respect to the sleeve: port P is connected to T through the unit housing, while ports A and B are blocked. Figure 22.8, instead, represents the unit in its working position: if the driver steers to the left, the spool immediately moves with respect to the sleeve. The axial slots in the spool, as visible from the cross section of Figure 22.8, orchestrate the following connections:

i. P is connected to some of the chambers of the orbit motor. In this configuration, the oil is supplied from P to the motor, which starts turning concordant to the steering wheel.
ii. The flow exiting the motor is sent to port A (connected to the steering cylinder) through the spool slots.
iii. The return flow from the cylinder enters the unit from port B and returns to the tank, passing through the housing of the unit.

While the motor turns, realizing the movement of the steering cylinder, the sleeve also follows the cardan shaft. When the motor has turned the same amount of turns as the steering wheel, the
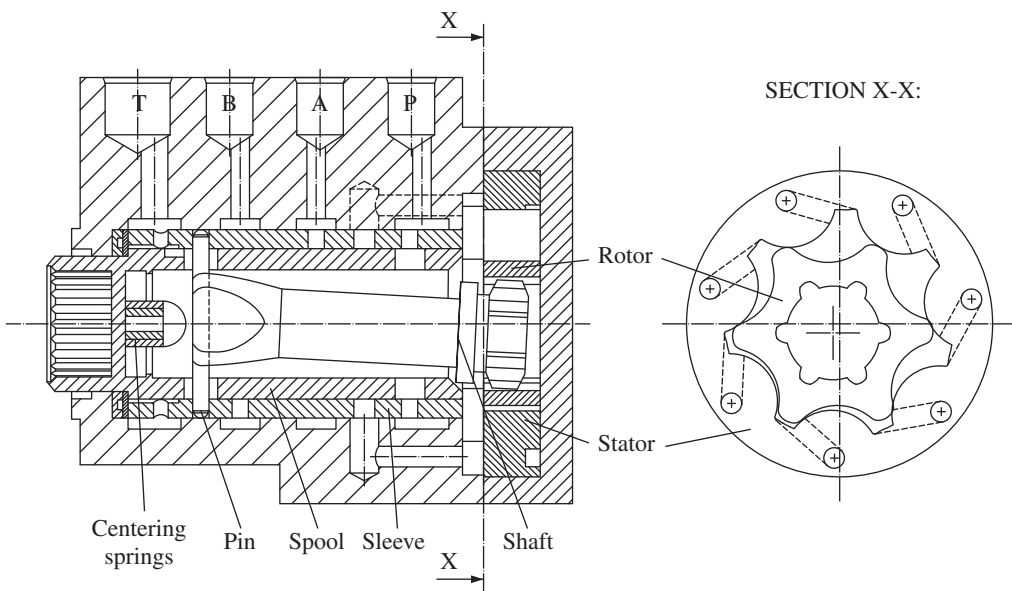
Figure 22.7 Simplified cross-section of a hydrostatic steering unit.
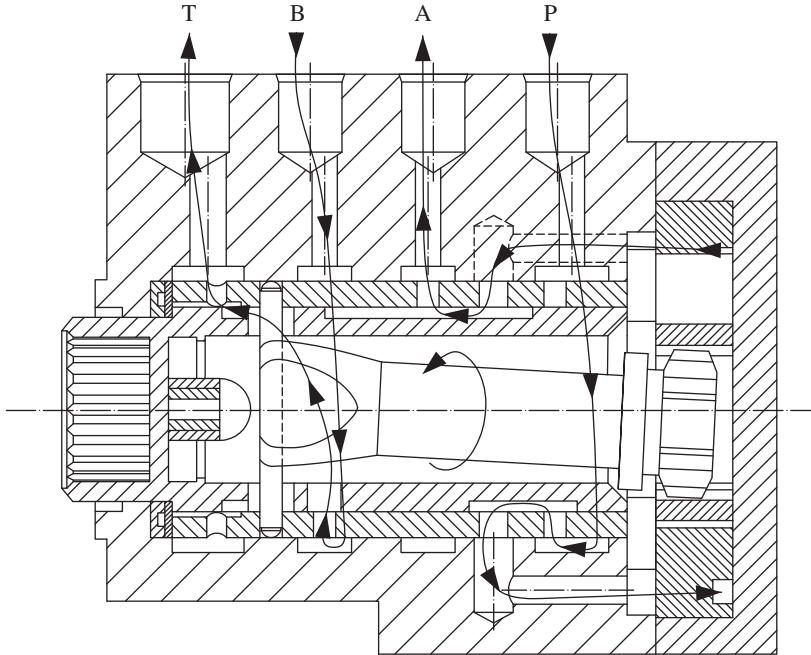
Figure 22.8 Hydrostatic steering unit in the operating position.

spool and sleeve return into the relative neutral position, and the unit stops delivering flow to the steering cylinder.

The pin linking the shaft and the sleeve plays an important role in terms of safety. In fact, in case the flow supply to the power unit is lost (e.g. dead engine or failed pump), the pin, after a certain rotation, engages the sleeve (the sleeve has a slot cut into it, so when the pin hits the end of the slot, the two are locked together). When this happens, the orbit unit is rigidly connected to the steering wheel. In this case, the unit becomes a hand-operated pump that, sucking oil from the check valve connected to T, delivers flow to the steering cylinders. For more detailed descriptions of these components, the reader can refer to [1].

Example 22.1   Steering unit sizing

An open center steering unit is used to supply a double rod steering cylinder. A fixed displacement pump rotating at 1500 *rpm* supplies the unit. The maximum force on the cylinder is 35 000 *N*, while the cylinder strokes of 25 *cm* in either direction from the center position. The cylinder rod is 25 *mm* in diameter.

Draw a system schematic. Calculate the size of the cylinder bore and the displacement of the steering unit and of the pump.

Assume the following data:

- Full steering (max left to max right) shall be accomplished in six turns of the steering wheel
- Max steering angular velocity is 1.5 turns per second
- Max operator steering torque is 150 *Nm*.
- Steering system sized for a max pressure of 138 *bar*

In case of loss of the pump supply, calculate the maximum steering force that the operator can apply on the wheels. Assume all units ideal during the calculation.

Given:

- A steering system with a maximum cylinder force, $F_{max} = 35\,000\ N$
- Cylinder rod diameter, $d_R = 25\ mm$
- Total cylinder stroke, $x_{max} = 50\ cm\ (25 + 25)$ or $500\ mm$
- Number of turns lock to lock, 6
- Maximum operator steering speed, $n_{st} = 1.5\ rev/s$
- Maximum operator torque, $T_m = 150\ Nm$
- Max pressure, $p_{max} = 138\ bar$
- Fixed displacement pump rotating at $n_P = 1500\ rpm$

Find:

- Cylinder bore diameter d_B
- Steering unit displacement V_{st}
- Steering pump displacement V_P
- Max force during emergency steering F_{em}

Solution:

The schematic of the system is represented below:
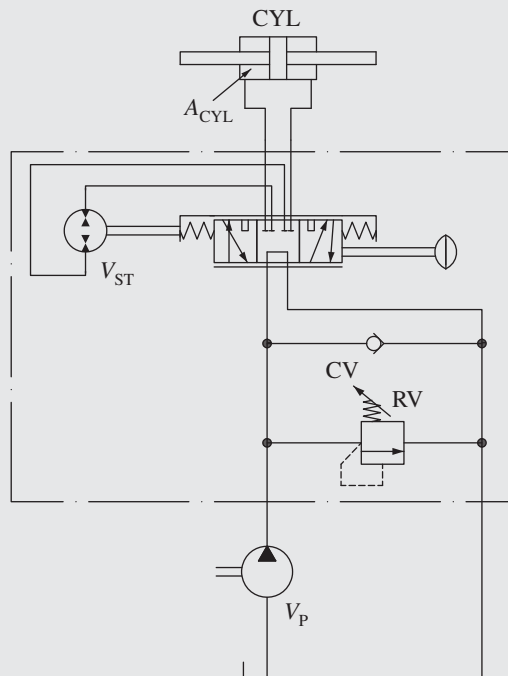
The cylinder bore area could be sized based on the maximum system pressure:

$$F_{max} = A_{cyl} \cdot p_{max} = \frac{\pi}{4} \left(d_B^2 - d_R^2 \right) \cdot p_{max}$$

Example 22.1 (Continued)

Therefore, considering the max pressure $p_{max} = 138$ [*bar*]:

$$d_B = \sqrt{\frac{4\,F_{max}}{\pi\,p_{max}} + d_R^2} = \sqrt{\frac{4 \cdot 35\,000\,[N]}{\pi\,138\,[bar]} \cdot 10 + 25^2\,[mm^2]} = 62\,mm$$

The volume of oil that needs to be displaced by the steering unit from lock to lock is

$$V_{max} = A_{cyl} \cdot x_{max} = \frac{\pi}{4}\left(d_B^2 - d_R^2\right) \cdot x_{max} = \frac{\pi}{4}(62^2 - 25^2)[mm^2] \cdot 500\,mm$$
$$= 1\,264\,061\,[mm^3] = 1264\,cm^3$$

The steering unit needs to supply V_{max} in six turns; therefore, $V_{st} = 1264/6 = 210\,cm^3/r$.

The maximum rotational speed of the steering wheel is 1.5 *n/s*, i.e. 90 *rpm*. This corresponds to a flow rate of

$$Q_{st} = V_{st} \cdot n_{st} = 210\,[cm^3/r] \cdot 90\,[r/min] = 18.9\,l/min$$

The pump displacement providing such flow at 1500 *rpm* corresponds to $V_P = 12.6\,cm^3/r$.

When the operator runs the steering in emergency mode, the steering unit acts as a pump supplied through the check valve (CV). The max torque from the operator is 150 *Nm* which corresponds to a pressure of:

$$p_{em} = \frac{2\pi \cdot T_m}{V_{st}} = \frac{20\pi \cdot 150\,[Nm]}{210\,[cm^3/r]} = 45\,bar$$

The maximum force of the steering cylinder in emergency mode will be

$$F_{em} = A_{cyl} \cdot p_{em} = \frac{\pi}{40}(62^2 - 25^2)\,[mm^2] \cdot 45\,[bar] = 113\,765\,N$$

22.4.2 Types of Hydrostatic Steering Units

As mentioned at the beginning of the chapter, hydrostatic steering units are available in different configurations depending on the type of circuit they are used. Figure 22.9 summarizes the available configurations.

A constant flow supply is usually used in combination with open center steering units. In the power beyond configuration, when the steering unit is in neutral, the flow is recirculated through port power beyond (PB), and can be used in a secondary circuit. Closed center steering units are combined with pressure supplies. The load sensing (LS) units are implemented in the traditional LS configuration, in which the flow to the steering is controlled by the LS margin, and the spool throttle area.

Another way to classify the units depends on their work-port configuration when in neutral. The steering can be *reactive* or *non-reactive*, as summarized in Figure 22.10. When a vehicle is driving the ground, forces usually tend to re-center the steering wheels. These forces are affected by the shape of the ground, as well as by the vehicle velocity. A nonreactive unit has the work-ports blocked in neutral; therefore, when the operator is not steering, the wheels are locked in their position. Vice versa, a reactive steering allows the fluid to recirculate from the steering actuator to the steering unit. Therefore, the ground forces cause the steering wheel to return to a straight position. This effect needs to be counteracted by the operator, who must hold the wheel while the vehicle is turning in order to maintain the desired steering angle.
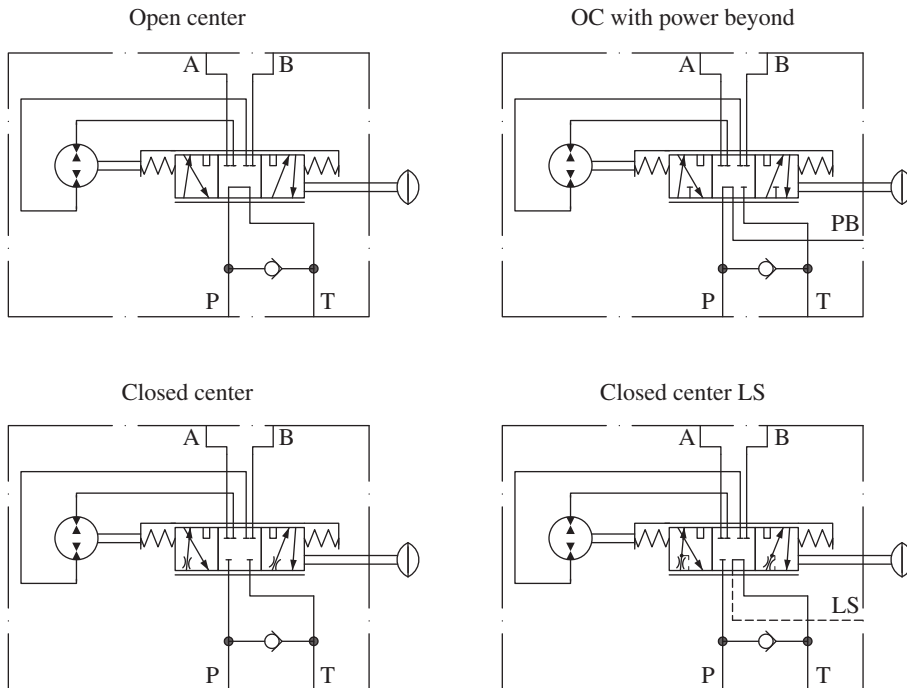
Open center

OC with power beyond

Closed center

Closed center LS

Figure 22.9 Different types of hydrostatic steering units.

<u>Non-reactive</u> steering: the steering ports are blocked in neutral, holding the wheel position when the operator releases the steering wheel. Suitable for rough terrain vehicles.

<u>Reactive</u> steering: if the steering wheel is released, the steering wheel returns to an approximately straight position. Suitable for vehicles traveling at higher speeds or on paved roads.

Figure 22.10 Reactive and nonreactive steering units.

22.5 Priority Valves

Priority valves are elements characterized by one inlet and two outlet flow paths, usually referred to as *controlled* and *excess flow*. The controlled flow path supplies the priority functions of the system. The excess flow path, instead, supplies the secondary functions. Priority valves ensure that the priority functions always receive the desired amount of flow, independent of the configuration of the rest of the circuit.

Priority valves are used in many applications, but they are very commonly utilized in steering circuits, characterized by a shared flow supply. Two types of priority valves are usually encountered. One is used in combination with a fixed displacement pump flow supply, while another is used in LS systems. This section illustrates both design architectures, applied to steering circuits.
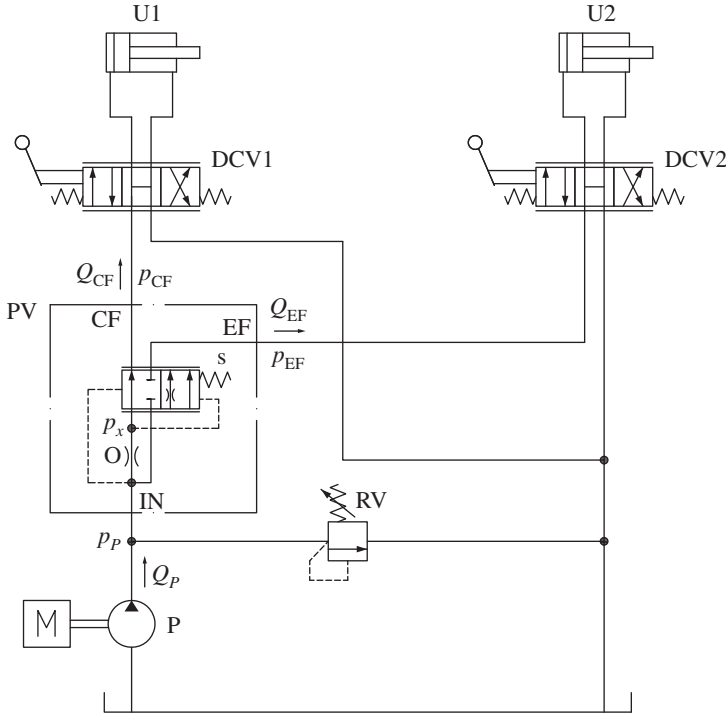
Figure 22.11 Priority circuit for fixed displacement pump flow supply.

22.5.1 Priority Valve for a Fixed Displacement Flow Supply

The simplest type of priority valve is the one used in combination with a flow supply. Figure 22.11 represents the hydraulic symbol of the valve (PV) within a two-actuator circuit. Valve PV has three ports: IN is connected to the pump outlet, CF is the *controlled flow* port, and EF is the *excess flow* port. CF and EF supply two actuators, U1 and U2, through two directional control valves, DCV1 and DCV2.

The priority valve PV consists of two elements: an orifice, O, and a four-way two position spool downstream of that orifice. In a neutral condition, the spool is open to CF and closed to EF. In a shifted condition, the spool opens to EF and restricts the opening to CF. However, it should be noted that the spool never fully closes the opening area toward CF. Three forces determine the spool position: the spring *s*, acting concordant to the pressure p_x (the pressure sensed downstream of O), and the inlet pressure p_P, acting on the other side of the spool. In other words, the spool imposes the typical compensator condition:

$$p_X = p_P - s \tag{22.5}$$

Under this condition, the flow through the metering orifice O, i.e. the controlled flow, becomes

$$Q_{CF} = C_f \cdot \Omega_O \sqrt{\frac{2s}{\rho}} \tag{22.6}$$

Unlike an LS compensator (which is usually a two-way spool), the spool of PV is connected to two outlet flow paths. The spool can create a restriction (i.e. compensator orifice) in both paths, depending on the operating conditions – see Figure 22.12.

The valve itself can have two different modes of operation, depending on the pressures at the two outlets of the spool.
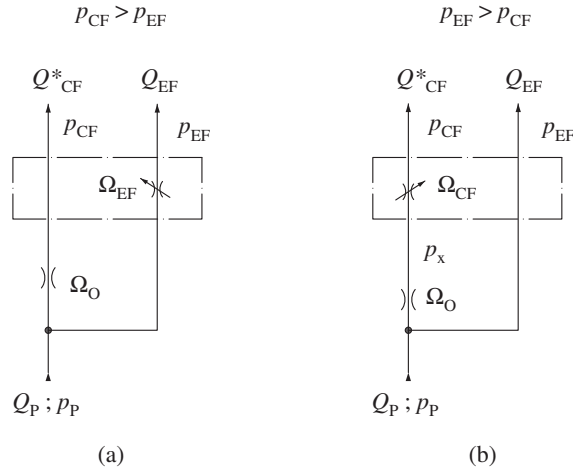
Figure 22.12 Operating modes of the priority valve.

In the first case, the **pressure at CF is higher than EF** ($p_{CF} > p_{EF}$). This is the case, for example, when DCV1 is commanded, while DCV2 remains in neutral. In this situation, the path of least resistance for the oil is represented by EF. Intuitively, one can understand that the valve has to create an additional restriction in the EF line to maintain the controlled flow Q^*_{CF} to the priority actuator. This situation is represented in Figure 22.12a). The pressure p_X is equal to p_{CF}, the highest of the two. Therefore, the pump pressure is

$$p_P = p_{CF} + s \tag{22.7}$$

Since $p_{CF} > p_{EF}$, the spool imposes a restriction (Ω_{EF}) in the excess flow line to satisfy the condition:

$$Q_{EF} = Q_P - Q^*_{CF} \tag{22.8}$$

The value of Ω_{EF} satisfying such condition is

$$\Omega_{EF} = \frac{C_f}{Q_P - Q^*_{CF}} \cdot \sqrt{\frac{2\left(p_P - p_{EF}\right)}{\rho}} \tag{22.9}$$

In the second case, the **pressure at EF is higher than CF** ($p_{CF} \leq p_{EF}$), for example, when DCV2 is actuated while DCV1 remains in neutral. In this condition, the path to CF becomes the one of least resistance; therefore, the spool reacts by creating a restriction on the CF line (Ω_{CF}). This situation is represented in Figure 22.12b). The path to EF is open, and therefore the pump pressure is

$$p_P = p_{EF} \tag{22.10}$$

In order to satisfy Eq. (22.5), the value of the intermediate pressure is $p_X = p_{EF} - s$. Therefore, the corresponding value of Ω_{CF} becomes

$$\Omega_{CF} = \frac{C_f}{Q^*_{CF}} \sqrt{\frac{2\left(p_{EF} - p_{CF} - s\right)}{\rho}} \tag{22.11}$$

In a nutshell, the priority valve (PV) acts as a compensator selectively in the CF or EF line, depending on which one has the highest load, in to maintain a set value for the flow to CF. Thus, the priority valve is different from a three-way flow control (such as that in Chapter 8). The latter, in fact, can control the flow under condition a) above, but is not designed to compensate

Orifice detail
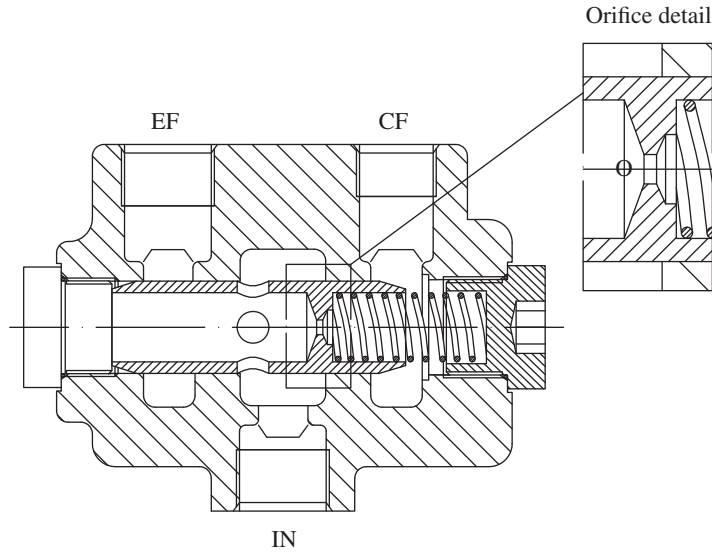
Figure 22.13 Cross-section of constant flow priority valve.

on the CF line. The priority valve is also different from a flow divider, because while the flow divider splits the input flow according to a set ratio, it does not control the value of the flow to the ports.

Figure 22.11 illustrates the flow supply: in the chosen schematic, the pump P is driven by a combustion engine, which usually operates at a variable speed. The priority valve is particularly useful in such applications, because the input flow can significantly vary between low and high idle, while it is desired to maintain a constant flow on the CF port.

The cross-section in Figure 22.13 shows a typical architecture for the priority valve, PV, for fixed displacement pump circuits. The inlet port communicates to CF and EF through four radial holes in the spool. The orifice O is achieved through a cross drilling in the spool, visible in the detailed view. In neutral condition, the flow path to EF is blocked, while the one to CF is open. As the spool shifts to the right, flow path to EF opens, while the other one is restricted.

Simply, Figure 22.11 shows two spools controlling the U1 and U2 actuators. In reality, U1 is very often represented by an open center steering unit. This common case is covered in the next example.

Example 22.2   Priority valve and power beyond feature

The circuit below represents a typical solution for power steering systems with fixed displacement pumps. The steering is controlled with a "power beyond" type steering unit. The steering circuit is always supplied with the desired flow Q_{CF}, but in neutral condition, the return flow from the unit goes through port PB and merges with the excess flow, Q_{EF},

going to the actuator U2. However, when steering is actuated, the return flow from the steering unit goes directly to the tank. In this way, the steering flow is not lost when the vehicle is not steering. One can say that the power beyond steering unit features a tandem connection with the actuators located downstream.
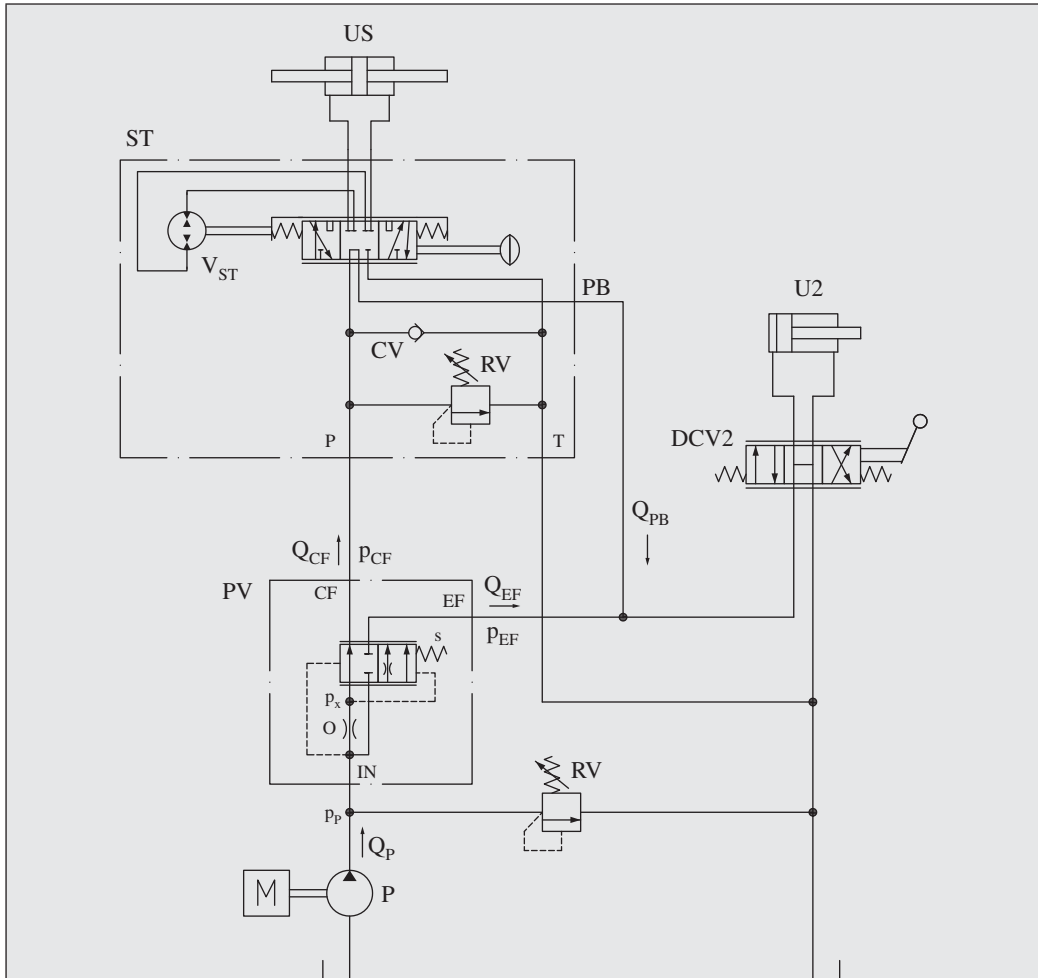
The pump flow is 60 *l/min*, the steering flow is 20 *l/min*, and the priority valve spring is set to 15 bar. Calculate pump pressure, pump power, and wasted power under the following three conditions:

(1) Steering at 80 *bar*, U2 at rest
(2) Steering at rest, U2 activated (full flow) at 150 *bar*
(3) Steering at 80 *bar* and U2 activated (full flow) at 150 *bar*

Given:
A steering circuit with power beyond steering unit where

Pump flow, $Q_P = 60$ *l/min*
Steering flow, $Q_{CF} = 20$ *l/min*
Priority valve spring rate, $s = 20$ *bar*
Steering pressure, $p_{CF} = 80$ *bar*
Excess flow actuator pressure, $p_{EF} = 150$ *bar*

Example 22.2 (Continued)

Find:

Pump pressure p_P, pump power P_P, and wasted power P_W for three different conditions

Solution:

In the first condition, the steering pressure at CF is higher than the pressure at EF:

$$p_{P,1} = p_{CF} + s = 100 \, bar$$

In the second condition, the EF pressure prevails. However, the power beyond port is pressurized to the load pressure; therefore, the CF port also sees the load ($p_{CF} = p_{EF}$):

$$p_{P,1} = p_{CF} + s = p_{EF} + s = 170 \, bar$$

In the third condition, however, the power beyond function is not used and the two functions operate at different pressure levels. The load at U2 prevails:

$$p_{P,3} = p_{EF} = 150 \, bar$$

In all cases, the pump power is equal to

$$P_{P,i} \, [kW] = \frac{Q_P \, [l/min] \cdot p_{P,i} \, [bar]}{600}$$

This leads to the following results: $P_{P,1} = 10 \, kW$, $P_{P,2} = 17 \, kW$, and $P_{P,3} = 15 \, kW$.

In the first condition, steering is working while EF is at rest; therefore, the excess flow is responsible for the wasted power:

$$P_{W,1} = \left(Q_P - Q_{CF} \right) \cdot p_{P,i} = \frac{40 \, [l/min] \cdot 100 \, [bar]}{600} = 6.7 \, kW$$

The reader should note that two-thirds of the pump power generates losses caused by the priority valve compensator.

In the second case, the steering is at rest and the steering flow merges with the excess flow. The only loss is caused by the priority valve spring:

$$P_{W,2} = Q_P \cdot s = \frac{60 \, [l/min] \cdot 20 \, [bar]}{600} = 2 \, kW$$

In the third case, the power loss is instead caused by the priority compensator reducing the pump pressure to the level of p_{CF}:

$$P_{W,3} = Q_{CF} \cdot \left(p_{P,3} - p_{CF} \right) = \frac{20 \, [l/min] \cdot (150 - 80) \, [bar]}{600} = 2.3 \, kW$$

It is important to point out that the speed of the actuator U2 is different in the two last cases. In case 2), the actuator sees the full pump flow, while in case 3) the excess flow is limited to 40 *l/min*.

22.5.2 Priority Valve for Load Sensing Circuits

The second type of priority valve is used in LS circuits, typically supplied by a variable displacement pump. A circuit representative of such an application is shown in Figure 22.14. The actuator with priority is an LS steering unit, while the excess flow user is, for sake of simplicity, an LS valve

Figure 22.14 Priority valve for LS circuit.

without compensators. The considerations valid for the circuit in Figure 22.14 can also be extended to load sensing pressure compensated (LSPC) circuits.

The supply flow to the CF line is not fixed as in the previous case. According to the LS principle, the steering flow is set by the position of the metering valve of the steering unit. The priority valve PV does not need to include a metering element (because this is within steering unit [ST]), and it functions just as a three-way compensator, similarly to the previous one. The spring chamber of the valve is connected to the LS pressure of the steering actuator, i.e. p_{U1}. The valve PV imposes the condition:

$$p_{CF} = p_{U1} + s_C \tag{22.12}$$

As in the previous case, the valve PV can selectively operate as a compensator on the EF or CF line, depending on which actuator requires the highest pressure. PV ensures that the margin pressure across ST is always equal to s_C.

In case of flow saturation, caused for example by a large amount of flow demanded by DCV2, PV ensures that ST receives the nominal flow demand, Q_{CF}, even if the value of p_{U1} is greater than p_{U2}. Only the remaining flow is diverted to DCV2.

Figure 22.15   LS priority valve cartridge style architecture.

Figure 22.15 shows an example of architecture of a LS priority valve, based on a cartridge construction. The LS pressure acts on the spring chamber. The CF pressure is reported to the bottom of the cartridge (to the left) through two radial holes in the spool. The orifice located inside the spool is a dynamic orifice, used to dampen the pilot pressure inside the chamber.

Problems

22.1   A steering unit supplies a double rod steering cylinder. The cylinder bore is 85 mm, while the rod is 32 mm. The overall cylinder stroke is 420 mm. Full steering (max left to max right) should be accomplished in 4 turns of the steering wheel, assuming the operator can reach a maximum steering angular velocity of 1.35 turns per second. Calculate the theoretical displacement of the steering unit and the theoretical flow required by the unit to meet the specifications.

22.2   A wheel loader uses an articulated steering system based on two opposite single rod cylinders, connected as in the figure below. Each cylinder has a bore of 110 mm, and a rod of 45 mm, with a stroke of 650 mm. What is the ratio of the supply and return flow?
Full steering (max left to max right) should be accomplished in six turns of the steering wheel, and the operator can reach a maximum steering angular velocity is 1.65 turns per second. Calculate the theoretical displacement of the steering unit, and the theoretical flow required by the unit to meet the specifications.
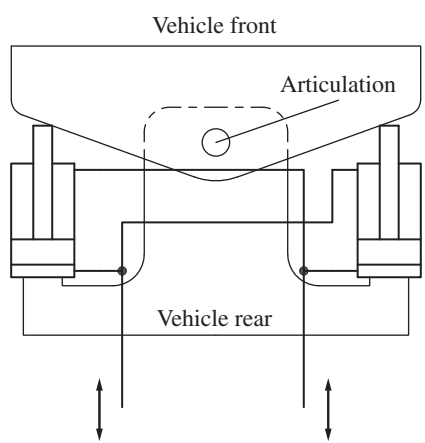
References

1 Nervegna, N. and Rundo, M. (2020). *Passi nell'oleodinamica* vol. 1–2, Epics.
2 Zarotti, G.L. (1997). Circuiti Oleodinamici – Nozioni e lineamenti introduttivi, Cemoter.

Part VI

Hydrostatic Transmissions and Hydrostatic Actuators

In fluid power, defining hydrostatic transmissions (HTs) is not an easy task. In principle, all hydraulic systems "transmit" mechanical power from a prime mover to hydrostatic actuators (HAs). Therefore, all hydraulic systems could be broadly referred to HTs. Therefore, categorizing a certain type of hydraulic control systems as an HT might confuse those who are studying hydraulic control technology. However, in common practice, HTs indicate only a certain subset of hydraulic concepts used to control rotary actuators (hydraulic motors).

Different classifications for HTs are defined in the literature or based on the industry practice, thereby often contradicting. In this book, the authors have decided to strictly refer to ISO standards 5598 and 4391 (basic definitions of fluid power systems and integral transmissions, as found in [1] and [2]): "combination of one or more hydraulic pumps and motors forming a unit designed to obtain a variation of speed or torque." Therefore, HTs refer to systems with only rotary actuators, regulated with various hydraulic control concepts, except for the metering control. Accordingly, HTs can be implemented in both open circuit and closed circuit configurations, using primary or secondary control (or a combination of both). A similar choice was made by Nervegna [3] and Zarotti [4]. This part of the book covers the description of these types of systems, expanding the principles introduced in Part III. Chapter 23 provides the basic definitions and describes the main layout architectures used to implement HTs and HAs. Chapter 24 further investigates the layout architectures of both open circuit and closed circuit HTs and their operating features. Chapter 25 focuses on the most common application of HT systems: the vehicle propulsion. This chapter introduces also more advanced technologies, such as hydromechanical power split and hydraulic hybrids, and presents a method for sizing basic HTs. Chapter 26 focuses solely on HAs to further differentiate them from HTs. Chapter 27 is dedicated to secondary controlled HTs, which are based on pressure supply and can be treated separately from the previous circuits based on flow supply.

Objectives

Part VI is entirely dedicated to HTs and HAs. HTs represent one of the most common applications of hydraulic control technology, particularly for vehicle propulsion. This part of the book will familiarize the reader with the most common layout architectures for HTs and their operating features as well as Has, which are related to a technology that is gaining increasing interest due to its easy integration with electric prime movers.

By reading each chapter of Part VI thoroughly, and by practicing on the proposed worked examples and the end-of-chapter problems, the reader will be able to

1) Recognize the different types of hydraulic circuits that can implement an HT or an HA, such as open and closed circuit.
2) Describe the operating behavior of an HT, in terms of transmission ratio and dynamic ratio.
3) Describe the characteristics (transmission ratio vs. dynamic ratio) of the basic HT architectures using either fixed or variable displacement units.
4) Explain the functions of all the main components present in an HT, including the need for flushing elements.
5) Understand the differences between primary and secondary control.
6) Illustrate the main features of displacement regulators used to control HTs.
7) Model the behavior of a hydrostatic transmission with a quasi-steady-state approach.
8) Discuss the requirements for a generic transmission system for vehicle propulsion and understand pros and cons of HTs compared to other technologies.
9) Classify the different architectures available for implementing a transmission system, including discrete variable ratio systems from continuously variable ratio systems (continuously variable transmissions [CVTs]).
10) Describe the use of HTs in complex transmission architectures such as hydromechanical power split transmissions and hydraulic hybrids.
11) Size the main components of a hydrostatic transmission.
12) Describe the operation, model, and size of HAs.
13) Describe the circuit and the operating features of a secondary controlled HT, based on pressure supply.

Chapter 23

Basics and Classifications

This chapter describes the basic concepts for hydrostatic transmissions (HTs) and hydrostatic actuators (HAs) and introduces the main parameters which are commonly used to describe HTs and HAs. Here, the different layout architectures, based on either open circuit and or closed-circuit design, are also presented and compared, with respect to some considerations on the main operating features for each design.

23.1 Hydrostatic Transmissions and Hydrostatic Actuators

23.1.1 Basic Definitions

Hydrostatic transmissions and **hydrostatic actuators** are based on primary or secondary control actuation[1]. The main difference between HTs and HAs is the type of application: an HT drives one or more rotary actuators, while an HA is used for linear actuators. The basic layouts of HTs and HAs are summarized in Figure 23.1.

> HTs and HAs perform hydraulic actuation without using metering control. They can both use primary control strategies. HTs can also be based on secondary control.

Figure 23.1 illustrates the basic layouts of HTs and HAs through simplified schematics: **closed circuit** (left column of the table) and **open circuit** (right column). The full circuit implementations will be described in Part IV.

In an open circuit configuration, it is always possible to identify the high-pressure (HP) line connecting the two units and the low-pressure (LP) line connecting the actuator to the tank, or sometimes to an LP accumulator. The location of both the HP and LP lines in the circuit is fixed, and it is not affected by the load. However, the pressure in the HP line of the circuit is defined by the external load and therefore its value changes with the operating conditions. Meanwhile, in the closed circuit architecture, the HP line and the LP line of the circuit can switch during the operation, depending on the commanded direction or the nature of the load (resistive or overrunning).

> In the **open circuit** configuration of HTs or HAs, the location of both the HP line and the low-pressure (LP) line does not change with the operating conditions. On the other hand, in **closed circuits** HTs or HAs, the HP and LP lines can switch during the operation, depending on the load conditions.

1 Secondary control can be applied only to HTs where the motor displacement can be adjusted.
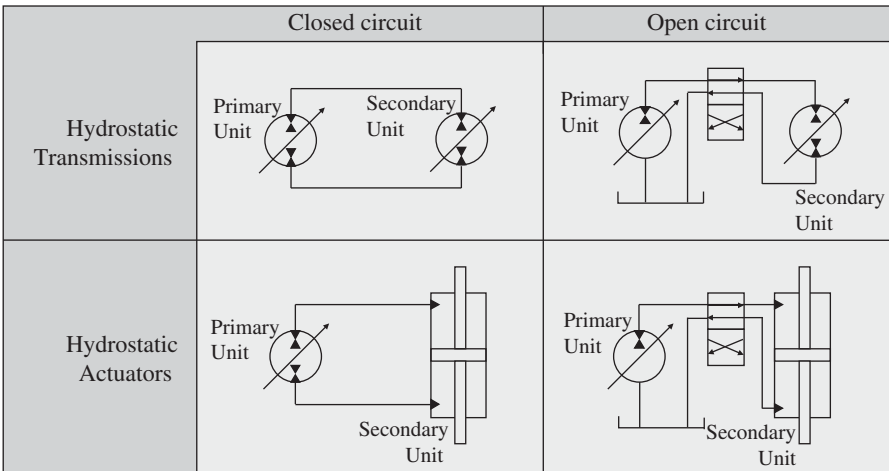
Figure 23.1 Conceptual schematic for hydrostatic transmissions and hydrostatic actuators with a single actuator.

In general, HTs and HAs can transfer energy between the prime mover and the hydraulic actuator in both directions. This is also why the rotating units in Figure 23.1 are represented with the pump/motor symbols. In other words, the unit connected to the prime mover operates as a pump when the load is resistive and can work as a motor if the load is overrunning. The unit connected to prime mover should be referred to as **primary unit**, while the unit connected to the function is the **secondary units**. The terms *primary* and *secondary* univocally refer to the physical location of the unit. However, the terms *pump* and *motor* are used to indicate the function of the unit from the energy transfer point of view, as explained in Part I. The primary/secondary nomenclature clarifies the confusion from mixing the location of a unit with the operating mode of the system. However, it is still a common practice in an HT to refer to *pump* as the unit connected to the prime mover, independently on the operating mode. Similarly the *motor* is the unit connected to the load. The use of the terms are correct, as long as their function during the system operation is further specified. Thus, we can refer to the primary unit as a pump working in either *pumping* or *motoring* mode, similar with a motor of an HT.

> The hydraulic unit connected to the prime mover is the **primary unit**, while the hydraulic unit connected to the actuator is the **secondary unit**. The terms pump and motor are commonly used for the primary unit and the secondary unit, respectively. In this case, it is recommended to further specify their functions, which can be either **pumping** or **motoring**.

The performance of HTs and HAs is usually evaluated with respect to four quadrants of operation. The quadrants are defined with a plot representing the actuator load on the horizontal axis and the actuator velocity on the vertical axis. For HAs, the load is the external force on the cylinder and the velocity is the measure of its traveling speed. However, for HTs the load is the torque on the motor shaft and the velocity is the angular velocity of the shaft. The positive and negative signs are determined with respect to a given frame of reference. In general, this reference is used so that when the two signs are concordant, the load is resistive because otherwise it is overrunning. Based on this assumption, quadrants 1 and 3 represent resistive load conditions, while quadrants 2 and 4 pertain to overrunning conditions.
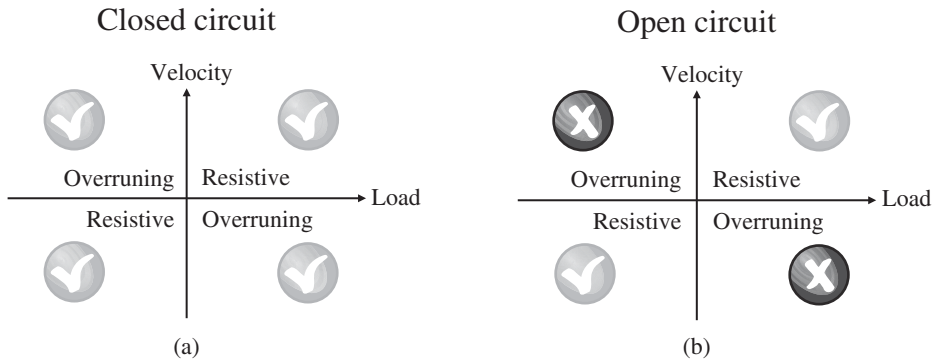
Figure 23.2 Four quadrant operation for an HT or HA: closed circuit configuration (a) and open circuit configuration (b).

Closed circuit HTs and HAs are known for their ability to cover all four quadrants of operation with a simple layout. Specifically, they have the capability of reversing the actuator motion as well as the power flow within the hydraulic circuit. The power goes from the prime mover to the actuator for resistive loads and from the actuator to the prime mover in case of overrunning loads. As it will be further discussed in Part IV, this feature can enable energy recovery.

In principle, open circuit HTs and HAs can also operate in all the four quadrants. However, open circuit architectures suitable for the four-quadrant operation are quite rare. Usually, they are unsuitable to handle cases where the load can transition between resistive and overrunning. For this reason, the most common open circuit solutions are designed to work in quadrants 2 and 4 (Figure 23.2). In this case, additional compensating elements (e.g. counterbalance valves, described in Chapter 14) can be utilized in the circuit to handle overrunning load conditions. When counterbalance valves handle overrunning loads, the load energy is dissipated.

In brief, typical open circuit HTs and HAs can operate on four quadrants but are not capable of recovering the load energy in quadrants 2 and 4, except for secondary control HTs with pressure supply. This type of open circuit layout can implement a four-quadrant operation without controllability issues in case of transitional loads. Energy recovery is achieved using HP accumulators. This particular type of layout will be explained separately in Chapter 27.

> Closed circuit HTs or HAs typically offer some advantages with respect to their open circuit counterpart, when handling overrunning load conditions.

One final difference between the closed and open circuit is the way in which the direction of motion is reversed. In the open circuit layout, a 4W2P directional element is used to switch the work-port of the secondary unit supplied by the primary flow. In the closed-circuit layout, however, the primary unit can reverse the flow direction. In some specific applications, this is accomplished by reversing the shaft rotation, but in most of the cases this is achieved with over-center primary units, which are described in Section 23.1.2.

23.1.2 Supply Concepts Used in Hydrostatic Transmissions and Hydrostatic Actuators

As mentioned in Chapter 11, primary and secondary control concepts can be combined with either a flow supply or a pressure type supply. In general, the majority of HTs and HAs use flow supplies. In other words, the hydraulic system is designed to control the actuator speed acting on the amount

of flow supplied by the primary unit. Flow-type supplies are included in either closed or open circuit layouts.

On the other hand, pressure supply is applied mostly in open circuits. Open circuit primary control with pressure supply is commonly used in presses (using linear actuators; therefore the circuit is a HA type) or fan drive circuits (which use rotary actuators; thus the circuit is a HT). The case of hydrostatic fan drives will be analyzed in more detail in Part VI. On the other hand, secondary control with pressure supply represents a category on its own among hydraulic systems. This concept is analyzed in depth in Chapter 27. The considerations made on HTs and HAs in this chapter and Chapters 24–25 might not apply to the particular case of secondary controlled HTs.

23.2 Primary Units for Hydrostatic Transmissions and Hydrostatic Actuators

Based on a primary control concept, the supply flow in HTs and Has can be regulated according to different methods as shown in Figure 23.3, which shows an electric motor as prime mover. However, the prime mover can be also an internal combustion engine (ICE).

23.2.1 Constant Speed Prime Mover and Variable Displacement Pump

Figure 23.3a represents a constant speed prime mover and a variable displacement pump. This architecture is suitable for applications using, for example, an engine running at a fixed speed or an induction-type electric motor without variable frequency drive. The shaft speed of the prime mover does not affect the regulation, and it can be selected based on the application flow requirements. The desired flow is controlled by adjusting the pump displacement, which is obtained through a displacement regulator.

23.2.2 Variable Speed Prime Mover and Fixed Displacement Pump

Figure 23.3b shows the alternative regulation methods based on a fixed displacement pump coupled with a variable speed prime mover. This solution is rarely seen in combination with combustion engines. The ICE shaft usually supplies energy to multiple functions, and its speed is often

Electric Motor (EM) - Hydraulic Unit (HU) combinations

(a) EM : constant speed
HU: variable displacement

(b) EM : variable speed
HU: fixed displacement

(c) EM : variable speed
HU: variable displacement
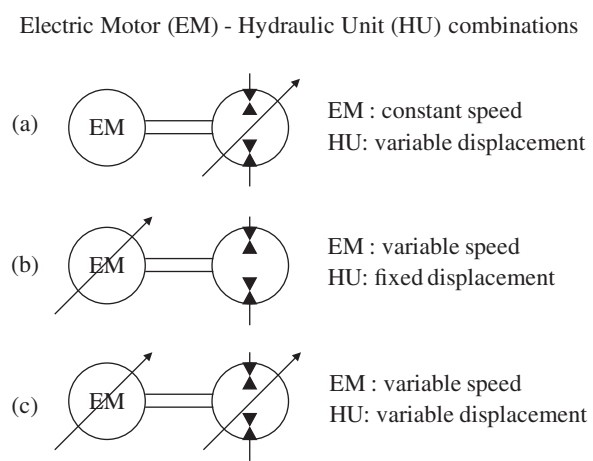
Figure 23.3 Different methods for implementing primary flow regulation: (a) constant speed prime mover and variable displacement pump (b) variable speed prime move and fixed displacement pump (c) variable speed prime move and fixed displacement pump.

limited by physical and functional constrains (idle and max governed speed). On the other hand, the method in Figure 23.3b is very well suited for systems using electric motors with variable frequency drives, which can vary their speed on a wide range. Unlike in Figure 23.3a, the variable motor–fixed pump solution permits using simpler hydraulic units (such as fixed displacement pumps) and requires more complexity on the electrical side.

23.2.3 Variable Speed Prime Mover and Variable Displacement Pump

Figure 23.3c shows the combination of the two variable units, which is by far the least economical. However, the complexity of using a variable speed prime mover coupled with a variable displacement pump can be compensated by the advantages enabled by the two degrees of freedom regulation. The methods in Figure 23.3a,b has only one variable, which needs to be controlled to meet the flow demand. However, with the solution in Figure 23.3c, the two controlled variables (shaft speed and pump displacement) can be regulated in such a way that the flow demand is satisfied at the most efficient condition for the system. In this way, the flow regulation can occur avoiding inefficient operation of the pump (such as operation at high pressures and low shaft speeds) or of the prime mover.

23.3 Over-center Variable Displacement Pump

Closed circuit layouts have the capability to reverse the flow direction without using directional elements. This can be achieved in two ways (Figure 23.4): the pump can reverse the flow by going over-center maintaining the same rotation (a), or the electric motor can reverse the direction of rotation (b), which is suitable for circuits based on fixed displacement units.

A representation of the operating modes of an over-center unit is given in Figure 23.5. The relationship between instantaneous displacement, V_D, and input command is given, i, by

$$V_D(i) = \epsilon(i) \cdot V_{D,\max} \tag{23.1}$$

The common convention indicates both the command and the instantaneous displacement with a positive sign when the pump supplies flow to the upper port. Vice versa, the negative sign is used to indicate that the pump supplies flow to the bottom port. These types of units are commonly based on a piston design (swash plate or sometimes bent axis). For the swash plate design similar to that in Chapter 6, the over-center unit can reverse the angle of the swash plate, thus reversing the flow direction. In this case, the command value is considered negative, as shown in Figure 23.5. The figure also highlights the presence of a deadband region for the input command, for which the unit is held at zero displacement. Despite being helpful when a zero flow is desired, this deadband
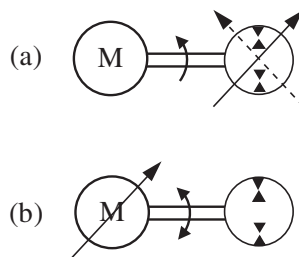
Figure 23.4 Different methods for implementing reversal of flow direction in closed circuit layouts: (a) single direction EM – over center pump (b) reversing EM, fixed displacement pump.
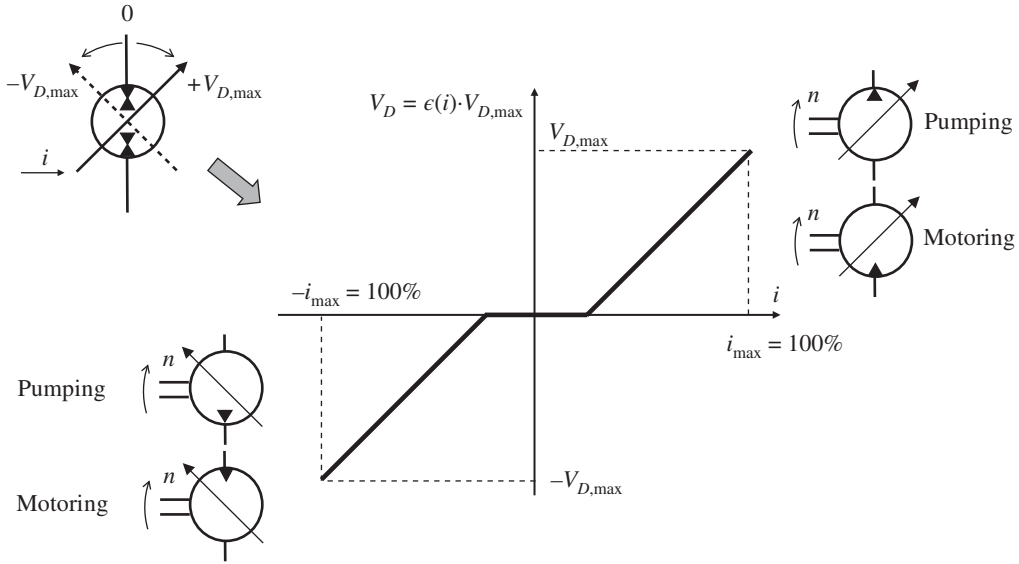
Figure 23.5 Over-center variable displacement pump/motor: relationship between input command and instantaneous displacement.

zone is not discussed further and the relationship between input command and displacement is considered purely linear.

In an over-center unit, for both pumping and motoring operation, the relationship between shaft rotational speed, flow rate, and fractional displacement is

$$Q_P(i) = n \cdot V_D(i) = n \cdot \epsilon(i) \cdot V_{D,\max} \tag{23.2}$$

Over-center units can also be found as secondary units in secondary controlled transmission (see Chapter 27).

23.4 Typical Applications

HTs are widely used in both industrial and mobile applications. Closed circuit systems are the preferred solution for several propulsion systems in off-road vehicles because of their ability to control overrunning load. Vehicles such as agricultural tractors, loaders, telehandlers, and many others can use closed circuit HTs for the propulsion systems. Open circuit systems are generally simpler and more economical than closed circuit HTs. They are used in applications such as cooling fan drives, small drilling machines, or compressor drives, where overrunning conditions are not an issue. Closed circuits can provide an easier and more efficient reversal of the flow (no need for directional elements that create additional pressure losses). Closed circuit, as it will be better described in the next Chapters, require also smaller reservoirs than open circuit HTs. Hence, the closed-circuit design is very successful in high-flow applications.

HAs achieve linear motion without introducing power losses associated with the metering regulation, as described in Parts III and V. Despite their energy efficiency advantage, HAs are still not very popular in mobile applications because, in systems with HAs, every actuator requires a dedicated pump. This significantly increases the size and cost of the system. However, HAs are successfully applied in industrial and aerospace applications such as injection molding machines and airplane landing gears. In these applications, the prime mover is an electric machine, often referred to as electrohydraulic actuator (EHA), whose components can be integrated in a self-contained and

compact arrangement that includes the reservoir, the supply pump and the electric motor, the control valves and the actuator (compact EHA). Compact EHAs are gaining popularity particularly in low power applications such as biomedical devices and human size robots.

23.5 Classification Summary

A schematic representation of the different types of HTs and HAs is presented in Figure 23.6. The figure divides different cases based on:

- the type of control (primary or secondary)
- the type of supply (flow supply or pressure supply)
- the type of actuator (rotary actuator or linear actuator)

The figure shows where HTs and HAs can be implemented and what are the possible architectures (open circuit or closed circuit). It also highlights the fact that the secondary control regulation strategy does not apply to HAs because this type of regulation would use hydraulic cylinders with variable piston or variable rod areas so that the actuator velocity can be varied by varying this area instead of varying the flow at the work-ports. Such cylinders are not commercially available nowadays. However, it is worth to note that the advantages of the secondary control regulation, particularly the ease of energy recuperation during overrunning load conditions, has pushed research for commercially viable solutions for variable area cylinders. Of particular interest is the solution recently proposed at Linkoping University in Sweden [5].
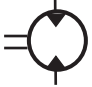
Figure 23.6 Classification and nomenclature of the different types of primary and secondary controlled systems.

Chapter 24

Hydrostatic Transmissions

This chapter focuses on the most common configurations of hydrostatic transmissions (HTs), which are used to drive rotary-type actuators (motors). The cases covered here include HTs based on primary controls, for both flow supply and pressure supply or for secondary control with only flow supply. Secondary controlled HTs with pressure supply are discussed in Chapter 27.

After presenting some important parameters common to all HTs, different circuit layouts are described in detail, highlighting the differences between the open and closed circuit solutions. This chapter illustrates the main functions of HTs and the basic control strategies.

24.1 Main Parameters for a Hydrostatic Transmission

Primary and secondary units of HTs are characterized by a unique set of parameters for each hydraulic unit (primary or secondary):

– V_D is the maximum displacement of the unit.
– ϵ represents the setting of the unit (intended as ratio between the current and maximum displacement).
– Δp represents the pressure difference between the high- and low-pressure lines of the transmission.
– Q is the volumetric flow rate across the unit.
– T represents the torque at the unit's shaft.
– n is the rotational speed of the unit.
– $\eta_T, \eta_v, \eta_{hm}$ represent the overall, volumetric, and hydromechanical efficiencies of the unit, respectively.

The detailed definition of the above parameters can be found in Chapter 6. In the following description, when a parameter is used for the primary unit, it will be indicated with the subscript *P*; the subscript *M* will be used for the secondary unit. Figure 24.1 implements most of these parameters for a generic HT.

Given the parameters for each unit, the HT can be further characterized by calculating three significant values: the *transmission ratio*, the *dynamic ratio*, and the *overall transmission efficiency*. These attributes are calculated under the assumptions of *flow and pressure coupling* of the two units, stating that the flow delivered by the primary is fully received by the secondary unit and that the pressure differential across the two units is equal.

1) The *transmission ratio* (τ) represents the ratio between the shaft speed of the secondary unit and the shaft speed of the primary unit. This is calculated by imposing the flow coupling condition.
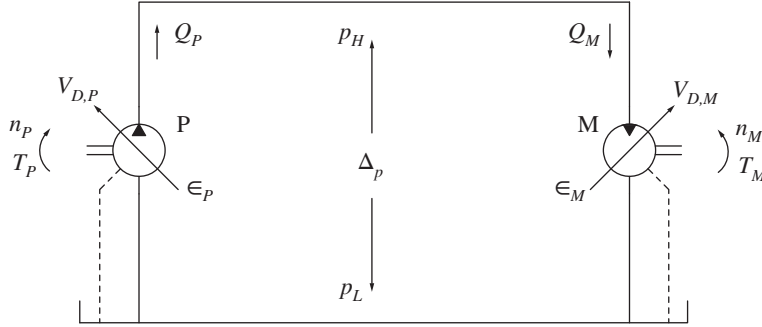
Figure 24.1 Parameters describing a generic hydrostatic transmission.

This means that the flow at the outlet of the primary unit is equal to the flow entering the secondary unit:

$$\tau = \frac{n_M}{n_P} = \frac{\epsilon_P \cdot V_{D,P}}{\epsilon_M \cdot V_{D,M}} \cdot \eta_{v,P} \cdot \eta_{v,M} \tag{24.1}$$

2) The *dynamic ratio* (κ) is the ratio between the shaft torque at the secondary unit and at the primary unit. This is calculated by imposing the pressure coupling condition:

$$\kappa = \frac{T_M}{T_P} = \frac{\epsilon_M \cdot V_{D,M}}{\epsilon_P \cdot V_{D,P}} \cdot \eta_{\mathrm{hm},P} \cdot \eta_{\mathrm{hm},M} \tag{24.2}$$

3) The *overall transmission efficiency* (η_{HT}) is the ratio between the power generated by the secondary unit and the power required by the primary unit:

$$\eta_{\mathrm{HT}} = \frac{P_M}{P_P} = \tau \cdot \kappa = \eta_{v,P} \cdot \eta_{v,M} \cdot \eta_{\mathrm{hm},P} \cdot \eta_{\mathrm{hm},M} = \eta_{T,P} \cdot \eta_{T,M} \tag{24.3}$$

The ratio between the shaft speed of the primary unit and the secondary unit is defined as the **transmission ratio**, τ. The ratio between the torque at the secondary unit shaft and the torque at the primary unit shaft is the **dynamic ratio**, κ. The product between τ and κ equals the **overall energy efficiency** of the transmission.

While the transmission ratio (τ) and dynamic ratio (κ) are fundamental parameters for hydromechanical transmissions or gearboxes, these two quantities are seldom utilized in the case of HTs. However, the overall efficiency is a key energy parameter for HTs and it is important, for example, for determining the cooling requirements of the system. The value of η_{HT} calculated above is affected only by the individual performance of primary and secondary units and does not include other contributions, such as line losses or charge pump losses (this item will be discussed in the next paragraphs). Another important observation is that the efficiency of the HT is not a constant value, but it is a function of the operating conditions.

In the case of an ideal system, the efficiency of the transmission is unitary; therefore, $\tau = 1/\kappa$.

Example 24.1 Properties of a hydrostatic transmission

A compact tracked vehicle is propelled by a hydraulic system including two HTs, one dedicated to each track. Each HT comprises a 20 cm^3/r variable pump and a 405 cm^3/r motor. The two pumps are powered by a 55 hp engine, which can run at a maximum speed of 2300 rpm. The

maximum operating pressure of the hydraulic system is 200 *bar*. The performance curves of pumps (at full displacement) and motors are shown below.

Pump efficiency (at 100% displacement)

Motor performance chart
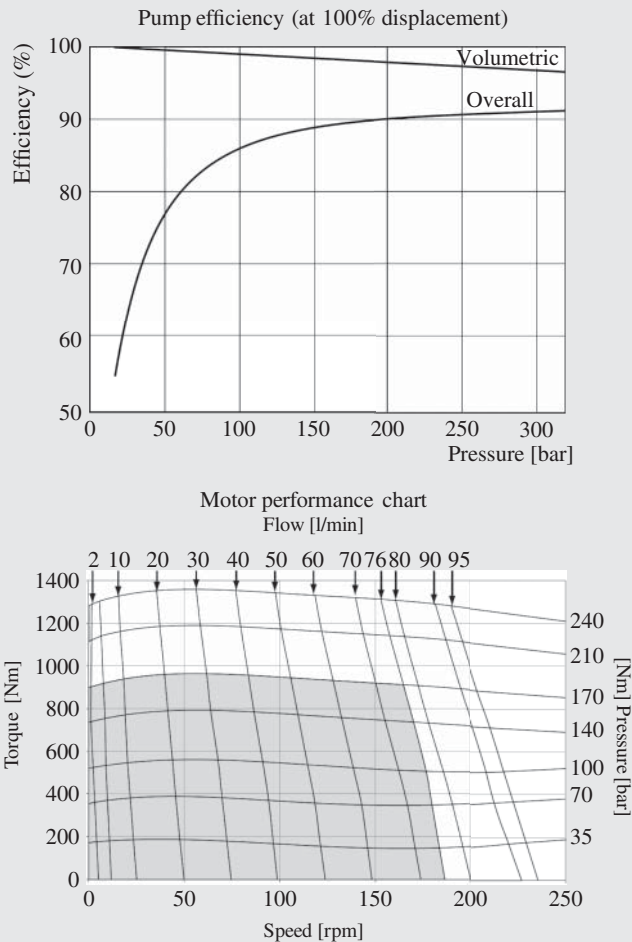
Answer to the following questions:

1) Calculate the values for the ideal transmission and dynamic ratio of each HT.
2) What is the overall efficiency of each transmission at maximum displacement and maximum pressure? Calculate the maximum power wasted by the real hydraulic system based on the provided charts.
3) Calculate the real values for transmission and dynamic ratio in the condition of maximum power.
4) How can the vehicle steering be achieved by such system?

Given:

Pump, $V_{D,P} = 20 \, cm^3/r$; $n_P = 2300 \, rpm$ max.
Motor, $V_{D,M} = 405 \, cm^3/r$
Maximum operating pressure, $p_{max} = 200 \, bar$
Engine power, $P_{eng} = 55 \, hp = 41 \, kW$

Example 24.1 (Continued)

Find:

1) Ideal transmission ratio τ and dynamic ratio κ
2) HT system efficiency and maximum system power loss
3) Real transmission ratio τ and dynamic ratio κ
4) Steering solution

Solution:

1) For each HT, the ideal transmission ratio is calculated as follows:

$$\tau = \frac{n_M}{n_P} = \frac{\epsilon_P \cdot V_{D,P}}{V_{D,M}} = \frac{\epsilon_P \cdot 20\,[cm^3/r]}{405\,[cm^3/r]} = \epsilon_P \cdot 0.049$$

The maximum value of τ corresponds to $\epsilon_P = 1$ and it is equal to 0.049.
The dynamic ratio is the inverse of τ and its minimum value is 20.25 ($\epsilon_P = 1$).

2) When the pump works at maximum displacement and at maximum pressure, the pump overall efficiency is 90%. The volumetric efficiency is approximately 97%. This means the flow delivered to the motor is

$$Q_{P,\max} = V_{D,P} \cdot n_P \cdot \eta_{v,P} = 20\,[cm^3/r] \cdot 2300\,[rpm] \cdot 0.97 \cdot \frac{1}{1000} = 44.6\,l/min$$

At this flow, based on the performance chart, the motor rotates at approximately 95 *rpm* delivering a torque of 1100 *Nm* (200 *bar*). This corresponds to an output power of

$$P_M = T_M \cdot \omega = 1100\,[N/m] \cdot 95 \cdot \frac{2\pi}{60}[rad/s] \cdot \frac{1}{1000} = 10.9\,kW$$

The ideal power at the motor is

$$P_{M,ideal} = Q_P \cdot p_{\max} = 44.6\,[l/min] \cdot 200\,[bar] \cdot \frac{1}{600} = 14.8\,kW$$

The motor overall efficiency is the ratio between the two power values: $\eta_{T,M} = 73.8\%$. This is a typical value for orbit motors, which are not the most efficient units available. The efficiency of the HT becomes

$$\eta_{HT} = \eta_{T,P} \cdot \eta_{T,M} = 66\%$$

The maximum power demand of each HT is

$$P_P = (Q_{P,\max} \cdot p_{\max})/\eta_{T,P} = 16.51\,kW$$

The overall wasted power corresponds to

$$P_{W,\max} = 2 \cdot (P_P - P_M) = 2 \cdot 3.84\,[kW] = 7.68\,kW$$

3) In the previous case, the volumetric and overall efficiency of the pump are known. Therefore, the hydromechanical efficiency can also be calculated by dividing the two. Therefore, $\eta_{hm,P} = 93\%$. The torque demanded by the pump at 200 *bar* is

$$T_P = \frac{V_{D,P} \cdot p_{\max}}{\eta_{hm,P}} = 20\,[cm^3/r] \cdot 200\,[bar] \cdot \frac{1}{20\pi} \cdot \frac{1}{0.93} = 68.5\,Nm$$

Therefore, the real ratios of the transmission are

$$\tau = \frac{n_M}{n_P} = \frac{95\,[rpm]}{2300\,[rpm]} = 0.041$$

$$\kappa = \frac{T_M}{T_P} = \frac{1100 \, [Nm]}{68.5 \, [Nm]} = 16$$

4) In tracked vehicles, the left and right tracks are usually controlled by two independent circuits and the steering function is achieved by changing the speed of one of the tracks. The track speed is changed by changing the pump displacement. The vehicle will steer in the direction of the track which is running at a lower speed.

24.2 Theoretical Layouts

Both primary and secondary units of an HT can have a fixed or variable displacement design. Four combinations are possible: pump and motor with fixed displacement (PFMF), variable displacement pump and fixed displacement motor (PVMF), fixed displacement pump and variable displacement motor (PFMV), and both pump and motor with variable displacement (PVMV). Each combination is characterized by different operating features as well as different transmission and dynamic ratios. For the sake of simplicity, the following theoretical analysis is provided assuming ideal units. The real case is then studied through qualitative charts. The transmission and dynamic ratio of a HT with ideal units are

$$\begin{cases} \tau = \dfrac{n_M}{n_P} = \dfrac{\epsilon_P \cdot V_{D,P}}{\epsilon_M \cdot V_{D,M}} \\[2mm] \kappa = \dfrac{T_M}{T_P} = \dfrac{\epsilon_M \cdot V_{D,M}}{\epsilon_P \cdot V_{D,P}} \end{cases} \tag{24.4}$$

In the ideal case, $\tau = \kappa^{-1}$.

Each theoretical layout is analyzed and compared to the other ones using two diagrams: the (τ, κ) diagram and the plot representing T_M and P_M as functions of τ. The (τ, κ) plane shows how the torque is transmitted at different output speeds and is also useful to understand the operating range of the transmission layout.

24.2.1 Pump and Motor with Fixed Displacement (PFMF)

This is the simplest combination, which is characterized by a single point of operation. In fact, in Eq. (24.4), the values of the displacement settings ϵ are unitary and the two ratios are constant:

$$\begin{cases} \tau = \dfrac{V_{D,P}}{V_{D,M}} \\[2mm] \kappa = \dfrac{V_{D,M}}{V_{D,P}} \end{cases} \tag{24.5}$$

The output torque T_M and power P_M of the transmission are solely a function of the load pressure Δp.

24.2.2 Variable Displacement Pump and Fixed Displacement Motor (PVMF)

This is the most common combination, and its conceptual schematic is represented in Figure 24.2. Here, the transmission configuration can be controlled by adjusting the setting of the primary unit
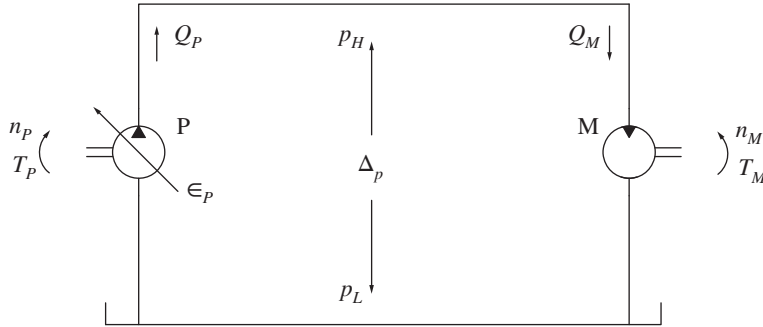
Figure 24.2 HT with variable displacement primary unit and fixed displacement secondary (PVMF).

ϵ_P (primary control). The values of the transmission and dynamic ratio are

$$
\begin{cases}
\tau = \dfrac{\epsilon_P \cdot V_{D,P}}{V_{D,M}} \\[4mm]
\kappa = \dfrac{V_{D,M}}{\epsilon_P \cdot V_{D,P}}
\end{cases}
\tag{24.6}
$$

As visible in Figure 24.3, in the (τ, κ) plane, the operating points of the transmission are described by the left half of a hyperbole. The values of $\tau_{\max}$ and $\kappa_{\min}$ correspond to the maximum setting of the pump displacement. The same figure also shows the trend of torque and output power at the motor shaft as a function of τ for different values of Δp: the first one is constant while the second one linearly increases with τ. In fact,

$$
\begin{aligned}
T_M &= V_{D,M} \cdot \Delta p \\
P_M &= T_M \cdot n_M = T_M \cdot n_P \cdot \tau
\end{aligned}
\tag{24.7}
$$

The charts in Figure 24.3 show how the PVMF layout allows reaching high output torque but it is limited in the velocity range of the motor shaft.

In the real case, considering the volumetric and hydromechanical losses of the units, the qualitative trends of torque, power, and efficiency of the PVMF transmission are represented in Figure 24.4, for a given value of Δp.

(a)

(b)
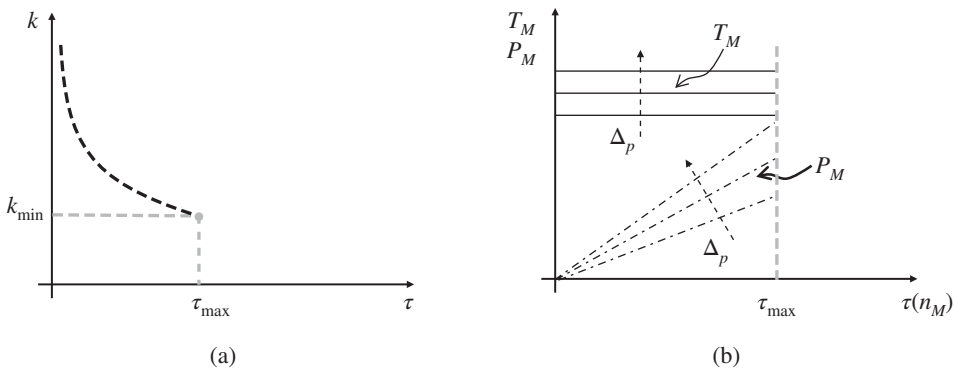
Figure 24.3 Transmission ratios (a), torque and power (b) for a PVMF transmission with ideal units.
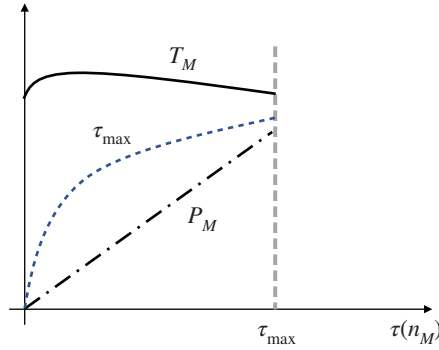
Figure 24.4　Torque, power, and efficiency curves for a PVMF transmission with real units.

24.2.3　Fixed Displacement Pump and Variable Displacement Motor (PFMV)

This combination, which is represented in Figure 24.5, is seldom encountered in HT applications. However, it is interesting to understand the implications of controlling the motor displacement (secondary control). The values of the two ratios become

$$\begin{cases} \tau = \dfrac{V_{D,P}}{\epsilon_M \cdot V_{D,M}} \\[4mm] \kappa = \dfrac{\epsilon_M \cdot V_{D,M}}{V_{D,P}} \end{cases} \tag{24.8}$$

The expressions of Eq. (24.8) are symmetrical with respect to Eq. (24.6); in fact, the operating points of the HT belong to the right half of a hyperbole, as shown in Figure 24.6. This points out how the PFMV layout allows reaching high output speeds, but it is limited in terms of motor velocity range. The transmission ratio is limited by a minimum value, meaning the motor cannot be controlled at low speeds. The values of $\tau_{\min}$ and $\kappa_{\max}$ correspond to the maximum setting of the motor displacement. The same figure represents the torque and power trends at the motor, which can be calculated as follows:

$$T_M = \epsilon_M \cdot V_{D,M} \cdot \Delta p = \frac{V_{D,P} \cdot \Delta p}{\tau}$$
$$P_M = T_M \cdot n_M = \frac{V_{D,P} \cdot \Delta p}{\tau} \cdot n_P \cdot \tau = V_{D,P} \cdot \Delta p \cdot n_P \tag{24.9}$$
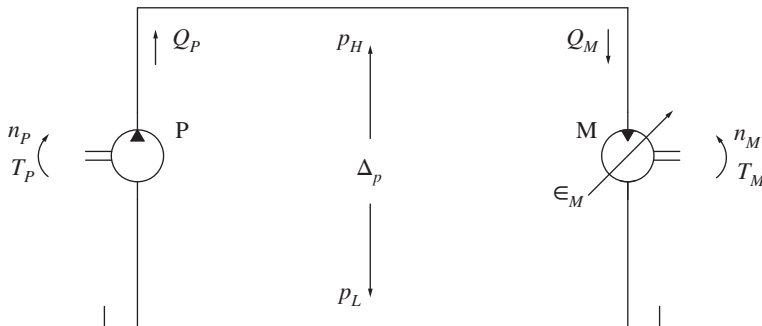
Figure 24.5　HT with fixed displacement primary unit and variable displacement secondary (PFMV).
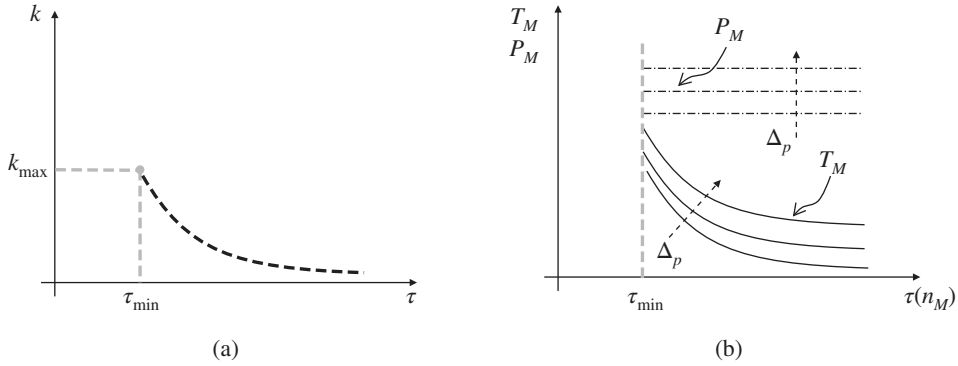
Figure 24.6 Transmission ratios (a), torque and power (b) for a PFMV transmission (ideal case).

Equation (24.9) shows that, for a given load Δp, the motor torque decreases with an increase of τ, following a segment of hyperbole. While τ increases, the motor displacement decreases. On the other hand, the power at the motor shaft is constant because the torque reduction is compensated by an increase in shaft velocity.

24.2.4 Variable Displacement Pump and Variable Displacement Motor (PVMV)

This combination (Figure 24.7) is the most complex to analyze because it is characterized by two degrees of freedom. The setting of both units can be simultaneously controlled, as each value of τ can correspond to different combinations of ϵ_M and ϵ_P.

The study of this configuration assumes that the control of the motor speed follows the scheme of Figure 24.8. At the null point, the pump displacement is zero ($\epsilon_P = 0$), while the motor is at maximum ($\epsilon_M = 1$). The motor speed is initially varied by increasing the pump displacement ϵ_P while keeping the motor at full displacement ($\epsilon_M = 1$). Only after the pump reaches the maximum displacement ($\epsilon_P = 1$ and $n_M = n_{M1}$), the motor decreases its displacement, until reaching the maximum speed n_{M2}.

In Figure 24.8, for $0 \leq n_M \leq n_{M1}$, the HT behaves as a PVMF transmission, while for $n_{M1} < n_M \leq n_{M2}$, the HT follows the principle of a PFMV configuration. The same behavior is shown in the characteristic diagrams of the PVMV transmission (Figure 24.9). In fact, the plots in this figure can be obtained by combining the curves in Figures 24.3 and 24.6. The values of τ^* and κ^* correspond to the condition $\epsilon_P = \epsilon_M = 1$ introduced in Eq. (24.4). The PVMV configuration
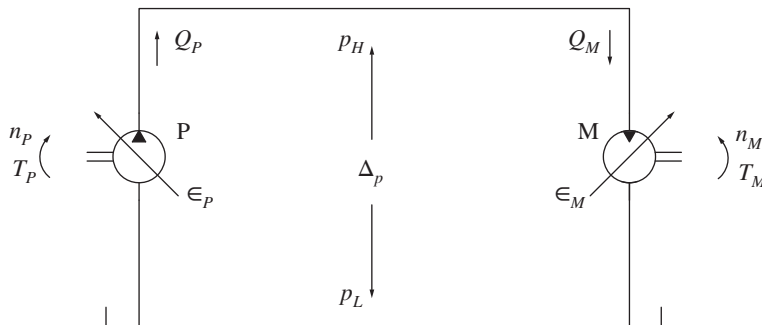
Figure 24.7 HT with variable displacement primary unit and variable displacement secondary (PVMV).
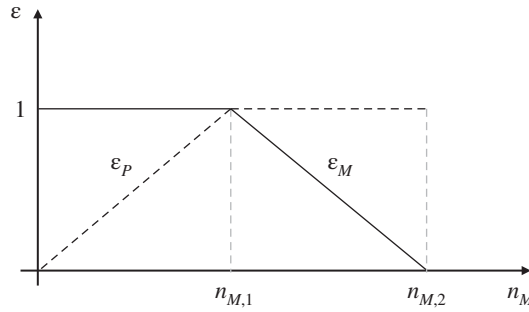
Figure 24.8 Control strategy for PVMV transmission.

can control the motor shaft speed over a wide range and it is still capable of producing high startup torques at the motor shaft.

The previous considerations are valid in the ideal case. If the losses of the pump and motor units were taken into consideration, the characteristic chart of the PVMV transmission would become similar to that in Figure 24.10. The torque on the motor T_M, for $\tau < \tau^*$ follows the same trend in Figure 24.4, approximating a constant value. For $\tau > \tau^*$, the value of T_M decreases as τ increases, following a segment of hyperbole, as in Figure 24.6. The lines at constant motor speed n_M are not vertical anymore, but they are inclined leftward. This indicates that for high values of T_M, the volumetric losses of the hydraulic units penalize the motor speed. The equal-efficiency lines show that the highest efficiency of the HT is located near the τ^* condition. This means that both the primary and the secondary units are at their maximum displacement. This observation is also intuitive, and it justifies the control considerations explained in Figure 24.8.
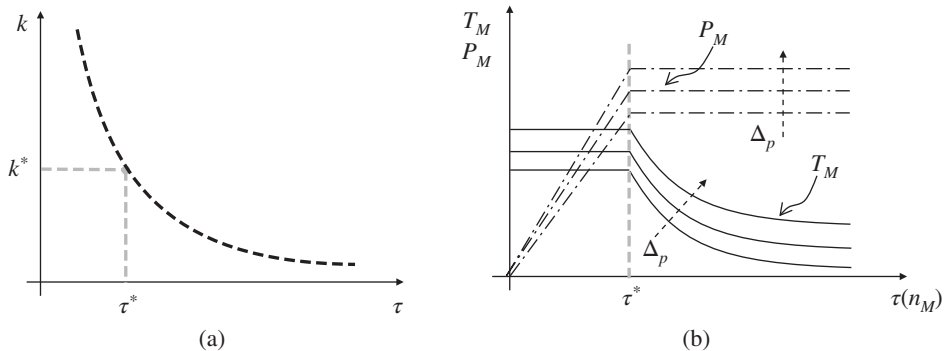
Figure 24.9 Transmission ratios (a), torque and power (b) for a PVMV transmission (ideal case).

24.2.5 Variable Displacement Pump and Dual Displacement Motor (PVM2)

The dual displacement motor setup is not only a special case of PVMV configuration but also quite common in certain applications. In this configuration, the motor displacement is not continuously adjustable, but it can be varied between two discrete settings, $V_{M,\min}$ ($\epsilon_M = \epsilon_{\min}$) and $V_{M,\max}$ ($\epsilon_M = 1$). In other words, the PVM2 configuration corresponds to two different PVMF configurations, one for each motor displacement. The conceptual schematic of the PVM2 layout is represented in Figure 24.11: the motor displacement is controlled by the valve directional valve (DV), which acts on the cylinder control piston (CC). When DV is in neutral position, the displacement is maximum. When DV is energized, the pump pressure acts against the soft spring of CC and reduces the motor displacement to its minimum value.
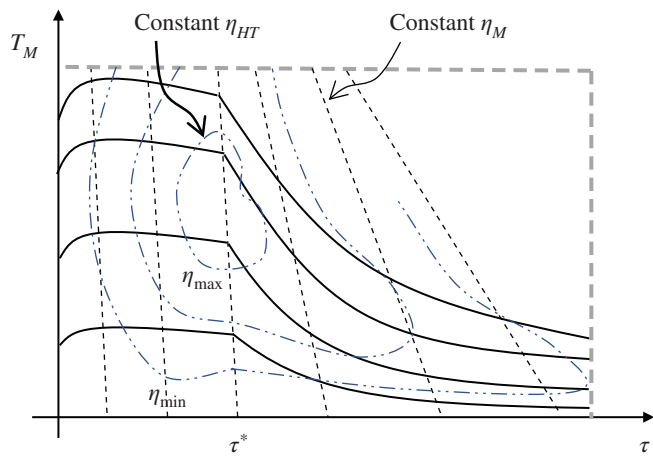
Figure 24.10 Characteristic diagram for a PVMV transmission considering real units.
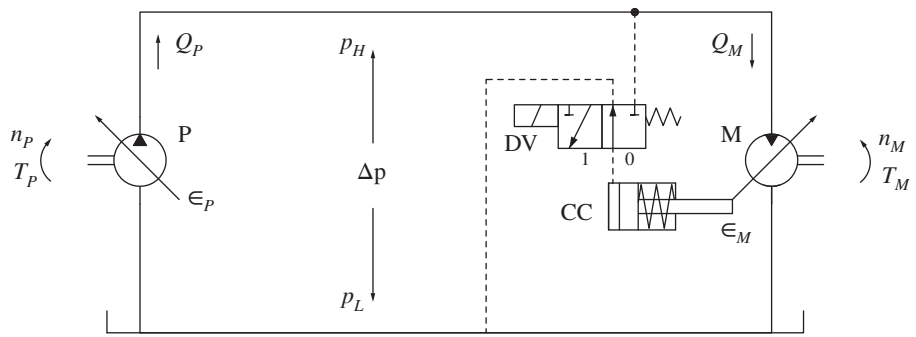
Figure 24.11 HT with variable displacement pump and dual displacement motor (PVM2).

When the motor is set at its maximum displacement ($\epsilon_M = 1$), the HT operates to maximize the output torque (hence, κ), while the motor shaft speed remains low. On the other hand, when the motor displacement is set to minimum ($\epsilon_M = \epsilon_{\min}$), the output speed can reach higher values (higher τ) at the expense of lower output torque values. In other words, the PVM2 configuration is a two-speed HT. Both speeds are often referred to as *first and second gears*. The operating characteristic of a PVM2 transmission is represented in Figure 24.12. It is important to note that the output power of (τ_1, κ_1) and (τ_2, κ_2) are the same.
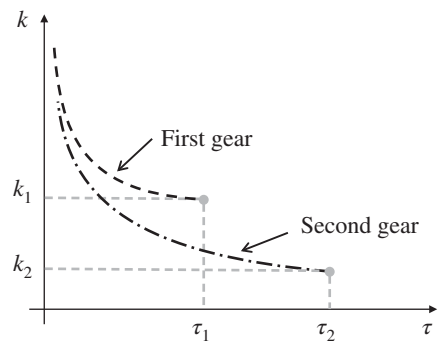
Figure 24.12 Ratios for a PVM2 hydrostatic transmission.

Example 24.2   Hydrostatic transmission layouts

An HT with a PVMV configuration is used to drive a drilling attachment. The pump has a maximum displacement of 85 cm^3/r, while the motor displacement varies between 60 and 24 cm^3/r. The pump rotates at 1200 rpm; the maximum operating pressure of the system is 350 bar. The pump at maximum displacement has a volumetric efficiency of 93%, while the motor has a volumetric efficiency approximately equal to 95% across the whole operating range.
  Answer to the following questions:

1) Calculate the minimum and maximum speed of the drill allowed by the HT.
2) What is the maximum speed at which the drill can still benefit from the maximum motor torque?
3) What is the pump and motor displacement to achieve a drilling speed of 2800 rpm?

Given:
Pump, $V_{P,max} = 85 \ cm^3/r$; $n_P = 1200 \ rpm$
  Pump volumetric efficiency, $\epsilon_P = 1$ is 0.93
  Motor, $V_{M,max} = 60 \ cm^3/r$; $V_{M,min} = 24 \ cm^3/r$
  Motor volumetric efficiency at all, $\epsilon_M = 0.95$
  Maximum operating pressure, $p_{max} = 350 \ bar$

Find:
1) Minimum and maximum value of n_M
2) Maximum value of n_M at which T_M is maximum
3) Values of V_P and V_M corresponding to $n_M = 2800 \ rpm$

Solution:

1) The variable displacement pump allows for a minimum setting $\epsilon_P = 0$, therefore making the minimum speed of the motor null. This would not have been the case for a PFMV configuration.
    The maximum motor speed is instead achieved for the case where the pump is at maximum displacement while the motor is at minimum. Applying Eq. (24.1), the value of τ_{max} is

$$\tau_{max} = \frac{n_{M,max}}{n_P} = \frac{V_{P,max}}{V_{M,min}} \cdot \eta_{v,P} \cdot \eta_{v,M} = \frac{85 \ [cm^3/r]}{24 \ [cm^3/r]} \cdot 0.93 \cdot 0.95 = 3.13$$

    The maximum speed of the motor is 3.13 times the speed of the pump, i.e. $n_{M, \ max} = 3754 \ rpm$.
2) The motor can produce maximum torque if it stays at its maximum displacement. Therefore, the condition of maximum speed and maximum torque (also referred to as corner power condition) is achieved when both units are at their maximum displacement. This situation is identified by the value previously indicated as τ^* and equal to

$$\tau^* = \frac{n_{M,T \ max}}{n_P} = \frac{V_{P,max}}{V_{M,max}} \cdot \eta_{v,P} \cdot \eta_{v,M} = \frac{85 \ [cm^3/r]}{60 \ [cm^3/r]} \cdot 0.93 \cdot 0.95 = 1.25$$

    The speed $n_{M, \ Tmax}$ is 1500 rpm.

Example 24.2 (Continued)

3) In this case, $n_M = 2800\,rpm$ and $n_P = 1200\,rpm$; therefore, the transmission ratio is

$$\overline{\tau} = \frac{n_M}{n_P} = \frac{2800\,[rpm]}{1200\,[rpm]} = 2.33$$

The same formula used at point (2) can be used to calculate the displacement of the units, thus obtaining a specific motor speed condition. In general,

$$\tau = \frac{n_M}{n_P} = \frac{\epsilon_P \cdot V_{P,\max}}{\epsilon_M \cdot V_{M,\max}} \cdot \eta_{v,P} \cdot \eta_{v,M} = \frac{\epsilon_P \cdot 85\,[cm^3/r]}{\epsilon_M \cdot 60\,[cm^3/r]} \cdot 0.93 \cdot 0.95 = 1.25 \cdot \frac{\epsilon_P}{\epsilon_M}$$

The ratio $\overline{\tau}$ is achieved for all the combinations of ϵ_P and ϵ_M satisfying the following:

$$\overline{\tau} = 1.25 \frac{\epsilon_P}{\epsilon_M} \rightarrow \frac{\epsilon_P}{\epsilon_M} = \frac{\overline{\tau}}{1.25} = \frac{2.33}{1.25} = 1.86$$

The value of $\overline{\tau} = 2.33$ is greater than τ^*, therefore applying the control strategy for a PVMV transmission represented in Figure 24.8, $\epsilon_P = 1$.
The value for ϵ_M is

$$\epsilon_M = 1/1.86 = 0.54$$

Therefore, the corresponding motor displacement is

$$V_M = 0.54 \cdot V_{M,\,\max} = 32.2\,cm^3/r.$$

24.3 Open Circuit Hydrostatic Transmissions

Among the possible classifications for HTs, a very common one consists in dividing HTs into open circuit or closed circuit layouts. This was also shown in classification in Figure 23.6. In an open circuit HT, it is always possible to locate the high-pressure and the low-pressure lines, independent on the operating conditions. This is very clear if one looks at the primary unit: the pump suction is always connected to tank, while the pump outlet port is the only one getting pressurized. This section focuses on the basic implementation of open circuit HTs with primary control.

24.3.1 Open Circuit HT with Flow Supply: Basic Circuit

The basic schematic of an open circuit HT is illustrated in Figure 24.13. The circuit is based on a variable displacement primary unit (P) and a fixed displacement secondary unit (M). The pump becomes a flow supply, as its displacement is one of the control variables.

The valve directional control valve (DCV) is an on/off valve. Depending on the selected working position, it sets the flow path between P and M. DCV does not function as a metering device and, ideally, it operates without introducing losses in the circuit. Figure 24.13 indicates also the sign convention used in the following paragraphs to indicate the direction of the shaft torque and velocity at both hydraulic units.

As mentioned in the previous chapters, the operation of the HT can be analyzed over four quadrants of operation, according to the direction of rotational velocity and torque at the motor shaft. The four possible circuit configurations that allow the operation of the HT in each quadrant are represented in Figure 24.14. In each quadrant, the torque and the speed of the units are represented with their current direction and the primary and secondary units are represented in their operating modes (pumping or motoring).
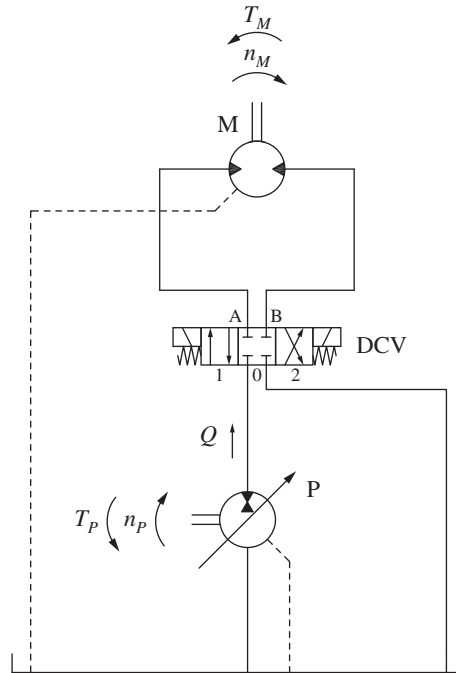
Figure 24.13 Basic schematic of an open circuit hydrostatic transmission.

In the two cases of resistive load (Q1 and Q3), the direction of rotation of the secondary unit is accomplished by switching the DCV to position 1 (clock wise [CW] rotation) or 2 (counterclock wise [CCW] rotation). For each position of the DCV, the actuator speed is controlled by varying the instantaneous displacement of the primary unit P (primary control). In those quadrants, P works always in pumping mode and since the load is resistive, while M works in motoring mode.

As shown in Figure 24.14, the circuit can also operate in the two quadrants where the load is overrunning (the second and the fourth quadrants of Figure 24.14). However, in these cases the system needs to change its configuration, in order to keep the same direction of rotation for the pump shaft, as required when a thermal engine is used as prime mover. In quadrants Q2 and Q4, the primary unit P operates in motoring mode, therefore requiring unit P to be in an over-center configuration[1]. The direction of the pump flow is opposite with respect to the previous cases of resistive load (Q1 and Q3). In Q2 and Q4, the secondary unit works in pumping mode. The DCV position that regulates the clockwise rotation of M is now 2, while the counterclockwise rotation is obtained in position 1.

At this point, it is important to observe that the same direction of the actuator shaft velocity, for the two load conditions (resistive and overrunning) is obtained with opposite configurations for the DCV position as well as the unit displacement. In other words, the load dictates the system configuration. This represents an issue for applications where the load is unpredictable or continuously switches from resistive to overrunning or vice versa (an example could be the swing function of an excavator). In these instances of load change, the open circuit HT must suddenly vary its configuration to follow the changes in load direction. This feature of operation implies significant control challenges, which make the implementation of the open circuit HT (as in Figure 24.13) unreasonable for applications that faces transitions between resistive and overrunning loads.

---

1 The system in Figure 24.14 can also be implemented with an electric machine as prime mover that can change the direction of rotation of the prime mover. In this case, instead of having P in over-center configuration, it is possible to invert the velocity of the prime mover.
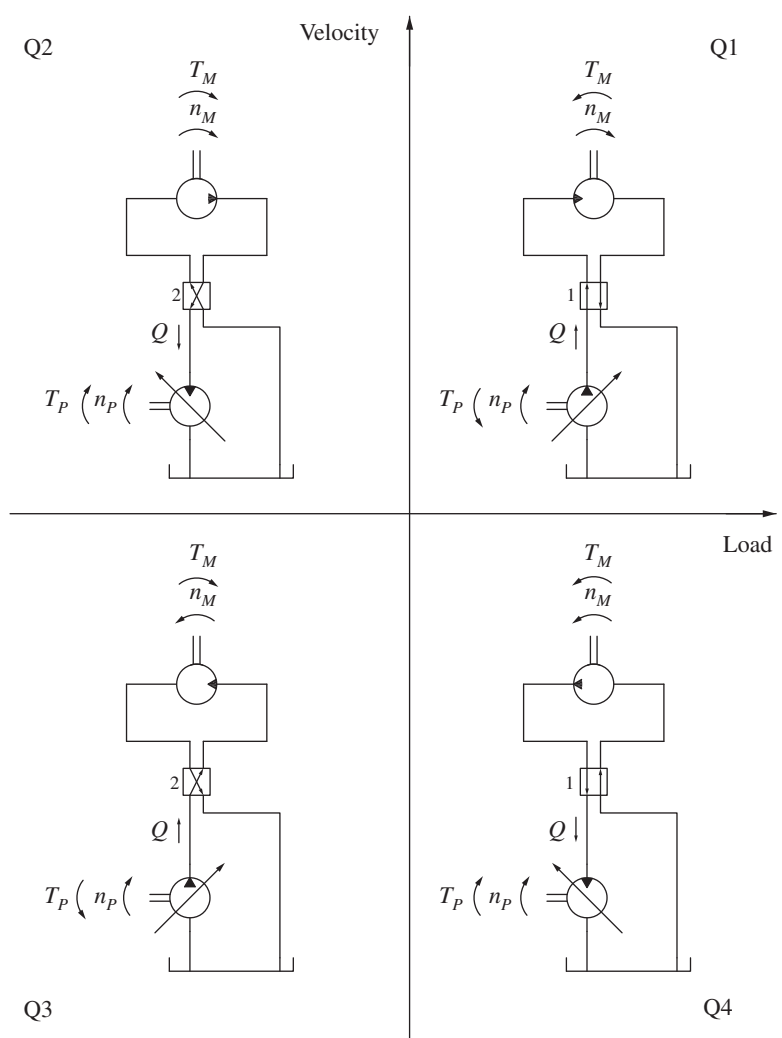
Figure 24.14 Operating modes for the basic circuit in Figure 24.13.

The basic open circuit HT in Figure 24.13 is suitable to control an actuator only when load conditions do not vary between resistive and overrunning during the motion. Transitions between these two load states present significant control challenges for the primary unit and the control valve.

The problem of smoothly overcoming changes in load directions can be addressed by the open circuit HT solution described in Section 24.3.2.

24.3.2 Open Circuit HT with Flow Supply: Common Implementation

A common implementation of an open circuit HT is represented in Figure 24.15. The circuit is very similar to that in Figure 24.13 but uses counterbalance valves (CBVs) to overcome loads rather than overrunning them. Similarly, the direction of the flow to the motor M is controlled by the DCV element, while the speed of M is controlled by the pump displacement.
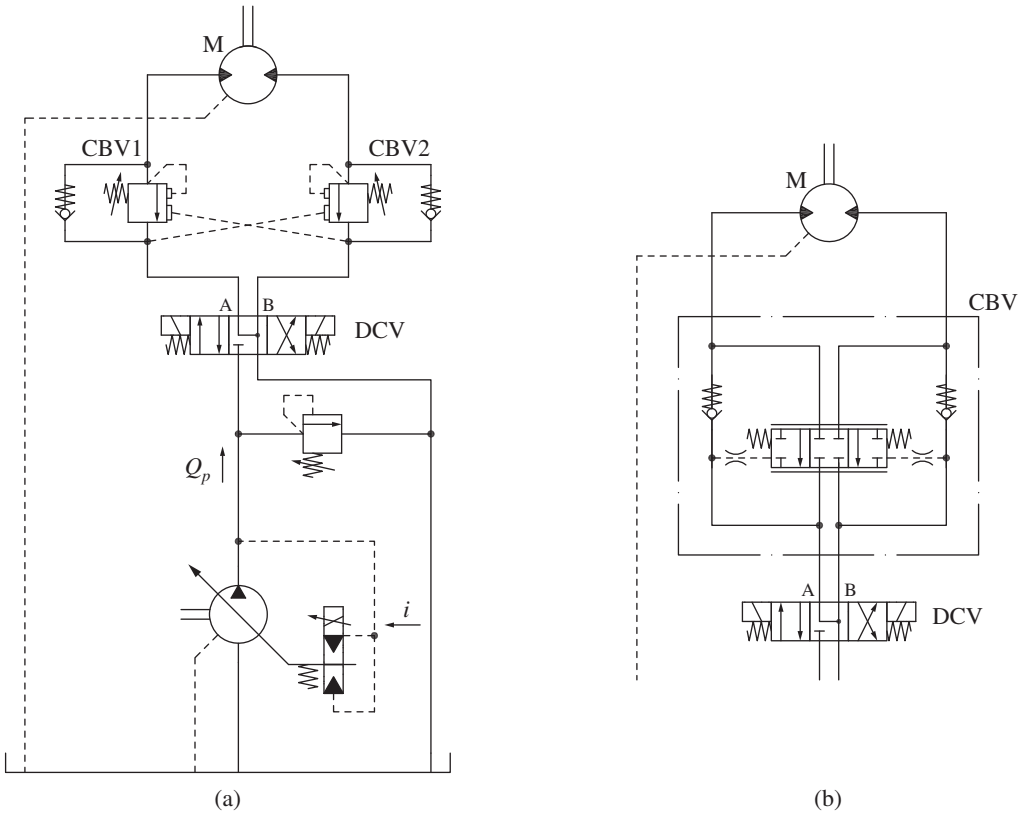
Figure 24.15 Typical schematic of an open circuit hydrostatic transmission: (a) complete schematic; (b) alternative counterbalance valve design typically used in propulsion applications.

The operation of the CBV valve follows the same explanation provided in Chapter 14. In the case of resistive loads, the CBV downstream the secondary unit, M, introduces only a small pressure loss considered by the primary unit, P, as an additional load. According to the CBV operation, this loss becomes negligible above a certain load threshold, which is determined by the CBV spring setting and its pilot ratio. In the case of overrunning loads, the compensating function of the CBV pressurizes the return of the secondary unit so that the supply pressure always stays positive. In other terms, the subsystem including the secondary unit and the CBV is always seen by the primary unit as a resistive load. In this way, the primary unit always operates in pumping mode.

The system in Figure 24.15 can easily operate in four quadrants but cannot recover energy. The energy provided to the hydraulic system by the overrunning loads is dissipated through the CBV, which works as a compensator. For the operation of this type of HT with resistive loads, effects of the CBV on the overall efficiency are usually negligible.

> Using meter-out elements such as CBVs, the open circuit HT can control loads in four quadrants to avoid controllability issues. However, the system does not recover energy during overrunning load conditions.

In the circuit in Figure 24.15, the pump presents an electric displacement control regulator (EDR), where the displacement is proportional to the input current i.
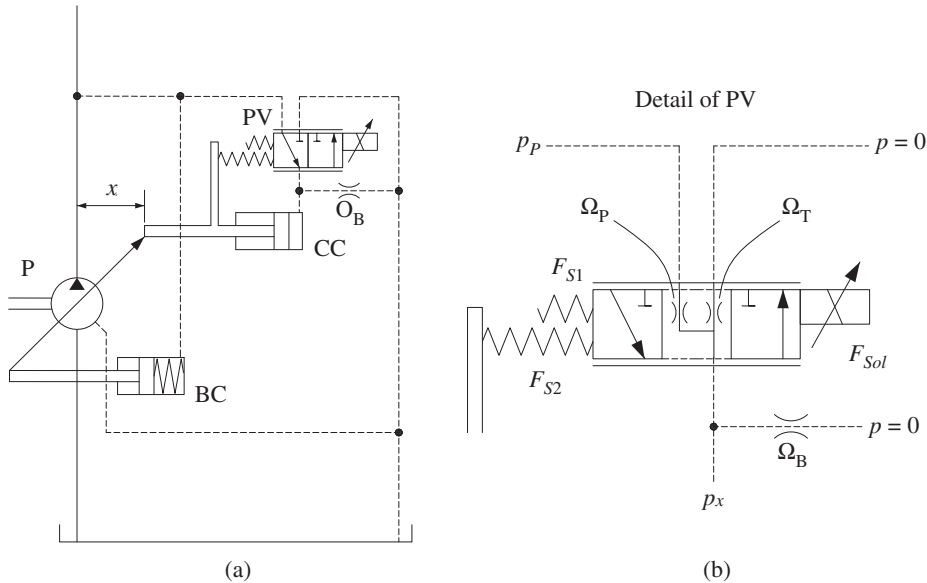
Figure 24.16 Displacement regulator for open circuit piston pumps with internal hydro-mechanical feedback.

Figure 24.15 also represents an alternative layout for the CBV. A single spool valve (CBV) is often used in propel circuits instead of the CBV1 and CBV2 elements. The spool valve does not present a zero-leakage characteristic. However, it achieves a braking effect that is "ramped" and not linked to a set pressure, as in traditional CBV designs, which can be encountered in open circuit propulsion systems.

Open Circuit Displacement Regulator

The displacement regulator for an open circuit variable displacement pump (generically indicated in Figure 24.15) can be implemented in different ways. The following paragraph analyzes the two most common solutions, based on a hydromechanical or electronic feedback.

Figure 24.16 shows a typical circuit of an electric displacement regulator for open circuit piston pumps using an internal hydromechanical feedback[2]. The swash plate mechanism of the pump is laid out in a similar style as the load sensing (LS) pumps presented in Chapter 16 (Figures 16.6–16.8). Two pistons, bias piston (BC) and CC, are used to control the position of the swash plate. In this case, the bias cylinder BC is located on the top and the control cylinder CC is located below the BC. A three-way proportional valve (PV) modulates the pressure in the control piston p_x. In this layout, a proportional solenoid controls the PV, while in the load sensing pump solution presented earlier, the three-way valves V1 and V2 were controlled by pressure signals. Even if the control of the valve is different, its functionality is basically the same for the two cases.

In the detailed view of valve PV represented in Figure 24.16, it is possible to observe how the spool position is determined from three force contributions:

1) F_{sol} is the solenoid force, which is proportional to the input current i.

---

2 When looking at the circuit, the reader should understand that the pump is represented at the standby condition (per ISO standards): the displacement is at maximum (per effect of the bias spring) and the control valve PV is de-energized. However, this configuration corresponds to the situation of pump non-rotating (engine off). As soon as the unit starts turning, the pump generates flow and the outlet pressure immediately access the control cylinder CC through PV bringing the displacement to ideally null value. At this point, the displacement can be increased by powering the solenoid of PV.

2) F_{S1} is the force of a soft bias spring. In first approximation, the value of F_{S1} can be considered as a constant, as the spool movement for this kind of valve is usually very limited.

3) F_{S2} is the force of a second spring acting between the spool and a feedback linkage rigidly connected to the displacement bias piston (BC). The travel of the BC piston (identified by x) is not negligible; therefore, the force F_{S2} changes with the piston position. The force F_{S2} is then equal to

$$F_{S2} = F_{S2,0} + k \cdot x \tag{24.10}$$

where k is the feedback spring stiffness and $F_{S2,0}$ is the spring preload.

An important observation is that the value of x is directly proportional to the value of the unit displacement. The relationship between x and V_d can be approximated as linear, since the swash plate max inclination is usually below 20°, and the sine of the swash plate angle can be approximated with the angle value itself (this assumption was explained in Example 16.3).

The spool of PV operates has two position, a stroking position, when the solenoid is energized and a de-stroking position when no energy is provided to the solenoid. Figure 24.16 highlights an intermediate position, which is very important to accomplish the regulation function of the system. In this intermediate position, the control pressure p_x is determined by the opening of the two small orifices, which are implemented inside PV, through a negative overlap between the spool lands and the internal ports in the valve body. The relation for this control pressure is

$$p_x = \left(\frac{\Omega_P^2}{\Omega_P^2 + \Omega_T^2} \right) \cdot p_P \tag{24.11}$$

The expression for Eq. (24.11) can be derived from the orifice equation applied at the two orifices implemented by PV in this intermediate position.

The control of the pump can be therefore described as a function of the command:

Neutral configuration ($i = 0$). The control piston is connected to the pump pressure. Therefore, the pump displacement is forced to zero. Note that Figure 24.16 shows the pump at full displacement, which would be the configuration of the system when the prime mover is turned off. However, with the prime mover on, the pump displacement will be (ideally) null.

Regulation ($i > i_0$). The regulation usually occurs with a command greater than i_0. i_0 is the current value that allows the PV to reach the left position in Figure 24.16. In this configuration, the pump can rapidly increase its displacement because of the decrease in the control pressure p_x, being the control line vented to tank. As the pump reduces its displacement, the internal mechanical feedback that connects the sleeve of PV and the pump causes the PV to operate in the intermediate configurations, where both the orifices Ω_P and Ω_T are partially open. The feedback that allows to have a relationship between the command i and the displacement x is based on the force F_{S2}. In fact, the force balance of the PV spool is

$$F_{\text{sol}} = m \cdot (i - i_0) = F_{S1} + F_{S2} = F_{S1} + F_{S2,0} + k \cdot x \tag{24.12}$$

In Eq. (24.12), m is a constant representative of the solenoid behavior (as explained in Chapter 8). The value of displacement set point is the following:

$$x = \frac{F_{S1} + F_{S2,0} + m \cdot (i - i_0)}{k} \tag{24.13}$$

Equation (24.13) sets a unique linear relationship between the current and the displacement. The two orifices Ω_P and Ω_T have a very small value, so that the internal leakages of the displacement adjustment system can be reduced.
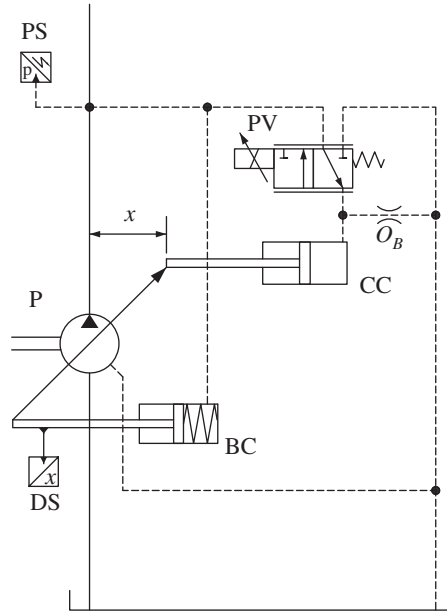
Figure 24.17 Displacement regulator for open circuit pumps with electric feedback.

Alternative Implementation with Electric Feedback

Figure 24.17 shows another type of regulator based on a different type of feedback. This hydraulic circuit is also very similar to those in Figures 16.6—16.8 of Chapter 16 (LS pump regulator). In the case of the LS pump in Figure 16.7, the pressure in the control piston is regulated by a three-way two-position proportional spool whose position is controlled by the pump outlet pressure, the load sensing pressure, and the margin spring. In Figure 24.17, the same 3/2 proportional valve is instead controlled by a solenoid. Furthermore, with respect to the circuit in Figure 24.16, the hydromechanical feedback is replaced by two sensors measuring the pump pressure and displacement. In such layout, the electronic signal to the pump is the result of a close control loop architecture (such as a proportional-integral-derivative control [PID]), which sets the pump to the desired displacement, or it creates a pressure-dependent displacement command. This type of control presents more challenges from the programming standpoint, but it allows improved flexibility (e.g. adjustable response rate) and presents less hydraulic components and internal leakage paths.

Open Circuit HTs with Pressure Supply

In some applications, open circuit HTs can be implemented with a pressure supply. This is typically convenient when the circuit is designed to control the torque at the shaft of the secondary unit. This type of circuit is common, for example, in hydrostatic fan drives. This particular case is taken as reference in this section to analyze open circuit HTs with pressure supply.

Figure 24.18 shows a typical circuit of a fan drive system: the motor shaft is connected to the cooling fan blades. The fan direction is controlled with the DCV element, which is a 2/4 solenoid actuated valve. The pump regulator implements a proportional pressure control, where the output pressure is a function of the input command i. The detailed schematic of the pump control resembles the one presented in Figure 16.8 where the pressure setting is controlled by a proportional relief valve (RV).

The fan is characterized by a unique and repeatable relationship between load (i.e. torque) and rotational speed. This follows a quadratic function that is represented in Figure 24.19:

$$T_m = k \cdot n_f^2 \tag{24.14}$$
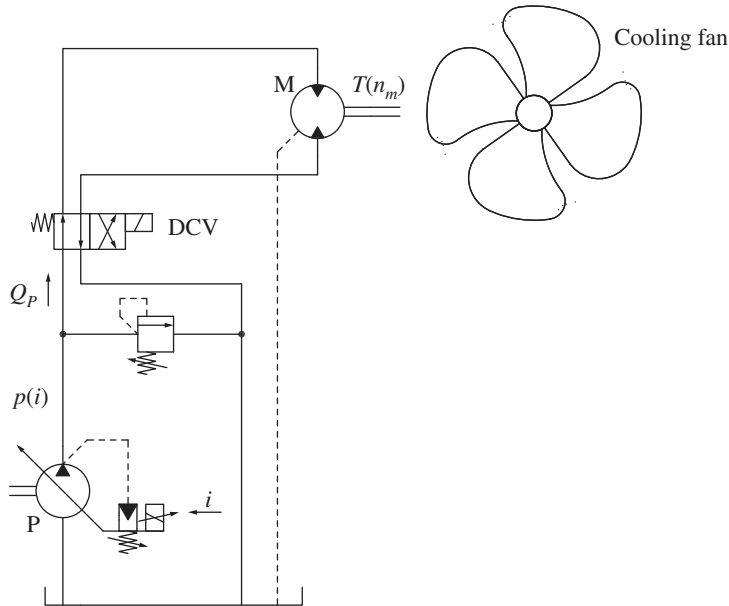
Figure 24.18 Typical circuit for a hydrostatic fan drive based on a pressure supply.

The pressure at the pump $p(i)$ corresponds to a precise torque at the motor. Therefore, the command i is directly related to the resulting fan speed. In the ideal case, the torque at the motor is be equal to

$$T_m = p(i) \cdot V_m \tag{24.15}$$

The fan speed in indirectly controlled by modulating the pump outlet pressure. The relationship between the two parameters is obtained by combining Eqs. (24.14) and (24.15):

$$n_f = \sqrt{\frac{p(i) \cdot V_m}{k}} \tag{24.16}$$

Hydrostatic fan drives are often implemented with open circuit HTs with pressure supply. The output shaft speed (fan) can be easily controlled by varying the supply pressure.
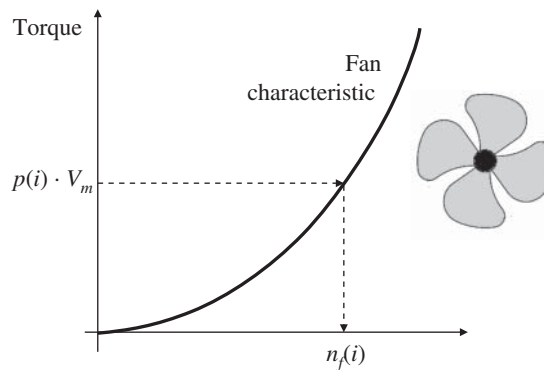
Figure 24.19 Quadratic relationship between fan speed and torque. The pressure setpoint of the pump corresponds to a precise fan speed.
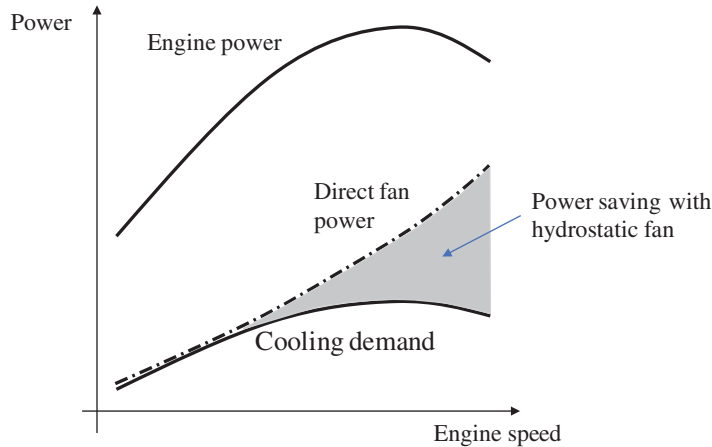
Figure 24.20 Engine and fan power considerations for mechanical and hydraulic driven fan.

The Case of Hydrostatic Fan Drives

The commercial success of hydrostatic fan drives, particularly in the field of mobile hydraulics, comes from the significant power savings that are achievable with respect to mechanically driven fans. A direct mechanical transmission between the engine shaft and the fan, through a belt, has a very high energy efficiency. However, it also has a fixed transmission ratio. This penalizes the design of the cooling system, which must be sized for the worst-case scenario (maximum cooling requirement of the engine). A mechanically driven fan provides air flow, which is solely a function of the engine speed. However, a hydrostatic fan drive allows for a continuously variable control of the fan to match precisely with the cooling demands. In this case, the fan speed is a function of the temperature of the cooling fluids.

Figure 24.20 shows how the maximum cooling demand for a diesel engine usually corresponds to the peak power condition, which is reached at a speed lower than the maximum speed (usually around the peak torque). Therefore, mechanically driven fans produce a significant excessive cooling at higher speeds. Due to the quadratic relationship previously explained (which becomes a cubic relationship in the power plot of Figure 24.20), the excessive cooling results in a significant power demand that is effectively wasted and subtracted from the power available to the other functions of the machine. This can be avoided with hydrostatic fan drives, which can easily follow the cooling demand and save a significant amount of power.

Example 24.3   Fan drive sizing

A 23-ton excavator uses a hydrostatic fan drive to cool an engine coolant, hydraulic oil, and engine charge air. The fan drive hydraulic system uses a variable displacement pump and a fixed displacement motor, according to the schematic in Figure 24.18. The maximum fan power is 16 *hp* at a maximum fan speed of 1600 *rpm*. The engine speed can be adjusted between 900 and 2100 *rpm*. The maximum cooling demand is reached at 1450 *rpm*. The hydraulic system is sized for a maximum operating pressure of 250 *bar*.

Calculate:

1) The size of the fan motor.

2) The size of the fan pump.
3) The maximum speed of the fan achievable at engine idle condition.
4) The pump displacement setting at maximum engine speed and maximum fan speed.

Assume the following motor efficiencies: $\eta_{v,M} = 0.94$, $\eta_{hm,M} = 0.91$. The pump efficiencies are as follows: $\eta_{v,P} = 0.96$, $\eta_{hm,P} = 0.93$

Given:

Fan max power, $P_{f,max} = 16\,hp$ at $n_f = 1600\,rpm$
Engine speed range, $n_e = 900{-}2100\,rpm$
Engine speed for max cooling, $n_e^* = 1450\,rpm$
Max system pressure, $p^* = 250\,bar$
Motor efficiencies, $\eta_{v,M} = 0.94$, $\eta_{hm,M} = 0.91$
Pump efficiencies, $\eta_{v,P} = 0.96$, $\eta_{hm,P} = 0.93$

Find:

1) Fan motor displacement, V_M
2) Fan pump max displacement, $V_{P,max}$
3) Motor max speed if $n_P = 900\,rpm$
4) Pump displacement setting ϵ_P if $n_P = 2100\,rpm$ and $n_M = 1600\,rpm$

Solution:

1) The maximum fan power corresponds to a motor torque requirement of

$$T_{M,max}\,[Nm] = \frac{P_{f,max}}{n_{f,max}} = \frac{16\,[hp] \cdot 0.75\,[kW/hp]}{1600\,[rpm]} \cdot \frac{30\,000}{\pi} = 71.5\,Nm$$

The motor displacement capable of generating such torque at the system maximum pressure is calculated as follows:

$$V_M\,[cm^3/r] = 2\pi \cdot \frac{T_{M,max}}{p^* \cdot \eta_{hm,M}} = 2\pi \cdot \frac{71.5\,[Nm]}{250\,[bar] \cdot 0.91} \cdot 10 = 19.7\,cm^3/r$$

This displacement value is only theoretical. The motor should be selected within a series of available displacements. Assuming the available values are 18, 20, and 22 cm^3/r, the selection should be close to a value slightly higher than the theoretical one. In this case $V_M = 20\,cm^3/r$. Since the motor actual displacement is slightly higher than the theoretical value, the maximum fan power is reached at a slightly lower pressure:

$$p_{max} = p^* \frac{19.7\,[cm^3/r]}{20\,[cm^3/r]} = 246\,bar$$

2) The flow required by the motor is

$$Q_{M,max}\,[l/min] = \frac{V_M\,[cm^3/r] \cdot n_{M,max}\,[rpm]}{1000 \cdot \eta_{v,M}} = \frac{20\,[cm^3/r] \cdot 1600\,[rpm]}{1000 \cdot 0.94} = 34.0\,l/min$$

The minimum engine speed at which the pump needs to provide $Q_{M,\,max}$ is $n_e^* = 1450\,rpm$. Therefore, the pump required displacement is

$$V_{P,max}\,[cm^3/r] = 1000 \cdot \frac{Q_{M,max}\,[l/min]}{n_e^*\,[rpm] \cdot \eta_{v,P}} = 1000 \cdot \frac{34.0\,[l/min]}{1450\,[rpm] \cdot 0.96} = 24.4\,cm^3/r$$

Example 24.3 (Continued)

The same results could have been obtained applying Eq. (24.1), because the value of τ is known.

Similarly to the motor, the pump also needs to be selected based on the available displacements. Assuming these are 20, 25 and 31.5 cm^3/r, the selection leads to $V_{P,\max} = 25$ cm^3/r. The pump max pressure limiter should be set at $p_{\max} = 246$ bar, as previously calculated.

3) The transmission ratio of the system is given by

$$\tau = \frac{n_M}{n_P} = \frac{\epsilon_P \cdot V_{P,\max}}{V_M} \cdot \eta_{v,P} \cdot \eta_{v,M} = \epsilon_P \cdot \frac{25\,[cm^3/r] \cdot 0.94 \cdot 0.96}{20\,[cm^3/r]} = \epsilon_P \cdot 1.13$$

If the engine runs at idle (900 rpm) and the pump is at maximum flow, the resulting motor speed is

$$n_M = 1.13 \cdot 900\,[rpm] = 1017\ rpm.$$

4) If the engine runs at 2100 *rpm* and the motor at 1600 *rpm*, the system pressure is 246 *bar* and the pump displacement setting is

$$\epsilon_P = \frac{n_M}{n_P} \cdot \frac{1}{1.13} = \frac{1600\,[rpm]}{2100\,[rpm]} \cdot \frac{1}{1.13} = 0.67$$

24.4 Closed Circuit Hydrostatic Transmissions

The principle of operation of a closed circuit HT is often represented with a pump and a motor connected as in Figure 24.21. This representation is very intuitive and can be used for a simple description of the operating features of the HT. However, the actual circuit of an HT must include several additional elements (Figure 24.22) that are necessary for the correct system operation. This section provides a step-by-step description of the complete architecture of a closed circuit HT, starting from the conceptual representation of Figure 24.21, and adding one by one the supplementary elements to form a complete working system.

24.4.1 Charge Circuit and Filtration

A charge circuit is always present in a closed circuit HT as in Figure 24.23, which shows again the conceptual circuit in Figure 24.21 but highlights the presence of external case drains. External drains are necessary for both the primary and secondary units, to guarantee a proper internal lubricating flow, as it was described in Chapter 6. Internal drain connections, which are possible

Figure 24.21 Conceptual representation of a closed circuit HT.
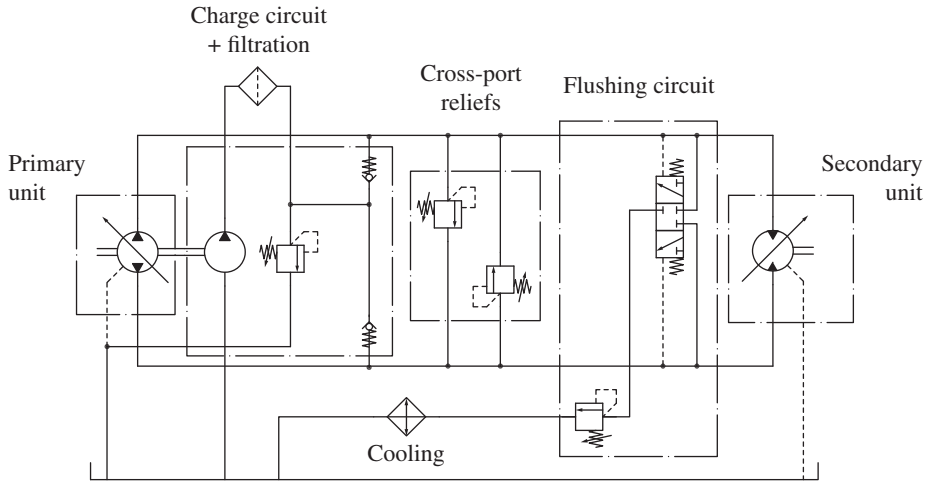
Figure 24.22 Detailed schematic of a closed circuit HT.

for open circuit HTs, are not possible in closed circuit HTs because the low pressure (LP) line is not defined a priori, but its location depends on the operating conditions.

The flow lost (due to internal leakages and, eventually, control losses) at each drain port is indicated by $Q_{P,d}$ (for the pump) and $Q_{M,d}$ (for the motor). In closed circuit units, external drains are always directly connected to the tank.

In Figure 24.23, the fluid lost through the drains causes imbalance in the flow between the HP and LP line. The overall flow lost $Q_L = Q_{P,d} + Q_{M,d}$ would reduce the pressure in the LP line (see also the pressure build-up equation in Chapter 4). The pump would operate under severe cavitation, and the entire transmission would fail in a short amount of time. To avoid this issue, the HT is equipped with a charge circuit, represented in Figure 24.24, which replenishes the leakage flow Q_L to the LP line. The charge circuit includes a charge pump (CP) a relief valve, RV1, and two check valves, CV1 and CV2, connecting the delivery of CP to the power lines of the HT.

The displacement of the charge pump is selected in order to satisfy the condition $Q_{CP} > Q_L$, in the worst-case scenario (usually corresponding to high pressure, low oil viscosity and low shaft speeds). This assumption implies that the flow through the relief valve RV1 is always greater than
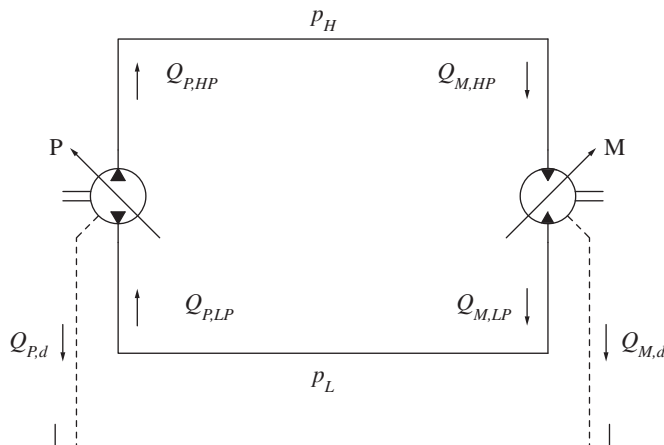
Figure 24.23 Case drain flows lost in a closed circuit.
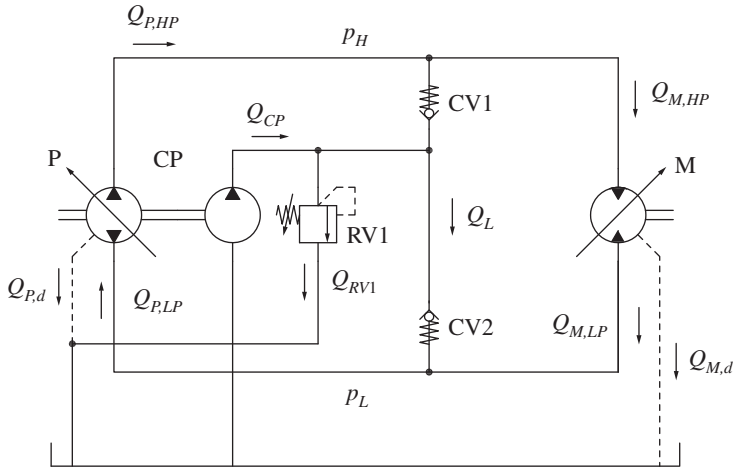
Figure 24.24 Charge circuit in a closed circuit HT.

zero $(Q_{RV1} > 0)$[3]. Consequently, the pressure at the delivery of CP is equal to p_{RV1}^*, setting RV1. The check valves CV1 and CV2 connect the charge circuit to the main lines of the HT and prevent the pressure in each line to fall below p_{RV1}^*. In other words, the charge circuit always sets the value of the LP line:

$$p_{LP} = p_{RV1}^* \tag{24.17}$$

In an HT, the charge circuit defines the suction pressure of the primary unit. The value of p_{RV1}^* is usually in the range of 10–25 bar. This is significantly higher than the tank pressure, which is usually the suction pressure for open circuit. In general, closed circuit hydrostatic pumps can operate at much higher speeds than open circuit units as cavitation is less of an issue, thanks to the charge circuit.

In summary, the **charge circuit** accomplishes the functions of

- making up for the external drain flows of both the primary and secondary units;
- setting a pressure reference for the low-pressure line LP. The pressure level at the high-pressure line is defined by the load (torque) acting on the secondary unit shaft.

Additional functions of the charge circuit are

- supplying pilot pressure to the displacement regulators of both primary and secondary units[4].
- providing fresh flow from the reservoir in exchange of the case drain flow, which is usually at higher temperature. This feature will be better described in Section 24.4 dedicated to the flushing circuit.

Considering the functions described above, the charge pump is often sized for flow rates significantly higher than the maximum value of overall leakages Q_L. As a rule of thumb, the charge pump displacement is at least 20% of the primary unit.

Despite the positive features accomplished by the charge circuit, the charge pump causes a power loss, which should be considered in the calculation of the system efficiency. The power consumed

---

3 This is always true when the flushing circuit is absent, which will be described in a later section. In case the HT uses a flushing valve, the flow rate though the valve RV can be null.
4 This is valid for the majority of the closed circuit HTs. In some instances, a circuit separated from the charge circuit is used for this pilot pressure functions.
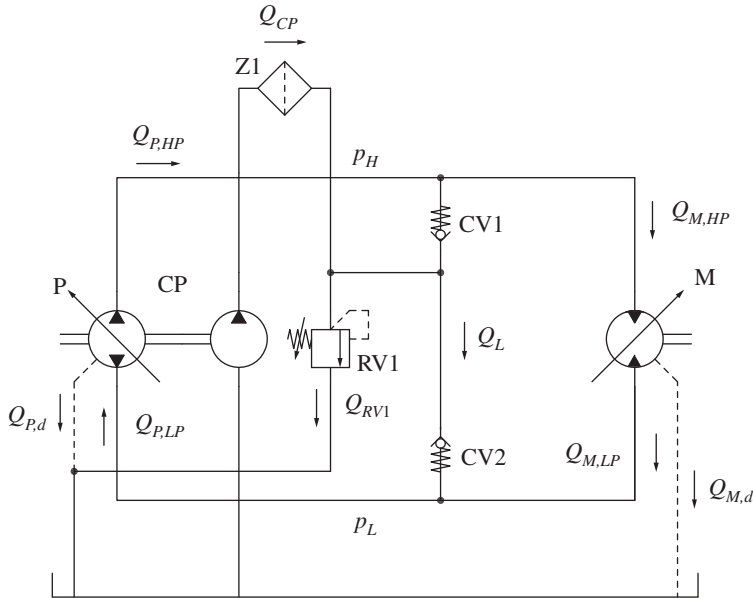
Figure 24.25 Charge pump circuit inclusive of filtration (Z1).

by the charge pump is

$$P_{CP} = Q_{CP} \cdot p_{RV1}^* \tag{24.18}$$

The outlet of the charge pump is often the preferred location for the filtration element of the circuit. A filter placed at the outlet of the charge pump, as represented in the circuit in Figure 24.25, ensures that the oil entering the loop is clean. This layout protects the primary and secondary units from contaminants that can be sucked in or generated by the charge pump. It also prevents a charge pump failure from leading to a catastrophic failure of the whole transmission circuit.

24.4.2 Cross-port Pressure Relief Valves

Figures 24.23 and 24.24 do not present any element for limiting the maximum pressure in the HP line. In closed circuit HTs, this function is mostly accomplished using two relief valves located between the two power lines and relieving in opposite directions. This layout is simply referred to as cross-port relief valves, represented in Figure 24.26 (RV2 and RV3). If the torque of the motor increases to the relief valves setting, the pump flow $Q_{P,HP}$ is diverted to one cross port relief (RV2, in Figure 24.26), so that the maximum pressure in the system cannot exceed p_{RV}^*.

It is important to notice that when p_{HP} reaches the setting of the cross-port relief p_{RV2}^*, the hydraulic motor unit operates with an inlet flow $Q_{M,HP}$ lower than the pump flow $Q_{P,HP}$. Consequently, the shaft velocity at the secondary unit decreases with respect to the nominal condition of $p_{HP} < p_{RV2}^*$, up to a complete stop or a reversal of the shaft rotation.

> Cross-port pressure relief valves are used to limit the maximum pressure within a closed circuit HT.

As shown in Figure 24.26, the cross-port relieves to the LP line, in parallel with the secondary unit. Its flow is not diverted to tank, as it commonly does in open circuits. In this way, $Q_{P,HP} = Q_{P,LP}$, meaning that the pump inlet flow is not affected by the operation of the cross-port relief. It is important to remark that in a closed circuit HT, the oil relieved by RV2 and RV3 remains in the
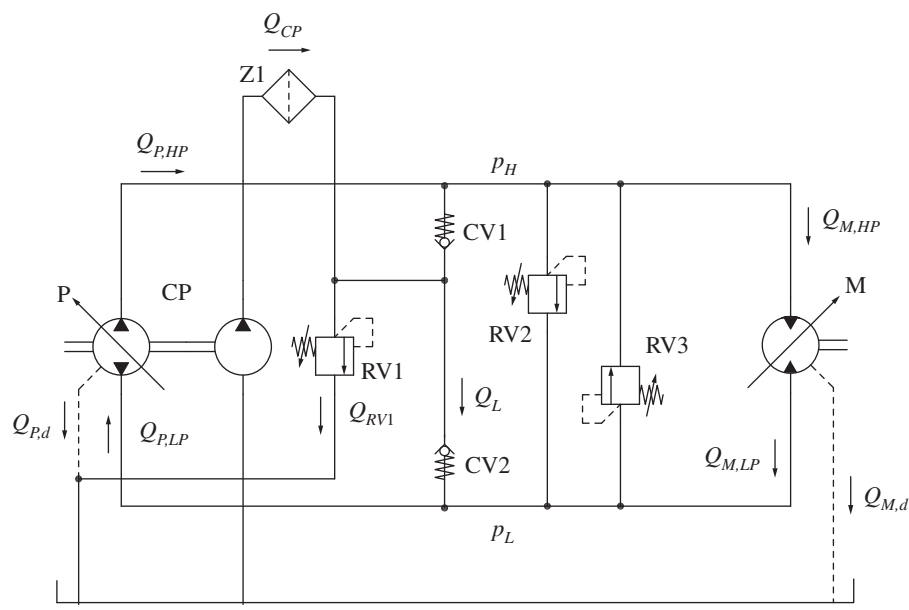
Figure 24.26 Cross-port relief valves (RV2 and RV3) in a closed circuit HT.

circuit. Therefore, in the case of a frequent operation of the cross-port relief valve, the oil can quickly overheat within the circuit. This even in the case the oil in the tank is at a much colder temperature.

Figure 24.27 shows an alternative arrangement for the cross-port relief valves RV2 and RV3. In this case, the pressure relief is merged with the anticavitation functionality, to manage the direction
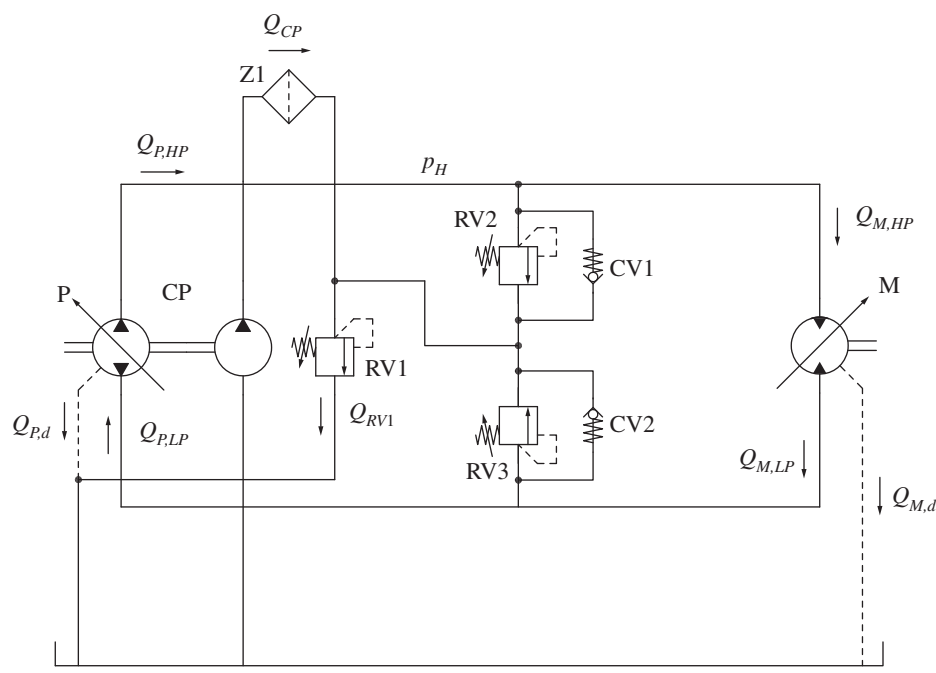
Figure 24.27 Solution with integrated cross-port relief valves and charge pump check valves.
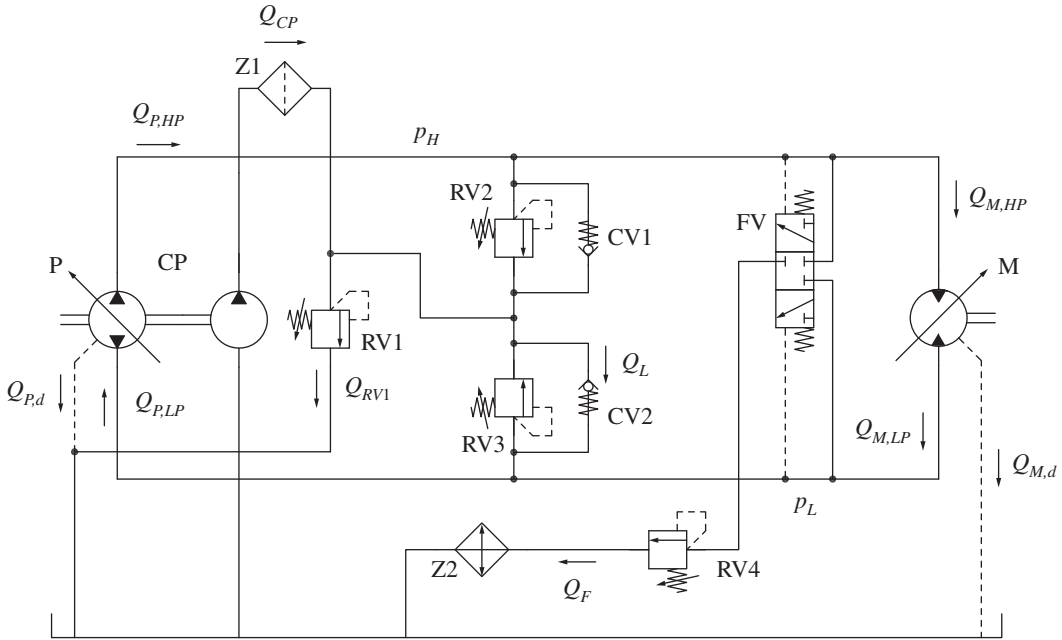
Figure 24.28 Closed circuit HT inclusive of the flushing circuit and filtration

of the charge flow. This arrangement is quite common when the valves are integrated in the housing of the primary unit. In Figure 24.27, in case of overpressurization, the flow diverted by one cross-port relief merges the charge pump flow, Q_{CP}, before merging the LP line through a check valve.

24.4.3 Flushing Circuit

A closed circuit HT should incorporate a *flushing valve* (FV in the circuit in Figure 24.28), which always connects the LP line to an additional pressure relief valve, RV4. The pressure relief valve RV4 is used to discharge the fluid to the tank, passing through a cooler. The system is represented in Figure 24.28.

The symbol of the flushing valve is represented in Figure 24.29. This valve consists of a 3/3 DCV whose position is determined by two centering springs and by two pilot pressures, p_A and p_B. During the operation of the HT, these values are equal to the pressure in the working lines. The force of the centering springs is very low, and it is neglected when studying the valve operation. In general, these centering springs are used to ensure that the valve returns to neutral when the system is turned off. The flushing valve is also referred to as "inverse shuttle valve": the outlet port C is connected to the input port (A or B), which has the lowest pressure.
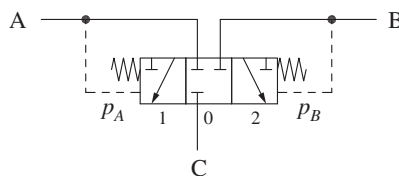
Figure 24.29 Flushing valve symbol.

With the charge circuit presented previously and represented in Figure 24.24, the pump CP replenishes the case drain leakages. The amount of flow exchanged between the closed circuit and the tank equals the case drain flow, Q_L. The value of Q_L can be tiny, especially under conditions of low load, and it cannot ensure a proper exchange of oil between the closed circuit of the HT and the tank. In other words, with the circuit in Figure 24.24, the difference between the oil temperature in the closed circuit loop and in the tank can be significant.

This issue can easily be overcome by utilizing a flushing circuit, as the one represented in Figure 24.28. In this circuit, the setting of the relief valve RV4 is lower than RV1 ($p_{RV4}^* < p_{RV1}^*$). Therefore, ideally $Q_{RV1} = 0$ and the entire flow provided by the charge pump, Q_{CP} enters the LP line. With this solution, the flow exchanged between the inner loop of the closed circuit HT and the tank equals the charge pump flow Q_{CP}. The flow discharged to tank thorough RV4 is

$$Q_F = Q_{CP} - Q_L \tag{24.19}$$

In Figure 24.28, the pressure level at the LP line is determined by RV4. In other words, $p_{LP} = p_{RV4}^*$. The flushing flow Q_F is properly filtered and cooled.

> The flushing circuit in close circuit HT allows for a proper cooling of the HT.

In some cases, the flushing valve is integrated within the motor, and the flushing line is arranged as represented in Figure 24.30. The flow discharged through flow control valve (FCV) is sent through the motor case and merges with the case drain flow. This is a common circuit especially for heavy-duty applications (high speeds and pressures) where the motor housing could overheat.

In Figure 24.30, an orifice downstream of FCV is used to control the flushing flow instead of a pressure relief valve. This is a very common solution: the operation of this circuit is slightly different from the previous one.

The flushing circuit can also guarantee the proper function of the HT during harsh dynamic conditions. For example, a fast reduction of the pump displacement, operated to reduce the shaft speed of the secondary unit, might require the presence of the flushing valve. In fact, the speed of the motor might not immediately follow a rapid change commanded to the pump displacement
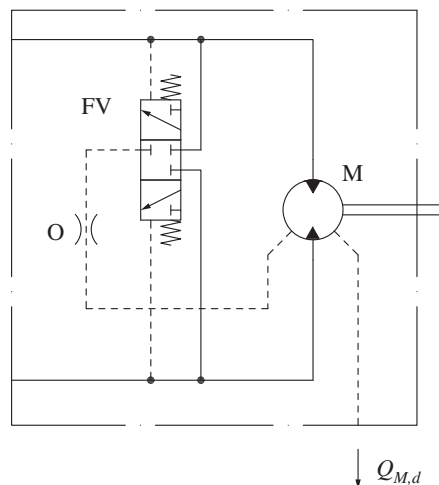
Figure 24.30 The flushing flow can be used to cool the motor housing.

adjustment system. This implies an instantaneous value of $Q_{M,LP}$ larger than $Q_{P,LP}$. This extra flow available at the LP line can be discharged to the tank through the flushing valve circuit.

An important detail of the flushing valve FV is the neutral position, which should have a closed center. If the neutral position were open center, during the commutations between LP and HP (such as a reversing of the secondary rotation), the fluid from HP line would go to directly to the reservoir, stalling the HT. In most of the closed circuit HTs, the valves RV4 and FV are mounted on the end plate of the secondary unit, so that its entire case is cooled by the flow Q_F.

Example 24.4 Sizing the flushing circuit and the charge pump for a HT

An HT presents a single pump (P) supplying two motors (M1 and M2) in parallel. The charge pump CP supplies flow to the low-pressure side of the circuit through two check valves CV1 and CV2. The charge pressure $p_{ch}^* = 18\ bar$ is set by the relief valve RV1. Each motor is equipped with a flushing valve (FV1 and FV2) and an orifice downstream it (O1 and O2). The flow discharged through each orifice is connected to the motor case drain and both drain lines convey through a hydraulic cooler. The performance characteristic of the cooler is given by the manufacturer and it is shown below in the cooling power vs. flow circuit.
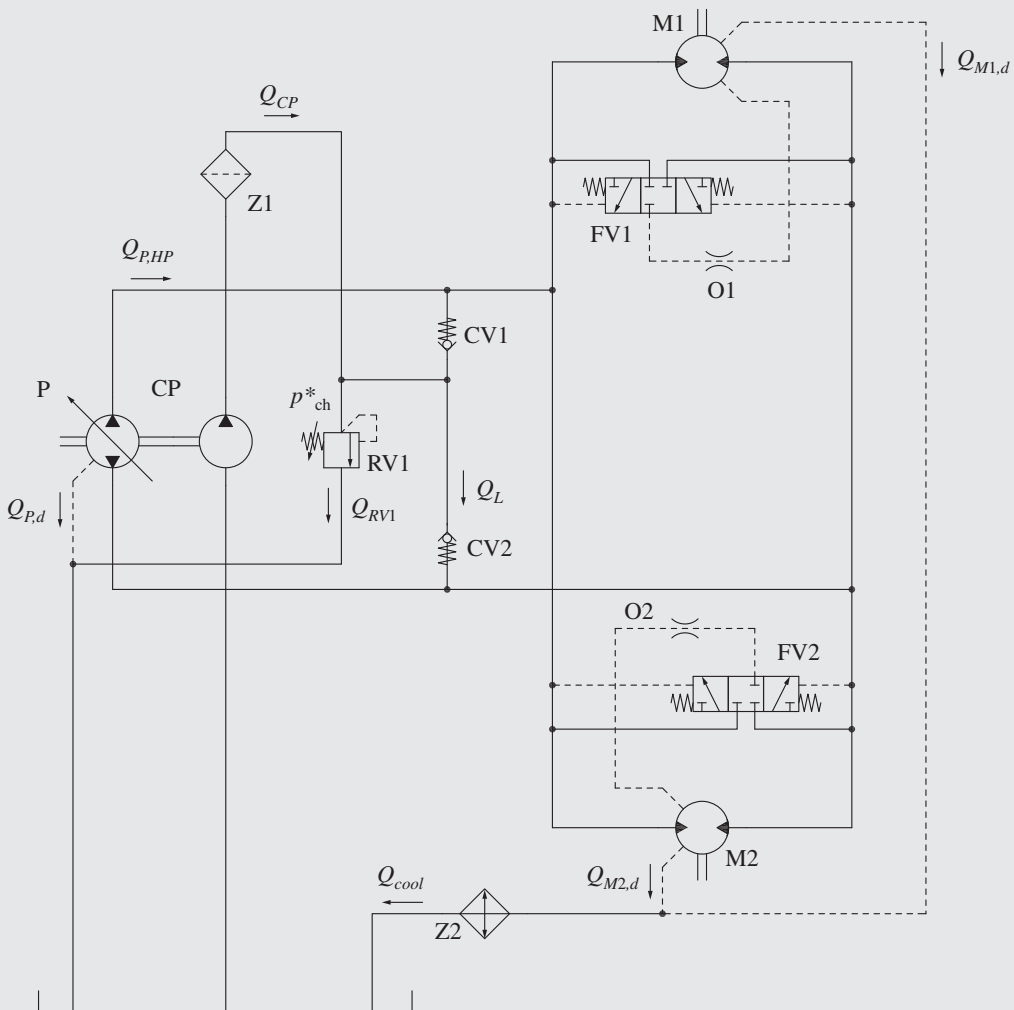
(Continued)

Example 24.4 (Continued)
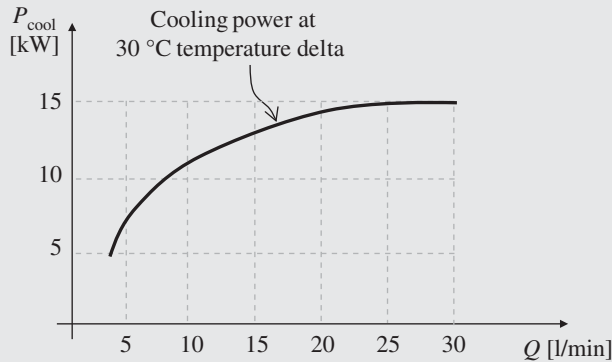
Cooler characteristic at 30 °C temperature difference (oil-ambient)

The hydrostatic pump has a displacement equal to $V_{D,P} = 83$ *cc/r* and it is driven by an 85 *kW* electric motor rotating at 1750 *rpm*. The pump (working at max displacement) has an overall efficiency $\eta_{t,P} = 0.92$ and a volumetric efficiency $\eta_{v,P} = 0.95$. The motors have the following efficiency values: $\eta_{t,M} = 0.93$ and $\eta_{v,P} = 0.96$. Select the proper size of the charge pump CP and of the orifices O1 and O2, assuming an oil density of 850 *kg/m³* and an orifice coefficient of 0.65.

Given:

1) Pump speed, $n_P = 1750$ *rpm*
2) Pump displacement, $V_P = 83$ *cc/r*
3) Pump overall and volumetric efficiency, $\eta_{t,P} = 0.92$ and $\eta_{v,P} = 0.95$
4) Motor overall and volumetric efficiency, $\eta_{t,M} = 0.93$ and $\eta_{v,M} = 0.96$
5) Charge pressure, $p_{ch}^* = 18$ *bar*
6) Cooler Z2 characteristic
7) Transmission max power, $P_T = 85$ *kW*
8) Orifice coefficient, $C_f = 0.65$
9) Oil density, $\rho = 850$ *kg/m³*

Find:

1) The charge pump displacement $V_{P,ch}$
2) The size of the flushing orifices O1 and O2

Solution:

The charge pump needs to be able to make up for the loss of fluid in the transmission due to the volumetric losses of the units. Additionally, it supplies the oil that is discharged by the flushing valves and the O1 and O2 orifices.

The maximum ideal pump flow output is the following:

$$Q_{P,i} = V_{D,P} \cdot n_P = 83 \, [cm^3/r] \cdot 1750 \, [rpm] \cdot 0.001 = 145.3 \, l/min$$

The flow loss through the pump internal leakage is

$$Q_{L,P} = Q_{P,i} \cdot (1 - \eta_{v,P}) = 145.3 \, [l/min] \cdot 0.05 = 7.3 \, l/min$$

The flow loss through the motors internal leakage is

$$Q_{L,M} = Q_{P,i} \cdot \eta_{v,P} \cdot (1 - \eta_{v,M}) = 145.3 \: [l/min] \cdot 0.95 \cdot 0.04 = 5.5 \: l/min$$

The flow lost in the transmission because of the internal leakages in the primary and secondary units is

$$Q_{L,\text{tot}} = Q_{L,P} + Q_{L,M1} + Q_{L,M2} = 7.3 \: [l/min] + 5.5 \: [l/min] = 12.8 \: l/min$$

In order to calculate the flushing flow, the worst-case cooling power demand needs to be calculated first as follows:

$$P_{\text{cool}} = P_T \cdot (1 - \eta_{t,P} \cdot \eta_{t,M}) = 85 \: [kW] \cdot (1 - 0.86) = 11.9 \: [kW]$$

Based on the cooler performance curve, the flow required to generate P_{cool} is approximately $Q_{\text{cool}} = 12 \: l/min$. Therefore, the flow coming from each flushing valve needs to equate the difference between the cooling flow requirement and the flow lost through the internal leakages of the motors:

$$Q_{\text{FV}} = 0.5 \cdot [Q_{\text{cool}} - Q_{P,i} \cdot \eta_{v,P} \cdot (1 - \eta_{v,M})] = 0.5 \cdot (12 \: [l/min] - 145.3 \: [l/min] \cdot 0.95 \cdot 0.04)$$
$$= 3.2 \: l/min$$

Considering the charge pressure is p_{ch}^*, the orifice diameter providing the required flow Q_{FV} is

$$d = \left(\frac{4}{\pi} \frac{Q_{\text{FV}}}{C_f} \sqrt{\frac{\rho}{2 \, p_{\text{ch}}^*}} \right)^{\frac{1}{2}} = 1.21 \: mm$$

In reality it is always recommended to apply a safety factor of 120–130% when sizing HTs charge and cooling system. Using a 125% safety factor, the cooling flow becomes $Q_{\text{FV}} = 4 \: l/min$. Therefore, the corrected orifice diameter is larger (1.36 mm), which can be approximated with a more realistic 1.4 mm.

With this increased orifice diameter, the flushing flow becomes 4.23 l/min.

Therefore, O1 and O2 should be 1.4 mm diameter orifices.

The charge pump needs to be able to make up for the internal leakages (safety factor should be applied) and guarantee the cooling flow:

$$Q_{\text{CP}} = Q_{L,\text{tot}} \cdot 125\% + 2 \cdot Q_{\text{FV}} = 24.5 \: l/min$$

Considering a volumetric efficiency of 0.9, the theoretical minimum displacement of the charge pump becomes 15.5 cm^3/r. The ratio between the displacement of the primary unit and the charge pump is approximately 20%, which is a very common value in practical applications.

24.5 Closed Circuit Displacement Regulators

In an HT, both primary and secondary units can continuously vary their displacements. Multiple regulator types and designs are available. These regulators can be grouped into two categories: regulators using external signals and those using internal signals. In the first case, the setting of the unit is defined by an external command acting on the regulator, which can be either manual, hydraulic, or electric. In the second case (regulator with internal signals), the regulator automatically adjusts the unit setting based on the manipulation of internal pressure signals. In this section, four types

of closed circuit HTs regulators are presented: two for pumps and two for motors. Two of those are external, and the other two internal controls. Other implementations for these regulators are present in today's commercial unit.

The regulators that will be introduced for the pumps are strictly for closed circuit applications, while the ones for motors can work both in closed and open circuit HTs.

24.5.1 Electrohydraulic Displacement Regulator for Closed Circuit Pumps

This regulation can be viewed as a type of displacement control from external signals. Closed circuit pumps present a different displacement control architecture with respect to open circuit pumps (presented in earlier). In an open circuit, the oil to control the stroking pistons is taken directly from the pump outlet. However, in a closed circuit unit, the charge pressure is used to supply the displacement regulator because closed circuit units are always bidirectional machines, capable of delivering flow in both directions. Therefore, in order to handle the transition across zero displacement (which corresponds to null outlet pressure), a separate pressure source is required.

Using charge pressure for pilot control is more efficient because the regulator consumes oil from a lower pressure source. However, the size of the control pistons should increase with respect to the previous case. Figure 24.31 represents the circuit of an electrohydraulic proportional control with position feedback. The displacement of the primary unit P is controlled with a double rod cylinder (CC) with centering springs. The travel of this cylinder is indicated with the letter x and it is proportional to the pump displacement. If x is negative, the unit reverses the direction of the flow.

In Figure 24.31 the chambers of the double rod cylinder are supplied by a 4/3 proportional DCV, which is supplied by the charge pump line at a pressure equal to p_L. DCV has a sliding sleeve, which is connected to CC by a linkage to implement the control feedback.

If the solenoid Y1 is energized with a given current i (enough to win the force F_{S2}), the spool moves to the left. The spool travel (in this case in the positive direction) is indicated with x_S. In this
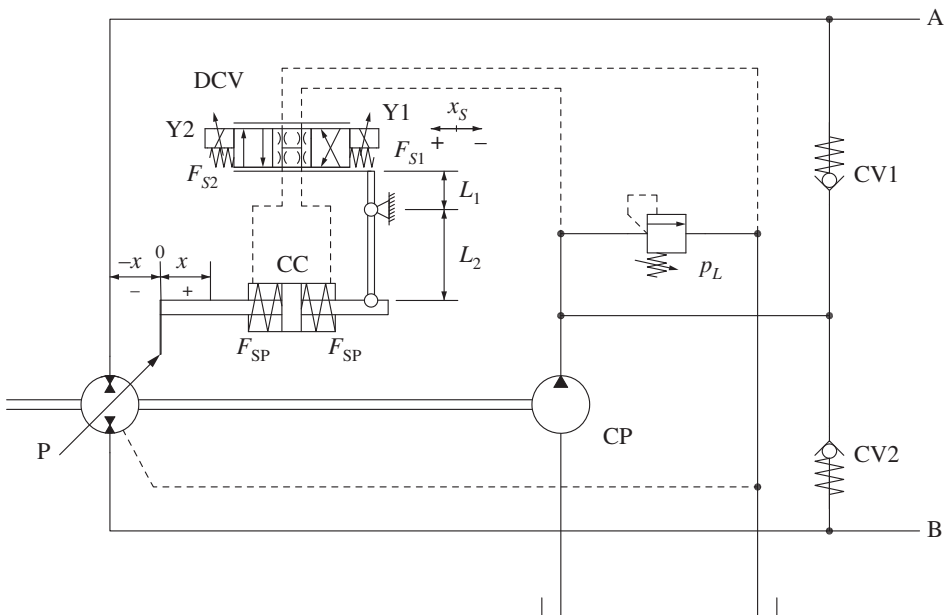
Figure 24.31 Displacement regulator for a closed circuit primary unit based on internal position feedback with amplification.

position, the left chamber of CC is supplied with oil from p_L, while the right chamber is connected to the tank. Therefore, the piston CC travels to the right, the value of x increases, and the pump displacement rises. As the rod of the piston CC moves, the sleeve of the valve follows until the valve is returned in neutral position and the displacement is held at the value corresponding to x. The relationship between the spool and piston travel is as follows:

$$x = \frac{L_2}{L_1} \cdot x_S \tag{24.20}$$

The centering springs included in CC are not considered in this analysis because the force they exert is negligible. Their main function is to return the displacement to null value if the machine is turned off and the charge pressure p_L is lost.

24.5.2 Automotive Control for Closed Circuit Pumps

Automotive-type controls have been specifically conceived for propulsion applications to emulate the behavior of a continuously variable transmission. In all the HT circuits and problems described before, the prime mover speed has been considered as a constant value for the system analysis. However, if the pump displacement is maintained at a certain set value by an electro-hydraulic (EH) displacement regulator, the output flow of the pump changes with the prime mover speed. In other words, an HT with variable speed prime mover has at least two degrees of freedom that can be controlled independently: the pump speed and the pump displacement. On the other hand, in a propulsion application, the driver's expectation is usually to have a vehicle speed increase resulting from pushing the gas pedal to increase the engine speed. In order to mimic such behavior, the control of an HT applied to a propulsion system has to create a link between the prime mover speed to the setting of the pump displacement. In this case, the motor is considered as a fixed displacement unit. This type of control is known as *automotive control* and it is based on internal signals.

Conceptual Schematic
Figure 24.32 shows the schematic implementing the automotive control. The main pump (P) is driven by a variable speed engine, where the throttle is controlled by the foot pedal. A second smaller fixed displacement pump, also referred as tachometric pump (TP), is also connected to the same shaft. This TP (displacement V_{TP}) generates the flow rate Q_{st}, which is directly proportional to n_P. An orifice[5] is located downstream of TP: the outlet pressure of the tachometric pump, p_{st}, is a function of the shaft speed:

$$p_{st} = \left(\frac{n_P \cdot V_{TP}}{c_f \cdot \Omega_{st}} \right)^2 \tag{24.21}$$

In Figure 24.32, the pressure generated by TP is used to control the displacement of the main pump. The pressure p_{st} acts against the control spring F_S. During idling conditions for the engine, p_{st} cannot overcome the force of the spring; therefore, the main pump remains at zero displacement. As the engine speed increases, the pump starts increasing its displacement following a parabolic curve, which is described by the equation below:

$$V_{D,P} \propto \left(\frac{n_P \cdot V_{TP}}{c_f \cdot \Omega_{st}} \right)^2 - \frac{F_S}{A_{CC}} \tag{24.22}$$

---

5 The orifice with area Ω_{st} is represented in the schematic as a variable orifice because it can be adjusted during the initial tuning process. However, during the system operation, this orifice remains fixed.
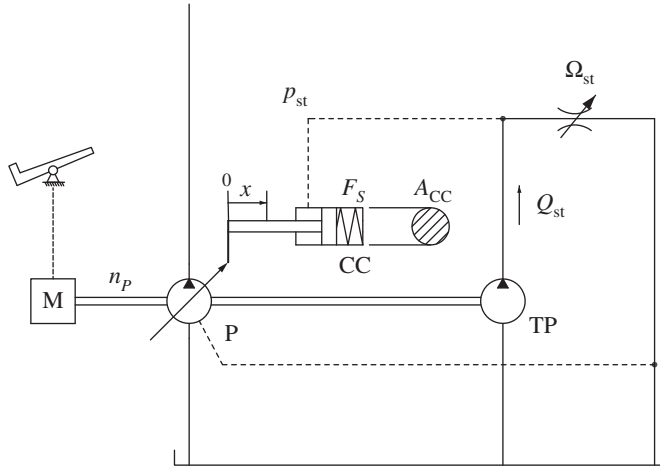
Figure 24.32 Conceptual schematic of the automotive control.

Figure 24.33 shows the trends of displacement and flow rate for the automotive controlled unit. The range of displacement control is between n_1 and n_2. If the engine reaches speeds higher than n_2, above this value the flow rate increases linearly with the speed.

Actual Implementation

The automotive control is actually implemented utilizing the circuit in Figure 24.34. The charge pump is also used as a TP, and the orifice O_{ST} to sense the pump speed. The control pressure sent to the piston CC is generated by a particular type of proportional pressure reducing valve (PV1). The setting of PV is not constant, but it is affected by the pressure difference between the charge pump outlet pressure p_{CP} and the charge relief pressure p_L. The setting of PV1 becomes

$$p_{st} = p^* + (p_{CP} - p_L) = p^* + \left(\frac{n_P \cdot V_{CP}}{c_f \cdot \Omega_{st}} \right)^2 \tag{24.23}$$

The valve DCV is now a simple on/off valve, which has the function of controlling the direction of the flow. In fact, this control also works in reverse gear. There is no feedback between DCV and the pump displacement.
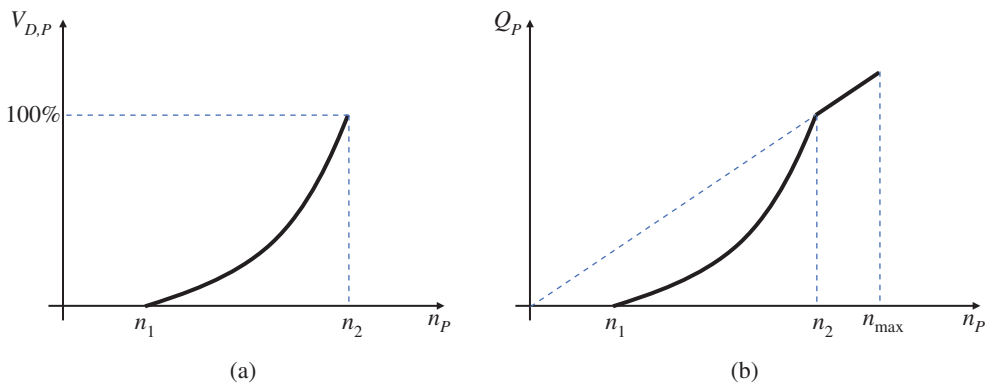
Figure 24.33 Displacement (a) and flow rate (b) of the main pump vs. engine speed.

Figure 24.34 Implementation of automotive control in a closed circuit pump.

24.5.3 Electrohydraulic Displacement Regulator for Motors

Variable displacement secondary units are usually controlled in the same way as open circuit pumps with hydromechanical feedback (as described previously regarding open circuit HTs). An example of this type of external signal regulator is shown in Figure 24.35: the pilot pressure to control the motor is taken internally with the shuttle valve SH, which selects the higher pressure between ports A and B. The control cylinder CC is biased to $V_{M,\,max}$, thanks to a spring. The working pressure selected by SH is also connected to the rod end of CC. The pressure to the bore side of CC is controlled through the proportional valve PV, which acts very similarly to valve PV shown in Figure 24.16. When the current to PV is null the bore chamber of CC is vented to the

Figure 24.35 Example of electrohydraulic displacement regulator for motors.

Figure 24.36 Example of automatic pressure regulator for motors.

tank, so the motor stays at maximum displacement. As the current increases, the control cylinder is pressurized and moves toward the minimum displacement setting. Thanks to the feedback linkage between CC and PV, the control achieves a linear relationship between input current and actual displacements, with a relationship similar to Eq. (24.13).

24.5.4 Automatic Pressure Regulator for Motors

This type of control adjusts the motor displacement based on an internal pressure signal. The control layout is presented in Figure 24.36: one important difference with respect to the previous case is that the motor is normally biased to minimum displacement. In the hydraulic schematic, the convention for minimum and maximum displacement is opposite with respect to the displacement regulator previously shown in Figure 24.35. When the working pressure (selected by valve SH) overcomes the spring setting p^*, valve CV starts shifting and the control cylinder CC starts moving to the left, increasing the motor displacement.

The control performance is represented in Figure 24.37. If the working pressure is smaller than p^*, the motor stays at minimum displacement. Therefore, for a given supply flow, the motor achieves
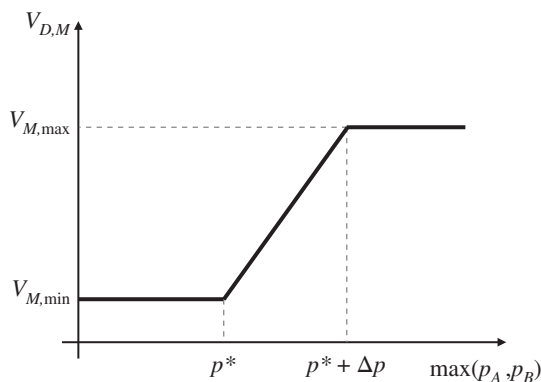
Figure 24.37 Displacement vs. pressure chart for an automatic pressure regulator.

the maximum speed with low torque output. When the pressure hits the threshold value, p^*, the displacement increases linearly with the pressure. The motor shaft slows down, but its torque output value increases. The maximum displacement is reached when the working pressure is $p^* + \Delta p$. The value of Δp is defined by the stiffness of the feedback spring.

From an operational standpoint, the automatic pressure regulator automatically reacts to the load conditions. In fact, the motor shaft automatically decelerates if the load increases. During the regulation range, the output power is constant, and the decrease in speed is compensated by the torque increase. Thus, this type of control is often referred to as *constant power* regulator.

Problems

24.1 An HT for a mower utilizes a circuit based on a variable displacement pump and a fixed displacement motor. The pump is connected to an internal combustion engine, which rotates at $n_P = 1000$ rpm. The pump maximum displacement is $V_P = 14\,\text{cm}^3/\text{rev}$, and its efficiencies are $\eta_{v, P} = 0.95$ and $\eta_{hm, P} = 0.92$. At the maximum velocity condition, the motor shaft has to rotate as close as possible to $n_M = 100$ rpm. For this purpose, the following options are available for the motor:

	Motor 1	Motor 2	Motor 3	Motor 4
V_M	90 cm³/rev	120 cm³/rev	150 cm³/rev	200 cm³/rev
$\eta_{v, M}$	0.92	0.94	0.94	0.95
$\eta_{hm, M}$	0.87	0.88	0.88	0.89
p_{max}	250 bar	250 bar	250 bar	250 bar
$n_{M, max}$	200 rpm	180 rpm	160 rpm	150 rpm

Find:
a) The motor that best matches the required maximum velocity requirement
b) The actual shaft speed of the motor, for the chosen option
c) The actual transmission ratio of the transmission
d) The maximum shaft torque of the motor to operate the system safely
e) The overall efficiency of the HT
f) The maximum power at the motor shaft
g) The maximum power at the pump shaft
h) If the maximum power of the combustion engine is 20% below, the maximum power of the HT at the pump shaft, determine the maximum pump displacement that avoids stalling the transmission (meaning exceeding the maximum torque available)
i) The maximum angular velocity of the motor shaft when the maximum power of the engine is 20% less the maximum power of the transmission

Both pump and motor efficiencies can be assumed constant throughout the problem.

24.2 The following data is available for the HT shown in the figure below:
Pump displacement, $V_P = 100\,\text{cm}^3/\text{rev}$
Pump volumetric efficiency, $\eta_{v, P} = 0.95$
Pump hydromechanical efficiency, $\eta_{hm, P} = 0.97$
Motor displacement, $V_M = 100\,\text{cm}^3/\text{rev}$
Motor volumetric efficiency, $\eta_{v, M} = 0.95$

Motor hydromechanical efficiency, $\eta_{\mathrm{hm},M} = 0.99$
Pump rotational speed, $n_P = 1475$ rpm
Pump input torque (at shaft), $T_P = 100$ Nm

a) Calculate the overall efficiency of the HT $\eta_{v,\mathrm{HT}}$, assuming no losses in the circuit connecting the pump and the motor.
b) Calculate the rotation speed nm and shaft torque T_M of the motor.
c) Calculate the transmission ratio τ and the torque ratio κ of the transmission.
d) In order to limit the output torque T_M of the motor to 80 Nm, an orifice is used between the pump outlet and the motor inlet. Determine the area of the orifice assuming an orifice coefficient equal to 0.7 and a fluid density of 870 kg/m³.

24.3 An open circuit HT is used to drive two wheels of a given vehicle. Using the data in the table below, solve the following points, assuming ideal components:

a) What is the function of valve V1? Describe it by listing the function for the three positions for V1.
b) What is the function of valve V2? Describe it by listing the function for the three positions for V2.

Assuming V1 in position 1 (parallel arrows) and equal load at the two motors:

c) What is the maximum tractive force (N) of the vehicle for position 1 of V2?
d) What is the maximum tractive force (N) of the vehicle for position 2 of V2?
e) What is the maximum speed (m/s) of the vehicle for position 1 of V2?
f) What is the maximum speed (m/s) of the vehicle for position 2 of V2?
g) What is the transmission ratio for the HT for position 2 of V2?
h) What is the transmission ratio for the HT for position 1 of V2?
i) Calculate the power (W) requested by the combustion engine M under full load.
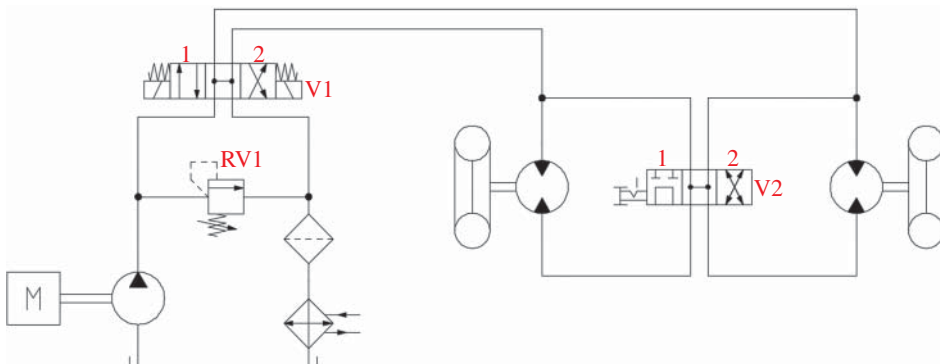
The parameters of the HR are listed below:

Symbol	Description	Value
D	Diameter of wheels	0.8 m
n	Shaft speed of the combustion engine driving the pump	1500 rpm
p_{RV1}*	Pressure setting of the relief valve RV1	210 bar
V_m	Displacement for both hydraulic motors	160 cc/rev
V_P	Pump displacement	50 cc/rev

24.4 An HT is used to move a rotary load with an electric motor, as represented in the schematic below. All the components can be considered as ideal (no losses), except for the pump and the hydraulic motor, for which the efficiencies are known. Both the pump and the hydraulic motor operate at maximum displacement.
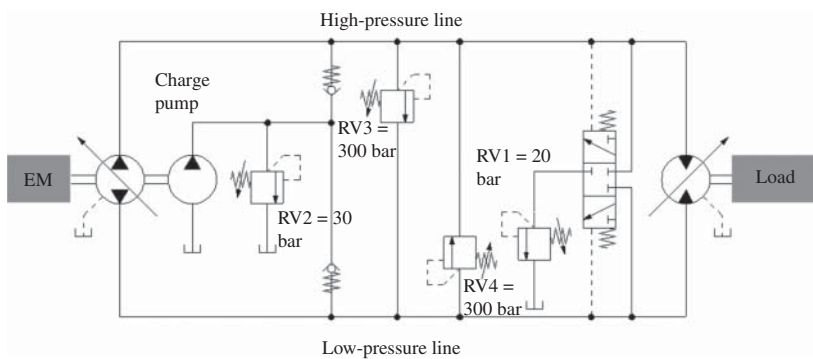
Symbol	Description	Value
T_M	Torque on the motor	120 Nm
n	Speed of the electric motor driving the pump	1490 rpm
p_{RV1}*	Pressure setting of the relief valve RV1	20 bar
V_{CH}	Charge pump displacement	10 cc/rev
V_P	Pump displacement	40 cc/rev
V_M	Motor displacement	32 cc/rev
$\eta_{mh,PCH}$	Charge pump hydromechanical efficiency	0.96
$\eta_{mh,P}$	Pump hydromechanical (or torque) efficiency	0.95
$\eta_{mh,M}$	Motor hydromechanical (or torque) efficiency	0.92
$\eta_{v,PCH}$	Charge pump volumetric efficiency	0.97
$\eta_{v,P}$	Pump volumetric efficiency	0.93
$\eta_{v,M}$	Motor volumetric efficiency	0.94

Find:

a) The flow rate (l/min) delivered by the pump and the rotational speed (rpm) of the hydraulic motor in the ideal case (assume ideal pump and hydraulic motor with 100% efficiency).

b) The actual flow rate (l/min) delivered by the pump.

c) The actual flow rate (l/min) generated by the charge pump.

d) The actual rotational speed (rpm) of the hydraulic motor.

e) The torque (Nm) requested by the charge pump.

f) The pressure (bar) at the delivery of the pump (equal to the pressure at the motor inlet), considering the values of the motor hydromechanical efficiency and of the pressure (bar) at the low-pressure line.

g) The actual torque requested by the main pump.

h) The total torque (Nm) required by the electric motor to drive both pumps.

i) The flow rate (l/min) discharged by the pressure relief valve RV1 (due to the difference between the flow rate at the pump inlet and the flow rate at the outlet of the hydraulic motor).

j) The power (W) requested by the electric motor.

k) The power (W) provided to the load (at the hydraulic motor shaft).

l) The power (W) dissipated in the hydraulic system (according to what calculated in *j* and *k*).

24.5 An open circuit HR is used to drive a fan with following characteristic:

$$T = 7 \times 10^{-6}\, n^2$$

$n_{max,f} = 3000\ \text{rpm}$
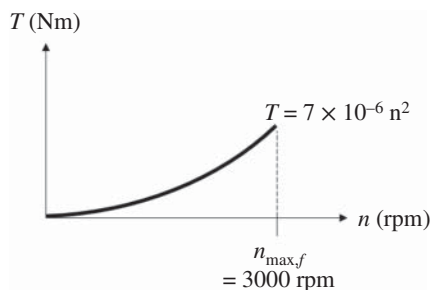
The HT needs to drive the fan from 0 to 3000 rpm ($n_{max,f}$).
The following options are available:
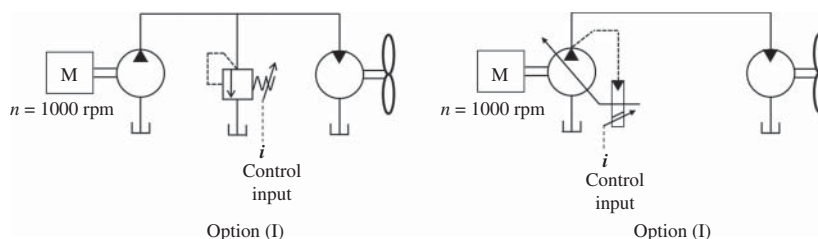
Option (I)   Option (I)

a) Does option (I) allow for speed regulation?

b) Does option (II) allow for speed regulation?

c) Considering the case of fan at $n_{max,f}$ (maximum speed allowable for the HT), does option (I) require higher/lower/same power at the prime mover when compared to option (II)? Explain your choice.

d) Select the motor capable of reaching n$_{\text{max, f}}$ from the table below:

Motors	A	B	C	D	E	F
Displacement (cc/rev)	5	5	10	10	20	20
p_{max} (bar)	220	220	220	220	220	220
n_{max} (rpm)	2000	4000	2000	4000	2000	4000
η_v	0.95	0.95	0.95	0.95	0.95	0.95
η_{hm}	0.95	0.95	0.95	0.95	0.95	0.95

e) Determine the motor flow rate at $n_{\text{max}, f}$ (maximum speed of the fan).

f) Determine the size of the pump assuming $\eta_{v, \text{pump}} = 0.95$.

g) Determine the power consumed by the prime mover at $n_{\text{max}, f}$ assuming $\eta_{\text{hm, pump}} = 0.9$.

h) Determine the system pressure to achieve $n_{\text{fan}} = \frac{n_{\text{max}, f}}{2}$.

i) Determine the motor flow rate at $n_{\text{fan}} = \frac{n_{\text{max}, f}}{2}$.

Chapter 25

Hydrostatic Transmissions Applied to Vehicle Propulsion

Vehicle propulsion is one of the most common applications for hydrostatic transmissions (HTs). This chapter will guide the reader toward the understanding of the basic needs for a vehicle transmission, as it describes the convenience of having a continuously variable transmission (CVT) system. A classification of the different technologies available for CVTs is also provided. In this way, the reader will be familiarized with the possible solutions that the hydraulic technology can offer. Starting with the basic application of HTs, the chapter further expands to the more advanced concepts of hydromechanical power split transmission and hydraulic hybrids, along with a systematic procedure for sizing basic HT architectures, which can be important to solve practical dimensioning problems.

25.1 Basic of Vehicle Transmission

The focus of this section is to provide generic considerations regarding propulsion systems for vehicles. The propulsion system includes the *vehicle transmission*, which represents the intermediate element between the prime mover and the wheels (Figure 25.1). The features of the vehicle transmission are identified by analyzing the typical characteristics of the prime mover and the load.

> The vehicle **transmission** is the intermediate element between the prime mover and the vehicle wheels.

The left chart in Figure 25.1 shows the typical torque and power characteristic for a combustion engine – Diesel engine (prime mover). The right side of the figure shows a typical vehicle resistance curve. Without entering into the specifics of the engine operation (more details in the Appendix), the following observations can be made from the two charts:

- The engine has a minimum shaft speed, usually referred to as *idle speed*, $n_{\min}$, at which it can operate. Therefore, it cannot provide torque from rest.
- The maximum power of the engine, $P_{\max}$ is achieved at a specific shaft speed value $n_{P_{\max}}$. Moreover, the power at full throttle is an increasing function for most of the range of operation of the engine.
- The maximum engine torque $T_{\max}$, is achieved at a shaft speed $n_{T_{\max}} \neq n_{P_{\max}}$.
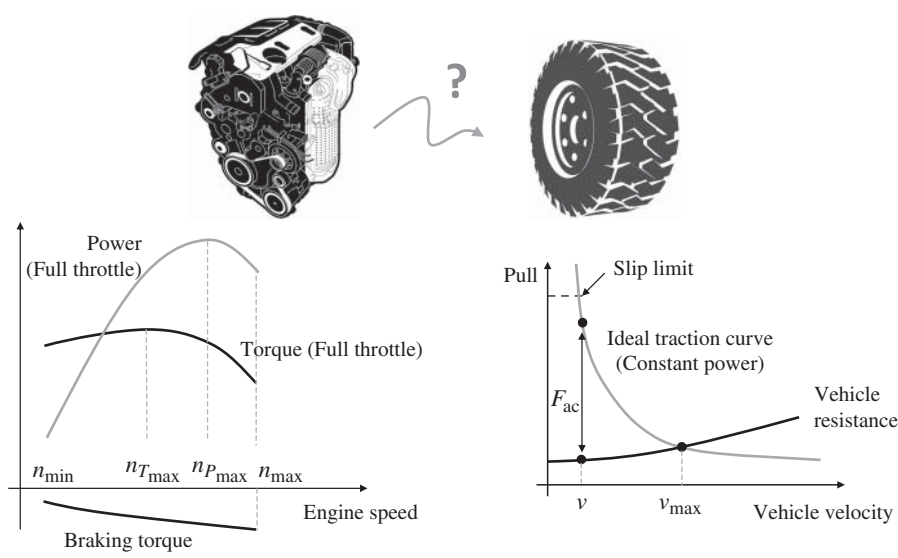
Figure 25.1 A transmission is the intermediate system between the engine and the wheels.

The typical vehicle resistance curve shown in Figure 25.1 results from the vehicle mass, the ground profile (slope), the rolling friction, and the aerodynamic resistance. For vehicles operating at low velocities such as in agriculture or construction fields, this resistance is usually very low, or negligible, therefore resulting in the resistance curve as a horizontal line. The resistance chart in Figure 25.1 shows also the constant power curve equal to the engine-rated power P_{max}. The maximum velocity that can be reached by the vehicle for a given resistance line is identified by the intersection point between the two curves, and the maximum acceleration force at a given velocity F_{ac} by the difference between these curves. Ideally, the vehicle acceleration is maximum at zero speed, while, as the vehicle moves faster, the acceleration monotonically decreases, thus providing the operator comfort and an easy control of the vehicle velocity [6].

In reality, the engine does not follow the ideal power hyperbole depicted in Figure 25.1 as the output torque is limited to the value T_{max}. The plot in Figure 25.2 represents a direct connection between engine and wheels through a gearbox with a ratio τ. The intersection between the two
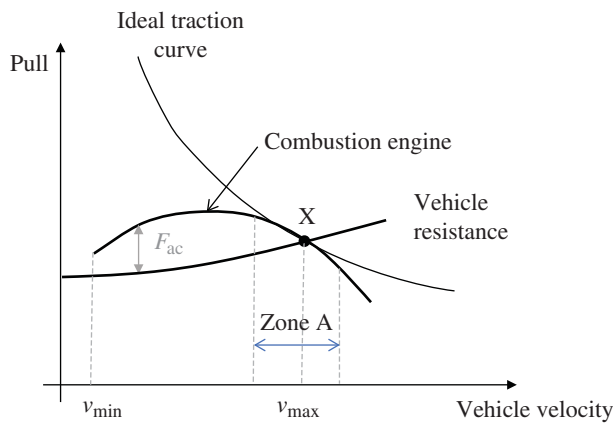
Figure 25.2 Hypothetical direct connection between the combustion engine and the vehicle wheels.

curves defines the maximum velocity that can be reached, v_{max}, which can be calculated as follows:

$$n_{P_{max}} \cdot R_R = \tau \cdot v_{max} \tag{25.1}$$

The parameter R_R represent the rolling radius, which is approximately equal to the wheel radius. A further analysis of Figure 25.2 leads to the following considerations:

- Low vehicle velocities cannot be achieved due to the engine speed limitation n_{min}.
- The acceleration at full throttle is not a monotonic function. This creates an irregular acceleration for the vehicle perceived by the operator.
- The engine can be stalled in case of increased vehicle resistance, due to an increase of vehicle payload or slope.

Figure 25.2 shows that a transmission with a single ratio provides a traction curve much different from the ideal curve, over the full vehicle speed range. The engine characteristics approximates the ideal traction curve only in a limited zone, defined by the intersection point X and its surroundings (marked as Zone A).

> The ideal transmission characteristic for a vehicle can be achieved by an engine and a transmission system that has the capability of varying the ratio between the engine and the wheels.

This can be accomplished in several ways. For example, Figure 25.3 shows a manual gearbox with four gears that can achieve a discrete variation for the transmission ratio τ. High vehicle resistances can be overcome by the engine with low gears. Shifting to higher gears, the vehicle can overcome less resistances and also reach higher vehicle velocities. The maximum driver comfort can be reached if the vehicle operator can switch gears at points close to the ideal traction curve. This is usually obtained when the engine operates between $n_{T_{max}}$ and $n_{P_{max}}$.
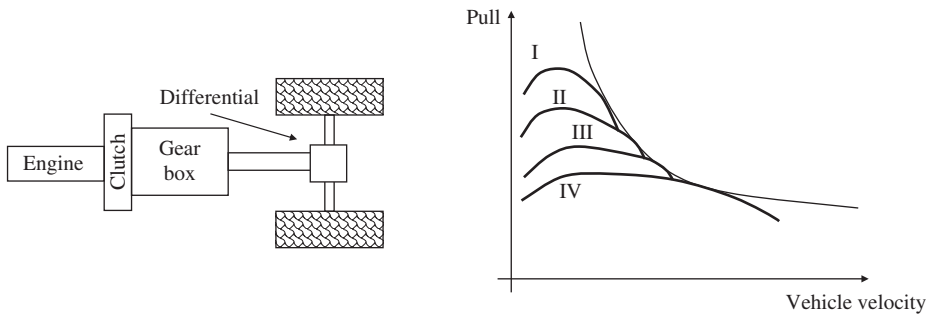
Figure 25.3 Four gears can be used to approximate the ideal traction curve.

> By implementing a variable transmission ratio, the vehicle transmission allows to operate the system in a wide range of traction force, also approximating the ideal traction conditions.

This concept is graphically shown in Figure 25.4.

From Chapter 24, it is clear how an HT can help in achieving a variable transmission ratio between the engine and the wheel axle, as schematically shown in Figure 25.5. Depending on the layout of the HT, different characteristics for the transmission ratio and the dynamic ratio can be obtained. This was discussed in Chapter 24, for the PVMF, the pump fixed displacement, motor variable displacement (PFMV), and the PVMV basic layouts, respectively.
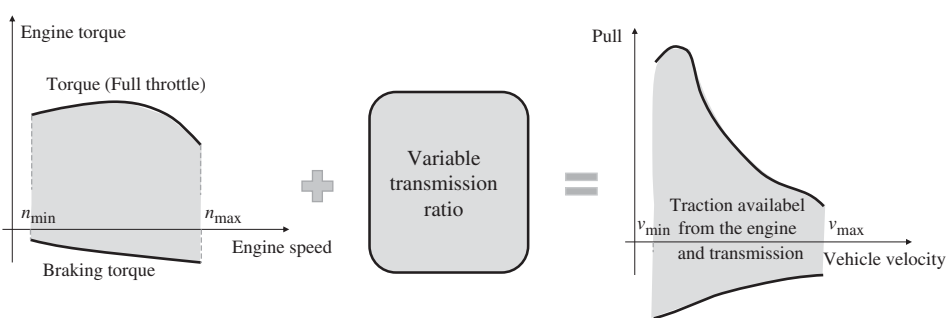
Figure 25.4 Combining an engine with a transmission with a variable ratio.
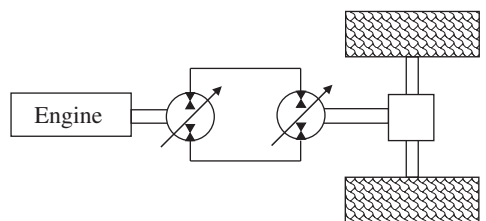
Figure 25.5 Hydrostatic transmission used for propulsion.

25.2 Classification for Variable Ratio Transmission Systems

HTs in propulsion applications, as discussed previously, should be used as a transmission system that can implement an infinitely variable transmission ratio.

Although the main focus of this book is on the analysis of HTs in terms of "fluid power," the reader should be given with a complete picture of the state of the art for variable transmission systems for propulsion applications. Figure 25.6 provides a general overview of the available technologies for implementing the vehicle propulsion. While the features of an HT with respect
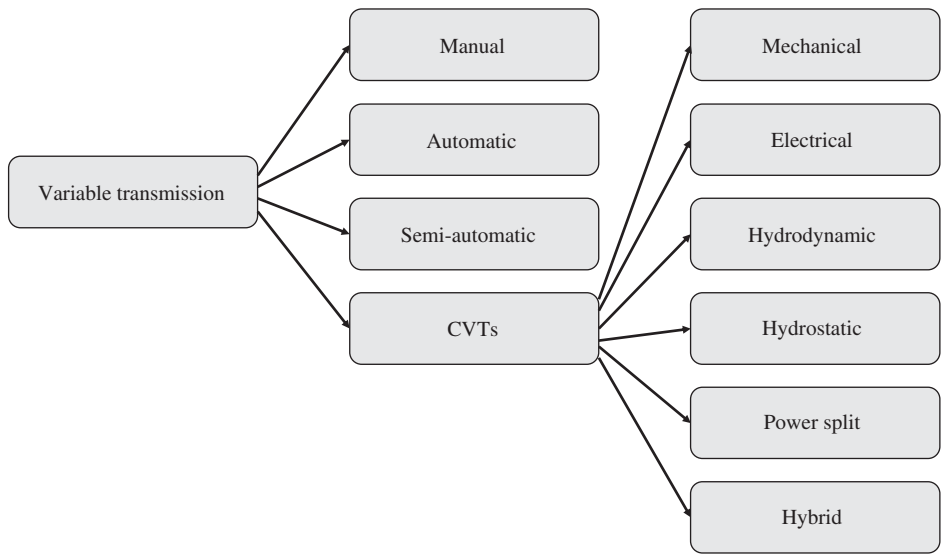
Figure 25.6 Technologies for variable ratio transmission systems.

to a discretely variable transmission has been introduced previously, in reality, the spectrum of available options is much broader.

Manual transmissions are systems usually comprised of sequential gearboxes, which include clutches to allow shifting the sequence of the gears that are engaged, as in Figure 25.3. These systems have been very popular for passenger vehicles, due to their low cost, high efficiency, and high reliability. However, a skilled driver should operate them to optimize vehicle mileage, despite the push toward the automation of the vehicle functions. Hence, the shares of these transmissions in automotive applications are gradually shrinking.

Semi-automatic transmissions represent an advancement toward the automation of the vehicle functions, relaxing the driver from controlling the clutch, which is performed by an electrical control unit. These kinds of transmissions found a relatively good commercial success in automotive applications, although nowadays most of the automotive vehicles with automated gear shifting adopt fully automatic transmissions.

Automatic transmissions are currently dominating the market of passenger cars. They can achieve very good performance in terms of driving comfort to the vehicle passengers, although the cost, reliability, and transmission efficiency is normally lower than those of manual transmission systems (for the same number of gears). The structure of such a transmission can be simplified with the schematic in Figure 25.7. A discrete-variable transmission gearbox is still present; however, between the engine and the gearbox, there is an additional element, the *torque converter*, also a basic element of a hydrodynamic CVT. The torque converter provides a fluid coupling between the engine shaft and the gearbox shaft, allowing to partially decouple the engine speed and torque from the transmission speed and torque. The ability of the torque converter to efficiently transmit torque and power highly depends on the speed ratio between the gearbox shaft and the engine shaft. In more detail, only for a speed ratio close to 1, the torque converter reaches a good energy efficiency. Thus, a variable gearbox with multiple speed ratios is used in modern transmissions to maintain the overall efficiency of the transmission sufficiently high (nowadays it is common to have 6 or more ratios). A lock-up clutch, typically included in the torque converter, is typically used to mechanically lock the two shafts to achieve the maximum transmission efficiency when the two shafts reaches the same rotational speed.

In general, all the transmission systems mentioned above are normally referred to as discrete variable transmissions. This also in the case of a torque converter used in the automatic transmissions, which would imply a CVT system. Figure 25.6 also sub-categorizes the different technologies that can be implemented to implement a **continuously variable transmission** system.
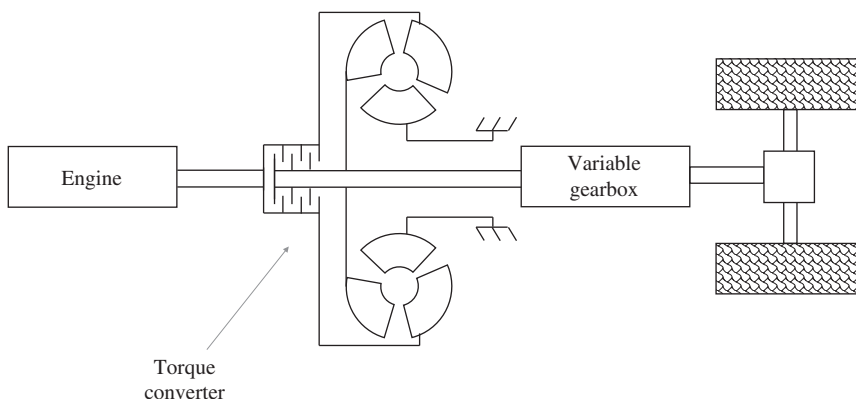
Figure 25.7 Schematic representation of an automatic transmission.

Purely **mechanical CVTs** are popular in several low torque applications (such as light motorcycles). Different mechanical systems have been proposed to implement a CVT. Among these, toroidal CVTs and the variable diameter pulleys are quite popular. It is not within the scope of this chapter to provide details on these latter systems. The interested reader is encouraged to consult other sources, such as Costa and Sepehri [7] for a simplified description, or to more specialized literature on mechanical CVTs, like [8].

Electric machines can also be used to implement a CVT. Substantially, an electric generator would be connected to the engine shaft (for vehicle still using a combustion engine; while a purely electric vehicle will use a battery as an energy source), while an electric motor to the wheel axle. This can be seen as the electric counterpart of an HT, although for the same power-rating electric components are still bulkier and heavier than hydraulic components. Nevertheless, there is a significant research trend for combining the two electric machines (generator and motor) into a single electric machine, to improve the power-to-weight ratio of the electric transmission. Electric transmissions systems are particularly interesting for the easy implementation of hybrid CVTs.

A **hydrodynamic** transmission system is typically implemented by a torque converter. HTs and hydrodynamic transmissions have in common the principle of realizing a fluid coupling between the input shaft (connected to the engine) and the output shaft. For this reason, these two technologies can be generally referred to as **hydraulic transmission systems**. However, there is an essential functional difference between the two transmission types, which is on the principle used by the hydraulic energy conversion elements. In an HT, hydrostatic units (pumps and motors) are used for the mechanical/hydraulic energy conversions. However, in a hydrodynamic transmission, hydrodynamic units (an impeller pump and a turbine) are used to accomplish the same energy conversion function. While hydrostatic pumps and motors operate with the principle of positive displacement machines (as described in Chapter 6), hydrodynamic machines (impeller pumps and turbine) base operate based on the fluid momentum principle. In simple words, the fluid velocity across the pump, or the turbine, is modified to achieve a positive or negative shaft torque. Textbooks on fluid mechanics and fluid machinery usually well describe the basic theory of these rotating machines. In hydraulics, hydrodynamic machines are not used for their inability to reach high operating pressures. In addition, their pressure vs. flow characteristic shows a very high dependency on the flow through the machine with the operating pressure. This makes these units unsuitable for hydraulic control systems, except for application in torque converters due to the operating features of hydrodynamic units (i.e. the low operating pressure), as depicted in Figure 25.8. The impeller accelerates the oil providing fluid momentum that is harvested at the
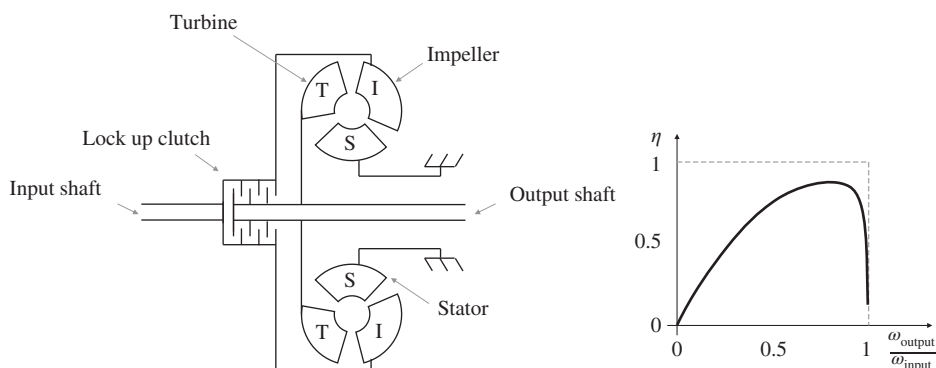
Figure 25.8 Schematic representation of a torque converter and realistic transmission efficiency.

turbine, which provides rotational power to the output shaft. The fluid exiting the turbine needs to be properly re-directed back to the impeller, with a proper inlet velocity. This latter function is implemented by the stator.

The energy conversion process briefly summarized above occurs at a high efficiency only at a certain design point, given by the relative velocity between the input and the output shafts. For this reason, the shaft speed ratio is an important parameter to consider when using torque converters. The right side of Figure 25.8 provides a realistic plot of the energy efficiency for a torque converter. The low efficiency of the torque converter beyond the optimal transmission ratio is the main reason behind the implementation of the automatic transmission layout in Figure 25.7. Very seldom a vehicle utilizes a torque converter without a gearbox with a variable transmission ratio.

Hydrostatic Transmissions, extensively covered in Chapter 24, represent instead a very common transmission system, particularly of heavy-duty applications. More details on the sizing of a HT for propulsion will be provided below.

Finally, Figure 25.6 shows how the power-split and hybrid transmissions are both technologies capable of realizing CVTs. Both power-split and hybrid transmission can be related to HTs and they will be more carefully described in Section 25.3.

25.3 Power-split Transmissions

The principle of power-split transmissions is to combine two technologies into a single transmission system. In relevant applications, a pure mechanical drive is coupled to another CVT system, either mechanical, electric, or hydraulic. The main purpose is to benefit of both advantages of the two systems: the high energy efficiency of the mechanical transmission and the variable transmission ratio of the CVT.

A **power-split transmission** typically combines a pure mechanical drive with a CVT, either mechanical, electric, or hydraulic, to benefit from the advantages of both the technologies integrated within the transmission.

According to the definition made by the first pioneer work published by John Deere [9], there are different alternatives for realizing a power split transmission (Figure 25.9):

The power-split transmission splits the power between the efficient mechanical transmission path and the flexible CVT path. Depending on how the mechanical power is input to the CVT, it is possible to distinguish the case of **input-coupled** (Figure 25.9a) from **output-coupled** (Figure 25.9b) power-split transmission.

In an input-coupled power split, there is a direct connection (i.e. fixed ratio) between the input shaft speed ω_E and the speed of the CVT. However, in the output-coupled power split, there is a direct connection between the output shaft speed of the transmission ω_T and the speed of the CVT.

The **compound power-split** solution (Figure 25.9c) is a combination of both input-coupled and output-coupled power split.

a) Input coupled

b) Output coupled
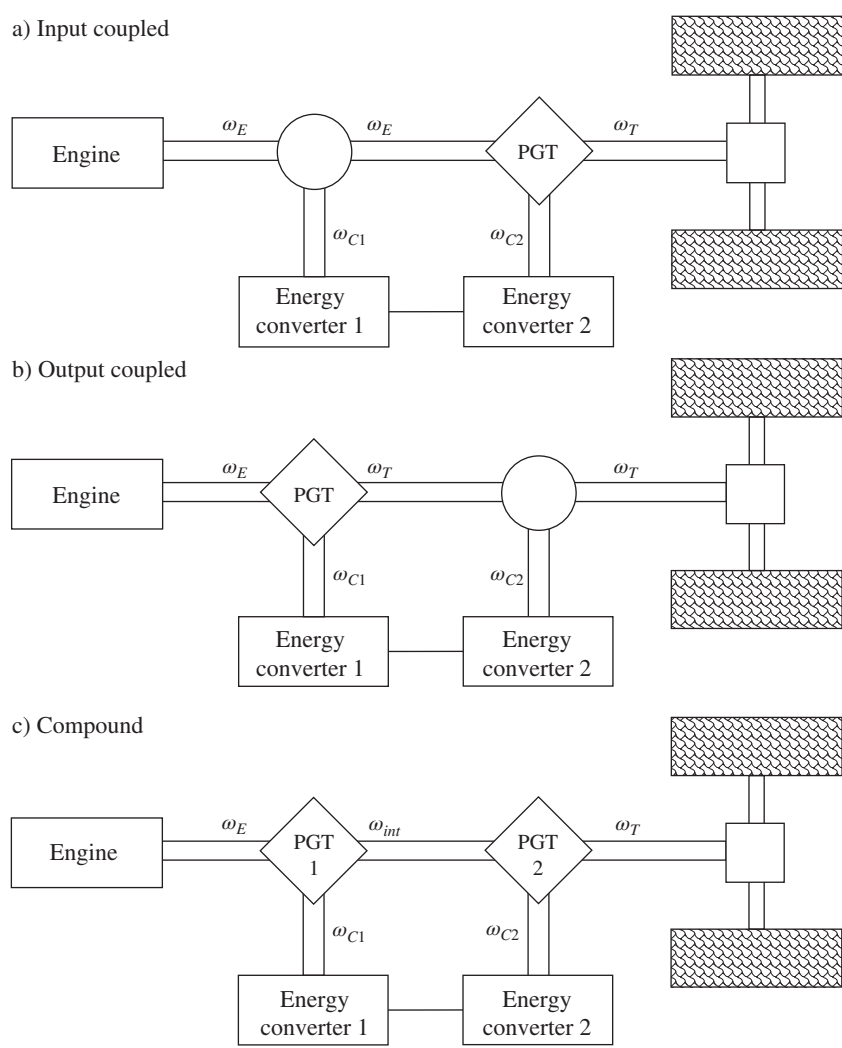
c) Compound

Figure 25.9 Generic schematics for power-split transmissions. (a) Input-coupled. (b) Output-coupled. (c) Compound.

25.3.1 Planetary Gear Train

At the base of a power split transmission, there is the planetary gear train (PGT), which is a device that allows the mechanical power to be either split or combined between three separated mechanical paths. In a PGT, the engagement between the gears occurs both on the outer (between the sun gear and the planet gears) and on the inner circumference (between the ring gear and the planet gears). The planets and the sun are supported by a rotating element, the carrier. The outer gear (the ring) is placed outside the planet gears. Figure 25.10 shows the implementation of a PGT (right figure) along with the common symbolic representation (left figure). The PGT presents three input/output mechanical connections, each one connected to the three different energy paths. Different PGTs can implement different shaft connection arrangements. In Figure 25.10, the sun and the carrier are rigidly connected to two mechanical shafts. These can be connected to the engine and to the wheel axle. However, the ring could present a PTO connection for driving, for example, a hydraulic unit.
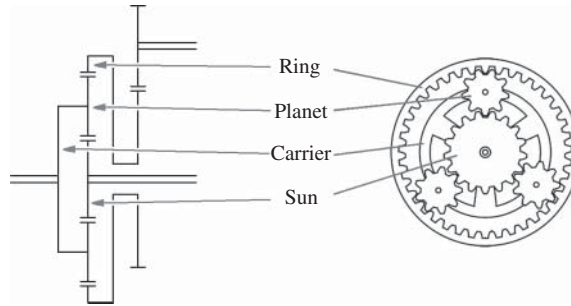
Figure 25.10 Planetary gear train (PGT): elements and symbolic representation.

Planetary gear trains are at the base of power split transmissions, allowing to either split or combine the mechanical power between three separated paths.

As shown in Figure 25.11, there is a linear relation between the angular velocities of the sun (ω_S), of the carrier (ω_C), and of the ring gear (ω_R). This is expressed by the fundamental formula for PGTs, also known as the Willis equation, found in [10] or [11]:

$$\omega_S - \tau_0 \omega_R - \left(1 - \tau_0\right) \omega_C = 0 \tag{25.2}$$

where the constant τ_0 is determined by the number of teeth of the ring gear (Z_R) and of the sun gear (Z_S):

$$\tau_0 = -\frac{Z_R}{Z_S} \tag{25.3}$$

Therefore, due to Eq. (25.2), the PGT has two degrees of freedom for the angular velocities of gear sets. If the angular velocity of two gear sets is defined, there will be a specific velocity for the third gear set according to the Willis equation.

In contrast, the torque transferred through the PGT gearsets has only one degree of freedom. In fact, from the torque balance on the PGT, it is possible to write the following relations:

$$\begin{cases} T_c = \left(\tau_0 - 1\right) T_s \\ T_R = -\tau_0 T_s \end{cases} \tag{25.4}$$

Therefore, a certain torque on one gear set yields to specific torque values on the other two gear sets.

These properties of variable speed ratios and fixed torque ratios between the gear sets allow the PGT to split the power between the three gear sets. This power split can be varied by adjusting the
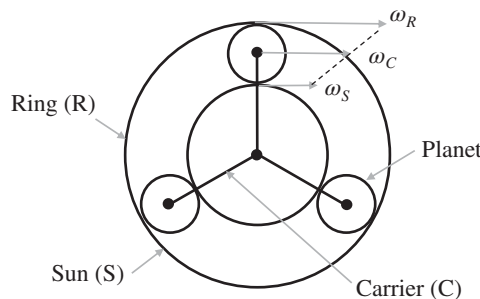
Figure 25.11 Linear dependence between the angular velocities of the elements of a PGT.
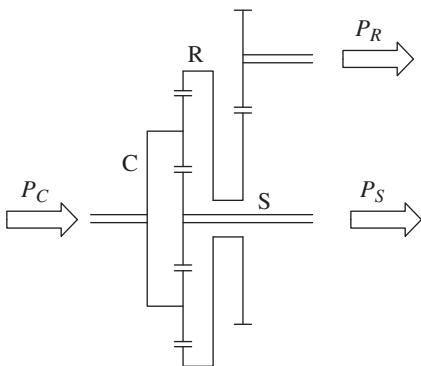
Figure 25.12 Power split obtained with a PGT.

relative speeds of the input and the output shafts. In more detail, considering the power at each gear set as $P = T\omega$, and considering that

$$P_S + P_C + P_R = 0 \tag{25.5}$$

from the Eqs. (25.2) and (25.4) it is possible to write the following power relations:

$$
\begin{aligned}
P_S &= \frac{P_C}{\tau_0 \dfrac{\omega_R}{\omega_S} - 1} \\
P_R &= \frac{-i_o P_C}{\tau_o - \dfrac{\omega_S}{\omega_R}}
\end{aligned}
\tag{25.6}
$$

These two relations are clearer with the graphical representation of Figure 25.12, which highlights the fundamental principle of power-split drives. It is very important to notice that the sign of the power terms can be either positive or negative, as in Figure 25.13. This means that the PGT can split the input power, but it can also operate as power summation, enabling power recirculation modes within the transmission.

PGT operation	PGT vector representation	Rotational direction	Torque direction	Power direction	Power flow
Summer		+ + +	+ − +	in out in	
Splitter		− + +	+ − +	out out in	

Figure 25.13 PGT operation as power summation or power splitting.

25.3.2 Hydromechanical Power-split Transmission

In a **hydromechanical power-split**, the PGT is used to combine a mechanical transmission with an HT.

(a)

(b)

(c)
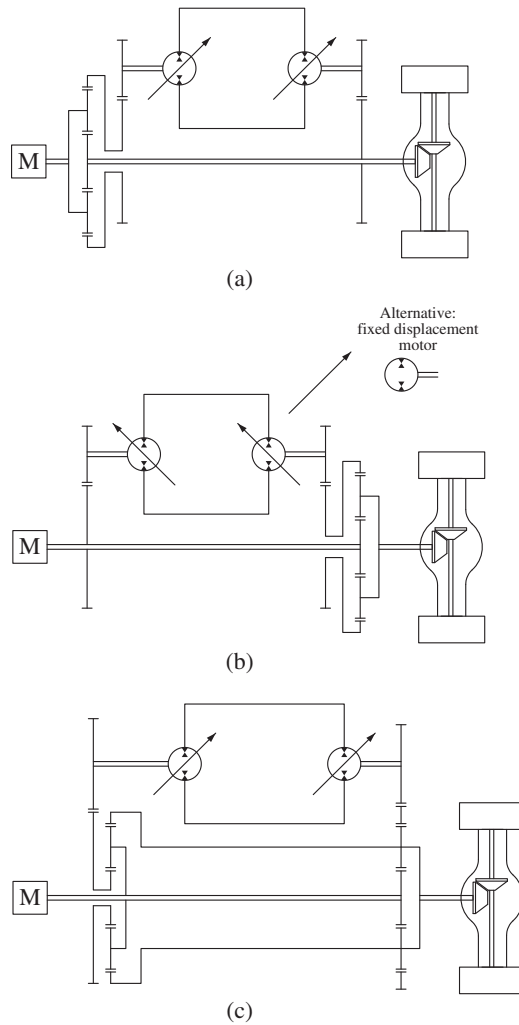
Figure 25.14 Hydromechanical power-split transmissions. (a) Output-coupled. (b) Input-coupled. (c) Compound.

Three different configurations can be used to implement a hydromechanical power-split: **input-coupled**, **output-coupled**, and **compound** hydromechanical power splits. These configurations are shown in the simplified schematics in Figure 25.14. The HT part in this figure are simplified for easy reference. The components necessary to run the HT, such as the flushing or charge circuit, are omitted. Figure 25.15 shows the complete circuit for an output coupled power-split hydrodynamic transmission (PST). This circuit has two peculiarities: the primary unit is bidirectional, and, therefore, the charge pump is located externally.

The high transmission efficiency of the hydromechanical power-split transmission is the key reason for the commercial success of this technology for vehicle propulsion. Mobile vehicles with intensive utilization, such as agricultural tractors, are nowadays equipped in most cases with PSTs. Current technology for PSTs spams from the basic architectures in Figure 25.14 to more complicated structures, including multiple stages PGTs [12], whose description is outside the scope of this book. The following subsections further describe the cases of output- and input-coupled PSTs. The reader interested in learning more on the compound PSTs in encouraged to look to specialized literatures, such as [13].
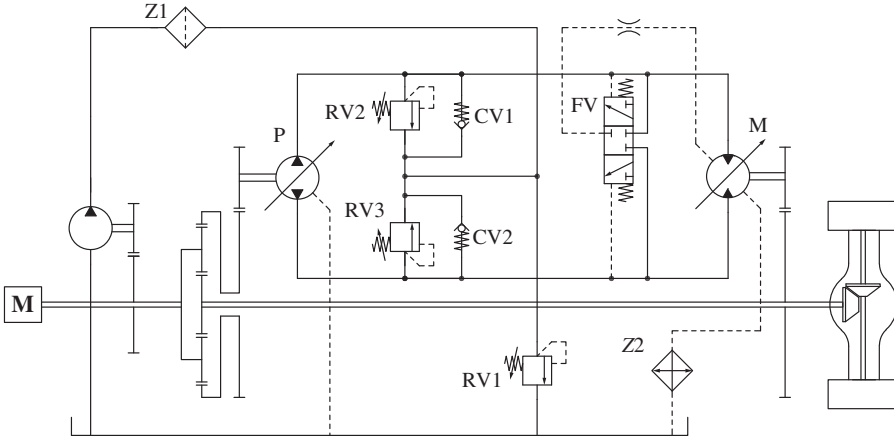
Figure 25.15 Detailed schematic for an output-coupled hydromechanical power-split transmission.

Analysis of an Output Coupled Hydromechanical Power Split Transmission

The simplified schematic for the output coupled hydromechanical PST is represented in Figure 25.16. PGT has the carrier gear set connected to the engine, while the sun, to the axle output gearbox; the ring gear set is connected to the primary unit of the HT. The speed ratio between the engine and the primary unit of the HT is no longer constant, as it was for a traditional HT. However, the speed of the secondary unit of the HT is in constant ratio with the vehicle speed. In normal operation, the power from the engine is split at the PGT, and the summing point is at the gearbox connected with the output shaft of the transmission. However, the power summing and power splitting function can also be reversed for certain operating conditions.

The overall hydromechanical transmission behaves as a CVT. In fact, with reference to Figure 25.15, it is possible to analyze the behavior of the PGT, in which:

- ω_S is the vehicle speed (assumed as an independent variable for the study)
- ω_C is the engine speed (assumed as an independent variable for the study)
- ω_R is determined by the Willis Eq. (25.2)
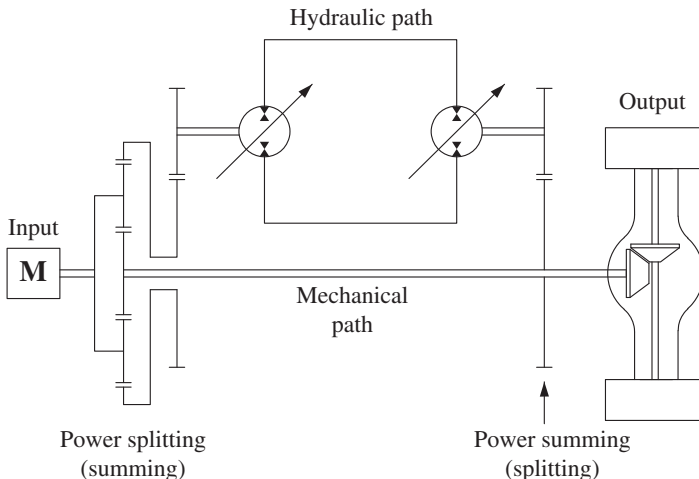
Figure 25.16 Simplified schematic for an output-coupled hydromechanical power-split transmission.
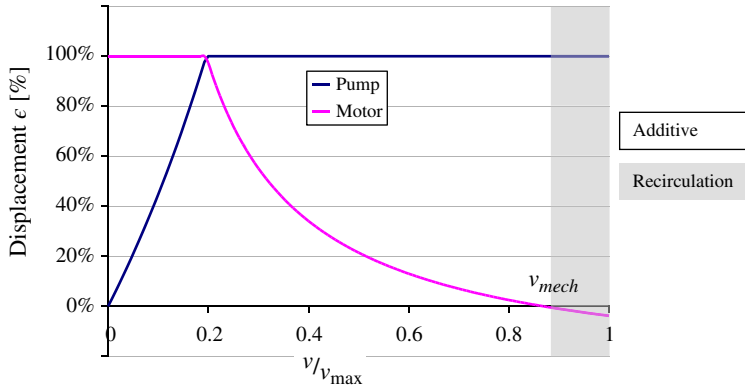
Figure 25.17 Sequential control of the primary and secondary units for an output-coupled power-split transmission.

Before the detailed analysis of the CVT operation, it is important to make some comments on the setting of the hydrostatic units. The primary and secondary displacement control logic is based on the vehicle speed and follows a path similar to the sequential control described above for the PVMV transmission (previous chapter). This is summarized with the plot in Figure 25.17. The reader should know that the pump speed decreases with the vehicle velocity until stopping at a velocity equal to a characteristic value v_{mech}. At this point the pump is at full stroke while the motor at null. Details on the primary unit speed will be clarified as follows.

At this point, four modes of the transmission can be analyzed as a function of the vehicle speed:

Case 1. Zero vehicle speed (fully hydraulic). When the vehicle speed approaches zero ($\omega_S = 0$), from Eq. (25.6) one can write

$$P_R = \frac{-\tau_0 P_C}{\tau_0 - \dfrac{\omega_S}{\omega_R}} = -P_C \tag{25.7}$$

which means that all the power is transferred hydrostatically. This situation can be shown in Figure 25.18. The pump is at zero displacement, while the motor is at maximum displacement.
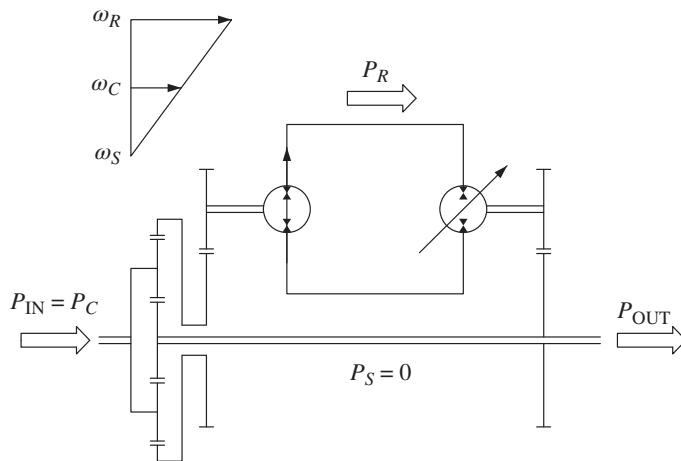
Figure 25.18 Behavior of the output-coupled hydromechanical power-split transmission at zero vehicle speed.

Case 2. Moderate vehicle speed (additive mode). As the vehicle speed increases (increasing ω_S), the velocity of the ring gear set (connected to the primary unit) decreases. This means that, according to Eq. (25.6), the percentage of power going through the hydraulic path decreases. Simultaneously, the power transferred to the more efficient mechanical path is increasing. This can be graphically represented with the circuit in Figure 25.19, which also shows the pump and motor setting (pump at partial displacement, motor at full displacement). This state for the transmission can be referred as power additive mode. The power from the mechanical path and from the HT are summed at the output shaft of the transmission, and they are split at the PGT.
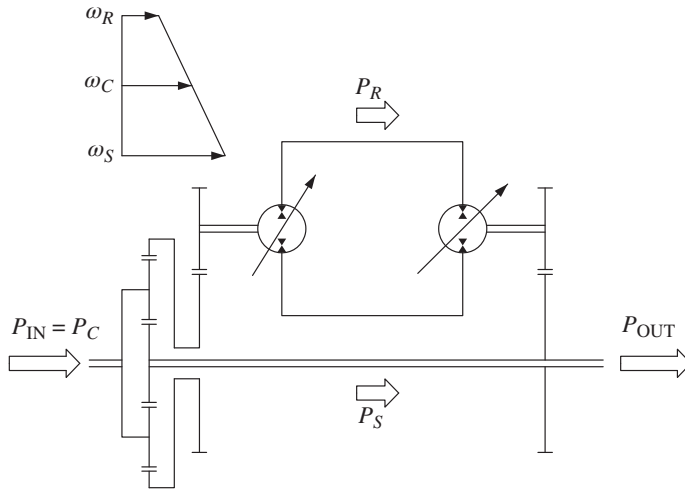
Figure 25.19 Behavior of the output-coupled hydromechanical power-split transmission at moderate vehicle velocities.

As the vehicle speeds up, the pump speed decreases (and with it, also the hydraulic power P_R), eventually reaching zero at the characteristic value v_{mech}. This is condition is also known as the "full mechanical point."

Case 3. Full mechanical point. In this condition, the angular velocity of the ring gear set is null ($\omega_R = 0$), and according to the Willis Eq. (25.2), the sun gear set velocity is related to the carrier angular velocity:

$$\omega_S = (1 - \tau_0)\, \omega_C \tag{25.8}$$

The whole power is transmitted mechanically, according to Eq. (25.6). This condition is achieved by setting the displacement of the secondary unit (the motor of the HT) equal to zero. This is also represented with the schematic in Figure 25.20.

It is important to remark that the full mechanical point is related to a particular engine speed. By varying the engine speed, the full mechanical point becomes a full mechanical range.

Case 4. High vehicle velocities (power recirculation). Beyond the full mechanical point ($v > v_{mech}$), the angular velocity of the ring gearset (connected to the pump) becomes negative. In addition, the sun gear set angular velocity increases, as represented in Figure 25.21. To maintain the HT correct operation, the secondary unit has to be set to a slightly negative displacement, thus working in pumping mode. According to Eq. (25.6), the power through the ring gear set
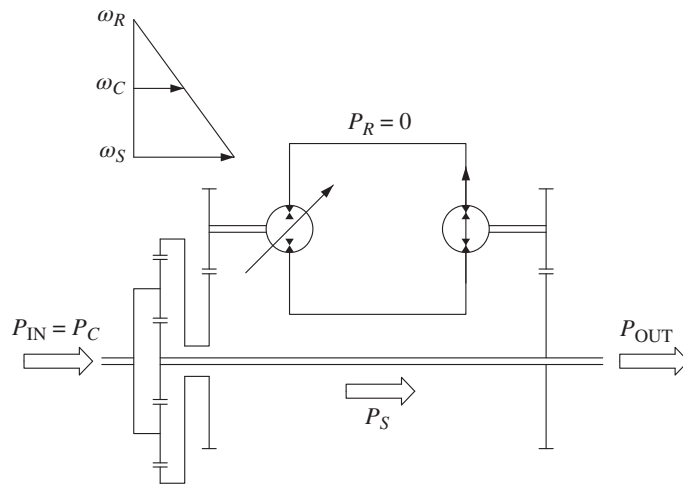
Figure 25.20 Behavior of the output-coupled hydromechanical power-split transmission at the full mechanical point.

further increases (hydrostatic path), as well as the power through the sun gear set (mechanical path). The transmission attains **a power recirculation mode**, which is characterized by lower efficiencies. The power between the hydraulic path and the mechanical path is split at the output shaft gear, and it is summed at the PGT.
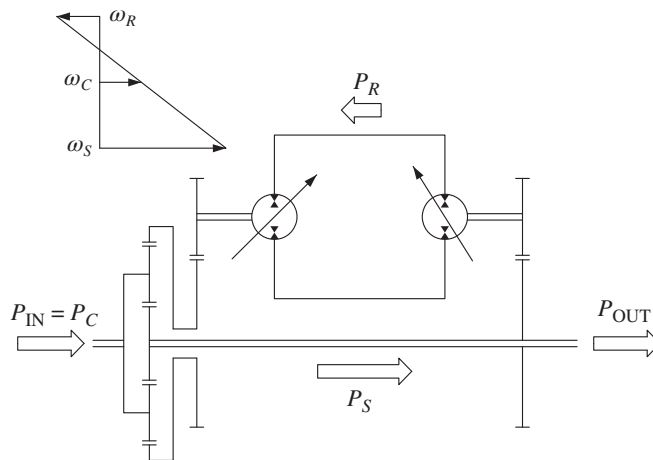
Figure 25.21 Behavior of the output-coupled hydromechanical power-split transmission above the full mechanical point.

A summary of the power flow within the output coupled hydromechanical transmission for the different operating modes is graphically presented in Figure 25.22.

Figure 25.23 shows a qualitative comparison between an optimally sized HT with respect to two optimally sized hydromechanical power-split transmissions. The power-split transmission enables
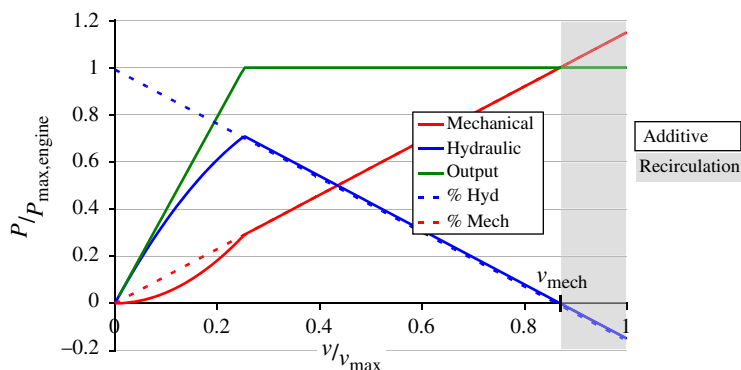
Figure 25.22 Summary of the operation modes for an output-coupled hydromechanical power-split transmission.

a significantly higher efficiency, especially in the higher speed range, because, in these conditions, most of the power is transferred to the vehicle axle through the more efficient mechanical path. Figure 25.23 also shows the effect of different choices for the full mechanical point of the transmission, which implies different geometries for the PGT gearsets.
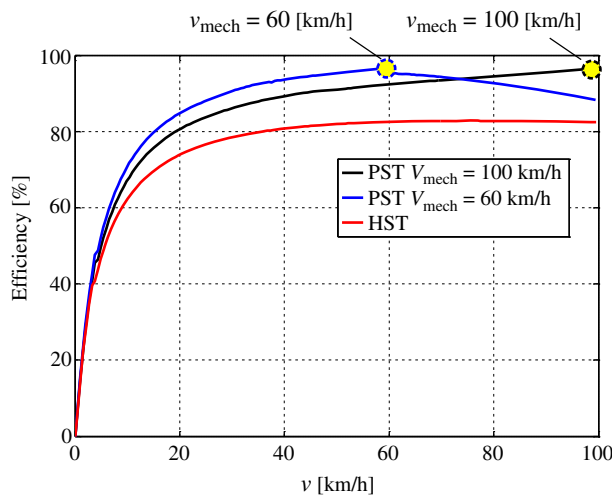
Figure 25.23 Qualitative transmission efficiencies for an HT and for an output-coupled hydromechanical power-split transmission (full mechanical point above 100 km/h). Source: Mikeska and Ivantysynova [14].

Analysis of an Input-coupled Hydromechanical Power-split Transmission

The input-coupled hydromechanical PST has operating features opposite to the output coupled, described in section Analysis of an Output Coupled Hydromechanical Power Split Transmission. The simplified schematic of the system is shown in Figure 25.24. The speed of the primary unit of the HT has now a fixed ratio to the engine speed. However, the speed ratio between the secondary unit and the vehicle speed is no longer constant. In normal operation, the power is split at the gearbox connecting the primary unit, while the PGT accomplishes the power summing function. For certain vehicle velocities, however, these power functions can be reversed.
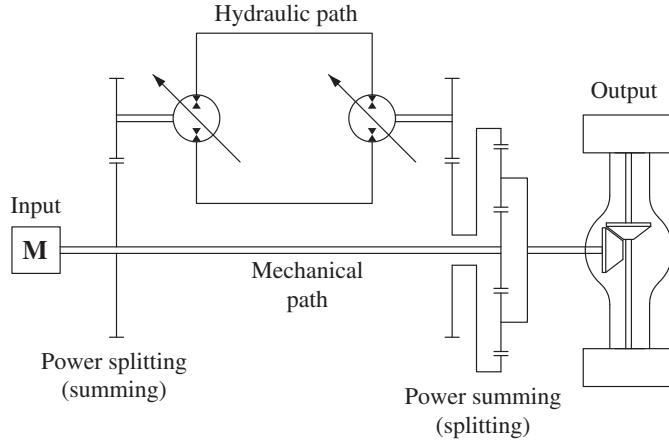
Figure 25.24 Simplified schematic for an input-coupled hydromechanical power-split transmission.

For the input coupled hydromechanical PST the PGT connects the shafts so that

- ω_S is the engine speed (which is the independent variable for the study)
- ω_C is the vehicle speed (which is the independent variable for the study)
- ω_R is determined by the Willis Eq. (25.2).

In this case the control logic for the setting of the hydrostatic units follows a different path, described in Figure 25.25. Both units start from the -100% position (over center). With the vehicle speeding up, the pump is first increased up to 100%. The full displacement condition for both units is called "saturation point." After reaching the saturation point, the motor displacement is also varied sequentially, to further increase the vehicle speed.

The operational modes of the transmission can be again analyzed as a function of the vehicle speed.

Case 1. Zero vehicle speed (full power recirculation). When the vehicle speed approaches zero ($\omega_C = 0$), from the Willis Eq. (25.2), the sun angular velocity is

$$\omega_S = \tau_0 \omega_R \tag{25.9}$$

Therefore, from the power relations of Eq. (25.6):

$$P_R = \omega_C T_C = -\omega_C \tau_0 T_S = -P_S \tag{25.10}$$
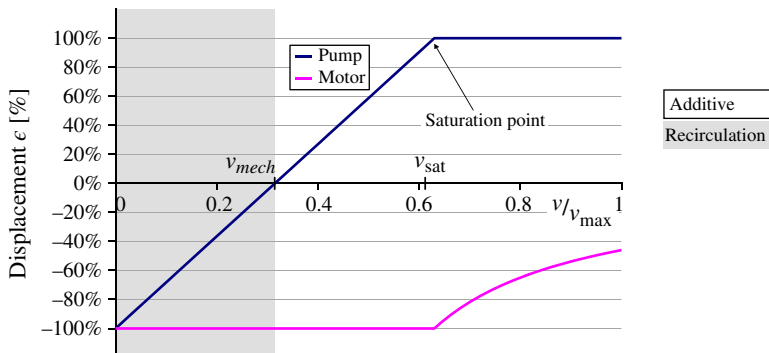
Figure 25.25 Sequential control for the HT for an input-coupled power-split transmission.
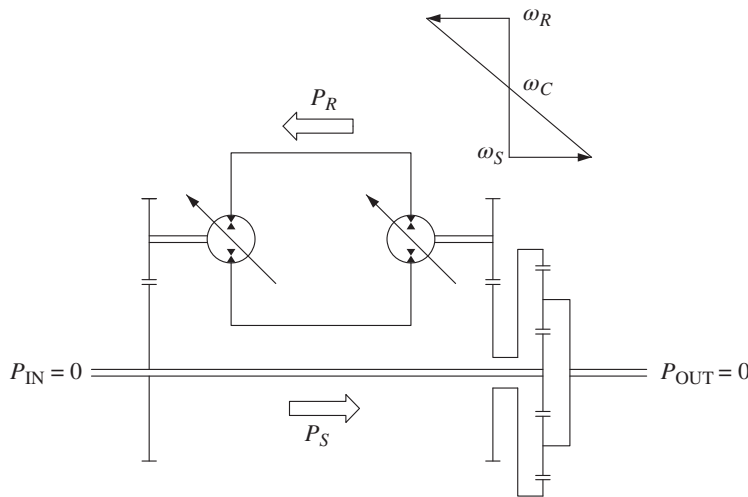
Figure 25.26 Behavior of the input-coupled hydromechanical power-split transmission at zero vehicle speed.

which means that at zero vehicle velocity, there is complete power recirculation, the engine provides only a very small amount of power, to cover losses. The recirculated power can be considerably high, compared to the power provided by the engine. This is shown by the arrows in Figure 25.26 (pump at −100% displacement and motor at 100% displacement).

Case 2. Moderate vehicle speed (power recirculation mode). As the velocity of the vehicle increases, ω_R decreases, as it is shown by the graphical representation of the Willis Eq. (25.2) in Figure 25.27. The magnitude of the ratio P_R/P_S decreases with the decrease of ω_R:

$$P_R = \omega_R T_R = -\omega_R \tau_0 T_S = -\omega_R \tau_0 \frac{P_S}{\omega_S} \tag{25.11}$$
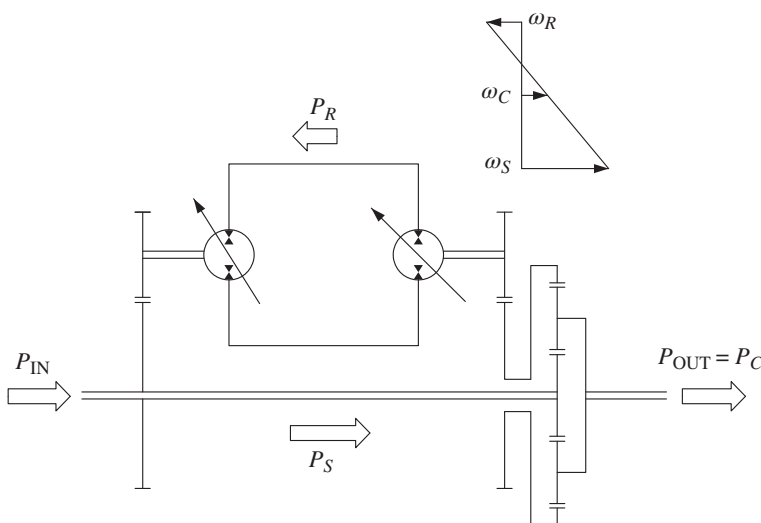
Figure 25.27 Behavior of the input-coupled hydromechanical power-split transmission at moderate vehicle speed.
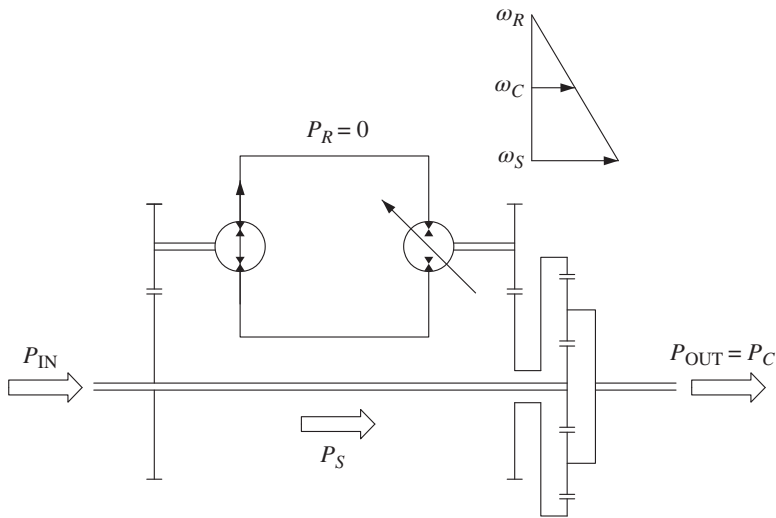
Figure 25.28 Behavior of the input-coupled hydromechanical power-split transmission at full mechanical mode.

The power from the mechanical path is recirculated through the HT. This amount of recirculated power decreases as the vehicle speed increases. The pump is at partial (negative) displacement, while the motor at full displacement.

Case 3. Full mechanical point. The angular velocity of the ring gear set, ω_R, eventually becomes zero as the vehicle speed further increases to a condition v_{mech}. This corresponds to reaching the condition of **full mechanical mode**. The magnitude of P_R reaches zero, and all the power to the output shaft is transferred though the mechanical path. Physically, this is achieved by setting the displacement of the primary unit of the HT to zero, as shown in Figure 25.28. The secondary unit is still at full displacement.
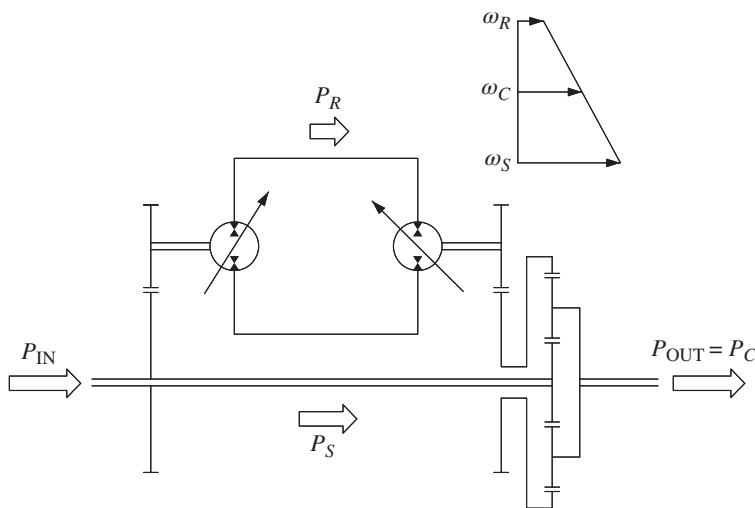
Figure 25.29 Behavior of the input-coupled hydromechanical power-split transmission at high vehicle speed.

Case 4. High vehicle speed (power additive mode). For velocities above v_{mech}, the ring gear set (connected to the pump) changes direction of rotation. Its power becomes power input to the transmission. For this reason, the primary unit displacement should be set as opposite with respect to the previous cases (overcenter unit). In the power formulas of Eq. (25.6), the ratio P_R/P_C increases, and at the limit of infinite velocity:

$$\lim_{\omega_R \to \infty} \frac{P_R}{P_C} = \lim_{\omega_R \to \infty} \frac{-\tau_0}{\tau_0 - \dfrac{\omega_S}{\omega_R}} = -1 \qquad (25.12)$$

Similarly, as the ratio P_S/P_C decreases,

$$\lim_{\omega_R \to \infty} \frac{P_S}{P_C} = \lim_{\omega_R \to \infty} \frac{1}{\tau_0 \dfrac{\omega_R}{\omega_S} - 1} = 0 \qquad (25.13)$$

This means that at high vehicle velocities more power tends to be transferred hydraulically. Therefore, the overall efficiency transmission tends to drop as the vehicle velocity exceeds v_{mech}. As the primary unit reaches 100% displacement, the saturation velocity point is reached. In this condition, the maximum engine power is also reached. The vehicle velocity can be further increased by lowering the displacement of the secondary unit.

The overall operation of the input coupled hydromechanical PST can be summarized with the plot in Figure 25.30. The figure also shows the setting for the instantaneous displacement of both primary and secondary units.

In the input coupled PST, one can adopt a PVMF layout using a fixed displacement motor and an over-center pump. This will still allow the vehicle velocity regulation (only below the saturation point) with a simpler architecture.

It is then understandable how the output coupled PST tends to have higher transmission efficiencies, although it requires a more sophisticated control strategy. To give a relative comparison between the two solutions, Figure 25.31 shows the efficiency trends for the two options of input-coupled and output-coupled PSTs.
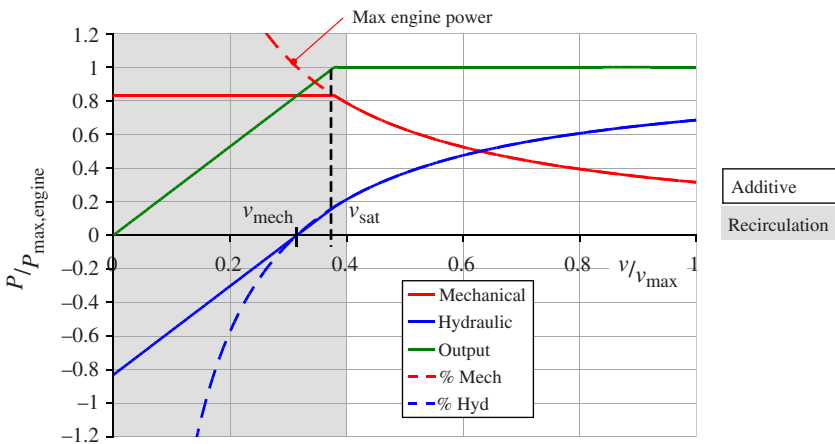
Figure 25.30 Summary of the operation modes for an input-coupled hydromechanical power-split transmission.
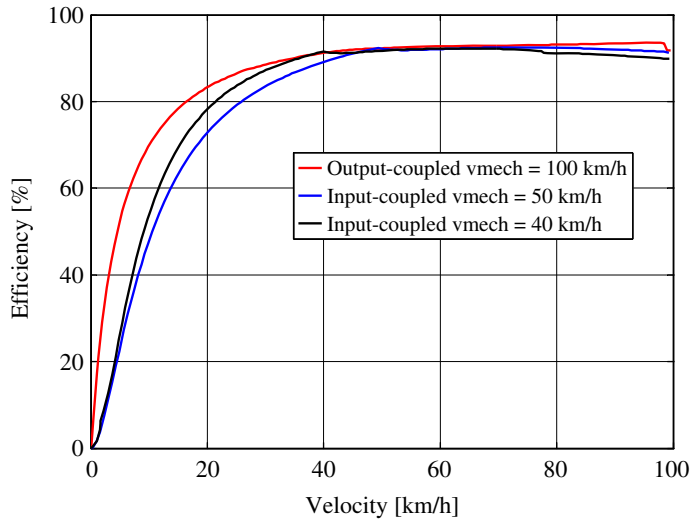
Figure 25.31 Qualitative transmission efficiencies for both input-coupled and output-coupled hydrome-chanical power-split transmissions. Source: From Mikeska and Ivantysynova [14]. Copyright 2002, Professional Engineering.

25.4 Hybrid Transmissions

The term "hybrid" is often used in different contexts. When referring to a transmission system, the denomination of a hybrid vehicle implies "any vehicle in which propulsion energy is available from at least two types of *energy sources* on board the vehicle" [15].

"Energy source" indicates any device capable of storing and release energy. This energy can be chemical (a battery or a fuel tank), electrical (a capacitor), mechanical (flywheel), or hydraulic (accumulator). During the operation of the vehicle, the quantity of energy stored within the energy source at a certain time is usually referred as *state of charge*. The state of charge of an accumulator is given by the instantaneous pressure; however, for a flywheel, it is the angular velocity.

According to the definition of hybrid given above, possible examples of hybrid vehicles are:

- A car with a combustion engine, a battery, and an electric motor
- A car with a combustion engine, a capacitor, and an electric motor
- A car with a combustion engine, a hydraulic accumulator, and a hydraulic motor
- A human powered bicycle with a battery and electric motor assist
- A human powered bicycle with a hydraulic accumulator and a hydraulic motor

However, the following examples are not hybrid vehicles:

- A car with a combustion engine
- A pure plug-in electric car
- A twin-engine vehicle
- A tandem bicycle

To further classify the different architectures for hybrid vehicles, it is convenient to further define what is an *energy converter*. An energy converter is a device that converts energy from one form to

another. In this sense, the combustion engine is an energy converter (it releases chemical energy to convert it into mechanical energy). Hydraulic pumps and motors are also energy converters.

Hybrid transmissions that found commercial applications are electric hybrids (that use combustion engines and electric motors) as well as hydraulic hybrids (that use the combustion engines and HTs). Hydraulic hybrids are currently a controversial topic within the fluid power industry. Research and development on this type of transmissions started in the late 1970s after the oil crisis and yielded to units commercially available in the late 1990s and early 2000s. Thanks to the integration of electronic controls, they were able to reach very high fuel efficiency improvements for applications like city buses or trucks. However, economic factors (like the drop in the oil price after 2008 as well as the development of alternative fuels like natural gas) did not play in favor of this technology and the adoption rate for hydraulic hybrids turned out to be very low. In addition, the rise in popularity of electric hybrids determined a further disincentive toward the adoption of hydraulic hybrids. The hydraulic hybrid technology can be still be considered as one of the most efficient transmission technologies, but it will require for further macro-economic catalysts (such as a significant raise in the oil price, or a shortage of materials for batteries) to become again attractive.

25.4.1   Series Hybrids

In a series hybrid vehicle, all the propulsion power comes from one energy converter. The energy converters and the energy sources are in a series layout. The general schematic is shown in Figure 25.32. Only the energy converter "2" provides the propulsion power.

Considering the case of hydraulic units, the series hydraulic hybrid can be represented with the schematics in Figure 25.33 and Figure 25.34. The simplified schematic (Figure 25.33) indicates how the hydraulic units are used as intermediate energy converters between the hydraulic accumulator. It is important to observe that the secondary hydraulic unit (the motor) needs to be variable displacement to implement a proper regulation. For a given state of charge of the accumulator (i.e. its pressure), the only way to vary the torque output is by varying the displacement of the secondary unit (secondary control).

Figure 25.34 shows one possible realistic implementation of a series hydraulic hybrid vehicle.

Series hydraulic hybrids have the advantage of an easy layout arrangement. Moreover, given that it is the engine decoupled from the wheel axle, it has a wide freedom in controlling the engine operating point. However, series hydraulic hybrids also have important disadvantages. First, the hydrostatic units realizing the CVT reach optimal efficiency only in a narrow operating range. Therefore, it is difficult to obtain high transmission efficiency with such system. In addition, the
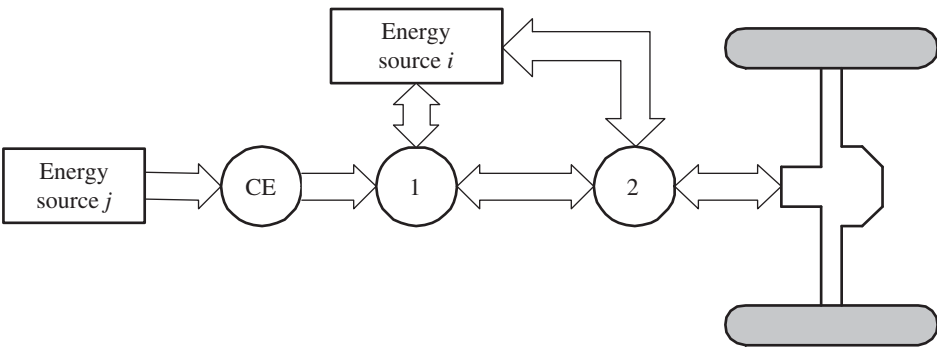
Figure 25.32   Series hybrid vehicle. 1 and 2 indicate energy converters.
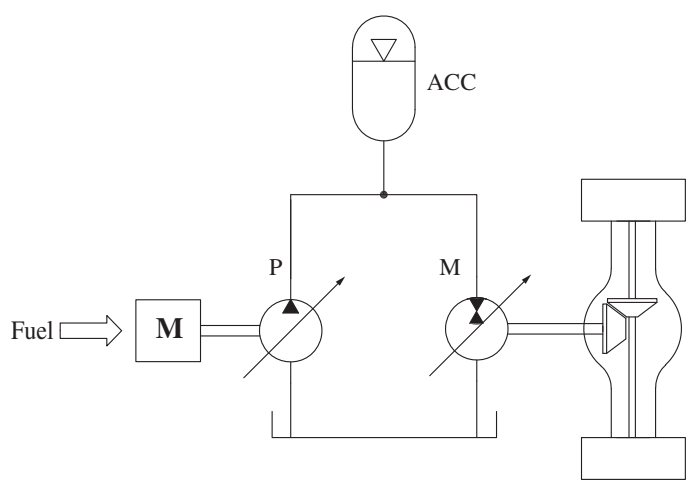
Figure 25.33 Series hydraulic hybrid (simplified schematic).

state of charge of the accumulator (i.e. its pressure) limits the maximum torque and power output of the system. This means that the accumulator pressure always needs to be adjusted to meet the torque requirement of the application.

Hydraulic series hybrid found a relative success in commercial applications. A well-known example is the UPS hydraulic hybrid vehicle commercialized in the early year 2000s, as mentioned in [16] and [17]. A version for city buses was also tested by Parker Hannifin with Altair Product design and the US Federal Transit Administration, reaching a 109% increase in fuel economy over conventional city buses [18]. The same work also reports a 29% increase in fuel economy with respect to the most efficient electric hybrid bus available at the time of the test campaign.
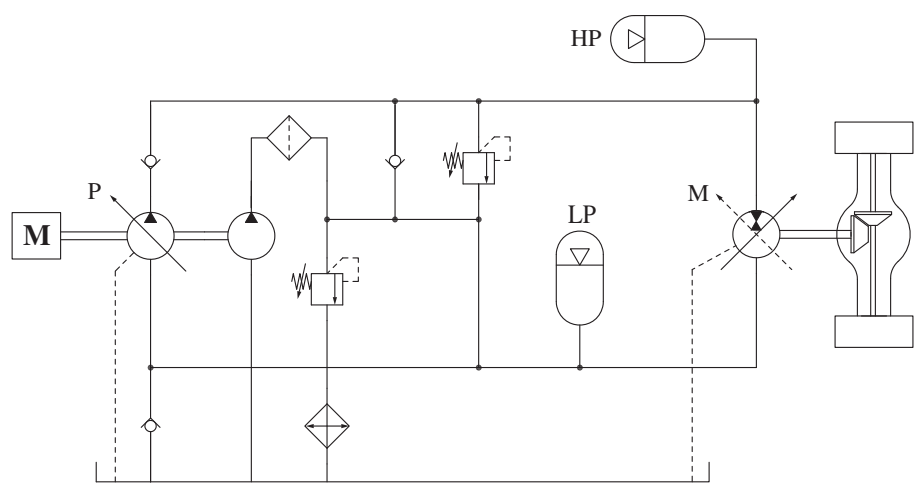
Figure 25.34 Series hydraulic hybrid (realistic circuit).

25.4.2 Parallel Hybrids

In a parallel hybrid vehicle, the propulsion power comes simultaneously from one or more energy converters. The energy converters and the energy sources have a parallel layout configuration, as
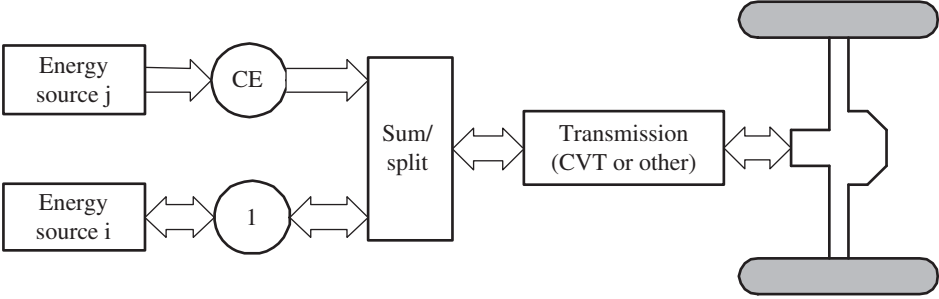
Figure 25.35 Parallel hybrid vehicle.

shown in the general schematic in Figure 25.35, which shows the combustion engine operating in parallel with another energy source/converter.

The simplified schematic showing the implementation of a parallel hydraulic hybrid transmission is given in Figure 25.36. The output torque is given by the sum of the output torque of the hydraulic unit (controlled by its instantaneous displacement) and the torque output from the combustion engine (controlled by the engine throttle). The hydraulic unit can operate in both pumping mode and motoring mode. This means that the accumulator can be changed either by the engine (for example, during instances of excess engine power) or by the vehicle (i.e. breaking instances). A more realistic implementation in shown in Figure 25.37, which shows the use of a torque converter and a discrete variable gearbox sharing the same shaft of the hydraulic unit.

The parallel hybrid configuration has the advantage of offering a direct, highly efficient, mechanical path between the engine and the wheel axle, when a CVT is not needed. It also offers the potential of engine downsizing, since the hydraulic accumulator can compensate for peaks of energy request. However, the drawback is a limited potential for engine management. In fact, the engine is typically directly coupled to the wheels through a non-CVT transmission.

The parallel hydraulic hybrid configuration found some commercial application. An example is the Ford hydraulic launch assist system, simplified with the schematic in Figure 25.38. Note that this system does not implement a CVT transmission. The parallel hybrid configuration was
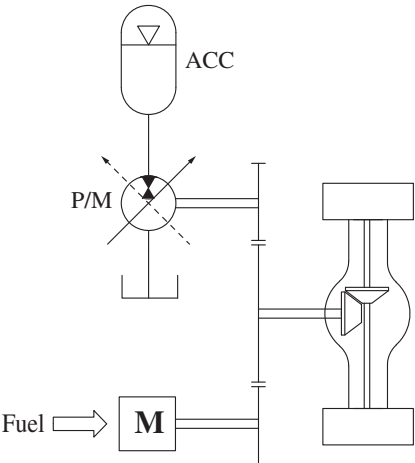
Figure 25.36 Parallel hydraulic hybrid (simplified schematic).
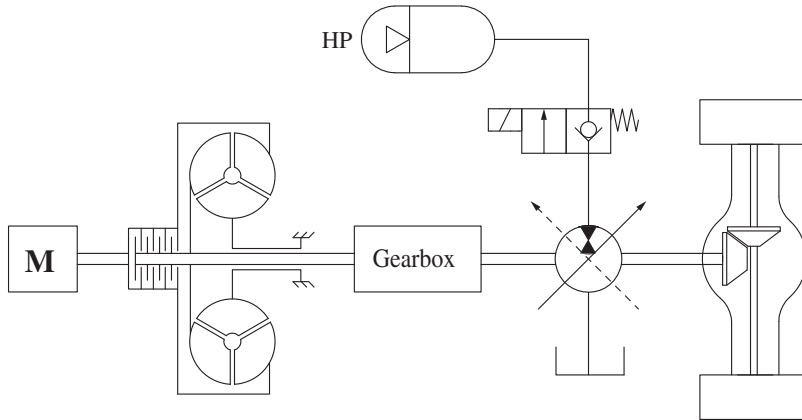
Figure 25.37 Parallel hydraulic hybrid (realistic schematic).

also used by Honda in the Insight model [20]. In this case the transmission is electric hybrid, not hydraulic hybrid.

25.4.3 Series-parallel Hybrids (or Power-split Hybrids)

A hybrid vehicle that implements both the series and the parallel configurations is called a series-parallel hybrid. The conceptual schematic of the transmission system is shown in Figure 25.39, where basically a PST includes an additional energy source (indicated with *i*, in Figure 25.39). For this reason, this configuration can be referred as **power split hybrid**.

An example of implementation of a hydraulic series-parallel hybrid is shown in Figure 25.40. The HT is open circuit and both units are variable displacement. The power output of the transmission comes from both the secondary unit of the HT and the engine. This can be shown by observing that $P_{out} = T_{out}\omega_{out}$ so that the power output can be discussed from an expression for the torque output, T_{out}. The torque output of the transmission can be found by elaborating the torque expression for the PGT, Eq. (25.4):

$$T_{out} = T_S + \frac{T_2}{\tau_2} \tag{25.14}$$

where T_2 is the torque of the secondary unit of the HT and τ_2 is the transmission ratio at the output gearbox.
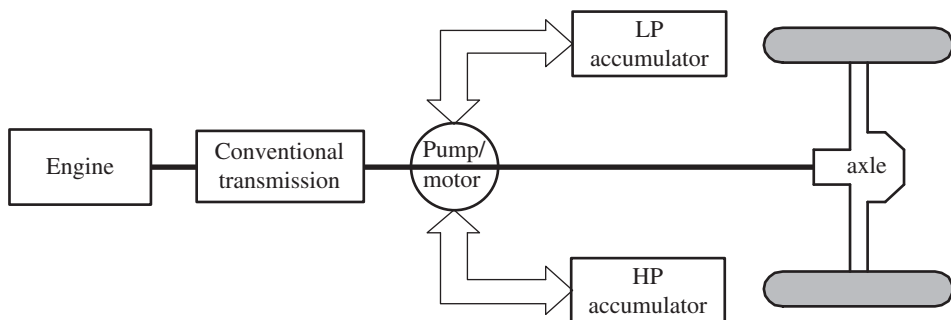
Figure 25.38 Simplified schematic of the Ford hydraulic launch assist system. Source: Modified from Kepner 2002 [19].
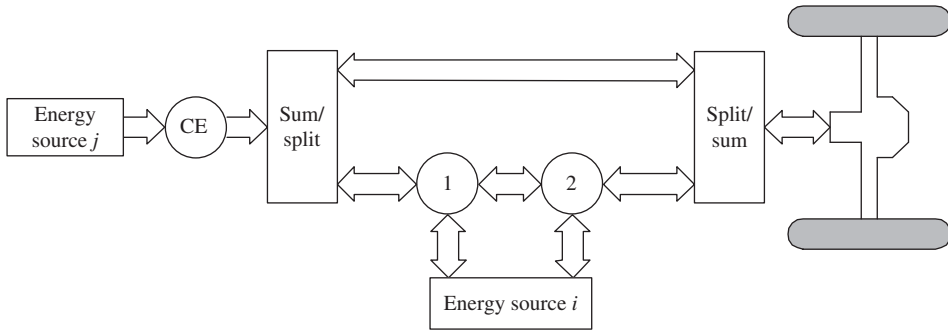
Figure 25.39 Series-parallel hybrid vehicle.

By using the basic relations for the hydrostatic pumps and motors, the previous Eq. (25.14) becomes

$$T_{\text{out}} = T_S + \frac{\epsilon_2 V_2 \Delta p}{\tau_2} \tag{25.15}$$

where Δp represent the state of charge of the accumulator.

Considering the geometrical ratio of the PGT, τ_0,

$$T_{\text{out}} = \frac{T_R}{\tau_0} + \frac{\epsilon_2 V_2 \Delta p}{\tau_2} \tag{25.16}$$

The torque loading at the ring is given by the primary unit of the HT; therefore,

$$T_{\text{out}} = \frac{\epsilon_1 V_1 \Delta p \tau_1}{\tau_0} + \frac{\epsilon_2 V_2 \Delta p}{\tau_2} \tag{25.17}$$

The last expression points out how the regulation of the instantaneous displacement of both the hydrostatic units, ϵ_1 and ϵ_2, determines respectively the torque (and therefore the power) requested at the engine (through ϵ_1) and at the hydraulic accumulator (through ϵ_2). More clearly, the power at the secondary unit is

$$P_2 = \omega_2 T_2 = \omega_2 \epsilon_2 V_2 \Delta p \tag{25.18}$$
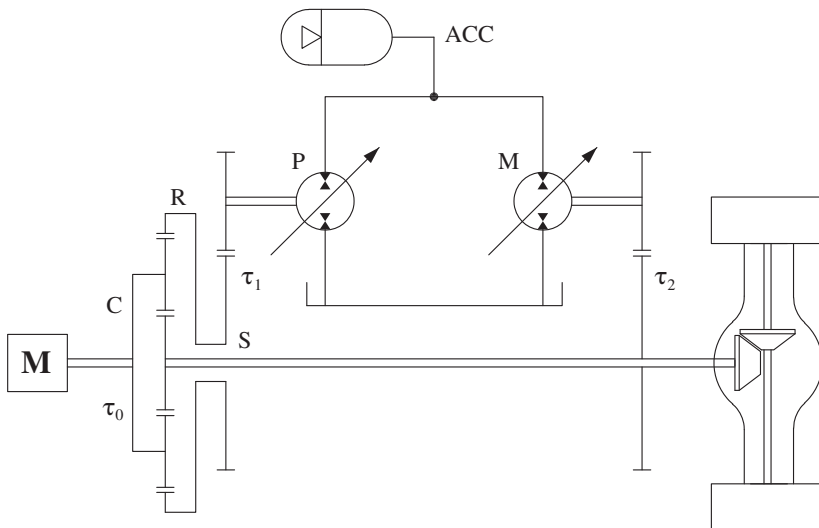
Figure 25.40 Hydraulic power-split hybrid system (output coupled).

while the power at the engine is

$$P_{CE} = \omega_{CE} T_{CE} = \omega_{CE} T_C = \omega_{CE} \left(\frac{1}{\tau_0} - 1 \right) T_R = \omega_{CE} \left(\frac{1}{\tau_0} - 1 \right) \varepsilon_1 V_1 \Delta p \tau_1 \tag{25.19}$$

Equations (25.18) and (25.19) highlight not only how the overall power comes from two separate sources, the engine and the accumulator (being a feature of the parallel configuration) but also how the overall power transmitted by the transmission is limited by the state of charge of the accumulator (which is a feature of the series configuration).

The primary unit of the HT has a very important role since it determines the power discharged by both the accumulator and the engine. In fact, for the accumulator,

$$P_{acc} = \Delta p Q_a = \Delta p \left(Q_2 - Q_1 \right) = \Delta p \left(\varepsilon_2 V_2 \omega_2 - \varepsilon_1 V_1 \omega_1 \right) \tag{25.20}$$

while, for the engine, the relationship with ε_1 was already highlighted in Eq. (25.19).

In general, the hybrid power split offers the advantage of freedom in the engine management (like in the series hybrid). This also allows it to transmit power through the highly efficient mechanical path, like in the parallel hybrid. The drawback of this solution is mainly due to the complexity and the overall cost. In fact, at least three energy converters (in Figure 25.40 with the engine and the two hydraulic units of the HT) and the PGT are needed to implement such configuration.

Notwithstanding the cost of the solution, the high energy efficiency advantage of the power split hybrid transmission made this solution particularly successful in the automotive market, but with the electric implementation. In particular the output-coupled transmission has been used by several passenger cars such as Toyota Prius, Toyota Camry, and Ford Escape. The electric hybrid compound type, with two PGTs, has been used in General Motors buses. In 2015, the PSA Peugeot-Citroen tested their concept series hydraulic hybrid passenger car, with the marketing name "Hybrid Air," and declared fuel economy improvement of 45% in city driving over the conventional mechanical transmission system [21].

25.5 Sizing Hydrostatic Transmissions for Propel Applications

This section presents a method for sizing a basic HT. The case of reference for this section is the propulsion of a vehicle. However, this procedure can also be applied for other cases where the requested torque of the application is given.

Sizing a HT for a propel application requires two things: first the most appropriate theoretical layout, among the ones described in the previous chapter. Then the displacements of both the primary and secondary units. Additional complexity is added by the fact that the designer can change the transmission ratios at the wheels, at the axle, or at the pump, if driven through a gearbox or a PTO.

Although the sizing of a HT is a commonly difficult task in hydraulics, a universally recognized sizing method does not exist. Several sizing procedures can be found in the literature. Among these, the authors decided to follow and expand the one suggested by Zarotti [22], which is broad and methodical. This procedure is valid for both open circuit and closed circuit HTs, and it is developed for the case of vehicle propulsion. With proper considerations, the method could also be extended to other applications of HTs.

The method is iterative because the designer, during the sizing process, must make a number of assumptions, like the efficiency of the units (when they are still unknown) or the maximum working pressure. At the end of the process, these assumptions need to be verified, and eventually, the sizing needs to be reviewed.

The problem starts with data that should be known. In a propulsion sizing problem, these are usually:

- vehicle mass (M) and maximum pull force (F_D)
- wheel rolling radius (R_R) and number of hydraulic drive motors (z_M)
- maximum slope (θ) the vehicle needs to overcome
- maximum speed of the vehicle on flat ground (v_{max})
- maximum vehicle acceleration ($\dot{v}_{max}$)
- type of surface on which the vehicle runs
- prime mover speed (n_E) and power (P_E)

Once the designer knows the data listed above, the sizing procedure adopts the following steps.

25.5.1 Step 1: Maximum Tractive Effort Calculation

The first step consists in finding what is the maximum tractive effort: i.e. the maximum force the vehicle needs to develop to meet the requirements expressed by the data previously listed.

The evaluation of the maximum tractive effort depends on the specific requirements of the application. The designer must ensure to include in the maximum tractive effort the most demanding condition for the HT. For the case of vehicle propulsion, it is common to include in the tractive effort a combination of vehicle weight, acceleration, pulling force and rolling resistance. With reference to Figure 25.41, F_T equals

$$F_T = M\left(g \cdot \sin\,\theta + \dot{v}_{max}\right) + F_D + F_R \tag{25.21}$$

The term F_R is often referred as "rolling resistance" and it is caused by the friction between the wheels and the ground. The value of F_R is calculated as follows:

$$F_R = Mg \cdot \cos\,\theta \cdot f_R \tag{25.22}$$

The parameter f_R represents the rolling resistance factor, which can be selected from Table 25.1, depending on the type of surface the vehicle can travel on.

Usually vehicles driven by HTs do not travel at high speeds (approximately greater than 50 km/h); therefore, the effect of the air drag is neglected in the force balance of Eq. (25.21).

Once F_T is determined, the torque on the driving wheels T_W can be calculated as follows:

$$T_W = F_T \cdot R_R \tag{25.23}$$
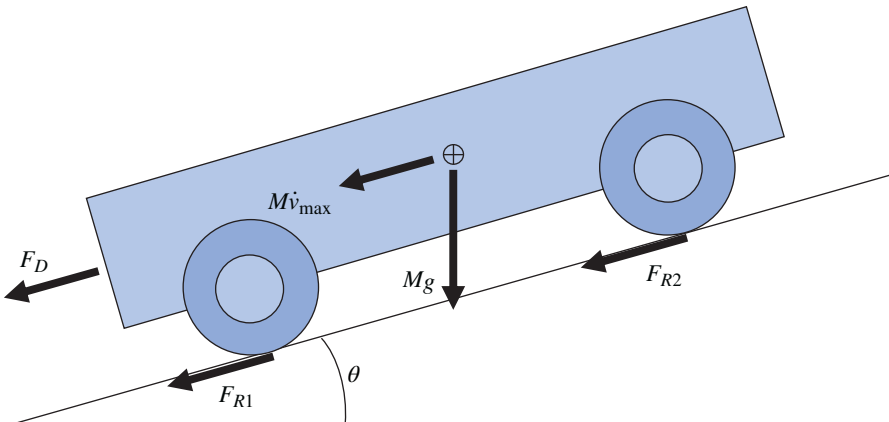
Figure 25.41 Force balance on the vehicle for calculating the tractive effort.

Table 25.1 Non-dimensional values for the rolling resistance factor.

Surface	Vehicle type	
	Wheeled	**Tracked**
Concrete	0.01–0.02	0.03–0.04
Asphalt	0.012–0.022	0.03–0.04
Paved road	0.015–0.037	0.035–0.045
Gravel road	0.025–0.04	0.035–0.05
Compressed soil	0.04–0.075	0.04–0.06
Soft soil	0.05–0.09	0.06–0.08
Sand and gravel mix	0.1–0.14	0.05–0.09

Source: Zarotti [22].

25.5.2 Step 2: Fixed or Variable Displacement Motor Selection

The layout of a HT for propulsion applications always includes a variable displacement pump (PV). The selection of the type of motor architecture (fixed, motor, fixed displacement [MF], variable, motor, variable displacement [MV], or dual, M2, displacement) can be performed by calculating the torque conversion factor of the HT, torque conversion factor (TCF):

$$\text{TCF} = \frac{v_{\max} \cdot F_T}{P_E} \tag{25.24}$$

The value of TCF represents the ratio between the corner power of the hydraulic transmission (a fictitious value given by the maximum force at the maximum required vehicle velocity) and the power of the prime mover. A graphical representation of the two power values is provided in Figure 25.42. A useful rule of thumb states that

- if TCF < 1.5 the HT can be sized using fixed displacement motors.
- if TCF > 2, the designer should consider a variable displacement motor.

If the HT has a PVMF (variable pump fixed motor) layout, the transmission corner power represented in Figure 25.42 is an operating point that is potentially achievable by the system, if the prime mover were large enough to satisfy this condition. However, the maximum input power is usually lower than the HT corner power (i.e. TCF > 1); thus, the system is characterized by an area of operating points that are not achievable because of the existing limitations (*stall area*, highlighted in gray in Figure 25.42). If the system tried to operate in this area (high pump displacement under high pressure), the prime mover would stall because of the load torque exceeding its limit. In a
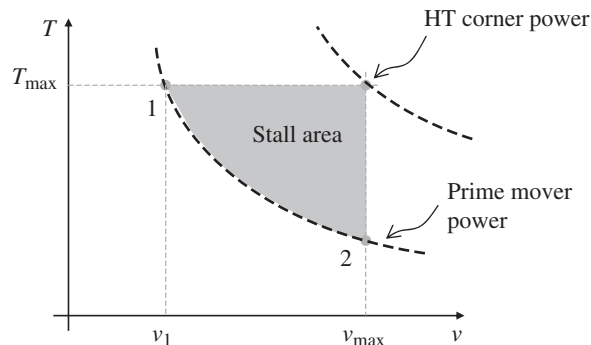
Figure 25.42 HT corner power and prime move power.

PVMF layout, the higher the value of TCF, the larger the stall area, and the installed pump power will significantly exceed the prime mover power[1].

For this reason, for higher values of TCF, the PVMF (primary variable, motor fixed) layout is not a viable solution for performance and cost reasons. Instead, a PVMV (primary variable, motor variable) or a PVM2 (primary variable, motor dual) layout allows to better match the vehicle's high speed requirements with the available prime mover (as shown in Figure 24.9 or 24.12) using smaller motors. When the motor has a variable displacement, the corner power of the HT is represented by the combination of maximum torque (motor at maximum displacement) and maximum speed (motor at minimum displacement). Therefore, this point of operation is not real but just a fictitious assumption. In general, the PVMV layout is preferred when the vehicle speed needs to be seamlessly adjusted over a wide range, as in an agricultural tractor. However, the PVM2 layout is acceptable for less demanding applications, such as compact construction vehicles, where the operator can select a turtle/rabbit drive mode.

25.5.3 Step 3: Sizing of the Motor (Secondary Unit)

This step of the sizing process can follow two different procedures depending on the gearbox ratio at the wheels (τ_M) being a given datum or a design parameter.

Given wheel ratio
If τ_M is provided together with the gearbox efficiency η_W (usually in the range 0.9–0.95), the torque on each hydraulic motor is calculated as follows:

$$T_M = \frac{T_W}{\eta_W \cdot \tau_M \cdot z_M} \tag{25.25}$$

To proceed with the sizing, the designer needs to make some assumptions which will need to be verified during or at the end of the sizing process:

- Volumetric ($\eta_{v,M}$) and hydromechanical efficiency ($\eta_{hm,M}$) of the hydraulic motor
- Volumetric ($\eta_{v,P}$) and hydromechanical efficiency ($\eta_{hm,P}$) of the hydraulic pump
- Maximum system pressure (p_{max})

These values can be initially selected based on the type of units that the designer intends to apply. An experienced designer can rapidly determine if the application is light-duty (maximum pressure usually lower than 250 bar, using piston pumps combined with gear or orbit motors), medium-duty (maximum pressure in the range of 250–350 bar, usually using piston units), or heavy-duty (maximum pressure higher than 350 bar, using piston pumps and motors). Based on this, a selection on a particular line of products can be made, to help with the preliminary assumptions on the energy efficiency parameters.

Based on these assumptions, the ideal motor maximum displacement can be calculated based on the torque requirement:

$$V_{M,i} = \frac{T_M}{\eta_{hm,M} \cdot \Delta p_{M,max}} \tag{25.26}$$

The reader should note that in Eq. (25.26) $\Delta p_{M,max}$ corresponds with the maximum pressure of the secondary unit for an open circuit HT. Instead, for a closed circuit HT, $\Delta p_{M,max}$ is the maximum differential pressure at the secondary unit considering the pressure value of the low pressure line. The motor displacement should be selected from the ones available to satisfy $V_M \geq V_{M,i}$.

Unknown wheel ratio
In this case the combined selection of the motor and gearbox transmission ratio can be optimized for maximizing the power density, leading to the most compact solution. The two equations useful

---

1 The reader should notice that, in this situation, the system will often operate at a combination of high pressure and low pump displacement, which is a usually characterized by very poor pump efficiency values.

for sizing motor and gearbox are the conditions of maximum pull and maximum velocity (points 1 and 2, respectively, in Figure 25.42):

$$T_W = V_{M,\max} \cdot \Delta p_{M,\max} \cdot \eta_{\mathrm{hm},M} \cdot z_M \cdot \tau_M \cdot \eta_W \tag{25.27}$$

and

$$\tau_M \cdot v_{\max} = R \cdot n_{M,\max} \tag{25.28}$$

The values $n_{M,\max}$ and $\Delta p_{M,\max}$ represent the maximum speed and pressure at which the motor can operate. The value of τ_M is still unknown, but the parameter can be eliminated (for the moment) by calculating the expression of τ_M from the second equation and substituting it into the other. In this way, the ideal motor displacement can be expressed as a function of known parameters:

$$V_{M,i} = \frac{v_{\max} \cdot T_W}{R \cdot n_{M,\max} \cdot \Delta p_{M,\max} \cdot z_M \cdot \eta_W\, \eta_{\mathrm{hm},M}} \tag{25.29}$$

The values of $n_{M,\max}$, $\Delta p_{M,\max}$ and $\eta_{\mathrm{hm},M}$ can be iteratively selected from the motor catalog. The designer starts with selecting three tentative values and obtains a result for the ideal motor displacement. At this point the value is re-calculated utilizing the correct values for the candidate displacement, selected from the catalogs of available products. The displacement selection $V_{M,\max}$ should be greater than the ideal value $V_{M,i}$.

If a variable displacement motor is being utilized (based on the TCF analysis), the value of $n_{M,\max}$ represents the maximum speed at minimum displacement, while $\Delta p_{M,\max}$ is the maximum continuous differential pressure at maximum displacement. Equation (25.29) somehow represents the ratio between the corner power of the vehicle (maximum speed and maximum pull) and the corner power of the hydraulic motor. For this reason, this process is also referred as the *corner power method*.

Once the motor displacement is selected, the gearbox ratio becomes

$$\tau_M \approx \frac{T_W}{V_{M,\max} \cdot \Delta p_{M,\max} \cdot z_M \cdot \eta_W \cdot \eta_{\mathrm{hm},M}} \tag{25.30}$$

25.5.4 Step 4: Sizing of the Pump (Primary Unit)

Once the motor size is determined, the speed of the secondary unit can be calculated for the conditions of maximum torque (n_{M1}) and maximum speed (n_{M2}):

$$n_{M1} = \frac{P_E \cdot \eta_{t,P} \cdot \eta_{t,M} \cdot \eta_W \cdot \tau_M}{F_T \cdot R_R \cdot z_M} \quad ; \quad n_{M2} = \frac{v_{\max} \cdot \tau_M}{R_R} \tag{25.31}$$

The pump needs to be able to provide enough flow to satisfy both conditions. If the motor is a fixed displacement type unit, the condition of maximum speed n_{M2} prevails; otherwise, if the motor has a variable displacement setup, the two conditions need to be compared to find the one requesting the highest flow.

Given pump-engine speed ratio

If the ratio between the pump shaft speed and the prime mover shaft speed (τ_P) is given, the pump displacement is calculated as follows:

$$V_{P,\max} = \frac{z_{M,\max}\left(n_{M1} \cdot V_{M,\max} ; n_{M2} \cdot V_{M,\min}\right)}{n_E \cdot \tau_P \cdot \eta_{v,M} \cdot \eta_{v,P}} \tag{25.32}$$

In Eq. (25.32), it is considered that a variable motor will operate at the minimum displacement at the maximum vehicle velocity, and at maximum displacement at the maximum torque condition. Obviously, if the HT uses a fixed displacement motor, Eq. (25.32) will use $V_{M,\min} = V_{M,\max} = V_M$. The actual pump will be selected to be as close as possible to size $V_{P,\max}$ resulting from the above Eq. (25.32).

Unknown pump ratio

If instead the ratio τ_P is unknown, the designer should size the HT to run the pump at the maximum allowable value of shaft speed, to optimize the power density. To achieve that, one can select the tentative ratio τ_P from the maximum allowable shaft speed of the pump:

$$\tau_P \approx \frac{n_{P,\max}}{n_E} \tag{25.33}$$

The value of the pump displacement is then given by Eq. (25.32).

The value of $n_{P,\max}$ often depends on the pump size, so the choice of τ_P has to be revisited after finding the value of $V_{P,\max}$. Therefore, the selection of the values of τ_P, $V_{P,\max}$ follows an iterative procedure.

25.5.5 Step 5: Check Results

At this point, after the main parameters of the HT are found, the designer should perform the following checks:

1) The HT performance meets all the given requirements.
2) The various efficiencies assumed during the calculations should match the final selection of the units (the primary unit – or pump, the secondary unit – or motor, the gearboxes).
3) The maximum speed of the motor falls within its operating range:

$$n_{M,\max} = \frac{n_E \cdot \tau_P \cdot V_{P,\max} \cdot \eta_{v,P} \cdot \eta_{v,M}}{V_{M,\min}} \tag{25.34}$$

4) The maximum speed of the pump $n_P = n_E \cdot \tau_P$ is within the allowable pump operating range. In particular, the condition of maximum speed for the prime mover needs to be carefully verified.
5) The maximum system pressure is within the allowable range of the selected units.
6) The maximum power demand at the prime mover is lesser or equal to its available power.

Example 25.1 Sizing a hydrostatic transmission for a small wheel loader

Design a HT for a wheel loader with the properties summarized in the following table:

Parameters	Value	Unit
Engine speed	2000	rpm
Engine/pump ratio	1	
Engine power	60	kW
Vehicle mass (total)	8.85	ton
Rolling radius	0.588	m
Max roading velocity	13	km/h
0-max speed	23	s
Max pulling force	21	kN
Max slope on gravel	30	%
Number of driving motors	1	

The motor is connected to the central differential gearbox as shown in the figure below.
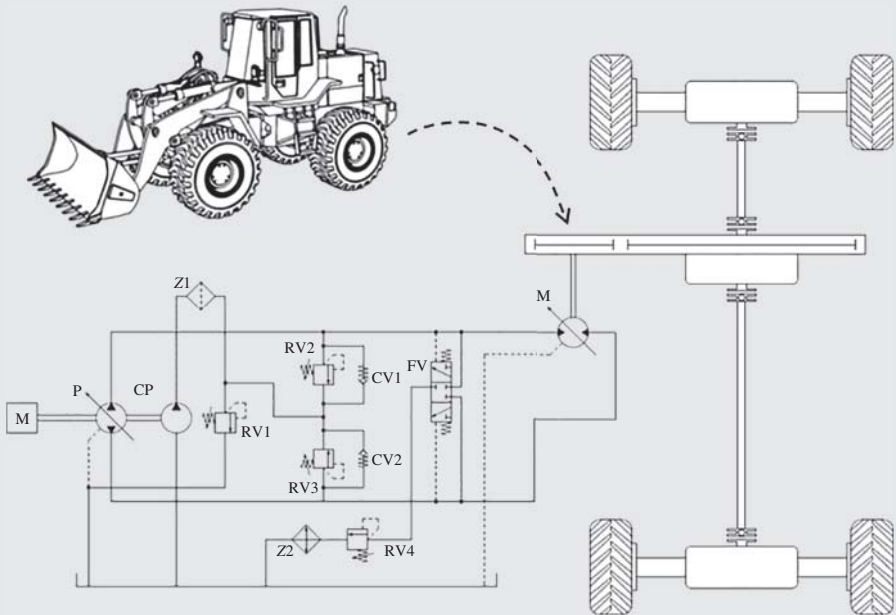
Select the primary and the secondary units from the following tables:

	Motor 1	Motor 2	Motor 3	Motor 4	Motor 5
Max displacement (cm³/rev)	60	80	40	60	80
Min displacement (cm³/rev)	60	80	12	18 cm³/rev	24
Max shaft speed (rpm)	5600	5000	6500 (minimum displacement) 4450 (maximum displacement)	5600 (minimum displacement) 3600 (maximum displacement)	5000 (minimum displacement) 3100 (maximum displacement)
Max operating pressure (bar)	420	420	420	420	420

	Pump 1	Pump 2	Pump 3
Max displacement (cm³/rev)	60	70	90
Max shaft speed (rpm)	3600	3300	3000
Maximum operating pressure (bar)	420	420	420

(Continued)

Example 25.1 (Continued)

Assume 20 *bar* as pressure setting for the charge pump. The available values for the overall gear ratio from the motor to the wheels are 50, 75, 100, and 125, and the overall gearbox and axle efficiency can be assumed as 0.93. For pumps and motors, assume efficiencies proper of piston units.

Given:

1) Engine speed, $n_E = 2000\ rpm$
2) Pump ratio, $\tau_P = 1$
3) Engine power, $P_E = 60\ kW$
4) Vehicle mass, $M = 8850\ kg$
5) Rolling radius, $R_R = 0.588\ m$
6) Max vehicle speed on flat, $v_{max} = 13\ km/h = 3.6\ m/s$
7) Maximum acceleration, $\dot{v}_{max} = \frac{v_{max}}{\Delta t} = 0.565\ m/s^2\ (\Delta t = 23\ s)$
8) Maximum pulling force, $F_D = 21\,000\ N$
9) Maximum slope, $\theta = 30\% = 18.4°$
10) Possible motor and pump choices (see table above)
11) Values for the overall gear ratio between the motor and the wheel, $\tau_W = 50, 75, 100, 125$
12) Overall efficiency of the gearbox and axle mechanical transmission, $\eta_W = 0.93$
13) Charge pump pressure, $p_{ch} = 20\ bar$

Find:

1) The motor displacement V_M and the motor type (fixed or variable)
2) The pump displacement V_P
3) The axle ratio τ_W

Solution:
The problem is a typical sizing of a HT, with unknown gearbox ratio at the motor. The tractive effort of the vehicle is the following:

$$F_T = M \left[g \cdot (\sin\ \theta + \cos\ \theta \cdot f_R) + \dot{v}_{max} \right] + F_D$$
$$= 8850\ [kg]\ \left[9.81\ [m/s^2] \cdot (0.31 + 0.95 \cdot 0.032) + 0.565\ [m/s^2] \right] + 21\,000\ N = 55\,700\ N$$

The coefficient of rolling resistance for gravel road has been assumed as $f_R = 0.032$, based on the values of Table 25.1. In this case, the motor is not connected to a wheel, but to a central case driving both front and rear axles. Thus, T_W represents the overall torque at the wheel hubs:

$$T_W = F_T \cdot R_R = 55\,700\ [N] \cdot 0.588\ [m] = 32\,751\ Nm$$

The sizing of the hydraulic units starts with the selection of the hydraulic motor, or secondary unit. The choice of a fixed or a variable displacement motor can be done based on the torque conversion factor, which for this case is

$$\text{TCF} = \frac{v_{max} \cdot F_T}{P_E} = \frac{3.6\ [m/s] \cdot 55\,700\ [N]}{60\ [kW] \cdot 1000} = 3.4$$

The high value of TCF suggests the choice of a variable displacement motor (the candidates are motors 3, 4, and 5 from the data table). A PVMV or a PVM2 layout can be chosen.

Since the final gear ratio is not given, the motor displacement and the combined gear ratios of transfer case and axles can be calculated with the corner power method.

Motor 4 is taken as initial reference; this can operate at a maximum speed of 5600 *rpm* and with a maximum pressure of 420 *bar*. An HT has a charge pressure of 20 *bar*, therefore the useful pressure difference at the motor is 400 *bar*. Based on these numbers the ideal maximum motor displacement results:

$$V_{M,i} = \frac{v_{\max} \cdot T_W}{R \cdot n_{M,\max} \cdot \Delta p_{M,\max} \cdot z_M \cdot \eta_W \, \eta_{hm,M}}$$

$$= \frac{3.6 \, [m/s] \cdot 32\,751 \, [Nm]}{0.588 \, [m] \cdot (0.1 \cdot 5600) \, [rad/s] \cdot 400 \cdot 10^5 \, [Pa] \cdot 0.93 \cdot 0.94} = 10.2 \, cm^3/rad$$

$$= 64.3 \, cm^3/r$$

The calculated ideal motor displacement is greater than the selected displacement of motor 4, equal to 60 cm^3/r. Therefore, the calculation should be repeated assuming the maximum performance values of motor 5, which max allowed speed is 5000 *rpm*:

$$V_{M,i} = \frac{v_{\max} \cdot T_W}{R \cdot n_{M,\max} \cdot \Delta p_{M,\max} \cdot z_M \cdot \eta_W \, \eta_{hm,M}} = 72 \, cm^3/r$$

The displacement of motor 5 is 80 cm^3/r, which is higher than the ideal value, $V_{M,i}$. Therefore, motor 5 is the correct motor for the application. With this choice, the ideal axle ratio becomes

$$\tau = \frac{T_W}{V_M \cdot (p_{\max} - p_{ch}) \cdot \eta_W \, \eta_{hm,M}} = \frac{2\pi \cdot 32\,751 \, [Nm]}{80 \cdot 10^{-6} \cdot \frac{1}{2\pi} \, [m^3] \cdot 400 \cdot 10^5 \, [Pa] \cdot 0.93 \cdot 0.94} = 73.5$$

The closest available ratio is 75.

Motor 5 can reach a minimum displacement of 24 cm^3/rev. Since no information is provided about the necessary torque at maximum speed, the authors will keep the 24 *cc/r* setting for the motor. This can eventually be adjusted to higher values.

At this point, the pump can be selected based on the flow requirements of the motor. In the condition of vehicle maximum pull, the motor speed can be calculated based on the available engine power:

$$n_{M1} = \frac{P_E \cdot \eta_{t,P} \, \eta_{t,M} \, \eta_W \cdot \tau_M}{F_T \cdot R_R \cdot z_M} = \frac{60 \, [kW] \cdot 0.85 \cdot 0.91 \cdot 0.93 \cdot 75}{\frac{55\,700}{1000} \, [kN] \cdot 0.588 \, [m]} = 98.8 \, [rad/s] = 943 \, rpm$$

In the condition of vehicle maximum speed instead, the motor speed results:

$$n_{M2} = \frac{v_{\max} \cdot \tau}{R_R} = \frac{3.6 \, [m/s] \cdot 75}{0.588 \, [m]} = 459 \, [rad/s] = 4383 \, rpm$$

The ideal pump displacement is

$$V_{P,i} = \frac{\max \left(n_{M1} \cdot V_{M,\max} ; n_{M2} \cdot V_{M,\min} \right)}{n_E \tau_P \cdot \eta_{v,M} \, \eta_{v,P}}$$

$$= \frac{\max \left(943 \cdot 80; 4383 \cdot 24 \right) \left([rpm] \cdot [cm^3/r] \right)}{2000 \, [rpm] \cdot 0.96 \cdot 0.94} = 58.2 \, cm^3/r$$

The manufacturer's catalog includes a 60 *cc/r* axial piston pump (Pump 1), which perfectly fits the application. It is important to notice that the maximum flow requirement is set by the maximum speed, when the motor is at minimum displacement.

(Continued)

Example 25.1 (Continued)

Summary: The final sizing presents a 60 *cc/r* PV and an 80 *cc/r* variable displacement motor (min displacement 24 *cc/r*). The maximum system pressure is 420 *bar*. The charge pressure is 20 *bar*.

Verification of the sizing:

1) Transmission performance
   The maximum torque at the axle is given by

   $$T_{\max} = \frac{V_{M,\max} \cdot \Delta p_{M,\max} \cdot \eta_{hm,M}}{2\pi} = \frac{80\,[cm^3/r] \cdot 400\,[bar] \cdot 0.94}{62.8} = 479\,Nm$$

   This will provide a tractive effort of

   $$F_{\max} = \frac{T_{\max} \cdot \tau \cdot \eta_W}{R_R} = \frac{479\,[Nm] \cdot 75 \cdot 0.95}{0.588\,[m]} = 58\,042\,N$$

   The tractive effort is slightly higher than the requirement. The maximum motor speed is

   $$n_{M,\max} = \frac{n_E \tau_P \cdot V_{P,\max} \cdot \eta_{v,P}\eta_{v,M}}{V_{M,\min}} = \frac{2000\,[rpm] \cdot 60\,[cm^3/r] \cdot 0.94 \cdot 0.96}{24\,[cm^3/r]} = 4512\,rpm$$

   This corresponds to a vehicle speed of

   $$v_{\max} = \frac{n_{M,\max} \cdot R_R}{\tau} = \frac{4512\,[rpm] \cdot 0.588\,[m]}{75 \cdot 9.54} = 3.70\,m/s$$

   All parameters satisfy the initial requirements.
2) Efficiencies
   The bent axis motor and the piston pump satisfy the efficiencies assumed during the solution.
3) Maximum motor speed
   As calculated before the maximum motor speed is 4512 *rpm*. The selected bent axis motor allows a maximum speed of 3100 *rpm* at max displacement and 5000 *rpm* at minimum. Therefore, the selection is correct.
4) Maximum pump speed
   The operating speed of 2000 *rpm* is well within the pump specifications (max speed of 3900 *rpm*).
5) Maximum system pressure
   The maximum allowed pressure for the motor is 420 *bar*, while it is 450 *bar* for the pump.
6) Maximum engine power
   When the vehicle is requiring the maximum tractive effort and the pump is at full displacement, the power at the pump shaft is

   $$P_{\max} = \frac{n_P \cdot V_{P,\max} \cdot p_{\max}}{2\pi \cdot \eta_{t,P}} = \frac{2000\,[rpm] \cdot 60\,[cm^3/r] \cdot 400\,[bar]}{62.8 \cdot 0.90 \cdot 9.54} = 89\,kW$$

   The system can theoretically over-power the engine and cause it to stall. The system should include an anti-stall feature, which limits the maximum displacement of the pump at higher pressures.

Problems

25.1 A small street sweeper uses a closed-loop HT for the drive circuit. The transmission should provide a maximum tractive effort of 2500 lbf while the maximum vehicle speed on flat surface is 30 mph. The vehicle wheels have a rolling radius of 0.355 m and they are driven through an axle with 5.38 drive ratio. The 75 hp engine runs up to 2600 rpm; the pump is driven directly from the engine bell housing. Size the pump and motors for the application: first calculate the theoretical displacements assuming a max pressure of 300 bar. Second, search for online available pump and motor displacements and provide a sizing using commercial units. Assume the proper efficiencies for the units.

25.2 Repeat the previous problem, but assuming the axle drive ratio not known. This can be selected with values between 6.2 and 14.5. How does the sizing changes?

25.3 A crane with an engine of 35 kW uses a separate closed loop hydrostatic transmission for driving the swing function. The swing is driven by two motors with gearbox connected in parallel, each one having a gearbox ratio of 40.6. The efficiency of the gearbox is 0.92. The maximum swing angular velocity corresponds to a full 360 degrees rotation in 9 seconds. The transmission must be able to drive the swing from zero to the maximum swing velocity. The swing requires a maximum accelerating torque of 16500 Nm. The pump is directly coupled to the engine flywheel (1:1 ratio), this running at a speed of 2300 rpm.
   a) Determine if the most suitable hydraulic transmission architecture. Should the transmission use a fixed displacement pump or a variable displacement pump? Should the transmission use a fixed displacement motors or a variable displacement one? Motivate your answer.
   b) Draw a fully functional ISO schematic of the transmission.
   c) Calculate the motor displacements assuming a max pressure of 280 bar, and a pressure of the charge system of 30 bar. As efficiency for each motor, assume 0.9 for the hydromechanical and 0.93 for the volumetric.
   d) Determine the pump displacement. The pump efficiency is 0.92 for the hydromechanical and 0.95 for the volumetric.
   e) Determine the volumetric losses (in L/min) for the maximum speed of the swing.
   f) Considering the charge pump also rotating at 2300 rpm, determine the size of the charge pump (cc/rev), considering a flow requirement that doubles the volumetric losses. Assume a volumetric efficiency for the charge pump of 0.95.
   g) Estimate the size of the tank, considering an average resident time of each oil particle in the tank of 1 min.

Chapter 26

Hydrostatic Actuators

Hydrostatic actuators (HAs) implement a primary control strategy to obtain the motion of linear actuators. This type of system, which is also referred to as *pump control* or *displacement control* actuation, represents a very efficient control technique because it acts directly on the flow or pressure supply without requiring metering elements, which are often responsible for power losses. HAs have a lot in common with hydrostatic transmissions. For example, the circuit layouts (open or closed) and the pump regulators are the same as the ones presented in the previous chapter. However, when the consumer is a single rod cylinder (as in most of the cases), HAs need to account for the difference between supply and return flow. This becomes critical, especially in closed circuit layouts.

An interesting family among HAs is represented by electrohydraulic actuators (EHAs). Here the flow supply is achieved using an electric prime mover. EHAs are commonly used in many aerospace applications and they are becoming popular also in mobile equipment due to the recent trend of electrically powered vehicles.

This chapter describes in detail both open and closed circuit HAs. Particular focus is given to the second case, which allows four-quadrant operation, with the possibility of recovering energy from the actuator. Single rod cylinders are also considered because this represents the most generic and complex case.

26.1   Open Circuit Hydrostatic Actuators

The common architecture of an open-circuit HA is shown in Figure 26.1. The figure represents the case of a fixed speed prime mover and variable displacement pump; however, the same circuit architecture could be used with the flow supply solutions previously described in Figure 23.3.

The circuit in Figure 26.1 is very similar to that in Figure 24.15, except that in the former, the actuator is a cylinder instead of a motor. The velocity of the actuator varies with the commanded pump displacement: $v_{\text{ext}}(i) = Q_p(i)/A$ in extension, and $v_{\text{ret}}(i) = Q_p(i)/a$ in retraction. Directional control valve (DCV) is used to control the flow direction and the two CBVs are used to manage overrunning loads and for load holding.

An interesting HA solution can be implemented when the direction of the external force is always the same, for example, in a forklift. Here the load is always pushing on the single acting cylinder controlling the lift function. In this case (circuit in Figure 26.2), a fixed displacement pump/motor is connected to a variable speed electric motor capable of reversing direction of rotation. The poppet-type solenoid valve (SV) holds the load in neutral position and allows flow to enter the cylinder bore chamber (lifting). When the cylinder needs to be retracted the SV is actuated and the rotating unit works in motoring mode. In this case the system operates in the
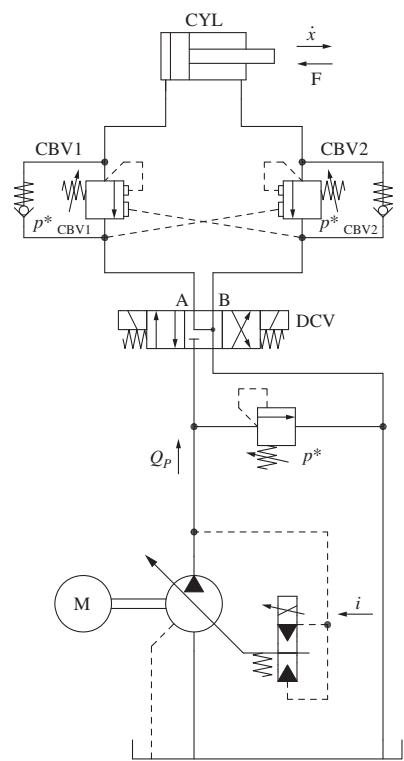
Figure 26.1 Open circuit hydrostatic actuator using counterbalance valves.
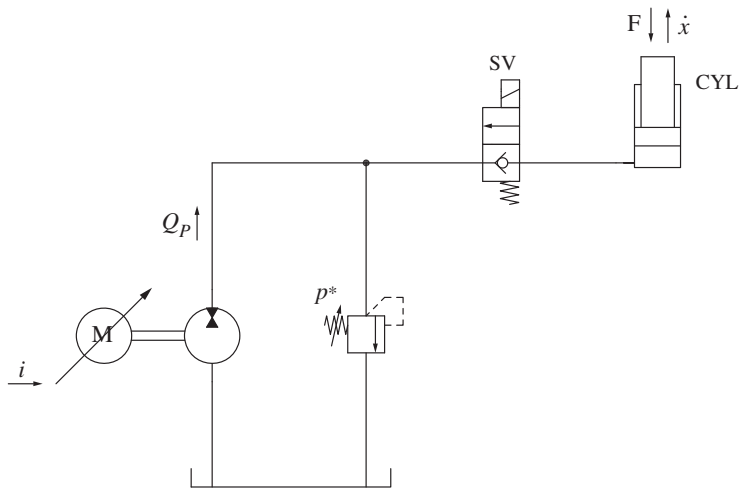
Figure 26.2 HA circuit with single acting cylinder.

second quadrant (similar to that in Figure 24.14) and the electric unit can utilize the overrunning load to generate electric power which, for example, can be stored in the batteries.

26.2 Closed Circuit Hydrostatic Actuators

The basic schematic of a closed-circuit HA with a single rod cylinder is represented in Figure 26.3. The figure refers again to a variable displacement pump, although the concept could be easily extended to the other variable flow supply architectures in Figure 23.3.

The primary unit has over-center capability and can work in four quadrants, as described in Figure 23.5. As for HTs, a charge pump (CP) is used to set, through the relief valve (RV), the lower value of the pressure in the system, p_L. The CP makes up for the leakages and can provide supplementary cooling flow. In Figure 26.3, an accumulator is also present in the low-pressure line to help the CP compensating for the cylinder differential flow. The function of the accumulator will be examined in detail. If the accumulator were not present, the charge pump would have to supply also the differential flow. This could imply a significant increase in the charge pump displacement, with a negative impact on the system size and efficiency.

The operation of the closed circuit system in Figure 26.3 is analyzed in the following pages, separating the case of cylinder extension and retraction. In this analysis, the authors have assumed the accumulator size to be large enough to compensate for the differential flow of the cylinder. Furthermore, for sake of simplicity, the low pressure p_L is assumed constant during the cylinder motion. Therefore, the CP has the singular function of making up for the case drain leakages of the primary unit. A more detailed analysis of the accumulator and CP interaction will be presented subsequently.

26.2.1 Cylinder Extension

The cylinder extension occurs when a positive command is given to the pump. When this happens in the circuit in Figure 26.3, the flow circulates clockwise. The cylinder extension condition needs to be further divided in two cases, which are defined by the magnitude and direction of the load. With reference to Figure 26.3, the force balance equation at the cylinder is:

$$F = p_A A - p_a a \tag{26.1}$$

A significant load value F^* is defined when p_L is present at both the cylinder chambers:

$$F^* = p_L \cdot (A - a) \tag{26.2}$$
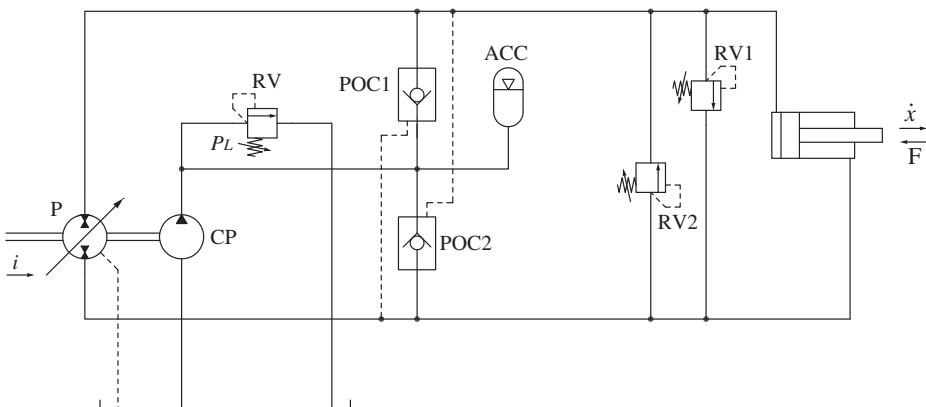
Figure 26.3 Primary control of a differential cylinder in closed circuit.

F^* represents the threshold condition separating the system operation between first and fourth quadrants. If the force on the actuator is greater than F^*, the pressure at the outlet of the primary unit is higher than the one at the inlet. This is also referenced as *pumping mode* and pertains to the first operating quadrant. Vice versa, if the load is smaller than F^*, the primary unit inlet pressure becomes higher than the outlet. In this case, the load can be slightly resistive ($0 < F < F^*$) or overrunning ($F < 0$). This condition is also referred to as *motoring mode* and belongs to the fourth operating quadrant.

26.2.1.1 Extension in Pumping Mode ($F > F^*$)

This is the operation corresponding to resistive loads higher than F^*. In this case, the high pressure p_H is present in the upper leg of the circuit, supplied by the outlet port of the primary unit. The accumulator sets the low pressure p_L in the opposite leg of the circuit, i.e. at the inlet port of the primary unit, connected to the actuator return port, as shown in Figure 26.4. The pump flow enters the piston chamber, so that the extension velocity equals:

$$\dot{x} = \frac{Q_P}{A} \tag{26.3}$$

The flow returning from the actuator Q_a merges with the flow supplied by the accumulator, Q_{acc}, to compensate for the effect of the differential area. Q_{acc} passes through POC2, which is kept fully open by p_H:

$$Q_{acc} = Q_a \cdot (\varphi - 1) \tag{26.4}$$

In this case, the pressure differential across the primary unit is positive (outlet pressure is higher than inlet pressure). The unit is working as a pump, requesting power from the prime mover (pumping mode).

The system efficiency is expressed as ratio between power output ($F \cdot v$) and the power input. Besides the power requested by the primary pump, $Q_P \cdot \Delta p_P$, the charge pump and the accumulator represent the two other input contributions:

$$\eta_S = \frac{F \cdot \dot{x}}{Q_P \cdot \Delta p_P + \left(Q_{acc} + Q_{CP}\right) \cdot p_L} \tag{26.5}$$
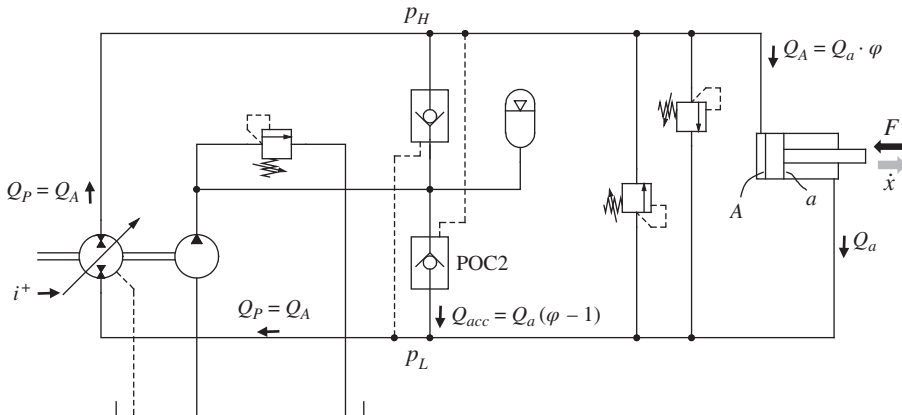
Figure 26.4 System behavior for the case of cylinder extension with resistive loads ($F > F^*$).

Analyzing Eq. (26.5), it is possible to observe that the CP contribution is the only effective loss of the system. In fact, neglecting the charge pump flow[1], the system efficiency becomes unitary:

$$\eta_S = \frac{F \cdot \dot{x}}{Q_P \cdot \Delta p_P + Q_{acc} \cdot p_L} = \frac{F \cdot \dot{x}}{Q_P \cdot (p_H - p_L) + Q_P \cdot p_L \cdot \left(1 - \frac{1}{\varphi}\right)} = 1 \tag{26.6}$$

Equation (26.6) shows that the efficiency of a primary controlled system with ideal units is unitary. This was not the case in metering concepts, where the system efficiency was always lower than one, also in the case of ideal units. The power losses in a HA are caused only by the primary unit losses and by the presence of the CP.

26.2.1.2 Extension in Motoring Mode ($F < F^*$)

In this case the loads are smaller than F^*. As represented in Figure 26.5, the higher pressure p_H is present in the lower leg of the circuit, connected to the inlet of the primary unit (or the cylinder rod side). On the other hand, the pressure p_L defined by the charge pump and the accumulator is seen at the unit outlet, i.e. the actuator inlet. Consequently, the extension velocity is set by the inlet flow of the primary unit and corresponds to a higher value with respect to the previous case:

$$\dot{x} = \frac{Q_P}{a} \tag{26.7}$$

In this case the accumulator flow calculated in Eq. (26.4), which balances the differential flow, merges with the outlet flow of the primary unit through POC1, supplying the actuator bore chamber.

The pressure differential across the primary unit is now negative, meaning that the inlet pressure is higher than the outlet. In this condition, it operates as a motor (motoring mode). As for closed circuit HTs, the power associated with the motion of the actuator under overrunning loads is not dissipated within the hydraulic systems, but it is returned at the primary unit shaft. This power can be:

a) Dissipated by the prime mover (e.g. engine braking). In this case the power is not utilized or stored, but the dissipation does not increase the temperature of the hydraulic fluid.
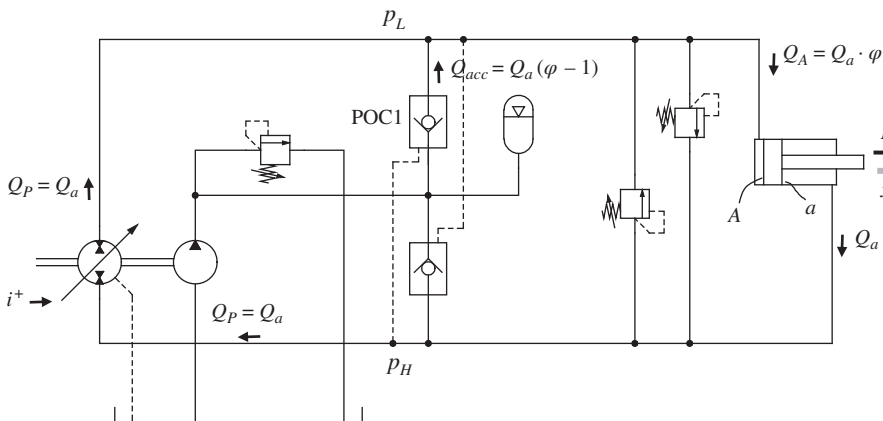
Figure 26.5 System behavior for the case of cylinder extension with low resistive or overrunning loads ($F < F^*$).

---

1 This is possible assuming the primary pump ideal, without case drain leakages.
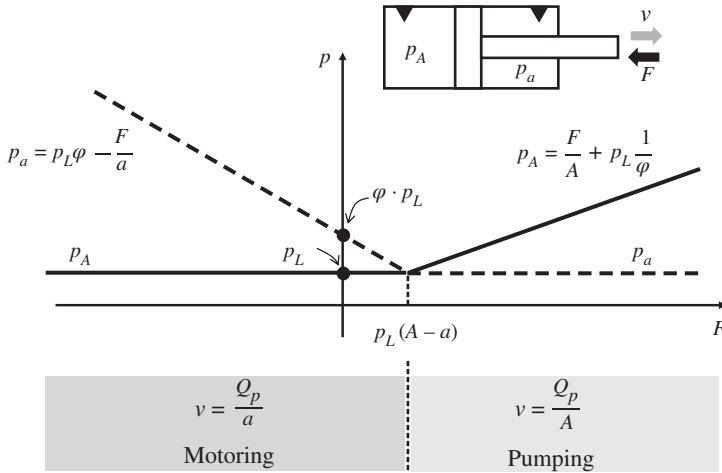
Figure 26.6 System pressures for the case of cylinder extension.

b) Transferred to other functions, such as another hydraulic pump powered by the same prime mover or an auxiliary function (e.g. AC compressor or engine cooling fan). In this case the power recirculates in the machine and the prime mover output demand is reduced.

c) Recovered by the prime mover. This is, for example, a case of an electric prime mover that, during motoring mode, can turn into a generator charging batteries.

Since the primary unit has the possibility of operating in motoring mode, it should be indicated in the hydraulic circuit as a reversible unit, as shown in Figure 26.3.

The system efficiency is measured for the energy recovery mode: the load now is the power input to the system, while the output is the energy at the pump shaft:

$$\eta_S = \frac{Q_P \cdot \Delta p_P}{F \cdot \dot{x} + \left(Q_{acc} + Q_{CP}\right) \cdot p_L} \tag{26.8}$$

If the charge pump contribution is neglected, the pump system efficiency becomes unitary. One important observation is that looking at Eqs. (26.5) and (26.8), the contribution of the accumulator is always at the denominator of the formulas because during extension, the accumulator needs to introduce fluid into the circuit to compensate for the differential volume of the cylinder. Neglecting the contribution of the accumulator would lead to efficiencies greater than unity, and it is conceptually wrong.

Figure 26.6 represents a snapshot of the cylinder extension case, summarizing the actuator speed and pressures as a function of the external force.

26.2.2 Cylinder Retraction

The cylinder retraction is obtained by providing a negative command to the pump displacement control. Under this condition, the unit works over center; in the system in Figure 26.3, the flow circulates counterclockwise.

In addition, the same two conditions (motoring and pumping modes) can be identified for the cylinder retraction. It is important to observe how the force F is still assumed positive if pushing

against the cylinder bore. Therefore, a positive value of F implies an overrunning load during retraction. With this assumption, the threshold value of the force separating pumping and motoring mode is the same as $F^* = p_L \cdot (A - a)$.

26.2.2.1 Retraction in Motoring Mode ($F > F^*$)

In Figure 26.7, the force is positive and has the same direction of the piston motion; therefore, the load is overrunning. The low-pressure system (accumulator and CP) controls the pressure value p_L at the bottom of the circuit, connected to the rod side of the actuator. The higher pressure p_H is set at the piston chamber, connected to the upper leg of the circuit.

As shown in Figure 26.7, the flow returning from the actuator enters the primary unit inlet, which is now on top. The pilot operated check valve POC2 is open under the action of the high pressure p_H acting on its pilot line. POC2 discharges the excess flow into the accumulator (and eventually to the low-pressure relief valve). This flow equals the differential flow $Q_{acc} = Q_a(\varphi - 1)$. The cylinder retraction velocity becomes:

$$\dot{x} = \frac{Q_P}{A} \tag{26.9}$$

The pressure differential, Δp_P, across the primary unit is negative, with respect to its over-center configuration. This means that the power in the system flows from the actuator back to the primary unit shaft. In other terms, the unit behaves as a hydraulic motor and the system operates in the second quadrant.

The system efficiency is equal to:

$$\eta_S = \frac{Q_P \cdot \Delta p_P + Q_{acc} \cdot p_L}{F \cdot \dot{x} + Q_{CP} \cdot p_L} = 1 \tag{26.10}$$

Also in this case, if the charge pump contribution is neglected, the system efficiency becomes unitary.
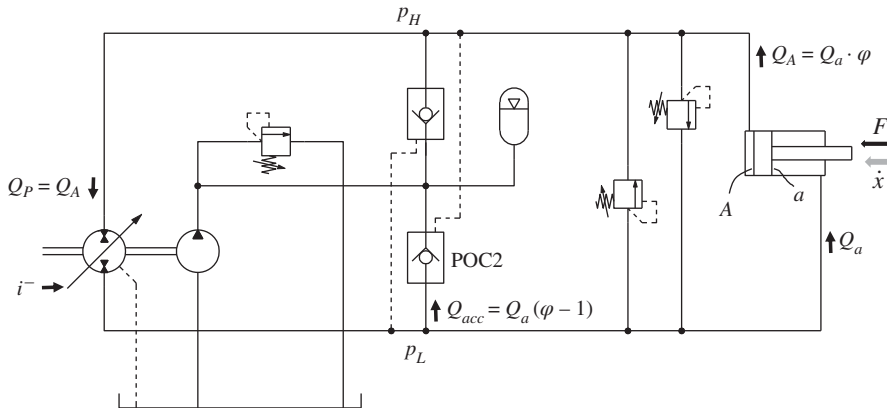
Figure 26.7 System behavior for the case of cylinder retraction with assistive loads ($F > F^*$).

26.2.2.2 Retraction in Pumping Mode ($F < F^*$)

The operation of the system in case of retraction under resistive load conditions (or light overrunning load conditions) are summarized with the schematic in Figure 26.8. In this case, the high pressure level, p_H, is set at the inlet of the actuator (cylinder rod side), while the low pressure level,
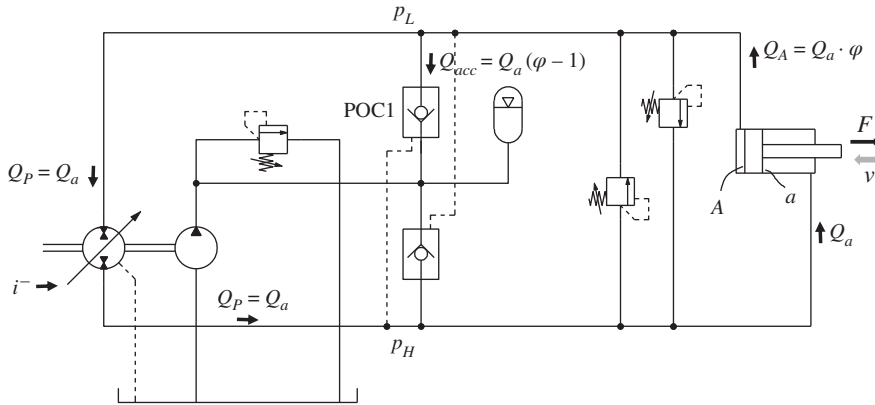
Figure 26.8 System behavior for the case of cylinder retraction with resistive loads ($F < F^*$).

p_L, at the return (piston side). POC1 is forced open by the value of p_H, letting the differential flow $Q_{acc} = Q_a(\varphi - 1)$ entering the low-pressure lines.

In this case, the cylinder retraction velocity becomes:

$$\dot{x} = \frac{Q_P}{a} \tag{26.11}$$

The supply pump sees a positive pressure differential, meaning that the pump operates in pumping mode, requesting energy at its shaft. The system operates in the third quadrant.

The same considerations are valid for the system efficiency, which now is:

$$\eta_S = \frac{F \cdot \dot{x} + Q_{acc} \cdot p_L}{Q_P \cdot \Delta p_P + Q_{CP} \cdot p_L} = 1 \tag{26.12}$$

In general, during cylinder retraction, for both resistive and overrunning loads, the differential flow is taken out from the main loop and enters the low-pressure accumulator. This flow is stored within the accumulator and it is made available for the subsequent extension case.

Also for the cylinder retraction, the ideal system has a theoretical unitary energy efficiency for both resistive and overrunning load conditions. This efficiency would be lower than 1 in case the
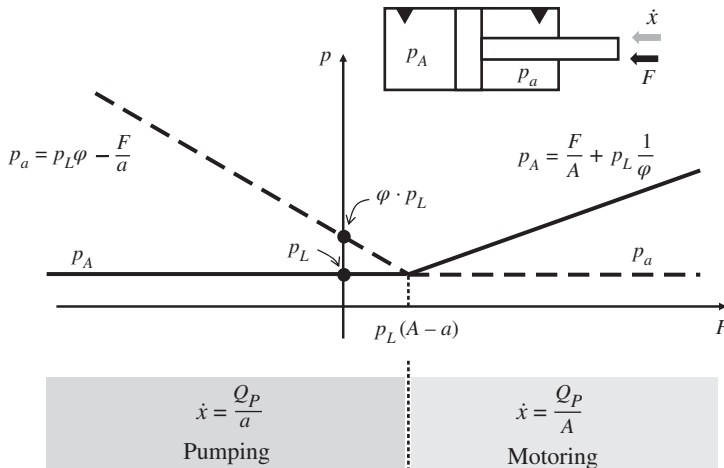
Figure 26.9 System pressures for the case of cylinder retraction.
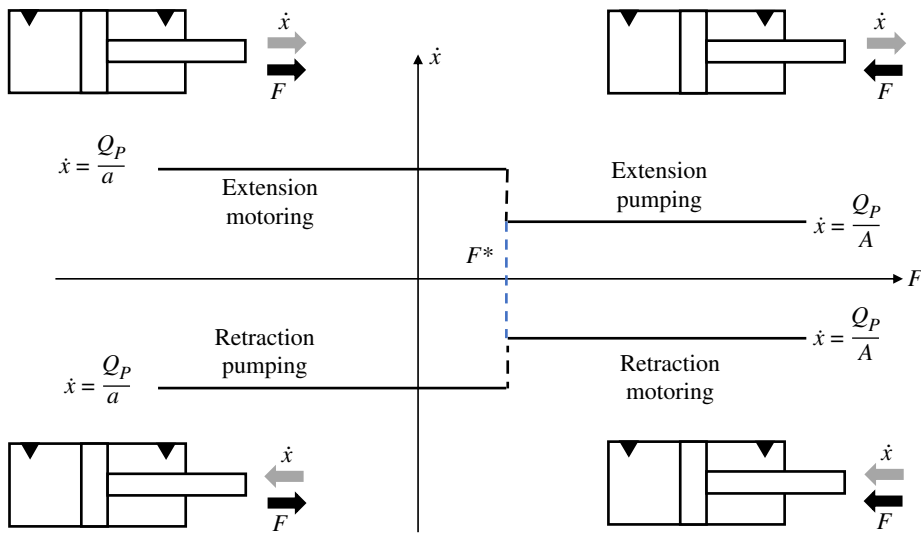
Figure 26.10 Summary of the operating conditions for the hydrostatic actuator in Figure 26.3.

flow sent to the low-pressure line would not be taken into consideration while studying the energy flows within the system. Figure 26.9 shows a summary of forces, speeds, and pressures for the case of cylinder retraction.

A summary plot for all the operating conditions of the closed circuit primary control actuation system in Figure 26.3 is shown in Figure 26.10. The figure highlights the four possible quadrants of operation of the system, depending on the possible configurations of load and speed directions. The chart highlights the values of the actuator velocities as a function of the load and the level of the low pressure p_L set by RV. The velocity switches from Q_P/A to Q_P/a when the load transitions across the critical value F^*, Which could cause problems in applications with varying loads that require accurate speed control.

26.3 Further Considerations on the Charge Pump and the Accumulator

In the previous analysis, several simplifying assumptions have been made on the operation of the accumulator and the charge pump. For example, it was supposed that the accumulator is large enough to compensate for the cylinder differential volume and for keeping a constant value of p_L. It was also supposed that the charge pump does not play a role during the cylinder movement and it is only sized to make up for the primary unit volumetric losses.

In reality, the accumulator pressure is not constant and, for a given accumulator volume and precharge, it varies depending on the volume of fluid stored according to formulas described in Chapter 9. In particular, the accumulator pressure will be within two limits, p_{ac-h} and p_{ac-l}. The upper limit, p_{ac-h}, is reached when the cylinder is fully retracted, and the bore side volume is null. In this situation the accumulator is full. Vice versa, the lower limit, p_{ac-l}, is reached at the opposite cylinder configuration when the minimum amount of oil is present in the accumulator.

At this point, the careful reader should foresee an issue concerning the interaction between charge pump, charge relief, and accumulator. In fact, with the circuit in Figure 26.3, if the setting of the charge relief, RV, was higher than p_{ac-h}, the CP would continuously charge the accumulator.
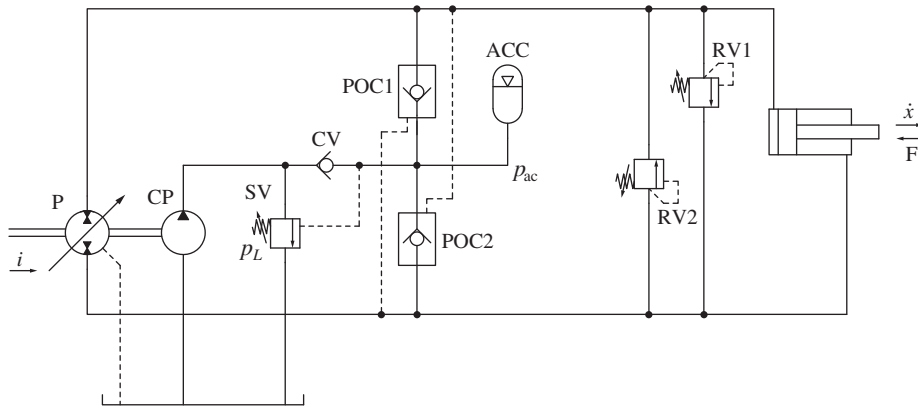
Figure 26.11 Closed circuit HA with accumulator and charge circuit sequence valve.

With a full accumulator the excess return flow during retraction would be discharged through RV. On the other hand, if the setting of the RV is equal to p_{ac-l}, the accumulator would always stay at a constant pressure p_{ac-l} and never contribute to the system operation. Hence, the circuit in Figure 26.3 does not represent a viable solution for realizing a closed circuit HA using an accumulator to balance the differential volume of the cylinder. The abovementioned issues can be resolved with the layout represented in Figure 26.11. Here, the check valve (CV) prevents the accumulator from discharging through the sequence valve SV. This latter is set to p_L and it is actuated by the accumulator pressure p_{ac}. If the accumulator is charged to a pressure above p_L, the sequence valve is open, and the charge pump returns to tank at ideally null pressure. Thus, the power consumption of CP is also null. When the accumulator pressure drops below p_L, the charge pump introduces oil in the low-pressure line of the circuit.

Example 26.1   Sizing a hydrostatic actuator with accumulator circuit

An HA is designed according to the circuit in Figure 26.11. The cylinder bore is 60 *mm* and the rod is 35 *mm*. The cylinder stroke is 450 *mm*. The force on the cylinder has always positive sign (according to the sign convention presented in the same figure) and can reach a maximum value of 58 *kN*. The cylinder should reach a maximum velocity of 150 *mm/s* during extension. Calculate the pump size knowing that the prime mover rotates at 2500 *rpm*. Calculate the maximum retraction speed.

Size the charge pump and the accumulator knowing that the primary pump has a volumetric efficiency of 93% and that the value of the low side pressure should oscillate between 10 and 14 *bar*.

Given:

1) Cylinder bore, $d_b = 60\ mm$
2) Cylinder rod, $d_r = 35\ mm$
3) Cylinder stroke, $s = 450\ mm$
4) Maximum force, $F = 58\,000\ N$
5) Maximum extension velocity, $v_{ext} = 150\ mm/s$
6) Pump speed, $n_P = 2500\ rpm$
7) Pump volumetric efficiency, $\eta_{v,\,P} = 0.93$
8) Sequence valve setting, $p_L = 10\ bar$
9) Maximum accumulator pressure, $p_{ac-h} = 14\ bar$

Find:

1) The primary pump displacement, V_P
2) The maximum cylinder retraction speed, v_{ret}
3) The maximum pump pressure, p_{max}
4) The charge pump displacement, V_{CP}
5) Accumulator volume, V_{ac} and precharge, p_0

Solution:

The cylinder has the following properties:

$$
\begin{cases}
A = \dfrac{\pi \cdot d_b^2}{4} = \dfrac{\pi \cdot 3600\,[mm^2]}{4} = 2827\,mm^2 \\[2mm]
a = \dfrac{\pi \cdot \left(d_b^2 - d_r^2\right)}{4} = \dfrac{\pi \cdot (3600 - 1225)\,[mm^2]}{4} = 1865\,mm^2 \\[2mm]
\Delta V = \dfrac{\pi \cdot d_r^2}{4} \cdot s = \dfrac{\pi \cdot 1225\,[mm^2]}{4} \cdot 450\,[mm] = 0.43\,l
\end{cases}
$$

A is the bore area, a is the rod side annular area, and ΔV is the differential volume of the cylinder. The area ratio is $\varphi = 1.51$.

The flow rate corresponding to the desired extension speed is:

$$
Q_{\text{ext}} = A \cdot v_{\text{ext}} = 2827\,[mm^2] \cdot 150\,[mm/s] = 424\,050\,[mm^3/s] = 25.4\,l/min
$$

The necessary pump displacement results:

$$
V_P = \frac{Q_{\text{ext}}}{n_P \cdot \eta_V} = \frac{25.4\,[l/min]}{2500\,[rpm] \cdot 0.93} = 11\,cm^3/r
$$

The maximum cylinder retraction speed results:

$$
v_{\text{ret}} = \varphi \cdot v_{\text{ext}} = 1.5 \cdot 150\,[mm/s] = 225\,mm/s
$$

The maximum system pressure can be calculated using the cylinder force balance formula:

$$
p_{\text{max}} = \frac{F}{A} + \frac{p_{\text{ac}-h}}{\varphi} = \frac{58\,000\,[N]}{2827\,[mm^2]} \cdot 10 \frac{[bar]}{[N/mm^2]} + \frac{14\,[bar]}{1.5} = 215\,bar
$$

The charge pump needs to be able to make up for the volumetric losses of the primary unit; therefore, its displacement needs to be at least:

$$
V_P = \frac{Q_{\text{ext}} \cdot \left(1 - \eta_V\right)}{n_P} = \frac{25.4\,[l/min] \cdot (1 - 0.93)}{2500\,[rpm]} = 0.7\,cm^3/r
$$

According to the design guidelines explained in Chapter 9, the accumulator precharge pressure can be selected as 90% of the minimum operating pressure:

$$
p_0 = 0.9 \cdot p_{\text{ac}-l} = 0.9 \cdot 10\,[bar] = 9\,bar
$$

Using the sizing formula presented in the same chapter, the accumulator volume results:

$$
V_{\text{ac}} = \frac{\left(\dfrac{p_{\text{ac}-h}}{p_{\text{ac}-l}}\right)^{\frac{1}{n}} \cdot \Delta V}{\left(\dfrac{p_0}{p_{\text{ac}-l}}\right)^{\frac{1}{n}} \cdot \left[\left(\dfrac{p_{\text{ac}-h}}{p_{\text{ac}-l}}\right)^{\frac{1}{n}} - 1\right]} = \frac{\left(\dfrac{14}{10}\right)^{\frac{1}{1.4}} \cdot 0.43\,[l]}{\left(\dfrac{9}{10}\right)^{\frac{1}{1.4}} \left[\left(\dfrac{14}{10}\right)^{\frac{1}{1.4}} - 1\right]} = 5 \cdot 0.43\,l = 2.2\,l
$$

26.4   Final Remarks on Hydrostatic Actuators

Primary control is a very efficient solution for controlling a single actuator. Especially in closed circuits, if the accumulator is properly sized for compensating the differential area effect, the CP can be relatively small, and this represents the only loss in the circuit. Furthermore, the possibility of recovering the energy in motoring mode opens many interesting scenarios such as downsizing of the prime mover, reducing the size of the cooling system, and recovering energy through batteries.

However, open and closed circuit HAs imply several challenges for the system design:

1) The real closed circuit pump/motor unit has internal leakages, which makes it challenging to hold an actuator under load at a constant position with the simple circuit shown in Figure 26.3. Possible solutions using position feedback of the actuator or load holding valves can become very complex to implement because they complicate the circuit and pose severe control challenges that usually reduce the efficiency of the system. The open circuit in Figure 26.1 does not have this issue because it uses counterbalance valves, but at the same time, it does not allow recovery energy.

2) In a closed circuit primary control system, the primary unit flow always limits the speed of the actuator, also under overrunning load. This can be a limitation in controlling functions that require fast cycle times during overrunning conditions (for example, the boom lowering in a wheel loader). Here, an open circuit or a metering system can use unloaded meter out designs that, in conjunction with anticavitation valves, can achieve very high speed of the actuator under assistive loads.

3) When primary control is extended to several actuators that are operating simultaneously, each actuator will need to be controlled by an independent pump. Therefore, in order to meet the individual cycle times, the installed pumps power can grow significantly with respect to a metering solution, where a single pump supplies multiple actuators. This is more evident for systems that are designed to work in flow saturation, i.e. where each single actuator can require high pump flows when working individually. This design implies high installation costs (pumps and gearboxes).

4) When multiple units are installed, the parasitic losses (pumps and gearboxes) can become very relevant and should be considered in the energy balance of the system. For example, a 75 cm^3/r unit at zero outlet flow rotating at 1800 rpm can require up to 2.5–3 kW of power.

Chapter 27

Secondary Controlled Hydrostatic Transmissions

The general classification provided in Chapter 10 introduces the basic concepts of secondary control. Flow and pressure supply have been discussed separately. In Chapter 23, a more specific classification for hydrostatic transmissions (HTs) has been presented, and secondary control HT with flow supply has been treated as part of the HTs presented in Chapter 24. In this chapter, the pressure supply will be discussed. In hydraulics, *secondary control hydrostatic transmissions* usually refer to the type of secondary controlled systems based on a constant pressure supply. This type of system warrants its own chapter because of its unique feature: the actuator speed is controlled indirectly as a result of the balance between the torque generated by the load and the torque generated by the secondary hydraulic unit.

Another interesting fact about this system is that it can only apply to rotary actuators. Nowadays, practical solutions for realizing a linear actuator with continuously adjustable area of influence are not available or are extremely complex to implement.

27.1 Basic Implementation

Secondary controlled systems were first created in the late 1970s by Prof. Nikolaus of the Army University of Hamburg, Germany [23]. At that time, the main aim of his research was the development of valveless hydraulic systems for the control of rotary units supplied by a constant pressure.

> This concept somehow mimics the idea of electric power distribution networks, where the supply voltage is kept constant and each consumer draws the current needed to achieve the desired operation (e.g. your home appliances).

In a secondary controlled system (Figure 27.1), the supply unit maintains a constant operating pressure (p^*) in the power lines; therefore, the torque provided by the actuator is solely a function of the motor displacement, whose value is directly controlled by the input command i:

$$T_M = V_M(i) \cdot p^* \tag{27.1}$$

However, the desired output of the regulation is usually the shaft speed. Newton's second law outlines the relationship between the shaft speed, n_M, the motor torque, T_M, and load torque T_L:

$$I\frac{\partial}{\partial t}n_M = T_M - T_L = V_M(i) \cdot p^* - T_L \tag{27.2}$$

In Eq. (27.2), I represents the overall shaft inertia, given by the combined effect of the load and the actuator rotating parts. Equation (27.2) explains how, in a secondary control system, the actuator
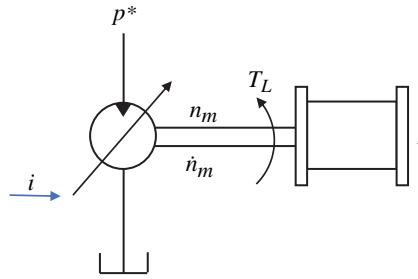
Figure 27.1 Variables involved in the control of a hydraulic motor through secondary control.

speed is controlled by acting on its derivative. The flow rate through the motor, Q_M, is a result of the equilibrium of Eq. (27.2), and it is given by the speed n_M and the displacement V_M.

Figure 27.2 shows the generic layout of a secondary control circuit (as in Chapter 10): the main elements of the system are the pressure-controlled variable displacement pump, the variable displacement motor, and the accumulator. Additionally, a check valve (CV) allows flow only from the pump to the accumulator. The accumulator plays a fundamental role, mainly for two reasons: first, during transitory phases, the dynamic response of the pump alone might not be able to guarantee the condition of constant pressure supply[1]. The accumulator ensures that this condition is always maintained. Second, the accumulator allows storage of the energy generated by overrunning loads; in fact, the motors used in secondary controlled systems can reverse their displacement ("over-center" condition) and, driven by the load, can behave as a pump and supply oil to the accumulator. The energy stored in the accumulator can be utilized in subsequent conditions of resistive loads, thus relieving the pump from producing this work.

The control of this type of system is more complex than most of the other hydraulic control systems described in this book. Therefore, the reader could question the motivations behind the development of this concept. The answer lies in the advantages allowed by the secondary control concept:

– The power is transferred from the primary to the secondary unit without throttling losses.
– The rotary actuator can work in four quadrants, i.e. as a motor and a pump, making energy recuperation possible in the case of overrunning loads.
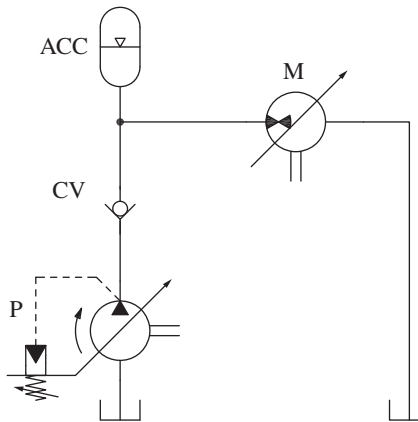
Figure 27.2 Basic implementation of the secondary control principle inclusive of primary and secondary units and accumulator.

---

1 In transitory phases such as rapid accelerations, the flow demand of the motor could exceed the pump capacity.

– Energy recovery also occurs without throttling losses.
– Constant pressure operation of the actuator permits very fast response to load transients. As a matter of fact, flow-imposed types of regulation, are dynamically limited by the compressibility effects (oil pressurization, hose expansions) associated with changes in pressure. Such phenomena that can delay the system response (for positive pressure gradients) or create local over-pressurization (negative gradients) are not present in the secondary controlled systems.
– The system can easily be extended to multiple actuators in parallel and the energy can freely flow from one to another.

On the other hand, the biggest challenges of such a system lie in the stability of the control loop, since the speed of the actuator is controlled indirectly by managing the actuator torque, according to Eq. (27.2). Another relates to the overall system efficiency when the hydraulic units operate at low displacement values. Although the system efficiency is ideally unitary (throttling losses are avoided), the overall efficiency of both the actual units can become significantly poor at low displacement.

Nowadays, secondary control circuits are well established in some niche applications, such as large winches and marine cranes, off-shore heave compensation systems and industrial test benches. All these applications benefit from the high accuracy of control and the energy recovery features offered by this kind of solution.

27.2 Secondary Control Circuit with Tachometric Pump

Figure 27.3 represents one of the first secondary controlled HT circuits implemented and it is purely based on a hydraulic feedback of the actuator speed. The main components of the circuit are the primary pressure-controlled pump P, the secondary unit M, and the accumulator AC. In particular, the displacement of the unit M is controlled through the double acting linear actuator control piston
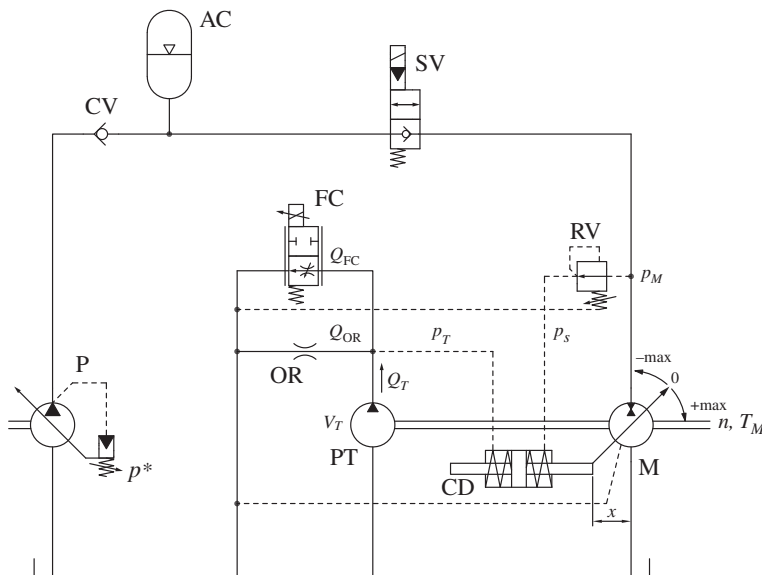
Figure 27.3 One of the first concepts for controlling the displacement of a secondary unit is based on a tachometric pump.

(CP), provided with two centering springs. The right chamber of the actuator (which increases the unit displacement) is supplied by a reducing valve (RV) set to a constant pressure value p_S. The left chamber of actuator CP is instead supplied with a pressure p_T generated by a separate circuit. This circuit comprises a fixed displacement pump PT (often referred as *tachometric pump*) whose outlet is connected to an orifice OR and, in parallel, to a two-way pressure compensated flow control valve FC (as seen in Chapter 8). The valve FC is normally closed and its setting is adjustable by mean of a proportional solenoid. The tachometric pump is coupled on the same shaft as the unit M, rotating at the same speed n. The flow generated by the tachometric pump is throttled through FC and OR, generating the resulting pressure p_T, which is sent to the actuator CP. The equilibrium between the pressure p_T and the pressure p_S at both sides of CP determines the instantaneous displacement of the secondary unit M.

Operation with resistive load. In the initial situation, the valve SV is closed, the rotary actuator M is not rotating, and its displacement is in the null position ($x = x_0$). The accumulator is charged by the pump P at a pressure equal to p^*. When SV is shifted, the pressure p^* is connected to the motor inlet port ($p_M = p^*$). The RV generates the pressure p_S which moves the motor M toward maximum displacement, because the value of p_T is initially null. As the displacement (i.e. x) increases, so does the torque at the output shaft T_M. When T_M reaches values greater than the load torque T_L, the actuator starts accelerating. As the actuator shaft moves ($n > 0$), the unit rotates, and the tachometric pump PT starts producing flow, where $Q_T = V_T \cdot n$. The flow rate through the orifice OR is:

$$Q_{OR} = Q_T - Q_{FC}(i) \tag{27.3}$$

$Q_{FC}(i)$ is the setting of the two-way FC valve, which is a function of the input current i.

In this condition, the orifice OR works as a compensator, and the flow area being Ω_{OR}, the resulting pressure p_T acting on the CP becomes:

$$p_T = \frac{\rho}{2(c_f \Omega_{OR})^2} \cdot [V_T n - Q_{FC}(i)]^2 \tag{27.4}$$

The value of p_T is a function exclusively of the rotational speed and of the setting of the two-way FC valve.

As the speed increases, the value of p_T also increases, counteracting the effect of p_S in the force balance of the CP. The system finds the equilibrium condition when the pressure p_S equals the tachometric pressure p_T. This corresponds to a specific value of the speed n, established at the motor shaft. The equilibrium at the CP can be graphically represented in Figure 27.4: p_T follows a parabolic trend with respect to the motor speed (as expressed by Eq. (27.4)), and the intersection with the set pressure p_S (horizontal dotted line) determines the resulting setpoint of the motor speed, n^*. The value of n^* is controlled by varying the setting of FC (i.e. the value of Q_{FC}). Increasing the current i, the parabola representing p_T shifts to the right; therefore, n^* is increased. Figure 27.4 shows an important feature of the regulation system: for a given input command, the resulting shaft speed of the unit is not exactly n^* but it ranges in an area Δn around the setpoint, depending on the value of the external load T_L. This is due to the effect of the centering springs inside the CP, whose force on the stroking mechanism is not negligible. In fact, the equilibrium at the CP, considering the springs, can be written as:

$$p_T = p_S - k(x - x_0) \tag{27.5}$$

where k is representative of the spring's stiffness. The ideal set-point value n^* represented in Figure 27.4 is true in a null load condition ($T_L = 0$). For resistive loads (positive T_L), the motor M works at positive displacements, $\epsilon > 0$, and ($x - x_0$) is also positive. This implies a controlled
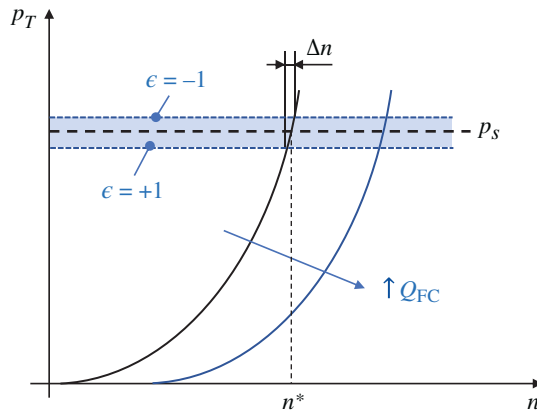
Figure 27.4 Regulation of the velocity of the secondary unit for the system of Figure 27.3.

speed lower than n^*, with the minimum value reached at the maximum resistive load $T_{L,\max}$, when M works at its maximum displacement $V_{M,\max}$.

Operation with overrunning load: However, if the load is overrunning (T_L negative), the motor works over-center, i.e. $\epsilon < 0$, and $(x - x_0)$ is negative. As a consequence, the shaft speed becomes higher than n^*, with the minimum value reached at the maximum overrunning load $-T_{L,\max}$, when M is at its minimum displacement $-V_{M,\max}$.

In overrunning load conditions, the direction of rotation of the unit is the same, but the direction of the flow is reversed: the unit M works as a pump supplying oil into the accumulator AC. The primary unit P stays at null stroke, separated from the rest of the circuit by the check valve CV. The power generated by the overrunning the load is recuperated and stored in the accumulator, which needs to be properly sized. When the load returns to resistive, the flow is initially supplied to the unit M by the accumulator, while the pump remains at null displacement.

27.3 Secondary Control Circuit with Tachometric Pump and Internal Force Feedback

The control schematic in Figure 27.3 is quite intuitive and clearly illustrates how a tachometric pump can be used to implement the shaft speed control of the secondary unit. However, its regulation presents several undesired features:

1) *Control range*. The set speed n^* is not controlled exactly, but within a range, as shown in Figure 27.4. This is caused by the stiffness of the centering springs in the control spool.
2) *Fluctuations of the control pressure p_T can easily lead to instability*. When the unit M modifies its displacement (i.e. every time the input command or the load change), the CP moves, which implies the displacement of a certain amount of fluid and leads to an instantaneous flow rate, which is either added or subtracted to the tachometric pump outlet, which is connected to the left chamber of CP[2]. This flow perturbation becomes part of Eq. (27.3), and, in turn, causes a change in the control pressure p_T. This phenomenon affects the robustness of the control system, resulting in potential undesired oscillations of the shaft speed n.

———

2 The area of the CP is not negligible with respect to the flow produced by PT.
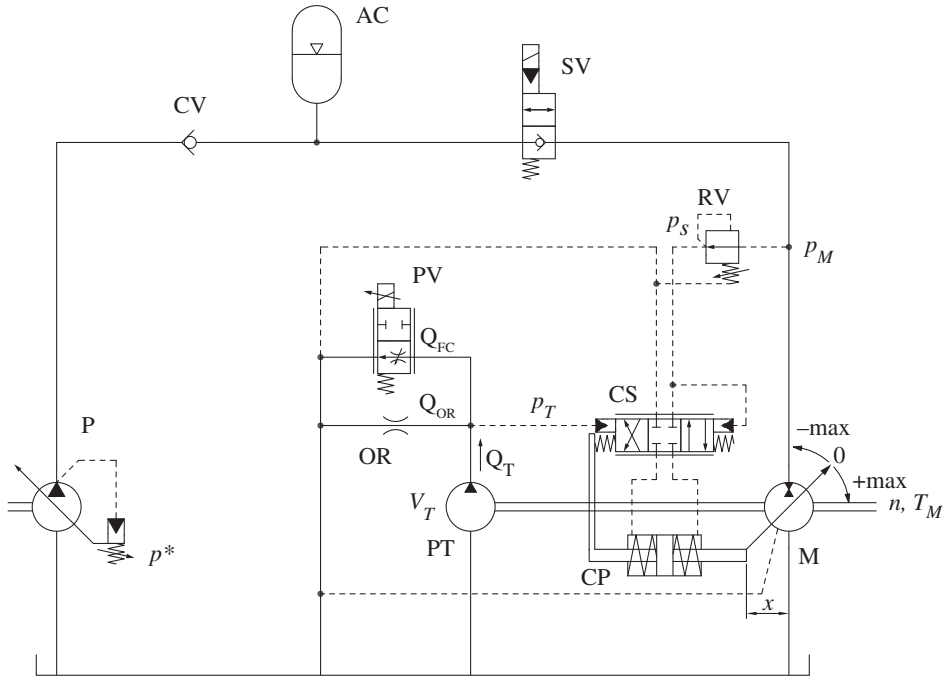
Figure 27.5 Secondary control circuit with tachometric pump and additional force feedback at the control piston CP.

These issues have been overcome through an improved control schematic, which also adds an additional feedback between the secondary unit displacement and the control signal, as represented in Figure 27.5. Here, the displacement of the unit M is changed through the linear actuator CP which, in turn, is controlled with a 4/3 valve with critical center (CV). The tachometric pressure p_T, and the constant pressure p_S are acting on the control spool of CV, which, in turn, controls the supply to the chambers of the actuator CP. The control also presents a mechanical force feedback between CP and CV, realizing a typical *hydraulic servomechanism* with force feedback. The operation of the servomechanism implemented by CP and CV can be described as follows: the position of the spool CV is determined by the effect of two centering springs and by the pressure force related to the difference between the pressure p_S and p_T. If $p_S > p_T$, the spool of CV moves to the left, compressing the centering spring of CV located on the left side. As a consequence of the connection established by the CV, the CP shifts to the left, increasing the unit displacement. With the point A moving to the left, the linkage pivoted in point B further compresses the left side spring of the CV. This additional spring compression pushes the CV spool toward the right until a new equilibrium position is found. This is reached only when the spool returns at its neutral condition, with the left side spring of CV compressed by the effect of the difference $p_S - p_T$. In this way, the CP travels proportionally to the value of $p_S - p_T$.

The servomechanism implemented by the CV and the CP introduces a first order dynamic between p_S and p_T and the position x of the CP (more details on the dynamics of servomechanisms can be found in [22]), with a time constant related to the stiffness of the spring used in CV. This dynamic behavior permits attenuation of the uncontrolled acceleration problem mentioned before.

The servomechanism also avoids fluctuations of the control pressure p_T. In fact, the movement of CP does not affect the flow rate of the tachometric pump. This is still connected to one of the CV

spool ends; however, the diameter and travel of the spool are much smaller than CP. Therefore, the flow contribution generated by the spool CV moving is negligible with respect to Q_T.

27.4 Secondary Control Circuit with Electronic Control

The secondary control circuits in Figures 27.3 and 27.5 implement an electric control of the actuator speed (proportional to the current to the valve PV) with a fully hydraulic feedback of the rotational speed through the tachometric pump. These were some of the original secondary control circuits developed after the initial research in the 1980s and, in this book, they are very useful to understand the challenges related to this type of control, as well as to appreciate the elegance of such solutions created by the pioneers of secondary control.

Besides the complexity of the above described circuits and the losses associated with the tachometric pump circuit, these control solutions do not allow the unit to fully work on four quadrants (i.e. when the shaft speed is reversed) because the tachometric pump is not bidirectional. A four-quadrant fully hydraulic solution – based on a bidirectional tachometric pump – is possible with such control but becomes very complex, for example, in [24].

Modern solutions for implementing secondary controls take advantage of electric sensors for implementing the feedback signals of pressure, displacement, and speed. The displacement control is achieved with an electric proportional directional control valve, as represented in Figure 27.6. The response of the system is significantly improved because the full system pressure p^* is supplied to the CP. The control of the system is further improved by having an electronic speed sensor (such as a quadrature encoder) united to a displacement sensor and a spool position sensor, which allow a very controllable and repeatable behavior of the valve DCV.

The control valve DCV has a bias position 0 where both ports of CD are vented to tank, thus setting the actuator M to a null displacement at rest. As the current to DCV increases, the spool
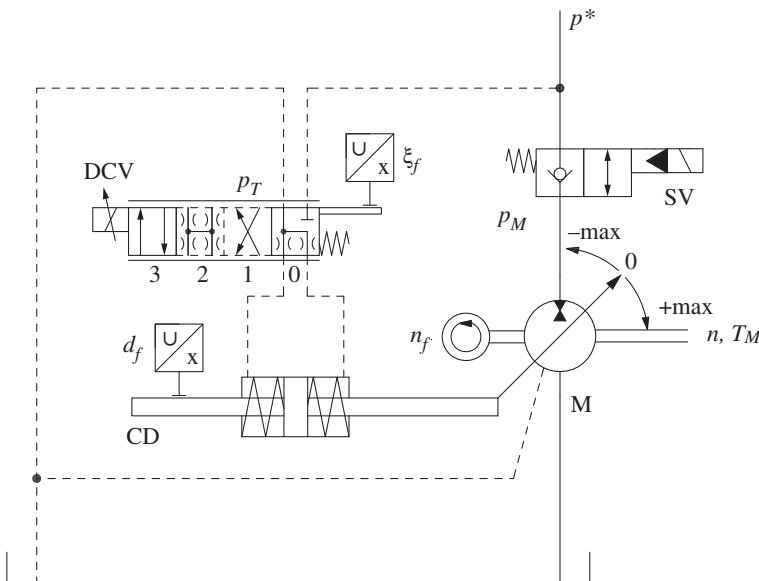
Figure 27.6 Secondary control unit with full electronic feedback of speed, displacement, and spool position.
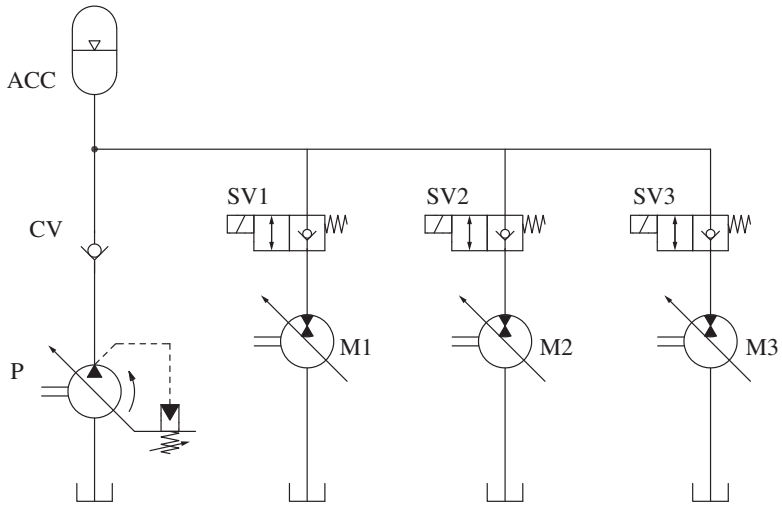
Figure 27.7 Secondary control circuit with multiple actuators.

shifts in position 1 (crossed arrow), which decreases the unit's displacement; position 2, which holds the displacement at the desired position (underlapped region, as described in Chapter 8); and position 1, which increases the displacement. During normal operation of the unit, the spool moves between positions 2 and 3 and positions 2 and 1.

27.5 Multiple Actuators

Despite the challenges represented by the control of the individual rotary actuators, the biggest advantage of secondary control systems is that the implementation of multiple actuator systems is extremely simple and efficient. Each actuator is connected in parallel and supplied from the primary unit. The pump and the accumulator are sized considering the duty cycle of the machine, namely the resistive and overrunning loads on each actuator. In fact, during the operation of the circuit, power can recirculate not only between the actuators and the accumulator, as seen before, but also between the actuators without involving the accumulator.

As shown in Figure 27.7, the circuit can control three actuators without any metering device. In case a linear function is also required in the system, this can be accomplished through a separate circuit or by using the same constant pressure supply and a metering element.

Problems

27.1 A secondary controlled HT is used to propel a hydraulic fan drive. The fan load characteristic follows the quadratic relationship $T[\text{Nm}] = 7 \cdot 10^{-6} \cdot n^2 \ [\text{rpm}^2]$. The fan needs to be controlled up to 4000 rpm, while the primary pump pressure compensator is set to 3000 psi. Determine the ideal sizes of the pump and motor for the transmission in order to achieve the required max speed. In addition, create a diagram representing the fan speed vs. the motor displacement in [%].

References

1 ISO 5598:2020 (2020). *Fluid power systems and components – Vocabulary*. https://www.iso.org/standard/67985.html.

2 ISO 4391:1983 (1983). *Hydraulic fluid power – Pumps, motors and integral transmissions – Parameter definitions and letter symbols*. https://www.iso.org/standard/10288.html.

3 Nervegna, N. and Rundo, M. (2020). *Passi nell'oleodinamica* vol. 1–2, Epics.

4 Zarotti, G.L. (1997). *Circuiti Oleodinamici – Nozioni e lineamenti introduttivi*. Cemoter.

5 Heybroek, K. and Sahlman, M. (2018). A hydraulic hybrid excavator based on multi-chamber cylinders and secondary control – design and experimental validation. *International Journal of Fluid Power* 19 (2): 91–105.

6 Heywood, J.B. (2018). *Internal Combustion Engine Fundamentals*, 2e. McGraw Hill.

7 Costa, G. and Sepehri, N. (2015). *Hydrostatic Transmissions and Actuators: Operation, Modelling and Applications*. Wiley.

8 Zorowski, C.F. (2016). *Design of Mechanical Power Transmissions, CreateSpace Independent Publishing Platform*, 1e.

9 Kress, J.H. (1968). Hydrostatic Power-Splitting Transmissions for Wheeled Vehicles – Classification and Theory of Operation. *SAE Paper No. 680549*.

10 Willis, R. (1841). *Principles of Mechanisms*. London: Longmans, Green.

11 Levai, Z. (1968). Structure and analysis of planetary gear trains. *Journal of Mechanisms* 3: 131–148.

12 Mistry, S.I. and Sparks, G.E. (2002). Infinitely Variable Transmission (IVT) of John Deere 7000 TEN Series Tractors. *ASME International Mechanical Engineering Congress Nov. 17–22 New Orleans. Paper IMECE2002-39347*. New York, NY: American Society of Mechanical Engineers.

13 De Pinto, S. and Matriota, G. (2013). A simple model for compound split transmissions. *Proceedings of the Institution of Mechanical Engineers, Part D: Journal of Automobile Engineering* 228 (5): 549–564.

14 Mikeska, D. and Ivantysynova, M. (2002). Virtual prototyping of power split drives. *Proceedings of Bath Workshop on Power Transmission and Motion Control PTMC*, Bath, UK, pp. 95–111.

15 Wouk, V. (1995). Hybrids: then and now. *IEEE Spectrum* 32 (7): 16–21.

16 Associated Press (2005). Hybrid-hydraulic powertrain generates world wide interest. *Detroit News* (29 June).

17 Brusstar, M. (2006). *Hydraulic Hybrids*. U.S. Environmental Protection Agency.

18 Wendel, G., Baseley, S., O'Brien, J., et al. (2007). Hydraulic hybrid vehicle system panel. *Michigan Clean Fleet Conference*. Detroit, MI.

19 Kepner, R. P. (2002). Hydraulic power assist – A demonstration of hydraulic hybrid vehicle regenerative braking in a road vehicle application. *SAE Technical Paper 2002-01-3128*.

20 Kelly, K. J., Mihalic, M., and Zolot, M. (2002). Battery usage and thermal performance of the Toyota Prius and Honda insight during chassis dynamometer testing. *The Seventeenth Annual Battery Conference on Applications and Advances*.

21 PSA-Peugeot-Citroen (2015). Hybrid air, an innovative full hybrid gasoline system. https://www.groupe-psa.com/en/newsroom/automotive-innovation/hybrid-air/.

22 Zarotti, G.L. (2003). *Trasmissioni Idrostatiche – Nozioni e lineamenti introduttivi*. Cemoter.

23 Nikolaus, H. (1977). Antriebssystem mit hydrostatischer Kraftübertragung. Deutsches Pat. P 27 39 968.4.

24 Kordak, R. (1996). Hydrostatic drives with secondary control. In: Mannesmann Rexroth Hydraulic Trainer Series, vol. 6. Mannesmann Rexroth GmbH.

Appendix A

Prime Movers and Their Interaction with the Hydraulic Circuit

The chapters of the book that presented the different layouts of hydraulic control systems, particularly Part III, Part IV, Part V, and Part VI, put their attention on the description of the hydraulic system behavior. The focus was mostly on the interaction between the components of the circuit and the effect of different loads. No particular considerations on the nature of the prime mover was made. This Appendix fills this gap, and it provides some descriptions on the interaction between different types of prime mover with the hydraulic system. Although the prime mover is not usually considered as a part of the hydraulic system, there is often a bidirectional cause–effect relationship between the behavior of the hydraulic system and the prime mover. To understand this mutual dependence, it is necessary to first understand the basics of prime movers. A designer familiar with the basic concepts of prime mover can optimize the hydraulic system design and make the best use of the primary source of power. In this Appendix, after some generic considerations, the fundamentals of diesel engines are first presented. These engines are the most common prime movers used in mobile equipment. The second part of the Appendix provides an overview of different electric motor technologies. The basics of operation and the different characteristics of electric machines are discussed. The last part of the Appendix focuses on power limiting controls for hydraulic pumps. These can be used to maximize the utilization of prime movers, without never exceeding the available power.

Objectives

This Appendix complements the contents of the book chapters in order to familiarize the reader with the different types of prime mover used in hydraulic systems. The reader will learn about the different types of prime mover and, more in particular, the interaction between the hydraulic system and the prime mover. After studying the contents of this Appendix, the reader will be able to:

1. Elaborate on the complexity of controlling the power transferred from a prime mover to a hydraulic system.
2. Describe the concepts of corner power and stall.
3. Formulate criteria for regulating the speed of a diesel engine based on the hydraulic torque demand.
4. Gain some familiarity with the most common types of electric motors, based on AC or DC supply.
5. Size electric power units for different applications.
6. Illustrate the concept of power limiting and torque limiting in a hydraulic pump.
7. Choose between the most commonly types of power controls available for hydraulic systems.

A.1   Corner Power Method and its Limitations

Before analyzing the different types of prime movers, it is important to recall some concepts regarding the power consumed by a hydraulic system. Some of these concepts were already mentioned in Chapter 25, which covered the sizing of hydrostatic transmissions.

When analyzing the coupling between a hydraulic pump and a prime mover, the first and easiest considerations can be made on the basis of the **corner power**. This is defined as the product between the maximum flow generated by the pump (i.e. when the prime mover reaches maximum speed) and the maximum pressure the loads can develop at the pump outlet. A hydraulic system is sized with the *corner power method* if the pump is selected so that its maximum demanded power does not exceed the prime mover available power. This is valid if the prime mover size is given. Vice versa, if the hydraulic pump size is given, the corner power method implies that the prime mover is chosen to satisfy the corner power of the hydraulic system. The corner power method represents a safe way of designing a system. It always ensures a consistent and continuous operation. Most of the systems studied in the book chapters assumes that the pump cannot overpower the prime mover.

> The **corner power** is the product between the maximum pressure and the maximum flow the supply pump can reach. A system designed according to the *corner power method* is such that the prime mover power is equal to the corner power.

The corner power method is a very good sizing method for systems designed for continuous and steady operation. However, very few hydraulic systems are designed following the corner power method, particularly in mobile applications. In fact, if the pump size is given, the corner power method leads to the selection of very large engines (or electric motors). Consequently, the cost and complexity of the overall system increases beyond reasonable values. Instead, if the engine size is a given parameter, this sizing method leads to relatively small pumps, thus limiting the machine performance.

Furthermore, it should be note that, in common applications, the simultaneous occurrence of high loads and high speeds is quite rare. Therefore, a system sized for the worst-case scenario would very seldom capitalize on the installed power. The prime mover would result in working most of the time far from the optimal efficiency. One significant example for understanding this aspect is the case of a hydraulic crane (shown in Figure A.1). The performance of this machine is mainly defined by two parameters: the load capacity and the lifting speed. When designing a new machine, these parameters are usually requirements the system needs to meet. Therefore, the designer will use these parameters to select of the and size of hydraulic components. The corner power method would lead to a system capable of delivering the maximum lifting speed at the maximum load. However, for a crane, this situation of simultaneous maximum speed and maximum load is unpractical and also dangerous. When the operator is handling a very heavy load, most of the times, he/she will command slow motion for the actuators. Instead, fast motions are desired when the crane is unloaded and is reaching the next working position.

The considerations made for the crane can easily be extended to several other machines, especially to mobile equipment where space and weight constraints are very important. At this point, if the corner power method is not the answer, what is the best way to select the right size prime
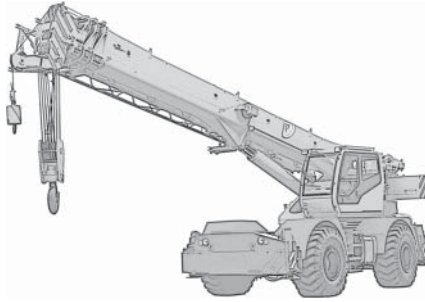
Figure A.1 A crane is a typical example of application where the combination of maximum load and maximum speed is not a desirable situation.

mover and pump for a given application? The best way to design these systems consists in choosing hydraulic components so that the hydraulic system has a corner power higher than the engine power. Such system will need to be equipped with a solution for limiting the power required by the pump(s), so that this power request is less or equal to the power available at the prime mover. This allows using the full pump capacity (flow) at low loads (pressures), while the available output flow decreases as the load increases.

> In many applications, particularly mobile equipment, the corner power of the hydraulic system is higher than the power available at the prime mover. In this case, the power requested by the hydraulic system should be limited, to avoid stalling the prime mover with excessive power demands.

A.2   Diesel Engine and its Interaction with a Hydraulic Pump

Many mobile hydraulic equipment is powered by diesel engines, contrary to passenger cars where most engines are of the gasoline type. This is because diesel engines better fit the operating conditions of hydraulic components.

Figure A.2 compares the full-throttle characteristic curves for a gasoline versus a diesel engine, of approximately the same size. The diesel engine works in a narrower speed range (typically from 700 to 2500 rpm) and achieves also its maximum power delivering a high torque (530 Nm, for Figure A.2) at a relatively low speed (1800 rpm). Contrarily, the gasoline engine operates on a much wider speed range (1000–6000 rpm), but it has a peak torque less than half of the diesel.

Hydraulic pumps are usually designed for working at speeds below 3000–3500 rpm, but this value usually goes down as the pump displacement increases. The only pumps that are designed to operate above 4000 rpm are found in aerospace applications., where the prime mover (a gas turbine) rotates at considerably higher speed reciprocating engines. Another important consideration pertains to the shape of the torque curve. For the case of the figure, the diesel engine torque curve is relatively flat above 1200 rpm. However, the gasoline engine torque decays quickly after it peaks at around 3800 rpm. Therefore, the diesel engine suits better the operating range allows for a more consistent operation of the hydraulic pumps, because the pump speed is less affected by the load variations.
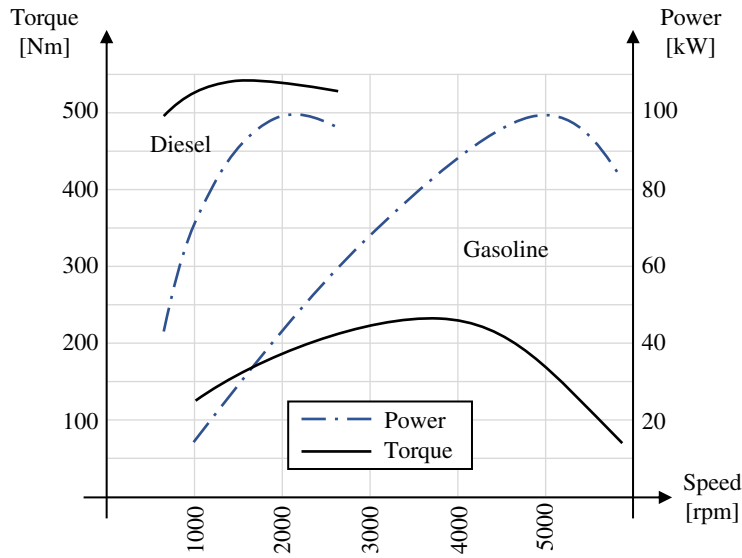
Figure A.2 Comparison of available torque (continuous line) and power (dotted line) for a gasoline and a diesel engine of similar size.

The diesel engine is more suitable to provide power to hydraulic pumps than gasoline engines. This is mainly due to their typical shaft speed range, which is convenient for most pump designs. Also, the diesel engine has an almost flat torque output curve, which makes the engine output torque not dependent on the loading conditions transmitted by the hydraulic circuit.

A.2.1 Diesel Engine Regulation

In operation the steady-state rotational speed of a diesel engine depends mainly on two parameters: the amount of fuel injected (or engine throttle) into the cylinders and the external load. Suppose a condition where the engine is running at a given speed. If the shaft load increases with no change in the amount of fuel injected, the engine will slow down. On the other hand, if the load decreases, the engine will speed up. The engine speed is kept within certain limits (idle and max speed) by the governing device.

The torque characteristic of the diesel engine for various throttle commands is detailed in Figure A.3. The figure shows various curves: the continuous line is the upper boundary and represents the maximum torque output of the engine, achieved at full throttle. This is usually the curve provided by manufacturers, as in the case in Figure A.2. However, the dotted curves represent the available torque for lower values of the throttle position, which relate to the fuel injection amount.

Figure A.4 takes as reference the situation where a diesel engine drives a hydraulic pump of a fixed displacement type. This basic coupling and can be used to illustrate the principle of the engine–pump interaction.

As initial condition, it is assumed that the engine throttle is set to the curve f_1 and the external load drives the pump at a certain pressure p_1, which generates a torque T_1. In this situation, the initial operating point of the engine is represented by X_1 and the resulting speed is n_{X1}.
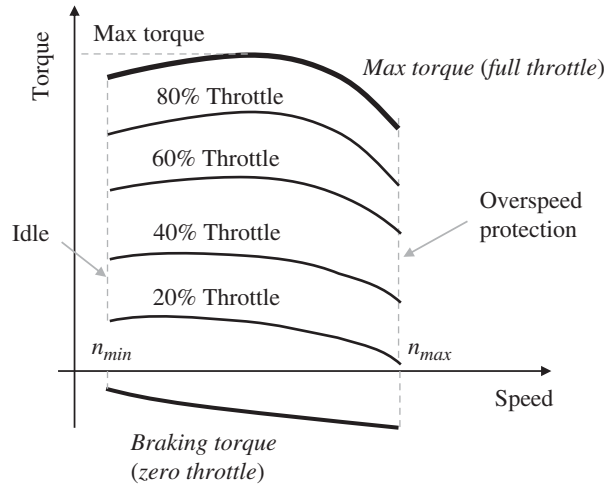
Figure A.3 Torque and power curves for a diesel engine. The chart shows how the torque is characteristic is a family of curves, which correspond to different levels of fuel injection.

If the external load changes, causing the pump pressure to raise to the value p_2, the resistive torque increases to T_2. At this point, there are two possible scenarios:

– *Torque-controlled engines.* The engine throttle stays at the value f_1; therefore, the operating point moves along the constant throttle torque curve to X_{2A}. The engine speed slows down to the value n_{2A}.
– *Speed-controlled engines.* The engine throttle increases to the level f_2, as reaction to the increased load. The constant engine throttle f_2 is indicated with a dotted line in Figure A.4). Therefore, the operating point moves vertically to X_{2B} with the speed staying at n_{X1}.
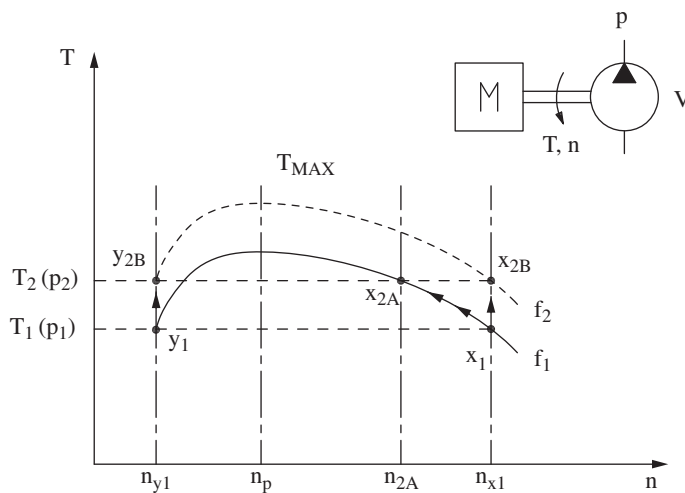
Figure A.4 Interaction between diesel engine and hydraulic pump.
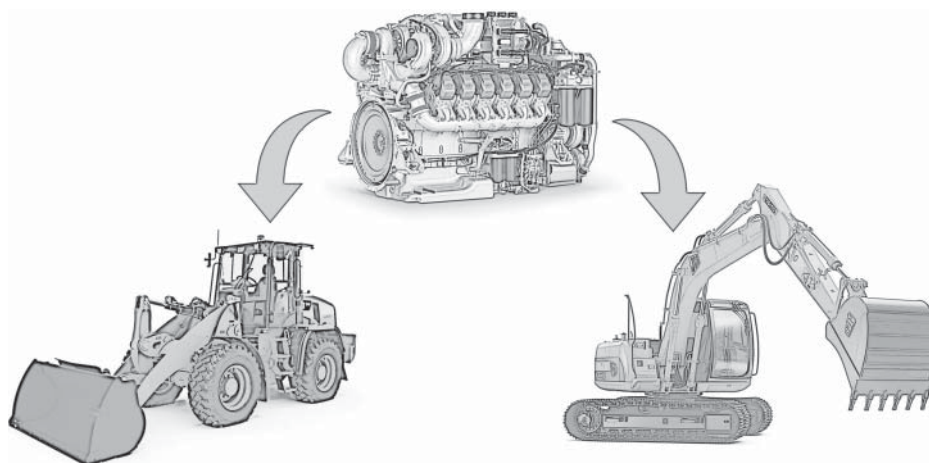
Figure A.5 Examples of machines powered by a diesel engine with different operating modes. The torque-controlled is typical for wheel loaders and the speed-controlled for excavators.

> There are two typical cases of engine regulators. In **torque-controlled** engines, the fuel injection is controlled by an input signal (e.g. gas pedal position) and, for a given input, it is maintained constant. On the other hand, **speed-controlled** engines are capable of automatically adjust the throttle in order to maintain a set speed.

These two types of regulation are found in most of the traditional applications (Figure A.5). A hydraulic excavator is a common example of speed-controlled engine: when the machine is running, the operator selects the engine speed in the cab. The engine governor adjusts the fuel injection in order to maintain the preset speed, while the torque changes as the external loads vary during the digging cycle. On the other hand, a wheel loader is an example of torque-controlled engine: here the operator pushes on the gas pedal that controls directly the amount of fuel injected to the cylinders. The engine speed is then determined by the torque generated by the balance of the various loads versus the fuel injected. In the case of torque-controlled engines, the speed governor intervenes at idle and for over-speed protection.

The design of engine speed governors has progressed throughout the last century, involving several solutions such as mechanical, hydraulic, and electronic devices (this is the case of most of the modern applications). The detailed design of the engine governor is not within the scope of this Appendix. More details can be found in the literature specific to internal combustion engines, for example, [1]. It is instead of interest to describe how the engine governor interacts with the hydraulic units connected to the engine.

A.2.2 Engine Stall

An interesting observation is about the shape of the engine torque curve, which usually has a slight downward concavity. In this curve, the torque peak T_{max} is located at an intermediate speed between the idle and the max speed. In the previous case, the operating point X_1 was located right of the peak. Therefore, a decrease in the engine speed was followed by an increase in the torque output. An interesting situation occurs when the operating point is located at the left of the peak torque. This can be the case of a system working at point Y_1 in Figure A.4. Here, a torque increases

to T_2, without a change to the fuel injection, would causes the engine to progressively reduce its speed, until a complete stop. This condition is generally indicated as **engine stall**. Usually, in a torque-controlled engine, the stall can be avoided by the operator (who feels the speed decreasing) by pushing on the gas pedal and increasing the fuel injection. In a speed-controlled engine, this occurs automatically, and the engine moves to point Y_{2B}. This consideration is valid until the fuel injection is below maximum. Once the fuel injection reaches the upper boundary curve, f_{max}, the speed-controlled engine behaves as a torque controlled. In both cases, the engine stalls if the external load overcomes the maximum engine torque at f_{max}.

A.2.3 Overrunning Loads

Diesel engines have the capability to operate with overrunning loads. This condition is represented by the low throttle curve in Figure A.3, which goes into the negative torque region. This feature is very important, for example, in passenger vehicles, where downhill roading conditions can be handled by the engine operating as a brake, so that the wheel brakes are not requested. For this reason, the braking capability of a diesel engine can be an important feature for certain vehicles using hydrostatic transmissions for the propulsion. In these systems (described in Part VI), the primary unit, which usually works as a pump, can also work in motoring mode (e.g. when the vehicle is braking or going downhill). In this case, the torque on the engine shaft is negative, meaning that the power flow is going from the primary unit to the engine. Modern electric controlled engines are capable of detecting this condition and automatically shut off the fuel injection, optimizing the fuel consumption.

A.2.4 Fuel Consumption

The operating point of the engine, which is determined by the loading of the hydraulic system, has important implications on the fuel consumption. For this reason, it can be useful to consider the consumption map of the engine. This consumption is normally expressed as **brake-specific fuel consumption**, in g/kWh. This parameter can be interpreted as the energy efficiency of the engine. A typical representation of the brake-specific fuel consumption for a diesel engine is shown with the contour line representation in Figure A.6.
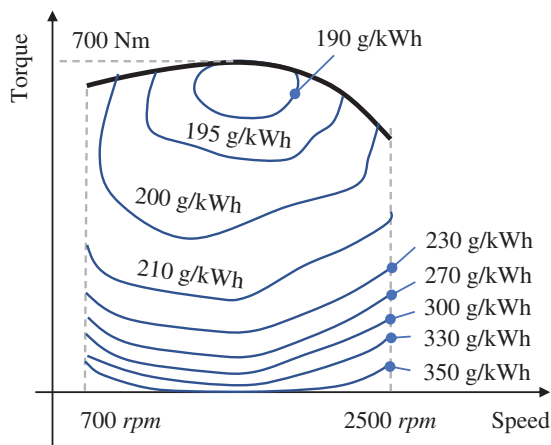
Figure A.6   Example of brake-specific fuel consumption map for 150 kW to 700 Nm diesel engine.

The knowledge of the efficiency map similar to Figure A.6 can be very useful for selecting the default speed of operation of a certain application, to promote higher fuel economy. During the last decades, several works have also described advanced engine controllers that use this kind of efficiency map to set the engine speed and throttle to meet the torque demand while always maximizing the engine efficiency.

A.3 Electric Prime Movers

When an electric motor is the prime movers of choice for the hydraulic system, two different scenarios can be encountered. In the first one, the electric motor is directly powered by AC from the grid. This is case, for example, of stationary industrial applications such as presses or injection molding machines. In the second scenario, the prime mover is powered by batteries, acting as a constant DC voltage supply. This is the case, for example, of industrial machines such as forklifts or mobile elevating work platforms. In the last years, the popularity of electric prime movers has increased among mobile applications. In fact, more and more stringent environmental and noise regulations are driving manufacturer to develop more and more electric hybrid (with downsized engine) or fully electric solutions.

This section covers the basic principles and the mechanical characteristics of three types of motors, which are commonly used in hydraulic applications. **Brushed DC motors** are the simplest type of motors used in combination with batteries. **Induction motors** are the most common type of motors used in industrial applications. **Synchronous permanent magnet motors** instead are gaining popularity in both mobile and industrial applications, due to their high efficiency and high power density. Similar to the Section A.2 dedicated to the diesel engine, the purpose of this section is to provide just a brief overview of the motor operation and point out the main features of the interaction between the hydraulic units used in a hydraulic system. Several textbooks are available to the reader interested in learning the basic principles behind the operation of electric machines, as well as their construction. Significant examples are [2–4].

A.3.1 Brushed DC Electric Motors

The principle of operation of *brush-type* DC motors is based on the interaction between two magnetic fields in relative motion: one is fixed and the other rotates with the motor shaft. Figure A.7 depicts this principle: the fixed magnetic field $\vec{B}$ is generated by the poles N and S. These are part
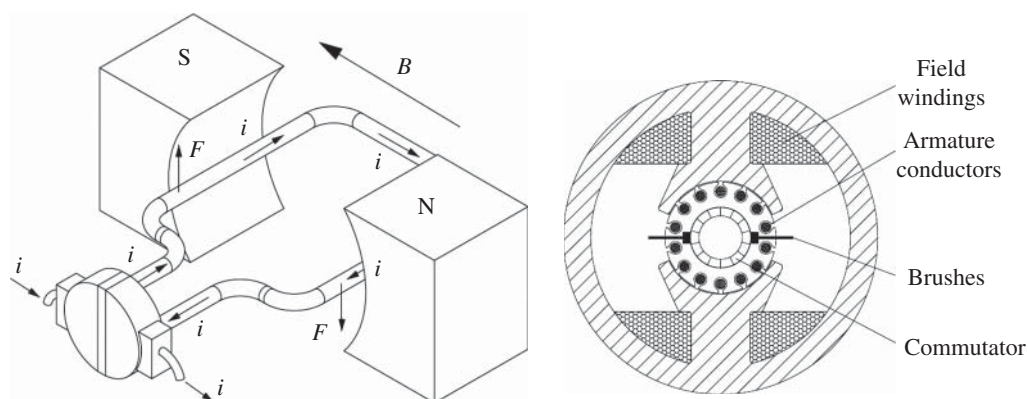
Figure A.7 Operating principle and simplified implementation of a DC brushed motor.

of the *stator*. The *armature* instead consists of a ring-shaped conductive material, which is free to rotate around the axis $\overline{AA'}$. The electrical current I flows around the armature and this loop generates the rotating magnetic field. The interaction between the two fields results in a torque propelling the shaft, rigidly connected to the armature.

One important part of these motors is the *commutator*. The commutator reverses the direction of the current in the armature every 180 degrees of rotation. In this way, the mechanical torque on the shaft maintains the same direction over the full shaft revolution. The commutator is equipped with contacts and *brushes*. These are usually considered one of the limiting factors of this type of motors. The brushes imply a certain amount of friction and, because of this, wear out over time. Their wear degrades the motor performance. Furthermore, the brushes are source of electrical noise and their design limits the amount of current that can be put into the armature. An excessive current would cause arcing.

Brushed electric motors are divided into two main design architectures: *self-excited* and *separately excited* motors. These are summarized in Figure A.8.

In *self-excited motors*, the magnetic field of the stator is generated utilizing field windings which are excited with the same voltage supply of the armature. If the windings are connected in series with the armature the motor is referred as *series wound*. In this case, the windings carry the same current as the armature.

If the stator windings are connected in parallel with the armature winding, the motor is referred as parallel wound, or also *shunt wound*. In this architecture, the full voltage is applied across the winding which sees a relatively small current (approximately 5%) of the rated armature current. It is also possible to realize motors where part of the winding is in series and part in parallel, these are known as *compound wound* motors.

In *separately excited motors*, the field winding is supplied from a separate power source, being electrically separated from the armature circuit. A particular case is represented by *permanent magnet DC motors*. In this design, the magnetic field of the stator is realized by using materials that retain their magnetic properties also in the absence of an inducing field or current. Permanent magnets are used to realize brushed motors, but they are very important in the implementation of brushless motors, which will be described in Section A.3.3.

The torque vs. speed performance of the various types of motors is visible in Figure A.9. Series wound motors present a very high torque at startup (zero speed), which quickly decays with speed. For this reason, they are usually applied as engine starters, for example, in cars. Shunt wound
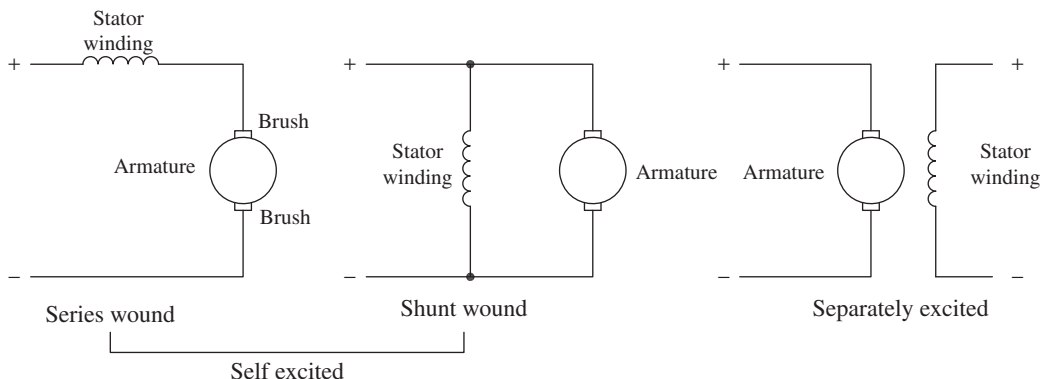
Figure A.8 Classification of DC brush motors based on type of excitation.
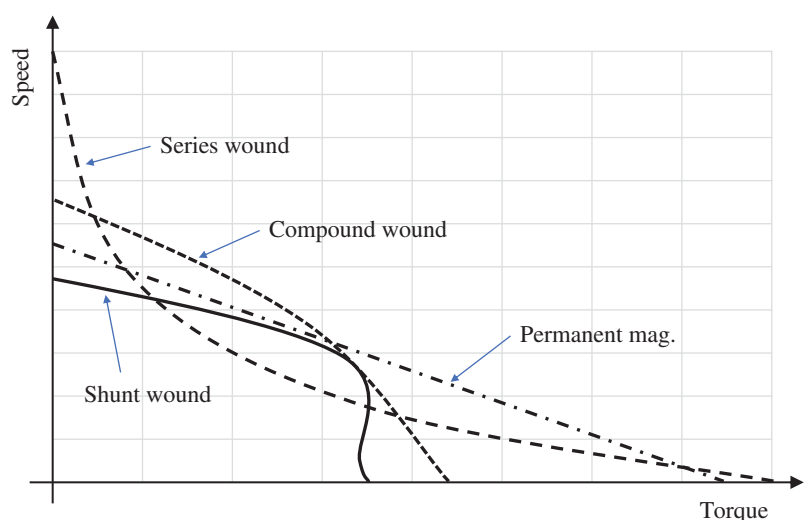
Figure A.9 Torque vs. speed curves for different types of DC brushed motors.

motors provide a lower startup torque, but this torque is more constant across the operating range. Compound wound motors combine the advantages of the two layouts, with an extended operating range with respect to the shunt wound. Permanent magnet brushed motors present the best performance curve with a linear characteristic and high startup torque. All these motor types can be used as prime movers for hydraulic systems.

A.3.1.1 DC Hydraulic Power Units

The combination of a DC motor with a hydraulic pump (in most cases of fixed displacement) is usually known as *hydraulic power unit* (**shown in** Figure A.10). DC brushed motors are usually combined with fixed displacement pumps and used in battery powered vehicles, where the power supply is provided by one or more electric batteries. Common supply voltages on mobile vehicles are 12, 24, and 48 V. The typical power range of such power units is up to 5 kW.

Motors applied to DC power units are usually permanent magnet type for applications below 1 kW or compound wound type for larger power requirements.
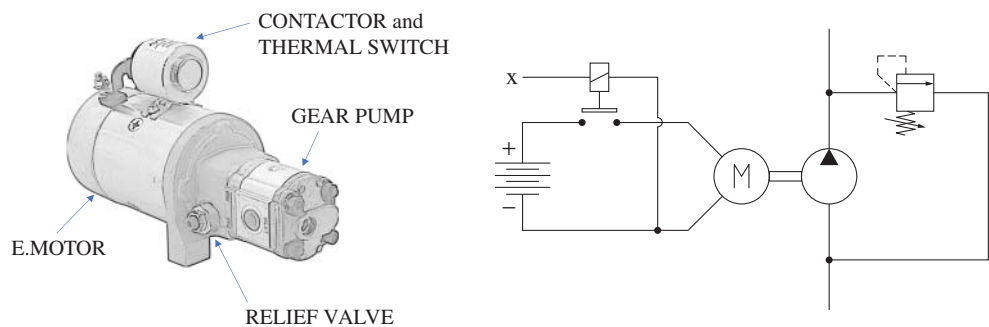
Figure A.10 DC power unit and equivalent schematic. A thermal switch (not represented) disables the contactor if the motor temperature exceeds a safety value.
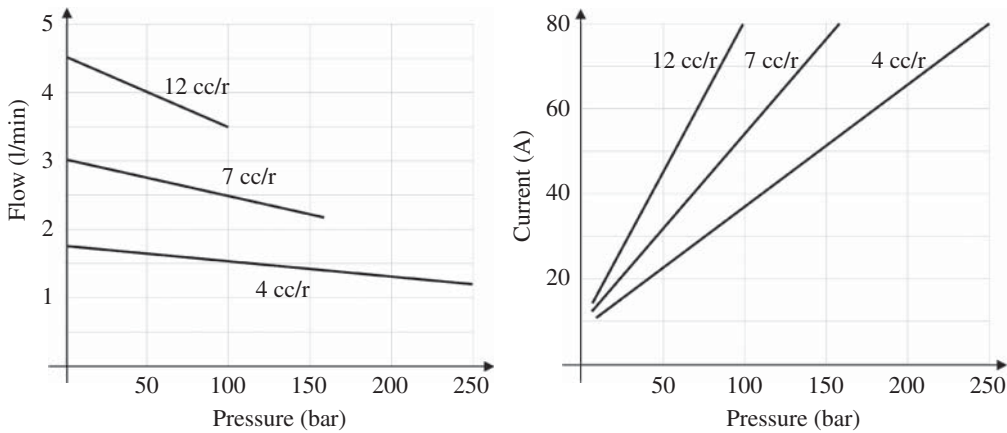
Figure A.11   Performance curves of a DC power unit using a PM motor for different pump sizes.

The characteristic of a DC power unit is obtained combining the torque vs. speed curve of the motor with the performance curve of the pump (i.e. pump efficiency). This is usually presented with a flow vs. pressure and a current vs. pressure charts. An example is shown in Figure A.11. The flow delivered to the system is not constant, but it is a function of the load pressure. As the load increases, the motor slows down and the current draw increases.

An important aspect that needs to be taken into consideration when using DC power units pertains to the duty cycle. In fact, these motors are not provided with a continuous cooling circuit. Furthermore, being the DC power units supplied by batteries, they are rarely applied to functions with continuous operation. A typical example of application can be small electric forklifts. In this machine, the power unit can be used for the lifting circuit. The lifting function is activated only intermittently, and after every lifting event there is a rest time in which the function is not used.

The duty cycle classification of electric rotating machines is described by standard IEC 60034. For the case of DC power units, three different duty cycle ratings are important:

i) *Continuous running duty* (S1). S1 usually indicates the operating limit (current) at which the motor can run continuously without overheating.
ii) *Short time duty* (S2). S2 represents the number of minutes at which the unit can run before reaching the thermal limit. S2 is a function of motor current (hydraulic pressure): the higher the current, the lower S2.
iii) *Intermittent periodic duty* (S3). A sequence of identical duty cycles consists of a time of operation at constant load and a time de-energized and at rest. S3 is usually indicated in % and represents the ratio between the "on" time and the overall cycle time for a given condition.

The power unit supplier usually specifies these ratings on a chart, as in Figure A.12. In this case, for example, the area S1 of continuous use is below 30 amp. Continuous currents above this value would overheat the motor, causing the thermal protection to stop it. If the operating point is, for example, 50 amp, the value of S2 is 7.5 minutes while S3 is 27%. This means that if the motor is used at 50 amp, it can run for maximum 7.5 minutes before overheating. When operating in intermittent cycles, the motor must rest for 73% of the time. For example, in a 10-minute period, the motor can work at 50 amp for 2.7 minutes and needs to rest for the remaining 7.3 minutes. On a 20-minute period, it can run for 5.4 minute and must rest for the following 14.6 minutes.
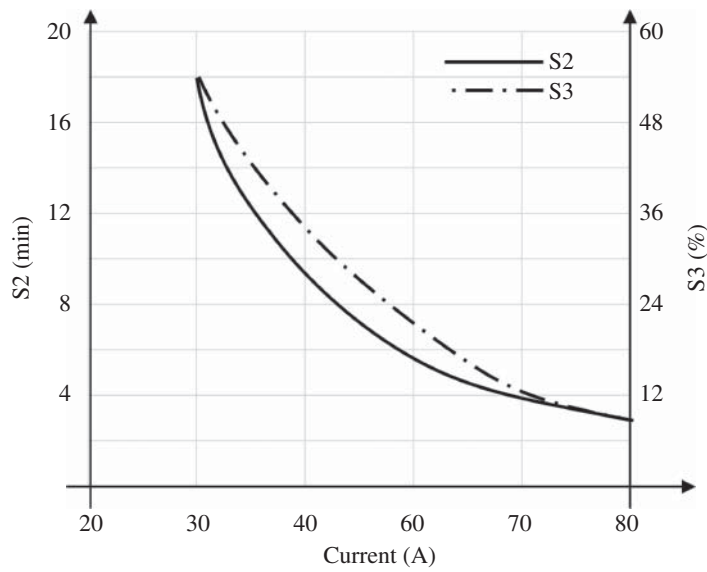
Figure A.12   Example of duty cycle ratings for a DC power unit.

The considerations made above assume that the DC power unit is controlled as an on/off device. This is typically achieved through a contactor. When the contactor is activated, the motor starts running and the operating speed is defined by the hydraulic load (current draw).

In certain applications, the DC power unit can be controlled in a proportional way. This means that the operator (or the controller) can set the flow delivered by the pump by regulating the motor speed. For DC brushed motors, this is achieved by controlling the current to either the armature or to the field winding. The current reduction shifts the torque curve downward, similarly to the effect of the fuel injection on the diesel torque characteristic previously described. The control of the current can be implemented in several ways: two very simple methods are shown in Figure A.13. This type of control of the motor current implies dissipation of power across the variable resistor.
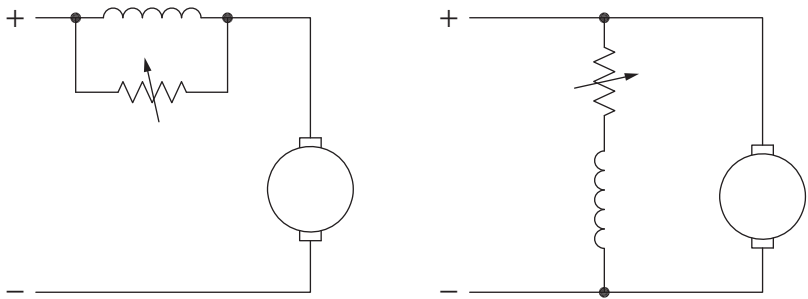
Figure A.13   Two simple methods for controlling the speed of DC motors. The variable resistor adjusts the current passing through the field winding.

Example A.1   DC power unit sizing

A trailer is equipped with a lifting platform powered by a DC power unit running from the truck battery of 24 *V*. This platform is used to load or unload the trailer and it is moved by a lifting cylinder whose piston volume (to obtain a full extension) is 4.5 *l*. The lifting of the platform requires up to 140 *bar* and it needs to be accomplished in less than 45 *s*. During the loading or the unloading of the trailer, the lifting system can be operated once every 9 *min*. The charts below represent the operating characteristics of four different power units built combining the same 2 *kW* DC motor with four different pumps. Select the pump with the correct displacement for the application.
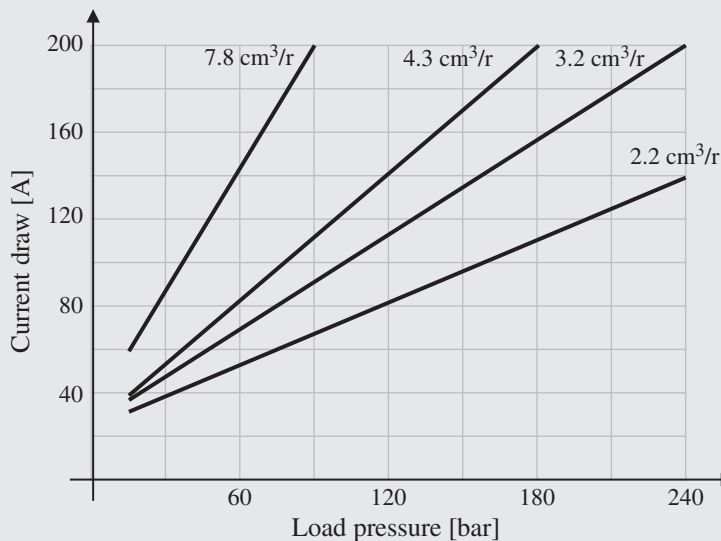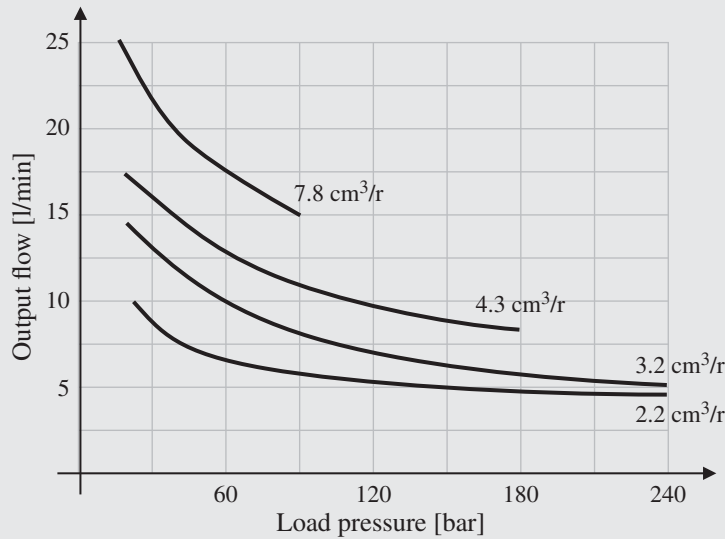
Example A.1 (Continued)
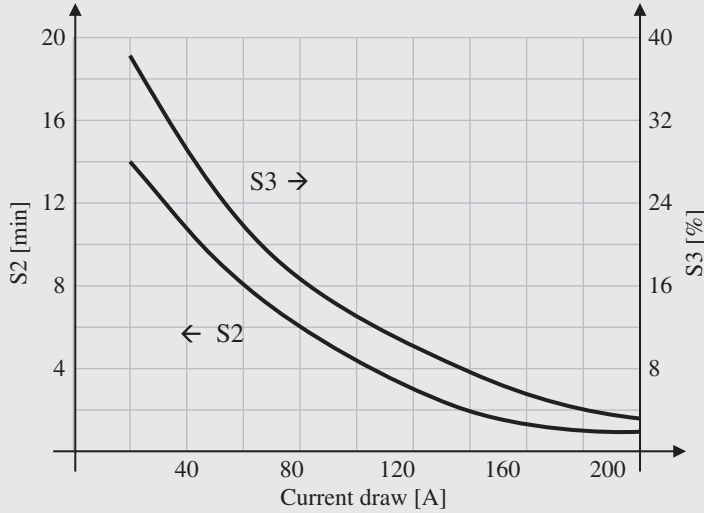
Given:
System voltage: 24 V (DC)
Electric motor rated power: 2 *kW*
Lift cylinder volume, $V_C = 4.5\,l$
Max lifting pressure, $p_{max} = 140$ *bar*
Maximum lift time, $t_{max} = 45\,s$
Duty cycle: one lift every 9 *min*

Find:
Pump displacement V_D

Solution:
Knowing the cylinder volume and the maximum allowed time, the minimum flow rate of the power unit needs to be

$$Q_{PU,min} = \frac{V_C}{t_{max}} = \frac{4.5\,[l]}{45\,[s]} \cdot 60 = 6\,l/min$$

The flow needs to be reached at a working pressure of 140 *bar*.

Looking at the first chart one can notice that the 7.8 cm^3/r pump cannot reach the desired pressure because it would overload the electric motor. Also, the 2.2 cm^3/r cannot provide the desired flow rate.

The first option, to maximize the lifting speed, is to select the 4.3 cm^3/r pump. This provides approximately 9 *l/min* at 140 *bar*. Looking at the second chart, the current draw by this power unit at 140 *bar* is 165 *A*. Using these data in the duty chart, 160 *A* corresponds to an S2 of 1.4 *min* and an S3 of 5%.

In other words, since the power unit provides 9 *l/min*, the lifting cycle can be achieved in

$$t_{4.4} = \frac{V_C}{Q_{PU}} = \frac{4.5\,[l]}{9\,[l/min]} \cdot 60 = 30\,s$$

This value is below the short time duty S2 of 1.4 *min*. The value of S3 defines an intermittent duty of one cycle (30 *s*) every interval Δt, where

$$\Delta t = \frac{t_{4.4}}{S3} = \frac{30\,[s]}{5[\%]} \cdot 100 = 600\,s = 10\,min$$

This value is too high, since the requirement is to run the unit at most once every 9 *min*.

Therefore, the lower pump displacement (3.2 *cm³/r*) needs to be investigated. In this case the power unit provides a flow of 6.5 *l/min* at 140 *bar*. The current draw is 130 *A* and S2 is 2 *min* and S3 is 8%.

Since the power unit provides 6.5 *l/min*, the lifting cycle can be achieved in

$$t_{3.2} = \frac{V_C}{Q_{PU}} = \frac{4.5\,[l]}{6.5\,[l/min]} \cdot 60 = 41.5\,s$$

This value is below the short time duty S2. The intermittent duty allows one cycle (41.5 *s*) every interval Δt, where

$$\Delta t = \frac{t_{3.2}}{S3} = \frac{41.5\,[s]}{8[\%]} \cdot 100 = 520\,s = 8\,min\ and\ 40\,s$$

This value is acceptable; therefore, the 3.2 *cm³/r* is the correct pump sizing for the application.

A.3.2 Induction Motor (or Asynchronous Motor)

Induction motors, often also referred to as *asynchronous motors*, are the most common prime movers encountered in industrial stationary applications because of their simplicity and good efficiency and especially because they operate with AC voltage supply, which is available from the network. However, when induction motors are used in mobile applications, the voltage supply usually comes from batteries and an inverter is required to generate AC.

From a very high level, the principle of operation of the asynchronous machine is based on the interaction of two magnetic fields, rotating at different speeds. This creates a mechanical torque on the shaft. Figure A.14 provides a simple representation of a conductive loop inside a magnetic field $\vec{B}$. The field is rotating at a given angular velocity ω around the axis $\overline{AA'}$. Consequently, a current is induced inside the loop (Faraday's law). This induced current creates another magnetic
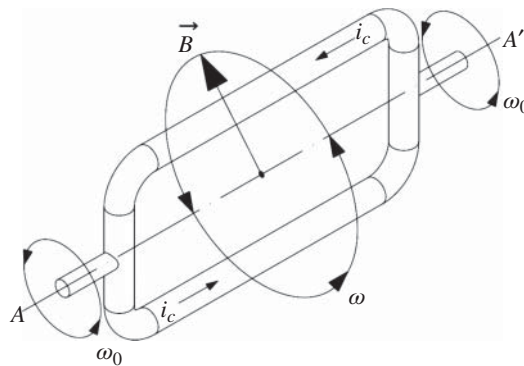
Figure A.14 The principle of operation of AC motors can be represented as a conductive ring surrounded by a rotating magnetic field.
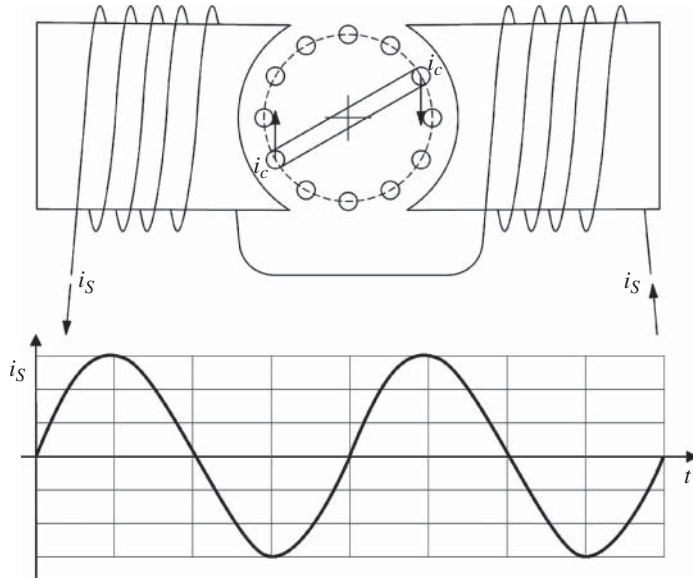
Figure A.15   Induction motor implementation with a single-phase current.

field, perpendicular to $\vec{B}$, which opposes to the change produced by $\vec{B}$ (Lenz's law). The interaction between the two fields causes the ring to turn around the same axis $\overline{AA'}$, with a speed ω_0. The above considerations are valid until the rotating speeds of the magnetic field ω and the ring ω_0 are different. If the two speeds were the same, the torque generated on the ring would be null. From this fact, this motor is named asynchronous: the speed of the rotor will always be smaller than the speed of the magnetic field.

Figure A.15 shows a simplified cross-section of an induction motor, based on a single-phase current. The magnetic field $\vec{B}$ is generated by the alternating current i_S. The windings carrying i_S are referred to as *poles*. A motor presents always an even number of poles, in this case two. The rotor is implemented with an armature holding several staggered shorted wire loops. This assembly is often referred to as *squirrel cage*. Since the supply current i_S follows a sinusoidal trend, the field $\vec{B}$ appears to the squirrel cage as a rotating field. This generates the induced opposing magnetic field in the rotor, which results in the induced current i_C.

Fluid power applications using induction motors typically use a three-phase induction motor type. An example of such layout is represented in Figure A.16: each phase (A, B, and C) presents three two-pole (or one pole pair) stator windings. One important property of this layout comes from the fact that the three-phase sinusoidal currents are shifted by 120°: this generates a rotating magnetic field of constant magnitude.

The value of the synchronous speed n_s is affected by the architecture of the motor. The one presented in Figure A.16 has two poles, i.e. one pole pair for each phase. The relationship between the number of poles N and the value of n_s is the following:

$$n_s \left[rpm \right] = \frac{f \ [Hz]}{N} \cdot 120 \tag{A.1}$$

f is the frequency of the supply, and it is usually equal to 50 or 60 Hz. A motor with two pole pairs with 60 Hz supply has a synchronous speed of 3600 rpm. In industrial hydraulic power units, motors with four poles are very common. This corresponds to a value of $n_s = 1800$ rpm. This is the main reason for which most industrial pumps are optimized for the operation at such speed.
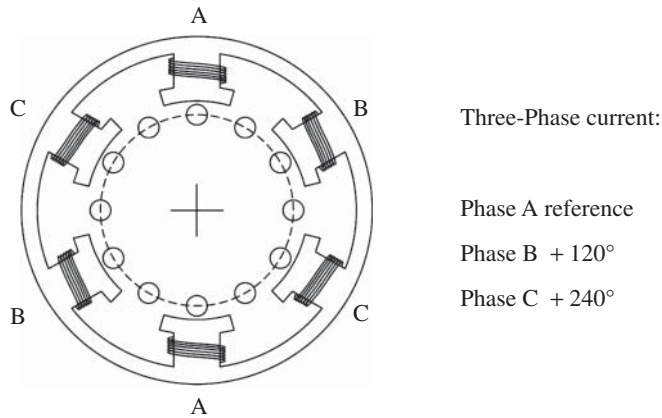
Figure A.16 Three-phase and two-pole induction motor: the rotating magnetic field is created by the sequential excitation of the pole pairs by the three-phase supply.

The performance characteristic of an induction AC motor is usually represented in a torque vs. speed chart. A typical representation of this curve, which provides the torque delivered by the motor at different shaft speeds, is shown in Figure A.17. This figure indicates following important parameters of the motor:

- *Breakaway rotor torque (starting torque).* This is the minimum torque, which the motor develops at rest for all angular positions of the rotor.
- *Breakdown torque (peak torque).* This is the maximum torque the motor can develop. This is an intermittent point of operation and usually is much higher than the rated torque for continuous use. For example, in the chart of Figure A.17, the breakdown torque is almost three times the rated load torque.
- *Pull-up torque.* This is the minimum torque developed by the motor when accelerating from rest to the breakdown torque point.
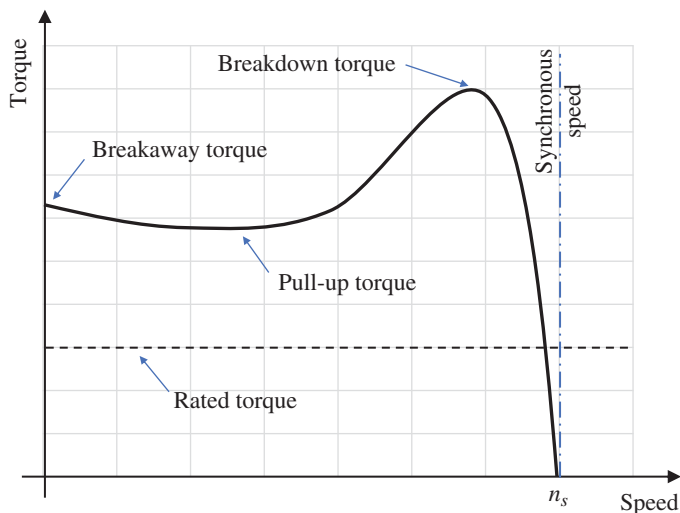
Figure A.17 Typical characteristic of an AC asynchronous induction motor.
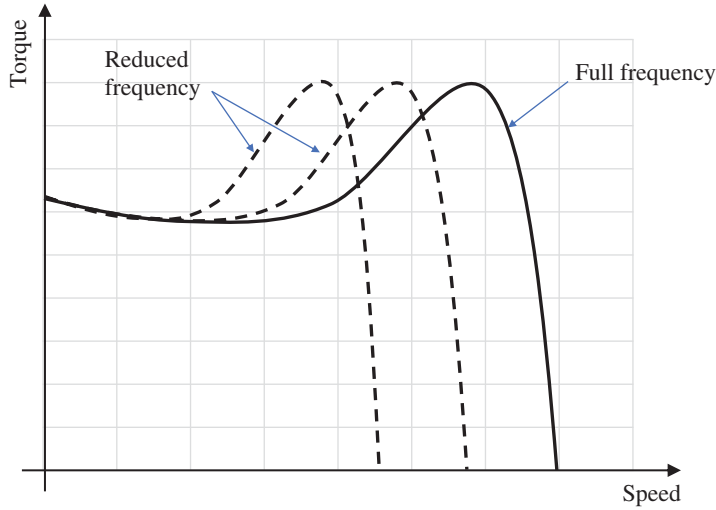
Figure A.18 Characteristic of an AC induction motor with variable frequency drive.

- *Rated load torque*. This is the maximum torque the motor can continuously produce (S1 duty) without overheating. Operating a motor overloaded for an extended period will cause an excessive heat buildup in the motor and may eventually burn up the motor windings. The AC induction motors in hydraulic power units are usually conceived for continuous applications; therefore, the maximum hydraulic torque is selected within the limit of the rated load.

In Figure A.17, the upper limit of the motor speed is represented by the synchronous speed n_s, which corresponds to a zero-torque value. In other words, the motor can never exceed the speed n_s. During regular motor operation, the motor works at a load lesser or equal than the rated torque. In this area the torque curve is almost vertical, and the speed is very close to the synchronous value. The difference (in percentage) between the synchronous speed n_s and the actual speed n_m of the motor is usually defined as *slip s*:

$$s\ [\%] = \frac{n_s - n_m}{n_s} \cdot 100 \tag{A.2}$$

Typical values for the slip are in the range of 0.5–5%.

Equation (A.1) also shows how the synchronous speed varies with the supply frequency. This method is commonly used to achieve speed control of induction motors. **Inverters** and **variable frequency drives** are electrical machines capable of continuously varying the motor supply frequency and they are commonly used to control induction motors. Figure A.18 shows the characteristic torque of a motor with an inverter realizing a *variable frequency drive*.

Induction motors are relatively simple machines, they do not require permanent magnets, brushes, commutator rings, or shaft position sensors. On the other hand, one of the main limits of common industrial AC induction motors is represented by their current consumption at startup. The area of the characteristic located at the left of the pull-up torque is usually characterized by a poor motor efficiency. Therefore, the current demand can easily spike to high values. For this reason, in hydraulic power units, the pumps driven by the AC motor are usually provided with an unloading valve, that is used at startup for minimizing the current consumption. Figure A.19 shows the example of a typical power unit with a variable displacement piston pump.
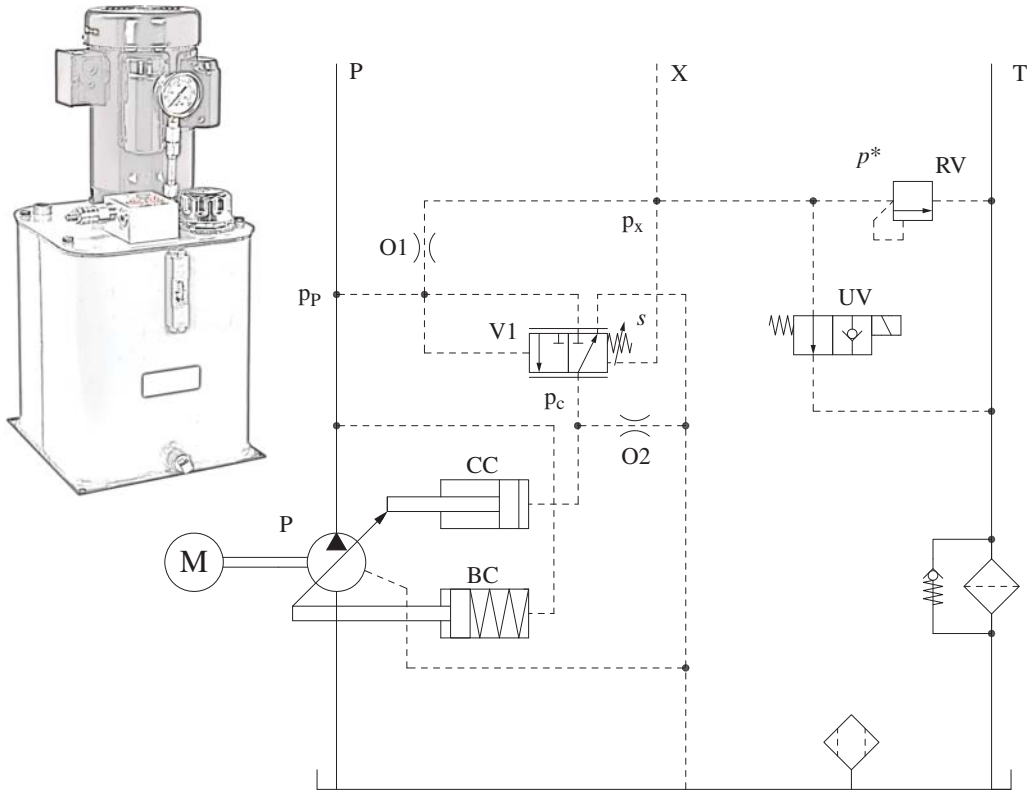
Figure A.19 Hydraulic power unit with induction motor and variable displacement pump equipped with unloading valve.

A.3.3 Synchronous Motor

The principle of operation of synchronous motors is also based on the interaction between two magnetic fields. One of the fields is rotating at synchronous speed and it is generated with poles and wires, in the same fashion as for the induction motor. In this case, the rotor is made of a permanent magnet material, which intrinsically provides a constant magnetic field. As represented in Figure A.20, north and south poles of the permanent magnet align with the opposite poles of the
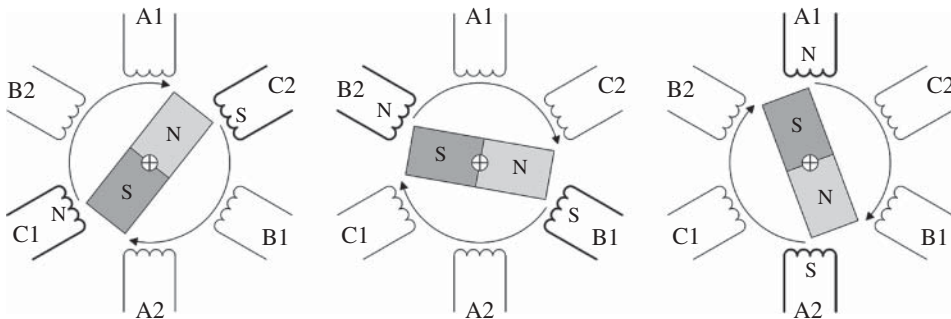
Figure A.20 Principle of operation of a synchronous motor with three pole pairs. The permanent magnet follows the rotating field at the same speed.
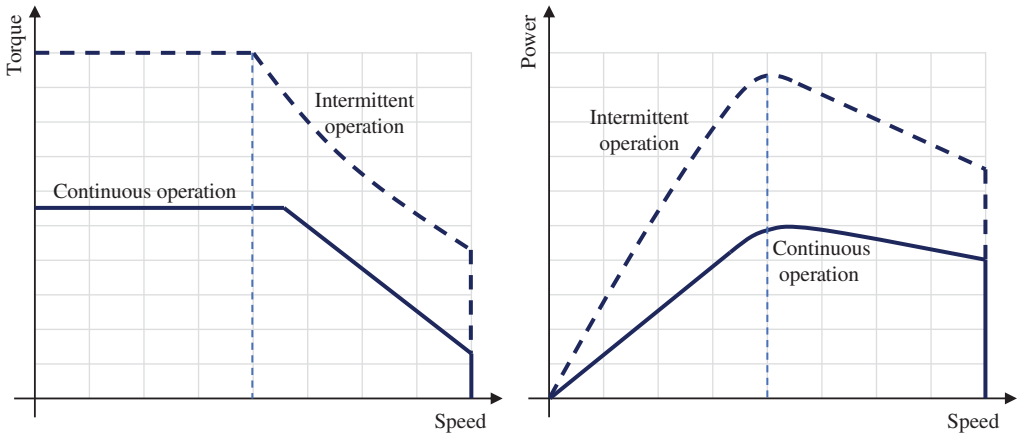
Figure A.21   Typical torque and power characteristics of a synchronous motor.

rotating field. In other words, the rotor gets locked to the rotating field and follows it with the same synchronous speed.

Synchronous motors always need a controller to manage the current through the poles and thus control the speed of the magnetic field. Figure A.21 shows the typical torque vs. speed characteristics of these machines. The motor can deliver full torque at zero motor speed. The continuous rating of the motor is affected by the type of cooling utilized. When the motors are liquid cooled, they can deliver a very high torque and power in a very compact package.

With respect to asynchronous motors, synchronous machines have much higher power density (approximately 30% gain) and they can work much more efficiently over a wide speed range. In fact, the absence of the squirrel cage loops results in higher efficiency since there are no current dissipations.

On the other hand, this energy performance gains come with a price due to

– the rare earth magnetic material used for the rotor;
– the more complex control structure, often requiring position feedback encoders, used for example to align the magnetic fields at startup.

Permanent magnet motors are becoming increasingly popular in mobile applications, where size, weight, and efficiency are very important. However, there are other motor designs using electromagnets instead of permanent magnets. These machines are usually applied to very large applications (like locomotive or power plants), which fall outside the scope of the book. For more insights on design, control and other features of synchronous motors, the reader can refer to [2–4].

A.4   Power Limitation in Hydraulic Pumps

As shown in Section A.2, every prime mover has a limited amount of torque that can be delivered at the shaft, which is usually a function of the rotational speed. When the prime mover is coupled to one or more hydraulic pumps, the pump displacement and the working pressures can be selected in such a way that the shaft torque remains below the prime mover torque limit. As mentioned at the beginning of the Appendix, this sizing principle is known as *corner power method*. This method is conservative and works well for applications that operates around a known pressure. However, for less predictable applications, this method can easily underutilize the available installed power,

which is reached only at high pressures. In this case, the productivity of the system can be enhanced by equipping the hydraulic circuit with solutions for controlling the amount of torque required by the hydraulic units. A high torque can be reached with high flows and low pressures, as well as low flows and high pressures. The following Sections A.4.1 and A.4.2 present some simple methods for implementing a torque limited supply (often referred as power limited supply), using fixed or variable displacement pumps.

One important remark is that all torque limiting devices act on the supply pump(s) by reducing the output flow for increasing load pressures. Therefore, when the torque limiter is active, the output of the pump decreases, and the function speeds might not meet the operator demand (flow saturation). For this reason, systems using torque limited pumps are often equipped with flow sharing valves.

A.4.1 Torque Limiting Using Fixed Displacement Pumps

The simplest way to create a power limited system is to use two fixed displacement pumps, arranged as in the circuit shown in Figure A.22. Pump P1 is the primary unit and it always supplies flow to the system. The pressure of P1 is limited by the pressure relief valve PC1 set to the pressure p_1^*. Pump P2 also supplies flow to the system, but its maximum pressure is limited by PC2. Differently from PC1, PC2 is not a pressure relief valve but instead a sequence valve, which is controlled by the outlet pressure of P1. The two pump outlets are connected by a check valve, CV1, which allows free flow from P2 to P1 but blocks the opposite path. The setting of the sequence valve PC2 is p_2^*, which must be lower than p_1^*.

Figure A.23 represents the operating characteristic of the system: when the load pressure is below p_2^*, both pumps supply flow to the hydraulic circuit. If the load pressure reaches or overcomes the value p_2^*, the sequence valve PC2 completely opens and the pump P2 is unloaded to the tank, ideally at zero pressure. Under this condition only P1 is supplying the system. It is important to remark that PC2 is not a relief valve. In case a pressure relief valve is used in place of PC2, the pump P2 would remain at p_2^*, causing a significant energy loss. However, the sequence valve allows to completely open its passage to the tank, when the load pressure overcomes p_2^*. The flow of P2 is then returned
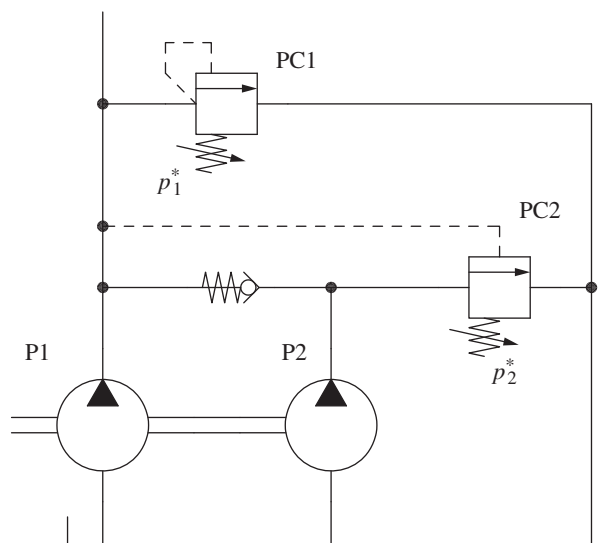
Figure A.22 Torque limitation using two fixed displacement pumps.
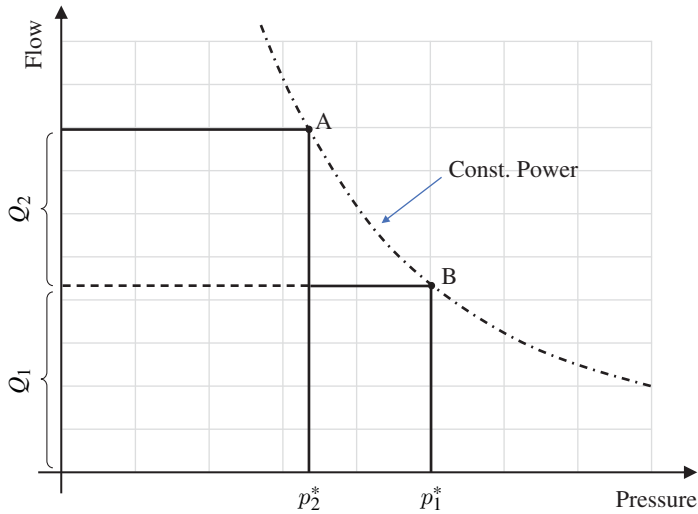
Figure A.23   Operating areas of a power limited supply using two fixed displacement pumps.

to the tank from a low-pressure value, ideally null, but in reality determined by the pressure drop across the fully open valve.

The values or the pump displacements and the pressure setting of the two valves OC1 and PC2 are not arbitrary. They need to be selected in order to have points A and B (on the chart in Figure A.23) located on the constant power curve, matching the available power from the prime mover.

A.4.2   Torque Limiting Using Variable Displacement Pumps

Torque limiting becomes more interesting when variable displacement piston pumps are utilized. In fact, in this case, it is possible to generate control mechanisms capable of accurately following a constant power curve.

A common type of torque limiting control applied to a swash plate piston pump is shown in Figure A.24. The pump displacement is adjusted by a control piston (CP) and a bias piston (BP) similarly to what shown in Chapters 16 and 17.

The bias piston (located at the top of the figure) is always connected to the pump outlet pressure and pushes the pump on-stroke. The control piston (at the bottom of the figure), has a larger diameter and it is supplied by a variable pressure, determined by the position of a 3/2 proportional valve (PV). When the valve PV is in neutral position 0, the control piston is drained to the tank and the pump is kept at maximum displacement by the bias piston BP. When the valve PV shifts toward position 1, the pressure to the control piston is increased and the pump displacement is reduced. The position of PV is determined by the effect of a soft spring (without adjustment arrow) and a plunger, which is in contact with an L-shaped linkage. On the other side of the plunger, the linkage is in contact with a stiff spring, which the load can be externally adjusted. The bias piston BP contains also a third piston actuator, TA: this is supplied by the pump outlet pressure and travels together with BP. TA is in contact with the bottom arm of the L-shaped linkage.

Figure A.25 shows a better insight on the operation of the power limiting control: the adjustable spring is set to the value *s*. The L-shaped linkage pushes against this spring. The soft spring on the opposite end does not provide a significant force, but it is used to keep PV in contact with the linkage. The contact point is indicated as C.
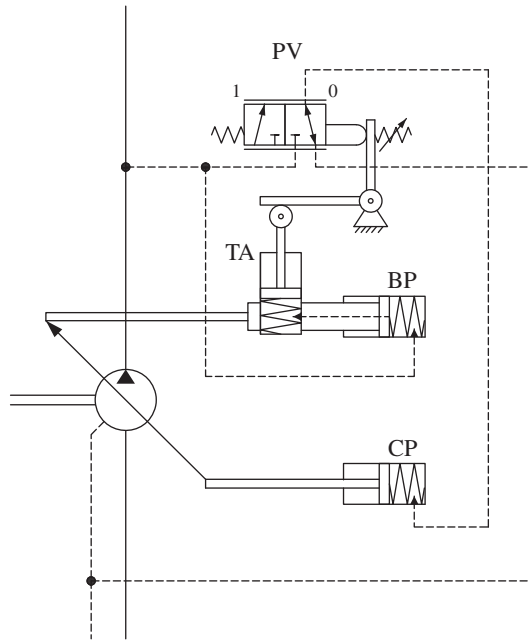
Figure A.24 Common method for limiting the torque for an axial piston pump.

The linkage is identified by three significant points: A is the point of contact between TA and the horizontal lever, B is the pivot point, and C is the point of contact between the vertical lever and the spring *s*. The torque actuator TA is supplied by the pump pressure *p* and moves together with the bias piston BP; therefore, the length of the segment $\overline{AB} = x$ varies with the pump displacement. In particular, when the displacement of the pump is set to zero, $x = x_0$. When the pump is at full displacement $x = x_{max}$. On the other hand, the distance $\overline{BC}$ is constantly equal to *y*.

The torque actuator TA has an area of influence Ω and it is subject to the force of a spring (with value F_s) and to the pump outlet pressure. Therefore, the resulting horizontal force against the adjustable spring *s* is:

$$h = \frac{(F_s + p\Omega) \cdot x}{y} \tag{A.3}$$
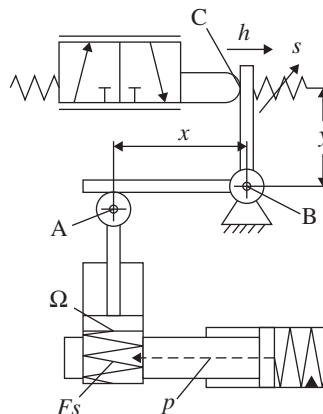
Figure A.25 Detailed operation of the power limiting device.

When the outlet pressure of the pump is null, PV is in neutral position and the pump delivers full flow. As the outlet pressure increases, the force h also increases according to Eq. (A.3), until becoming greater than the force of the adjustable spring s. This causes the spool to shift and the pump to reduce its displacement, since the control piston pressure is increased. Meanwhile, the reduced displacement decreases the value of x, which, in turn, decreases the value of h. The pump displacement mechanism sets to a new equilibrium position characterized by a higher pressure and a reduced displacement.

Assuming in the first approximation that the relationship between x and the pump displacement is the following[1]:

$$d = k \cdot \left(x - x_{\min}\right) \tag{A.4}$$

where k is a constant, the equilibrium position of this swash plate as a function of the outlet pressure is defined as follows:

$$d = k \left(\frac{sy}{F_s + p\Omega} - x_{\min}\right) \tag{A.5}$$

Equation (A.5) defines the relationship between the pump allowed displacement vs. outlet pressure. This relationship is hyperbolic, which corresponds to a constant power condition (assuming the prime mover speed remains constant) as in Figure A.26.

Figure A.27 shows how the power limiting control can be integrated with a pressure limiter (PVP) and a load sensing spool (PVL). These work in the same fashion as the ones described in Chapter 16, for the LS pump. The torque limiter PVT spool, which was previously connected to the internal drain, is now connected to the signal generated by the LS and max pressure control spools. In this way the torque limiter can reduce the pump displacement command coming from PVP and PVL but it cannot increase it.

Besides the arm linkage mechanisms shown in the previous example, another common power limiting control architecture is based on a cam actuated relief valve. The principle is shown in Figure A.28. The pump is equipped with a load sensing control (PVL spool) with two relief valves, RV1 and RV2, connected in parallel to the load sensing signal line. The pump control mechanism
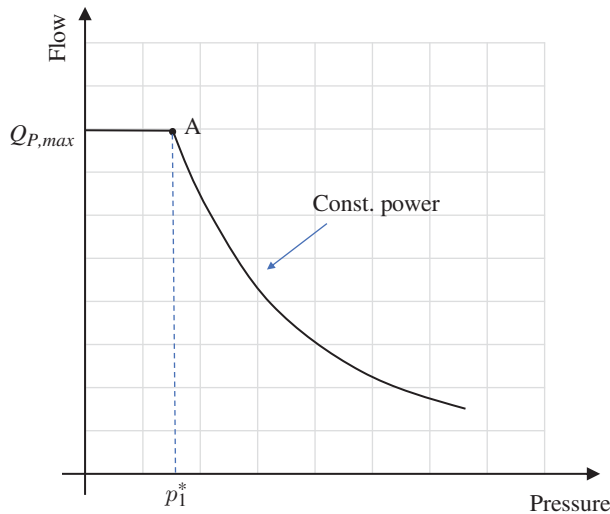
Figure A.26 Pressure–flow characteristic of a variable displacement pump with power (torque) limiter.

---

[1] This assumes that the relationship between displacement and swash plate angle is linear, which is a good assumption for small swash plate angles.

Figure A.27 Power limiting control integrated with load sensing and max pressure spools.

Figure A.28 Torque limiting control based on a cam-adjusted relief valve.
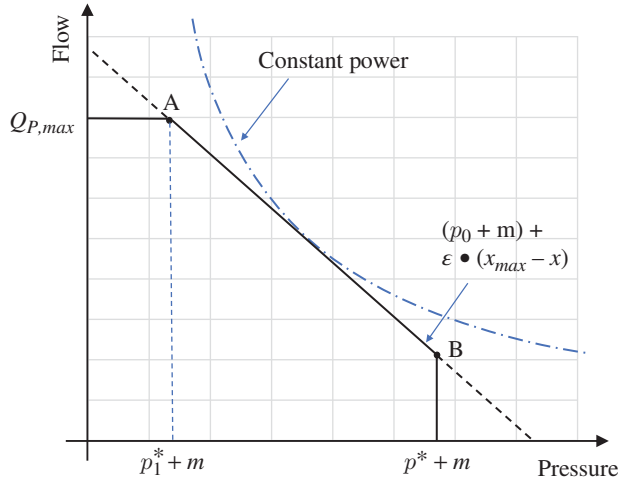
Figure A.29 Operating area for a cam-operated torque limiting control.

it is also furnished with a cone-shaped cam, built in the stroking piston rod. This cam acts on the spring of RV2, so that its spring load p_t^* is minimum at full displacement and increases while the pump reduces its setting. If x is the displacement of the pump, the setting of RV2 can be expressed as follows:

$$p_t^*(x) = p_0 + \varepsilon \cdot (x_{\max} - x) \tag{A.6}$$

where p_0 is the minimum spring load and ε is a constant value, comprehensive of the spring stiffness and the cam shape angle. For every pump configuration, the maximum pump pressure is determined by the minimum between the setting of RV1 and RV2:

$$p_{\max}(x) = \min\left(p^*, p_t^*(x)\right) + m \tag{A.7}$$

Based on Eq. (A.7), the torque limiter provides a linear relationship between flow and pressure of the pump. This is shown in Figure A.29, where the operating area of the pump is defined by a trapezoid. The torque limitation is active between point A and point B, where the pressure limit of RV1 is reached. Differently from the arm-linkage mechanism previously presented, the cam-relief concept is capable only of approximating the constant power condition. The hyperbolic trend can be better approximated by properly shaping the cam or by using nested springs on RV2. Furthermore, the reader should notice that the cam-relief control limits the torque by acting on the maximum pressure allowed at the pump outlet. Vice versa, the arm-linkage control reduces the pump displacement based on the pressure. This latter concept sounds more natural, as usually the pump pressure is defined by the external loads.

References

1 Heywood, J.B. (2018). *Internal Combustion Engine Fundamentals*, 2e. McGraw Hill.

2 Chapman, S.J. (2004). *Electric Machinery Fundamentals*, 4e. MxGraw-Hill Higher Education.

3 Fitzgerald, A.E., Kingsley, C., and Umans, S.D. (2005). *Electric Machinery*, 6e. McGraw-Hill.

4 Krause, P.C., Sudhoff, S.D., and Wasynczuk, O. (2002). *Analysis of Electric Machinery and Drive Systems*, 2e. Wiley.

Index

WILEY END USER LICENSE AGREEMENT

Go to www.wiley.com/go/eula to access Wiley's ebook EULA.